



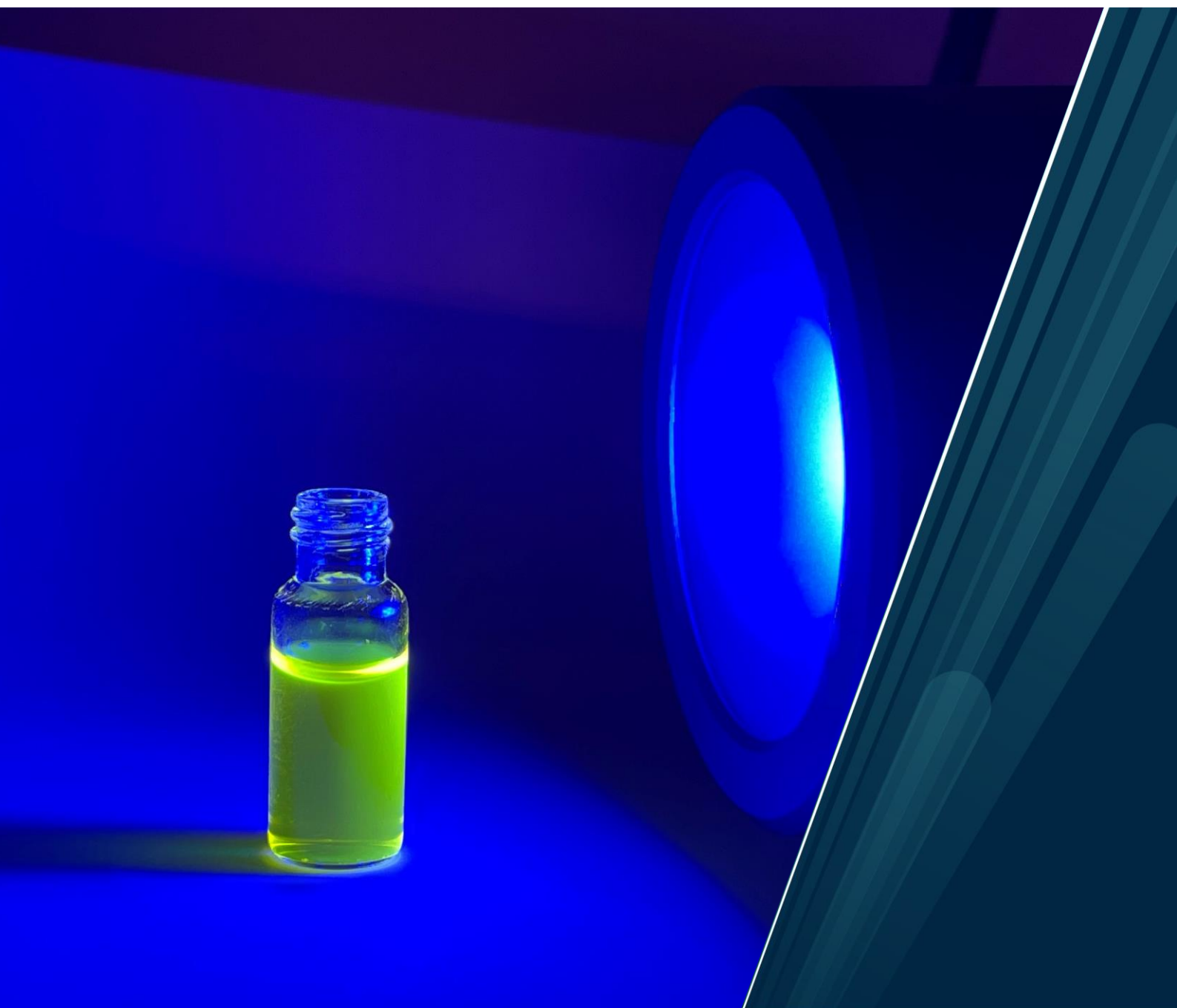
UiT The Arctic University of Norway

Faculty of Science and Technology

Visible light-mediated alkyl radical additions to alkenyl and alkynyl silanes

Floriane Baussière

A dissertation for the degree of Philosophiae Doctor – October 2024



“One more experiment and it should be done!”

Famous last words

Acknowledgements

To all the people who have been part of my PhD journey, thank you, I couldn't have done it without you. A single page is extremely short to thank everyone properly, but here goes:

A special thank you to my incredible supervisor Marius for supporting me through it all and giving me the opportunity to work on this amazing chemistry in the first place. It has (mostly) been a blast! Thank you for all the talks, debates, encouragements and for stopping me from throwing my reaction vials and computer out the window during the challenging times. This PhD wouldn't have been possible without you. And this thesis would definitely not have been written without your help. I will dearly miss our conversations about otters and life, the tea/coffee/sweets breaks, the group activities and our karaoke time in Japan.

To Mateusz and Anna-Luisa, thank you for being amazing friends and office mates, I couldn't imagine my years in Tromsø without you. There's no one else I would rather share a lab/listen to 80's music/hunt down our favorite chemists with. These four years with you have been filled with adventures and scientific discoveries, I am so grateful. Thank you for all the laughs, support, nights out, gossip, drinks, dinners and passionate conversations about our most beloved/despised compounds. Mateusz, thank you for being your organized self and reminding me of all important dates/deadlines and keeping both our lives in check. I cannot wait to hear all about your next step and am looking forward to visiting you across the Atlantic, be it at Cornell, in British Columbia or while drinking cocktails on a beach at our dream conference. And if it all goes sideways, let's open our bakery! Anna, thank you for all the knitting evenings and ski trips, and your support during these writing months, I greatly appreciated it. You are getting all my house decorations when I move out of Tromsø!

To Jana, I am so grateful we have met. Thank you for all the trips and adventures, concerts, cooking sessions, choir practices, knitting times, bouldering evenings and all the great conversations, I look forward to visiting you in sunny South Africa.

Thank you to Jostein, Truls and Ronny for keeping the department running. To all my coworkers, thank you for the nice work environment, Friday cakes, great lunch conversations and fun parties, I've had a great four years thanks to you. A special thank you to Kumar and Sinduh for our time sharing an office, it was great fun. Thank you to Fredrik, Martin and Quentin for the Mansions of Madness game nights.

To all my friends who have endured my curiosity and patiently listened to all my long speeches about molecules, synthesis issues and mechanisms throughout the years, thank you. Fanny, Séverine, Alessia, Vicky, Thomas, Hélène, Kevin, Adrien, Yann and Loïc, thank you for being amazing friends and your endless support that started many years before this PhD. Thank you for all the times together, calls, and for always having my back and offering to come kidnap me when times get rough. I hope this thesis will help you understand what it is I do in my lab, it should be a lot clearer than my confused live explanations. A special thank you to Simon for staying in touch no matter where you are in the world, and for not ending our friendship over me missing your wedding (I promise I've tried finishing writing this thesis early, but it didn't work out).

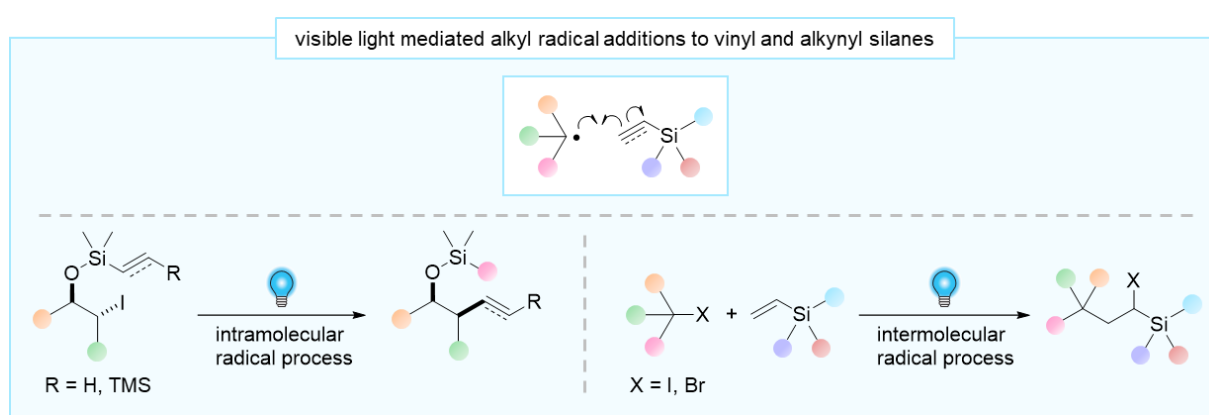
To my family, thank you! You've always supported my passion for science and chemistry, I am really grateful and miss you all (but you know that already). Thank you for being there for me, especially these last few months, and stopping me from running away and starting a new life under a new identity instead of writing this thesis. Most of all, I'd like to express my deepest gratitude to my mom and sister Caroline, for everything. You will be proud to know this page was written in complete last-minute frenzy!

Floriane Baussière
October 2024, Tromsø, Norway

Abstract

Radicals are reactive species that possess a unique reactivity, which enables them to form unusual bonds unreachable by ionic chemistry. In the last twenty years, radical chemistry has benefited from a renewed interest due to the emergence of methods that can initiate radical reactions under mild conditions. Among those, visible light-mediated radical chemistry has become established as a powerful synthetic strategy and is to this day a fast-growing field.

Organosilanes are a highly useful and versatile class of compounds that have found multiple applications in synthetic chemistry. Despite belonging to the same periodic table group, significant differences exist between carbon and silicon, which impact their reactivities. While radical additions to unsaturated C-C bonds are well known, similar additions to alkenyl and alkynyl silanes remain underexplored. The work presented in this thesis aimed to investigate and develop new methods for the visible light-mediated intra- and intermolecular addition of alkyl radicals onto vinyl and alkynyl silanes (Scheme i).



Scheme i. Alkyl radical addition to vinyl and alkynyl silane and generic reactions performed in this thesis.

First, we have developed a general protocol for the introduction of vinyl and alkynyl groups onto sp^3 carbons from activated and unactivated alkyl iodide radical precursors, using vinyl and alkynyl silyl tethers as radical acceptors. Mechanistic investigations revealed that the intramolecular photoredox catalyzed radical group transfer of the vinyl or alkynyl group from silicon to carbon proceeds through a pathway involving both single electron transfer (SET), halogen atom transfer (XAT) and chain propagation, which also includes radical cyclization and spontaneous ring fragmentation of the resulting cyclic intermediate. The protocol was successfully applied to a wide range of substrates and afforded the desired products in moderate to excellent yields with high diastereoselectivities.

Second, we investigated the photoredox catalyzed intermolecular radical addition of electron-deficient radicals onto divinyltetramethyldisiloxane. To our surprise, the anticipated radical cyclization did not take place, but a product resulting from an atom transfer radical addition (ATRA) process was formed instead. Thus, we turned our attention to the optimization of the intermolecular ATRA reaction. While this work requires further investigation, it orientated us towards our third objective.

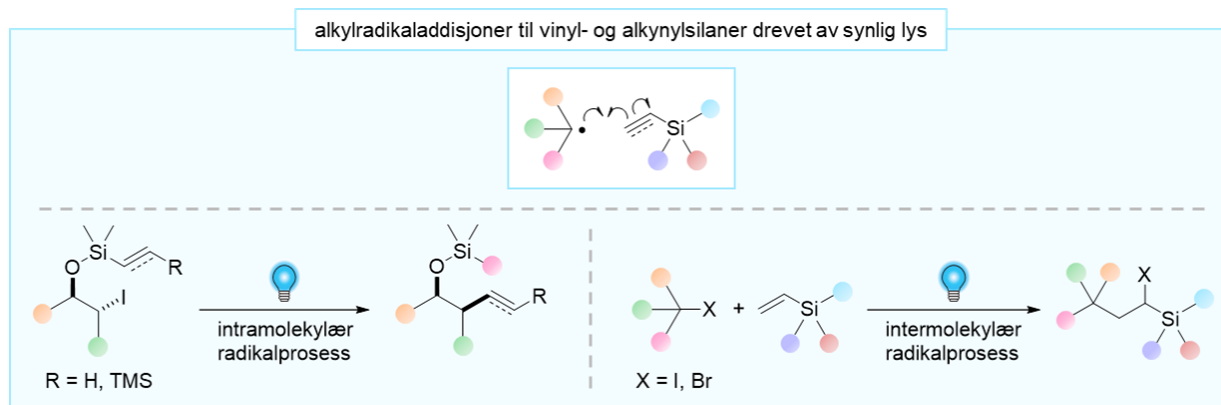
Finally, we developed a preliminary protocol for the photocatalyst-free visible light-mediated intermolecular ATRA reaction between α -iodoketones and trimethylvinylsilane. The protocol was successfully applied to a selection of substrates. However, a high variability of isolated yields was observed despite extensive screening of the reaction conditions, which suggests that the optimal conditions may be substrate dependent. We postulated that the desired ATRA reaction was initiated by photoexcitation of a halogen bond (XB) complex and operated through chain propagation.

Overall, we have successfully developed both inter- and intramolecular radical addition processes of alkyl radicals to vinylsilanes. Through our work, we have exploited multiple ways to generate alkyl radicals from alkyl halide precursors using visible light-mediated techniques, and have gained insight onto the different mechanisms of these reactions. We anticipate that these results will establish alkenyl and alkynyl silanes as radical acceptors in contemporary radical chemistry.

Sammendrag

Radikaler er reaktive spesier som innehar en unik reaktivitet, noe som gjør at de kan danne uvanlige bindinger som ikke er tilgjengelige gjennom ionisk kjemi. I løpet av de siste tjue årene har interessen rundt radikalkjemi blitt fornyet på grunn av fremveksten av metoder som kan initiere radikalreaksjoner under milde betingelser. Blant disse har radikalkjemi som er drevet av synlig lys blitt etablert som en slagkraftig syntesestrategi, og dette er fremdeles felt i rask vekst.

Organosilaner er en svært nyttig og allsidig klasse forbindelser som har funnet flere anvendelser i syntetisk kjemi. Til tross for at de tilhører samme gruppe i periodesystemet, er det betydelige forskjeller mellom karbon og silisium, noe som påvirker deres reaktiviteter. Mens radikaladdisjoner til umettede C-C-bindinger er veletablert, har lignende addisjoner til alkenyl- og alkynylsilaner blitt lite utforsket. Arbeidet presentert i denne avhandlingen hadde som mål å undersøke og utvikle nye metoder for intra- og intermolekulære addisjoner av alkylradikaler til vinyl- og alkynylsilaner drevet av synlig lys (Skjema ii).



Skjema ii. Alkylradikaladdisjon til vinyl- og alkynylsilan og generiske reaksjoner utført i denne avhandlingen.

Først har vi utviklet en generell protokoll for introduksjon av vinyl- og alkynylgrupper på sp^3 -karboner fra aktiverte og uaktiverede alkyljodid-radikalforløpere, ved bruk av forankrede vinyl- og alkynylsilaner som radikalakseptorer. Mekanistiske undersøkelser viste at den intramolekulære fotoredoks-katalyserte radikalgruppeoverføringen av vinyl- eller alkynyl-gruppen fra silisium til karbon skjer gjennom en trasé som involverer både enkeltelektronoverføring (SET), halogenatomoverføring (XAT) og propagering av en kjedereaksjon, og inkluderer også radikalsyklisering og spontan fragmentering av det resulterende sykliske intermediet som dannes i reaksjonen. Protokollen ble anvendt på et bredt spekter av substrater og ga de ønskede produktene i moderate til utmerkede utbytter med høy diastereoselektivitet.

Deretter undersøkte vi den fotoredoks-katalyserte intermolekulære radikaladdisjonen av elektronfattige radikaler til divinyltetrametyldisiloksan. Til vår overraskelse fant ikke den forventede radikalsykliseringen sted, men et produkt som er resultatet av en radikaladdisjon med atomoverføring (ATRA) ble dannet i stedet. Dermed rettet vi oppmerksomheten mot optimaliseringen av denne intermolekulære ATRA-reaksjonen. Selv om videre undersøkelser fortsatt er nødvendig i dette arbeidet, orienterte det oss også mot vårt tredje mål.

Til slutt utviklet vi en foreløpig protokoll for en fotokatalysator-fri intermolekulær ATRA-reaksjon drevet av synlig lys mellom α -jodketoner og trimetylvinyllsilan. Protokollen ble anvendt på et utvalg av substrater. Imidlertid ble det observert en høy variasjon i isolerte utbytter til tross for omfattende

screening av reaksjonsbetingelsene, noe som tyder på at de optimale betingelsene kan være substratavhengige. Vi postulerte at den ønskede ATRA-reaksjonen ble initiert ved fotoeksitasjon av et halogenbindingskompleks (XB-kompleks) og opererte gjennom kjedepropagering.

Samlet sett har vi lykket i å utvikle både inter- og intramolekulære radikaladdisjonsprosesser av alkylradikaler til vinylsilaner. Gjennom arbeidet vårt har vi utnyttet flere måter å generere alkylradikaler fra alkylhalidforløpere ved hjelp av teknikker drevet av synlig lys, og har fått innsikt i de forskjellige mekanismene for disse reaksjonene. Vi forventer at disse resultatene vil etablere alkenyl- og alkynylsilaner som radikalakseptorer i moderne radikalkjemi.

Summary of papers and author contributions

Paper I

Radical Group Transfer of Vinyl and Alkynyl Silanes Driven by Photoredox Catalysis

Floriane Baussière and Marius M. Haugland

J. Org. Chem. **2023**, 88, 12451-12463.

Paper summary

In Paper I, we investigated the photoredox catalyzed group transfer of vinyl and alkynyl groups from silyl tethers to sp^3 carbons. To this end, a wide scope of activated and unactivated alkyl halide radical precursors were synthesized and applied in the protocol, giving the desired homoallylic and homopropargylic alcohols in moderate to high yields and excellent diastereoselectivities. The mechanism of the reaction was investigated.

My contribution

I contributed to the planning and development of the synthetic strategy. I synthesized all the compounds and analyzed all analytical data. I contributed to the elucidation of the reaction mechanism. I wrote the first draft of the manuscript and contributed to the revision of the paper.

Paper II

Light-promoted synthesis of complex α -iodoalkylsilanes

Floriane Baussière and Marius M. Haugland

Manuscript

Paper summary

In Paper II, we investigated the visible light-mediated photocatalyst-free intermolecular ATRA reaction between α -iodoketones and trimethylvinylsilane. To this end, an extensive screening of the reaction conditions was performed with a panel of prepared substrates. The mechanism of the reaction was investigated.

My contribution

I contributed to the planning and development of the synthetic strategy. I synthesized all the compounds and analyzed all analytical data. I contributed to the elucidation of the reaction mechanism. I wrote the first draft of the manuscript and contributed to its revision.

Abbreviations

4CzIPN	2,4,5,6-Tetrakis(9 <i>H</i> -carbazol-9-yl) isophthalonitrile
A	Electron acceptor
AIBN	Azobisisobutyronitrile
APCI	Atmospheric pressure chemical ionization
ATRA	Atom transfer radical addition
BDE	Bond dissociation energy
BP	Benzoyl peroxide
bpy	2,2'-Bipyridyl
CDMV	Chlorodimethylvinylsilane
D	Electron donor
DIPEA	<i>N,N</i> -Diisopropylethylamine
DLP	Dilauroyl peroxide
DMAP	4-Dimethylaminopyridine
DMF	Dimethylformamide
dtbbpy	4,4'-Di- <i>tert</i> -butyl-2,2'-bipyridyl
DVTMDS	Divinyltetramethyldisiloxane
EDA	Electron donor-acceptor
EDMS	Ethyldimethylsilyl
EPR	Electron paramagnetic resonance
E_{red}	Reduction potential
ESI	Electrospray ionization
EWG	Electron-withdrawing group
GC-MS	Gas chromatography-mass spectrometry
HAT	Hydrogen atom transfer
HE	Hantzsch ester
HOMO	Highest occupied molecular orbital

HPLC	High-performance liquid chromatography
HRMS	High-resolution mass spectrometry
IR or FTIR	Infrared
<i>J</i>	Coupling constant
LC-HRMS	Liquid chromatography-high resolution mass spectrometry
LDA	Lithium diisopropylamide
LED	Light-emitting diode
LUMO	Lowest unoccupied molecular orbital
<i>m</i> -CPBA	<i>meta</i> -Chloroperbenzoic acid
MesAcr	Mesityl acridinium
NBS	<i>N</i> -Bromosuccinimide
NIS	<i>N</i> -Iodosuccinimide
NISac	<i>N</i> -Iodosaccharin
NMR	Nuclear magnetic resonance
NOE	Nuclear Overhauser effect
PC	Photocatalyst
PMP	1,2,2,6,6-Pentamethylpiperidine
PPTS	<i>para</i> -Toluenesulfonate
ppy	[2-Phenylpyridinato- <i>C</i> ² , <i>N</i>]
<i>R</i> _f	Retention factor
rt	Room temperature
SET	Single electron transfer
SOMO	Singly occupied molecular orbital
TBAF	Tetrabutylammonium fluoride
TBAI	Tetrabutylammonium iodide
TBSCl	Tributylsilyl chloride
TEDMS	[2-(trimethylsilyl)ethynyl]dimethylsilyl

TEMPO	2,2,6,6-Tetramethylpiperidine 1-oxyl
TES	Triethylsilyl
THF	Tetrahydrofuran
TLC	Thin-layer chromatography
TMS	Trimethylsilyl
TTMSS	Tris(trimethylsilyl)silane
TTMSSOH	Tris(trimethylsilyl)silanol
UV	Ultraviolet
UV-vis	Ultraviolet-visible light
XAT	Halogen atom transfer
XB	Halogen-bond
Δ	Heat
δ	Chemical shift
ν_{\max}	Wavelength of maximum absorbance

Table of Contents

Acknowledgements	i
Abstract	iii
Sammendrag	v
Summary of papers and author contributions	vii
Abbreviations	ix
1. Introduction	1
1.1 Radical chemistry.....	1
1.1.1 Background.....	1
1.1.2 Radical addition to unsaturated bonds	2
1.1.3 C-centered radicals	2
1.1.4 Visible light photocatalysis.....	3
1.1.5 Photoredox catalysis	4
1.1.6 Atom transfer radical addition (ATRA).....	6
1.1.7 Halogen atom transfer (XAT).....	7
1.1.8 Halogen-bond (XB) complexes	9
1.2 Organosilanes.....	11
1.2.1 Silanes in organic chemistry	11
1.2.2 α -Haloalkylsilanes	12
1.2.3 Silyl tethers in radical chemistry	13
1.3 Radical addition to alkenyl and alkynyl silanes	15
1.3.1 Intramolecular radical addition to alkenyl silyl tethers.....	15
1.3.2 Intramolecular radical group transfer with silyl tethers	15
1.3.3 Intermolecular radical addition to alkenyl silanes	18
2. Aim of the thesis.....	25
3. Results	27
3.1 Radical Group Transfer of Vinyl and Alkynyl Silanes Driven by Photoredox Catalysis (Paper I)	27
3.1.1 Introduction.....	27
3.1.2 Initial results	27
3.1.3 Summary of Paper I.....	29
3.1.4 Conclusion	37
3.2 Intermolecular ATRA reaction between activated alkyl bromides and divinylsiloxane.....	38
3.2.1 Introduction.....	38
3.2.2 Synthetic strategy towards radical homoallylation of alkyl halides	38

3.2.3 Initial results	39
3.2.4 Initial optimization of intermolecular ATRA reaction	40
3.2.5 Conclusion	42
3.3 Light-promoted synthesis of complex α -iodoalkylsilanes (Paper II)	43
3.3.1 Introduction.....	43
3.3.2 Initial results	43
3.3.3 Summary of Paper II.....	47
3.3.4 Conclusion	51
4. Conclusions and outlook	53
5. Additional compounds	55
5.1 Experimental methods.....	55
5.1.1 Compounds connected to chapter 3.1	56
5.1.2 Compounds connected to chapter 3.2.....	61
5.1.3 Compounds connected to chapter 3.3	62
5.2 NMR spectra	64
5.2.1 Compounds connected to chapter 3.1	64
5.2.2 Compounds connected to chapter 3.2.....	80
5.2.3 Compounds connected to chapter 3.3	83
6. References	89

1. Introduction

1.1 Radical chemistry

*Visible light-mediated radical chemistry has received a lot of attention in the last two decades and is a vast and fast-growing field. Therefore, giving a complete overview of literature precedence on all aspects of this topic would be a colossal task, which falls outside the scope of this thesis. Instead, an overview of the main concepts directly relevant to our work is presented in this chapter. The readers are referred to a selection of excellent reviews for a more extensive perspective of the field.*¹⁻²²

1.1.1 Background

Radicals are high-energy species with different reactivities than their corresponding ionic analogues. Indeed, due to their electron-deficient nature, radicals are not bound by the same chemical rules as ions and can be used to achieve transformations and exotic chemical bonds not reachable by traditional, ionic chemistry.²³⁻²⁴ For this reason, these reactive species have been intensively studied in the last fifty years as chemists are always looking for new ways to generate chemical bonds, especially the valued C-C bond. One important aspect of open-shell chemistry is that radical reactions generate new radical intermediates that can continue reacting, until this chain of reactions is terminated. Therefore, radical transformations can enable the formation of complex chemical scaffolds in few synthetic steps as multiple chemical bonds can be generated one after the other in a single reaction, a process named radical cascade.²⁵ Another significant advantage of radical chemistry over ionic chemistry is that radical reactions can be performed in nucleophilic solvents and tolerate protic functional groups, which expands the applicability of such reactions.¹⁴ Therefore, radical chemistry offers a powerful alternative to ionic chemistry to tackle challenges in synthetic chemistry.

Despite the attractive applications of radical chemistry in synthesis, the field has long suffered from a bad reputation.²⁶ Indeed, the first radical transformations were developed prior to chemists having any fundamental understanding of radicals, which led to the historically accepted notion that these reactive species lacked selectivity and were uncontrollable and of no practical value.²⁷⁻²⁸ This misguided concept was a result of the high reactivity of open-shell species, which typically react at rates close to the diffusion limit. Uncontrolled radical chain terminations would result in the formation of numerous products.²⁹ Additionally, up until the last twenty years, radical process initiation was intimately associated with the use of highly toxic reagents, harsh reaction conditions and inaccessible technical equipment, such as high-intensity ultraviolet (UV) light sources.⁹ For these reasons, radical chemistry has long been overshadowed by ionic reactions.

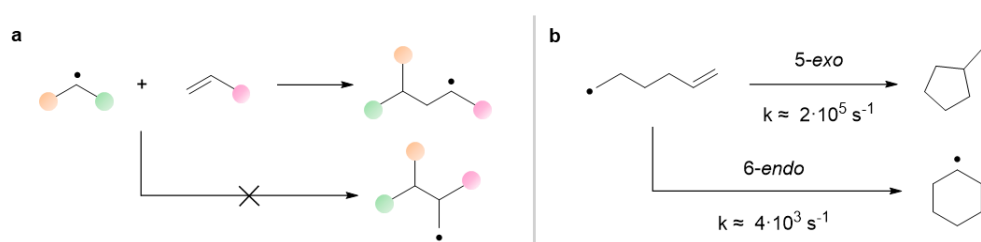
In recent years, radical chemistry has benefited from a renewed interest with the emergence of techniques able to generate radicals under mild conditions, with photoredox catalysis and electrochemistry revitalizing the use of open-shell intermediates in organic synthesis.⁵ Furthermore, the reactivity of different radical species and the factors governing radical processes have been intensively studied and are now well understood,³⁰ making it possible to design transformations with controlled outcomes through selective chemical bond formation.³¹ Nowadays, radical processes are regularly implemented in synthetic strategies, and photoredox catalysis in particular has found numerous applications notably in small molecule synthesis,^{2, 4-5} dual catalysis with metals,^{6, 12} medicinal chemistry,³² and natural product synthesis.³³

1.1.2 Radical addition to unsaturated bonds

Despite the high reactivity of open-shell species, radical reactions do not take place at random. In fact, contrary to previous beliefs, radical processes proceed with specific selectivity. The main modes of reactivity of such reactions are now well established.²⁶ Additionally, radical transformations are regulated by set reaction rates, which makes it possible to predict the outcome of synthetic reactions by comparing rate constants of competing reactions and tuning reaction systems to promote the desired transformations.³⁴ Through knowledge of philicity (see below) and reaction rates of typical radical processes, most radical reactions are highly predictable and controllable.²⁹

Among typical reactions of open-shell species are alkyl radical addition to alkenes and alkynes.³⁴ These processes have been thoroughly studied and are regularly implemented in synthetic strategies to form new C-C bonds.³⁵ Electronic effects have a strong impact on the rates of such reactions.³⁶ Indeed, radical additions onto unsaturated C-C bonds are favored by polarity match of the coupling partners, which is explained by frontier orbital theory.³⁷ Therefore, C-centered radical additions onto unsaturated bonds can generally be organized into two categories depending on the nature of the substituents present on the radical and on the radical acceptor;³⁵ addition of electron-deficient (i.e. relatively electrophilic) radicals onto electron-rich olefins, among which are the famous Minisci-type reactions,³⁸ and addition of electron-rich/neutral (nucleophilic) radicals onto electron-deficient olefins (commonly called Giese reactions).³⁹

In addition to electronic effects, C-centered radical additions onto unsaturated bonds are modulated by steric effects. As a rule, intermolecular alkyl radical additions take place on the less substituted position of unsaturated bonds (Scheme 1a).⁴⁰ Not only is the position less sterically hindered, but the resulting radical adduct is stabilized by the adjacent substituents.³⁰ Interestingly, regioselectivity of intramolecular radical additions onto unsaturated bonds differs from the selectivity of intermolecular reactions. Indeed, these small ring forming processes are kinetically controlled, and 5-*exo* ring closure is favored over 6-*endo* due to a better overlap between the π system of the unsaturated bond and the singly occupied molecular orbital (SOMO) of the alkyl radical, which confers it a higher reaction rate k (Scheme 1b).³⁴



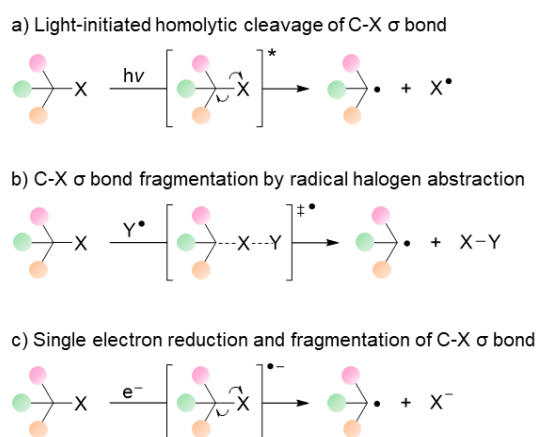
Scheme 1. Regioselectivity of (a) inter- and (b) intramolecular alkyl radical addition to π bonds.^{34, 40}

1.1.3 C-centered radicals

Alkyl radicals are the most commonly encountered open-shell species in organic synthesis. They typically have a relatively nucleophilic character as their SOMO is an unhybridized p orbital of sp^2 hybridized carbons, which is stabilized by electron density donation from the surrounding substituents.³⁰ Therefore, in hydrocarbon compounds, tertiary alkyl radicals are the most stable and have the most nucleophilic character. However, the philicity of C-centered radicals is strongly influenced by the nature

of their α -substituents, and in presence of electron-withdrawing groups (EWGs) alkyl radicals can have an electrophilic character.³⁰

In addition to being formed as intermediates during radical processes, C-centered radicals can be obtained in various ways to initiate desired radical reactions. Alkyl radicals can be obtained by homolytic cleavage of labile C-N or C-O bonds or hydrogen atom transfer (HAT), a process during which a hydrogen atom is abstracted from an appropriate carbon. However, the most common way to generate alkyl radicals is by breaking carbon-halogen (C-X) σ bonds, either by light-initiated homolytic cleavage of the bond, halogen abstraction by another radical species, or by single electron reduction followed by halide anion dissociation (Scheme 2).⁹



Scheme 2. Modes of generation of C-centered radicals from alkyl halides: (a) Light-initiated homolytic cleavage. (b) Halogen atom abstraction. (c) Single electron reduction and fragmentation.⁴¹

The strength of C-X bonds is an important factor for the generation of alkyl radicals from alkyl halides, and the ease with which said radicals are formed is inversely proportional to the bond dissociation energy (BDE) of C-X bonds, which follows the trend C-Cl > C-Br > C-I.⁴¹ While alkyl radicals are easily generated from most alkyl halides by reaction with tin-centered radicals, they are harder to form under milder reaction conditions due to the C-X BDEs, especially from alkyl chlorides.⁹ Therefore, alkyl iodides are typically used as radical precursors in light-mediated radical initiation protocols. However, C-X bonds can be weakened – or “activated” – by EWGs in the α -position and benzylic substituents, and electron-deficient bromides are also commonly used in radical photochemistry.³

1.1.4 Visible light photocatalysis

Unlike UV light irradiation, visible light irradiation is an advantageous way to initiate radical reactions as it is not harmful, does not require expensive setups and is readily available using commercially available light-emitting diode (LED) lamps. Indeed, compared to earlier radical initiation methods that typically required toxic reagents, visible light photocatalysis constitutes a successful step towards greener chemistry as it enables the generation of radicals under very mild conditions. This field has received significant attention in the last two decades.⁴²⁻⁴³

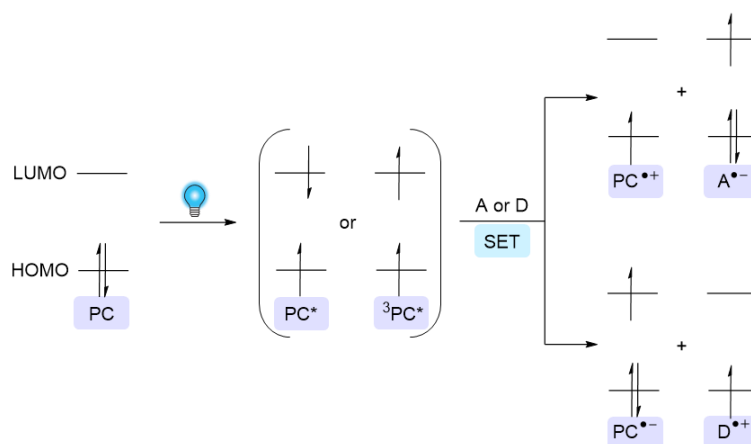
Ultimately, alkyl radical generation by direct photoexcitation of radical precursors and subsequent homolytic cleavage of the desired bond represent the holy grail of visible light photocatalysis, and a few examples of such reactions have been reported.^{14, 20} However, most organic molecules do not absorb light in the visible range and the presence of additional photoexcitable reagents are often required to

initiate radical reactions. Such compounds are referred to as photocatalysts (PCs).⁹ Alternatively, complexes that absorb visible light can be formed between radical precursors and specific additives as another way to promote light-mediated radical initiation.¹⁵ While from an atom economy perspective the use of photocatalysts and additives is a drawback, this strategy has the advantage of producing only a single photoexcitable species of molecule or complex, thereby increasing the selectivity of what radicals are generated and thus the selectivity of reactions as a whole.^{1,5} Alkyl radicals can be generated from alkyl halides under visible light irradiation *via* several different mechanisms, and the main pathways for this are discussed below.

1.1.5 Photoredox catalysis

Nowadays, photoredox catalysis is the most widespread method for light-mediated initiation of radical reactions. This approach benefits from an increased sustainability profile compared to the previously used initiation methods as it is generally more energy efficient, safer and has a reduced environmental impact.⁴⁴⁻⁴⁵ Indeed, photoredox catalysis relies on the use of bench stable and relatively non-toxic PCs, which can catalyze radical initiation at room temperature using extremely low catalyst loadings.³

The key principle of photoredox catalysis is single electron transfer (SET). Upon visible light irradiation, promotion of a single electron of the photocatalyst leads to the formation of an excited singlet or triplet state, which results in two partially filled orbitals (Scheme 3). SET between the excited photocatalyst and an electron donor (D) or electron acceptor (A) results in two radical ions, each of which can in turn initiate radical processes.^{3,5}

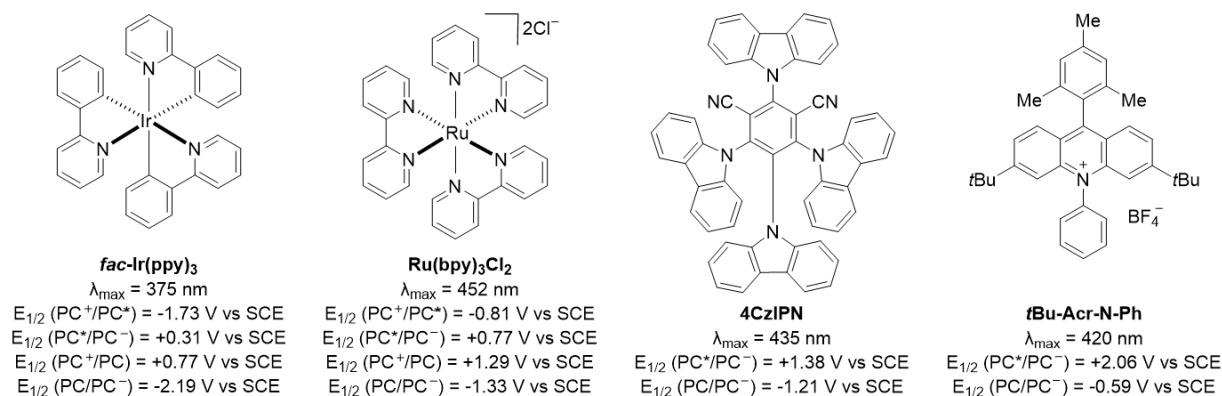


Scheme 3. Radical generation by visible light photoexcitation of PC and SET from/to D or A.^{3,5}

Photoredox catalysis has revived the interest of chemists for photochemistry and is a hot and fast-growing field.¹⁻⁵ As a result, a wide range of PCs have been applied to visible light-mediated radical processes and new PCs are continuously being developed as interactions between PCs and other reagents are regulated by the photo- and electrochemical properties of PCs. Indeed, SET between a photoexcited PC and A can only occur if the oxidation potential of the excited PC is stronger than the reduction potential of A to its corresponding radical anion. Similarly, SET between an excited PC and D requires redox match between the reduction potential of the excited PC and oxidation potential of D. Therefore, the redox potentials of all reagents involved must be considered when designing photoredox catalyzed reactions.³

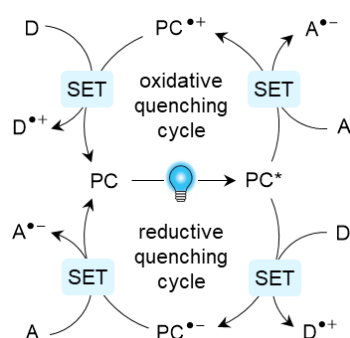
The most commonly employed PCs in photoredox catalysis are variations of iridium and ruthenium polypyridyl complexes, which absorb visible light in the blue-green range (Scheme 4).³ These

complexes benefit from long-lived excited states and generally high redox potentials. Additionally, these redox potentials can be finely tuned to fit specific reactions by modifying the ligands surrounding the central metal atom. However, the cost and finite supply of iridium and ruthenium is a long-term sustainability issue for PCs based on these metals. Luckily, metal-free alternatives are available, and numerous organic PCs have been developed and successfully applied to photoredox catalyzed reactions. 4CzIPN and mesityl acridinium (MesAcr, e.g. *t*Bu-Acr-N-Ph) PCs, in particular, are regularly implemented in synthetic strategies (Scheme 4).^{5, 46}



Scheme 4. Photophysical properties of some PCs commonly encountered in photoredox catalysis.^{3, 47-48}

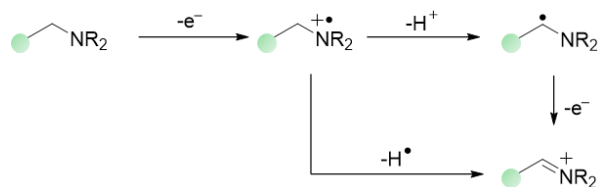
As already illustrated in Scheme 3, upon light irradiation SET can occur between an excited PC and either A or D. Therefore, two different photocatalytic cycles can take place depending on which reagent quenches the excited state PC. These two possible pathways are known as oxidative and reductive quenching cycles (Scheme 5). The mode of reactivity of a specific reaction depends on how well the redox potentials match between the different reagents involved. However, irrespective of which mechanistic cycle the reaction operates through, it typically requires a sacrificial electron acceptor or donor to turn over the photocatalytic cycle and regenerate the ground state of the photocatalyst. Common sacrificial electron acceptors include aryldiazonium salts, dinitrobenzenes and peroxides, while the most common sacrificial electron donors are tertiary amines.^{5, 47}



Scheme 5. Oxidative and reductive quenching pathways of PCs.⁵

When amines are used as electron donors, they undergo single electron oxidation of the amine to its corresponding aminium radical cation (Scheme 6). This significantly lowers the pK_a of protons in the α -position of the nitrogen, which therefore offers two different fates for the aminium radical cation. Due to its lowered pK_a , the radical cation can easily be deprotonated to an α -amino radical, which is stabilized by delocalization onto the nitrogen atom. This species can then undergo another single electron

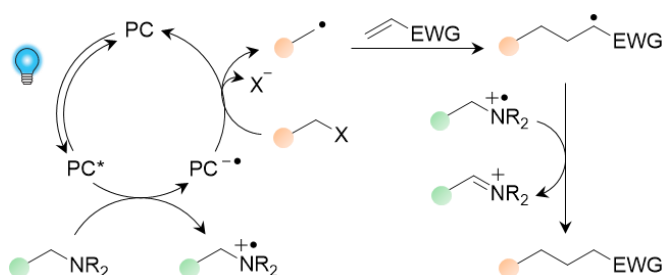
oxidation to yield its corresponding iminium ion.⁴⁹⁻⁵¹ Alternatively, the weakened C(α)-H bond means that the hydrogen atom can be easily abstracted by a hydrogen atom acceptor, and the aminium radical cation can be directly converted to the iminium ion by HAT. This makes aminium radical cations excellent hydrogen atom donors during photoredox catalyzed reactions.^{3, 52}



Scheme 6. Fate of intermediates from single electron oxidation of amines.³

Alkyl radical generation by single electron reduction of alkyl halides and subsequent C-X bond fragmentation (see Scheme 2c) is also frequently achieved by photoredox catalysis. The reduction potentials of such radical precursors are correlated with the C-X BDEs, which is why activated alkyl iodides and activated alkyl bromides (e.g., 2-bromoacetophenone, $E_{\text{red}} = -1.45 \text{ V vs SCE}^{53}$) are extensively used as substrates for such transformations. Whereas reduction of unactivated alkyl iodides (e.g., ethyl iodide, $E_{\text{red}} = -1.67 \text{ V vs SCE}^{54}$) can be achieved with strongly reducing metal-based PCs, most photoredox catalyzed processes cannot be applied to unactivated alkyl bromides (e.g., ethyl bromide, $E_{\text{red}} = -2.13 \text{ V vs SCE}^{55}$) and alkyl chlorides (e.g., ethyl chloride, $E_{\text{red}} = -2.79 \text{ V vs SCE}^{56}$) due to limitations in the redox potentials of available PCs.⁹

Photoredox catalysis systems involving alkyl halides as radical precursors and amines as sacrificial electron donors allow the transformation of alkyl halides into either simpler or more complex molecular scaffolds through reactions such as reductive dehalogenations,⁵⁷⁻⁵⁸ reductive radical cyclizations,⁵⁹⁻⁶⁰ radical cascades,⁶¹ and Giese reactions (transformation illustrated in Scheme 7).⁶² These transformations are overall reductive in nature as the substrates undergo single electron reduction and HAT during the reaction. As a result of the mild reaction conditions needed for such open-shell processes and the high tolerance of radical processes towards many functional groups, photoredox catalyzed transformations can be applied for late-stage functionalization of complex alkyl halides, which renders this strategy particularly valuable in synthetic chemistry.



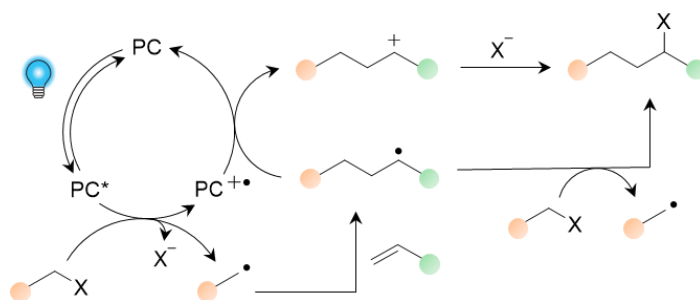
Scheme 7. Generic example of a photoredox catalyzed reaction (Giese reaction) involving an alkyl halide and an amine.

1.1.6 Atom transfer radical addition (ATRA)

Not all reactions involving alkyl halides as radical precursors are net reductive. Indeed, alkyl halides can undergo radical additions to π bonds that are net redox-neutral, through a mechanism known as atom

transfer radical addition (ATRA). In this process, the substrate undergoes both single electron reduction and single electron oxidation at different points in the mechanism. ATRA reactions are synthetically useful as they allow intra- and intermolecular dual functionalization of alkenes and alkynes with anti-Markovnikov selectivity. Additionally, they benefit from high atom efficiency as all atoms of the reagents are present in the product as well, which makes these transformations highly attractive from a sustainability perspective.⁶³⁻⁶⁶

Typically, ATRA reactions are initiated by transition metals.⁶³⁻⁶⁶ However, they can also be initiated by photoredox catalysis. In this mechanism, upon light irradiation, SET takes place between the photoexcited PC and the alkyl halide, which generates an alkyl radical that can add to a π bond (Scheme 8). Chain propagation between the radical adduct and the substrate affords the desired ATRA product. Alternatively, SET between the radical adduct and the oxidized PC provides the corresponding carbocation that may be trapped by the halogen anion to afford the desired ATRA product. The latter pathway is known as radical-polar crossover. Mechanistic studies of different photoredox initiated ATRA reactions have concluded that both the chain propagation and radical-polar crossover pathways take place during such reactions.^{57-58, 67} Therefore, no sacrificial electron donors are necessary to turn over the catalytic cycle of photoredox catalyzed ATRA reactions. Moreover, these reactions benefit from a lack of hydrogen atom donors in the reaction mixtures to avoid HAT with the radical intermediates.³

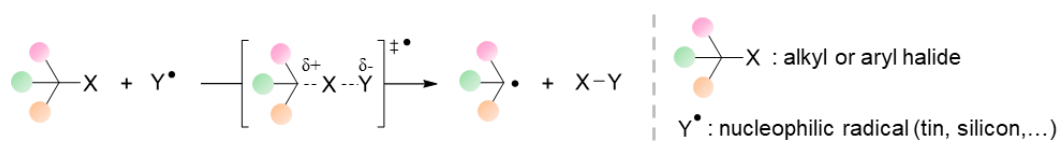


Scheme 8. Mechanism of a generic photoredox catalyzed intermolecular ATRA reaction involving both chain propagation and radical-polar crossover pathways.³

1.1.7 Halogen atom transfer (XAT)

Direct homolysis of C-X bonds under UV irradiation and single electron reduction of alkyl halides are not the only ways to generate alkyl radicals from alkyl halides using light. Indeed, halogen-atom transfer (XAT) has emerged as another powerful synthetic tool to easily access these open-shell species.⁴¹

By contrast to SET processes, the alkyl halide radical precursor does not interact with a PC during XAT. Therefore, XAT reactions are not limited by matching the redox potential of PCs and organic halides, and XAT can enable radical generation from radical precursors with high reduction potentials such as unactivated alkyl and even from the highly challenging aryl halides.⁶⁸ In XAT processes, the halogen atom is effectively abstracted from the radical precursor by another, nucleophilic radical XAT reagent through a colinear transition state (Scheme 9).

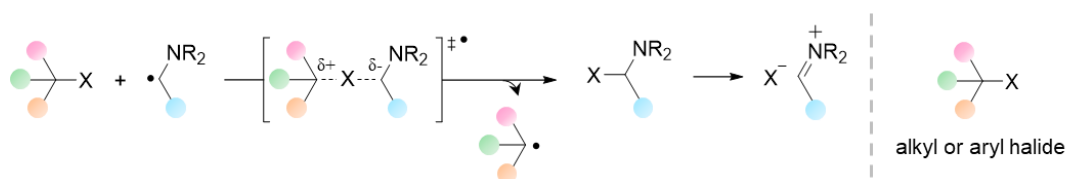


Scheme 9. XAT between organic halide and nucleophilic radical *via* colinear transition state.⁴¹

The two main factors governing XAT are polar effects and BDE, which control the kinetics and the thermodynamics of the reaction, respectively. The halogen atom transfer proceeds through a colinear transition state, during which a partial negative charge builds on the carbon bound to the halide while a partial positive charge builds on the halogen-abstracting atom (Scheme 9). Therefore, polarity plays an important role on the kinetics of the halogen atom transfer. XAT reagents able to stabilize a partial positive charge and radical precursors able to stabilize a partial negative charge can better stabilize the charge transfer during the transition state, which facilitates the halogen atom transfer and thus the generation of the desired alkyl radical. For this reason, XAT proceeds faster with electron-deficient organic halides and nucleophilic radicals as XAT reagents. Notably, inductive and steric effects also affect the rate of XAT reactions, albeit on a smaller scale than polarity, which remains the dominant factor.⁴¹

XAT is also facilitated by favorable changes in enthalpy. This is the case when the newly formed σ bond between the halogen atom and the XAT reagent is stronger than the initial C-X bond of the organic halide. Therefore, the feasibility of XAT is also dictated by differences in BDEs between the substrate and the product. XAT is facilitated by weak C-X bonds, therefore organic iodides proceed through XAT faster than organic bromides and chlorides due to their lower C-X BDEs. For the same reason, XAT is accelerated with activated organic halides. The stability of the resulting C-centered radical also has an impact on the efficiency of XAT processes, as BDEs of C-X bonds are lowered for substrates resulting in more stable radicals. Tin, silicon, germanium, boron and phosphorus radicals are commonly used as XAT reagents due to the high BDEs of the Y-X σ bonds formed, which are higher than the BDEs of C-X σ bonds.⁴¹ Additionally, aryl radicals are typical XAT reagents known to react with alkyl iodides at rates close to diffusion control.⁶⁹

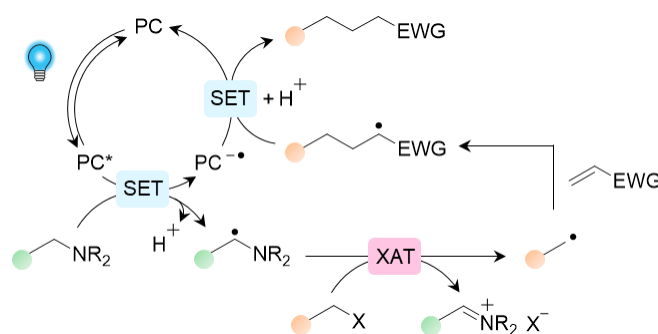
While enthalpic gain typically drives XAT processes, the atom transfer can also be initiated by radicals that form σ bonds of similar strengths than those of the initial C-X bonds if XAT is followed by irreversible fragmentation of the XAT reagent. This is the case when α -aminoalkyl and α -hydroxyalkyl radicals are used as XAT reagents (Scheme 10). Upon halogen atom abstraction, the resulting species rapidly fragment into stable iminium and carbonyl compounds, respectively, which is the overall driving force of these reactions.⁴¹



Scheme 10. XAT between organic halide and α -aminoalkyl radical followed by irreversible fragmentation of the α -haloamine to a more stable iminium ion, which provides the overall driving force of the reaction.⁴¹

The latter strategy benefits from the use of less toxic XAT reagents. Indeed, α -aminoalkyl radicals can easily be obtained by single electron oxidation of tertiary amines, which are inexpensive and widely available. This oxidation to generate the XAT reagent can be performed by photoredox catalysis, as previously discussed, making alkyl radical generation achievable under mild reaction conditions through a combination of photoredox catalysis and XAT. This synthetic strategy has been applied to a number of chemical reactions,^{68,70} as illustrated by the photoredox/XAT catalyzed Giese reaction (Scheme 11). Light-promoted SET between a photoexcited PC and a tertiary amine generates the α -aminoalkyl radical, which undergoes XAT with an alkyl halide. The resulting alkyl radical regioselectively adds to

an electron-deficient olefin, while the α -haloamine fragments into an iminium cation and iodide anion. Subsequent SET between the reduced PC and radical adduct affords a carbanion, which is protonated to afford the desired Giese product.⁶⁸

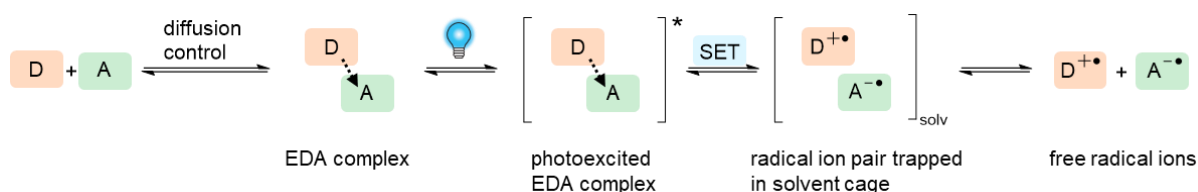


Scheme 11. Mechanism of a generic photoredox/XAT catalyzed Giese reaction.⁶⁸

1.1.8 Halogen-bond (XB) complexes

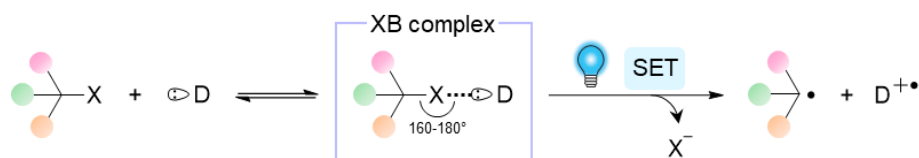
Another method to generate alkyl radicals from organohalides in a light-mediated fashion is by photoexcitation of light-absorbing complexes. Most organic compounds are colorless and therefore do not absorb light in the visible range. However, upon addition of additives, some molecules form colored electron donor-acceptor (EDA) complexes, which can be used to generate radicals by photoexcitation.^{15-16, 18-19} While photoredox catalysis and XAT are extremely powerful and versatile techniques that allow the generation of radicals under very mild conditions, they both require the use of complex and often expensive PCs to absorb visible light and initiate their respective processes. EDA complexes, on the other hand, are formed between relatively simple molecules. Therefore, the atom efficiency of radical reactions initiated by photoexcitation of EDA complexes is arguably higher than the ones of reactions initiated by SET and XAT.^{14, 20}

EDA complexes are formed between ground state electron donors (D) and electron acceptors (A) through weak interactions controlled by diffusion.⁷¹ Typically, Ds are electron-rich compounds with low ionization potentials such as amines, Hantzsch ester (HE) and *N*-hydroxyphthalimide esters.^{16, 18} On the other hand, As are electron-deficient molecules with low reduction potentials such as alkyl pyridinium salts (also known as Katritzky salts) and nitrobenzene derivatives.⁷¹ EDA complexes absorb light at a longer wavelength than their individual components, an effect known as a bathochromic shift. Therefore, most EDA complexes are colored and can be characterized by UV-vis spectroscopy.⁷¹ Upon light irradiation at their new absorption wavelength, EDA complexes form excited states that can trigger SET between their components (Scheme 12). The resulting radical ion pairs are initially trapped in solvents cages, from which they must escape to generate free radical ions and thus initiate radical reactions.^{15, 71}



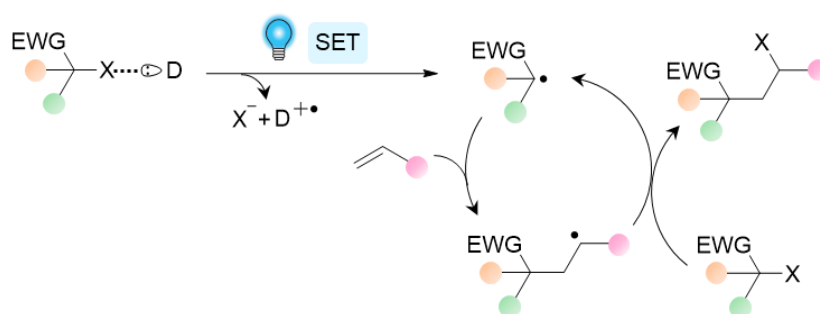
Scheme 12. Radical initiation by visible light irradiation of EDA complexes.^{18, 71}

Interestingly, C-centered radical generation from alkyl or aryl halides by light irradiation of colored complexes occurs through a slightly different mechanism. While the principle remains that photoexcitation of colored complexes formed from colorless compounds leads to subsequent fragmentation into radical species upon SET, the interaction between the partners in the complex differs. Indeed, while they are overall electronegative, halides covalently bound to carbon atoms exhibit an area of local positive surface potential on the halide, diametrically opposite to the C-X bond, which is known as a σ -hole.⁷² This electron-deficient region can interact with an electron donor through a supramolecular interaction between the σ^* orbital of the C-X bond and a filled non-bonding orbital of D.⁷³ Partial charge transfer across this orbital interaction results in a non-covalent halogen-bond (XB), which forms a 160° to 180° angle with the C-X bond.²¹ In this way, XB complexes are formed by σ -hole interactions between electron donors, which are typically amines, phosphines and sulfides, and C-bound halides.²¹ Similarly to EDA complexes, XB complexes display a bathochromic shift in UV-vis spectroscopy as they absorb light at a longer wavelength than their separate components. Beyond UV-vis, complexes can also be characterized by nuclear magnetic resonance (NMR), infrared (IR) and electron paramagnetic resonance (EPR) spectroscopy.²¹ Photoexcitation of XB complexes induces SET between the components, which upon fragmentation of the C-X bond results in a C-centered radical, the radical cation of the electron donor, and a halide anion (Scheme 13).²¹



Scheme 13. Alkyl radical generation by light irradiation of a XB complex.²¹

Synthetic strategies relying on σ -hole XB complexes have successfully been implemented with radical reactions using perfluoroalkyl, alkyl, aryl and alkenyl halides as radical precursors.²¹ Notably, this approach has also been applied to light-driven ATRA reactions between activated alkyl halides and terminal alkenes (Scheme 14). These reactions were promoted by XB complexation between organohalide radical precursors and amines as electron donors, and proceeded *via* chain propagation.⁷⁴⁻⁷⁶



Scheme 14. Mechanism of a generic ATRA reaction initiated by photoexcitation of an XB complex.⁷⁴⁻⁷⁶

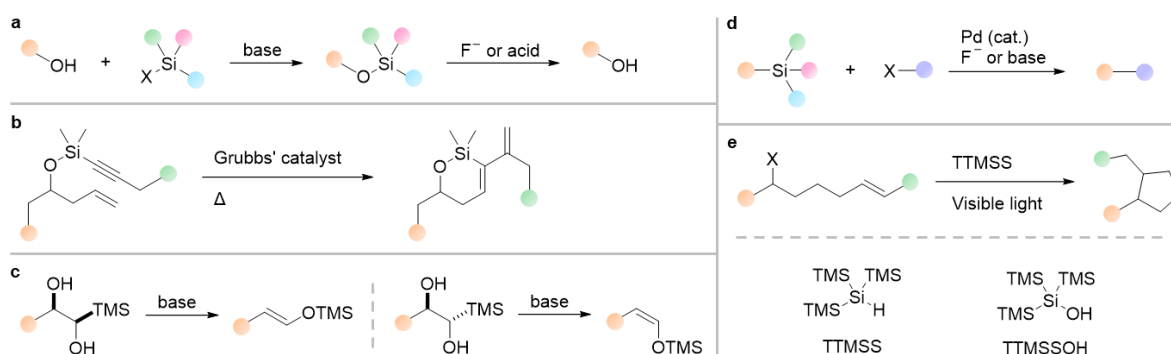
1.2 Organosilanes

Organosilanes are a highly useful and versatile class of compounds that have found multiple applications in synthetic chemistry, including radical chemistry. As this thesis focuses on intra- and intermolecular addition of C-centered radicals to vinyl and alkynyl organosilanes, the properties and main applications of organosilanes are introduced below, with an emphasis on radical chemistry.

1.2.1 Silanes in organic chemistry

Silicon is a non-toxic element found in high abundance in the Earth's crust.⁷⁷ Despite belonging to the same periodic table group as carbon, significant differences exist between the two elements, which impact their relative chemical reactivities. Not only is silicon less electronegative than carbon, but it is also a larger atom. Moreover, it can access additional electronic energy levels through employing *d* orbitals, which extends the possible coordination number of silicon and allows it to form five- and six-coordinated hypervalent complexes. Furthermore, the lengths of Si-Y covalent bonds differ from the lengths of the corresponding C-Y bonds (where Y is any other atom). These properties provide organosilanes with a unique reactivity, which has found crucial applications in the fields of polymer synthesis,⁷⁸ electronic devices,⁷⁹⁻⁸⁰ and medicinal chemistry.⁸¹⁻⁸² Moreover, organosilanes have proved highly useful reagents and intermediates in organic chemistry. In nature, silicon is only found in the form of inorganic compounds.⁷⁷ However, the formation of Si-C bonds has been thoroughly investigated, and nowadays organosilanes are widely accessible through well-developed synthetic strategies.⁸³ Additionally, a wide selection of such compounds are commercially available.

One of the main uses of organosilanes in synthetic chemistry is the protection of alcohols (Scheme 15a).⁸⁴⁻⁸⁵ Indeed, silyl ether protecting groups are easily introduced in molecules by reaction between alcohols and halosilanes under mild conditions. The resulting silyl ethers are stable under most reaction conditions and are effortlessly and selectively cleaved upon treatment with a fluoride source or acid. Therefore, silyl ether protecting groups are highly popular. For the same reasons, silyl ethers are excellent temporary tethers and are used extensively to improve the regio- and stereoselectivities of cross-coupling reactions (Scheme 15b).⁸⁶⁻⁸⁸ Indeed, these types of selectivity are easier to control in intramolecular processes, which is why temporary tethers are such a valuable synthetic strategy. Moreover, silyl groups are commonly used to control the stereochemistry of various reactions, such as the geometry of the double bond in β -eliminations (Scheme 15c).⁸⁹ Another important application of organosilanes is their use as reagents for the Hiyama coupling, which is a palladium catalyzed cross-coupling reaction (Scheme 15d).⁹⁰⁻⁹¹ In the past, organosilicon hydrides have also been used to replace highly toxic tin compounds as radical initiators.⁹² However, this approach had limited success.⁹ Nonetheless, organosilanes have found a new application in radical chemistry with the emergence of light-mediated XAT methods, as several organosilanes – among which tris(trimethylsilyl)silane (TTMSS) and tris(trimethylsilyl)silanol (TTMSSOH) are the most popular – have been shown to be highly potent XAT reagents (Scheme 15e).⁴¹



Scheme 15. Generic examples of the main applications of organosilanes in organic chemistry: **(a)** Protecting groups for alcohols.⁸⁴ **(b)** Temporary tethers for cross-coupling reactions.⁸⁶ **(c)** Control of stereochemistry.⁸⁹ **(d)** Coupling partner in the Hiyama cross-coupling.⁹⁰ **(e)** Halogen atom abstractor (XAT reagent) for radical chemistry.⁴¹

The silyl groups themselves play a crucial role in the reactivity of organosilanes, as they have the ability to stabilize negative charges in their α -position and positive charges in their β -position by hyperconjugation. These effects are known as the α - and β -silicon effects, respectively (Scheme 16).⁹³⁻⁹⁴ While both effects can influence chemical transformations, it is noteworthy that ion stabilization by the β -silicon effect is a stronger effect, and has therefore found more numerous applications in synthesis. Interestingly, silyl groups have also been shown, to a lesser extent, to stabilize α - and β -alkyl radicals.⁹⁵⁻¹⁰¹ This effect has been proposed to result from hyperconjugation and partial delocalization of the unpaired electron through a π -type bonding interaction between the half-filled p orbital of C and an empty d orbital of Si, which is known as the $(p-d)\pi$ bonding effect.⁹⁷⁻⁹⁹ Computational studies have suggested that contrary to the stabilization of ions, the stabilization of radicals by a silyl group is stronger for alkyl radicals in α -position compared to ones in β -position.¹⁰²



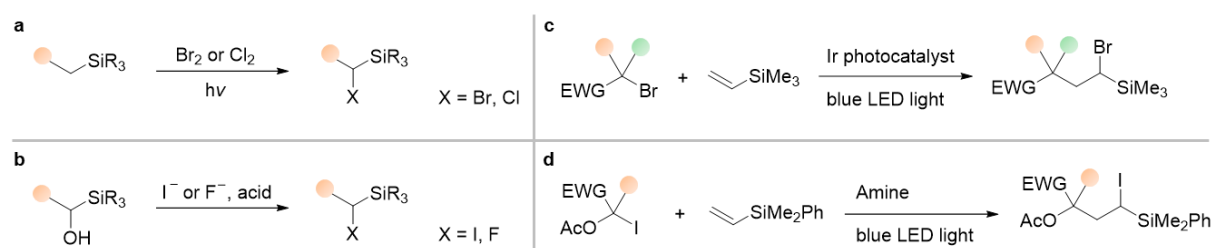
Scheme 16. Stabilizing effect of silyl groups on **(a)** cations, **(b)** anions and **(c)** radicals.⁹³⁻¹⁰¹

1.2.2 α -Haloalkylsilanes

α -Haloalkylsilanes are interesting synthetic intermediates that can be used in a variety of useful transformations.¹⁰³ Through metalation, they can be derived to Grignard reagents, which can react with electrophiles to afford more complex and valuable compounds.¹⁰⁴ Indeed, α -haloalkylsilanes find their main application as precursors for the Peterson olefination.¹⁰⁵ Alternatively, they can be used to introduce different nucleophilic substituents in the α -position of silicon by substitution of the halide.¹⁰³ An important α -haloalkylsilane reagent is the Ruppert-Prakash reagent, which is widely used for trifluoromethylation reactions.¹⁰⁶ More recently, α -haloalkylsilanes have been used as electrophiles for an enantioselective metal-catalyzed cross-coupling reaction.¹⁰⁷ This category of compounds is also highly interesting for radical chemistry, as silyl tethers containing α -haloalkylsilane moieties can be used as radical precursors for intramolecular radical cyclizations (see subchapter 1.2.3).

The applications of α -haloalkylsilanes in organic processes are limited by the challenging synthesis of these compounds, which often requires harsh conditions or highly reactive reagents.¹⁰³ α -Iodo- and α -fluoroalkylsilanes are especially difficult to access. While α -bromo- and α -chloroalkylsilanes can be

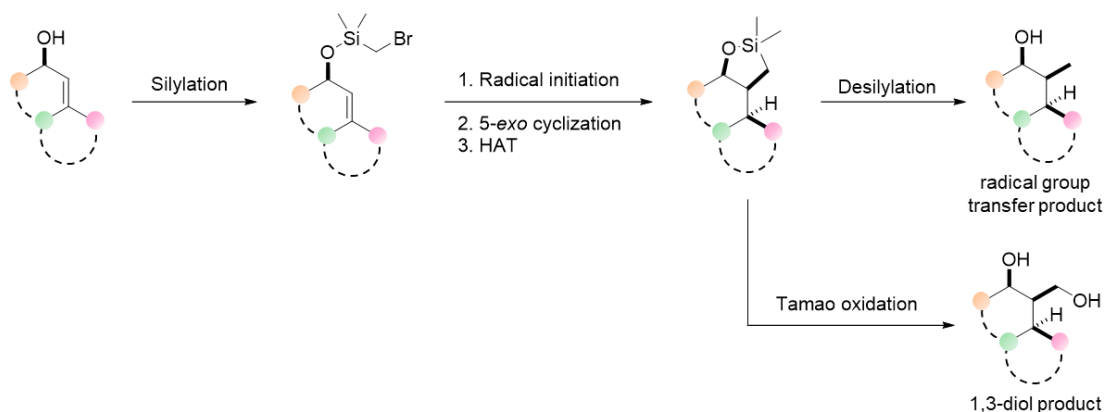
prepared by direct radical halogenation of alkylsilanes (Scheme 17a), this process is not applicable for the iodo- and fluoro- analogues.¹⁰⁸⁻¹⁰⁹ The latter compounds are typically synthesized by halogen substitution of α -hydroxyalkylsilanes (Scheme 17b), a strategy that is limited by the availability of the α -silyl alcohol precursors.^{103, 110} Radical chemistry can also be applied to prepare α -haloalkylsilanes (see subchapter 1.3.3). In the last few years, photoredox catalyzed ATRA reaction between alkyl bromides and vinylsilanes has been used to afford α -bromoalkylsilanes *via* radical chemistry (Scheme 17c).¹¹¹ More recently, α -iodoalkylsilanes were successfully synthesized by a combination of photoexcitation of an XB complex and ATRA reaction (Scheme 17d).¹¹² However, the two latter reports are the only precedent of α -haloalkylsilane synthesis through intermolecular visible light-mediated ATRA reaction between alkyl halides and vinylsilanes (see subchapter 1.3.3 for details).¹¹¹⁻¹¹⁵



Scheme 17. Generic conditions for the synthesis of (a) α -bromo- and α -chloroalkylsilanes, (b) α -iodo- and α -fluoroalkylsilanes, and visible light-mediated intermolecular ATRA reactions for the synthesis of (c) α -bromoalkylsilanes and (d) α -iodoalkylsilanes.¹⁰⁸⁻¹¹²

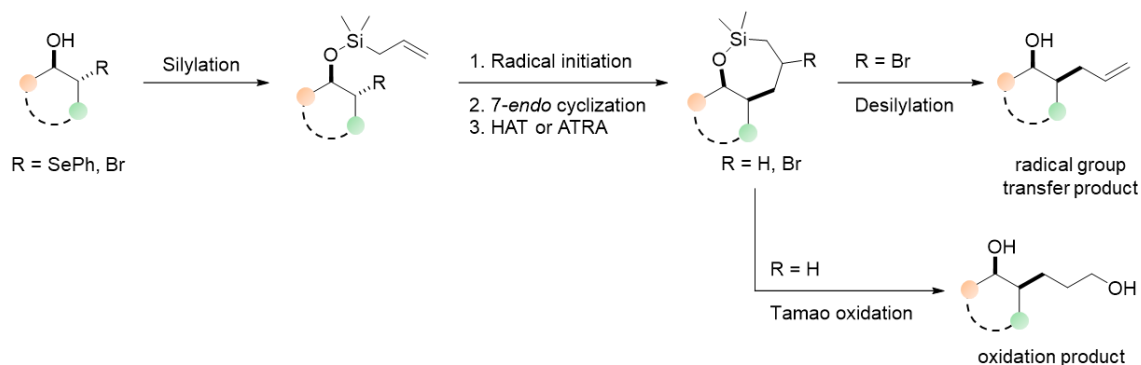
1.2.3 Silyl tethers in radical chemistry

As discussed in subchapter 1.2.1, temporary silyl tethers are widely used in organic synthesis to improve the regio- and stereoselectivity of chemical reactions by locking the reagents in intramolecular systems, before removing the tether by simple desilylation at the end of the reaction.¹¹⁶ Similarly to ionic chemistry, this powerful strategy can be applied to radical chemistry to optimize the desired transformations by bringing the reactants closer together, thus increasing the reaction rates and reducing the number of potential side-reactions.¹¹⁶ Additionally, the stereoselectivity of such transformations is high due to new C-C bonds being formed *via* radical cyclization, which is a highly controlled process (Scheme 18). Indeed, reaction from cyclic substrates allows the introduction of multiple stereocenters in a single synthetic step.¹¹⁷⁻¹¹⁸ Typically, the substrates of such radical cyclization reactions are homoallylic alcohols, which are silylated with α -bromomethylsilanes to form the required radical precursors. After the radical transformation, the resulting cyclic products can be desilylated to afford the formal radical group transfer products.¹¹⁷⁻¹²¹ Alternatively, the cyclic intermediates can be subjected to Tamao oxidation to afford 1,3-diol products.¹²²⁻¹²³



Scheme 18. Silyl tethers are regularly used in radical chemistry to stereoselectively introduce C-C bonds *via* radical cyclization.¹¹⁶⁻¹²¹

Although the most well-established strategy is to have the radical precursor on the silyl tether, this is not a requirement for radical cyclization to operate. Indeed, temporary silyl tethers can be used to introduce alkene radical acceptors instead (Scheme 19). This synthetic strategy towards the stereoselective formation of quaternary centers has been successfully used for the synthesis of branched nucleosides and nucleotides *via* radical cyclization and subsequent ring fragmentation through desilylation or Tamao oxidation.¹²²⁻¹²⁴ Moreover, it has been applied to open-chain substrates to achieve control of the stereoselectivity of newly formed C-C bonds.¹²⁵



Scheme 19. Example of radical cyclizations using silyl tethers with unsaturated substituents to control the stereoselectivity of the newly formed C-C bond.¹²²⁻¹²⁵

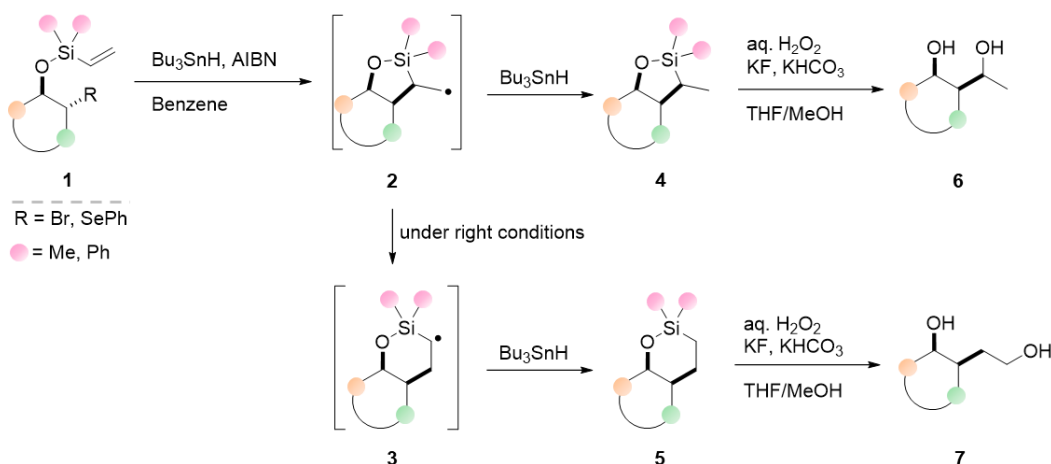
1.3 Radical addition to alkenyl and alkynyl silanes

As discussed in subchapter 1.1.2, C-C bond formation by addition of carbon-centered radicals to olefins is well known.³⁴⁻³⁵ Among these, however, relatively few examples of radical addition to alkenyl and alkynyl silanes have been reported.

1.3.1 Intramolecular radical addition to alkenyl silyl tethers

The first radical cyclization with alkenyl silyl tethers as radical acceptors was reported as a single example that formed part of a larger study of radical cyclizations.¹²⁶ This chemistry was later developed more systematically for the stereoselective synthesis of branched nucleosides. Indeed, intramolecular processes are known to enable control of the stereoselectivity of the reaction products, which makes radical cyclizations through 5-membered ring intermediates particularly interesting for the synthesis of *syn*-substituted products. In the first report of radical cyclization with silyl ethers as radical acceptors, the authors discovered that the nature of the cyclic intermediate of the radical reaction could be controlled by the reaction conditions (Scheme 20).¹²⁷ C-X σ bond cleavage of the alkyl bromide or phenylselenide radical precursor **1** by radical initiation with tributyltin hydride (Bu_3SnH) and azobisisobutyronitrile (AIBN) successfully led to a kinetically favored 5-*exo* radical cyclization.¹²⁸ Depending on the reaction temperature and the concentration of Bu_3SnH in the mixture, the resulting radical cyclic intermediate **2** could rearrange to thermodynamically more stable radical cyclic intermediate **3**. HAT between **2** or **3** and Bu_3SnH afforded the dehalogenated products **4** and **5**, respectively, which were transformed into products **6** and **7** upon Tamao oxidation. Therefore, the nature of the substituent to be introduced onto the product could be controlled by the reaction conditions of the radical reaction.¹²⁷ This synthetic strategy employing radical cyclization and ring opening by Tamao oxidation was successfully applied to the synthesis of various branched nucleosides and glycosides.¹²⁹⁻

136

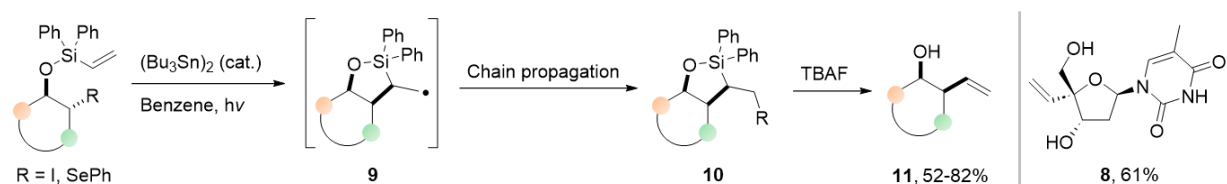


Scheme 20. Radical ring rearrangement depending on the reaction conditions.¹²⁷

1.3.2 Intramolecular radical group transfer with silyl tethers

Introduction of vinyl groups onto radical precursors *via* radical addition to tethered alkenyl silanes and subsequent ring fragmentation was first investigated for the synthesis of biologically active branched-sugar nucleoside **8** (Scheme 21).¹³⁷ The key step of this synthetic strategy was the regio- and diastereoselective introduction of the vinyl group onto the sugar ring, which required a temporary vinyl silyl ether as radical acceptor. This step was performed one-pot by a telescoped radical cyclization/desilylation procedure. Indeed, the authors proposed that upon radical initiation with

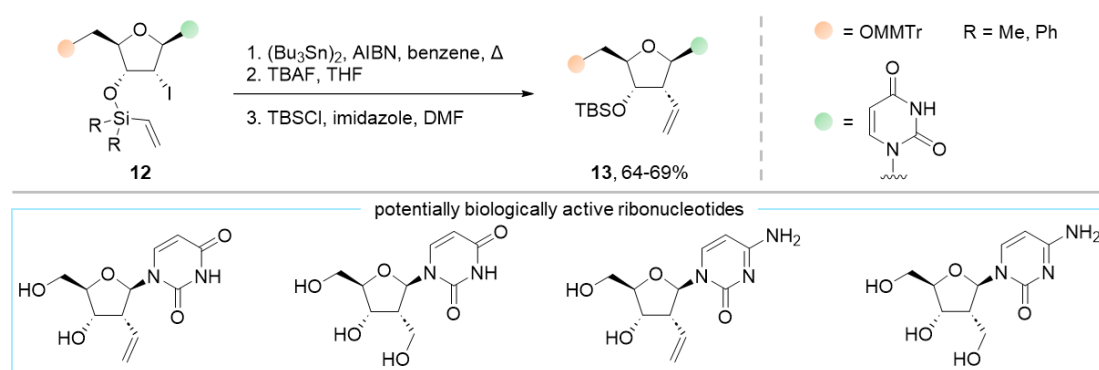
(Bu_3Sn)₂ in benzene under mercury lamp irradiation, 5-*exo* cyclic radical intermediate **9** was obtained by intramolecular addition of the formed alkyl radical to the vinyl silane. Due to the lack of a hydrogen atom donor in the reaction mixture, no dehalogenated cyclic product was formed. Instead, radical chain propagation afforded the labile cyclic ATRA product **10**, which fragmented to afford the desired group transfer product **11** upon elimination and desilylation with a fluoride source. The *syn* diastereoselectivity of the radical group transfer products was confirmed by ¹H NMR coupling constants and nuclear Overhauser effect (NOE) experiments. The authors explained this selectivity by the known *syn* selectivity of 5,5-ring fusions formed by radical cyclization reactions.²⁹



Scheme 21. Radical group transfer of a vinyl group through radical cyclization and desilylation.¹³⁷

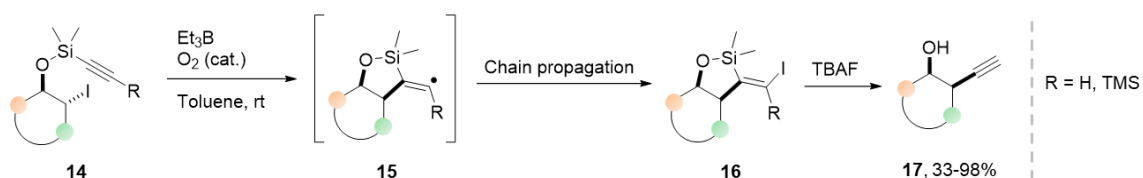
This procedure was successfully applied to a range of cyclic alkyl iodide radical precursors with vinyl silyl ether substituents and yielded the desired vinyl group transfer products **11** in 52-82% yields. In contrast, the radical reaction did not operate with the corresponding alkyl phenylselenide and alkyl bromide radical precursors. This lack of reactivity was attributed to C-Se and C-Br bonds being more stable than C-I bonds due to their higher BDEs. Indeed, the authors observed that an analogous alkyl phenylselenide substrate, which was activated by the selenide group being in a benzylic position, underwent the anticipated transformation and afforded the desired product in 53% yield. The protocol was successfully implemented as the last step of the synthesis of target nucleoside **8**, affording the desired product in 61% yield.¹³⁷

In the following year, the same synthetic strategy for radical group transfer *via* intramolecular radical addition of a C-centered radical to a vinyl silyl ether and subsequent ring fragmentation was used to diastereoselectively introduce a vinyl substituent onto a ribonucleotide, which was further converted into different potentially biologically active derivatives (Scheme 22).¹³⁸ In this study, radical cyclization was initiated by refluxing alkyl iodide radical precursor **12** with substoichiometric amounts of (Bu_3Sn)₂ and AIBN in benzene. Treatment of the cyclic intermediate with tetrabutylammonium fluoride (TBAF) followed by protection of the resulting homoallylic alcohol with tributylsilyl chloride (TBSCl) afforded the desired ribonucleoside **13** in 64-69% yield, depending on the substituents on the silane in the substrate.



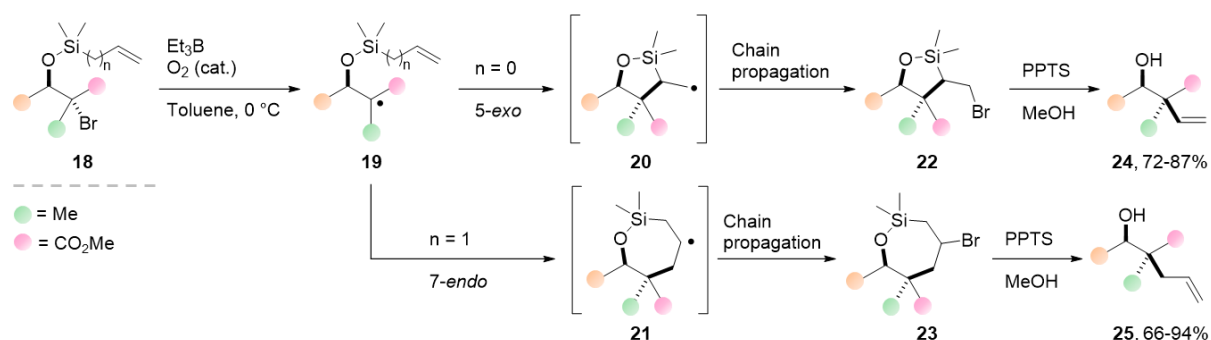
Scheme 22. Synthesis of ribonucleotide derivatives through radical group transfer of a vinyl group.¹³⁸

Further work in the field revealed that temporary silyl tethers could similarly be used to introduce alkynyl groups onto cyclic sp^3 carbons (Scheme 23).¹³⁹⁻¹⁴⁰ Indeed, 5-*exo* cyclization by radical addition to ethynyldimethylsilyl (EDMS) and [2-(trimethylsilyl)ethynyl]dimethylsilyl (TEDMS) ethers operated similarly to the intramolecular radical addition to vinyl silyl ethers discussed above. Radical initiation by treatment of alkyl iodide substrate **14** with triethylborane (Et_3B) and trace amounts of oxygen afforded cyclic radical intermediate **15**, which under these conditions further formed the labile cyclic ATRA product **16** by abstracting an iodine atom through chain propagation. Telescoped desilylation of the crude cyclic intermediate **16** by fluoride addition afforded the desired alkynylated product **17**. The protocol was successfully applied to a range of cyclic alkyl iodide EDMS and TEDMS ether substrates, diastereoselectively affording the desired alkynylated products **17** in 33-88% yields.¹³⁹ While the radical group transfer reaction indistinctly operated with EDMS and TEDMS ethers, the use of fluoride as a desilylation reagent resulted exclusively in ethynyl-substituted products **17**. This synthetic strategy was further used to introduce ethynyl groups onto various nucleosides derivatives with excellent regio- and diastereoselectivity in high yields (up to 98%).¹⁴⁰⁻¹⁴¹



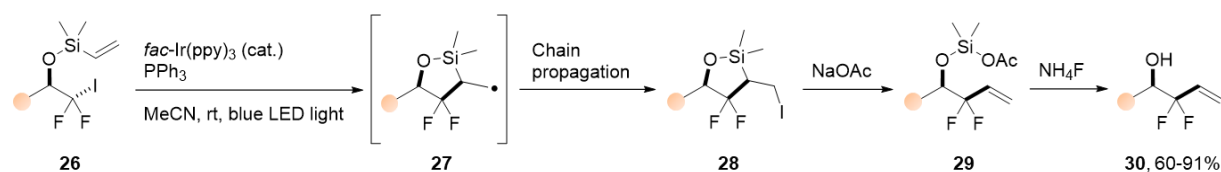
Scheme 23. Introduction of alkynyl groups onto sp^3 carbons *via* radical group transfer.¹³⁹⁻¹⁴¹

Regio- and stereoselective radical group transfer of vinyl and allyl groups onto sp^3 carbons in open-chain substrates was achieved a few years later according to a similar radical cyclization/ring fragmentation strategy (Scheme 24).¹²⁵ Tertiary acyclic alkyl radicals **19** were obtained by treatment of activated bromide substrates **18** with Et_3B and trace amounts of O_2 . Subsequent cyclization by radical attack on the vinyl or allyl silyl tether led to 5-*exo* or 7-*endo* cyclic radical intermediates **20** and **21**, respectively. Radical chain propagation afforded the corresponding cyclic ATRA intermediates **22** and **23**, which provided the desired radical group transfer products **24** and **25** with high diastereoselectivity upon elimination under mild acidic conditions with pyridinium *para*-toluenesulfonate (PPTS). The ATRA product intermediates **22** and **23** were too labile to be isolated. However, the envisioned mechanism of radical group transfer *via* a radical cyclization/elimination pathway was supported by formation of dehalogenated reduction products when the radical reaction was performed in the presence of an equivalent of Bu_3SnH as a hydrogen atom donor. The protocol was successfully used for the synthesis of a variety of quaternary vinylated and allylated products with a controlled *syn* diastereoselectivity, affording the desired products **24** and **25** in 72-87% and 66-94% yields, respectively.¹²⁵



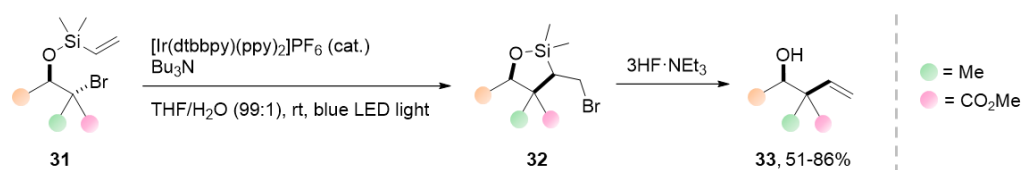
Scheme 24. Radical group transfer of vinyl and allyl groups through radical cyclization and desilylation.¹²⁵

More recently, silyl tethers were effectively used for intramolecular radical transfer of vinyl groups onto perfluorinated sp^3 carbons (Scheme 25).¹⁴² Unlike previously reported studies utilizing similar synthetic strategies, this work used photoredox catalysis to generate radicals from alkyl iodides *via* an oxidative quenching catalytic cycle. Indeed, the authors proposed that, in this one-pot reaction, the radical process was initiated by single electron reduction and following fragmentation of the activated C-I σ bond of perfluorinated radical precursor **26** with photoexcited iridium photocatalyst *fac*-Ir(ppy)₃ under blue light irradiation. Triphenylphosphine (PPh₃) was added to the reaction mixture to further activate the substrate by forming a halogen-bond complex with the iodide. The authors proposed that upon radical cyclization, the radical intermediate **27** underwent chain propagation. The labile ATRA intermediate **28** subsequently underwent nucleophilic attack by an acetate anion present in the reaction mixture, which triggered an elimination to reform the desired vinyl moiety in product **29**. Finally, the telescoped addition of a fluoride source afforded the desired homoallylic alcohol products **30** in 60-91% yields.



Scheme 25. Photoredox catalyzed radical group transfer of vinyl groups from activated alkyl iodides.¹⁴²

Most recently, a protocol for photoredox catalyzed vinyl group transfer by radical cyclization/ring fragmentation using vinyl silyl ether as a temporary tether was developed for activated alkyl bromide substrates (Scheme 26).¹⁴³ In this procedure, alkyl radicals were generated by C-Br σ bond cleavage upon SET between the radical precursor **31** and an iridium photocatalyst excited by blue light. The catalytic cycle was turned over by using a tertiary amine as sacrificial electron donor. Radical cyclization followed by chain propagation afforded the cyclic ATRA intermediate **32**. Fluoride promoted elimination led to the desired homoallylic alcohol product **33** in good to excellent yields. The origin of the high diastereoselectivity of the radical group transfer process was supported by computational studies of the reaction mechanism. This protocol was successfully used as a key step in the synthesis of complex nucleoside analogues.¹⁴³

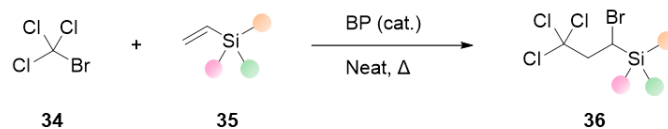


Scheme 26. Photoredox catalyzed radical group transfer of vinyl groups from activated alkyl bromides.¹⁴³

1.3.3 Intermolecular radical addition to alkenyl silanes

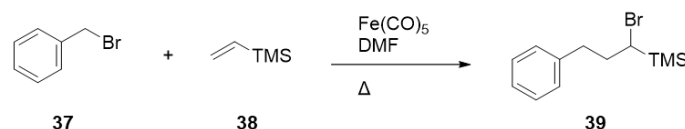
The intermolecular radical addition of C-centered radicals onto vinyl silanes was first reported as part of a larger systematic study of the reactivity of alkyl radicals with alkenyl-substituted silanes with different substituents at Si (Scheme 27).¹⁴⁴ In this study, a combination of benzoyl peroxide (BP) and heat was used to generate a C-centered radical by bromine abstraction from bromotrichloromethane **34** by the activated radical initiator. The relative rates of radical addition of the electron-deficient trichloromethyl radical onto different vinyl silanes **35** were recorded. Due to the chosen reaction conditions, all reactions resulted in their corresponding ATRA products **36**. The authors reported that the rates of radical addition onto vinyl silanes with all-carbon Si substituents were correlated with steric

factors, with the rate decreasing as the bulkiness of the substituents increased. Additionally, analysis of a similar reaction with mono- and trichloro vinyl silanes revealed that the number of inductively electron-withdrawing groups on the silane impacted the radical addition rate of the alkyl radical onto the unsaturated bond, with trichlorovinylsilane being the least reactive coupling partner.



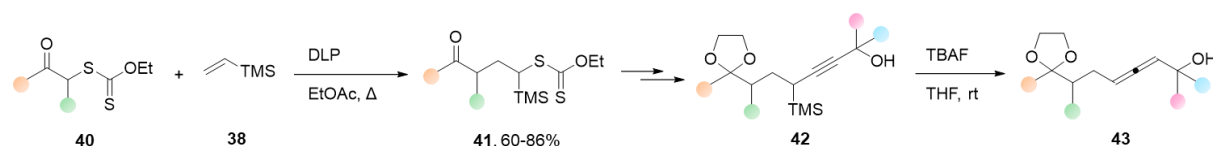
Scheme 27. Generic reaction scheme of peroxide-initiated ATRA reaction between trichloromethyl radical and vinyl silanes bearing alkyl or electron-withdrawing substituents.¹⁴⁴

The ATRA reaction between benzyl bromide **37** and trimethylvinylsilane **38** was used as a reference reaction in studies focused on benzyl radical additions onto olefins bearing substituents with different electronic properties (Scheme 28).¹¹³⁻¹¹⁵ Indeed, trimethylvinylsilane **38** proved a strategic standard coupling partner for competitive kinetics experiments due to the rate of ATRA reaction between benzyl radical and **38**, which afforded ATRA product **39**, falling into the middle range of the other ATRA reaction rates.¹¹⁵ In these studies, radical reactions were initiated from benzyl bromide **37** by a combination of substoichiometric amounts of $\text{Fe}(\text{CO})_5$, dimethylformamide (DMF) and heat.¹¹³⁻¹¹⁵



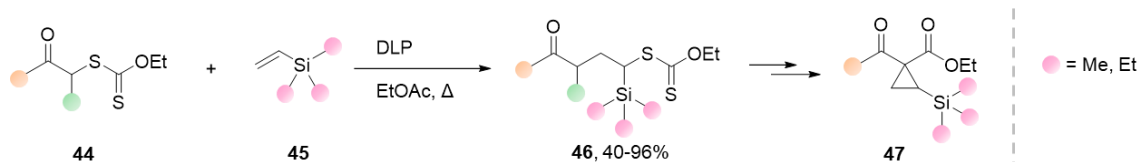
Scheme 28. ATRA reaction between benzyl radical and trimethylvinylsilane initiated by $\text{Fe}(\text{CO})_5$ and heat.¹¹³⁻¹¹⁵

Further work on ATRA reactions between alkyl radicals and vinyl silanes showed the utility of intermolecular radical additions to vinyl silanes as key steps in the synthesis of various chemical moieties. Among alkyl radical precursors, xanthates have received particular attention for such transformations due to the reversibility of the reaction between the alkyl radical and its radical precursor. In these processes the alkyl radical mostly exists as a xanthate adduct that is not prone to termination by dimerization, and continuously releases the alkyl radical into the reaction mixture.¹⁴⁵ This facilitates relatively slow radical processes such as intermolecular radical addition to olefins. ATRA reactions between xanthates and vinyl silanes was first implemented as the first step of the synthetic pathway to obtain trimethylsilyl (TMS)-substituted propargyl alcohols and 2,3-allenols (Scheme 29).¹⁴⁶ A combination of dilauroyl peroxide (DLP) and heat was successfully used to initiate the ATRA reaction between alkyl radicals obtained from α -keto xanthates **40** and trimethylvinylsilane **38**, which resulted in the desired ATRA products **41** in 60-86% yields. Further transformation of these products afforded TMS-substituted propargyl alcohols **42** in two steps, which could in turn be transformed into 2,3-allenols **43**.



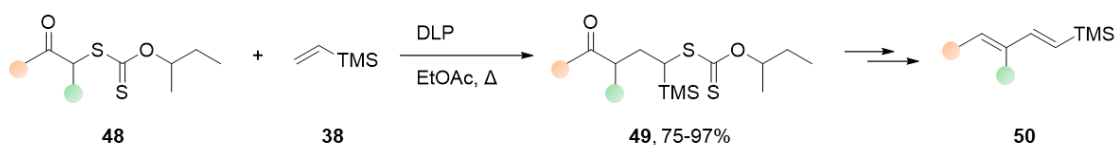
Scheme 29. Use of ATRA reaction between α -keto alkyl radicals and trimethylvinylsilane as the key step for the synthesis of TMS-substituted propargyl alcohols and 2,3-allenols.¹⁴⁶

In a follow-up study, a similar DLP/heat radical initiation protocol was used as a key step in the synthesis of silyl-substituted cyclopropanes (Scheme 30), which demonstrated another interesting synthetic application of radical addition of xanthates to vinylsilanes.¹⁴⁷ Addition of alkyl radicals generated from α -keto xanthates **44** to trialkylvinylsilane **45** afforded ATRA products **46** in 40-96% yields. These products were further transformed into the desired silyl-substituted cyclopropanes **47** in two steps.



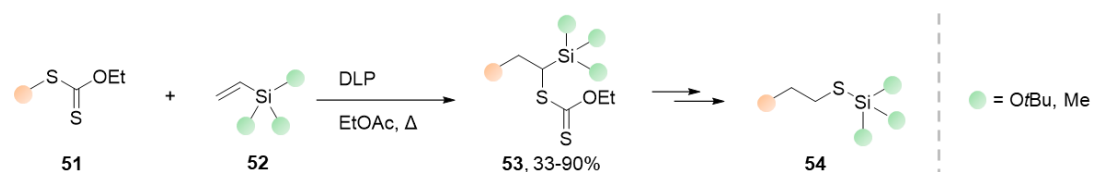
Scheme 30. Use of ATRA reaction in the multi-step synthesis of silyl-substituted cyclopropanes.¹⁴⁷

Additionally, by modifying the chain of the xanthate group, this radical protocol was successfully applied in the multi-step synthesis of synthetically useful dienylsilanes (Scheme 31).¹⁴⁸ Indeed, radical xanthate addition of α -keto xanthates **48** to trimethylvinylsilane **38** afforded the key ATRA intermediates **49** in 75-97% yields, which enabled the further synthesis of the desired (1*E*,3*E*)-TMS dienes **50** via cyclization and elimination.



Scheme 31. ATRA reaction in synthetic strategy to afford (1*E*,3*E*)-TMS dienes.¹⁴⁸

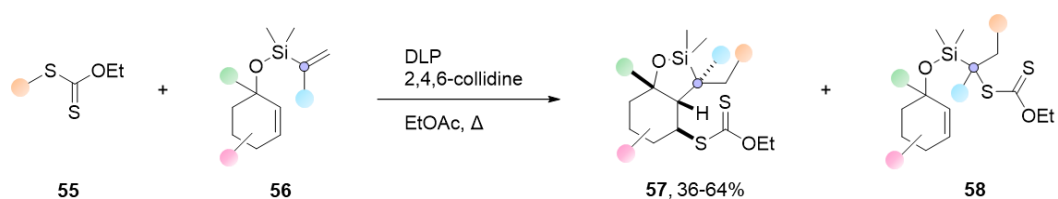
ATRA reactions between xanthates and vinyl silanes have not been limited to trialkylvinylsilanes as radical acceptors. The authors of the three previously mentioned studies reported that their protocol could additionally be applied to such reactions with trialkoxyvinylsilanes to afford trialkoxyalkylsilanes, which are otherwise challenging to prepare (Scheme 32).¹⁴⁹ Indeed, upon radical initiation with DLP and heat, an ATRA reaction between xanthates **51** and trialkoxyvinylsilanes **52** afforded the desired products **53** in 33-90% yields. The authors attributed the lowest yields to partial desilylation of the products during purification, due to the known hydrolytic sensitivity of trialkoxysilanes. This issue was overcome by replacing trimethoxyvinylsilane with more robust trialkoxyvinylsilanes, which improved the isolated yields of several products. Interestingly, in a follow-up study, further treatment of compounds **53** resulted in a radical thia-Brook rearrangement, which afforded products **54** and thus broadened the synthetic applications of radical addition to vinyl silanes even further.¹⁵⁰



Scheme 32. ATRA reaction between xanthates and trialkoxyvinylsilanes.¹⁴⁹⁻¹⁵⁰

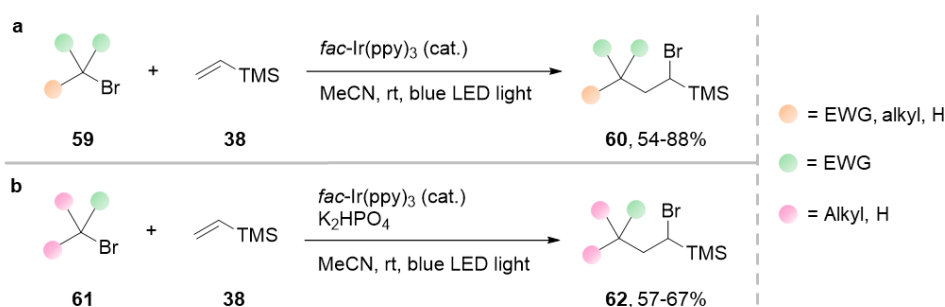
While intermolecular additions of C-centered radicals to vinylsilanes have mostly been applied to the synthesis of synthetically useful ATRA products, this strategy has also been successfully used in a

radical cascade to control the stereoselectivity of formation of fused ring systems.¹¹⁸ To that end, a protocol was developed for a radical cascade with regioselective attack by an alkyl radical – formed from xanthate radical precursor **55** – onto vinylsilane-derivatized cyclic allylic alcohols **56** as the first step, which resulted in the desired xanthate-substituted bicyclic products **57** (Scheme 33). This reaction allowed the formation of three stereocenters in a single step. Radical reaction was initiated by addition of DLP to a mixture of silylated alcohol **56** and xanthate **55** under reflux, while the proton scavenger 2,4,6-collidine was added to the reaction mixture to avoid acidic desilylation. The radical cascade to bicyclic product **57** was favored over the alternative ATRA reaction to unwanted open-chain product **58** by performing the reaction at high dilution. Nonetheless, the competing radical reaction could not be entirely eliminated. The protocol was successfully applied to a wide selection of silylated alcohols and xanthates and afforded the desired bicyclic products **57** in 36-64% yields with high diastereoselectivity.



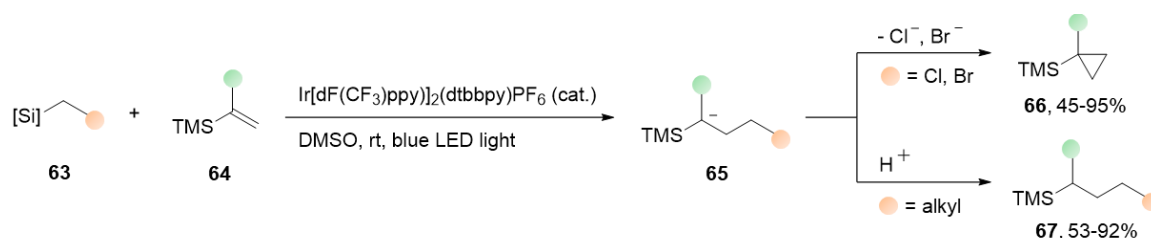
Scheme 33. Intermolecular radical cascade involving intermolecular radical addition to a vinylsilane.¹¹⁸

More recently, in 2021, an elegant photoredox-catalyzed ATRA protocol for the synthesis of α -bromoalkylsilanes by radical coupling between electron-deficient alkyl radicals and trimethylvinylsilane **38** was developed.¹¹¹ SET between blue light-excited *fac*-Ir(ppy)₃ and the radical precursors **59** led to fragmentation of the activated C-Br σ bonds to afford the corresponding alkyl radicals, which regioselectively added onto the relatively electron-rich double bond of radical acceptor **38** (Scheme 34a). Radical propagation and/or SET between the radical adduct and the oxidized photocatalyst followed by nucleophilic trapping of a bromide anion afforded the desired ATRA product **60**. The methodology was successfully applied to a range of alkyl bromides bearing two or three electron-withdrawing groups, affording the desired products **60** in 54-88% yields. The authors reported that only trace amounts of ATRA product were obtained when subjecting substrates bearing a single electron-withdrawing group **61** to the initial reaction conditions. This issue was overcome by increasing the loading of photocatalyst and trimethylvinylsilane **38**, as well as by introducing an equivalent of K₂HPO₄ to the reaction mixture to exploit the known ability of inorganic bases to facilitate similar radical reactions (Scheme 34b).⁵⁸ Under these new conditions, radical coupling between singly-activated alkyl bromides **61** and trimethylvinylsilane **38** afforded the desired ATRA products **62** in 57-67% yields. Additionally, an α -chloroalkylsilane product was successfully synthesized with the developed protocol.



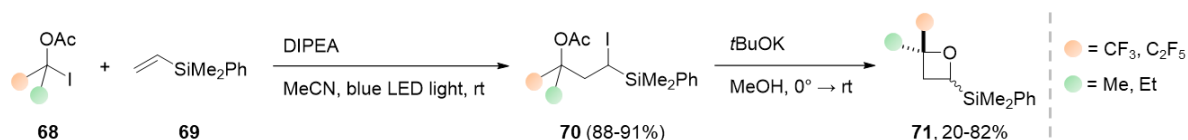
Scheme 34. Photoredox-catalyzed ATRA reaction between activated alkyl bromides and trimethylvinylsilane.¹¹¹

Later that year, a photoredox catalyzed radical-polar crossover protocol was published for the synthesis of silyl-substituted cyclopropanes and Giese-type products *via* intermolecular addition of alkyl radicals to vinylsilanes (Scheme 35).¹⁰¹ In this overall redox-neutral process, SET between the photo-excited iridium photocatalyst and a silicate alkyl radical precursor **63** generated a C-centered radical, which regioselectively added onto vinylsilane **64**. Single electron oxidation of the reduced photocatalyst by the radical adduct turned over the catalytic cycle and afforded anion **65**, which the authors suggested was the key intermediate of the transformation. Indeed, depending on the nature of the silicate used as radical precursor, two different products could be obtained from **65**. Under the same reaction conditions, reactions with chloro- and bromomethyl silicates afforded silyl-substituted cyclopropanes **66** *via* 3-*exo* cyclization of **65**, whereas Giese-type products **67** were obtained by protonation of intermediate **65** when an alkyl silicate was used instead. The protocol was successfully used for the synthesis of a range of silyl-substituted cyclopropanes and Giese-type products, affording the desired compounds **66** and **67** in 45-95% and 53-92% yields, respectively. Mechanistic investigations confirmed that the reaction proceeded *via* a radical-polar crossover process. The authors proposed that single electron reduction of the radical adduct to anion **65** was assisted by the stabilizing effect of the silyl group, thus showcasing the importance of the silyl group for the reaction.



Scheme 35. Photoredox-catalyzed overall redox-neutral reaction between alkyl radicals and vinylsilanes.¹⁰¹

Most recently, in 2024, radical initiation *via* visible light irradiation of XB complexes was successfully applied to prompt ATRA reaction between highly activated alkyl iodides and vinylsilanes through chain propagation (Scheme 36).¹¹² Upon photoexcitation of an XB complex formed between the alkyl iodide radical precursor **68** and an amine (DIPEA) and subsequent C-I σ bond fragmentation, the C-centered radical regioselectively added onto vinylsilane **69**. Chain propagation between the resulting radical adduct and **68** afforded the desired α -iodoalkylsilane ATRA product **70**, which was further transformed into oxetane **71** under basic conditions. A small substrate scope was shown to successfully afford the desired oxetane products **71** in 20-82% yields, with low diastereoselectivity. While the authors reported good NMR yields for the ATRA product afforded by the ATRA reaction between their original substrate and **69** under their optimized conditions (88-91%), yields of the other ATRA intermediates were not reported as the oxetane products were synthesized through a telescoped method.



Scheme 36. ATRA reaction between electron-deficient C-centered radicals and vinylsilanes initiated by visible-light photoexcitation of XB complexes.¹¹²

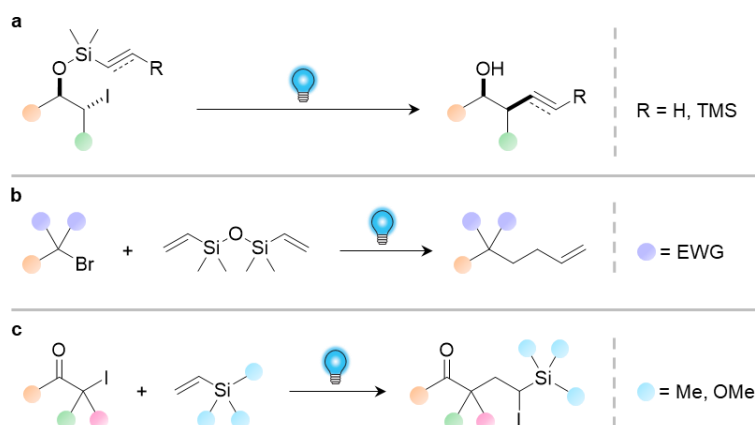
In conclusion, the first general protocols for silyl tethered radical group transfer through radical cyclization and ring fragmentation relying on modern radical initiation methods have emerged in the

last decade. While these protocols improved the sustainability of these reactions by removing the need of hazardous radical initiators and widened the scope of products that could be afforded *via* such transformations, their application remains limited to activated alkyl halides as radical precursors. Intermolecular alkyl radical additions to vinylsilanes, on the other hand, remain largely underexplored beyond a few notable examples. Nonetheless, examples of such transformations mediated by visible light have started to emerge in recent years.

2. Aim of the thesis

The aim of this thesis was to investigate and develop new methods for the intra- and intermolecular alkyl radical addition onto vinyl and alkynyl silanes, using visible light to initiate the radical reactions. Alkyl halides were chosen as radical precursors due to the lability of C-X σ bonds and the well-established visible light mediated methods to initiate radical reactions from such precursors.^{3,9,21,41} The work presented in this thesis is divided into three parts, each connected to one of the following objectives:

1. Develop a visible light mediated radical protocol for the intramolecular radical group transfer of vinyl and alkynyl groups onto sp^3 carbons *via* radical cyclization and ring fragmentation by desilylation, using a vinyl or alkynyl silyl tether as radical acceptor (Scheme 37a).
The work connected to this objective is described in chapter 3.1 and Paper I.
2. Investigate the introduction of homoallyl chains onto sp^3 carbons through visible light mediated intermolecular radical addition of electron-deficient C-centered radicals to tetramethyldivinylsiloxane, radical cyclization and subsequent desilylation (Scheme 37b).
The work connected to this objective is described in chapter 3.2.
3. Investigate and develop a visible light mediated radical method to synthesize α -iodoalkylsilanes *via* an intermolecular ATRA reaction between α -iodoketones and trialkylvinylsilanes (Scheme 37c).
The work connected to this objective is described in chapter 3.3 and Paper II.



Scheme 37. Reactions envisaged for (a) objective 1, (b) objective 2, (c) objective 3.

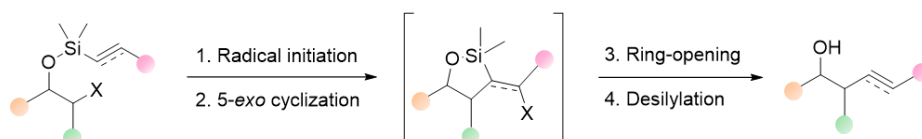
3. Results

In the following chapters, compounds that can be found in papers I and II are designated with the same numerology as in the accompanying papers, with the prefix **PI** and **PII** indicating their paper of reference. Experimental procedures and NMR spectra of compounds not included in these papers can be found in chapter 5.

3.1 Radical Group Transfer of Vinyl and Alkynyl Silanes Driven by Photoredox Catalysis (Paper I)

3.1.1 Introduction

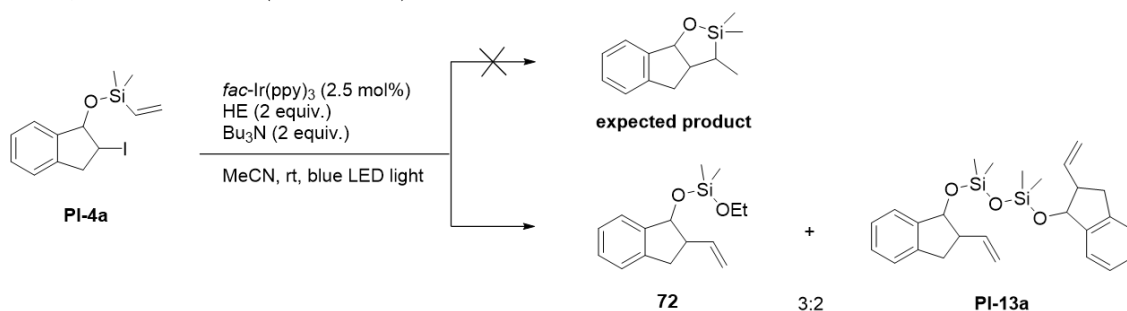
As discussed in chapter 1, C-centered radical addition to alkenyl and alkynyl silanes is still underexplored, despite the advantages of using silicon tethers for the diastereoselective introduction of alkene and alkyne moieties onto sp^3 carbons *via* intramolecular radical cyclization and subsequent ring-opening of the intermediate (Scheme 38). While a few examples of such transformations have been reported (see subchapter 1.3.2),^{118, 125, 138-140, 142-143} they either relied on toxic reagents or required activated organohalides as radical precursors. Additionally, all previous examples used a fluoride source to remove the silyl tether after the reaction. We set out to contribute to the field by developing a general photoredox catalyzed method for such intramolecular transformations under milder conditions on a wider range of substrates than previously reported.



Scheme 38. Radical cyclization/ring-opening strategy for the introduction of alkenes and alkynes onto sp^3 carbons.

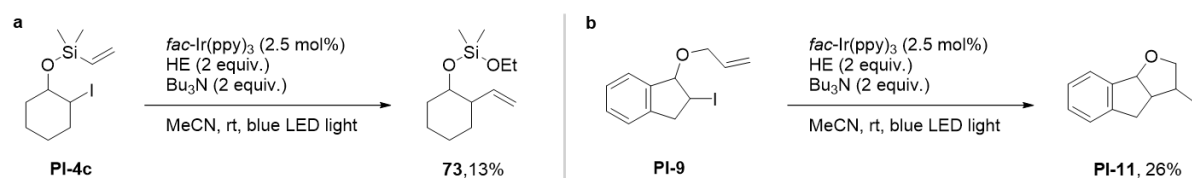
3.1.2 Initial results

We started our investigation by subjecting substrate **PI-4a** to a literature protocol for photoredox catalyzed radical formation from unactivated alkyl iodides.⁵⁹ Our choice of substrate was motivated by the ease of synthesis of **PI-4a** (see the Supporting Information of Paper I for details), as well as by the UV-activity of the compound which facilitated monitoring the progress of the reaction and potential side-reactions by TLC. To our surprise, no expected reduced cyclic product was obtained under these conditions, despite the presence of two good potential hydrogen atom donors, Hantzsch ester (HE) and tributylamine, in the reaction mixture. Instead, the reaction resulted in an inseparable 3:2 mixture of two products, **72** and **PI-13a** (Scheme 39).



Scheme 39. Initial photoredox catalyzed radical cyclization. The expected reduced cyclic product was not formed. Instead, a 3:2 mixture of ring-opened products **72** and **PI-13a** was obtained.

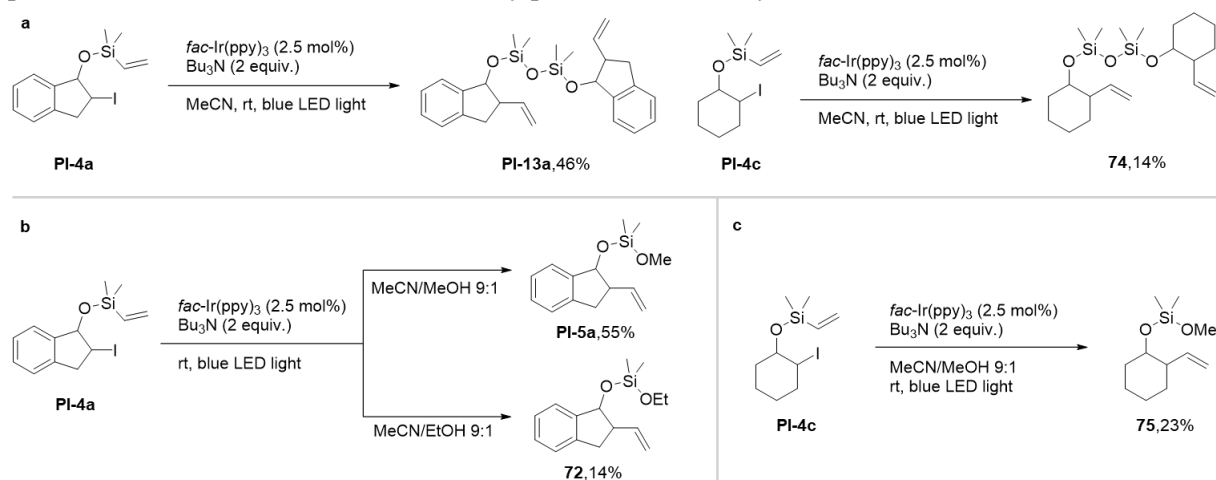
Intrigued by the evident group transfer of the vinyl moiety, which indicated spontaneous fragmentation of the cyclic intermediate without the need for a fluoride source, the same reaction conditions were applied to **PI-4c** to examine whether the direct ring-opening was substrate-dependent. To our delight, this reaction resulted in the sole formation of product **73** (Scheme 40a). However, purification of the product was challenging, and **73** was isolated in 13% yield. This result supported our hypothesis that the cyclic intermediate undergoes spontaneous fragmentation under our reaction conditions.



Scheme 40. Photoredox catalyzed reactions with (a) silyl ether and (b) ether substrates.

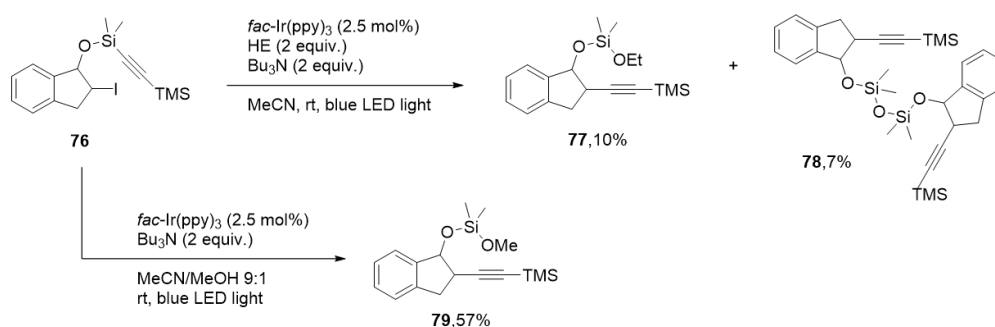
To determine the role of silicon in this fragmentation process, a control experiment was performed with carbon analogue **PI-9** (Scheme 40b). ^1H NMR analysis of the crude mixture showed complete conversion of **PI-9** into reduced cyclic product **PI-11**, which indicated that in the absence of silicon in the compound any cyclic intermediate does not undergo fragmentation to the group transfer product, but is rather reduced in the expected HAT process instead. Purification of product **PI-11** was challenging, and the product was isolated in 26% yield despite the relatively pure ^1H NMR spectrum of the crude reaction mixture.

Based on the reagents employed in our protocol, we postulated that the observed ethoxy groups connected to the silyl ethers in products **72** and **73** originated from HE. Upon operating the reaction without the HE but otherwise under the same conditions, dimeric products **PI-13a** and **74** were afforded as the only products from **PI-4a** and **PI-4c** in 46% and 14% yield, respectively (Scheme 41a), which confirmed the source of the ethoxy groups. The mechanism through which the ethoxy group was transferred from HE to the silane was not investigated. However, we theorized that the nature of the substituent introduced onto the silane during the reaction could be regulated by addition of specific nucleophiles to the reaction mixture. We were pleased to observe that, upon reaction in a 9:1 mixture of MeCN and MeOH, radical precursor **PI-4a** afforded product **PI-5a** as the only product in 55% yield (Scheme 41b). Further modification the solvent system to MeCN/EtOH 9:1 afforded product **72** in 14% yield (Scheme 41b), which supported our hypothesis. Similarly, subjecting substrate **PI-4c** to the protocol in MeCN/MeOH 9:1 afforded only product **75** in 23% yield (Scheme 41c).



Scheme 41. (a) Reaction without HE. (b and c) Effect of adding a nucleophile to the reaction mixture on the substituent introduced onto the silyl ether during the reaction.

Next, we decided to investigate whether a similar intramolecular radical cyclization/ring fragmentation process could take place with alkynyl silanes as temporary tethers. Substrate **76** was irradiated with blue LED light under the initial reaction conditions with HE mentioned above. To our delight, the reaction afforded a 1:1 mixture of products **77** and **78**, which were isolated in 10% and 7% yields respectively (Scheme 42). Due to the relatively clean profile of the reaction, we attributed these low yields to degradation of the products on silica column during purification. This result suggested that intramolecular radical alkynyl group transfer was also achievable by spontaneous fragmentation of cyclic intermediate when using silyl tethers. Similarly to reactions with vinyl silane substrates **PI-4a** and **PI-4c**, reaction of **75** in MeCN/MeOH 9:1 in the absence of HE afforded methoxy siloxane product **79** in 57% yield.



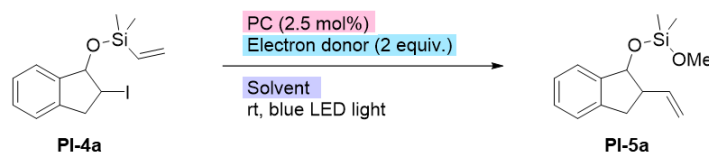
Scheme 42. Photoredox catalyzed radical group transfer of alkynyl group from silyl ether to sp^3 carbon.

As previously mentioned, it was globally observed that HE only complicated the reaction and could be removed without impacting the yield. Additionally, performing the photoredox catalyzed process in a mixture of MeCN and MeOH afforded a single product, which could be isolated more easily and in higher yields than the corresponding dimer product. With these initial results at hand, we set out to optimize and investigate the photoredox catalyzed intramolecular radical group transfer of vinyl and alkynyl silanes using alkyl iodides as radical precursors (Paper I).

3.1.3 Summary of Paper I

3.1.3.1 Optimization of reaction conditions

Optimization of the reaction conditions was performed by varying the following three parameters: the photocatalyst, the sacrificial electron donor and the solvent of the reaction (Scheme 43).



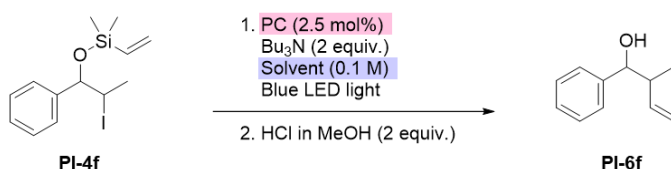
Scheme 43. Parameters varied during the optimization of the reaction conditions.

We began our optimization by screening ten photocatalysts with appropriate redox potentials for reaction with alkyl iodides. Our selection of PCs intended to cover both organic and organometallic PCs, as well as PCs expected to operate *via* oxidative and reductive quenching pathways under these reaction conditions. The screening was performed with substrate **PI-4a** and Bu_3N as sacrificial electron donor in MeCN/MeOH 9:1 under blue light irradiation with LED strips. All PCs successfully catalyzed the desired radical process to afford **PI-5a** in good to excellent yields (61-88%, Paper I, Table 1, entries

1-10), out of which the highest yield (88%) was achieved with 4CzIPN, while the fastest conversion (0.5 h) was catalyzed by $[\text{Ir}(\text{dtbbpy})(\text{ppy})_2]\text{PF}_6$ (see Scheme 45 for the structure of this PC).

Next, the three most efficient PCs in terms of yields and reaction times (4CzIPN, perylene and $[\text{Ir}(\text{dtbbpy})(\text{ppy})_2]\text{PF}_6$) were selected to evaluate the effect of the amine electron donor on the reaction (Paper I, Table 1, entries 11-16). Upon screening of three amines (Et_3N , Bu_3N and DIPEA) with the three PCs, the combination of 4CzIPN and Bu_3N were selected as the optimal reagents for the attempted reaction (88%, 2 h), while $[\text{Ir}(\text{dtbbpy})(\text{ppy})_2]\text{PF}_6/\text{Bu}_3\text{N}$ was considered the second-best combination for the transformation (81%, 0.5 h).

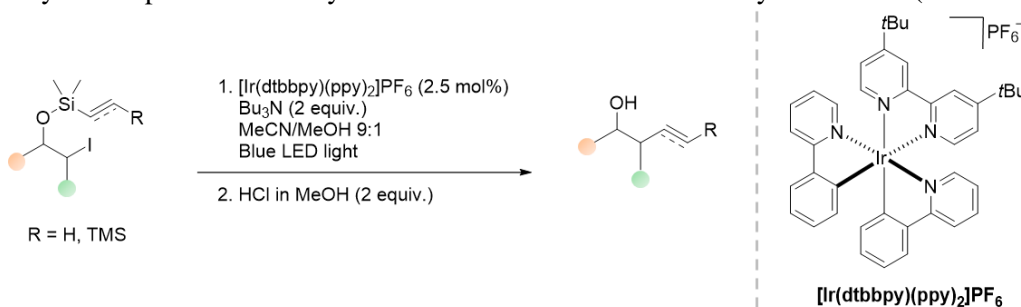
To assess the broadness of applicability of our optimized protocol, open-chain substrate **PI-4f** was subjected to the photoredox catalyzed reaction in a telescoped procedure involving acid-catalyzed silyl ether solvolysis (Scheme 44). This transformation successfully afforded the desired homoallylic alcohol **PI-6f** in 54% yield. However, full conversion of the radical process required 6 h of light irradiation (Paper I, Table 2, entry 1). When 4CzIPN was replaced with the more time-efficient $[\text{Ir}(\text{dtbbpy})(\text{ppy})_2]\text{PF}_6$, **PI-6f** was afforded in 57% in 2 h (Paper I, Table 2, entry 2). Therefore, all further reactions were performed with this iridium PC, despite 4CzIPN being a more attractive PC due to its metal-free nature and lower cost.



Scheme 44. Optimization of reaction conditions on an open-chain substrate. The photoredox catalyzed process was followed by acid-catalyzed desilylation to afford the homoallylic alcohol.

A screening of different polar aprotic solvents clearly indicated that the reaction operated fastest when performed in nitrile-based solvent systems (Paper I, Table 2, entries 2-9). Indeed, full conversion of **PI-4f** to **PI-6f** was achieved in 1-3 h in MeCN, MeCN/MeOH 9:1 and *t*-BuCN, whereas more than 20 h were needed to reach full conversion in CH_2Cl_2 , EtOAc, DMF, THF and THF/ H_2O 99:1. Moreover, higher yields were obtained in the three first mentioned solvent systems, with MeCN/MeOH 9:1 providing the highest yield (57%).

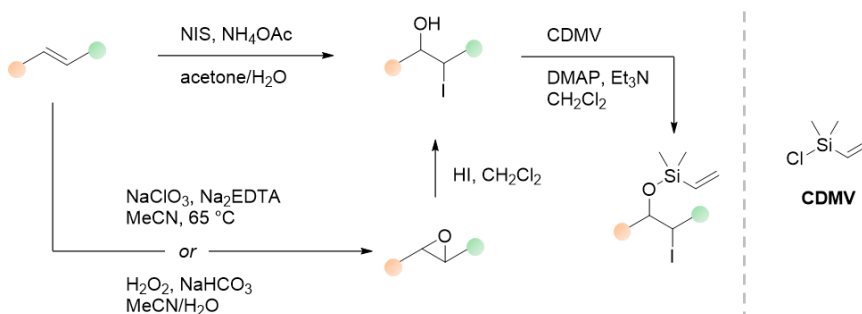
Based on these results, all further photoredox catalyzed intramolecular radical cyclization/ring opening reactions were performed under blue light irradiation (LED strips) in anhydrous MeCN/MeOH 9:1, with $[\text{Ir}(\text{dtbbpy})(\text{ppy})_2]\text{PF}_6$ as photocatalyst and Bu_3N as sacrificial electron donor. The radical process was followed by telescoped acidic desilylation to afford the desired homoallylic alcohols (Scheme 45).



Scheme 45. Optimized reaction conditions for the envisioned photoredox catalyzed transformation followed by desilylation under acidic conditions.

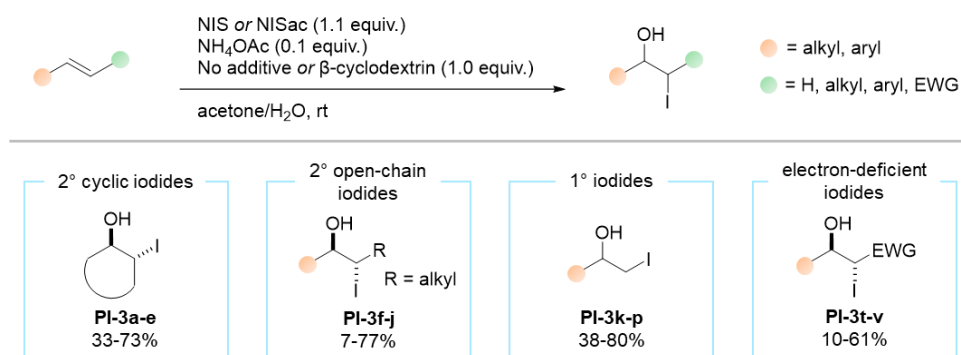
3.1.3.2 Substrate synthesis

With the optimized reaction conditions in hand, we set out to apply our protocol to a wide range of substrates to determine the limits of the method. To that end, a variety of alkyl iodide silyl ethers were synthesized from commercially available reagents according to the general two-step synthetic strategy displayed in Scheme 46. In the first step, iodohydrins were synthesized from alkenes, either directly or *via* an epoxide, depending on the desired position of the iodide in the product. Silylation of the alcohol with chlorodimethylvinylsilane (CDMV) as a second step afforded the desired alkyl iodide silyl ether radical precursors.



Scheme 46. Synthetic strategy towards substrates for the intended photoredox catalyzed radical group transfer. Some compounds required modification of these standard protocols (see paragraphs below for details).

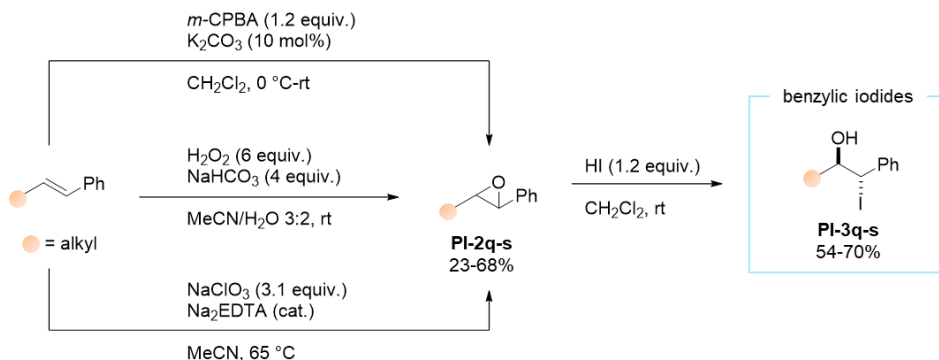
Iodohydrins with iodides in secondary cyclic, secondary open-chain, primary and electron-deficient positions were synthesized by direct iodohydroxylation of the corresponding alkenes (Scheme 47) with *N*-iodosuccinimide (NIS) and substoichiometric amounts of ammonium acetate (NH₄OAc) in H₂O/acetone 1:4, in accordance with a literature procedure.¹⁵¹ While this method afforded most desired iodohydrins in moderate to good yields (33-80% over 14 substrates, with one lower yield of 7% for one particular compound due to partial hydrolysis of another functional group in the substrate under the reaction conditions) some compounds required slight modifications of the protocol. Firstly, not all substrates were soluble in the solvent system for this reaction. These solubility issues were overcome by introducing β -cyclodextrin, a cyclic carbohydrate chain with hydrophobic cavities, into the reaction mixture.¹⁵² Secondly, iodohydroxylation of electron-deficient olefins required replacing NIS with *N*-iodosaccharin (NISac), a stronger, more electrophilic iodinating reagent.¹⁵³ Using these protocol modifications as needed allowed the synthesis of five additional iodohydrins in 10-61% yields.



Scheme 47. Iodohydroxylation of alkenes to afford iodohydrins with iodides in secondary cyclic, secondary open-chain, primary and electron-deficient positions. The reagents were combined as needed to afford the desired products.

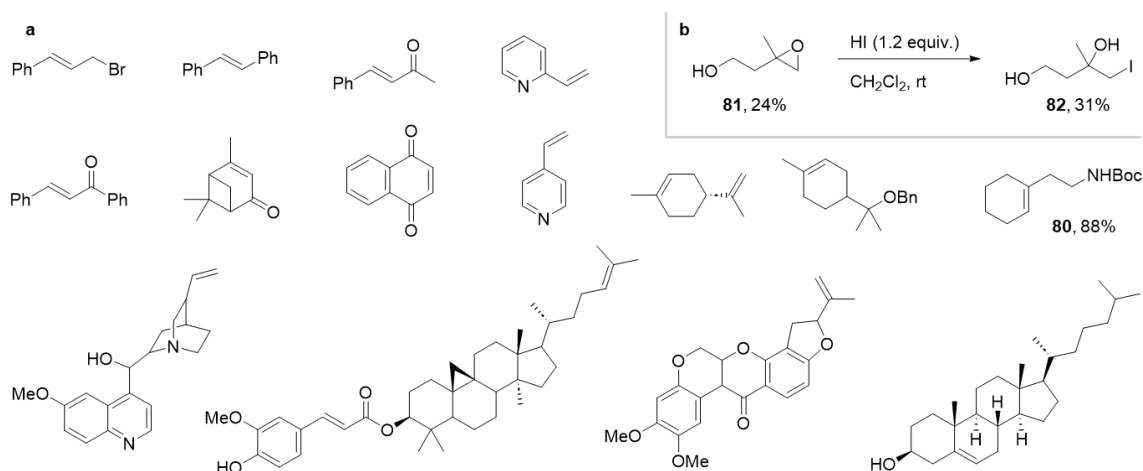
To achieve the desired regioselectivity, iodohydrins with iodides in benzylic positions were synthesized through epoxidation of olefins conjugated with aromatic rings and subsequent epoxide opening with

hydroiodic acid (Scheme 48). To this end, three literature procedures utilizing *meta*-chloroperbenzoic acid (*m*-CPBA), sodium carbonate-activated hydrogen peroxide, or sodium chlorite as oxidizing agents were followed.¹⁵⁴⁻¹⁵⁶ Epoxidation of electron-deficient alkenes operated smoothly after substrate-dependent selection of the oxidizing agent and afforded the desired products in moderate to good yields (23-68%, see the Supporting Information of Paper I for additional details). Interestingly, the protocol with *m*-CPBA as oxidizing agent was never the optimal method for epoxidation of our selected olefins and was therefore not included in the experimental section of Paper I. Subsequent ring opening of the epoxides in acidic conditions led to iodohydrins with the desired regioselectivity in 54-70% yields.



Scheme 48. Synthetic strategies towards iodohydrins with benzylic iodides through epoxidation and acid-catalyzed ring opening to afford the desired regioselectivity.

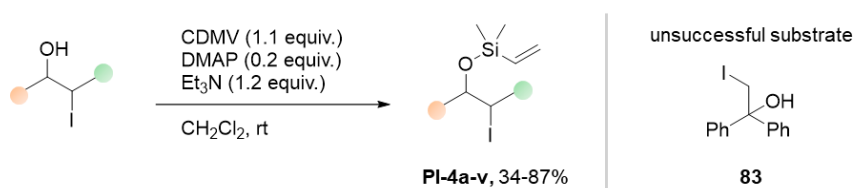
Despite our best efforts, not all targeted iodohydrins could be synthesized (Scheme 49a). Indeed, iodohydroxylation of some electron-deficient alkenes remained elusive, including olefins conjugated to heteroaromatic rings. Moreover, no iodohydrins with iodides in tertiary positions could be synthesized *via* epoxidation of trisubstituted olefins followed by treatment of the resulting epoxides with hydroiodic acid. Multiple epoxidations with the oxidizing agents mentioned above were performed on different trisubstituted olefins – including on protected substrate **80**, which was synthesized for that purpose – without success. This finding is in agreement with literature reports that tertiary iodides are notoriously unstable and challenging to synthesize.¹⁵⁷ The only productive substrate synthesis involving a trisubstituted alkene was treatment of isoprenol with sodium carbonate-activated hydrogen peroxide, which afforded epoxide **81** in 24% yield. Subsequent ring-opening in acidic conditions, however, led to iodohydrin **82** with the opposite regioselectivity to the intended product, in 31% yield (Scheme 49b).



Scheme 49. Unsuccessful substrates for (a) iodohydroxylation and (b) acidic epoxide opening with undesired regioselectivity.

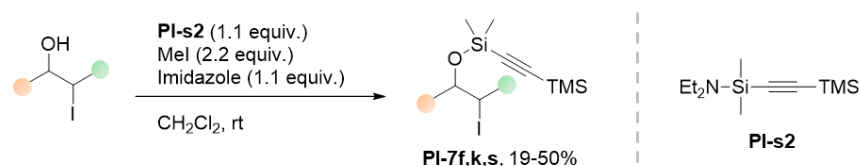
Next, we set out to extend our substrate scope by including derivatives of natural products. Therefore, iodohydroxylation of quinine, γ -oryzanol, rotenone and cholesterol (Scheme 49a) was attempted with NIS and NISac, according to the procedures described above. However, no reaction took place with any of the four substrates. Iodohydroxylation *via* epoxidation and ring opening was also unsuccessful, with no epoxide derivative isolated for any of these natural products despite subjecting each substrate to the three different oxidation systems. At this point, functionalization of natural products was abandoned.

All synthesized iodohydrins successfully underwent 4-dimethylaminopyridine (DMAP)-catalyzed silylation with CDMV in basic conditions (Scheme 50) and afforded the desired silyl ether products in moderate to excellent yields (34-87% over 22 compounds). Iodohydrin **83** was the only exception, as it decomposed under the reaction conditions.



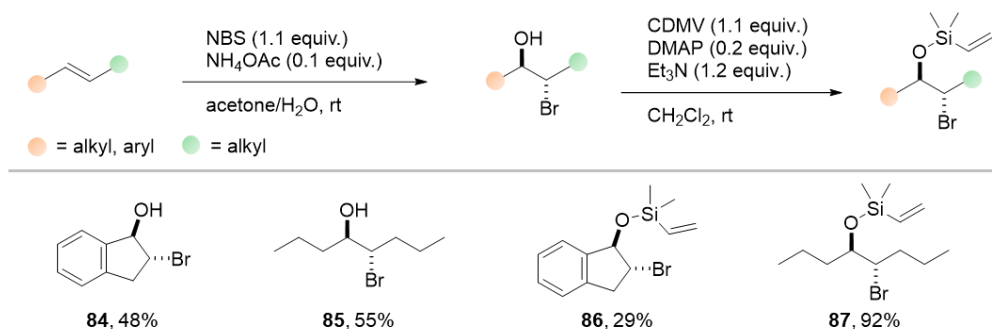
Scheme 50. DMAP-catalyzed silylation of iodohydrins to produce the desired radical precursors.

Additionally, alkynyl silyl ether derivatives of three selected compounds were obtained by silylation of their corresponding iodohydrins with a previously synthesized aminoalkynylsilane **PI-s2**,¹⁴¹ methyl iodide and imidazole in yields of 19-50%, according to a literature procedure (Scheme 51).¹⁴¹



Scheme 51. Synthesis of alkynyl silyl ether derivatives of alkyl iodide radical precursors.

Finally, alkyl bromide analogues of substrates **PI-4a** and **PI-4g** were synthesized according to the same synthetic strategy as the alkyl iodide substrates (Scheme 52) by substituting NIS with *N*-bromosuccinimide (NBS) in the halohydroxylation step, which afforded bromohydrins **84** and **85** in 48% and 55% yields, respectively. Subsequent silylation with CDMV in the previously mentioned conditions afforded the desired products **86** and **87** in 29% and 92% yields, respectively.

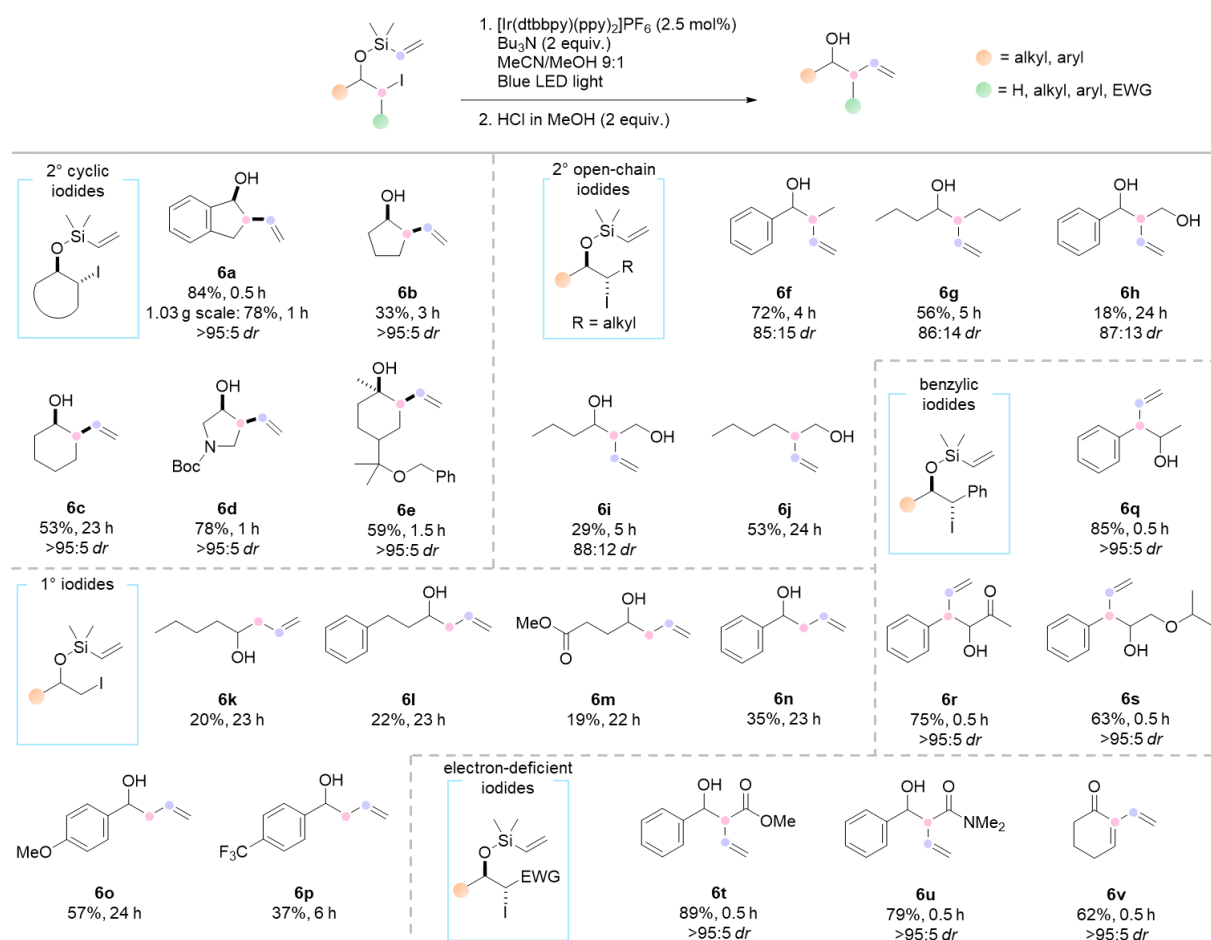


Scheme 52. Synthesis of alkyl bromide silyl ether radical precursors.

3.1.3.3 Summary of substrate scope

As previously mentioned, the scope of radical precursors subjected to our photoredox catalyzed radical group transfer method was limited by the synthesis of the substrates, with iodohydroxylation being the restricting step of the synthetic strategy. Nonetheless, our protocol was applied to a scope of twenty-two alkyl iodide vinyl silanes, three alkyl iodide alkynyl silanes and two alkyl bromide vinyl silanes.

All alkyl iodide vinyl silane substrates successfully underwent the envisioned photoredox catalyzed radical vinyl group transfer onto sp^3 carbons and afforded their corresponding primary, secondary or tertiary homoallylic alcohols **PI-6a-v** in 18-89% yields (Scheme 53). We were pleased to observe that the radical reaction could be initiated from radical precursors with both activated and unactivated C-I bonds. Additionally, the protocol presented broad functional group tolerance, high diastereoselectivity, and could be performed at gram scale without impacting the yield.

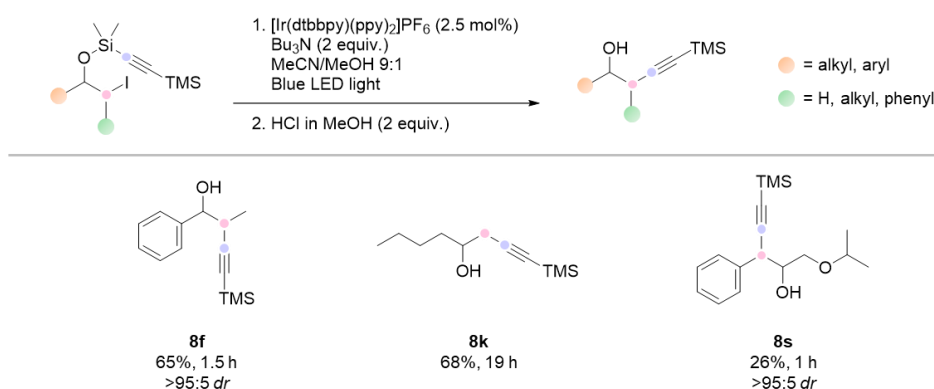


Scheme 53. Photoredox catalyzed radical group transfer of vinyl group from silane to sp^3 carbon. The products are organized in different categories depending on the position of the iodide on the substrate. The C-C σ bonds formed during the reaction are highlighted with pink and violet dots.

Interestingly, we generally noticed that lower isolated yields were obtained with reactions requiring longer reaction times, which suggested the radical process might compete with a slower side-reaction. Unsurprisingly, this effect was particularly evident for reactions involving substrates generating primary alkyl radicals (**PI-4k-p**), which are known to be less stable than secondary and tertiary alkyl radicals due to a lack of stabilization by electron-density donation from the surrounding alkyl groups. Primary

alkyl radicals are thus generated at slower rates than secondary and tertiary alkyl radicals.³⁰ Control experiments subjecting primary iodide substrates **PI-4k** and **PI-4n** to our photoredox catalyzed protocol, albeit in the absence of PC, revealed that the substrates underwent only minor background degradation under the reaction conditions and were recovered in 92% and 91% yields, respectively, after 24 h of reaction. However, upon reaction under the original conditions, only 40% yields of each of the desired products were obtained after 24 h, meaning 60% of each compound were lost during the photoredox catalyzed step. Despite this, the reactions appeared remarkably clean, with only the desired product apparent by analysis of the crude material with ¹H NMR. We therefore associated the loss of material with a relatively slow polymerization process, which could compete when radical processes are also relatively slow.

Intramolecular radical cyclization/ring fragmentation and subsequent acidic silyl ether deprotection of alkynyl silane radical precursors **PI-7f**, **PI-7k** and **PI-7s** successfully afforded homopropargylic alcohols **PI-8f**, **PI-8k** and **PI-8s** in 26–68% yields with high diastereoselectivity (> 95:5 *dr*), without losing the trimethylsilyl substituent of the alkyne (Scheme 54). Pleasingly, these results not only showed that radical alkynyl group transfer was successfully achievable with our protocol, but they also revealed the advantage of cleaving the silyl ether in acidic condition over using a fluoride source as it enabled selective *O*-desilylation of the products.



Scheme 54. Photoredox catalyzed radical group transfer of alkynyl groups from silane to *sp*³ carbon. The C-C σ bonds formed during the reaction are highlighted with pink and violet dots.

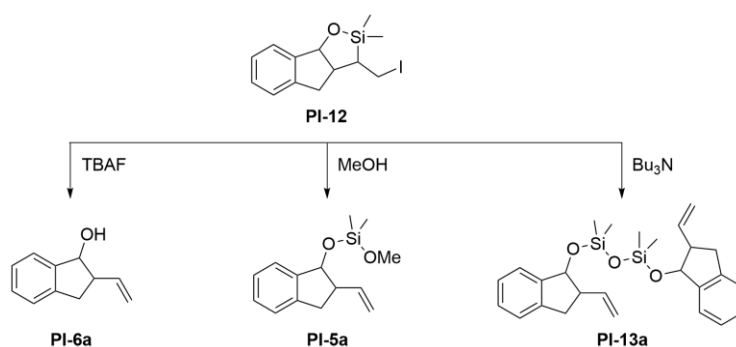
The anticipated radical process did not operate with bromo-substrates **86** and **87** under our reaction conditions, however, and the starting materials were fully recovered. The observed lack of radical initiation was attributed to the strengths of C-Br σ bonds, which are significantly higher than those of analogous C-I σ bonds and thus harder to break.⁴¹

3.1.3.4 Summary of mechanistic investigations

The radical nature of the photoredox catalyzed reaction was confirmed by subjecting **PI-4a** to our standard conditions, albeit in the absence of the photocatalyst, light and Bu₃N, respectively, which showed that no reaction occurred if one of these reagents was missing (see the Supporting Information of Paper I). Despite significant efforts, the radical nature of the reaction could not be additionally confirmed by trapping of radical intermediates. Indeed, reaction in the presence of the well-established radical trap 2,2,6,6-tetramethylpiperidine 1-oxyl (TEMPO) did not yield any isolatable radical adduct. An attempt was made to observe the expected radical adducts by gas chromatography-mass spectrometry (GC-MS). However, no such species could be observed, which was attributed to potential thermal

degradation of the radical adducts. We considered analyzing the crude reaction mixture by liquid chromatography-high resolution mass spectrometry (LC-HRMS). However, silyl ethers are known to have limited stability on columns. While the column of the LC-HRMS instrument of our department is a reverse-phase C18 column, which should significantly reduce the risks of silyl ethers getting stuck, we ultimately decided not to analyze our crude reaction mixture with this method to avoid possible contamination of the high-performance liquid chromatography (HPLC) column.

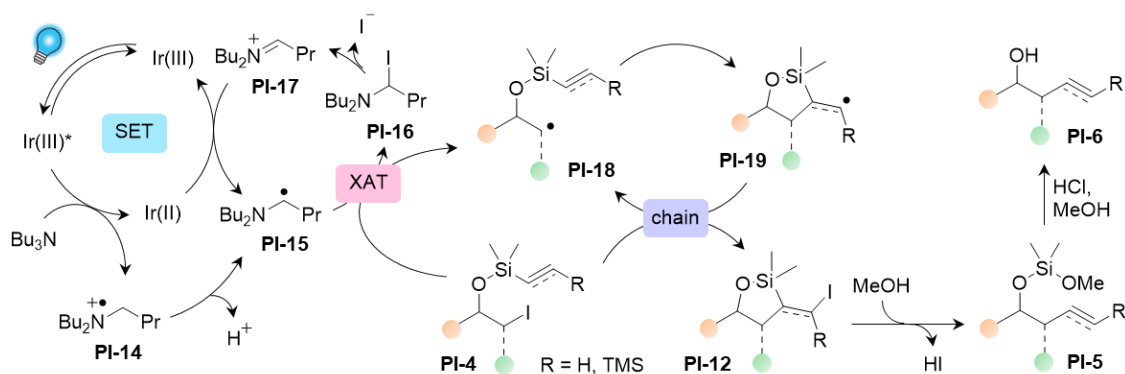
Through mechanistic investigations (see Paper I for details), we confirmed that silicon played a vital role in the spontaneous ring fragmentation of the cyclic intermediate. Additionally, we showed that *in situ* ring opening of the cyclic iodide **PI-12**, a presumed intermediate in our reaction, could be prompted by different nucleophiles, which lead to the formation of a variety of products (Scheme 55).



Scheme 55. Fate of the cyclic iodide intermediate depending on the nucleophile used to induce ring fragmentation.

Further investigations (see Paper I for details) revealed that alkyl radical generation from the alkyl iodide starting material operated *via* an XAT mechanism, and that radical chain propagation was an important mode of reactivity in the reaction mechanism. Additionally, full conversion of the substrate to the desired product was obtained with catalytic amounts of amine in the reaction mixture. This suggested that the iminium ion side product resulting from XAT initiation could be reduced back to the α -aminoalkyl radical capable of performing XAT.

Based on these results, we proposed the following reaction mechanism (Scheme 56). Upon light irradiation, SET between the photoexcited Ir(III)* PC and Bu₃N generated aminium radical **PI-14**. Subsequent deprotonation of **PI-14** afforded α -aminoalkyl radical **PI-15**, which proceeded through XAT with alkyl iodide **PI-4** to generate α -iodoamine **PI-16** and alkyl radical **PI-18**. Rapid fragmentation of **PI-16** to iminium ion **PI-17** and subsequent SET between **PI-17** and Ir(II) turned over the photoredox catalytic cycle and regenerated XAT reagent **PI-15**. Meanwhile, 5-*exo* radical cyclization of **PI-18** led to intermediate **PI-19**, which afforded cyclic alkyl or vinyl iodide **PI-12** by iodine abstraction from alkyl iodide **PI-4** *via* radical chain propagation. Nucleophilic attack on **PI-12** by the solvent prompted ring fragmentation and elimination to siloxane **PI-5**, which afforded the desired homoallylic or homopropargylic alcohol **PI-6** upon desilylation under acidic conditions.



Scheme 56. Proposed mechanism of the photoredox catalyzed radical group transfer of vinyl and alkynyl groups from silanes.

3.1.4 Conclusion

Our initial investigation of photoredox catalyzed intramolecular C-centered radical addition to unsaturated silyl ether tethers revealed that under our reaction conditions the cyclic intermediate underwent spontaneous fragmentation. This *in situ* ring opening resulted in the effective radical group transfer of a vinyl group from a silane to an sp^3 carbon. Moreover, radical alkynyl group transfer was also achieved under the same conditions. Intrigued by these results, we decided to further investigate this reaction and develop a broadly applicable method for the targeted photoredox catalyzed intramolecular radical transformation using alkyl iodides as radical precursors.

To that end, a wide selection of alkyl iodide silyl ethers were synthesized from commercially available alkenes. This two step – or three, depending on whether epoxidation was required to introduce the iodide onto the desired position of the molecule – synthesis was largely successful, although iodohydroxylation of some strongly electron-deficient alkenes remained elusive. Additionally, no tertiary iodides or iodohydrins derived from natural products could be synthesized.

Nevertheless, we have successfully developed a photoredox catalyzed protocol for the intramolecular radical group transfer of vinyl and alkynyl groups from silyl tethers, which proved efficient for a wide range of activated and unactivated alkyl iodides as radical precursors. The methods showed excellent functional group tolerance and high diastereoselectivity. Additionally, ring fragmentation of the identified cyclic intermediate was mediated by nucleophilic attack by the solvent, which eliminated the need for a fluoride source to afford the desired homoallylic or homopropargylic alcohol.

The mechanism of the reaction was investigated and revealed that the reaction proceeded *via* a combination of SET, XAT and radical chain propagation. Interestingly, we found that the key XAT reagent was regenerated by reduction of an iminium ion side-product through unusual double catalytic cycles that simultaneously regenerated the ground state of the PC in the photoredox catalytic cycle.

3.2 Intermolecular ATRA reaction between activated alkyl bromides and divinylidisiloxane

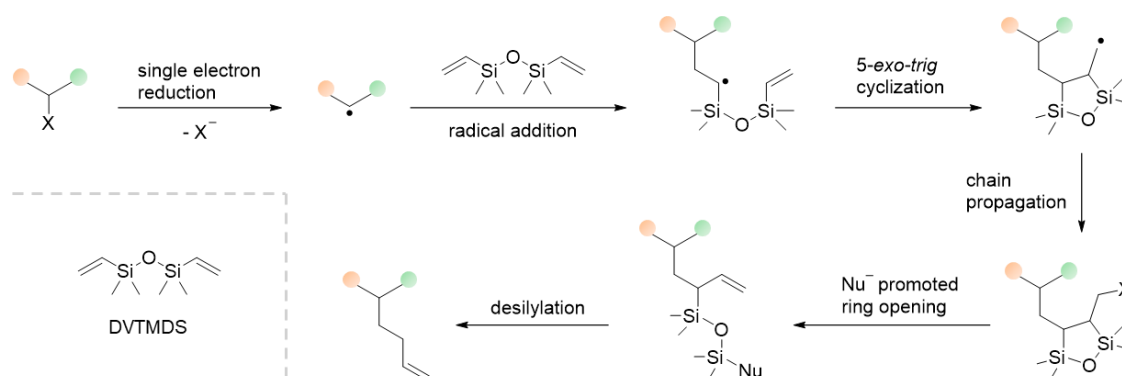
3.2.1 Introduction

Pleased with the intramolecular radical group transfer discovered during the initial phase of our previous investigation (chapter 3.1), we set out to investigate similar reactions in intermolecular systems. Indeed, our radical cyclization/ring fragmentation synthetic strategy would benefit from being applicable to intermolecular systems as it would no longer be dependent on having an appropriate functional group for silane tethering in α -position of the alkyl halide radical precursor. Additionally, synthetic applications of intermolecular C-centered radical addition to vinylsilanes remains underexplored and few examples of such transformations have been reported in the literature (see subchapter 1.3.3).^{101, 111-115, 118, 144-150} Therefore, we set out to contribute to the field by developing a photoredox catalyzed protocol for the introduction of homoallylic moieties onto sp^3 carbons using activated alkyl bromides as radical precursors. Interestingly, our target transformation could not be achieved as radical cyclization did not take place and ATRA reaction proceeded instead.

This work was done in parallel to the previous one (chapter 3.1), with our understanding of the chemistry involved developing underway. Although a significant amount of work remains to be done to complete the project described in this chapter, we decided to include it in this thesis to prepare the ground for chapter 3.3.

3.2.2 Synthetic strategy towards radical homoallylation of alkyl halides

Based on the vital role played by silicon in the spontaneous fragmentation of cyclic intermediates discovered during our work on intramolecular radical group transfer of vinyl and alkynyl groups from silicon to sp^3 carbons (chapter 3.1), we hypothesized that this unique behavior could be similarly exploited in the homoallylation of alkyl halides *via* an intermolecular radical cascade. To this end, we planned the strategy pathway illustrated in Scheme 57 involving the following succession of steps: photoredox catalyzed alkyl radical generation by single electron reduction of C-X bonds and subsequent σ bond fragmentation, intermolecular radical addition to π bond, *5-exo-trig* cyclization, chain propagation, ring opening prompted by nucleophilic attack on silicon, and desilylation.



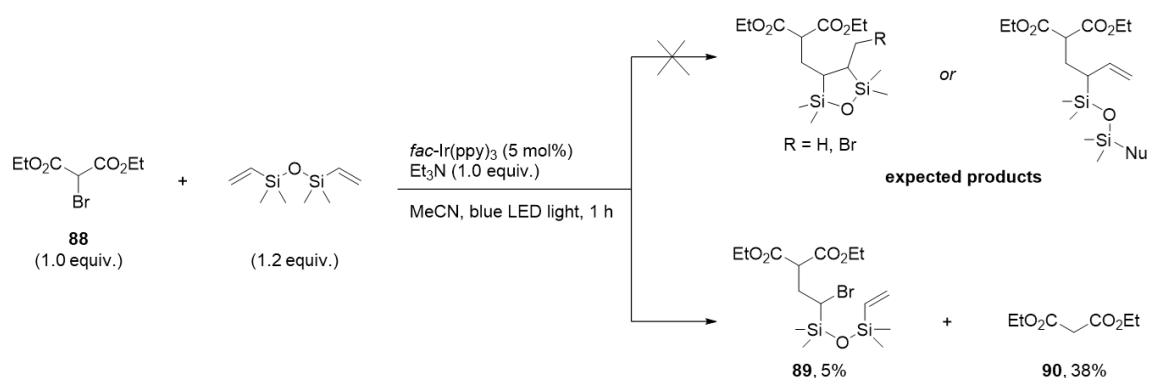
Scheme 57. Synthetic strategy towards radical homoallylation of alkyl halides *via* a radical cascade involving *5-exo-trig* cyclization and silicon promoted nucleophilic ring fragmentation of the cyclic intermediate.

Our choice of divinyltetramethyldisiloxane (DVTMDS) as radical acceptor was motivated by the symmetry of the compound. Additionally, we postulated that upon radical addition to one of the vinyl

groups, 5-*exo-trig* cyclization would form the desired β -halo silane intermediate, which could undergo the nucleophilic promoted ring fragmentation required to afford the targeted homoallylic product.

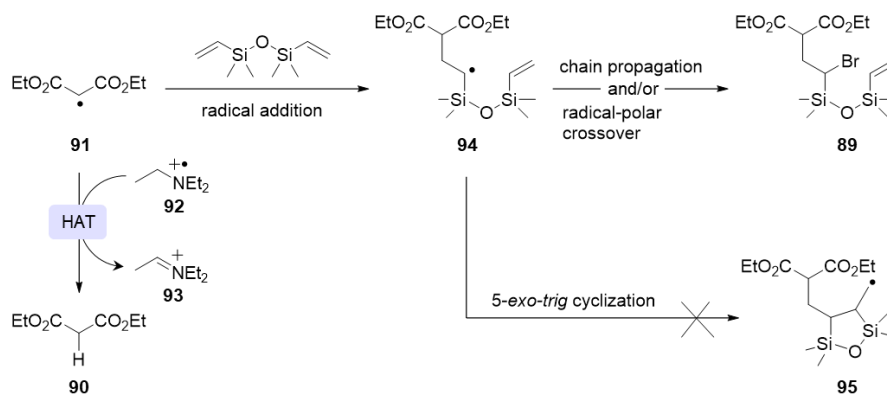
3.2.3 Initial results

We began our investigation by subjecting DVTMDS and diethyl bromomalonate **88** to a generic set of photoredox catalysis conditions for alkyl radical generation from alkyl halides. Diethyl bromomalonate **88** was chosen as the initial substrate for the investigation due to the two EWGs in α -position of the C-Br bond, which make reduction of this σ bond easier and allows radical initiation to happen *via* SET with photocatalysts with relatively weak reduction potentials.³ A mixture of the coupling partners, iridium PC *fac*-Ir(ppy)₃ and sacrificial electron donor Et₃N in acetonitrile was irradiated with blue light from LED strips for 1 h (Scheme 58). To our surprise, no formation of bromo- and hydro-cyclic intermediates or radical group transfer products were observed. Instead, the reaction resulted in a mixture of ATRA product **89** and diethyl malonate **90**, which were isolated in 5% and 38% yields, respectively. The structure of **89** was verified by analysis of 2D NMR spectra and HRMS. Additionally, the HRMS spectrum of this compound displayed the doublet character distinctive for bromides, confirming that the product was brominated.



Scheme 58. Photoredox catalyzed radical addition of electron-deficient C-centered radical to DVTMDS resulting in ATRA reaction and reduction of the alkyl bromide substrate.

Based on these initial results, we reasoned that upon single electron reduction of the alkyl bromide and subsequent C-Br σ bond fragmentation, the resulting C-centered radical **91** was involved in two different pathways (Scheme 59). We hypothesized that alkyl radical **91** underwent HAT with aminium radical cation **92**, which was generated during the photoredox catalytic cycle. This resulted in reduced substrate **90** and iminium ion **93**. In parallel, alkyl radical **91** added onto one of the π bonds of DVTMDS. The observed regioselectivity of the radical attack on the alkene can be rationalized by steric effects,⁴⁰ as well as stabilization of the resulting α -silyl radical **94** by silicon.⁹⁵⁻¹⁰¹ Bromination of the resulting α -silyl radical **94** through chain propagation and/or radical-polar crossover afforded the ATRA product **89**.

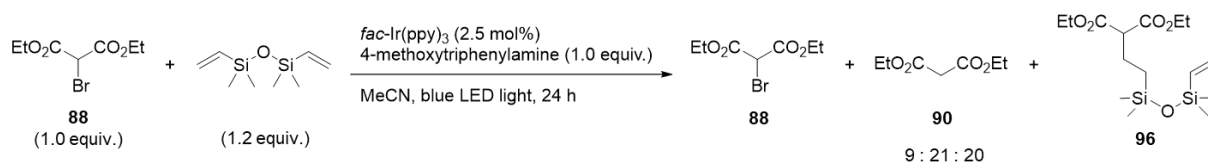


Scheme 59. Proposed mechanistic pathways underwent by alkyl radical **91**.

The factors favorizing formation of ATRA product **89** over *5-exo-trig* radical cyclization of intermediate **94** to cyclic intermediate **95** remained elusive (Scheme 59). Indeed, α -silyl radicals are known to go through intramolecular radical cyclization with alkenes.¹¹⁶⁻¹²¹ However, to the best of our knowledge, no radical cyclization of α -silyl radicals derived from vinyl disiloxanes have been reported. We hypothesized that the observed lack of radical cyclization was a result of the ATRA product formation occurring at a higher rate than *5-exo-trig* cyclization under these conditions.³⁴ While multiple factors might impact these reaction rates, we reasoned that the methyl substituents on the silicon atoms can disfavor ring formation by preventing the cyclic radical **94** from adopting the conformation necessary to cyclize, by unfavorable steric effects and/or raising the bond rotation energy barrier. This intermediate might also suffer from an unfavorable geometry due to the significantly longer Si-C/O bond lengths compared to C-C/O bonds.⁷⁷ Moreover, the high steric congestion of the cyclized radical intermediate **95** could force the newly formed ring into a conformation unsuitable for radical stabilization by the silicon atom through stereoelectronic effects, thereby raising the activation energy for cyclization.¹¹⁶ Due to the unsuccessful *5-exo-trig* cyclization, a decision was made to focus on the synthesis of the ATRA product **89**.

3.2.4 Initial optimization of intermolecular ATRA reaction

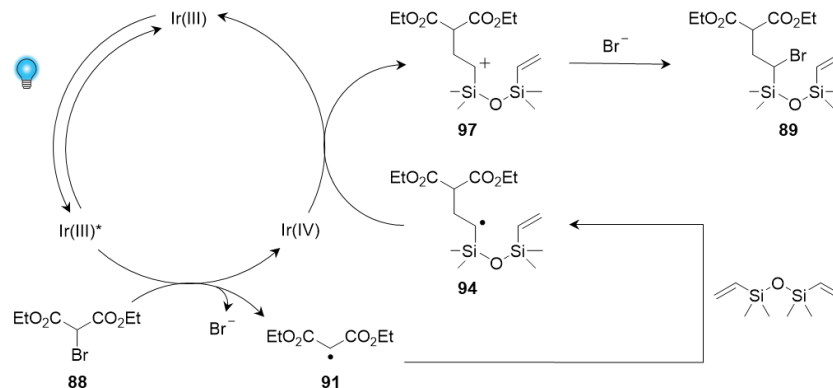
Inspired by literature precedence, we set to overcome the undesired HAT side-reaction by replacing Et₃N with 4-methoxytriphenylamine as sacrificial electron-donor, a tertiary amine with no C(α)-H bonds.⁵⁷ However, under these conditions, no desired ATRA product **89** was obtained (Scheme 60). Instead, the reaction resulted in a 9:21:20 mixture of unreacted substrate **88**, diethyl malonate **90** and reduced product **96**. The origin of the hydrogens found in the structures of **90** and **96** was not investigated. However, we hypothesized that it might derive from the solvent, the substrate or the methoxy group of the amine.



Scheme 60. Photoredox catalyzed reaction with 4-methoxytriphenylamine as sacrificial electron donor.

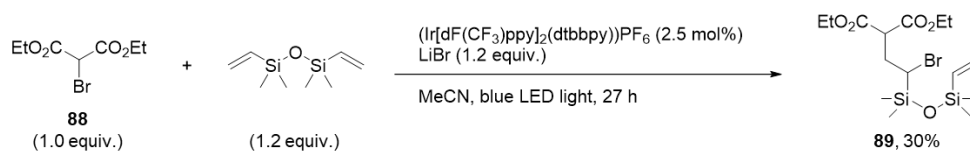
Since the use of amines as sacrificial electron donors was an issue, we decided to simplify our reaction mixture by removing the amine altogether. Since our focus had shifted from intermolecular radical

addition and subsequent radical cyclization to intermolecular ATRA reaction, we reasoned that external electron donors were no longer needed to complete the photoredox catalytic cycle (Scheme 61). Indeed, the turnover step of the iridium PC cycle could in this case be achieved *via* a radical-polar crossover pathway by SET between the oxidized PC and the radical adduct **94**, which would afford α -silyl cation **97** that could be trapped by the bromide anion to afford the desired ATRA product **89**.



Scheme 61. Proposed mechanism for the synthesis of ATRA product **89** through photoredox catalyzed radical-polar crossover pathway.

Based on literature precedence, LiBr was introduced as an additive to the reaction mixture to facilitate the radical initiation (Scheme 62).⁵⁸ Indeed, Lewis acids are known to activate α -bromo esters towards single electron reduction. Additionally, *fac*-Ir(ppy)₃ was replaced with (Ir[dF(CF₃)ppy]₂(dtbbpy))PF₆. This change of PC was motivated by the redox potentials of the PCs in the turnover step. While both PCs were strong enough ($E_{1/2}(\text{PC}^+/\text{PC}^*)_{\text{fac-Ir(ppy)}_3} = -1.73 \text{ V vs SCE}^3$; $E_{1/2}(\text{PC}^+/\text{PC}^*)_{(\text{Ir[dF(CF}_3\text{)ppy]}_2(\text{dtbbpy)})\text{PF}_6} = -1.21 \text{ V vs SCE}^{58}$) to promote single electron reduction of diethyl bromomalonate **88** ($E_{\text{red}} = -1.00 \text{ V vs SCE}^{158}$), we hypothesized that the desired ATRA reaction would be optimized with the latter PC due to its higher reduction potential ($E_{1/2}(\text{PC}^+/\text{PC})_{\text{fac-Ir(ppy)}_3} = +0.77 \text{ V vs SCE}^3$; $E_{1/2}(\text{PC}^+/\text{PC})_{(\text{Ir[dF(CF}_3\text{)ppy]}_2(\text{dtbbpy)})\text{PF}_6} = +1.69 \text{ V vs SCE}^{58}$). Under these conditions, ATRA product **89** was isolated in a significantly improved yield of 30%. Analysis of the crude material revealed that while conversion was not complete and approximately one third of the unreacted remaining material remained, only trace amounts of side reactions or degradation processes were visible. Therefore, the moderate isolated yield of **89** was attributed to incomplete conversion, and purification issues as the product partially degraded during silica during column chromatography.



Scheme 62. Photoredox catalyzed intermolecular ATRA reaction without sacrificial electron donor.

We later learned that the scientific article we used as reference for the redox potential values of (Ir[dF(CF₃)ppy]₂(dtbbpy))PF₆ had itself obtained these potentials from another research paper, which has recently been corrected. Indeed, the authors of the initial study realized that an arithmetic error had been made, and that the correct oxidation potential of this photoexcited PC was in fact weaker than first reported ($E_{1/2}(\text{PC}^+/\text{PC}^*) = -0.89 \text{ V vs SCE}^{159}$). Based on this new value, we hypothesized that the

reaction would benefit from being catalyzed by *fac*-Ir(ppy)₃ after all, due to better potential match with the substrate. Moreover, the protocol could be applied to a larger scope of alkyl bromide radical precursors due to the higher oxidation potential of the photoexcited *fac*-Ir(ppy)₃. However, due to time constraints, the photoredox catalyzed intermolecular ATRA reaction between activated alkyl bromides and DVTMDS with *fac*-Ir(ppy)₃ remains to be fully optimized.

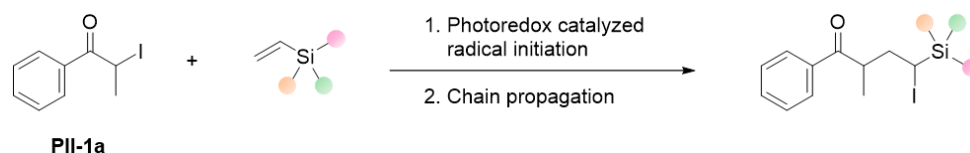
3.2.5 Conclusion

Our initial investigation of addition of electron-deficient C-centered radicals onto DVTMDS revealed that the anticipated radical cyclization did not take place under these conditions and that an ATRA reaction was favored instead. Therefore, this synthetic strategy could not be applied towards the envisaged radical introduction of alkyl chains onto alkyl halides, as the critical radical cyclic intermediate was not formed. We thus turned our attention to the observed ATRA reaction. While this work requires further investigation to develop a general protocol for the envisaged photoredox catalyzed transformation in the absence of a sacrificial electron donor, it re-focused our attention to orient us towards intermolecular ATRA reactions between alkyl halides and vinylsilanes. Further work will include reaction optimization with a PC with stronger redox potentials, to extend the applicability of the method, as well as investigating the substrate scope.

3.3 Light-promoted synthesis of complex α -iodoalkylsilanes (Paper II)

3.3.1 Introduction

Intrigued by the unexpected formation of the ATRA product upon intermolecular radical addition of C-centered radicals onto DVTMDS described in chapter 3.2, we decided to investigate the challenging photoredox catalyzed synthesis of α -haloalkylsilanes, which are useful versatile intermediates for the synthesis of complex molecules (see subchapter 1.2.2), *via* an ATRA reaction (Scheme 63). To that end, 2-iodo-1-phenyl-1-propanone (**PII-1a**, see the Supporting Information of Paper II for details about the synthesis) was selected as the initial substrate for the attempted reaction due to its labile activated C-I σ bond, and its absorption in the UV-range that facilitated monitoring the reaction by TLC. DVTMDS was replaced with simpler vinylsilanes as radical acceptors to reduce the number of possible side-reactions through radical addition to both π bonds and/or cleavage of the disiloxane moiety during the reaction. Additionally, we reasoned that reducing the steric hindrance of the substituents on the silane would enhance alkyl radical addition to the double bond, therefore improving the desired ATRA reaction.

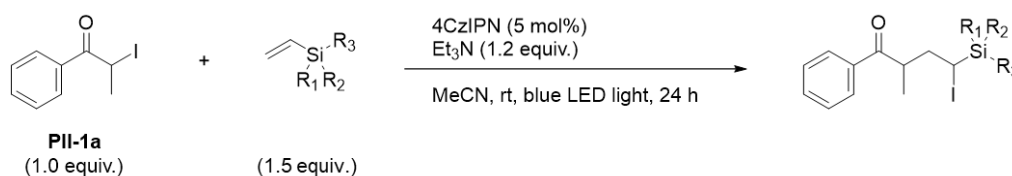


Scheme 63. Synthetic strategy towards intermolecular photoredox catalyzed ATRA reaction between alkyl iodides and vinylsilanes.

3.3.2 Initial results

We began our investigation by screening commercially available vinylsilanes **PII-2** and **98-99** as radical acceptors for the envisioned ATRA reaction to examine the effect of the silicon substituents on the radical addition (Table 1, entries 1 and 3-4). Silane **100** was synthesized by treatment of CDMV with MeOH in basic conditions to complete the scope of the screening (entry 2). This synthesis was challenging due to the volatility of the product, which was isolated by distillation, and **100** was obtained in 11% yield. A standard photoredox catalysis system involving 4CzIPN as PC and Et₃N as sacrificial electron donor was selected to initiate the desired radical reaction upon blue light irradiation with LED strips.

Table 1. Screening of vinylsilanes as radical acceptors for the desired ATRA reaction^a

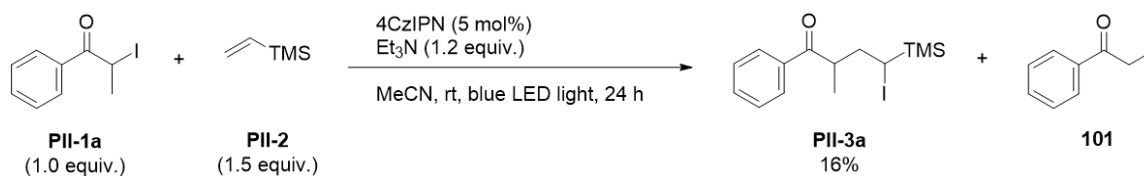


entry	vinylsilane	R ₁	R ₂	R ₃	yield (%) ^b
1	PII-2	Me	Me	Me	16
2	100	Me	Me	OMe	8
3	98	Me	OMe	OMe	4
4	99	OMe	OMe	OMe	0

^aReaction scale: 0.20 mmol. ^bYield determined by ¹H NMR with ethylene carbonate as internal standard.

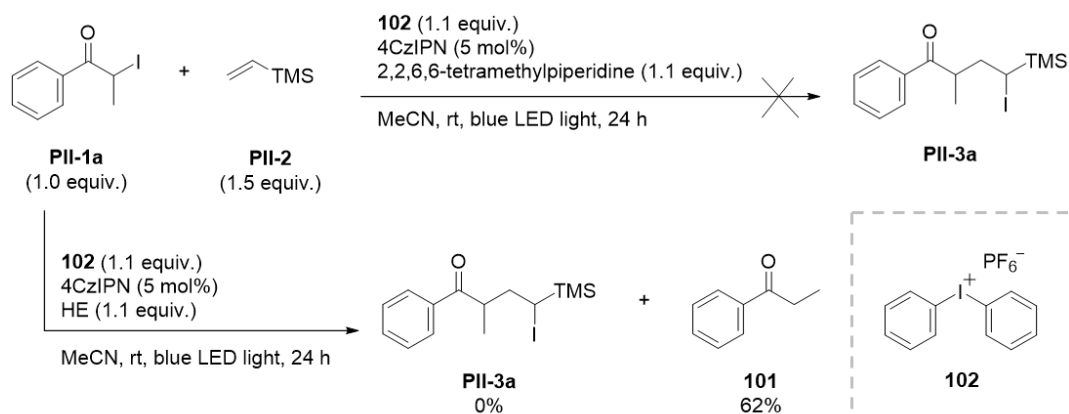
Unfortunately, all yields were low and had to be determined by analysis of ^1H NMR spectra of the crude mixtures as the desired products could not be isolated due to instability to column chromatography. To this end, ethylene carbonate was added to the reaction mixtures before light irradiation to serve as internal standard. A clear correlation was observed between the number of methoxy groups on the silane and conversion to the desired ATRA products (Table 1), with trimethylvinylsilane **PII-2** affording the highest conversion to the desired ATRA product in 16% yield (entry 1). Indeed, methoxy groups are inductively electron-withdrawing, and radical addition of the electron-deficient C-centered radical into more electron-rich vinylsilanes is favored due to better polarity match between the coupling partners.^{34, 36, 144}

Based on these results, we went on to optimize the intermolecular ATRA reaction between activated alkyl iodides and vinylsilanes with trimethylvinylsilane **PII-2**. The desired ATRA product **PII-3a** was isolated in 16% yield upon increasing the reaction mixture concentration from 0.1 M to 0.5 M (Scheme 64). However, the reaction produced a non-negligible amount of the reduced starting material, 2-propiophenone **101**. Substrate **PII-1a** was fully recovered when the reaction was operated in the dark, which ruled out nucleophilic degradation of this alkyl iodide. Therefore, we postulated that HAT was also operating between the aminium radical cation generated during the photoredox catalytic cycle and the alkyl radical produced from **PII-1a**. Competing HAT reaction is a well-known issue with ATRA reactions performed with tertiary amines as sacrificial electron-donors (see chapter 1.1.5 for details on aminium radical cations as hydrogen atom donors).⁵⁷ No conversion to the desired ATRA product **PII-3a** was observed upon substitution of Et_3N with amines that could not serve as hydrogen atom donors, such as 4-methoxytriphenylamine, 2,2,6,6-tetramethylpiperidine, and quinuclidine, which suggested the reaction might proceed *via* an XAT mechanism.



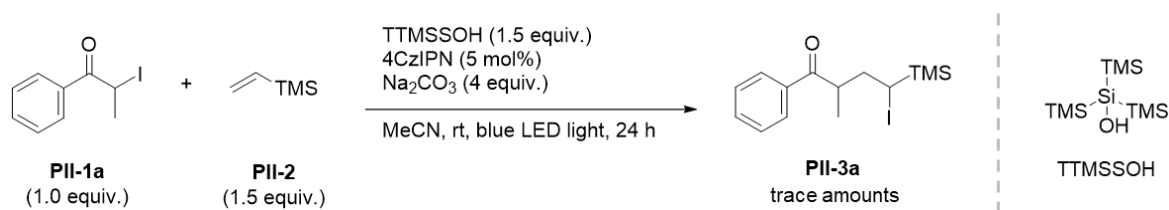
Scheme 64. Photoredox catalyzed ATRA reaction between **PII-1a** and **PII-2** under initial reaction conditions.

If the reaction proceeds through XAT, the HAT issue cannot be solved by using an amine with no C(α)-H. We therefore set out to resolve this issue by initiating the radical reaction with different XAT reagents. To this end, a photoredox catalyzed reaction was attempted with 2,2,6,6-tetramethylpiperidine as sacrificial electron donor and the commercially available diphenyliodonium hexafluorophosphate **102** as XAT agent precursor (Scheme 65). Upon single electron reduction, this hypervalent iodide derivative is known to fragment into iodobenzene and an aryl radical, which proceeds through XAT with alkyl iodides at a reaction rate close to the diffusion limit.¹⁶⁰⁻¹⁶¹ However, under these conditions, no desired product was formed. The amine was then replaced by the better electron donor HE, as we postulated that the XAT reaction rate might be high enough to favor XAT over undesirable HAT under these conditions. However, this reaction resulted exclusively in reduced substrate **101**, which was isolated in 62% yield.



Scheme 65. Attempted ATRA reactions with hypervalent iodide salt **C-d** as XAT reagent precursor.

Photoredox catalyzed XAT radical initiation was next performed with tris(trimethylsilyl)silanol (TTMSSOH) as XAT reagent precursor, in the presence of an inorganic base to neutralize the acid generated during the XAT reagent activation (Scheme 66).⁴¹ While trace amounts of the desired ATRA product **PII-3a** were obtained, the reaction was not optimized further because substrate degradation was observed even without light irradiation under these conditions.

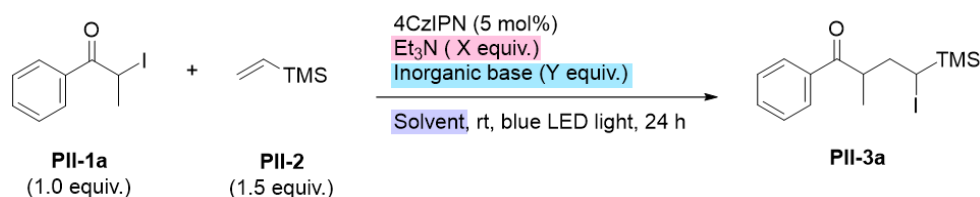


Scheme 66. Attempted ATRA reaction with TTMSSOH as XAT agent precursor.

Due to these unsuccessful results, we decided to go back to our amine-based system (Table 2, entry 1). Inspired by our results in chapter 3.1, attempts were made to operate the reaction with catalytic amounts of amine in the presence of an inorganic base (Table 2, entries 2-6). Indeed, we postulated that similarly to the mechanism discovered in chapter 3.1, the α -aminoalkyl radical XAT reagent might be regenerated through double catalytic cycles, which would reduce the amount of amine required in the reaction mixture and thus reduce the unproductive HAT pathway. Moreover, ATRA reactions involving alkyl halides have been shown to be enhanced in the presence of inorganic bases.^{111, 162} To our delight, reducing the amount of Et₃N to 0.2 equivalent and introducing an equivalent of K₂CO₃ resulted in an increased yield of 28% (entry 2). When K₂CO₃ was replaced with Na₂CO₃, the yield dropped to 6% (entry 3). However, it increased back to 15% with Cs₂CO₃ (entry 4), although this base was not fully soluble in MeCN at the required concentration. Therefore, an attempt was performed in MeCN/H₂O 9:1 to fully solubilize the salt and thereby optimize the light absorption of the reaction mixture, which pleasingly afforded **PII-3a** in 27% (entry 5). For comparison, operating the reaction in a similar solvent system with K₂CO₃ resulted in 26% of the desired ATRA product (entry 6). A subsequent solvent screening indicated that while the desired ATRA product **PII-3a** was successfully synthesized in all solvents tested (Table 2, entries 7-16), MeCN afforded the highest conversion to **PII-3a** with a 42% ¹H NMR yield (entry 7). Unlike the previous experiments reported in Table, the yields of the solvent screening (entries 7-16) were determined by ¹H NMR with ethylene carbonate as internal standard to

ensure reliable direct yields comparison by removing small fluctuations that might rise during purification by column chromatography.

Table 2. Optimization of reaction conditions for the envisioned ATRA reaction^a



entry	amine	X	inorganic base	Y	solvent	yield (%)
1	Et ₃ N	1.2	none	-	MeCN	16
2	Et ₃ N	0.2	K ₂ CO ₃	1.0	MeCN	28
3	Et ₃ N	0.2	Na ₂ CO ₃	1.0	MeCN	6
4	Et ₃ N	0.2	Cs ₂ CO ₃	1.0	MeCN	15
5	Et ₃ N	0.2	Cs ₂ CO ₃	1.0	MeCN/H ₂ O 9:1	27
6	Et ₃ N	0.2	K ₂ CO ₃	1.0	MeCN/H ₂ O 9:1	26
7	Et ₃ N	0.2	K ₂ CO ₃	1.0	MeCN	42 ^b
8	Et ₃ N	0.2	K ₂ CO ₃	1.0	MeCN- <i>d</i> ₃ /D ₂ O 9:1	35 ^b
9	Et ₃ N	0.2	K ₂ CO ₃	1.0	CH ₂ Cl ₂	39 ^b
10	Et ₃ N	0.2	K ₂ CO ₃	1.0	DCE	37 ^b
11	Et ₃ N	0.2	K ₂ CO ₃	1.0	DMF	34 ^b
12	Et ₃ N	0.2	K ₂ CO ₃	1.0	THF	19 ^b
13	Et ₃ N	0.2	K ₂ CO ₃	1.0	DMSO- <i>d</i> ₆	8 ^b
14	Et ₃ N	0.2	K ₂ CO ₃	1.0	Toluene	3 ^b
15	Et ₃ N	0.2	K ₂ CO ₃	1.0	Et ₂ O	4 ^b
16	Et ₃ N	0.2	K ₂ CO ₃	1.0	EtOAc	7 ^b
17	PMP	0.2	K ₂ CO ₃	1.0	MeCN	4
18	PMP	1.2	none	-	MeCN	36
19 ^c	PMP	1.2	none	-	MeCN	49
20 ^c	PMP	1.2	none	-	CH ₂ Cl ₂	44

^aReaction scale: 0.20 mmol. ^bYield determined by ¹H NMR with ethylene carbonate as internal standard. ^c3.0 equiv. of trimethylvinylsilane.

Next, an attempt was made to replace Et₃N with the more sterically hindered amine 1,2,2,6,6-pentamethylpiperidine (PMP, Table 2, entries 17-20), as we hypothesized that steric hindrance might disfavor HAT between the aminium radical cation and the C-centered radical derived from **PII-1a**. The yields of these experiments were isolated yields, to be directly comparable with the ones from previous experiments (entries 1-6). While only 4% of product **PII-3a** was isolated when operating the reaction with a combination of PMP and K₂CO₃ (entry 17), 36% of the desired product was generated upon operating the reaction with PMP on its own (entry 18). This promising result was further improved by increasing the amount of radical acceptor **PII-2** to 3.0 equivalents with respect to alkyl iodide radical precursor **PII-1a** (entry 19). With these higher quantities of **PII-2**, formation of a white precipitate was observed during the reaction. Due to the importance of light absorption for the conversion of the substrate, we were interested in knowing if the presence of precipitate impacted the yield. An attempt was therefore performed in CH₂Cl₂ (entry 20), in which the precipitate was soluble. Interestingly, the

reaction was not further improved by the solvent change. Therefore, acetonitrile was selected as the solvent for all further reactions as it provided the highest yield.

Having developed a promising preliminary method for intermolecular ATRA reaction between activated alkyl iodides and trimethylvinylsilane **PII-2**, we set out to further improve our protocol to increase the applicability of the reaction (Paper II).

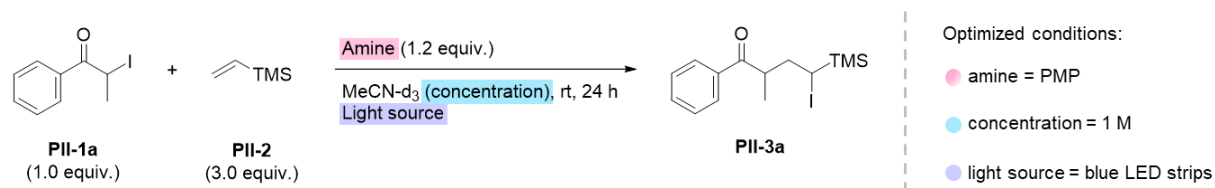
3.3.3 Summary of Paper II

3.3.3.1 Optimization of photocatalyst-free reaction conditions

We started our investigation by verifying the radical nature of the reaction. To this end, alkyl iodide **PII-1a** was submitted to the standard reaction conditions described above, albeit in absence of blue light, amine, PC, and amine and PC, respectively (Paper II, Table 1). All experiments were performed in duplicates to assure the reproducibility of the results. These experiments revealed that while no reaction occurred in the absence of light or amine, similar yields were obtained in presence or absence of PC (43-49% and 44-47%, respectively), which implied that the radical process was not initiated by SET or XAT. ATRA product **PII-3a** was, admittedly, afforded in 8% (NMR yield) upon reaction in absence of both PC and amine in one attempt, but no desired product was obtained in the duplicate experiment. This result could suggest that radical initiation can partially occur through spontaneous C-I σ bond homolysis upon blue light irradiation but that it was not the main mechanistic pathway. Moreover, material contamination with trace amounts of amine could not be ruled out. Due to the difference in the temperature between the inside of the light irradiation setup (34 °C) and room temperature, a control experiment was conducted to ensure that blue light irradiation was necessary for the desired transformation to take place, and that the reaction was not driven by heat instead. To this end, a reaction mixture containing all reagents was stirred at 34 °C in the dark for 24 h, but did not yield any desired ATRA product. Finally, **PII-1a** was subjected to the standard reaction conditions in the presence of the radical trap TEMPO (see the Supporting Information of Paper II for details). Manual purification of the crude reaction mixture did not allow the isolation of adducts between any of the radical intermediates and TEMPO. Therefore, despite our initial unwillingness to load silylated compounds onto the HPLC column of the LC-HRMS instrument of our department (see subchapter 3.1.3.4), the crude mixture was analyzed by LC-HRMS. The main compound of this analysis was the alkyl radical-TEMPO adduct **PII-SI-A1**, which confirmed that the reaction was a radical process.

We reasoned that if the radical reaction was not initiated by SET, XAT or light-driven C-I bond cleavage, it was likely initiated by excited-state halogen-bond (XB) complex fragmentation (see chapter 1.1.8 for details on XB complexes). Therefore, we set out to optimize the reaction conditions for the ATRA reaction under photocatalyst-free conditions (Scheme 67). A screening of secondary and tertiary amines was performed in the absence of any PC to identify an appropriate halogen-bond acceptor (Paper II, Table 2, entries 1-9). Reaction with PMP afforded the desired ATRA product **PII-3a** in the highest yields (53-65%, reaction performed in triplicate). Therefore, all further reactions were performed with PMP as the XB acceptor. A subsequent brief screening of light sources confirmed that the irradiation wavelength had to be in the blue light range for the desired ATRA reaction to take place (Paper II, Table 2, entries 6 and 10-13). Interestingly, similar yields were obtained when irradiating the standard reaction mixture with broad-emission blue light LED strips and when using a high intensity lamp with a narrower wavelength distribution. Finally, the desired ATRA product **PII-3a** was afforded in 72-83% (reaction

performed in triplicate) upon increasing the concentration of the reaction mixture to 1 M (Paper II, Table 2, entries 6 and 14-15). Further increase of the concentration did not provide higher yields.

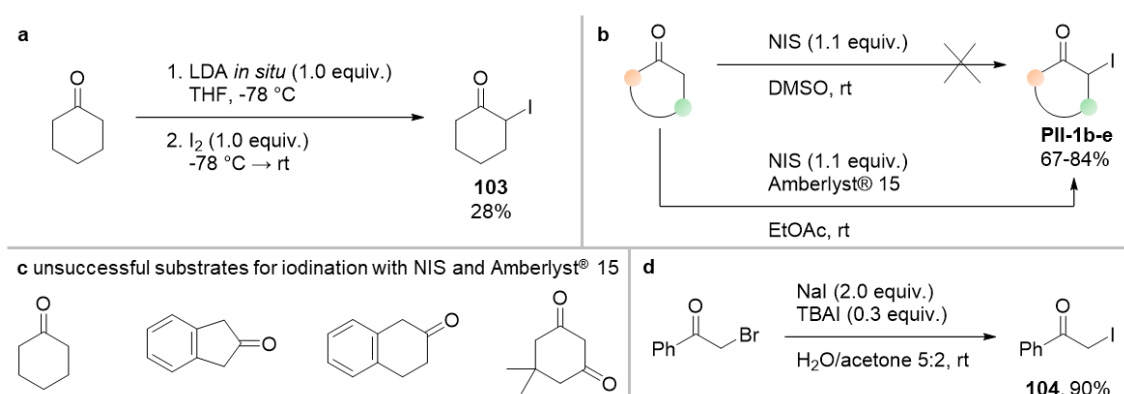


Scheme 67. Conditions optimized for the envisioned visible light-mediated intermolecular ATRA reaction.

Based on these results, the intermolecular ATRA reaction between α -keto alkyl iodide **PII-1a** and **PII-2** initiated by XB complex photoexcitation was optimal in a 1 M reaction mixture with PMP as the XB acceptor and light irradiation from blue LED strips (Scheme 67).

3.3.3.2 Substrate synthesis

With the optimized conditions in hand, we set out to apply our method to a selection of substrates. To this end, various synthetic strategies of α -halogenation of ketones were tested to synthesize the desired cyclic α -iodoketone radical precursors (Scheme 68). Firstly, an attempt was made to obtain compound **103** by enolization of the ketone with lithium diisopropylamide (LDA), which was generated *in situ* from *n*-butyllithium (*n*-BuLi) and diisopropylamine, followed by iodination with iodine (Scheme 68a).¹⁶³⁻¹⁶⁴ While this method did afford the desired product **103** in 28% isolated yield, it required multiple manipulations and was time consuming. Therefore, alternative protocols were investigated.



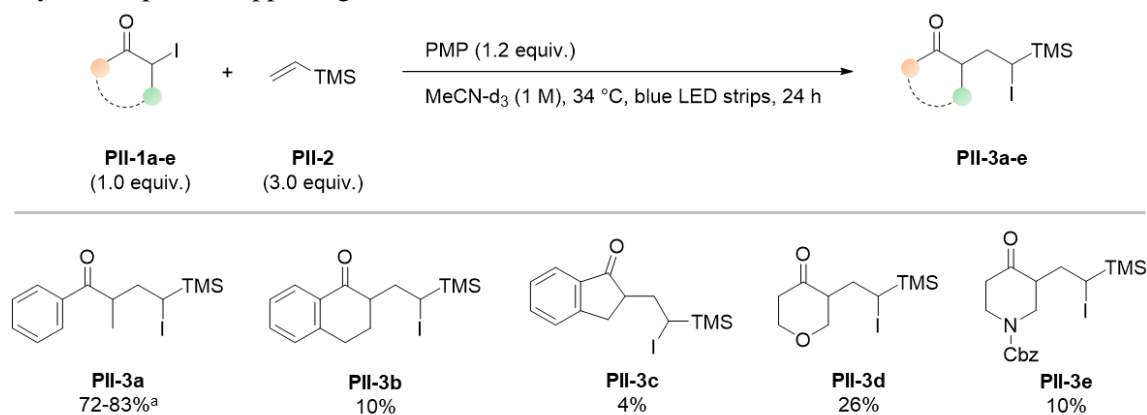
Scheme 68. Synthetic strategies towards α -keto alkyl iodides, relying on (a) enolate reaction with iodine or (b) NIS. (c) Unsuccessful substrates. (d) Alternative strategy relying on the Finkelstein reaction.¹⁶³⁻¹⁶⁷

Inspired by literature precedence on catalyst-free α -halogenation of ketones, some compounds were treated with NIS as the iodinating agent in DMSO (Scheme 68b).¹⁶⁵ In our case, however, no desired α -iodoketones were obtained *via* this method. Iodination was, however, successfully achieved by treatment of the carbonyl compounds with NIS in presence of the Amberlyst[®] 15 catalyst in EtOAc, which afforded compounds **PII-1b-e** in 67-84% isolated yields (Scheme 68b).¹⁶⁶ However, despite our best efforts, α -iodination of some carbonyl compounds remained elusive under these conditions (Scheme 68c). Due to time constraints, a decision was made to limit our substrate scope to compounds **PII-1a-e**.

Additionally, compound **104** was synthesized but not used for the investigation of the substrate scope as, unlike substrates **PII-1a-e**, it did not possess a secondary iodide (Scheme 68d). Nevertheless, it was subjected to one of our visible light protocols (see subchapter 3.3.3.3). Compound **104** was synthesized by a Finkelstein reaction according to literature precedence.¹⁶⁷ Indeed, treatment of 2-bromoacetophenone with sodium iodide and tetrabutylammonium iodide (TBAI) in H₂O/acetone 5:2 afforded the desired product **104** in 90% yield.

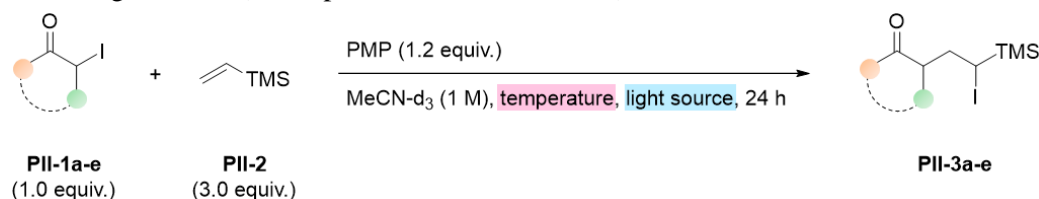
3.3.3.3 Summary of the substrate scope

In the interest of time, all the reactions of the substrate scope were performed in MeCN-*d*₃ and the yields were determined by ¹H NMR with ethylene carbonate as internal standard. Despite high conversion of the substrates, the desired ATRA products **PII-3b-e** were formed in low to moderate yields (4-26%) under our optimized reaction conditions (Scheme 69). Control experiments with 4CzIPN in the reaction mixtures revealed that substrates **PII-1d-e** underwent the desired intermolecular ATRA reaction with trimethylvinylsilane **PII-2** in higher yields in the presence of a PC (43-85%, Paper II, Supporting Information). However, no evident yield increase was observed for **PII-3b-c** (9-10%). Therefore, we reasoned that going through a photoredox catalyzed system would not provide a generally applicable solution for all substrates. Instead, we aimed to optimize our PC-free protocol by modifying the additive to improve XB complex formation between the amine and iodides in cyclic secondary positions. A supplementary amine screen was performed with substrate **PII-1b** (see the Supporting Information of Paper II for details), which also included a selection of pyridine-based amines known to form XB complexes with electron-deficient alkyl bromides.^{74-75, 168-169} Interestingly, this screening confirmed that PMP was the best additive for our targeted transformation as it afforded the desired product **PII-3b** in 18% yield (Paper II, Supporting Information).



Scheme 69. Intermolecular ATRA reaction between alkyl iodides **PII-1a-e** and trimethylvinylsilane **PII-2** under the initial optimized conditions. ^aExperiment performed in triplicate.

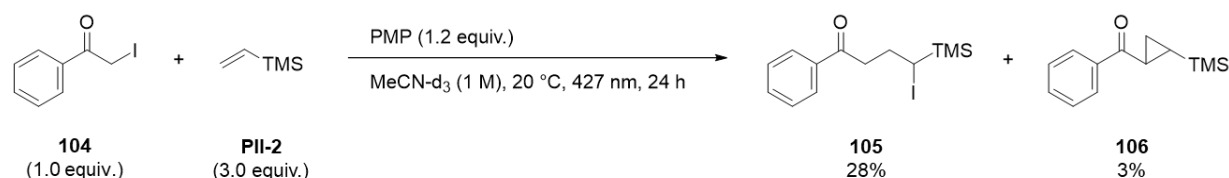
Next, we turned our attention to other parameters of the reaction (Scheme 70). Unfortunately, no clear correlation was observed with the yield of products **PII-3a-e** upon modification of the temperature and the irradiation light source (see Paper II, Table 3 for details).



Scheme 70. Conditions modified for optimization of the ATRA reaction between substrates **PII-1a-e** and **PII-2**.

While our investigation revealed that the overall conversion-to-yield ratio of the different substrates tested was at its maximum when the reactions were operated at 20 °C, the optimal irradiation wavelength seemed to be substrate dependent, with 456 nm affording the overall highest yields (Paper II, Table 3). This was interesting as we did not expect open-chain and cyclic analogues – **PII-1a** and **PII-1b**, respectively – to require different wavelengths for the photoexcitation of their corresponding XB complexes with PMP. Moreover, aromatic substrates with a fused ring moiety – **PII-1b** and **PII-1c** – continuously afforded their respective ATRA products in low yields, independently of the irradiation wavelength. Therefore, no optimal conditions were yet set for our desired transformation as further work is required to establish a general protocol for the intermolecular ATRA reaction between α -iodoketones and trimethylvinylsilane.

In addition to the results presented in Paper II, another ATRA reaction was performed with a primary alkyl iodide radical precursor (Scheme 71). Substrate **104** was subjected to our protocol at 20 °C under blue light irradiation with a Kessil 427 nm lamp, which afforded a mixture of the desired ATRA product **105** and TMS-substituted cyclopropane **106**, which were isolated in 28% and 3% yields, respectively.

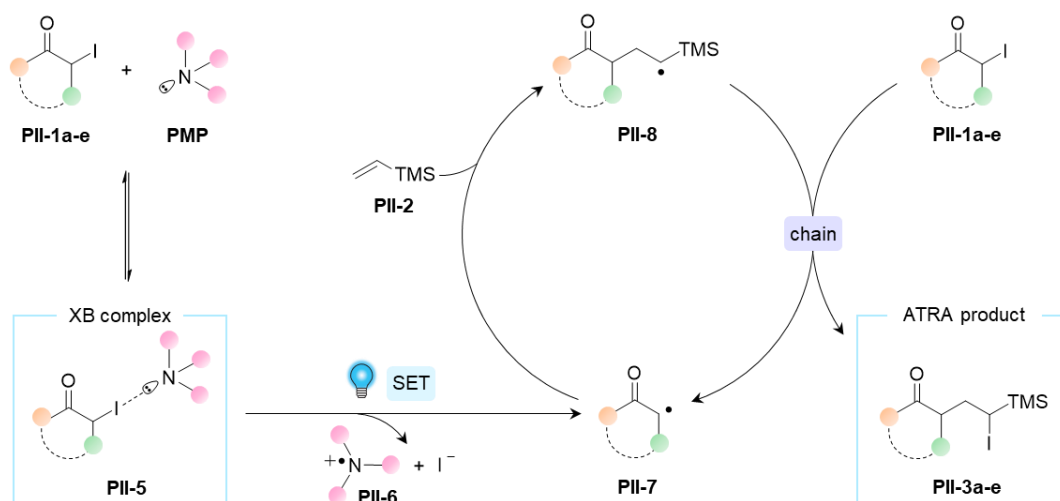


Scheme 71. ATRA reaction between **104** and **PII-2**.

The unexpected cyclopropanated product **106** was presumably formed from **105** by intramolecular nucleophilic attack by an enolate on the alkyl iodide moiety. This result was encouraging, as it suggests a possible modification or extension of the protocol for application towards the synthesis of silylated cyclopropanes, which are useful building blocks with numerous applications in organic synthesis.¹⁷⁰ This is only one of several interesting applications of the structurally complex α -iodosilanes that are accessible from our XB complex-mediated ATRA protocol.

3.3.3.4 Summary of the mechanistic investigations

Based on literature precedence, attempts were made to observe XB complexation between **PII-1a** and PMP by recording the UV-vis, ¹H NMR and ¹³C NMR spectra of **PII-1a** in acetonitrile on its own as well as in mixtures with PMP and PMP/**PII-2** (see Paper II and its Supporting Information for details).²¹ However, no new absorption band from the anticipated XB complex was visible in the UV-vis spectra upon mixing **PII-1a** and PMP. Similarly, no changes of chemical shifts of the α -proton and α -carbon of **PII-1a** were observed in the spectra of the mixtures, compared to pure **PII-1a**. Therefore, the expected XB complex formation was not confirmed by these methods. However, based on literature precedence and our initial findings that no PC was required for the reaction to operate despite proceeding through a radical process, as confirmed by radical trapping with TEMPO, we postulated that the reaction was initiated by the visible light photoexcitation of an XB complex and proceeded *via* an ATRA chain mechanism (Scheme 72). Upon light irradiation, SET proceeded between the components of the photoexcited XB complex **PII-5**, which generated the electron-deficient alkyl radical **PII-7**, an aminium radical cation **PII-6** and an iodide anion. Regioselective radical addition of **PII-7** onto trimethylvinylsilane **PII-2** generated α -silyl radical **PII-8**, which afforded the desired ATRA product **PII-3a-e** through radical chain propagation.



Scheme 72. Postulated mechanism of the visible light-mediated intermolecular ATRA reaction between α -iodoketones **PII-1a-e** and trimethylvinylsilane **PII-2**.

3.3.4 Conclusion

We successfully developed a preliminary method for the visible light-mediated intermolecular ATRA reaction between electron-deficient alkyl iodides and vinylsilanes. While the radical reaction was first believed to be initiated by XAT between the alkyl iodide radical precursor and an α -aminoalkyl radical, further investigations revealed that no PC was required for the reaction to proceed despite the radical nature of the reaction. Therefore, we hypothesized that the reaction proceeded *via* photoexcitation of an XB complex formed between the alkyl iodide radical precursor and the amine.

The initial PC-free protocol was applied to a selection of α -iodoketone substrates, which were synthesized by direct α -halogenation of ketones under mild conditions. All substrates successfully afforded the desired ATRA products under the initial reaction conditions, albeit in a wide range of yields. Therefore, attempts were made to optimize the conditions by varying the temperature of the reaction setup as well as the wavelength of the light source. While these factors impacted the conversion of the substrates and the yields of the desired ATRA products, no clear trend could be identified to optimize the desired transformation for all substrates.

Formation of an XB complex between the substrate and PMP was investigated by UV-vis, ^1H NMR and ^{13}C NMR. However, no complexation was observed with these methods, and the formation of the XB complex could not be unambiguously confirmed. Nevertheless, based on our initial results and literature precedence, we postulated that the reaction proceeded *via* photoexcitation of an XB complex and an ATRA chain mechanism.

While this work requires further investigation, we expect that this XB/ATRA process will allow the synthesis of a wide variety of structurally complex α -iodosilanes, a category of compounds which are typically difficult to obtain but have many interesting applications in organic synthesis. Moreover, early results suggest that this synthetic strategy could be applied towards the synthesis of silylated cyclopropanes.

4. Conclusions and outlook

Radical chemistry remains an important and highly active area within organic chemistry. In this thesis, we have successfully developed new protocols for the intra- and intermolecular visible light driven radical addition of C-centered radicals onto vinyl and alkynyl silanes, a class of radical acceptors that have previously been underexplored.

The photoredox catalyzed protocol developed in chapter 3.1 (connected to objective 1 of this thesis and Paper I) enabled the radical group transfer of vinyl and alkynyl groups from silyl ethers to sp^3 carbons on a wide range of activated and unactivated alkyl iodide radical precursors. The method showed good functional group tolerance and high diastereoselectivity due to the formation of the new C-C bond *via* radical cyclization. Mechanistic studies revealed that the reaction proceeded *via* a combination of SET, XAT and chain propagation, which resulted in radical cyclization followed by spontaneous ring fragmentation of the cyclic intermediate. The telescoped addition of an acid to the reaction mixture enabled the cleavage of the resulting silyl ether, which afforded the desired homoallylic and homopropargylic alcohols in moderate to excellent yields. Our investigation also showed that the XAT reagent was regenerated from an iminium ion side product through an unusual double catalytic cycle.

The envisaged radical homoallylation reaction investigated in chapter 3.2 (connected to objective 2 of this thesis), which was based on the photoredox catalyzed intermolecular radical addition of electron-deficient C-centered radicals to DVTMDS, did not occur as planned. Initial investigations revealed that the anticipated radical cyclization of an addition intermediate did not take place. Instead, the key radical intermediate underwent chain propagation, which afforded the ATRA product. Thus, we turned our attention to the intermolecular ATRA reaction. While this work requires further investigation due to time constraints, it redirected our focus towards the intermolecular ATRA reaction between electron-deficient alkyl radicals and vinylsilanes (chapter 3.3).

A photocatalyst-free protocol was developed in chapter 3.3 (connected to objective 3 of this thesis and Paper II) for the visible light-mediated intermolecular radical addition of electron-deficient alkyl radicals to trimethylvinylsilane. Based on the results of our initial mechanistic investigation and literature precedence, we postulated that the radical reaction was initiated by photoexcitation of an XB complex formed between the α -iodoketone radical precursors and an amine, and that the ATRA reaction proceeded through chain propagation. The protocol was successfully applied to a selection of α -iodoketones to obtain the desired α -iodoalkylsilanes. An extensive screening of the reaction conditions indicated that the optimal conditions were relatively substrate-specific. Exciting preliminary results revealed that the ATRA products can proceed to form the corresponding substituted cyclopropanes, which is an example of the high utility of these α -iodoalkylsilane compounds.

Further investigation of the intermolecular ATRA reaction between activated alkyl halides and vinylsilanes is required to identify the optimal conditions of a general protocol that is applicable on a wider range of substrates, not limited to α -iodoketones, in reasonable yields. Moreover, we expect that the scope of complex α -iodosilanes reachable through this XB/ATRA process can be increased by performing the ATRA reaction with alkenyl and alkynyl silanes other than trimethylvinylsilane.

Overall, this work has demonstrated the potential of alkenyl and alkynyl silanes as radical acceptors in contemporary radical chemistry. We expect that these visible light-mediated intra- and intermolecular

transformations can be applied in the introduction of substituents and functional groups into complex molecules, as well as in the synthesis of highly useful intermediates.

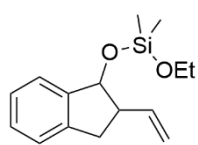
5. Additional compounds

This chapter includes additional experimental procedures and NMR spectra for compounds from chapter 3 not included in papers I and II.

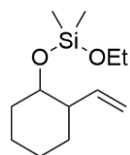
5.1 Experimental methods

All reagents purchased from chemical suppliers were used as received. All air and/or water sensitive reactions were carried out under an atmosphere of argon in flame-dried glassware using standard Schlenk techniques. Anhydrous solvents were dried by pre-storing over activated 4 Å molecular sieves and purged by argon sparging. Light irradiation was performed with RGB LED strips (5.4 W) set to blue and a 427 nm Kessil LED PR160L lamp. For experiments with blue LED strips, reaction flasks were placed 1 cm away from the light source. The intensity of the Kessil lamp was set to the maximum (max 45 W). The experiments with the Kessil LED PR160L lamp were performed in an EvoluChem PhotoRedOx Box TC™ coupled with a Julabo 310F refrigerated bath equipped with a Julabo CORIO™ CD circulator. Reactions were monitored by thin-layer chromatography (TLC) on pre-coated aluminum-based plates (TLC Silica gel 60 F₂₅₄, Supelco). The plates were developed under UV irradiation (254 nm) or with vanillin or KMnO₄ staining and subsequent heating. Column chromatography was performed with silica gel (Silica gel 60, irregular 40–63 μm for flash chromatography, VWR Chemicals). ¹H NMR spectra were recorded at room temperature on a 400 MHz Bruker 9.4 Tesla Avance III HD system equipped with a SmartProbe (broad band). ¹³C NMR spectra (¹H decoupled) were recorded at room temperature on the same machine operating at 101 MHz. All chemical shifts (δ) are reported in parts per million (ppm) with internal reference to residual protons/carbons in CDCl₃ (δ 7.26/77.16) or MeCN-d₃ (δ 1.94/118.26). Coupling constants (*J*) are given in Hz with an accuracy of 0.1 Hz. Infrared (IR) spectra were recorded as thin films or liquids on an Agilent Technologies Cary 630 FTIR 318 spectrometer. Wavelength of maximum absorbance (*v*_{max}) are reported in wavenumbers (cm⁻¹). Only selected characteristic resonances are reported. High-resolution mass spectra (HRMS) were recorded by direct injection of the compounds as solutions in MeOH on a Thermo Scientific Orbitrap Exploris 120 Mass spectrometer, using dual electrospray ionization (ESI) and atmospheric pressure chemical ionization (APCI) probes.

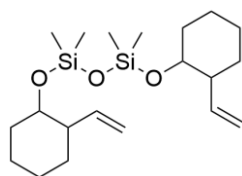
5.1.1 Compounds connected to chapter 3.1



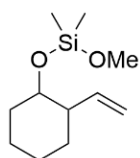
Ethoxydimethyl((2-vinyl-2,3-dihydro-1H-inden-1-yl)oxy)silane 72. Silylated substrate **PI-4a** (41 mg, 0.12 mmol, 1.0 equiv.) was added to a mixture of *fac*-Ir(ppy)₃ (2.0 mg, 3.0 μmol, 2.5 mol%) and Bu₃N (55 μL, 0.23 mmol, 2.0 equiv.) in dry MeCN/EtOH 9:1 (1.2 mL) under Ar. The mixture was degassed by Ar sparging for 5 min before placing the reaction vial 1 cm away from the blue LED strip light source. A fan was placed on top of the setup to keep the reaction environment at room temperature. The reaction mixture was stirred under light irradiation for 1 h before being reduced *in vacuo*. The crude was purified by column chromatography (Et₂O/pentane 3%) to afford **72** (4.4 mg, 0.02 mmol, 14%) as a colorless oil. **R_f** (Et₂O/pentane 3%) 0.35; **IR** (liquid, $\nu_{\max}/\text{cm}^{-1}$) 2970, 2910, 1261, 1108, 1067, 1022, 989, 955, 918, 884, 844, 795, 754, 724; **¹H NMR** (400 MHz, CDCl₃) δ 7.37 – 7.31 (m, 1H, ArH), 7.25 – 7.17 (m, 3H, ArH), 6.01 (ddd, $J = 17.3, 10.3, 7.9$ Hz, 1H, CHCH₂), 5.25 (d, $J = 5.6$ Hz, 1H, CHO), 5.19 – 5.12 (m, 1H, CHCH₂), 5.09 (dd, $J = 10.2, 2.1$ Hz, 1H, CHCH₂), 3.74 (qq, $J = 7.0, 3.3$ Hz, 2H, OCH₂CH₃), 3.09 – 3.00 (m, 1H, CH), 3.00 – 2.89 (m, 2H, CH₂), 1.20 (t, $J = 7.0$ Hz, 3H, OCH₂CH₃), 0.17 (s, 3H, Si(CH₃)), 0.15 (s, 3H, Si(CH₃)); **¹³C NMR** (101 MHz, CDCl₃) δ 144.6, 142.9, 138.5, 128.3, 126.6, 124.9, 124.8, 115.8, 77.7, 58.3, 50.4, 36.5, 18.5, -2.2, -2.3; **HRMS** (ESI) calc. for C₁₅H₂₂O₂SiNa ([M+Na]⁺) 285.1281, found 285.1284.



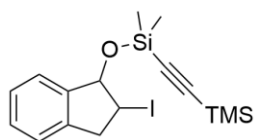
Ethoxydimethyl((2-vinylcyclohexyl)oxy)silane 73. Silylated substrate **PI-4c** (0.20 g, 0.66 mmol, 1.0 equiv.) was added to a mixture of *fac*-Ir(ppy)₃ (17 mg, 26 μmol, 4 mol%), Hantzsch ester (0.33 g, 1.32 mmol, 2.0 equiv.) and Bu₃N (0.78 mL, 1.26 mmol, 1.9 equiv.) in dry MeCN (6.5 mL) under Ar. The mixture was degassed by Ar sparging for 5 min before placing the reaction vial 1 cm away from the blue LED strip light source. A fan was placed on top of the setup to keep the reaction environment at room temperature. The reaction mixture was stirred under light irradiation for 24 h before being reduced *in vacuo*. The crude was purified by column chromatography (Et₂O/pentane 5%) to afford **73** (19 mg, 0.08 mmol, 13%) as a colorless oil. **R_f** (Et₂O/pentane 5%) 0.40; **¹H NMR** (400 MHz, CDCl₃) δ 5.90 (ddd, $J = 17.6, 10.5, 7.4$ Hz, 1H), 5.05 – 4.93 (m, 2H), 3.98 (dt, $J = 5.5, 2.8$ Hz, 1H), 3.74 (q, $J = 7.0$ Hz, 2H), 2.19 – 2.06 (m, 1H), 1.80 – 1.57 (m, 5H), 1.54 – 1.32 (m, 4H), 1.20 (t, $J = 7.0$ Hz, 3H), 0.09 (d, $J = 2.0$ Hz, 6H); **¹³C NMR** (101 MHz, CDCl₃) δ 141.6, 114.0, 71.1, 58.1, 46.7, 33.4, 26.7, 24.6, 20.9, 18.5, -2.4, -2.5.



1,1,3,3-Tetramethyl-1,3-bis((2-vinylcyclohexyl)oxy)disiloxane 74. Silylated substrate **PI-4c** (36 mg, 0.12 mmol, 1.0 equiv.) was added to a mixture of *fac*-Ir(ppy)₃ (2.0 mg, 3.0 μmol, 2.5 mol%) and Bu₃N (52 μL, 0.22 mmol, 1.9 equiv.) in dry MeCN (1.2 mL) under Ar. The mixture was degassed by Ar sparging for 5 min before placing the reaction vial 1 cm away from the blue LED strip light source. A fan was placed on top of the setup to keep the reaction environment at room temperature. The reaction mixture was stirred under light irradiation for 20 h before being reduced *in vacuo*. The crude was purified by column chromatography (Et₂O/pentane 0-1%) to afford **74** (3.1 mg, 8.1 μmol, 14%) as a colorless oil. **R_f** (Et₂O/pentane 1%) 0.64; **IR** (liquid, $\nu_{\max}/\text{cm}^{-1}$) 2933, 2858, 1745, 1644, 1451, 1376, 1261, 1201, 1100, 1056, 1022, 911, 873, 847, 829, 799; **¹H NMR** (400 MHz, CDCl₃) δ 5.90 (ddd, $J = 17.6, 10.5, 7.4$ Hz, 2H, 2 x CHCH₂), 5.06 – 4.91 (m, 4H, 2 x CHCH₂), 4.04 – 3.91 (m, 2H, 2 x CHO), 2.15-2.09 (m, 2H, 2 x CH(CHCH₂)), 1.74-1.61 (m, 8H, 4 x CH₂), 1.50 – 1.24 (m, 8H, 4 x CH₂), 0.07 (m, 12H, 2 x Si(CH₃)₂); **¹³C NMR** (101 MHz, CDCl₃) δ 141.8 (2C), 113.8 (2C), 70.8 (2C), 46.7 (2C), 33.3 (2C), 26.9 (2C), 24.6 (2C), 20.9 (2C), -0.1 (2C), -0.3 (2C); **HRMS** (ESI) calc. for C₂₀H₃₈O₃Si₂Na ([M+Na]⁺) 405.2257, found 405.2255.

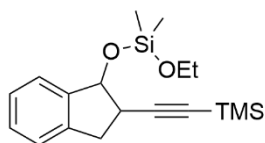


Methoxydimethyl((2-vinylcyclohexyl)oxy)silane 75. Silylated substrate **PI-4c** (82 mg, 0.26 mmol, 1.0 equiv.) was added to a mixture of *fac*-Ir(ppy)₃ (4.1 mg, 6.0 μmol, 2.5 mol%) and Bu₃N (0.12 mL, 0.49 mmol, 1.9 equiv.) in dry MeCN/MeOH 9:1 (2.6 mL) under Ar. The mixture was degassed by Ar sparging for 5 min before placing the reaction vial 1 cm away from the blue LED strip light source. A fan was placed on top of the setup to keep the reaction environment at room temperature. The reaction mixture was stirred under light irradiation for 5 h before being reduced *in vacuo*. The crude was purified by column chromatography (Et₂O/pentane 3%) to afford **75** (13 mg, 0.06 mmol, 23%) as a colorless oil. **R_f** (Et₂O/pentane 3%) 0.33; **IR** (liquid, $\nu_{\text{max}}/\text{cm}^{-1}$) 2933, 2858, 1644, 1451, 1261, 1197, 1089, 1063, 1026, 911, 877, 851, 829, 799, 732; **¹H NMR** (400 MHz, CDCl₃) δ 5.91 (ddd, $J = 17.6, 10.5, 7.4$ Hz, 1H, CH(CHCH₂)), 5.01 (ddd, $J = 10.2, 2.1, 1.1$ Hz, 1H, CH(CHCH₂)), 4.98 (q, $J = 1.7$ Hz, 1H, CH(CHCH₂)), 3.98 (dt, $J = 5.6, 2.8$ Hz, 1H, CHO), 3.48 (s, 3H, OCH₃), 2.14 (tt, $J = 10.3, 2.7$ Hz, 1H, CH(CHCH₂)), 1.76 – 1.60 (m, 4H, 4 x CH₂), 1.53 – 1.24 (m, 4H, 4 x CH₂), 0.10 (s, 3H, Si(CH₃)), 0.10 (s, 3H, Si(CH₃)); **¹³C NMR** (101 MHz, CDCl₃) δ 141.6, 114.1, 71.1, 50.2, 46.6, 33.4, 26.7, 24.6, 20.8, -3.0, -3.1; **HRMS** (ESI) calc. for C₁₁H₂₃O₂Si ([M+H]⁺) 215.1462, found 215.1462.



((2-Iodo-2,3-dihydro-1H-inden-1-yl)oxy)dimethyl((trimethylsilyl)ethynyl)silane 76. According to a literature procedure,¹⁴¹ a 2.0 M methyl iodide solution in *tert*-butyl methyl ether (0.96 mL, 1.9 mmol, 2.7 equiv.) was added dropwise to a solution of aminosilane **PI-s2** (0.21 g, 0.92 mmol, 1.3 equiv.) in dry CH₂Cl₂

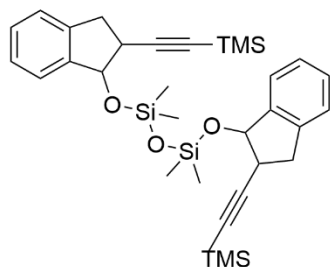
(4 mL) under Ar. The reaction mixture was stirred at room temperature 1 h before being cannulated into a mixture of imidazole (58 mg, 0.85 mmol, 1.2 equiv.) and iodohydrin **PI-3a** (0.19 g, 0.71 mmol, 1.0 equiv.) in dry CH₂Cl₂ (5 mL) under Ar. The mixture was stirred 2.5 h, reduced *in vacuo* and the crude was redissolved in EtOAc. The organic layer was washed with an aqueous 10% Na₂S₂O₃ solution and brine, dried over anhydrous Na₂SO₄, filtered and reduced *in vacuo*. The crude was purified by column chromatography (CH₂Cl₂/pentane 10%) to afford **76** (56 mg, 0.14 mmol, 19%) as a colorless oil. **¹H NMR** (400 MHz, CDCl₃) δ 7.59 – 7.48 (m, 1H, ArH), 7.31 – 7.23 (m, 2H, ArH), 7.23 – 7.17 (m, 1H, ArH), 5.57 (d, $J = 5.4$ Hz, 1H, CHO), 4.31 (td, $J = 7.1, 5.4$ Hz, 1H, CHI), 3.70 – 3.58 (m, 1H, CH₂), 3.30 (dd, $J = 16.4, 7.0$ Hz, 1H, CH₂), 0.43 (s, 3H, Si(CH₃)₂), 0.37 (s, 3H, Si(CH₃)₂), 0.22 (s, 9H, Si(CH₃)₃); **¹³C NMR** (101 MHz, CDCl₃) δ 142.7, 141.2, 128.7, 127.4, 124.9, 124.4, 115.8, 111.2, 86.0, 43.0, 30.1, 1.4, 1.1, -0.0 (3C). Data consistent with literature values.¹⁴⁰



Ethoxydimethyl((2-((trimethylsilyl)ethynyl)-2,3-dihydro-1H-inden-1-yl)oxy)silane 77. Silylated substrate **76** (0.10 g, 0.25 mmol, 1.0 equiv.) was added to a mixture of *fac*-Ir(ppy)₃ (7.5 mg, 12 μmol, 5 mol%), Hantzsch ester (0.12 g, 0.49 mmol, 2.0 equiv.) and Bu₃N 0.12 mL, 0.48 mmol, 2.0 equiv.) in dry

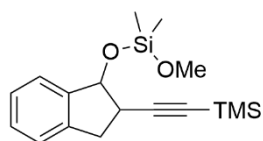
MeCN (2.4 mL) under Ar. The mixture was degassed by Ar sparging for 5 min before placing the reaction vial 1 cm away from the blue LED strip light source. A fan was placed on top of the setup to keep the reaction environment at room temperature. The reaction mixture was stirred under light irradiation for 18 h before being reduced *in vacuo*. The reaction produced a 10:7 mixture of **77** and **78**. The products were separated by column chromatography (Et₂O/pentane 4%) to afford **77** (8.5 mg, 0.03 mmol, 10%) as a colorless oil. **R_f** (Et₂O/pentane 4%) 0.33; **IR** (liquid, $\nu_{\text{max}}/\text{cm}^{-1}$) 2959, 1257, 1115, 1071, 847, 799, 758; **¹H NMR** (400 MHz, CDCl₃) δ 7.38 – 7.33 (m, 1H, ArH), 7.26 – 7.17 (m, 3H, ArH), 5.23 (d, $J = 5.0$ Hz, 1H, CHO), 3.78 (qd, $J = 7.0, 4.1$ Hz, 2H, OCH₂CH₃), 3.29 – 3.20 (m, 2H, CH₂), 3.17 – 3.07 (m, 1H, CHCCSi(CH₃)₃), 1.21 (t, $J = 7.0$ Hz, 3H, OCH₂CH₃), 0.27 (s, 3H, Si(CH₃)₃), 0.18-0.17 (m, 12H, Si(CH₃)₃ and Si(CH₃)₂); **¹³C NMR** (101 MHz, CDCl₃) δ 143.6, 142.2, 128.6, 126.9,

125.2, 124.9, 106.4, 86.9, 76.1, 58.3, 39.1, 37.7, 18.5, 0.3 (3C), -2.0, -2.3; **HRMS** (ESI) calc. for $C_{18}H_{28}O_2Si_2Na$ ($[M+Na]^+$) 355.1520, found 355.1523.

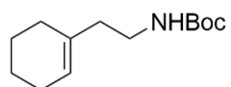


1,1,3,3-Tetramethyl-1,3-bis-((2-(prop-1-yn-1-yl)-2,3-dihydro-1H-inden-1-yl)oxy)disiloxane 78. Silylated substrate **76** (0.10 g, 0.25 mmol, 1.0 equiv.) was added to a mixture of *fac*-Ir(ppy)₃ (7.5 mg, 12 μmol, 5 mol%), Hantzsch ester (0.12 g, 0.49 mmol, 2.0 equiv.) and Bu₃N (0.12 mL, 0.48 mmol, 2.0 equiv.) in dry MeCN (2.4 mL) under Ar. The mixture was degassed by Ar sparging for 5 min before placing the reaction vial 1 cm away from the blue LED strip light source. A fan was placed on top

of the setup to keep the reaction environment at room temperature. The reaction mixture was stirred under light irradiation for 18 h before being reduced *in vacuo*. The reaction produced a 10:7 mixture of **77** and **78**. The products were separated by column chromatography (Et₂O/pentane 4%) to afford **78** (9.8 mg, 0.02 mmol, 7%) as a colorless oil. **R_f** (Et₂O/pentane 4%) 0.46; **IR** (liquid, ν_{max}/cm^{-1}) 2959, 2918, 2188, 1257, 1119, 1089, 1056, 1026, 981, 892, 847, 803, 754; **¹H NMR** (400 MHz, CDCl₃) δ 7.41 – 7.28 (m, 2H, ArH), 7.25 – 7.09 (m, 6H, ArH), 5.26 – 5.17 (m, 2H, CHO), 3.34 – 3.16 (m, 4H, 2 x CH₂), 3.16 – 2.98 (m, 2H, 2 x CHCCSi(CH₃)₃), 0.28 (d, $J = 1.3$ Hz, 6H, 2 x Si(CH₃)₃), 0.16–0.14 (m, 24H, 4 x Si(CH₃)₃, 4 x Si(CH₃)₂); **¹³C NMR** (101 MHz, CDCl₃) δ 143.7 (2C), 142.0 (2C), 128.5 (2C), 126.9 (2C), 125.3 (2C), 124.8 (2C), 106.5 (2C), 86.8 (2C), 76.1 (2C), 39.0 (2C), 37.8 (2C), 0.4 (10C); **HRMS** (ESI) calc. for $C_{32}H_{46}O_3Si_4Na$ ($[M+Na]^+$) 613.2416, found 613.2414.

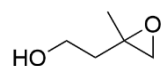


Methoxydimethyl(2-((trimethylsilyl)ethynyl)-2,3-dihydro-1H-inden-1-yl)-oxy)silane 79. Silylated substrate **76** (85 mg, 0.21 mmol, 1.0 equiv.) was added to a mixture of *fac*-Ir(ppy)₃ (4.1 mg, 6.2 μmol, 3.0 mol%) and Bu₃N (0.12 mL, 0.49 mmol, 2.3 equiv.) in dry MeCN/MeOH 9:1 (2.1 mL) under Ar. The mixture was degassed by Ar sparging for 5 min before placing the reaction vial 1 cm away from the blue LED strip light source. A fan was placed on top of the setup to keep the reaction environment at room temperature. The reaction mixture was stirred under light irradiation for 1 h before being reduced *in vacuo*. The crude was purified by column chromatography (Et₂O/pentane 5%) to afford **79** (37 mg, 0.12 mmol, 57%) as a colorless oil. **R_f** (Et₂O/pentane 5%) 0.30; **IR** (liquid, ν_{max}/cm^{-1}) 2962, 2840, 2188, 1719, 1365, 1257, 1223, 1115, 1086, 1067, 1022, 978, 892, 840, 799, 754; **¹H NMR** (400 MHz, CDCl₃) δ 7.22 – 7.16 (m, 1H, ArH), 7.12 – 7.00 (m, 3H, ArH), 5.04 (d, $J = 5.0$ Hz, 1H, CHO), 3.33 (s, 3H, OCH₃), 3.13 – 3.02 (m, 2H, CHCH₂, CHCH₂), 3.01 – 2.90 (m, 1H, CHCH₂), 0.09 (s, 3H, Si(CH₃)₂), 0.00 (m, 12H, Si(CH₃)₂, Si(CH₃)₃); **¹³C NMR** (101 MHz, CDCl₃) δ 143.5, 142.2, 128.7, 127.0, 125.2, 124.9, 106.3, 86.9, 76.2, 50.4, 39.0, 37.7, 0.3, -2.6, -2.8; **HRMS** (ESI) calc. for $C_{17}H_{27}O_2Si_2$ ($[M+H]^+$) 319.1544, found 319.1552.

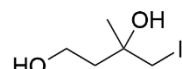


tert-Butyl (2-(cyclohex-1-en-1-yl)ethyl)carbamate 80. 2-(1-Cyclohexenyl)ethylamine (0.43 mL, 3.00 mmol, 1.0 equiv.) was added to a solution of di-*tert*-butyl dicarbonate (0.79 g, 3.60 mmol, 1.2 equiv.) and Et₃N (0.50 mL, 3.60 mmol, 1.2 equiv.) in dry CH₂Cl₂ (3 mL) under Ar. The reaction mixture was stirred at room temperature for 1.5 h before being quenched with water and a saturated aqueous K₂CO₃ solution. The mixture was extracted with CH₂Cl₂. The combined organic layers were dried over anhydrous Na₂SO₄, filtered, and reduced *in vacuo*. The crude was purified by column chromatography (Et₂O/pentane 10%) to afford **80** (0.59 g, 2.64 mmol, 88%) as a colorless oil. **¹H NMR** (400 MHz, CDCl₃) δ 5.49–5.41 (1H, m, CH₂CHC), 4.47 (1H, br s, NH), 3.19 (2H, q, $J = 6.6$ Hz, CH₂CH₂NH), 2.09 (2H, t, $J = 6.9$ Hz, CH₂CH₂NH), 1.99 (2H, ddt, $J = 6.1, 4.1, 2.0$ Hz, CH₂), 1.91 (2H, dq, $J = 6.4, 3.2, 2.5$ Hz, CH₂), 1.66–1.58 (2H, m, CH₂), 1.56

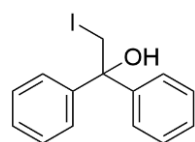
(2H, ddd, $J = 7.8, 5.2, 2.1$ Hz, CH_2), 1.44 (9H, s, 3 x CH_3); ^{13}C NMR (CDCl_3 , 101 MHz) δ 156.0, 134.8, 123.5, 79.2, 38.5, 38.3, 28.6 (3C), 28.0, 25.4, 23.0, 22.5. Data consistent with literature values.¹⁷¹



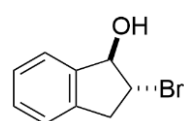
2-(2-Methyloxiran-2-yl)ethan-1-ol 81. Based on a literature procedure,¹⁵⁵ 3-methyl-3-buten-1-ol (0.42 mL, 4.00 mmol, 1.0 equiv.) was added to a mixture of H_2O_2 (30 wt % in H_2O , 1.9 mL, 24.00 mmol, 6.0 equiv.) and NaHCO_3 (1.34 g, 16.00 mmol, 4.0 equiv.) in $\text{MeCN}/\text{H}_2\text{O}$ 3:2 (80 mL), and the reaction mixture was stirred 3 h at room temperature. It was slowly quenched with an aqueous 1 M $\text{Na}_2\text{S}_2\text{O}_3$ solution until no more peroxide was detected by starch paper. The mixture was reduced *in vacuo* before being extracted with EtOAc . The combined organic layers were washed with brine, dried over anhydrous Na_2SO_4 and reduced *in vacuo* to afford **81** (96.2 mg, 0.94 mmol, 24%) as a colorless oil. ^1H NMR (400 MHz, CDCl_3) δ 3.72 (2H, pt, $J = 11.3, 4.9$ Hz, CH_2OH), 2.82 (1H, d, $J = 4.4$ Hz, CH_2O), 2.64 (1H, d, $J = 4.4$ Hz, CH_2O), 2.13 (1H, t, $J = 5.3$ Hz, OH), 2.03–1.91 (1H, m, CH_2), 1.86 (1H, ddd, $J = 14.7, 6.2, 4.6$ Hz, CH_2), 1.38 (3H, s, CH_3); ^{13}C NMR (CDCl_3 , 101 MHz) δ 59.1, 56.3, 52.8, 37.4, 21.8. Data consistent with literature values.¹⁷²



4-Iodo-3-methylbutane-1,3-diol 82. Hydroiodic acid (57 wt % in H_2O , 25 μL , 0.19 mmol, 0.2 equiv.) was added to a mixture of **81** (96 mg, 0.94 mmol, 1.0 equiv.) and TBAI (0.44 g, 1.18 mmol, 1.3 equiv.) in CH_2Cl_2 (2 mL), and the reaction mixture was stirred 16 h at room temperature in the dark. The mixture was reduced *in vacuo*, and the residue was redissolved in EtOAc . It was washed with aqueous 10% NaHCO_3 and 10% $\text{Na}_2\text{S}_2\text{O}_3$ solutions, dried over anhydrous Na_2SO_4 , filtered, and reduced *in vacuo*. The crude was purified by column chromatography ($\text{Et}_2\text{O}/\text{pentane}$ 20-50%) to afford **82** (66 mg, 0.29 mmol, 31%) as a colorless oil. \mathbf{R}_f ($\text{Et}_2\text{O}/\text{pentane}$ 20%) 0.30; \mathbf{IR} (thin film, $\nu_{\text{max}}/\text{cm}^{-1}$) 3327, 2936, 2931, 1457, 1412, 1376, 1212, 1189, 1163, 1111, 1050, 1018; ^1H NMR (400 MHz, CDCl_3) δ 3.99–3.82 (2H, m, CH_2OH), 3.38 (2H, q, $J = 10.1$ Hz, CH_2I), 3.04 (1H, s, OH), 2.48–2.41 (1H, m, OH), 2.02 (1H, ddd, $J = 14.7, 7.1, 4.2$ Hz, CH_2), 1.87 (1H, ddd, $J = 14.7, 7.1, 4.3$ Hz, CH_2), 1.41 (3H, s, CH_3); ^{13}C NMR (CDCl_3 , 101 MHz) δ 71.9, 60.1, 40.3, 27.0, 21.0; \mathbf{HRMS} (APCI) calc. for $\text{C}_5\text{H}_{11}\text{IO}_2\text{Na}$ ($[\text{M}+\text{Na}]^+$) 252.9696, found 252.9696.

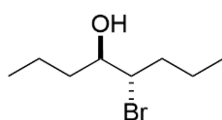


2-Iodo-1,1-diphenylethan-1-ol 83. Based on a literature procedure,¹⁵¹ NIS (0.75 g, 3.32 mmol, 1.2 equiv.) and H_2O (2.7 mL) were added to a mixture of 1,1-diphenylethylene (0.50 mL, 2.75 mmol, 1.0 equiv.) and NH_4OAc (22 mg, 0.28 mmol, 0.1 equiv.) in acetone (10 mL). The reaction mixture was stirred 6 h at room temperature in the dark before being concentrated *in vacuo*. H_2O (20 mL) was added, and the mixture was extracted with CH_2Cl_2 . The combined organic layers were washed with an aqueous 10% $\text{Na}_2\text{S}_2\text{O}_3$ solution and brine, dried over anhydrous Na_2SO_4 , filtered, and reduced *in vacuo*. The crude was purified by column chromatography ($\text{Et}_2\text{O}/\text{pentane}$ 10%) to afford **83** (0.71 g, 2.19 mmol, 80%) as a colorless oil. ^1H NMR (400 MHz, CDCl_3) δ 7.43–7.32 (4H, m, ArH), 7.32–7.23 (4H, m, ArH), 7.23–7.14 (2H, m, ArH), 3.94 (2H, s, CH_2I), 2.77 (1H, s, OH); ^{13}C NMR (CDCl_3 , 101 MHz) δ 143.5 (2C), 128.5 (4C), 127.8 (2C), 126.3 (4C), 76.8, 22.6 (2C). Data consistent with literature values.¹⁷³



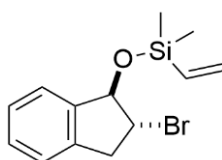
2-Bromo-2,3-dihydro-1H-inden-1-ol 84. Based on a literature procedure,¹⁵¹ NBS (0.54 g, 3.05 mmol, 1.2 equiv.) and H_2O (2.4 mL) were added to a mixture of indene (0.31 mL, 2.47 mmol, 1.0 equiv.) and NH_4OAc (19 mg, 0.24 mmol, 0.1 equiv.) in acetone (9 mL). The reaction mixture was stirred 23 h at room temperature in the dark before being concentrated *in vacuo*. H_2O (20 mL) was added, and the mixture was extracted with Et_2O . The combined organic layers were washed with an aqueous 10% $\text{Na}_2\text{S}_2\text{O}_3$ solution and brine, dried over anhydrous Na_2SO_4 , filtered, and reduced *in vacuo*. The crude was purified by recrystallization from

EtOAc to afford **84** (0.25 g, 1.18 mmol, 48%) as a light-brown solid. $^1\text{H NMR}$ (400 MHz, CDCl_3) δ 7.47–7.39 (1H, m, ArH), 7.34–7.28 (2H, m, ArH), 7.25–7.19 (1H, m, ArH), 5.32 (1H, t, $J = 5.8$ Hz, CHO), 4.29 (1H, td, $J = 7.3, 5.8$ Hz, CHBr), 3.59 (1H, dd, $J = 16.2, 7.2$ Hz, CH_2), 3.23 (1H, dd, $J = 16.2, 7.4$ Hz, CH_2), 2.30 (1H, d, $J = 5.9$ Hz, OH); $^{13}\text{C NMR}$ (CDCl_3 , 101 MHz) δ 141.8, 139.9, 129.2, 127.8, 124.7, 124.2, 83.6, 54.6, 40.6. Data consistent with literature values.¹⁷⁴



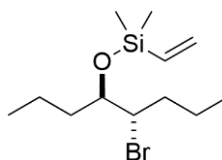
5-Bromo-2-octanol 85. Based on a literature procedure,¹⁵¹ NBS (0.54 g, 3.02 mmol, 1.2 equiv.) and H_2O (2.4 mL) were added to a mixture of trans-4-octene (0.40 mL, 2.47 mmol, 1.0 equiv.) and NH_4OAc (22 mg, 0.29 mmol, 0.1 equiv.) in acetone (9 mL). The reaction mixture was stirred 23 h at room temperature in the

dark before being concentrated *in vacuo*. H_2O (20 mL) was added, and the mixture was extracted with CH_2Cl_2 . The combined organic layers were washed with an aqueous 10% $\text{Na}_2\text{S}_2\text{O}_3$ solution and brine, dried over anhydrous Na_2SO_4 , filtered, and reduced *in vacuo*. The crude was purified by column chromatography (Et_2O /pentane 5–7%) to afford **85** (0.29 g, 1.36 mmol, 55%) as a colorless oil. $^1\text{H NMR}$ (400 MHz, CDCl_3) δ 4.20 (1H, dt, $J = 10.4, 3.3$ Hz, CHBr), 3.70 (1H, ddt, $J = 8.6, 6.7, 3.5$ Hz, CHOH), 1.93 (1H, d, $J = 6.6$ Hz, OH), 1.90–1.31 (8H, m, 4 x CH_2), 0.95 (6H, td, $J = 7.1, 4.0$ Hz, 2 x CH_3); $^{13}\text{C NMR}$ (CDCl_3 , 101 MHz) δ 74.7, 65.3, 35.4, 35.3, 21.4, 19.3, 14.2, 13.6. Data consistent with literature values.¹⁷⁵



((2-Bromo-2,3-dihydro-1H-inden-1-yl)oxy)dimethylvinylsilane 86.

Chloro(dimethyl)vinylsilane (0.20 mL, 1.41 mmol, 1.2 equiv.) was added to a mixture of **84** (0.25 g, 1.17 mmol, 1.0 equiv.), DMAP (29 mg, 0.24 mmol, 0.2 equiv.), and Et_3N (0.20 mL, 1.41 mmol, 1.2 equiv.) in dry CH_2Cl_2 (7 mL) under Ar. The reaction mixture was stirred 20 min at room temperature in the dark. The reaction was quenched by slowly adding a few drops of isopropanol, and the mixture was concentrated *in vacuo*. The residue was redissolved in water and extracted with Et_2O . The combined organic layers were washed with a saturated aqueous NaHCO_3 solution and brine, dried over anhydrous Na_2SO_4 , filtered and reduced *in vacuo*. The crude was purified by column chromatography (Et_2O /pentane 1.5%) to afford **86** (0.10 g, 0.34 mmol, 29%) as a light-yellow oil. $^1\text{H NMR}$ (400 MHz, CDCl_3) δ 7.31–7.23 (3H, m, ArH), 7.22–7.16 (1H, m, ArH), 6.29 (1H, dd, $J = 20.3, 14.9$ Hz, SiCHCH $_2$), 6.10 (1H, dd, $J = 14.9, 3.8$ Hz, SiCHCH $_2$), 5.88 (1H, dd, $J = 20.3, 3.8$ Hz, SiCHCH $_2$), 5.32 (1H, d, $J = 5.6$ Hz, CHO), 4.27 (1H, td, $J = 7.3, 5.6$ Hz, CHBr), 3.57 (1H, dd, $J = 16.2, 7.3$ Hz, CH_2), 3.19 (1H, dd, $J = 16.2, 7.4$ Hz, CH_2), 0.36 (3H, s, Si(CH_3)), 0.34 (3H, s, Si(CH_3)); $^{13}\text{C NMR}$ (CDCl_3 , 101 MHz) δ 142.7, 139.7, 137.5, 134.0, 128.7, 127.5, 124.5, 124.3, 83.9, 54.7, 40.8, -1.0, -1.1. Data consistent with literature values.¹²⁷

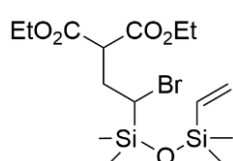


((5-Bromo-2-octan-4-yl)oxy)dimethylvinylsilane 87. Chloro(dimethyl)vinylsilane (0.23 mL, 1.62 mmol, 1.2 equiv.) was added to a mixture of **85** (0.28 g, 1.33 mmol, 1.0 equiv.), DMAP (33 mg, 0.27 mmol, 0.2 equiv.), and Et_3N (0.23 mL, 1.65 mmol, 1.2 equiv.) in dry CH_2Cl_2 (7 mL) under Ar. The reaction mixture was stirred

20 min at room temperature in the dark. The reaction was quenched by slowly adding a few drops of isopropanol, and the mixture was washed with water. The aqueous layer was extracted with Et_2O . The combined organic layers were washed with a saturated aqueous NaHCO_3 solution and brine, dried over anhydrous Na_2SO_4 , filtered and reduced *in vacuo*. The crude was purified by column chromatography (Et_2O /pentane 1%) to afford **87** (0.36 g, 1.23 mmol, 92%) as a colorless oil. R_f (Et_2O /pentane 0.5%) 0.36; IR (liquid, $\nu_{\text{max}}/\text{cm}^{-1}$) 2960, 1740, 1368, 1251, 1230, 1219, 1087, 1042, 825, 784; $^1\text{H NMR}$ (400 MHz, CDCl_3) δ 6.18 (1H, dd, $J = 20.2, 14.9$ Hz, SiCHCH $_2$), 6.02 (1H, dd, $J =$

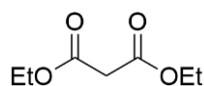
14.9, 4.0 Hz, SiCHCH₂), 5.79 (1H, dd, *J* = 20.2, 4.0 Hz, SiCHCH₂), 3.98 (1H, dt, *J* = 8.8, 4.3 Hz, CHBr), 3.79 (1H, ddd, *J* = 7.8, 4.3, 3.2 Hz, CHO), 1.75 (2H, tdd, *J* = 9.2, 6.9, 4.5 Hz, CH₂), 1.70–1.56 (2H, m, CH₂), 1.55–1.21 (4H, m, 2 x CH₂), 0.92 (6H, td, *J* = 7.2, 4.0 Hz, 2 x CH₃), 0.23 (6H, m, Si(CH₃)₂); ¹³C NMR (CDCl₃, 101 MHz) δ 138.0, 133.3, 76.1, 62.2, 36.6, 36.1, 21.2, 18.8, 14.2, 13.6, -1.1, -1.1; HRMS (ESI) calc. for C₁₂H₂₅BrOSiNa ([M+Na]⁺) 315.0750/316.0784/317.0730, found 315.0750/316.0789/317.0729.

5.1.2 Compounds connected to chapter 3.2



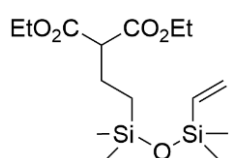
Diethyl 2-(2-bromo-2-(1,1,3,3-tetramethyl-3-vinylidisiloxanyl)ethyl)malonate **89**.

A mixture of diethyl bromomalonate (78 mg, 0.30 mmol, 1.0 equiv.), (Ir[dF(CF₃)ppy]₂(dtbbpy))PF₆ (8 mg, 8 μmol, 2.5 mol%), LiBr (31 mg, 0.36 mmol, 1.2 equiv.) and divinyltetramethyldisiloxane (89 μL, 0.38 mmol, 1.3 equiv.) was prepared in dry MeCN (3 mL) under Ar. The reaction mixture was degassed 5 min by Ar sparging, irradiated with blue light from LED strips at 34 °C for 27 h, and reduced *in vacuo*. The crude was purified by column chromatography (Et₂O/pentane 10%) to afford **89** (38.4 mg, 0.09 mmol, 30%) as a colorless oil. *R*_f (Et₂O/pentane 10%) 0.36; IR (liquid, ν_{max}/cm⁻¹) 2960, 1733, 1254, 1152, 1038, 839, 786, 706; ¹H NMR (400 MHz, CDCl₃) δ 6.12 (1H, dd, *J* = 20.2, 14.8 Hz, Si(CH₃)₂CHCH₂), 5.94 (1H, dd, *J* = 14.9, 3.9 Hz, Si(CH₃)₂CHCH₂), 5.73 (1H, dd, *J* = 20.2, 4.0 Hz, Si(CH₃)₂CHCH₂), 4.26–4.16 (4H, m, 2 x OCH₂), 3.86 (1H, dd, *J* = 10.7, 3.6 Hz, COCHCO), 3.15 (1H, dd, *J* = 13.0, 2.5 Hz, CHBr), 2.55–2.48 (1H, m, COCHCH₂), 2.17–2.09 (1H, m, COCHCH₂), 1.27 (6H, td, *J* = 7.1, 4.9 Hz, 2 x CH₃), 0.23 (6H, s, Si(CH₃)₂), 0.17 (6H, s, Si(CH₃)₂); ¹³C NMR (CDCl₃, 101 MHz) δ 169.5, 168.9, 139.0, 132.2, 61.7, 61.6, 51.2, 40.7, 32.0, 14.2, 14.2, 0.4 (2C), -1.2, -2.0; HRMS (ESI) calc. for C₁₅H₂₉BrO₅Si₂Na ([M+Na]⁺) 447.0629/449.0609, found 447.0630/449.0610.



Diethyl malonate **90**. A mixture of diethyl bromomalonate (65 μL, 0.35 mmol, 1.0 equiv.), *fac*-Ir(ppy)₃ (6 mg, 9 μmol, 2.5 mol%), triethylamine (49 μL, 0.35 mmol, 1.0 equiv.) and divinyltetramethyldisiloxane (0.10 mL, 0.44 mmol, 1.3 equiv.) was

prepared in dry MeCN (3.5 mL) under Ar. The reaction mixture was degassed 5 min by Ar sparging, irradiated 1 h with blue light from LED strips at 34 °C, and reduced *in vacuo*. The crude was purified by column chromatography (Et₂O/pentane 5–20%) to afford **90** (21 mg, 0.13 mmol, 38%) as a colorless oil. ¹H NMR (400 MHz, CDCl₃) δ 4.21 (4H, q, *J* = 7.1 Hz, 2 x CH₂), 3.36 (2H, s, COCH₂CO), 1.28 (6H, t, *J* = 7.1 Hz, 2 x CH₃); ¹³C NMR (CDCl₃, 101 MHz) δ 61.7 (2C), 41.8, 14.2 (2C). Data consistent with literature values.¹⁷⁶

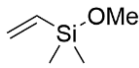


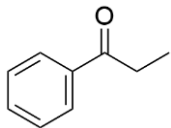
Diethyl 2-(2-bromo-2-(1,1,3,3-tetramethyl-3-vinylidisiloxanyl)ethyl)malonate **96**.

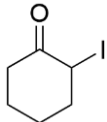
A mixture of diethyl bromomalonate (65 μL, 0.35 mmol, 1.0 equiv.), *fac*-Ir(ppy)₃ (6 mg, 9 μmol, 2.5 mol%), 4-methoxytriphenylamine (0.10 g, 0.35 mmol, 1.0 equiv.) and divinyltetramethyldisiloxane (0.11 mL, 0.46 mmol, 1.3 equiv.) was prepared in dry MeCN (3.5 mL) under Ar. The reaction mixture was degassed 5 min by Ar sparging, irradiated 24 h with blue light from LED strips at 34 °C, and reduced *in vacuo*. The crude was purified by column chromatography (CH₂Cl₂/pentane 30–50%) to afford an inseparable 2:5 mixture of diethyl bromomalonate and **96** (20.9 mg, 0.06 mmol, 17%) as a colorless oil. *Mass of product and NMR data extrapolated from NMR of mixture.* *R*_f (CH₂Cl₂/pentane 50%) 0.55; ¹H NMR (400 MHz, CDCl₃) δ 6.10 (1H, dd, *J* = 20.2, 14.8 Hz, Si(CH₃)₂CHCH₂), 5.92 (1H, dd, *J* = 14.8, 4.0 Hz, Si(CH₃)₂CHCH₂), 5.70 (1H, dd, *J* = 20.3, 4.0 Hz, Si(CH₃)₂CHCH₂), 4.22–4.16 (4H, m, 2 x OCH₂), 3.27 (1H, t, *J* = 7.5 Hz, COCHCO), 1.95–1.88 (2H, m, COCH(CH₂CH₂)CO), 1.26 (6H, t, *J* = 7.1 Hz, 2 x CH₃), 0.56–0.51 (2H,

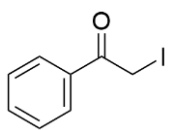
m, $\text{CH}_2\text{Si}(\text{CH}_3)_2$), 0.13-0.07 (12H, m, 2 x $\text{Si}(\text{CH}_3)_2$); ^{13}C NMR (CDCl_3 , 101 MHz) δ 169.6 (2C), 139.6, 131.8, 61.3 (2C), 55.0, 23.1, 16.2, 14.2 (2C), 0.5 (2C), 0.3 (2C).

5.1.3 Compounds connected to chapter 3.3

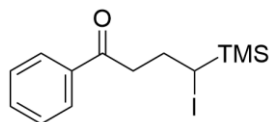
 **Vinyldimethylmethoxysilane 100.** A solution of TMSCl (5.0 mL, 35.13 mmol, 1.0 equiv.) in dry Et_2O (10 mL) was added dropwise at 0 °C over 45 min to a mixture of dry MeOH (1.4 mL, 35.13 mmol, 1.0 equiv.) and Bu_3N (8.8 mL, 36.89 mmol, 1.1 equiv.) in dry Et_2O (60 mL). The reaction mixture was stirred overnight at room temperature before being filtered. The filtrate was purified by fractional distillation (37 °C, 1000 mbar) to afford **100** (0.46 g, 3.93 mmol, 11%) as a colorless oil. ^1H NMR (400 MHz, CDCl_3) δ 6.21–5.98 (2H, m, CH, CH_2), 5.80 (1H, dd, J = 19.6, 4.6 Hz, CH_2), 3.43 (3H, s, OCH₃), 0.19 (6H, s, 2 x $\text{Si}(\text{CH}_3)_2$); ^{13}C NMR (CDCl_3 , 101 MHz) δ 137.0, 133.6, 50.6, -2.5 (2C).

 **Propiophenone 101.** A mixture of α -iodoketone **PII-1a** (78 mg, 0.30 mmol, 1.0 equiv.), 4CzIPN (12 mg, 16 μmol , 5 mol%), Hantzsch ester (84 mg, 0.33 mmol, 1.1 equiv.), diphenyliodonium hexafluorophosphate (0.14 g, 0.33 mmol, 1.1 equiv.) and trimethylvinylsilane (66 μL , 0.45 mmol, 1.5 equiv.) was prepared in dry MeCN (0.6 mL) under Ar. The reaction mixture was irradiated with blue light from LED strips at 34 °C for 24 h before being reduced *in vacuo*. The crude was purified by column chromatography (Et_2O /pentane 3%) to afford **101** (25 mg, 0.19 mmol, 62%) as a light-yellow oil. ^1H NMR (400 MHz, CDCl_3) δ 8.02–7.91 (2H, m, ArH), 7.61–7.50 (1H, m, ArH), 7.47–7.43 (2H, m, ArH), 3.00 (2H, q, J = 7.2 Hz, CH_2), 1.23 (3H, t, J = 7.3 Hz, CH_3); ^{13}C NMR (CDCl_3 , 101 MHz) δ 200.9, 137.0, 133.0, 128.7 (2C), 128.1 (2C), 31.9, 8.4. Data consistent with literature values.¹⁷⁷

 **2-Iodocyclohexan-1-one 103.** Based on a combination of two literature procedures.¹⁶³⁻¹⁶⁴ A solution of *n*-BuLi (1.7 M in hexanes, 2.9 mL, 5.0 mmol, 1.0 equiv.) was slowly added to a solution of dry diisopropylamine (0.71 mL, 5.0 mmol, 1.0 equiv.) in dry THF (8 mL) at 0 °C under Ar. The reaction mixture was stirred 15 min at 0 °C before being cooled to -78 °C. A solution of cyclohexanone (0.52 mL, 5.0 mmol, 1.0 equiv.) in dry THF (8 mL) was added dropwise over 30 min. The resulting reaction mixture was stirred 30 min at -78 °C. The setup was protected from light with aluminum foil while kept at this temperature, and a solution of iodine (1.27 g, 5.0 mmol, 1.0 equiv.) in dry THF (25 mL) was added dropwise over 30 min in the dark. The reaction mixture was stirred an additional 30 min at -78 °C before being allowed to slowly reach room temperature. The reaction was quenched with aqueous sat. $\text{Na}_2\text{S}_2\text{O}_3$ solution, which was added dropwise until the reaction mixture turned colorless. The layers were separated, and the aqueous layer was further extracted with Et_2O . The combined organic layers were dried over anhydrous Na_2SO_4 and reduced *in vacuo*. The crude was purified by column chromatography (Et_2O /pentane 20%) to afford **103** (0.31 g, 1.4 mmol, 28%) as a light-yellow oil. ^1H NMR (400 MHz, CDCl_3) δ 4.68 (1H, t, J = 4.7 Hz, CHI), 3.26–3.18 (1H, m, CH_2), 2.36–2.30 (1H, m, CH_2), 2.22–2.15 (1H, m, CH_2), 2.12–1.91 (3H, m, CH_2), 1.81–1.71 (2H, m, CH_2); ^{13}C NMR (CDCl_3 , 101 MHz) δ 204.9, 37.4, 36.4, 32.5, 26.8, 22.6. Data consistent with literature values.¹⁷⁸

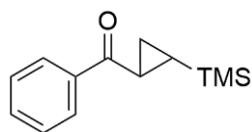
 **2-Iodoacetophenone 104.** Based on a literature procedure.¹⁷⁹ 2-Bromoacetophenone (2.00 g, 10.00 mmol, 1.0 equiv.) was added to a mixture of sodium iodide (3.03 g, 20.23 mmol, 2.0 equiv.) and tetrabutylammonium iodide (0.93 g, 2.52 mmol, 0.3 equiv.) in H_2O /acetone 5:2 (70 mL) and the reaction mixture was stirred in the dark. Upon completion as indicated by TLC, the reaction mixture was concentrated *in vacuo* and the remaining

aqueous mixture was extracted with Et₂O (3 x 20 mL). The combined organic layers were washed with an aqueous 10% Na₂S₂O₃ solution and brine, dried over anhydrous Na₂SO₄ and reduced *in vacuo*. The crude was purified by column chromatography (Et₂O/pentane 30%) to afford **104** (2.21 g, 8.98 mmol, 90%) as a yellow oil. ¹H NMR (400 MHz, CDCl₃) δ 8.05–7.93 (2H, m, ArH), 7.65–7.54 (1H, m, ArH), 7.54–7.43 (2H, m, ArH), 4.37 (2H, s, CH₂I); ¹³C NMR (CDCl₃, 101 MHz) δ 192.9, 134.0, 133.6, 129.2 (2C), 129.0 (2C), 1.8. Data consistent with literature values.¹⁸⁰



4-Iodo-1-phenyl-4-(trimethylsilyl)butan-1-one 105. A mixture of **104** (0.15 g, 0.60 mmol, 1.0 equiv.), PMP (0.13 mL, 0.72 mmol, 1.2 equiv.) and trimethylvinylsilane (0.26 mL, 1.80 mmol, 3.0 equiv.) was prepared in dry MeCN (0.6 mL) under Ar. The reaction vial was placed into the photoreactor

(see the Supporting Information of Paper II for a picture of the setup) and the reaction mixture was irradiated with a Kessil 427 nm light at 20 °C for 24 h. The mixture was reduced *in vacuo* and the residual material was purified by column chromatography (Et₂O/pentane 5%) to afford a mixture of **105** and **106**. The products were separated by further purification on a second column chromatography in CH₂Cl₂ 100%) to afford **105** (59 mg, 0.17 mmol, 28%) as a colorless oil. *R*_f 0.30 (Et₂O/pentane 5%); IR (liquid, $\nu_{\max}/\text{cm}^{-1}$) 2953, 2898, 1684, 1599, 1449, 1360, 1249, 1225, 1198, 1181, 1158, 1076, 1003, 975, 836, 741, 690; ¹H NMR (400 MHz, CDCl₃) δ 8.01–7.99 (2H, m, ArH), 7.60–7.57 (1H, m, ArH), 7.50–7.46 (2H, m, ArH), 3.36 (1H, ddd, *J* = 17.6, 8.1, 4.7 Hz, COCH₂), 3.25–3.14 (2H, m, COCH₂, CHI), 2.23–2.14 (1H, m, CH₂CHI), 2.05–1.95 (1H, m, CH₂CHI), 0.20 (9H, s, Si(CH₃)₃); ¹³C NMR (CDCl₃, 101 MHz) δ 199.5, 137.0, 133.3, 128.8 (2C), 128.2 (2C), 41.1, 28.4, 23.9, -2.0 (3C); HRMS (ESI) calc. for C₁₃H₁₉IOSiNa ([M+Na]⁺) 369.0142, found 369.0142.



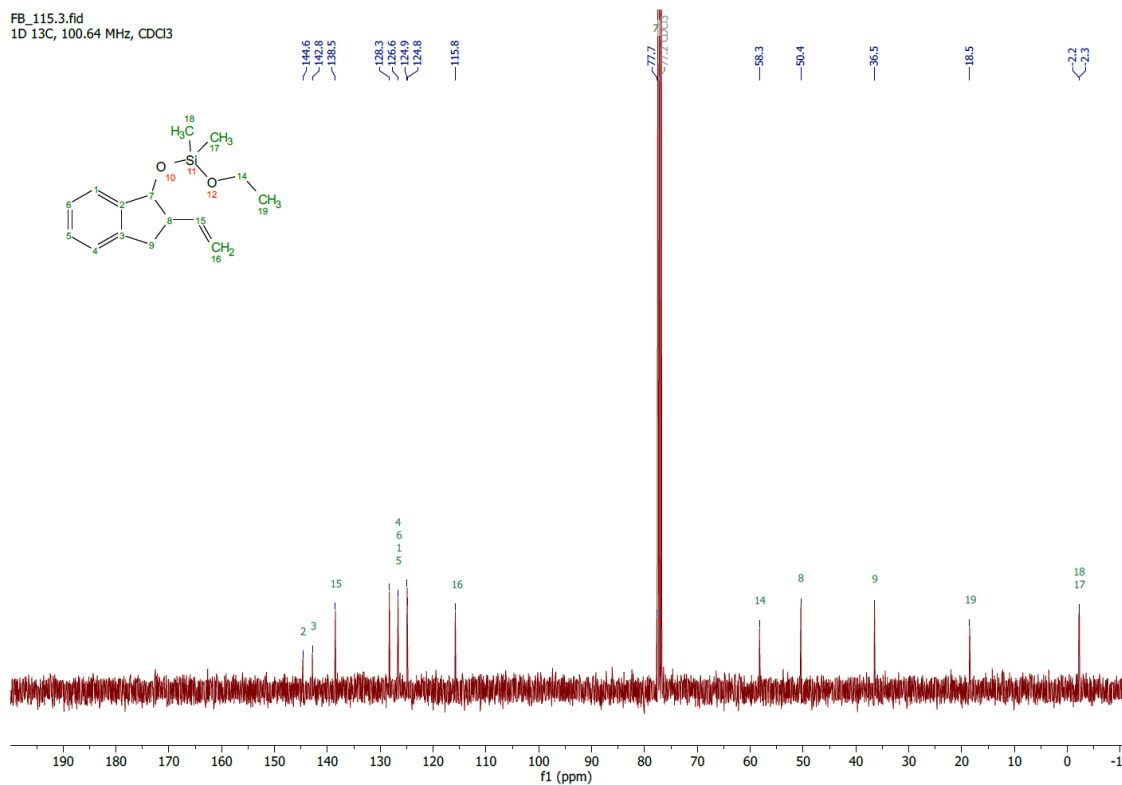
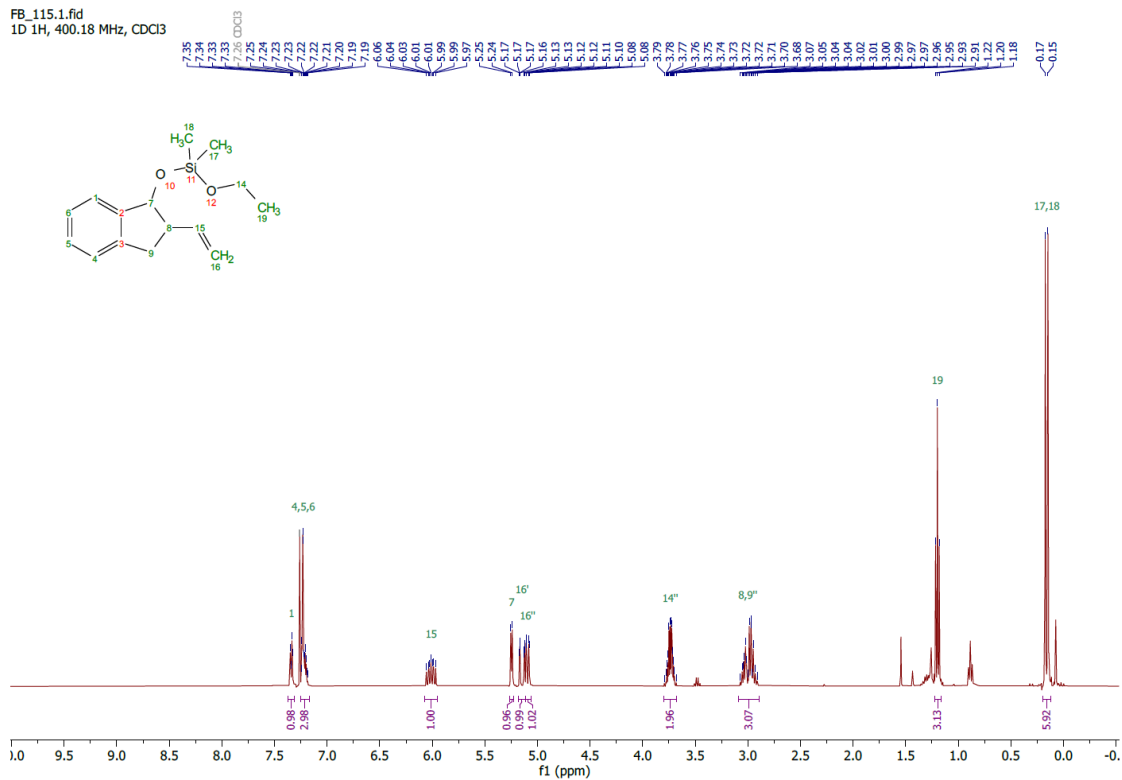
Phenyl(2-(trimethylsilyl)cyclopropyl)methanone 106. A mixture of **104** (0.15 g, 0.60 mmol, 1.0 equiv.), PMP (0.13 mL, 0.72 mmol, 1.2 equiv.) and trimethylvinylsilane (0.26 mL, 1.80 mmol, 3.0 equiv.) was prepared in dry MeCN (0.6 mL) under Ar. The reaction vial was placed into the photoreactor (see

the Supporting Information of Paper II for a picture of the setup) and the reaction mixture was irradiated with a Kessil 427 nm light at 20 °C for 24 h. The mixture was reduced *in vacuo* and the residual material was purified by column chromatography (Et₂O/pentane 5%) to afford a mixture of **105** and **106**. The products were separated by further purification on a second column chromatography in CH₂Cl₂ 100%) to afford **106** (4 mg, 0.02 mmol, 3%) as a colorless oil. *R*_f 0.30 (Et₂O/pentane 5%); IR (thin film, $\nu_{\max}/\text{cm}^{-1}$) 2957, 1748, 1740, 1735, 1670, 1451, 1385, 1251, 1223, 1018, 980, 839; ¹H NMR (400 MHz, CDCl₃) δ 8.06–7.94 (2H, m, ArH), 7.63–7.52 (1H, m, ArH), 7.52–7.42 (2H, m, ArH), 2.52 (1H, ddd, *J* = 7.2, 5.9, 4.1 Hz, CH₂), 1.49 (1H, ddd, *J* = 10.7, 4.1, 2.8 Hz, CH₂), 0.96 (1H, ddd, *J* = 8.4, 7.2, 2.8 Hz, CH₂), 0.71 (1H, ddd, *J* = 10.7, 8.5, 5.9 Hz, CH), 0.04 (9H, s, Si(CH₃)₃); ¹³C NMR (CDCl₃, 101 MHz) δ 200.8, 138.4, 132.8, 128.7 (2C), 128.1 (2C), 21.3, 15.5, 13.7, -2.3 (3C); HRMS (ESI) calc. for C₁₃H₁₈OSiNa ([M+Na]⁺) 241.1019, found 241.1018.

5.2 NMR spectra

5.2.1 Compounds connected to chapter 3.1

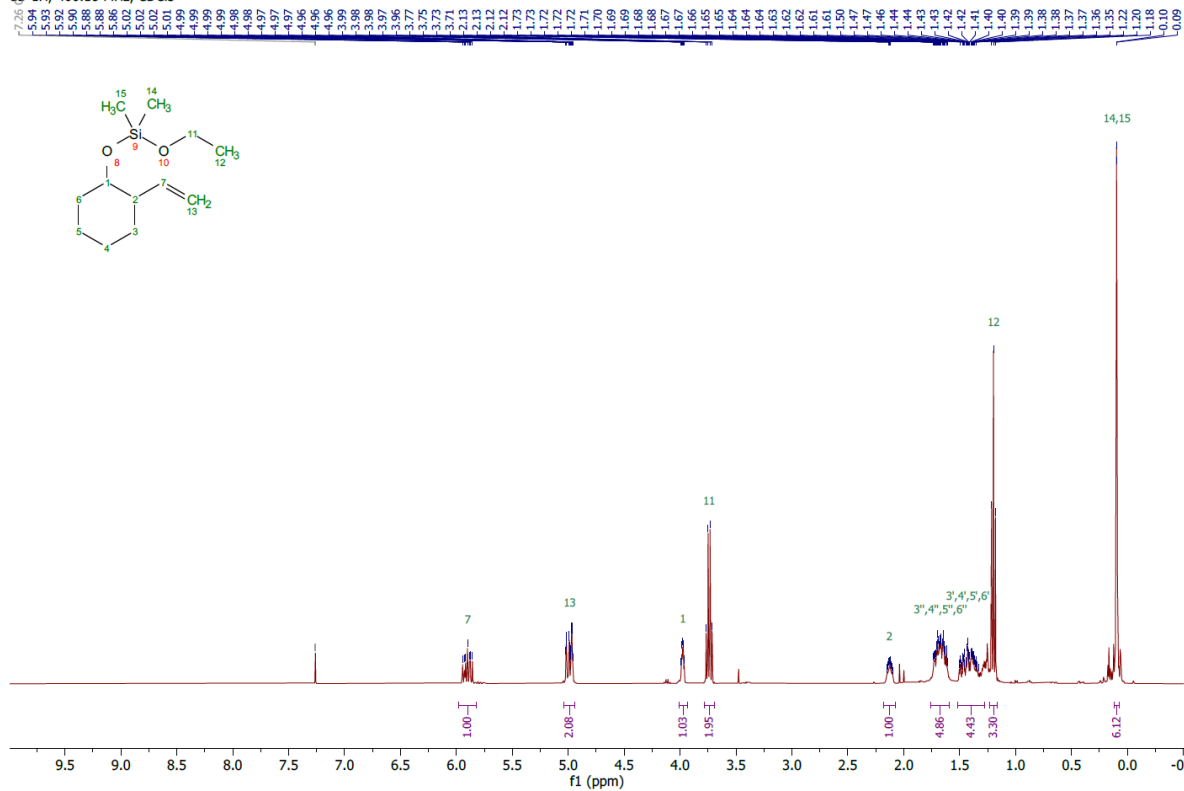
Ethoxydimethyl((2-vinyl-2,3-dihydro-1*H*-inden-1-yl)oxy)silane **72**



Ethoxydimethyl((2-vinylcyclohexyl)oxy)silane **73**

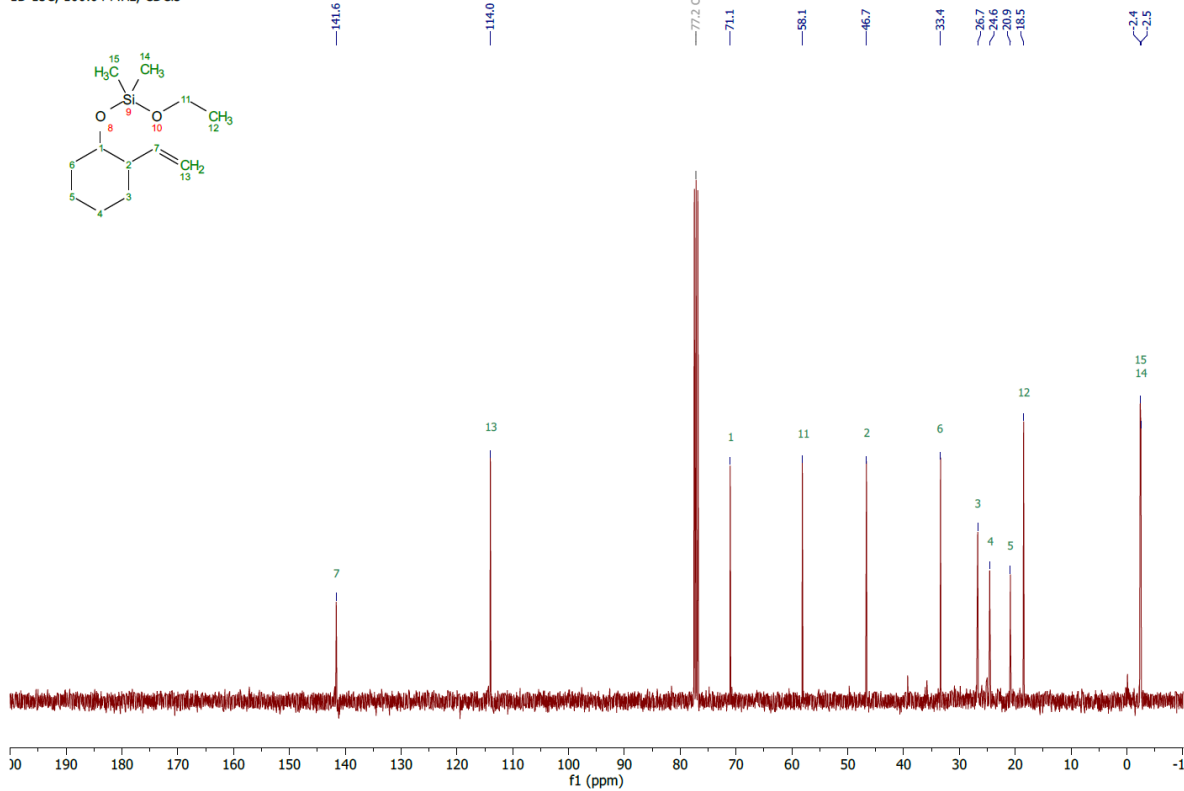
FB_71.1.fid

1D 1H, 400.18 MHz, CDCl3



FB_71.3.fid

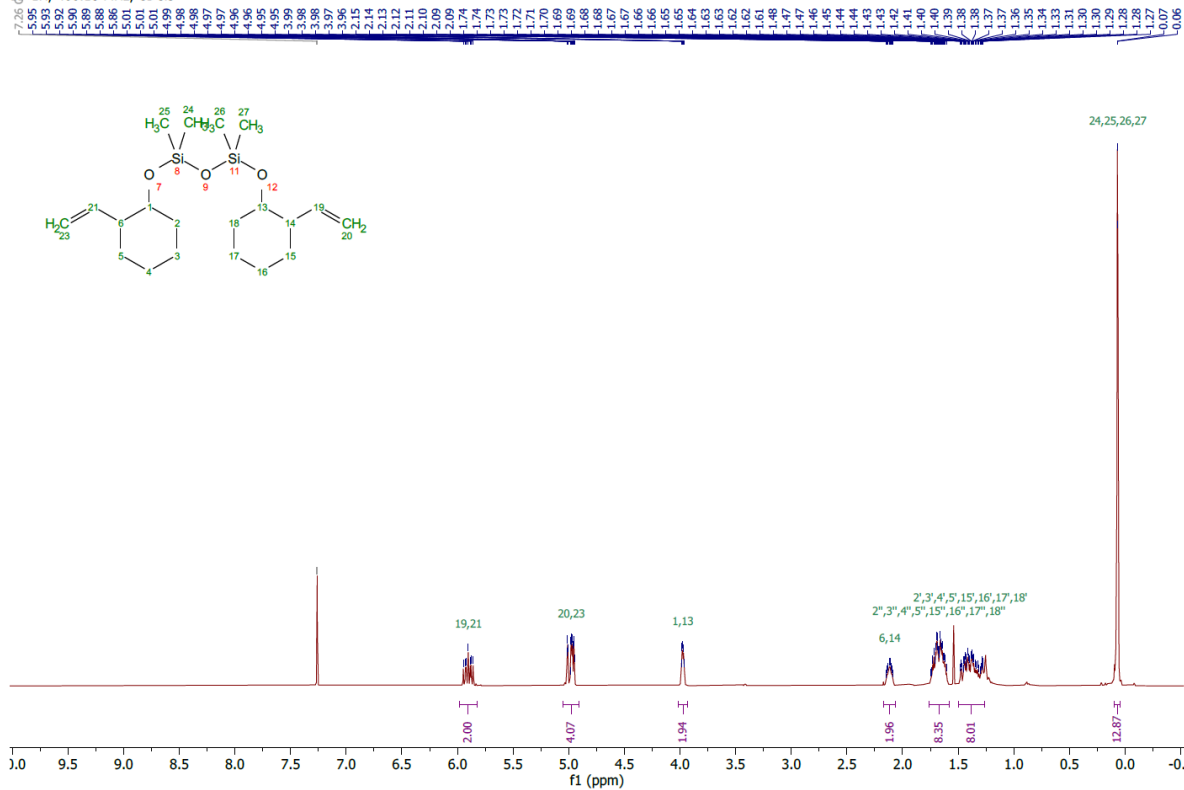
1D 13C, 100.64 MHz, CDCl3



1,1,3,3-Tetramethyl-1,3-bis((2-vinylcyclohexyl)oxy)disiloxane **74**

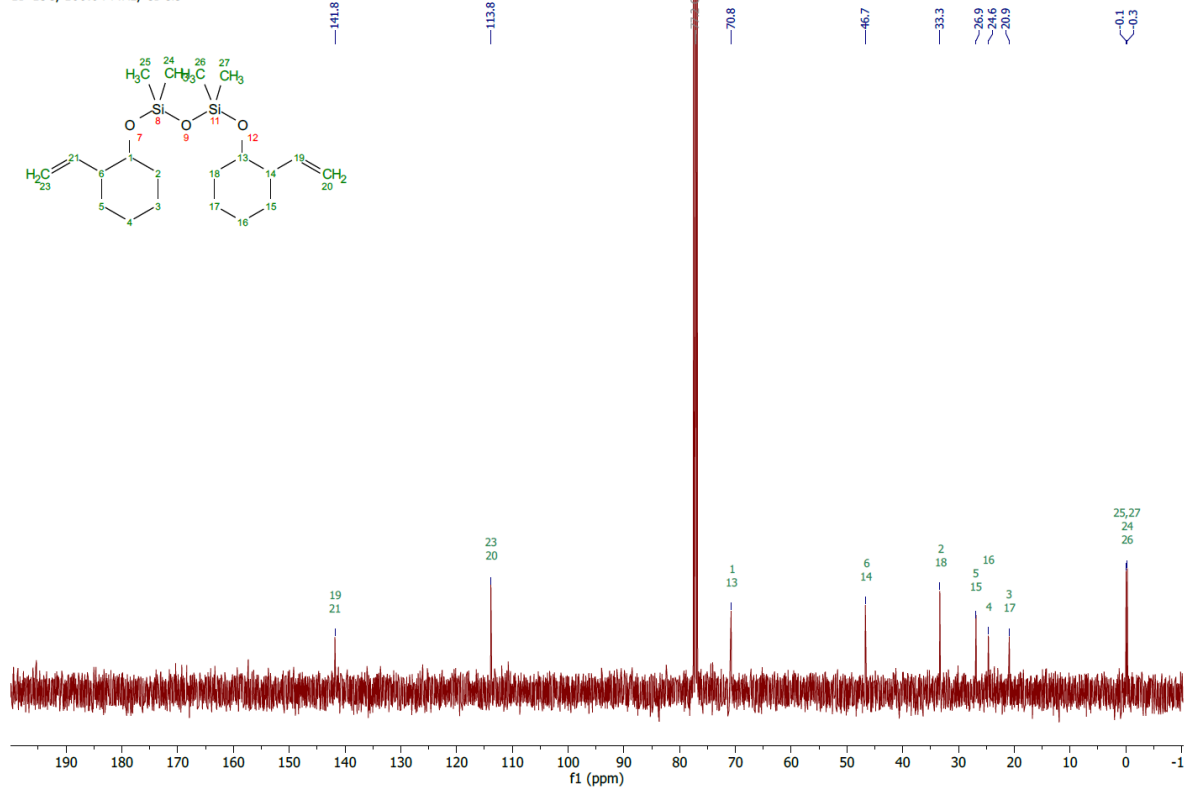
FB_116.1.fid

1D 1H, 400.18 MHz, CDCl3



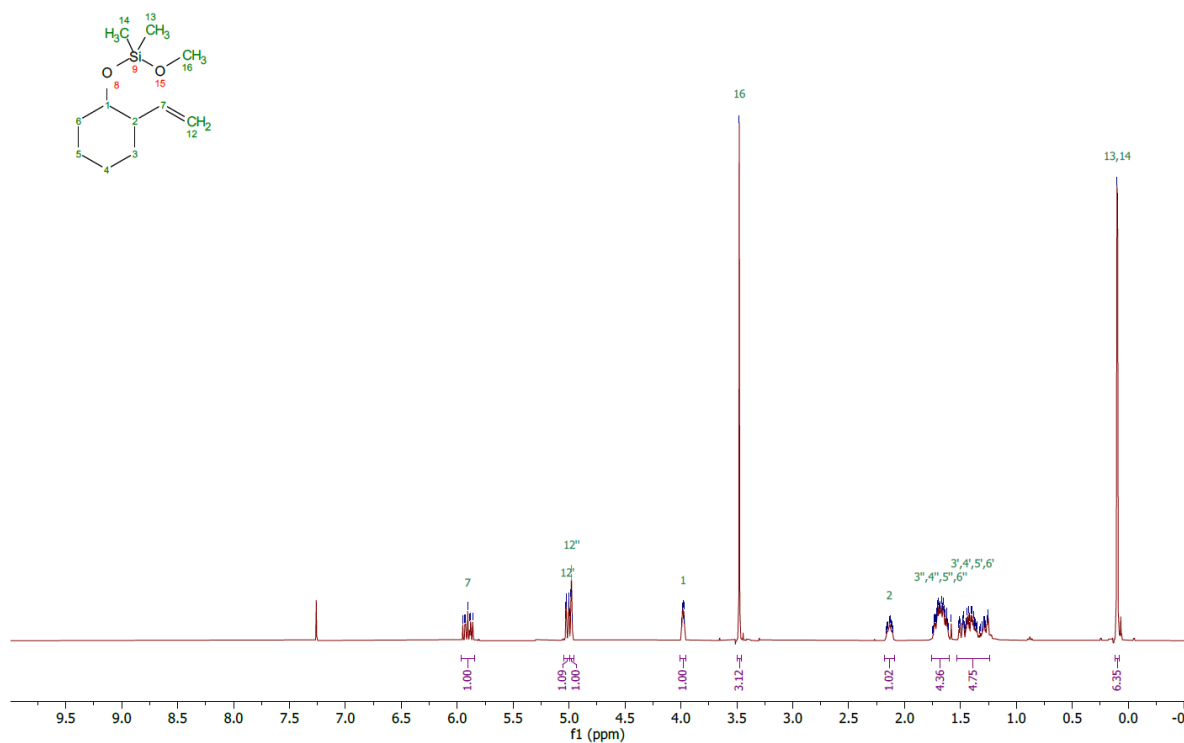
FB_116.3.fid

1D 13C, 100.64 MHz, CDCl3

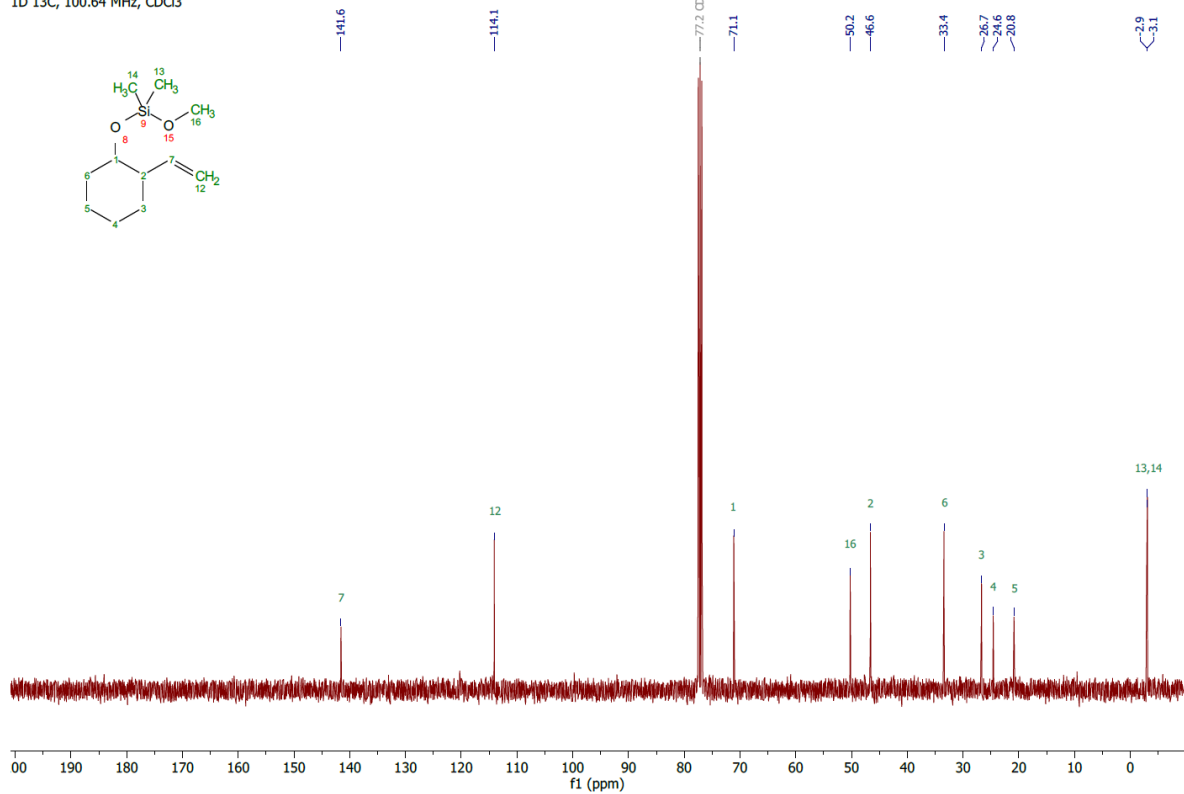


Methoxydimethyl((2-vinylcyclohexyl)oxy)silane **75**

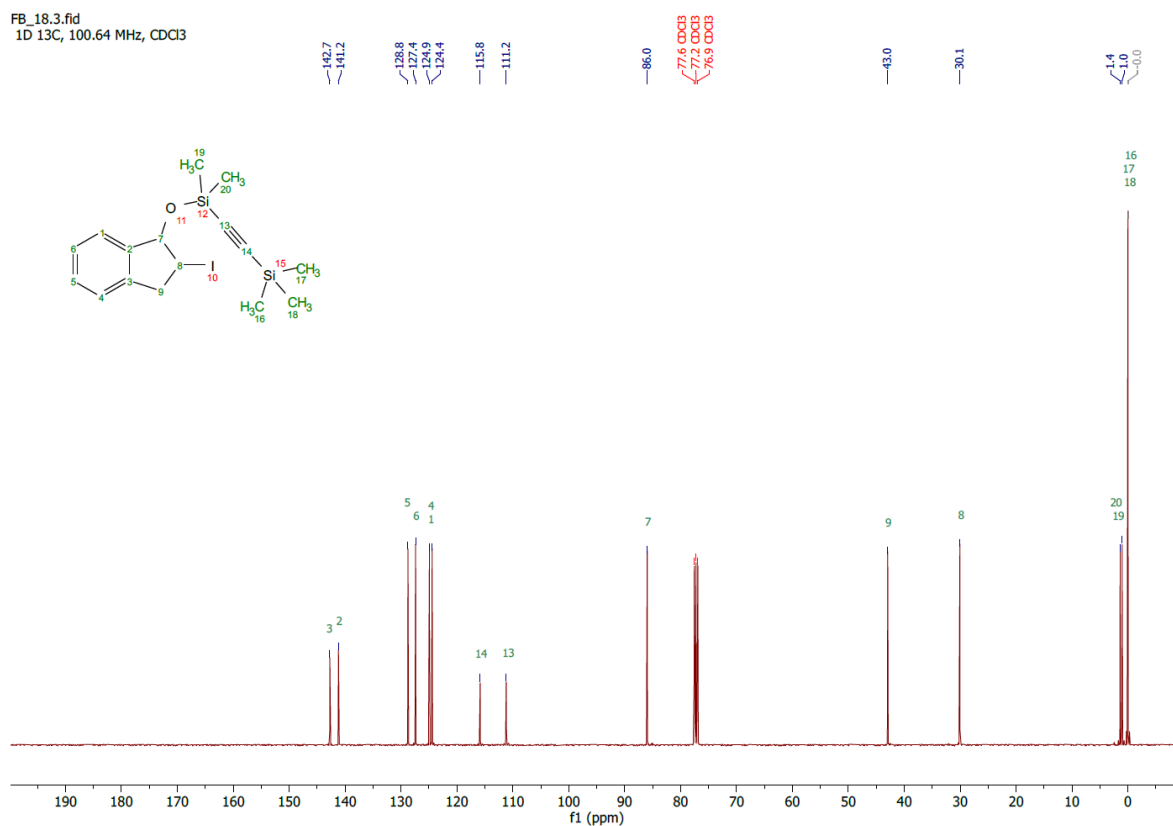
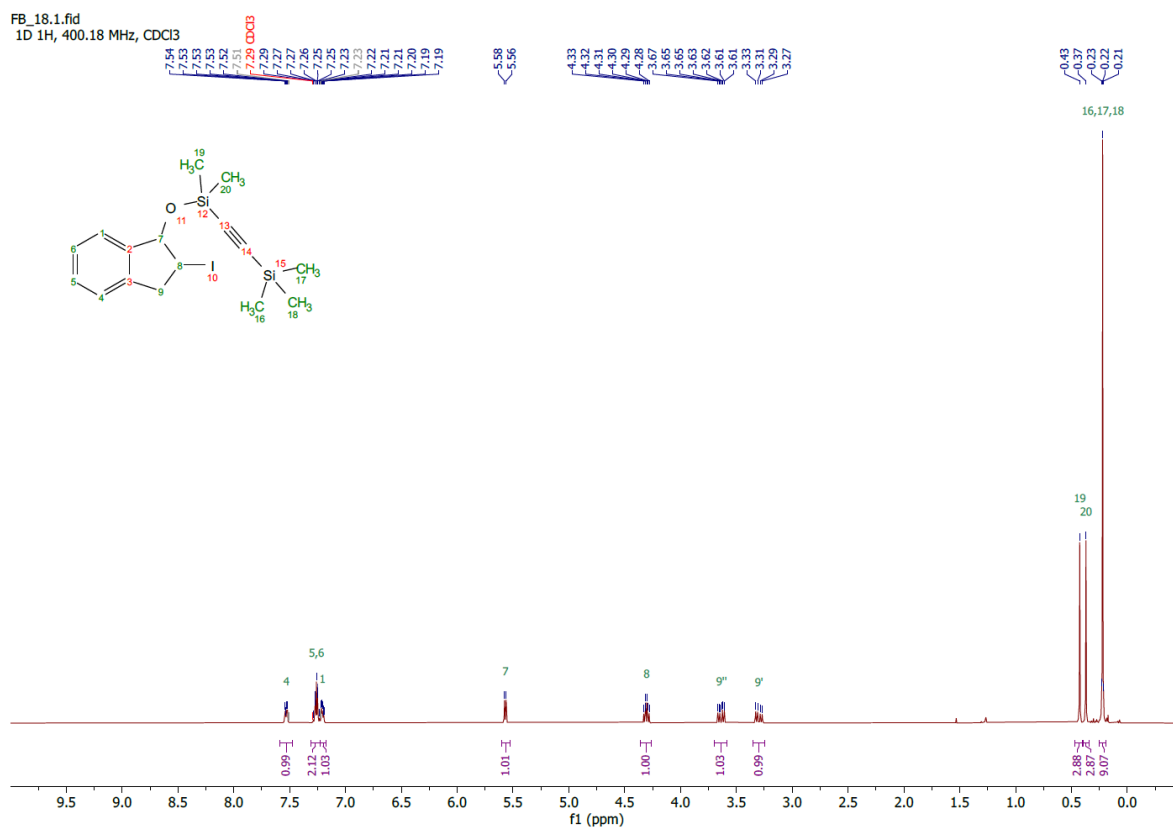
FB_100_yellow_2.3.fid
1D 1H, 400.78 MHz, CDCl3



FB_100_yellow_2.3.fid
1D 13C, 100.64 MHz, CDCl3

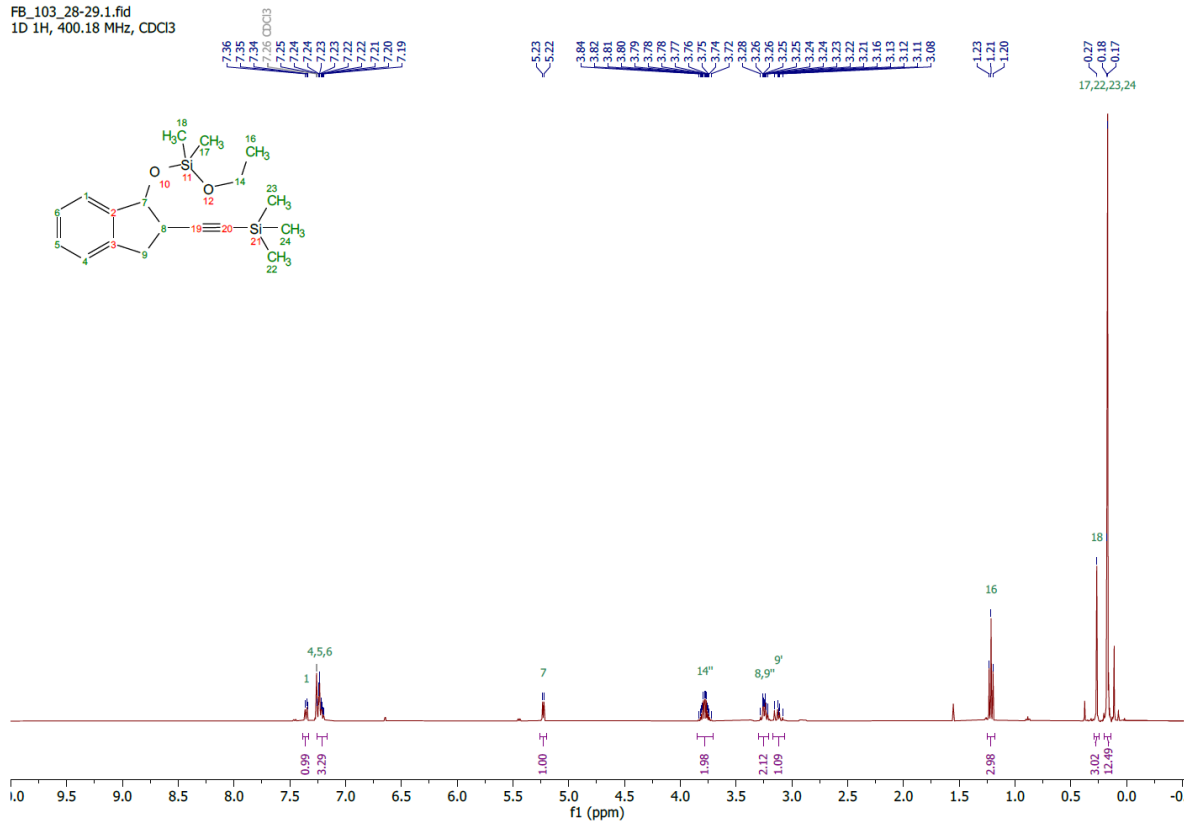


((2-Iodo-2,3-dihydro-1H-inden-1-yl)oxy)dimethyl((trimethylsilyl)ethynyl)silane **76**

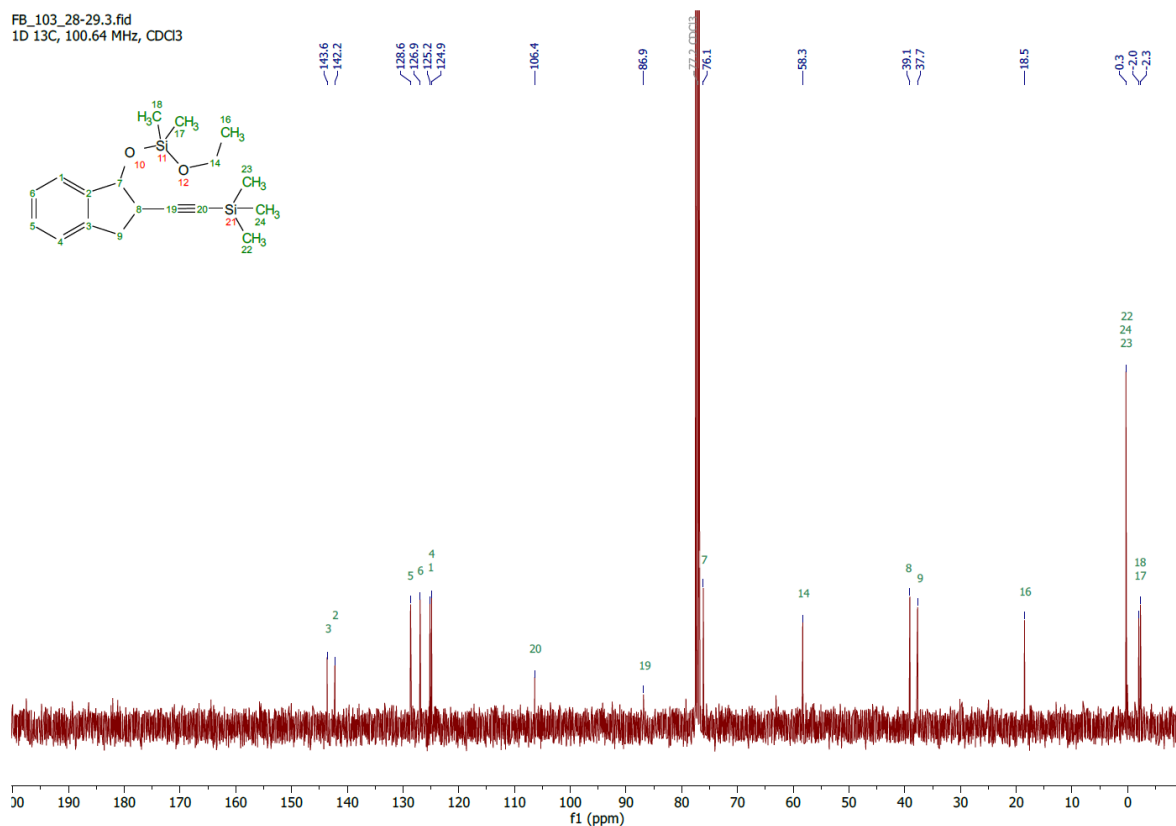


Ethoxydimethyl((2-((trimethylsilyl)ethynyl)-2,3-dihydro-1H-inden-1-yl)oxy)silane 77

FB_103_28-29.1.fid
1D 1H, 400.18 MHz, CDCl3

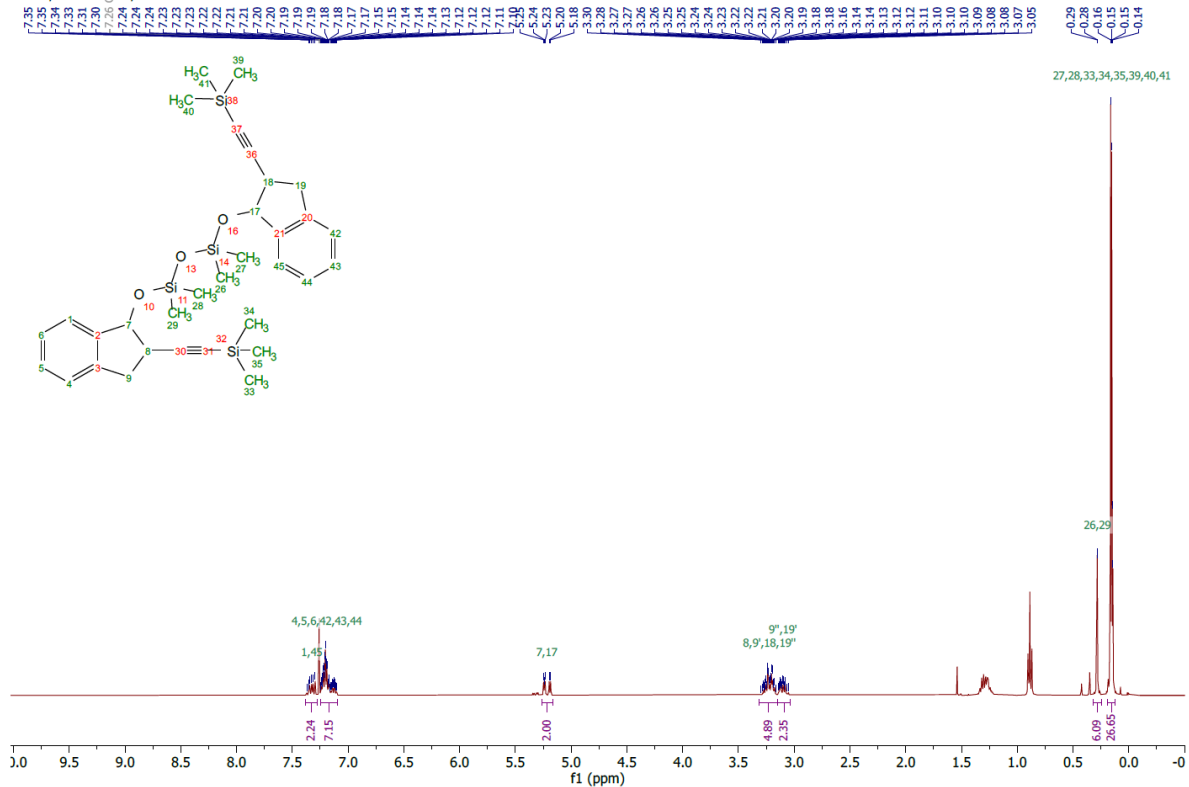


FB_103_28-29.3.fid
1D 13C, 100.64 MHz, CDCl3

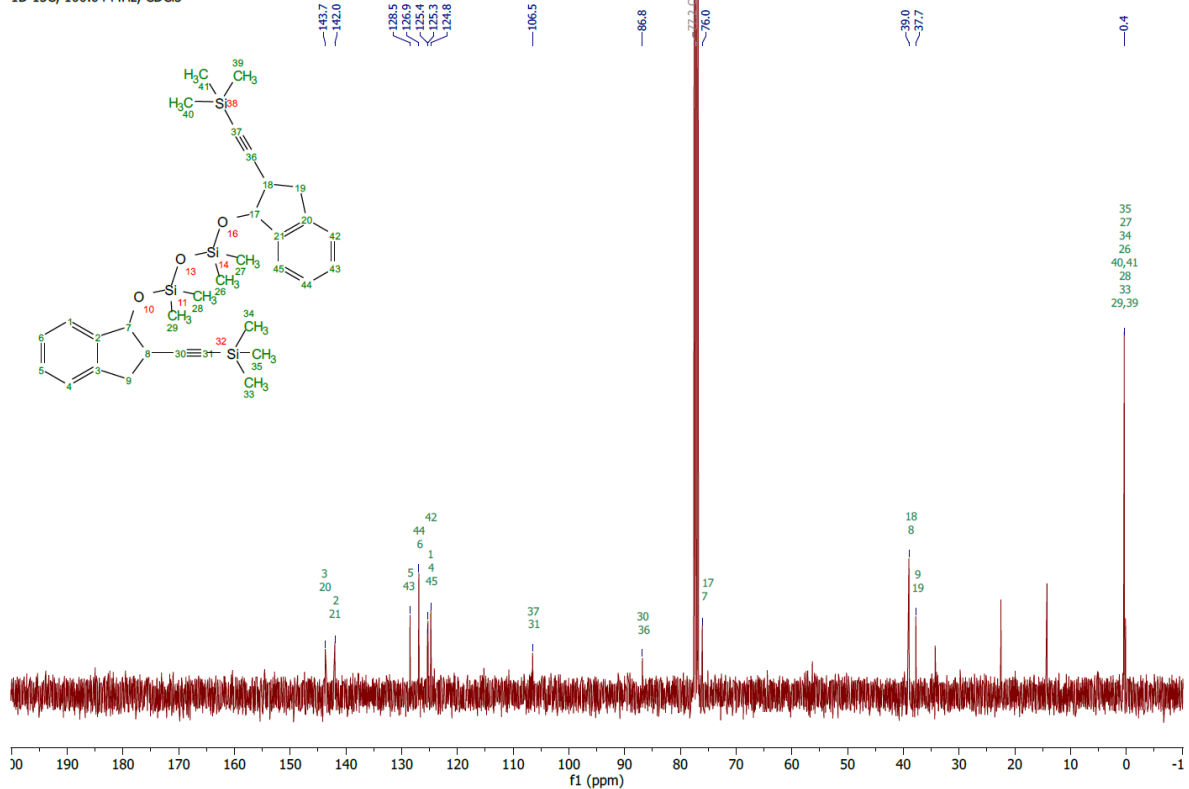


1,1,3,3-Tetramethyl-1,3-bis-((2-(prop-1-yn-1-yl)-2,3-dihydro-1H-inden-1-yl)oxy)disiloxane **78**

FB_103_25-26.1.fid
1D 1H, 400.18 MHz, CDCl3

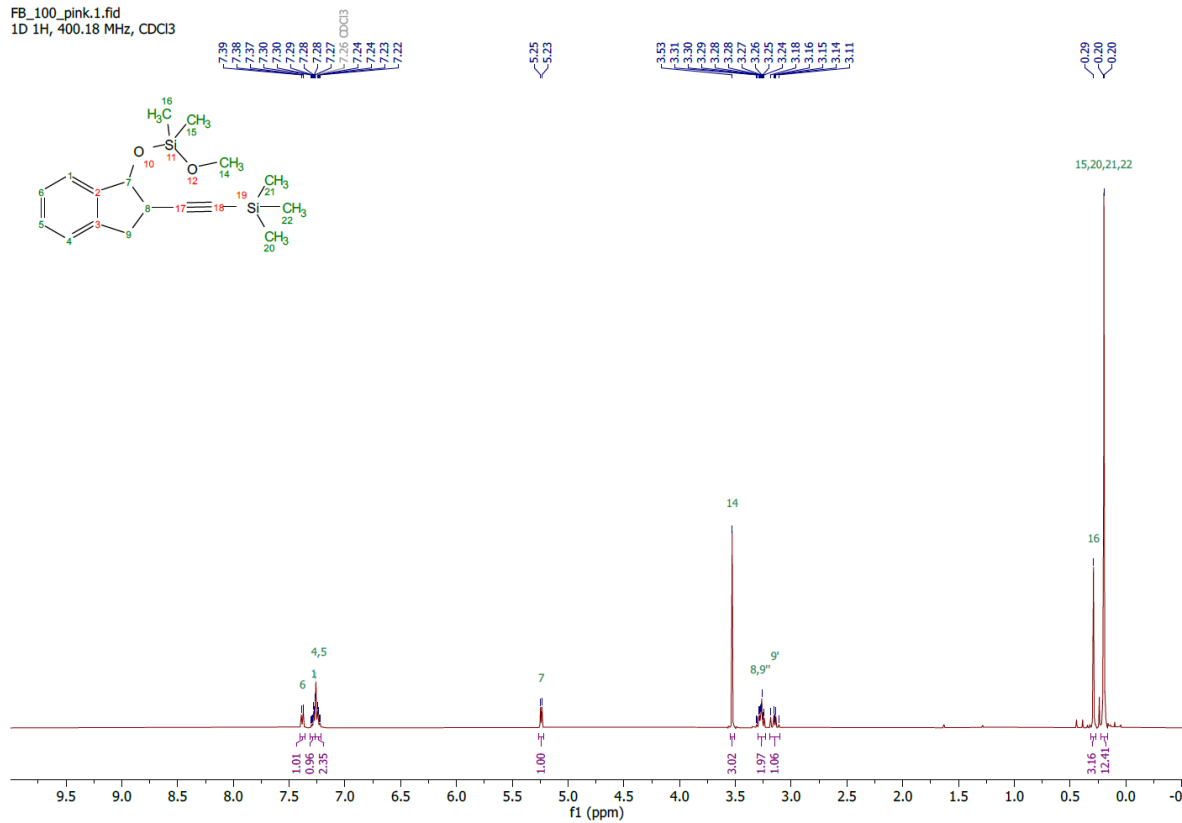


FB_103_25-26.3.fid
1D 13C, 100.64 MHz, CDCl3

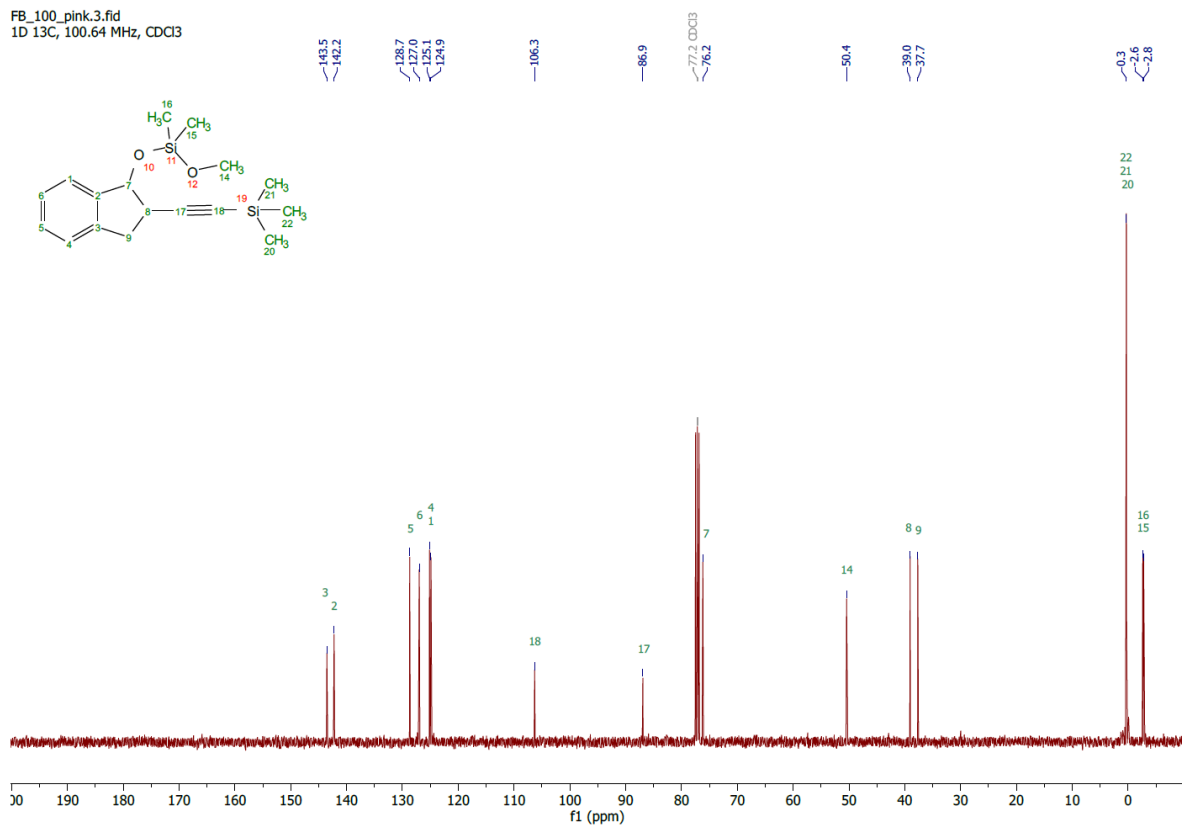


Methoxydimethyl((2-((trimethylsilyl)ethynyl)-2,3-dihydro-1H-inden-1-yl)oxy)silane **79**

FB_100_pink.1.fid
1D 1H, 400.18 MHz, CDCl3

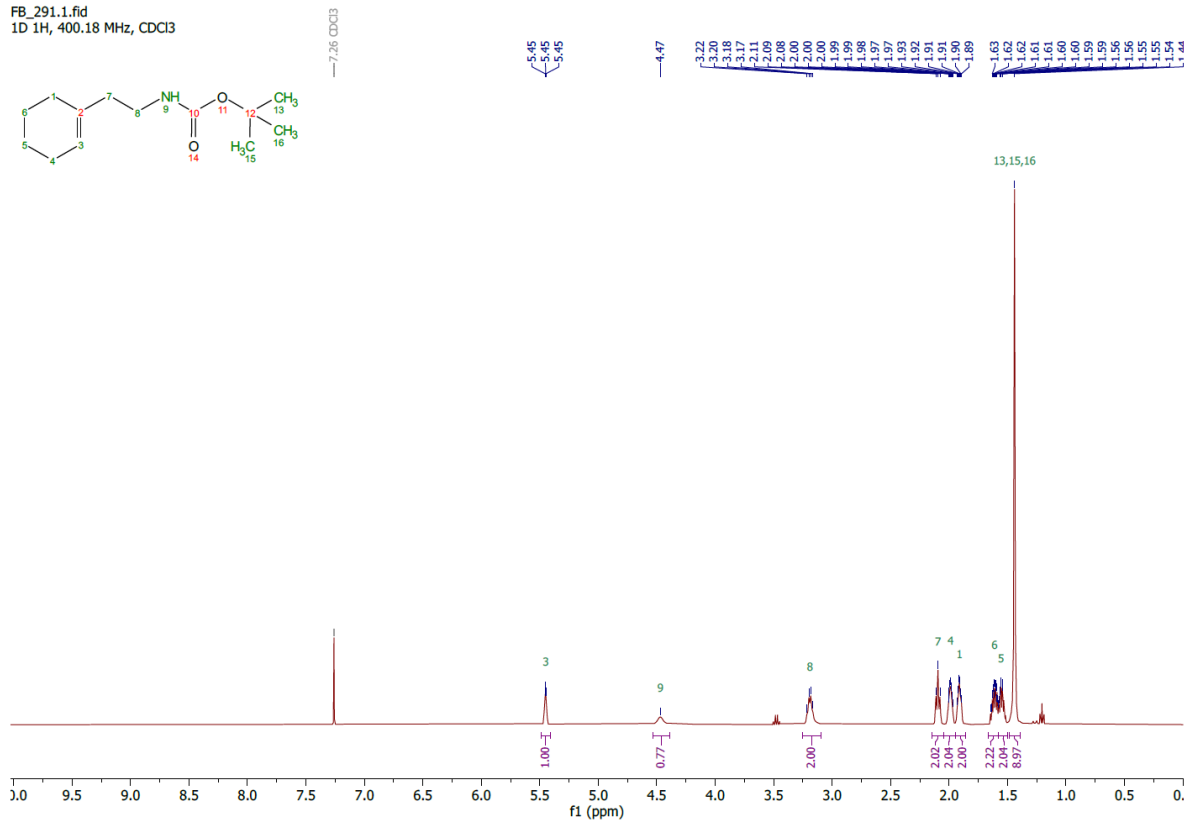


FB_100_pink.3.fid
1D 13C, 100.64 MHz, CDCl3

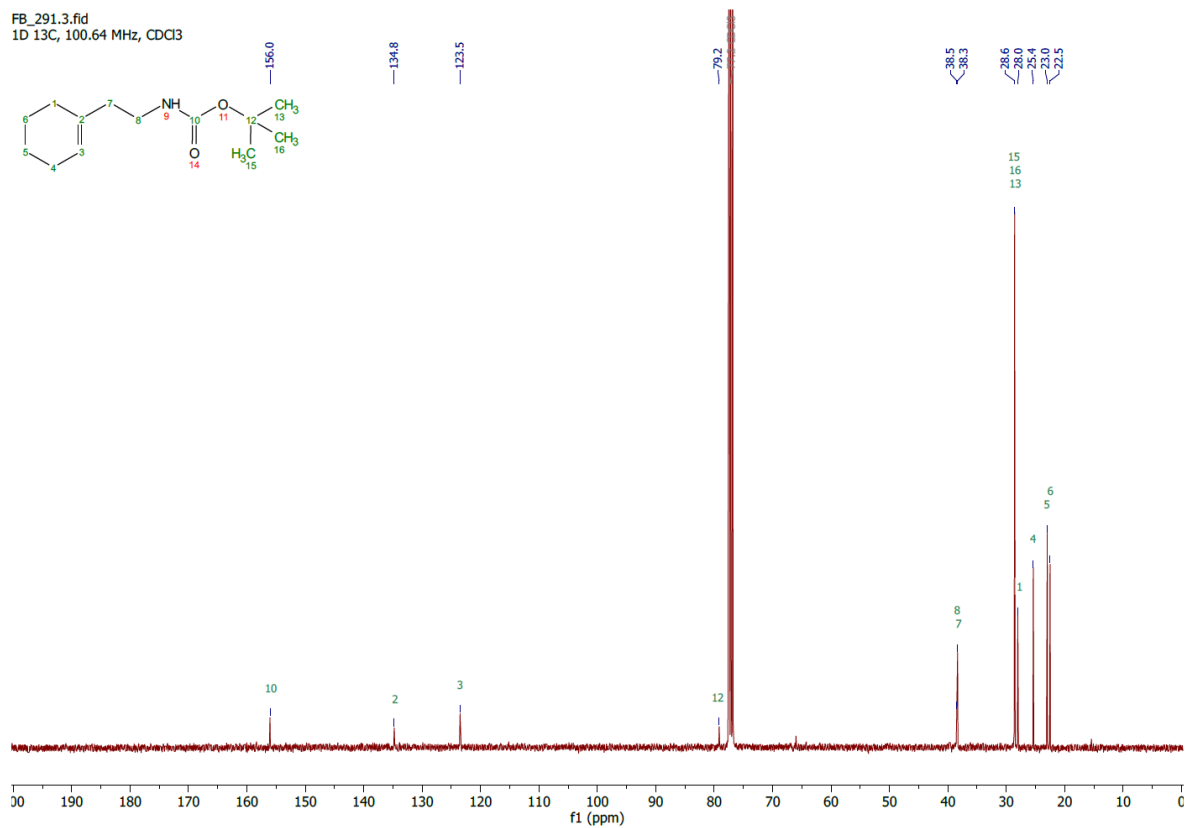


tert-Butyl (2-(cyclohex-1-en-1-yl)ethyl)carbamate **80**

FB_291.1.fid
1D 1H, 400.18 MHz, CDCl₃

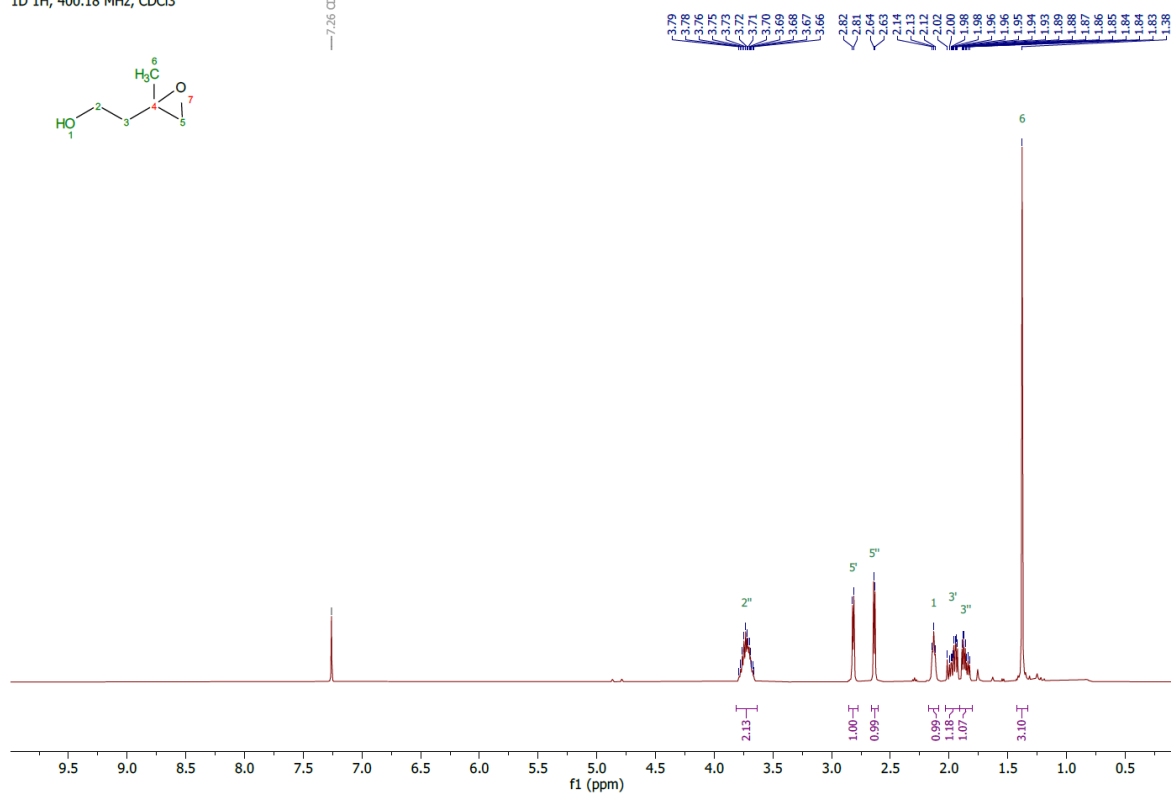
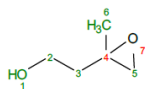


FB_291.3.fid
1D 13C, 100.64 MHz, CDCl₃

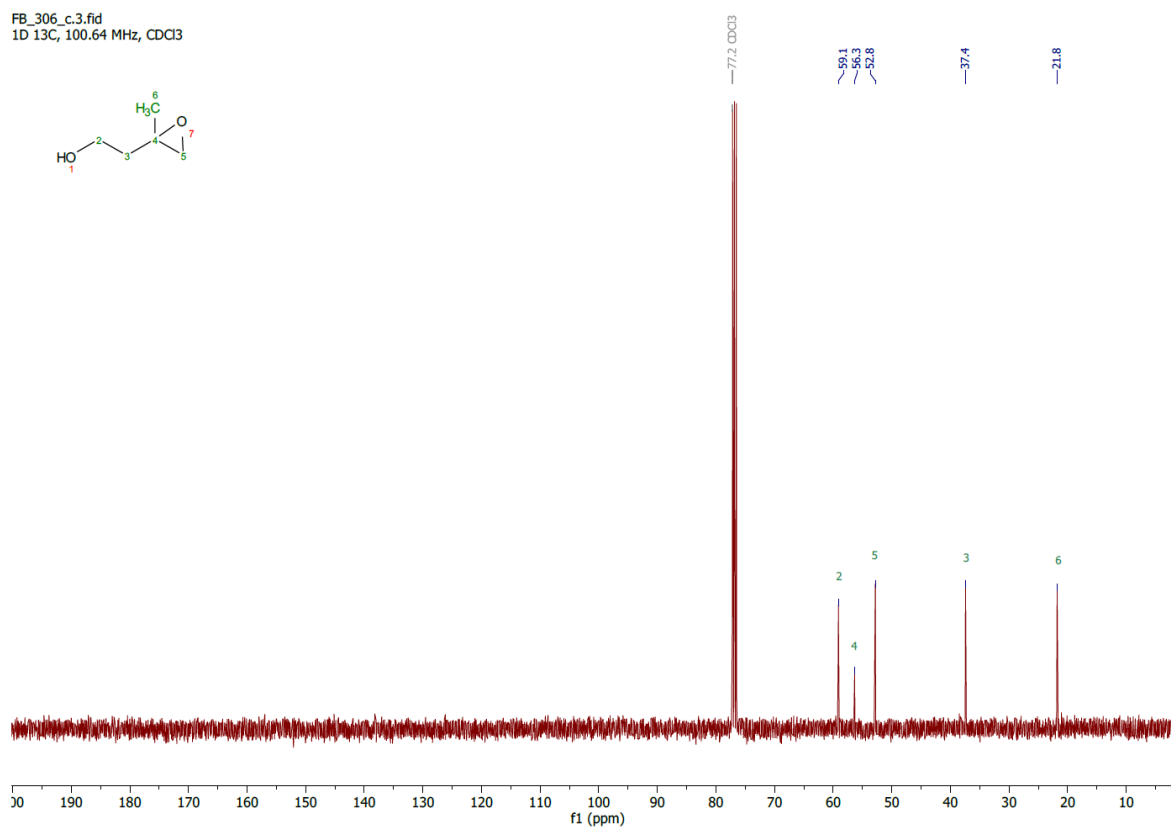
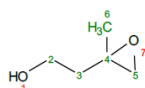


2-(2-Methyloxiran-2-yl)ethan-1-ol **81**

FB_306_c.1.fid
1D 1H, 400.18 MHz, CDCl3

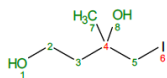


FB_306_c.3.fid
1D 13C, 100.64 MHz, CDCl3

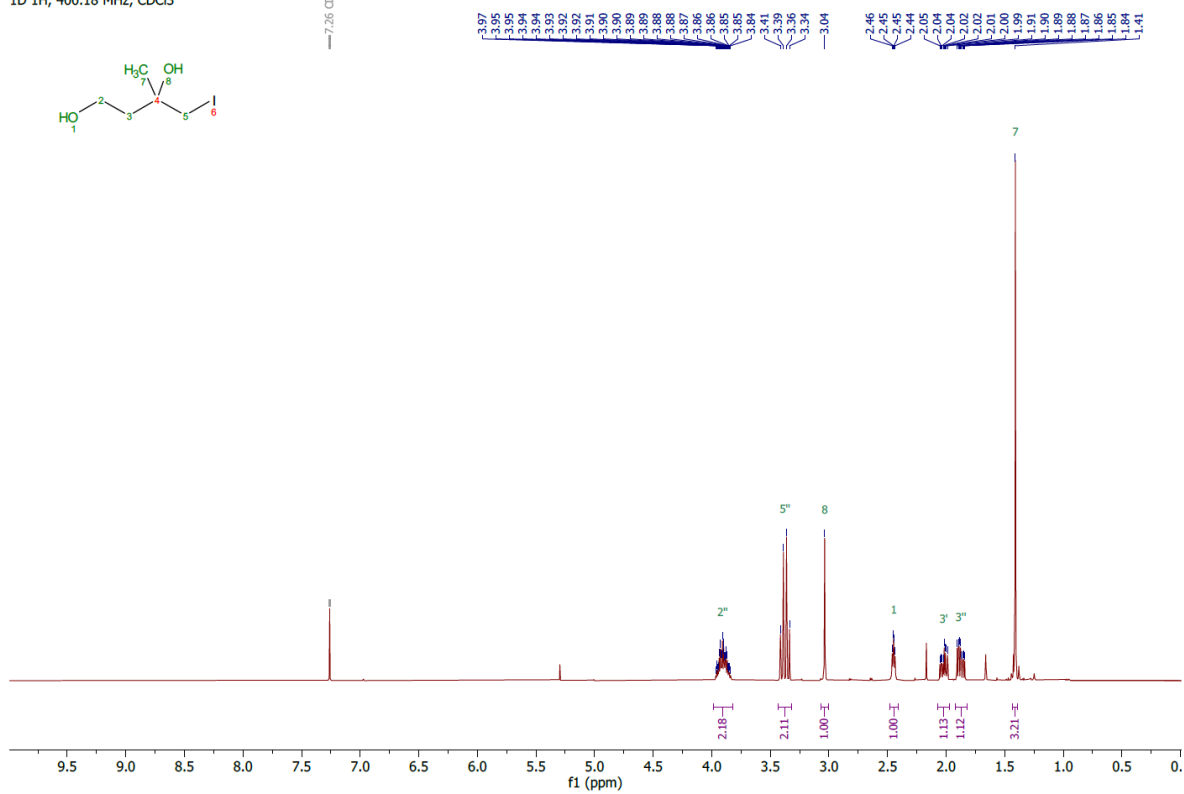


4-Iodo-3-methylbutane-1,3-diol **82**

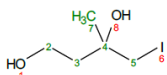
FB_308_23-33.1.fid
1D 1H, 400.18 MHz, CDCl3



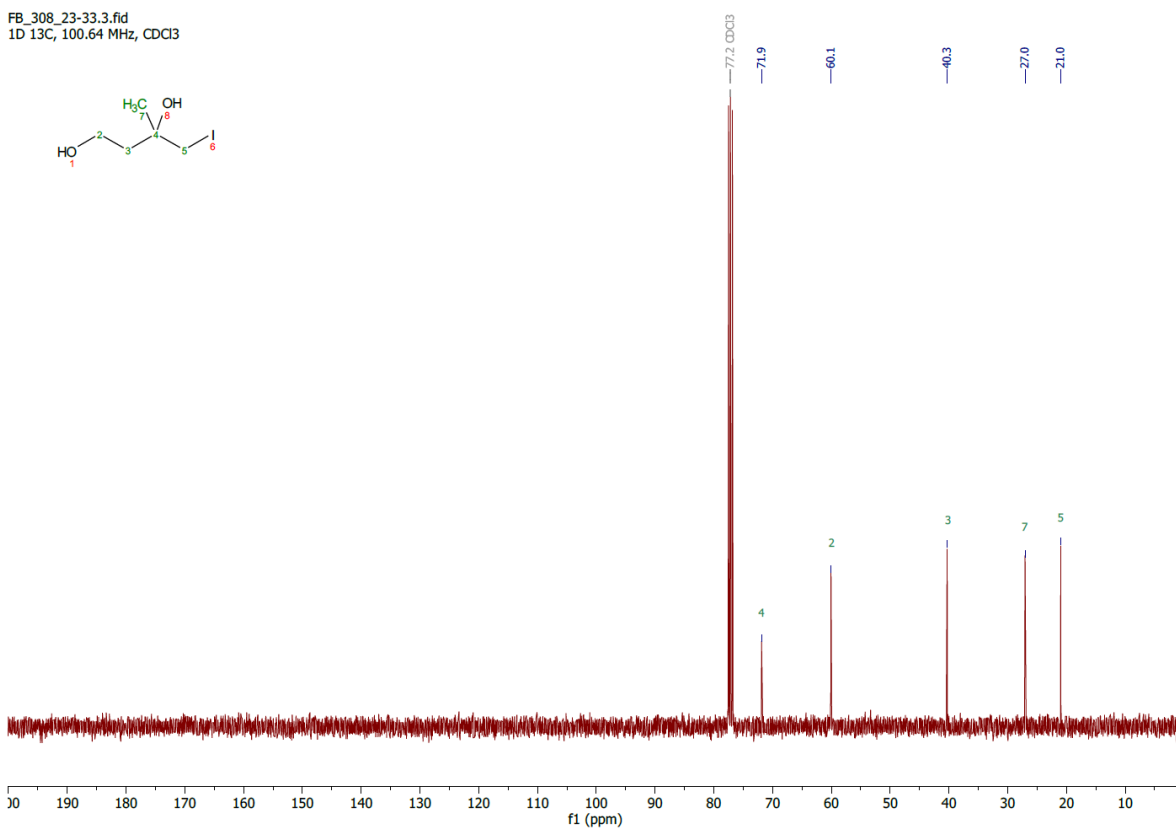
77.26 CDCl3



FB_308_23-33.3.fid
1D 13C, 100.64 MHz, CDCl3

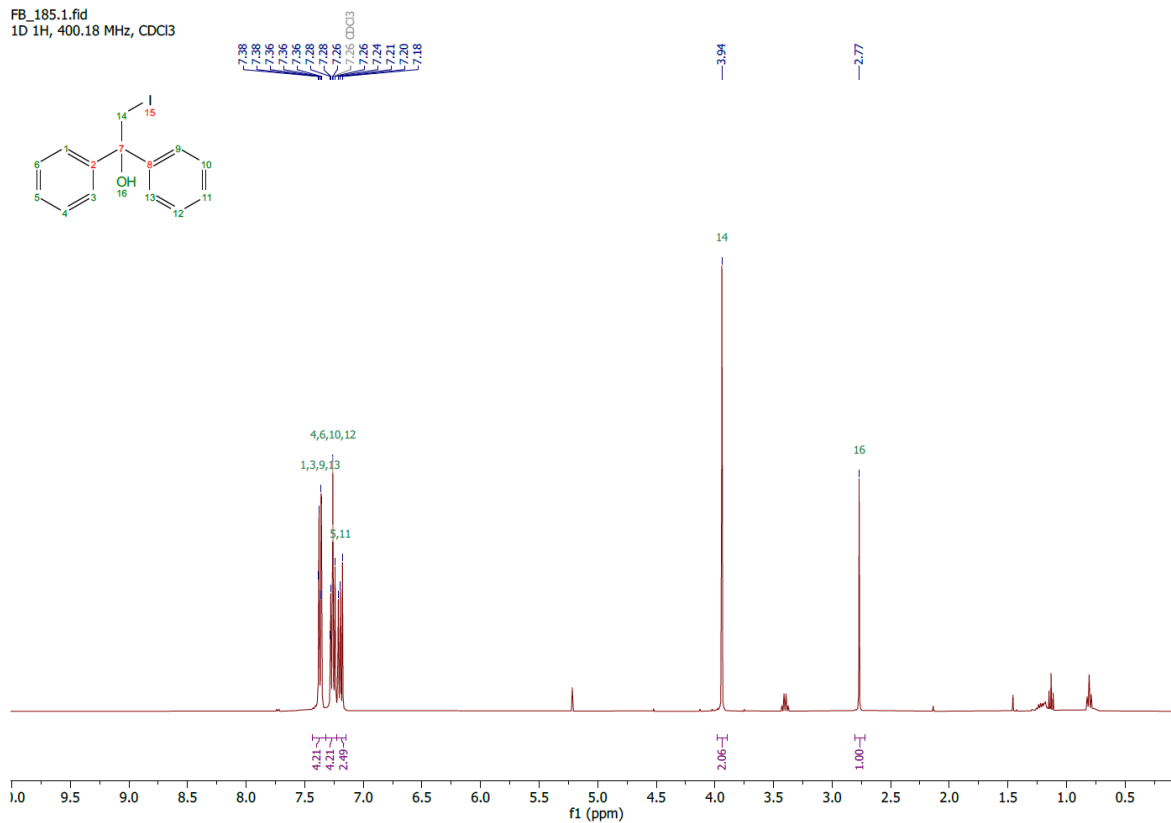


77.2 CDCl3

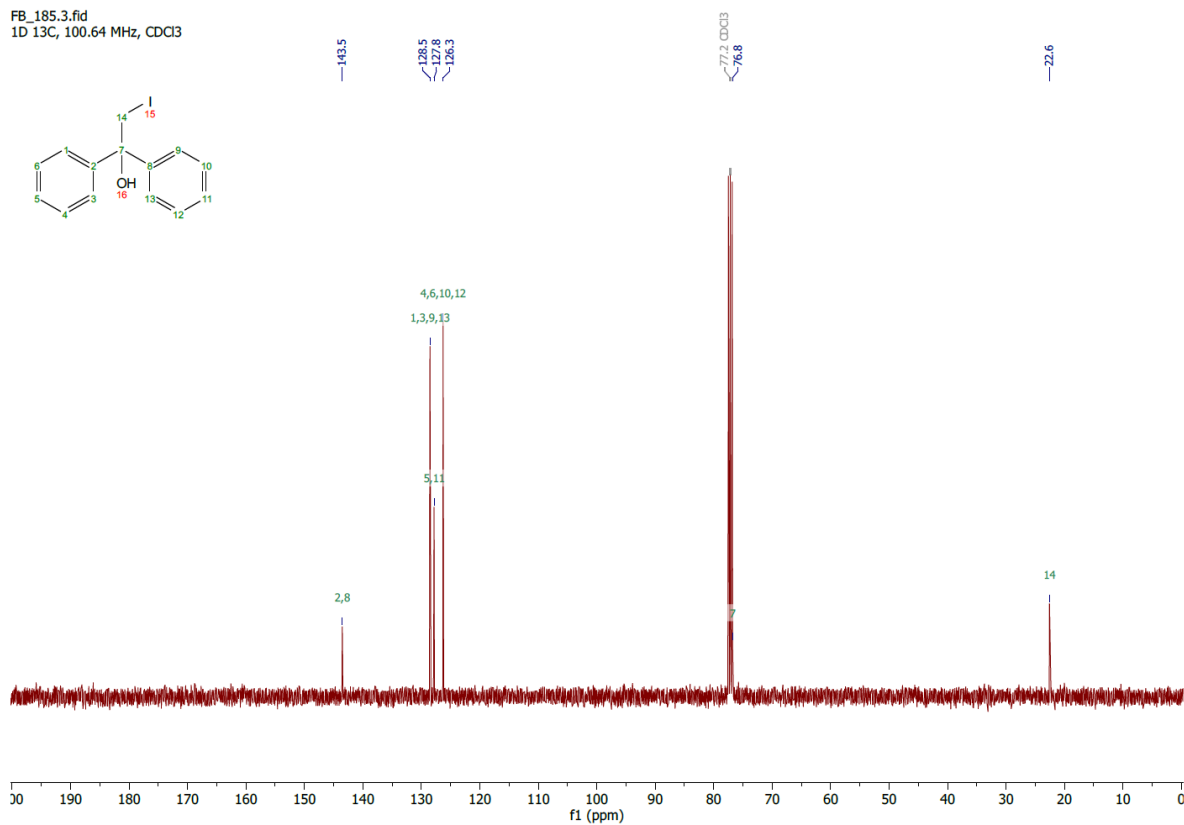


2-Iodo-1,1-diphenylethan-1-ol **83**

FB_185.1.fid
1D 1H, 400.18 MHz, CDCl3

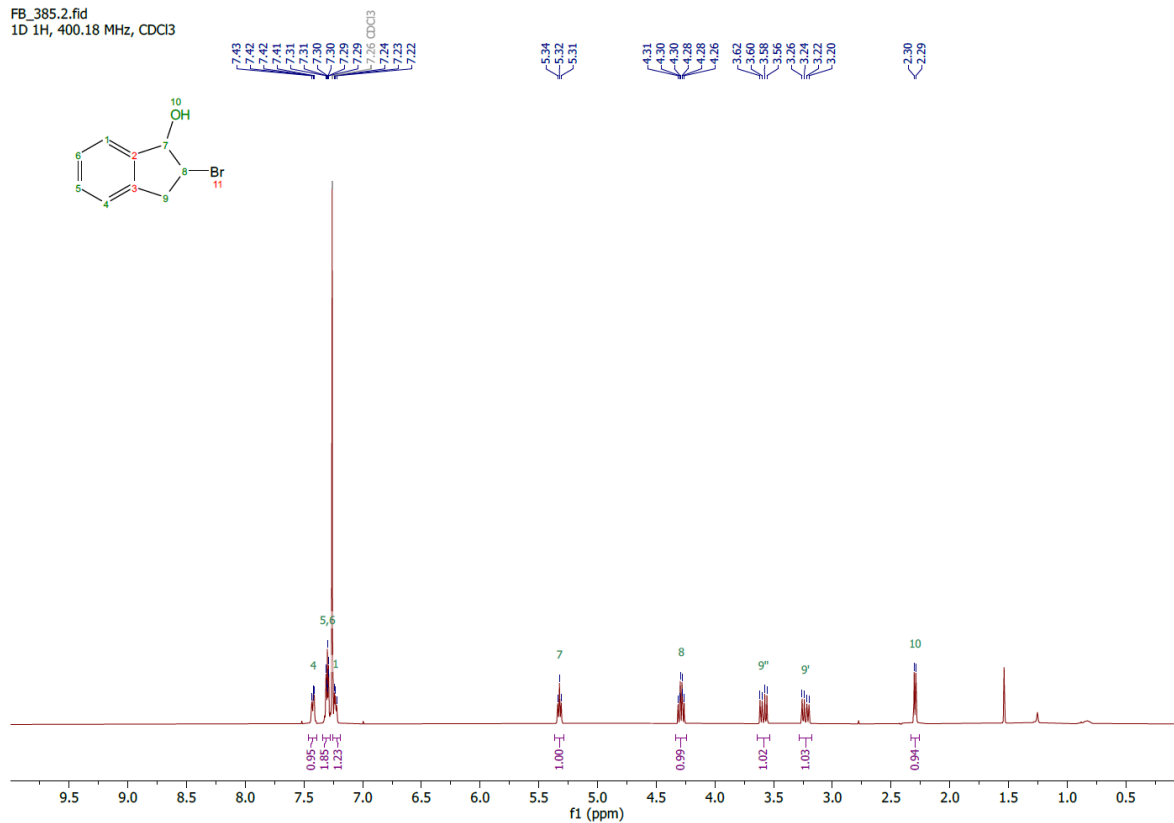


FB_185.3.fid
1D 13C, 100.64 MHz, CDCl3

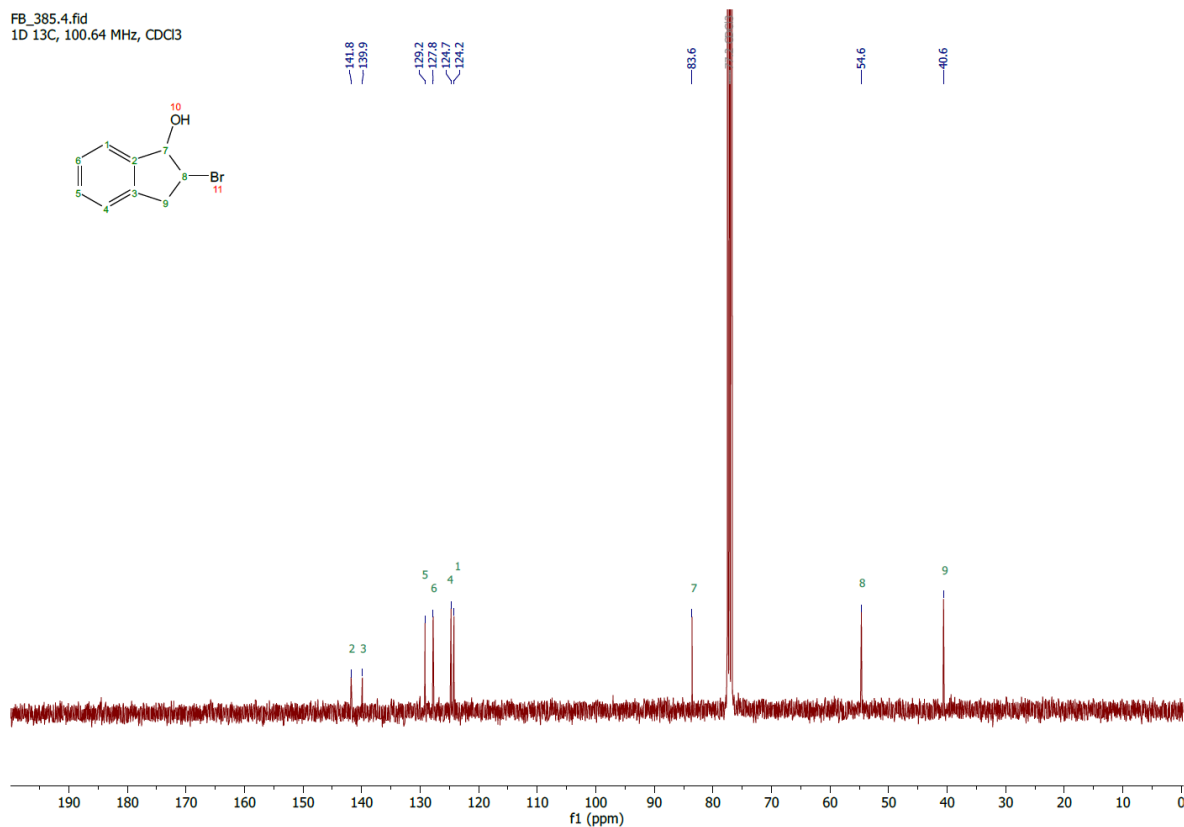


2-Bromo-2,3-dihydro-1*H*-inden-1-ol **84**

FB_385.2.fid
1D 1H, 400.18 MHz, CDCl₃



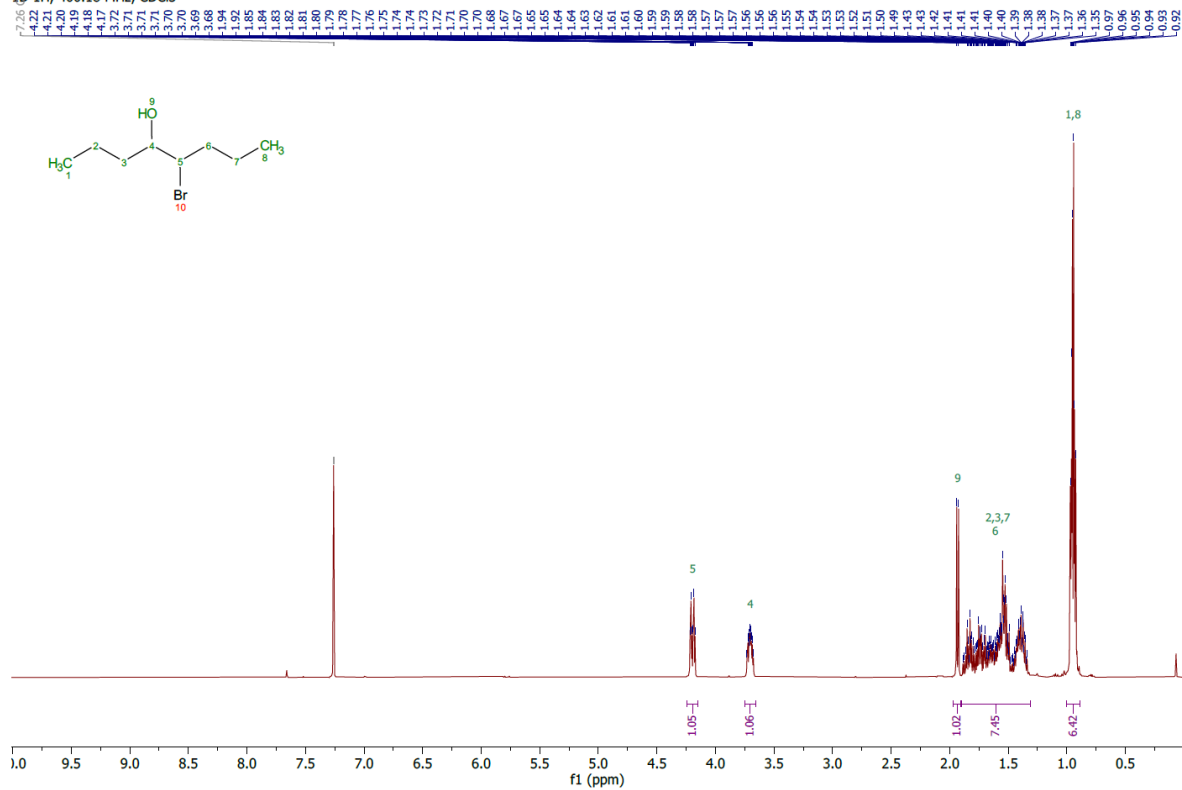
FB_385.4.fid
1D 13C, 100.64 MHz, CDCl₃



5-Bromo-octan-4-ol **85**

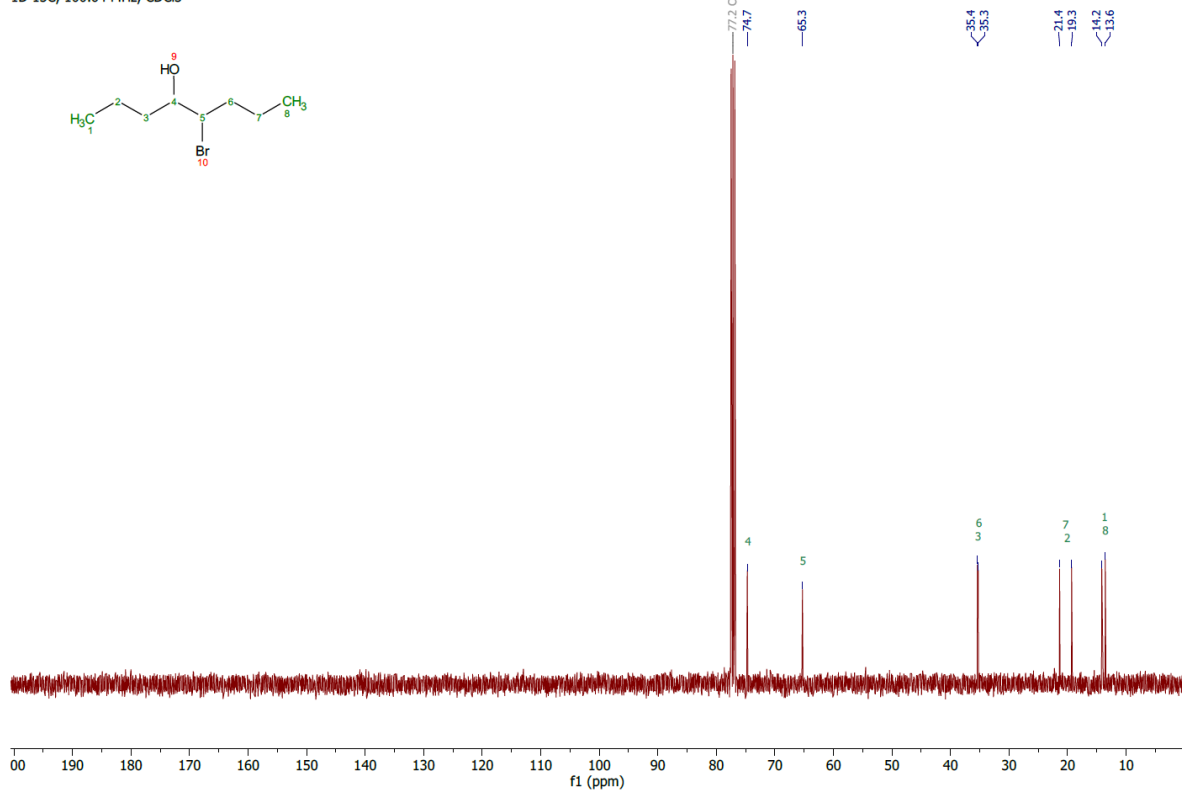
FB_386.1.fid

1D 1H, 400.18 MHz, CDCl3



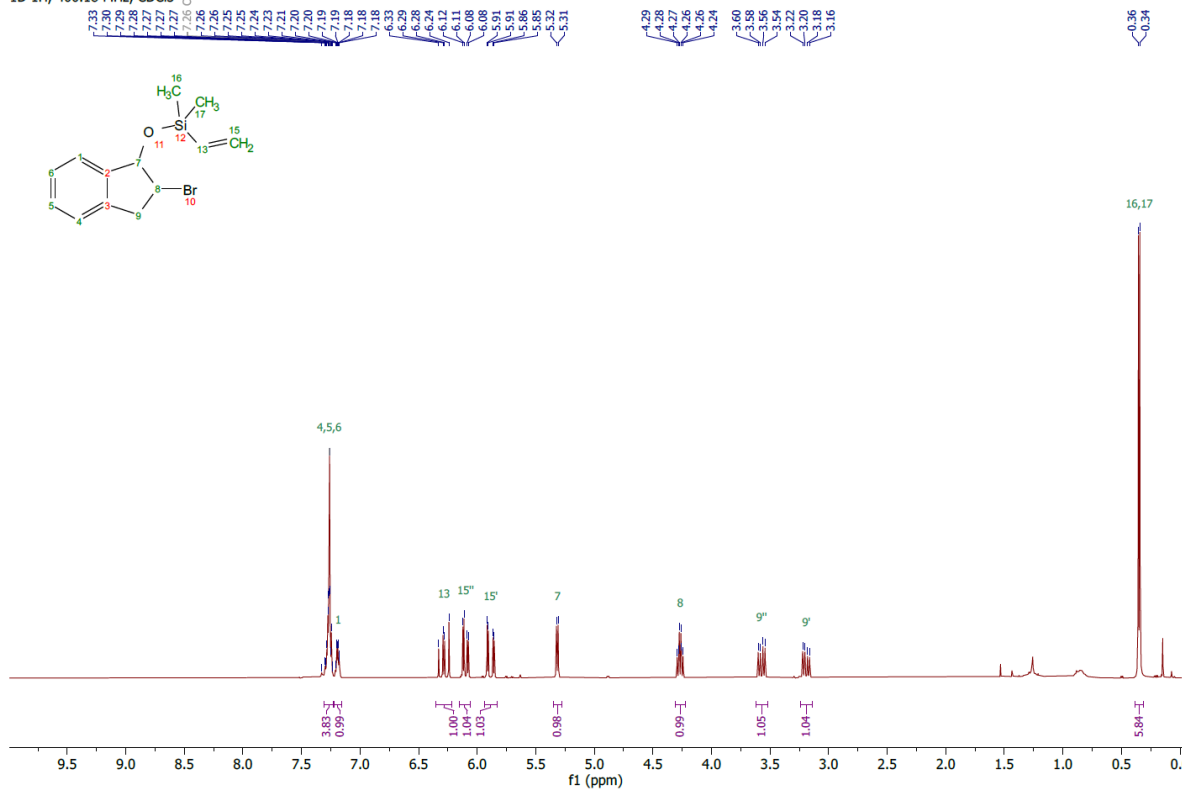
FB_386.3.fid

1D 13C, 100.64 MHz, CDCl3

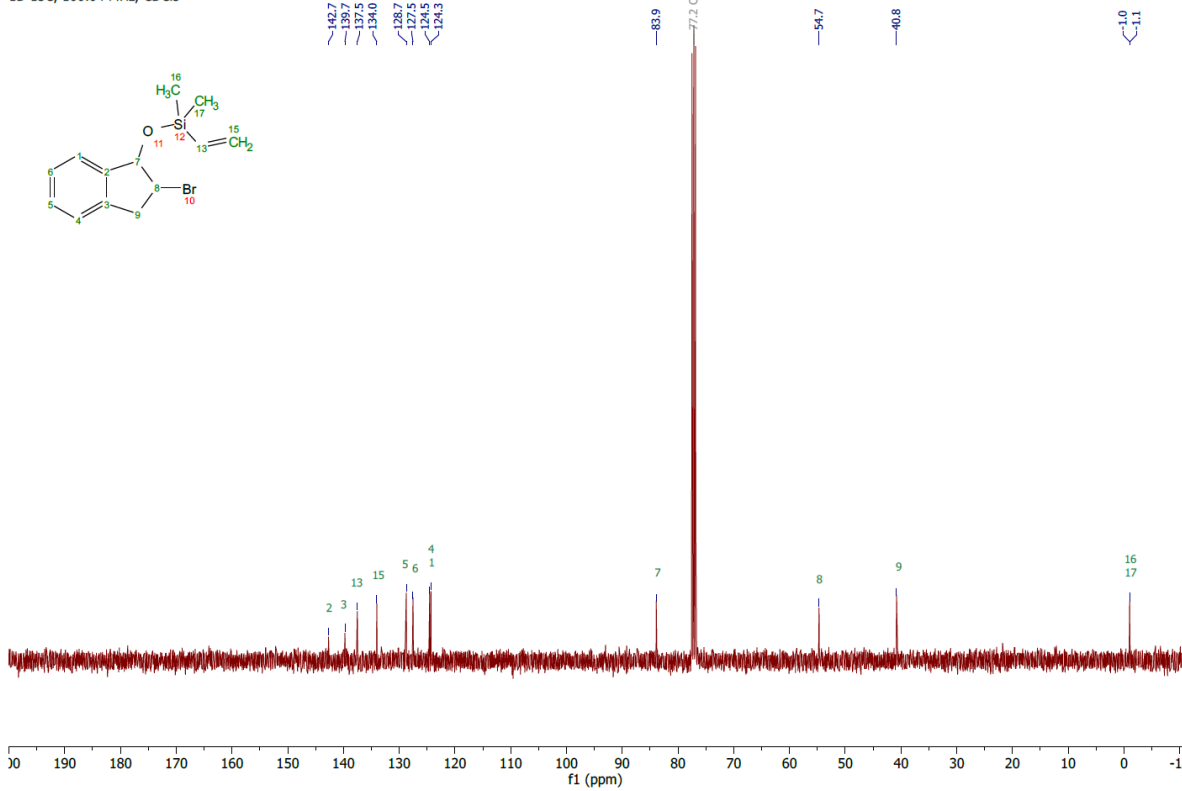


((2-Bromo-2,3-dihydro-1*H*-inden-1-yl)oxy)dimethylvinylsilane 86

FB_392_4-7.1.fid
1D 1H, 400.18 MHz, CDCl₃



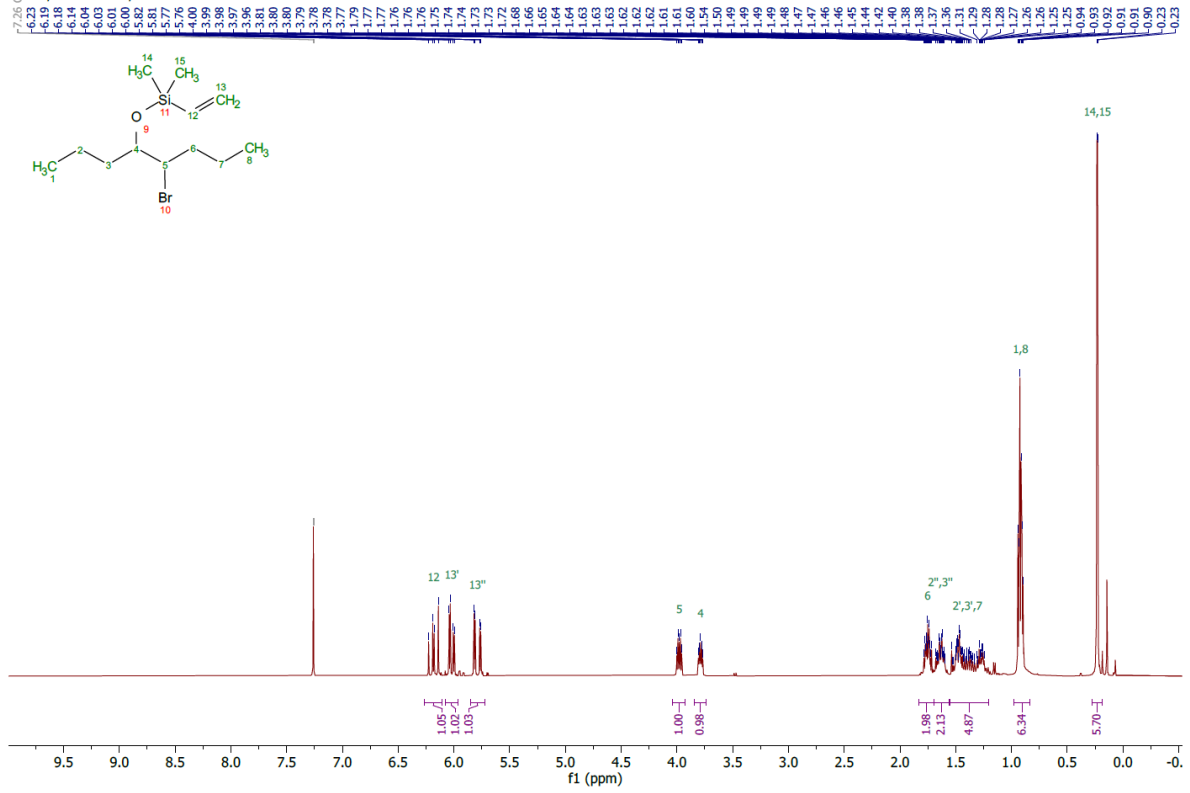
FB_392_4-7.3.fid
1D 13C, 100.64 MHz, CDCl₃



((5-Bromooctan-4-yl)oxy)dimethylvinylsilane **87**

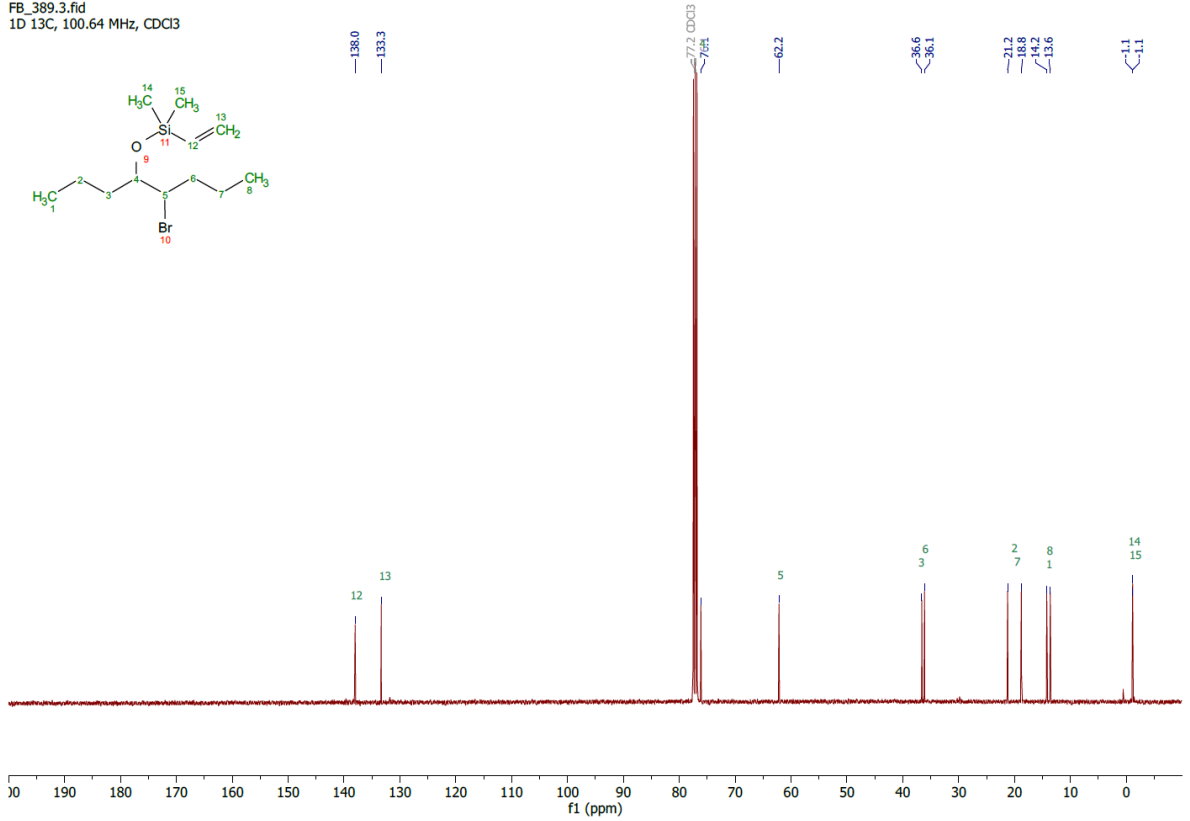
FB_389.1.fid

1D 1H, 400.18 MHz, CDCl3



FB_389.3.fid

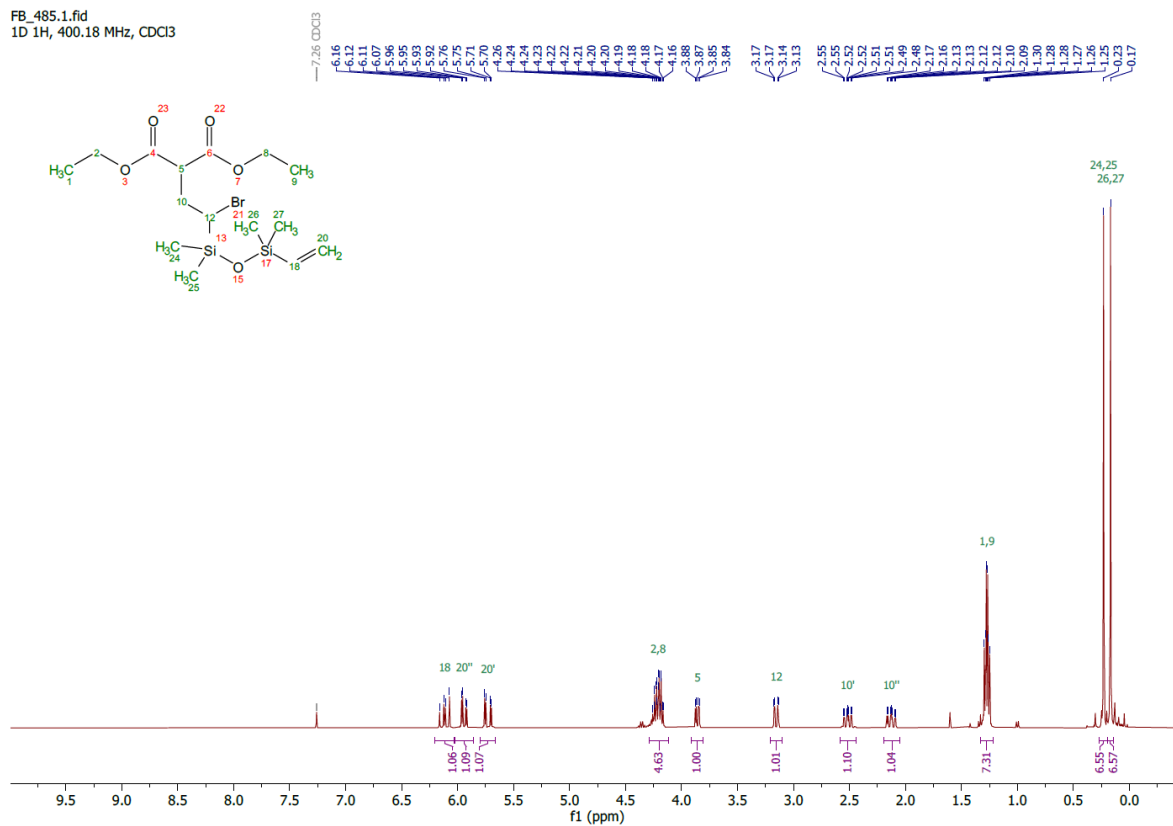
1D 13C, 100.64 MHz, CDCl3



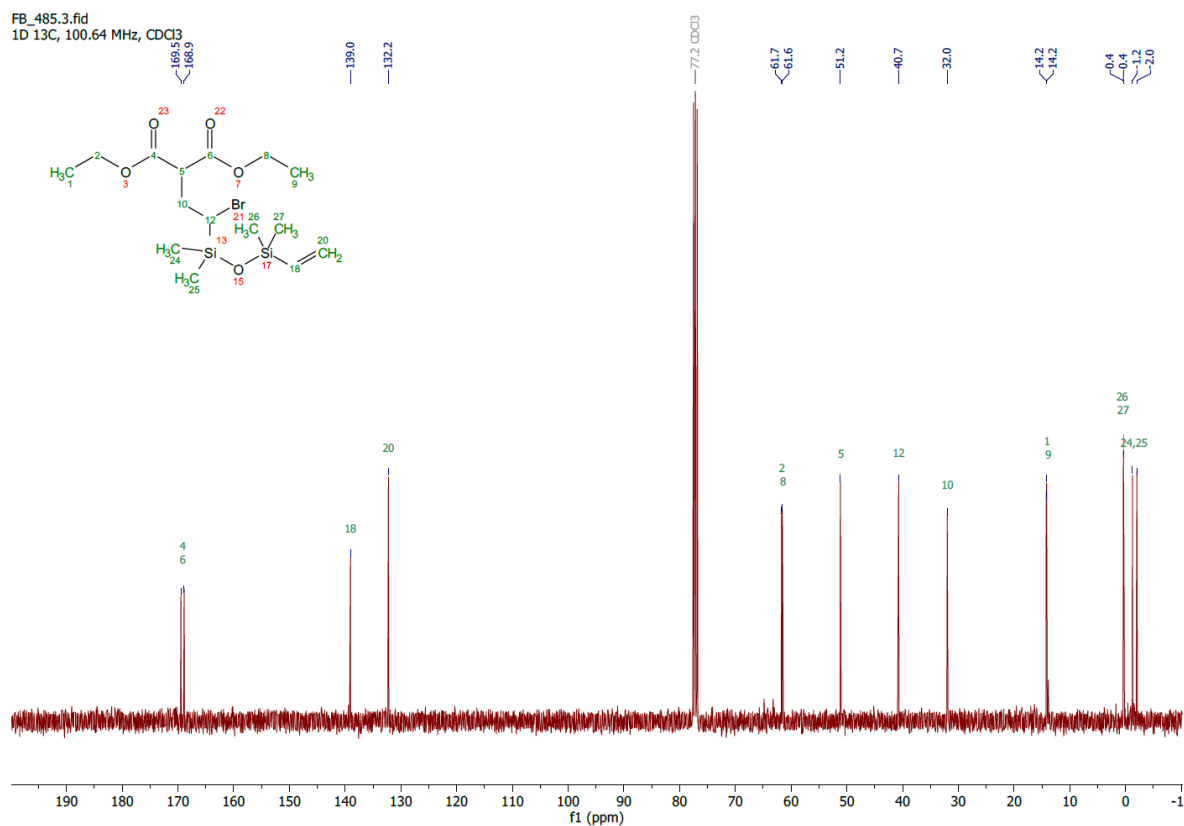
5.2.2 Compounds connected to chapter 3.2

Diethyl 2-(2-bromo-2-(1,1,3,3-tetramethyl-3-vinylidisiloxanyl)ethyl)malonate **89**

FB_485.1.fid
1D 1H, 400.18 MHz, CDCl₃

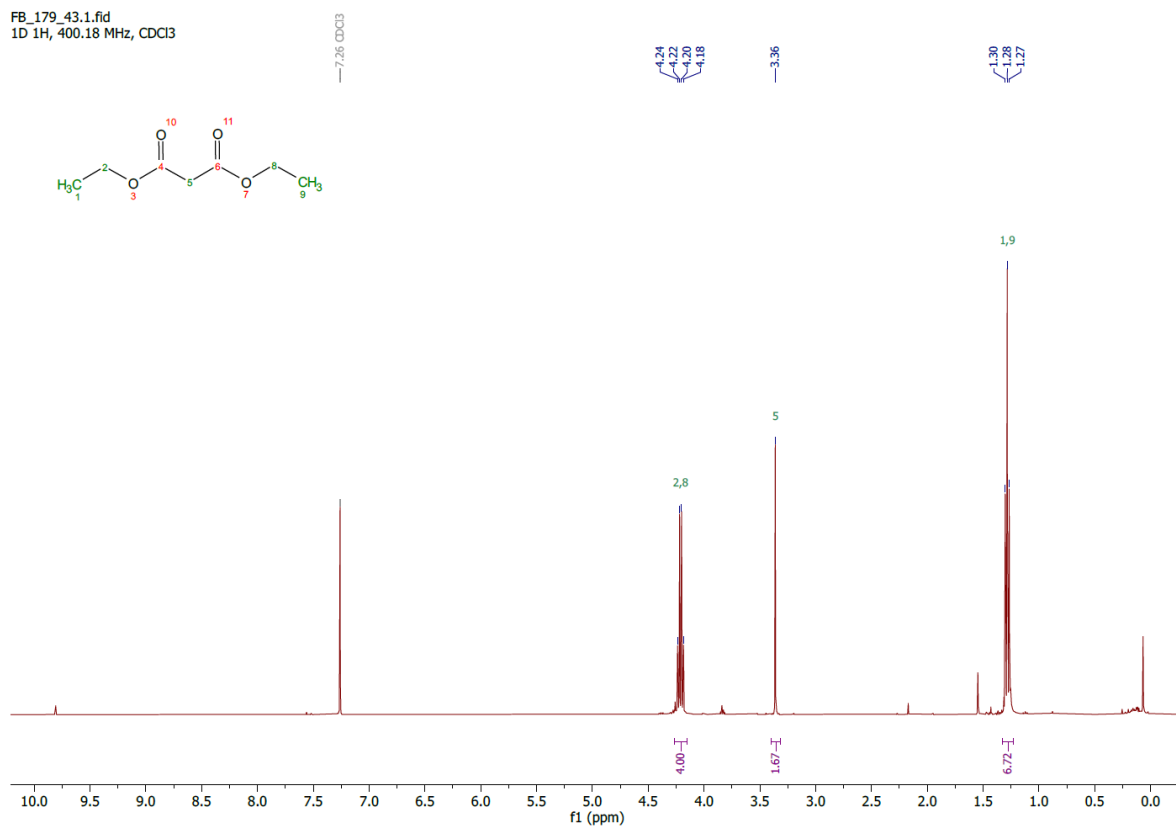


FB_485.3.fid
1D 13C, 100.64 MHz, CDCl₃

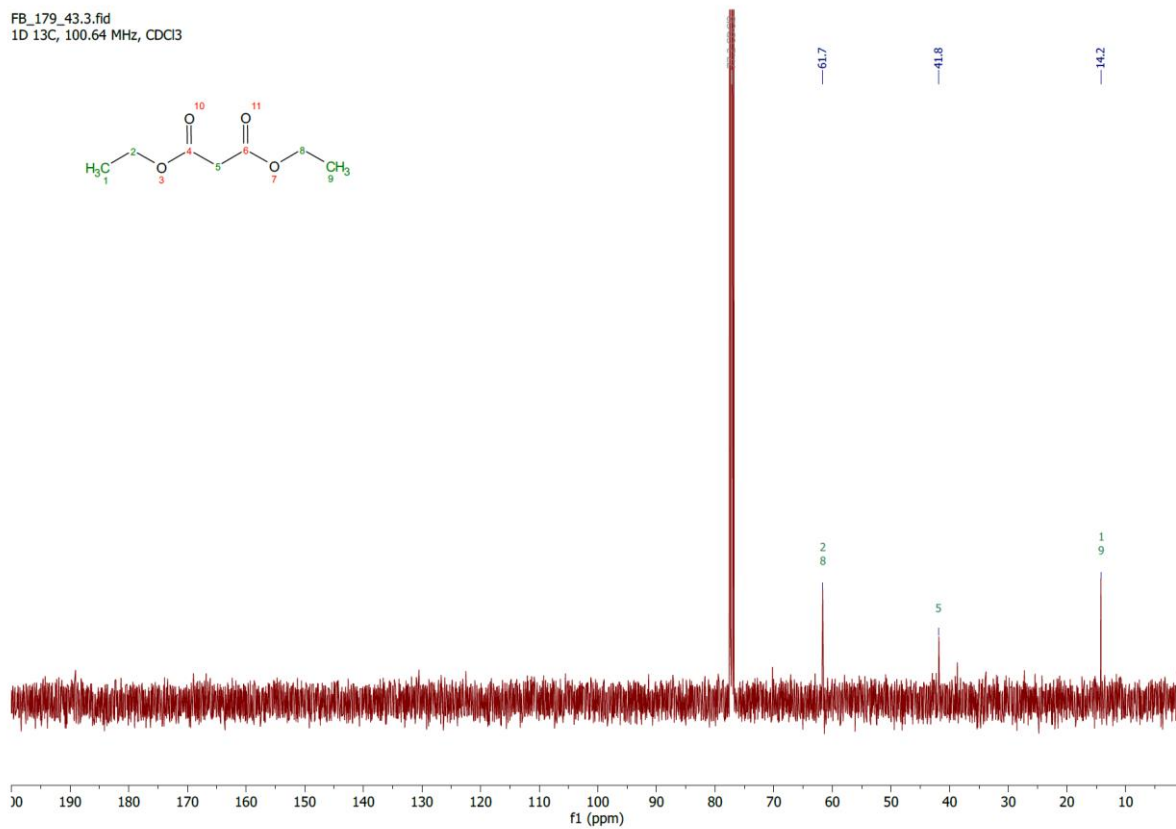


Diethyl malonate 90

FB_179_43.1.fid
1D 1H, 400.18 MHz, CDCl3

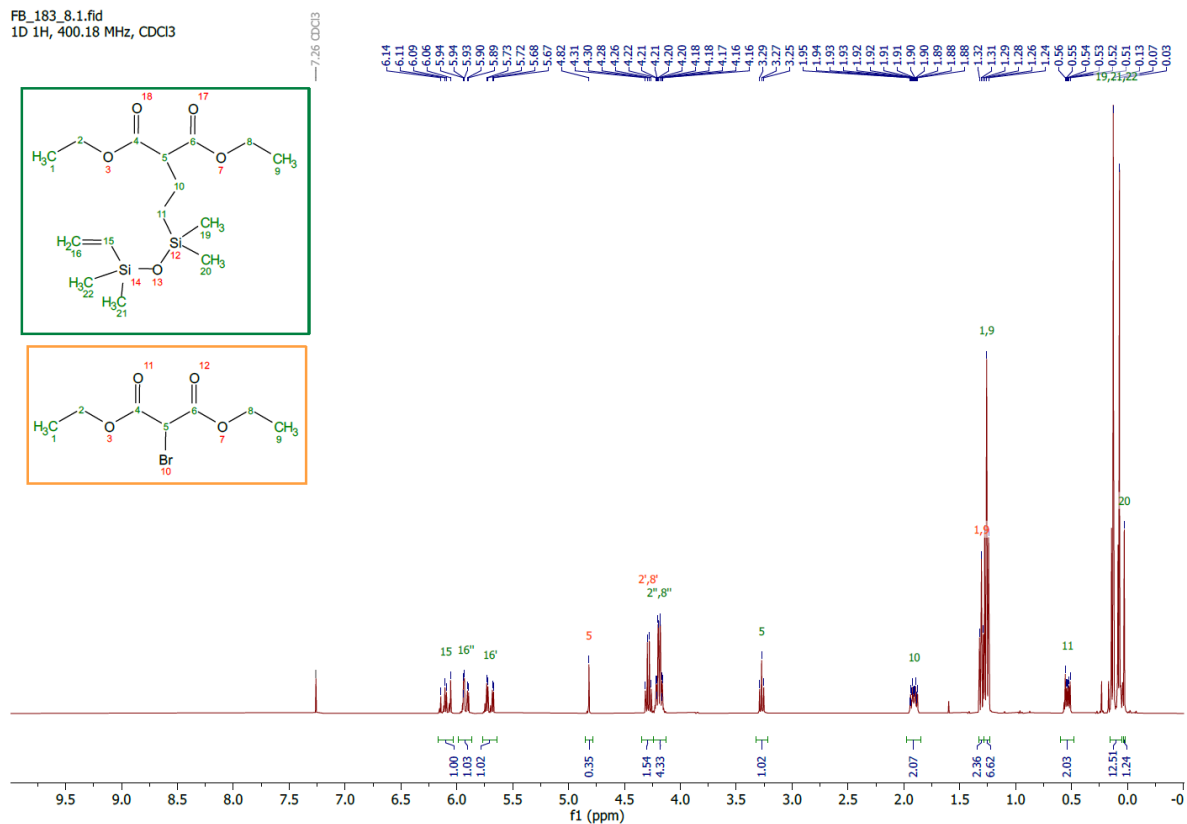


FB_179_43.3.fid
1D 13C, 100.64 MHz, CDCl3

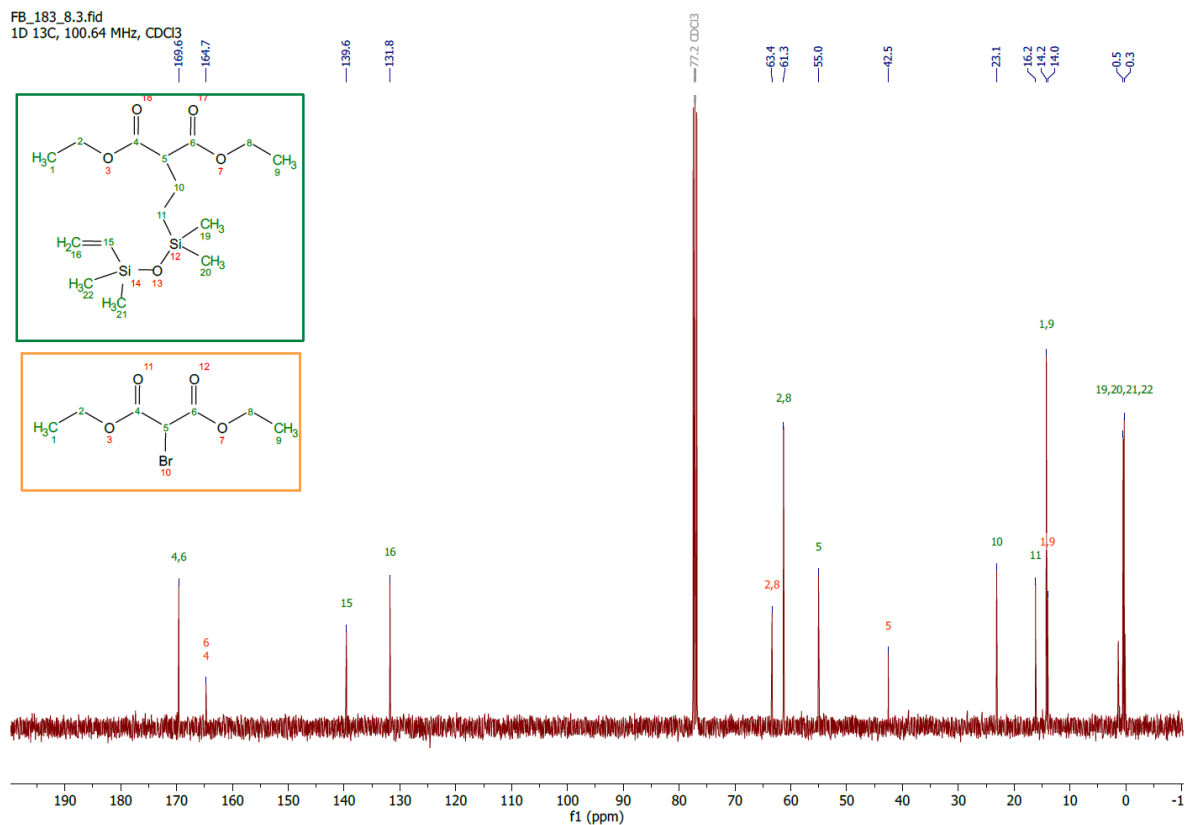


Inseparable 2:5 mixture of diethyl bromomalonate **88** and diethyl2-(2-bromo-2-(1,1,3,3-tetramethyl-3-vinyldisiloxaneyl)ethyl)malonate **96**

FB_183_8.1.fid
1D 1H, 400.18 MHz, CDCl3



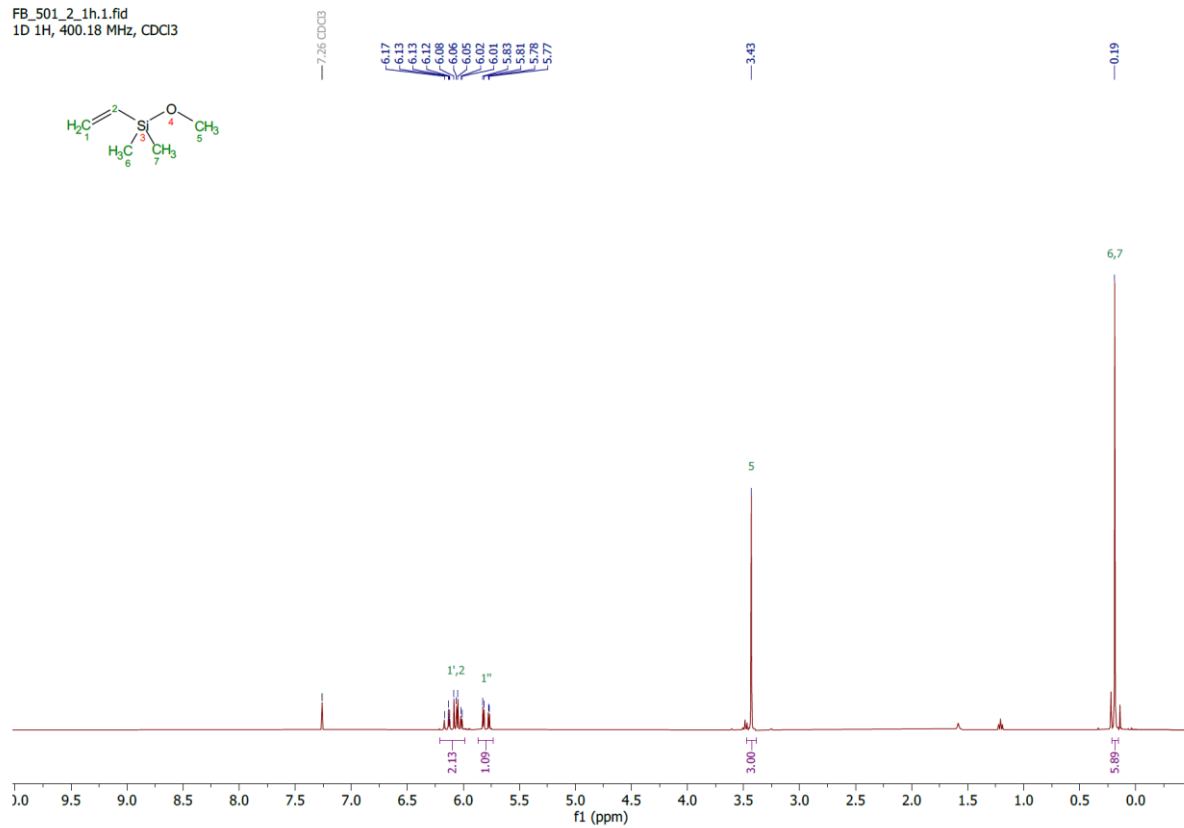
FB_183_8.3.fid
1D 13C, 100.64 MHz, CDCl3



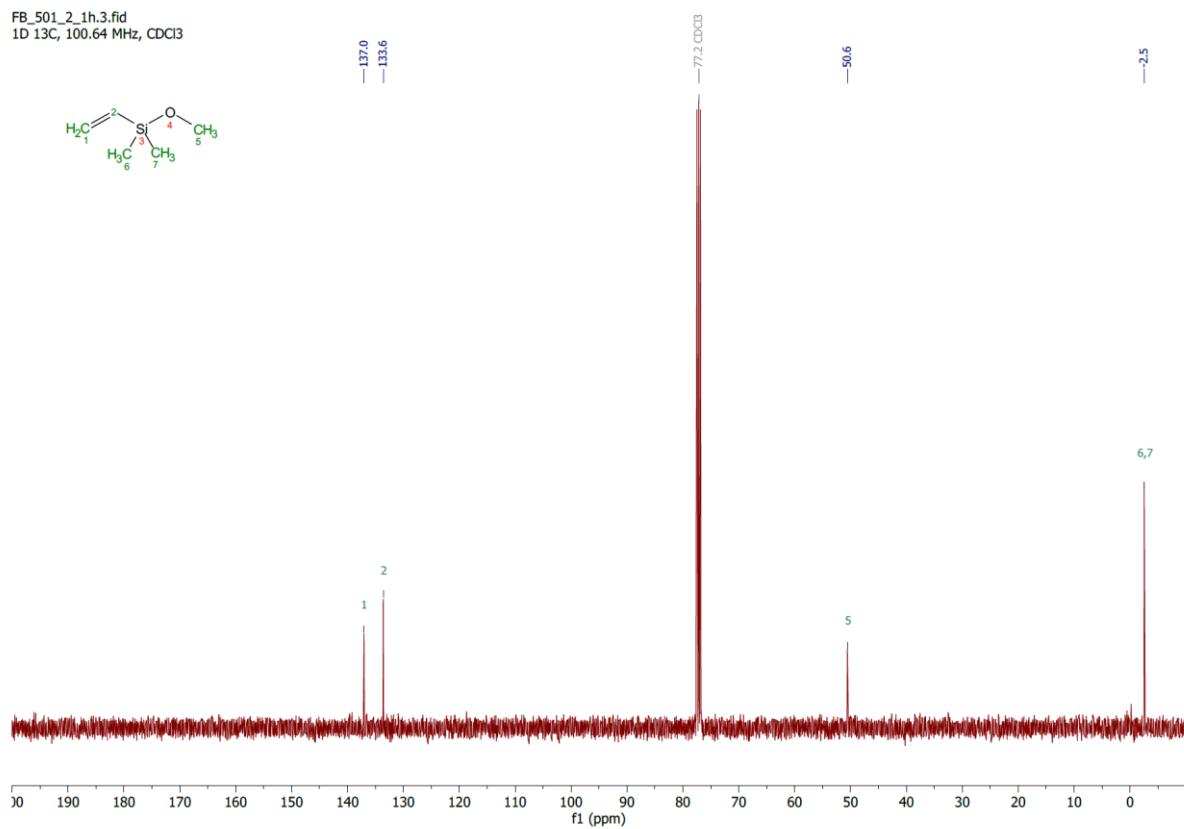
5.2.3 Compounds connected to chapter 3.3

Vinyldimethylmethoxysilane **100**

FB_501_2_1h.1.fid
1D 1H, 400.18 MHz, CDCl₃

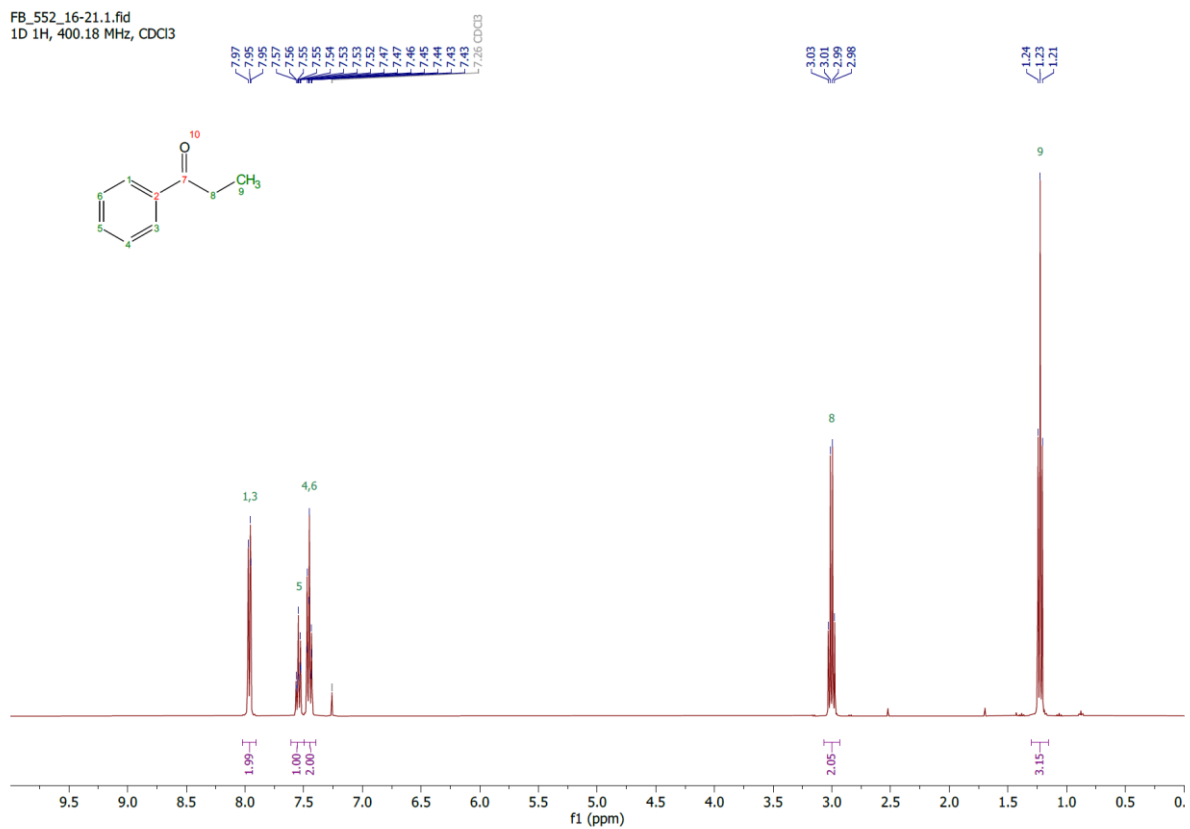


FB_501_2_1h.3.fid
1D 13C, 100.64 MHz, CDCl₃

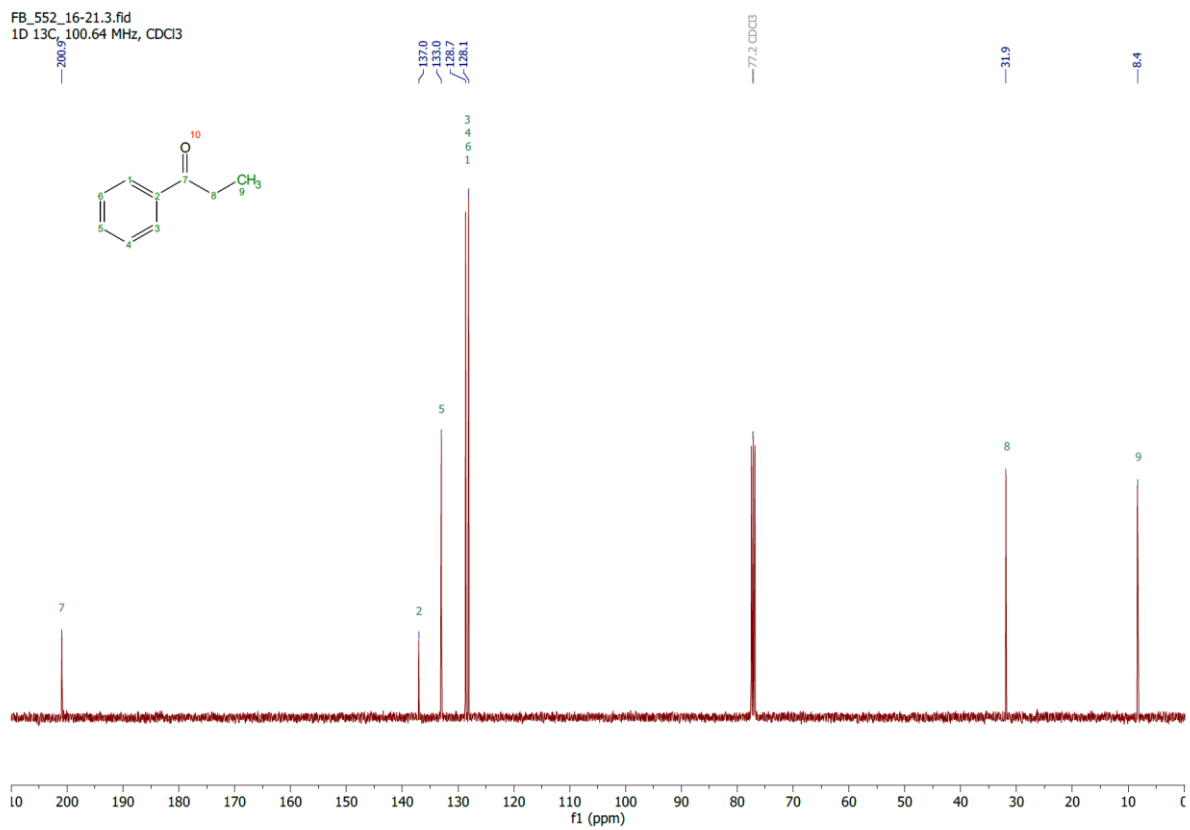


Propiophenone 101

FB_552_16-21.1.fid
1D 1H, 400.18 MHz, CDCl3

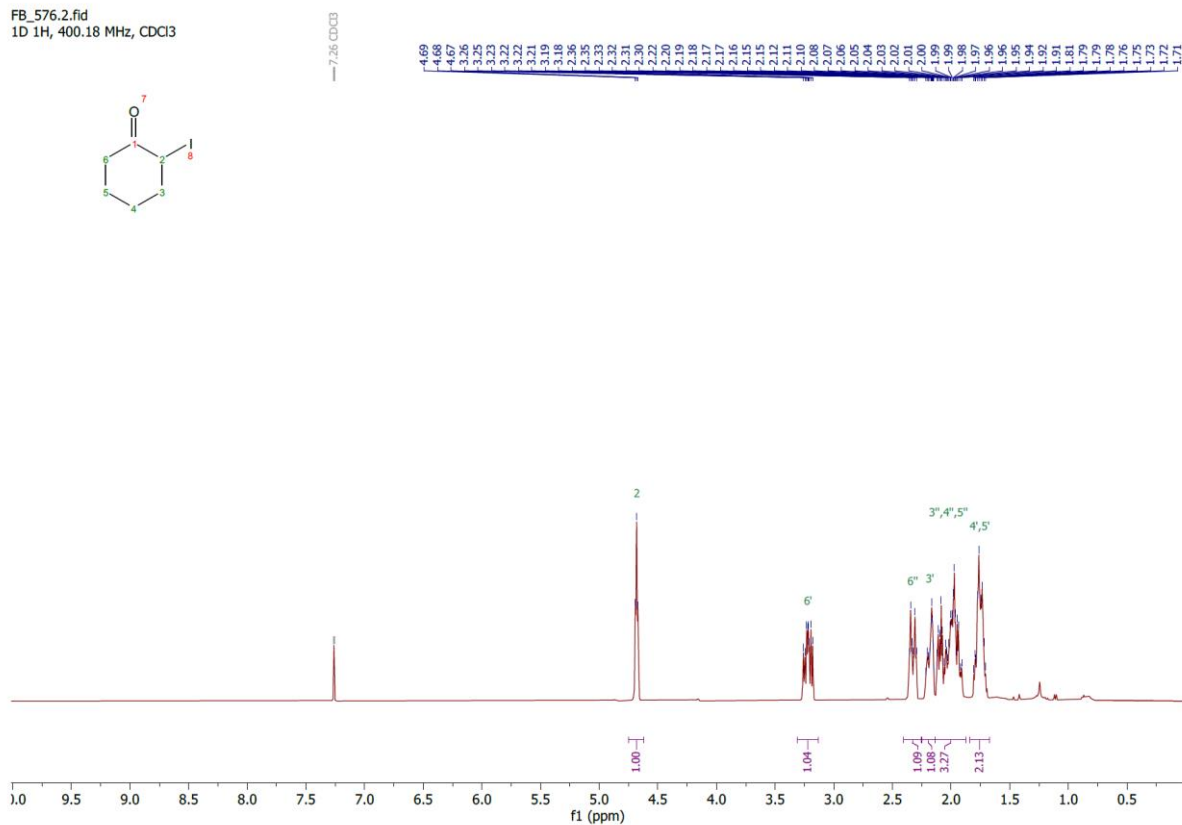
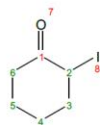


FB_552_16-21.3.fid
1D 13C, 100.64 MHz, CDCl3

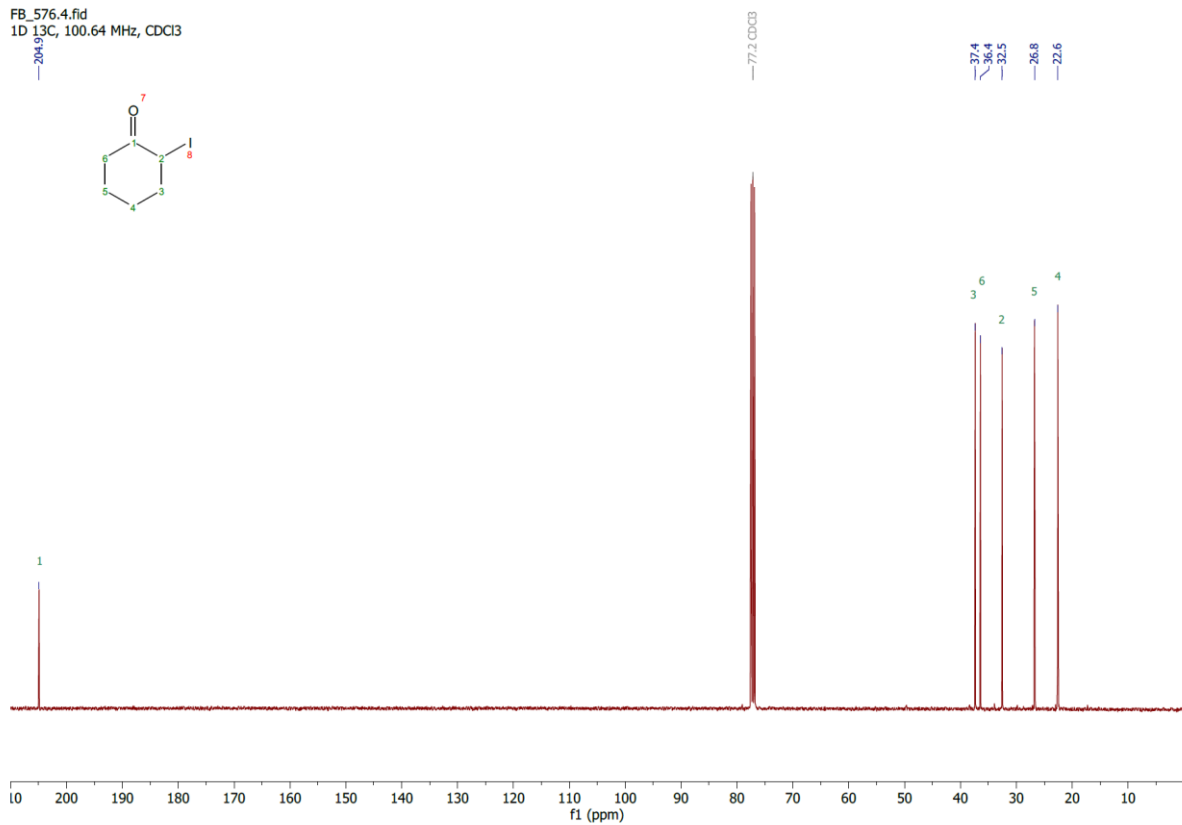
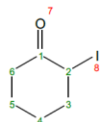


2-Iodocyclohexan-1-one **103**

FB_576.2.fid
1D 1H, 400.18 MHz, CDCl3

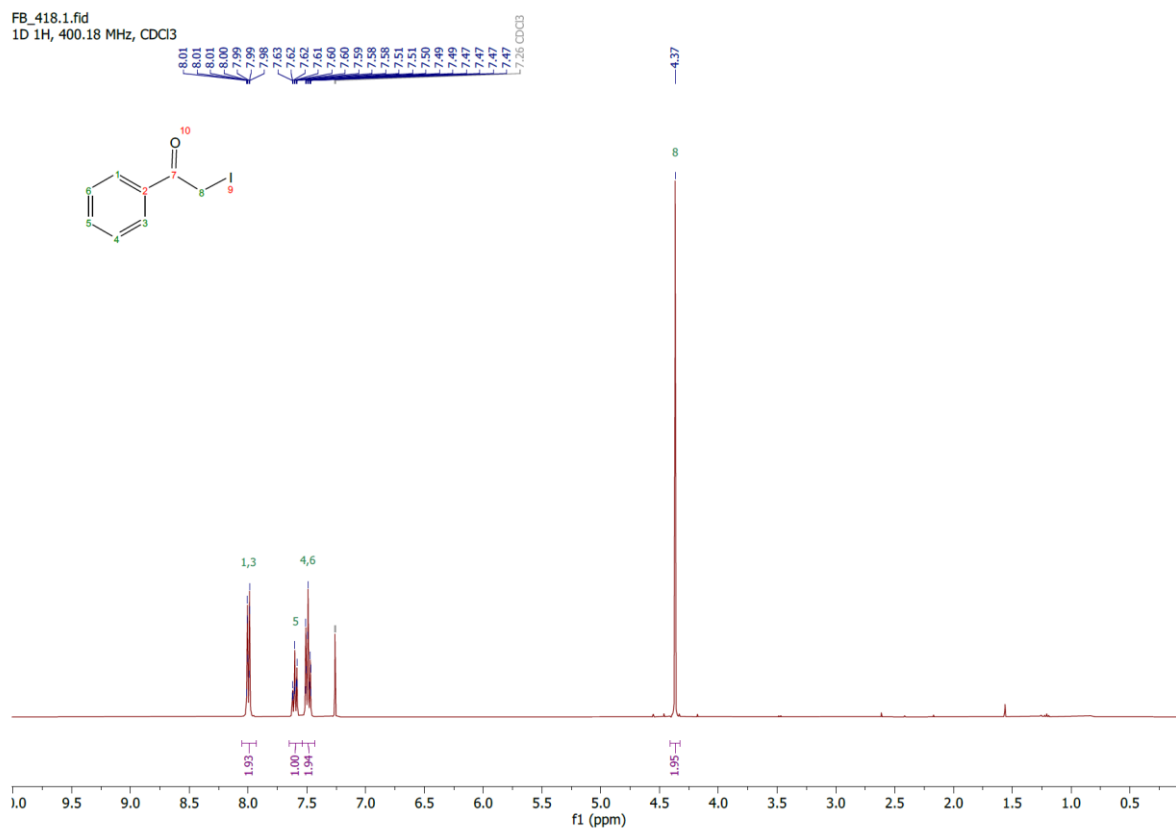


FB_576.4.fid
1D 13C, 100.64 MHz, CDCl3

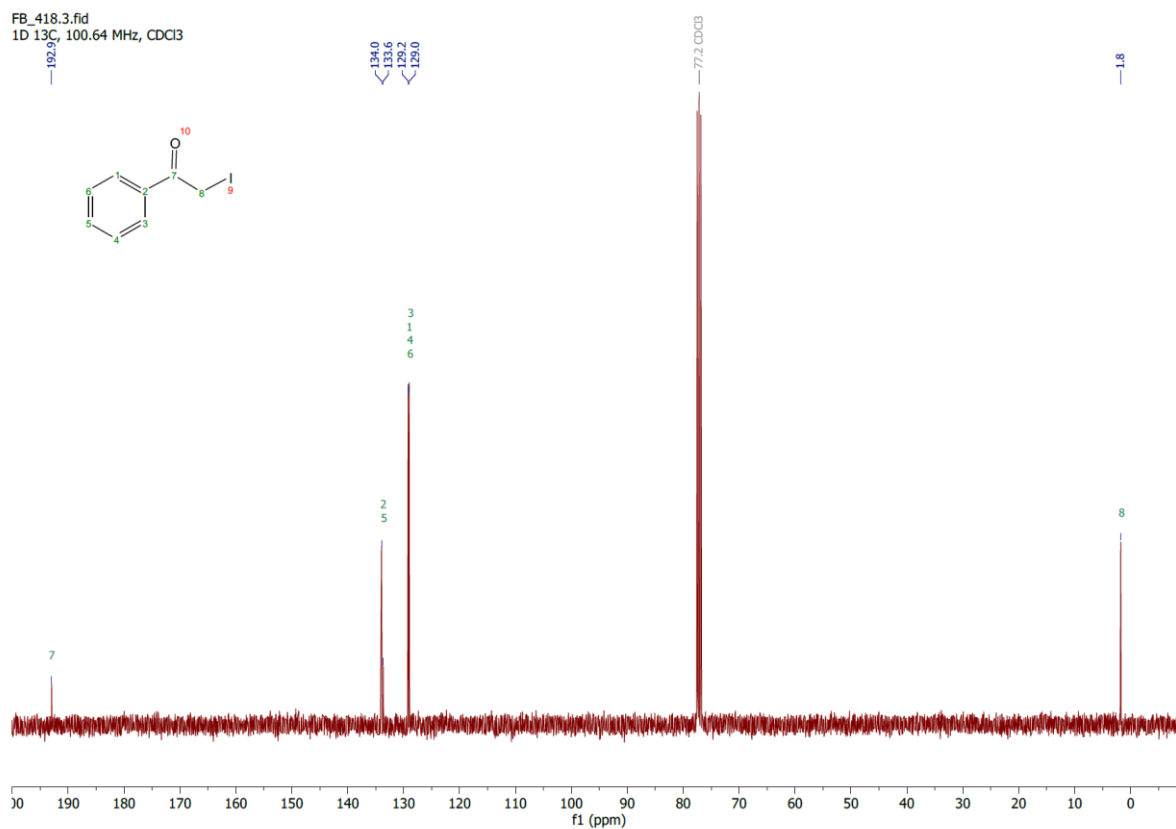


2-Iodoacetophenone 104

FB_418.1.fid
1D 1H, 400.18 MHz, CDCl3

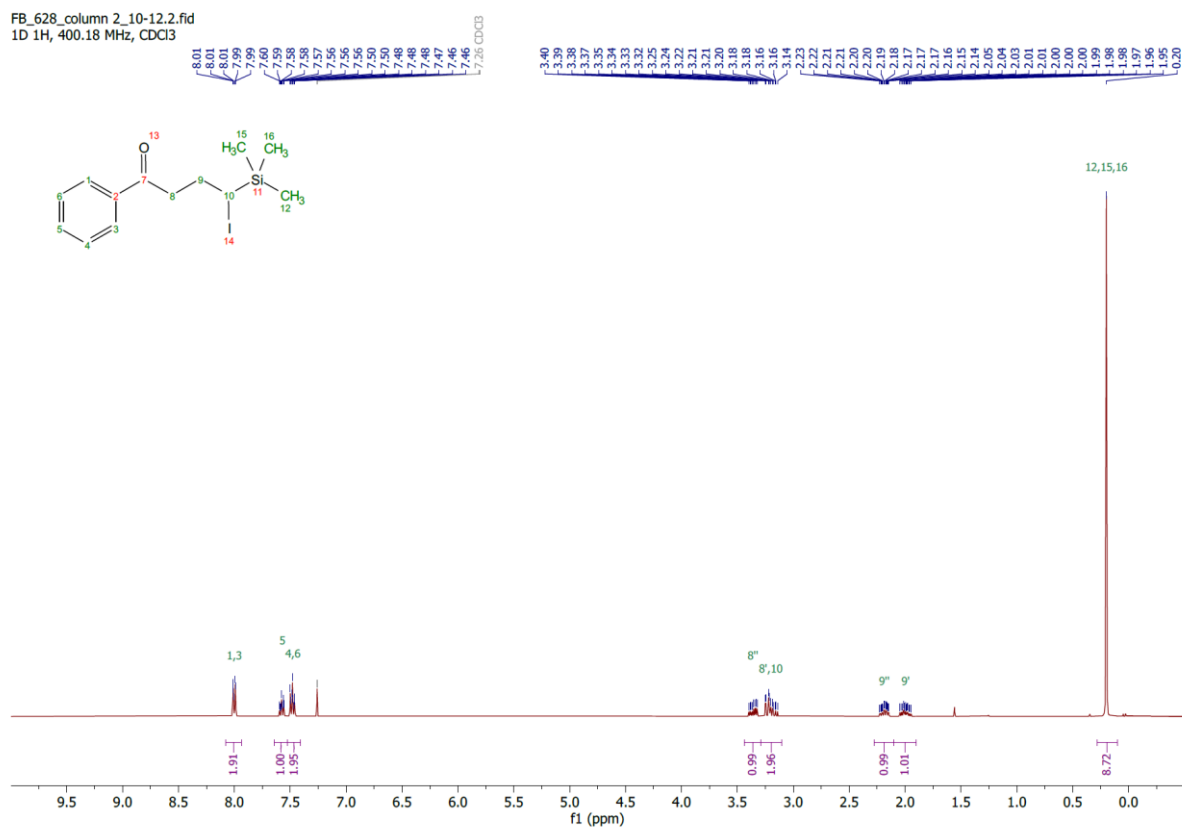


FB_418.3.fid
1D 13C, 100.64 MHz, CDCl3

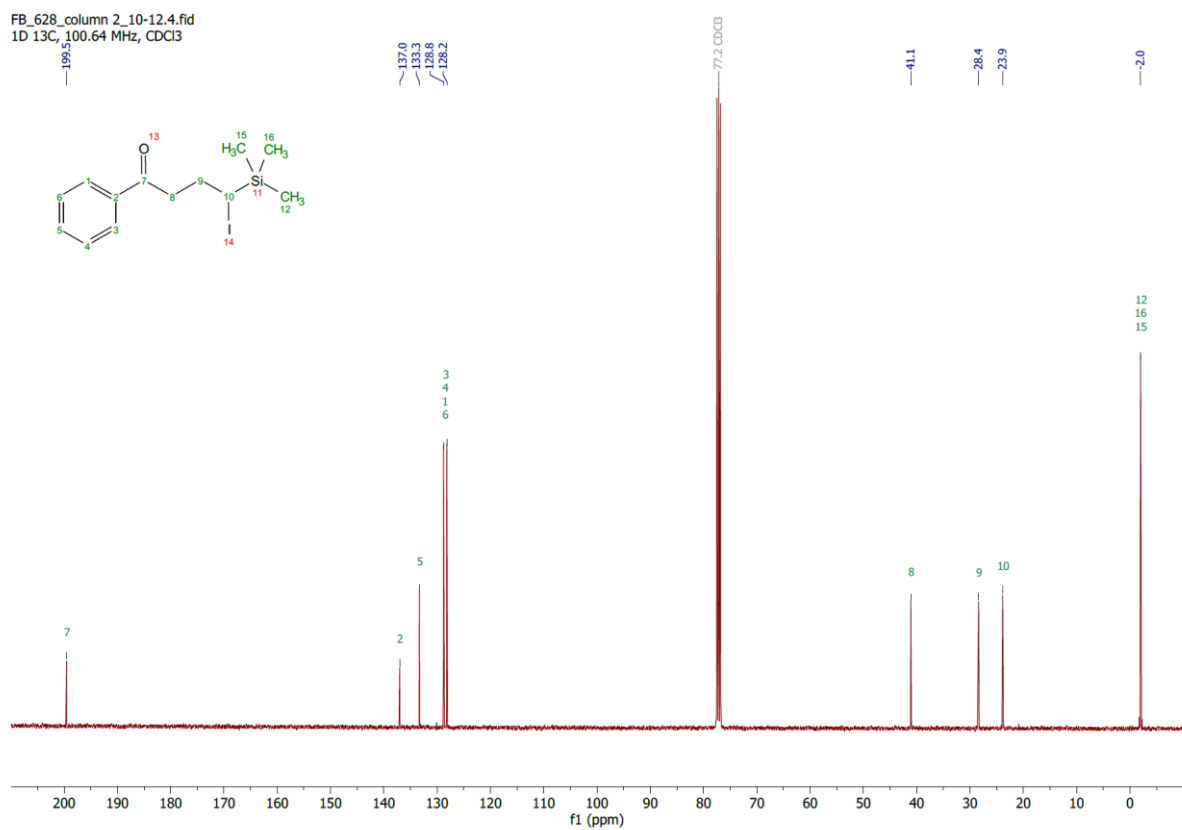


4-Iodo-1-phenyl-4-(trimethylsilyl)butan-1-one **105**

FB_628_column 2_10-12.2.fid
1D 1H, 400.18 MHz, CDCl₃

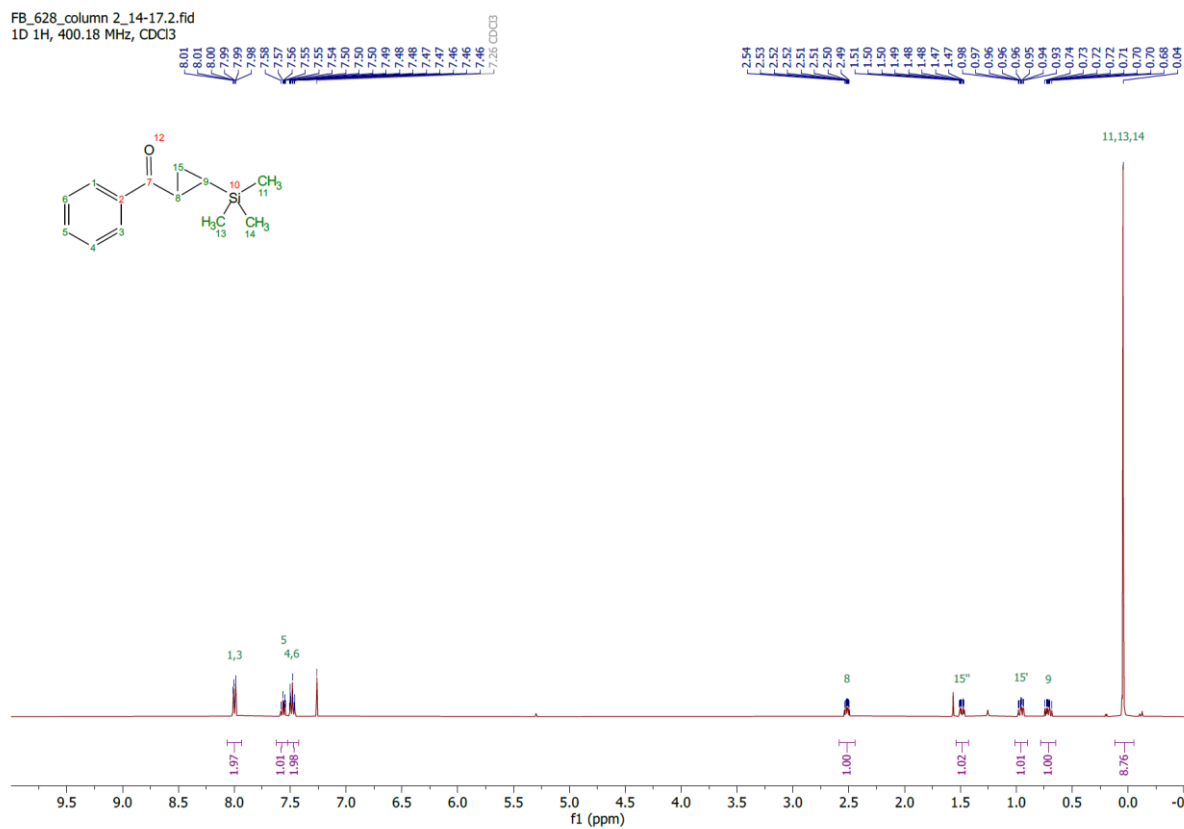


FB_628_column 2_10-12.4.fid
1D 13C, 100.64 MHz, CDCl₃

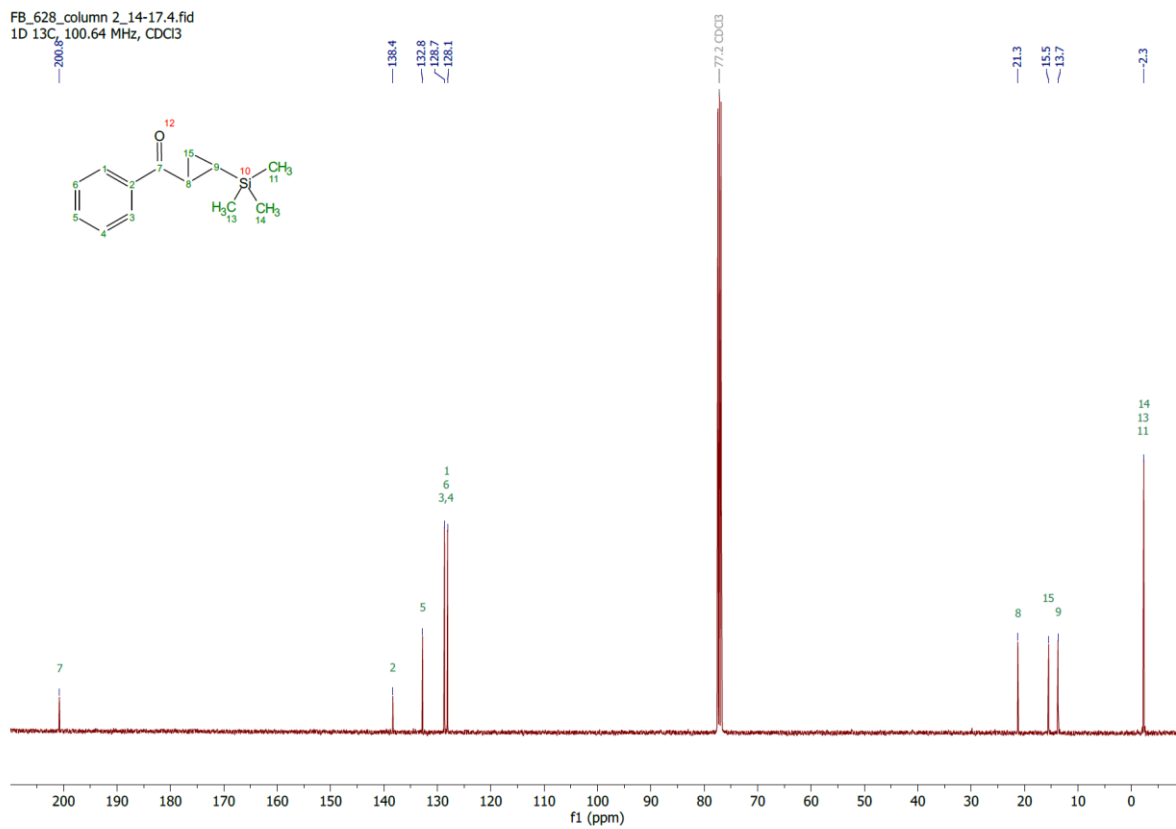


Phenyl(2-(trimethylsilyl)cyclopropyl)methanone **106**

FB_628_column 2_14-17.2.fid
1D 1H, 400.18 MHz, CDCl3



FB_628_column 2_14-17.4.fid
1D 13C, 100.64 MHz, CDCl3



6. References

1. Narayanam, J. M.; Stephenson, C. R., Visible light photoredox catalysis: applications in organic synthesis. *Chem. Soc. Rev.* **2011**, *40* (1), 102-13.
2. Tucker, J. W.; Stephenson, C. R., Shining light on photoredox catalysis: theory and synthetic applications. *J. Org. Chem.* **2012**, *77* (4), 1617-22.
3. Prier, C. K.; Rankic, D. A.; MacMillan, D. W. C., Visible Light Photoredox Catalysis with Transition Metal Complexes: Applications in Organic Synthesis. *Chem. Rev.* **2013**, *113* (7), 5322-5363.
4. Shaw, M. H.; Twilton, J.; MacMillan, D. W., Photoredox Catalysis in Organic Chemistry. *J. Org. Chem.* **2016**, *81* (16), 6898-926.
5. Romero, N. A.; Nicewicz, D. A., Organic Photoredox Catalysis. *Chem. Rev.* **2016**, *116* (17), 10075-10166.
6. Skubi, K. L.; Blum, T. R.; Yoon, T. P., Dual Catalysis Strategies in Photochemical Synthesis. *Chem. Rev.* **2016**, *116* (17), 10035-10074.
7. Twilton, J.; Le, C.; Zhang, P.; Shaw, M. H.; Evans, R. W.; MacMillan, D. W. C., The merger of transition metal and photocatalysis. *Nat. Rev. Chem.* **2017**, *1*, 0052.
8. Chen, Y.; Lu, L.-Q.; Yu, D.-G.; Zhu, C.-J.; Xiao, W.-J., Visible light-driven organic photochemical synthesis in China. *Sci. China Chem.* **2019**, *62*, 24-57.
9. Crespi, S.; Fagnoni, M., Generation of Alkyl Radicals: From the Tyranny of Tin to the Photon Democracy. *Chem. Rev.* **2020**, *120* (17), 9790-9833.
10. Yu, X. Y.; Chen, J. R.; Xiao, W. J., Visible Light-Driven Radical-Mediated C-C Bond Cleavage/Functionalization in Organic Synthesis. *Chem. Rev.* **2021**, *121* (1), 506-561.
11. Candish, L.; Dollins, K. D.; Cook, G. C.; Douglas, J. J.; Gómez-Suárez, A.; Jolit, A.; Keess, S., Photocatalysis in the Life Science Industry. *Chem. Rev.* **2022**, *122* (2), 2907-2980.
12. Chan, A. Y.; Perry, I. B.; Bissonnette, N. B.; Buksh, B. F.; Edwards, G. A.; Frye, L. I.; Garry, O. L.; Lavagnino, M. N.; Li, B. X.; Liang, Y.; Mao, E.; Millet, A.; Oakley, J. V.; Reed, N. L.; Sakai, H. A.; Seath, C. P.; MacMillan, D. W. C., Metallaphotoredox: The Merger of Photoredox and Transition Metal Catalysis. *Chem. Rev.* **2022**, *122* (2), 1485-1542.
13. Murray, P. R. D.; Cox, J. H.; Chiappini, N. D.; Roos, C. B.; McLoughlin, E. A.; Hejna, B. G.; Nguyen, S. T.; Ripberger, H. H.; Ganley, J. M.; Tsui, E.; Shin, N. Y.; Koronkiewicz, B.; Qiu, G.; Knowles, R. R., Photochemical and Electrochemical Applications of Proton-Coupled Electron Transfer in Organic Synthesis. *Chem. Rev.* **2022**, *122* (2), 2017-2291.
14. Sumida, Y.; Ohmiya, H., Direct excitation strategy for radical generation in organic synthesis. *Chem. Soc. Rev.* **2021**, *50*, 6320-6332.
15. Crisenza, G. E. M.; Mazzarella, D.; Melchiorre, P., Synthetic Methods Driven by the Photoactivity of Electron Donor-Acceptor Complexes. *J. Am. Chem. Soc.* **2020**, *142* (12), 5461-5476.
16. Saxena, B.; Patel, R. I.; Sharma, A., Recent Advances in Electron Donor-Acceptor (EDA)-Complex Reactions involving Quaternary Pyridinium Derivatives. *Adv. Synth. Catal.* **2023**, *365* (10), 1538-1564.
17. Capaldo, L.; Ravelli, D.; Fagnoni, M., Direct Photocatalyzed Hydrogen Atom Transfer (HAT) for Aliphatic C-H Bonds Elaboration. *Chem. Rev.* **2022**, *122* (2), 1875-1924.
18. Zheng, L. Y.; Cai, L. H.; Tao, K. L.; Xie, Z.; Lai, Y. L.; Guo, W., Progress in Photoinduced Radical Reactions using Electron Donor-Acceptor Complexes. *Asian J. Org. Chem.* **2021**, *10* (4), 711-748.
19. Yuan, Y.-Q.; Majumder, S.; Yang, M.-H.; Guo, S.-R., Recent advances in catalyst-free photochemical reactions via electron-donor-acceptor (EDA) complex process. *Tetrahedron Lett.* **2020**, *61* (8), 151506.
20. Lang, Y.; Li, C.-J.; Zeng, H., Photo-induced transition-metal and external photosensitizer-free organic reactions. *Org. Chem. Front.* **2021**, *8*, 3594-3613.
21. Piedra, H. F.; Valdes, C.; Plaza, M., Shining light on halogen-bonding complexes: a catalyst-free activation mode of carbon-halogen bonds for the generation of carbon-centered radicals. *Chem. Sci.* **2023**, *14* (21), 5545-5568.

22. Hoffmann, N., Photochemical Reactions as Key Steps in Organic Synthesis. *Chem. Rev.* **2008**, *108* (3), 1052-1103.
23. *Encyclopedia of Radicals in Chemistry, Biology and Materials*. John Wiley & Sons, Ltd.: Chichester, UK, 2012.
24. *Radicals in Organic Synthesis*. Wiley-VCH Verlag GmbH: 2001.
25. McCarroll, A. J.; Walton, J. C., Programming organic molecules: Design and management of organic syntheses through free-radical cascade processes. *Angew. Chem., Int. Ed. Engl.* **2001**, *40* (12), 2225-2248.
26. Yan, M.; Lo, J. C.; Edwards, J. T.; Baran, P. S., Radicals: Reactive Intermediates with Translational Potential. *J. Am. Chem. Soc.* **2016**, *138* (39), 12692-12714.
27. Walling, C., Some properties of radical reactions important in synthesis. *Tetrahedron* **1985**, *41* (19), 3887-3900.
28. Ingold, K. U., Kinetic and mechanistic studies of free radical reactions in the 21st century. *Pure Appl. Chem.* **1997**, *69* (2), 241-243.
29. Curran, D. P.; Porter, N. A.; Giese, B., *Stereochemistry of Radical Reactions: Concepts, Guidelines, and Synthetic Applications*. VCH: Weinheim, 1996.
30. Parsaee, F.; Senarathna, M. C.; Kannangara, P. B.; Alexander, S. N.; Arche, P. D. E.; Welin, E. R., Radical philicity and its role in selective organic transformations. *Nat. Rev. Chem.* **2021**, *5*, 486-499.
31. Studer, A.; Curran, D. P., Catalysis of Radical Reactions: A Radical Chemistry Perspective. *Angew. Chem., Int. Ed. Engl.* **2015**, *55* (1), 58-102.
32. Douglas, J. J.; Sevrin, M. J.; Stephenson, C. R. J., Visible Light Photocatalysis: Applications and New Disconnections in the Synthesis of Pharmaceutical Agents. *Org. Process Res. Dev.* **2016**, *20* (7), 1134-1147.
33. Nicholls, T. P.; Leonori, D.; Bissember, A. C., Applications of visible light photoredox catalysis to the synthesis of natural products and related compounds. *Nat. Prod. Rep.* **2016**, *33*, 1248-1254.
34. Zard, S. Z., *Radical Reactions in Organic Synthesis*. Oxford University Press: 2003.
35. Beniazza, R.; Liautard, V.; Poittevin, C.; Ovadia, B.; Mohammed, S.; Robert, F.; Landais, Y., Free-Radical Carbo-Alkenylation of Olefins: Scope, Limitations and Mechanistic Insights. *Chem. Eur. J.* **2017**, *23* (10), 2439-2447.
36. Fischer, H.; Radom, L., Factors Controlling the Addition of Carbon-Centered Radicals to Alkenes - An Experimental and Theoretical Perspective. *Angew. Chem., Int. Ed. Engl.* **2001**, *40* (8), 1340-1371.
37. Giese, B., Formation of CC Bonds by Addition of Free-Radicals to Alkenes. *Angew. Chem., Int. Ed. Engl.* **1983**, *22* (10), 753-764.
38. Proctor, R. S. J.; Phipps, R. J., Recent Advances in Minisci-Type Reactions. *Angew. Chem., Int. Ed. Engl.* **2019**, *58* (39), 13666-13699.
39. Kanegusuku, A. L. G.; Roizen, J. L., Recent Advances in Photoredox-Mediated Radical Conjugate Addition Reactions: An Expanding Toolkit for the Giese Reaction. *Angew. Chem., Int. Ed. Engl.* **2021**, *60* (39), 21116-21149.
40. Tedder, J. M., Which Factors Determine the Reactivity and Regioselectivity of Free-Radical Substitution and Addition-Reactions. *Angew. Chem., Int. Ed. Engl.* **1982**, *21* (6), 401-410.
41. Julia, F.; Constantin, T.; Leonori, D., Applications of Halogen-Atom Transfer (XAT) for the Generation of Carbon Radicals in Synthetic Photochemistry and Photocatalysis. *Chem. Rev.* **2022**, *122* (2), 2292-2352.
42. Bonfield, H. E.; Knauber, T.; Lévesque, F.; Moschetta, E. G.; Susanne, F.; Edwards, L. J., Photons as a 21st century reagent. *Nat. Commun.* **2020**, *11*, 804.
43. Marzo, L.; Pagire, S. K.; Reiser, O.; König, B., Visible-Light Photocatalysis: Does It Make a Difference in Organic Synthesis? *Angew. Chem., Int. Ed. Engl.* **2018**, *57* (32), 10034-10072.
44. Sheldon, R. A., Metrics of Green Chemistry and Sustainability: Past, Present, and Future. *ACS Sustain. Chem. Eng.* **2018**, *6* (1), 32-48.
45. Crisenza, G. E. M.; Melchiorre, P., Chemistry glows green with photoredox catalysis. *Nat. Commun.* **2020**, *11*, 803.
46. Vega-Penalosa, A.; Mateos, J.; Companyo, X.; Escudero-Casao, M.; Dell'Amico, L., A Rational Approach to Organo-Photocatalysis: Novel Designs and Structure-Property Relationships. *Angew. Chem., Int. Ed. Engl.* **2021**, *60* (3), 1082-1097.

47. Motz, R. N.; Sun, A. C.; Lehnerr, D.; Ruccolo, S., High-Throughput Determination of Stern-Volmer Quenching Constants for Common Photocatalysts and Quenchers. *ACS Org. Inorg. Au* **2023**, *3* (5), 266-273.
48. Wu, Y. Y.; Kim, D.; Teets, T. S., Photophysical Properties and Redox Potentials of Photosensitizers for Organic Photoredox Transformations. *Synlett* **2021**, *33* (12), 1154-1179.
49. Nicholas, A. M. d. P.; Arnold, D. R., Thermochemical Parameters for Organic Radicals and Radical Ions. Part 1. The Estimation of the pKa of Radical Cations Based on Thermochemical Calculations. *Can. J. Chem.* **1982**, *60*, 2165-2179.
50. Nelsen, S. F.; Ippoliti, J. T., On the Deprotonation of Trialkylamine Cation Radicals by Amines. *J. Am. Chem. Soc.* **1986**, *108*, 4879-4881.
51. Dinnocenzo, J. P.; Banach, T. E., Deprotonation of Tertiary Amine Cation Radicals. A Direct Experimental Approach. *J. Am. Chem. Soc.* **1989**, *111*, 8646-8653.
52. Condie, A. G.; Gonzalez-Gomez, J. C.; Stephenson, C. R., Visible-light photoredox catalysis: aza-Henry reactions via C-H functionalization. *J. Am. Chem. Soc.* **2010**, *132* (5), 1464-1465.
53. Speckmeier, E.; Fuchs, P. J. W.; Zeitler, K., A synergistic LUMO lowering strategy using Lewis acid catalysis in water to enable photoredox catalytic, functionalizing C-C cross-coupling of styrenes. *Chem. Sci.* **2018**, *9* (35), 7096-7103.
54. Howes, K. R.; Bakac, A.; Espenson, J. H., Reactions of the 17-Electron Bis(Dimethylglyoximate)(Triphenylphosphine)Rhodium(I) Radical. *Inorg. Chem.* **1988**, *27* (18), 3147-3151.
55. Lambert, F. L.; Kobayashi, K., Polarography of Organic Halogen Compounds .1. Steric Hindrance and the Half-Wave Potential in Alicyclic and Aliphatic Halides. *J. Am. Chem. Soc.* **1960**, *82* (20), 5324-5328.
56. Lambert, F. L.; Ingall, G. B., Voltammetry of Organic Halogen Compounds .4. Reduction of Organic Chlorides at Vitreous (Glassy) Carbon Electrode. *Tetrahedron Lett.* **1974**, (36), 3231-3234.
57. Wallentin, C. J.; Nguyen, J. D.; Finkbeiner, P.; Stephenson, C. R. J., Visible Light-Mediated Atom Transfer Radical Addition via Oxidative and Reductive Quenching of Photocatalysts. *J. Am. Chem. Soc.* **2012**, *134* (21), 8875-8884.
58. Nguyen, J. D.; Tucker, J. W.; Konieczynska, M. D.; Stephenson, C. R. J., Intermolecular Atom Transfer Radical Addition to Olefins Mediated by Oxidative Quenching of Photoredox Catalysts. *J. Am. Chem. Soc.* **2011**, *133* (12), 4160-4163.
59. Nguyen, J. D.; D'Amato, E. M.; Narayanam, J. M.; Stephenson, C. R., Engaging unactivated alkyl, alkenyl and aryl iodides in visible-light-mediated free radical reactions. *Nat. Chem.* **2012**, *4* (10), 854-859.
60. Tucker, J. W.; Nguyen, J. D.; Narayanam, J. M. R.; Krabbe, S. W.; Stephenson, C. R. J., Tin-free radical cyclization reactions initiated by visible light photoredox catalysis. *Chem. Comm.* **2010**, *46* (27), 4985-4987.
61. Tucker, J. W.; Narayanam, J. M. R.; Krabbe, S. W.; Stephenson, C. R. J., Electron Transfer Photoredox Catalysis: Intramolecular Radical Addition to Indoles and Pyrroles. *Org. Lett.* **2010**, *12* (2), 368-371.
62. Aycock, R. A.; Wang, H.; Jui, N. T., A mild catalytic system for radical conjugate addition of nitrogen heterocycles. *Chem. Sci.* **2017**, *8* (4), 3121-3125.
63. Kharasch, M. S.; Urry, W. H.; Jensen, E. V., Addition of derivatives of chlorinated acetic acids to olefins. *J. Am. Chem. Soc.* **1945**, *67* (9), 1626.
64. Clark, A. J., Atom transfer radical cyclisation reactions mediated by copper complexes. *Chem. Soc. Rev.* **2002**, *31* (1), 1-11.
65. Muñoz-Molina, J. M.; Belderrain, T. R.; Pérez, P. J., Atom Transfer Radical Reactions as a Tool for Olefin Functionalization - On the Way to Practical Applications. *Eur. J. Inorg. Chem.* **2011**, (21), 3155-3164.
66. Clark, A. J., Copper Catalyzed Atom Transfer Radical Cyclization Reactions. *Eur. J. Org. Chem.* **2016**, *2016* (13), 2231-2243.
67. Shen, Y.; Cornella, J.; Juliá-Hernández, F.; Martín, R., Visible-Light-Promoted Atom Transfer Radical Cyclization of Unactivated Alkyl Iodides. *ACS Catal.* **2017**, *7* (1), 409-412.

68. Constantin, T.; Zanini, M.; Regni, A.; Sheikh, N. S.; Julia, F.; Leonori, D., Aminoalkyl radicals as halogen-atom transfer agents for activation of alkyl and aryl halides. *Science* **2020**, *367* (6481), 1021-1026.
69. Caiger, L.; Zhao, H.; Constantin, T.; Douglas, J. J.; Leonori, D., The Merger of Aryl Radical-Mediated Halogen-Atom Transfer (XAT) and Copper Catalysis for the Modular Cross-Coupling-Type Functionalization of Alkyl Iodides. *ACS Catal.* **2023**, *13*, 4985-4991.
70. Constantin, T.; Juli, F.; Sheikh, N. S.; Leonori, D., A case of chain propagation: alpha-aminoalkyl radicals as initiators for aryl radical chemistry. *Chem. Sci.* **2020**, *11* (47), 12822-12828.
71. Lima, C. G. S.; Lima, T. D.; Duarte, M.; Jurberg, I. D.; Paixao, M. W., Organic Synthesis Enabled by Light-Irradiation of EDA Complexes: Theoretical Background and Synthetic Applications. *ACS Catal.* **2016**, *6* (3), 1389-1407.
72. Breugst, M.; Koenig, J. J., σ -Hole Interactions in Catalysis. *Eur. J. Org. Chem.* **2020**, (34), 5473-5487.
73. Gilday, L. C.; Robinson, S. W.; Barendt, T. A.; Langton, M. J.; Mullaney, B. R.; Beer, P. D., Halogen Bonding in Supramolecular Chemistry. *Chem. Rev.* **2015**, *115* (15), 7118-7195.
74. Matsuo, K.; Yamaguchi, E.; Itoh, A., In Situ-Generated Halogen-Bonding Complex Enables Atom Transfer Radical Addition (ATRA) Reactions of Olefins. *J. Org. Chem.* **2020**, *85* (16), 10574-10583.
75. Matsuo, K.; Kondo, T.; Yamaguchi, E.; Itoh, A., Photoinduced Atom Transfer Radical Addition Reaction of Olefins with α -Bromo Carbonyls. *Chem. Pharm. Bull.* **2021**, *69* (8), 796-801.
76. Rrapi, M.; Batsika, C. S.; Nikitas, N. F.; Tappin, N. D. C.; Triandafillidi, I.; Renaud, P.; Kokotos, C. G., Photochemical Synthesis of Lactones, Cyclopropanes and ATRA Products: Revealing the Role of Sodium Ascorbate. *Chem. Eur. J.* **2024**, *30* (21), e20240253.
77. Pawlenko, S., *Organosilicon Chemistry*. Walter de Gruyter GmbH: 1986.
78. Pouget, E.; Tonnar, J.; Lucas, P.; Lacroix-Desmazes, P.; Ganachaud, F.; Boutevin, B., Well-Architected Poly(dimethylsiloxane)-Containing Copolymers Obtained by Radical Chemistry. *Chem. Rev.* **2010**, *110* (3), 1233-1277.
79. Nekrashevich, S. S.; Gritsenko, V. A., Electronic structure of silicon dioxide (a review). *Phys. Solid State* **2014**, *56* (2), 207-222.
80. Kakiage, K.; Nakada, Y.; Kogure, T.; Yamamura, M.; Kyomen, T.; Unno, M.; Hanaya, M., Applicability of silanol to sensitizing dye for dye-sensitized solar cell. *Silicon Chem.* **2008**, *3*, 303-305.
81. Showell, G. A.; Mills, J. S., Chemistry challenges in lead optimization: silicon isosteres in drug discovery. *Drug Discov. Today* **2003**, *8* (12), 551-556.
82. Gately, S.; West, R., Novel therapeutics with enhanced biological activity generated by the strategic introduction of silicon isosteres into known drug scaffolds. *Drug Dev. Res.* **2007**, *68* (4), 156-163.
83. Patai, S., *The Chemistry of Organic Silicon Compounds*. Wiley: Chinchester England, 1989.
84. Crouch, R. D., Recent Advances in Silyl Protection of Alcohols. *Synth. Commun.* **2013**, *43* (17), 2265-2279.
85. Schelhaas, M.; Waldmann, H., Protecting group strategies in organic synthesis. *Angew. Chem., Int. Ed. Engl.* **1996**, *35* (18), 2056-2083.
86. Čusak, A., Temporary Silicon-Tethered Ring-Closing Metathesis: Recent Advances in Methodology Development and Natural Product Synthesis. *Chem. Eur. J.* **2012**, *18*, 5800-5824.
87. Bracegirdle, S.; Anderson, E. A., Recent advances in the use of temporary silicon tethers in metal-mediated reactions. *Chem. Soc. Rev.* **2010**, *39*, 4114-4129.
88. Parasram, M.; Gevorgyan, V., Silicon-Tethered Strategies for C-H Functionalization Reactions. *Acc. Chem. Res.* **2017**, *50* (8), 2038-2053.
89. Fleming, I.; Barbero, A.; Walter, D., Stereochemical control in organic synthesis using silicon-containing compounds. *Chem. Rev.* **1997**, *97* (6), 2063-2192.
90. Nakao, Y.; Hiyama, T., Silicon-based cross-coupling reaction: an environmentally benign version. *Chem. Soc. Rev.* **2011**, *40* (10), 4893-4901.
91. Denmark, S. E.; Sweis, R. F., Design and implementation of new, silicon-based, cross-coupling reactions: Importance of silicon-oxygen bonds. *Acc. Chem. Res.* **2002**, *35* (10), 835-846.
92. Chatgililoglu, C., Organosilanes as Radical-Based Reducing Agents in Synthesis. *Acc. Chem. Res.* **1992**, *25* (4), 188-194.

93. Roberts, D. D.; McLaughlin, M. G., Strategic Applications of the beta-Silicon Effect. *Adv. Synth. Catal.* **2022**, *364* (14), 2307-2332.
94. Lambert, J. B.; Zhao, Y.; Emblidge, R. W.; Salvador, L. A.; Liu, X. Y.; So, J. H.; Chelius, E. C., The β effect of silicon and related manifestations of σ conjugation. *Acc. Chem. Res.* **1999**, *32* (2), 183-190.
95. Wilt, J. W.; Kolewe, O., α -Silyl Radicals. The Peroxide-Induced Decarbonylation of Triphenylsilylacetaldehyde. *J. Am. Chem. Soc.* **1965**, *87* (9), 2071-2072.
96. Wilt, J. W.; Kolewe, O.; Kraemer, J. F., The Search for Radical Rearrangement in Organosilicon Systems. I. α -Silyl Radicals from Silaneophyl Systems. *J. Am. Chem. Soc.* **1969**, *91* (10), 2624-2631.
97. Krusic, P. J.; Kochi, J. K., Electron Spin Resonance of Group IV Organometallic Alkyl Radicals in Solution. *J. Am. Chem. Soc.* **1969**, *91* (22), 6161-6164.
98. Kawamura, T.; Kochi, J. K., Hyperconjugative and p-d homoconjugative effects of silicon, germanium, and tin on alkyl radicals from electron spin resonance studies. *J. Am. Chem. Soc.* **1972**, *94* (2), 648-650.
99. Wilt, J. W.; Aznavoorian, P. M., Favored reduction of α -chlorosilane vs. α -chloroalkanes with tri-n-butyltin hydride. *J. Org. Chem.* **1978**, *43* (6), 1285-1286.
100. Wilt, J. W.; Chwang, W. K.; Dockus, C. F.; Tomiuk, N. M., Aryl Shifts from Silicon to Carbon Via Gamma-Silyl and Delta-Silyl Radicals. *J. Am. Chem. Soc.* **1978**, *100* (17), 5534-5540.
101. Yang, N. Y.; Fang, Y. W.; Xu, F. F.; Zhou, R.; Jin, X. P.; Zhang, L.; Shi, J. X.; Fang, J. H.; Wu, H.; Zhang, Z. Y., Application of the stabilization effect of a silyl group in radical-polar crossover reactions enabled by photoredox-neutral catalysis. *Org. Chem. Front.* **2021**, *8* (19), 5303-5309.
102. Ibrahim, M. R.; Jorgensen, W. L., Ab Initio Investigations of the β -Silicon Effect on Alkyl and Cyclopropyl Carbenium Ions and Radicals. *J. Am. Chem. Soc.* **1989**, *111* (3), 819-824.
103. Lawrence, N. J., *Science of Synthesis*. Thieme: 2002; Vol. 4.
104. van Delft, F. L.; de Kort, M.; van der Marel, G.; van Boom, J., Use of a Novel α -Hydroxyethylating Reagent in the Stereoselective Synthesis of Lincosamine. *J. Org. Chem.* **1996**, *61* (5), 1883-1885.
105. Hudrlik, P. F.; Agwarambo, E. L. O.; Hudrlik, A. M., Concerning the Mechanism of the Peterson Olefination Reaction. *J. Org. Chem.* **1989**, *54* (23), 5613-5618.
106. Cai, Y. Y.; Zhu, W. J.; Zhao, S. J.; Dong, C. J.; Xu, Z. C.; Zhao, Y. C., Difluorocarbene-Mediated Cascade Cyclization: The Multifunctional Role of Ruppert-Prakash Reagent. *Org. Lett.* **2021**, *23* (9), 3546-3551.
107. Schwarzwald, G. M.; Matier, C. D.; Fu, G. C., Enantioconvergent Cross-Couplings of Alkyl Electrophiles: The Catalytic Asymmetric Synthesis of Organosilanes. *Angew. Chem., Int. Ed. Engl.* **2019**, *58* (11), 3571-3574.
108. Hauser, C. R.; Hance, C. R., Preparation and Reactions of α -Halo Derivatives of Certain Tetra-substituted Hydrocarbon Silanes. Grignard Syntheses of Some Silyl Compounds. *J. Am. Chem. Soc.* **1952**, *74* (20), 5091-5096.
109. Tamao, K.; Kumada, M., Preparation of Certain Bromomethyl-Substituted and Iodomethyl-Substituted Disilanes. *J. Organomet. Chem.* **1971**, *30* (3), 329-337.
110. Barrett, A. G. M.; Flygare, J. A., Triply Convergent, Stereospecific Alkene Formation via Peterson Olefination. *J. Org. Chem.* **1991**, *56*, 638-642.
111. Ehrnsberger, P. Photoredox-catalyzed ATRA reactions and related processes in a new light. PhD thesis. University of Regensburg, 2021.
112. Gatazka, M. R.; Parikh, S. G.; Rykaczewski, K. A.; Schindler, C. S., Ketyl Radical Enabled Synthesis of Oxetanes. *Synthesis* **2024**, *56* (16), 2513-2520.
113. Vasil'eva, T. T.; Gapusenko, S. I.; Terent'ev, A. B.; Pinyaskin, V. V.; Strankevich, I. V.; Chistyakov, A. L.; Mysov, E. I., Radical-type addition of benzyl bromide to vinyl chloride: the kinetics and activation energy of the process. *Russ. Chem. Bull.* **1993**, *42*, 840-842.
114. Vasil'eva, T. T.; Gapusenko, S. I.; Vitt, S. V.; Terent'ev, A. B., Homolytic addition of benzyl bromide to unsaturated compounds in conditions of metal-complex initiation. *Bull. Russ. Acad. Sci.: Chem.* **1992**, *41*, 1841-1845.
115. Terent'ev, A. B.; Gapusenko, S. I.; Vasil'eva, T. T.; Vitt, S. V., Relative kinetics of the radical addition of benzyl bromide to unsaturated compounds. *Bull. Russ. Acad. Sci.: Chem.* **1992**, *41*, 1567-1571.

116. Bols, M.; Skrydstrup, T., Silicon-Tethered Reactions. *Chem. Rev.* **1995**, *95* (5), 1253-1277.
117. Stork, G.; Kahn, M., Control of Ring Junction Stereochemistry via Radical Cyclization. *J. Am. Chem. Soc.* **1985**, *107* (2), 500-501.
118. Mikhaylov, A. A.; Zard, S. Z., Extension to the Silyl-Tethered Radical Cyclization: Cyclohex-2-en-1-oxy Vinyl Silanes in Stereoselective Radical Addition/Cyclization Cascades. *Org. Lett.* **2017**, *19* (7), 1866-1869.
119. Nishiyama, H.; Kitajima, T.; Matsumoto, M.; Itoh, K., Silylmethyl Radical Cyclization - New Stereoselective Method for 1,3-Diol Synthesis from Allylic Alcohols. *J. Org. Chem.* **1984**, *49* (12), 2298-2300.
120. Stork, G.; Sofia, M. J., Stereospecific Reductive Methylation via a Radical Cyclization-Desilylation Process. *J. Am. Chem. Soc.* **1986**, *108* (21), 6826-6828.
121. Stork, G.; Mah, R., Introduction of angular methyl groups via radical cyclization. *Tetrahedron Lett.* **1989**, *30* (28), 3609-3612.
122. Shuto, S.; Terauchi, M.; Yahiro, Y.; Abe, H.; Ichikawa, S.; Matsuda, A., Stereoselective synthesis of α and β -C-glucosides via radical cyclization with an allylsilyl tether.: Control of the stereoselectivity by changing the conformation of the pyranose ring. *Tetrahedron Lett.* **2000**, *41* (21), 4151-4155.
123. Terauchi, M.; Yahiro, Y.; Abe, H.; Ichikawa, S.; Tovey, S. C.; Dedos, S. G.; Taylor, C. W.; Potter, B. V. L.; Matsuda, A.; Shuto, S., Synthesis of 4,8-anhydro-D-glycero-D-ido-nonanitol 1,6,7-trisphosphate as a novel IP receptor ligand using a stereoselective radical cyclization reaction based on a conformational restriction strategy. *Tetrahedron* **2005**, *61* (15), 3697-3707.
124. Kanazaki, M.; Ueno, Y.; Shuto, S.; Matsuda, A., Highly nuclease-resistant phosphodiester-type oligodeoxynucleotides containing 4' α -C-aminoalkylthymidines form thermally stable duplexes with DNA and RNA.: A candidate for potent antisense molecules. *J. Am. Chem. Soc.* **2000**, *122* (11), 2422-2432.
125. Duplessis, M.; Waltz, M. E.; Bencheqroun, M.; Cardinal-David, B.; Guindon, Y., Stereoselective Quaternary Center Construction via Atom-Transfer Radical Cyclization Using Silicon Tethers on Acyclic Precursors. *Org. Lett.* **2009**, *11* (14), 3148-3151.
126. Wilt, J. W., Effect of the Silicon Site on the Cyclization of Sila-5-Hexen-1-Yl Radicals - the Unusual Effect of Alpha-Silicon. *J. Am. Chem. Soc.* **1981**, *103* (17), 5251-5253.
127. Shuto, S.; Kanazaki, M.; Ichikawa, S.; Matsuda, A., A novel ring-enlargement reaction of (3-oxa-2-silacyclopentyl)methyl radicals into 4-oxa-3-silacyclohexyl radicals. Stereoselective introduction of a hydroxyethyl group via unusual 6-endo-cyclization products derived from 3-oxa-4-silahexenyl radicals and its application to the synthesis of a 4'- α -branched nucleoside. *J. Org. Chem.* **1997**, *62* (17), 5676-5677.
128. Beckwith, A. L. J.; Easton, C. J.; Serelis, A. K., Some Guidelines for Radical Reactions. *Chem. Commun.* **1980**, (11), 482-483.
129. Shuto, S.; Kanazaki, M.; Ichikawa, S.; Minakawa, N.; Matsuda, A., Stereo- and regioselective introduction of 1- or 2-hydroxyethyl group via intramolecular radical cyclization reaction with a novel silicon-containing tether.: An efficient synthesis of 4' α -branched 2'-deoxyadenosines. *J. Org. Chem.* **1998**, *63* (3), 746-754.
130. Ueno, Y.; Nagasawa, Y.; Sugimoto, I.; Kojima, N.; Kanazaki, M.; Shuto, S.; Matsuda, A., Nucleosides and nucleotides.: 174.: Synthesis of oligodeoxynucleotides containing 4'-C-[2-[[N-(2-aminoethyl)carbonyl]oxy]ethyl]thymidine and their thermal stability and nuclease-resistance properties. *J. Org. Chem.* **1998**, *63* (5), 1660-1667.
131. Sugimoto, I.; Shuto, S.; Mori, S.; Shigeta, S.; Matsuda, A., Nucleosides and nucleotides.: 183.: Synthesis of 4' α -branched thymidines as a new type of antiviral agent. *Bioorg. Med. Chem. Lett.* **1999**, *9* (3), 385-388.
132. Yahiro, Y.; Ichikawa, S.; Shuto, S.; Matsuda, A., Synthesis of C-glycosides via radical cyclization reactions with a vinylsilyl tether.: Control of the reaction course by a change in the conformation of the pyranose ring due to steric repulsion between adjacent bulky protecting groups. *Tetrahedron Lett.* **1999**, *40* (30), 5527-5531.
133. Kodama, T.; Shuto, S.; Nomura, M.; Matsuda, A., An efficient method for the preparation of 1' α -branched-chain sugar pyrimidine ribonucleosides from uridine: The first conversion of a natural nucleoside into 1'-substituted ribonucleosides. *Chem. Eur. J.* **2001**, *7* (11), 2332-2340.

134. Shuto, S.; Yahiro, Y.; Ichikawa, S.; Matsuda, A., Synthesis of 3,7-anhydro-D-glycero-D-idoctitol 1,5,6-trisphosphate as an IP3 receptor ligand using a radical cyclization reaction with a vinylsilyl tether as the key step.: Conformational restriction strategy using steric repulsion between adjacent bulky protecting groups on a pyranose ring. *J. Org. Chem.* **2000**, *65* (18), 5547-5557.
135. Sakaguchi, N.; Hirano, S.; Matsuda, A.; Shuto, S., Radical reactions with 2-bromobenzylidene group, a protecting/radical-translocating group for the 1,6-radical hydrogen transfer reaction. *Org. Lett.* **2006**, *8* (15), 3291-3294.
136. Xi, Z.; Rong, J. H.; Chattopadhyaya, J., Diastereospecific Synthesis of 2'-C-Branched or 3'-C-Branched Nucleosides through Intramolecular Free-Radical Capture by Silicon-Tethered Acetylene. *Tetrahedron* **1994**, *50* (17), 5255-5272.
137. Sugimoto, I.; Shuto, S.; Matsuda, A., A one-pot method for the stereoselective introduction of a vinyl group via an atom-transfer radical-cyclization reaction with a diphenylvinylsilyl group as a temporary connecting tether. Synthesis of 4'-alpha-C-vinylthymidine, a potent antiviral nucleoside. *J. Org. Chem.* **1999**, *64* (19), 7153-7157.
138. Sukeda, M.; Shuto, S.; Sugimoto, I.; Ichikawa, S.; Matsuda, A., Synthesis of pyrimidine 2'-deoxy ribonucleosides branched at the 2'-position via radical atom-transfer cyclization reaction with a vinylsilyl group as a radical-acceptor tether. *J. Org. Chem.* **2000**, *65* (26), 8988-8996.
139. Sukeda, M.; Ichikawa, S.; Matsuda, A.; Shuto, S., A new entry to the stereoselective introduction of an ethynyl group by a radical reaction: Synthesis of the potential antimetabolite 2'-deoxy-2'-C-ethynyluridine. *Angew. Chem., Int. Ed. Engl.* **2002**, *41* (24), 4748-4750.
140. Sukeda, M.; Ichikawa, S.; Matsuda, A.; Shuto, S., The first radical method for the introduction of an ethynyl group using a silicon tether and its application to the synthesis of 2'-deoxy-2'-C-ethynyl nucleosides. *J. Org. Chem.* **2003**, *68* (9), 3465-3475.
141. Haugland, M. M.; El-Sagheer, A. H.; Porter, R. J.; Pena, J.; Brown, T.; Anderson, E. A.; Lovett, J. E., 2'-Alkynyl nucleotides: A Sequence- and Spin Label-Flexible Strategy for EPR Spectroscopy in DNA. *J. Am. Chem. Soc.* **2016**, *138* (29), 9069-9072.
142. Panferova, L. I.; Struchkova, M. I.; Dilman, A. D., Vinylation of Iododifluoromethylated Alcohols via a Light-Promoted Intramolecular Atom-Transfer Reaction. *Synthesis* **2017**, *49* (18), 4124-4132.
143. Becerril-Jimenez, F.; Lussier, T.; Leblanc, L.; Eymard, C.; Dostie, S.; Prevost, M.; Guindon, Y., Photoredox-Catalyzed Stereoselective Radical Reactions to Synthesize Nucleoside Analogues with a C2'-Stereogenic All-Carbon Quaternary Center. *J. Org. Chem.* **2019**, *84* (22), 14795-14804.
144. Sakurai, H.; Hosomi, A.; Kumada, M., Addition of trichloromethyl radicals to alkenylsilylanes. *J. Org. Chem.* **1969**, *34* (6), 1764-1768.
145. Zard, S. Z., On the trail of xanthates: Some new chemistry from an old functional group. *Angew. Chem., Int. Ed. Engl.* **1997**, *36* (7), 673-685.
146. Li, Z.; Zard, S. Z., A Flexible Radical-Based Approach to TMS-Substituted Propargyl Alcohols and to 2,3-Allenols. *Org. Lett.* **2009**, *11* (13), 2868-2871.
147. Li, S. G.; Zard, S. Z., Novel Route to Triethylsilyl-Substituted Cyclopropanes. *Org. Lett.* **2014**, *16* (23), 6180-6183.
148. Goh, K. K.; Kim, S.; Zard, S. Z., A synthesis of (1E,3E)-TMS dienes from keto-xanthates via Chugaev-type elimination. *J. Org. Chem.* **2013**, *78* (23), 12274-12279.
149. Quiclet-Sire, B.; Yanagisawa, Y.; Zard, S. Z., A direct, versatile route to functionalized trialkoxysilanes. *Chem. Comm.* **2014**, *50* (18), 2324-2326.
150. Quiclet-Sire, B.; Zard, S. Z., A radical thia-Brook rearrangement. *Chem. Comm.* **2014**, *50* (45), 5990-5992.
151. Das, B.; Venkateswarlu, K.; Damodar, K.; Suneel, K., Ammonium acetate catalyzed improved method for the regioselective conversion of olefins into halohydrins and haloethers at room temperature. *J. Mol. Catal. A Chem.* **2007**, *269* (1-2), 17-21.
152. Narender, M.; Reddy, M. S.; Nageswar, Y. D.; Rao, K. R., Aqueous phase synthesis of vic-halohydrins from olefins and N-halosuccinimides in the presence of beta-cyclodextrin. *J. Mol. Catal. A Chem.* **2006**, *258* (1-2), 10-14.
153. Urankar, D.; Rutar, I.; Modec, B.; Dolenc, D., Synthesis of bromo- and iodohydrins from deactivated alkenes by use of N-bromo- and N-iodosaccharin. *Eur. J. Org. Chem.* **2005**, (11), 2349-2353.

154. Derouet, D.; Cauret, L.; Brosse, J. C., Study of the addition of monoalkylphosphonic acids onto trialkyl-substituted epoxides. *J. Org. Chem.* **2001**, *66* (11), 3767-3774.
155. Yao, H. R.; Richardson, D. E., Epoxidation of alkenes with bicarbonate-activated hydrogen peroxide. *J. Am. Chem. Soc.* **2000**, *122* (13), 3220-3221.
156. Geng, X. L.; Wang, Z.; Li, X. Q.; Zhang, C., A simple method for epoxidation of olefins using sodium chlorite as an oxidant without a catalyst. *J. Org. Chem.* **2005**, *70* (23), 9610-9613.
157. Miller, L. I.; Hoffmann, A. K., Electrochemical Formation of Carbonium and Iodonium Ions from Alkyl and Aryl Iodides. *J. Am. Chem. Soc.* **1967**, *89* (3), 593-597.
158. Wang, M.; Rörich, I.; Ramanan, C.; Blom, P. W. M.; Huang, W.; Li, R.; Zhang, K. A. I., Electron donor-free photoredox catalysis *via* an electron transfer cascade by cooperative organic photocatalysts. *Catal. Sci. Technol.* **2018**, *8*, 3539-3547.
159. Lowry, M. S.; Goldsmith, J. I.; Slinker, J. D.; Rohl, R.; Pascal, R. A.; Malliaras, G. G.; Bernhard, S., Single-Layer Electroluminescent Devices and Photoinduced Hydrogen Production from an Ionic Iridium(III) Complex. *Chem. Mat.* **2005**, *17*, 5712-5719.
160. Danen, W. C.; Winter, R. L., Halogen Abstraction Studies .2. Free-Radical Abstraction of Iodine from Aliphatic Iodides - Evidence to Support Anchimeric Assistance by Neighboring Halogen in Homolytic Reactions. *J. Am. Chem. Soc.* **1971**, *93* (3), 716-720.
161. Kryger, R. G.; Lorand, J. P.; Stevens, N. R.; Herron, N. R., Radicals and Scavengers .7. Diffusion Controlled Scavenging of Phenyl Radicals and Absolute Rate Constants of Several Phenyl Radical Reactions. *J. Am. Chem. Soc.* **1977**, *99* (23), 7589-7600.
162. Hossain, A.; Engl, S.; Lutsker, E.; Reiser, O., Visible-Light-Mediated Regioselective Chlorosulfonylation of Alkenes and Alkynes: Introducing the Cu(II) Complex [Cu(dap)Cl] to Photochemical ATRA Reactions. *ACS Catal.* **2019**, *9* (2), 1103-1109.
163. Barluenga, J.; Suero, M. G.; Pérez-Sánchez, I.; Flórez, J., Diastereoselective cyclopropanation of ketone enols with Fischer carbene complexes. *J. Am. Chem. Soc.* **2008**, *130* (9), 2708-2709.
164. Groenewegen, P.; Kallenberg, H.; Vandergen, A., Aldehyde Enolates .3. Direct Sulfonylation and Iodination of Aldehyde Anions. *Tetrahedron Lett.* **1979**, (30), 2817-2820.
165. Sreedhar, B.; Reddy, P. S.; Madhavi, M., Rapid and catalyst-free α -halogenation of ketones using halosuccinamides in DMSO. *Synth. Commun.* **2007**, *37* (22-24), 4149-4156.
166. Meshram, H. M.; Reddy, P. N.; Sadashiv, K.; Yadav, J. S., Amberlyst-15-promoted efficient 2-halogenation of 1,3-keto-esters and cyclic ketones using N-halosuccinimides. *Tetrahedron Lett.* **2005**, *46* (4), 623-626.
167. Saiter, J.; Guérin, T.; Donnard, M.; Panossian, A.; Hanquet, G.; Leroux, F. R., Direct Trifluoromethoxylation without OCF-Carrier through In Situ Generation of Fluorophosgene. *Eur. J. Org. Chem.* **2021**, (22), 3139-3147.
168. Marotta, A.; Fang, H.; Adams, C. E.; Marcus, K. S.; Daniliuc, C. G.; Molloy, J. J., Direct Light-Enabled Access to α -Boryl Radicals: Application in the Stereodivergent Synthesis of Allyl Boronic Esters. *Angew. Chem., Int. Ed. Engl.* **2023**, *62* (34), e202307540.
169. Wang, Y. X.; Wang, J. H.; Li, G. X.; He, G.; Chen, G., Halogen-Bond-Promoted Photoactivation of Perfluoroalkyl Iodides: A Photochemical Protocol for Perfluoroalkylation Reactions. *Org. Lett.* **2017**, *19* (6), 1442-1445.
170. Paquette, L. A., Silyl-Substituted Cyclopropanes as Versatile Synthetic Reagents. *Chem. Rev.* **1986**, *86* (5), 733-750.
171. Herbort, J. H.; Bednar, T. N.; Chen, A. D.; RajanBabu, T. V.; Nagib, D. A., γ C-H Functionalization of Amines via Triple H-Atom Transfer of a Vinyl Sulfonyl Radical Chaperone. *J. Am. Chem. Soc.* **2022**, *144* (29), 13366-13373.
172. Yamazaki, S., Methyltrioxorhenium-Catalyzed Epoxidation of Homoallylic Alcohols with Hydrogen Peroxide. *J. Org. Chem.* **2012**, *77* (21), 9884-9888.
173. Zhang, M. Z.; Wang, X.; Gong, M. Y.; Chen, L.; Shi, W. B.; He, S. H.; Jiang, Y.; Chen, T. Q., An efficient iodine pentoxide-triggered iodocarbocyclization for the synthesis of iodooxindoles in water. *Org. Biomol. Chem.* **2018**, *16* (28), 5197-5202.
174. Palmer, M. J.; Kenny, J. A.; Walsgrove, T.; Kawamoto, A. M.; Wills, M., Asymmetric transfer hydrogenation of ketones using amino alcohol and monotosylated diamine derivatives of indane. *J. Chem. Soc., Perkin Trans. 1* **2002**, (3), 416-427.

175. Denmark, S. E.; Burk, M. T.; Hoover, A. J., On the Absolute Configurational Stability of Bromonium and Chloronium Ions. *J. Am. Chem. Soc.* **2010**, *132* (4), 1232-1233.
176. Li, Z.; Zhang, L.; Ding, R.; Wang, J.; Chen, D. F.; Ren, Z.; Ding, C.; Chen, K.; Wang, J.; Wang, Z., Mechanochemical reduction of alkyl and aryl halides using mesoporous zinc oxide. *Chem. Commun.* **2024**, *60*, 6146-6149.
177. Chang, X.; Cheng, X.; Liu, X. T.; Fu, C.; Wang, W. Y.; Wang, C. J., Stereodivergent Construction of 1,4-Nonadjacent Stereocenters via Hydroalkylation of Racemic Allylic Alcohols Enabled by Copper/Ruthenium Relay Catalysis. *Angew. Chem., Int. Ed. Engl.* **2022**, *61* (36), e20226517.
178. Shiroodi, R. K.; Dudnik, A. S.; Gevorgyan, V., Stereocontrolled 1,3-Phosphatylxy and 1,3-Halogen Migration Relay toward Highly Functionalized 1,3-Dienes. *J. Am. Chem. Soc.* **2012**, *134* (16), 6928-6931.
179. Sayyahi, S.; Saghanezhad, J., An efficient method for synthesis of phenacyl derivatives under homogeneous phase transfer catalyst condition in aqueous media. *Chinese Chem. Lett.* **2011**, *22* (3), 300-302.
180. Klahn, P.; Erhardt, H.; Kotthaus, A.; Kirsch, S. F., The Synthesis of α -Azidoesters and Geminal Triazides. *Angew. Chem., Int. Ed. Engl.* **2014**, *53* (30), 7913-7917.

Paper I

Radical Group Transfer of Vinyl and Alkynyl Silanes Driven by Photoredox Catalysis

Floriane Baussière and Marius M. Haugland

J. Org. Chem. **2023**, 88, 12451-12463

Radical Group Transfer of Vinyl and Alkynyl Silanes Driven by Photoredox Catalysis

Floriane Baussière and Marius M. Haugland*



Cite This: *J. Org. Chem.* 2023, 88, 12451–12463



Read Online

ACCESS |



Metrics & More

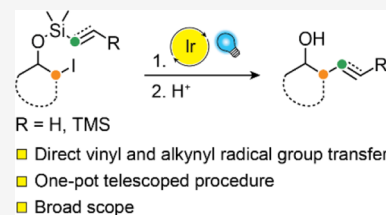


Article Recommendations



Supporting Information

ABSTRACT: Radical group transfer is a powerful tool for the formation of C–C bonds. These processes typically involve radical addition to C–C π bonds, followed by fragmentation of the resulting cyclic intermediate. Despite the advantageous lability of organosilanes in this context, silicon-tethered radical acceptor groups have remained underexplored in radical group transfer reactions. We report a general photoredox-catalyzed protocol for the radical group transfer of vinyl and alkynyl silanes onto sp^3 carbons, using activated and unactivated iodides as radical precursors. Our method displays high diastereoselectivity and excellent functional group tolerance, and enables direct formation of group transfer products by in situ ring opening. Mechanistic investigations revealed that the reaction proceeds via an unusual dual catalytic cycle, resulting in an overall redox-neutral process.



INTRODUCTION

Radical cyclizations are a powerful strategy to forge C–C bonds. These intramolecular processes benefit from very rapid kinetics, can generate multiple bonds in one transformation, and enable unique reactivity pathways for the synthesis of complex scaffolds.^{1–3} Although radical processes have traditionally relied on harmful reagents and harsh conditions, photoredox catalysis has emerged as a method of choice for performing radical chemistry under mild, non-toxic conditions.^{4,5} Radical cyclizations typically involve the addition of a carbon-centered radical to a C–C π bond, leading to cyclic products (Scheme 1a).^{2,6} This strategy has been widely employed to produce both saturated and unsaturated all-carbon rings and heterocycles.^{1,3,7} Stereoselective radical cyclizations, moreover, have been used to access enantio-enriched cyclic frameworks, which feature, e.g., in many pharmaceuticals and natural products.^{8–13}

The use of silicon-substituted alkenes and alkynes in radical cyclizations has, however, remained relatively underexplored. Due to the controllable lability of organosilanes, the cyclic products of these reactions can undergo ring-opening, which leads to an overall group transfer reaction of the vinyl or alkynyl substituent from silicon to carbon. Radical group transfer reactions of vinyl and alkynyl silanes have previously been performed using traditional radical initiators, e.g., on cyclic alkyl iodide substrates (Scheme 1b).^{14–16} Following the radical cyclization reaction, addition of a fluoride source results in elimination and desilylation. A similar strategy has also been applied to activated, tertiary bromides¹⁷ and in a radical cyclization cascade to set multiple contiguous stereocenters.¹⁸

More recently, two examples of radical cyclizations with vinyl silanes initiated by photoredox catalysis have been shown. Alkene group transfer was achieved with electronically activated alkyl iodides using an Ir(III) photocatalyst and

irradiation with blue light (Scheme 1c).¹⁹ Similarly, irradiation of an Ir(III) photocatalyst resulted in alkene group transfer of tertiary, activated alkyl bromides (Scheme 1d).²⁰ Beyond these successful initial demonstrations, a general method for group transfer reactions of silicon-tethered alkenes and alkynes has not yet been reported.

In this work, we present a general photoredox-catalyzed method for the radical group transfer of vinyl and alkynyl silanes. Using activated as well as unactivated alkyl iodides as radical precursors, we demonstrate the installation of alkenes and alkynes on sp^3 carbon atoms across a broad range of substrates. Our protocol exhibits excellent functional group tolerance and high diastereoselectivity, and enables the removal of the siloxane tether without the use of a fluoride source. Mechanistic investigations, moreover, reveal an unusual dual catalytic mechanism that enables an overall redox-neutral process. We expect the in-depth understanding of this reactivity to facilitate future use of vinyl and alkynyl silanes in radical chemistry.

RESULTS AND DISCUSSION

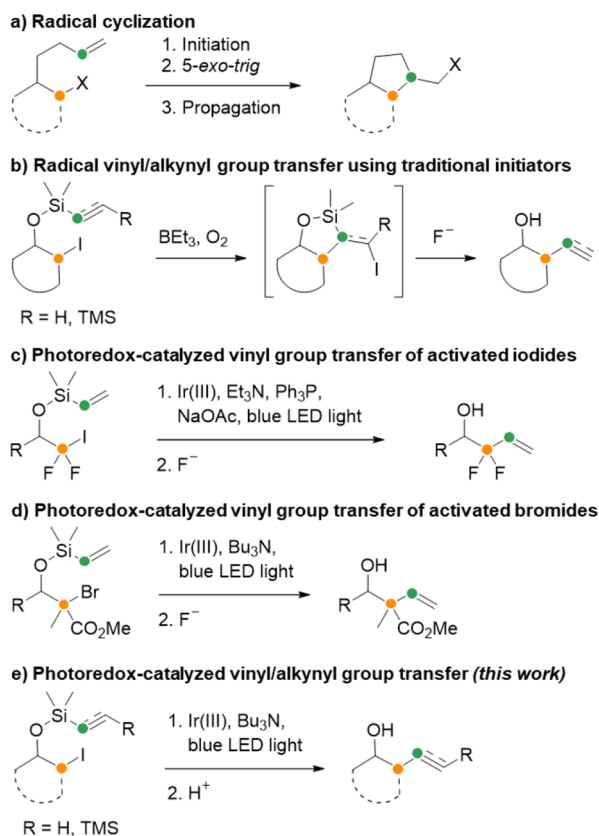
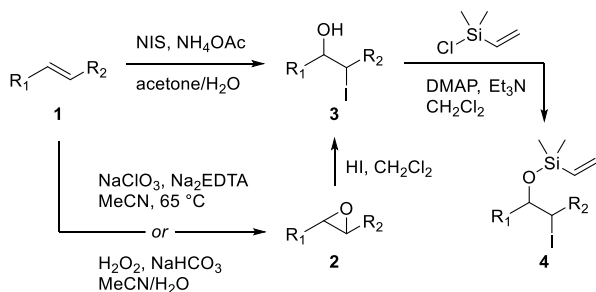
Substrates for the envisaged radical group transfer were prepared according to the general route shown in Scheme 2. Alkenes (1) were transformed, either directly or via an epoxide intermediate (2), into iodohydrins (3), which were further derivatized into vinyl siloxanes (4).

Received: June 1, 2023

Published: August 15, 2023



Scheme 1. Radical Cyclizations and Group Transfers

Scheme 2. Main Routes for Substrate Synthesis^a

^aA few substrates required modification of these standard protocols (see the [Supporting Information](#) for details).

We began our investigation with a screening of different potential metal-based and organic photocatalysts for the photoredox-catalyzed group transfer (Table 1, entries 1–10). Inspired by a previously reported method for heterolytic cleavage of unactivated C–I bonds,²¹ we subjected iodide **4a** to a range of photocatalysts in the presence of an amine electron donor under irradiation by blue LED lights. To our surprise, we observed the direct formation of the alkene group transfer product **5a**. Previous studies have reported the formation of a cyclized intermediate that requires the addition of a fluoride source to facilitate ring-opening/elimination.²⁰ Under our conditions, however, no fluoride appears to be required.

Unexpectedly, all the photocatalysts tested proved capable of catalyzing the reaction. No clear distinction in the yield was seen between photocatalysts typically going through oxidative (Table 1, entries 1–6) and reductive (Table 1, entries 7–10)

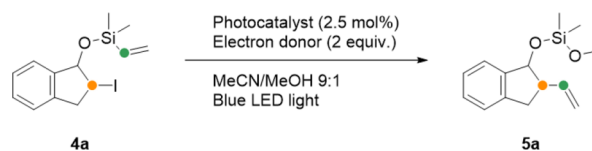
quenching pathways, nor between metal-based (Table 1, entries 1, 8–10) and organic (Table 1, entries 2–7) photocatalysts. In line with previous reports of atom transfer radical addition of activated halides with alkenes and alkynes, complete conversion from **4a** to **5a** generally proceeded faster with photocatalysts that undergo reductive quenching.²² 4CzIPN (Table 1, entry 7) was selected as the most promising photocatalyst due to its fast reaction time and high yield.

The effect of the tertiary amine used as an electron donor was studied next, with perylene, 4CzIPN, and [Ir(dtbbpy)(ppy)₂]PF₆ (Table 1, entries 3, 7, 9, and 11–16). While all three electron donors gave comparable reaction times and yields with [Ir(dtbbpy)(ppy)₂]PF₆, the choice of tertiary amine had an impact on the conversion rate with perylene and 4CzIPN. Tributylamine was chosen as the best electron donor as it had a faster conversion rate than triethylamine and DIPEA (Table 1, entries 7, 13, and 14) and provided higher yields.

Based on these results, we applied our selected reaction conditions (Table 1, entry 7) to an open-chain substrate **4f** in a telescoped procedure where the siloxane is cleaved upon treatment with HCl. Unexpectedly, this open-chain analogue of **4a** required 6 h to reach complete conversion (Table 2, entry 1). To improve the reaction rate, 4CzIPN was replaced by the more efficient photocatalyst [Ir(dtbbpy)(ppy)₂]PF₆ for further development. A solvent screening performed with **4f** confirmed acetonitrile/methanol 9:1 (Table 2, entry 2) as the best solvent system.

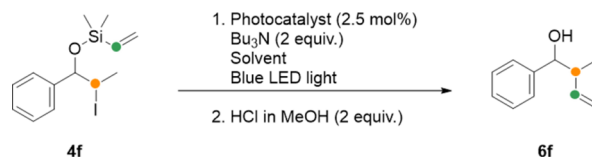
Next, the optimized photoredox reaction/acidic desilylation procedure was successfully applied to a wide range of substrates (Scheme 3). Although most radical group transfers produced secondary homoallylic alcohols, the protocol also proved applicable to primary (**6j**) and tertiary (**6e**) alcohols. Moreover, the method showed good functional group tolerance toward ketones (**6r**, **6v**), esters (**6m**, **6t**), amides (**6u**), carbamates (**6d**), ethers (**6e**, **6s**), and electron-rich as well as deficient aryl groups (**6o–p**). The reaction could also be performed at gram scale with a similar isolated yield (**6a**, Scheme 3). In contrast, no conversion was observed when attempting the reaction with bromide analogues of substrates **4a** and **4g**. This is not surprising, as halogen abstraction of alkyl bromides is known to be more challenging than alkyl iodides due to the higher bond strength of the C–Br bond.²³

Group transfer reactions of alkyl iodides at secondary positions generally occurred notably faster in cyclic systems (**6a–e**) than in open-chain counterparts (**6f–j**). The slower reaction rates of open-chain systems could be attributed to their higher entropic degrees of freedom. We were happy to observe that the radical group transfer reaction occurred with high diastereoselectivity in cyclic systems **6a–6e**, while open-chain systems **6f–6i** produced 12–15% of a minor diastereomer. The reaction at primary positions (**6k–p**), however, was slow and gave modest to moderate yields despite complete consumption of the substrates. Primary alkyl radicals are known to be unstable due to the lack of hyperconjugative donation of electron density from adjacent alkyl groups.²⁴ This can result in a higher activation energy for the formation of such radicals, thereby explaining the longer reaction times. Benzylic radicals, on the other hand, are known to be stabilized by delocalization.^{25,26} Indeed, we were pleased to observe rapid reactions and high isolated yields at benzylic positions (**6q–s**). Similarly, reactions at electron-deficient positions also proceeded rapidly and gave high yields (**6t–v**). This has been attributed to the ease of activation of the carbon-iodine

Table 1. Optimization of Reaction Conditions^a

entry	photocatalyst	electron donor	time	yield (%) ^b
1	<i>fac</i> -Ir(ppy) ₃	Bu ₃ N	4 h	75
2	7-(diethylamino)-3-(thiophen-2-yl)-2 <i>H</i> -chromen-2-one	Bu ₃ N	22 h	70
3	perylene	Bu ₃ N	4 h	74
4	eosin Y	Bu ₃ N	4 h	66
5	bengal rose	Bu ₃ N	4 h	70
6	rhodamine B	Bu ₃ N	4 h	61
7	4CzIPN	Bu ₃ N	2 h	88
8	Ru(bpy) ₃ Cl ₂	Bu ₃ N	23 h	79
9	[Ir(dtbbpy)(ppy) ₂] ₂ PF ₆	Bu ₃ N	0.5 h	81
10	[Ir(dF(CF ₃)ppy) ₂ (dtbbpy)]PF ₆	Bu ₃ N	1.5 h	72
11	perylene	Et ₃ N	18 h	79
12	perylene	DIPEA	1 h	74
13	4CzIPN	Et ₃ N	4 h	73
14	4CzIPN	DIPEA	4 h	85
15	[Ir(dtbbpy)(ppy) ₂] ₂ PF ₆	Et ₃ N	0.5 h	74
16	[Ir(dtbbpy)(ppy) ₂] ₂ PF ₆	DIPEA	0.5 h	78

^aReaction scale: 90 μmol. ^bYield determined by quantitative ¹H NMR with ethylene carbonate as an internal standard.

Table 2. Solvent Screening^a

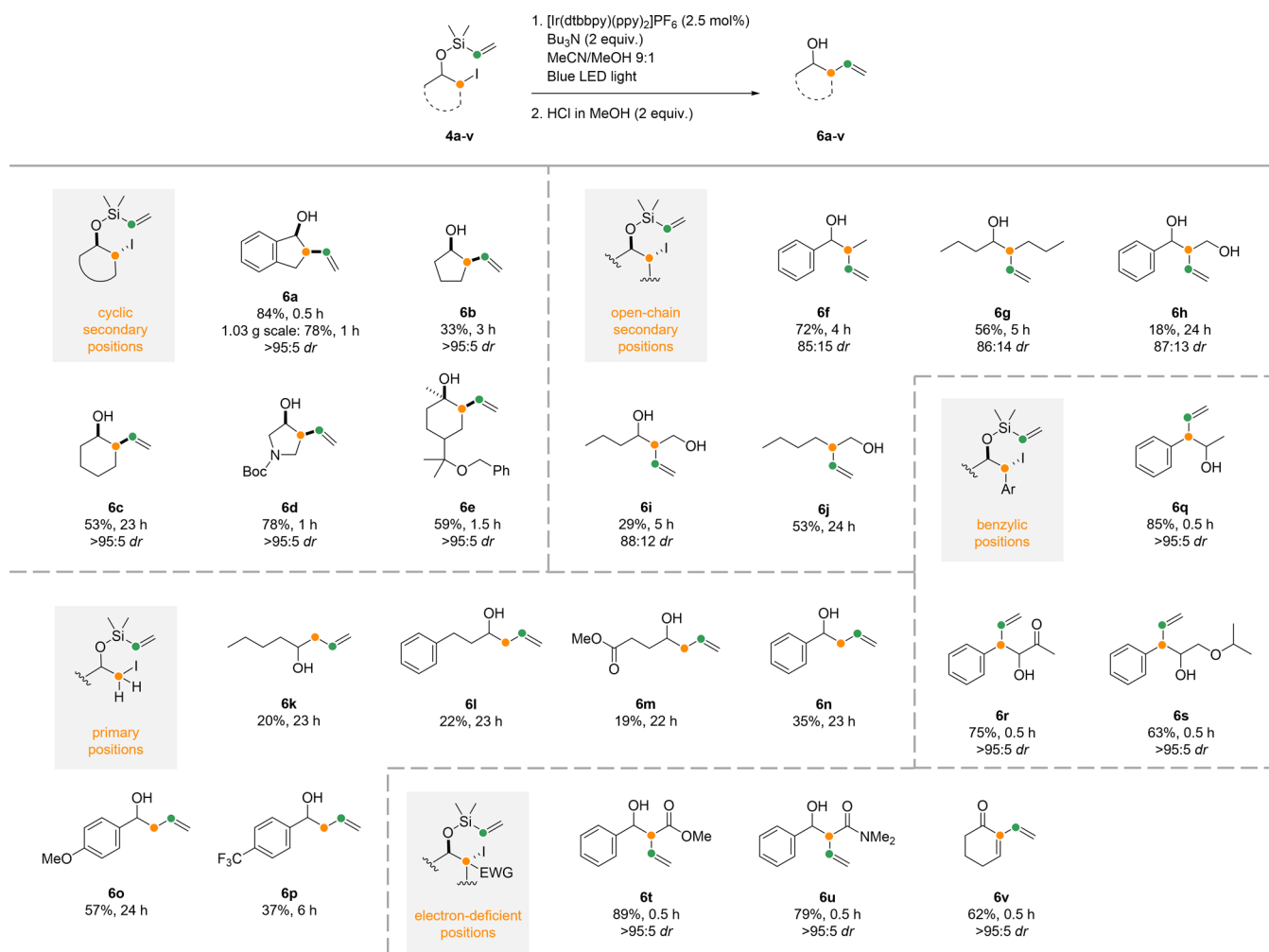
entry	photocatalyst	solvent	time ^b	yield (%) ^c
1	4CzIPN	MeCN/MeOH 9:1	6 h	54
2	[Ir(dtbbpy)(ppy) ₂] ₂ PF ₆	MeCN/MeOH 9:1	2 h	57
3	[Ir(dtbbpy)(ppy) ₂] ₂ PF ₆	MeCN	3 h	55
4	[Ir(dtbbpy)(ppy) ₂] ₂ PF ₆	CH ₂ Cl ₂	24 h	36
5	[Ir(dtbbpy)(ppy) ₂] ₂ PF ₆	EtOAc	24 h	n.d. ^d
6	[Ir(dtbbpy)(ppy) ₂] ₂ PF ₆	DMF	24 h	57
7	[Ir(dtbbpy)(ppy) ₂] ₂ PF ₆	<i>t</i> -BuCN	1 h	42
8	[Ir(dtbbpy)(ppy) ₂] ₂ PF ₆	THF	22.5 h	n.d. ^d
9	[Ir(dtbbpy)(ppy) ₂] ₂ PF ₆	THF/H ₂ O 99:1	22.5 h	n.d. ^d

^aReaction scale: 70 μmol. ^bPhotoredox catalysis reaction time; acidic desilylation reaction time: 10 min. ^cYield determined by quantitative ¹H NMR with ethylene carbonate as an internal standard. ^dNot determined.

bonds in substrates **4q–v**.²⁷ The resulting radical intermediates, moreover, are electrophilic and thus polarity-matched for reaction with the electron-rich vinyl silane moiety.²⁴ Interestingly, the radical alkene group transfer in open-chain benzylic and electron-deficient systems **6q–6v** also proceeded with high diastereoselectivity. A similar effect has been reported previously in group transfer reactions of other vinyl silanes with electron-deficient radicals.²⁰ We were pleased to obtain the β,γ-unsaturated carboxylic acid derivatives **6t–u** with no migration of the double bond.²⁸ Only in ketone **6v** did we observe elimination of the intermediate homoallylic alcohol to produce a conjugated system.

In general, longer reaction times correlated with lower isolated yields, which suggests that the radical group transfer is competing with a slower side reaction. To investigate this hypothesis, the reaction with **4k** was performed in MeCN-*d*₃/CD₃OD 9:1, and, upon full consumption of the starting

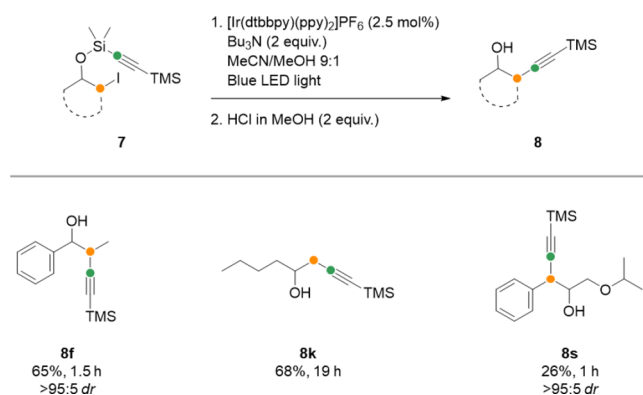
material, directly subjected to analysis by ¹H NMR with an internal standard. The yield at this stage was 40%, with no sign of elimination or other decomposition products despite the reaction being run in a closed system. ¹H NMR analysis was repeated after acidic desilylation and after aqueous workup. The yield did not change during desilylation, while a further 25% of the material was lost during the workup. Additional control experiments with **4n** verify that the starting material and product only undergo minor background degradation under the reaction conditions, but that 60% of the material is lost during the photoredox-catalyzed reaction (see the Supporting Information). Replacing Bu₃N with the more sterically hindered amine 1,2,2,6,6-pentamethylpiperidine results in similar isolated yields, which suggests little or no degradation through S_N2 substitution of the alkyl iodide. Although no side products could be observed by ¹H NMR or isolated, we hypothesize that degradation can occur through

Scheme 3. Radical Group Transfer of Vinyl Silanes^a

^aThe products are organized in five categories, depending on the position of the iodide before the radical reaction. Reaction scale: 0.30 mmol.

polymerization when the rate of the group transfer reaction is slow.

To our delight, the protocol could also be extended to radical group transfer of alkynes (Scheme 4). Analogous alkynyl silane substrates **7f**, **7k**, and **7s** were prepared from iodohydrins **3** by treatment with an alkynyl aminosilane (see the Supporting Information). After subjecting this material to

Scheme 4. Radical Group Transfer of Alkynyl Silanes^a

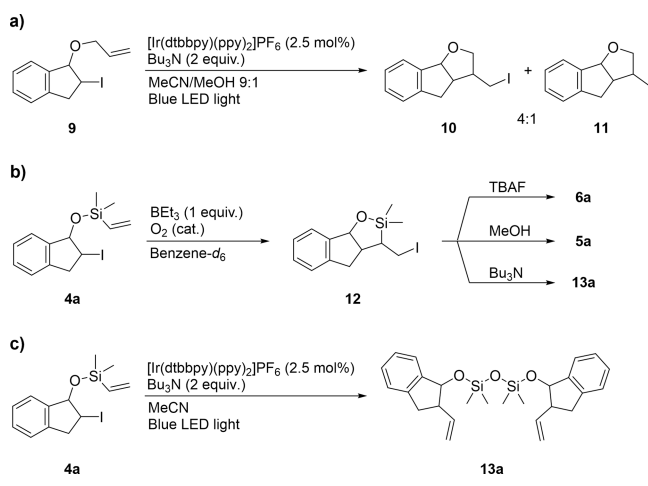
^aReaction scale: 0.30 mmol.

radical group transfer and desilylation, we obtained products alkynylated at secondary (**8f**), primary (**8k**), and benzylic (**8s**) positions. Under the acidic desilylation conditions, the trimethylsilyl substituent on the alkyne remains intact.

Mechanistic Investigations. Intrigued by the direct formation of the alkene group transfer product, in contrast to previous studies, we turned our attention to investigating the mechanism of the reaction. No conversion was observed when the reaction was performed in the absence of either the photocatalyst, Bu₃N, or visible light irradiation (see the Supporting Information) which strongly suggests that the reaction goes through a radical mechanism. In an attempt to trap any radical intermediates with a sufficiently long lifetime, we performed the radical alkene transfer reaction in the presence of 2,2,6,6-tetramethylpiperidine 1-oxyl (TEMPO) as a radical trap. However, no adducts between TEMPO and radical intermediates could be observed.

Next, we set out to investigate the importance of the silicon atom for the group transfer reaction. We subjected the allylic ether **9**, which can be considered an all-carbon analogue of vinyl silane **4a**, to the alkene transfer reaction conditions (Scheme 5a). This resulted in the formation of a 4:1 mixture of halogenated and reduced cyclic products **10** and **11**, respectively, through a 5-exo-trig radical cyclization. If vinyl silanes **4** undergo the same cyclization, this implies that the

Scheme 5. (a–c) Mechanistic Investigations



silicon atom can facilitate a subsequent ring-opening process under the reaction conditions. To verify this, iodide **4a** was subjected to BEt_3 and trace levels of oxygen in benzene- d_6 with ^1H NMR monitoring. Under these conditions, the cyclized iodide **12** is formed via a radical chain mechanism (Scheme 5b). Addition of tetrabutylammonium fluoride facilitated the formation of the ring-opened and desilylated product **6a**. Addition of methanol or Bu_3N was also found to promote rapid ring opening, to **5a** and the dimeric disiloxane **13a**, respectively, with methanol reacting faster (see the Supporting Information for details). We therefore propose that under the photoredox-catalyzed reaction conditions, the intermediate siloxane **5** (see Table 1) is formed by nucleophilic attack on the silicon atom of **12**. Notably, as nucleophilic/Lewis basic species coordinate to BEt_3 and prevent radical generation with O_2 , group transfer reactions with in situ ring opening cannot be performed with this initiator.

When the photoredox-catalyzed reaction was performed in the absence of methanol, the only observed product was a disiloxane-bridged dimer **13a** (Scheme 5c). This suggests that under these conditions, the reaction proceeds through a silylium ion stabilized by a Lewis base (e.g., MeCN or Bu_3N).²⁹ Silylium ions are known to be extremely reactive toward nucleophiles, and even traces of water are known to result in disiloxane formation.²⁹ We therefore performed the radical group transfer reaction in a gas-tight NMR tube with direct monitoring by ^1H NMR spectroscopy, in the presence or absence of methanol- d_4 (Figure 1a,b, respectively). As expected, when methanol was present in the reaction mixture, we observed rapid formation of product **5a** with no detectable intermediates (Figure 1a). In pure acetonitrile, however, the reaction proceeded via an intermediate that could be clearly observed at the start of the reaction. This intermediate was gradually converted into the dimeric product **13a** as the reaction progressed. Thus, we postulate that the observed intermediate is the solvent-stabilized silylium ion, which is subsequently captured by trace amounts of water to produce the dimeric product **13a**.

We were surprised to find that all the photocatalysts tested proved capable of catalyzing the reaction (Table 1). Unactivated halides are known to have more negative reduction potentials (e.g., ethyl iodide, $E_{\text{red}} = -1.67$ V vs SCE³⁰) than activated halides (α -carbonyl, α -heteroatom, benzylic or allylic) and therefore normally require strongly

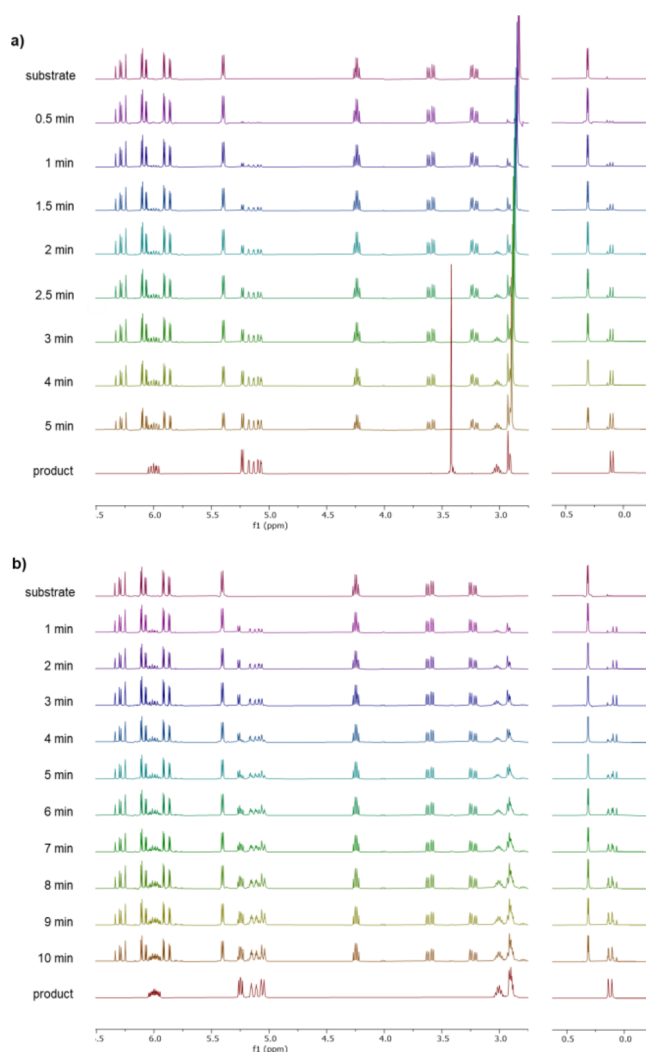
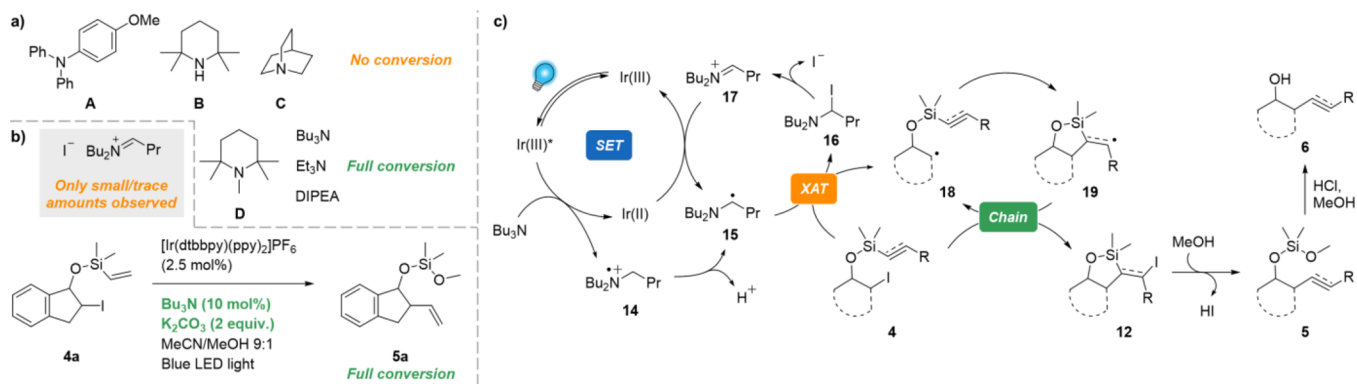


Figure 1. NMR monitoring of the reaction in deuterated solvents (see the Supporting Information for full spectra). Reactions were irradiated with blue LED light for the indicated time, interrupted for ^1H NMR analysis, and resubmitted to further light irradiation. (a) MeCN- d_3 /CD $_3$ OD 9:1; (b) MeCN- d_3 .

reducing photocatalysts for efficient radical formation by single-electron transfer (SET).^{21,26,31} This suggests that the reaction rather proceeds via a halogen-atom transfer (XAT) mechanism, where facile SET between photocatalysts and amines with subsequent deprotonation generates α -aminoalkyl radicals. Such radicals are highly potent halogen abstractors that can rapidly generate alkyl radicals from alkyl halides. At the same time, α -haloamines are formed, which in turn dissociate into iminium halide salts.^{32,33} Control experiments substituting Bu_3N with 4-methoxytriphenylamine (A), 2,2,6,6-tetramethylpiperidine (B), or quinuclidine (C), which cannot participate in XAT, led to no conversion, thereby confirming that the reaction is initiated by an XAT process (Scheme 6a). The reaction could, however, be promoted by 1,2,2,5,5-pentamethylpiperidine (D) and other amines containing the α -hydrogens required for XAT. At the same time, we were surprised to only observe very small or even trace amounts of the iminium halide or related hydrolysis products, even though these side products are expected in stoichiometric quantities in XAT reactions. Moreover, full conversion could also be achieved using 10 mol % of Bu_3N in the presence of

Scheme 6. (a–c) Mechanistic Observations and Proposed Mechanism



stoichiometric K_2CO_3 (Scheme 6b). Given the well-matched reduction potentials of iminium ions (e.g., 1-(4-fluorophenyl)ethan-1-iminium: $E_{red} = -1.10$ V vs SCE³⁴) and $[Ir(dtbbpy)(ppy)_2]PF_6$ ($E_{red} = -1.51$ V vs SCE), we propose that the iminium ion can be reduced back to the α -aminoalkyl radical by the reduced photocatalyst in our system, thereby turning over the photocatalytic cycle. Although similar reductions have been reported previously,³⁴ we believe this to be the first example of a coupled XAT/iminium SET reduction, leading to an overall process that is catalytic with respect to the amine.

Based on these results, we propose the following mechanism for the photoredox-catalyzed radical group transfer of vinyl and alkynyl groups from silanes (Scheme 6c). Following irradiation with visible light, the excited photocatalyst $Ir(III)^*$ effects the single-electron oxidation of Bu_3N . Subsequent deprotonation of the resulting aminium radical **14** generates the key α -aminoalkyl radical **15**, which partakes in XAT with iodide **4**. The resulting α -iodoamine **16** rapidly collapses into iminium ion **17**, which is then reduced by $Ir(II)$ to regenerate the ground-state photocatalyst and the α -aminoalkyl radical **15**. Alkyl radical **18**, meanwhile, undergoes fast 5-*exo* cyclization to radical **19**, which propagates the reaction through a radical chain mechanism. Nucleophilic attack on the cyclized iodide intermediate **12** by methanol leads to the ring-opened siloxane **5**. Once the group transfer reaction is complete, addition of acid triggers solvolysis into alcohol **6**.

CONCLUSIONS

We have successfully developed a general protocol for the photoredox-catalyzed radical group transfer of vinyl and alkynyl silanes. Our method enables the incorporation of alkenes and alkynes on sp^3 positions, using either activated or unactivated alkyl iodides as radical precursors. The protocol exhibits high diastereoselectivity and broad functional group tolerance and does not require the use of a fluoride source to drive the ring-opening of the cyclic siloxane intermediate. Instead, we have found that the use of a nucleophilic solvent, which is not compatible with established conventional radical initiators, can promote ring opening to directly yield the group transfer product. Having investigated the mechanism of the reaction, we have identified an XAT reaction coupled with reductive regeneration of the α -aminoalkyl radical halogen abstractor. This unusual dual catalytic cycle results in an overall redox-neutral radical group transfer reaction that can be performed with catalytic amounts of amine. We expect that this process can also be applied in the initiation of other radical transformations, and that the improved understanding of the

reactivity of silicon-based radical acceptors can be exploited in the synthesis of complex molecular scaffolds through radical cyclization/fragmentation strategies.³⁵

EXPERIMENTAL SECTION

All reagents, purchased from Acros, Alfa, Sigma-Aldrich, TCI and VWR, were used as supplied. All air- and/or water-sensitive reactions were carried out under an atmosphere of argon in flame-dried glassware using standard Schlenk techniques. Anhydrous solvents were dried by pre-storing over activated 3 Å (MeOH) or 4 Å (all other solvents) molecular sieves and purged by argon sparging. Blue light irradiation was performed with RGB LED strips (5.4 W). Reactions were monitored by thin-layer chromatography (TLC) on pre-coated aluminum-based plates (TLC Silica gel 60 F₂₅₄, Supelco). The plates were developed under UV irradiation (254 nm) or with vanillin or $KMnO_4$ staining and subsequent heating. Column chromatography was performed with silica gel (Silica gel 60, irregular 40–63 μm for flash chromatography, VWR Chemicals). ¹H NMR spectra were recorded at room temperature on a 400 MHz Bruker 9.4 Tesla Avance III HD system equipped with a SmartProbe (broad band). ¹³C NMR spectra (¹H decoupled) were recorded at room temperature on the same machine operating at 101 MHz. All chemical shifts (δ) are reported in parts per million (ppm) with internal reference to residual protons/carbons in $CDCl_3$ (δ 7.26/77.16) or $MeCN-d_3$ (δ 1.94/118.26). Coupling constants (J) are given in Hz with an accuracy of 0.1 Hz. Infrared (IR) spectra were recorded as thin films or liquids on an Agilent Technologies Cary 630 FTIR 318 spectrometer. Wavelength of maximum absorbance (λ_{max}) is reported in wavenumbers (cm^{-1}). Only selected characteristic resonances are reported. High-resolution mass spectra (HRMS) were recorded by direct injection of the compounds as solutions in MeOH on a Thermo Scientific Orbitrap Exploris 120 Mass spectrometer, using dual electrospray ionization (ESI) and atmospheric pressure chemical ionization (APCI) probes. Characterization of compounds **1–4v** and ¹H and ¹³C NMR spectra of all compounds are provided in the Supporting Information.

Procedure 1 for the Synthesis of Epoxides 2. Based on a literature procedure,³⁶ aqueous 2 M NaOH was added to an aqueous 4×10^{-4} M EDTA solution (0.3 M with respect to the olefin) until pH 4. The mixture was added to a solution of olefin (1.0 equiv) in acetonitrile (85 mM with respect to the olefin). Sodium chlorite (3.1 equiv) was added, the reaction flask was equipped with a condenser, and the reaction mixture was stirred at 65 °C overnight. The colorless mixture turned yellow. It was cooled to 0 °C, and the mixture was slowly quenched by dropwise addition of an aqueous 1 M $Na_2S_2O_3$ solution until no more peroxide was detected by starch/iodide paper. The colorless quenched mixture was reduced in vacuo before being extracted with CH_2Cl_2 (3×15 mL). The combined organic layers were washed with water and brine, dried over anhydrous Na_2SO_4 , filtered, and concentrated in vacuo. The crude material was purified by column chromatography to afford the desired epoxide.

Procedure II for the Synthesis of Epoxides 2. Based on a literature procedure,³⁷ hydrogen peroxide (30% in water, 6.0 equiv) was added to a mixture of olefin (1.0 equiv) and sodium bicarbonate (4.0 equiv) in acetonitrile/water 3:2 (50 mM with respect to the olefin). The reaction mixture was stirred at room temperature for 48 h before being quenched by slow addition of 1 M Na₂S₂O₃ until no more peroxide was detected by starch/iodide paper. The mixture was reduced in vacuo, and the residue was extracted with EtOAc (3 × 10 mL). The combined organic layers were washed with brine, dried over anhydrous Na₂SO₄, filtered and concentrated in vacuo. The crude material was purified by column chromatography to afford the desired epoxide.

Procedure A for the Synthesis of Iodohydrins 3. Based on a literature procedure,³⁸ N-iodosuccinimide (1.1 equiv) and distilled water (1.0 M with respect to the olefin) were added to a mixture of olefin (1.0 equiv) and ammonium acetate (0.1 equiv) in acetone (0.25 M with respect to the olefin). The reaction mixture was stirred in the dark at room temperature. Upon completion as indicated by TLC, the mixture was concentrated in vacuo, and the residue was redissolved in water and extracted with ethyl acetate (3 × 10 mL). The combined organic layers were washed with an aqueous 10% solution of Na₂S₂O₃, dried over anhydrous Na₂SO₄, filtered, and concentrated in vacuo. The crude material was purified by column chromatography to afford the desired iodohydrin.

Procedure B for the Synthesis of Iodohydrins 3. Hydroiodic acid (57 wt % in H₂O, 1.2 equiv) was added to a solution of epoxide 2 (1.0 equiv) in CH₂Cl₂ (0.5 M with respect to the epoxide), and the reaction mixture was stirred in the dark at room temperature. Upon completion as indicated by TLC, the mixture was diluted with CH₂Cl₂ (20 mL). It was washed with an aqueous 10% solution of NaHCO₃, an aqueous 10% solution of Na₂S₂O₃, dried over anhydrous Na₂SO₄, filtered, and concentrated in vacuo. The crude material was purified by column chromatography to afford the desired iodohydrin.

Procedure C for the Synthesis of Vinyl Silanes 4. Chloro-(dimethyl)vinylsilane (1.1 equiv) was added to a mixture of iodohydrin 3 (1.0 equiv), 4-dimethylaminopyridine (0.2 equiv), and Et₃N (1.2 equiv) in dry CH₂Cl₂ (0.1 M with respect to the iodohydrin) under Ar. The reaction mixture was stirred for 20 min in the dark at room temperature. The reaction was quenched by slowly adding a few drops of isopropanol, and the mixture was concentrated in vacuo. The residue was redissolved in water and extracted with Et₂O (3 × 10 mL). The combined organic layers were washed with a saturated aqueous NaHCO₃ solution and brine, dried over anhydrous Na₂SO₄, filtered, and concentrated in vacuo. The crude material was purified by column chromatography to afford the desired vinyl silane.

Procedure D for the Synthesis of Siloxanes 5. Vinyl silane 4 (1.0 equiv) was added to a mixture of [Ir(dtbbpy)(ppy)₂](PF₆)₂ (2.5 mol %) and Bu₃N (2.0 equiv) in dry MeCN/MeOH 9:1 (0.1 M with respect to the silane) under Ar. The mixture was degassed by Ar sparging for 5 min before placing the reaction vial 1 cm away from the light source. A fan was placed on top of the setup to keep the reaction environment at room temperature. The reaction mixture was irradiated with blue LED light until full consumption of the substrate as indicated by TLC. The mixture was reduced in vacuo, and the crude material was purified by column chromatography to afford the desired siloxane.

Methoxydimethyl((2-vinyl-2,3-dihydro-1H-inden-1-yl)oxy)-silane (5a) was synthesized from vinyl silane 4a (42 mg, 0.12 mmol, 1.0 equiv), [Ir(dtbbpy)(ppy)₂](PF₆)₂ (2.5 mg, 2.7 μmol, 2.2 mol %), and Bu₃N (58 μL, 0.24 mmol, 2.0 equiv) in MeCN/MeOH 9:1 (1.2 mL) according to Procedure D. The crude was purified by column chromatography (Et₂O/pentane 5%) to afford siloxane 5a (20 mg, 79 μmol, 65%) as a colorless oil. *R*_f 0.27 (Et₂O/pentane 2.5%); IR (liquid, ν_{\max} /cm⁻¹) 2962, 2940, 2910, 2840, 1261, 1063, 1022, 989, 888, 851, 799, 754; ¹H NMR (400 MHz, CDCl₃) δ 7.40–7.34 (1H, m, ArH), 7.30–7.26 (1H, m, ArH), 7.23 (2H, m, ArH), 6.05 (1H, ddd, *J* = 17.3, 10.3, 7.8 Hz, CHCH₂), 5.26 (1H, d, *J* = 5.4 Hz, CHO), 5.18 (1H, ddd, *J* = 17.4, 2.1, 0.9 Hz, CHCH₂), 5.13 (1H, ddd, *J* = 10.4, 2.1, 0.6 Hz, CHCH₂), 3.49 (3H, s, OCH₃), 3.11–2.92 (3H, m, CH(CHCH₂), CH₂), 0.20 (3H, s, Si(CH₃)₂), 0.17 (3H, s, Si(CH₃)₂);

¹³C{¹H} NMR (CDCl₃, 101 MHz) δ 144.6, 142.9, 138.4, 128.3, 126.7, 124.9, 124.8, 115.9, 77.7, 50.39, 50.37, 36.5, -2.76, -2.81; HRMS (ESI) calc. for C₁₄H₂₀O₂SiNa ([M + Na]⁺) 271.1125, found 271.1124.

Methoxydimethyl(oct-1-en-4-yloxy)silane (5k) was synthesized from vinyl silane 4k (0.21 g, 0.68 mmol, 1.0 equiv), [Ir(dtbbpy)(ppy)₂](PF₆)₂ (15 mg, 16 μmol, 2.4 mol %), and Bu₃N (0.35 mL, 1.5 mmol, 2.2 equiv) in MeCN/MeOH 9:1 (7.7 mL) according to Procedure D. The crude was purified by column chromatography (Et₂O/pentane 2.5%) to afford an inseparable 1:2 mixture of substrate 4k (6.3 mg, 20 μmol) and siloxane 5k (8.7 mg, 40 μmol, 6%) as a colorless oil. *Note: the NMR data were extracted from the analysis of the inseparable mixture.* *R*_f 0.26 (Et₂O/pentane 2.5%); IR (liquid, ν_{\max} /cm⁻¹) 2959, 2933, 2862, 1256, 1085, 1057, 914, 837, 788, 729; ¹H NMR (400 MHz, CDCl₃) δ 5.90–5.75 (1H, m, CHCH₂), 5.12–4.99 (2H, m, CHCH₂), 3.80 (1H, m, CHO), 3.49 (3H, s, OCH₃), 2.25 (2H, m, CHOCH₂CHCH₂), 1.54–1.40 (2H, m, CH₂CHO), 1.40–1.19 (4H, m, 2 × CH₂), 0.94–0.85 (3H, m, CH₃), 0.13 (6H, s, Si(CH₃)₂); ¹³C{¹H} NMR (CDCl₃, 101 MHz) δ 135.4, 117.0, 72.3, 50.3, 42.1, 36.7, 27.9, 22.9, 14.2, -2.87, -2.92; HRMS (ESI) calc. for C₁₁H₂₄O₂SiNa ([M + Na]⁺) 239.1438, found 239.1437.

Methoxydimethyl((1-phenylbut-3-en-1-yl)oxy)silane (5n) was synthesized from vinyl silane 4n (1.0 g, 3.1 mmol, 1.0 equiv), [Ir(dtbbpy)(ppy)₂](PF₆)₂ (65 mg, 71 μmol, 2.3 mol %), and Bu₃N (1.4 mL, 5.9 mmol, 1.9 equiv) in MeCN/MeOH 9:1 (30 mL) according to Procedure D. The crude was purified by column chromatography (Et₂O/pentane 5%) to afford siloxane 5n (0.17 g, 0.73 mmol, 24%) as a colorless oil. *R*_f 0.37 (Et₂O/pentane 5%); IR (liquid, ν_{\max} /cm⁻¹) 2961, 2836, 1258, 1193, 1081, 1068, 994, 916, 845, 795, 700; NMR (400 MHz, CDCl₃) δ 7.36–7.28 (4H, m, ArH), 7.26–7.21 (1H, m, ArH), 5.78 (1H, ddt, *J* = 17.2, 10.2, 7.0 Hz, CHCH₂), 5.09–4.99 (2H, m, CHCH₂), 4.81 (1H, m, CHO), 3.34 (3H, s, OCH₃), 2.59–2.39 (2H, m, CHOCH₂), 0.10 (3H, s, Si(CH₃)₂), 0.02 (3H, s, Si(CH₃)₂); ¹³C{¹H} NMR (CDCl₃, 101 MHz) δ 144.5, 135.1, 128.3 (2C), 127.3, 126.1 (2C), 117.3, 74.7, 50.3, 45.0, -2.99, -3.05; HRMS (ESI) calc. for C₁₃H₂₀O₂SiNa ([M + Na]⁺) 259.1125, found 259.1122.

Procedure E for the Synthesis of Homoallylic Alcohols 6 and Homopropargylic Alcohols 8. Silylated substrate 4 or 7 (1.0 equiv) was added to a mixture of [Ir(dtbbpy)(ppy)₂](PF₆)₂ (2.5 mol %) and Bu₃N (2.0 equiv) in dry MeCN/MeOH 9:1 (0.1 M with respect to the silane) under Ar. The mixture was degassed by Ar sparging for 5 min before placing the reaction vial 1 cm away from the light source. A fan was placed on top of the setup to keep the reaction environment at room temperature. The reaction mixture was irradiated with blue LED light until full consumption of the substrate as indicated by TLC. After turning off the blue LED light, a solution of HCl 1.25 M in MeOH (2.0 equiv) was added, and the reaction mixture was stirred for 10 min at room temperature. Brine (2 mL) was added before concentrating the mixture in vacuo. The residue was further diluted with brine (10 mL) before being extracted with EtOAc (3 × 5 mL). The combined organic layers were washed with an aqueous 10% NaHCO₃ solution and brine, dried over anhydrous Na₂SO₄, filtered, and concentrated in vacuo. The crude material was purified by column chromatography to afford the desired product.

2-Vinyl-2,3-dihydro-1H-inden-1-ol (6a) was synthesized from vinyl silane 4a (0.11 g, 0.31 mmol, 1.0 equiv; *gram scale: 1.0 g, 3.0 mmol, 1.0 equiv*), [Ir(dtbbpy)(ppy)₂](PF₆)₂ (6.4 mg, 7.0 μmol, 2.4 mol %; *gram scale: 59 mg, 65 μmol, 2.2 mol %*), Bu₃N (0.14 mL, 0.59 mmol, 1.9 equiv; *gram scale: 1.4 mL, 6.0 mmol, 2.0 equiv*) in MeCN/MeOH 9:1 (3 mL; *gram scale: 30 mL*) and HCl 1.25 M in MeOH (0.50 mL, 0.63 mmol, 2.0 equiv; *gram scale: 4.8 mL, 6.0 mmol, 2.0 equiv*) according to Procedure E. The crude was purified by column chromatography (IPA/CH₂Cl₂ 1%) to afford 6a (42 mg, 0.26 mmol, 84%; *gram scale: 0.38 g, 2.3 mmol, 78%*) as a colorless oil. ¹H NMR (400 MHz, CDCl₃) δ 7.44 (1H, d, *J* = 6.8 Hz, ArH), 7.28 (3H, d, *J* = 3.6 Hz, ArH), 5.99 (1H, ddd, *J* = 17.8, 10.5, 7.8 Hz, CHCH₂), 5.30 (1H, d, *J* = 9.0 Hz, CHCH₂), 5.27 (1H, s, CHCH₂), 5.10 (1H, t, *J* = 5.2 Hz, CHO), 3.15 (1H, p, *J* = 7.1 Hz, CH(CHCH₂)), 3.02 (2H, d, *J* = 7.1 Hz, CH₂), 1.82 (1H, d, *J* = 4.8 Hz, OH); ¹³C{¹H} NMR

(CDCl₃, 101 MHz) δ 144.3, 142.7, 137.0, 128.6, 126.9, 125.1, 124.9, 117.9, 77.2, 49.6, 35.4. Data consistent with literature values.³⁹

2-Ethynylcyclopentanol (6b) was synthesized from vinyl silane **4b** (91 mg, 0.31 mmol, 1.0 equiv), [Ir(dtbbpy)(ppy)₂]₂PF₆ (6.4 mg, 7.0 μ mol, 2.2 mol %), Bu₃N (0.14 mL, 0.59 mmol, 1.9 equiv) in MeCN/MeOH 9:1 (3 mL), and HCl 1.25 M in MeOH (0.50 mL, 0.63 mmol, 2.0 equiv) according to Procedure E. The crude was purified by column chromatography (IPA/CH₂Cl₂ 0.5%) to afford **6b** (11 mg, 0.10 mmol, 33%) as a colorless oil. ¹H NMR (400 MHz, CDCl₃) δ 5.95 (1H, ddd, *J* = 17.3, 10.6, 6.8 Hz, CHCH₂), 5.24–5.10 (2H, m, CHCH₂), 4.16 (1H, dh, *J* = 6.7, 2.2 Hz, CHOH), 2.47 (1H, tddt, *J* = 8.1, 6.7, 4.4, 1.4 Hz, CH(CHCH₂)), 1.86 (2H, tdd, *J* = 12.4, 9.1, 5.9 Hz, CH₂), 1.79–1.53 (4H, m, 2 \times CH₂), 1.42 (1H, d, *J* = 3.0 Hz, OH); ¹³C{¹H} NMR (CDCl₃, 101 MHz) δ 137.7, 117.0, 75.4, 49.8, 34.2, 27.5, 22.1. Data consistent with literature values.⁴⁰

2-Vinylcyclohexan-1-ol (6c) was synthesized from vinyl silane **4c** (94 mg, 0.30 mmol, 1.0 equiv), [Ir(dtbbpy)(ppy)₂]₂PF₆ (6.3 mg, 7.0 μ mol, 2.3 mol %), Bu₃N (0.14 mL, 0.59 mmol, 1.9 equiv) in MeCN/MeOH 9:1 (3 mL), and HCl 1.25 M in MeOH (0.50 mL, 0.63 mmol, 2.1 equiv) according to Procedure E. The crude was purified by column chromatography (IPA/CH₂Cl₂ 1%). A short second column chromatography (IPA/CH₂Cl₂ 0.5%) afforded **6c** (20 mg, 0.16 mmol, 53%) as a colorless oil. ¹H NMR (400 MHz, CDCl₃) δ 5.94 (1H, ddd, *J* = 17.3, 10.6, 6.6 Hz, CHCH₂), 5.25–5.02 (2H, m, CHCH₂), 3.86 (1H, s, CHOH), 2.27 (1H, dd, *J* = 10.4, 5.8 Hz, CH(CHCH₂)), 1.83–1.20 (9H, m, 4 \times CH₂, OH); ¹³C{¹H} NMR (CDCl₃, 101 MHz) δ 140.0, 116.1, 69.4, 45.4, 32.3, 25.7, 24.4, 21.0. Data consistent with literature values.⁴¹

tert-Butyl 3-hydroxy-4-vinylpyrrolidine-1-carboxylate (6d) was synthesized from vinyl silane **4d** (0.12 mg, 0.29 mmol, 1.0 equiv), [Ir(dtbbpy)(ppy)₂]₂PF₆ (6.4 mg, 7.0 μ mol, 2.4 mol %), Bu₃N (0.14 mL, 0.59 mmol, 2.0 equiv) in MeCN/MeOH 9:1 (3 mL), and HCl 1.25 M in MeOH (0.50 mL, 0.63 mmol, 2.1 equiv) according to Procedure E. The crude was purified by column chromatography (IPA/CH₂Cl₂ 2%) to afford **6d** (49 mg, 0.23 mmol, 78%) as a colorless oil. ¹H NMR (400 MHz, CDCl₃, mixture of rotamers) δ 5.89 (1H, dddd, *J* = 14.8, 11.0, 6.9, 4.5 Hz, CH(CHCH₂)), 5.31–5.12 (2H, m, CH(CHCH₂)), 4.24 (1H, dd, *J* = 3.6, 2.1 Hz, CHOH), 3.61–3.40 (3H, m, 3 \times CH₂), 3.34 (1H, dt, *J* = 12.4, 10.5 Hz, CH₂), 2.84–2.71 (1H, m, CH(CHCH₂)), 2.27 (1H, dd, *J* = 48.5, 3.5 Hz, OH), 1.43 (9H, s, 3 \times CH₃); ¹³C{¹H} NMR (CDCl₃, 101 MHz, mixture of rotamers) δ 154.8, 133.9, 133.7, 119.0, 118.6, 79.5, 72.8, 72.2, 54.3, 54.2, 48.1, 47.7, 47.2, 47.1, 28.6. Data consistent with literature values.⁴²

4-(2-Benzoyloxy)propan-2-yl)-1-methyl-2-vinylcyclohexan-1-ol (6e) was synthesized from vinyl silane **4e** (0.14 g, 0.30 mmol, 1.0 equiv), [Ir(dtbbpy)(ppy)₂]₂PF₆ (6.3 mg, 7.0 μ mol, 2.4 mol %), Bu₃N (0.14 mL, 0.60 mmol, 2.0 equiv) in MeCN/MeOH 9:1 (3 mL), and HCl 1.25 M in MeOH (0.50 mL, 0.63 mmol, 2.1 equiv) according to Procedure E. The crude was purified by column chromatography (IPA/CH₂Cl₂ 0.5–1%). A short second column chromatography (Et₂O/pentane 30%) afforded **6e** (51 mg, 0.18 mmol, 59%) as a colorless oil. *R*_f 0.35 (Et₂O/pentane 40%); IR (thin film, ν_{\max} /cm⁻¹) 2969, 2933, 2869, 1455, 1385, 1368, 1174, 1129, 1088, 1059, 1030, 998, 911, 734, 698; ¹H NMR (400 MHz, CDCl₃) δ 7.39–7.19 (5H, m, ArH), 5.94 (1H, ddd, *J* = 17.2, 10.5, 8.1 Hz, CHCH₂), 5.19–5.02 (2H, m, CHCH₂), 4.44 (2H, s, OCH₂Ph), 2.00 (1H, ddd, *J* = 12.0, 8.1, 3.6 Hz, CH(CHCH₂)), 1.79 (1H, dt, *J* = 9.8, 2.6 Hz, CH₂C(CH₃)OH), 1.73–1.56 (3H, m, 2 \times CH₂, CHC(CH₃)₂), 1.53–1.34 (3H, m, 2 \times CH₂, CH₂C(CH₃)OH), 1.23 (7H, d, *J* = 2.7 Hz, C(CH₃)₂, OH), 1.19 (3H, s, C(CH₃)OH); ¹³C{¹H} NMR (CDCl₃, 101 MHz) δ 140.2, 139.5, 128.4 (2C), 127.3 (2C), 127.1, 116.3, 77.3, 70.1, 63.3, 50.9, 46.1, 40.0, 29.3, 28.6, 23.1, 23.0, 22.7; HRMS (ESI) calc. for C₁₉H₂₈O₂Na ([M + Na]⁺) 311.1982, 311.1981.

2-Methyl-1-phenylbut-3-en-1-ol (6f) was synthesized from vinyl silane **4f** (0.10 g, 0.30 mmol, 1.0 equiv), [Ir(dtbbpy)(ppy)₂]₂PF₆ (6.2 mg, 7.0 μ mol, 2.2 mol %), Bu₃N (0.14 mL, 0.59 mmol, 2.0 equiv) in MeCN/MeOH 9:1 (3 mL), and HCl 1.25 M in MeOH (0.50 mL, 0.63 mmol, 2.1 equiv) according to Procedure E. The crude was purified by column chromatography (IPA/CH₂Cl₂ 1%) to afford an

inseparable 87:13 diastereomers mixture of **6f** (35 mg, 0.22 mmol, 72%) as a colorless oil. *Note: the NMR data were extracted from the analysis of the inseparable mixture.* ¹H NMR (400 MHz, CDCl₃, major) δ 7.45–7.12 (5H, m, ArH), 5.79 (1H, dt, *J* = 17.8, 9.1 Hz, CHCH₂), 5.25–5.08 (2H, m, CHCH₂), 4.33 (1H, d, *J* = 7.9 Hz, CHOH), 2.46 (1H, h, *J* = 7.5 Hz, CHCH₃), 2.18 (1H, s, OH), 0.85 (3H, d, *J* = 6.8 Hz, CH₃); ¹³C NMR (CDCl₃, 101 MHz, major) δ 142.6, 140.8, 128.3 (2C), 127.7, 127.0 (2C), 116.9, 78.0, 46.4, 16.6. ¹H NMR (400 MHz, CDCl₃, minor) δ 7.45–7.12 (5H, m, ArH), 5.70 (1H, d, *J* = 8.6 Hz, CHCH₂), 5.09–4.93 (2H, m, CHCH₂), 4.57 (1H, t, *J* = 4.3 Hz, CHOH), 2.56 (1H, q, *J* = 6.8 Hz, CHCH₃), 0.99 (3H, d, *J* = 6.9 Hz, CH₃); ¹³C{¹H} NMR (CDCl₃, 101 MHz, minor) δ 142.7, 140.4, 128.2 (2C), 127.4, 126.6 (2C), 115.6, 77.4, 44.8, 14.1. Data consistent with literature values.⁴³

5-Vinylcyclohexan-1-ol (6g) was synthesized from vinyl silane **4g** (0.10 g, 0.30 mmol, 1.0 equiv), [Ir(dtbbpy)(ppy)₂]₂PF₆ (6.6 mg, 7.2 μ mol, 2.4 mol %), Bu₃N (0.14 mL, 0.59 mmol, 1.9 equiv) in MeCN/MeOH 9:1 (3 mL), and HCl 1.25 M in MeOH (0.50 mL, 0.63 mmol, 2.1 equiv) according to Procedure E. The crude was purified by column chromatography (IPA/CH₂Cl₂ 0.5%) to afford an inseparable 86:14 diastereomers mixture of **6g** (27 mg, 0.17 mmol, 56%) as a colorless oil. *Note: the NMR data were extracted from the analysis of the inseparable mixture.* *R*_f 0.36 (IPA/CH₂Cl₂ 1%); IR (thin film, ν_{\max} /cm⁻¹) 3351, 2958, 2930, 2874, 1639, 1467, 1459, 1423, 1380, 1119, 1060, 1022, 912, 848; ¹H NMR (400 MHz, CDCl₃, major) δ 5.63 (1H, m, (CHCH₂)), 5.22–5.00 (2H, m, (CHCH₂)), 3.45 (1H, m, CHOH), 2.04–1.96 (1H, m, CH(CHCH₂)), 1.60–1.13 (9H, m, 4 \times CH₂, OH), 0.90 (6H, m, 2 \times CH₃); ¹³C{¹H} NMR (CDCl₃, 101 MHz, major) δ 139.1, 117.8, 73.5, 50.3, 37.0, 33.1, 20.6, 19.1, 14.3, 14.2. ¹H NMR (400 MHz, CDCl₃, minor) δ 5.63 (1H, m, (CHCH₂)), 5.22–5.00 (2H, m, (CHCH₂)), 3.45 (1H, m, CHOH), 2.12–2.07 (1H, m, CH(CHCH₂)), 1.60–1.13 (9H, m, 4 \times CH₂, OH), 0.90 (6H, m, 2 \times CH₃); ¹³C{¹H} NMR (CDCl₃, 101 MHz, minor) δ 139.5, 117.1, 74.3, 50.7, 36.2, 32.3, 20.6, 19.4, 14.2 (2C); HRMS (ESI) calc. for C₁₀H₂₀O₂Na ([M + Na]⁺) 179.1406, found 179.1406.

1-Phenyl-2-vinylpropane-1,3-diol (6h) was synthesized from vinyl silane **4h** (0.14 g, 0.30 mmol, 1.0 equiv), [Ir(dtbbpy)(ppy)₂]₂PF₆ (6.8 mg, 7.3 μ mol, 2.4 mol %), Bu₃N (0.14 mL, 0.59 mmol, 1.9 equiv) in MeCN/MeOH 9:1 (3 mL), and HCl 1.25 M in MeOH (0.50 mL, 0.63 mmol, 2.1 equiv) according to Procedure E. The crude was purified by column chromatography (Et₂O/pentane 20%). A short second column chromatography (IPA/CH₂Cl₂ 1–5%) afforded an inseparable 87:13 diastereomers mixture of **6h** (9.6 mg, 54 μ mol, 18%) as a colorless oil. *Note: the NMR data were extracted from the analysis of the inseparable mixture.* ¹H NMR (400 MHz, CDCl₃, major) δ 7.35–7.11 (5H, m, ArH), 5.74 (1H, ddd, *J* = 17.4, 10.5, 8.7 Hz, CHCHCH₂), 5.24–5.16 (1H, m, CHCHCH₂), 5.10 (1H, m, CHCHCH₂), 4.75 (1H, m, ArCHOH), 3.55 (2H, m, CH₂OH), 2.53 (1H, m, ArCH(OH)CH), 2.35 (1H, d, *J* = 3.2 Hz, ArCHOH), 1.66–1.63 (1H, m, CH₂OH); ¹³C{¹H} NMR (CDCl₃, 101 MHz, major) δ 142.2, 135.4, 128.5 (2C), 127.9, 126.6 (2C), 119.9, 75.1, 63.9, 53.7. ¹H NMR (400 MHz, CDCl₃, minor) δ 7.36–7.10 (5H, m, ArH), 5.53 (1H, m, CHCHCH₂), 5.03–4.90 (2H, m, CHCHCH₂), 4.71 (1H, m, ArCHOH), 3.83–3.75 (1H, m, CH₂OH), 3.71 (1H, m, CH₂OH), 2.60 (2H, m, ArCH(OH)CH, ArCHOH); ¹³C{¹H} NMR (CDCl₃, 101 MHz, minor) δ 142.7, 135.6, 128.5 (2C), 128.0, 126.8 (2C), 118.4, 77.3, 65.0, 52.3. Data consistent with literature values.⁴⁴

2-Vinylhexan-1,3-diol (6i) was synthesized from vinyl silane **4i** (0.13 g, 0.29 mmol, 1.0 equiv), [Ir(dtbbpy)(ppy)₂]₂PF₆ (6.4 mg, 7.0 μ mol, 2.3 mol %), Bu₃N (0.14 mL, 0.59 mmol, 2.0 equiv) in MeCN/MeOH 9:1 (3 mL), and HCl 1.25 M in MeOH (0.50 mL, 0.63 mmol, 2.2 equiv) according to Procedure E. The crude was purified by column chromatography (IPA/CH₂Cl₂ 1–5%). A short second column chromatography (Et₂O/pentane 10–100%) afforded an inseparable 88:12 diastereomers mixture of **6i** (12 mg, 84 μ mol, 29%) as a colorless oil. *Note: the NMR data were extracted from the analysis of the inseparable mixture.* ¹H NMR (400 MHz, CDCl₃, major) δ 5.85 (1H, ddd, *J* = 17.3, 10.4, 8.8 Hz, CH(CHCH₂)), 5.27–5.24 (1H, m, CH(CHCH₂)), 5.16–5.15 (1H, m, CH(CHCH₂)), 3.83–3.73 (3H, m, CHOH, CH₂OH), 2.33–2.27 (1H, m, CH(CHCH₂)),

2.24 (1H, m, CHO), 2.18–2.17 (1H, m, CH₂OH), 1.52–1.30 (4H, m, 4 × CH₂), 0.94–0.91 (3H, m, CH₃); ¹³C{¹H} NMR (CDCl₃, 101 MHz, *major*) δ 134.9, 119.1, 72.7, 64.9, 50.9, 37.2, 19.1, 14.2. ¹H NMR (400 MHz, CDCl₃, *minor*) δ 5.69–5.60 (1H, m, CH(CHCH₂)), 5.27–5.08 (2H, m, CH(CHCH₂)), 3.83–3.73 (3H, m, CHO, CH₂OH), 2.33–2.27 (1H, m, CH(CHCH₂)), 2.24 (1H, m, CHO), 2.18–2.17 (1H, m, CH₂OH), 1.52–1.30 (4H, m, 4 × CH₂), 0.94–0.91 (3H, m, CH₃); ¹³C{¹H} NMR (CDCl₃, 101 MHz, *minor*) δ 136.4, 118.2, 74.6, 65.4, 51.7, 37.8, 18.6, 14.2. Data consistent with literature values.⁴⁵

2-Vinylhexan-1-ol (6j) was synthesized from vinyl silane **4j** (99 mg, 0.29 mmol, 1.0 equiv), [Ir(dtbbpy)(ppy)₂]₂PF₆ (6.5 mg, 7.1 μmol, 2.5 mol %), Bu₃N (0.14 mL, 0.59 mmol, 2.1 equiv) in MeCN/MeOH 9:1 (3 mL), and HCl 1.25 M in MeOH (0.50 mL, 0.63 mmol, 2.2 equiv) according to Procedure E. The crude was purified by column chromatography (IPA/CH₂Cl₂ 1%). A short second column chromatography (Et₂O/pentane 50%) afforded **6j** (20 mg, 0.15 mmol, 53%) as a colorless oil. ¹H NMR (400 MHz, CDCl₃) δ 5.58 (1H, dt, *J* = 18.0, 9.6 Hz, CHCH₂), 5.13 (2H, dd, *J* = 13.7, 9.6 Hz, CHCH₂), 3.55 (1H, q, *J* = 5.4 Hz, CH₂OH), 3.40 (1H, t, *J* = 9.4 Hz, CH₂OH), 2.30–2.08 (1H, m, CH(CHCH₂)), 1.51 (1H, s, OH), 1.46–1.16 (6H, m, 3 × CH₂), 0.88 (3H, t, *J* = 6.6 Hz, CH₃); ¹³C{¹H} NMR (CDCl₃, 101 MHz) δ 140.3, 117.3, 65.8, 47.2, 30.5, 29.4, 22.9, 14.1. Data consistent with literature values.⁴⁶

Oct-1-en-4-ol (6k) was synthesized from vinyl silane **4k** (78 mg, 0.25 mmol, 1.0 equiv), [Ir(dtbbpy)(ppy)₂]₂PF₆ (5.2 mg, 5.7 μmol, 2.3 mol %), Bu₃N (0.12 mL, 0.48 mmol, 1.9 equiv) in MeCN/MeOH 9:1 (2.5 mL), and HCl 1.25 M in MeOH (0.40 mL, 0.51 mmol, 2.1 equiv) according to Procedure E. The crude was purified by column chromatography (IPA/CH₂Cl₂ 0.5%) to afford **6k** (6.2 mg, 48 μmol, 20%) as a colorless oil. ¹H NMR (400 MHz, CDCl₃) δ 5.83 (1H, ddd, *J* = 17.4, 14.7, 7.7 Hz, CHCH₂), 5.22–5.04 (2H, m, CHCH₂), 3.64 (1H, t, *J* = 6.3 Hz, CHO), 2.31 (1H, dt, *J* = 11.6, 5.3 Hz, CH₂CHCH₂), 2.14 (1H, dt, *J* = 14.7, 7.9 Hz, CH₂CHCH₂), 1.63–1.20 (9H, m, 3 × CH₂, OH), 0.91 (3H, t, *J* = 6.8 Hz, CH₃); ¹³C{¹H} NMR (CDCl₃, 101 MHz) δ 135.1, 118.2, 70.8, 42.1, 36.7, 28.0, 22.9, 14.2. Data consistent with literature values.⁴⁷

1-Phenylhex-5-en-3-ol (6l) was synthesized from vinyl silane **4l** (59 mg, 0.16 mmol, 1.0 equiv), [Ir(dtbbpy)(ppy)₂]₂PF₆ (3.4 mg, 3.8 μmol, 2.3 mol %), Bu₃N (76 μL, 0.32 mmol, 1.9 equiv) in MeCN/MeOH 9:1 (1.7 mL) and HCl 1.25 M in MeOH (0.27 mL, 0.34 mmol, 2.1 equiv) according to Procedure E. The crude was purified by column chromatography (IPA/CH₂Cl₂ 1%) to afford **6l** (6.2 mg, 35 μmol, 22%) as a colorless oil. ¹H NMR (400 MHz, CDCl₃) δ 7.47–7.12 (5H, m, ArH), 5.86 (1H, ddd, *J* = 17.2, 14.6, 7.7 Hz, CHCH₂), 5.28–5.09 (2H, m, CHCH₂), 3.82–3.62 (1H, m, CHO), 2.86 (1H, m, CH₂CH₂CHO), 2.73 (1H, m, CH₂CH₂CHO), 2.37 (1H, m, CHOCH₂CH), 2.23 (1H, m, CHOCH₂CH), 1.84 (2H, m, CH₂CH₂CHO), 1.65 (1H, m, OH); ¹³C{¹H} NMR (CDCl₃, 101 MHz) δ 142.2, 134.7, 128.6 (2C), 128.5 (2C), 126.0, 118.5, 70.1, 42.2, 38.6, 32.2. Data consistent with literature values.⁴⁸

Methyl 4-hydroxyhept-6-enoate (6m) was synthesized from vinyl silane **4m** (0.10 g, 0.30 mmol, 1.0 equiv), [Ir(dtbbpy)(ppy)₂]₂PF₆ (6.6 mg, 7.2 μmol, 2.4 mol %), Bu₃N (0.14 mL, 0.59 mmol, 2.0 equiv) in MeCN/MeOH 9:1 (3 mL) and HCl 1.25 M in MeOH (0.50 mL, 0.63 mmol, 2.1 equiv) according to Procedure E. The crude was purified by column chromatography (IPA/CH₂Cl₂ 2%). A short second column chromatography (Et₂O/pentane 50%) afforded **6m** (8.8 mg, 56 μmol, 19%) as a colorless oil. *R*_f 0.31 (IPA/CH₂Cl₂ 5%); IR (thin film, ν_{max}/cm⁻¹) 3457, 2952, 2923, 1738, 1441, 1357, 1219, 1208, 1170, 1082, 1074, 998, 918; ¹H NMR (400 MHz, CDCl₃) δ 5.82 (1H, m, CHCH₂), 5.20–5.07 (2H, m, CHCH₂), 3.68 (4H, s, CHO, CH₃), 2.48 (2H, td, *J* = 7.3, 2.5 Hz, C(O)CH₂), 2.35–2.24 (1H, m, CH(OH)CH₂CH), 2.19 (1H, m, CH(OH)CH₂CH), 1.92–1.79 (2H, m, CH₂CH(OH), OH), 1.73 (1H, m, CH₂CH(OH)); ¹³C{¹H} NMR (CDCl₃, 101 MHz) δ 174.6, 134.5, 118.6, 70.1, 51.8, 42.2, 31.7, 30.6; HRMS (ESI) calc. for C₈H₁₄O₃Na ([M + Na]⁺) 181.0835, found 181.0834.

1-Phenylbut-3-en-1-ol (6n) was synthesized from vinyl silane **4n** (0.10 g, 0.30 mmol, 1.0 equiv), [Ir(dtbbpy)(ppy)₂]₂PF₆ (6.6 mg, 7.2

μmol, 2.4 mol %), Bu₃N (0.14 mL, 0.59 mmol, 1.9 equiv) in MeCN/MeOH 9:1 (3 mL), and HCl 1.25 M in MeOH (0.50 mL, 0.63 mmol, 2.1 equiv) according to Procedure E. The crude was purified by column chromatography (IPA/CH₂Cl₂ 1%) to afford **6n** (16 mg, 0.11 mmol, 35%) as a colorless oil. ¹H NMR (400 MHz, CDCl₃) δ 7.31–7.10 (5H, m, ArH), 5.71 (1H, ddt, *J* = 17.2, 10.1, 7.2 Hz, CHCH₂), 5.14–4.99 (2H, m, CHCH₂), 4.63 (1H, m, CHO), 2.50–2.32 (2H, m, CHOCH₂), 1.96 (1H, m, OH); ¹³C{¹H} NMR (CDCl₃, 101 MHz) δ 144.0, 134.6, 128.6 (2C), 127.7, 125.9 (2C), 118.6, 73.4, 44.0. Data consistent with literature values.⁴⁹

1-(4-Methoxyphenyl)but-3-en-1-ol (6o) was synthesized from vinyl silane **4o** (0.11 g, 0.30 mmol, 1.0 equiv), [Ir(dtbbpy)(ppy)₂]₂PF₆ (6.6 mg, 7.2 μmol, 2.4 mol %), Bu₃N (0.14 mL, 0.59 mmol, 2.0 equiv) in MeCN/MeOH 9:1 (3 mL) and HCl 1.25 M in MeOH (0.50 mL, 0.63 mmol, 2.1 equiv) according to Procedure E. The crude was purified by column chromatography (IPA/CH₂Cl₂ 0–4%) to afford **6o** (30 mg, 0.17 mmol, 57%) as a colorless oil. ¹H NMR (400 MHz, CDCl₃) δ 7.28 (2H, dd, *J* = 8.6, 1.7 Hz, ArH), 6.89 (2H, dd, *J* = 8.6, 1.8 Hz, ArH), 5.89–5.71 (1H, m, CHCH₂), 5.25–5.06 (2H, m, CHCH₂), 4.76–4.62 (1H, m, CHO), 3.81 (3H, d, *J* = 1.7 Hz, OCH₃), 2.50 (2H, t, *J* = 6.9 Hz, CH(OH)CH₂), 1.96 (1H, dd, *J* = 3.1, 1.6 Hz, OH); ¹³C{¹H} NMR (CDCl₃, 101 MHz) δ 159.2, 136.2, 134.8, 127.2 (2C), 118.4, 114.0 (2C), 73.1, 55.4, 43.9. Data consistent with literature values.⁵⁰

1-(4-(Trifluoromethyl)phenyl)but-3-en-1-ol (6p) was synthesized from vinyl silane **4p** (0.12 g, 0.30 mmol, 1.0 equiv), [Ir(dtbbpy)(ppy)₂]₂PF₆ (7.2 mg, 7.9 μmol, 2.6 mol %), Bu₃N (0.14 mL, 0.59 mmol, 1.9 equiv) in MeCN/MeOH 9:1 (3 mL) and HCl 1.25 M in MeOH (0.50 mL, 0.63 mmol, 2.1 equiv) according to Procedure E. The crude was purified by column chromatography (IPA/CH₂Cl₂ 0.5%) to afford **6p** (24 mg, 0.11 mmol, 37%) as a colorless oil. ¹H NMR (400 MHz, CDCl₃) δ 7.61 (2H, d, *J* = 8.1 Hz, ArH), 7.54–7.41 (2H, m, ArH), 5.87–5.70 (1H, m, CH(OH)-CH₂CHCH₂), 5.25–5.12 (2H, m, CH(OH)CH₂CHCH₂), 4.80 (1H, dt, *J* = 8.1, 3.9 Hz, CHO), 2.60–2.39 (2H, m, CH(OH)-CH₂CHCH₂), 2.19 (1H, d, *J* = 3.3 Hz, OH); ¹³C{¹H} NMR (CDCl₃, 101 MHz) δ 147.9, 133.8, 129.8 (q, ²J_{C-F} = 32.3 Hz), 126.2 (2C), 125.5 (2C, d, ³J_{C-F} = 3.8 Hz), 124.3 (q, ¹J_{C-F} = 272.2 Hz), 119.4, 72.7, 44.0. Data consistent with literature values.⁵¹

3-Phenylpent-4-en-2-ol (6q) was synthesized from vinyl silane **4q** (0.10 g, 0.30 mmol, 1.0 equiv), [Ir(dtbbpy)(ppy)₂]₂PF₆ (6.6 mg, 7.2 μmol, 2.4 mol %), Bu₃N (0.14 mL, 0.59 mmol, 1.9 equiv) in MeCN/MeOH 9:1 (3 mL) and HCl 1.25 M in MeOH (0.50 mL, 0.63 mmol, 2.1 equiv) according to Procedure E. The crude was purified by column chromatography (IPA/CH₂Cl₂ 10.5–1%) to afford **6q** (42 mg, 0.26 mmol, 85%) as a colorless oil. ¹H NMR (400 MHz, CDCl₃) δ 7.37–7.22 (5H, m, ArH), 6.20–6.11 (1H, m, CHCH₂), 5.28–5.24 (2H, m, CHCH₂), 4.01 (1H, dq, *J* = 7.7, 6.2 Hz, CH(CHCH₂)), 3.20 (1H, t, *J* = 8.4 Hz, CHO), 1.96 (1H, m, OH), 1.11 (3H, d, *J* = 6.2 Hz, CH₃); ¹³C{¹H} NMR (CDCl₃, 101 MHz) δ 141.6, 138.6, 128.8 (2C), 128.1 (2C), 126.8, 118.1, 70.3, 59.3, 20.7. Data consistent with literature values.⁵²

3-Hydroxy-4-phenylhex-5-en-2-one (6r) was synthesized from vinyl silane **4r** (0.11 g, 0.30 mmol, 1.0 equiv), [Ir(dtbbpy)(ppy)₂]₂PF₆ (6.6 mg, 7.2 μmol, 2.4 mol %), Bu₃N (0.14 mL, 0.59 mmol, 1.9 equiv) in MeCN/MeOH 9:1 (3 mL) and HCl 1.25 M in MeOH (0.50 mL, 0.63 mmol, 2.1 equiv) according to Procedure E. The crude was purified by column chromatography (IPA/CH₂Cl₂ 0.5–1%). A short second column chromatography (Et₂O/pentane 50%) afforded **6r** (43 mg, 0.22 mmol, 75%) as a yellow oil. ¹H NMR (400 MHz, CDCl₃) δ 7.41–7.32 (4H, m, ArH), 7.27 (1H, m, ArH), 6.09 (1H, ddd, *J* = 17.1, 10.3, 8.9 Hz, CHCH₂), 5.25–5.09 (2H, m, CHCH₂), 4.48 (1H, dd, *J* = 4.9, 3.4 Hz, CHO), 3.76 (1H, dd, *J* = 8.9, 3.5 Hz, CH(CHCH₂)), 3.55 (1H, d, *J* = 5.0 Hz, OH), 2.19 (3H, s, CH₃); ¹³C{¹H} NMR (CDCl₃, 101 MHz) δ 208.6, 140.6, 135.1, 128.8 (2C), 128.2 (2C), 127.1, 118.3, 80.4, 52.8, 26.2. Data consistent with literature values.⁵³

1-Isopropoxy-3-phenylpent-4-en-2-ol (6s) was synthesized from vinyl silane **4s** (82 mg, 0.20 mmol, 1.0 equiv), [Ir(dtbbpy)(ppy)₂]₂PF₆ (4.5 mg, 4.9 μmol, 2.4 mol %), Bu₃N (92 μL, 0.39 mmol, 1.9 equiv) in MeCN/MeOH 9:1 (2 mL) and HCl 1.25 M in MeOH (0.33 mL,

0.41 mmol, 2.0 equiv) according to Procedure E. The crude was purified by column chromatography (IPA/CH₂Cl₂ 0.5–1%) to afford **6s** (28 mg, 0.13 mmol, 63%) as a light-yellow oil. *R*_f 0.26 (Et₂O/pentane 30%); IR (thin film, $\nu_{\text{max}}/\text{cm}^{-1}$) 2972, 2868, 1454, 1382, 1370, 1128, 1076, 916, 760, 701; ¹H NMR (400 MHz, CDCl₃) δ 7.37–7.17 (5H, m, ArH), 6.20 (1H, ddd, *J* = 17.1, 10.3, 8.3 Hz, CHCH₂), 5.25–5.08 (2H, m, CHCH₂), 3.98 (1H, ddt, *J* = 8.1, 6.8, 3.4 Hz, CHOH), 3.48 (1H, p, *J* = 6.1 Hz, CH(CH₃)₂), 3.41 (1H, t, *J* = 8.2 Hz, CH(CH₂CH₂)), 3.33 (1H, dd, *J* = 9.5, 3.1 Hz, CH₂O), 3.15 (1H, dd, *J* = 9.5, 6.8 Hz, CH₂O), 2.51 (1H, d, *J* = 3.7 Hz, OH), 1.11 (6H, dd, *J* = 6.1, 2.2 Hz, 2 × CH₃); ¹³C{¹H} NMR (CDCl₃, 101 MHz) δ 141.3, 138.7, 128.7 (2C), 128.2 (2C), 126.8, 117.1, 73.2, 72.2, 70.1, 53.5, 22.2, 22.1; HRMS (APCI) calc. for C₁₄H₂₁O₂ ([M + H]⁺) 221.1536, found 221.1536.

Methyl 2-(hydroxy(phenyl)methyl)but-3-enoate (6t) was synthesized from vinyl silane **4t** (0.12 g, 0.31 mmol, 1.0 equiv), [Ir(dtbbpy)(ppy)₂]₂PF₆ (6.6 mg, 7.2 μ mol, 2.3 mol %), Bu₃N (0.14 mL, 0.59 mmol, 1.9 equiv) in MeCN/MeOH 9:1 (3 mL) and HCl 1.25 M in MeOH (0.50 mL, 0.63 mmol, 2.0 equiv) according to Procedure E. The crude was purified by column chromatography (IPA/CH₂Cl₂ 0.5–1%). A short second column chromatography (Et₂O/pentane 50%) afforded **6t** (57 mg, 0.28 mmol, 89%) as a colorless oil. ¹H NMR (400 MHz, CDCl₃) δ 7.29 (5H, m, ArH), 6.03–5.85 (1H, m, CHCH₂), 5.25 (1H, m, CHCH₂), 5.14 (1H, m, CHCH₂), 5.01 (1H, m, CHO), 3.59 (3H, m, OCH₃), 3.33 (1H, m, CH(CH₂CH₂)), 2.93 (1H, m, OH); ¹³C{¹H} NMR (CDCl₃, 101 MHz) δ 173.0, 140.8, 131.8, 128.4 (2C), 128.0, 126.4 (2C), 120.8, 74.0, 58.3, 52.1. Data consistent with literature values.⁵⁴

2-(Hydroxy(phenyl)methyl)-N,N-dimethylbut-3-enamide (6u) was synthesized from vinyl silane **4u** (0.13 g, 0.32 mmol, 1.0 equiv), [Ir(dtbbpy)(ppy)₂]₂PF₆ (7.3 mg, 8.0 μ mol, 2.5 mol %), Bu₃N (0.14 mL, 0.59 mmol, 1.9 equiv) in MeCN/MeOH 9:1 (3 mL) and HCl 1.25 M in MeOH (0.50 mL, 0.63 mmol, 2.0 equiv) according to Procedure E. The crude was purified by column chromatography (IPA/CH₂Cl₂ 1%) to afford **6u** (55 mg, 0.25 mmol, 79%) as a yellow oil. *R*_f 0.27 (Et₂O/pentane 80%); IR (thin film, $\nu_{\text{max}}/\text{cm}^{-1}$) 3391, 2931, 1618, 1493, 1453, 1400, 1145, 1058, 922, 702; ¹H NMR (400 MHz, CDCl₃) δ 7.33–7.13 (5H, m, ArH), 5.76 (1H, ddd, *J* = 17.4, 10.3, 8.1 Hz, CHCH₂), 5.21–5.11 (1H, m, CHCH₂), 5.08 (1H, m, CHO), 4.98–4.92 (1H, m, OH), 4.85 (1H, m, CHCH₂), 3.38 (1H, dd, *J* = 8.1, 3.3 Hz, CHCH₂), 2.90 (3H, s, NCH₃), 2.85 (3H, s, NCH₃); ¹³C{¹H} NMR (CDCl₃, 101 MHz) δ 173.7, 141.2, 131.1, 128.0 (2C), 127.3, 126.3 (2C), 120.0, 73.7, 53.4, 37.3, 35.6; HRMS (APCI) calc. for C₁₃H₁₈NO₂ ([M + H]⁺) 220.1332, found 220.1327.

2-Vinyl-2-cyclohexenone (6v) was synthesized from vinyl silane **4v** (97 mg, 0.30 mmol, 1.0 equiv), [Ir(dtbbpy)(ppy)₂]₂PF₆ (5.5 mg, 6.0 μ mol, 2.0 mol %), Bu₃N (0.14 mL, 0.59 mmol, 2.0 equiv) in MeCN/MeOH 9:1 (3 mL) and HCl 1.25 M in MeOH (0.50 mL, 0.63 mmol, 2.1 equiv) according to Procedure E. The crude was purified by column chromatography (IPA/CH₂Cl₂ 0.5–1%) to afford **6v** (23 mg, 0.19 mmol, 62%) as a colorless oil. ¹H NMR (400 MHz, CDCl₃) δ 7.02 (1H, t, *J* = 4.5 Hz, CCH), 6.53 (1H, dd, *J* = 17.7, 11.2 Hz, CHCH₂), 5.70–5.58 (1H, m, CHCH₂), 5.14 (1H, d, *J* = 11.2 Hz, CHCH₂), 2.44 (4H, m, 2 × CH₂), 1.99 (2H, m, CH₂); ¹³C{¹H} NMR (CDCl₃, 101 MHz) δ 198.5, 145.4, 136.7, 131.4, 115.8, 38.8, 26.4, 22.7. Data consistent with literature values.⁵⁵

Procedure F for the Synthesis of Alkynyl Silanes 7. Based on a literature procedure,⁵⁶ methyl iodide (2.2 equiv) was added dropwise to a solution of aminosilane **s2** (see the Supporting Information) (1.1 equiv) in dry CH₂Cl₂ (0.5 M with respect to the aminosilane) under Ar. The mixture was stirred for 1 h at room temperature before being cannulated into a mixture of iodohydrin **3** (1.0 equiv) and imidazole (1.1 equiv) in dry CH₂Cl₂ (0.2 M with respect to the iodohydrin) under Ar. After stirring for 1 h, the mixture was concentrated in vacuo. The residue was redissolved in EtOAc and was washed with an aqueous 10% Na₂S₂O₃ solution and brine. The organic layer was dried over anhydrous Na₂SO₄, filtered, and concentrated in vacuo. The crude material was purified by column chromatography to afford the desired product.

(2-Iodo-1-phenylpropoxy)dimethyl(trimethylsilyl)ethylsilane (7f) was synthesized from iodohydrin **3f** (0.30 g, 1.1 mmol, 1.0 equiv), aminosilane **s2** (0.26 g, 1.3 mmol, 1.1 equiv), methyl iodide (0.16 mL, 2.5 mmol, 2.3 equiv), and imidazole (83 mg, 1.2 mmol, 1.1 equiv) in dry CH₂Cl₂ (7.5 mL) according to Procedure F. The crude was purified by column chromatography (CH₂Cl₂/pentane 10%) to afford **7f** (0.24 g, 0.57 mmol, 50%) as a colorless oil. *R*_f 0.44 (CH₂Cl₂/pentane 10%); IR (liquid, $\nu_{\text{max}}/\text{cm}^{-1}$) 2960, 1452, 1251, 1131, 1045, 829, 789, 752, 699; ¹H NMR (400 MHz, CDCl₃) δ 7.40–7.26 (5H, m, ArH), 5.01 (1H, d, *J* = 5.1 Hz, CHO), 4.36 (1H, qd, *J* = 6.9, 5.0 Hz, CHI), 1.80 (3H, d, *J* = 6.9 Hz, CHICH₃), 0.32 (3H, s, Si(CH₃)₂), 0.13 (9H, s, 3 × Si(CH₃)₃), 0.12 (3H, s, Si(CH₃)₂); ¹³C{¹H} NMR (CDCl₃, 101 MHz) δ 141.5, 128.1 (2C), 127.9, 127.1 (2C), 115.5, 110.6, 80.7, 34.1, 22.7, 0.9, 0.6, –0.1 (3C); HRMS (APCI) calc. for C₁₆H₂₆IOSi₂ ([M + H]⁺) 417.0561, found 417.0560.

((1-Iodohexan-2-yl)oxy)dimethyl(trimethylsilyl)ethynylsilane (7k) was synthesized from iodohydrin **3k** (0.29 g, 1.3 mmol, 1.0 equiv), aminosilane **s2** (0.26 g, 1.3 mmol, 1.0 equiv), methyl iodide (0.16 mL, 2.5 mmol, 1.9 equiv), and imidazole (82 mg, 1.2 mmol, 0.95 equiv) in dry CH₂Cl₂ (7.5 mL) according to Procedure F. The crude was purified by column chromatography (CH₂Cl₂/pentane 5%) to afford **7k** (91 mg, 0.24 mmol, 19%) as a colorless oil. *R*_f 0.41 (CH₂Cl₂/pentane 5%); IR (liquid, $\nu_{\text{max}}/\text{cm}^{-1}$) 2960, 2862, 1251, 1036, 831, 792, 756; ¹H NMR (400 MHz, CDCl₃) δ 3.76 (1H, ddt, *J* = 7.5, 6.0, 4.6 Hz, CHO), 3.33–3.20 (2H, m, CH₂I), 1.69 (1H, dddd, *J* = 13.9, 9.3, 5.4, 2.9 Hz, CH₂CHO), 1.62–1.49 (1H, m, CH₂CHO), 1.43–1.22 (4H, m, 4 × CH₂), 0.91 (3H, t, *J* = 7.0 Hz, CH₃), 0.30 (3H, s, Si(CH₃)), 0.27 (3H, s, Si(CH₃)), 0.19 (9H, s, 3 × Si(CH₃)); ¹³C{¹H} NMR (CDCl₃, 101 MHz) δ 115.2, 111.0, 72.9, 36.3, 27.6, 22.7, 14.2, 13.5, 0.90, 0.86, –0.1 (3C); HRMS (APCI) calc. for C₁₃H₂₈IOSi₂ ([M + H]⁺) 383.0718, found 383.0717.

((1-Iodo-3-isopropoxy-1-phenylpropan-2-yl)oxy)dimethyl(trimethylsilyl)ethynylsilane (7s) was synthesized from iodohydrin **3s** (0.31 g, 0.96 mmol, 1.0 equiv), aminosilane **s2** (0.26 g, 1.2 mmol, 1.2 equiv), methyl iodide (0.14 mL, 2.3 mmol, 2.4 equiv), and imidazole (70 mg, 1.0 mmol, 1.1 equiv) in dry CH₂Cl₂ (4.2 mL) according to Procedure F. The crude was purified by column chromatography (Et₂O/pentane 5%) to afford an inseparable 62:38 diastereomers mixture of **7s** (0.17 g, 0.36 mmol, 37%) as a light-yellow oil. *Note: the NMR data were extracted from the analysis of the inseparable mixture.* *R*_f 0.48 (CH₂Cl₂/pentane 5%); IR (liquid, $\nu_{\text{max}}/\text{cm}^{-1}$) 2971, 1251, 1117, 1032, 825, 792, 755, 697; ¹H NMR (400 MHz, CDCl₃, major) δ 7.47–7.43 (2H, m, ArH), 7.30–7.18 (3H, m, ArH), 5.32 (1H, d, *J* = 5.6 Hz, CHI), 4.44 (1H, q, *J* = 5.5 Hz, CHOSi), 3.59 (1H, m, CH₂OCH(CH₃)₂), 3.51 (1H, m, CH(CH₃)₂), 3.40 (1H, m, CH₂OCH(CH₃)₂), 1.24–1.07 (6H, m, CH(CH₃)₂), 0.31–0.14 (15H, m, 5 × Si(CH₃)); ¹³C{¹H} NMR (CDCl₃, 101 MHz, major) δ 140.7, 129.6 (2C), 129.0, 128.2 (2C), 115.1, 111.3, 77.4, 72.2, 69.7, 34.1, 22.2, 1.3, 0.7, –0.1 (3C); ¹H NMR (400 MHz, CDCl₃, minor) δ 7.47–7.43 (2H, m, ArH), 7.30–7.18 (3H, m, ArH), 5.32 (1H, d, *J* = 5.6 Hz, CHI), 3.70 (1H, q, *J* = 5.3 Hz, CHOSi), 3.51 (1H, m, CH(CH₃)₂), 3.40 (2H, m, CH₂OCH(CH₃)₂), 1.24–1.07 (6H, m, CH(CH₃)₂), 0.31–0.14 (15H, m, 5 × Si(CH₃)); ¹³C{¹H} NMR (CDCl₃, 101 MHz, minor) δ 141.7, 128.4 (2C), 128.0, 127.9 (2C), 115.0, 111.4, 76.6, 72.2, 70.3, 39.0, 25.5, 1.3, 0.6, –0.1 (3C); HRMS (APCI) calc. for C₁₉H₃₃INO₂Si₂ ([M + NH₄]⁺) 492.1246, found 492.1246.

2-Methyl-1-phenyl-4-(trimethylsilyl)but-3-yn-1-ol (8f) was synthesized from **7f** (0.13 g, 0.30 mmol, 1.0 equiv), [Ir(dtbbpy)(ppy)₂]-PF₆ (6.3 mg, 6.9 μ mol, 2.3 mol %), Bu₃N (0.14 mL, 0.59 mmol, 2.0 equiv) in MeCN/MeOH 9:1 (3 mL) and HCl 1.25 M in MeOH (0.50 mL, 0.63 mmol, 2.1 equiv) according to Procedure E. The crude was purified by column chromatography (IPA/CH₂Cl₂ 0–0.2%) to afford **8f** (45 mg, 0.19 mmol, 65%) as a colorless oil. ¹H NMR (400 MHz, CDCl₃) δ 7.39–7.27 (5H, m, ArH), 4.48 (1H, dd, *J* = 7.2, 3.6 Hz, CHOH), 2.80 (1H, p, *J* = 7.0 Hz, CH(CC)), 2.66 (1H, d, *J* = 3.6 Hz, OH), 1.08 (3H, d, *J* = 7.0 Hz, CHCH₃), 0.18 (9H, s, Si(CH₃)₃); ¹³C{¹H} NMR (CDCl₃, 101 MHz) δ 141.4, 128.3 (2C), 128.1, 126.9

(2C), 107.8, 88.2, 77.5, 36.6, 17.3, 0.2 (3C). Data consistent with literature values.⁵⁷

1-(Trimethylsilyl)oct-1-yn-4-ol (8k) was synthesized from **7k** (72 mg, 0.19 mmol, 1.0 equiv), [Ir(dtbbpy)(ppy)₂]₂PF₆ (4.3 mg, 4.7 μmol, 2.5 mol %), Bu₃N (80 μL, 0.34 mmol, 1.8 equiv) in MeCN/MeOH 9:1 (1.8 mL), and HCl 1.25 M in MeOH (0.30 mL, 0.38 mmol, 2.0 equiv) according to Procedure E. The crude was purified by column chromatography (IPA/CH₂Cl₂ 0–0.5%) to afford **8k** (25 mg, 0.13 mmol, 68%) as a colorless oil. ¹H NMR (400 MHz, CDCl₃) δ 3.78–3.66 (1H, m, CHOH), 2.45 (1H, dd, *J* = 16.8, 4.7 Hz, CH₂CCSi(CH₃)₃), 2.34 (1H, dd, *J* = 16.8, 6.9 Hz, CH₂CCSi(CH₃)₃), 1.97 (1H, d, *J* = 4.8 Hz, OH), 1.52 (2H, m, CH₂CHOH), 1.46–1.23 (4H, m, 4 × CH₂), 0.90 (3H, t, *J* = 7.1 Hz), 0.15 (9H, s, Si(CH₃)₃); ¹³C{¹H} NMR (CDCl₃, 101 MHz) δ 103.5, 87.7, 70.0, 36.0, 29.0, 27.9, 22.7, 14.1, 0.2 (3C). Data consistent with literature values.⁵⁸

1-Isopropoxy-3-phenyl-5-(trimethylsilyl)pent-4-yn-2-ol (8s) was synthesized from **7s** (0.14 g, 0.30 mmol, 1.0 equiv), [Ir(dtbbpy)(ppy)₂]₂PF₆ (6.3 mg, 6.9 μmol, 2.3 mol %), Bu₃N (0.14 mL, 0.59 mmol, 2.0 equiv) in MeCN/MeOH 9:1 (3 mL), and HCl 1.25 M in MeOH (0.50 mL, 0.63 mmol, 2.1 equiv) according to Procedure E. The crude was purified by column chromatography (IPA/CH₂Cl₂ 0.5–1%). A short second column chromatography (Et₂O/pentane 70%) afforded **8s** (23 mg, 78 μmol, 26%) as a colorless oil. *R*_f 0.38 (Et₂O/pentane 70%); IR (thin film, *ν*_{max}/cm⁻¹) 2972, 2172, 1740, 1371, 1250, 1130, 1076, 842, 760, 701; ¹H NMR (400 MHz, CDCl₃) δ 7.43–7.37 (2H, m, ArH), 7.37–7.30 (2H, m, ArH), 7.27 (1H, qd, *J* = 5.0, 3.9, 1.6 Hz, ArH), 4.02 (1H, d, *J* = 5.5 Hz, CHCC), 3.87 (1H, p, *J* = 5.4 Hz, CHOH), 3.63–3.55 (1H, m, CH(CH₃)₂), 3.55–3.48 (1H, m, CH₂), 3.32 (1H, dd, *J* = 9.6, 5.7 Hz, CH₂), 2.36 (1H, d, *J* = 5.2 Hz, OH), 1.16 (6H, dd, *J* = 6.1, 4.1 Hz, (CH₃)₂), 0.20 (9H, s, Si(CH₃)₃); ¹³C{¹H} NMR (CDCl₃, 101 MHz) δ 138.1, 128.6 (2C), 128.5 (2C), 127.4, 104.6, 89.7, 74.1, 72.3, 69.2, 42.8, 22.2, 22.1, 0.2 (3C); HRMS (APCI) calc. for C₁₇H₂₇O₂Si ([M + H]⁺) 291.1775, found 291.1778.

1-(Allyloxy)-2-iodo-2,3-dihydro-1H-indene (9) was synthesized according to a literature procedure.⁵⁹ Indene (0.50 mL, 3.9 mmol, 1.0 equiv) and allyl alcohol (0.30 mL, 4.4 mmol, 1.1 equiv) were added to a solution of NIS (0.96 g, 4.3 mmol, 1.1 equiv) in dry CH₂Cl₂ (3.9 mL) at –78 °C under Ar. The reaction mixture was stirred 5 min at this temperature, before removing the cold bath. It was further stirred at room temperature overnight. The mixture was partially reduced in vacuo, and an aqueous 0.1 M Na₂S₂O₃ solution (10 mL) was added to the residue. The mixture was extracted with CH₂Cl₂ (3 × 8 mL), and the combined organic layers were dried over anhydrous Na₂SO₄ before being concentrated in vacuo. The crude was purified by column chromatography (Et₂O/pentane 4%) to afford **9** (0.39 g, 1.3 mmol, 33%) as a light-yellow oil. *R*_f 0.39 (Et₂O/pentane 5%); IR (liquid, *ν*_{max}/cm⁻¹) 3027, 3020, 2972, 2853, 1740, 1461, 1426, 1368, 1219, 1054, 923, 748; ¹H NMR (400 MHz, CDCl₃) δ 7.48–7.36 (1H, m, ArH), 7.35–7.16 (3H, m, ArH), 5.98 (1H, ddt, *J* = 17.3, 10.4, 5.7 Hz, OCH₂CHCH₂), 5.36 (1H, dq, *J* = 17.2, 1.6 Hz, OCH₂CHCH₂), 5.29–5.16 (2H, m, CHO, OCH₂CHCH₂), 4.48 (1H, ddd, *J* = 6.9, 4.9, 3.7 Hz, CHI), 4.32 (1H, ddt, *J* = 12.6, 5.5, 1.5 Hz, OCH₂), 4.24 (1H, ddt, *J* = 12.7, 5.8, 1.4 Hz, OCH₂), 3.74 (1H, dd, *J* = 16.9, 6.9 Hz, CH₂), 3.29 (1H, dd, *J* = 16.9, 4.8 Hz, CH₂); ¹³C{¹H} NMR (CDCl₃, 101 MHz) δ 141.6, 140.6, 134.8, 129.2, 127.3, 125.3, 124.8, 117.8, 91.4, 71.2, 43.7, 26.5; HRMS (ESI) calc. for C₁₂H₁₃OINa ([M + Na]⁺) 322.9903, found 322.9903.

3-(Iodomethyl)-3,3a,4,8b-tetrahydro-2H-indeno[1,2-*b*]furan (10) was synthesized from **9** (90 mg, 0.30 mmol, 1.0 equiv), [Ir(dtbbpy)(ppy)₂]₂PF₆ (5.8 mg, 6.3 μmol, 2.1 mol %), and Bu₃N (0.14 mL, 0.59 mmol, 2.0 equiv) in MeCN/MeOH 9:1 (3 mL) according to Procedure D. The crude was redissolved in EtOAc (5 mL) and was transferred into a separatory funnel containing an aqueous 1 M HCl solution (20 mL). The aqueous layer was extracted with EtOAc (3 × 5 mL), and the combined organic layers were washed with an aqueous 2 M HCl solution, a saturated NaHCO₃ solution, and brine. The organic layer was dried over anhydrous Na₂SO₄ and concentrated in vacuo. The crude was purified by column chromatography (Et₂O/pentane 20%) to afford an inseparable 4:1

mixture of **10** (44 mg, 0.15 mmol, 48%) and **11** (6.3 mg, 36 μmol, 12%). Note: the NMR data were extracted from the analysis of the inseparable mixture. *R*_f 0.33 (Et₂O/pentane 20%); IR (liquid, *ν*_{max}/cm⁻¹) 3024, 2922, 2848, 1740, 1459, 1368, 1219, 1184, 1180, 1021, 749; ¹H NMR (400 MHz, CDCl₃) δ 7.49–7.33 (1H, m, ArH), 7.33–7.10 (3H, m, ArH), 5.57 (1H, d, *J* = 6.7 Hz, CHO), 4.03 (1H, dd, *J* = 8.5, 6.7 Hz, OCH₂), 3.32–3.18 (2H, m, OCH₂, OCH₂CHCH₂), 3.18–3.05 (2H, m, CH₂I), 3.05–2.82 (3H, m, 2 × CH₂, CH); ¹³C{¹H} NMR (CDCl₃, 101 MHz) δ 143.3, 142.0, 129.1, 127.3, 125.5, 124.6, 88.2, 71.8, 46.7, 45.9, 30.7, 2.3; HRMS (ESI) calc. for C₁₂H₁₃OINa ([M + Na]⁺) 322.9903, found 322.9904.

3-Methyl-3,3a,4,8b-tetrahydro-2H-indeno[1,2-*b*]furan (11) was synthesized from **9** (90 mg, 0.30 mmol, 1.0 equiv), [Ir(dtbbpy)(ppy)₂]₂PF₆ (5.8 mg, 6.3 μmol, 2.1 mol %), and Bu₃N (0.14 mL, 0.59 mmol, 2.0 equiv) in MeCN/MeOH 9:1 (3 mL) according to Procedure D. The crude was redissolved in EtOAc (5 mL) and was transferred into a separatory funnel containing an aqueous 1 M HCl solution (20 mL). The aqueous layer was extracted with EtOAc (3 × 5 mL), and the combined organic layers were washed with an aqueous 2 M HCl solution, a saturated NaHCO₃ solution, and brine. The organic layer was dried over anhydrous Na₂SO₄ and concentrated in vacuo. The crude was purified by column chromatography (Et₂O/pentane 20%) to afford an inseparable 4:1 mixture of **10** (44 mg, 0.15 mmol, 48%) and **11** (6.3 mg, 36 μmol, 12%). Note: the NMR data were extracted from the analysis of the inseparable mixture. *R*_f 0.33 (Et₂O/pentane 20%); IR (liquid, *ν*_{max}/cm⁻¹) 3024, 2922, 2848, 1740, 1459, 1368, 1219, 1184, 1180, 1021, 749; ¹H NMR (400 MHz, CDCl₃) δ 7.46–7.35 (1H, m, ArH), 7.34–7.11 (3H, m, ArH), 5.49 (1H, d, *J* = 6.7 Hz, CHO), 3.90 (1H, dd, *J* = 8.3, 6.9 Hz, OCH₂), 3.32–3.18 (1H, m, CH₂), 3.18–3.05 (2H, m, OCH₂, CH), 3.05–2.80 (1H, m, CH₂), 2.57–2.41 (1H, m, CHCH₃), 1.01 (3H, d, *J* = 6.9 Hz, CH₃); ¹³C{¹H} NMR (CDCl₃, 101 MHz) δ 144.2, 142.9, 128.7, 127.0, 125.5, 124.5, 88.1, 73.3, 45.6, 37.1, 31.2, 12.3; HRMS (ESI) calc. for C₁₂H₁₄ONa ([M + Na]⁺) 197.0937, found 197.0937.

1,1,3,3-Tetramethyl-1,3-bis((2-vinyl-2,3-dihydro-1H-inden-1-yl)oxy)disiloxane (13a) was synthesized according to a modified Procedure D. A mixture of vinyl silane **4a** (0.10 g, 0.29 mmol, 1.0 equiv), [Ir(dtbbpy)(ppy)₂]₂PF₆ (6.7 mg, 7.4 μmol, 2.5 mol %), and Bu₃N (0.14 mL, 0.59 mmol, 2.0 equiv) in dry MeCN (3 mL) was prepared under Ar. The mixture was degassed 5 min by Ar sparging before placing the reaction vial 1 cm away from the light source. A fan was placed on top of the setup to keep the reaction environment at room temperature. The reaction mixture was irradiated with blue LED light until full consumption of the substrate as indicated by TLC. The mixture was reduced in vacuo, and the crude was purified by column chromatography (Et₂O/pentane 1%) to afford **12a** (43 mg, 95 μmol, 64%) as a colorless oil. *R*_f 0.38 (Et₂O/pentane 3%); IR (liquid, *ν*_{max}/cm⁻¹) 3076, 2960, 2906, 1258, 1113, 1046, 1019, 985, 916, 882, 844, 795, 751, 721; ¹H NMR (400 MHz, CD₃CN) δ 7.32 (2H, m, ArH), 7.26–7.12 (6H, m, ArH), 6.00 (2H, m, 2 × CHCH₂), 5.25 (2H, m, 2 × CHO), 5.13 (2H, m, 2 × CHCH₂), 5.06 (2H, m, 2 × CHCH₂), 3.07–2.95 (2H, m, 2 × CH(CHCH₂)), 2.95–2.84 (4H, m, 2 × CH₂), 0.12 (12H, m, 2 × Si(CH₃)₂); ¹³C{¹H} NMR (CD₃CN, 101 MHz) δ 145.7 (2C), 143.7 (2C), 139.6 (2C), 129.0 (2C), 127.3 (2C), 125.7 (2C), 125.6 (2C), 116.0 (2C), 78.2 (2C), 50.8 (2C), 36.7 (2C), 0.1 (2C), 0.0 (2C); HRMS (ESI) calc. for C₂₆H₃₄O₃Si₂Na ([M + Na]⁺) 473.1939, found 473.1941.

■ ASSOCIATED CONTENT

Data Availability Statement

The data underlying this study are available in the published article, in its Supporting Information, and openly available in DataverseNO at <https://doi.org/10.18710/USRNGE>.⁶⁰

Supporting Information

The Supporting Information is available free of charge at <https://pubs.acs.org/doi/10.1021/acs.joc.3c01213>.

Additional experimental details, characterization of compounds **1–4v**, and ^1H and ^{13}C NMR spectra for all compounds (PDF)

AUTHOR INFORMATION

Corresponding Author

Marius M. Haugland – Department of Chemistry, UiT The Arctic University of Norway, 9037 Tromsø, Norway;

orcid.org/0000-0001-7017-344X;

Email: marius.m.haugland@uit.no

Author

Floriane Baussière – Department of Chemistry, UiT The Arctic University of Norway, 9037 Tromsø, Norway

Complete contact information is available at:

<https://pubs.acs.org/10.1021/acs.joc.3c01213>

Author Contributions

The manuscript was written through contributions from both authors.

Notes

The authors declare no competing financial interest.

ACKNOWLEDGMENTS

The authors thank the Tromsø Research Foundation and UiT Centre for New Antibacterial Strategies (CANS) for a start-up grant (TFS project ID: 18_CANS).

REFERENCES

- (1) Liao, J. H.; Yang, X.; Ouyang, L.; Lai, Y. L.; Huang, J. Z.; Luo, R. S. Recent advances in cascade radical cyclization of radical acceptors for the synthesis of carbo- and heterocycles. *Org. Chem. Front.* **2021**, *8*, 1345–1363.
- (2) Wang, Y.; Wen, X.; Cui, X.; Zhang, X. P. Enantioselective Radical Cyclization for Construction of 5-Membered Ring Structures by Metalloradical C-H Alkylation. *J. Am. Chem. Soc.* **2018**, *140*, 4792–4796.
- (3) Plesniak, M. P.; Huang, H. M.; Procter, D. J. Radical cascade reactions triggered by single electron transfer. *Nat. Rev. Chem.* **2017**, *1*, No. 0077.
- (4) Prier, C. K.; Rankic, D. A.; MacMillan, D. W. C. Visible Light Photoredox Catalysis with Transition Metal Complexes: Applications in Organic Synthesis. *Chem. Rev.* **2013**, *113*, 5322–5363.
- (5) Romero, N. A.; Nicewicz, D. A. Organic Photoredox Catalysis. *Chem. Rev.* **2016**, *116*, 10075–10166.
- (6) Maust, M. C.; Hendy, C. M.; Jui, N. T.; Blakey, S. B. Switchable Regioselective 6-endo or 5-exo Radical Cyclization via Photoredox Catalysis. *J. Am. Chem. Soc.* **2022**, *144*, 3776–3781.
- (7) Adams, K.; Ball, A. K.; Birkett, J.; Brown, L.; Chappell, B.; Gill, D. M.; Lo, P. K. T.; Patmore, N. J.; Rice, C. R.; Ryan, J.; Raubo, P.; Sweeney, J. B. An iron-catalysed C-C bond-forming spirocyclization cascade providing sustainable access to new 3D heterocyclic frameworks. *Nat. Chem.* **2017**, *9*, 396–401.
- (8) Miyabe, H.; Kawashima, A.; Yoshioka, E.; Kohtani, S. Progress in Enantioselective Radical Cyclizations. *Chem. – Eur. J.* **2017**, *23*, 6225–6236.
- (9) Miyabe, H.; Takemoto, Y. Enantioselective Radical Cyclizations: A New Approach to Stereocontrol of Cascade Reactions. *Chem. – Eur. J.* **2007**, *13*, 7280–7286.
- (10) Kern, N.; Plesniak, M. P.; McDouall, J. J. W.; Procter, D. J. Enantioselective cyclizations and cyclization cascades of samarium ketyl radicals. *Nat. Chem.* **2017**, *9*, 1198–1204.
- (11) Brill, Z. G.; Grover, H. K.; Maimone, T. J. Enantioselective synthesis of an ophiobolin sesterterpene via a programmed radical cascade. *Science* **2016**, *352*, 1078–1082.
- (12) Hashimoto, T.; Kawamata, Y.; Maruoka, K. An organic thiol radical catalyst for enantioselective cyclization. *Nat. Chem.* **2014**, *6*, 702–705.
- (13) Biegasiewicz, K. F.; Cooper, S. J.; Gao, X.; Oblinsky, D. G.; Kim, J. B.; Garfinkle, S. E.; Joyce, L. A.; Sandoval, B. A.; Scholes, G. D.; Hyster, T. K. Photoexcitation of flavoenzymes enables a stereoselective radical cyclization. *Science* **2019**, *364*, 1166–1169.
- (14) Sakeda, M.; Shuto, S.; Sugimoto, I.; Ichikawa, S.; Matsuda, A. Synthesis of Pyrimidine 2'-Deoxy Ribonucleosides Branched at the 2'-Position via Radical Atom-Transfer Cyclization Reaction with a Vinylsilyl Group as a Radical-Acceptor Tether. *J. Org. Chem.* **2000**, *65*, 8988–8996.
- (15) Sakeda, M.; Ichikawa, S.; Matsuda, A.; Shuto, S. A New Entry to the Stereoselective Introduction of an Ethynyl Group by a Radical Reaction: Synthesis of the Potential Antimetabolite 2'-Deoxy-2'-C-Ethynyluridine. *Angew. Chem., Int. Ed.* **2002**, *41*, 4748–4750.
- (16) Sakeda, M.; Ichikawa, S.; Matsuda, A.; Shuto, S. The First Radical Method for the Introduction of an Ethynyl Group Using a Silicon Tether and its Application to the Synthesis of 2'-Deoxy-2'-C-Ethynylnucleosides. *J. Org. Chem.* **2003**, *68*, 3465–3475.
- (17) Duplessis, M.; Waltz, M. E.; Bencheqroun, M.; Cardinal-David, B.; Guindon, Y. Stereoselective Quaternary Center Construction via Atom-Transfer Radical Cyclization Using Silicon Tethers on Acyclic Precursors. *Org. Lett.* **2009**, *11*, 3148–3151.
- (18) Mikhaylov, A. A.; Zard, S. Z. Extension to the Silyl-Tethered Radical Cyclization: Cyclohex-2-en-1-oxy Vinyl Silanes in Stereoselective Radical Addition/Cyclization Cascades. *Org. Lett.* **2017**, *19*, 1866–1869.
- (19) Panferova, L. I.; Struchkova, M. I.; Dilman, A. D. Vinylation of Iododifluoromethylated Alcohols via a Light-Promoted Intramolecular Atom-Transfer Reaction. *Synthesis* **2017**, *49*, 4124–4132.
- (20) Becerril-Jiménez, F.; Lussier, T.; Leblanc, L.; Eymard, C.; Dostie, S.; Prévost, M.; Guindon, Y. Photoredox-Catalyzed Stereoselective Radical Reactions to Synthesize Nucleoside Analogues with a C2'-Stereoogenic All-Carbon Quaternary Center. *J. Org. Chem.* **2019**, *84*, 14795–14804.
- (21) Nguyen, J. D.; D'Amato, E. M.; Narayanam, J. M.; Stephenson, C. R. Engaging unactivated alkyl, alkenyl and aryl iodides in visible-light-mediated free radical reactions. *Nat. Chem.* **2012**, *4*, 854–859.
- (22) Wallentin, C. J.; Nguyen, J. D.; Finkbeiner, P.; Stephenson, C. R. J. Visible Light-Mediated Atom Transfer Radical Addition via Oxidative and Reductive Quenching of Photocatalysts. *J. Am. Chem. Soc.* **2012**, *134*, 8875–8884.
- (23) Zhang, J.; Jiang, M.; Wang, C. S.; Guo, K.; Li, Q. X.; Ma, C.; Ni, S. F.; Chen, G. Q.; Zong, Y.; Lu, H.; Xu, L. W.; Shao, X. X. Transition-metal free C-N bond formation from alkyl iodides and diazonium salts via halogen-atom transfer. *Nat. Commun.* **2022**, *13*, 7961.
- (24) Parsaee, F.; Senarathna, M. C.; Kannagara, P. B.; Alexander, S. N.; Arche, P. D. E.; Welin, E. R. Radical philicity and its role in selective organic transformations. *Nat. Rev. Chem.* **2021**, *5*, 486–499.
- (25) Dubois, M. A. J.; Rojas, J. J.; Sterling, A. J.; Broderick, H. C.; Smith, M. A.; White, A. J. P.; Miller, P. W.; Choi, C.; Mousseau, J. J.; Duarte, F.; Bull, J. A. Visible Light Photoredox-Catalyzed Decarboxylative Alkylation of 3-Aryloxyetanes and Azetidines via Benzylic Tertiary Radicals and Implications of Benzylic Radical Stability. *J. Org. Chem.* **2023**, *88*, 6476–6488.
- (26) Roslin, S.; Odell, L. R. Visible-Light Photocatalysis as an Enabling Tool for the Functionalization of Unactivated C(sp³)-Substrates. *Eur. J. Org. Chem.* **2017**, 1993–2007.
- (27) Zhou, Q. Q.; Düsel, S. J. S.; Lu, L. Q.; König, B.; Xiao, W. J. Alkenylation of unactivated alkyl bromides through visible light photocatalysis. *Chem. Commun.* **2019**, *55*, 107–110.
- (28) Zhang, S.; Duan, X. H.; Li, P. F. Access to Stereodefined Multifunctionalized β,γ -Unsaturated Ketones via Chemo-, Regio- and Diastereoselective Copper-Catalyzed Diborylation of Cross-Conjugated Enynones. *Chin. J. Chem.* **2021**, *39*, 590–596.

- (29) Klare, H. F. T.; Albers, L.; Süsse, L.; Keess, S.; Müller, T.; Oestreich, M. Silylium Ions: From Elusive Reactive Intermediates to Potent Catalysts. *Chem. Rev.* **2021**, *121*, 5889–5985.
- (30) Howes, K. R.; Bakac, A.; Espenson, J. H. Reactions of the 17-Electron Bis(Dimethylglyoximate)(Triphenylphosphine) Rhodium(II) Radical. *Inorg. Chem.* **1988**, *27*, 3147–3151.
- (31) Crespi, S.; Fagnoni, M. Generation of Alkyl Radicals: From the Tyranny of Tin to the Photon Democracy. *Chem. Rev.* **2020**, *120*, 9790–9833.
- (32) Juliá, F.; Constantin, T.; Leonori, D. Applications of Halogen-Atom Transfer (XAT) for the Generation of Carbon Radicals in Synthetic Photochemistry and Photocatalysis. *Chem. Rev.* **2022**, *122*, 2292–2352.
- (33) Constantin, T.; Zanini, M.; Regni, A.; Sheikh, N. S.; Juliá, F.; Leonori, D. Aminoalkyl radicals as halogen-atom transfer agents for activation of alkyl and aryl halides. *Science* **2020**, *367*, 1021–1026.
- (34) Leitch, J. A.; Rossolini, T.; Rogova, T.; Maitland, J. A. P.; Dixon, D. J. α -Amino Radicals via Photocatalytic Single-Electron Reduction of Imine Derivatives. *ACS Catal.* **2020**, *10*, 2009–2025.
- (35) A previous version of this work prior to peer review has been posted on a preprint server: Baussière, F.; Haugland, M. M. Radical Group Transfer of Vinyl and Alkynyl Silanes Driven by Photoredox Catalysis. *ChemRxiv* preprint; June 2, **2023**; ver. 1. DOI: [10.26434/chemrxiv-2023-fg16p](https://doi.org/10.26434/chemrxiv-2023-fg16p)
- (36) Geng, X. L.; Wang, Z.; Li, X. Q.; Zhang, C. A Simple Method for Epoxidation of Olefins Using Sodium Chlorite as an Oxidant without a Catalyst. *J. Org. Chem.* **2005**, *70*, 9610–9613.
- (37) Yao, H. R.; Richardson, D. E. Epoxidation of Alkenes with Bicarbonate-Activated Hydrogen Peroxide. *J. Am. Chem. Soc.* **2000**, *122*, 3220–3221.
- (38) Das, B.; Venkateswarlu, K.; Damodar, K.; Suneel, K. Ammonium acetate catalyzed improved method for the regioselective conversion of olefins into halohydrins and haloethers at room temperature. *J. Mol. Catal. A: Chem.* **2007**, *269*, 17–21.
- (39) Sugimoto, I.; Shuto, S.; Matsuda, A. A One-Pot Method for the Stereoselective Introduction of a Vinyl Group via an Atom-Transfer Radical-Cyclization Reaction with a Diphenylvinylsilyl Group as a Temporary Connecting Tether. Synthesis of 4' α -C-Vinylthymidine, a Potent Antiviral Nucleoside. *J. Org. Chem.* **1999**, *64*, 7153–7157.
- (40) Hegedus, L. S.; McKearin, J. M. Palladium-Catalyzed Cyclization of ω -Olefinic Tosamides. Synthesis of Non-Aromatic Nitrogen-Heterocycles. *J. Am. Chem. Soc.* **1982**, *104*, 2444–2451.
- (41) Launay, G. G.; Slawin, A. M. Z.; O'Hagan, D. Prins fluorination cyclisations: Preparation of 4-fluoro-pyran and -piperidine heterocycles. *Beilstein J. Org. Chem.* **2010**, *6*, 41.
- (42) Hocine, S.; Montagnon, C.; Vakiti, J. R.; Fourquez, J. M.; Hanessian, S. Stereoselective Synthesis of Oxabicyclic Pyrrolidines of Medicinal Relevance: Merging Chemoenzymatic and Catalytic Methods. *Eur. J. Org. Chem.* **2021**, *2021*, 274–283.
- (43) Haddad, T. D.; Hirayama, L. C.; Singaram, B. Indium-Mediated Asymmetric Barbier-Type Allylations: Additions to Aldehydes and Ketones and Mechanistic Investigation of the Organoinidium Reagents. *J. Org. Chem.* **2010**, *75*, 642–649.
- (44) Araki, S.; Kameda, K.; Tanaka, J.; Hirashita, T.; Yamamura, H.; Kawai, M. Umpolung of vinyloxiranes: Regio- and stereoselectivity of the In/Pd-mediated allylation of carbonyl compounds. *J. Org. Chem.* **2001**, *66*, 7919–7921.
- (45) Park, J. K.; McQuade, D. T. Iterative Asymmetric Allylic Substitutions: syn- and anti-1,2-Diols through Catalyst Control. *Angew. Chem., Int. Ed.* **2012**, *51*, 2717–2721.
- (46) Pérez, M.; Fañanás-Mastral, M.; Bos, P. H.; Rudolph, A.; Harutyunyan, S. R.; Feringa, B. L. Catalytic asymmetric carbon-carbon bond formation via allylic alkylations with organolithium compounds. *Nat. Chem.* **2011**, *3*, 377–381.
- (47) Hayashi, K.; Tanimoto, H.; Zhang, H.; Morimoto, T.; Nishiyama, Y.; Kakiuchi, K. Efficient Synthesis of α,β -Unsaturated Alkylimines Performed with Allyl Cations and Azides: Application to the Synthesis of an Ant Venom Alkaloid. *Org. Lett.* **2012**, *14*, 5728–5731.
- (48) Kashyap, B.; Phukan, P. Rapid access to homoallylic alcohols via Pd(OAc)₂ catalyzed Barbier type allylation in presence of DMAP. *Tetrahedron Lett.* **2013**, *54*, 6324–6327.
- (49) Kobayashi, S.; Nishio, K. Facile and Highly Stereoselective Synthesis of Homoallylic Alcohols Using Organosilicon Intermediates. *J. Org. Chem.* **1994**, *59*, 6620–6628.
- (50) Huang, X. R.; Pan, X. H.; Lee, G. H.; Chen, C. P. C₂-Symmetrical Bipyridyldiols as Promising Enantioselective Catalysts in Nozaki-Hiyama Allylation. *Adv. Synth. Catal.* **2011**, *353*, 1949–1954.
- (51) Dam, J. H.; Frstrup, P.; Madsen, R. Combined Experimental and Theoretical Mechanistic Investigation of the Barbier Allylation in Aqueous Media. *J. Org. Chem.* **2008**, *73*, 3228–3235.
- (52) Zhu, Y. X.; Colomer, I.; Thompson, A. L.; Donohoe, T. J. HFIP Solvent Enables Alcohols To Act as Alkylating Agents in Stereoselective Heterocyclization. *J. Am. Chem. Soc.* **2019**, *141*, 6489–6493.
- (53) McNally, A.; Evans, B.; Gaunt, M. J. Organocatalytic Sigmatropic Reactions: Development of a [2,3] Wittig Rearrangement through Secondary Amine Catalysis. *Angew. Chem., Int. Ed.* **2006**, *45*, 2116–2119.
- (54) Tiecco, M.; Testaferri, L.; Santi, C. Catalytic Oxyselenenylation-Deselenenylation Reactions of Alkenes – Stereoselective One-Pot Conversion of 3-Alkenols into 2,5-Dihydrofurans. *Eur. J. Org. Chem.* **1999**, 797–803.
- (55) Yadav, V. K.; Senthil, G.; Babu, K. G.; Parvez, M.; Reid, J. L. Heteroatom Influence on the π -Facial Selectivity of Diels-Alder Cycloadditions to 1-Oxa-4-thia-6-vinylspiro[4.5]dec-6-ene, 3-Methoxy-3-methyl-2-vinylcyclohexene, and 3-Methoxy-2-vinylcyclohexene. *J. Org. Chem.* **2002**, *67*, 1109–1117.
- (56) Haugland, M. M.; El-Sagheer, A. H.; Porter, R. J.; Peña, J.; Brown, T.; Anderson, E. A.; Lovett, J. E. 2'-Alkynyl nucleotides: A Sequence- and Spin Label-Flexible Strategy for EPR Spectroscopy in DNA. *J. Am. Chem. Soc.* **2016**, *138*, 9069–9072.
- (57) Hirashita, T.; Suzuki, Y.; Tsuji, H.; Sato, Y.; Naito, K.; Araki, S. Nickel-Catalyzed Indium(I)-Mediated syn-Selective Propargylation of Aldehydes. *Eur. J. Org. Chem.* **2012**, *2012*, 5668–5672.
- (58) Chemla, F.; Bernard, N.; Normant, J. A New Diastereodivergent Synthesis of 1,2-Disubstituted Homopropargylic Alcohols. *Eur. J. Org. Chem.* **1999**, 2067–2078.
- (59) Guisán-Ceinos, M.; Soler-Yanes, R.; Collado-Sanz, D.; Phapale, V. B.; Buñuel, E.; Cárdenas, D. J. Ni-Catalyzed Cascade Cyclization-Kumada Alkyl-Alkyl Cross-Coupling. *Chem. – Eur. J.* **2013**, *19*, 8405–8410.
- (60) Baussière, F.; Haugland, M. M. Replication Data for: Radical Group Transfer of Vinyl and Alkynyl Silanes Driven by Photoredox Catalysis. *DataVerseNO*, V1; 2023. DOI: [10.18710/USRNGE](https://doi.org/10.18710/USRNGE)

Supporting Information for:

Radical Group Transfer of Vinyl and Alkynyl Silanes Driven by Photoredox Catalysis

Floriane Baussière and Marius M. Haugland*

Department of Chemistry, UiT The Arctic University of Norway, 9037 Tromsø, Norway

* marius.m.haugland@uit.no

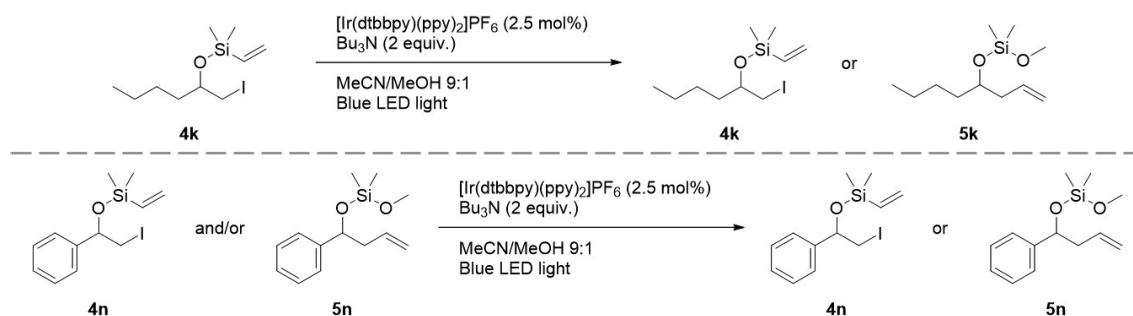
Contents

1. Stability experiments	S2
2. Control experiments – radical reaction	S2
3. ¹H NMR monitoring of the radical reaction initiated with BEt₃	S3
4. ¹H NMR monitoring of the reaction, full spectra	S3
5. ¹H NMR analysis of the fate of the iminium ion	S4
6. Experimental methods	S5
7. Photocatalysts synthesis	S5
8. Silanes synthesis	S6
9. Olefins 1e, 1i and 1s synthesis	S7
10. Epoxides 2q, 2r and 2s synthesis	S8
11. Iodohydrins 3a-v synthesis	S10
11.1 Procedure A	S10
11.2 Procedure B	S10
12. Vinyl silanes 4a-v synthesis	S18
12.1 Procedure C	S18
13. References	S28
14. NMRs	S30

1. Stability experiments

Stability experiments on **4k**, **4n** and **5n** were performed as follow. Mixtures of the investigated compounds (0.16 mmol, 1.0 equiv), [Ir(dtbbpy)(ppy)₂]₂PF₆ (see table) and Bu₃N (0.32 mmol, 2.0 equiv.) in MeCN-d₃/CD₃OD 9:1 (0.1 M with respect to the compound) were prepared under Ar. The reaction mixtures were degassed 5 min by Ar sparging, before transferring precise aliquots (0.40 mL) into NMR tubes together with precise volumes of ethynyl carbonate in MeCN-d₃ solution (0.10 mL). Quantitative ¹H NMR of each mixture were recorded. The mixtures in vials were irradiated by blue LED light for 24 h, before transferring precise aliquots (0.40 mL) into NMR tubes together with precise volumes of ethynyl carbonate in MeCN-d₃ solution (0.10 mL) again. Quantitative ¹H NMR of each mixture were recorded. For each NMR, the integral of the ethynyl carbonate peak was set to 4.00. The integral of one proton of **4k**, **4n** and **5n** was measured and reported in Table S1.

Table S1. Vinyl silanes 4k/n and siloxane 5n stability experiments

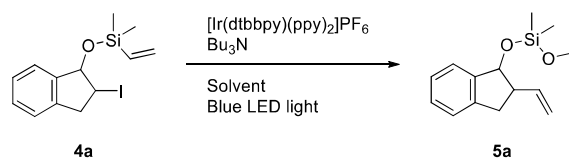


in the reaction mixture before blue LED light irradiation	[Ir(dtbbpy)(ppy) ₂] ₂ PF ₆	integral of one proton				yield (%) ^d
		at 0 h		at 24 h		
		4k/n	5k/n	4k/n	5k/n	
4k^a	no photocatalyst	1.09	-	1.00	-	92
4k^b	2.5 mol%	1.18	-	-	0.47	40
4n^c	no photocatalyst	1.00	-	0.91	-	91
4n	2.5 mol%	1.32	-	-	0.53	40
1:1 4n/5n mixture ^c	2.5 mol%	1.62	1.38	-	1.97	66
5n^c	2.5 mol%	-	2.79	-	2.38	85

^aReaction scale: 21 μmol. ^bReaction scale: 0.38 mmol. ^cReaction scale: 0.16 mmol. ^dStability yields were calculated from the integrals of **4k**, **4n** and **5n** before and after 24 h of reaction.

2. Control experiments – radical reaction

Table S2. Photoredox-catalyzed radical reaction control experiments^a



entry	[Ir(dtbbpy)(ppy) ₂] ₂ PF ₆	Bu ₃ N	solvent	blue LED light	time	yield (%) ^b
1	no photocatalyst	2 equiv.	MeCN/MeOH 9:1	yes	0.5 h	0
2	2.5 mol%	no base	MeCN/MeOH 9:1	yes	0.5 h	0
3	2.5 mol%	2 equiv.	MeCN/MeOH 9:1	no light	0.5 h	0

^aReaction scale: 0.10 mmol. ^bYield determined by ¹H NMR integral comparison between substrate and product.

3. ^1H NMR monitoring of the radical reaction initiated with BEt_3

A mixture of substrate **4a** (21 mg, 62 μmol , 1.0 equiv.) and 1 M solution of BEt_3 in hexenes (12 μL , 12 μmol , 0.2 equiv.) in benzene- d_6 (0.6 mL) was prepared in triplicates in gas-tight NMR tubes under Ar. Air was injected to initiate the radical reaction before sealing the tubes. The mixtures were shaken, and the reaction was monitored by ^1H NMR. TBAF (1 M in THF, 0.12 mL, 0.12 mmol, 2.0 equiv.), MeOH (4.0 μL , 0.10 mmol, 2.0 equiv.) and Bu_3N (24 μL , 0.10 mmol, 2.0 equiv.) were added to the different tubes, the mixtures were shaken, and the reactions were monitored by ^1H NMR. The appearance of the vinyl proton peak at approximately 6 ppm indicates that the ring opened.

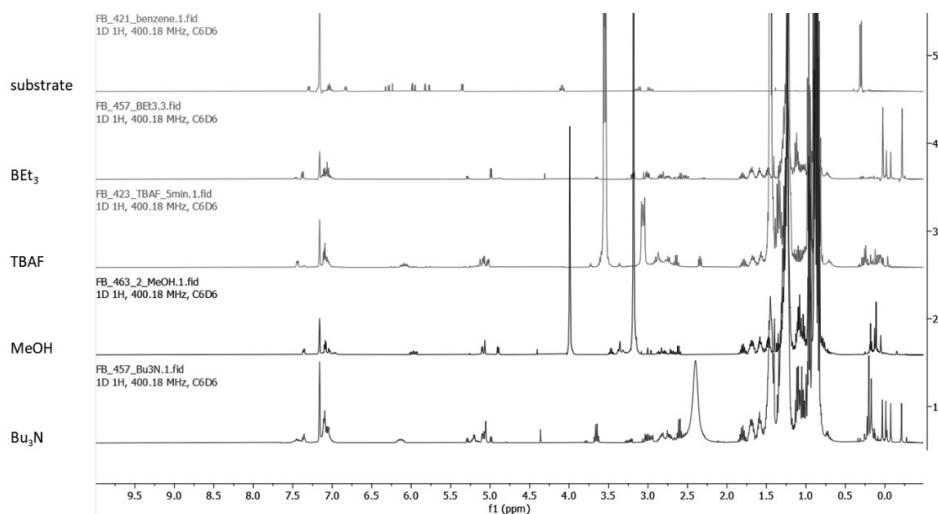


Figure S1. NMR following of the radical reaction initiated by BEt_3 in benzene- d_6 .

4. ^1H NMR monitoring of the reaction, full spectra

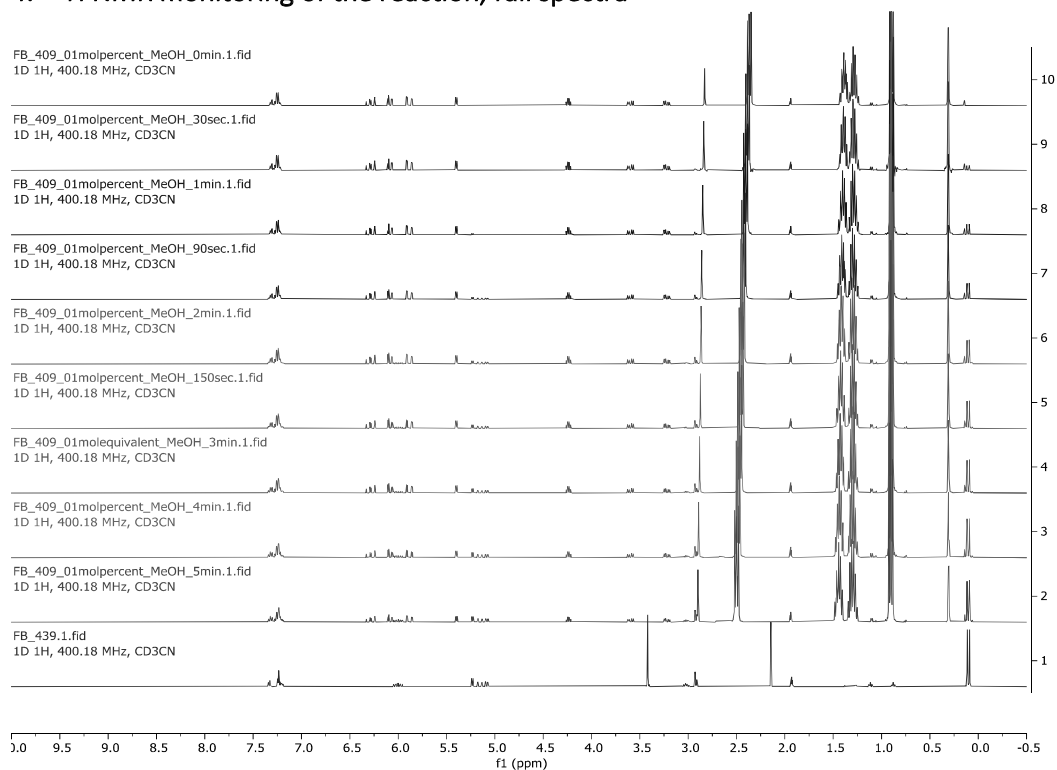


Figure S2. NMR following of the radical reaction in $\text{MeCN-}d_3/\text{CD}_3\text{OD}$ 9:1.

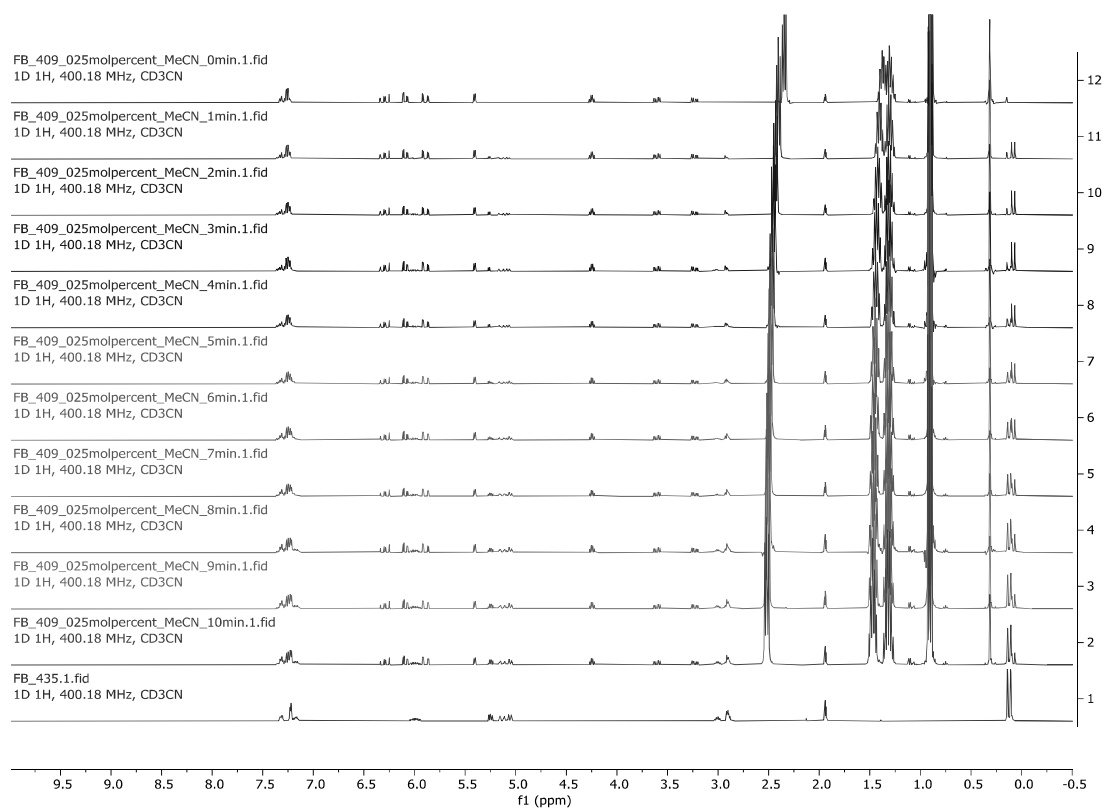


Figure S3. NMR following of the radical reaction in $\text{MeCN-d}_3/\text{CD}_3\text{OD}$ 9:1.

5. ^1H NMR analysis of the fate of the iminium ion

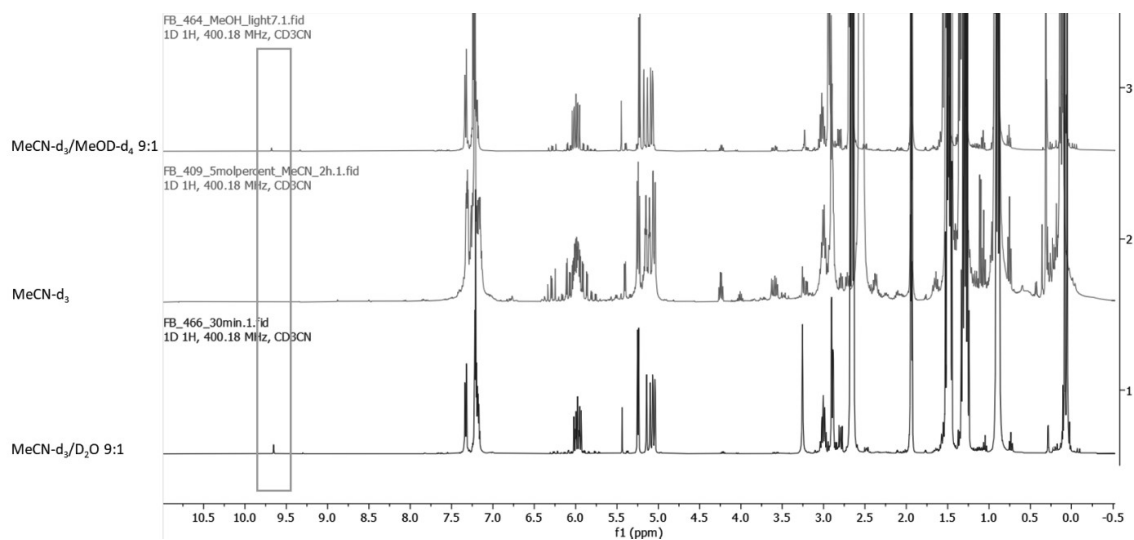
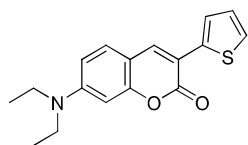


Figure S4. ^1H NMR analysis of the crude product of photoredox reactions of substrate **4a** performed in different solvents. Reactions were performed in deuterated solvents in gas-tight NMR tubes by direct irradiation. Reaction progress was monitored by ^1H NMR without opening the sealed NMR tubes. At full conversion, the amounts of butanal formed (relative to **6a** or **13a**) were <5% ($\text{MeCN-d}_3/\text{MeOD-d}_4$), trace (MeCN-d_3) and 8% ($\text{MeCN-d}_3/\text{D}_2\text{O}$).

6. Experimental methods

All reagents purchased from Acros, Alfa, Sigma-Aldrich, TCI and VWR were used as supplied. All air and/or water sensitive reactions were carried out under an atmosphere of argon in flame-dried glassware using standard Schlenk techniques. Anhydrous solvents were dried by pre-storing over activated 3 Å (MeOH) or 4 Å (all other solvents) molecular sieves and purged by argon sparging. Blue light irradiation was performed with RGB LED strips (IP20, 220-240 V, 5.4 W). Reactions were monitored by thin layer chromatography (TLC) on pre-coated aluminum-based plates (TLC Silica gel 60 F₂₅₄, Supelco). The plates were developed under UV irradiation (254 nm) or with vanillin or KMnO₄ staining and subsequent heating. Column chromatography was performed with silica gel (Silica gel 60, irregular 40-63 μm for flash chromatography, VWR Chemicals). ¹H NMR spectra were recorded at room temperature on a 400 MHz Bruker 9.4 Tesla Avance III HD system equipped with a SmartProbe (broad band). ¹³C NMR spectra (¹H decoupled) were recorded at room temperature on the same machine operating at 101 MHz. All chemical shifts (δ) are reported in parts per million (ppm) with internal reference to residual protons in CDCl₃ (δ 7.26 or 77.16) or MeCN-d₃ (δ 1.94 or 118.26). Coupling constants (*J*) are given in Hz with an accuracy of 0.1 Hz. Infrared (IR) spectra were recorded as thin films or liquids on an Agilent Technologies Cary 630 FTIR 318 spectrometer. Wavelength of maximum absorbance (*v*_{max}) are reported in wavenumbers (cm⁻¹). Only selections of characteristic resonances are reported. High-resolution mass spectra (HRMS) were recorded by direct injection of the compounds as solutions in MeOH on a Thermo Scientific Orbitrap Exploris 120 Mass spectrometer, using dual electrospray ionization (ESI) and atmospheric pressure chemical ionization (APCI) probes.

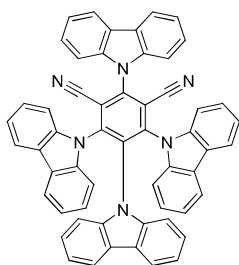
7. Photocatalysts synthesis



7-(Diethylamino)-3-(thiophen-2-yl)-2H-chromen-2-one was synthesized according to a procedure reported by Gualandi *et al.*¹ Triethylamine (2.0 mL, 14 mmol, 1.0 equiv.) was added to a mixture of 4-(diethylamino)salicylaldehyde (1.8 g, 9.3 mmol, 1.2 equiv.) and 2-thiopheneacetic acid (1.1 g, 7.6 mmol, 1.0 equiv.) in acetic anhydride (27 mL) under Ar. The reaction flask was topped with a condenser and the reaction mixture was refluxed for 3 h. The reaction mixture was allowed to reach room temperature before being cooled in an ice-water bath. The mixture was diluted with water (50 mL) and transferred into a separatory funnel where it was extracted with EtOAc (3 × 30 mL). The combined organic layers were washed with a saturated aqueous NaHCO₃ solution (7 × 50 mL), dried over anhydrous Na₂SO₄ and reduced *in vacuo*. The dark brown residue was purified by column chromatography (EtOAc/heptane 0-30%) to afford 7-(diethylamino)-3-(thiophen-2-yl)-2H-chromen-2-one as a yellow solid (0.79 g, 2.7 mmol, 35%).

¹H NMR (400 MHz, CDCl₃) δ 7.88 (1H, s, CH), 7.66 (1H, dd, *J* = 3.7, 1.2 Hz, SCH), 7.33 (1H, d, *J* = 8.8 Hz, NCCHCHC), 7.31 (1H, dd, *J* = 5.1, 1.2 Hz, SCCH), 7.08 (1H, dd, *J* = 5.1, 3.7 Hz, SCHCH), 6.61 (1H, dd, *J* = 8.8, 2.5 Hz, NCCHCHC), 6.53 (1H, d, *J* = 2.5 Hz, NCCHC), 3.43 (4H, q, *J* = 7.1 Hz, N(CH₂CH₃)₂), 1.22 (6H, t, *J* = 7.1 Hz, N(CH₂CH₃)₂); ¹³C{¹H} NMR (CDCl₃, 101 MHz) δ 160.7, 155.7, 150.6, 137.6, 137.0, 129.0, 127.4, 125.7, 125.0, 114.9, 109.4, 108.9, 97.3, 45.0 (2C), 12.6 (2C).

Data consistent with literature values.¹

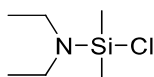


4CzIPN was synthesized according to a procedure reported by Filippini *et al.*² A solution of carbazole (1.7 g, 10 mmol, 5.0 equiv.) in dry THF (16 mL) was slowly added to a stirred solution of sodium hydride (60% dispersion in mineral oil, 0.62 g, 1.5 mmol, 7.6 equiv.) in dry THF (25 mL) under Ar. The mixture was stirred 30 min at room temperature before slowly adding a solution of tetrafluoroisophthalonitrile (0.41 g, 2.0 mmol, 1.0 equiv.) in dry THF (3 mL). The reaction mixture was stirred overnight at room temperature. Distilled water (0.2 mL) was added to quench the excess sodium hydride and the mixture was concentrated *in vacuo*. The crude was purified by column chromatography (CH₂Cl₂/pentane 25-80%) to afford 4CzIPN (1.4 g, 1.8 mmol, 86%) as a yellow solid.

¹H NMR (400 MHz, CDCl₃) δ 8.23 (2H, dt, *J* = 7.9, 1.0 Hz), 7.76–7.66 (8H, m), 7.49 (2H, ddd, *J* = 8.0, 6.6, 1.6 Hz), 7.33 (2H, dt, *J* = 7.6, 1.0 Hz), 7.25–7.19 (4H, m), 7.13–7.04 (8H, m), 6.87–6.78 (4H, m), 6.63 (2H, td, *J* = 7.7, 7.2, 1.2 Hz); ¹³C{¹H} NMR (CDCl₃, 101 MHz) δ 145.4, 140.1, 138.3, 137.1, 127.1, 125.9, 125.1, 124.9, 124.7, 124.0, 122.5, 122.1, 121.5, 121.1, 120.6, 119.8, 116.5, 111.8, 110.1, 109.62, 109.56.

Data consistent with literature values.²

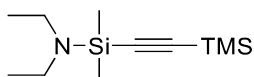
8. Silanes synthesis



Chloro(diethylamino)dimethylsilane s1 was synthesized according to a procedure reported by Haugland *et al.*³ A solution of diethylamine (8.6 mL, 83 mmol, 1.0 equiv.) in dry THF (11 mL) was added dropwise over 2 h to a suspension of dichlorodimethylsilane (10 mL, 83 mmol, 1.0 equiv.) and Et₃N (13 mL, 91 mmol, 1.1 equiv.) in dry THF (11 mL) under Ar at 0 °C. The reaction mixture was diluted with dry THF (35 mL), allowed to reach room temperature, and was stirred for 20 h. Dry pentane (20 mL) was added, and the mixture was filtered through celite under N₂ flow. The filtrate was reduced *in vacuo*. It was purified by vacuum distillation (68 °C under 90 mbar) to afford chloro(diethylamino)dimethylsilane **s1** (3.3 g, 20 mmol, 24%) as a colorless oil.

¹H NMR (400 MHz, CDCl₃) δ 2.89 (4H, q, *J* = 7.0 Hz, 2 x CH₂CH₃), 1.04 (6H, t, *J* = 7.1 Hz, 2 x CH₂CH₃), 0.46 (6H, s, Si(CH₃)₂); ¹³C{¹H} NMR (CDCl₃, 101 MHz) δ 40.0 (2C), 15.4 (2C), 2.1 (2C).

Data consistent with literature values.³

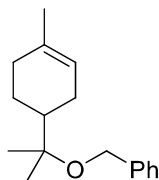


Trimethylsilylethynyl(diethylamino)dimethylsilane s2 was synthesized according to a procedure reported by Haugland *et al.*³ n-BuLi 2.3 M in hexenes (5.8 mL, 13 mmol, 1.1 equiv.) was added dropwise over 20 min to a solution of TMSA (1.7 mL, 12 mmol, 1.0 equiv.) in dry THF (20 mL) under Ar at -78 °C. After 30 min of stirring at room temperature, the mixture was added dropwise to a solution of chloro(diethylamino)dimethylsilane **s1** (2.0 g, 12 mmol, 1.0 equiv.) in dry THF (1.3 mL) under Ar at -78 °C. The mixture was allowed to slowly reach room temperature while stirring overnight. THF (5 mL) was added to quench the unreacted n-BuLi and the mixture was reduced *in vacuo*. The crude was purified by vacuum distillation to afford trimethylsilylethynyl(diethylamino)dimethylsilane **s2** (1.9 g, 8.5 mmol, 70%) as a colorless oil.

$^1\text{H NMR}$ (400 MHz, CDCl_3) δ 2.85 (4H, q, $J = 7.0$ Hz, 2 x CH_2CH_3), 1.01 (6H, t, $J = 7.0$ Hz, 2 x CH_2CH_3), 0.19 (6H, s, $\text{Si}(\text{CH}_3)_2$), 0.16 (9H, s, $\text{Si}(\text{CH}_3)_3$); $^{13}\text{C}\{^1\text{H}\}$ NMR (CDCl_3 , 101 MHz) δ 114.1, 112.6, 40.3 (2C), 15.6 (2C), 0.3 (2C), 0.1 (3C).

Data consistent with literature values.³

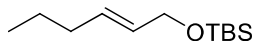
9. Olefins 1e, 1i and 1s synthesis



4-(1-(Benzyloxy)-1-methylethyl)-1-methylcyclohexene 1e. A solution of (-)- α -terpinol (0.96 g, 6.2 mmol, 1.0 equiv.) in dry THF (20 mL) was added dropwise over 30 min to a solution of sodium hydride (60% dispersion in mineral oil, 0.50 g, 13 mmol, 2.0 equiv.) in dry THF (40 mL) at 0 °C under Ar. The mixture was stirred 30 min at 0 °C, benzyl bromide (2.2 g, 13 mmol, 2.1 equiv.) was added dropwise and the reaction mixture was stirred 1 h before being allowed to slowly reach room temperature. It was stirred 1 h at room temperature before being stirred at 27 °C for 68 h. Isopropanol (5 mL) was slowly added to quench the residual sodium hydrate and the reaction mixture was concentrated *in vacuo*. The residue was redissolved in water and extracted with CH_2Cl_2 (3 x 30 mL). The combined organic layers were washed with brine, dried over anhydrous Na_2SO_4 , filtered and concentrated *in vacuo*. The crude was purified by column chromatography (Et_2O /pentane 0-2%) to afford 4-(1-(benzyloxy)-1-methylethyl)-1-methylcyclohexene **1e** (0.59 g, 2.4 mmol, 39%) as a colorless oil.

$^1\text{H NMR}$ (400 MHz, CDCl_3) δ 7.39–7.18 (5H, m, ArH), 5.47–5.35 (1H, m, $\text{C}(\text{CH}_3)\text{CH}$), 4.45 (2H, s, OCH_2Ar), 2.14–1.73 (6H, m, 2 x CH_2 , CH), 1.66 (3H, dd, $J = 2.2, 1.1$ Hz, $\text{C}(\text{CH}_3)\text{CH}$), 1.33 (1H, tt, $J = 12.1, 6.0$ Hz, CH_2), 1.22 (6H, d, $J = 1.0$ Hz, 2 x CH_3); $^{13}\text{C}\{^1\text{H}\}$ NMR (CDCl_3 , 101 MHz) δ 140.3, 134.2, 128.4 (2C), 127.3 (2C), 127.1, 121.1, 77.4, 63.2, 42.5, 31.3, 27.1, 24.2, 23.5, 23.2, 22.8.

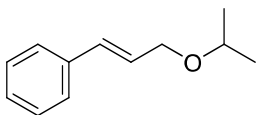
Data consistent with literature values.⁴



tert-Butyl(hex-2-en-1-yloxy)dimethylsilane 1i was synthesized according to a procedure reported by Wata *et al.*⁵ *tert*-Butylchlorodimethylsilane (0.74 g, 4.9 mmol, 1.2 equiv.) was added to a mixture of *trans*-hex-2-en-1-ol (0.49 mL, 4.0 mmol, 1.0 equiv.) and imidazole (0.41 g, 6.1 mmol, 1.5 equiv.) in dry CH_2Cl_2 (4 mL) under Ar at 0 °C. The reaction mixture was stirred overnight at room temperature before being quenched with water (15 mL). The mixture was extracted with CH_2Cl_2 (3 x 5 mL) and the combined organic layers were washed with brine, dried over anhydrous Na_2SO_4 , filtered and concentrated *in vacuo*. The crude was purified by column chromatography (EtOAc /heptane 1-4%) to afford *tert*-butyl(hex-2-en-1-yloxy)dimethylsilane **1i** (0.79 g, 3.7 mmol, 93%) as a colorless oil.

$^1\text{H NMR}$ (400 MHz, CDCl_3) δ 5.70–5.58 (1H, m, CHCH), 5.58–5.46 (1H, m, CHCH), 4.18–4.06 (2H, m, CH_2O), 2.06–1.95 (2H, m, CH_2), 1.40 (2H, h, $J = 7.4$ Hz, CH_2), 0.90 (12H, d, $J = 3.0$ Hz, CH_3 , $\text{C}(\text{CH}_3)_3$), 0.07 (6H, s, $\text{Si}(\text{CH}_3)_2$); $^{13}\text{C}\{^1\text{H}\}$ NMR (CDCl_3 , 101 MHz) δ 131.5, 129.4, 64.3, 34.4, 26.2 (3C), 22.5, 18.6, 13.8, -4.9 (2C).

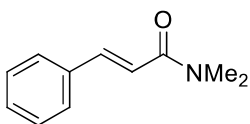
Data consistent with literature values.⁶



1-Phenyl-3-isopropoxy-1-propene 1s. Dry isopropanol (0.54 mL, 7.0 mmol, 1.0 equiv.) was added dropwise to a solution of sodium hydride (60% dispersion in mineral oil, 0.25 g, 11 mmol, 1.5 equiv.) in dry THF under Ar. The mixture was stirred 30 min at room temperature before being cooled to 0 °C. Cinnamyl bromide (1.6 mL, 11 mmol, 1.5 equiv.) was added dropwise. The mixture was stirred 15 min at 0 °C before being allowed to slowly reach room temperature. It was stirred at room temperature overnight. The reaction was quenched by slowly adding isopropanol (5 mL) and the mixture was reduced *in vacuo*. The residue was redissolved in water and extracted with EtOAc (3 x 20 mL). The combined organic layers were washed with brine, dried over anhydrous Na₂SO₄, filtered and concentrated *in vacuo*. The crude was purified by column chromatography (Et₂O/pentane 0-5%) to afford 1-phenyl-3-isopropoxy-1-propene **1s** (0.79 g, 4.5 mmol, 64%) as a light yellow oil.

¹H NMR (400 MHz, CDCl₃) δ 7.44–7.18 (5H, m, ArH), 6.61 (1H, dt, *J* = 16.0, 1.6 Hz, ArCH), 6.31 (1H, dt, *J* = 15.9, 6.0 Hz, CHCH₂O), 4.15 (2H, dd, *J* = 6.0, 1.5 Hz, CH₂O), 3.69 (1H, hept, *J* = 6.1 Hz, CH(CH₃)₂), 1.21 (6H, d, *J* = 6.1 Hz, 2 x CH₃); ¹³C{¹H} NMR (CDCl₃, 101 MHz) δ 137.0, 131.9, 128.6 (2C), 127.7, 127.0, 126.6 (2C), 71.1, 68.9, 22.3 (2C).

Data consistent with literature values.⁷

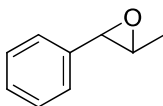


***N,N*-Dimethylcinnamamide 1u.** Oxalyl chloride (1.4 g, 11 mmol, 1.5 equiv.) and DMF (5 drops) were added to a solution of *trans*-cinnamic acid (1.2 g, 7.8 mmol, 1.0 equiv.) in dry CH₂Cl₂ (30 mL) under Ar. The reaction mixture was stirred at room temperature for 2 h before being cooled to 0 °C. A solution of dimethylamine 2 M in THF (15 mL, 30 mmol, 3.9 equiv.) was added dropwise to the cooled mixture. The reaction mixture was stirred 15 min at 0 °C before being stirred 2 h at room temperature. Water (25 mL) was slowly added to quench the reaction, and the mixture was reduced *in vacuo*. The residue was extracted with CH₂Cl₂ (3 x 10 mL), and the combined organic layers were washed with an aqueous 1 M HCl solution, a saturated aqueous NaHCO₃ solution and brine. The organic layer was dried over anhydrous Na₂SO₄, filtered and concentrated *in vacuo*. The crude was purified by column chromatography (MeOH/CH₂Cl₂ 5%) to afford *N,N*-dimethylcinnamamide **1u** (1.1 g, 6.0 mmol, 77%) as a light orange solid.

¹H NMR (400 MHz, CDCl₃) δ 7.67 (1H, dd, *J* = 15.4, 2.2 Hz, PhCH), 7.53 (2H, d, *J* = 7.0 Hz, ArH), 7.43–7.29 (3H, m, ArH), 6.89 (1H, dd, *J* = 15.5, 2.3 Hz, PhCHCHCO), 3.12 (6H, d, *J* = 41.2 Hz, CH₃); ¹³C{¹H} NMR (CDCl₃, 101 MHz) δ 166.8, 142.5, 135.6, 129.7, 128.9, 127.9, 117.6, 37.6, 36.1.

Data consistent with literature values.⁸

10. Epoxides 2q, 2r and 2s synthesis

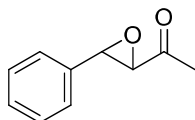


2-Methyl-3-phenyloxirane 2q was synthesized according to a procedure reported by Geng *et al.*⁹ Aqueous 2 M NaOH (4 μL) was added to an aqueous 4 · 10⁻⁴ M EDTA solution (9 mL) and the pH was adjusted to 4 with dilute aqueous NaOH. The mixture was added to a solution of *trans*-β-methylstyrene (0.40 mL, 3.1 mmol, 1.0 equiv.) in acetonitrile (36 mL). Sodium chlorite (1.1 g, 9.3 mmol, 3.1 equiv.) was added, the reaction flask was topped with a condenser and the reaction mixture was stirred at 65 °C overnight. The colorless mixture turned yellow. It was

cooled to 0 °C, and the mixture was slowly quenched by dropwise addition of an aqueous 1 M Na₂S₂O₃ solution until no more peroxide was detected by starch paper. The colorless quenched mixture was reduced *in vacuo* before being extracted with CH₂Cl₂ (3 x 15 ml). The combined organic layers were washed with water and brine, dried over anhydrous Na₂SO₄, filtered and concentrated *in vacuo*. The crude was purified by column chromatography (Et₂O/pentane 1:19-1:9) to afford 2-methyl-3-phenyloxirane **2q** (0.28 g, 2.1 mmol, 68%) as a colorless oil.

¹H NMR (400 MHz, CDCl₃) δ 7.37–7.21 (5H, m, ArH), 3.56 (1H, d, *J* = 2.0 Hz, ArCHO), 3.03 (1H, qd, *J* = 5.1, 2.1 Hz, CHO), 1.44 (3H, d, *J* = 5.1 Hz, CH₃); ¹³C{¹H} NMR (CDCl₃, 101 MHz) δ 137.9, 128.6 (2C), 128.2, 125.7 (2C), 59.7, 59.2, 18.1.

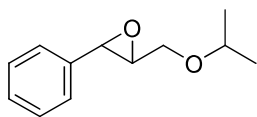
Data consistent with literature values.¹⁰



1-(3-Phenyloxiran-2-yl)ethan-1-one 2r was synthesized according to a procedure reported by Yao *et al.*¹¹ Hydrogen peroxide (30% in water, 3.7 mL, 48 mmol, 6.0 equiv.) was added to a mixture of benzalacetone (1.2 g, 8.0 mmol, 1.0 equiv.) and sodium bicarbonate (2.7 g, 32 mmol, 4.0 equiv.) in acetonitrile/water 3:2 (160 mL). The reaction mixture was stirred at room temperature for 48 h before being quenched by slow addition of 1 M Na₂S₂O₃ until no more peroxide was visible on starch paper. The mixture was reduced *in vacuo* and the residue was extracted with EtOAc (3 x 10 mL). The combined organic layers were washed with brine, dried over anhydrous Na₂SO₄, filtered and concentrated *in vacuo*. The crude was purified by column chromatography (Et₂O/pentane 10-20%) to afford a 3:2 mixture of 1-(3-phenyloxiran-2-yl)ethan-1-one **2r** (0.30 g, 1.9 mmol, 23%) and benzalacetone (0.20 g, 1.4 mmol) as a light-yellow oil. Due to the instability of the epoxide, the mixture was used without further purification for the next step.

¹H NMR (400 MHz, CDCl₃) δ 7.59–7.23 (5H, m), 4.01 (1H, d, *J* = 1.8 Hz), 3.49 (1H, d, *J* = 1.8 Hz), 2.20 (3H, s); ¹³C{¹H} NMR (CDCl₃, 101 MHz) δ 204.3, 135.2, 129.2, 128.9 (2C), 125.8 (2C), 63.6, 57.9, 24.9.

Data consistent with literature values.¹²



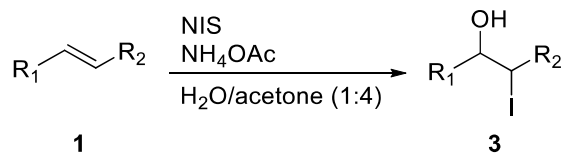
2-(Isopropoxymethyl)-3-phenyloxirane 2s was synthesized according to a procedure reported by Geng *et al.*⁹ Aqueous 2 M NaOH (6 μL) was added to an aqueous 4 · 10⁻⁴ M EDTA solution (13 mL) and the pH was adjusted to 4 with dilute aqueous NaOH. The mixture was added to a solution of 1-phenyl-3-isopropoxy-1-propene **1s** (0.79 g, 4.5 mmol, 1.0 equiv.) in acetonitrile (53 mL). Sodium chlorite (1.6 g, 14 mmol, 3.1 equiv.) was added, the reaction flask was topped with a condenser and the reaction mixture was stirred at 65 °C overnight. The colorless mixture turned yellow. It was cooled to 0 °C, and the mixture was slowly quenched by dropwise addition of an aqueous 1 M Na₂S₂O₃ solution until no more peroxide was detected by starch paper. The colorless quenched mixture was reduced *in vacuo* before being extracted with CH₂Cl₂ (3 x 15 ml). The combined organic layers were washed with water and brine, dried over anhydrous Na₂SO₄, filtered and concentrated *in vacuo*. The crude was purified by column chromatography (Et₂O/pentane 5-10%) to afford 2-(isopropoxymethyl)-3-phenyloxirane **2s** (0.23 g, 1.2 mmol, 26%) as a light-yellow oil.

R_f 0.24 (Et₂O/pentane 10%); IR (thin film, ν_{max}/cm⁻¹) 2974, 2926, 2921, 2871, 1466, 1382, 1371, 1150, 1130, 1091, 885, 751, 700; ¹H NMR (400 MHz, CDCl₃) δ 7.41–7.22 (5H, m, ArH), 3.80 (2H, dd, *J* = 11.4, 2.9 Hz, CHO, CH₂), 3.69

(1H, hept, $J = 6.1$ Hz, $\text{CH}(\text{CH}_3)_2$), 3.58 (1H, dd, $J = 11.5, 5.2$ Hz, CH_2), 3.20 (1H, ddd, $J = 5.3, 3.1, 2.1$ Hz, CHO), 1.20 (6H, t, $J = 5.8$ Hz, $2 \times \text{CH}_3$); $^{13}\text{C}\{^1\text{H}\}$ NMR (CDCl_3 , 101 MHz) δ 137.2, 128.6, 128.3, 125.9, 72.5, 68.2, 61.7, 56.2, 22.3, 22.1; HRMS (APCI) calc. for $\text{C}_{12}\text{H}_{17}\text{O}_2$ ($[\text{M}+\text{H}]^+$) 193.1223, found 193.1223.

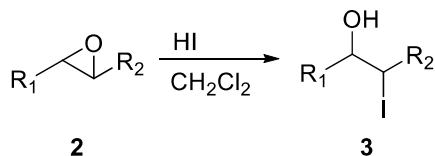
11. Iodohydrins 3a-v synthesis

11.1 Procedure A

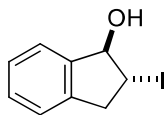


Based on a literature procedure.¹³ *N*-iodosuccinimide (1.1 equiv.) and distilled water (1.0 M with respect to the olefin) were added to a mixture of olefin (1.0 equiv.) and ammonium acetate (0.1 equiv.) in acetone (0.25 M with respect to the olefin). The reaction mixture was stirred in the dark at room temperature. Upon completion as indicated by TLC, the mixture was concentrated *in vacuo*, and the residue was redissolved in water and extracted with ethyl acetate (3×10 mL). The combined organic layers were washed with an aqueous 10% solution of $\text{Na}_2\text{S}_2\text{O}_3$, dried over anhydrous Na_2SO_4 , filtered and concentrated *in vacuo*. The crude was purified by column chromatography to afford the wanted iodohydrin **3**.

11.2 Procedure B



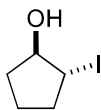
Hydroiodic acid (57 wt.% in H_2O , 1.2 equiv.) was added to a solution of epoxide **2** (1.0 equiv.) in CH_2Cl_2 (0.5 M with respect to the epoxide) and the reaction mixture was stirred in the dark. Upon completion as indicated by TLC, the mixture was diluted with CH_2Cl_2 (20 mL). It was washed with an aqueous 10% solution of NaHCO_3 , an aqueous 10% solution of $\text{Na}_2\text{S}_2\text{O}_3$, dried over anhydrous Na_2SO_4 , filtered and concentrated *in vacuo*. The crude was purified by column chromatography to afford the wanted iodohydrin **3**.



2-Iodo-2,3-dihydro-1H-inden-1-ol 3a was synthesized from indene (1.0 mL, 7.7 mmol, 1.0 equiv.), *N*-iodosuccinimide (1.9 g, 8.7 mmol, 1.1 equiv.) and NH_4OAc (65 mg, 0.83 mmol, 0.11 equiv.) in $\text{H}_2\text{O}/\text{acetone}$ 1:4 (38 mL) according to Procedure A. The crude was purified by column chromatography (EtOAc/pentane 20%) to afford 2-iodo-2,3-dihydro-1H-inden-1-ol **3a** (1.3 g, 5.0 mmol, 65%) as a white solid.

^1H NMR (400 MHz, CDCl_3) δ 7.48–7.39 (1H, m, *ArH*), 7.32–7.27 (2H, m, *ArH*), 7.25–7.21 (1H, m, *ArH*), 5.40 (1H, t, $J = 6.3$ Hz, CHOH), 4.22 (1H, ddd, $J = 8.0, 7.3, 6.4$ Hz, CHI), 3.60 (1H, dd, $J = 16.2, 7.3$ Hz, CH_2), 3.32 (1H, dd, $J = 16.2, 8.0$ Hz, CH_2), 2.31 (1H, d, $J = 6.2$ Hz, OH); $^{13}\text{C}\{^1\text{H}\}$ NMR (CDCl_3 , 101 MHz) δ 142.2, 141.1, 129.0, 127.7, 124.5, 124.0, 85.2, 42.4, 30.2.

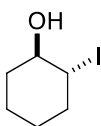
Data consistent with literature values.¹⁴



2-Iodocyclopentanol 3b was synthesized from cyclopentene (0.22 mL, 2.5 mmol, 1.0 equiv.), *N*-iodosuccinimide (0.63 g, 2.8 mmol, 1.1 equiv.) and NH_4OAc (26 mg, 0.33 mmol, 0.13 equiv.) in $\text{H}_2\text{O}/\text{acetone}$ 1:4 (12 mL) according to Procedure A. The crude was purified by column chromatography (EtOAc/heptane 30%) to afford 2-iodocyclopentanol **3b** (0.25 g, 1.2 mmol, 47%) as a colorless oil.

$^1\text{H NMR}$ (400 MHz, CDCl_3) δ 4.45 (1H, dd, $J = 6.6, 4.0$ Hz, *CHOH*), 4.04 (1H, q, $J = 5.9$ Hz, *CHI*), 2.37 (1H, dq, $J = 14.4, 7.3$ Hz, *CH_2*), 2.09 (2H, ddq, $J = 28.4, 13.9, 7.1$ Hz, *CH_2*), 1.95 (1H, d, $J = 3.5$ Hz, *OH*), 1.82 (2H, p, $J = 7.6$ Hz, *CH_2*), 1.65–1.51 (1H, m, *CH_2*); $^{13}\text{C}\{^1\text{H}\}$ NMR (CDCl_3 , 101 MHz) δ 82.3, 35.8, 34.3, 31.1, 22.2.

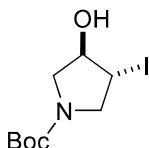
Data consistent with literature values.¹⁵



2-Iodocyclohexanol 3c was synthesized from cyclohexene (1.0 mL, 9.9 mmol, 1.0 equiv.), *N*-iodosuccinimide (2.5 g, 11 mmol, 1.1 equiv.) and NH_4OAc (79 mg, 1.0 mmol, 0.10 equiv.) in $\text{H}_2\text{O}/\text{acetone}$ 1:4 (50 mL) according to Procedure A. The crude was purified by column chromatography (EtOAc/pentane 20%) to afford 2-iodocyclohexanol **3c** (1.5 g, 6.8 mmol, 69%) as a colorless oil.

$^1\text{H NMR}$ (400 MHz, CDCl_3) δ 4.04 (1H, ddd, $J = 12.3, 9.7, 4.3$ Hz, *CHI*), 3.65 (1H, tdd, $J = 10.0, 4.5, 2.6$ Hz, *CHO*), 2.47 (1H, dqd, $J = 13.3, 3.6, 1.9$ Hz, *CHICH_2*), 2.31 (1H, d, $J = 2.7$ Hz, *OH*), 2.17–2.07 (1H, m, *CH_2CHOH*), 2.07–2.01 (1H, m, *CHICH_2*), 1.91–1.79 (1H, m, *CH_2CH_2CHOH*), 1.59–1.47 (1H, m, *CHICH_2CH_2*), 1.47–1.19 (3H, m, *CHICH_2CH_2*, *CH_2CH_2CHOH*, *CH_2CHOH*); $^{13}\text{C}\{^1\text{H}\}$ NMR (CDCl_3 , 101 MHz) δ 76.1, 43.6, 38.8, 33.8, 28.1, 24.6.

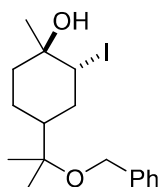
Data consistent with literature values.¹⁴



tert-Butyl 3-hydroxy-4-iodopyrrolidine-1-carboxylate 3d was synthesized according to a procedure reported by Narender *et al.*¹⁶ A solution of β -cyclodextrin (2.8 g, 2.5 mmol, 1.0 equiv.) in water (30 mL) was stirred at 65 °C until full dilution. A solution of *N*-Boc-2,5-dihydro-1*H*-pyrrole (0.45 mL, 2.5 mmol, 1.0 equiv.) in acetone (2 mL) was added dropwise to the warm solution, and the reaction mixture was allowed to cool to room temperature. *N*-iodosaccharin (0.88 g, 2.8 mmol, 1.1 equiv.) was added and the mixture was stirred in the dark at room temperature for 1 h. EtOAc (30 mL) was added, and the reaction mixture was filtered under reduced pressure. The filtrate was extracted with EtOAc (3 x 10 mL), the combined organic layers were washed with an aqueous 10% solution of $\text{Na}_2\text{S}_2\text{O}_3$, dried over anhydrous Na_2SO_4 , filtered and concentrated *in vacuo*. The crude was purified by column chromatography (EtOAc/heptane 50%) to afford *tert*-butyl 3-hydroxy-4-iodopyrrolidine-1-carboxylate **3d** (0.47 g, 1.5 mmol, 60%) as a colorless oil.

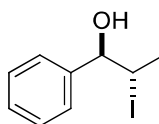
R_f 0.31 (EtOAc/heptane 50%); IR (thin film, $\nu_{\text{max}}/\text{cm}^{-1}$) 3387, 2977, 2928, 1670, 1421, 1369, 1167, 1116, 959, 869, 771; $^1\text{H NMR}$ (400 MHz, CDCl_3 , mixture of rotamers) δ 4.54 (1H, d, $J = 5.6$ Hz, *CHOH*), 4.16–4.03 (2H, m, *CHI*, *CH_2CHI*), 3.97–3.85 (1H, m, *CH_2CHOH*), 3.85–3.70 (1H, m, *CH_2CHI*), 3.37 (1H, t, $J = 11.5$ Hz, *CH_2CHOH*), 2.54 (1H, d, $J = 3.9$ Hz, *OH*), 1.47 (9H, s, 3 x *CH_3*); $^{13}\text{C}\{^1\text{H}\}$ NMR (CDCl_3 , 101 MHz, mixture of rotamers) δ 154.5 (2C), 80.3

(2C), 78.9, 78.0, 54.5, 54.0, 51.5, 51.1, 29.2, 28.6, 26.1, 25.7; **HRMS** (APCI) calc. for C₄H₉INO ([M-Boc+H]⁺) 213.9723, found 213.9721.



4-(2-(Benzyloxy)propan-2-yl)-2-iodo-1-methylcyclohexanol 3e was synthesized from 4-(1-(benzyloxy)-1-methylethyl)-1-methylcyclohexene **1e** (0.44 g, 1.8 mmol, 1.0 equiv.), *N*-iodosuccinimide (0.44 g, 2.0 mmol, 1.1 equiv.) and NH₄OAc (28 mg, 0.36 mmol, 0.20 equiv.) in H₂O/acetone 1:4 (8.2 mL) according to Procedure A. The crude was purified by column chromatography (Et₂O/pentane 50%) to afford 4-(2(benzyloxy)propan-2-yl)-2-iodo-1-methylcyclohexanol **3e** (0.23 g, 0.59 mmol, 33%) as a colorless oil.

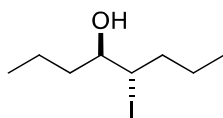
R_f 0.32 (Et₂O/pentane 50%); **IR** (thin film, ν_{\max} /cm⁻¹) 2974, 2934, 2879, 1454, 1384, 1320, 1230, 1207, 1167, 1128, 1086, 1059, 1029, 987, 948, 907, 885, 735, 698; **¹H NMR** (400 MHz, CDCl₃) δ 7.41–7.20 (5H, m, ArH), 4.54–4.39 (3H, m, OCH₂, CHI), 2.26–1.96 (4H, m, 3 x CH₂, CH), 1.70–1.53 (3H, m, 3 x CH₂), 1.51 (3H, s, C(CH₃)OH), 1.49–1.42 (1H, m, OH), 1.27 (3H, s, CH₃), 1.21 (3H, s, CH₃); **¹³C{¹H} NMR** (CDCl₃, 101 MHz) δ 140.0, 128.4 (2C), 127.5 (2C), 127.2, 76.8, 71.5, 63.3, 43.0, 41.0, 33.7, 33.3, 32.9, 23.7, 23.6, 22.5; **HRMS** (APCI) calc. for C₁₇H₂₉INO₂ ([M+NH₄]⁺) 406.1238, found 406.1237.



2-iodo-1-phenylpropan-1-ol 3f was synthesized from *trans*- β -methylstyrene (1.0 mL, 7.6 mmol, 1.0 equiv.), *N*-iodosuccinimide (2.1 g, 9.2 mmol, 1.2 equiv.) and NH₄OAc (60 mg, 0.78 mmol, 0.10 equiv.) in H₂O/acetone 1:4 (36 mL) according to Procedure A. The crude was purified by column chromatography (Et₂O/heptane 10%) to afford 2-iodo-1-phenylpropan-1-ol **3f** (1.4 g, 5.4 mmol, 71%) as a colorless oil.

¹H NMR (400 MHz, CDCl₃) δ 7.44–7.28 (5H, m, ArH), 4.96 (1H, t, *J* = 3.5 Hz, CHOH), 4.53 (1H, qd, *J* = 7.0, 3.7 Hz, CHI), 2.36 (1H, d, *J* = 3.4 Hz, OH), 1.74 (3H, d, *J* = 7.0 Hz, CH₃); **¹³C{¹H} NMR** (CDCl₃, 101 MHz) δ 139.9, 128.5 (2C), 128.2, 126.6 (2C), 78.6, 36.1, 21.4.

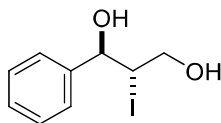
Data consistent with literature values.¹⁷



5-iodooctan-4-ol 3g was synthesized from *trans*-4-octene (1.0 mL, 6.2 mmol, 1.0 equiv.), *N*-iodosuccinimide (1.7 g, 7.5 mmol, 1.2 equiv.) and NH₄OAc (48 mg, 0.63 mmol, 0.10 equiv.) in H₂O/acetone 1:4 (29 mL) according to Procedure A. The crude was purified by column chromatography (Et₂O/pentane 10-20%) to afford 5-iodooctan-4-ol **3g** (1.2 g, 4.8 mmol, 77%) as a light-yellow oil.

R_f 0.38 (Et₂O/pentane 20%); **IR** (liquid, ν_{\max} /cm⁻¹) 3409, 2959, 2933, 2873, 1465, 1383, 1257, 1115, 1067, 1007, 847, 747; **¹H NMR** (400 MHz, CDCl₃) δ 4.34 (1H, dt, *J* = 10.5, 3.4 Hz, CHI), 3.38–3.25 (1H, m, CHOH), 1.95–1.79 (2H, m, OH, CH₂CHOH), 1.72–1.49 (5H, m, 3 x CH₂CH₂CH₃, 2 x CH₂CH₂CH₃), 1.47–1.30 (2H, m, 2 x CH₂CH₂CH₃), 1.02–

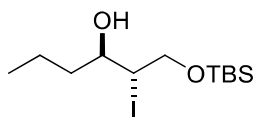
0.88 (6H, m, 2 x CH₃); ¹³C{¹H} NMR (CDCl₃, 101 MHz) δ 75.3, 49.9, 37.0, 36.8, 23.4, 19.3, 14.2, 13.4; HRMS (APCI) calc. for C₈H₂₁INO [(M+NH₄)⁺] 274.0662, found 274.0685.



2-iodo-1-phenylpropan-1,3-diol 3h was synthesized from cinnamyl alcohol (0.55 g, 4.0 mmol, 1.0 equiv.), *N*-iodosuccinimide (0.99 g, 4.4 mmol, 1.1 equiv.) and NH₄OAc (31 mg, 0.40 mmol, 0.10 equiv.) in H₂O/acetone 1:4 (19 mL) according to Procedure A. The crude was purified by column chromatography (Et₂O/pentane 50%) to afford 2-iodo-1-phenylpropan-1,3-diol **3h** (0.65 g, 2.3 mmol, 58%) as a white solid.

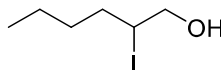
¹H NMR (400 MHz, CDCl₃) δ 7.45–7.28 (5H, m, ArH), 5.06 (1H, dd, *J* = 6.3, 4.1 Hz, CHOH), 4.46 (1H, ddd, *J* = 6.3, 5.4, 4.6 Hz, CHI), 3.97 (1H, ddd, *J* = 12.4, 6.8, 4.6 Hz, CH₂), 3.82 (1H, ddd, *J* = 12.3, 6.2, 5.4 Hz, CH₂), 2.92 (1H, d, *J* = 4.1 Hz, CHOH), 2.54 (1H, t, *J* = 6.5 Hz, CH₂OH); ¹³C{¹H} NMR (CDCl₃, 101 MHz) δ 141.0, 128.8 (2), 128.7, 126.7 (2), 78.7, 66.1, 41.6.

Data consistent with literature values.¹⁸



1-((tert-Butyldimethylsilyl)oxy)-2-iodohexan-3-ol 3i was synthesized from **1i** (0.78 g, 3.7 mmol, 1.0 equiv.), *N*-iodosuccinimide (0.93 g, 4.1 mmol, 1.1 equiv) and ammonium acetate (38 mg, 0.49 mmol, 0.10 equiv.) in H₂O/acetone 1:4 (18 mL) according to Procedure A. The crude was purified by column chromatography (EtOAc/heptane 5-50%) to afford 1-((tert-butylidimethylsilyl)oxy)-2-iodohexan-3-ol **3i** (88 mg, 0.25 mmol, 7%) as a colorless oil.

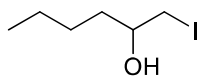
R_f 0.33 (Et₂O/pentane 10%); IR (liquid, ν_{max}/cm⁻¹) 2956, 2929, 2856, 1465, 1256, 1091, 1059, 835, 777; ¹H NMR (400 MHz, CDCl₃) δ 4.22 (1H, dt, *J* = 7.9, 5.4 Hz, CHI), 4.07 (1H, dd, *J* = 11.0, 4.8 Hz, CHICH₂), 3.91 (1H, dd, *J* = 10.9, 8.0 Hz, CHICH₂), 3.68 (1H, dtd, *J* = 8.5, 5.5, 2.9 Hz, CHOH), 2.99 (1H, d, *J* = 5.2 Hz, OH), 1.71 (1H, ddd, *J* = 12.7, 6.9, 3.5 Hz, CH₃CH₂), 1.61–1.47 (2H, m, CH₃CH₂, CH₃CH₂CH₂), 1.47–1.34 (1H, m, CH₃CH₂CH₂), 0.95 (3H, t, *J* = 7.1 Hz, CH₃CH₂), 0.91 (9H, s, C(CH₃)₃), 0.10 (5H, d, *J* = 2.0 Hz, Si(CH₃)₂); ¹³C{¹H} NMR (CDCl₃, 101 MHz) δ 74.5, 67.8, 41.5, 38.4, 25.9, 18.8, 18.3, 14.1, -5.2, -5.3; HRMS (APCI) calc. for C₁₂H₂₅IOSi [(M+H-H₂O)⁺] 341.0792, found 341.0792.



2-iodohexan-1-ol 3j was synthesized from 1-hexene (1.0 mL, 7.8 mmol, 1.0 equiv.), *N*-iodosuccinimide (2.1 g, 9.4 mmol, 1.2 equiv.) and NH₄OAc (62 mg, 0.79 mmol, 0.10 equiv.) in H₂O/acetone 1:4 (36 mL) according to Procedure A. The reaction produced a 1:4 mixture of 2-iodohexan-1-ol **3j** and 1-iodohexan-2-ol **3k**. The isomers were separated by column chromatography (Et₂O/pentane 0-30%) to afford 2-iodohexan-1-ol **3j** (0.25 g, 1.1 mmol, 14%) as a colorless oil.

R_f 0.33 (Et₂O/pentane 30%); IR (liquid, ν_{max}/cm⁻¹) 3367, 2955, 2926, 2859, 1459, 1380, 1231, 1154, 1099, 1053, 1034, 1002, 732; ¹H NMR (400 MHz, CDCl₃) δ 4.22 (1H, ddt, *J* = 9.4, 6.5, 4.9 Hz, CHI), 3.80–3.65 (2H, m, CH₂O), 1.96 (1H, m OH), 1.87 (1H, m, CH₂CHI), 1.77 (1H, m, CH₂CHI), 1.59–1.45 (1H, m, CH₂CH₂CHI), 1.45–1.26 (3H, m,

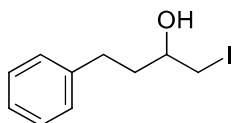
$\text{CH}_2\text{CH}_2\text{CHI}$, 2 x CH_3CH_2), 0.92 (3H, t, $J = 7.1$ Hz, CH_3); $^{13}\text{C}\{^1\text{H}\}$ NMR (CDCl_3 , 101 MHz) δ 68.7, 42.2, 36.1, 31.7, 22.1, 14.0; HRMS (ESI) calc. for $\text{C}_6\text{H}_{13}\text{IONa}$ ($[\text{M}+\text{Na}]^+$) 250.9903, found 250.9903.



1-iodohexan-2-ol 3k was synthesized from 1-hexene (1.0 mL, 7.8 mmol, 1.0 equiv.), *N*-iodosuccinimide (2.1 g, 9.4 mmol, 1.2 equiv.) and NH_4OAc (62 mg, 0.79 mmol, 0.10 equiv.) in $\text{H}_2\text{O}/\text{acetone}$ 1:4 (36 mL) according to Procedure A. The reaction produced a 1:4 mixture of 2-iodohexan-1-ol **3j** and 1-iodohexan-2-ol **3k**. The isomers were separated by column chromatography ($\text{Et}_2\text{O}/\text{pentane}$ 0-30%) to afford 1-iodohexan-2-ol **3k** (1.1 g, 4.8 mmol, 62%) as a colorless oil.

^1H NMR (400 MHz, CDCl_3) δ 3.57–3.46 (1H, m, CHOH), 3.40 (1H, dd, $J = 10.1, 3.5$ Hz, CH_2I), 3.23 (1H, dd, $J = 10.1, 6.8$ Hz, CH_2I), 1.93 (1H, d, $J = 5.3$ Hz, OH), 1.56 (2H, dtd, $J = 7.9, 5.9, 3.5$ Hz, CH_2CHOH), 1.48–1.27 (4H, m, $\text{CH}_2\text{CH}_2\text{CH}_3$, $\text{CH}_2\text{CH}_2\text{CH}_3$), 0.98–0.85 (3H, m, CH_3); $^{13}\text{C}\{^1\text{H}\}$ NMR (CDCl_3 , 101 MHz) δ 71.1, 36.5, 28.0, 22.7, 17.0, 14.1.

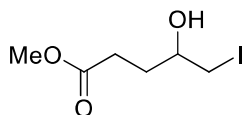
Data consistent with literature values.¹⁹



1-iodo-4-phenylbutan-2-ol 3l was synthesized from 4-phenyl-1-butene (0.60 mL, 4.0 mmol, 1.0 equiv.), *N*-iodosuccinimide (1.1 g, 4.8 mmol, 1.2 equiv.) and NH_4OAc (34 mg, 0.44 mmol, 0.11 equiv.) in $\text{H}_2\text{O}/\text{acetone}$ 1:4 (19 mL) according to Procedure A. The crude was purified by column chromatography ($\text{Et}_2\text{O}/\text{pentane}$ 0-40%) to afford 1-iodo-4-phenylbutan-2-ol **3l** (0.51 g, 1.9 mmol, 47%) as a colorless oil.

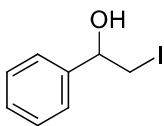
^1H NMR (400 MHz, CDCl_3) δ 7.38–7.21 (5H, m, ArH), 3.58 (1H, dddd, $J = 12.4, 6.8, 5.4, 3.5$ Hz, CHOH), 3.43 (1H, dd, $J = 10.2, 3.5$ Hz, CH_2I), 3.30 (1H, dd, $J = 10.2, 6.8$ Hz, CH_2I), 2.91–2.81 (1H, m, CH_2CHOH), 2.76 (1H, dt, $J = 13.8, 8.1$ Hz, CH_2CHOH), 2.04 (1H, d, $J = 5.4$ Hz, OH), 1.97–1.88 (2H, m, CH_2); $^{13}\text{C}\{^1\text{H}\}$ NMR (CDCl_3 , 101 MHz) δ 141.4, 128.7 (2C), 128.6 (2C), 128.6, 126.2, 70.3, 38.3, 32.1, 16.7.

Data consistent with literature values.²⁰



Methyl 4-hydroxy-5-iodopentanoate 3m was synthesized from methyl 4-pentanoate (0.31 g, 2.7 mmol, 1.0 equiv.), *N*-iodosuccinimide (0.68 g, 3.0 mmol, 1.1 equiv.) and NH_4OAc (28 mg, 0.35 mmol, 0.13 equiv.) in $\text{H}_2\text{O}/\text{acetone}$ 1:4 (12.5 mL) according to Procedure A. The crude was purified by column chromatography ($\text{Et}_2\text{O}/\text{pentane}$ 50-60%) to afford methyl 4-hydroxy-5-iodopentanoate **3m** (0.34 g, 1.3 mmol, 48%) as a colorless oil.

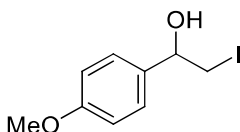
R_f 0.26 ($\text{Et}_2\text{O}/\text{pentane}$ 50%); IR (thin film, $\nu_{\text{max}}/\text{cm}^{-1}$) 3318, 2950, 2837, 1720, 1655, 1442, 1016; ^1H NMR (400 MHz, CDCl_3) δ 3.69 (3H, s, OCH_3), 3.61 (1H, dh, $J = 14.4, 3.9$ Hz, CHOH), 3.36 (1H, dd, $J = 10.2, 4.0$ Hz, CH_2I), 3.24 (1H, dd, $J = 10.2, 6.6$ Hz, CH_2I), 2.50 (2H, t, $J = 7.1$ Hz, $\text{CH}_3\text{OCOCH}_2$), 2.35 (1H, d, $J = 5.5$ Hz, OH), 1.96 (1H, dtd, $J = 14.5, 7.3, 3.5$ Hz, CH_2), 1.82 (1H, dtd, $J = 14.0, 8.8, 6.9$ Hz, CH_2); $^{13}\text{C}\{^1\text{H}\}$ NMR (CDCl_3 , 101 MHz) δ 174.2, 70.4, 52.0, 31.5, 30.4, 15.5; HRMS (APCI) calc. for $\text{C}_6\text{H}_{12}\text{IO}_3$ ($[\text{M}+\text{H}]^+$) 258.9826, found 258.9824.



2-Iodo-1-phenylethan-1-ol 3n was synthesized from styrene (0.30 mL, 2.6 mmol, 1.0 equiv.), *N*-iodosuccinimide (0.61 g, 2.7 mmol, 1.0 equiv.) and NH₄OAc (24 mg, 0.30 mmol, 0.12 equiv.) in H₂O/acetone 1:4 (12 mL) according to Procedure A. The crude was purified by column chromatography (Et₂O/pentane 30%) to afford 2-iodo-1-phenylethan-1-ol **3n** (0.44 g, 1.8 mmol, 69%) as an orange oil.

¹H NMR (400 MHz, CDCl₃) δ 7.38 (5H, m, ArH), 4.84 (1H, m, CHO), 3.50 (1H, m, CH₂I), 3.41 (1H, m, CH₂I), 2.51–2.37 (1H, m, OH); ¹³C{¹H} NMR (CDCl₃, 101 MHz) δ 141.2, 128.9, 128.5, 125.9, 74.2, 15.5.

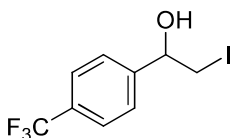
Data consistent with literature values.²¹



2-Iodo-1-(4-methoxyphenyl)ethan-1-ol 3o was synthesized from 1-methoxy-4-vinylbenzene (1.4 mL, 10 mmol, 1.0 equiv.), *N*-iodosuccinimide (2.4 g, 11 mmol, 1.1 equiv.) and NH₄OAc (0.11 g, 1.4 mmol, 0.14 equiv.) in H₂O/acetone 1:4 (48 mL) according to Procedure A. The crude was purified by column chromatography (Et₂O/pentane 30%) to afford 2-iodo-1-(4-methoxyphenyl)ethan-1-ol **3o** (1.5 g, 5.2 mmol, 52%) as a dark-red oil.

¹H NMR (400 MHz, CDCl₃) δ 7.30 (2H, d, *J* = 8.7 Hz, ArH), 6.90 (2H, d, *J* = 8.8 Hz, ArH), 4.80 (1H, d, *J* = 7.4 Hz, CHO), 3.81 (3H, s, OCH₃), 3.52–3.33 (2H, m, CH₂I), 2.42 (1H, s, OH); ¹³C{¹H} NMR (CDCl₃, 101 MHz) δ 159.8, 133.4, 127.1 (2C), 114.2 (2C), 73.9, 55.5, 15.7.

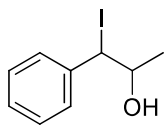
Data consistent with literature values.¹⁴



2-Iodo-1-(4-(trifluoromethyl)phenyl)ethan-1-ol 3p was synthesized from 4-(trifluoromethyl)styrene (0.37 mL, 2.5 mmol, 1.0 equiv.), *N*-iodosuccinimide (0.61 g, 2.7 mmol, 1.1 equiv.) and NH₄OAc (29 mg, 0.37 mmol, 0.15 equiv.) in H₂O/acetone 1:4 (12 mL) according to Procedure A. The crude was purified by column chromatography (Et₂O/pentane 20%) to afford 2-iodo-1-(4-(trifluoromethyl)phenyl)ethan-1-ol **3p** (0.32 g, 1.0 mmol, 41%) as a colorless oil.

¹H NMR (400 MHz, CDCl₃) δ 7.64 (2H, d, *J* = 8.1 Hz, ArH), 7.58–7.46 (2H, m, ArH), 4.88 (1H, dt, *J* = 8.0, 3.7 Hz, CHO), 3.52 (1H, dd, *J* = 10.4, 3.6 Hz, CH₂I), 3.39 (1H, dd, *J* = 10.4, 8.5 Hz, CH₂I), 2.54 (1H, d, *J* = 3.8 Hz, OH); ¹³C{¹H} NMR (CDCl₃, 101 MHz) δ 145.0, 130.5, 126.3 (2C), 125.8 (2C, q, ³J_{C-F} = 3.8 Hz), 73.4, 14.9. Note: The ¹³C signal for the CF₃ group was not visible due to its low intensity.

Data consistent with literature values.²²

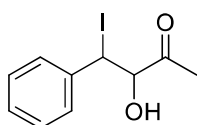


1-Iodo-1-phenylpropan-2-ol 3q was synthesized from 2-methyl-3-phenyloxirane **2q** (0.25 g, 1.9 mmol, 1.0 equiv.) and hydroiodic acid (57 wt.% in H₂O, 0.3 mL, 2.3 mmol, 1.2 equiv.) in CH₂Cl₂ (3.8 mL) according to Procedure B. The crude was purified by column chromatography (Et₂O/pentane 30%) to afford an inseparable 89:11 diastereomers mixture of 1-iodo-1-phenylpropan-2-ol **3q** (0.27 g, 1.0 mmol, 54%) as a colorless oil. *Note: the product degraded when kept under Ar at 8 °C overnight. It was resynthesized and used straight away for the next step. The NMR data were extracted from the inseparable mixture NMR.*

R_f 0.30 (Et₂O/pentane 30%); **IR** (thin film, $\nu_{\max}/\text{cm}^{-1}$) 3419, 2975, 1492, 1453, 1116, 1076, 942, 759, 698; **HRMS** (APCI) calc. for C₉H₁₂I₂O ([M+H]⁺) 262.9927, found 262.9925.

major: **¹H NMR** (400 MHz, CDCl₃) δ 7.53–7.20 (5H, m, ArH), 5.04 (1H, d, J = 6.8 Hz, CHI), 4.18 (1H, pd, J = 6.3, 3.8 Hz, CHOH), 2.04 (1H, d, J = 3.9 Hz, OH), 1.41 (3H, d, J = 6.1 Hz, CH₃); **¹³C{¹H} NMR** (CDCl₃, 101 MHz) δ 140.3, 129.0 (2C), 128.9 (2C), 128.6, 72.5, 41.5, 21.4.

minor: **¹H NMR** (400 MHz, CDCl₃) δ 7.53–7.20 (5H, m, ArH), 5.07–5.06 (1H, m, CHI), 4.06–3.98 (1H, m, CHOH), 2.34 (1H, d, J = 3.9 Hz, OH), 1.13 (3H, d, J = 6.1 Hz, CH₃); **¹³C{¹H} NMR** (CDCl₃, 101 MHz) δ 128.5 (2C), 128.1 (3C), 72.2, 47.4, 20.1.

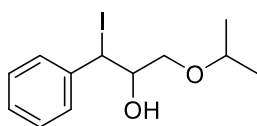


3-Hydroxy-4-iodo-4-phenylbutan-2-one 3r was synthesized from 1-(3-phenyloxiran-2-yl)ethan-1-one **2r** (0.30 g, 1.8 mmol, 1.0 equiv.) and hydroiodic acid (57 wt.% in H₂O, 0.29 mL, 2.3 mmol, 1.2 equiv.) in CH₂Cl₂ (3.7 mL) according to Procedure B. The crude was purified by column chromatography (Et₂O/pentane 20%) to afford an inseparable 86:14 diastereomers mixture of 3-hydroxy-4-iodo-4-phenylbutan-2-one **3r** (0.35 g, 1.2 mmol, 65%) as a light-yellow oil. *Note: the NMR data were extracted from the inseparable mixture NMR.*

R_f 0.30 (Et₂O/pentane 20%); **IR** (thin film, $\nu_{\max}/\text{cm}^{-1}$) 3442, 1719, 1455, 1357, 1239, 1194, 1101, 699; **HRMS** (APCI) calc. for C₁₀H₁₂I₂O₂ ([M+H]⁺) 290.9877, found 290.9876.

major: **¹H NMR** (400 MHz, CDCl₃) δ 7.53–7.44 (2H, m, ArH), 7.33–7.22 (3H, m, ArH), 5.54 (1H, d, J = 4.2 Hz, CH₂I), 4.59 (1H, dd, J = 4.9, 4.1 Hz, CHOH), 3.59 (1H, d, J = 4.8 Hz, OH), 2.15 (3H, s, CH₃); **¹³C{¹H} NMR** (CDCl₃, 101 MHz) δ 204.4, 138.7, 129.0, 128.8, 128.7, 128.7, 82.3, 29.9, 26.9.

minor: **¹H NMR** (400 MHz, CDCl₃) δ 7.62–7.59 (2H, m, ArH), 7.33–7.28 (3H, m, ArH), 5.51 (1H, d, J = 2.9 Hz, CH₂I), 4.01 (1H, dd, J = 5.9, 2.8 Hz, CHOH), 3.89 (1H, d, J = 5.9 Hz, OH), 2.28 (3H, s, CH₃); **¹³C{¹H} NMR** (CDCl₃, 101 MHz) δ 80.3, 34.3, 25.5. *Note: Carbonyl and aromatic carbons missing due to low intensity.*



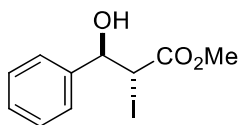
1-Iodo-3-isopropoxy-1-phenylpropan-2-ol 3s was synthesized from 2-(isopropoxymethyl)-3-phenyloxirane **2s** (0.23 g, 1.2 mmol, 1.0 equiv.) and hydroiodic acid (57 wt.% in H₂O, 0.19 mL, 1.4 mmol, 1.2 equiv.) in CH₂Cl₂ (2.3 mL) according to Procedure B. The crude was purified by column chromatography (Et₂O/pentane 20%) to afford

an inseparable 64:36 diastereomers mixture of 1-iodo-3-isopropoxy-1-phenylpropan-2-ol **3s** (0.26 g, 0.82 mmol, 70%) as a yellow oil. *Note: the NMR data were extracted from the inseparable mixture NMR.*

R_f 0.22 (Et₂O/pentane 20%); IR (thin film, $\nu_{\max}/\text{cm}^{-1}$) 3422, 2971, 2869, 1736, 1454, 1382, 1371, 1147, 1128, 1095, 926, 765, 697; HRMS (APCI) calc. for C₁₂H₁₇O₂Na ([M+Na]⁺) 343.0165, found 343.0166.

major: ¹H NMR (400 MHz, CDCl₃) δ 7.46 (2H, m, ArH), 7.36–7.21 (3H, m, ArH), 5.22 (1H, d, J = 7.9 Hz, CHI), 4.29 (1H, dtd, J = 7.9, 5.1, 3.9 Hz, CHOH), 3.74 (1H, m, CH₂), 3.69 (1H, m, CH₂), 3.61 (1H, m, CH(CH₃)₂), 2.59 (1H, d, J = 4.9 Hz, OH), 1.18 (6H, dd, J = 8.8, 6.1 Hz, 2 x CH₃); ¹³C{¹H} NMR (CDCl₃, 101 MHz) δ 140.7, 128.9, 128.8 (2C), 128.7 (2C), 74.4, 72.5, 69.9, 34.0, 22.2 (2C).

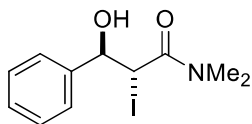
minor: ¹H NMR (400 MHz, CDCl₃) δ 7.46 (2H, m, ArH), 7.37–7.20 (3H, m, ArH), 5.26 (1H, d, J = 7.5 Hz, CHI), 3.85–3.78 (1H, m, CHOH), 3.52–3.44 (1H, m, CH(CH₃)₂), 3.35 (1H, m, CH₂), 3.22 (1H, m, CH₂), 2.73 (1H, d, J = 5.6 Hz, OH), 1.10 (6H, dd, J = 11.8, 6.1 Hz, 2 x CH₃); ¹³C{¹H} NMR (CDCl₃, 101 MHz) δ 141.4, 128.4, 128.3 (2C), 128.2 (2C), 74.7, 72.5, 68.7, 39.4, 22.3, 22.1.



Methyl 3-hydroxy-2-iodo-3-phenylpropanoate 3t was synthesized according to a procedure reported by Urankar *et al.*²³ Water (0.5 mL) was added to a mixture of methyl *trans*-cinnamate (0.42 g, 2.6 mmol, 1.0 equiv.) and *N*-iodosaccharin (0.89 g, 2.8 mmol, 1.1 equiv.) in acetonitrile (5 mL). The reaction mixture was stirred in the dark at room temperature for 48 h. The reaction mixture was reduced *in vacuo*, the residue was redissolved in Et₂O and was washed with a saturated aqueous solution of NaHCO₃ and an aqueous 10% solution of Na₂S₂O₄. The organic layer was dried over anhydrous Na₂SO₄, filtered and concentrated *in vacuo*. The crude was purified by column chromatography (EtOAc/heptane 30%) to afford methyl 3-hydroxy-2-iodo-3-phenylpropanoate **3t** (0.21 g, 0.70 mmol, 27%) as a white solid.

¹H NMR (400 MHz, CDCl₃) δ 7.43–7.30 (5H, m, 5 x ArH), 5.09 (1H, dd, J = 8.3, 5.8 Hz, CHOH), 4.59 (1H, d, J = 8.3 Hz, CHI), 3.78 (3H, s, OCH₃), 3.33 (1H, d, J = 5.8 Hz, OH); ¹³C{¹H} NMR (CDCl₃, 101 MHz) δ 171.9, 139.5, 128.9, 128.8 (2C), 127.1 (2C), 76.5, 53.3, 24.5.

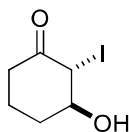
Data consistent with literature values.²³



3-Hydroxy-2-iodo-*N,N*-dimethyl-3-phenylpropanamide 3u. *N*-iodosaccharin (0.87 g, 2.8 mmol, 1.1 equiv.) was added to a mixture of *N,N*-dimethylcinnamamide **1u** (0.44 g, 2.5 mmol, 1.0 equiv.) and ammonium acetate (26 mg, 0.34 mmol, 0.14 equiv.) in H₂O/acetone 1:4 (12 mL). The reaction mixture was stirred in the dark at room temperature for 69 h before being reduced *in vacuo*. The crude was redissolved in CH₂Cl₂ and was washed with a saturated aqueous NaHCO₃ solution and an aqueous 10% Na₂S₂O₃ solution. The organic layer was dried over anhydrous Na₂SO₄, filtered and reduced *in vacuo*. The crude was purified by column chromatography (Et₂O/pentane 90%) to afford 3-hydroxy-2-iodo-*N,N*-dimethyl-3-phenylpropanamide **3u** (0.49 g, 1.5 mmol, 61%) as a colorless oil.

R_f 0.14 (Et₂O/pentane 80%); IR (thin film, $\nu_{\max}/\text{cm}^{-1}$) 3381, 2930, 1736, 1627, 1495, 1455, 1401, 1334, 1179, 1159, 1015, 760, 703; ¹H NMR (400 MHz, CDCl₃) δ 7.46–7.28 (5H, m, ArH), 5.14 (1H, t, J = 6.5 Hz, CHOH), 5.03 (1H, d, J = 6.6 Hz, OH), 4.65 (1H, d, J = 6.5 Hz, CHI), 2.93 (6H, d, J = 3.7 Hz, N(CH₃)₂); ¹³C{¹H} NMR (CDCl₃, 101 MHz) δ 170.8,

140.0, 128.6 (2), 128.4, 127.1 (2), 77.4, 38.1, 36.4, 24.0; **HRMS** (APCI) calc. for C₁₁H₁₅INO₂ ([M+H]⁺) 320.0142, found 320.0141.

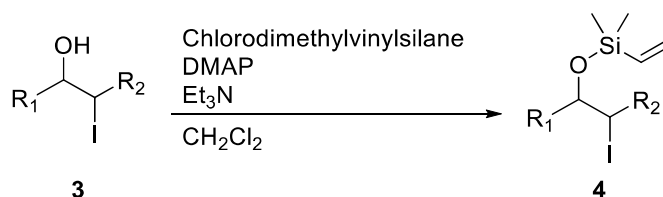


3-Hydroxy-2-iodocyclohexan-1-one 3v was synthesized according to a procedure reported by Narender *et al.*¹⁶ A solution of β -cyclodextrin (3.2 g, 2.8 mmol, 1.1 equiv.) in water (30 mL) was stirred at 65 °C until full dilution. A solution of 2-cyclohexen-1-one (0.26 mL, 2.5 mmol, 1.0 equiv.) in acetone (2 mL) was added dropwise to the warm solution, and the reaction mixture was allowed to cool to room temperature. *N*-iodosaccharin (0.87 g, 2.8 mmol, 1.1 equiv.) was added and the mixture was stirred in the dark at room temperature for 21 h. EtOAc (30 mL) was added, and the reaction mixture was filtered under reduced pressure. The filtrate was extracted with EtOAc (3 x 10 mL), the combined organic layers were washed with an aqueous 10% solution of Na₂S₂O₃, dried over anhydrous Na₂SO₄, filtered and concentrated *in vacuo*. The crude was purified by column chromatography (Et₂O/pentane 60%) to afford 3-hydroxy-2-iodocyclohexan-1-one **3v** (0.17 g, 0.71 mmol, 28%) as a light-orange oil.

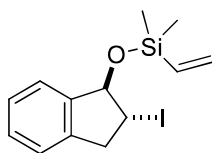
R_f 0.35 (Et₂O/pentane 60%); **IR** (liquid, ν_{\max} /cm⁻¹) 3391, 2951, 1701, 1420, 1222, 1059, 971; **¹H NMR** (400 MHz, CDCl₃) δ 4.54 (1H, d, *J* = 6.6 Hz, CHI), 4.17 (1H, dt, *J* = 7.0, 3.5 Hz, CHOH), 2.97 (1H, ddd, *J* = 14.0, 8.0, 5.4 Hz, COCH₂), 2.49–2.33 (2H, m, COCH₂, CH(OH)CH₂), 2.32 (1H, d, *J* = 3.0 Hz, OH), 2.19–2.03 (1H, m, CH₂), 1.85 (1H, dtd, *J* = 13.5, 7.6, 3.6 Hz, CH(OH)CH₂), 1.73 (1H, dtq, *J* = 17.7, 8.3, 4.1 Hz, CH₂); **¹³C{¹H} NMR** (CDCl₃, 101 MHz) δ 202.5, 76.0, 40.8, 37.2, 29.6, 20.4; **HRMS** (APCI) calc. for C₆H₁₀IO₂ ([M+H]⁺) 240.9720, found 240.9718.

12. Vinyl silanes 4a-v synthesis

12.1 Procedure C



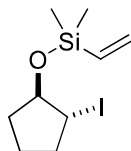
Chloro(dimethyl)vinylsilane (1.1 equiv.) was added to a mixture of iodohydrin **3** (1.0 equiv.), 4-dimethylaminopyridine (0.2 equiv.) and Et₃N (1.2 equiv.) in dry CH₂Cl₂ (0.1 M with respect to the iodohydrin) under Ar. The reaction mixture was stirred 20 min in the dark at room temperature. The reaction was quenched by slowly adding a few drops of isopropanol, and the mixture was reduced *in vacuo*. The residue was redissolved in water and extracted with Et₂O (3 x 10 mL). The combined organic layers were washed with a saturated aqueous NaHCO₃ solution and brine, dried over anhydrous Na₂SO₄, filtered and concentrated *in vacuo*. The crude was purified by column chromatography to afford the wanted silylated product **4**.



((2-iodo-2,3-dihydro-1H-inden-1-yl)oxy)dimethylvinylsilane 4a was synthesized from 2-iodo-2,3-dihydro-1H-inden-1-ol **3a** (0.92 g, 3.5 mmol, 1.0 equiv.), chlorodimethylvinylsilane (0.61 mL, 4.2 mmol, 1.2 equiv.), 4-dimethylaminopyridine (85 mg, 0.70 mmol, 0.2 equiv.) and Et₃N (0.59 mL, 4.2 mmol, 1.2 equiv.) in dry CH₂Cl₂ (20

mL) according to Procedure C. The crude was purified by column chromatography (Et₂O/pentane 2.5%) to afford ((2-iodo-2,3-dihydro-1*H*-inden-1-yl)oxy)dimethylvinylsilane **4a** (1.1 g, 3.1 mmol, 86%) as a colorless oil.

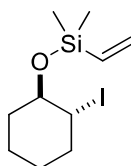
R_f 0.47 (Et₂O/pentane 2.5%); **IR** (liquid, $\nu_{\text{max}}/\text{cm}^{-1}$) 3048, 2955, 2854, 1719, 1596, 1465, 1410, 1361, 1257, 1220, 1179, 1127, 1086, 1041, 1011, 959, 862, 784, 747, 721, 706; **¹H NMR** (400 MHz, CDCl₃) δ 7.29 (1H, q, $J = 5.4$ Hz, ArH), 7.26–7.22 (2H, m, 2 \times ArH), 7.20 (1H, q, $J = 4.5$ Hz, ArH), 6.30 (1H, dd, $J = 20.3, 14.9$ Hz, Si(CHCH₂)), 6.10 (1H, dd, $J = 14.9, 3.8$ Hz, Si(CHCH₂)), 5.89 (1H, dd, $J = 20.3, 3.8$ Hz, Si(CHCH₂)), 5.40 (1H, d, $J = 5.8$ Hz, CHO), 4.21 (1H, td, $J = 7.4, 5.8$ Hz, CHI), 3.60 (1H, dd, $J = 16.3, 7.3$ Hz, CHICH₂), 3.28 (1H, dd, $J = 16.2, 7.6$ Hz, CHICH₂), 0.37 (3H, s, Si(CH₃)₂), 0.35 (3H, s, Si(CH₃)₂); **¹³C{¹H} NMR** (CDCl₃, 101 MHz) δ 143.0, 141.0, 137.6, 134.0, 128.6, 127.4, 124.4, 124.2, 85.5, 42.8, 30.4, -0.9 (2C); **HRMS** (ESI) calc. for C₁₃H₁₇IOSiNa ([M+Na]⁺) 366.9986, found 366.9988.



(2-Iodocyclopentyl)oxydimethylvinylsilane 4b was synthesized from 2-iodocyclopentanol **3b** (0.24 g, 1.1 mmol, 1.0 equiv.), chlorodimethylvinylsilane (0.20 mL, 1.4 mmol, 1.2 equiv.), 4-dimethylaminopyridine (40 mg, 0.32 mmol, 0.3 equiv.) and Et₃N (0.20 mL, 1.4 mmol, 1.2 equiv.) in dry CH₂Cl₂ (7.3 mL) according to Procedure C. The crude was purified by column chromatography (EtOAc/heptane 5%) to afford (2-iodocyclopentyl)oxydimethylvinylsilane **4b** (0.21 g, 0.70 mmol, 61%) as a colorless oil.

¹H NMR (400 MHz, CDCl₃) δ 6.14 (1H, dd, $J = 20.0, 14.9$ Hz, Si(CHCH₂)), 6.03 (1H, dd, $J = 14.9, 4.2$ Hz, Si(CHCH₂)), 5.79 (1H, dd, $J = 19.9, 4.2$ Hz, Si(CHCH₂)), 4.43 (1H, dt, $J = 6.9, 3.8$ Hz, CHO), 4.03 (1H, dt, $J = 8.3, 4.4$ Hz, CHI), 2.33 (1H, dq, $J = 14.5, 7.4$ Hz, CH₂), 2.05 (2H, dddd, $J = 21.5, 19.3, 8.2, 6.0$ Hz, CH₂), 1.79 (2H, p, $J = 8.0$ Hz, CH₂), 1.62–1.48 (1H, m, CH₂), 0.21 (3H, s, Si(CH₃)₂), 0.20 (3H, s, Si(CH₃)₂); **¹³C{¹H} NMR** (CDCl₃, 101 MHz) δ 137.6, 133.5, 82.7, 36.0, 34.8, 32.4, 22.5, -1.4 (2C).

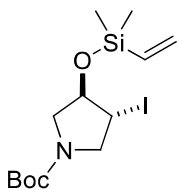
Data consistent with literature values.²⁴



(2-Iodocyclohexyl)oxydimethylvinylsilane 4c was synthesized from 2-iodocyclohexanol **3c** (0.31 g, 1.4 mmol, 1.0 equiv.), chlorodimethylvinylsilane (0.22 mL, 1.6 mmol, 1.2 equiv.), 4-dimethylaminopyridine (33 mg, 0.27 mmol, 0.2 equiv.) and Et₃N (0.22 mL, 1.6 mmol, 1.2 equiv.) in dry CH₂Cl₂ (7.2 mL) according to Procedure C. The crude was purified by column chromatography (EtOAc/heptane 5%) to afford (2-iodocyclohexyl)oxydimethylvinylsilane **4c** (0.35 g, 1.1 mmol, 82%) as a colorless oil.

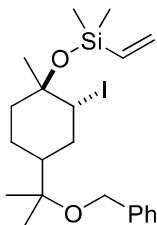
¹H NMR (400 MHz, CDCl₃) δ 6.21 (1H, dd, $J = 20.3, 14.9$ Hz, Si(CH₃)₂CHCH₂), 6.02 (1H, dd, $J = 14.9, 3.9$ Hz, Si(CH₃)₂CHCH₂), 5.81 (1H, dd, $J = 20.3, 3.9$ Hz, Si(CH₃)₂CHCH₂), 3.99 (1H, ddd, $J = 11.1, 8.7, 4.2$ Hz, CHI), 3.70 (1H, td, $J = 8.8, 4.4$ Hz, CHO), 2.49–2.36 (1H, m), 2.05–1.88 (2H, m), 1.78 (1H, qdd, $J = 7.3, 6.0, 3.7, 1.9$ Hz), 1.58–1.44 (1H, m), 1.43–1.17 (3H, m), 0.26 (3H, s, Si(CH₃)₂), 0.24 (3H, s, Si(CH₃)₂); **¹³C{¹H} NMR** (CDCl₃, 101 MHz) δ 138.1, 133.3, 76.4, 39.6, 38.0, 35.2, 27.4, 24.0, -1.0, -1.2.

Data consistent with literature values.²⁴



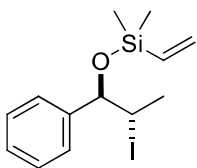
tert-Butyl 3-((dimethylvinylsilyl)oxy)-4-iodopyrrolidine-1-carboxylate 4d was synthesized from *tert*-butyl 3-hydroxy-4-iodopyrrolidine-1-carboxylate **3d** (0.47 g, 1.5 mmol, 1.0 equiv.), chlorodimethylvinylsilane (0.26 mL, 1.8 mmol, 1.2 equiv.), 4-dimethylaminopyridine (51 mg, 0.42 mmol, 0.3 equiv.) and Et₃N (0.26 mL, 1.9 mmol, 1.2 equiv.) in dry CH₂Cl₂ (9.6 mL) according to Procedure C. The crude was purified by column chromatography (EtOAc/heptane 15%) to afford *tert*-butyl 3-((dimethylvinylsilyl)oxy)-4-iodopyrrolidine-1-carboxylate **4d** (0.42 g, 1.1 mmol, 71%) as a light-yellow oil.

R_f 0.47 (EtOAc/heptane 15%); **IR** (thin film, $\nu_{\text{max}}/\text{cm}^{-1}$) 2974, 1702, 1400, 1367, 1255, 1168, 1111, 1081, 1009, 838, 782; **¹H NMR** (400 MHz, CDCl₃, mixture of rotamers) δ 6.19–6.01 (2H, m, Si(CHCH₂), Si(CHCH₂)), 5.80 (1H, dd, $J = 18.1, 5.9$ Hz, Si(CHCH₂)), 4.44 (1H, td, $J = 5.4, 2.5$ Hz, CHO), 4.02 (2H, d, $J = 10.5$ Hz, CHI, CH₂I), 3.89–3.64 (2H, m, CH₂I, CH₂CHO), 3.34–3.19 (1H, m, CH₂CHO), 1.47 (9H, d, $J = 2.6$ Hz, 3 x CH₃), 0.22 (3H, s, Si(CH₃)₂), 0.21 (3H, s, Si(CH₃)₂); **¹³C{¹H} NMR** (CDCl₃, 101 MHz, mixture of rotamers) δ 156.0 (2), 136.8 (2), 134.4 (2), 80.0 (2), 79.3, 78.4, 54.1, 54.0, 52.0, 51.5, 28.6 (6), 26.7 (2), -1.6 (4); **HRMS** (APCI) calc. for C₈H₁₇INO₂Si ([M-Boc+H]⁺) 298.0119, 298.0118.



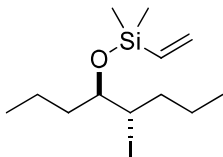
((4-(2-Benzyloxy)propan-2-yl)-2-iodo-1-methylcyclohexyl)oxydimethylvinylsilane 4e was synthesized from 4-(2-(benzyloxy)propan-2-yl)-2-iodo-1-methylcyclohexanol **3e** (0.22 g, 0.57 mmol, 1.0 equiv.), chlorodimethylvinylsilane (97 μ L, 0.68 mmol, 1.2 equiv.), 4-dimethylaminopyridine (16 mg, 0.13 mmol, 0.2 equiv.) and Et₃N (95 μ L, 0.69 mmol, 1.2 equiv.) in dry CH₂Cl₂ (3.1 mL) according to Procedure C. The crude was purified by column chromatography (Et₂O/pentane 2%) to afford ((4-(2-benzyloxy)propan-2-yl)-2-iodo-1-methylcyclohexyl)oxydimethylvinylsilane **4e** (0.17 g, 0.33 mmol, 63%) as a colorless oil.

R_f 0.34 (Et₂O/pentane 2%); **IR** (thin film, $\nu_{\text{max}}/\text{cm}^{-1}$) 2947, 1454, 1379, 1364, 1252, 1174, 1090, 1051, 1032, 1009, 833, 781, 733, 696; **¹H NMR** (400 MHz, CDCl₃) δ 7.41–7.20 (5H, m, ArH), 6.15 (1H, dd, $J = 20.2, 14.8$ Hz, Si(CHCH₂)), 5.95 (1H, dd, $J = 14.8, 3.8$ Hz, Si(CHCH₂)), 5.76 (1H, dd, $J = 20.2, 3.9$ Hz, Si(CHCH₂)), 4.46 (3H, q, $J = 11.1$ Hz, CHI, OCH₂), 2.25–1.88 (4H, m, 2 x CHICH₂, CHC(CH₃)₂O, C(CH₃)(OR)CH₂), 1.68–1.52 (3H, m, C(CH₃)(OR)CH₂, CH₂), 1.50 (3H, s, C(CH₃)(OR)), 1.26 (3H, s, C(CH₃)₂), 1.20 (3H, s, C(CH₃)₂), 0.19 (6H, s, Si(CH₃)₂); **¹³C{¹H} NMR** (CDCl₃, 101 MHz) δ 140.1, 139.4, 132.3, 128.4 (2C), 127.5 (2C), 127.1, 76.9, 74.5, 63.2, 44.6, 40.6, 34.4, 33.0, 32.0, 23.7, 23.5, 22.4, 0.7, 0.6; **HRMS** (APCI) calc. for C₂₁H₃₇INO₂Si ([M+NH₄]⁺) 490.1633, found 490.1633.



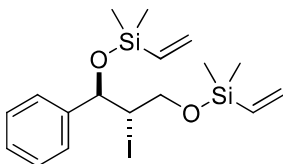
(2-iodo-1-phenylpropoxy)dimethylvinylsilane 4f was synthesized from 2-iodo-1-phenylpropan-1-ol **3f** (0.20 g, 0.77 mmol, 1.0 equiv.), chlorodimethylvinylsilane (0.16 mL, 1.1 mmol, 1.5 equiv.), 4-dimethylaminopyridine (24 mg, 0.20 mmol, 0.3 equiv.) and Et₃N (0.16 mL, 1.2 mmol, 1.5 equiv.) in dry CH₂Cl₂ (5.1 mL) according to Procedure C. The crude was purified by column chromatography (Et₂O/pentane 3%) to afford (2-iodo-1-phenylpropoxy)dimethylvinylsilane **4f** (0.22 g, 0.63 mmol, 82%) as a colorless oil.

R_f 0.51 (Et₂O/heptane 3%); IR (liquid, ν_{max}/cm⁻¹) 2954, 1497, 1455, 1408, 1252, 1072, 1051, 1008, 959, 834, 784, 747, 698; ¹H NMR (400 MHz, CDCl₃) δ 7.35–7.27 (5H, m, ArH), 6.09 (1H, dd, *J* = 20.0, 14.9 Hz, SiCHCH₂), 5.97 (1H, dd, *J* = 14.8, 4.2 Hz, SiCHCH₂'), 5.74 (1H, dd, *J* = 20.0, 4.2 Hz, SiCHCH₂), 4.87 (1H, d, *J* = 4.7 Hz, CH₂O), 4.32 (1H, qd, *J* = 6.9, 4.7 Hz, CHI), 1.76 (3H, d, *J* = 6.9 Hz, CH₃), 0.17 (3H, s, Si(CH₃)₂), 0.12 (3H, s, Si(CH₃)₂); ¹³C{¹H} NMR (CDCl₃, 101 MHz) δ 141.9, 137.4, 133.5, 128.1 (2C), 127.9, 127.0 (2C), 80.2, 34.6, 22.3, -1.3, -1.5; HRMS (APCI) calc. for C₁₃H₁₉IOSiNa ([M+Na]⁺) 369.0142, found 369.0141.



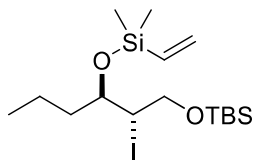
((5-iodooctan-4-yl)oxy)dimethylvinylsilane 4g was synthesized from 5-iodooctan-4-ol **3g** (0.31 g, 1.2 mmol, 1.0 equiv.), chlorodimethylvinylsilane (0.20 mL, 1.4 mmol, 1.2 equiv.), 4-dimethylaminopyridine (30 mg, 0.24 mmol, 0.2 equiv.) and Et₃N (0.20 mL, 1.4 mmol, 1.2 equiv.) in dry CH₂Cl₂ (6.4 mL) according to Procedure C. The crude was purified by column chromatography (Et₂O/pentane 0-1%) to afford ((5-iodooctan-4-yl)oxy)dimethylvinylsilane **4g** (0.36 g, 1.1 mmol, 87%) as a colorless oil.

R_f 0.55 (Et₂O/pentane 1%); IR (liquid, ν_{max}/cm⁻¹) 2959, 2936, 2873, 1465, 1410, 1257, 1149, 1127, 1078, 1041, 1011, 963, 907, 829, 788, 702; ¹H NMR (400 MHz, CDCl₃) δ 6.18 (1H, dd, *J* = 20.2, 14.9 Hz, Si(CHCH₂)), 6.02 (1H, dd, *J* = 14.8, 4.0 Hz, Si(CHCH₂')), 5.80 (1H, dd, *J* = 20.2, 4.0 Hz, Si(CHCH₂)), 4.13 (1H, dt, *J* = 10.0, 3.7 Hz, CHI), 3.33 (1H, ddd, *J* = 8.2, 4.1, 3.0 Hz, CHO), 1.87–1.71 (1H, m, CHICH₂), 1.68–1.54 (3H, m, CHICH₂, CHOCH₂, CHICH₂CH₂), 1.54–1.42 (2H, m, CHOCH₂, CHOCH₂CH₂), 1.39–1.30 (2H, m, CHOCH₂CH₂, CHICH₂CH₂), 0.92 (6H, m, 2 x CH₃), 0.24 (3H, s, Si(CH₃)₂), 0.23 (3H, s, Si(CH₃)₂); ¹³C{¹H} NMR (CDCl₃, 101 MHz) δ 137.9, 133.4, 76.0, 46.3, 37.9, 37.8, 23.2, 18.8, 14.3, 13.4, -1.08, -1.14.; HRMS (ESI) calc. for C₁₂H₂₅IOSiNa ([M+Na]⁺) 363.0612, found 363.0611.



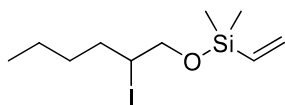
6-iodo-3,3,9,9-tetramethyl-5-phenyl-4,8-dioxa-3,9-disilaundeca-1,10-diene 4h was synthesized from 2-iodo-1-phenylpropan-1,3-diol **3h** (0.33 g, 1.2 mmol, 1.0 equiv.), chlorodimethylvinylsilane (0.36 mL, 2.6 mmol, 2.2 equiv.), 4-dimethylaminopyridine (29 mg, 0.24 mmol, 0.2 equiv.) and Et₃N (0.36 mL, 2.6 mmol, 2.2 equiv.) in dry CH₂Cl₂ (7.6 mL) according to Procedure C. The crude was purified by column chromatography (Et₂O/pentane 1%) to afford 6-iodo-3,3,9,9-tetramethyl-5-phenyl-4,8-dioxa-3,9-disilaundeca-1,10-diene **4h** (0.19 g, 0.43 mmol, 36%) as a colorless oil.

R_f 0.30 (Et₂O/pentane 1%); **IR** (thin film, $\nu_{\max}/\text{cm}^{-1}$) 2960, 1409, 1253, 1127, 1096, 1072, 1052, 1009, 959, 857, 838, 787, 701; **¹H NMR** (400 MHz, CDCl₃) δ 7.37–7.27 (5H, m, ArH), 6.20–5.90 (4H, m, 2 x Si(CHCH₂), 2 x Si(CHCH₂)), 5.75 (2H, ddd, J = 30.1, 19.8, 4.4 Hz, 2 x Si(CHCH₂)), 4.89 (1H, d, J = 5.9 Hz, CHO), 4.33 (1H, q, J = 5.8 Hz, CHI), 3.94 (1H, dd, J = 11.3, 6.0 Hz, CHICH₂O), 3.71 (1H, dd, J = 11.3, 5.5 Hz, CHICH₂O), 0.20 (6H, s, Si(CH₃)₂), 0.12 (3H, s, Si(CH₃)₂), 0.09 (3H, s, Si(CH₃)₂); **¹³C{¹H} NMR** (CDCl₃, 101 MHz) δ 141.8, 137.4, 137.2, 133.7, 133.4, 127.9 (3C), 127.4 (2C), 75.5, 64.8, 43.9, -1.4, -1.6, -1.9 (2C); **HRMS** (APCI) calc. for C₁₇H₂₈IO₂Si₂ ([M+H]⁺) 447.0667, found 447.0667.



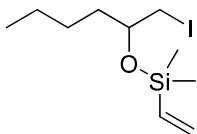
(1-((*tert*-Butyldimethylsilyloxy)-2-iodohexan-3-oxo)dimethylvinylsilane 4i was synthesized from 1-((*tert*-butyldimethylsilyloxy)-2-iodohexan-3-ol **3i** (0.19 g, 0.52 mmol, 1.0 equiv.), chlorodimethylvinylsilane (85 μ L, 0.70 mmol, 1.4 equiv.), 4-dimethylaminopyridine (16 mg, 0.13 mmol, 0.2 equiv.) and Et₃N (98 μ L, 0.70 mmol, 1.4 equiv.) in dry CH₂Cl₂ (3.7 mL) according to Procedure C. The crude was purified by column chromatography (Et₂O/pentane 2%) to afford 1-((*tert*-butyldimethylsilyloxy)-2-iodohexan-3-oxo)dimethylvinylsilane **4i** (0.15 g, 0.33 mmol, 65%) as a colorless oil.

R_f 0.60 (Et₂O/pentane 2%); **IR** (thin film, $\nu_{\max}/\text{cm}^{-1}$) 2957, 2930, 2861, 1473, 1466, 1254, 1100, 1090, 1059, 1054, 1050, 838, 785, 779; **¹H NMR** (400 MHz, CDCl₃) δ 6.17 (1H, dd, J = 20.2, 14.8 Hz, Si(CHCH₂)), 6.02 (1H, dd, J = 14.9, 3.9 Hz, Si(CHCH₂)), 5.80 (1H, dd, J = 20.2, 4.0 Hz, Si(CHCH₂)), 4.22 (1H, ddd, J = 7.9, 5.7, 4.1 Hz, CHI), 3.88 (1H, dd, J = 10.9, 5.7 Hz, CHICH₂O), 3.79 (1H, dd, J = 10.9, 8.1 Hz, CHICH₂O), 3.57 (1H, dt, J = 8.2, 3.1 Hz, CHO), 1.66–1.40 (3H, m, 2 x CH₃CH₂, CH₃CH₂CH₂), 1.38–1.22 (1H, m, CH₃CH₂CH₂), 0.90 (12H, s, CH₃, C(CH₃)₃), 0.23 (3H, s, Si(CH₃)₂(CHCH₂)), 0.22 (3H, s, Si(CH₃)₂(CHCH₂)), 0.07 (3H, s, Si(CH₃)₂C(CH₃)₃), 0.06 (3H, s, Si(CH₃)₂C(CH₃)₃); **¹³C{¹H} NMR** (CDCl₃, 101 MHz) δ 137.9, 133.4, 71.9, 66.1, 44.5, 37.5, 26.0 (3C), 18.6, 18.3, 14.2, -1.2, -1.3, -5.1, -5.3; **HRMS** (APCI) calc. for C₁₆H₃₆IO₂Si₂ ([M+H]⁺) 443.1293, found 443.1292.



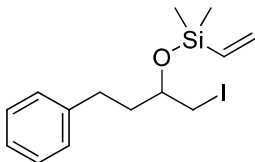
((2-iodohexyl)oxy)dimethylvinylsilane 4j was synthesized from 2-iodohexan-1-ol **3j** (0.11 g, 0.47 mmol, 1.0 equiv.), chlorodimethylvinylsilane (80 μ L, 0.56 mmol, 1.2 equiv.), 4-dimethylaminopyridine (13 mg, 0.11 mmol, 0.2 equiv.) and Et₃N (80 μ L, 0.58 mmol, 1.2 equiv.) in dry CH₂Cl₂ (2.5 mL) according to Procedure C. The crude was purified by column chromatography (Et₂O/pentane 1%) to afford ((2-iodohexyl)oxy)dimethylvinylsilane **4j** (0.11 g, 0.35 mmol, 76%) as a colorless oil.

R_f 0.34 (Et₂O/pentane 1%); **IR** (thin film, $\nu_{\max}/\text{cm}^{-1}$) 2957, 2931, 2871, 2860, 1408, 1252, 1077, 835, 783, 701; **¹H NMR** (400 MHz, CDCl₃) δ 6.21–6.07 (1H, m, Si(CHCH₂)), 6.04 (1H, ddd, J = 15.2, 4.8, 2.3 Hz, Si(CHCH₂)), 5.80 (1H, ddd, J = 19.7, 4.5, 2.1 Hz, Si(CHCH₂)), 4.14–3.99 (1H, m, CHI), 3.87 (1H, dd, J = 11.1, 5.0 Hz, CH₂O), 3.77–3.64 (1H, m, CH₂O), 1.85 (1H, d, J = 13.1 Hz, CH₂CHI), 1.79–1.63 (1H, m, CH₂CHI), 1.58–1.48 (1H, m, CH₃CH₂), 1.44–1.28 (3H, m, CH₃CH₂, 2 x CH₃CH₂), 0.92 (3H, dt, J = 7.9, 3.9 Hz, CH₃), 0.21 (6H, s, 2 x Si(CH₃)₂); **¹³C{¹H} NMR** (CDCl₃, 101 MHz) δ 137.1, 133.8, 68.9, 38.1, 35.8, 31.6, 22.1, 14.1, -1.9, -2.0; **HRMS** (APCI) calculated for C₁₀H₂₁IOSiNa ([M+Na]⁺) 335.0299, found 335.0299.



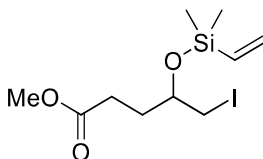
((1-iodohexan-2-yl)oxy)dimethylvinylsilane 4k was synthesized from 1-iodohexan-2-ol **3k** (0.30 g, 1.3 mmol, 1.0 equiv.), chlorodimethylvinylsilane (0.23 mL, 1.6 mmol, 1.2 equiv.), 4-dimethylaminopyridine (34 mg, 0.27 mmol, 0.2 equiv.) and Et₃N (0.22 mL, 1.6 mmol, 1.2 equiv.) in dry CH₂Cl₂ (7.2 mL) according to Procedure C. The crude was purified by column chromatography (Et₂O/pentane 1%) to afford ((1-iodohexan-2-yl)oxy)dimethylvinylsilane **4k** (0.34 g, 1.1 mmol, 82%) as a colorless oil.

R_f 0.38 (Et₂O /pentane 1%); IR (liquid, ν_{max}/cm⁻¹) 2959, 2936, 2862, 1410, 1257, 1037, 1011, 963, 940, 840, 817, 784, 698; ¹H NMR (400 MHz, CDCl₃) δ 6.17 (1H, dd, *J* = 20.1, 14.9 Hz, Si(CHCH₂)), 6.03 (1H, dd, *J* = 14.8, 4.0 Hz, Si(CHCH₂)), 5.80 (1H, dd, *J* = 20.1, 4.0 Hz, Si(CHCH₂)), 3.60 (1H, dq, *J* = 7.2, 5.1 Hz, CHO), 3.25–3.12 (2H, m, CH₂l), 1.72–1.57 (1H, m, CH₂CHO), 1.57–1.42 (1H, m, CH₂CHO), 1.42–1.18 (4H, m, CH₂CH₂CH₃, CH₂CH₂CH₃), 0.90 (3H, dd, *J* = 7.8, 6.2 Hz, CH₂CH₂CH₃), 0.23 (6H, s, 2 x Si(CH₃)₂); ¹³C{¹H} NMR (CDCl₃, 101 MHz) δ 137.7, 133.6, 72.2, 36.7, 27.6, 22.7, 14.2, 14.0, -1.2, -1.3; HRMS (APCI) calc. for C₁₀H₂₁IOSiNa ([M+Na]⁺) 335.0299, found 335.0299.



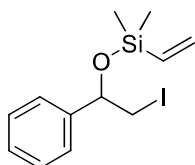
((1-iodo-4-phenylbutan-2-yl)oxy)dimethylvinylsilane 4l was synthesized from 1-iodo-4-phenylbutan-2-ol **3l** (0.48 g, 1.7 mmol, 1.0 equiv.), chlorodimethylvinylsilane (0.30 mL, 2.1 mmol, 1.2 equiv.), 4-dimethylaminopyridine (42 mg, 0.35 mmol, 0.2 equiv.) and Et₃N (0.29 mL, 2.1 mmol, 1.2 equiv.) in dry CH₂Cl₂ (9.3 mL) according to Procedure C. The crude was purified by column chromatography (Et₂O/pentane 3%) to afford ((1-iodo-4-phenylbutan-2-yl)oxy)dimethylvinylsilane **4l** (0.52 g, 1.5 mmol, 83%) as a colorless oil.

R_f 0.45 (Et₂O /pentane 3%); IR (liquid, ν_{max}/cm⁻¹) 2950, 1595, 1497, 1455, 1408, 1251, 1052, 959, 835, 783, 698; ¹H NMR (400 MHz, CDCl₃) δ 7.33–7.26 (2H, m, ArH), 7.23–7.15 (3H, m, ArH), 6.18 (1H, dd, *J* = 20.1, 14.8 Hz, SiCHCH₂), 6.04 (1H, dd, *J* = 14.9, 4.0 Hz, SiCHCH₂), 5.82 (1H, dd, *J* = 20.1, 4.0 Hz, SiCHCH₂), 3.71–3.62 (1H, m, CHO), 3.22 (2H, d, *J* = 5.4 Hz, CH₂l), 2.71 (1H, ddd, *J* = 13.7, 10.5, 5.7 Hz, CCH₂), 2.59 (1H, ddd, *J* = 13.7, 10.5, 5.9 Hz, CCH₂), 1.98 (1H, dddd, *J* = 13.7, 10.4, 5.9, 4.3 Hz, CH₂CHO), 1.86 (1H, dddd, *J* = 13.8, 10.5, 7.3, 5.7 Hz, CH₂CHO), 0.25 (3H, s, Si(CH₃)₂), 0.24 (3H, s, Si(CH₃)₂); ¹³C{¹H} NMR (CDCl₃, 101 MHz) δ 141.8, 137.6, 133.8, 128.6 (2C), 128.5 (2C), 126.1, 71.7, 38.7, 31.7, 13.4, -1.2, -1.3; HRMS (APCI) calc. for C₁₄H₂₁IOSiNa ([M+Na]⁺) 383.0299, found 383.0298.



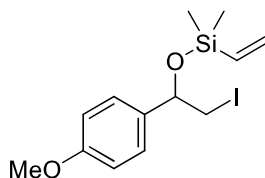
Methyl 4-((dimethylvinylsilyl)oxy)-5-iodopentanoate 4m was synthesized from methyl 4-hydroxy-5-iodopentanoate **3m** (0.34 g, 1.3 mmol, 1.0 equiv.), chlorodimethylvinylsilane (0.24 mL, 1.7 mmol, 1.4 equiv.), 4-dimethylaminopyridine (44 mg, 0.36 mmol, 0.3 equiv.) and Et₃N (0.24 mL, 1.7 mmol, 1.3 equiv.) in dry CH₂Cl₂ (8.4 mL) according to Procedure C. The crude was purified by column chromatography (Et₂O/pentane 10%) to afford methyl 4-((dimethylvinylsilyl)oxy)-5-iodopentanoate **4m** (0.23 g, 0.66 mmol, 50%) as a colorless oil.

R_f 0.29 (Et₂O /pentane 10%); IR (liquid, $\nu_{\max}/\text{cm}^{-1}$) 2954, 1736, 1438, 1252, 1171, 1100, 1066, 1008, 960, 837, 814, 783, 700; ¹H NMR (400 MHz, CDCl₃) δ 6.15 (1H, dd, $J = 19.9, 14.9$ Hz, Si(CHCH₂)), 6.04 (1H, dd, $J = 14.9, 4.2$ Hz, Si(CHCH₂)), 5.80 (1H, dd, $J = 19.9, 4.2$ Hz, Si(CHCH₂)), 3.67 (4H, s, OCH₃, CHOH), 3.17 (2H, dd, $J = 5.5, 2.6$ Hz, CH₂I), 2.37 (2H, td, $J = 7.8, 3.0$ Hz, COCH₂), 2.02 (1H, dtd, $J = 15.5, 7.7, 3.6$ Hz, CH₂), 1.81 (1H, dq, $J = 14.5, 7.4$ Hz, CH₂), 0.22 (6H, s, 2 x Si(CH₃)₂); ¹³C{¹H} NMR (CDCl₃, 101 MHz) δ 173.8, 137.3, 134.0, 70.9, 51.8, 31.8, 29.8, 12.6, -1.4, -1.5; HRMS (APCI) cal. for C₁₀H₁₉I O₃Si ([M+H]⁺) 343.0221, found 343.0220.



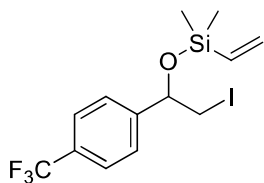
(2-Iodo-1-phenylethoxy)dimethylvinylsilane 4n was synthesized from 2-iodo-1-phenylethan-1-ol **3n** (0.26 g, 1.0 mmol, 1.0 equiv.), chlorodimethylvinylsilane (0.20 mL, 1.4 mmol, 1.4 equiv.), 4-dimethylaminopyridine (36 mg, 0.30 mmol, 0.3 equiv.) and Et₃N (0.20 mL, 1.4 mmol, 1.4 equiv.) in dry CH₂Cl₂ (6.7 mL) according to Procedure C. The crude was purified by column chromatography (Et₂O/pentane 1%) to afford (2-iodo-1-phenylethoxy)dimethylvinylsilane **4n** (0.21 g, 0.62 mmol, 61%) as a light-yellow oil.

R_f 0.38 (Et₂O /pentane 1%); IR (liquid, $\nu_{\max}/\text{cm}^{-1}$) 2961, 1407, 1252, 1098, 997, 889, 836, 811, 784, 699; ¹H NMR (400 MHz, CDCl₃) δ 7.39–7.21 (5H, m, ArH), 6.09 (1H, dd, $J = 19.9, 14.9$ Hz, Si(CHCH₂)), 5.98 (1H, dd, $J = 14.9, 4.4$ Hz, Si(CHCH₂)), 5.75 (1H, dd, $J = 19.8, 4.3$ Hz, Si(CHCH₂)), 4.80 (1H, dd, $J = 7.6, 4.9$ Hz, CHO), 3.42–3.26 (2H, m, CH₂I), 0.18 (3H, s, Si(CH₃)₂), 0.13 (3H, s, Si(CH₃)₂); ¹³C{¹H} NMR (CDCl₃, 101 MHz) δ 142.7, 137.3, 133.8, 128.6 (2C), 128.2, 126.2 (2C), 75.6, 14.8, -1.3, -1.5; HRMS (ESI) calc. for C₁₂H₁₇I OSiNa ([M+Na]⁺) 354.9986, found 354.9986.



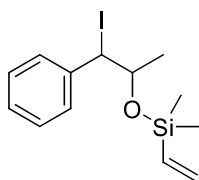
(2-Iodo-1-(4-methoxyphenyl)ethoxy)dimethylvinylsilane 4o was synthesized from 2-iodo-1-(4-methoxyphenyl)ethan-1-ol **3o** (1.5 g, 5.2 mmol, 1.0 equiv.), chlorodimethylvinylsilane (0.95 mL, 6.7 mmol, 1.3 equiv.), 4-dimethylaminopyridine (0.18 g, 1.4 mmol, 0.3 equiv.) and Et₃N (0.95 mL, 6.8 mmol, 1.3 equiv.) in dry CH₂Cl₂ (33 mL) according to Procedure C. The crude was purified by column chromatography (Et₂O/pentane 5%) to afford (2-iodo-1-(4-methoxyphenyl)ethoxy)dimethylvinylsilane **4o** (0.98 g, 2.7 mmol, 52%) as a colorless oil.

R_f 0.29 (Et₂O /pentane 5%); IR (liquid, $\nu_{\max}/\text{cm}^{-1}$) 2956, 1611, 1512, 1249, 1171, 1100, 1037, 999, 893, 837, 787; ¹H NMR (400 MHz, CDCl₃) δ 7.24 (2H, d, $J = 8.6$ Hz, ArH), 6.87 (2H, d, $J = 8.5$ Hz, ArH), 6.08 (1H, dd, $J = 19.9, 14.8$ Hz, Si(CHCH₂)), 5.98 (1H, dd, $J = 14.9, 4.4$ Hz, Si(CHCH₂)), 5.75 (1H, dd, $J = 19.8, 4.4$ Hz, Si(CHCH₂)), 4.76 (1H, t, $J = 6.4$ Hz, CHO), 3.81 (3H, s, OCH₃), 3.32 (2H, d, $J = 6.4$ Hz, CH₂I), 0.17 (3H, s, Si(CH₃)₂), 0.11 (3H, s, Si(CH₃)₂); ¹³C{¹H} NMR (CDCl₃, 101 MHz) δ 159.4, 137.4, 134.8, 133.6, 127.3 (2C), 113.9 (2C), 75.1, 55.4, 15.0, -1.3, -1.5; HRMS (ESI) calc. for C₁₃H₁₉I O₂SiNa ([M+Na]⁺) 385.0091, found 385.0091.



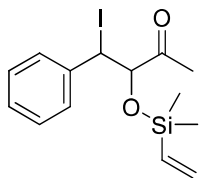
(2-Iodo-1-(4-(trifluoromethyl)phenyl)ethoxy)dimethylvinylsilane 4p was synthesized from 2-iodo-1-(4-(trifluoromethyl)phenyl)ethan-1-ol **3p** (0.32 g, 1.0 mmol, 1.0 equiv.), chlorodimethylvinylsilane (0.17 mL, 1.2 mmol, 1.2 equiv.), 4-dimethylaminopyridine (27 mg, 0.22 mmol, 0.2 equiv.) and Et₃N (0.17 mL, 1.2 mmol, 1.2 equiv.) in dry CH₂Cl₂ (6.5 mL) according to Procedure C. The crude was purified by column chromatography (Et₂O/pentane 2%) to afford (2-iodo-1-(4-(trifluoromethyl)phenyl)ethoxy)dimethylvinylsilane **4p** (0.29 g, 0.72 mmol, 71%) as a colorless oil.

R_f 0.53 (Et₂O /pentane 2%); **IR** (liquid, $\nu_{\text{max}}/\text{cm}^{-1}$) 2960, 1412, 1326, 1255, 1168, 1128, 1103, 1069, 890, 840, 790; **¹H NMR** (400 MHz, CDCl₃) δ 7.60 (2H, d, $J = 8.1$ Hz, ArH), 7.49–7.40 (2H, m, ArH), 6.16–5.94 (2H, m, Si(CHCH₂), Si(CHCH₂)), 5.76 (1H, dd, $J = 19.1, 5.0$ Hz, Si(CHCH₂)), 4.83 (1H, dd, $J = 7.2, 5.0$ Hz, CHO), 3.39–3.26 (2H, m, CH₂I), 0.21 (3H, s, Si(CH₃)₂), 0.15 (3H, s, Si(CH₃)₂); **¹³C{¹H} NMR** (CDCl₃, 101 MHz) δ 146.6, 136.9, 134.2, 130.3 (q, $^2J_{\text{C-F}} = 32.3$ Hz), 126.5 (2C), 125.5 (2C, q, $^3J_{\text{C-F}} = 3.8$ Hz), 124.3 (q, $^1J_{\text{C-F}} = 272.2$ Hz), 74.7, 13.8, -1.4, -1.6; **HRMS** (APCI) calc. for C₁₃H₁₇F₃IOSi ([M+H]⁺) 401.0040, found 401.0038.



((1-Iodo-1-phenylpropan-2-yl)oxy)dimethylvinylsilane 4q was synthesized from 1-iodo-1-phenylpropan-2-ol **3q** (0.31 g, 1.2 mmol, 1.0 equiv.), chlorodimethylvinylsilane (0.21 mL, 1.4 mmol, 1.2 equiv.), 4-dimethylaminopyridine (30 mg, 0.25 mmol, 0.2 equiv.) and Et₃N (0.20 mL, 1.5 mmol, 1.2 equiv.) in dry CH₂Cl₂ (6.5 mL) according to Procedure C. The crude was purified by column chromatography (Et₂O/pentane 5%) to afford ((1-iodo-1-phenylpropan-2-yl)oxy)dimethylvinylsilane **4q** (0.14 g, 0.40 mmol, 34%) as a light-yellow oil.

R_f 0.59 (Et₂O /pentane 5%); **IR** (liquid, $\nu_{\text{max}}/\text{cm}^{-1}$) 2953, 1453, 1376, 1250, 1090, 1076, 1059, 987, 960, 828, 783, 695; **¹H NMR** (400 MHz, CDCl₃) δ 7.48–7.15 (5H, m, ArH), 6.10–5.91 (2H, m, Si(CHCH₂), Si(CHCH₂)), 5.69 (1H, dd, $J = 17.4, 6.8$ Hz, Si(CHCH₂)), 4.95 (1H, d, $J = 6.7$ Hz, CHI), 4.12 (1H, p, $J = 6.2$ Hz, CHO), 1.37 (3H, d, $J = 6.0$ Hz, CH₃), 0.06 (3H, s, Si(CH₃)₂), 0.04 (3H, s, Si(CH₃)₂); **¹³C{¹H} NMR** (CDCl₃, 101 MHz) δ 141.5, 137.6, 133.4, 129.3 (2C), 128.3 (2C), 127.9, 73.5, 41.0, 23.2, -1.4, -1.7; **HRMS** (APCI) calc. for C₁₃H₂₀IOSi ([M+H]⁺) 347.0323, found 347.0322.

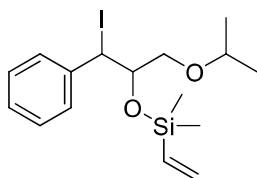


3-((Dimethylvinylsilyl)oxy)-4-iodo-4-phenylbutan-2-one 4r was synthesized from 3-hydroxy-4-iodo-4-phenylbutan-2-one **3r** (0.35 g, 1.2 mmol, 1.0 equiv.), chlorodimethylvinylsilane (0.21 mL, 1.4 mmol, 1.2 equiv.), 4-dimethylaminopyridine (30 mg, 0.24 mmol, 0.2 equiv.) and Et₃N (0.20 mL, 1.4 mmol, 1.2 equiv.) in dry CH₂Cl₂ (6.4 mL) according to Procedure C. The crude was purified by column chromatography (Et₂O/pentane 5-10%) to afford an inseparable 87:13 diastereomers mixture of 3-((dimethylvinylsilyl)oxy)-4-iodo-4-phenylbutan-2-one **4r** (0.18 g, 0.49 mmol, 41%) as a yellow oil. *Note: the NMR data were extracted from the inseparable mixture data.*

R_f 0.59 (Et₂O /pentane 5%); IR (liquid, $\nu_{\max}/\text{cm}^{-1}$) 2961, 1724, 1674, 1408, 1354, 1254, 1123, 1074, 871, 842, 789, 698; HRMS (APCI) calc. for C₁₄H₂₀IO₂Si ([M+H]⁺) 375.0272, found 375.0269.

major: ¹H NMR (400 MHz, CDCl₃) δ 7.44 (2H, dd, J = 7.9, 1.8 Hz, ArH), 7.30–7.23 (3H, m, ArH), 6.04 (1H, d, J = 2.7 Hz, Si(CHCH₂)), 6.01 (1H, d, J = 1.9 Hz, Si(CHCH₂)), 5.79–5.68 (1H, m, Si(CHCH₂)), 5.20 (1H, d, J = 6.3 Hz, CHI), 4.43 (1H, d, J = 6.2 Hz, CHO), 1.96 (3H, s, CH₃), 0.17 (3H, s, Si(CH₃)₂), 0.16 (3H, s, Si(CH₃)₂); ¹³C{¹H} NMR (CDCl₃, 101 MHz) δ 207.7, 139.5, 136.3, 134.6, 129.4 (2C), 128.6, 128.5 (2C), 84.0, 31.3, 26.0, -1.6, -1.8.

minor: ¹H NMR (400 MHz, CDCl₃) δ 7.81–7.79 (2H, m, ArH), 7.40–7.22 (3H, m, ArH), 6.63 (1H, s, CHO), 6.35–6.26 (1H, m, Si(CHCH₂)), 5.98–5.97 (1H, m, Si(CHCH₂)), 5.82–5.81 (1H, m, Si(CHCH₂)), 5.78–5.70 (1H, m, CHI), 2.44 (3H, s, CH₃), 0.36 (6H, s, Si(CH₃)₂); ¹³C{¹H} NMR (CDCl₃, 101 MHz) δ 195.5, 147.7, 138.6, 134.4, 132.6, 130.2 (2C), 128.6, 120.6, 77.4, 31.3, 25.3, -0.0 (2C).

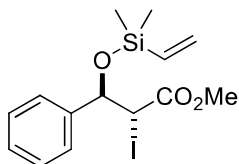


((1-iodo-3-isopropoxy-1-phenylpropan-2-yl)oxy)dimethylvinylsilane 4s was synthesized from 1-iodo-3-isopropoxy-1-phenylpropan-2-ol **3s** (0.26 g, 0.82 mmol, 1.0 equiv.), chlorodimethylvinylsilane (0.14 mL, 1.0 mmol, 1.2 equiv.), 4-dimethylaminopyridine (23 mg, 0.20 mmol, 0.2 equiv.) and Et₃N (0.14 mL, 1.0 mmol, 1.2 equiv.) in dry CH₂Cl₂ (4.4 mL) according to Procedure C. The crude was purified by column chromatography (Et₂O/pentane 1.5%) to afford a separable 80:20 diastereomers mixture of ((1-iodo-3-isopropoxy-1-phenylpropan-2-yl)oxy)dimethylvinylsilane **4s** (0.12 g, 0.29 mmol, 35%) as a colorless oil.

R_f 0.29 (Et₂O/pentane 1.5%); IR (thin film, $\nu_{\max}/\text{cm}^{-1}$) 2971, 1251, 1114, 1074, 960, 826, 784, 696; HRMS (APCI) calc. for C₁₆H₂₆IO₂Si ([M+Na]⁺) 405.0741, found 405.0742.

major: ¹H NMR (400 MHz, CDCl₃) δ 7.49–7.38 (2H, m, ArH), 7.30–7.17 (3H, m, ArH), 6.10 (1H, dd, J = 20.1, 14.9 Hz, Si(CHCH₂)), 5.97 (1H, dd, J = 14.8, 4.2 Hz, Si(CHCH₂)), 5.72 (1H, dd, J = 20.1, 4.2 Hz, Si(CHCH₂)), 5.25 (1H, d, J = 5.7 Hz, CHI), 4.27 (1H, q, J = 5.6 Hz, CHO), 3.49 (1H, dq, J = 12.2, 5.9 Hz, CH(CH₃)₂), 3.38 (2H, d, J = 5.5 Hz, CH₂O), 1.12 (6H, dd, J = 10.1, 6.1 Hz, CH(CH₃)₂), 0.15 (3H, s, Si(CH₃)₂), 0.14 (3H, s, Si(CH₃)₂); ¹³C{¹H} NMR (CDCl₃, 101 MHz) δ 140.9, 137.9, 133.3, 129.5 (2C), 128.2 (2C), 127.9, 77.0, 72.2, 70.4, 34.4, 22.1 (2C), -1.1, -1.4.

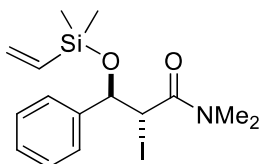
minor: ¹H NMR (400 MHz, CDCl₃) δ 7.47–7.38 (2H, m, ArH), 7.31–7.17 (3H, m, ArH), 6.06 (1H, dd, J = 19.8, 14.9 Hz, Si(CHCH₂)), 5.96 (1H, dd, J = 14.9, 4.5 Hz, Si(CHCH₂)), 5.74 (1H, dd, J = 19.7, 4.5 Hz, Si(CHCH₂)), 5.25 (1H, d, J = 5.4 Hz, CHI), 3.55–3.42 (2H, m, CHO, CH(CH₃)₂), 3.40–3.21 (2H, m, CH₂O), 1.10 (6H, dd, J = 10.5, 6.2 Hz, CH(CH₃)₂), 0.18 (3H, s, Si(CH₃)₂), 0.16 (3H, s, Si(CH₃)₂); ¹³C{¹H} NMR (CDCl₃, 101 MHz) δ 141.7, 137.9, 133.4, 129.0 (2C), 128.4 (2C), 128.1, 76.2, 72.2, 71.1, 39.7, 22.2, 22.1, -1.1, -1.2.



Methyl 3-((dimethylvinylsilyl)oxy)-2-iodo-3-phenylpropanoate 4t was synthesized from methyl 3-hydroxy-2-iodo-3-phenylpropanoate **3t** (0.21 g, 0.68 mmol, 1.0 equiv.), chlorodimethylvinylsilane (0.14 mL, 0.98 mmol, 1.4 equiv.), 4-dimethylaminopyridine (25 mg, 0.20 mmol, 0.3 equiv.) and Et₃N (0.14 mL, 1.0 mmol, 1.5 equiv.) in dry CH₂Cl₂ (4.5 mL) according to Procedure C. The crude was purified by column chromatography (Et₂O/pentane 5%)

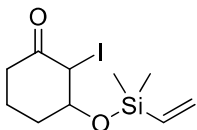
to afford methyl 3-((dimethylvinylsilyl)oxy)-2-iodo-3-phenylpropanoate **4t** (0.19 g, 0.48 mmol, 70%) as a colorless oil.

R_f 0.27 (Et₂O/heptane 5%); **IR** (liquid, $\nu_{\text{max}}/\text{cm}^{-1}$) 2952, 1740, 1252, 1168, 1050, 855, 836, 785, 698; **¹H NMR** (400 MHz, CDCl₃) δ 7.34 (5H, d, $J = 2.7$ Hz, ArH), 6.01–5.85 (2H, m, Si(CHCH₂)), Si(CHCH₂)), 5.71–5.57 (1H, m, Si(CHCH₂)), 5.07 (1H, d, $J = 10.2$ Hz, CHO), 4.39 (1H, d, $J = 10.2$ Hz, CHI), 3.80 (3H, s, OCH₃), 0.02 (3H, s, Si(CH₃)₂), -0.02 (3H, s, Si(CH₃)₂); **¹³C{¹H} NMR** (CDCl₃, 101 MHz) δ 171.0, 140.4, 136.9, 133.5, 128.8, 128.3 (2C), 127.9 (2C), 77.6, 52.9, 27.5, -1.6, -1.8; **HRMS** (APCI) calculated for C₁₄H₂₀O₃Si ([M+H]⁺) 391.0221, found 391.0220.



3-((Dimethylvinylsilyl)oxy)-2-iodo-*N,N*-dimethyl-3-phenylpropanamide 4u was synthesized from 3-hydroxy-2-iodo-*N,N*-dimethyl-3-phenylpropanamide **3u** (0.40 g, 1.3 mmol, 1.0 equiv.), chlorodimethylvinylsilane (0.21 mL, 1.5 mmol, 1.2 equiv.), 4-dimethylaminopyridine (34 mg, 0.28 mmol, 0.2 equiv.) and Et₃N (0.21 mL, 1.5 mmol, 1.2 equiv.) in dry CH₂Cl₂ (8.1 mL) according to Procedure C. The crude was purified by column chromatography (Et₂O/pentane 50%) to afford 3-((dimethylvinylsilyl)oxy)-2-iodo-*N,N*-dimethyl-3-phenylpropanamide **4u** (0.37 g, 0.92 mmol, 73%) as a yellow oil.

R_f 0.46 (Et₂O/pentane 50%); **IR** (liquid, $\nu_{\text{max}}/\text{cm}^{-1}$) 2956, 1655, 1496, 1455, 1400, 1251, 1065, 879, 855, 841, 787, 701; **¹H NMR** (400 MHz, CDCl₃) δ 7.43–7.26 (5H, m, ArH), 6.03–5.84 (2H, m, Si(CHCH₂)), Si(CHCH₂)), 5.61 (1H, dd, $J = 19.2, 5.0$ Hz, Si(CHCH₂)), 5.24 (1H, d, $J = 9.7$ Hz, CHO), 4.63 (1H, d, $J = 9.8$ Hz, CHI), 3.09 (3H, s, NCH₃), 3.00 (3H, s, NCH₃), 0.03 (3H, s, Si(CH₃)₂), 0.02 (3H, s, Si(CH₃)₂); **¹³C{¹H} NMR** (CDCl₃, 101 MHz) δ 169.6, 141.6, 137.5, 133.1, 128.4 (2C), 128.1, 127.9 (2), 77.5, 38.0, 36.7, 27.5, -1.5, -1.6; **HRMS** (APCI) calc. for C₁₅H₂₃INO₂Si ([M+H]⁺) 404.0537, found 404.0536.



3-((Dimethylvinylsilyl)oxy)-2-iodocyclohexan-1-one 4v was synthesized from 3-hydroxy-2-iodocyclohexan-1-one **3v** (0.17 g, 0.69 mmol, 1.0 equiv.), chlorodimethylvinylsilane (0.12 mL, 0.83 mmol, 1.2 equiv.), 4-dimethylaminopyridine (23 mg, 0.19 mmol, 0.3 equiv.) and Et₃N (0.12 mL, 0.83 mmol, 1.2 equiv.) in dry CH₂Cl₂ (4.4 mL) according to Procedure C. The crude was purified by column chromatography (Et₂O/pentane 5%) to afford a separable 71:29 diastereomers mixture of 3-((dimethylvinylsilyl)oxy)-2-iodocyclohexan-1-one **4v** (0.14 g, 0.44 mmol, 64%) as a colorless oil.

R_f 0.39 (*major*), 0.21 (*minor*) (Et₂O/pentane 5%); **IR** (liquid, $\nu_{\text{max}}/\text{cm}^{-1}$) 2955, 1716, 1254, 1114, 1065, 1007, 880, 851, 791; **HRMS** (APCI) calc. for C₁₀H₁₈IO₂Si ([M+H]⁺) 325.0115, found 325.0114

major: **¹H NMR** (400 MHz, CDCl₃) δ 6.20–6.07 (1H, m, Si(CHCH₂)), 6.04 (1H, d, $J = 9.7$ Hz, Si(CHCH₂)), 5.79 (1H, dd, $J = 18.9, 5.2$ Hz, Si(CHCH₂)), 4.32–4.22 (2H, m, CHI, CHO), 3.14 (1H, ddd, $J = 14.6, 12.2, 5.9$ Hz, CH₂O), 2.52–2.38 (1H, m, CH₂CHO), 2.29 (1H, dt, $J = 14.4, 4.5$ Hz, CH₂O), 2.22–2.06 (1H, m, CH₂), 1.84–1.69 (2H, m, CH₂CHO, CH₂), 0.20 (3H, s, Si(CH₃)₂), 0.19 (3H, s, Si(CH₃)₂); **¹³C{¹H} NMR** (CDCl₃, 101 MHz) δ 205.0, 136.9, 134.2, 75.8, 35.7, 32.4, 27.7, 20.3, -1.6 (2C).

minor: **¹H NMR** (400 MHz, CDCl₃) δ 6.13 (1H, dd, $J = 19.8, 14.7$ Hz, Si(CHCH₂)), 6.03 (1H, dd, $J = 15.0, 4.6$ Hz, Si(CHCH₂)), 5.80 (1H, dd, $J = 19.8, 4.3$ Hz, Si(CHCH₂)), 4.73–4.63 (1H, m, CHI), 3.36–3.25 (1H, m, CHO), 3.11 (1H, ddd, $J = 14.7, 11.0, 6.1$ Hz, CH₂O), 2.28 (1H, dt, $J = 14.7, 5.2$ Hz, CH₂O), 2.03–1.68 (3H, m, 2 x CH₂CHO, CH₂), 1.66–

1.50 (1H, m, CH₂), 0.23 (3H, s, Si(CH₃)₂), 0.22 (3H, s, Si(CH₃)₂); ¹³C{¹H} NMR (CDCl₃, 101 MHz) δ 203.6, 137.1, 134.2, 72.5, 44.5, 35.8, 31.8, 20.5, -1.4, -1.4.

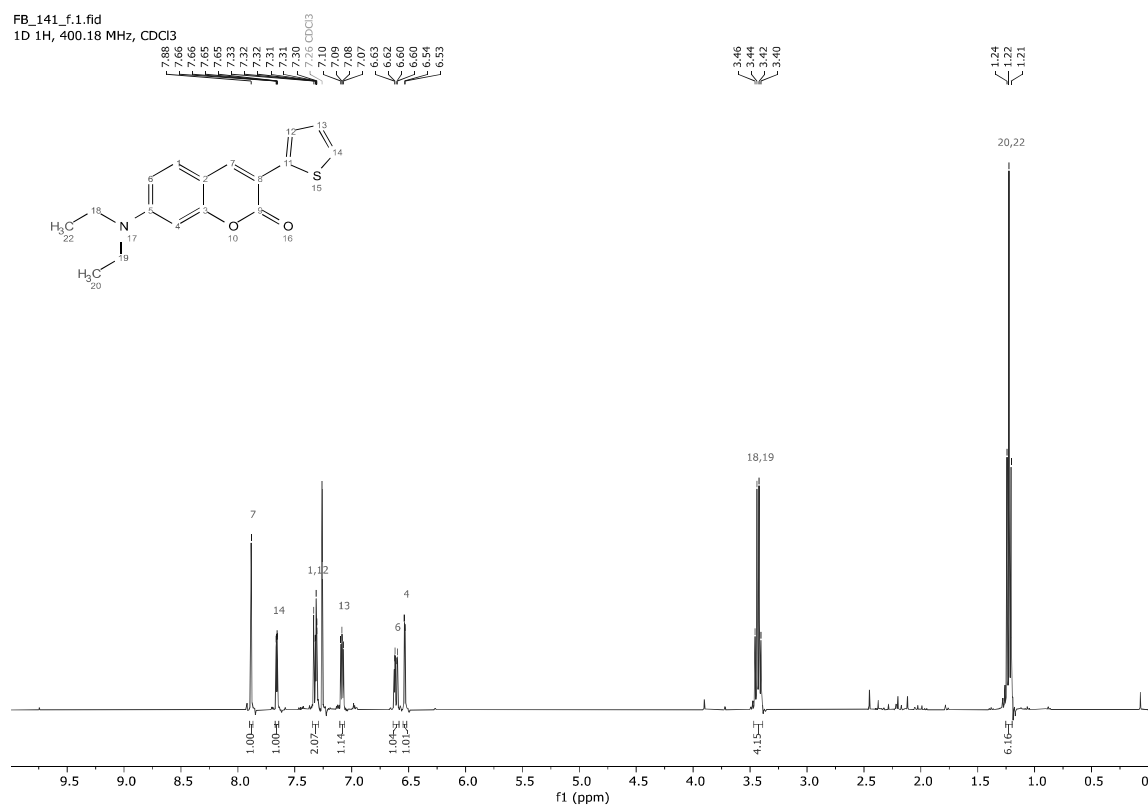
13. References

1. Gualandi, A.; Rodeghiero, G.; Della Rocca, E.; Bertoni, F.; Marchini, M.; Perciaccante, R.; Jansen, T. P.; Ceroni, P.; Cozzi, P. G., Application of coumarin dyes for organic photoredox catalysis. *Chem. Comm.* **2018**, *54* (72), 10044-10047.
2. Filippini, D.; Silvi, M., Visible light-driven conjunctive olefination. *Nat. Chem.* **2022**, *14*, 66-70.
3. Haugland, M. M.; El-Sagheer, A. H.; Porter, R. J.; Peña, J.; Brown, T.; Anderson, E. A.; Lovett, J. E., 2'-Alkynylnucleotides: A Sequence- and Spin Label-Flexible Strategy for EPR Spectroscopy in DNA. *J. Am. Chem. Soc.* **2016**, *138* (29), 9069-9072.
4. Yadav, J. S.; Reddy, B. V. S.; Narasimhulu, G.; Purnima, K. V., FeCl₃-catalyzed functionalization of monoterpenes via hydroalkylation of unactivated alkenes. *Tetrahedron Lett.* **2009**, *50* (42), 5783-5785.
5. Wata, C.; Hashimoto, T., Organoiodine-Catalyzed Enantioselective Intermolecular Oxyamination of Alkenes. *J. Am. Chem. Soc.* **2021**, *143* (4), 1745-1751.
6. Pospisil, J.; Marko, I. E., Efficient and stereoselective synthesis of allylic ethers and alcohols. *Org. Lett.* **2006**, *8* (26), 5983-5986.
7. Kelly, C. B.; Ovian, J. M.; Cywar, R. M.; Gosselin, T. R.; Wiles, R. J.; Leadbeater, N. E., Oxidative cleavage of allyl ethers by an oxoammonium salt. *Org. Biomol. Chem.* **2015**, *13* (14), 4255-4259.
8. Zhang, M. Z.; Wang, X.; Gong, M. Y.; Chen, L.; Shi, W. B.; He, S. H.; Jiang, Y.; Chen, T. Q., An efficient iodine pentoxide-triggered iodocarbocyclization for the synthesis of iodooxindoles in water. *Org. Biomol. Chem.* **2018**, *16* (28), 5197-5202.
9. Geng, X. L.; Wang, Z.; Li, X. Q.; Zhang, C., A simple method for epoxidation of olefins using sodium chlorite as an oxidant without a catalyst. *J. Org. Chem.* **2005**, *70* (23), 9610-9613.
10. Zhu, Y. X.; Colomer, I.; Thompson, A. L.; Donohoe, T. J., HFIP Solvent Enables Alcohols To Act as Alkylating Agents in Stereoselective Heterocyclization. *J. Am. Chem. Soc.* **2019**, *141* (16), 6489-6493.
11. Yao, H. R.; Richardson, D. E., Epoxidation of alkenes with bicarbonate-activated hydrogen peroxide. *J. Am. Chem. Soc.* **2000**, *122* (13), 3220-3221.
12. Ren, J.; Yu, P. C.; Zhang, M. J.; Zhao, Y. X.; Zhong, J.; Hu, K., Discovery of alpha-methylene-gamma-lactone-delta-epoxy derivatives with anti-cancer activity: synthesis, SAR study, and biological activity. *Med. Chem. Res.* **2022**, *31* (10), 1803-1817.
13. Das, B.; Venkateswarlu, K.; Damodar, K.; Suneel, K., Ammonium acetate catalyzed improved method for the regioselective conversion of olefins into halohydrins and haloethers at room temperature. *J. Mol. Catal. A: Chem.* **2007**, *269* (1-2), 17-21.
14. Yi, W.; Wang, P. F.; Lu, M.; Liu, Q. Q.; Bai, X.; Chen, K. D.; Zhang, J. W.; Liu, G. Q., Environmentally Friendly Protocol for the Oxidative Iodofunctionalization of Olefins in a Green Solvent. *ACS Sustain. Chem. Eng.* **2019**, *7* (19), 16777-16785.
15. Hu, Q. Y.; Rege, P. D.; Corey, E. J., Simple, catalytic enantioselective syntheses of estrone and desogestrel. *J. Am. Chem. Soc.* **2004**, *126* (19), 5984-5986.
16. Narender, M.; Reddy, M. S.; Nageswar, Y. D.; Rao, K. R., Aqueous phase synthesis of vic-halohydrins from olefins and N-halosuccinimides in the presence of β-cyclodextrin. *J. Mol. Catal. A: Chem.* **2006**, *258* (1-2), 10-14.
17. Shimizu, A.; Hayashi, R.; Ashikari, Y.; Nokami, T.; Yoshida, J., Switching the reaction pathways of electrochemically generated β-haloalkoxysulfonium ions - synthesis of halohydrins and epoxides. *Beilstein J. Org. Chem.* **2015**, *11*, 242-248.
18. Dhokale, R. A.; Seidl, F. J.; Shinde, A. H.; Mague, J. T.; Sathyamoorthi, S., Tethered Silanoxyiodination of Alkenes. *J. Org. Chem.* **2021**, *86* (13), 9233-9243.
19. Sanseverino, A. M.; de Mattos, M. C. S., Iodohydrins: An easy route to epoxides from alkenes. *Synth. Commun.* **1998**, *28* (3), 559-572.
20. Braun, H. A.; Meusinger, R.; Schmidt, B., 2-Iodoethanols from aldehydes, diiodomethane and isopropylmagnesium chloride. *Tetrahedron Lett.* **2005**, *46* (15), 2551-2554.
21. Sharma, S. M. L.; Singh, J., Envirocat (K10-MX)-Catalyzed Regioselective Transformation of Alkenes into Iodohydrins and β-Iodo Ethers and Further Conversion of Iodohydrins to Epoxides Using Al₂O₃-Na₂CO₃ Under MWI. *Synth. Commun.* **2012**, *42* (9), 1306-1324.
22. Luan, S. N.; Castanheiro, T.; Poisson, T., Electrochemical Synthesis of Iodohydrins. *Adv. Synth. Catal.* **2022**, *364* (16), 2741-2747.

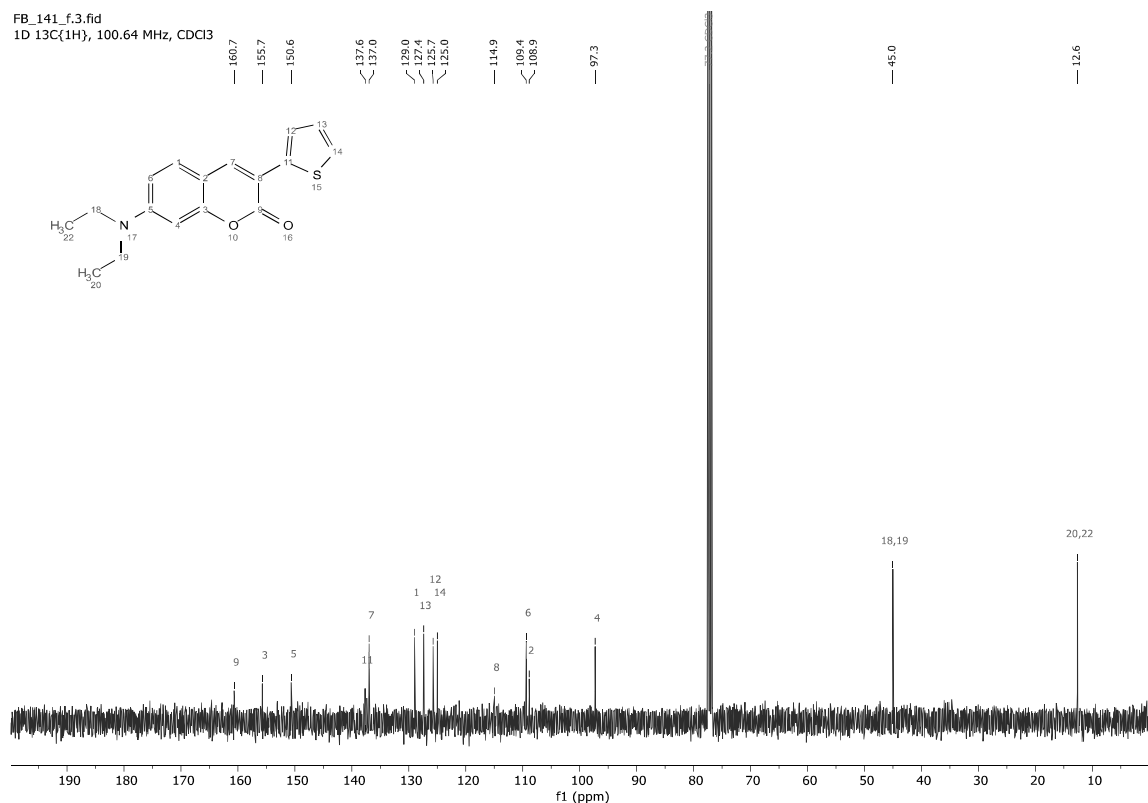
23. Urankar, D.; Rutar, I.; Modec, B.; Dolenc, D., Synthesis of bromo- and iodohydrins from deactivated alkenes by use of N-bromo- and N-iodosaccharin. *Eur. J. Org. Chem.* **2005**, *2005* (11), 2349-2353.
24. Someya, H.; Ohmiya, H.; Yorimitsu, H.; Oshima, K., Cobalt-catalyzed sequential cyclization/cross-coupling reactions of 6-halo-1-hexene derivatives with Grignard reagents and their application to the synthesis of 1,3-diols. *Tetrahedron* **2007**, *63* (35), 8609-8618.

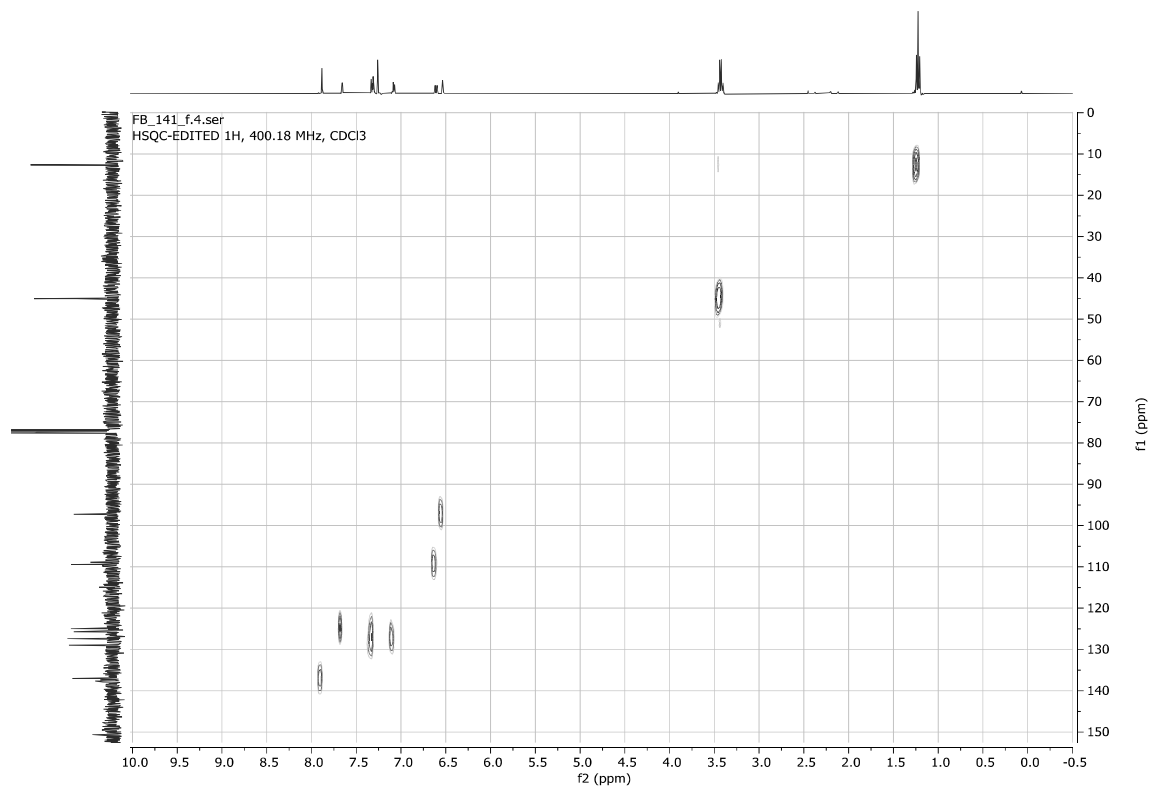
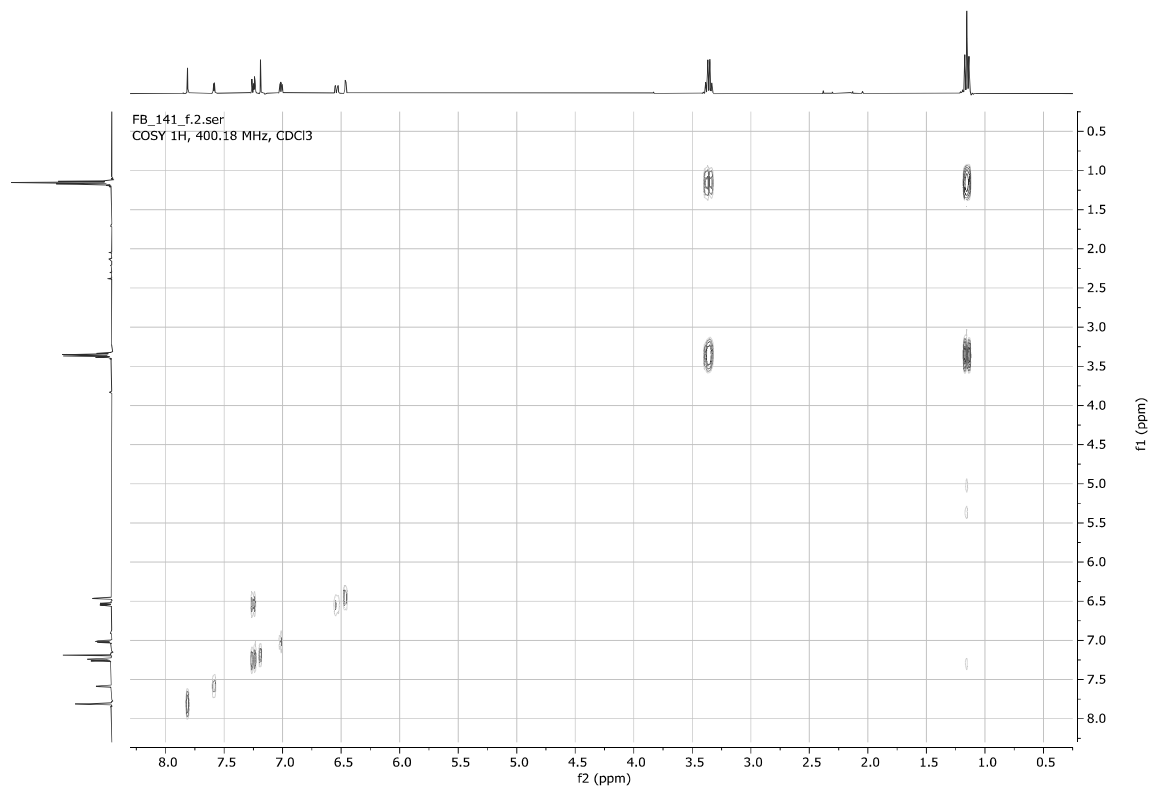
7-(Diethylamino)-3-(thiophen-2-yl)-2H-chromen-2-one

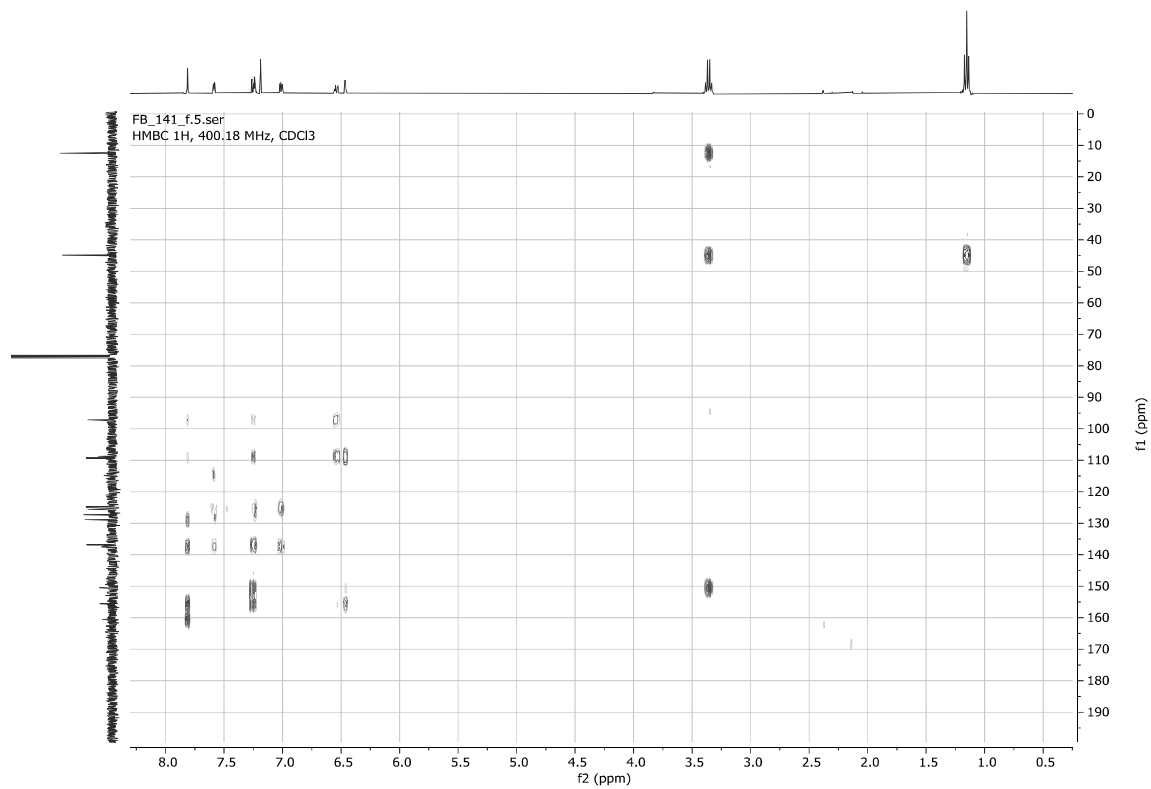
FB_141_f.1.fid
1D 1H, 400.18 MHz, CDCl3



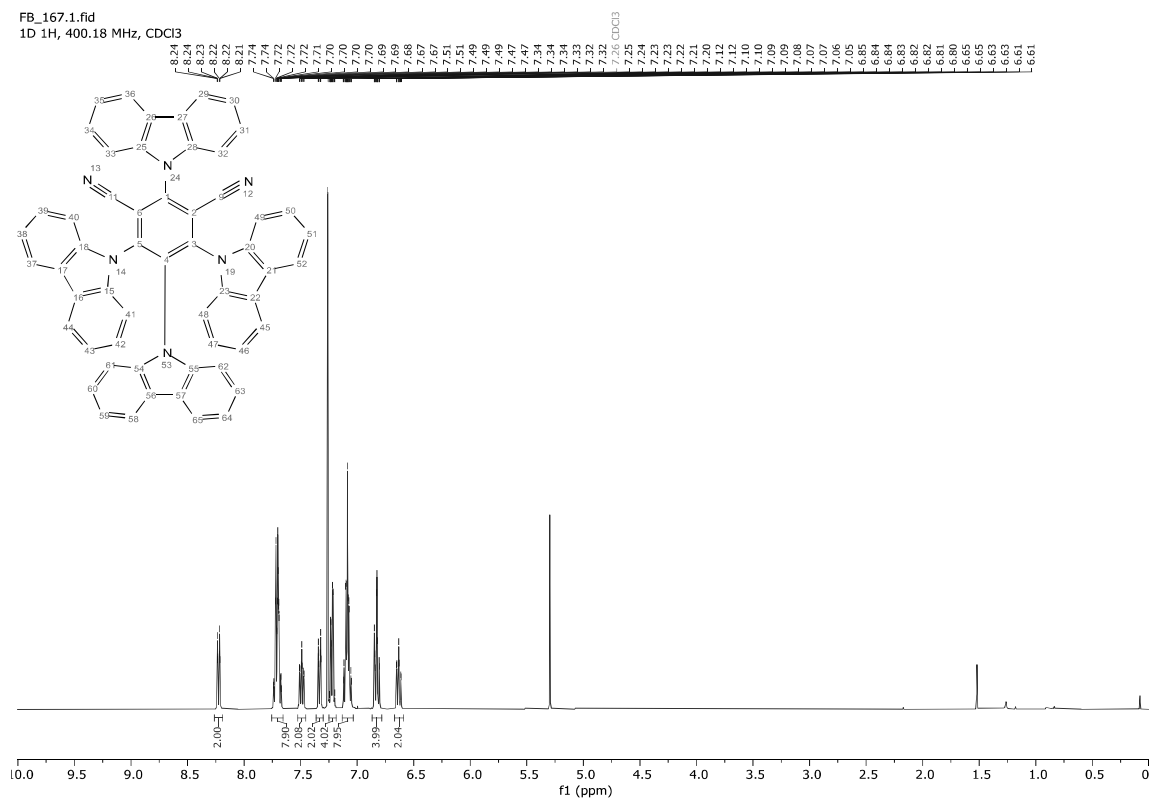
FB_141_f.3.fid
1D 13C(1H), 100.64 MHz, CDCl3



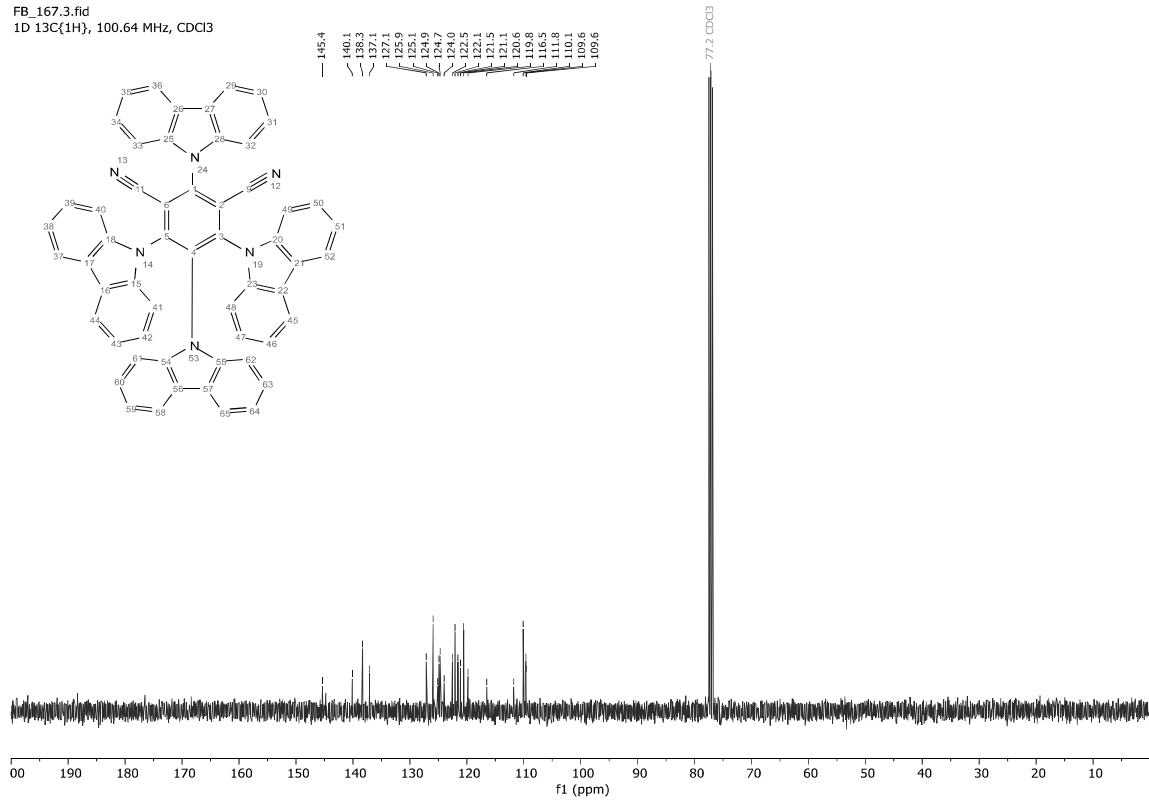




4CzIPN

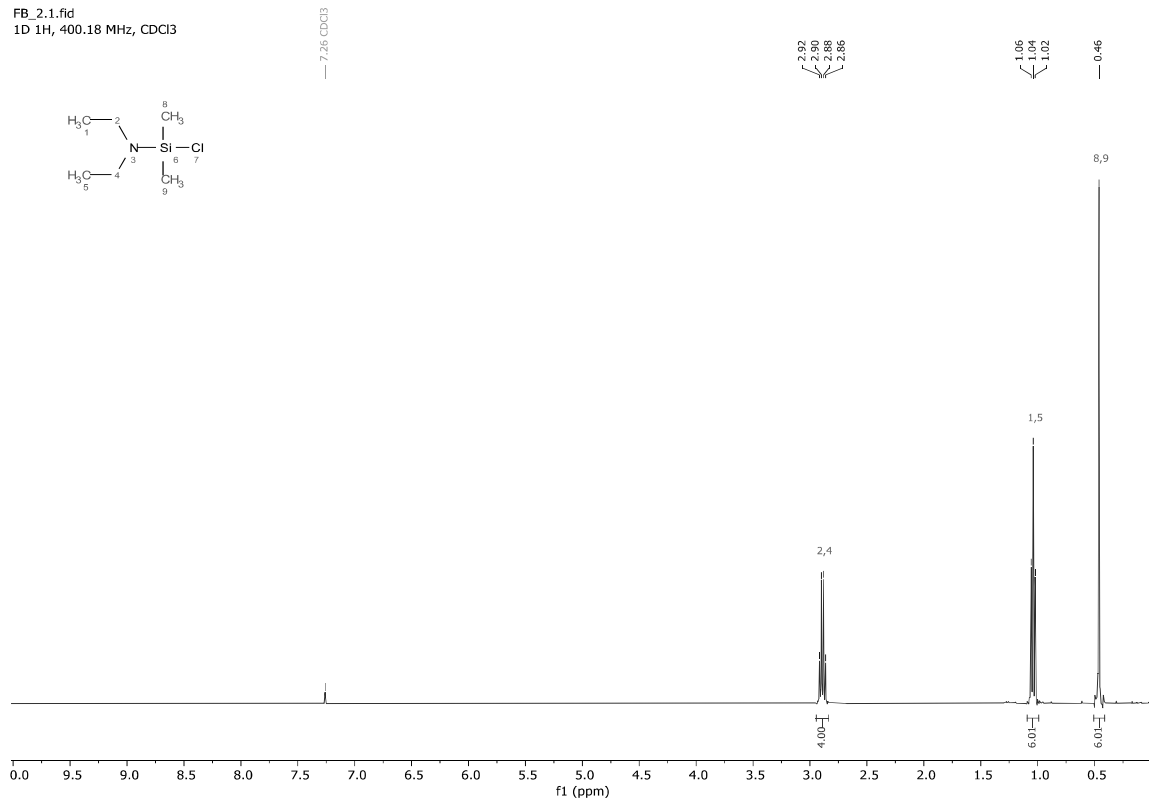


FB_167.3.fid
1D 13C{1H}, 100.64 MHz, CDCl3

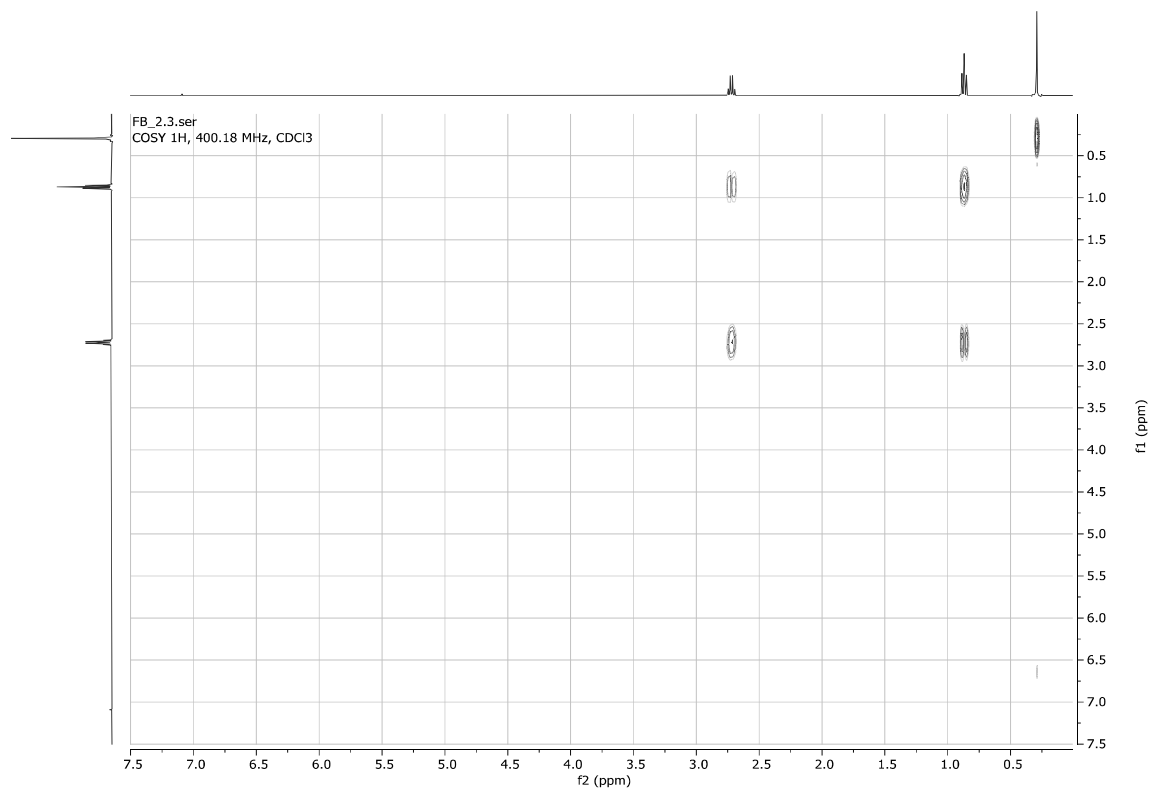
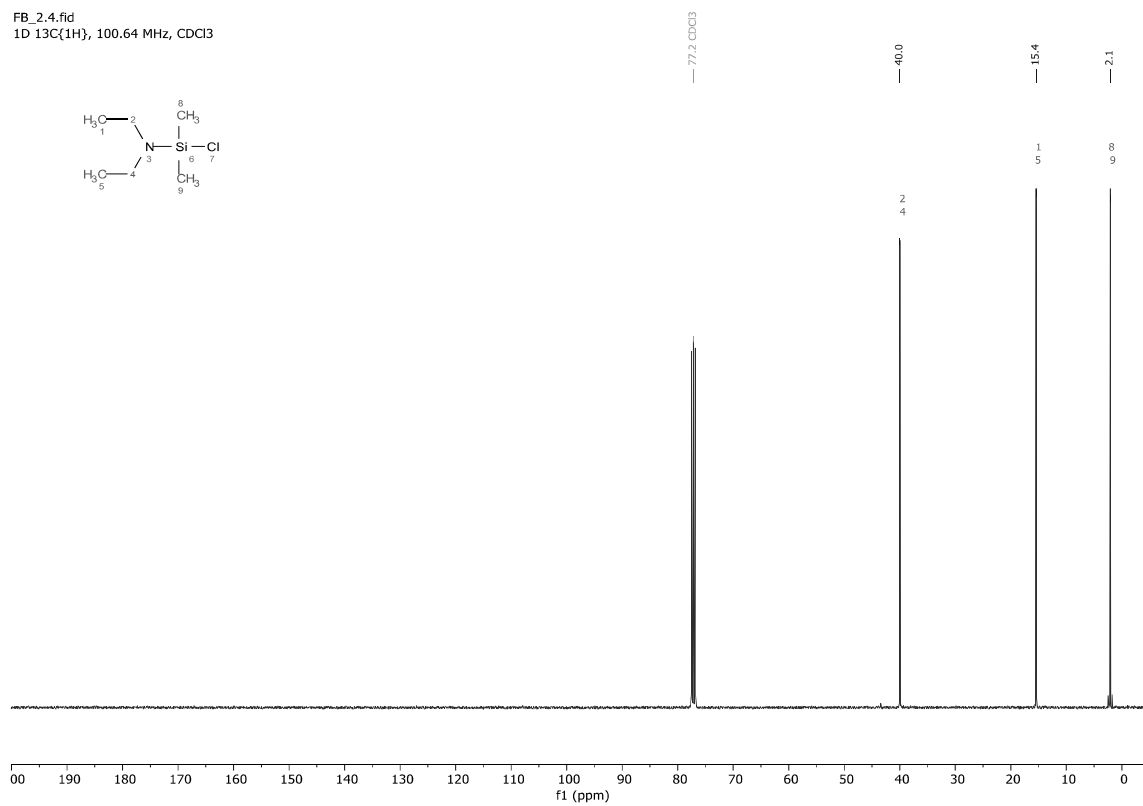


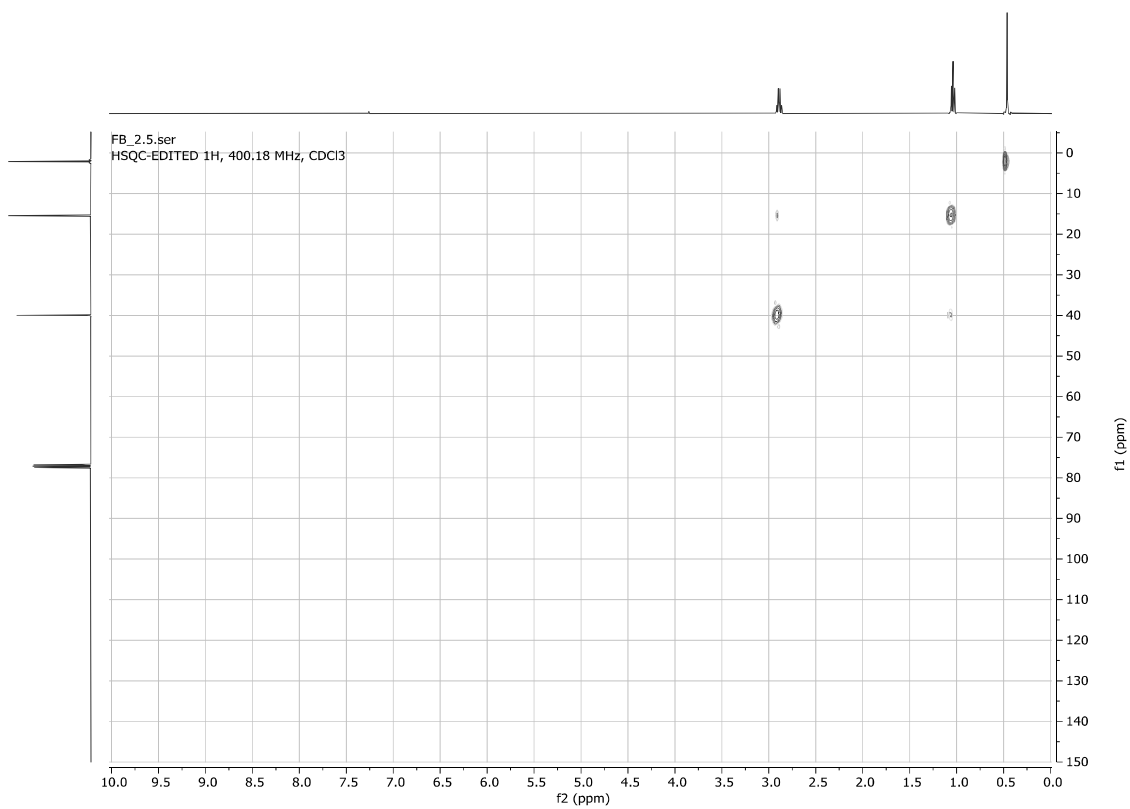
Chloro(diethylamino)dimethylsilane s1

FB_2.1.fid
1D 1H, 400.18 MHz, CDCl3



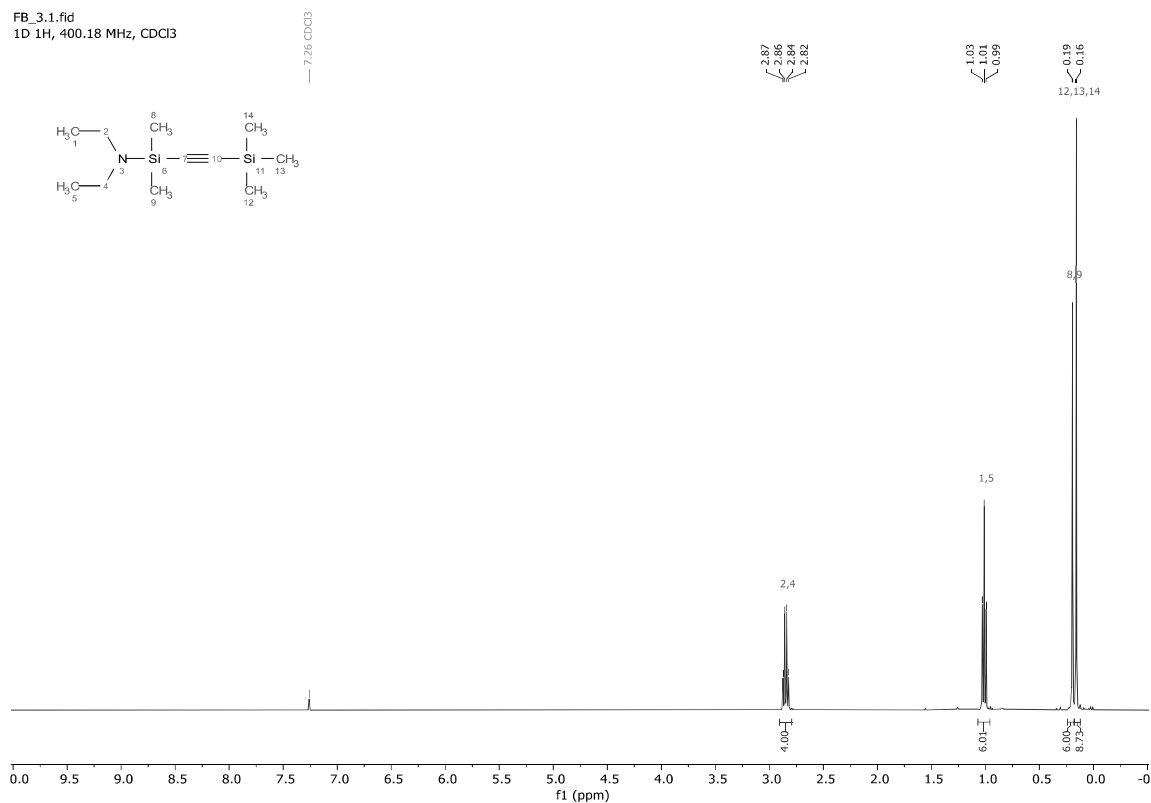
FB_2.4.fid
1D 13C{1H}, 100.64 MHz, CDCl3



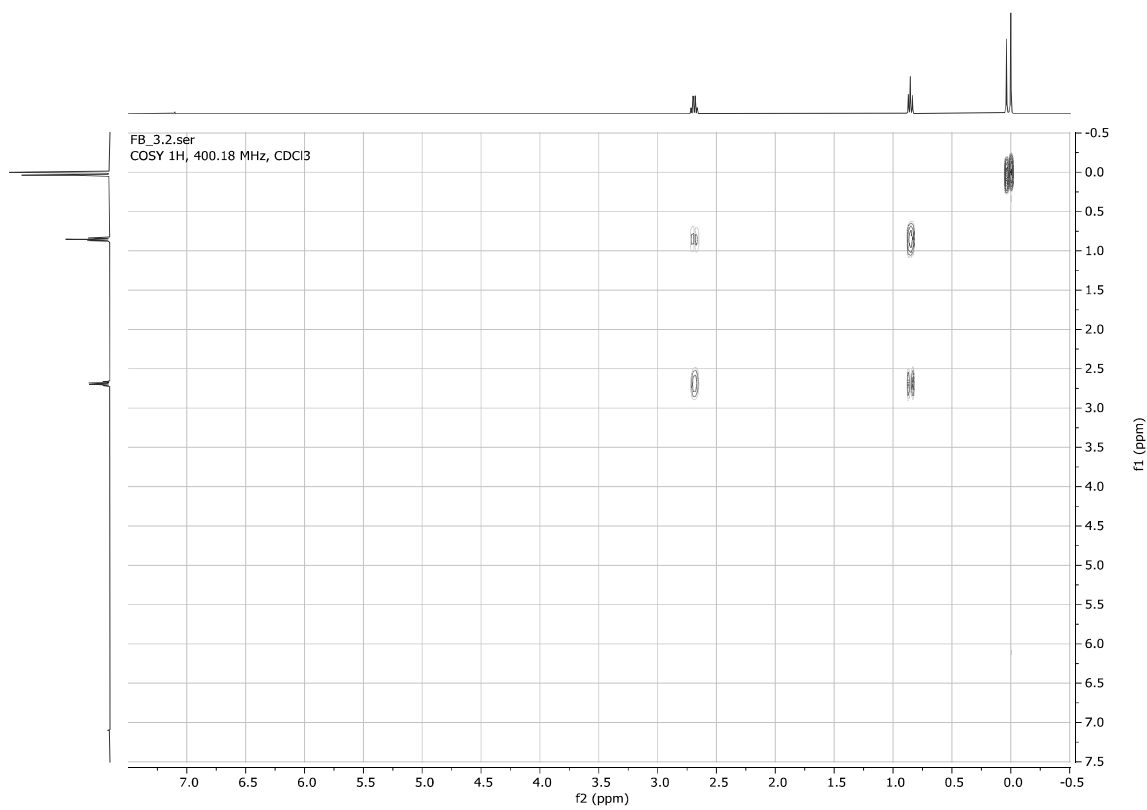
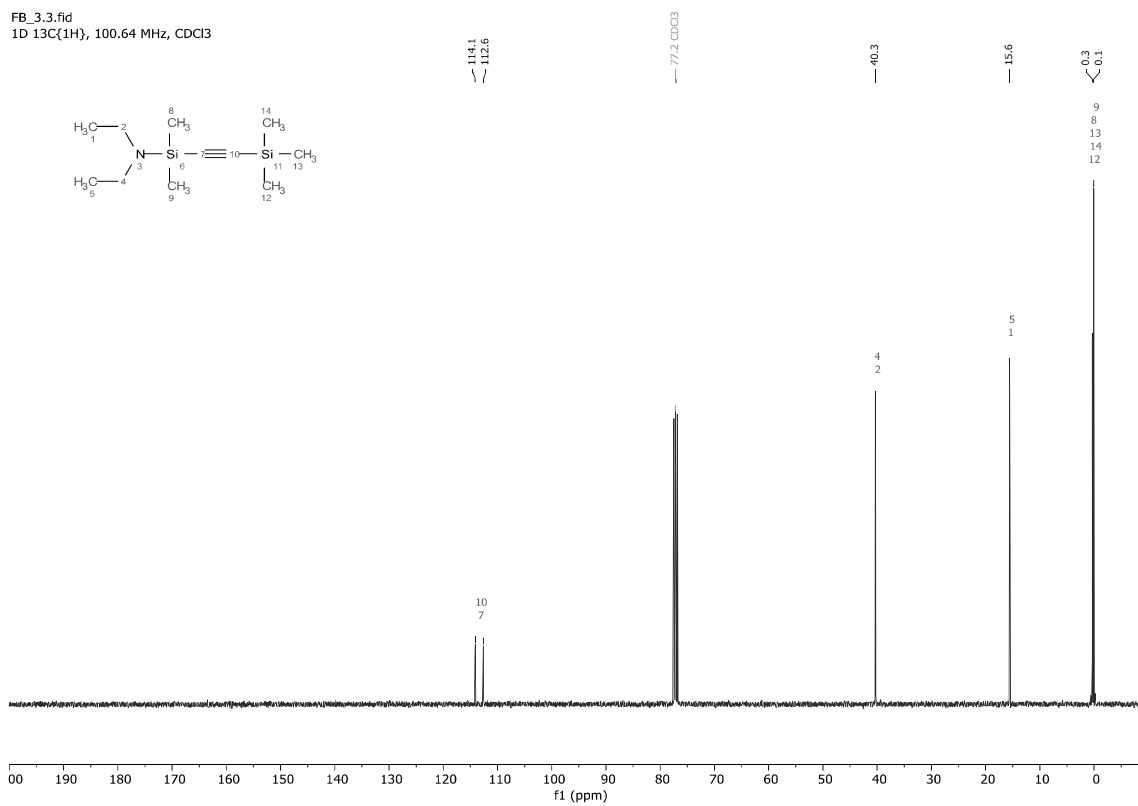


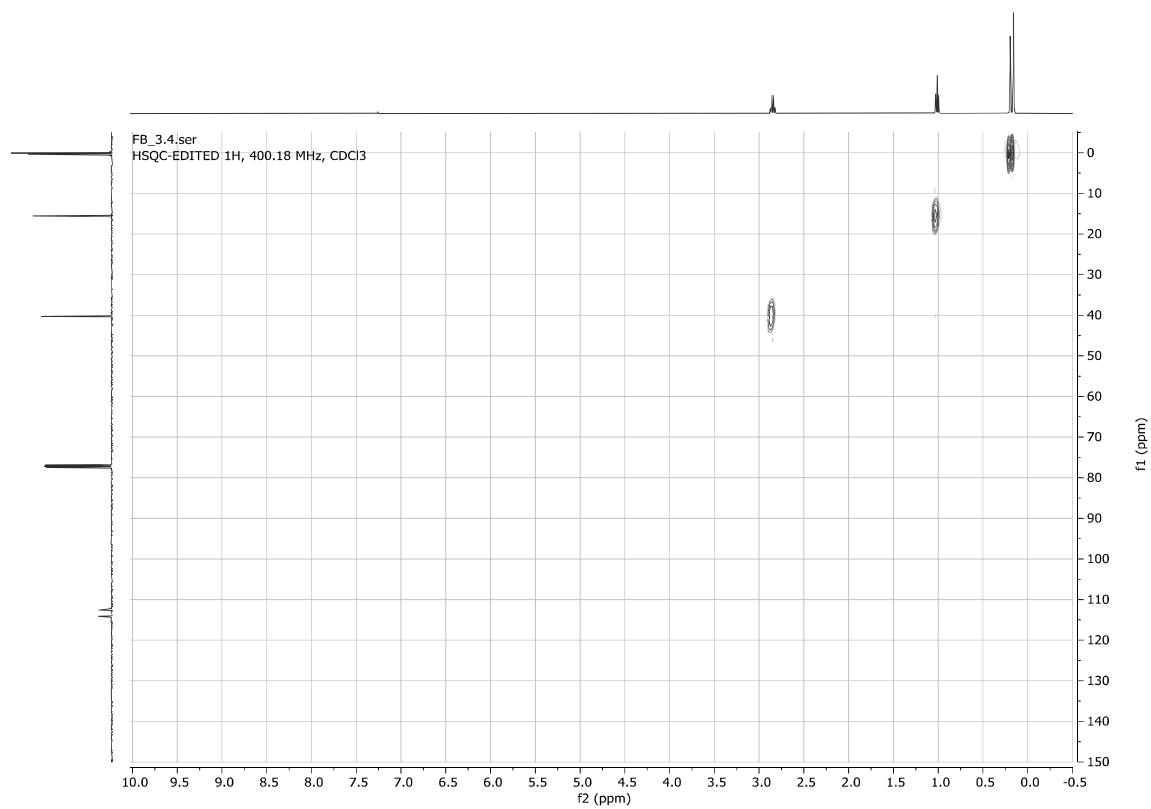
Trimethylsilylethynyl(diethylamino)dimethylsilane **s2**

FB_3.1.fid
1D 1H, 400.18 MHz, CDCl3

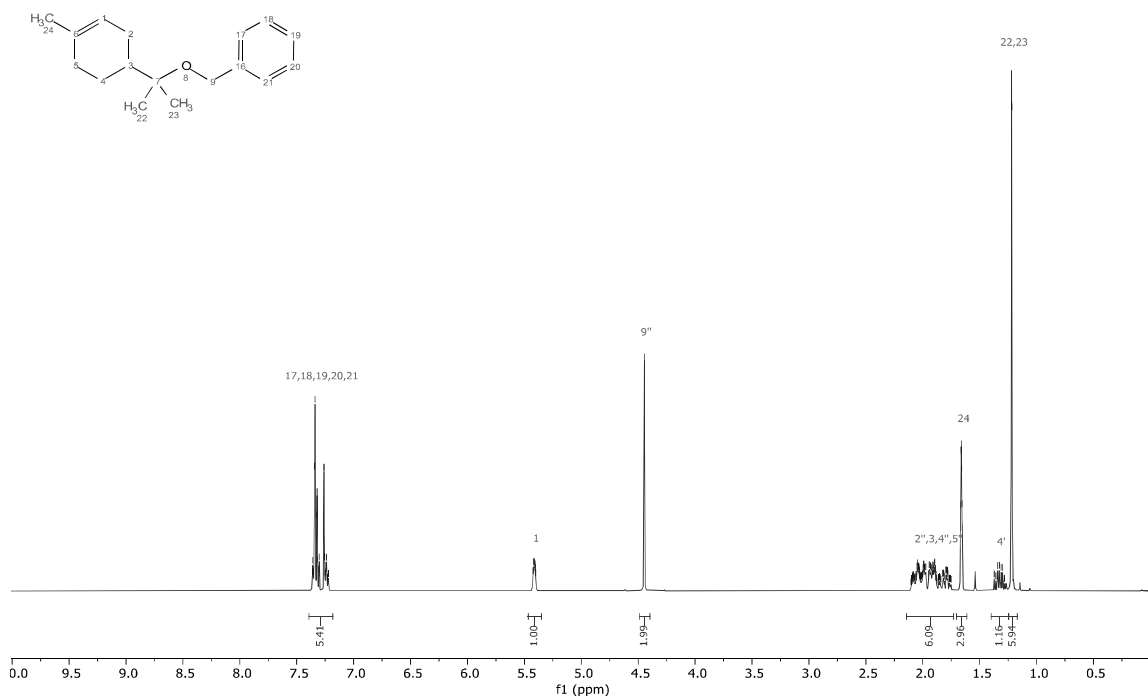


FB_3.3.fid
1D 13C{1H}, 100.64 MHz, CDCl3

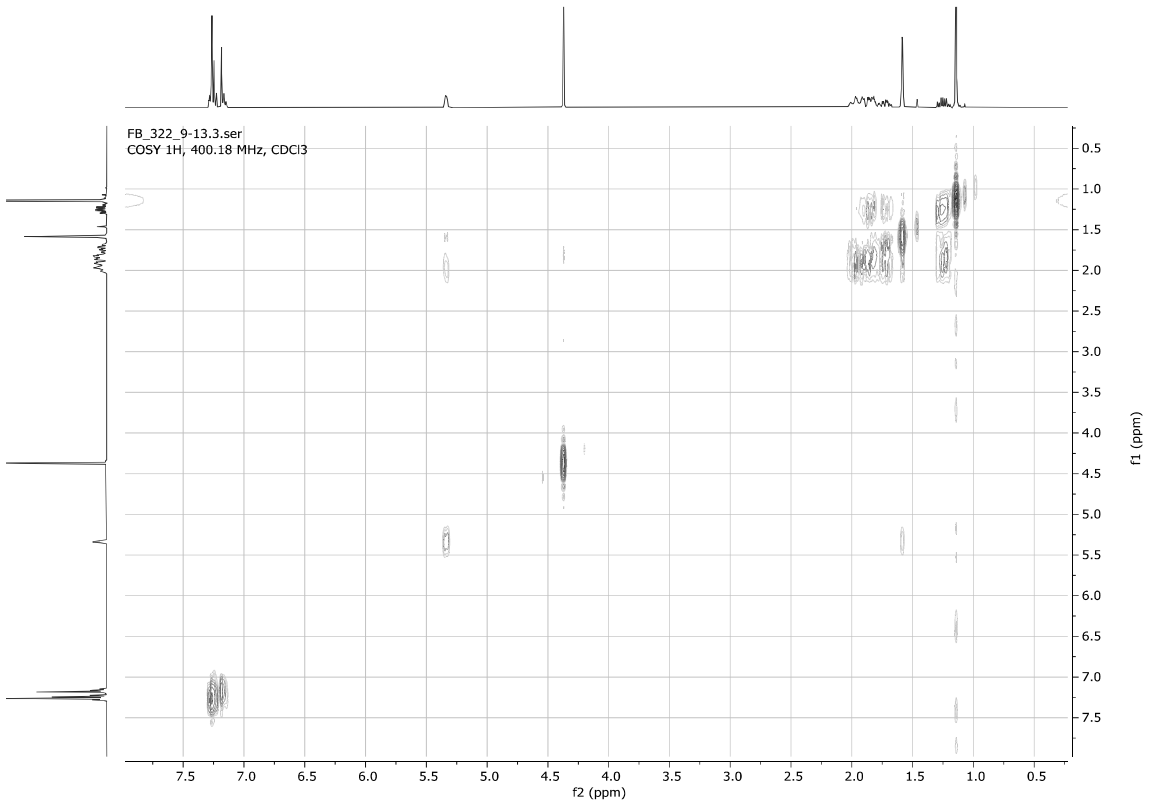
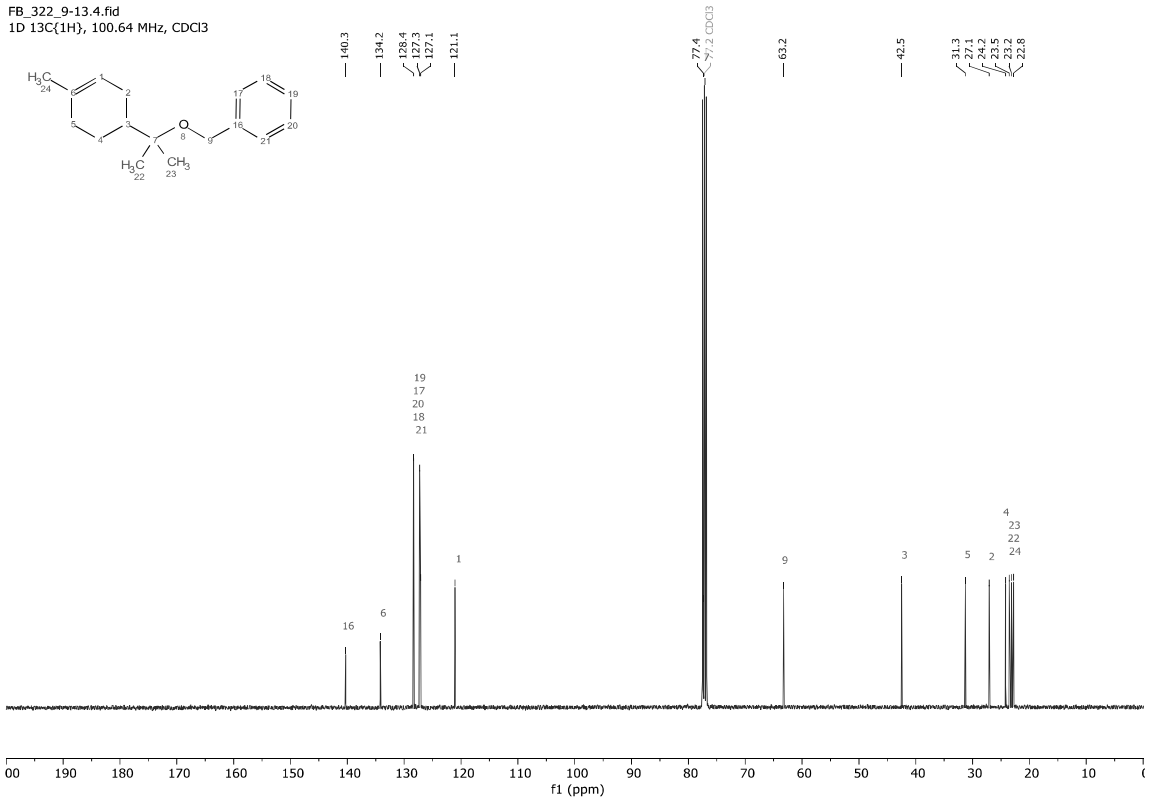


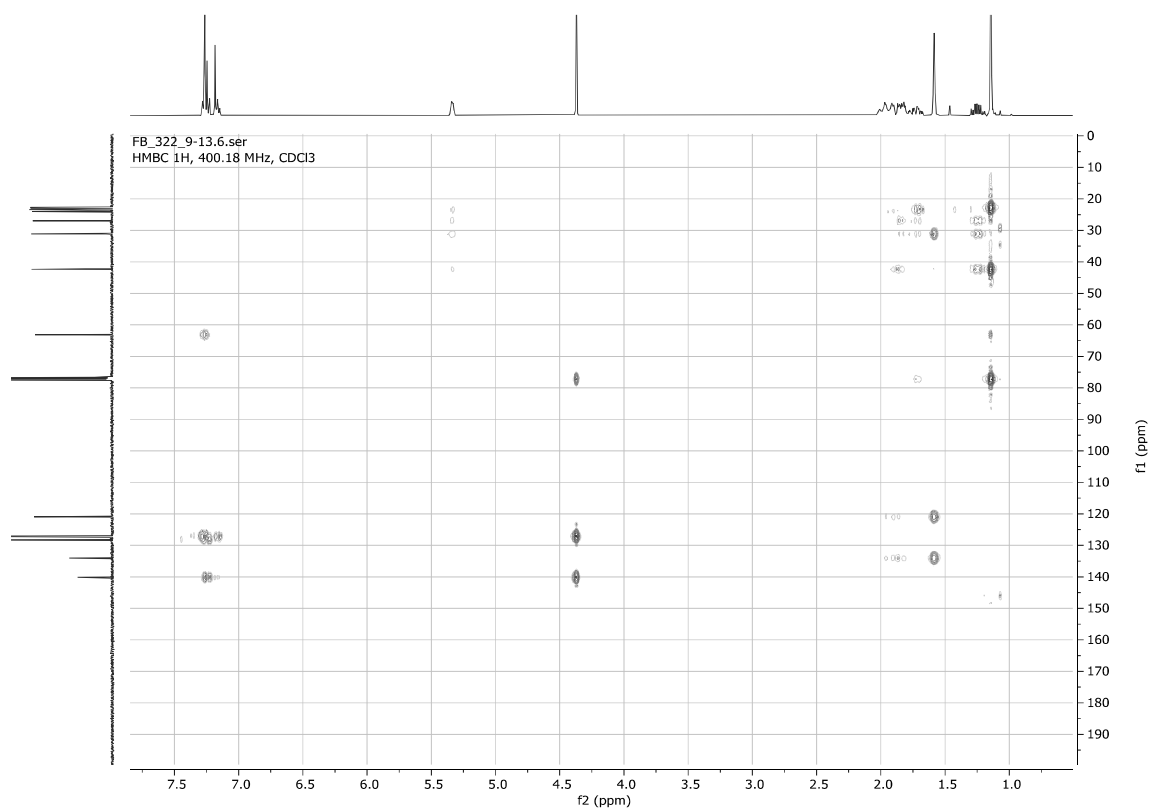
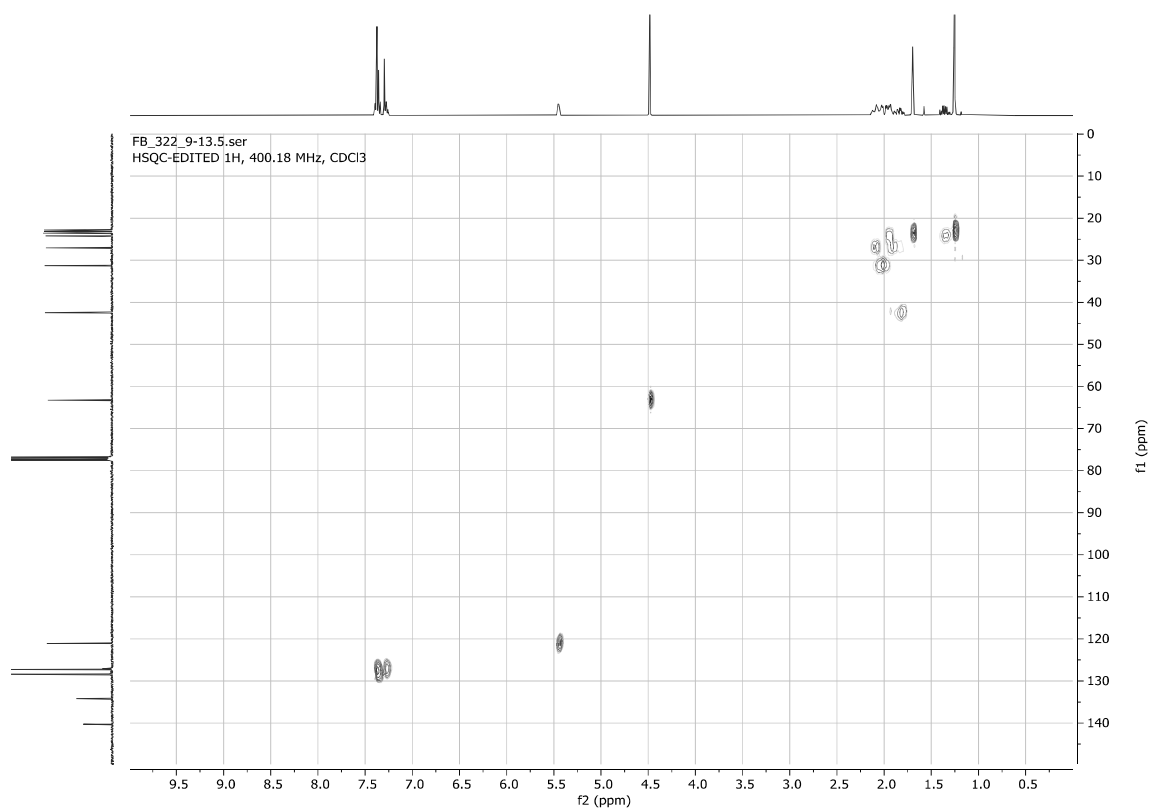


4-(1-(Benzyloxy)-1-methylethyl)-1-methylcyclohexene **1e**



FB_322_9-13.4.fid
1D 13C{1H}, 100.64 MHz, CDCl3



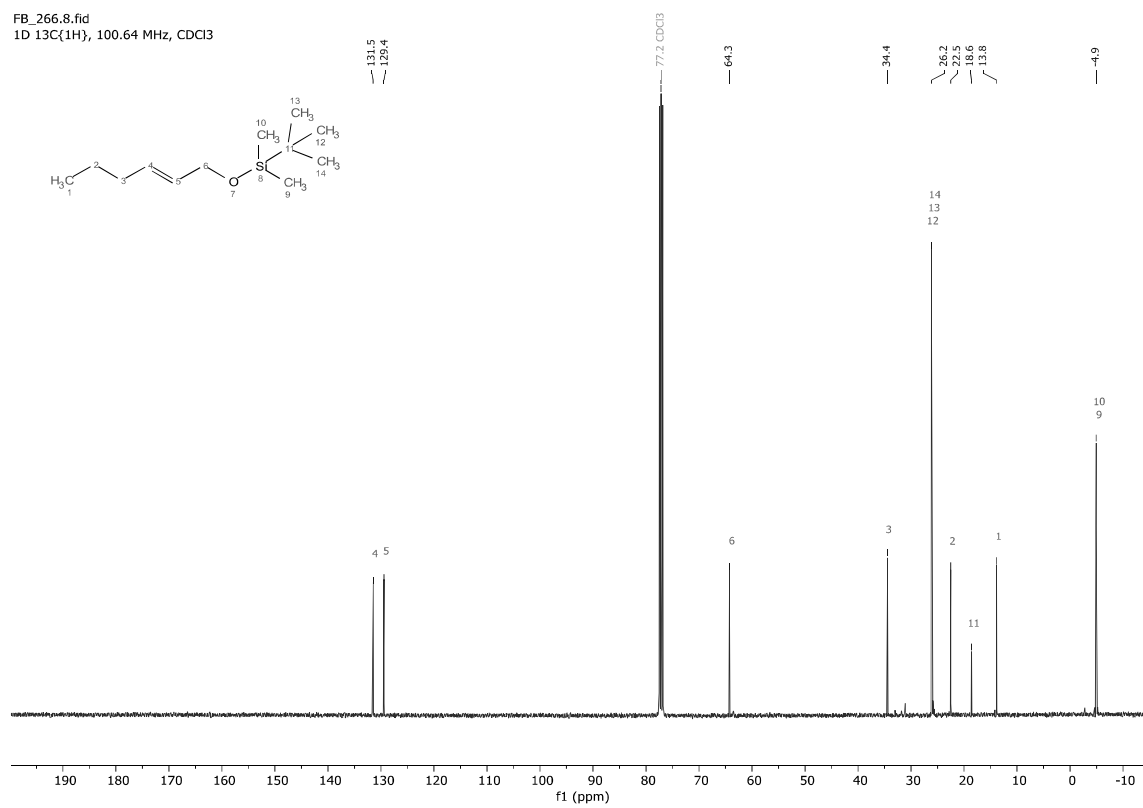


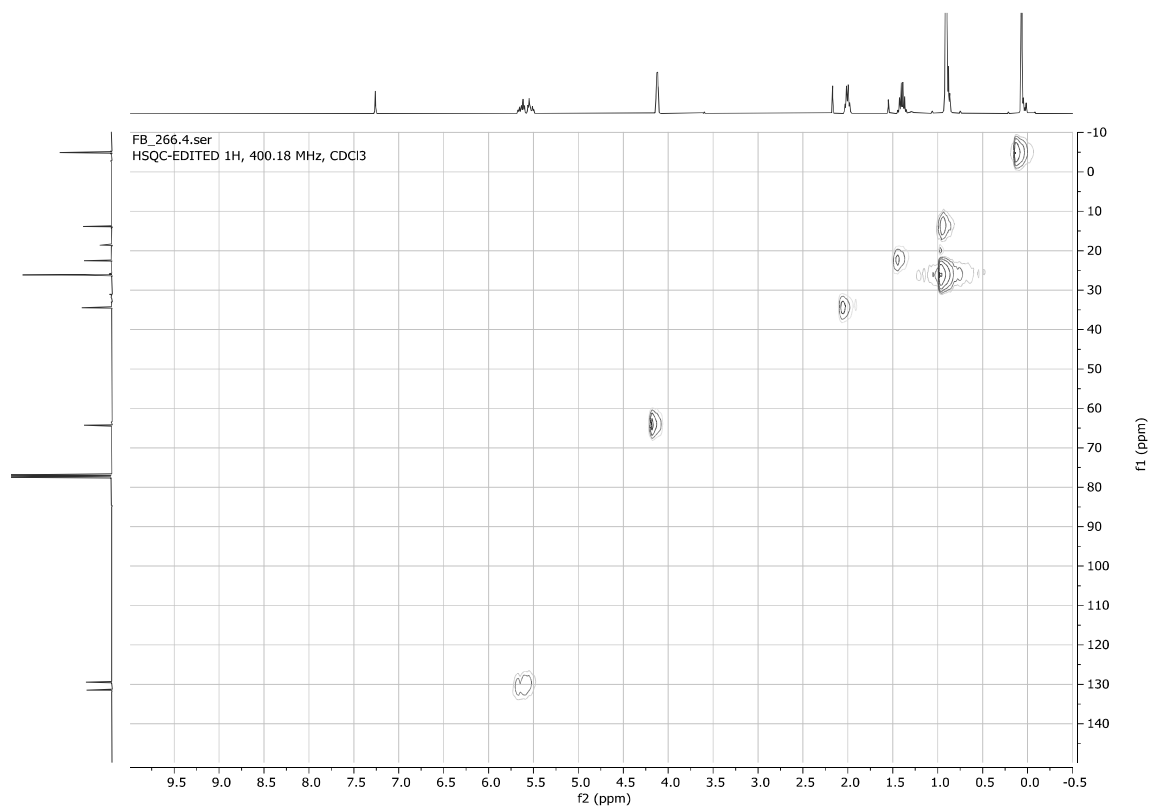
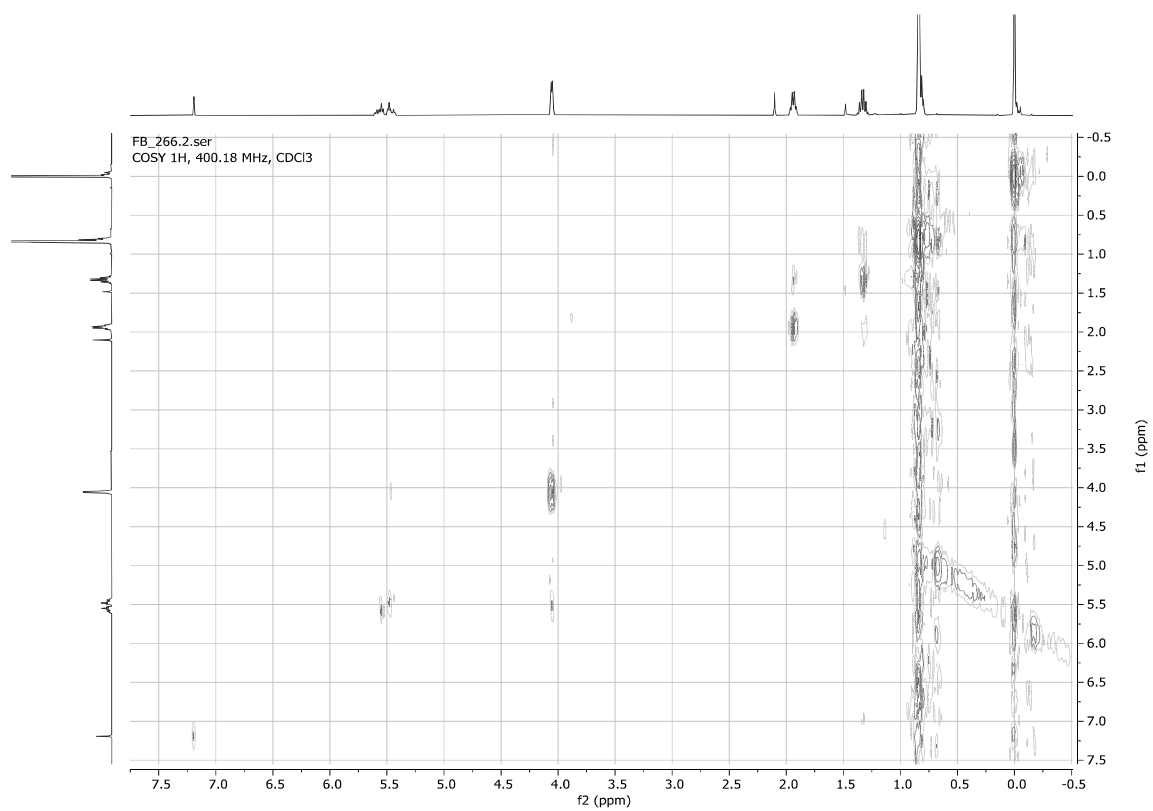
tert-Butyl(hex-2-en-1-yloxy)dimethylsilane **1i**

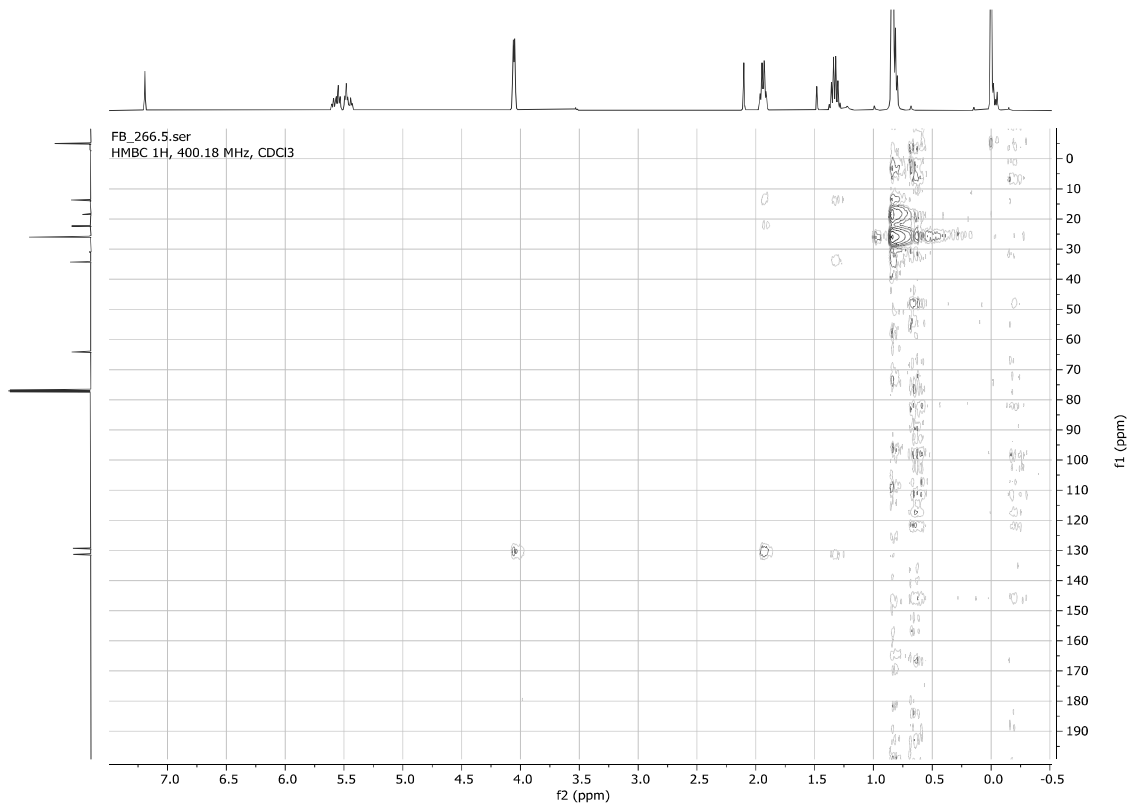
FB_266.6.fid
1D 1H, 400.18 MHz, CDCl3



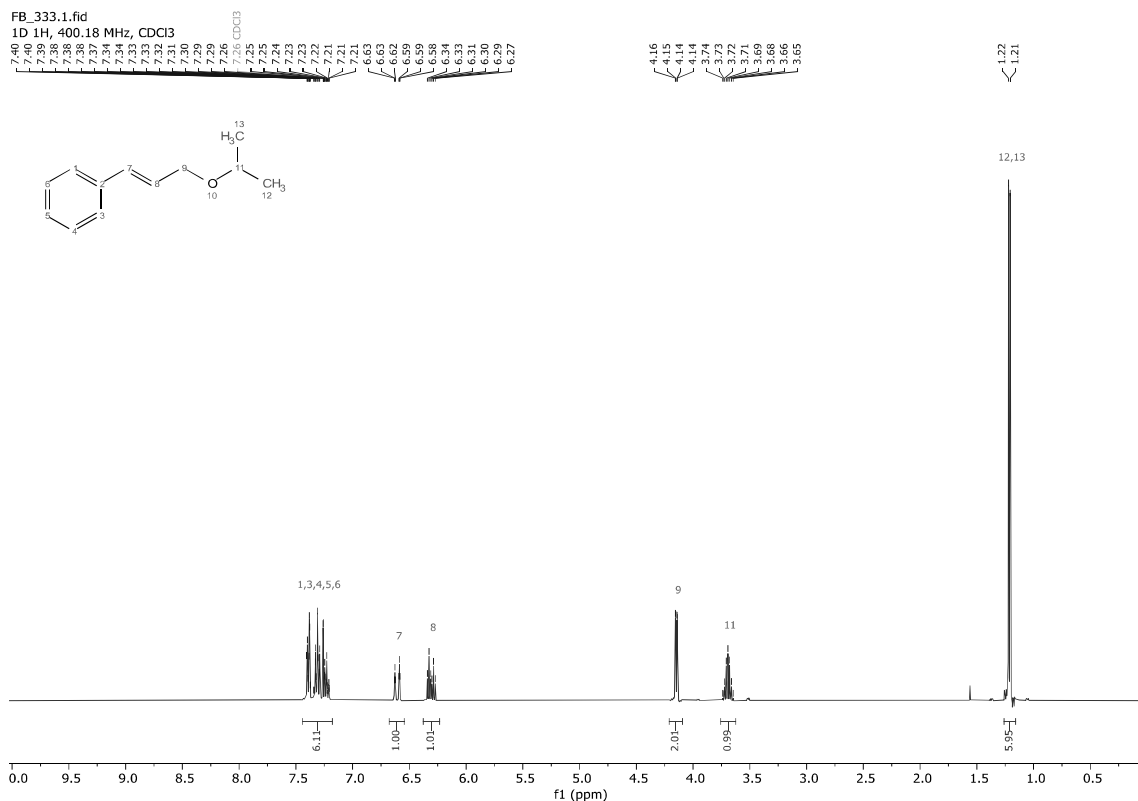
FB_266.8.fid
1D 13C(1H), 100.64 MHz, CDCl3



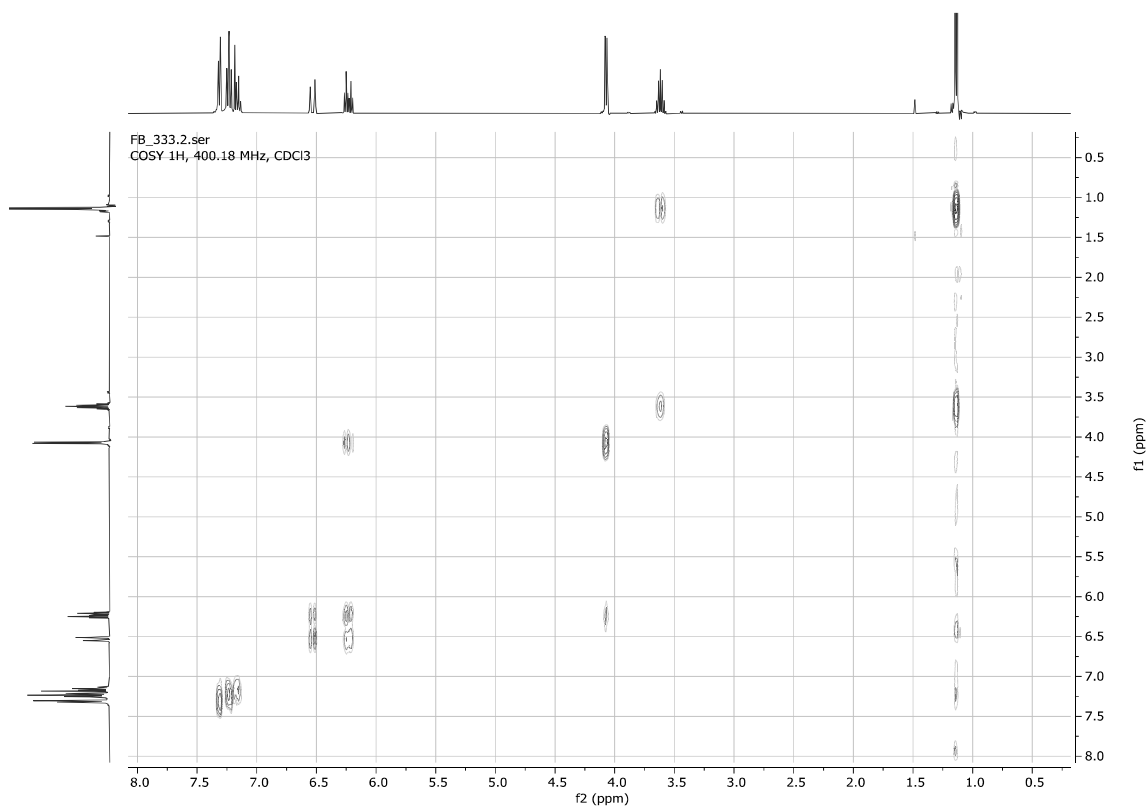
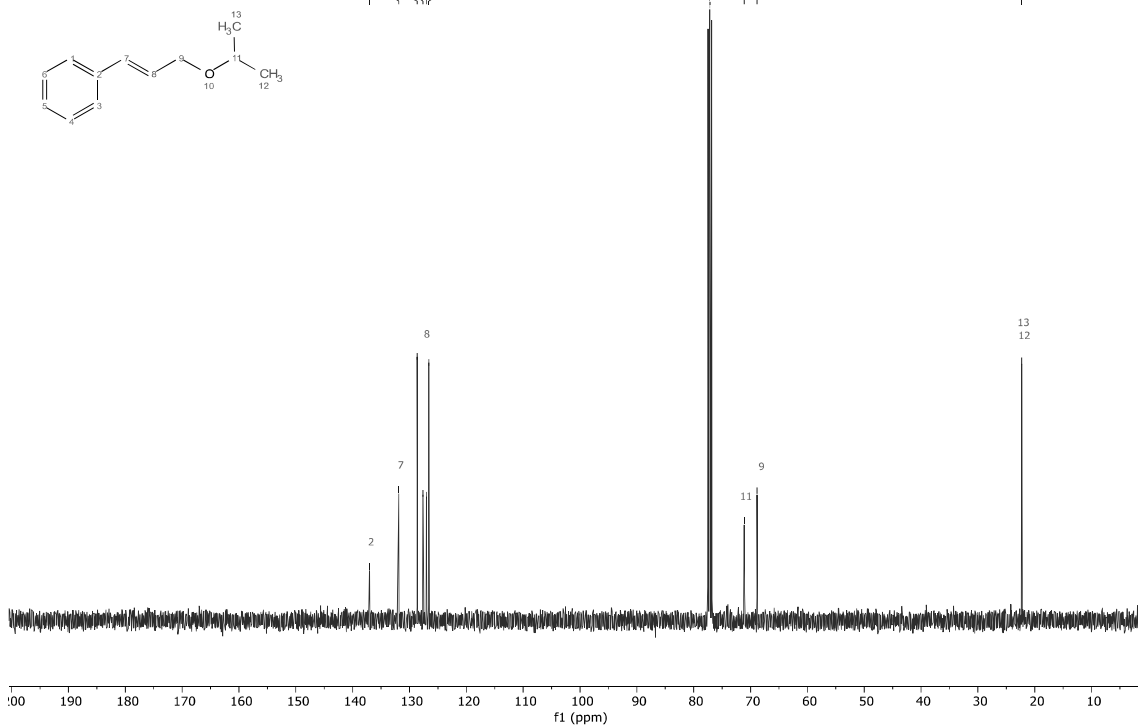


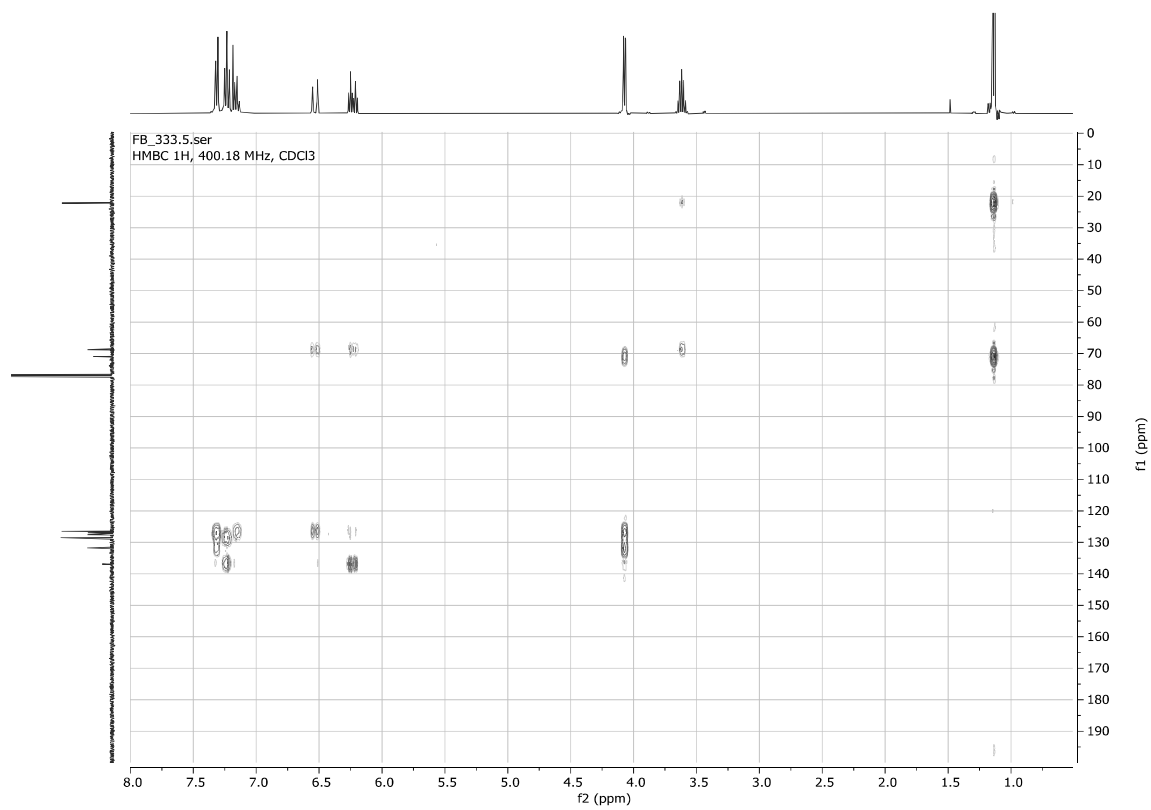
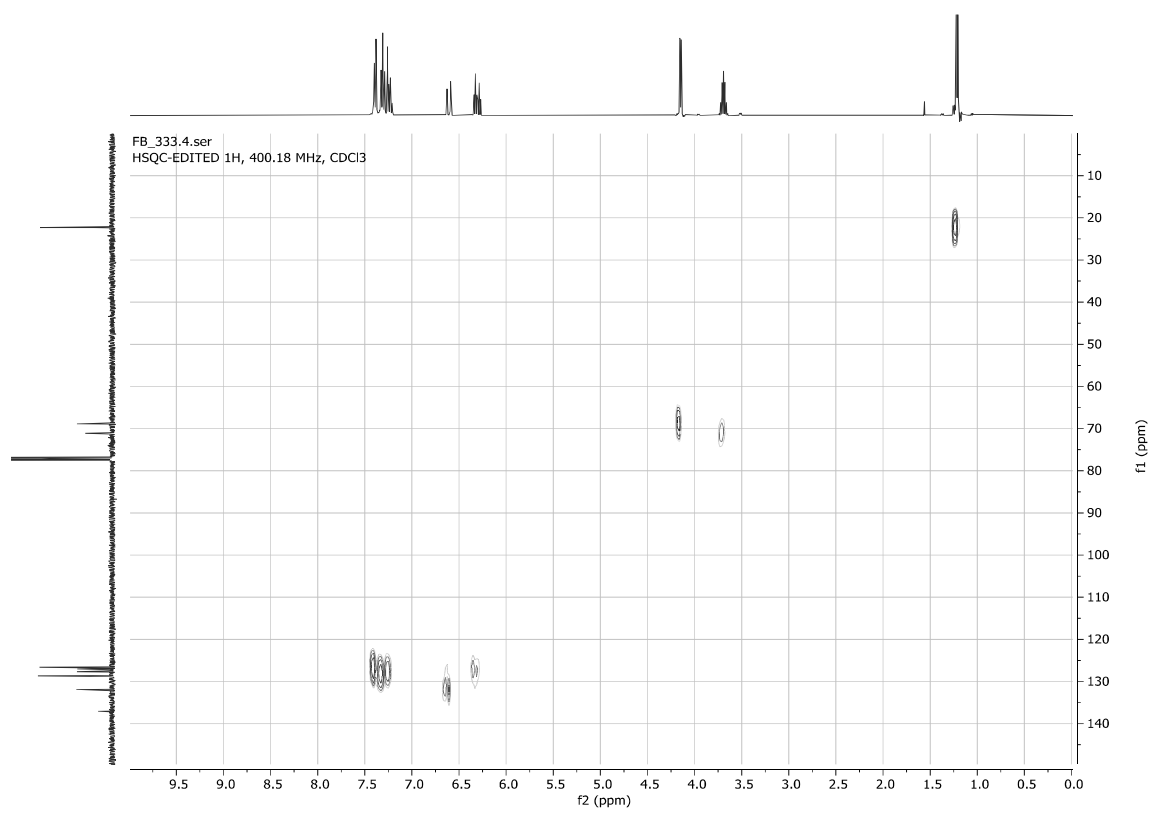


1-Phenyl-3-isopropoxy-1-propene **1s**



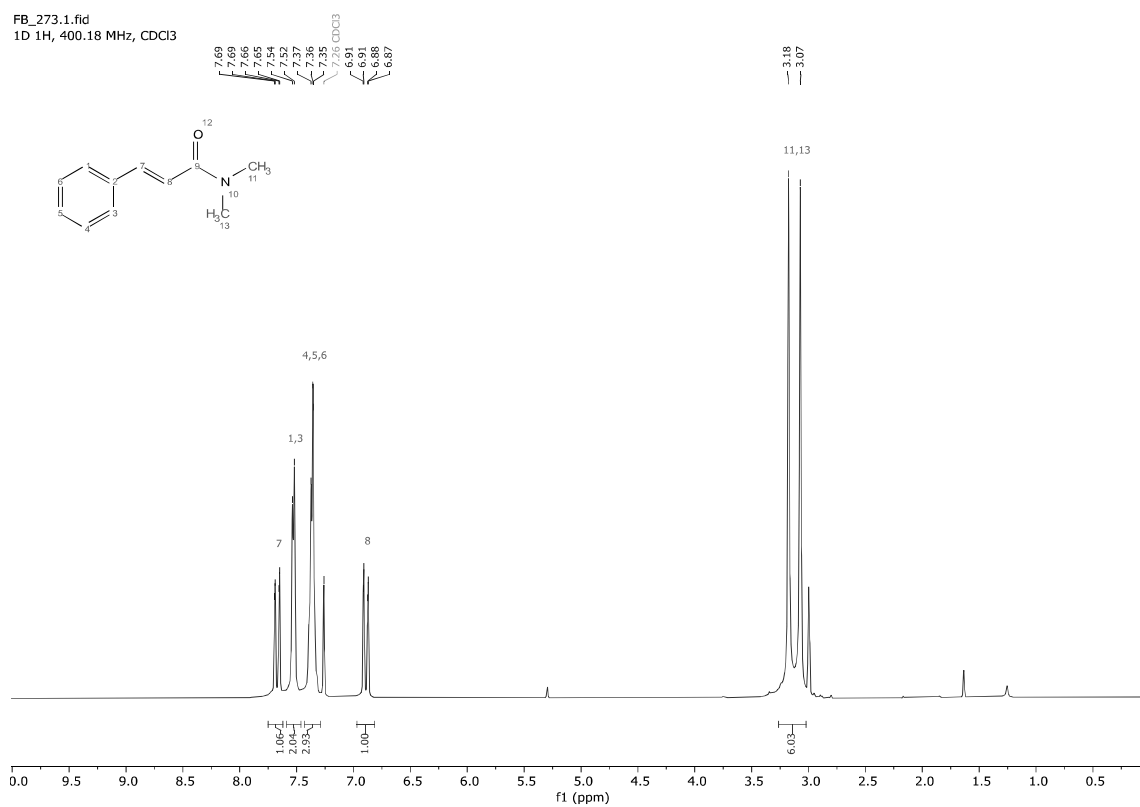
FB_333.3.fid
1D 13C{1H}, 100.64 MHz, CDCl3



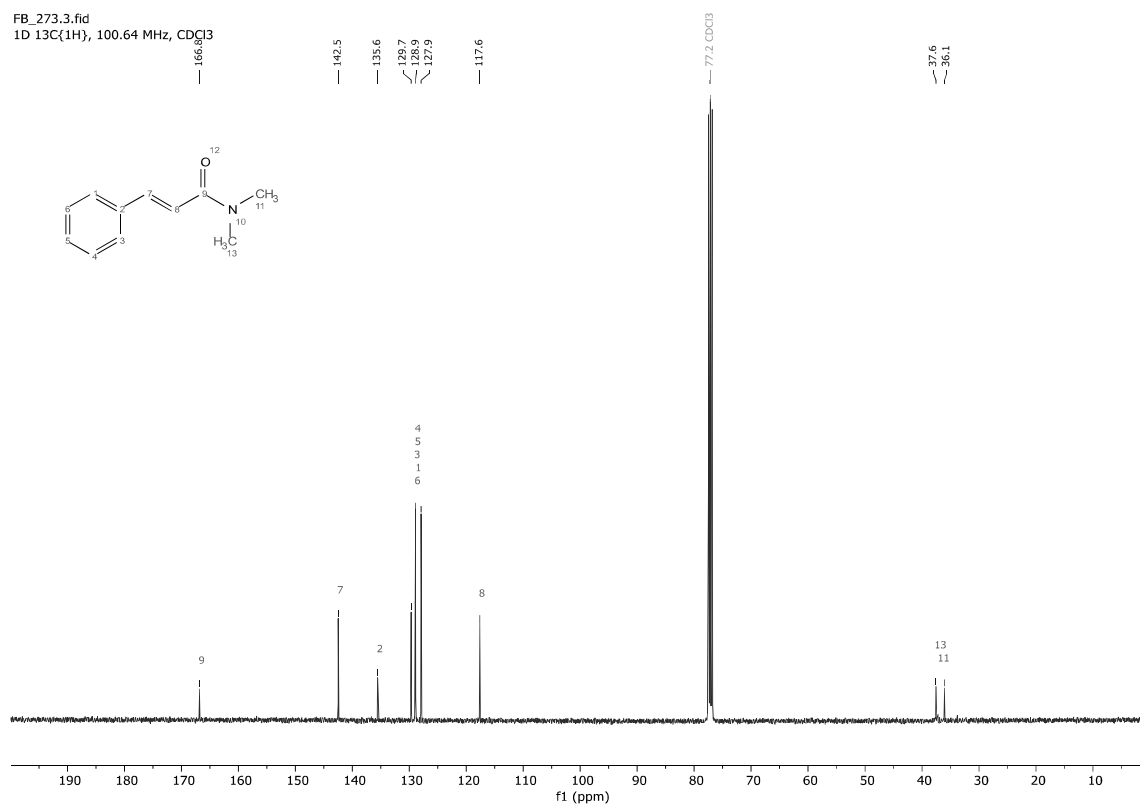


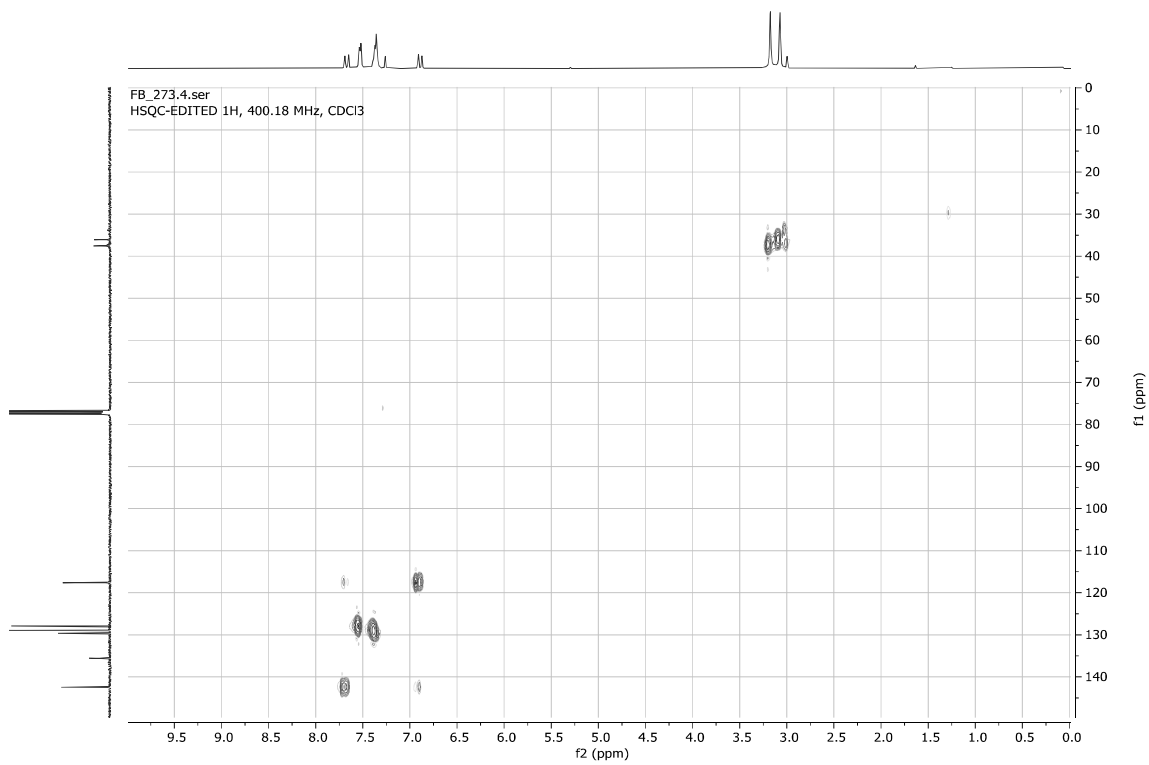
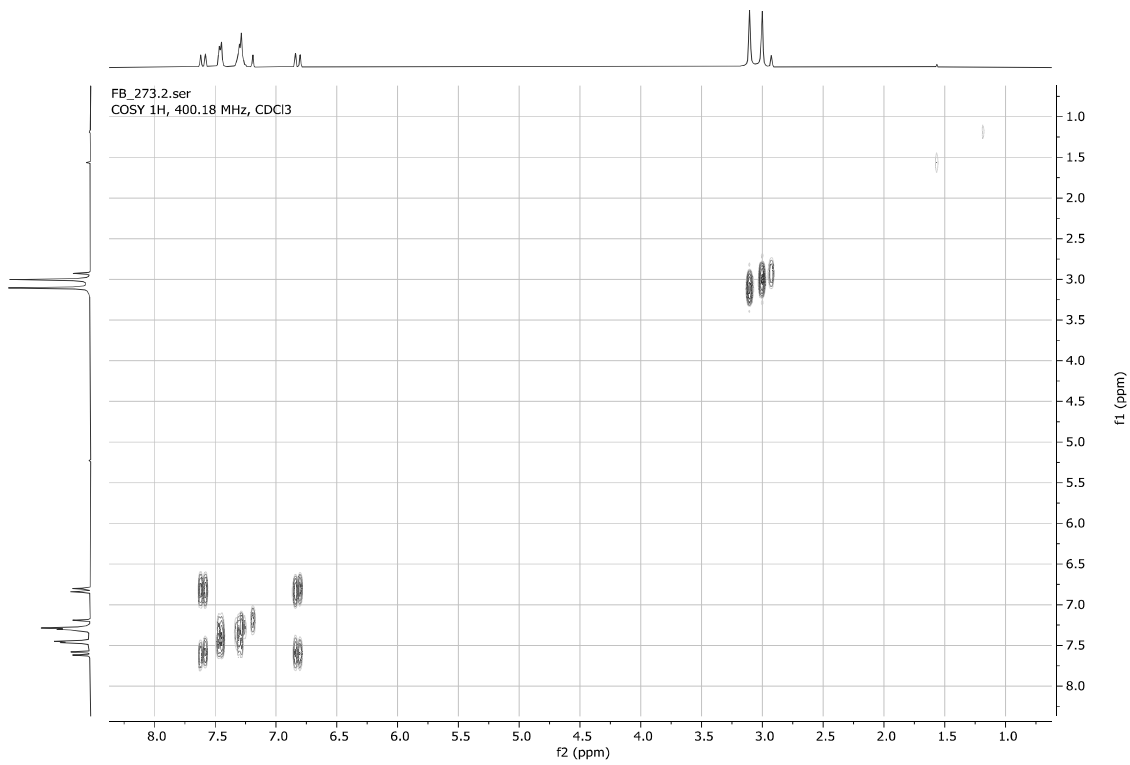
N,N-Dimethylcinnamamide **1u**

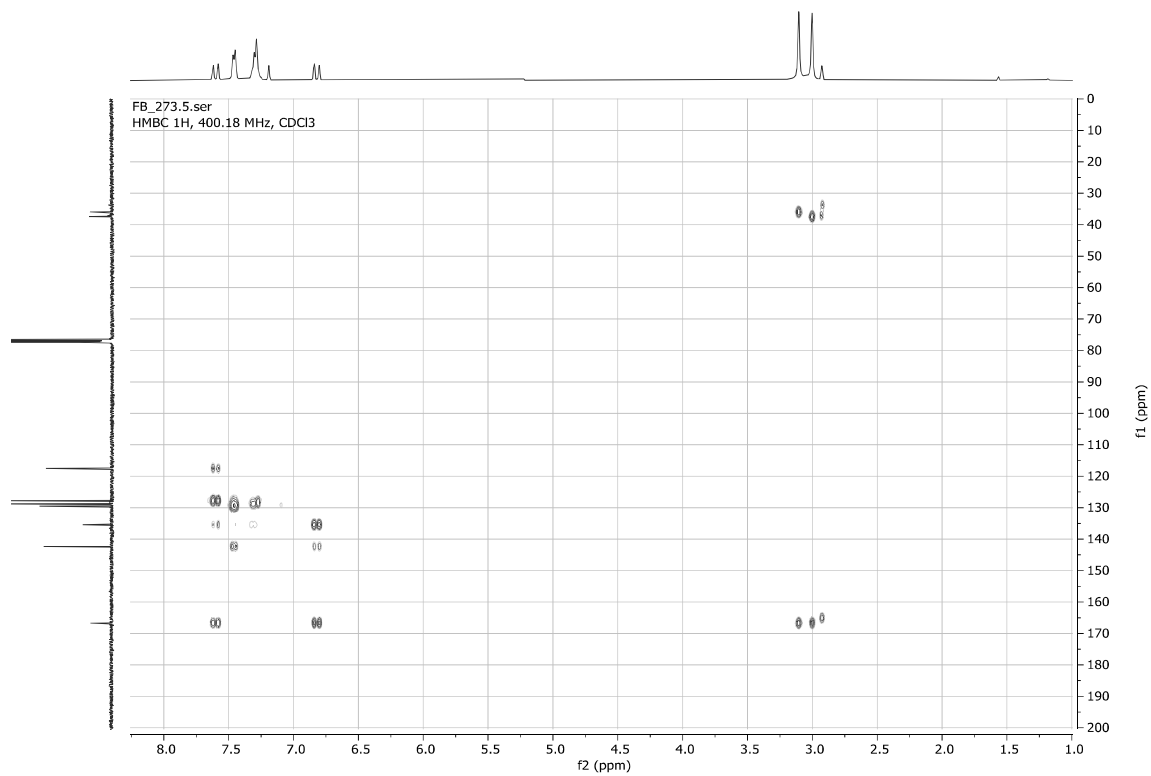
FB_273.1.fid
1D 1H, 400.18 MHz, CDCl₃



FB_273.3.fid
1D 13C{1H}, 100.64 MHz, CDCl₃

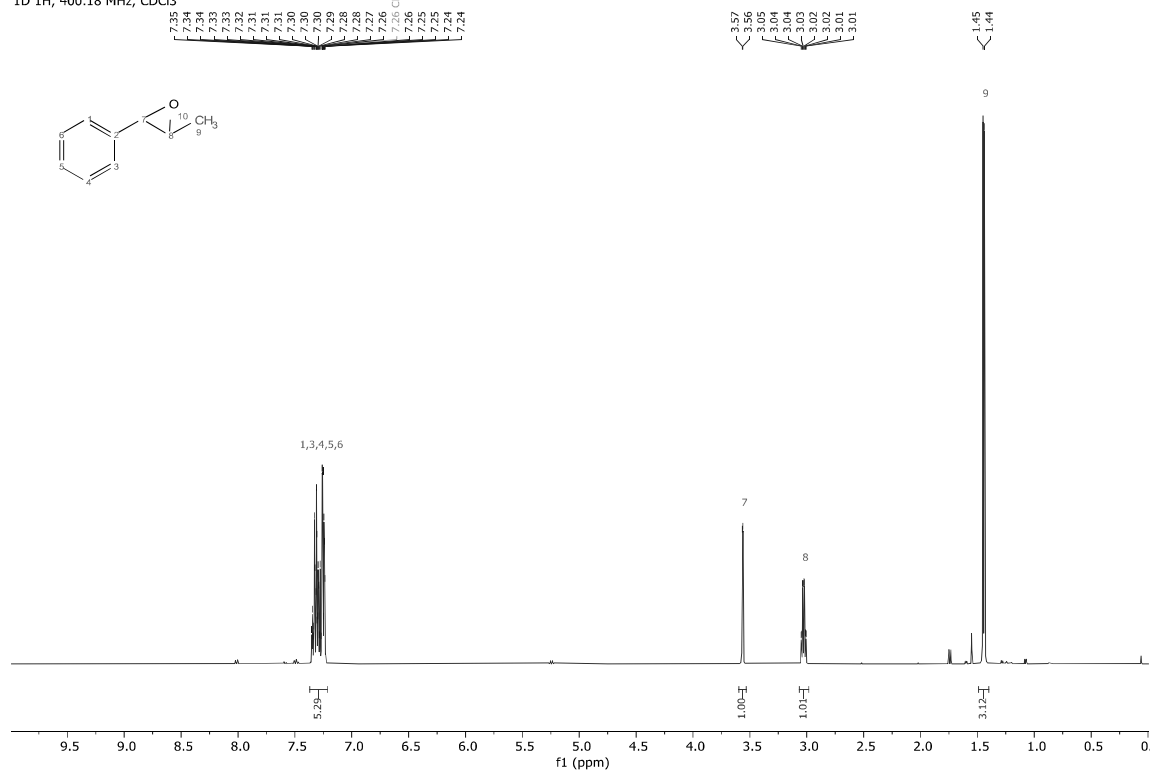
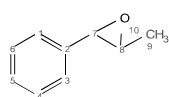




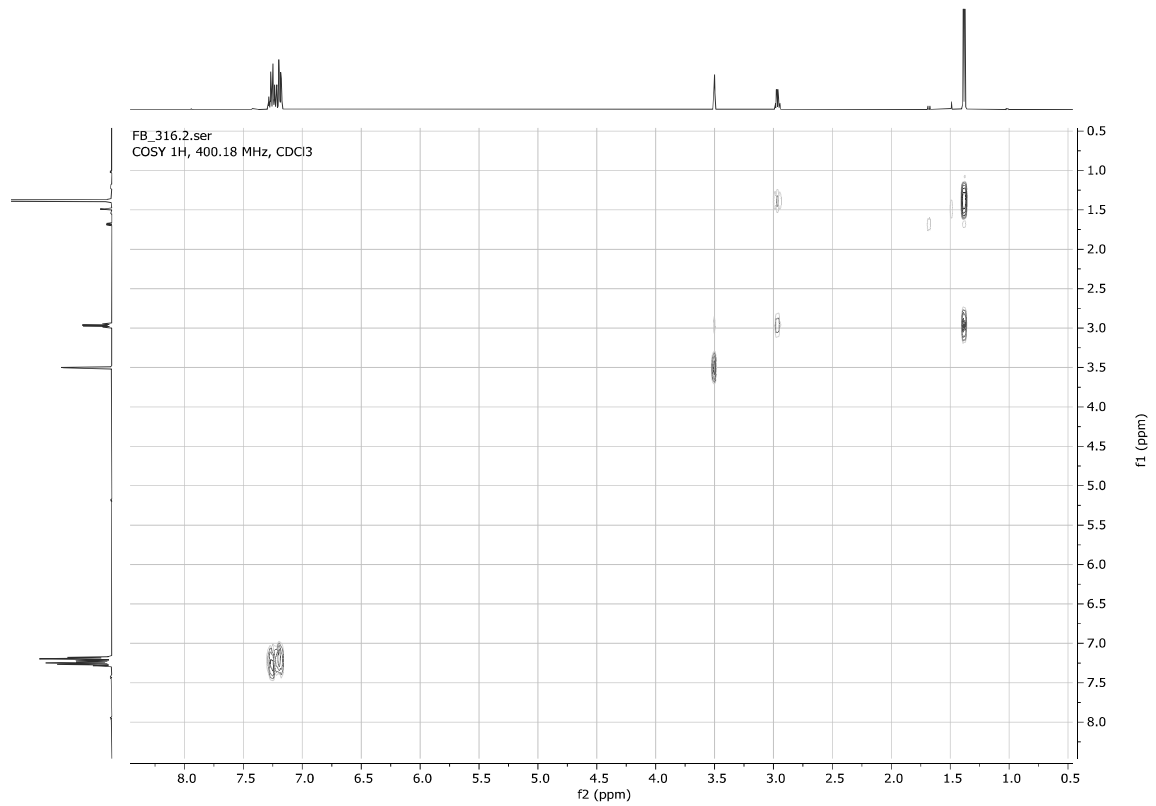
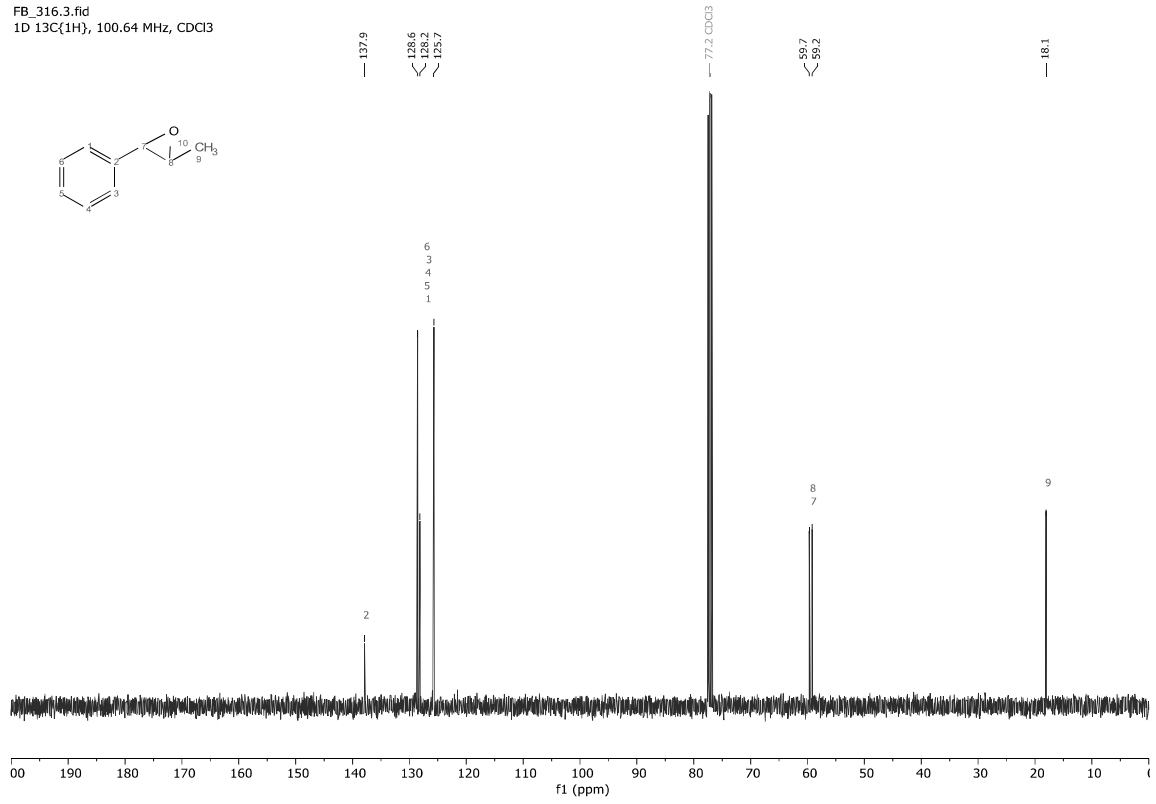


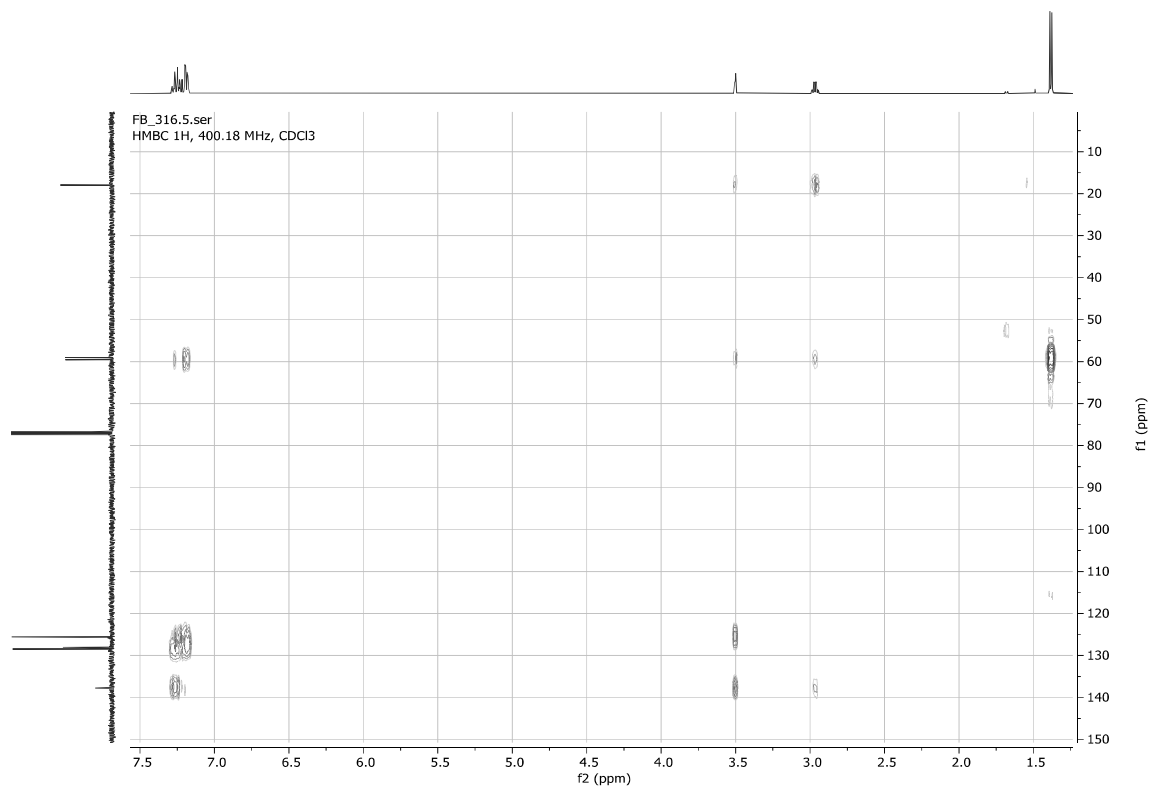
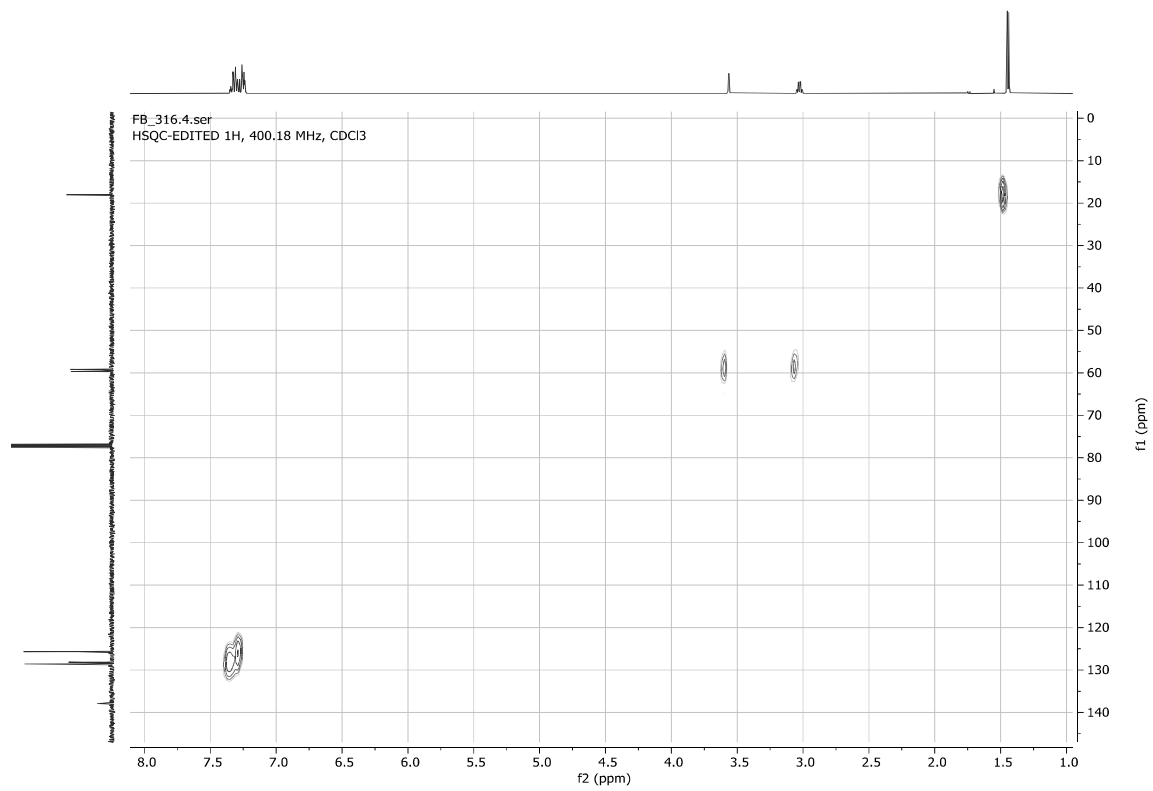
2-Methyl-3-phenyloxirane **2q**

FB_316.1.fid
1D 1H, 400.18 MHz, CDCl3



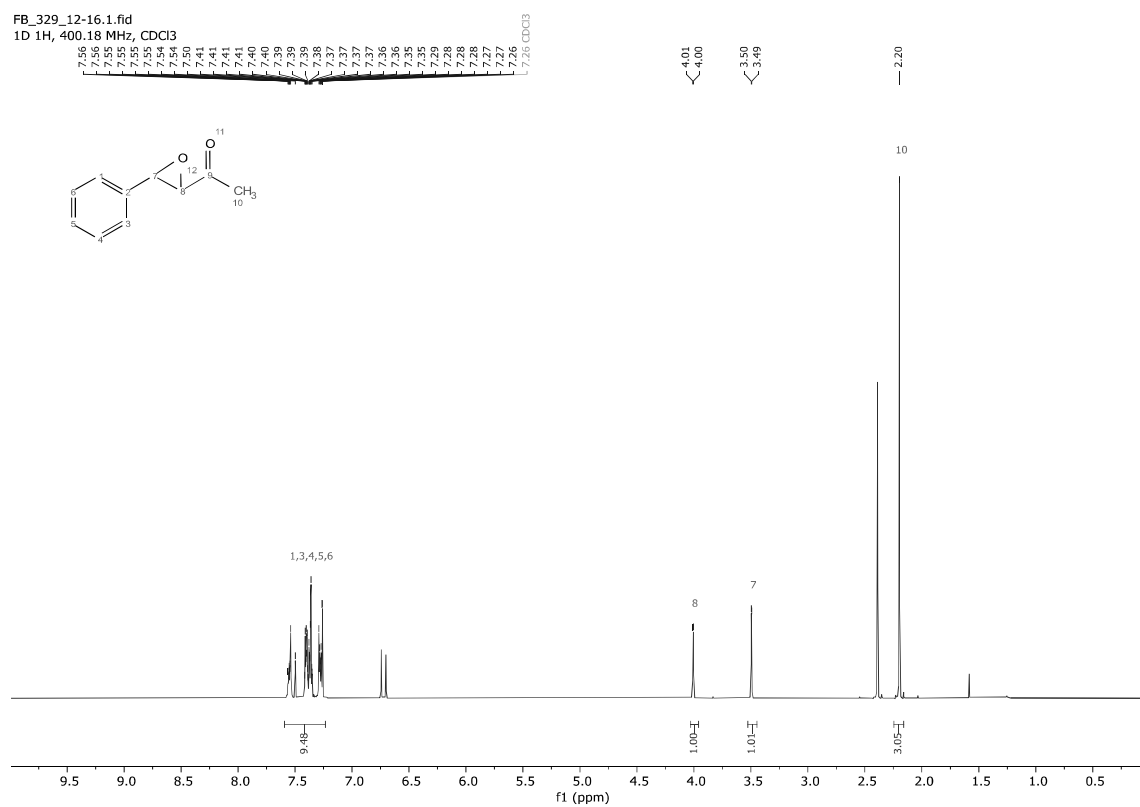
FB_316.3.fid
1D 13C{1H}, 100.64 MHz, CDCl3



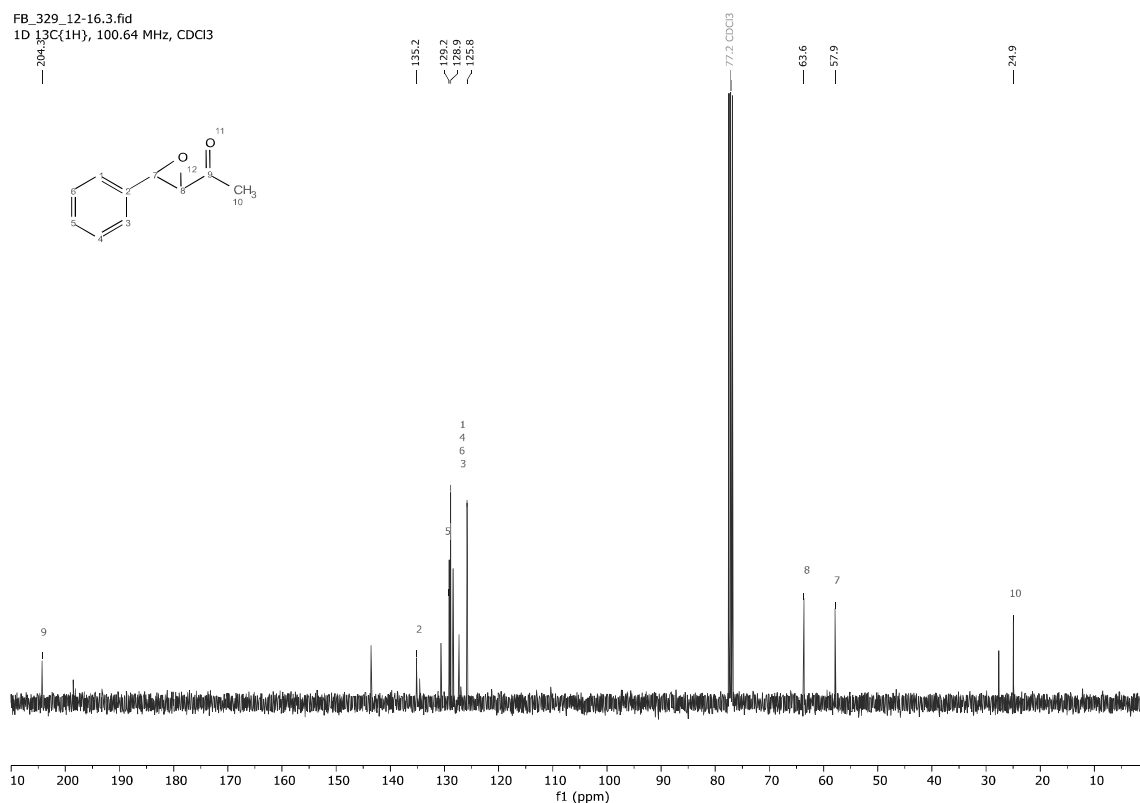


1-(3-Phenyloxiran-2-yl)ethan-1-one 2r

FB_329_12-16.1.fid
1D 1H, 400.18 MHz, CDCl3

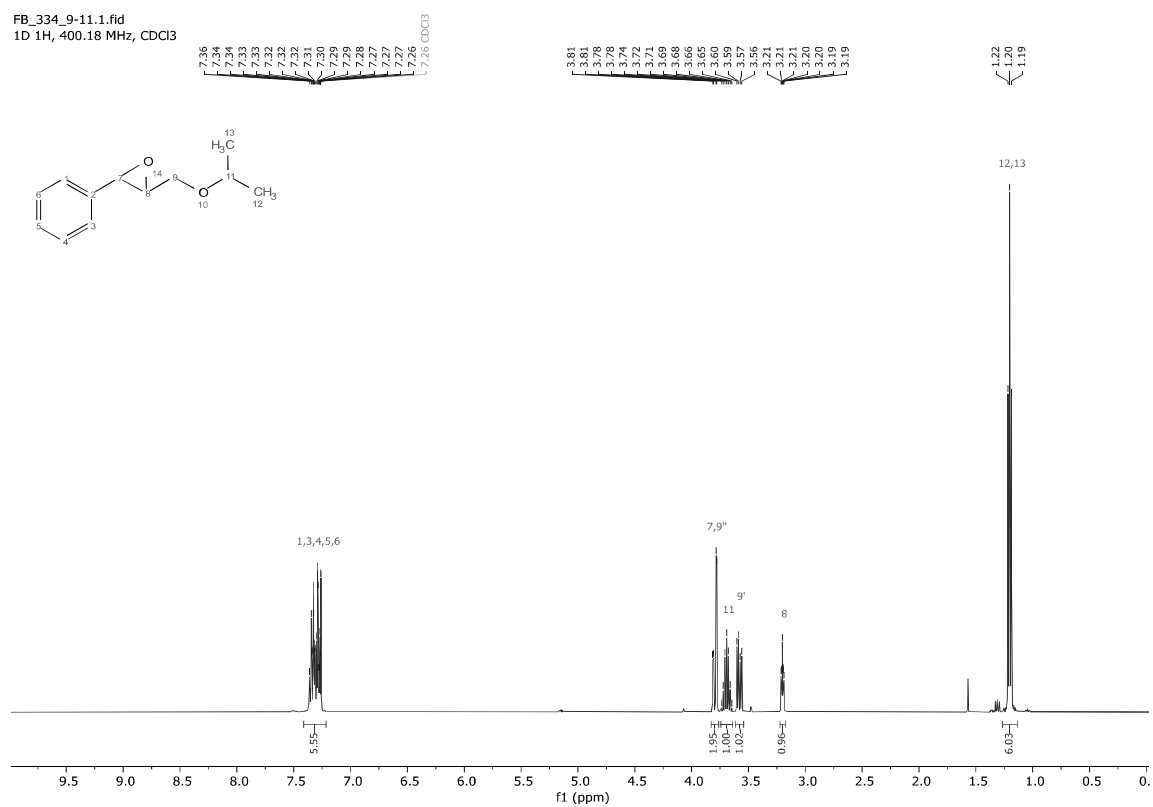


FB_329_12-16.3.fid
1D 13C(1H), 100.64 MHz, CDCl3

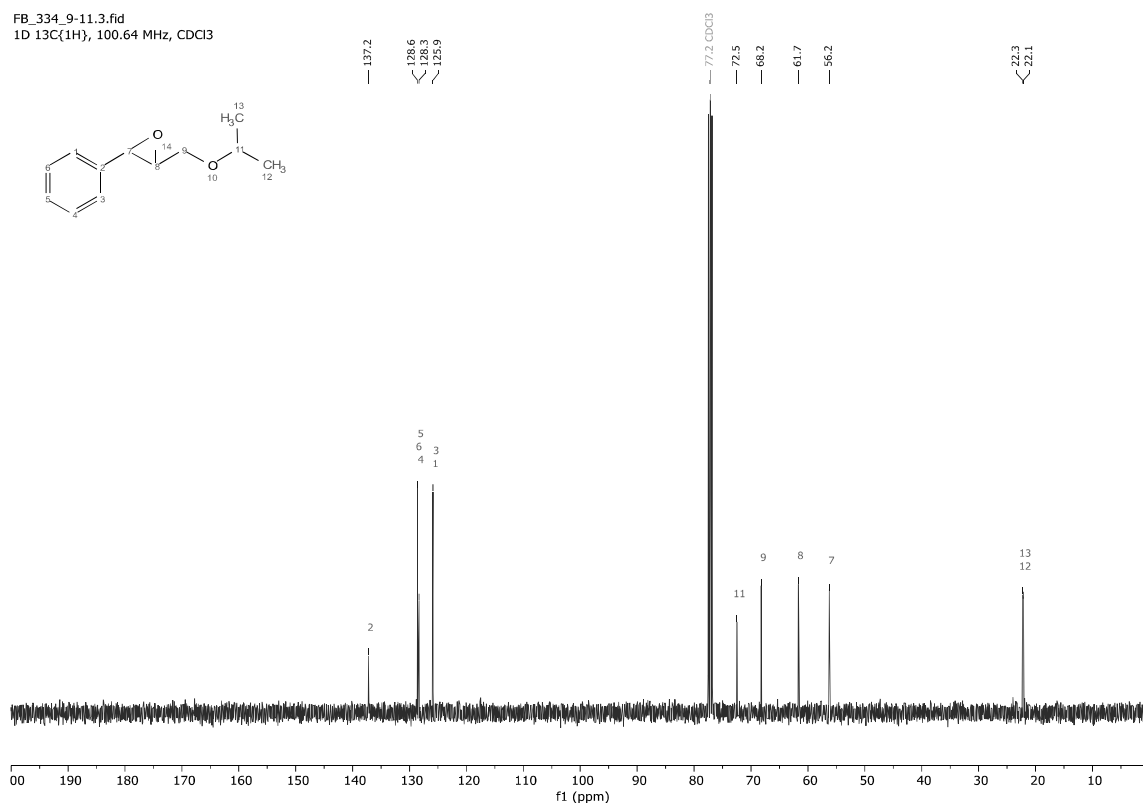


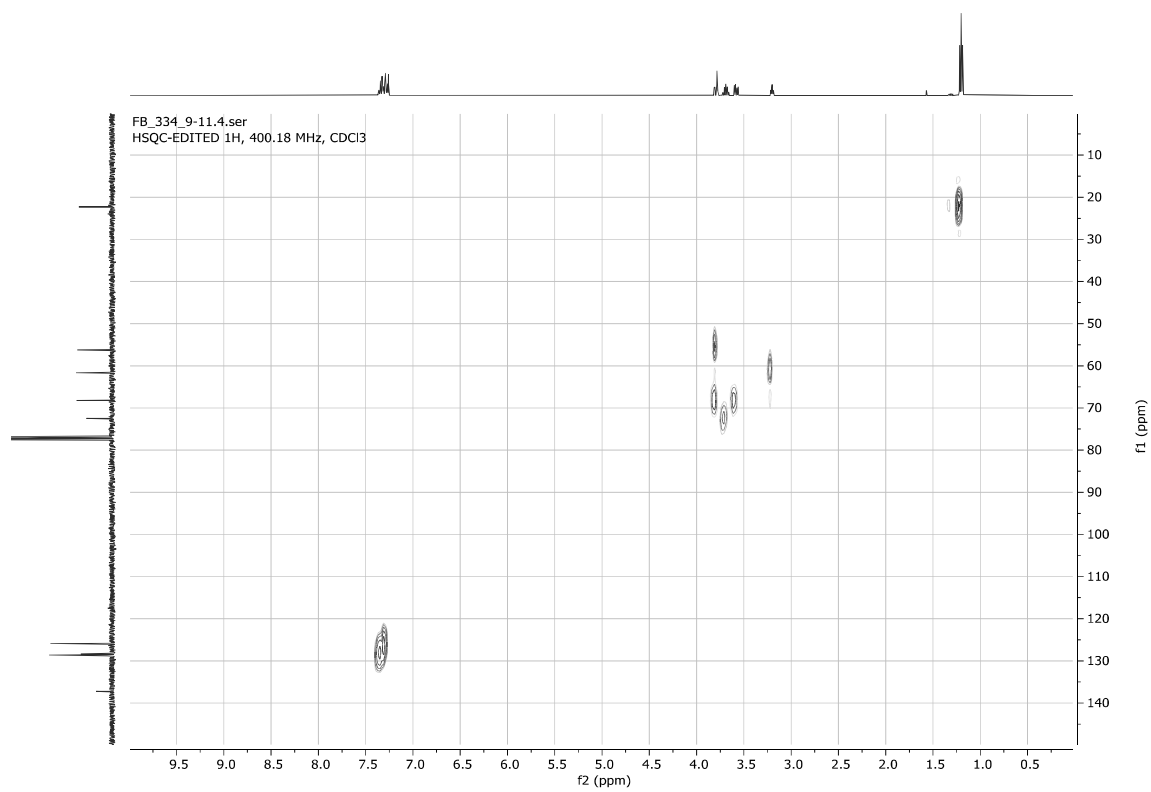
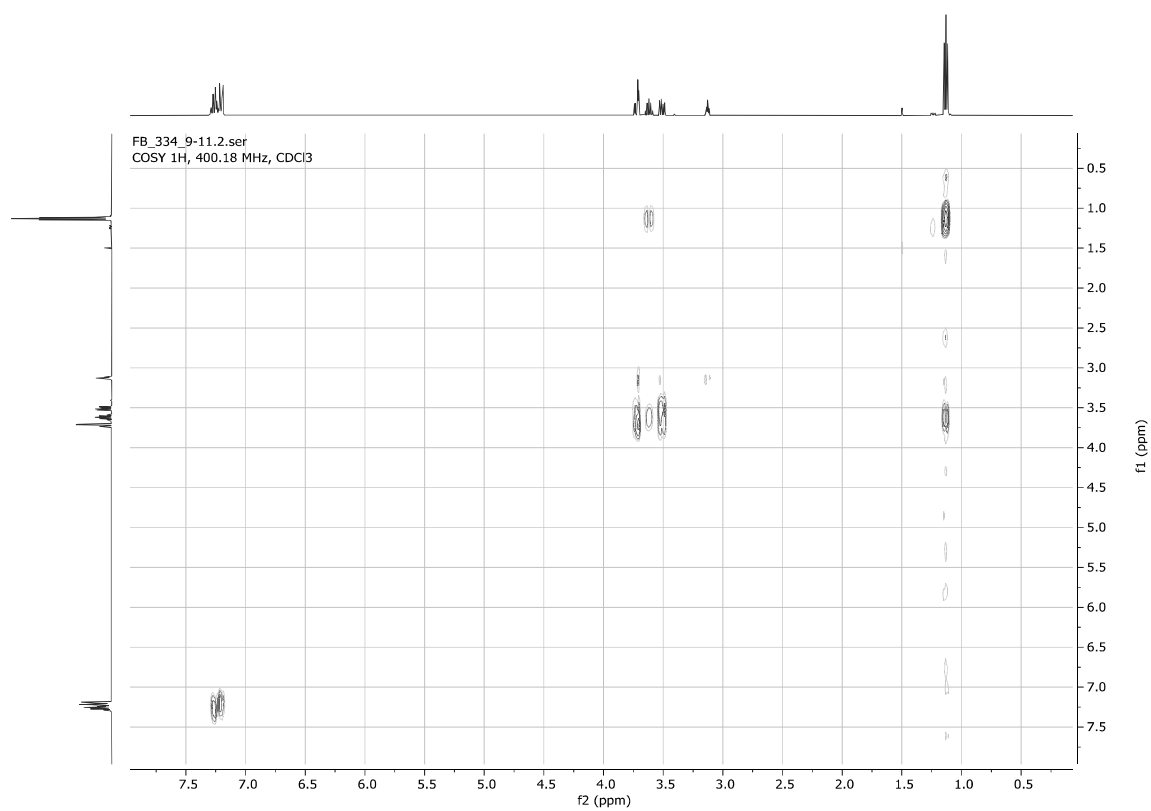
2-(Isopropoxymethyl)-3-phenyloxirane **2s**

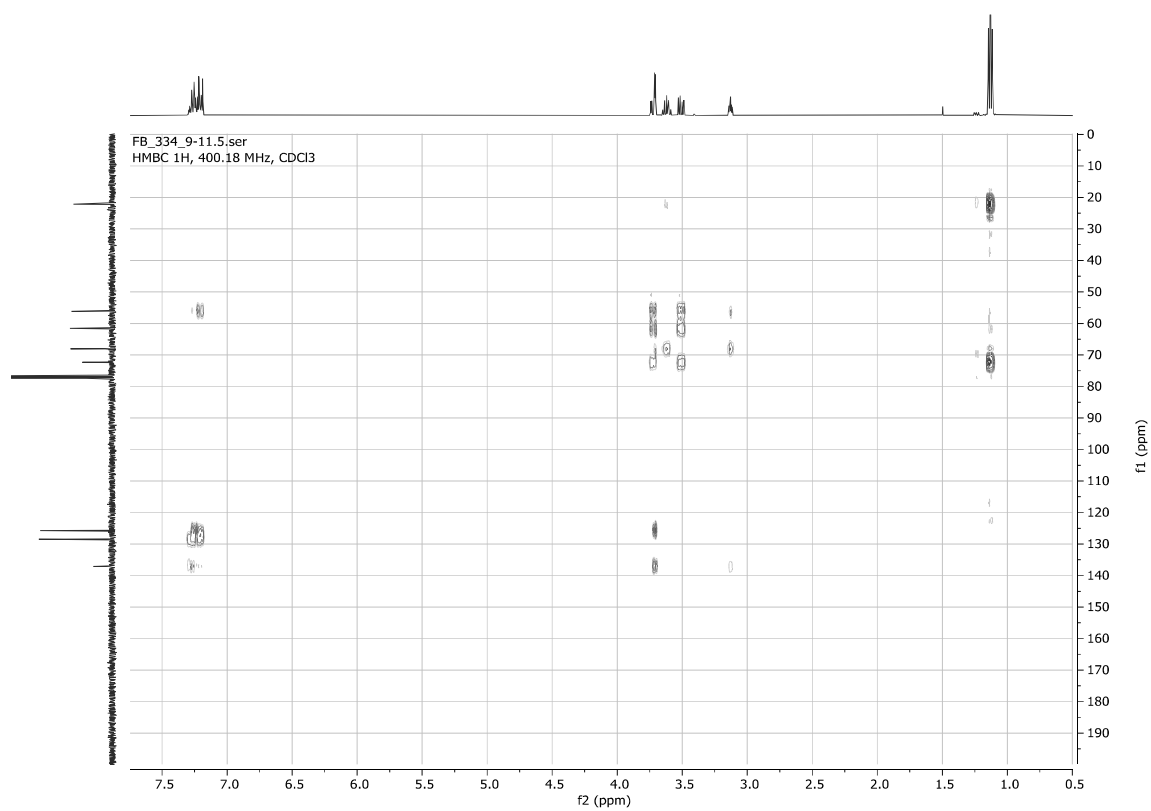
FB_334_9-11.1.fid
1D 1H, 400.18 MHz, CDCl3



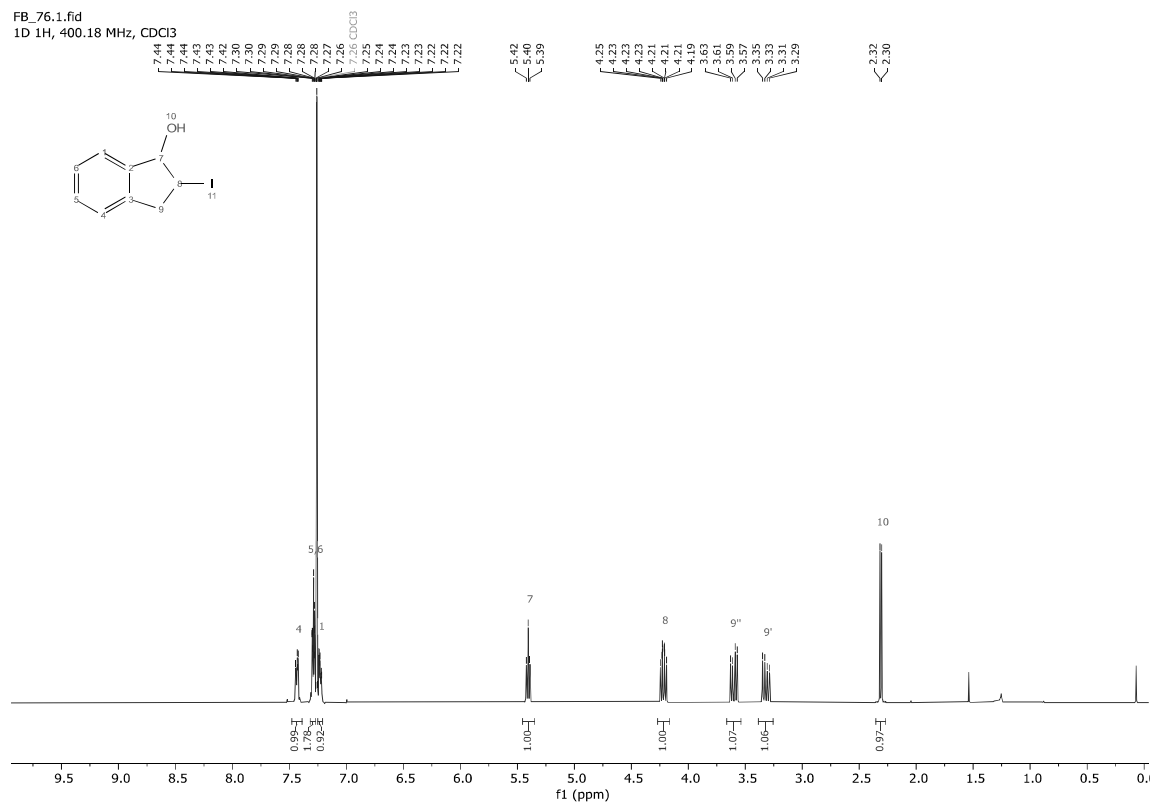
FB_334_9-11.3.fid
1D 13C(1H), 100.64 MHz, CDCl3



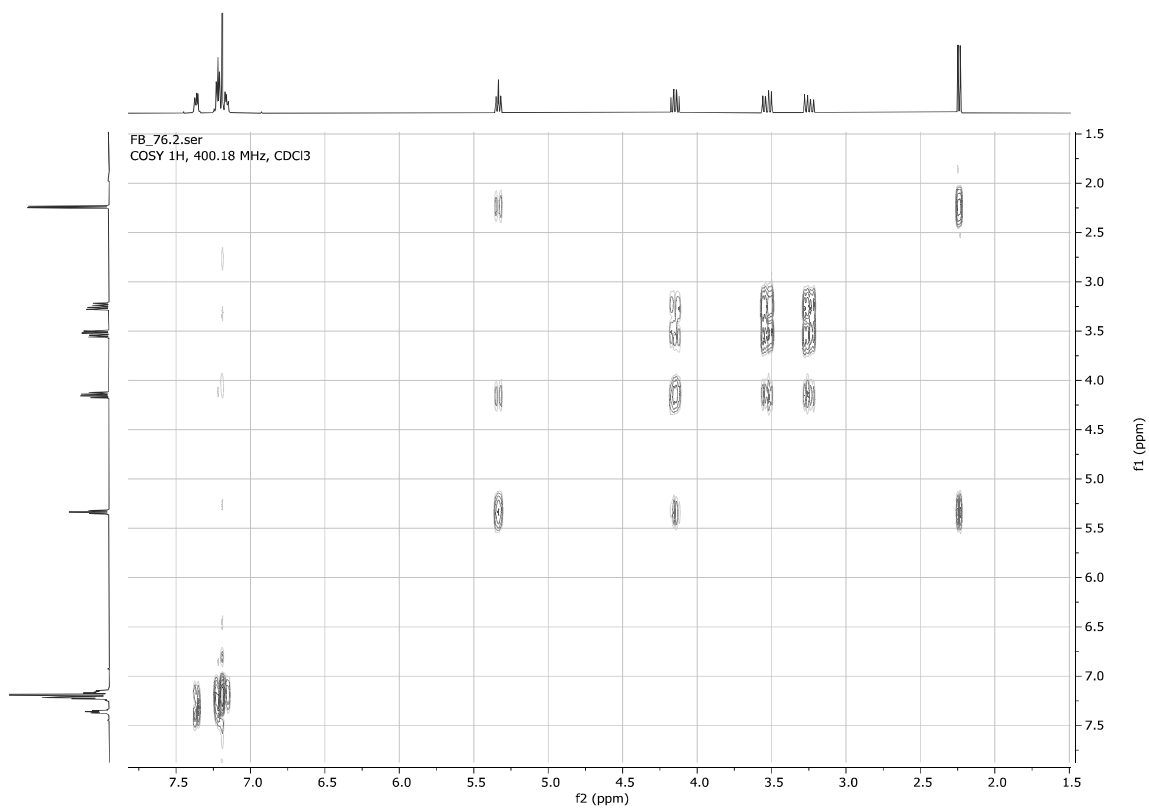
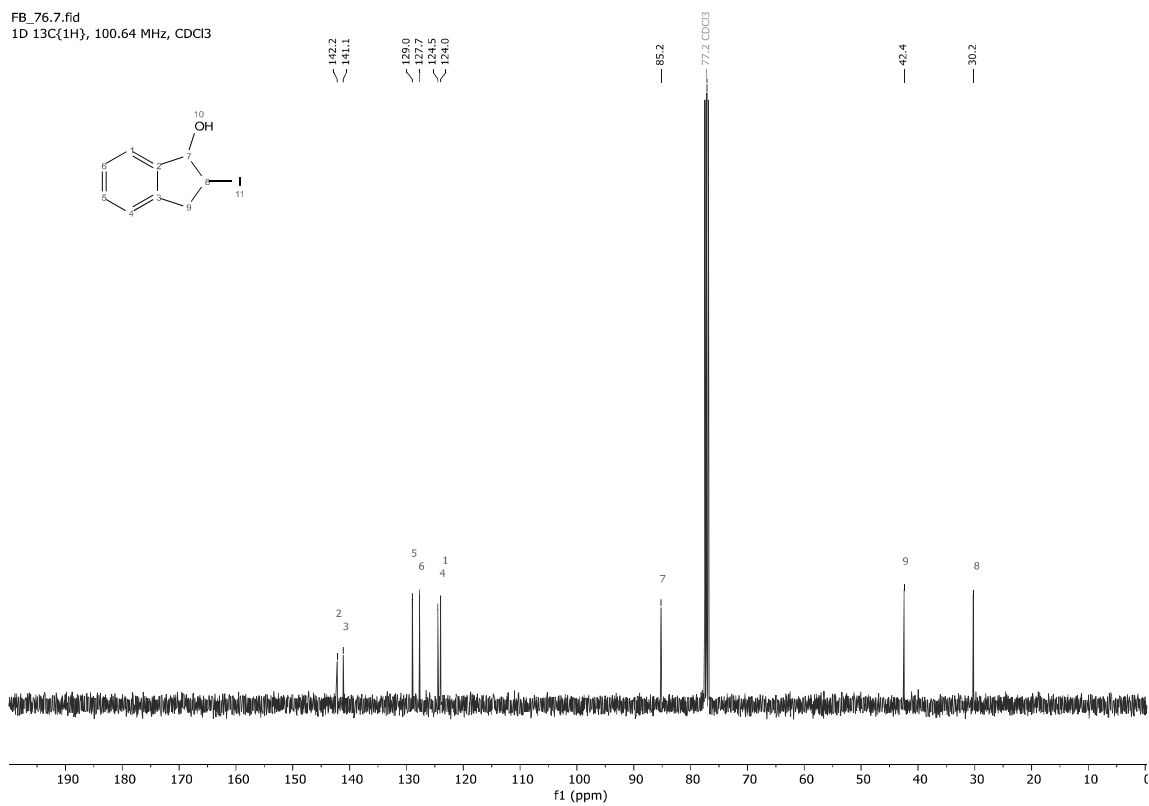
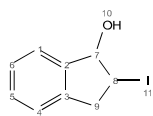


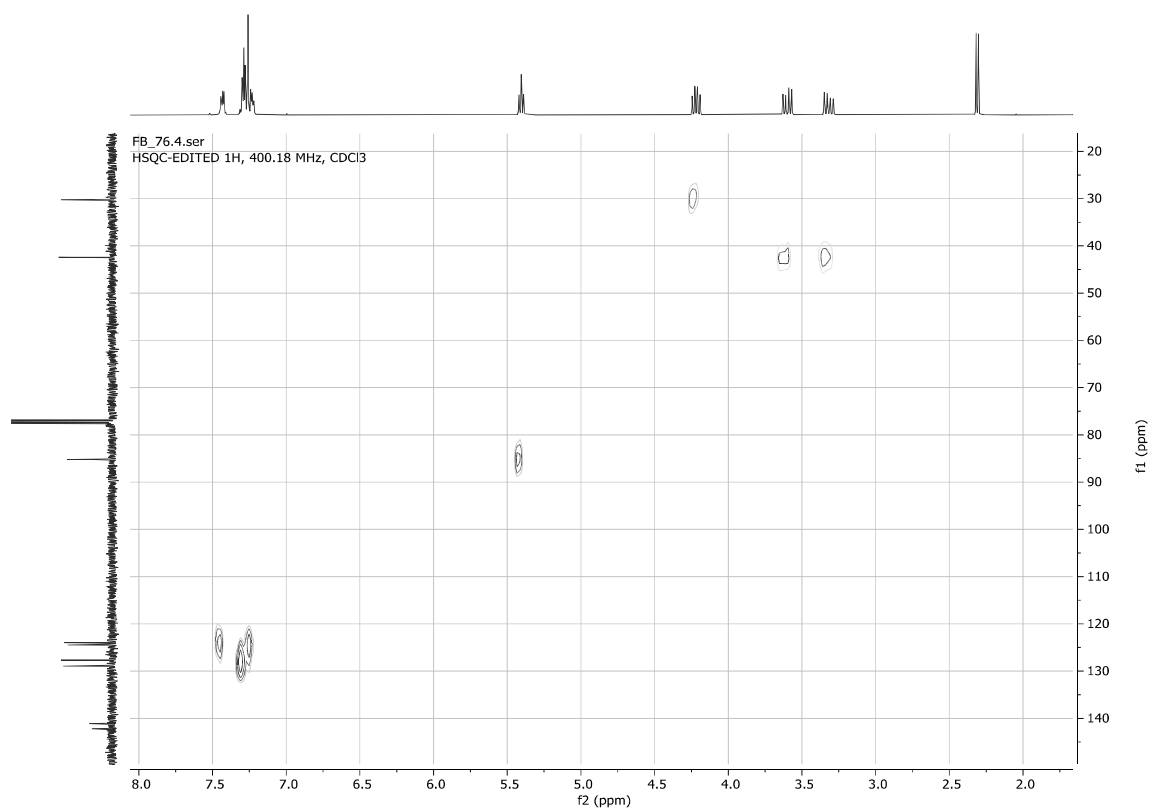


2-Iodo-2,3-dihydro-1H-inden-1-ol **3a**



FB_76.7.fid
1D 13C{1H}, 100.64 MHz, CDCl3

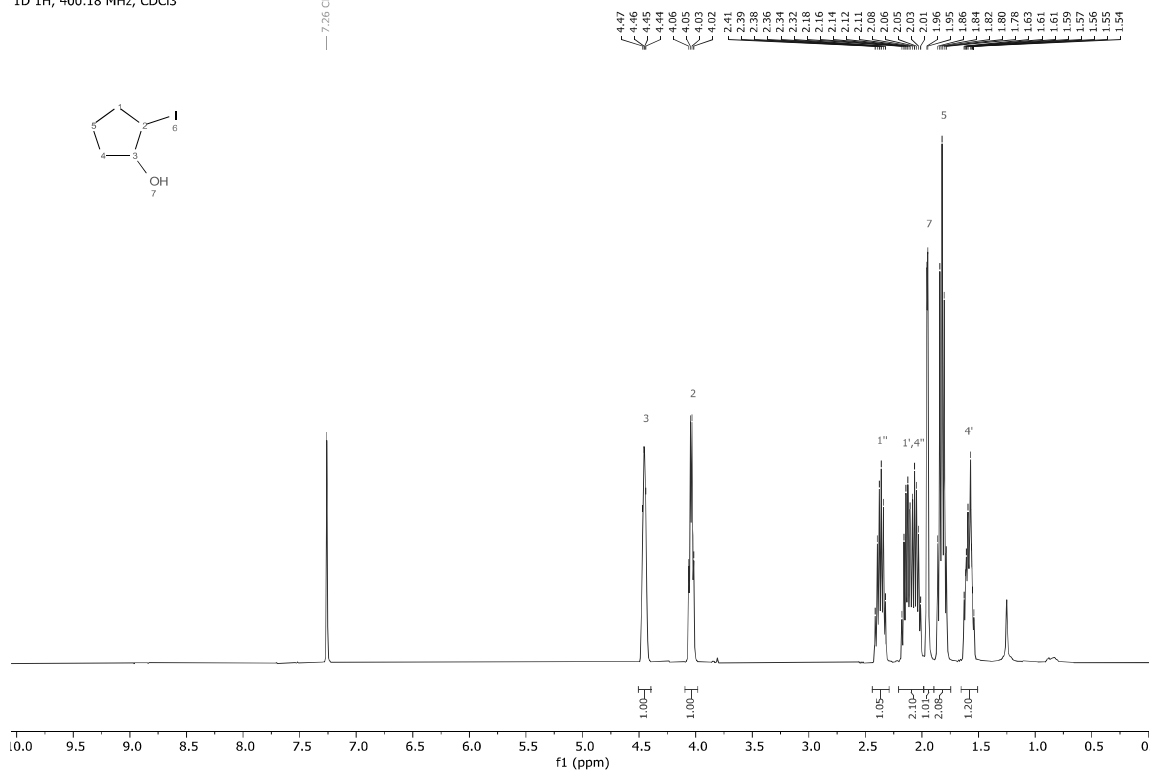
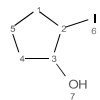




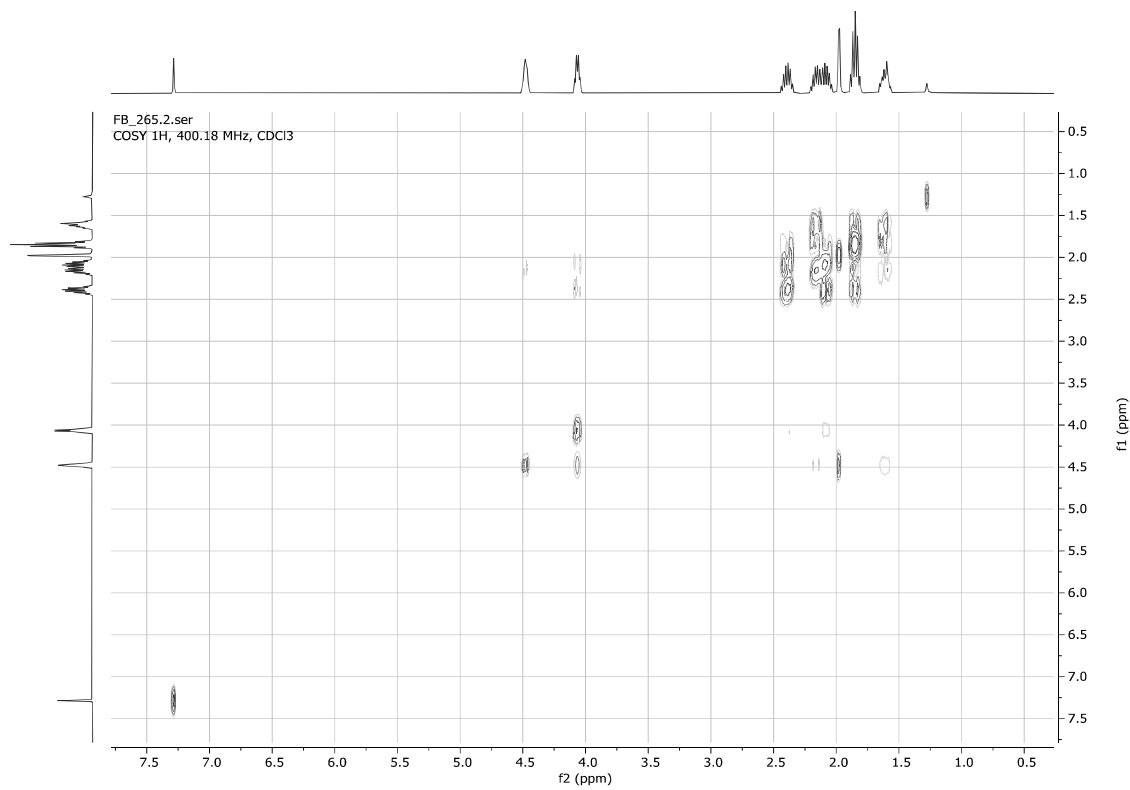
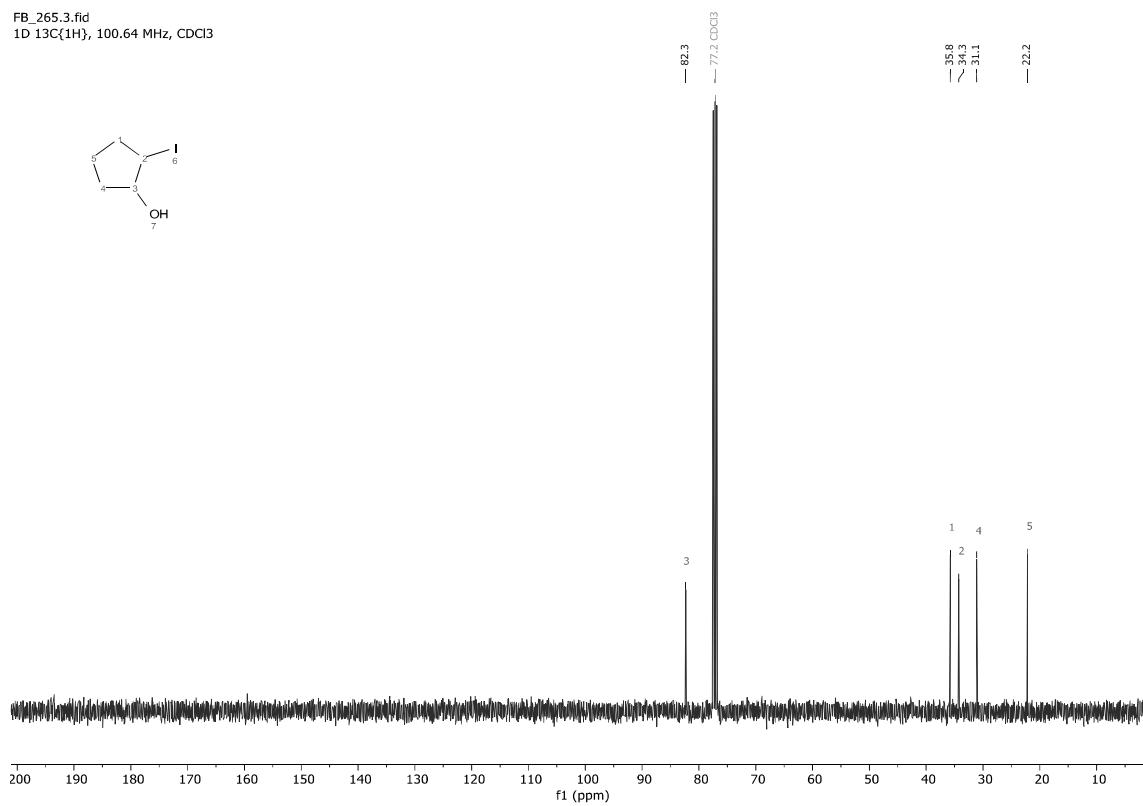
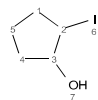
2-Iodocyclopentanol **3b**

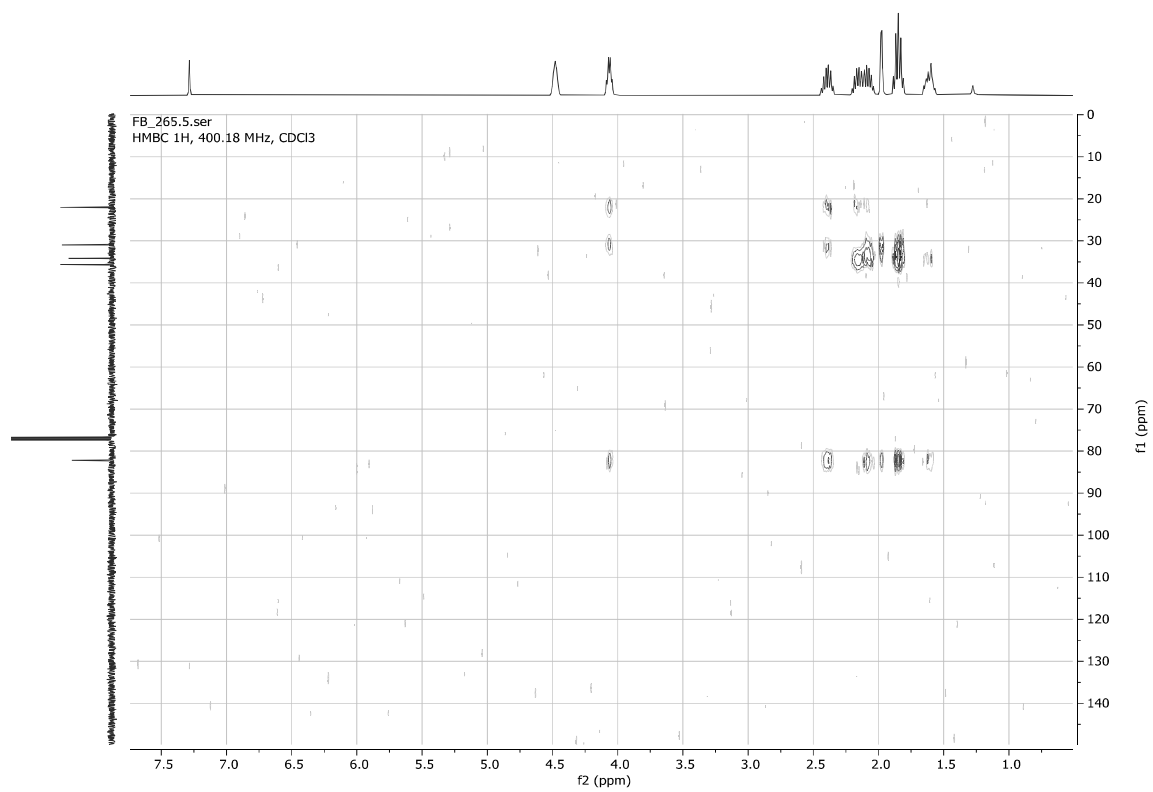
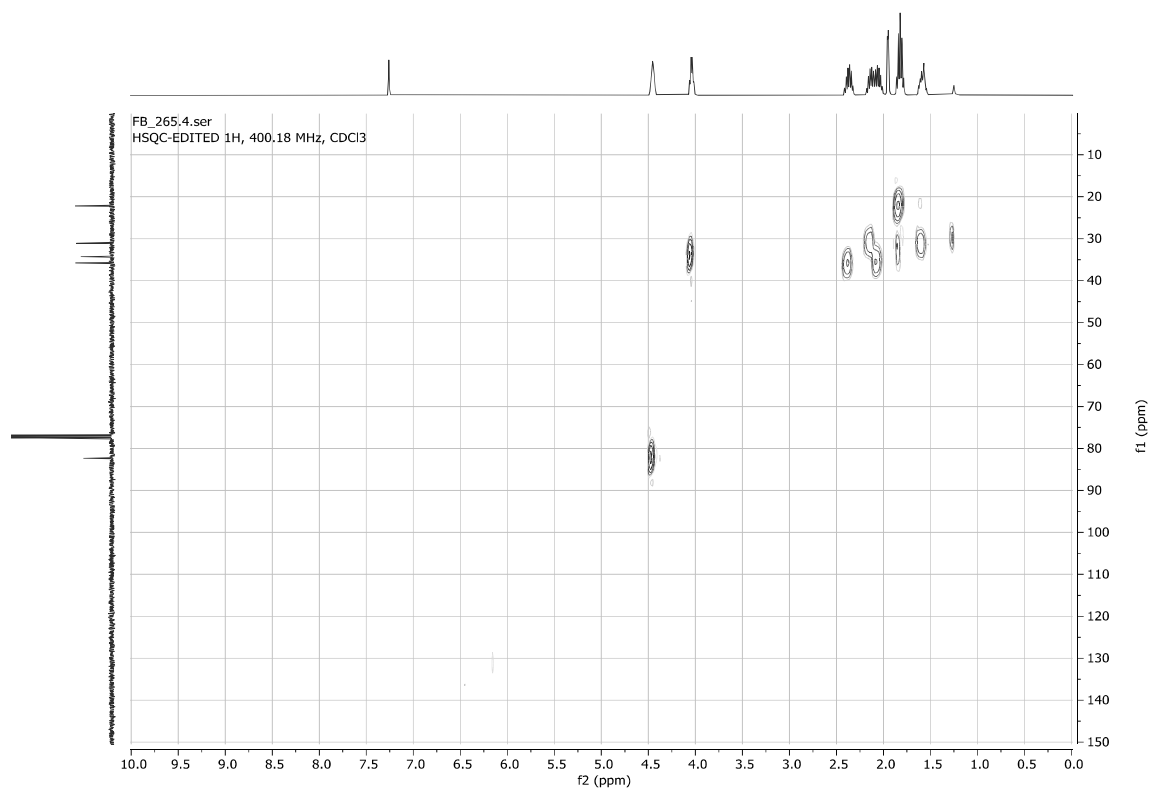
FB_265.1.fid
1D 1H, 400.18 MHz, CDCl3

— 7.26 CDCl3

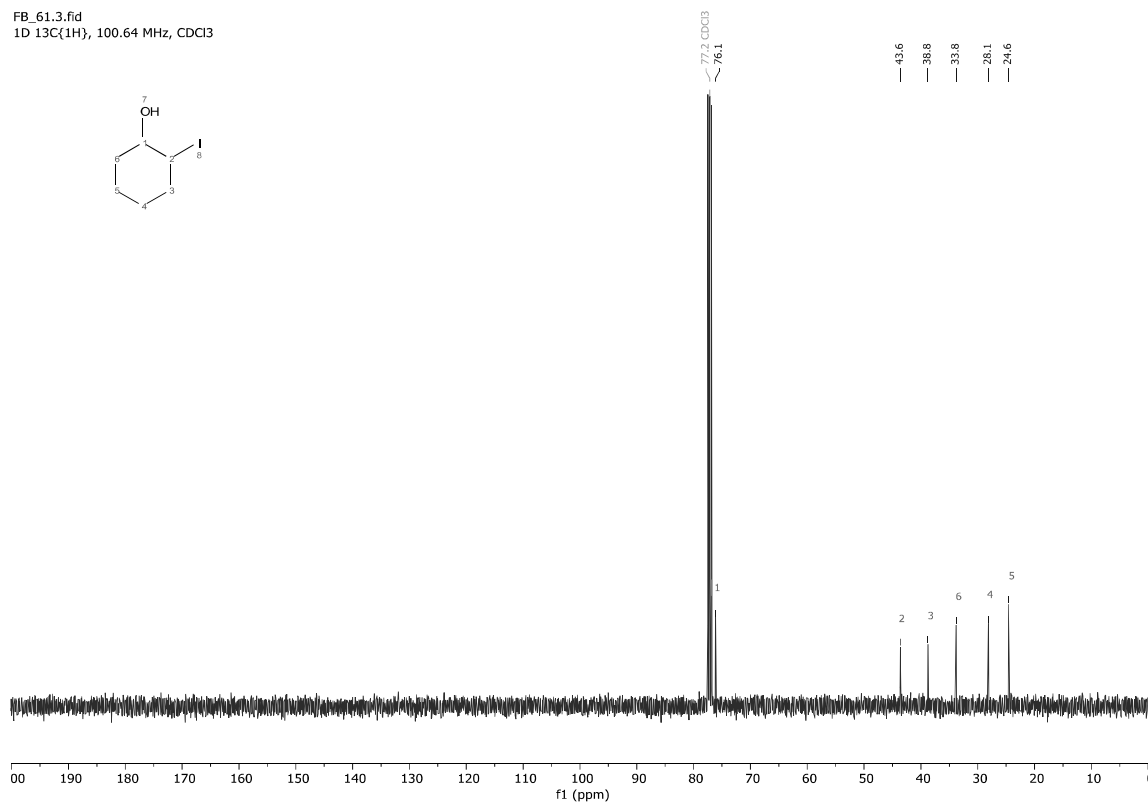
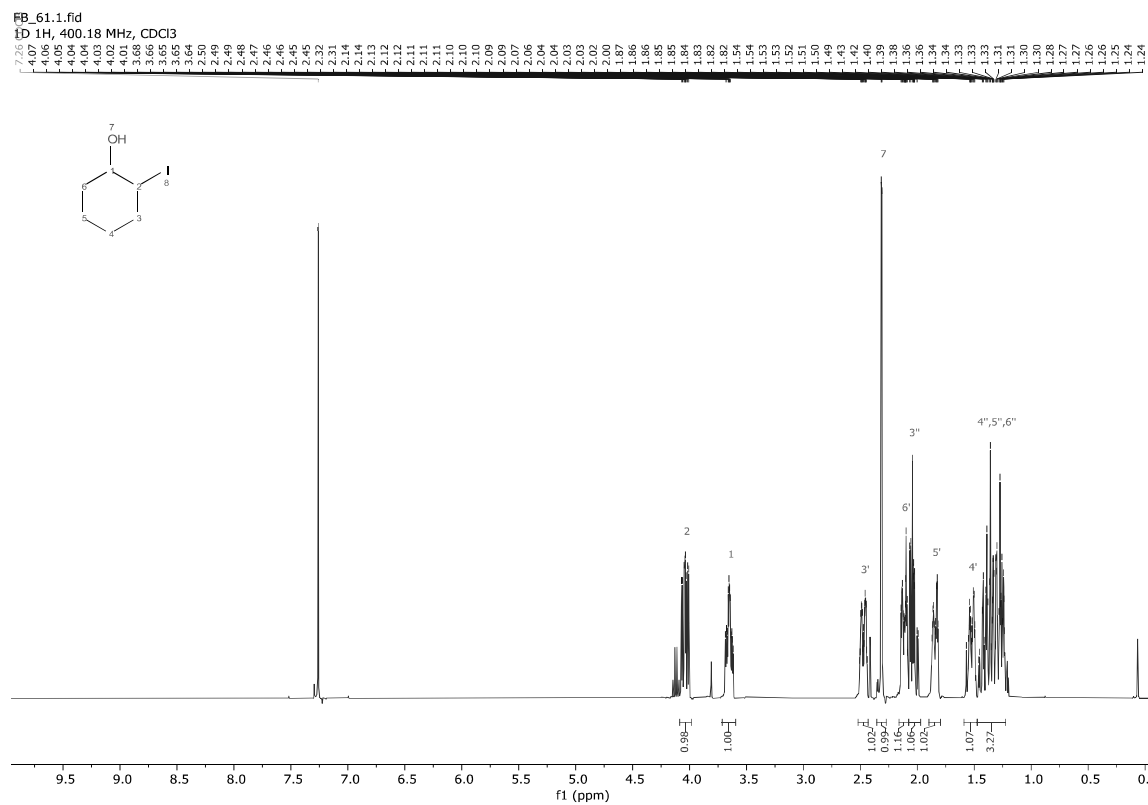


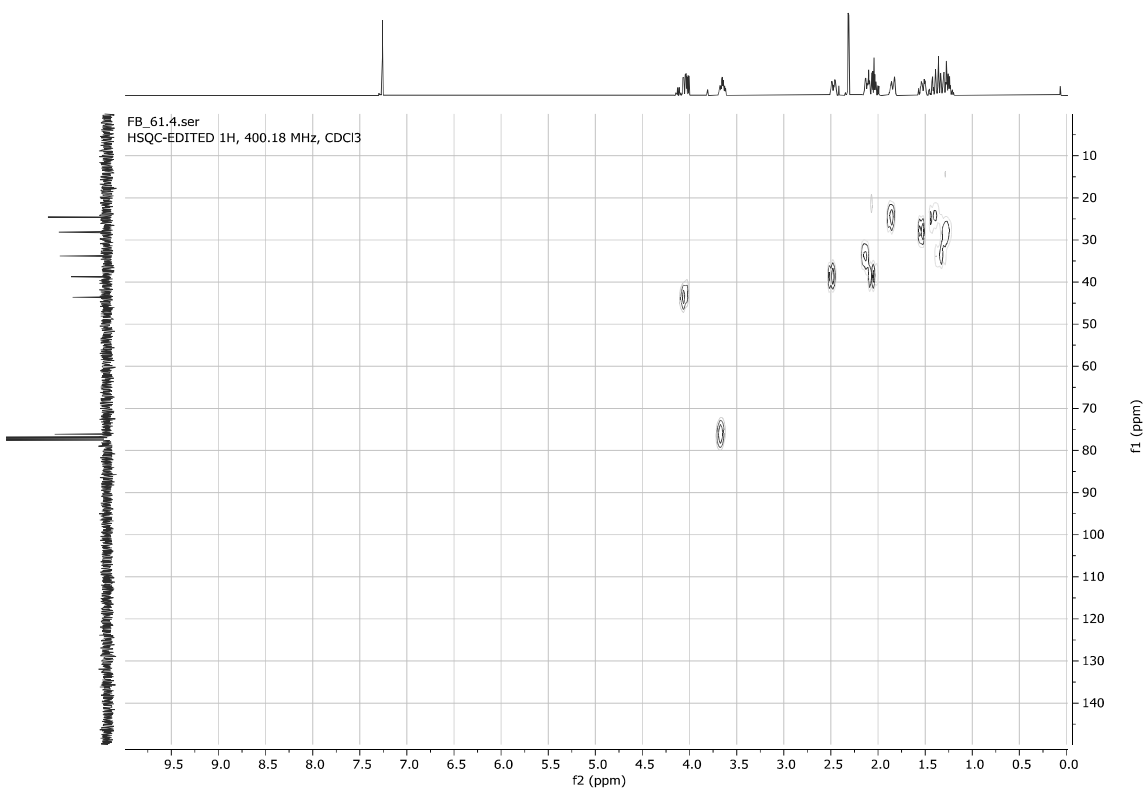
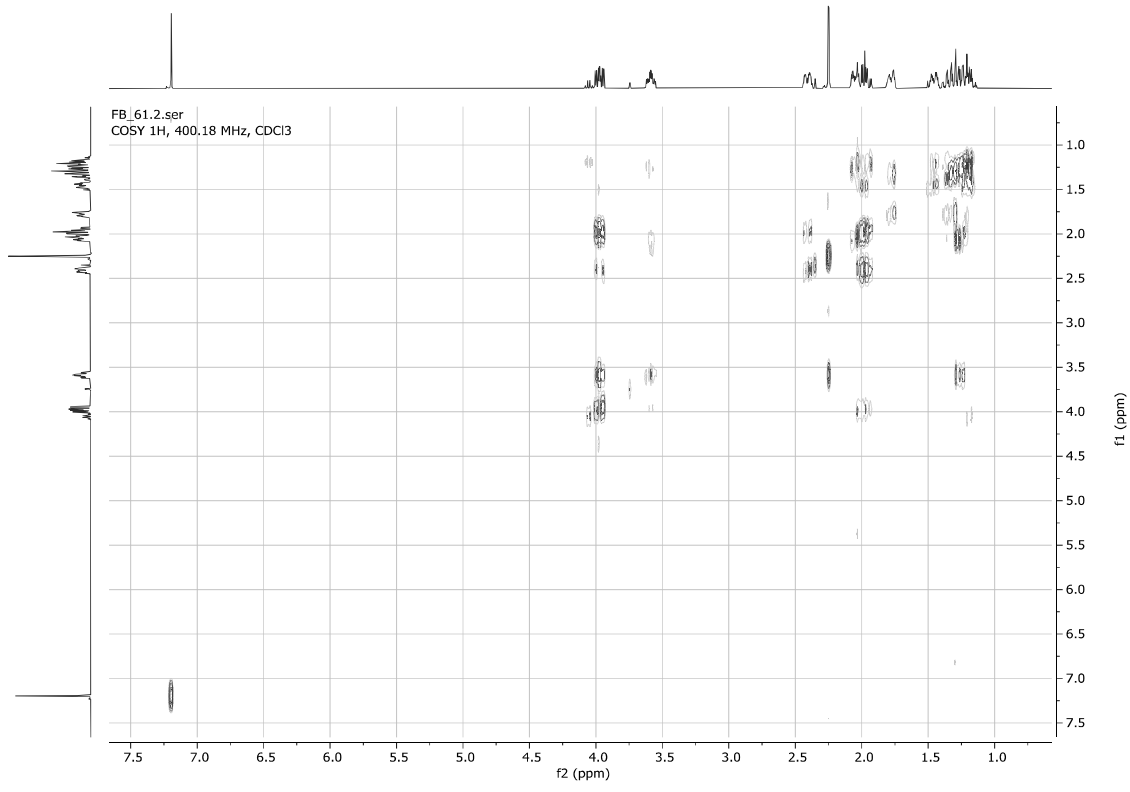
FB_265.3.fid
1D 13C{1H}, 100.64 MHz, CDCl3





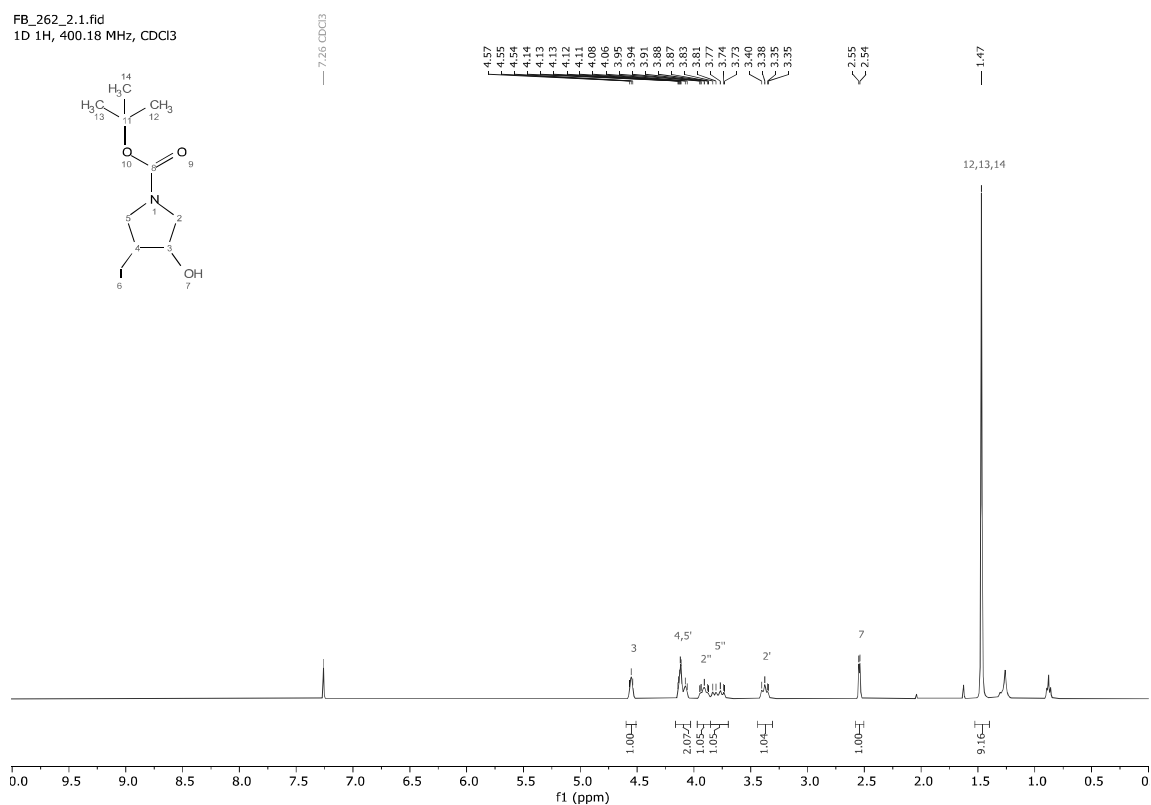
2-Iodocyclohexanol **3c**



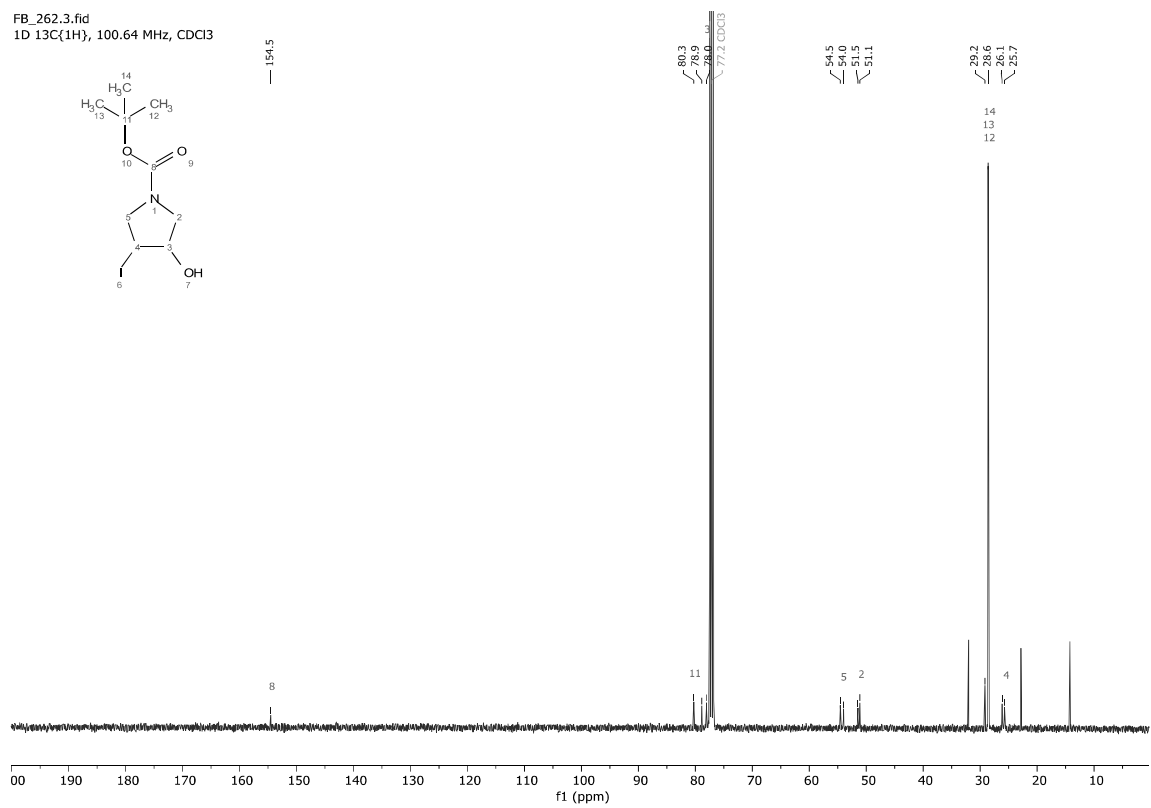


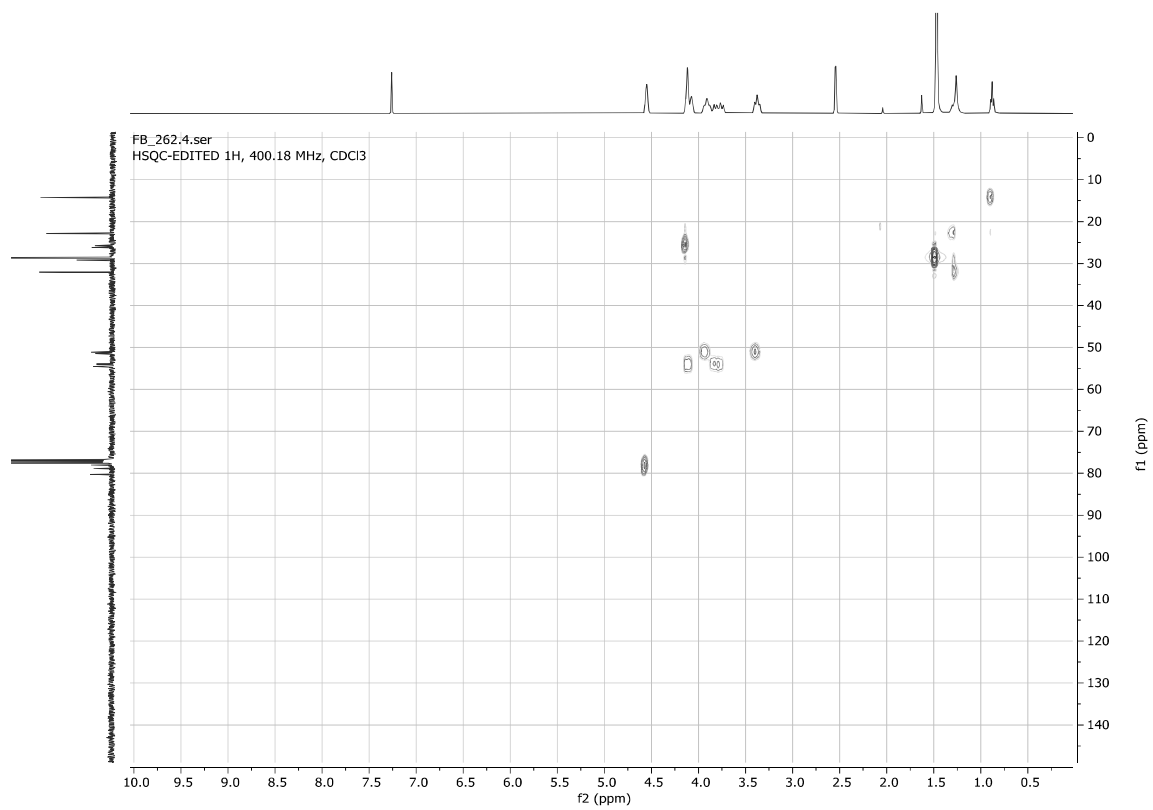
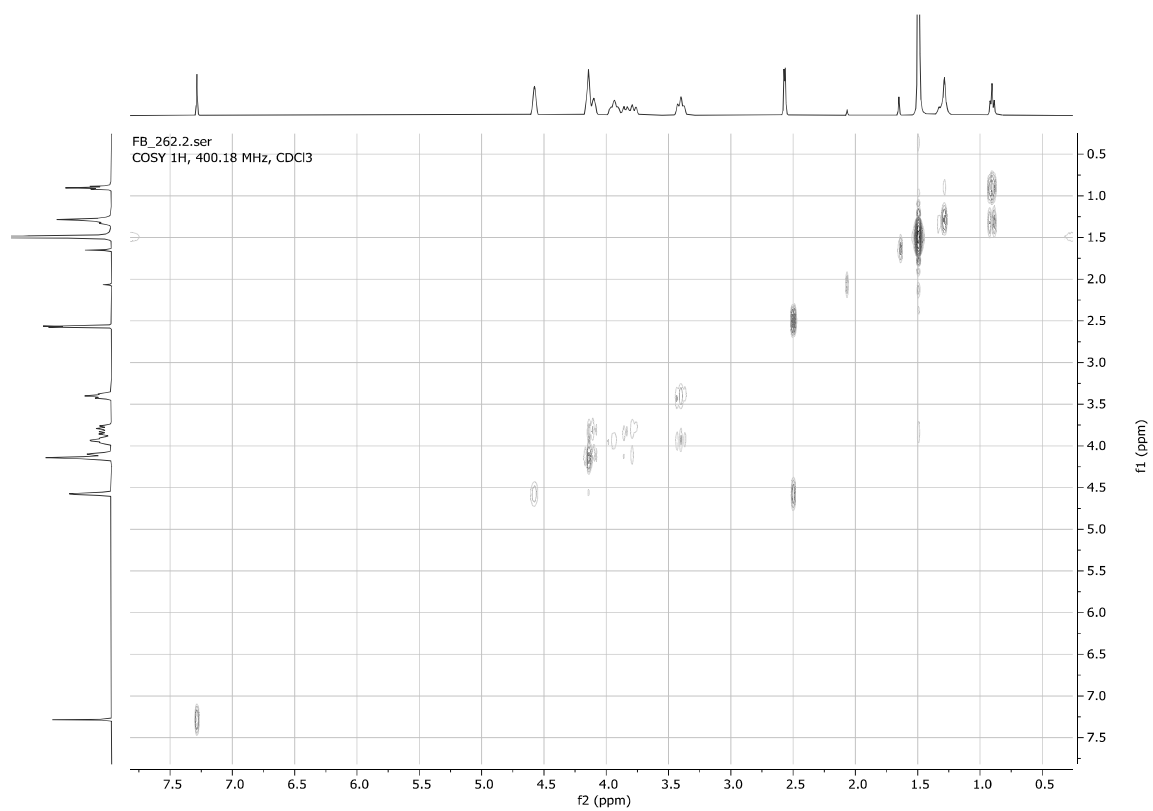
tert-Butyl 3-hydroxy-4-iodopyrrolidine-1-carboxylate **3d** (mixture of rotamers)

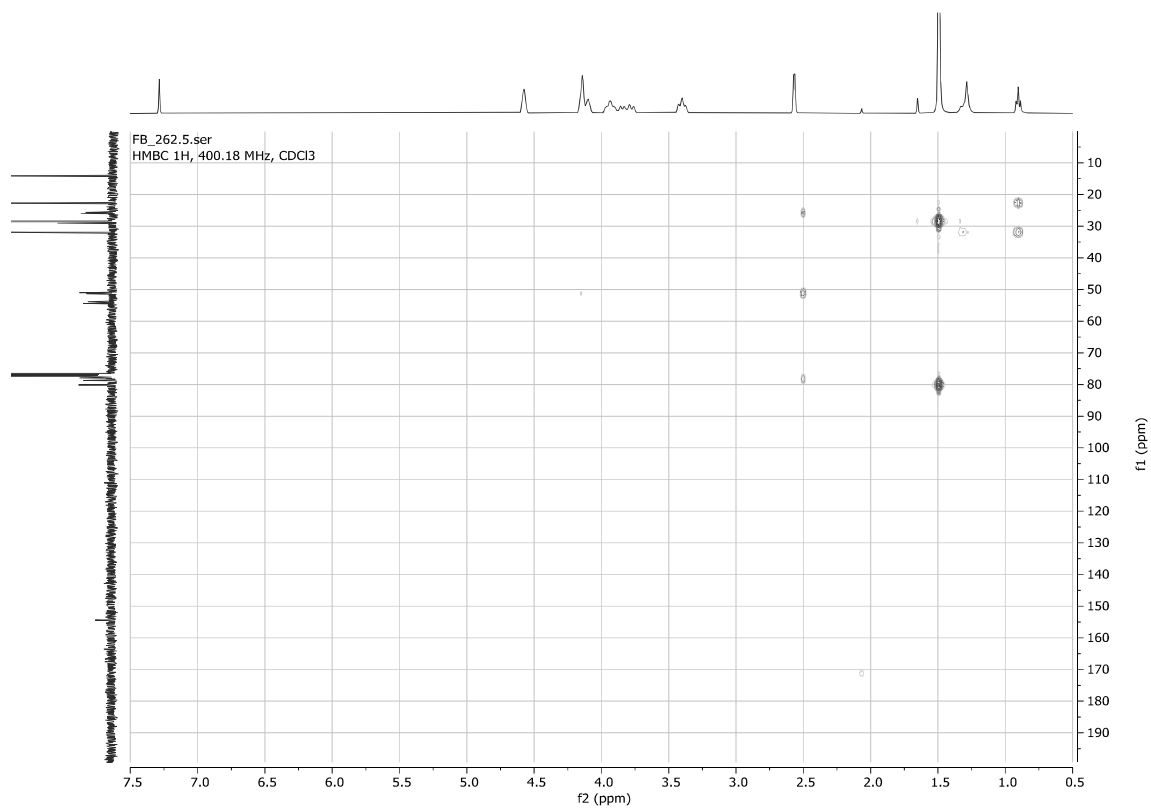
FB_262_2.1.fid
1D 1H, 400.18 MHz, CDCl₃



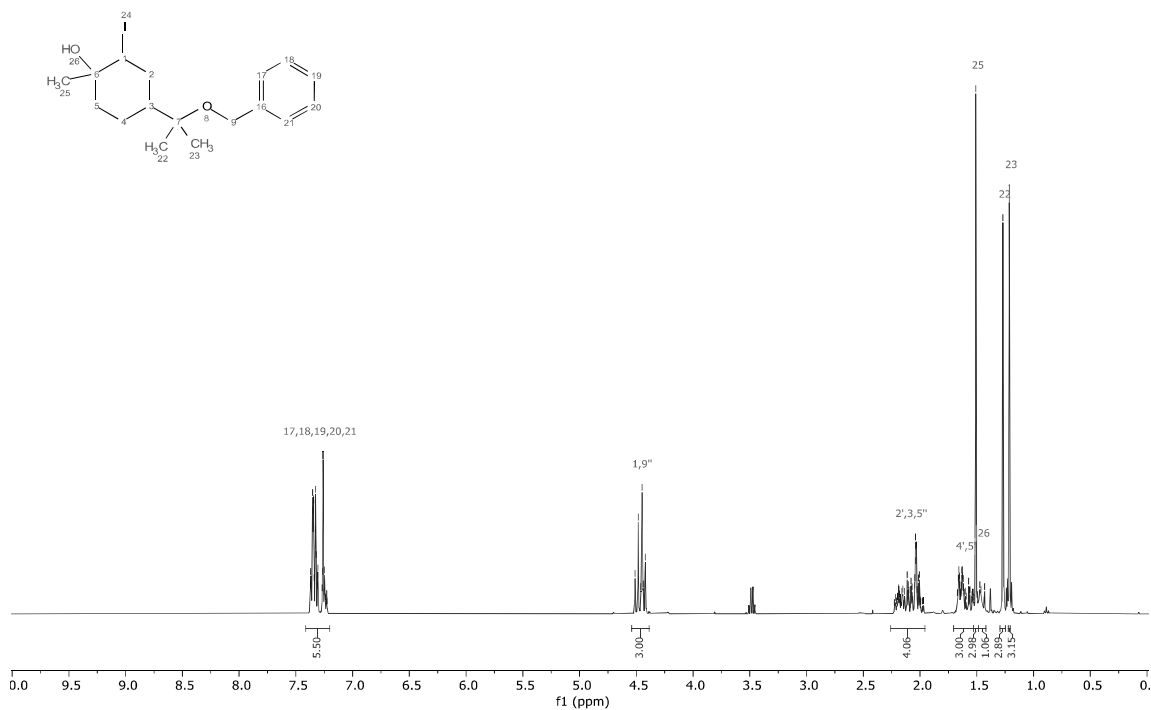
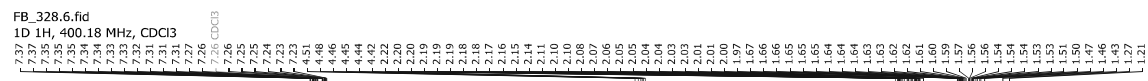
FB_262.3.fid
1D 13C{1H}, 100.64 MHz, CDCl₃



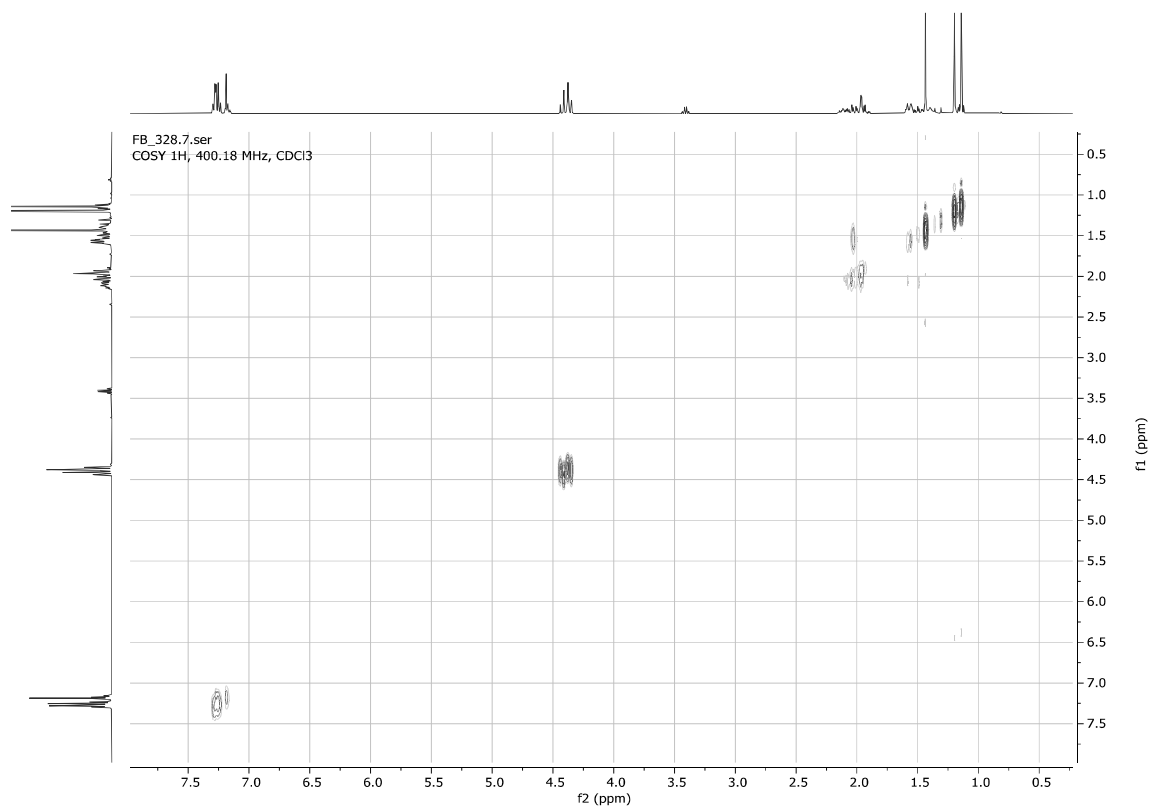
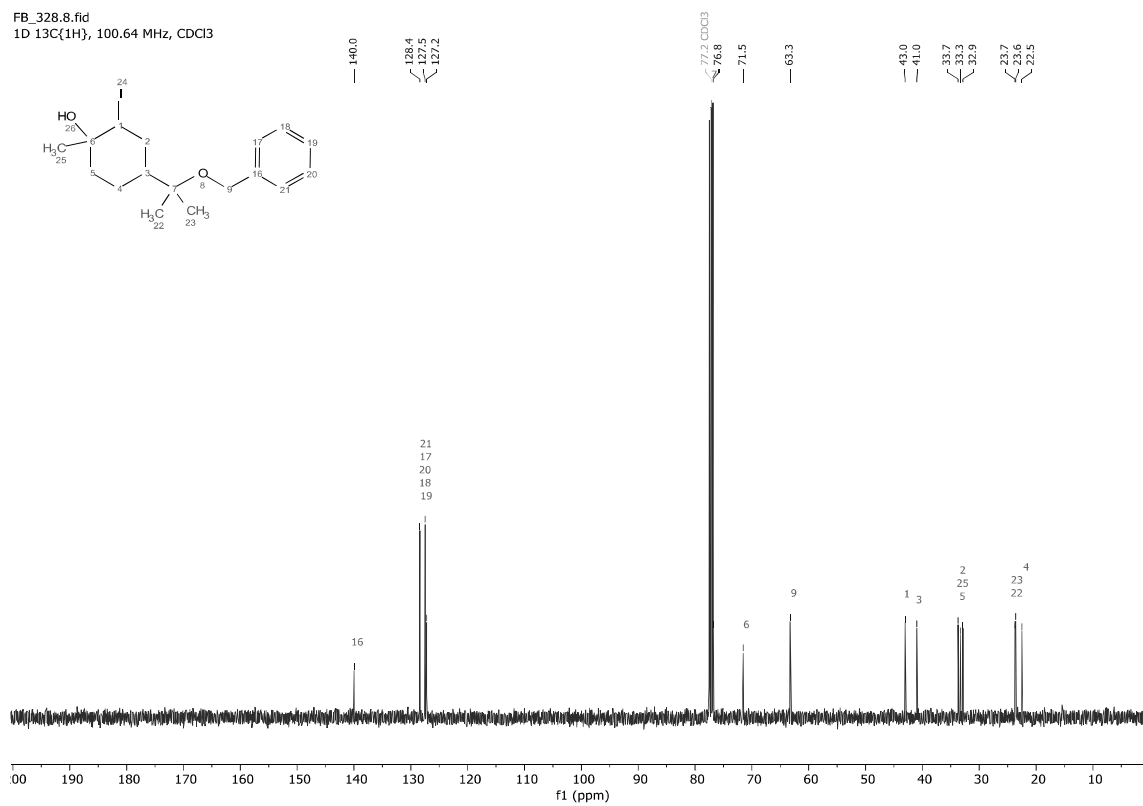


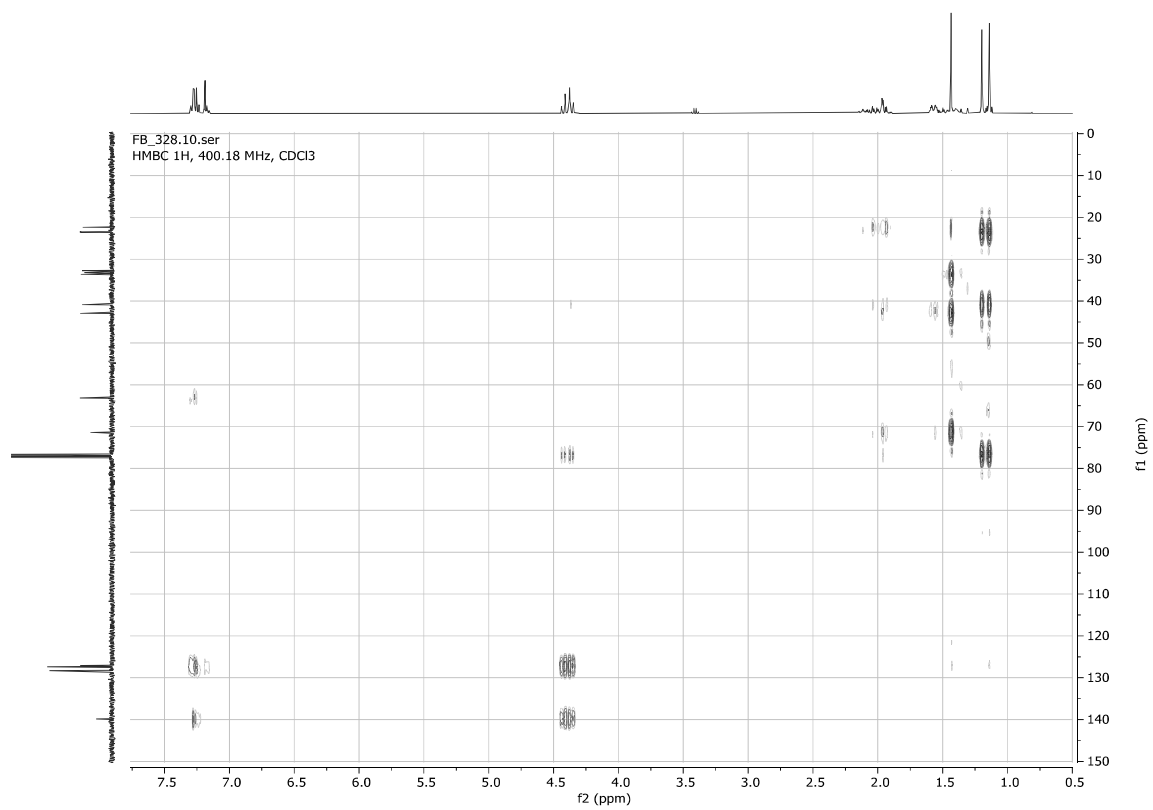
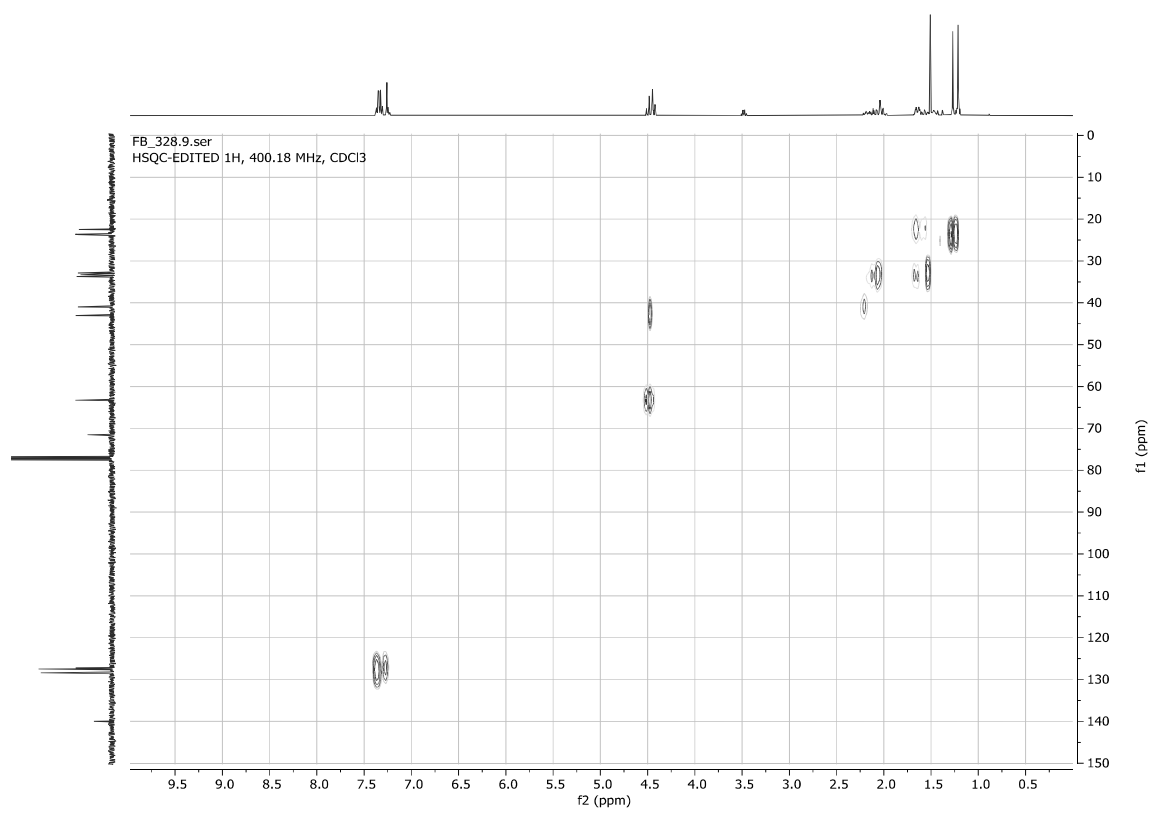


4-(2-(Benzyloxy)propan-2-yl)-2-iodo-1-methylcyclohexanol **3e**



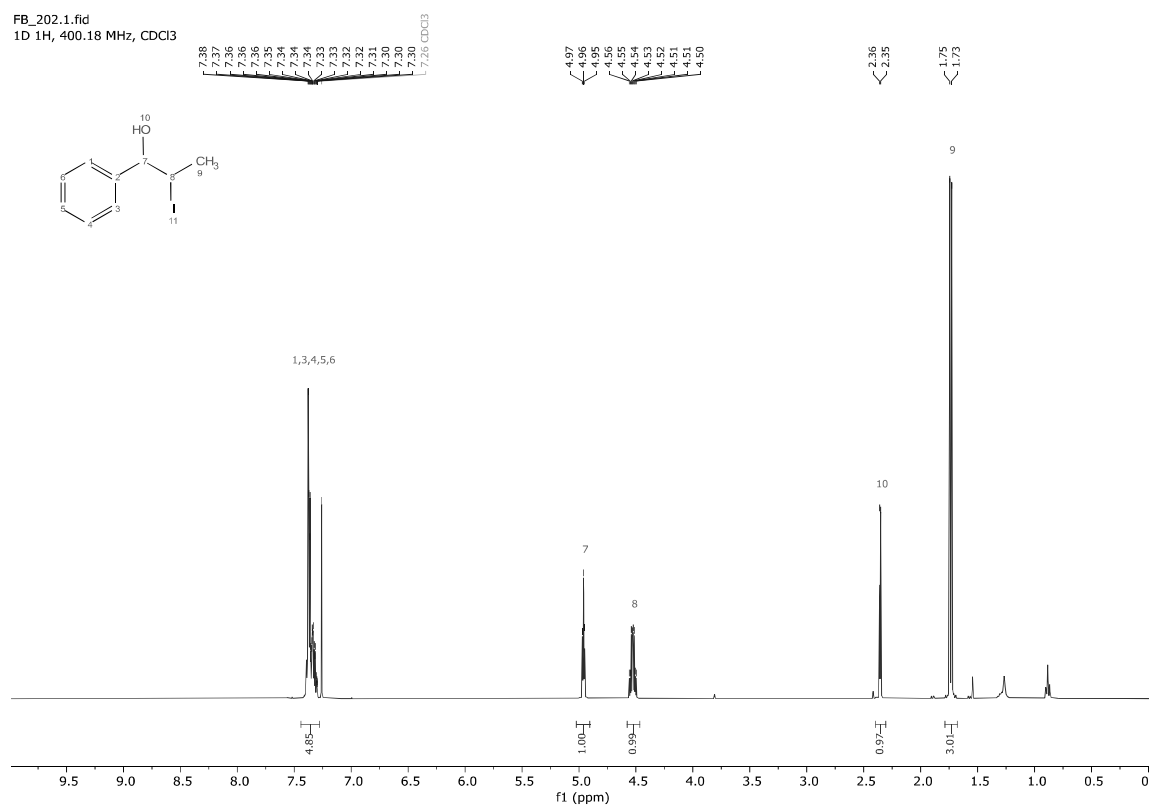
FB_328.8.fid
1D 13C{1H}, 100.64 MHz, CDCl3



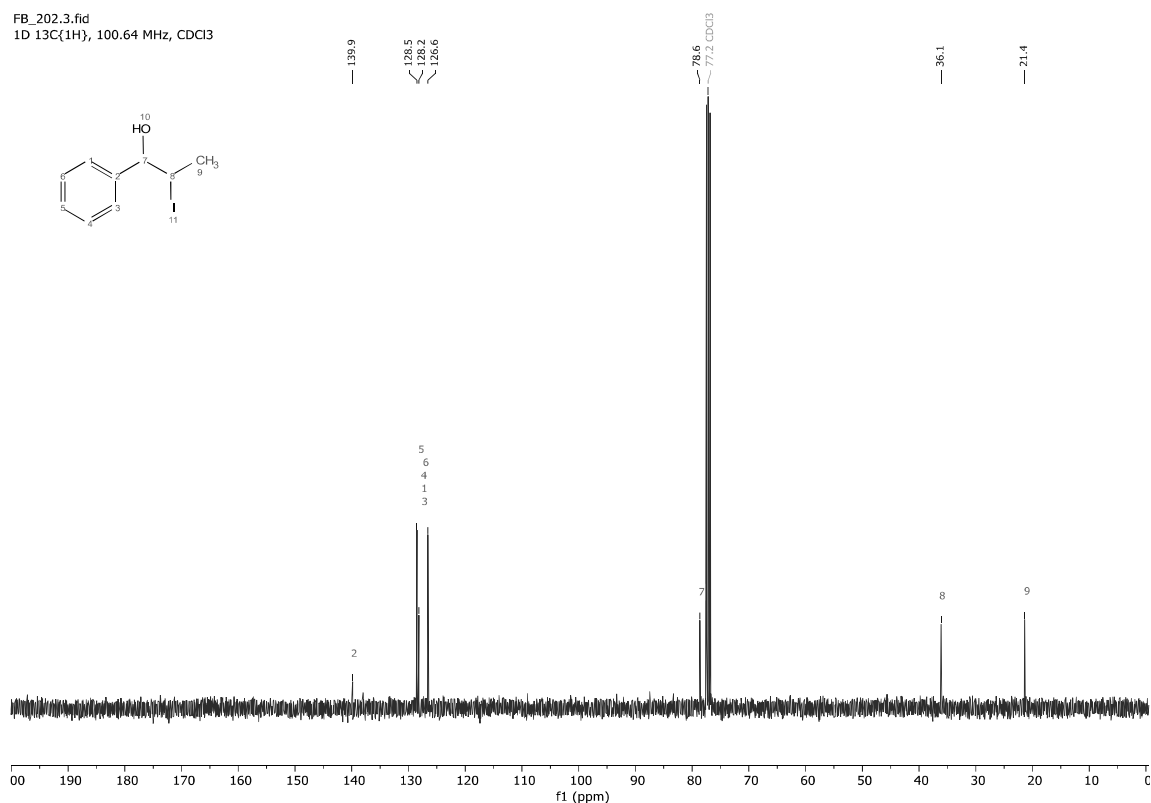


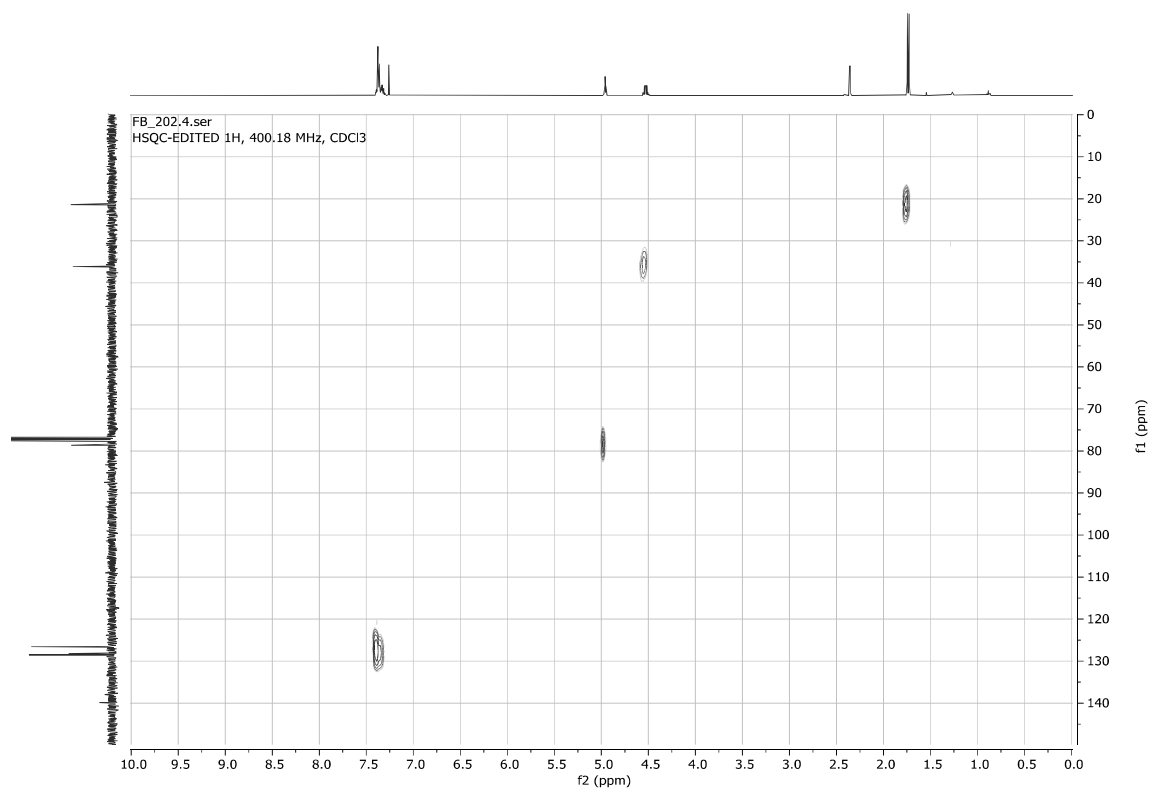
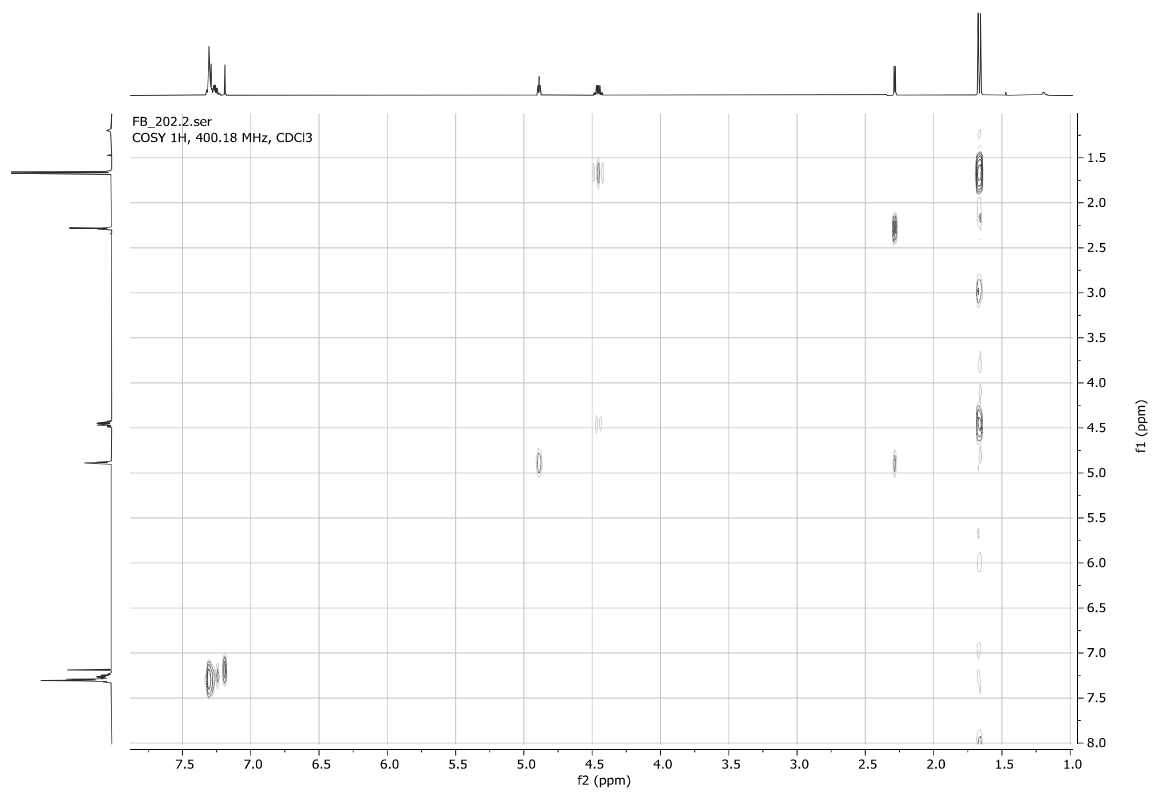
2-Iodo-1-phenylpropan-1-ol 3f

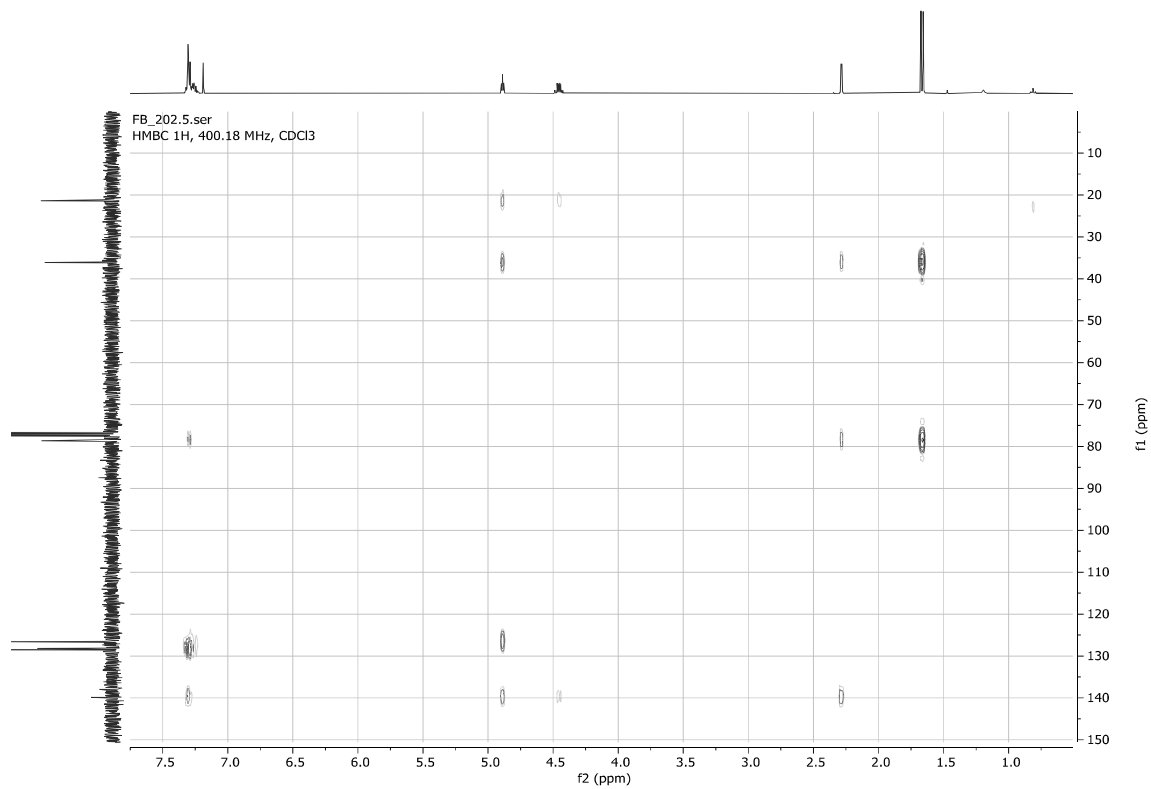
FB_202.1.fid
1D 1H, 400.18 MHz, CDCl3



FB_202.3.fid
1D 13C{1H}, 100.64 MHz, CDCl3



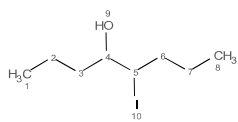
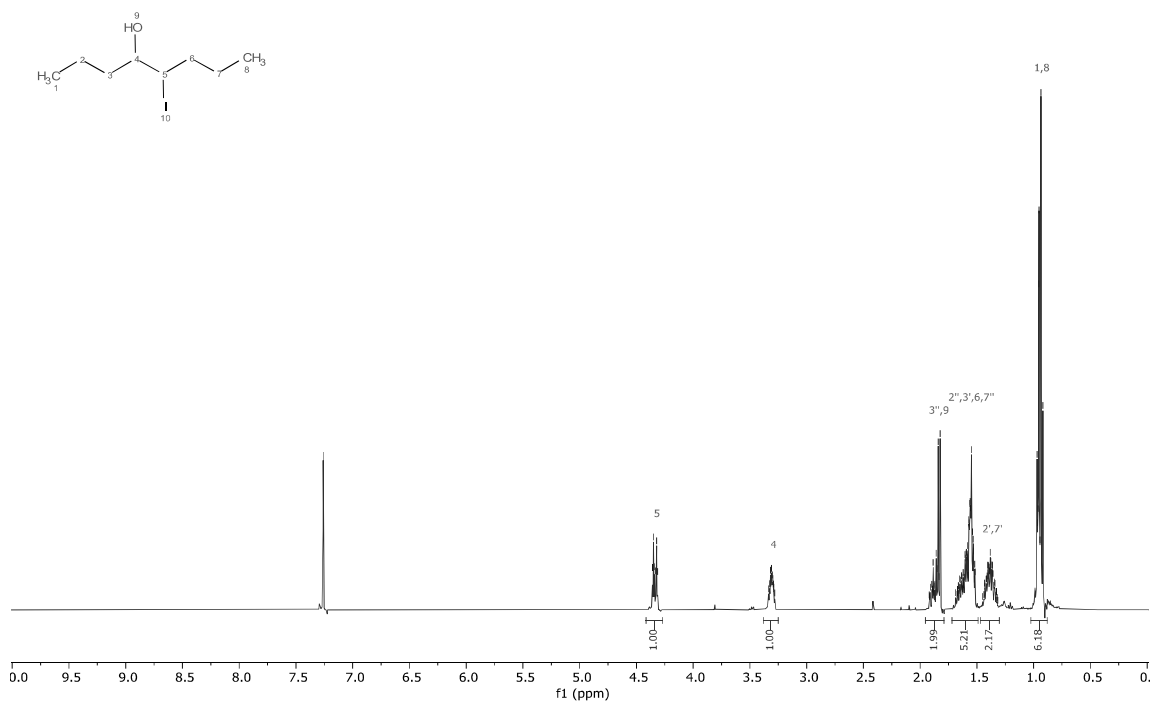




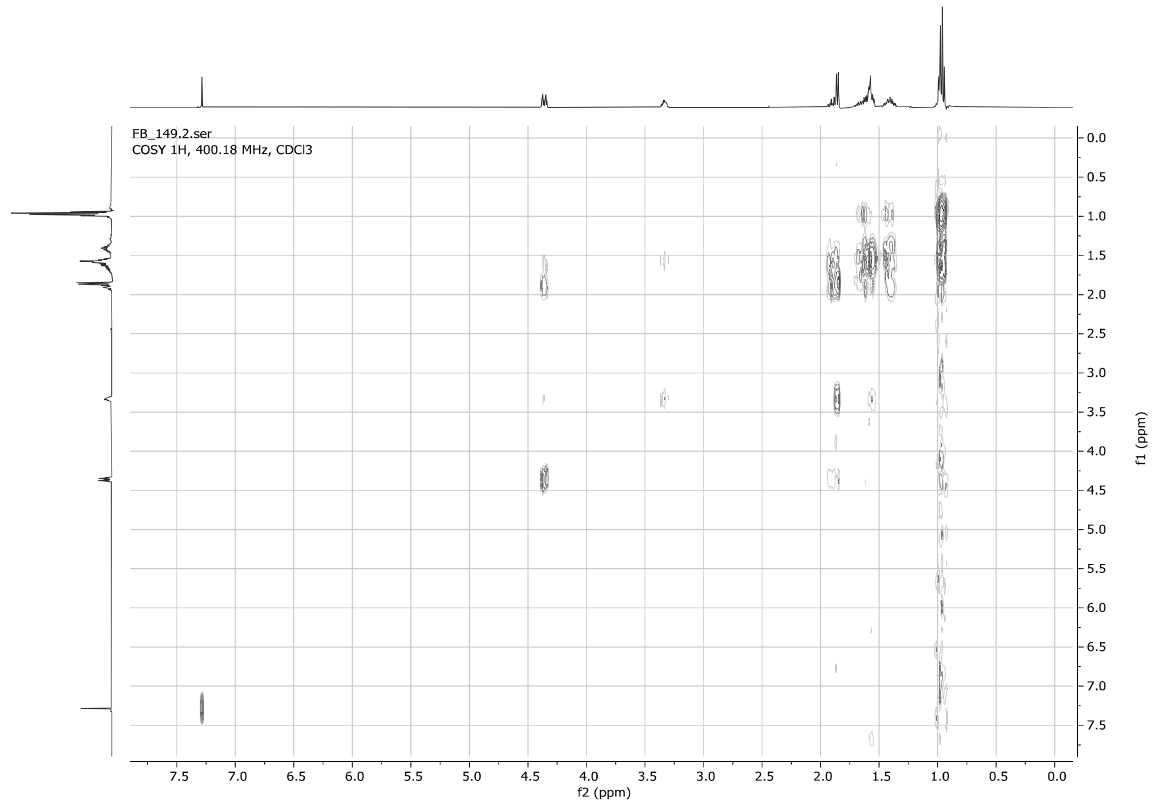
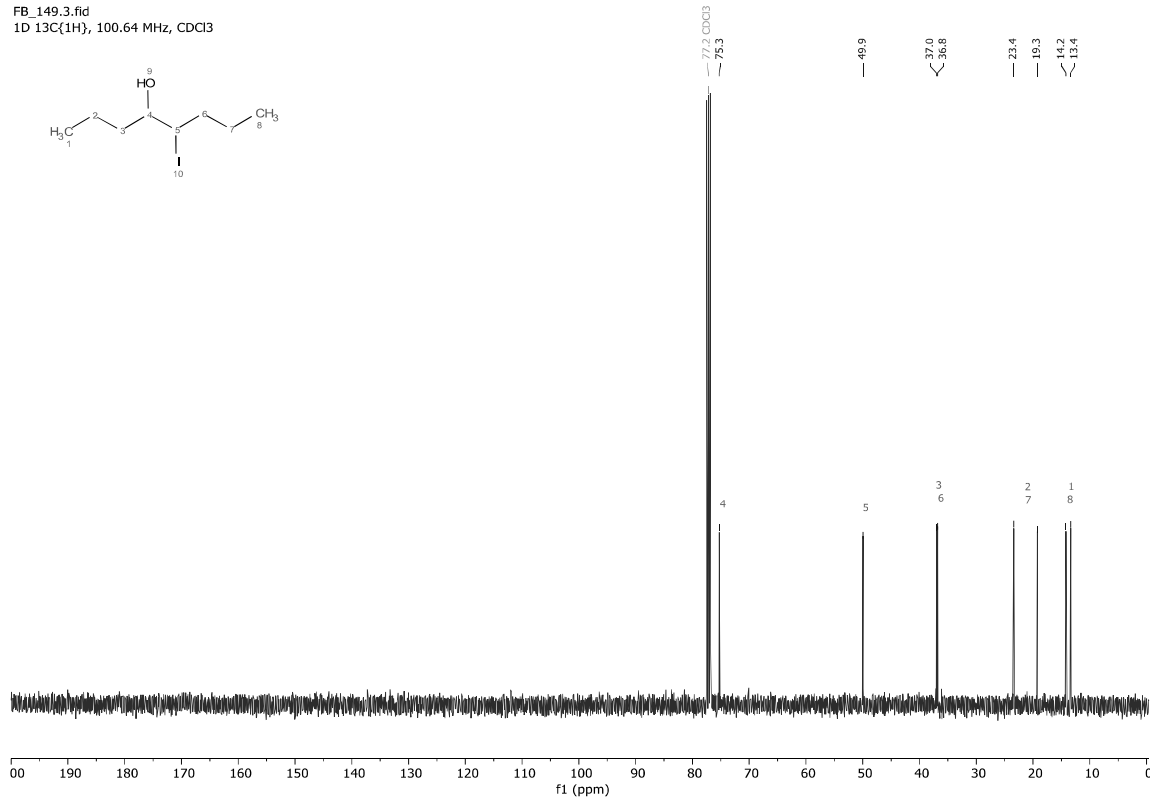
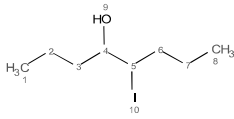
5-Iodooctan-4-ol **3g**

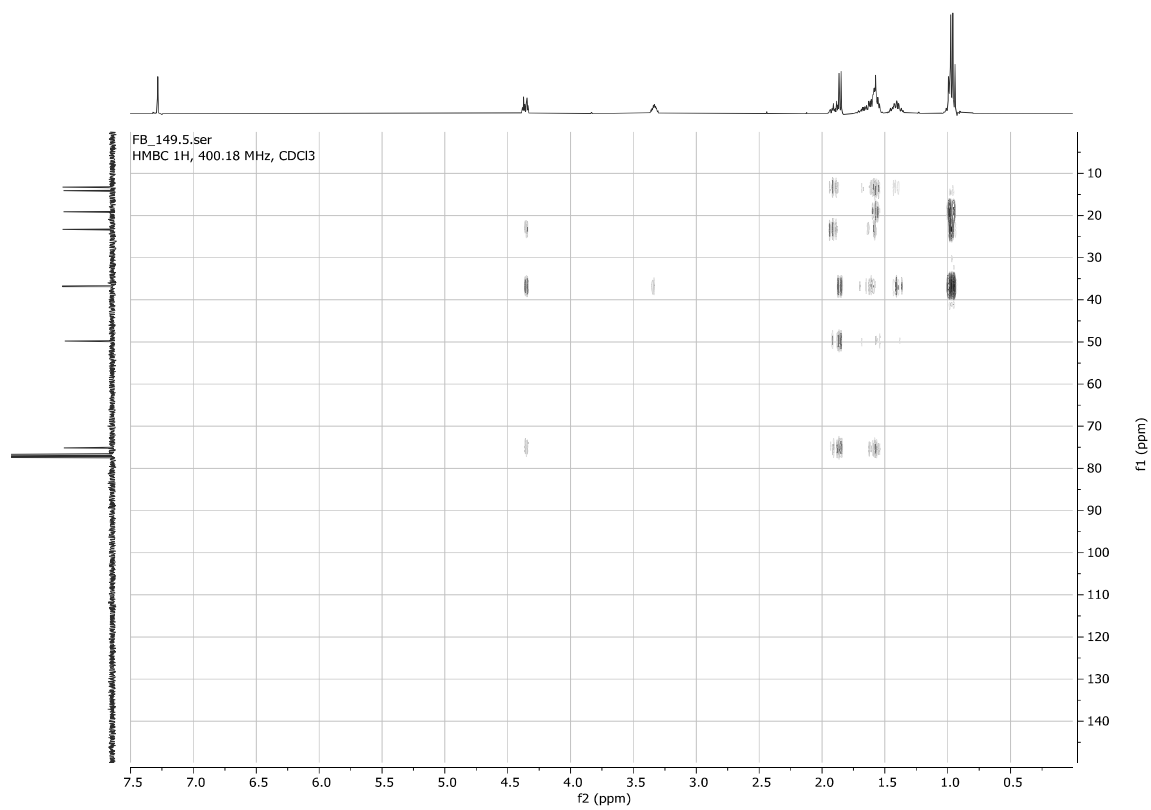
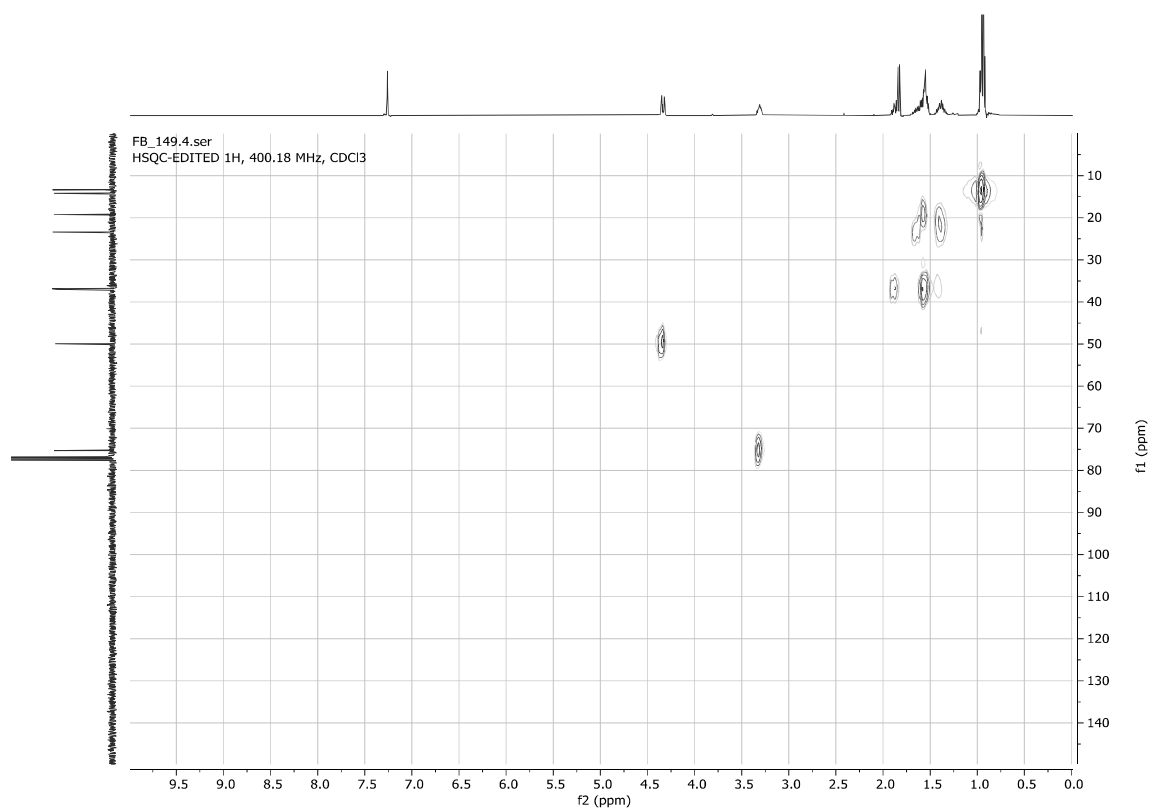
FB_149.1.fid
1D 1H, 400.18 MHz, CDCl3

7.26
4.36
4.35
4.34
4.33
4.32
4.31
3.34
3.33
3.32
3.31
3.30
3.29
3.28
4.10
1.89
1.88
1.87
1.86
1.85
1.84
1.83
1.82
1.67
1.66
1.65
1.64
1.63
1.62
1.61
1.60
1.59
1.58
1.57
1.56
1.55
1.54
1.53
1.52
1.51
1.43
1.42
1.41
1.40
1.40
1.39
1.38
1.38
1.37
1.36
1.35
1.34
1.33
0.97
0.96
0.95
0.94
0.94
0.92



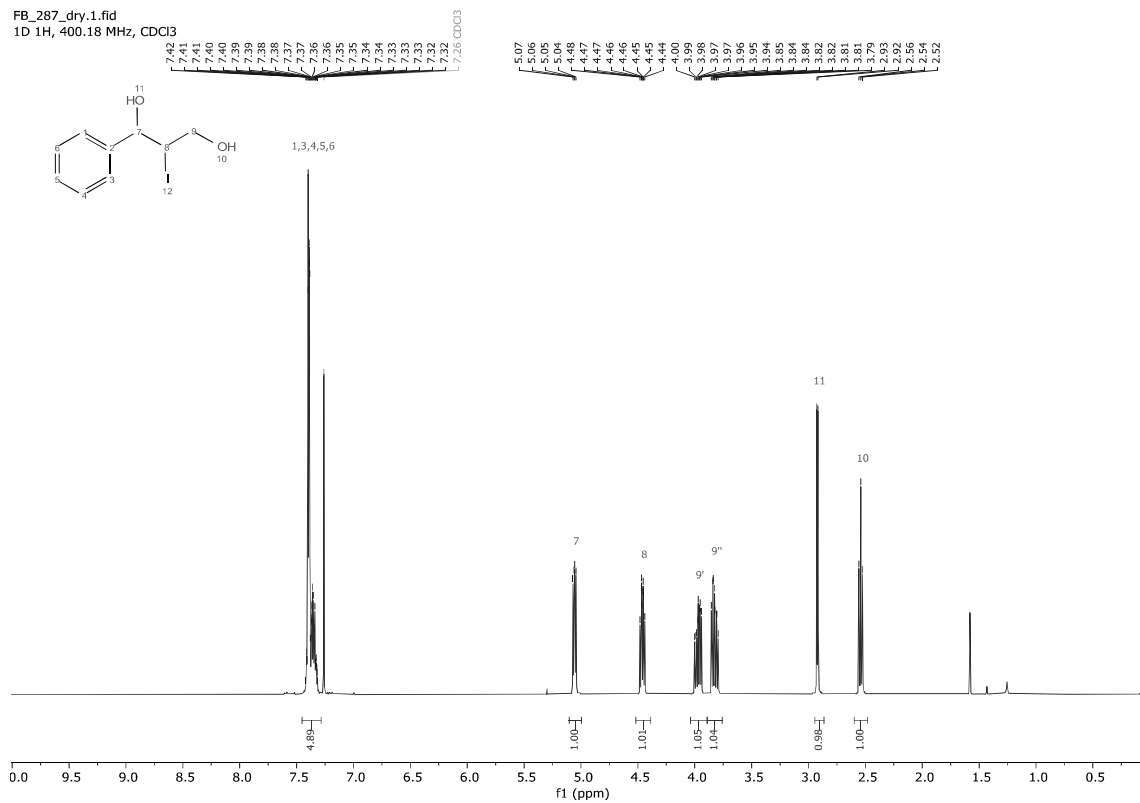
FB_149.3.fid
1D 13C{1H}, 100.64 MHz, CDCl3



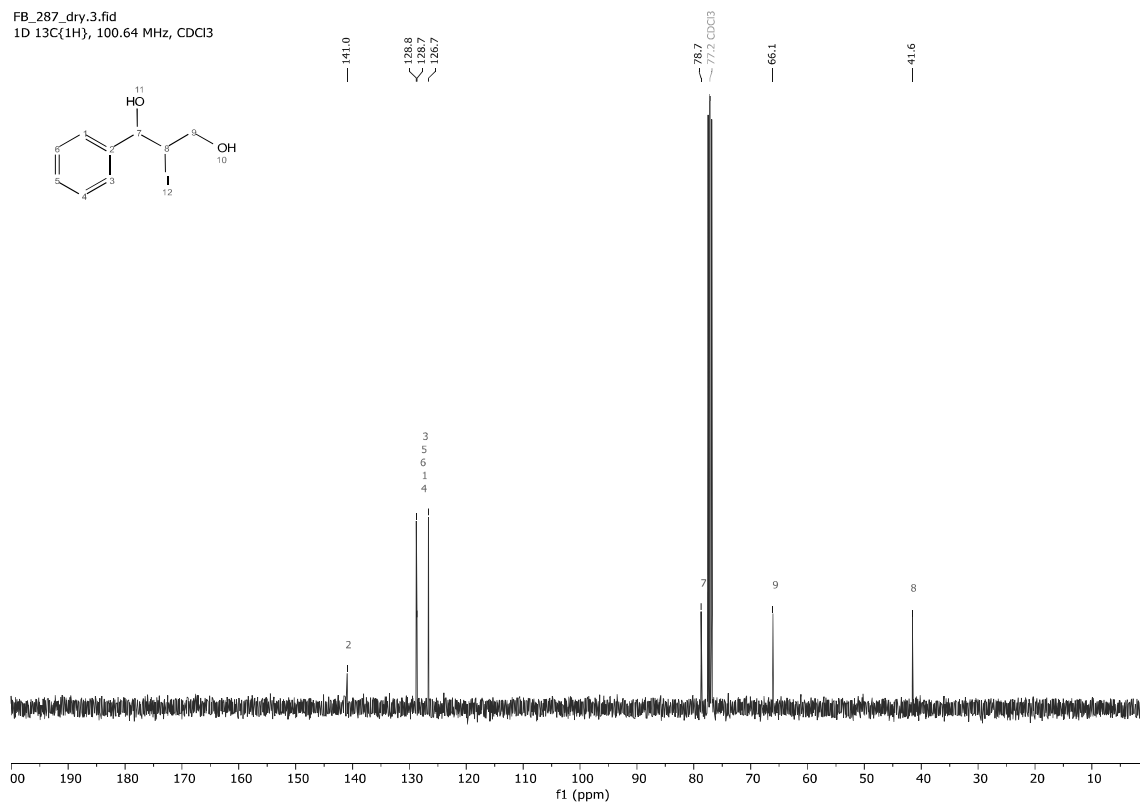


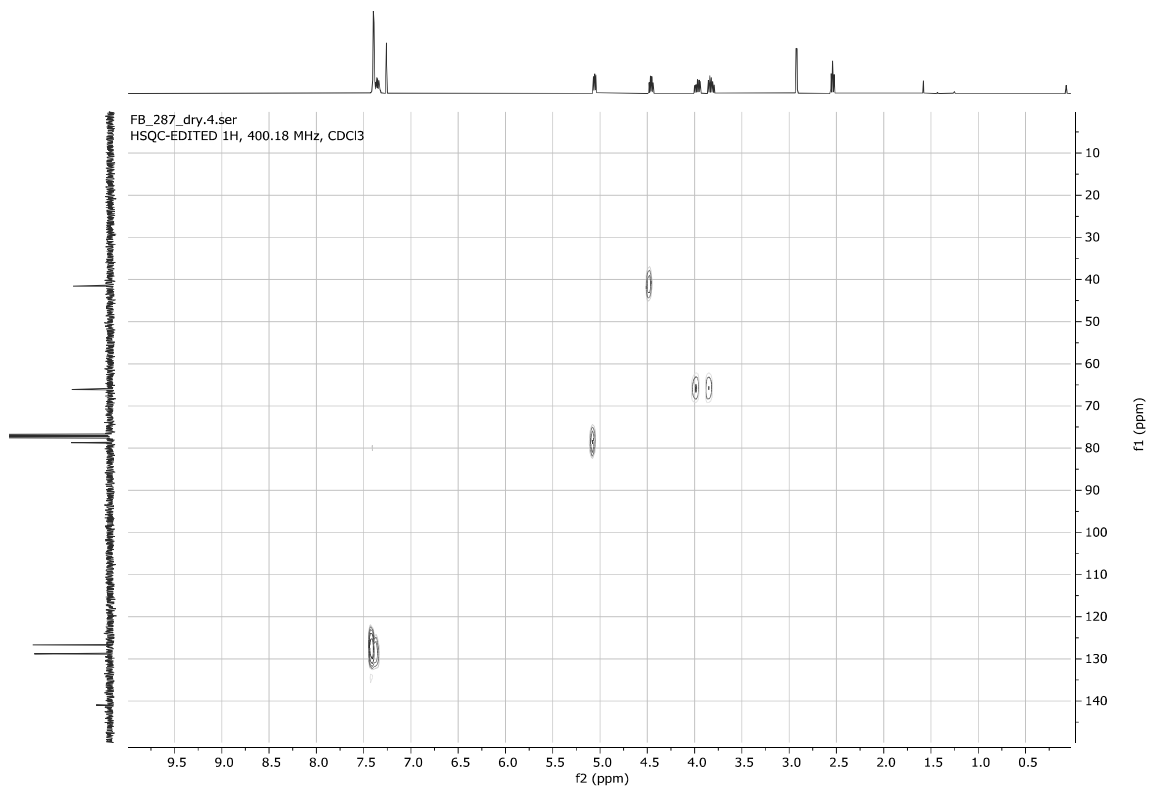
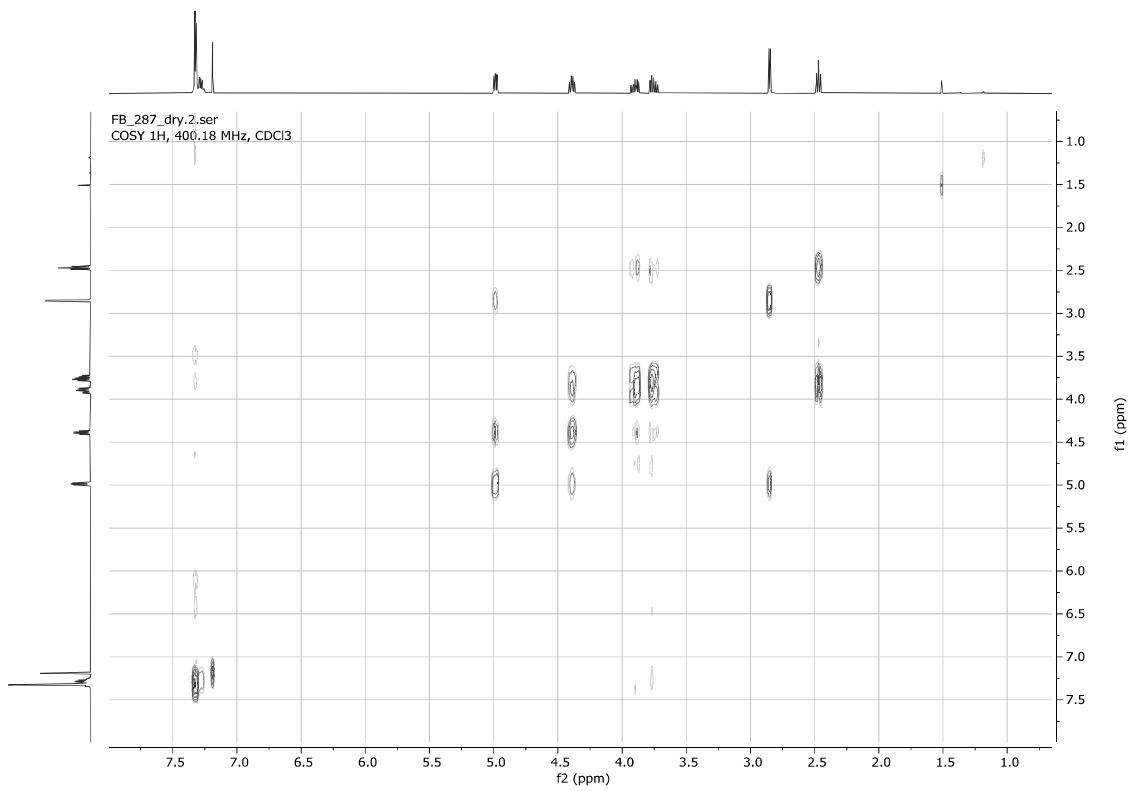
2-Iodo-1-phenyl-propan-1,3-diol **3h**

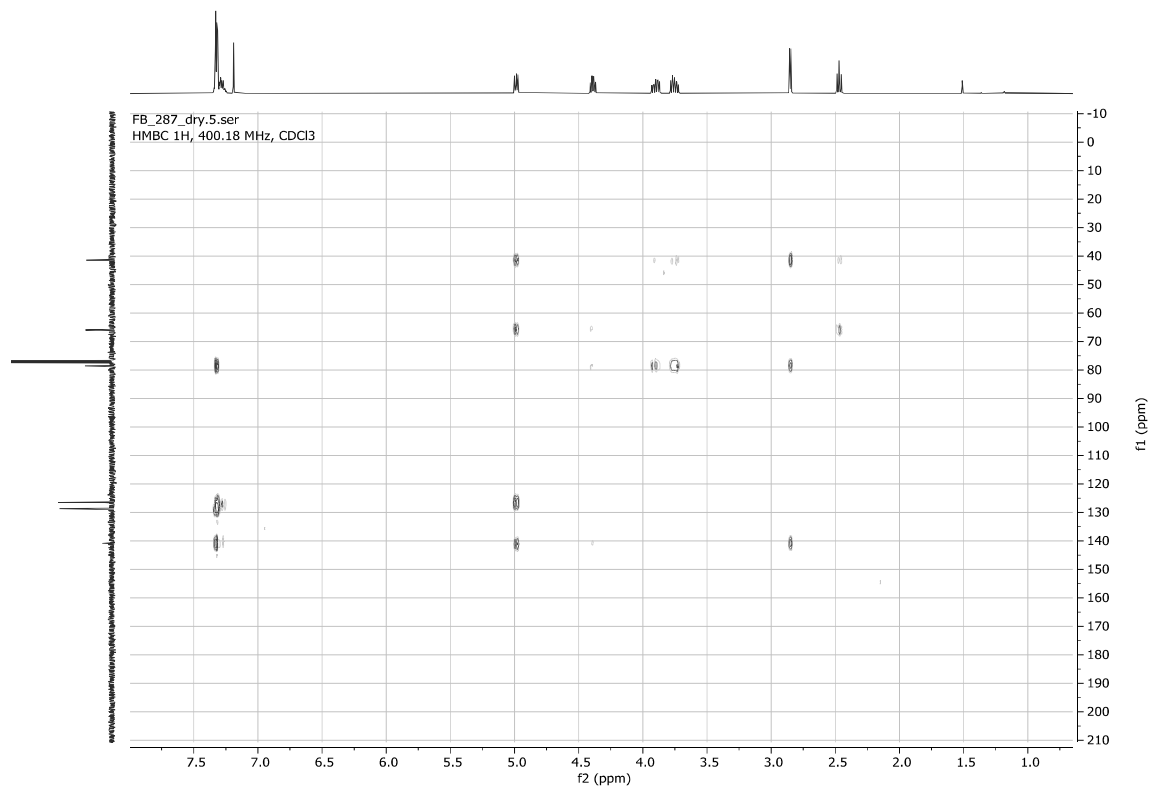
FB_287_dry.1.fid
1D 1H, 400.18 MHz, CDCl₃



FB_287_dry.3.fid
1D 13C(1H), 100.64 MHz, CDCl₃

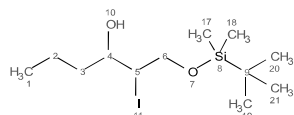
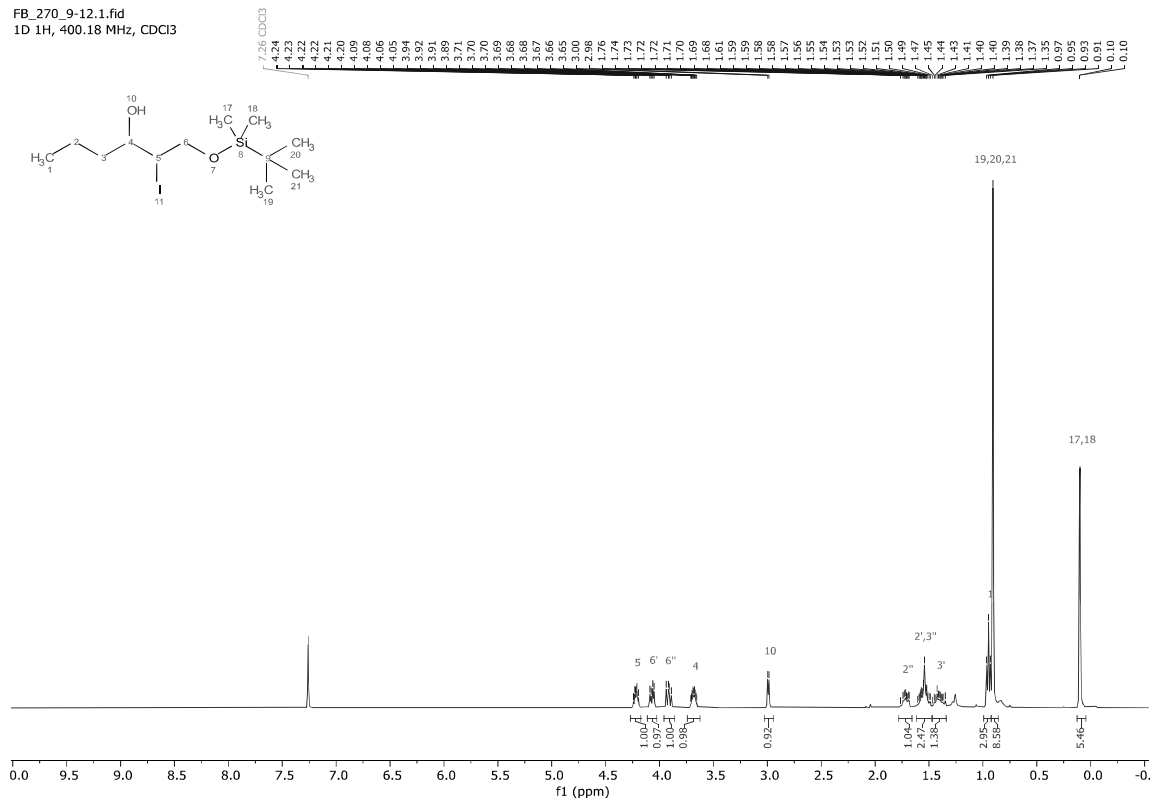




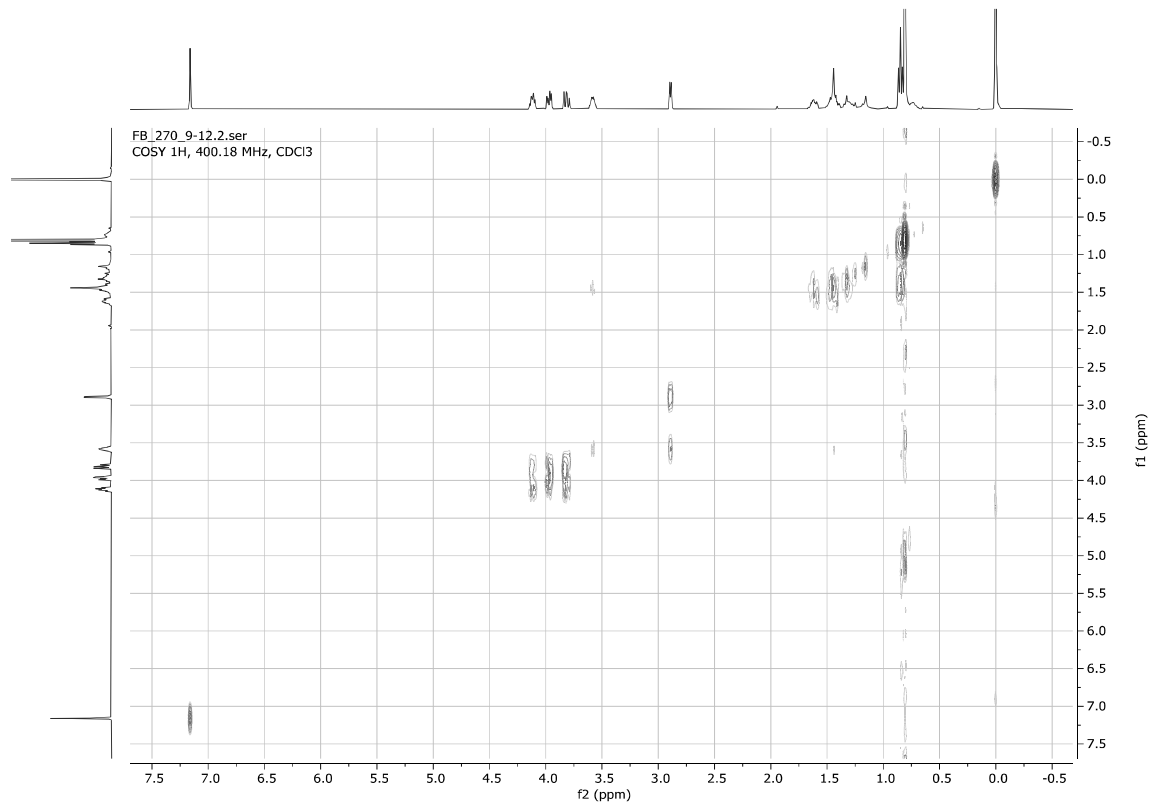
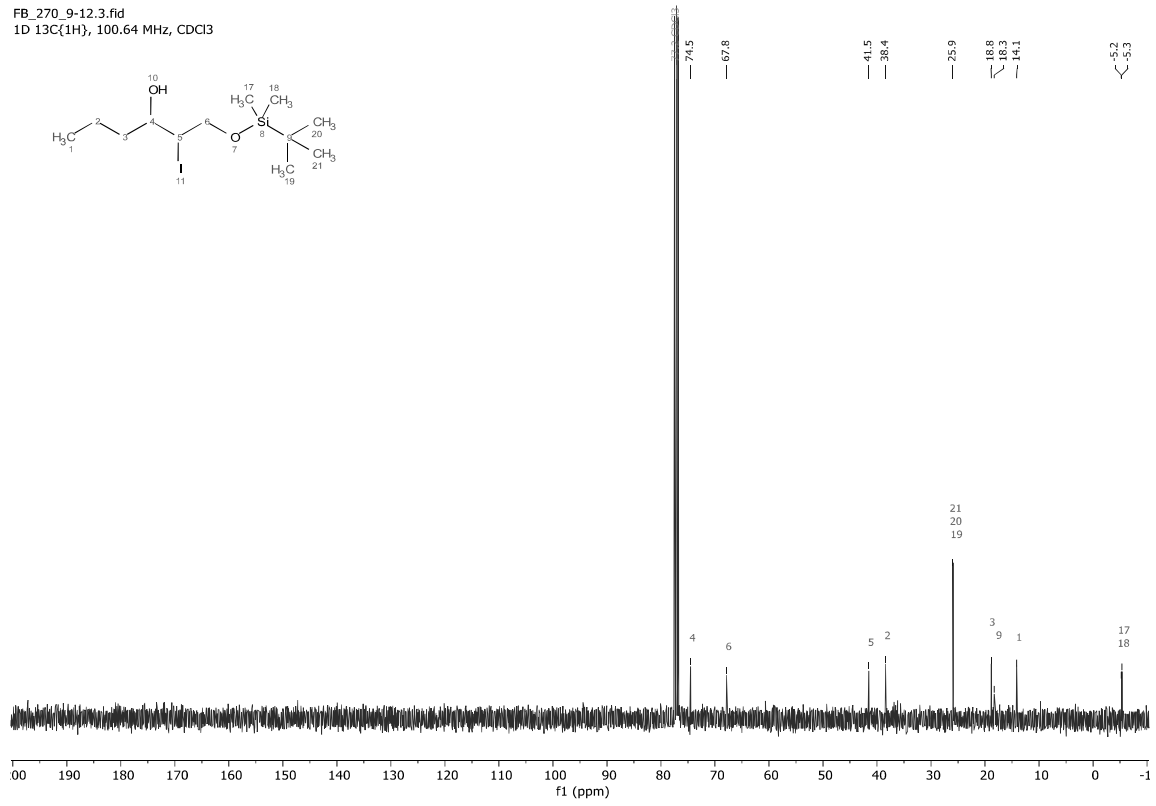


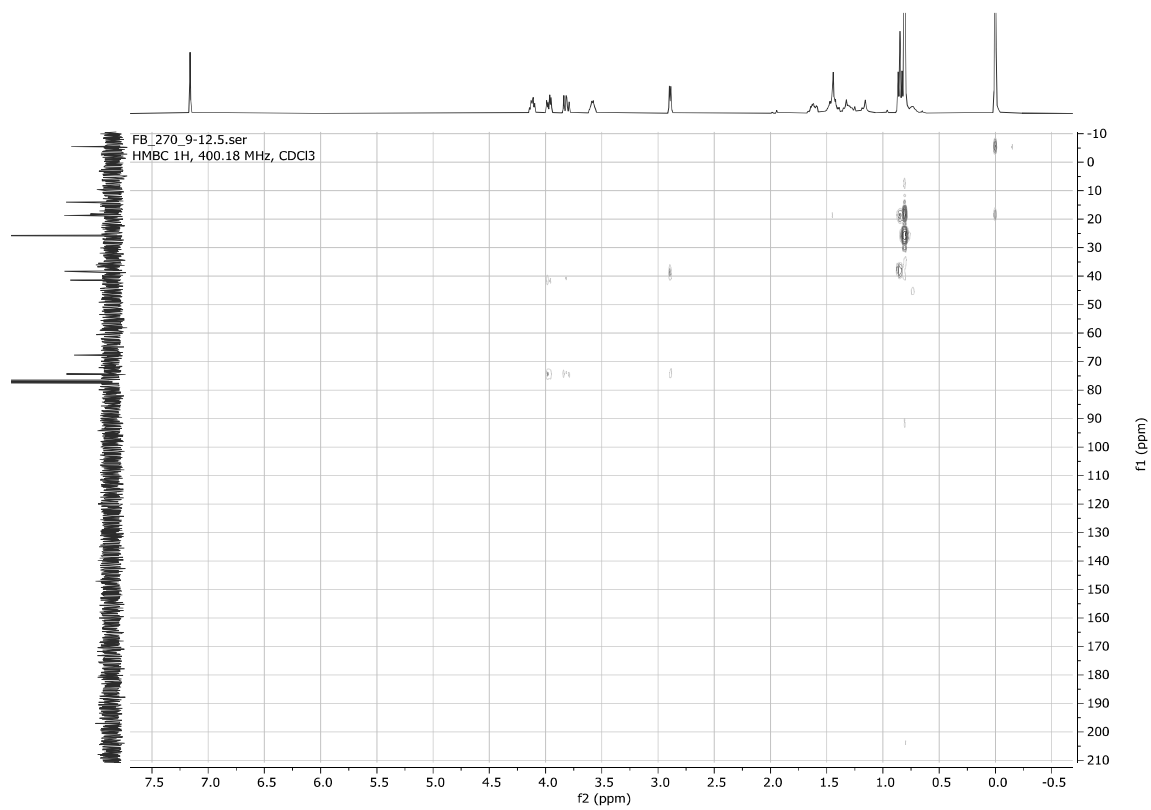
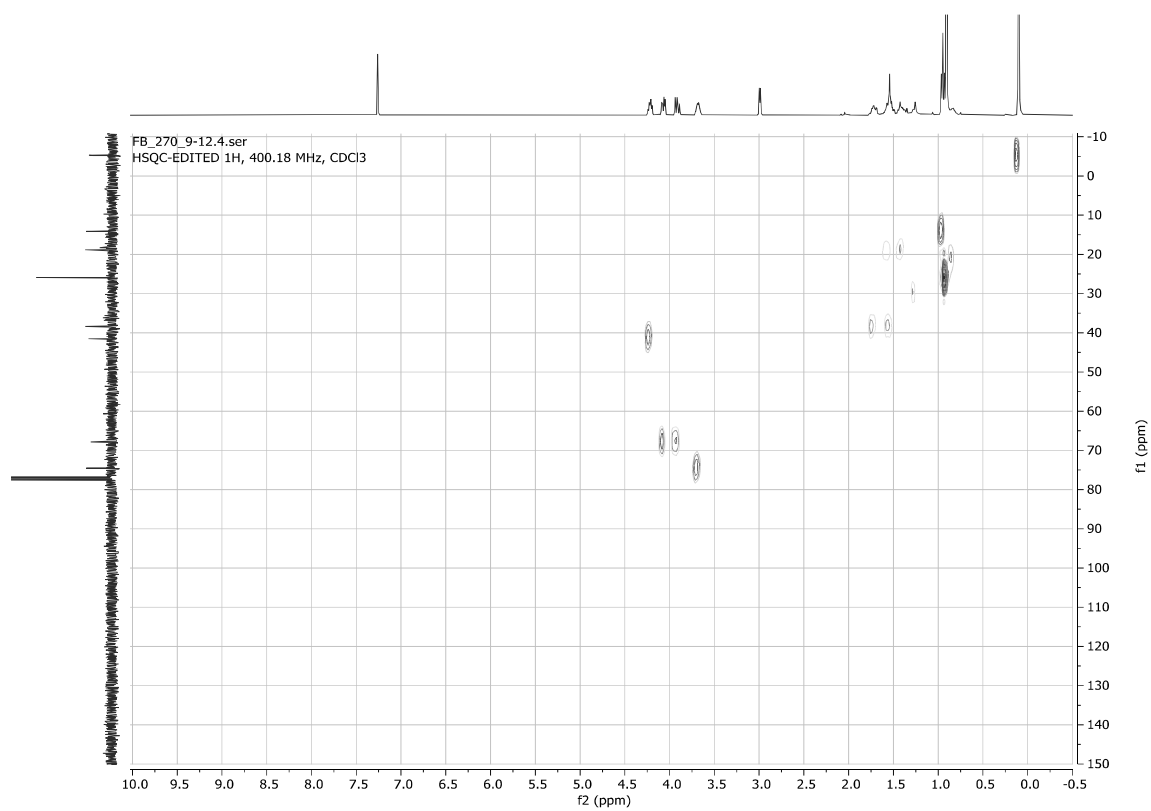
1-((*tert*-Butyldimethylsilyl)oxy)-2-iodohexan-3-ol **3i**

FB_270_9-12.1.fid
1D 1H, 400.18 MHz, CDCl3



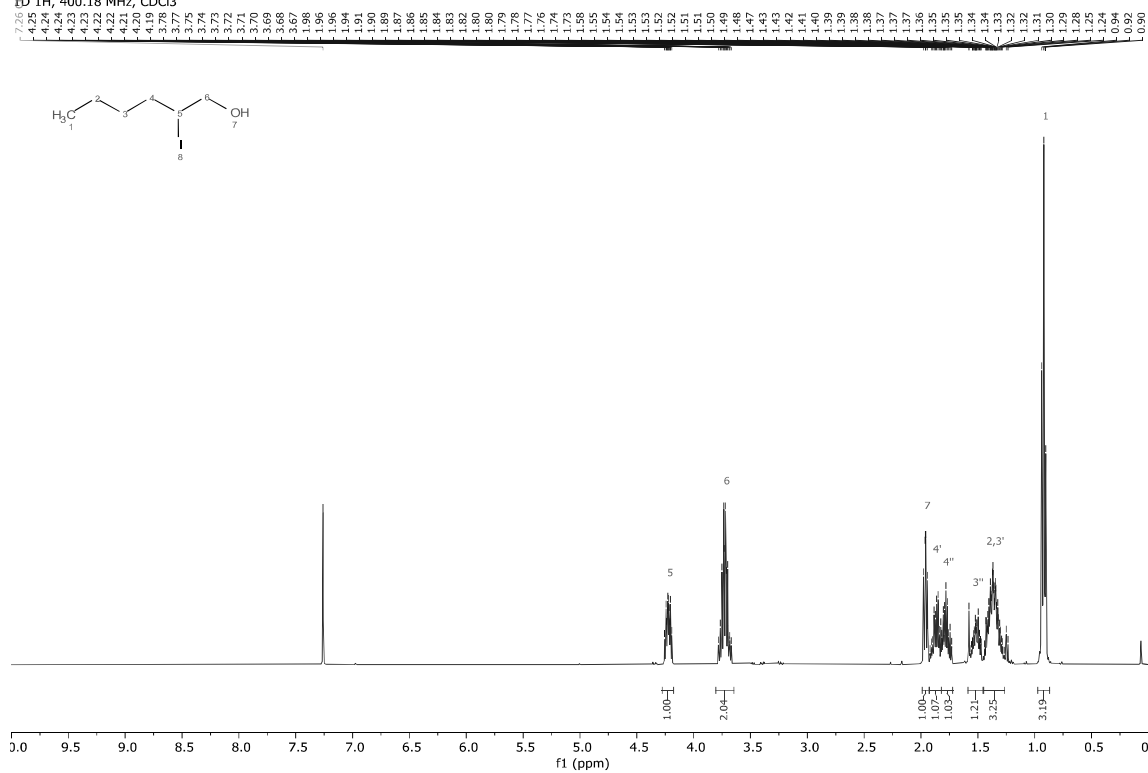
FB_270_9-12.3.fid
1D 13C{1H}, 100.64 MHz, CDCl3



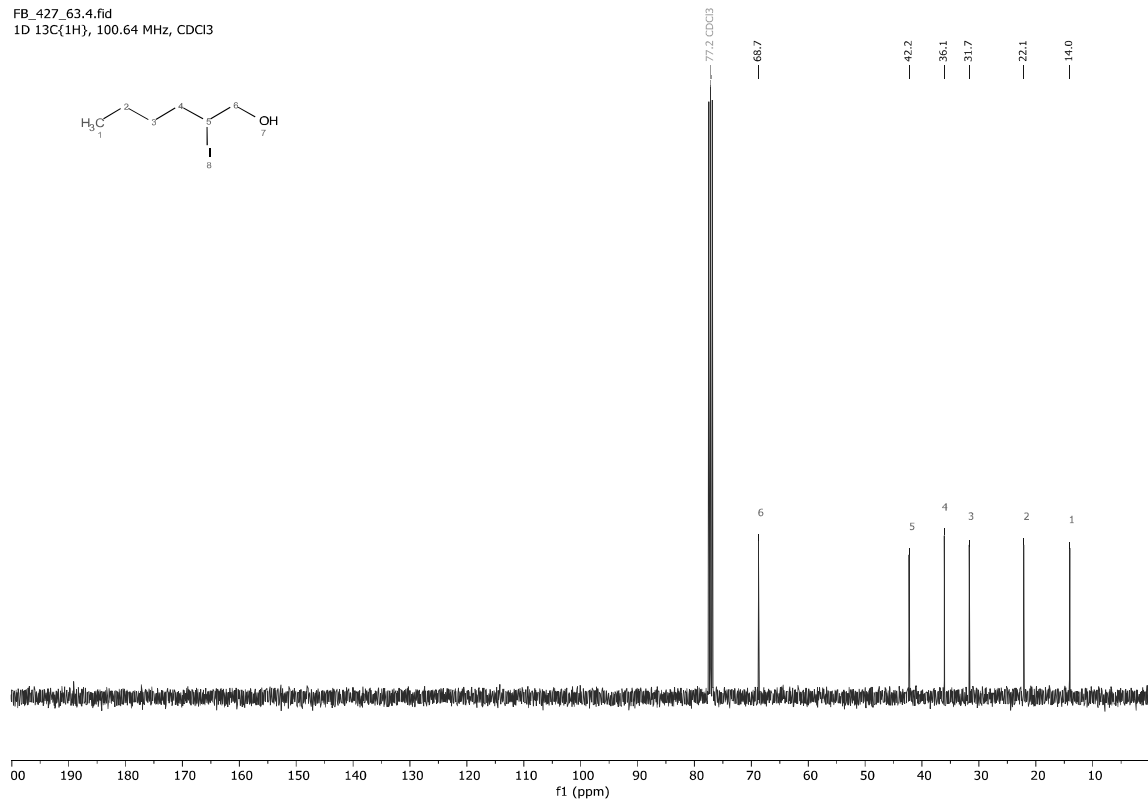


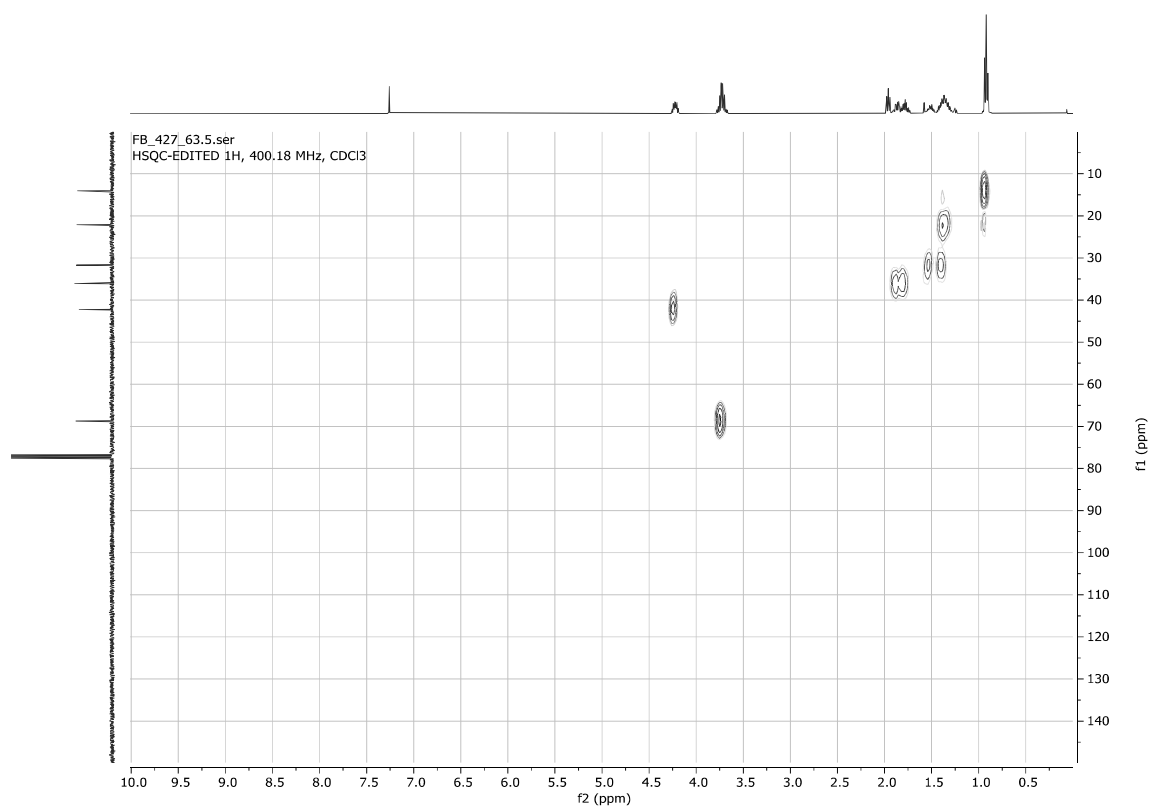
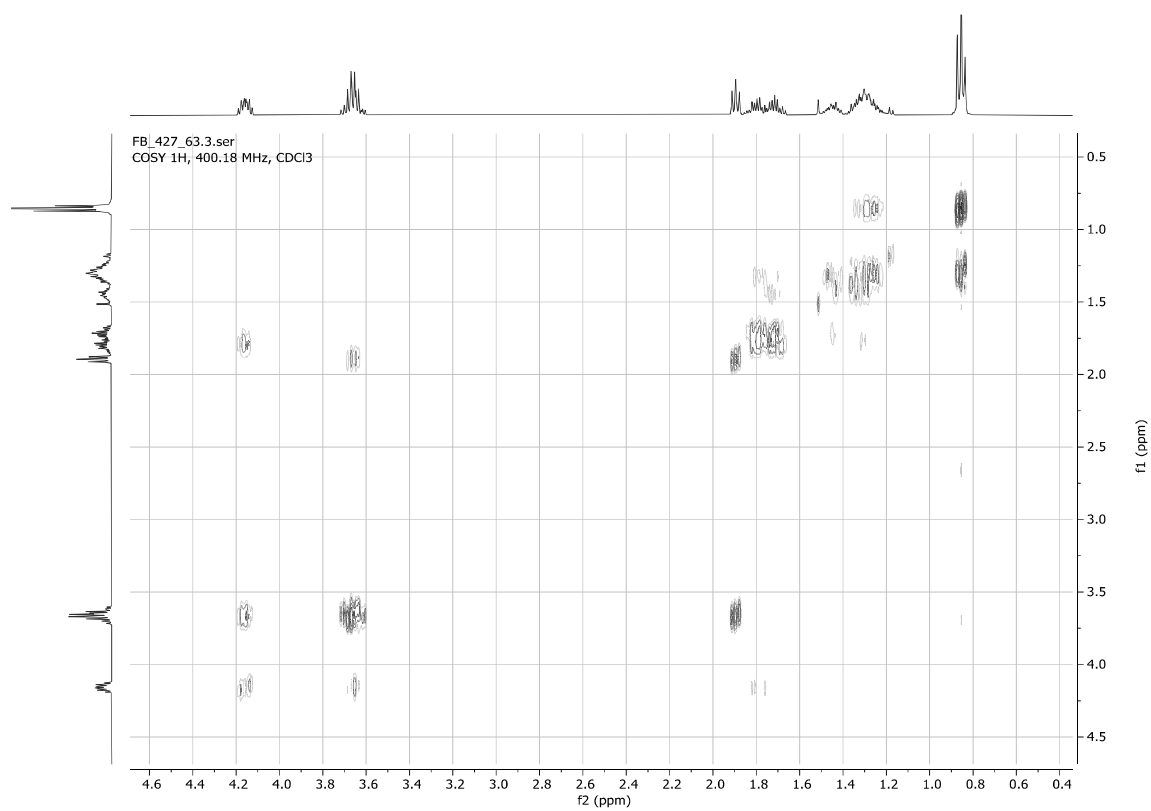
2-Iodohexan-1-ol 3j

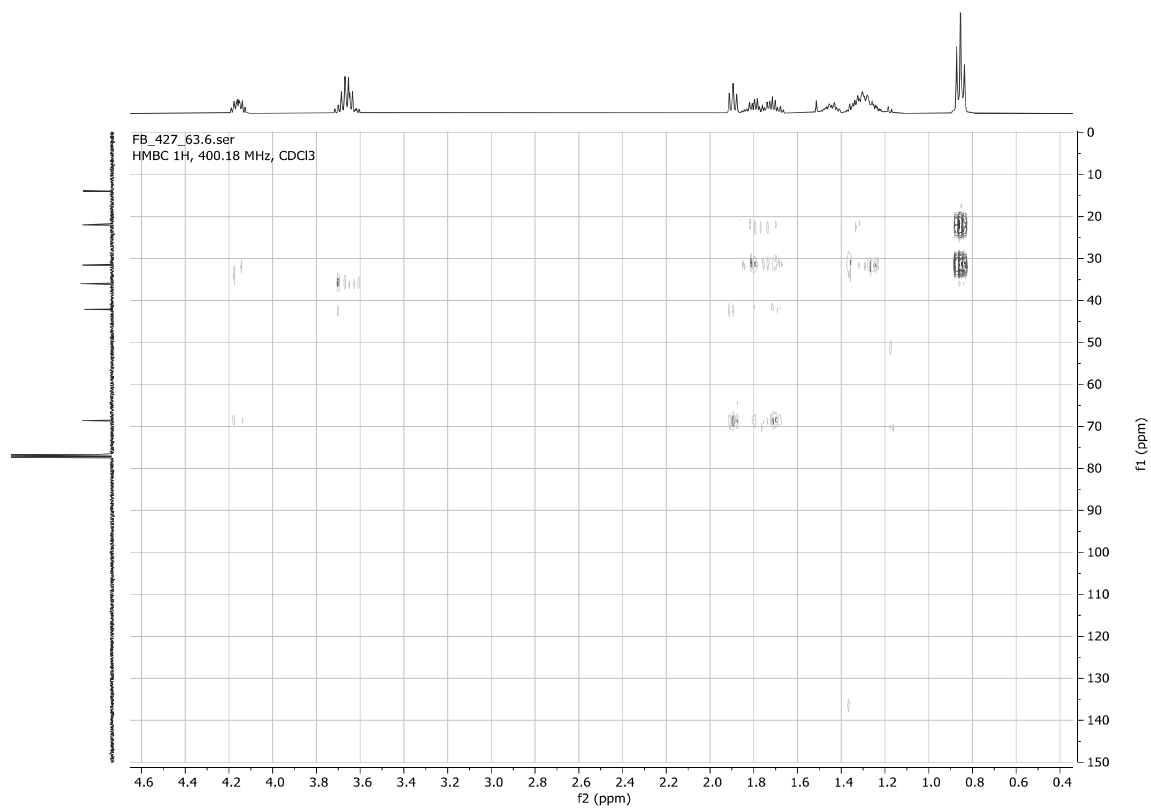
FB_427_63.1.fid
1D 1H, 400.18 MHz, CDCl3



FB_427_63.4.fid
1D 13C(1H), 100.64 MHz, CDCl3

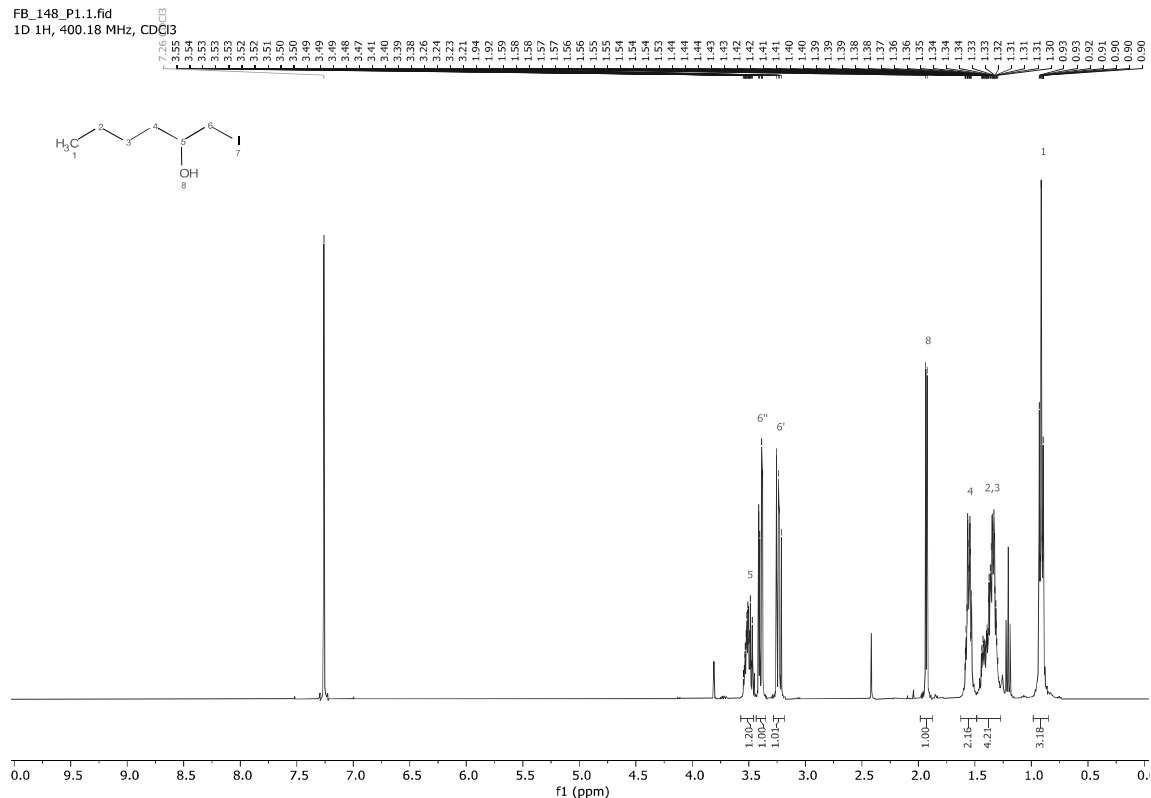




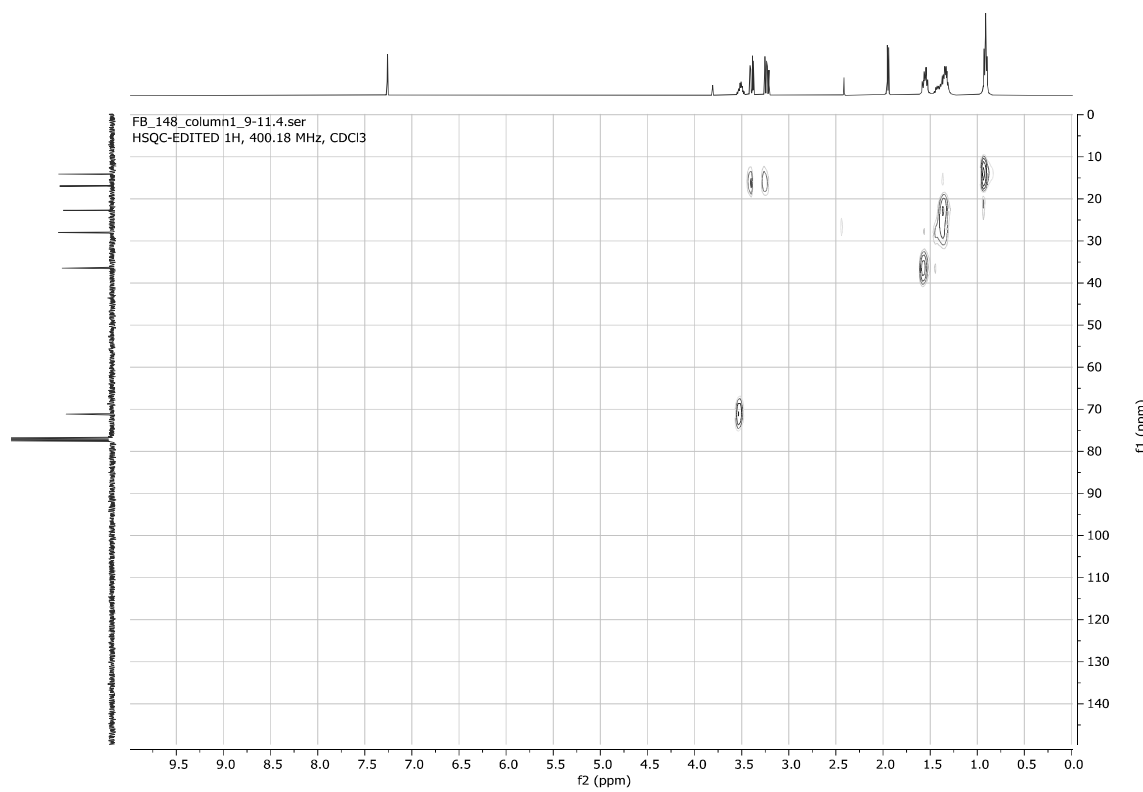
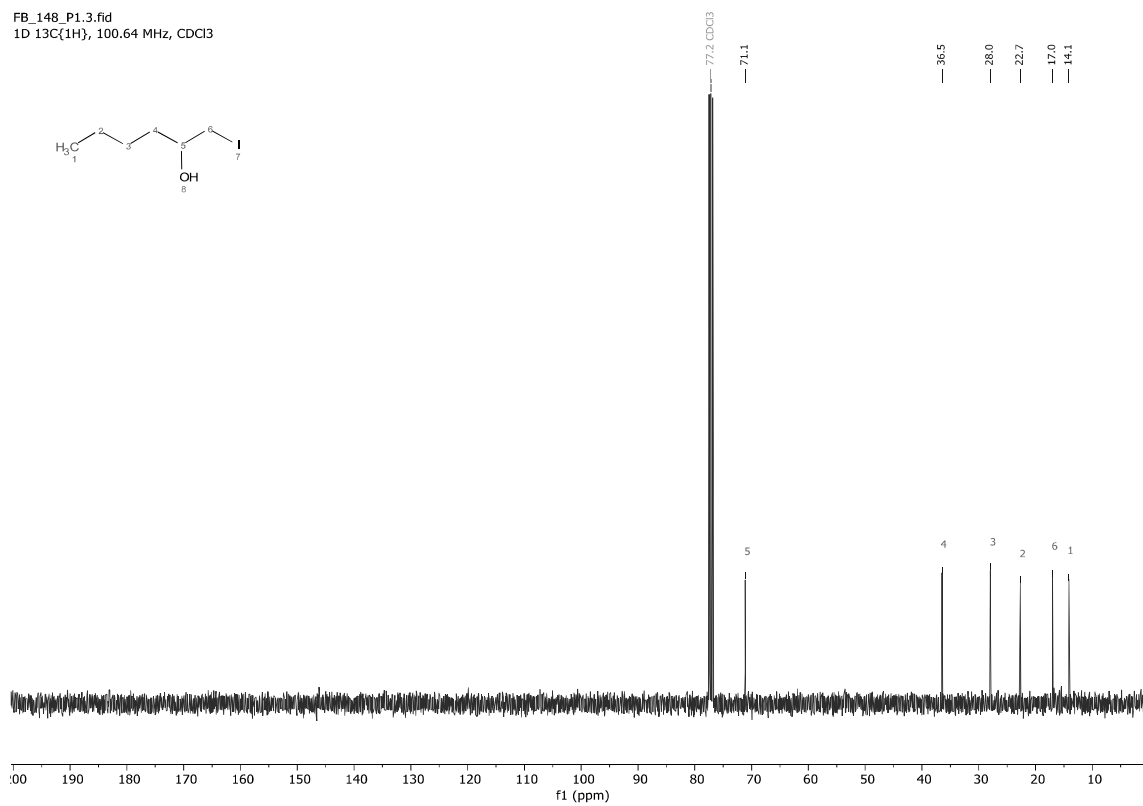
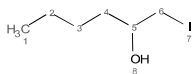


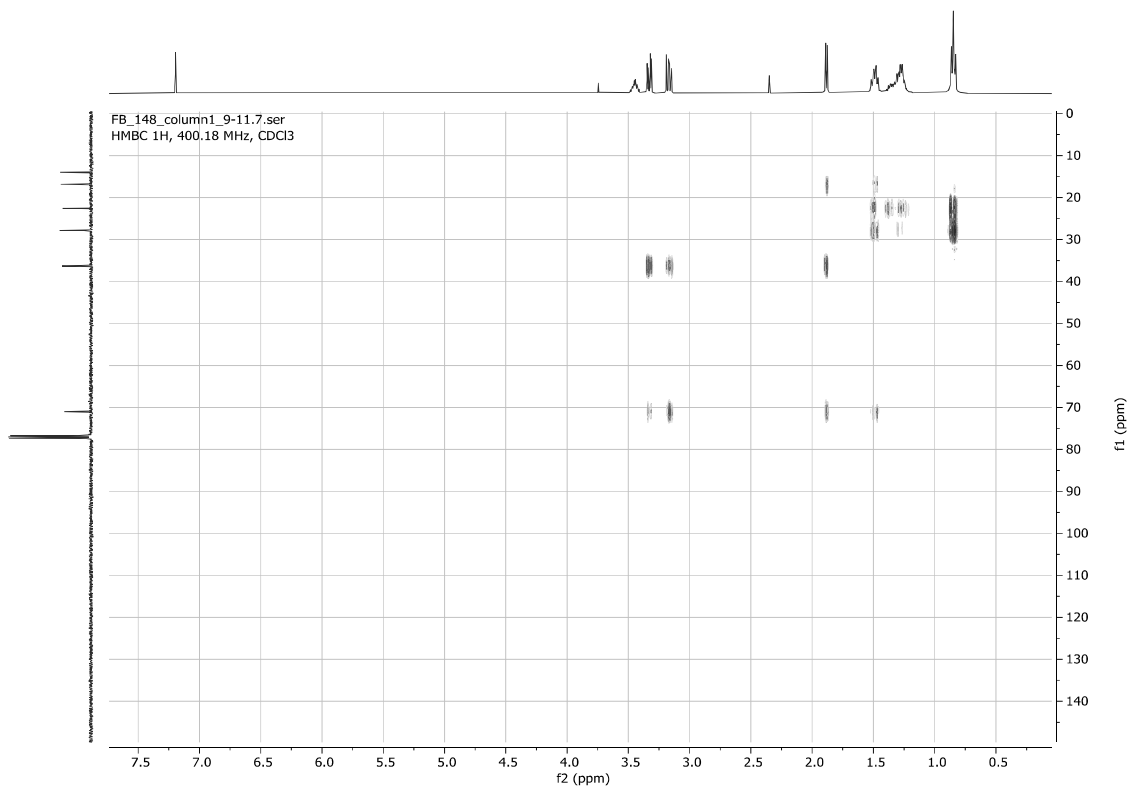
1-Iodohexan-2-ol **3k**

FB_148_P1.1.fid
1D 1H, 400.18 MHz, CDCl3



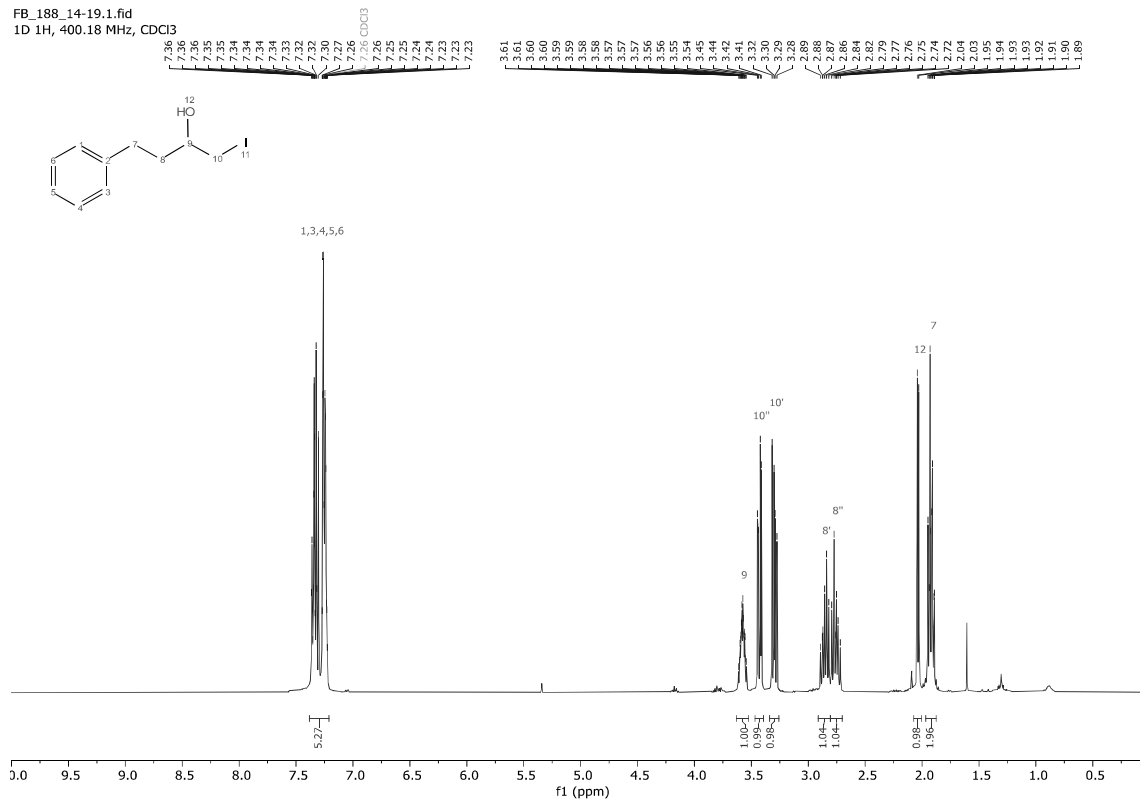
FB_148_P1.3.fid
1D 13C{1H}, 100.64 MHz, CDCl3



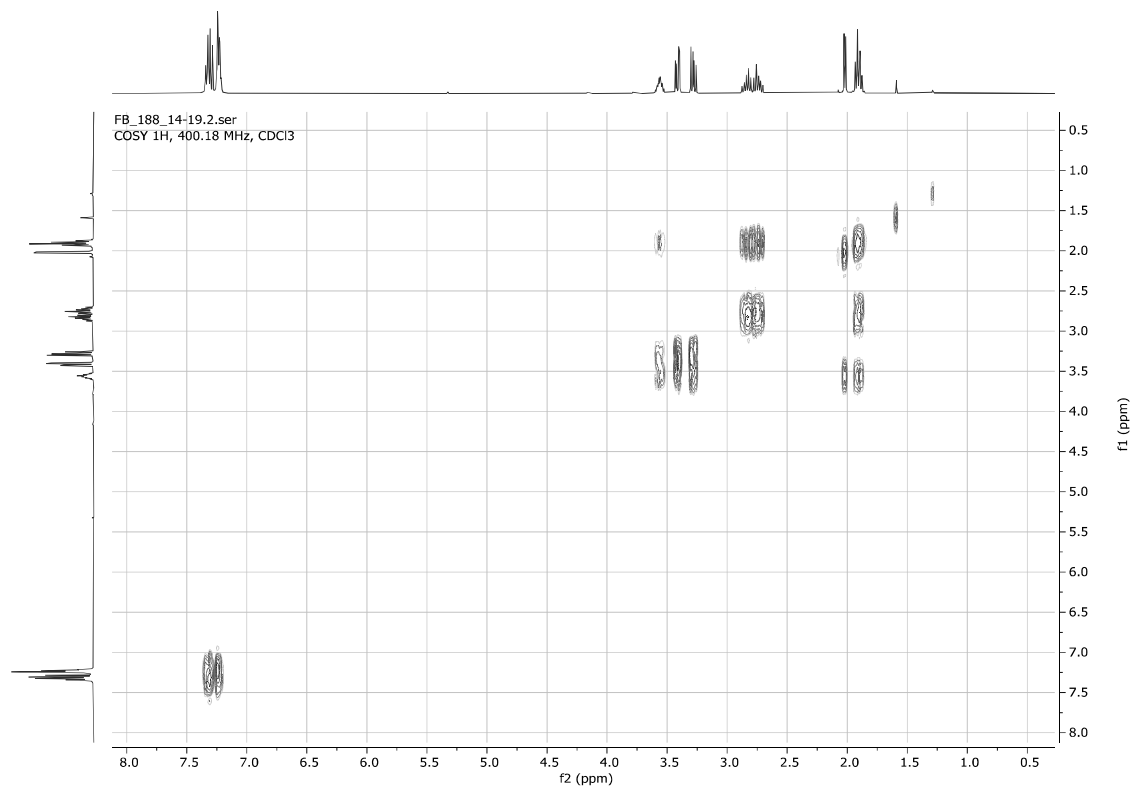
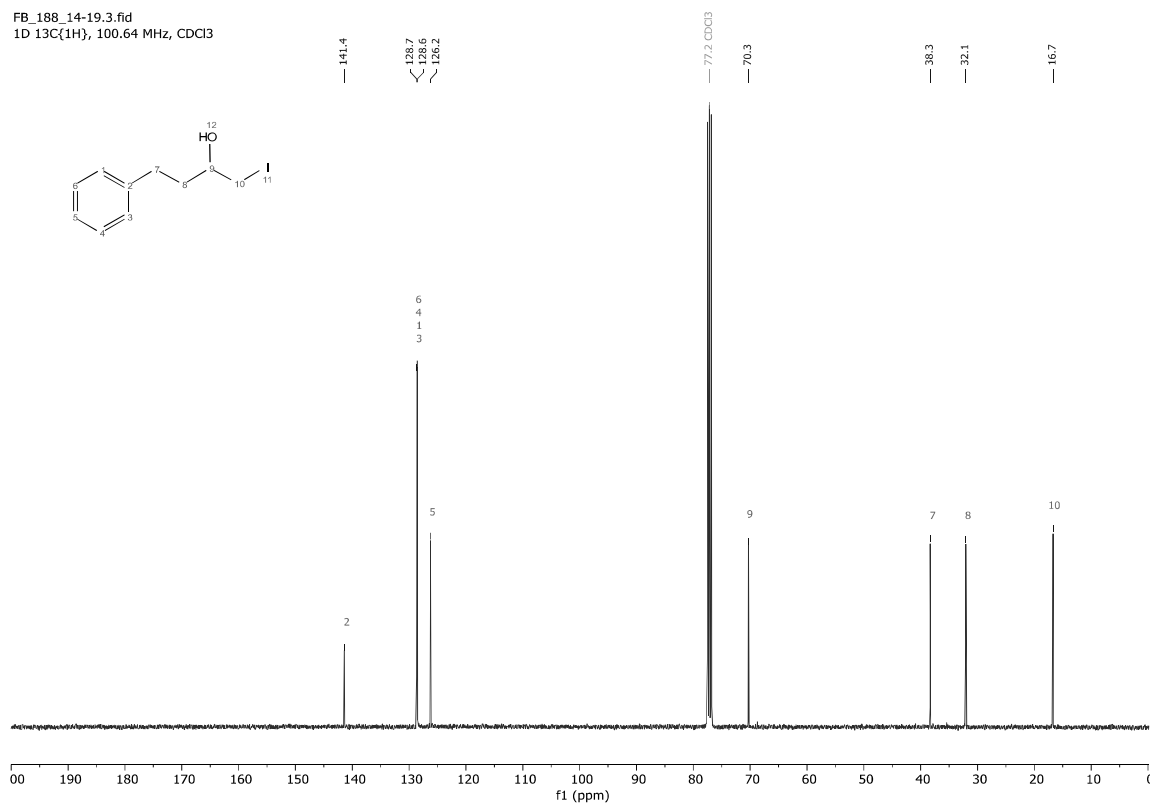


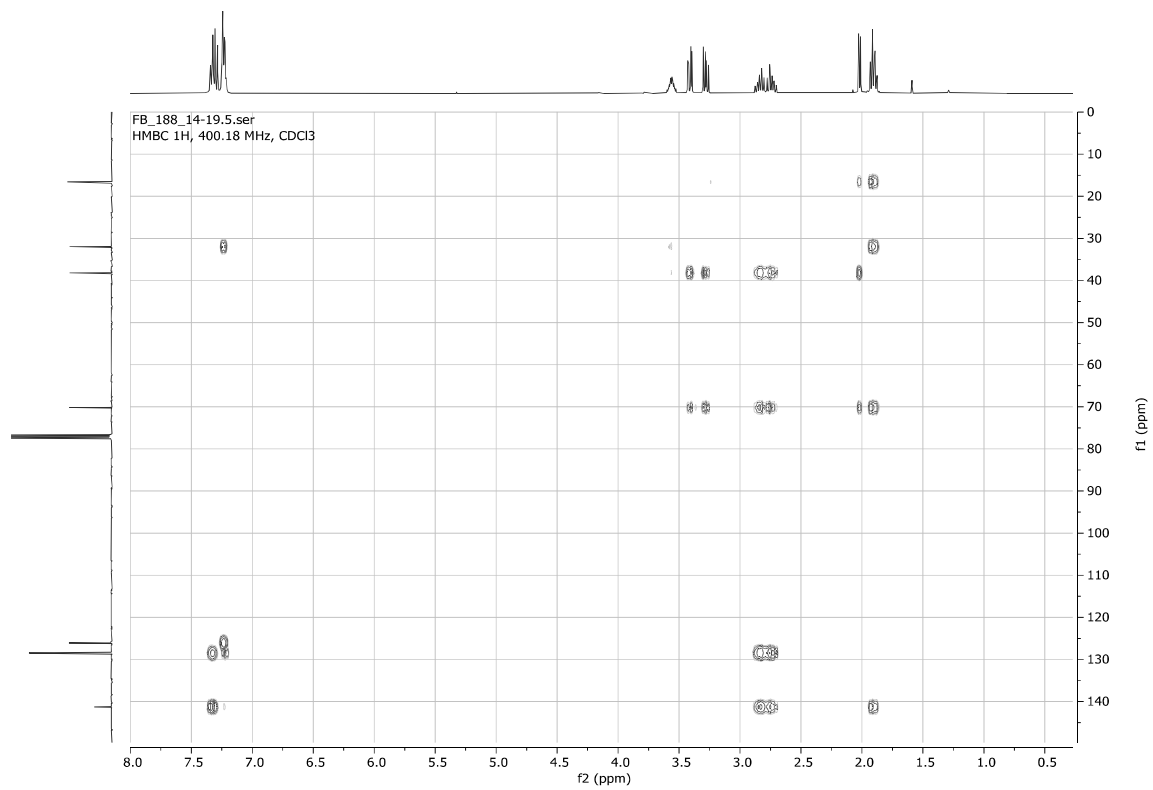
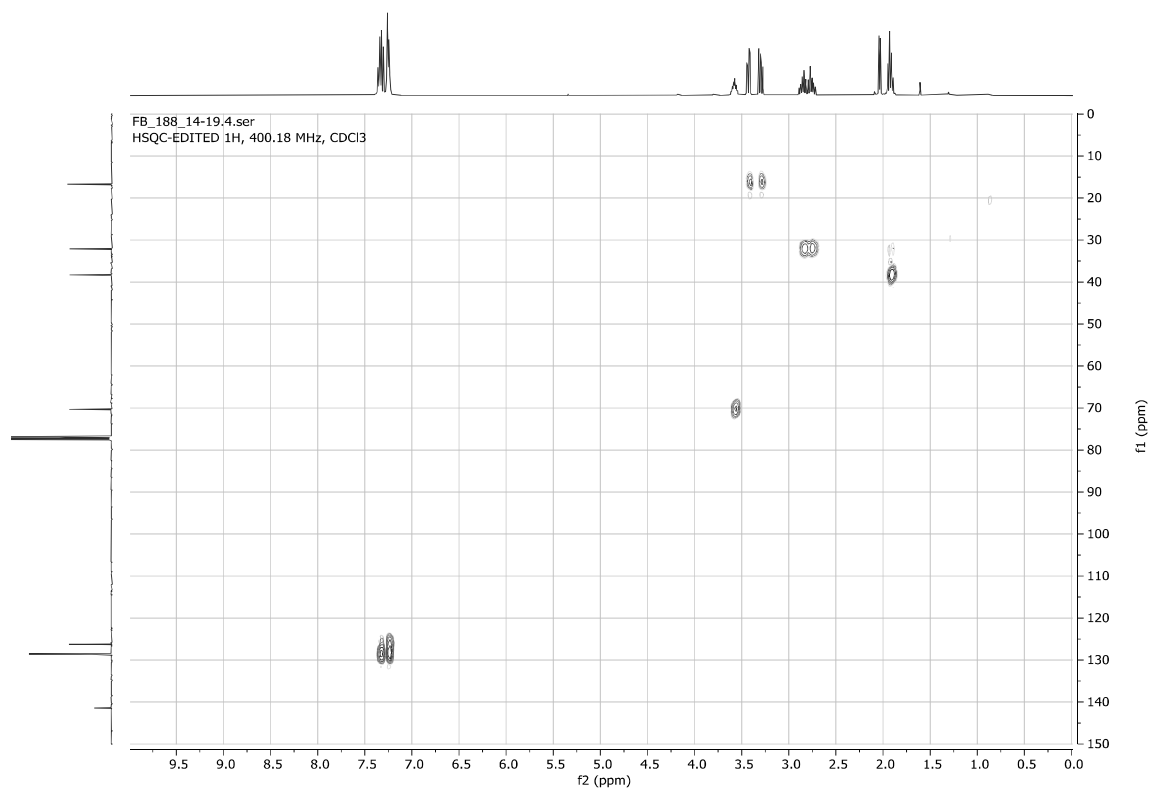
1-Iodo-4-phenylbutan-2-ol **31**

FB_188_14-19.1.fid
1D 1H, 400.18 MHz, CDCl3



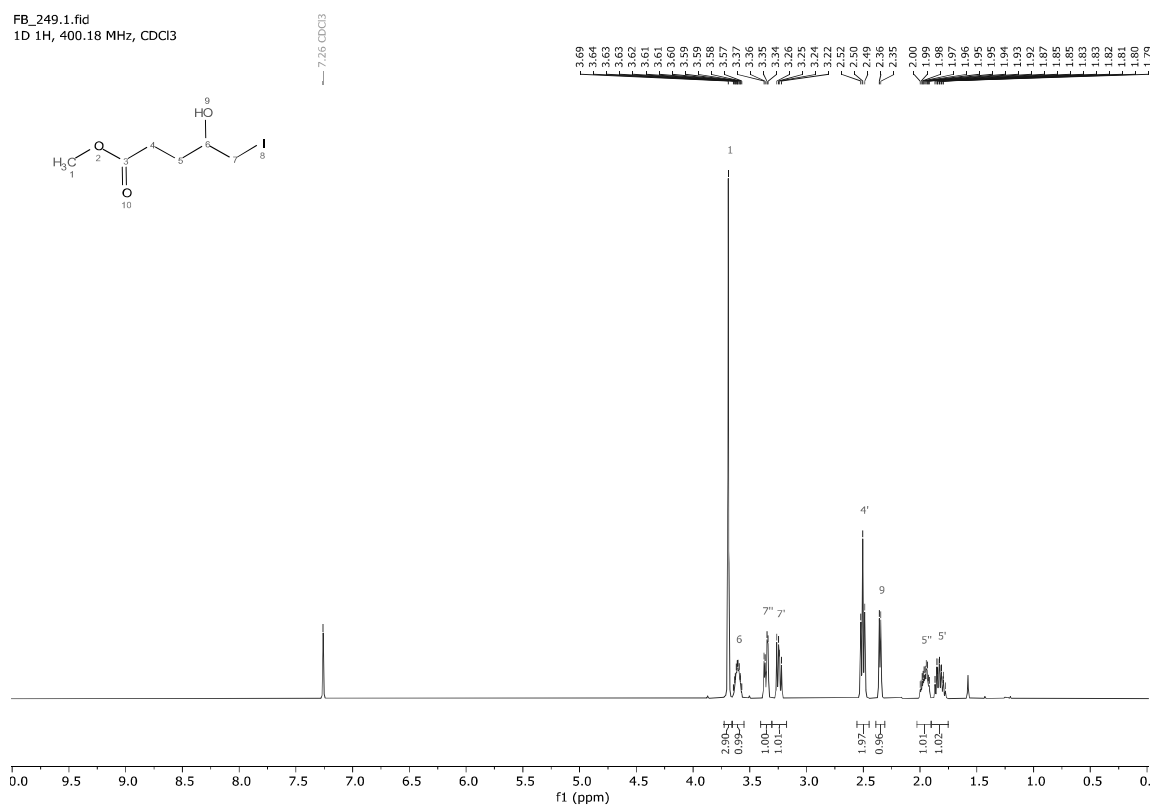
FB_188_14-19.3.fid
1D 13C{1H}, 100.64 MHz, CDCl3



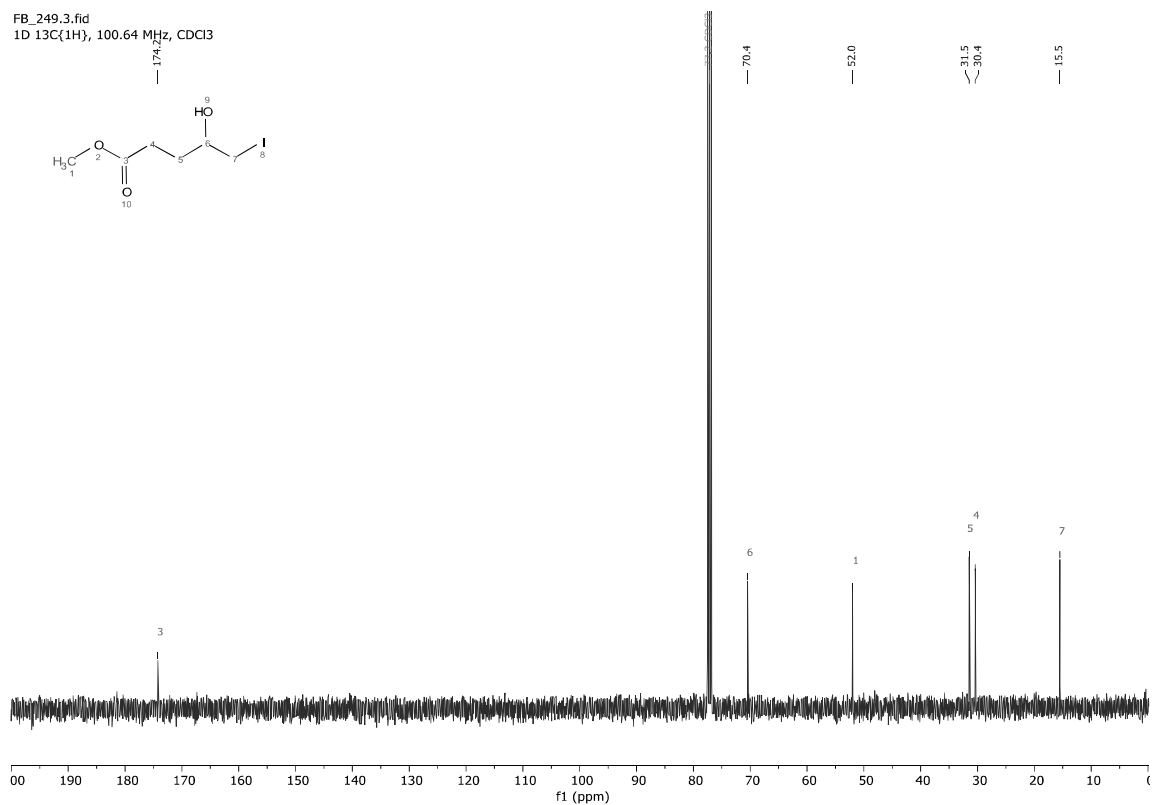


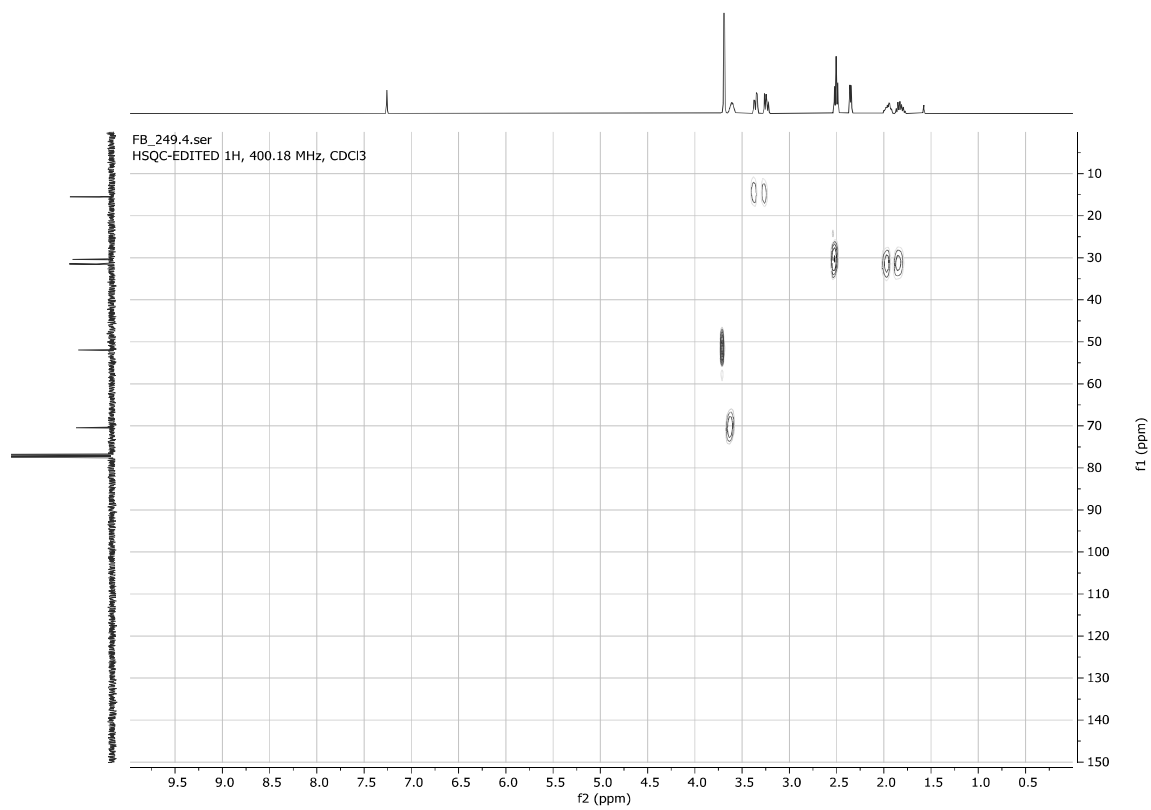
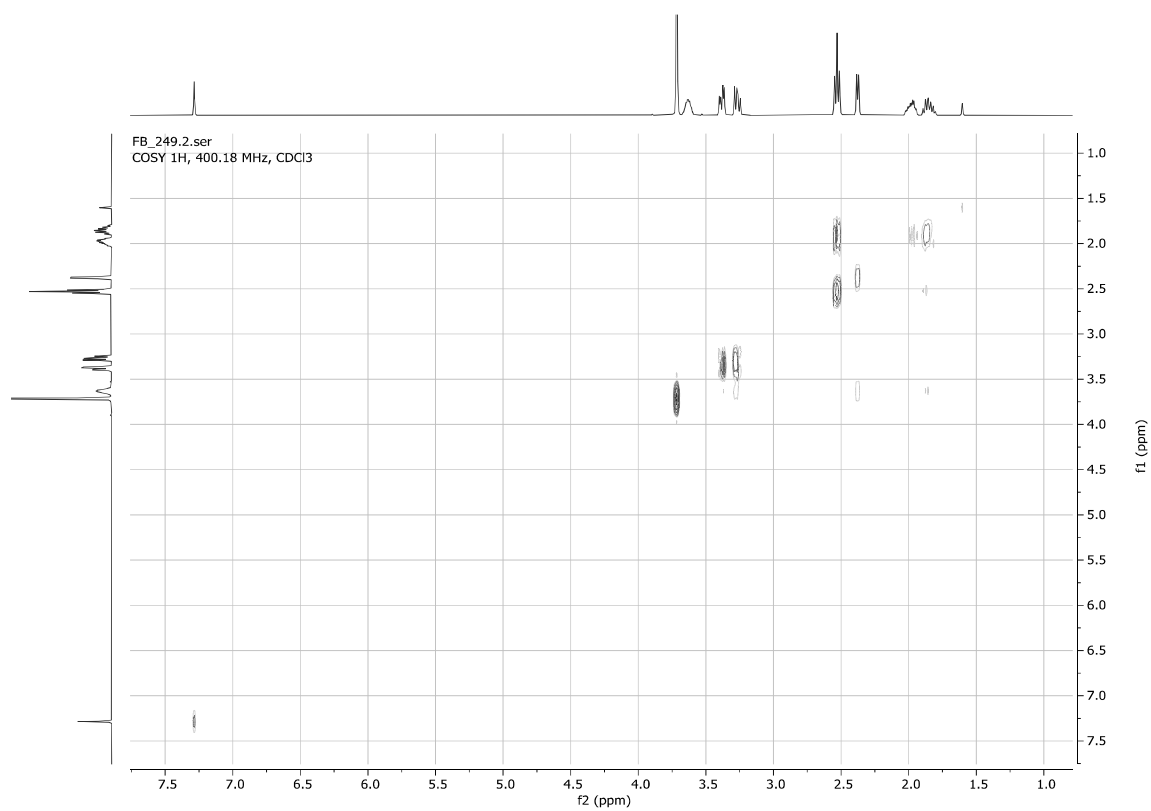
Methyl 4-hydroxy-5-iodopentanoate **3m**

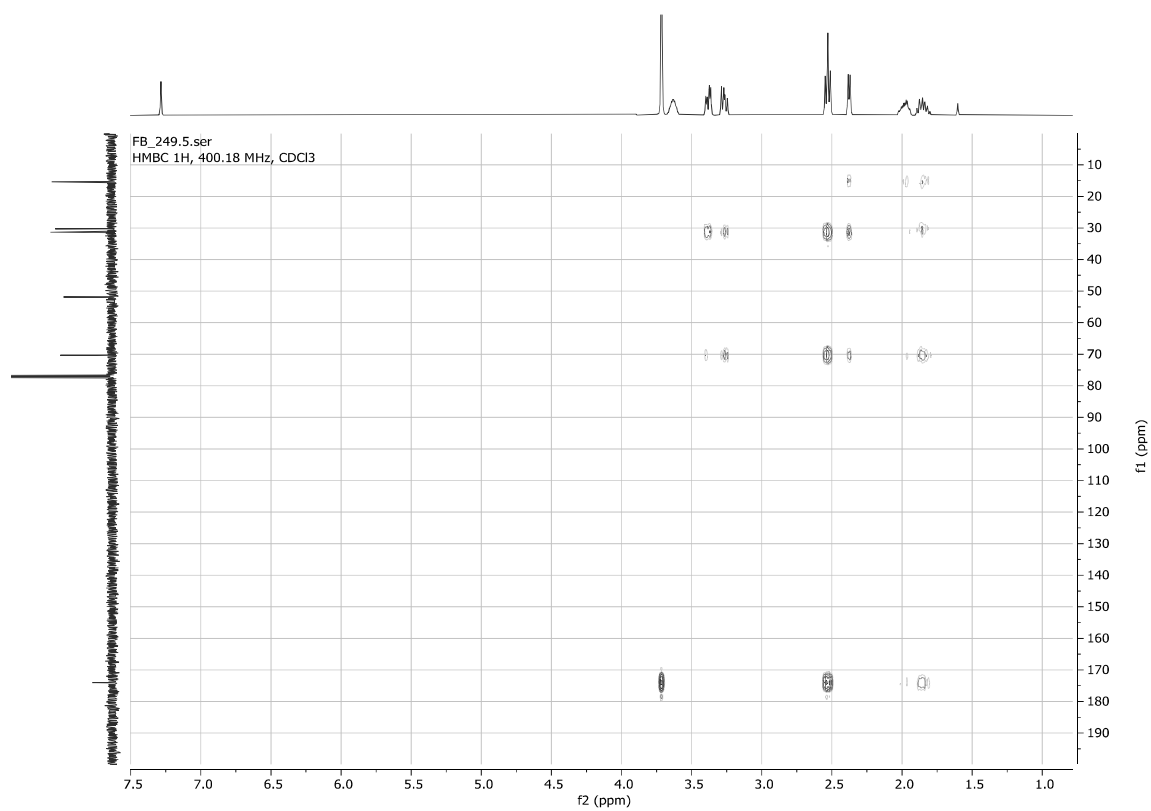
FB_249.1.fid
1D 1H, 400.18 MHz, CDCl₃



FB_249.3.fid
1D 13C(1H), 100.64 MHz, CDCl₃

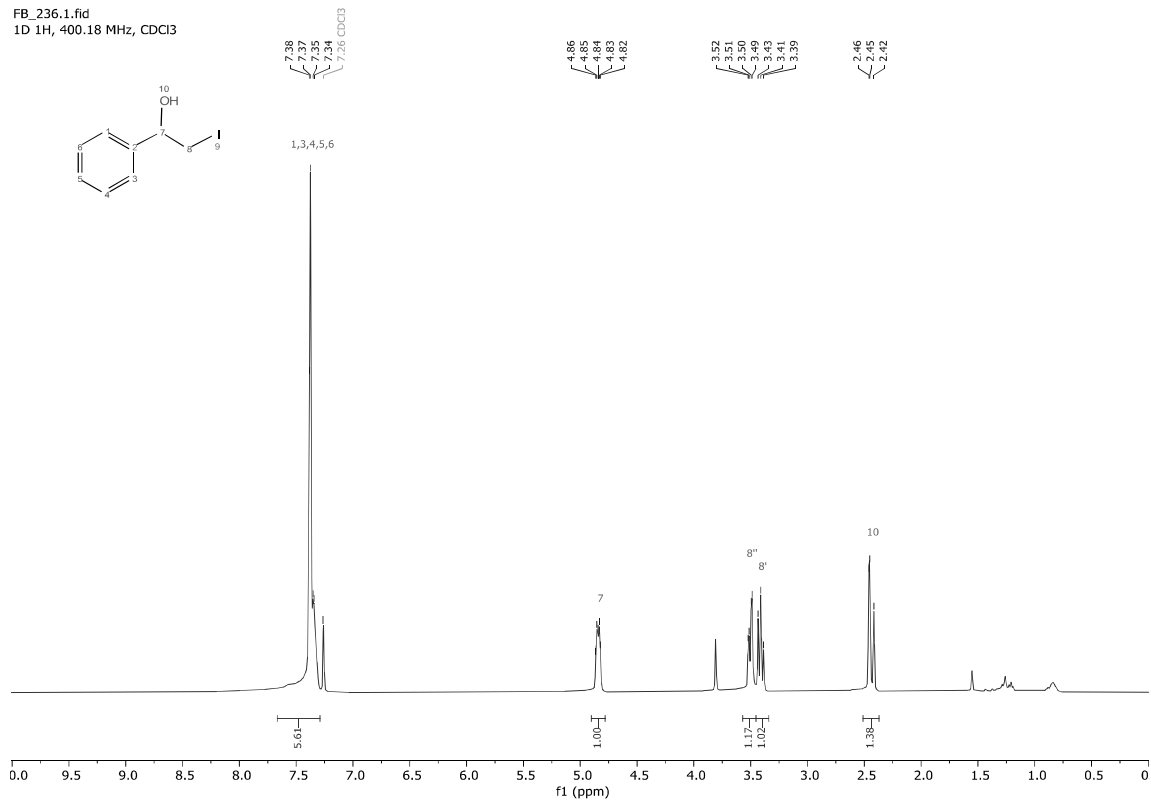




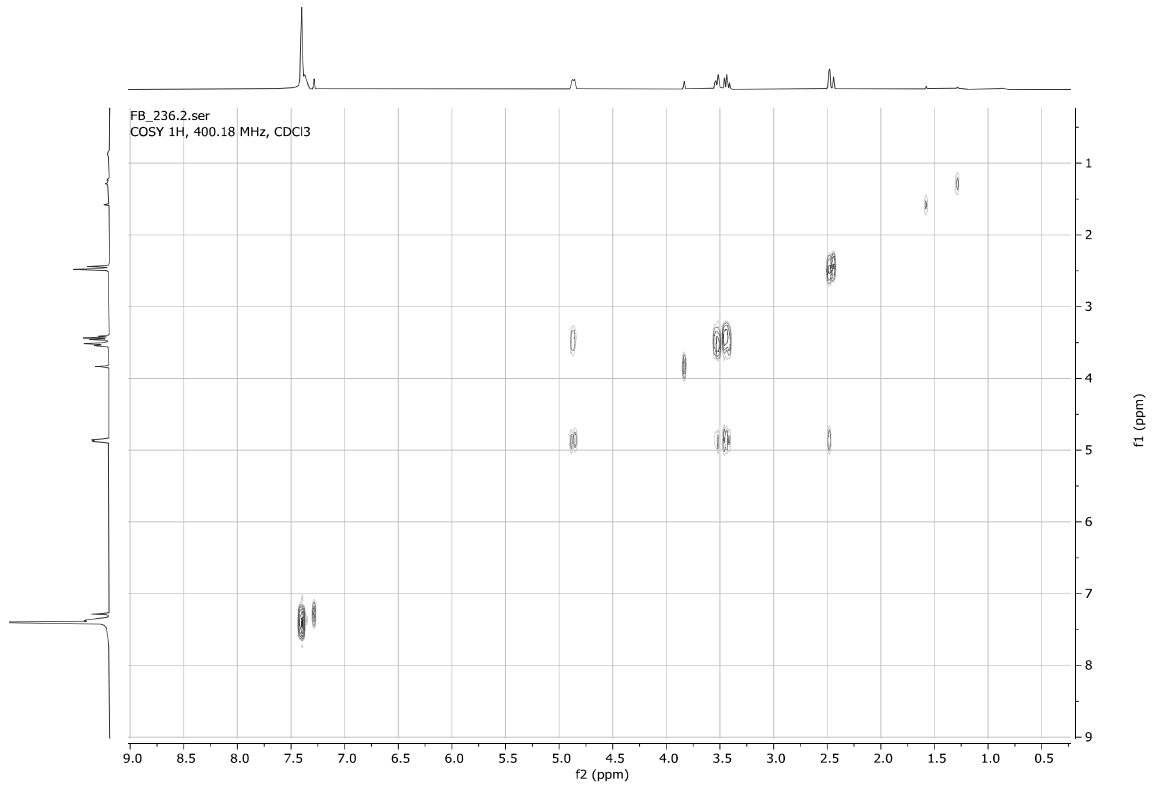
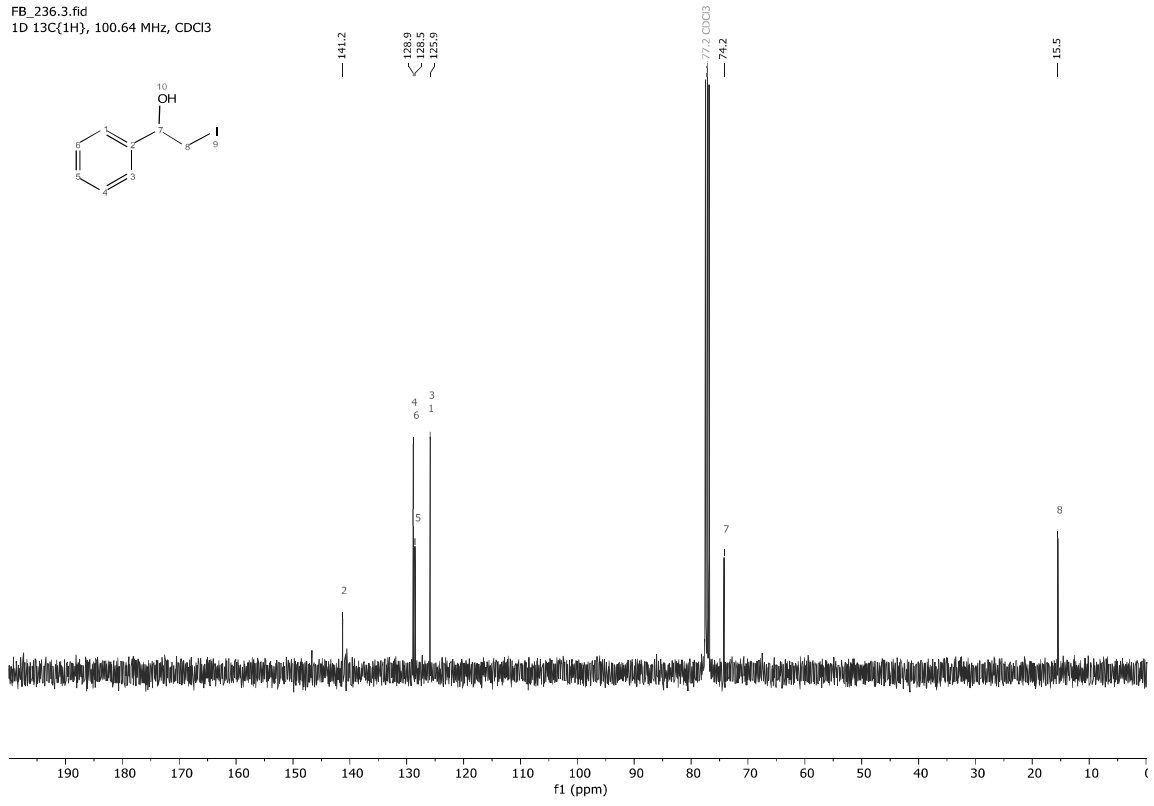
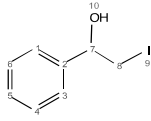


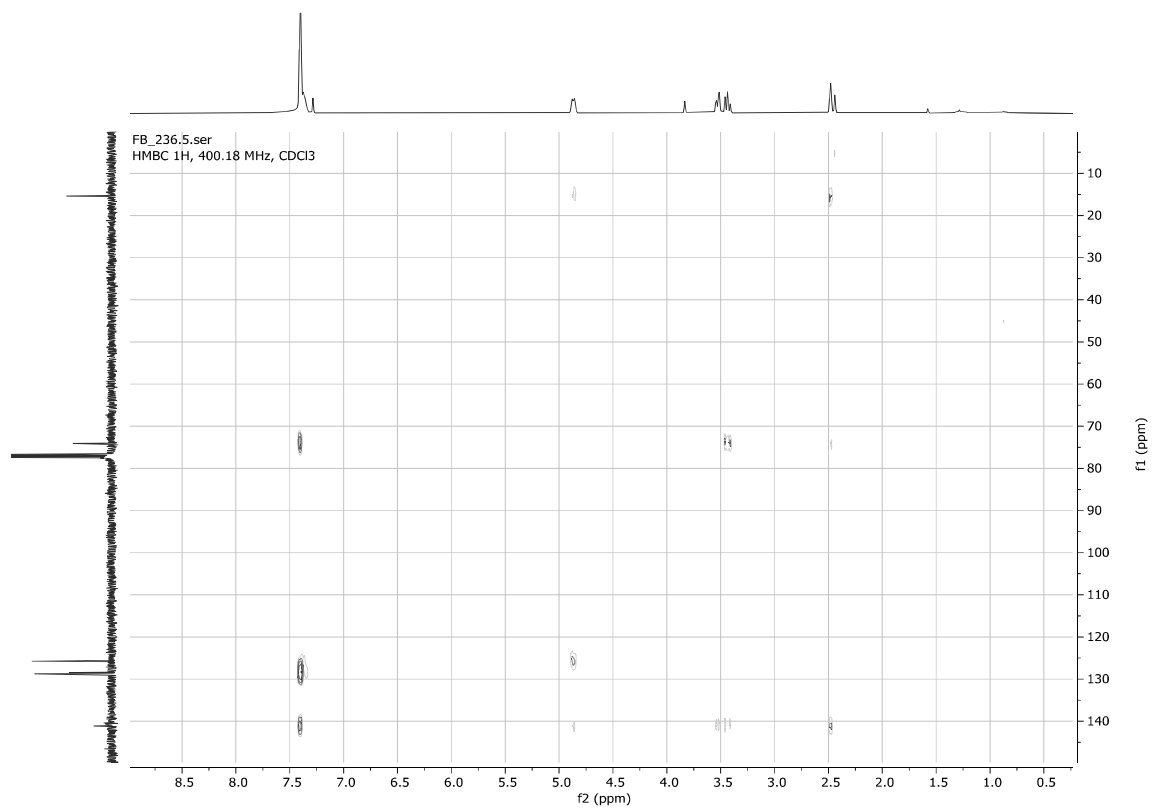
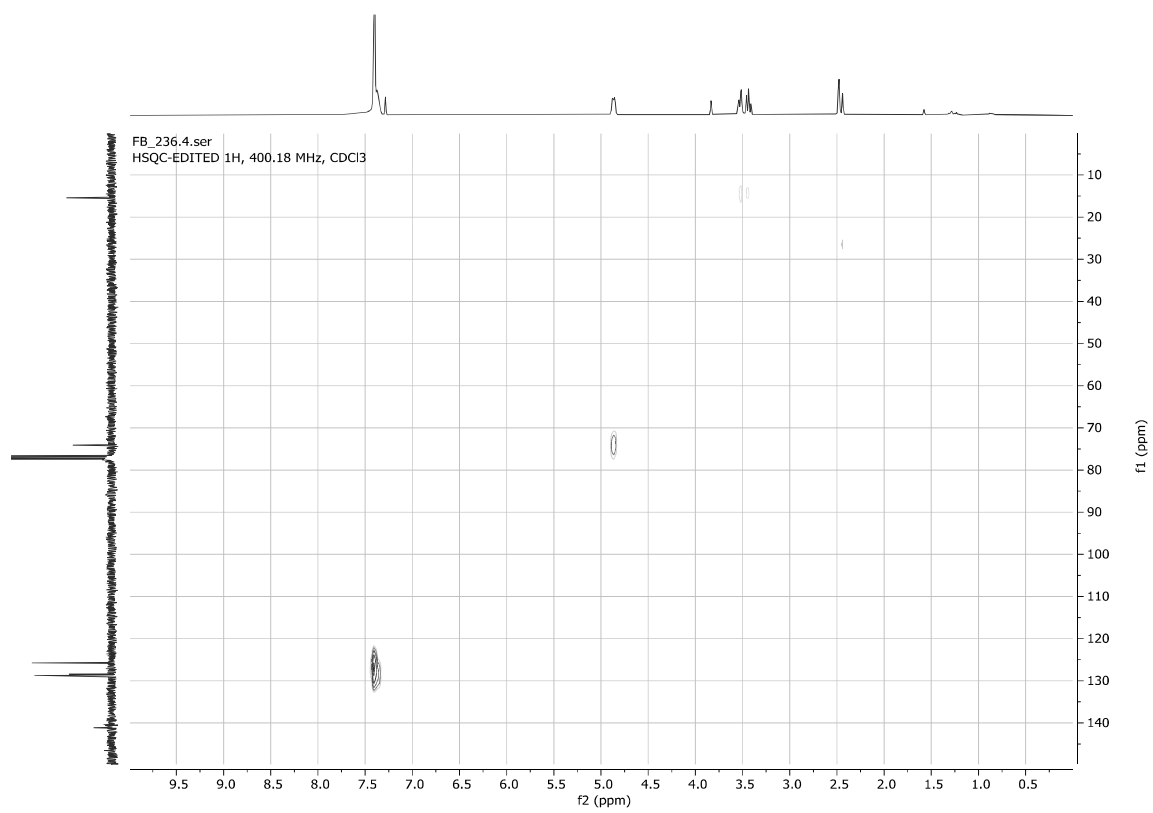
2-Iodo-1-phenylethan-1-ol **3n**

FB_236.1.fid
1D 1H, 400.18 MHz, CDCl3



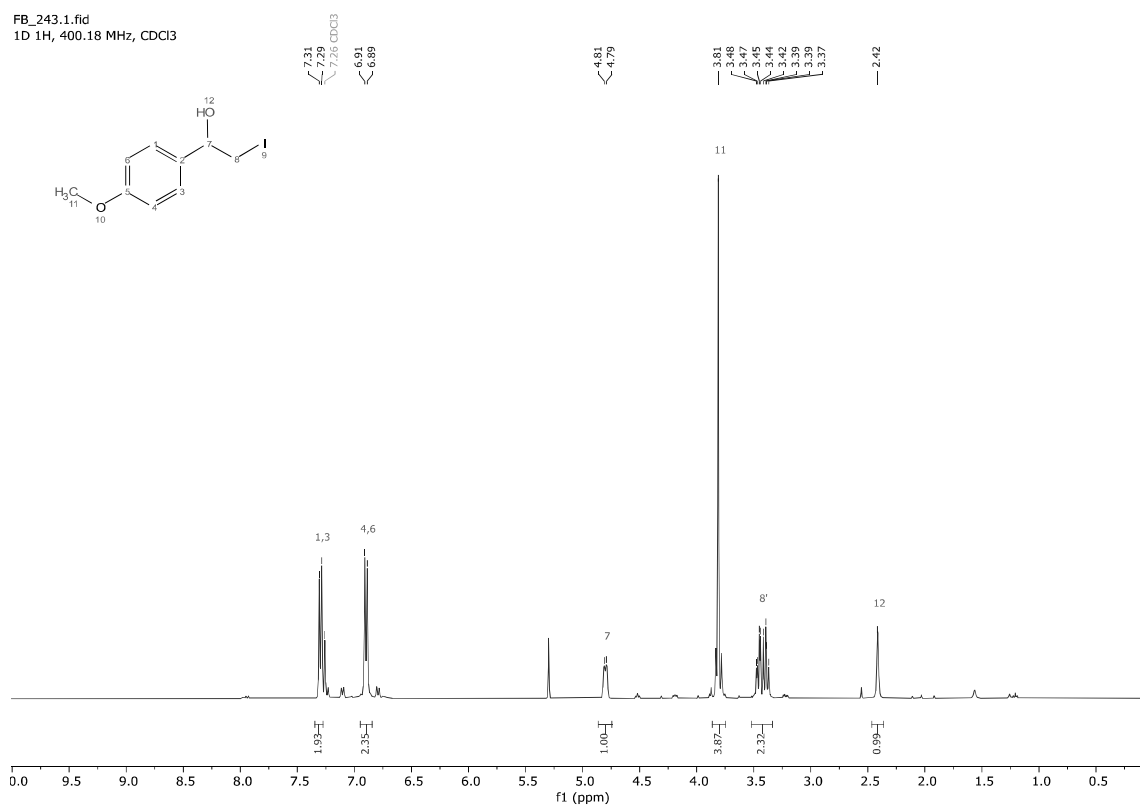
FB_236.3.fid
1D 13C{1H}, 100.64 MHz, CDCl3



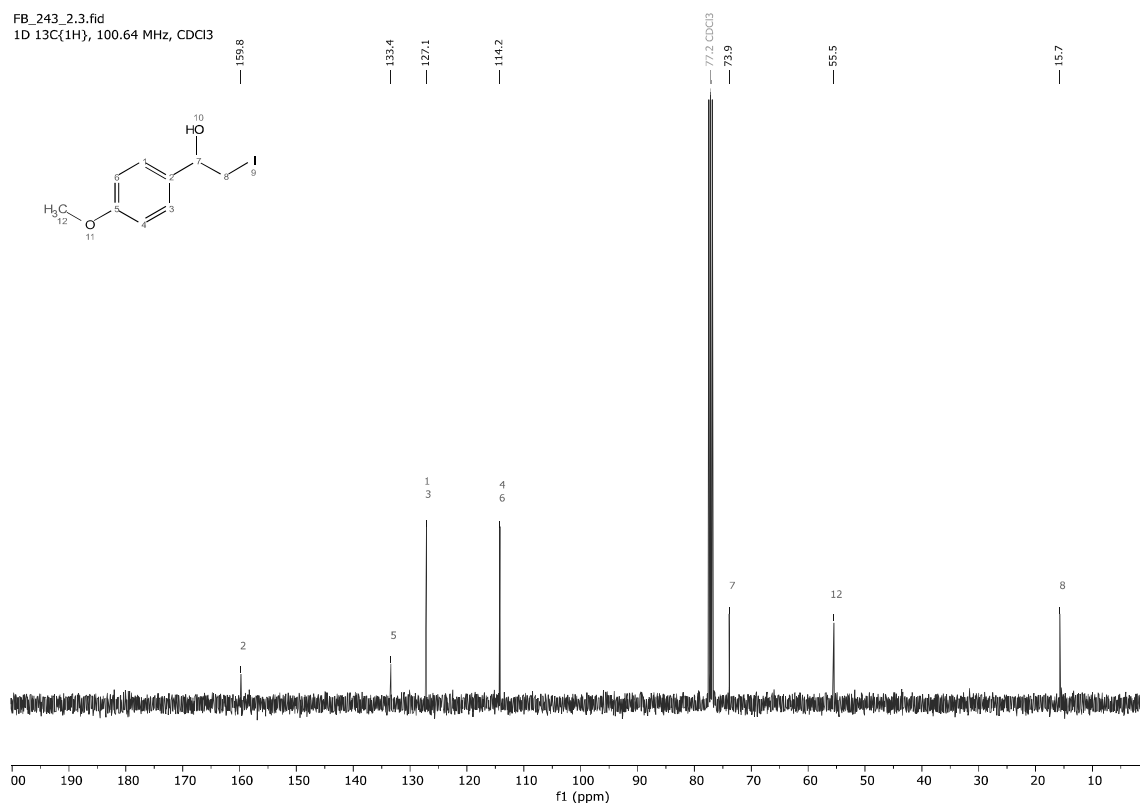


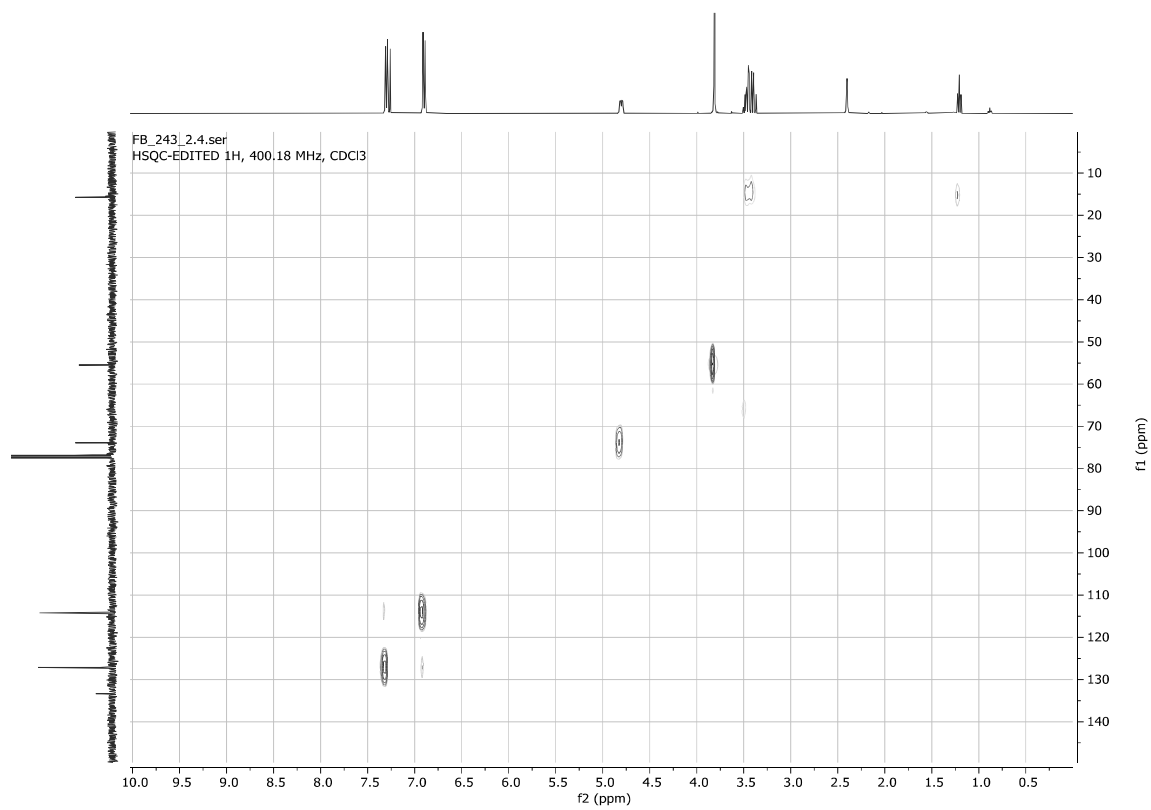
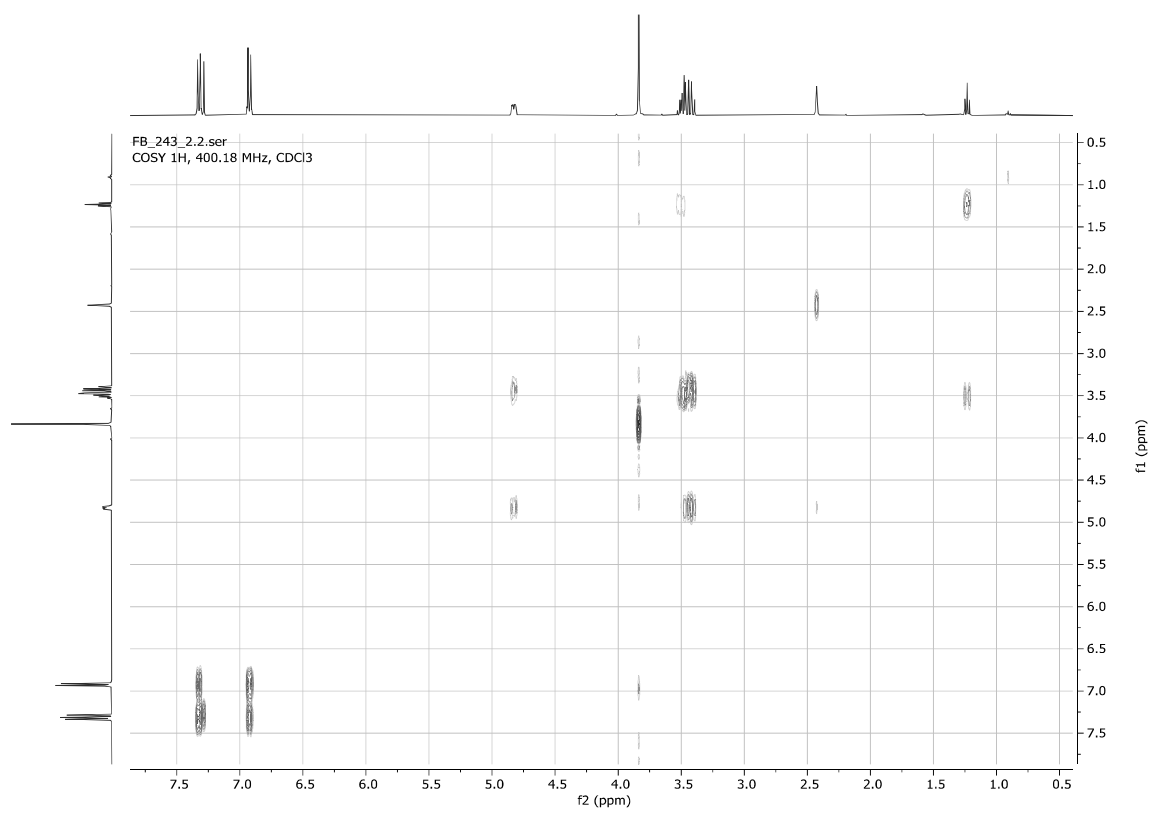
2-Iodo-1-(4-methoxyphenyl)ethan-1-ol **3o**

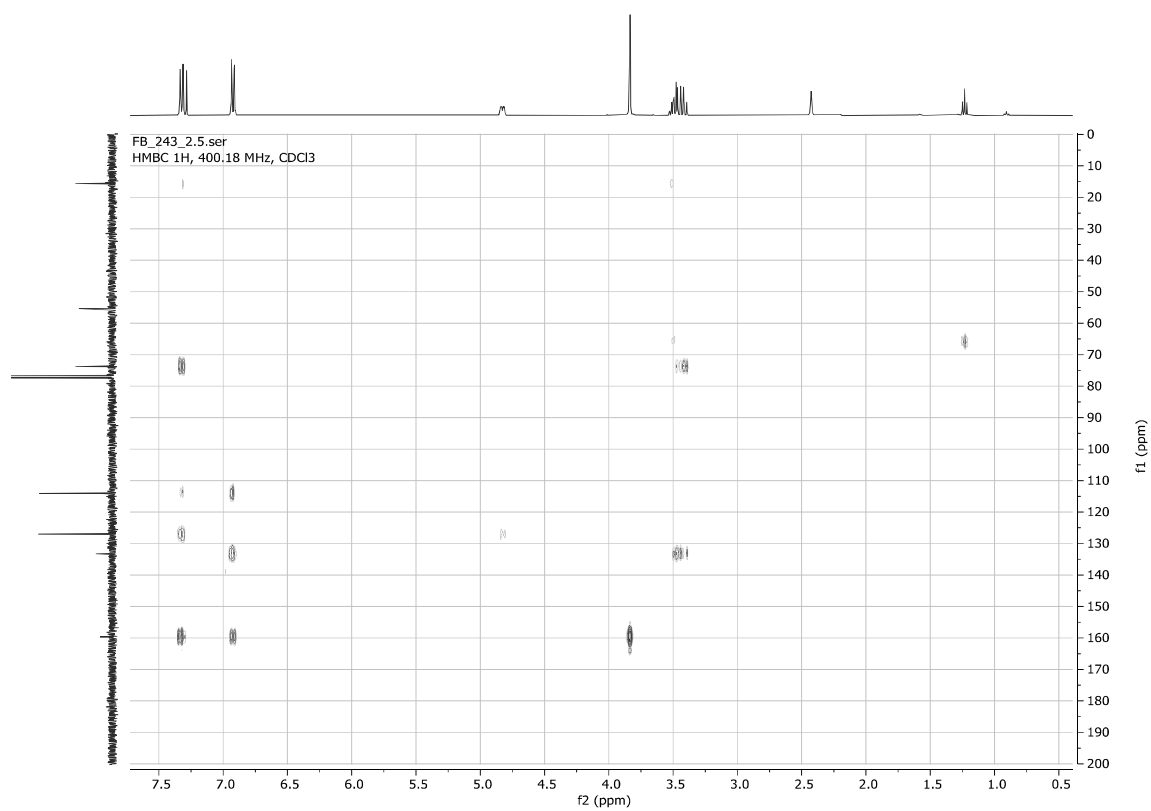
FB_243.1.fid
1D 1H, 400.18 MHz, CDCl3



FB_243_2.3.fid
1D 13C(1H), 100.64 MHz, CDCl3

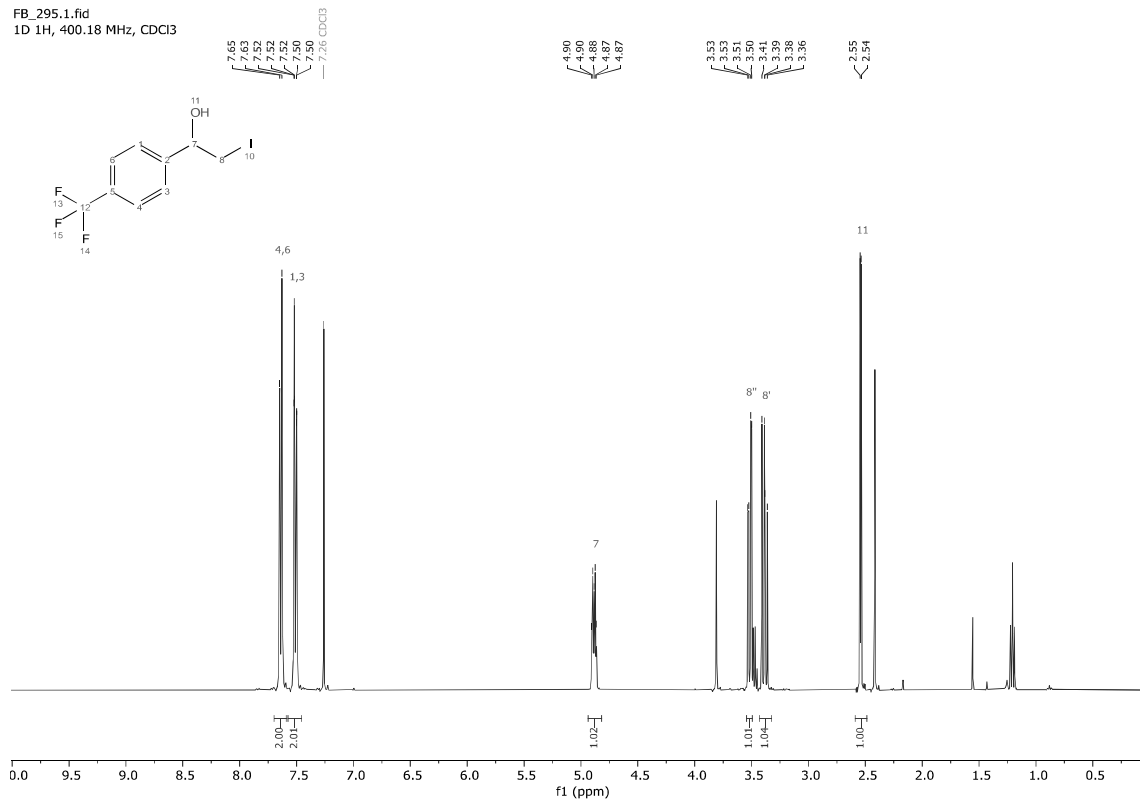




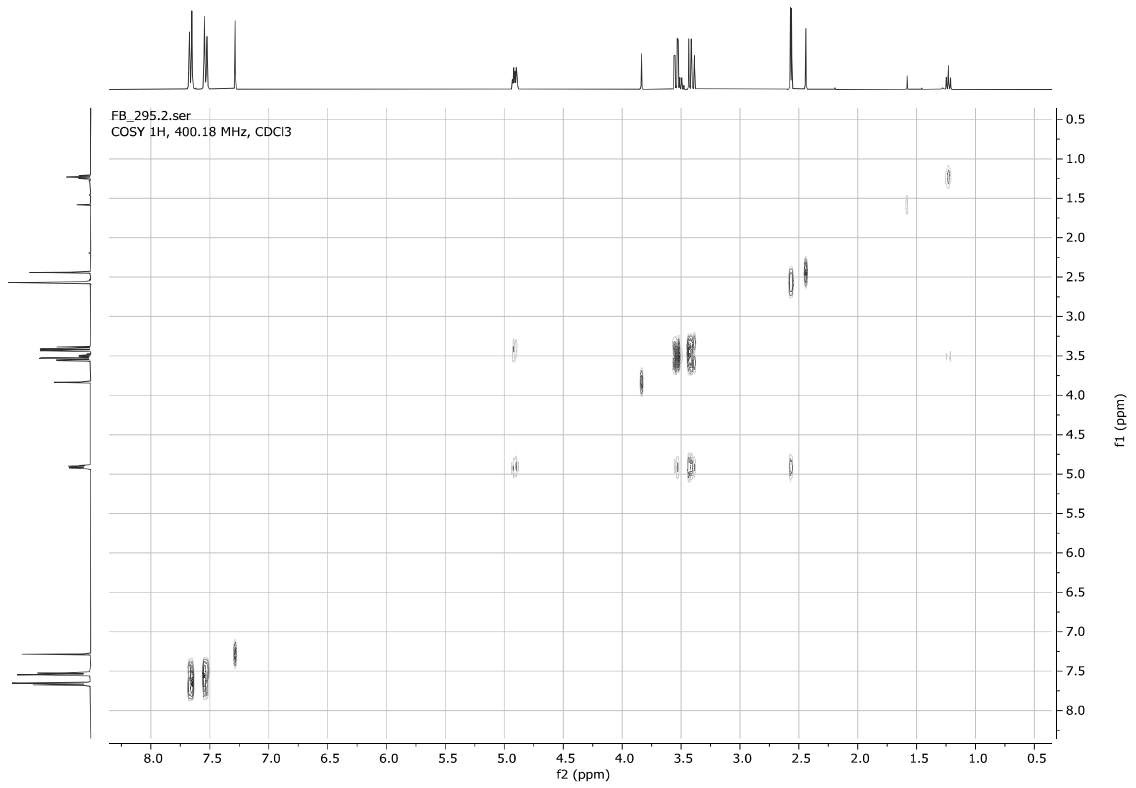
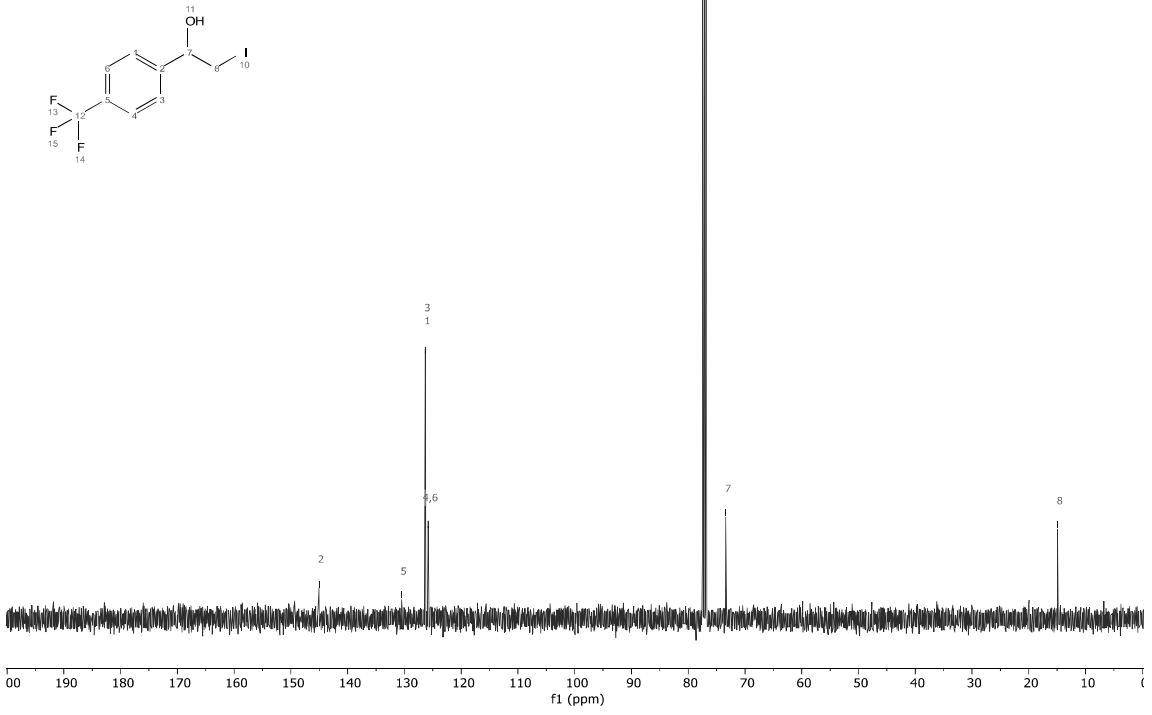


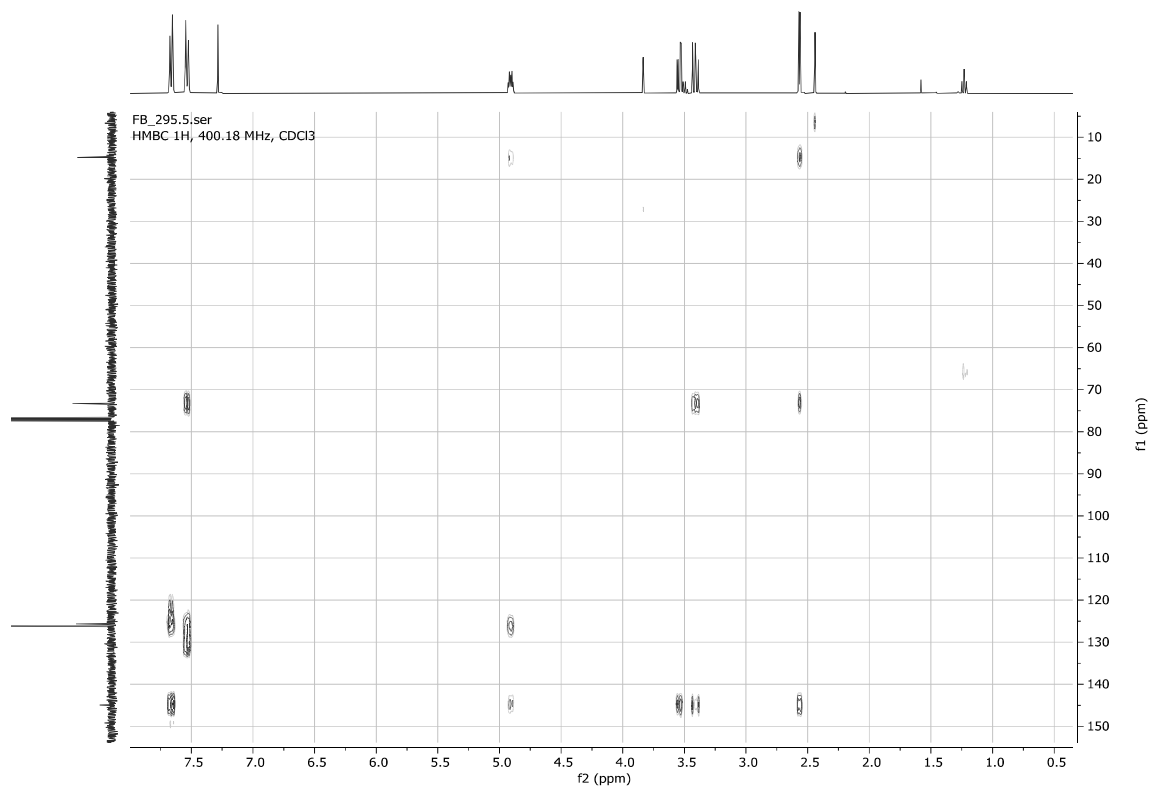
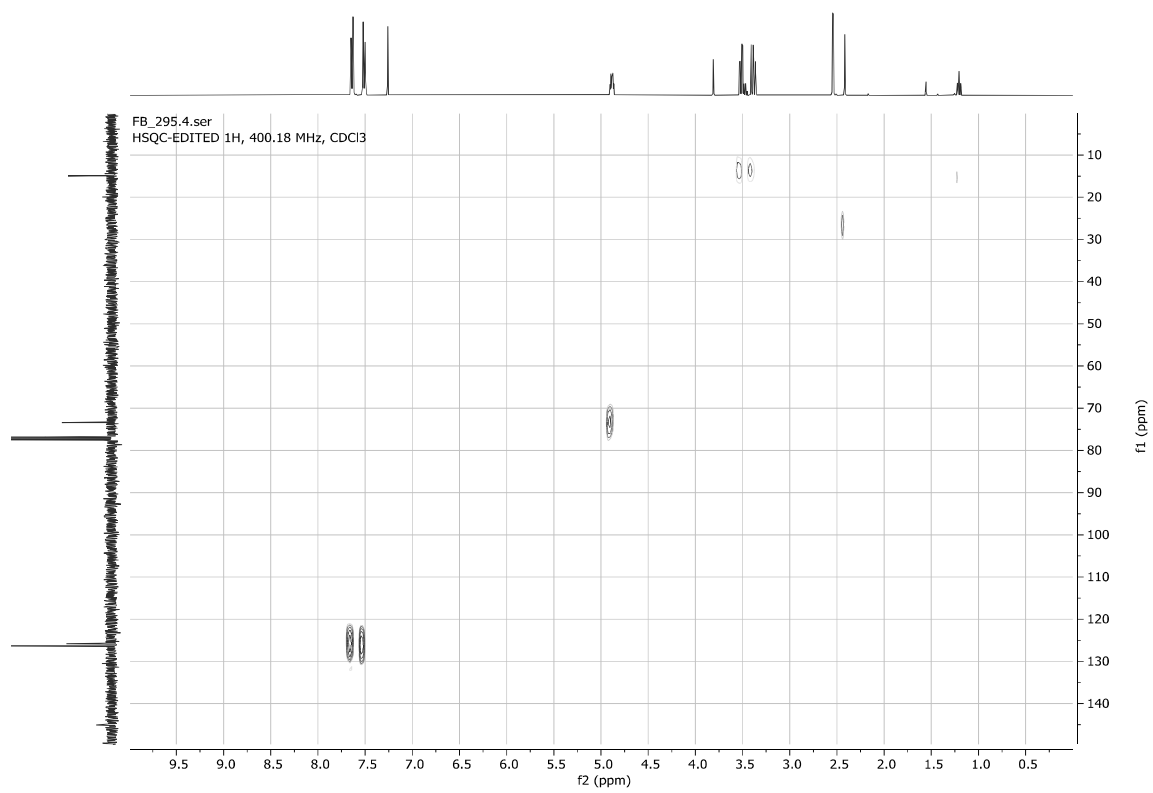
2-Iodo-1-(4-(trifluoromethyl)phenyl)ethan-1-ol **3p**

FB_295.1.fid
1D 1H, 400.18 MHz, CDCl3



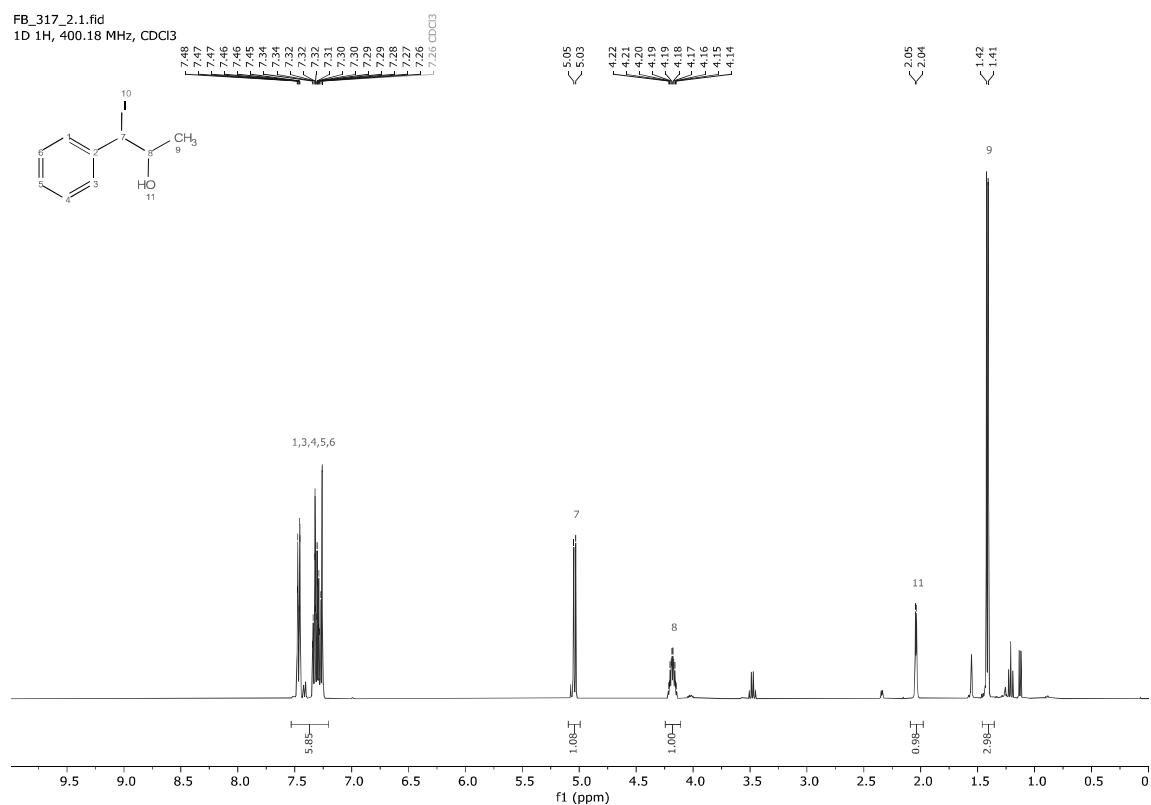
FB_295.3.fid
1D 13C{1H}, 100.64 MHz, CDCl3



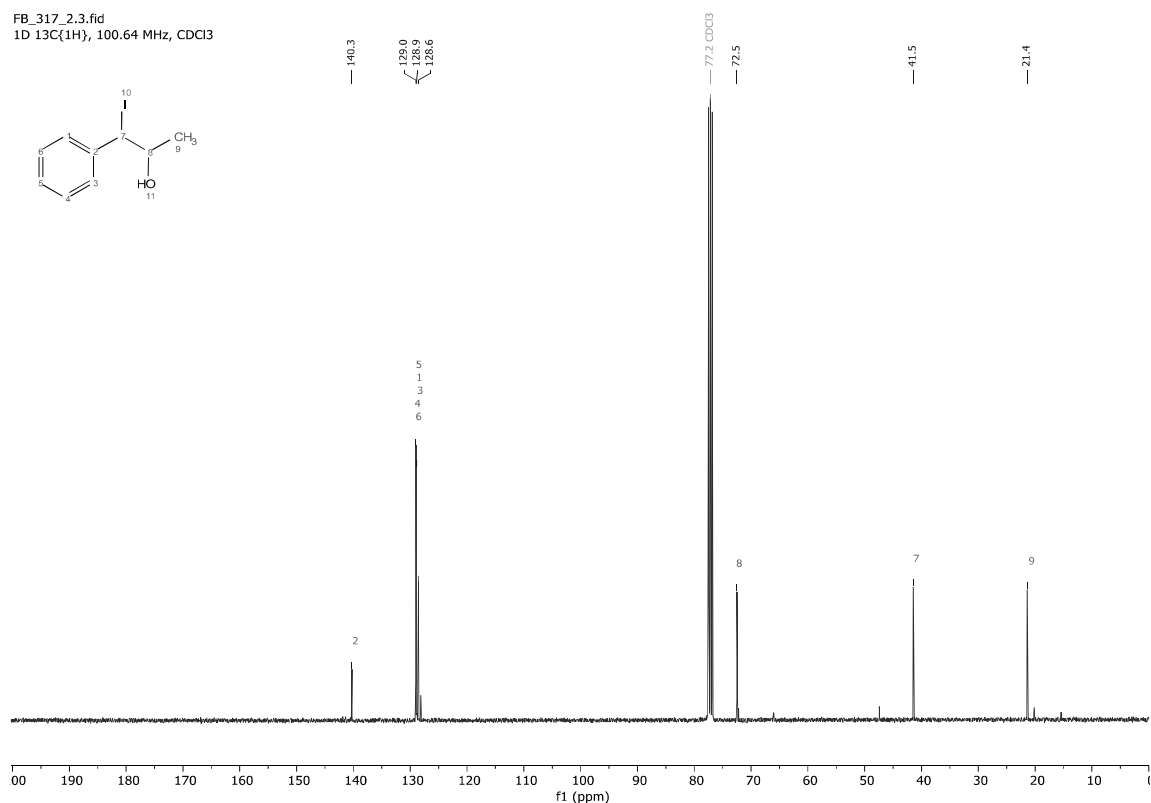


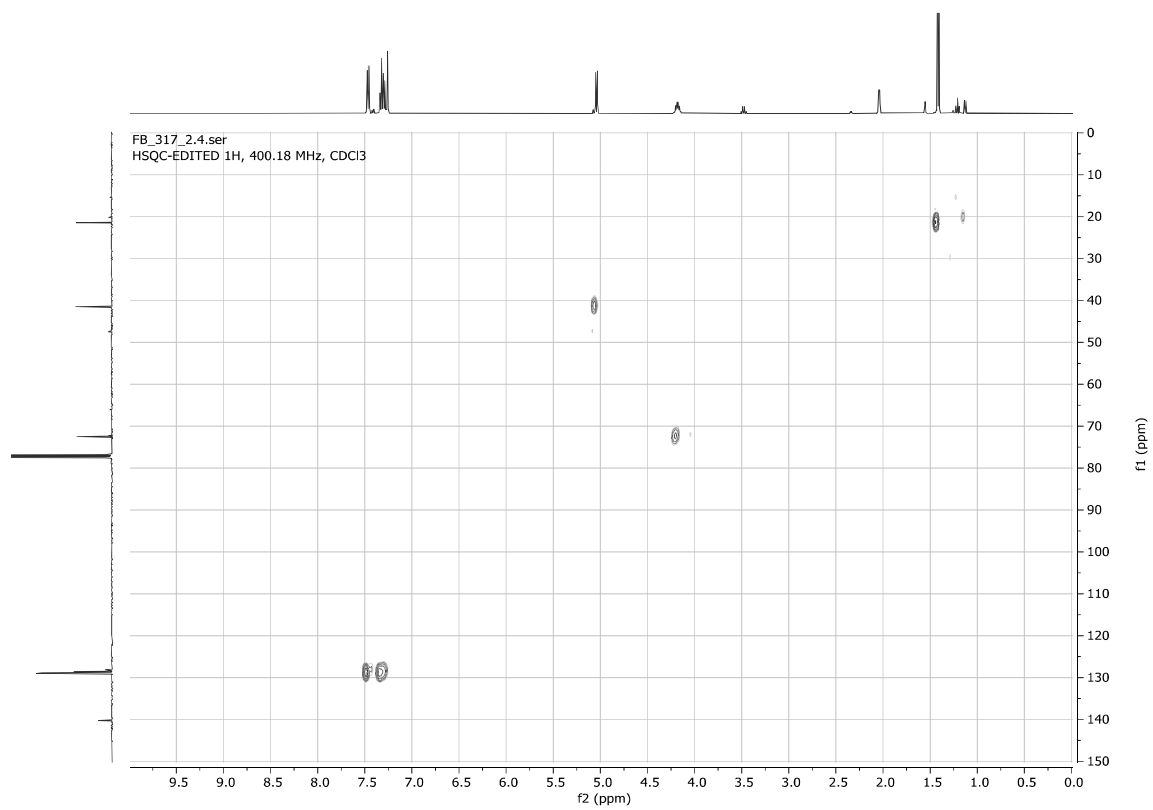
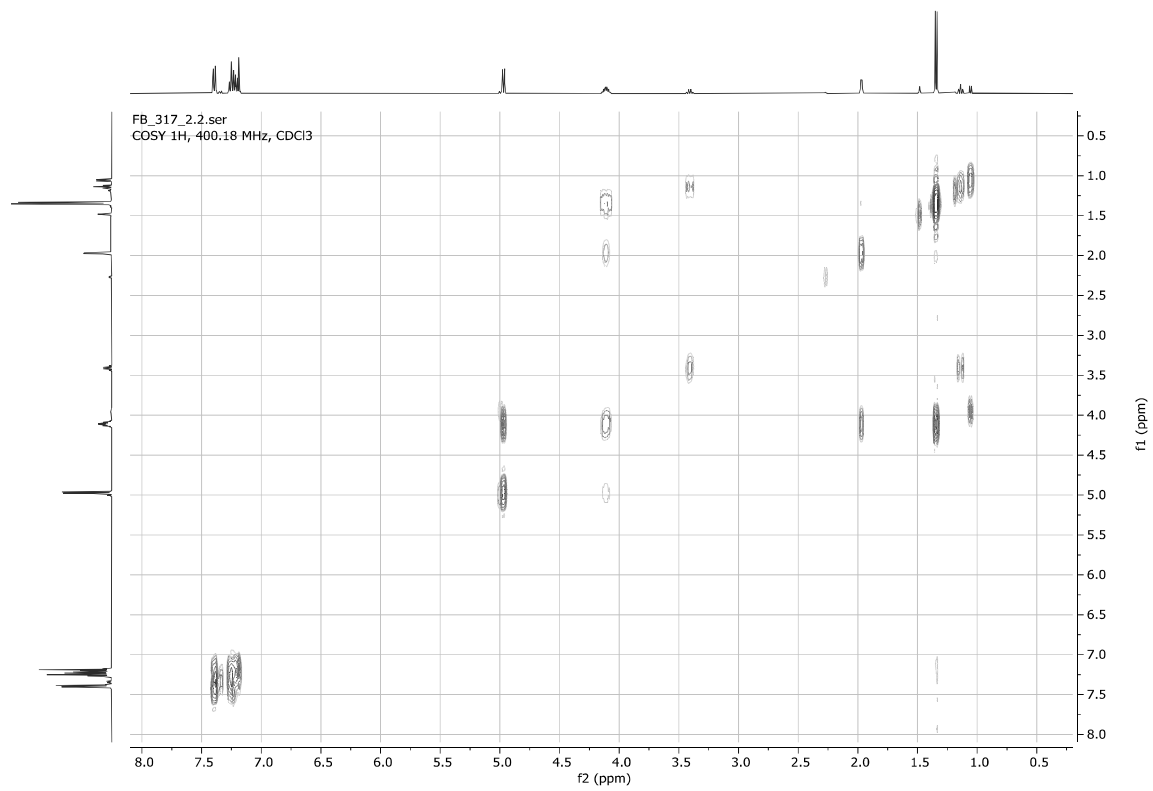
1-Iodo-1-phenylpropan-2-ol **3q** (*inseparable 89:11 diastereomers mixture*)

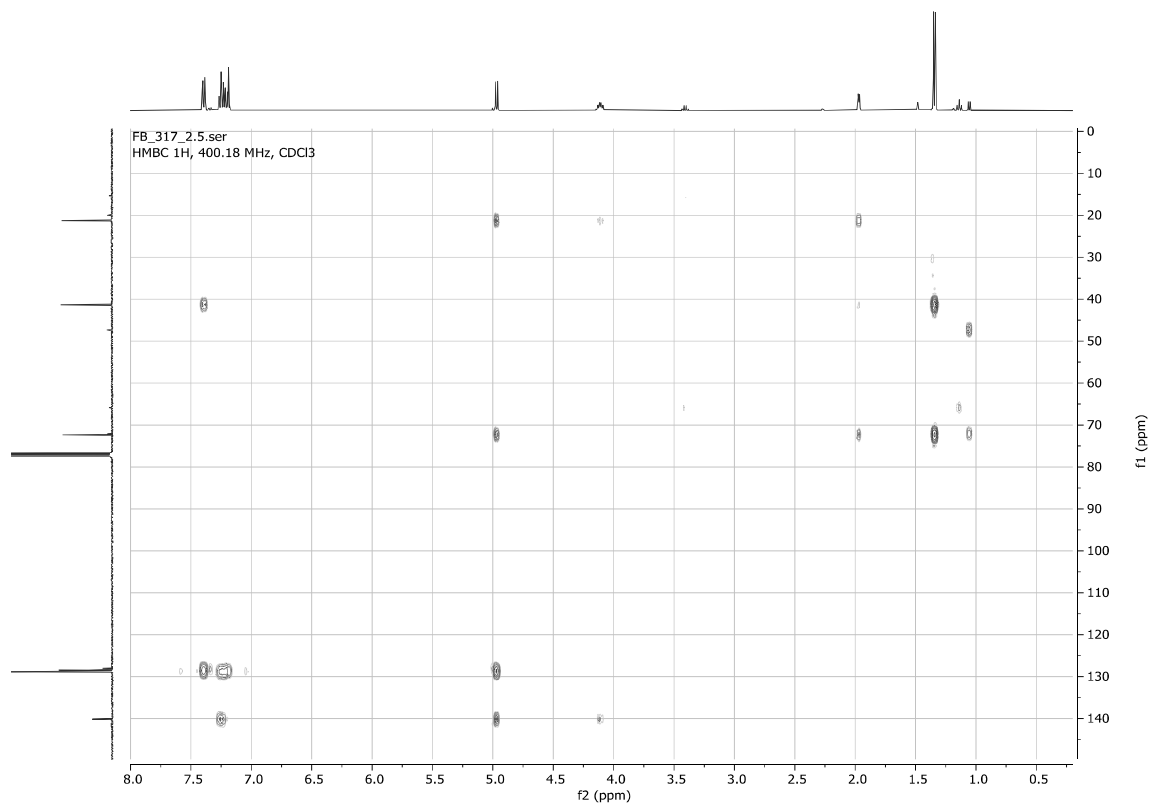
FB_317_2.1.fid
1D 1H, 400.18 MHz, CDCl₃



FB_317_2.3.fid
1D 13C(1H), 100.64 MHz, CDCl₃

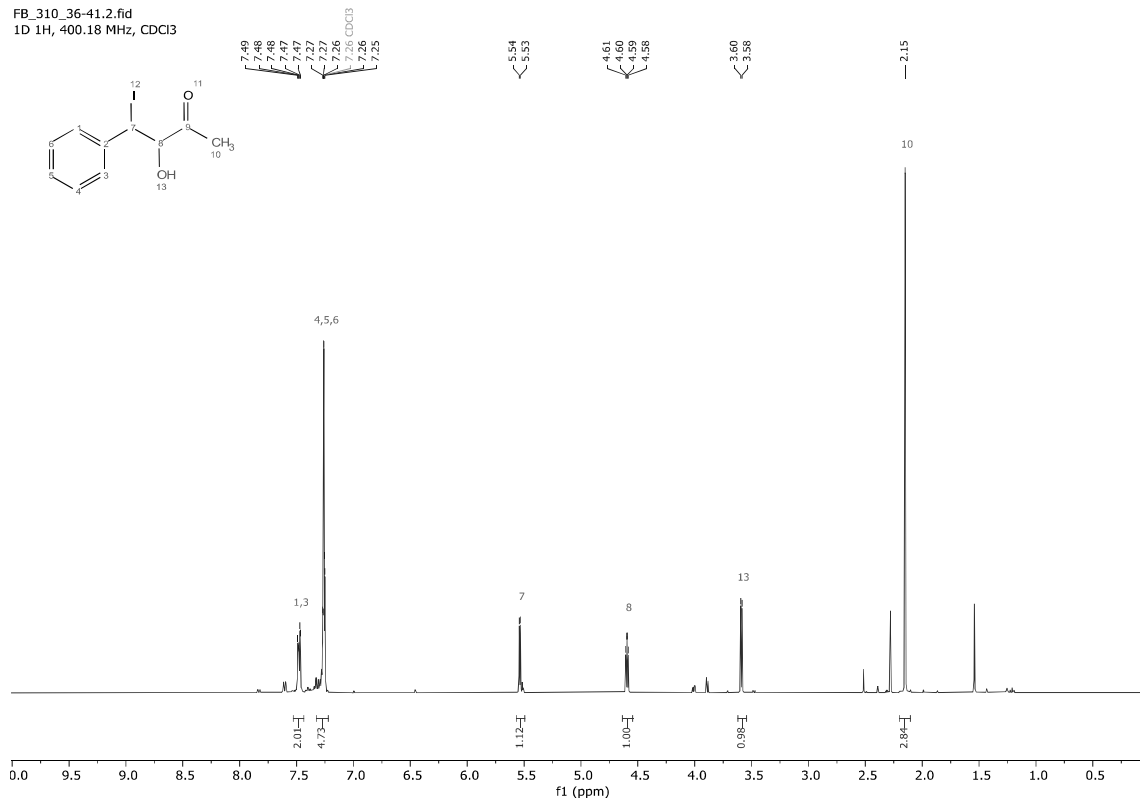




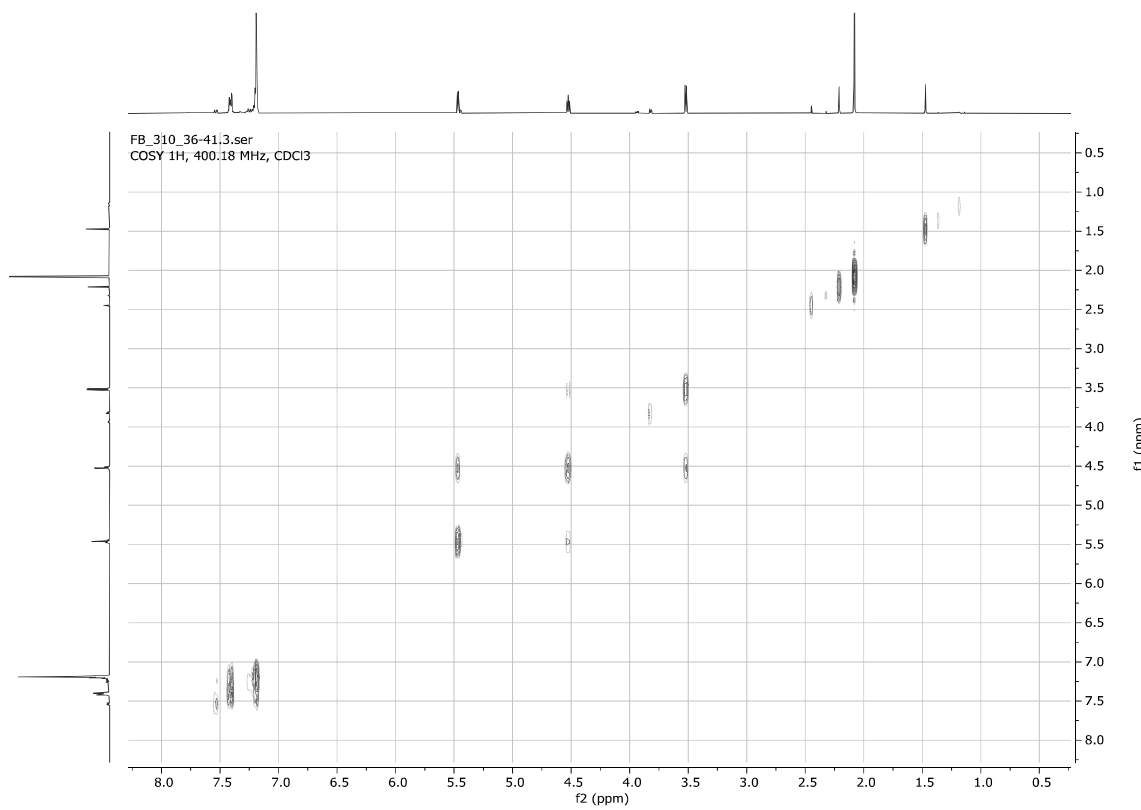
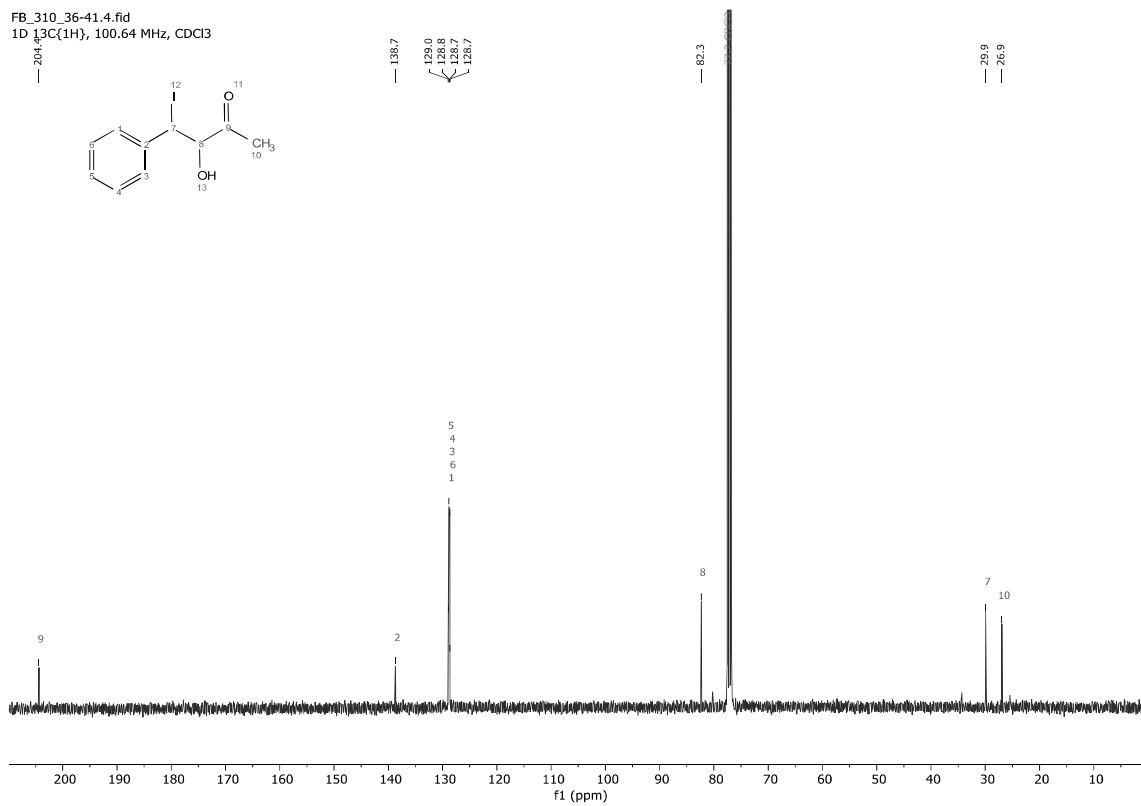


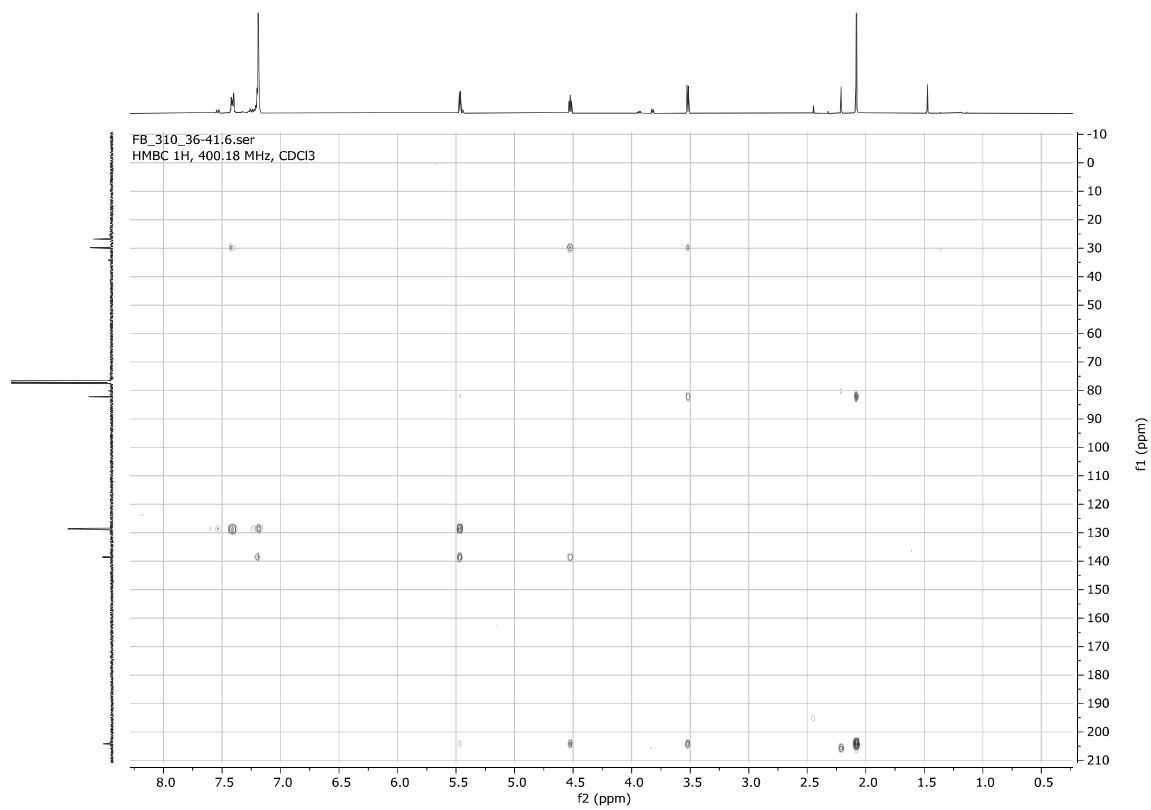
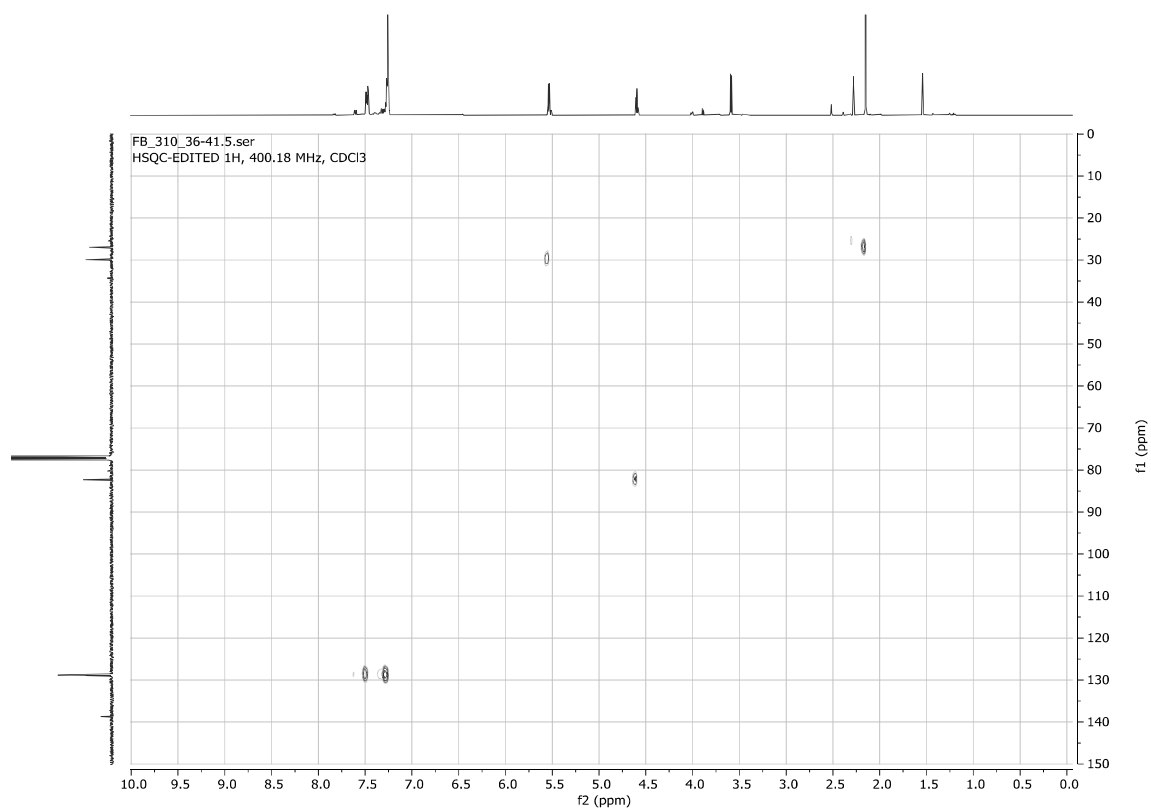
3-Hydroxy-4-iodo-4-phenylbutan-2-one **3r** (*inseparable 86:14 diastereomers mixture*)

FB_310_36-41.2.fid
1D 1H, 400.18 MHz, CDCl3

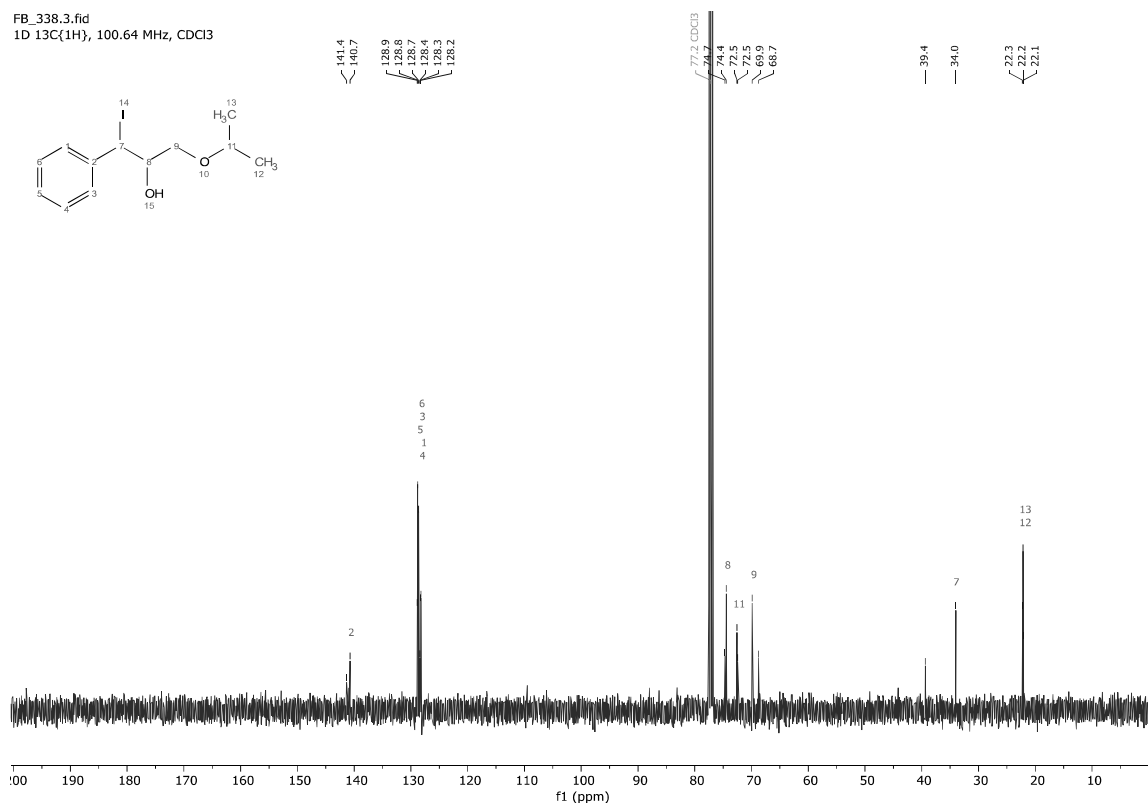
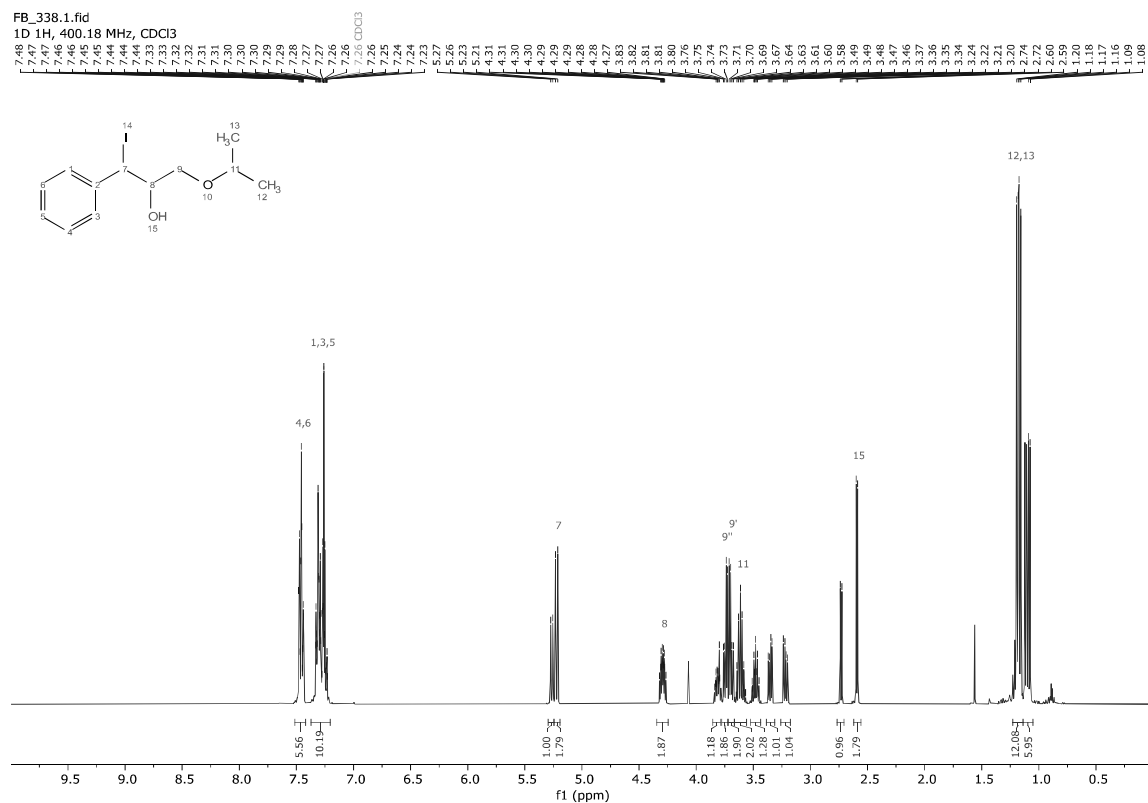


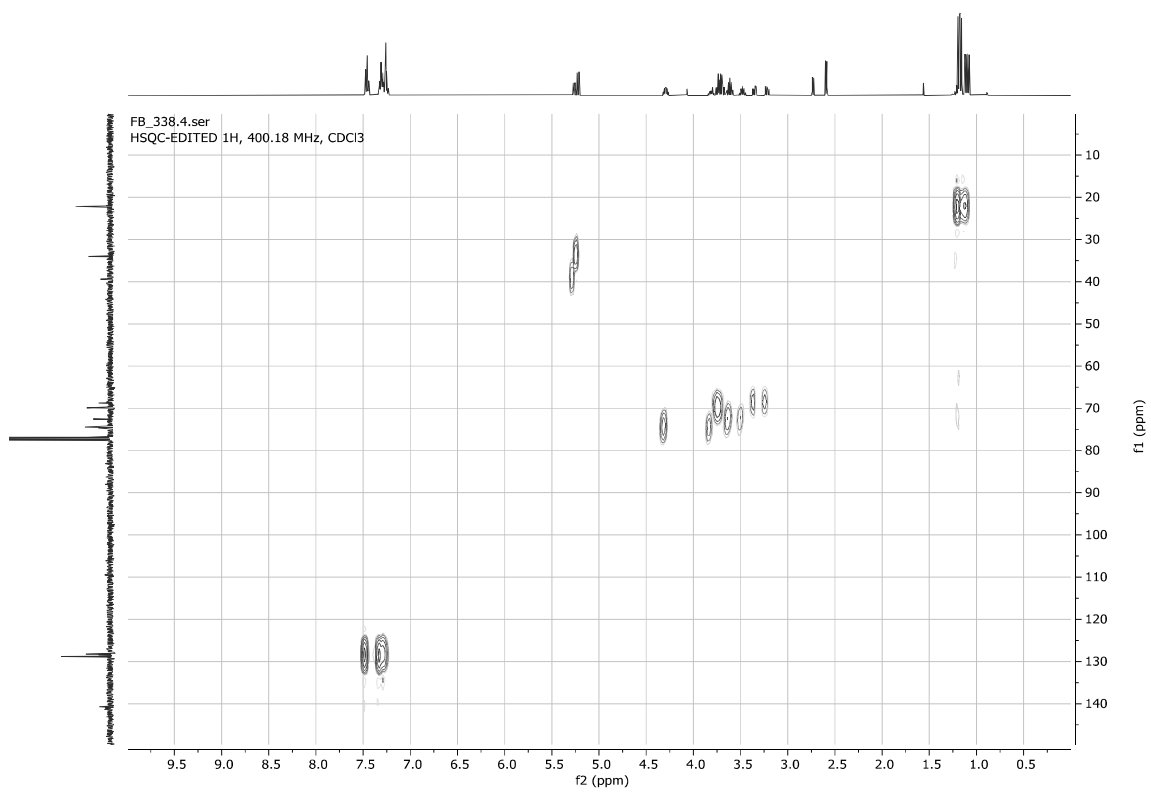
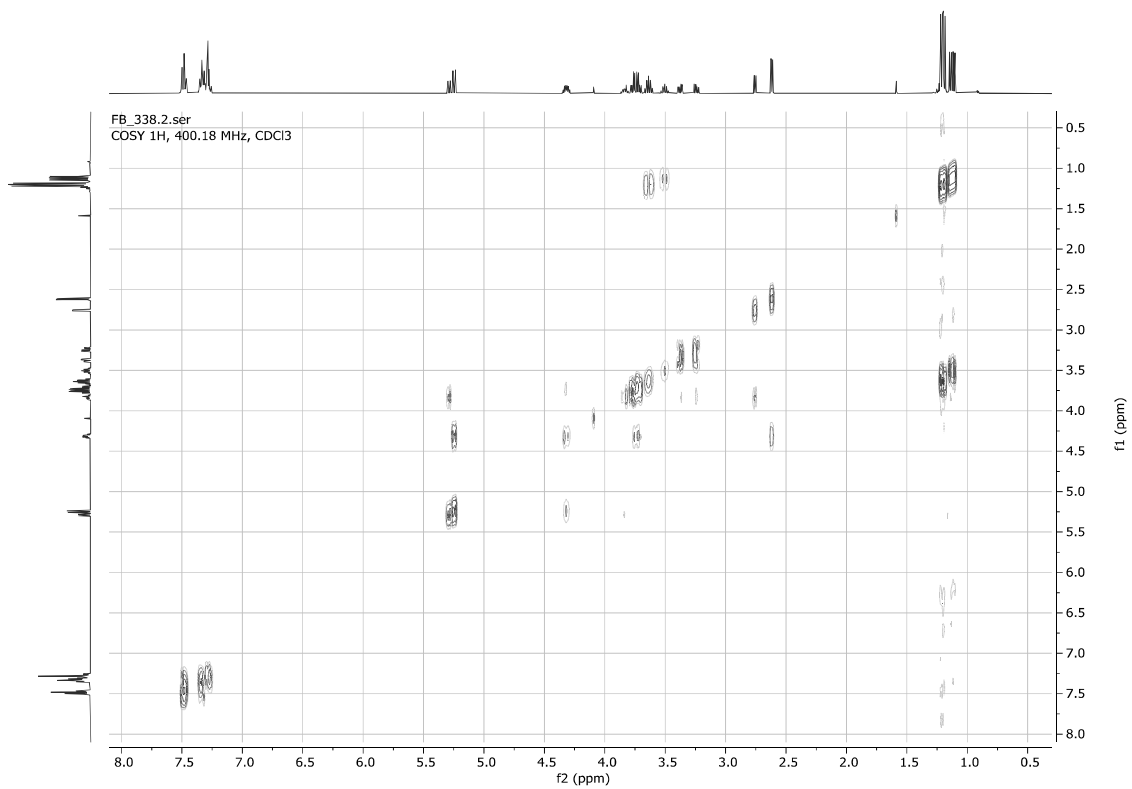
FB_310_36-41.4.fid
1D ¹³C{¹H}, 100.64 MHz, CDCl₃

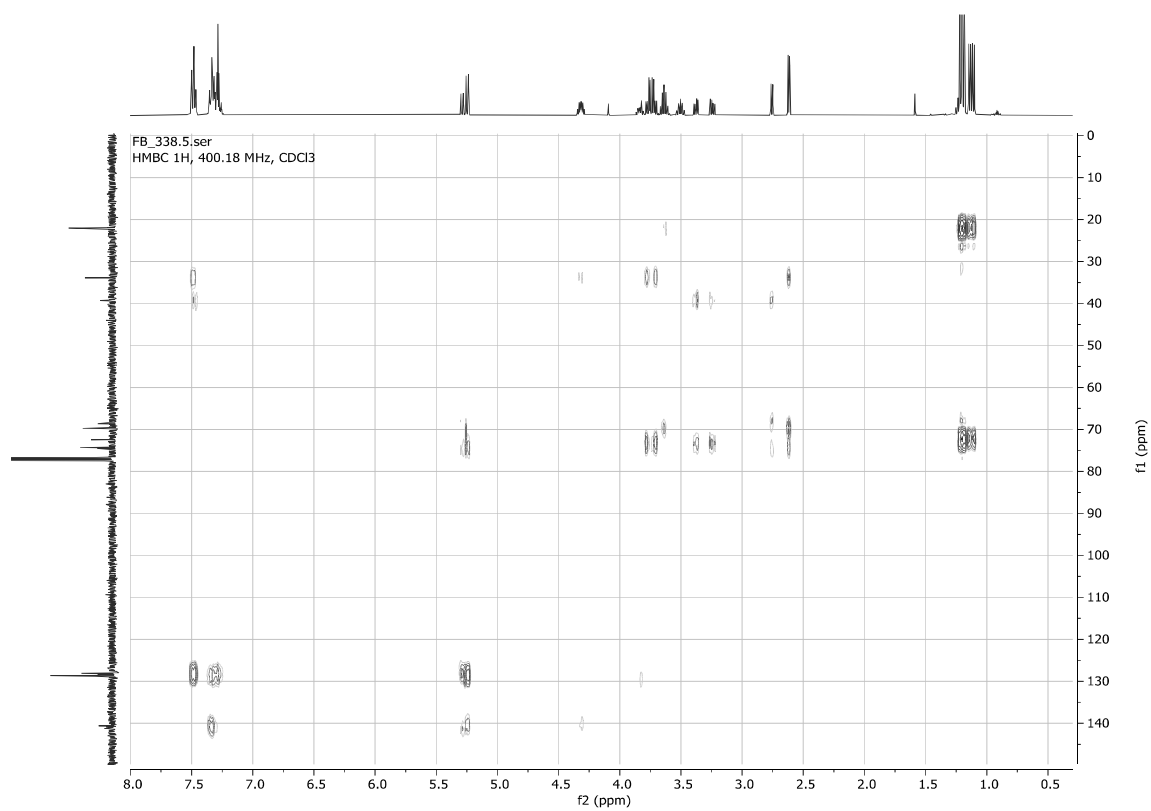




1-Iodo-3-isopropoxy-1-phenylpropan-2-ol **3s** (*inseparable 64:36 diastereomers mixture*)

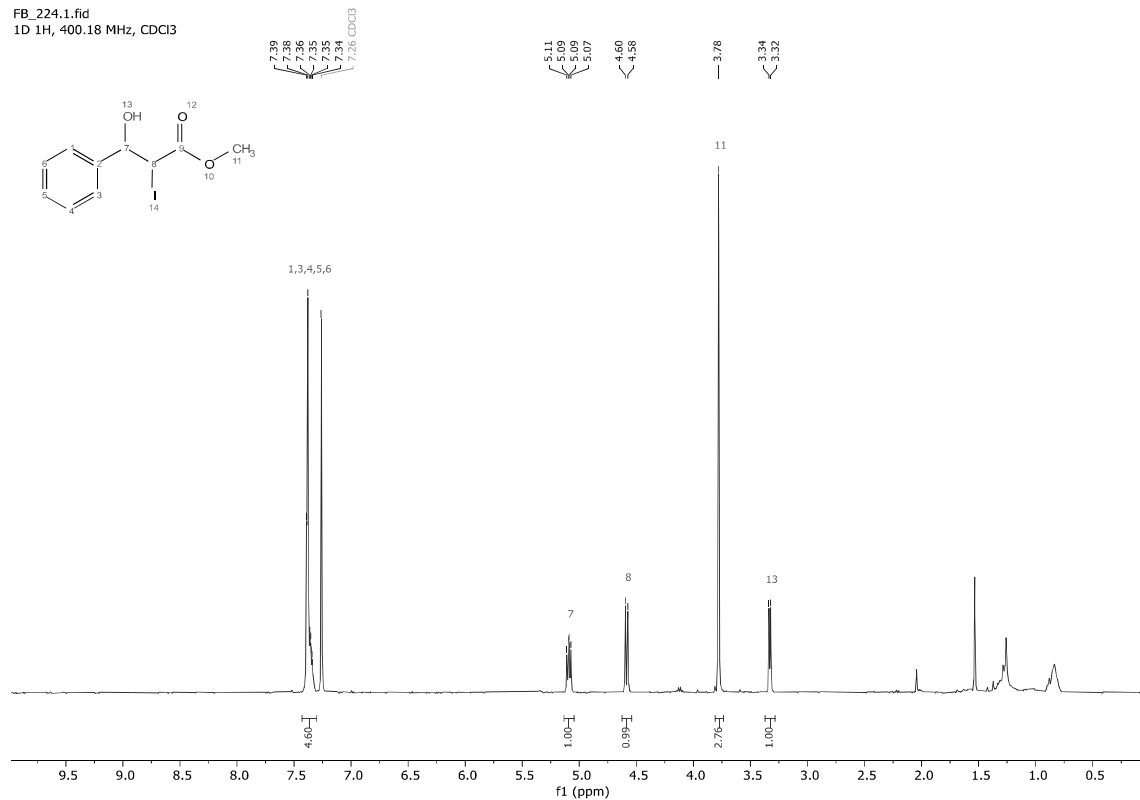




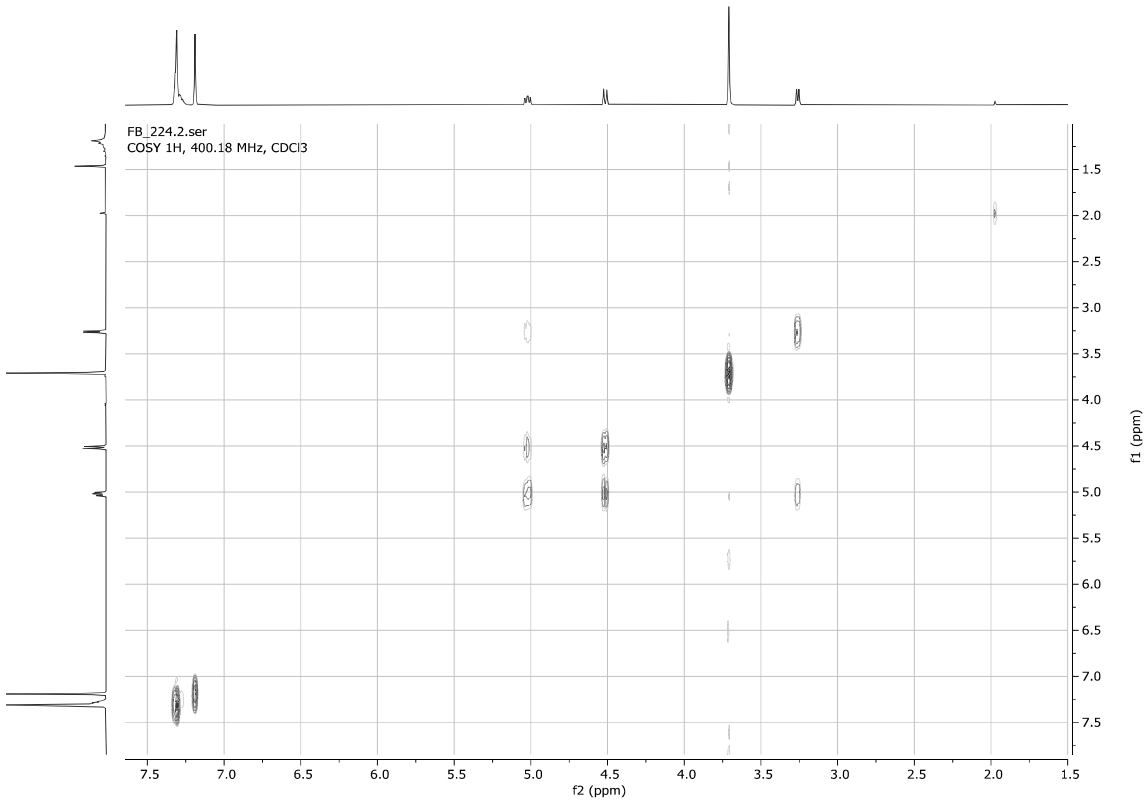
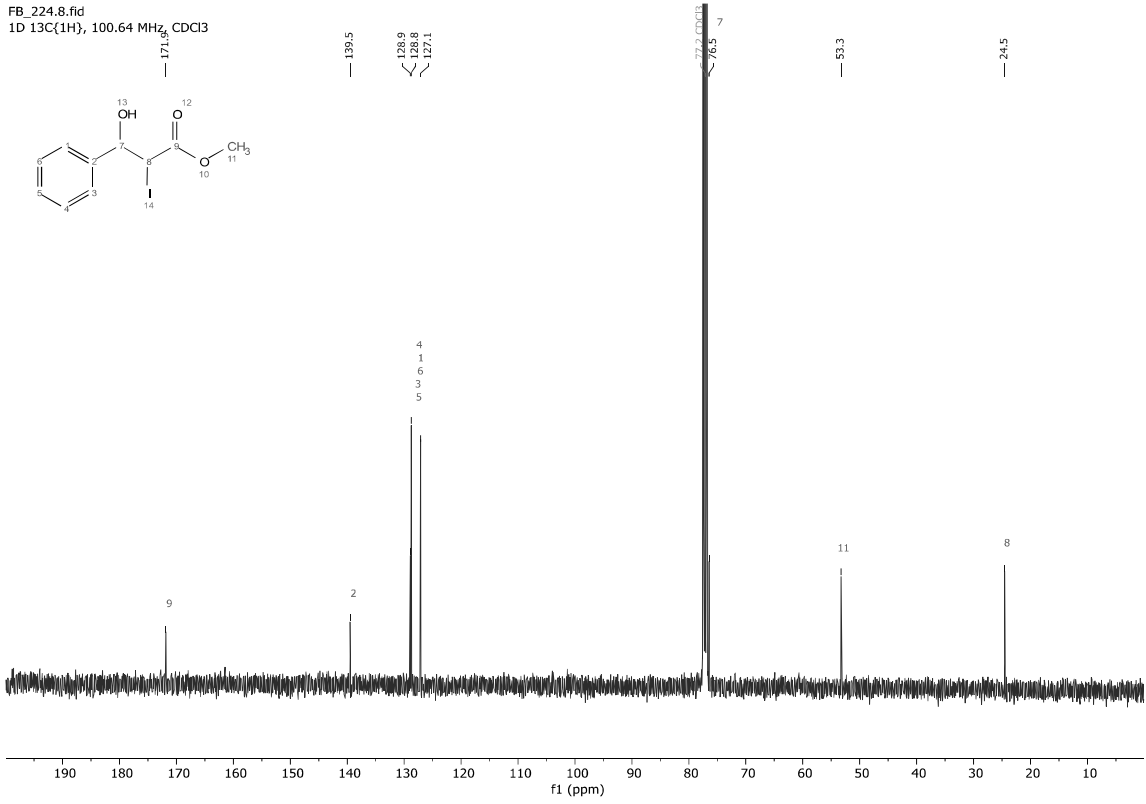


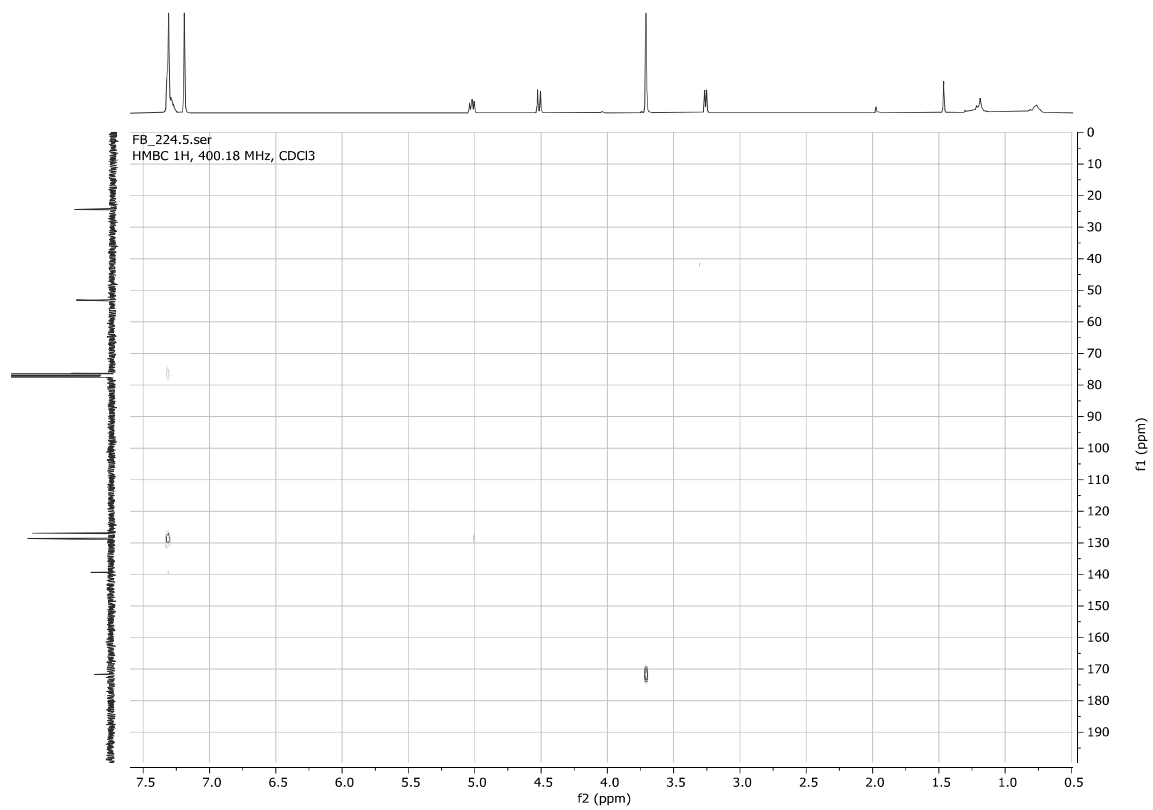
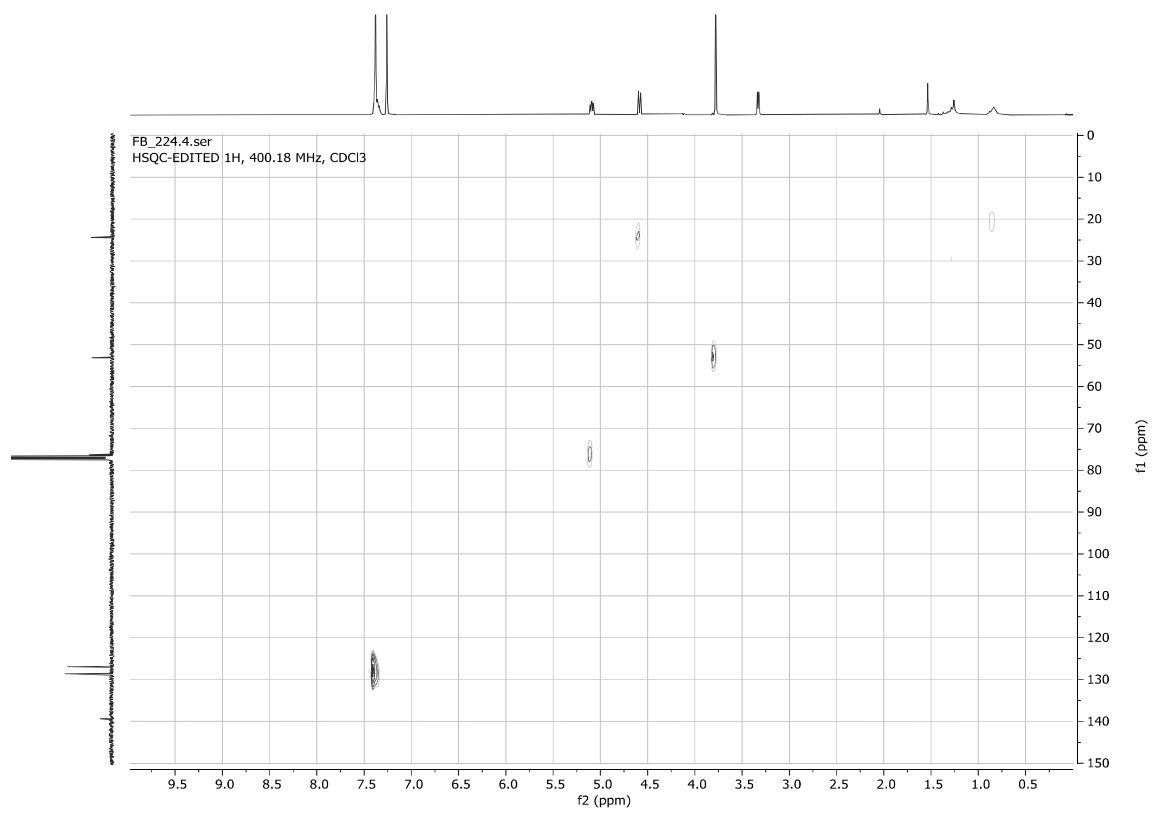
Methyl 3-hydroxy-2-iodo-3-phenylpropanoate 3t

FB_224.1.fid
1D 1H, 400.18 MHz, CDCl3



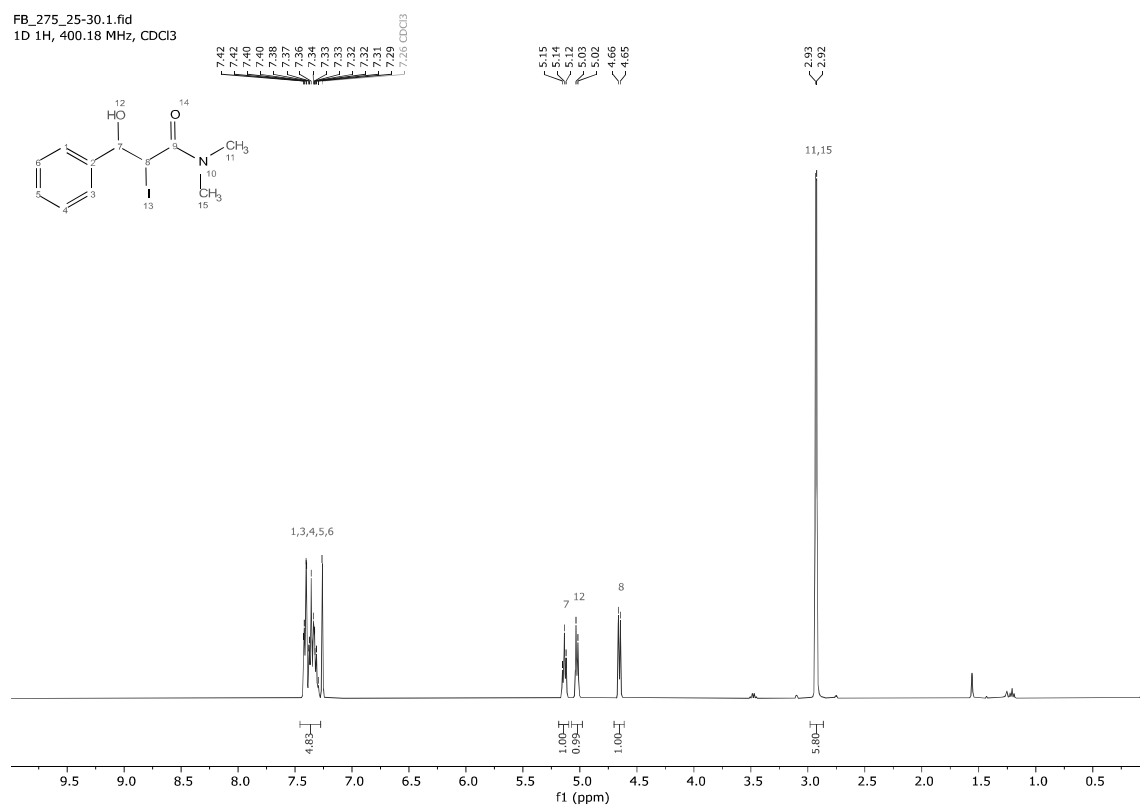
FB_224.8.fid
1D 13C{1H}, 100.64 MHz, CDCl3



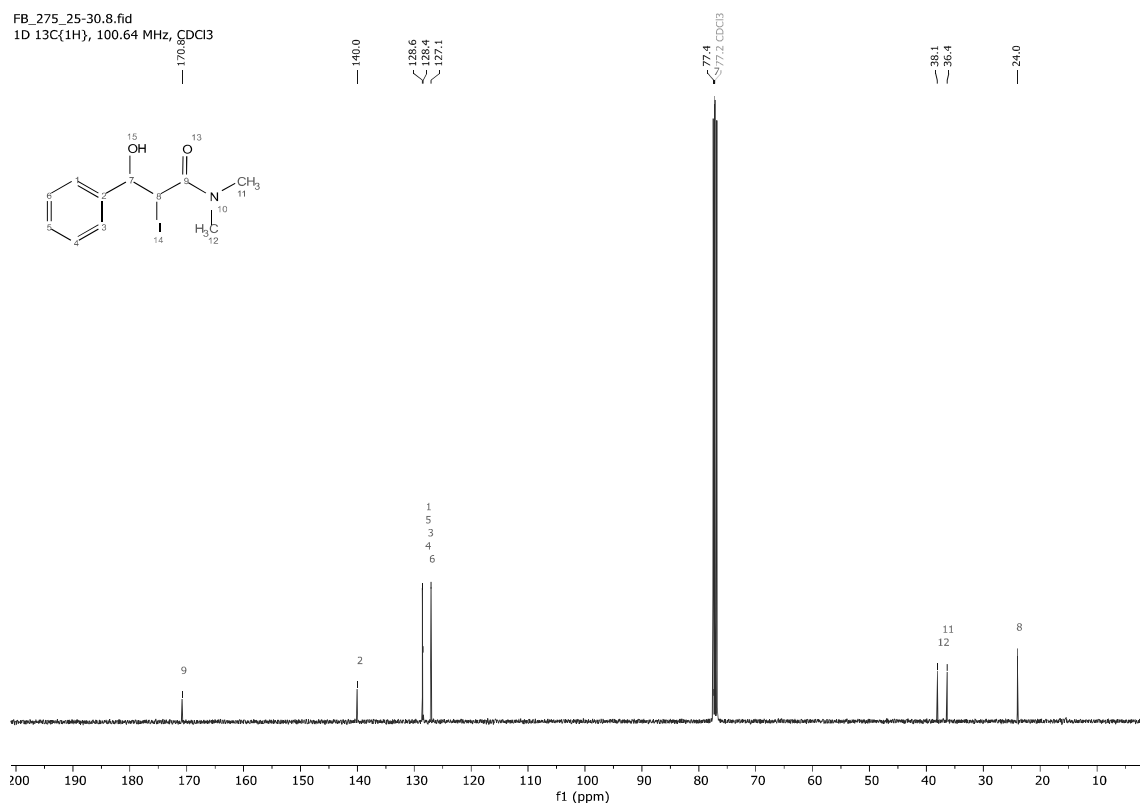


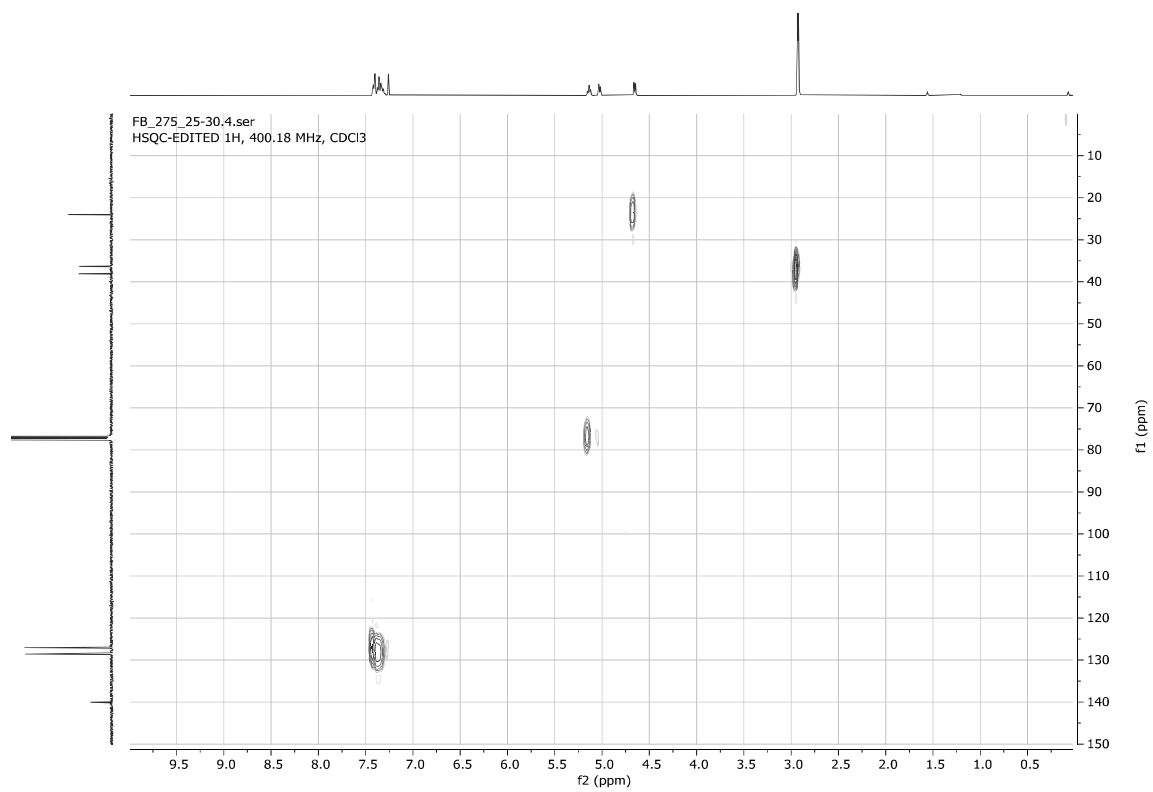
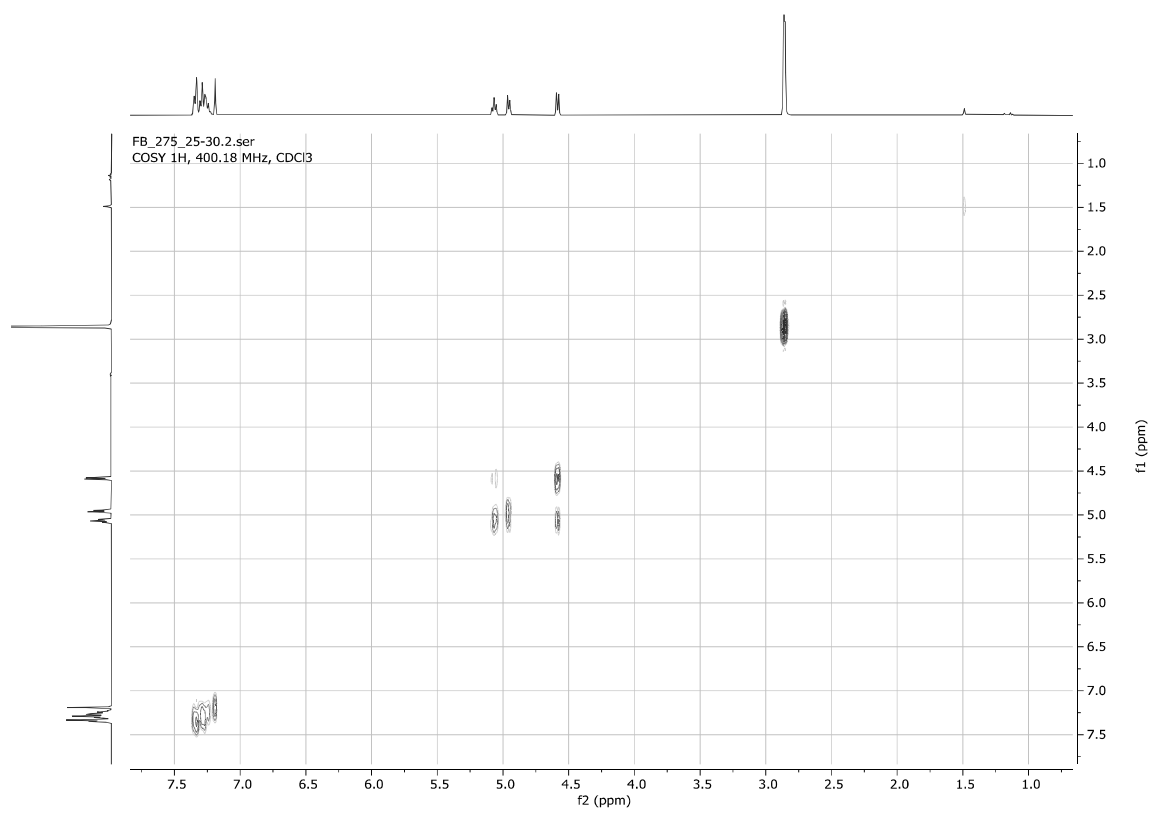
3-Hydroxy-2-iodo-*N,N*-dimethyl-3-phenylpropanamide **3u**

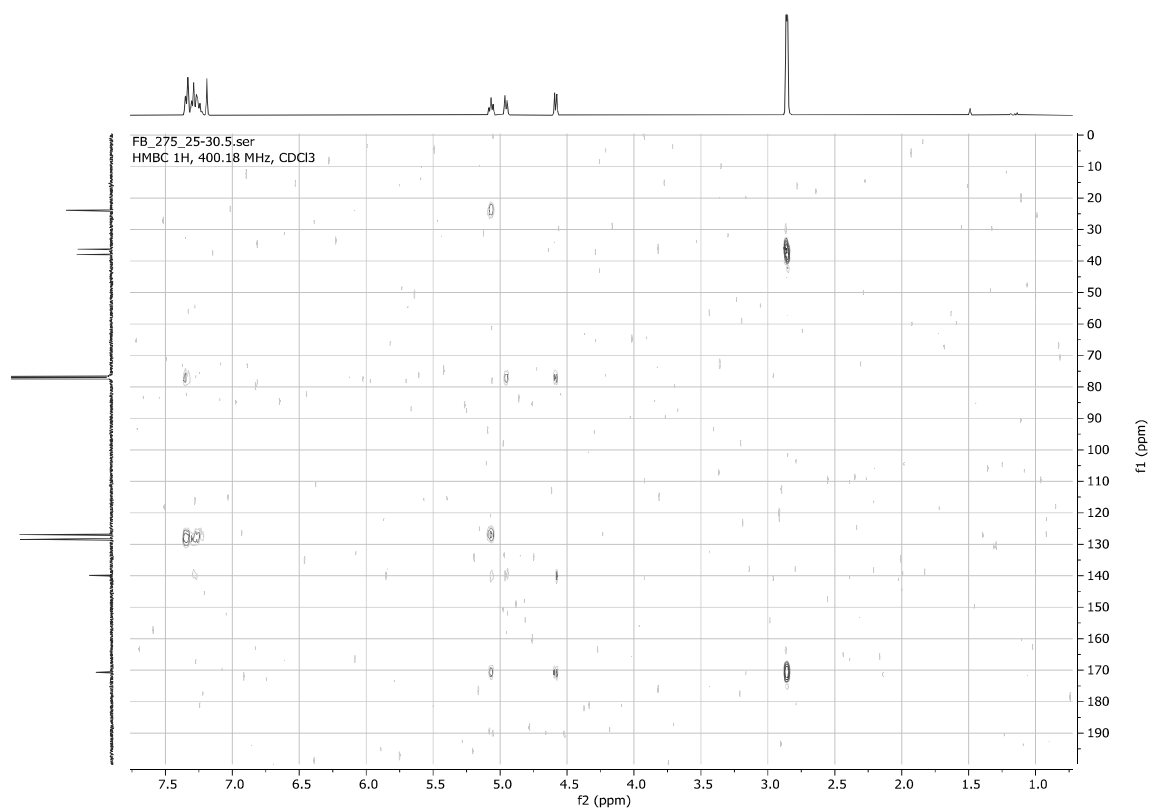
FB_275_25-30.1.fid
1D 1H, 400.18 MHz, CDCl₃



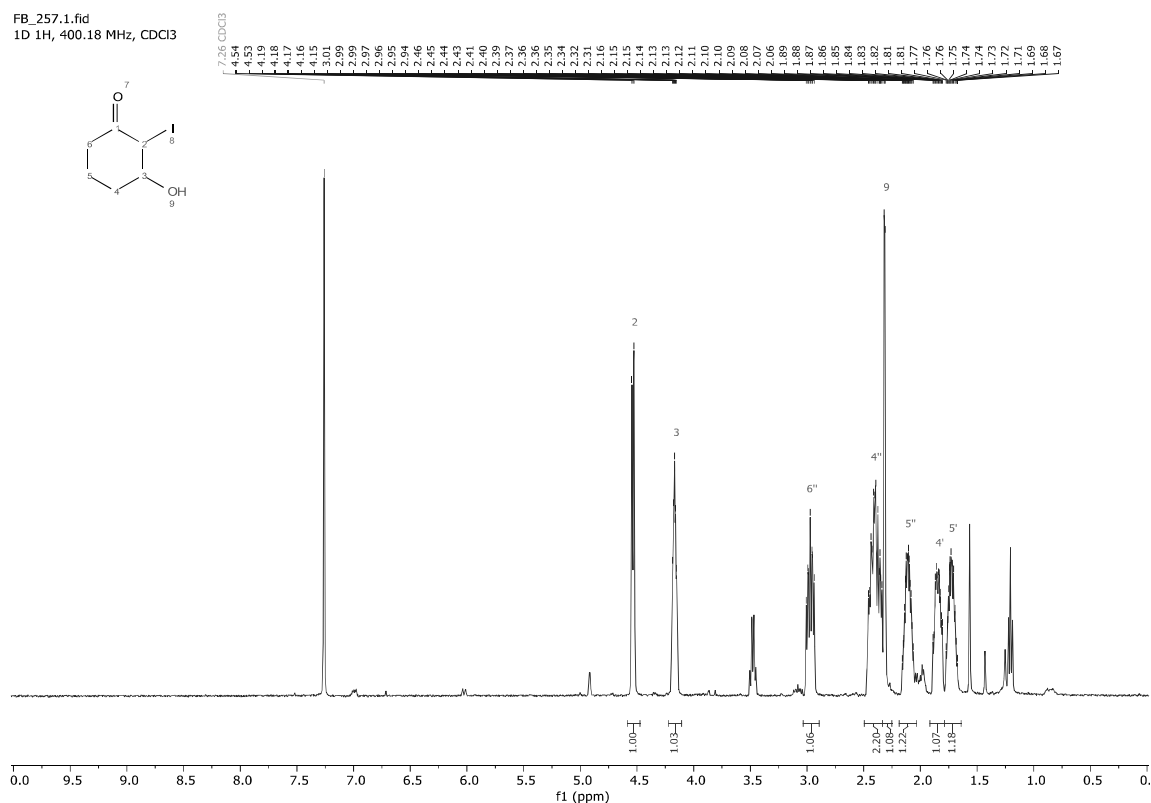
FB_275_25-30.8.fid
1D 13C(1H), 100.64 MHz, CDCl₃



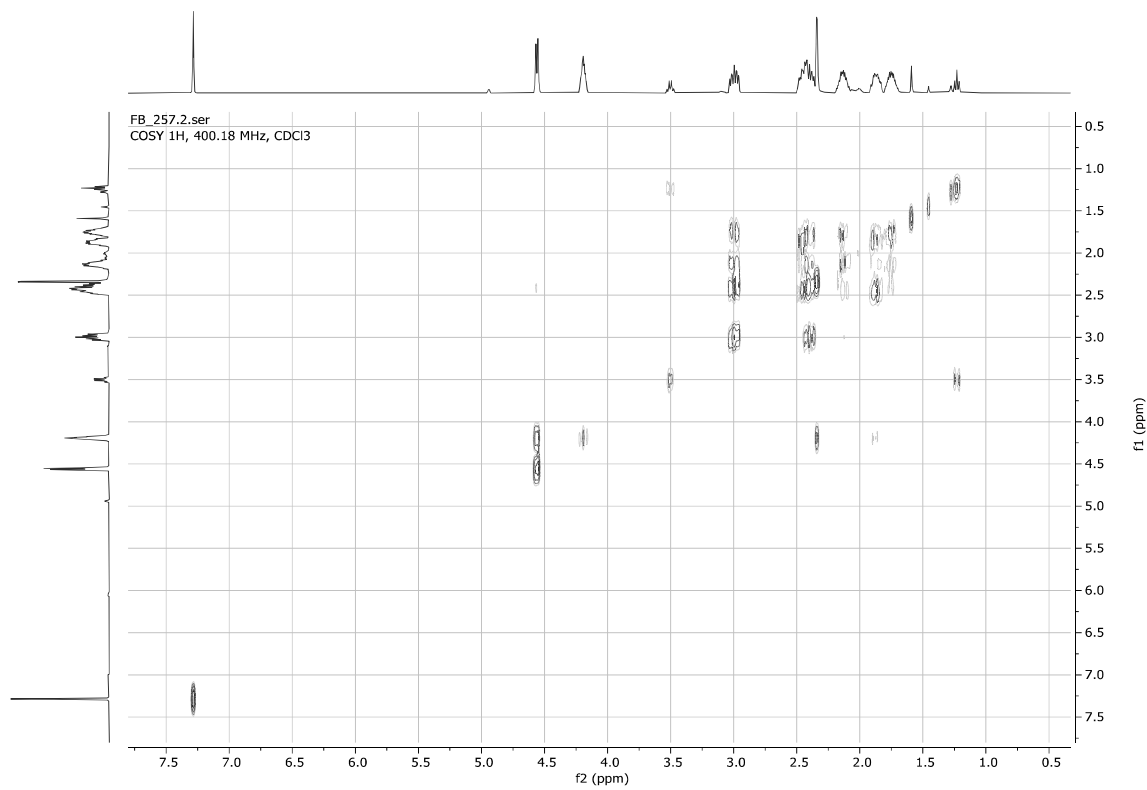
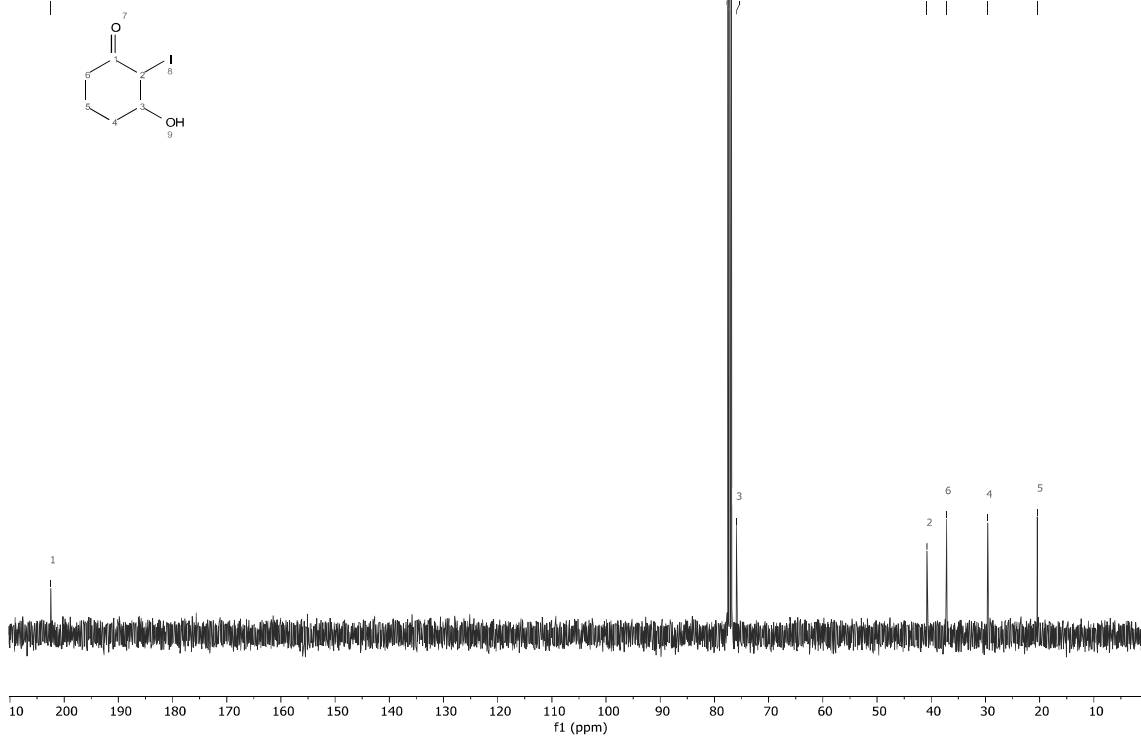


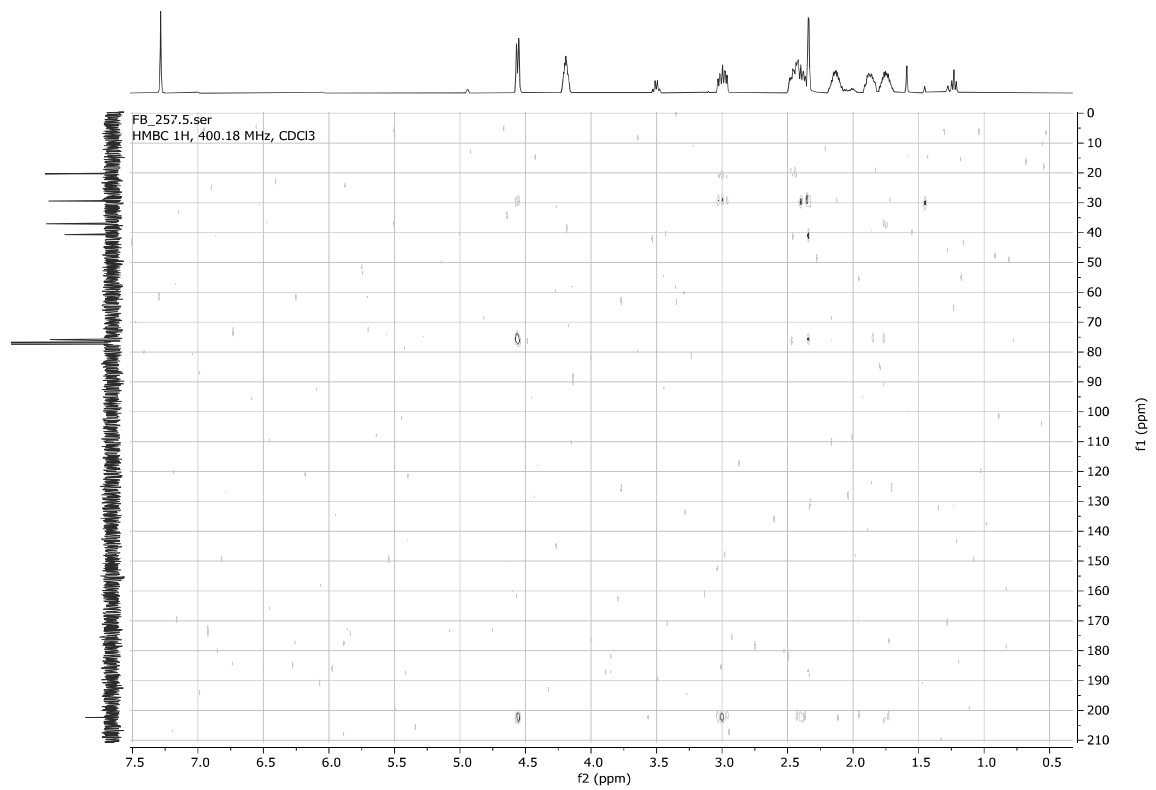
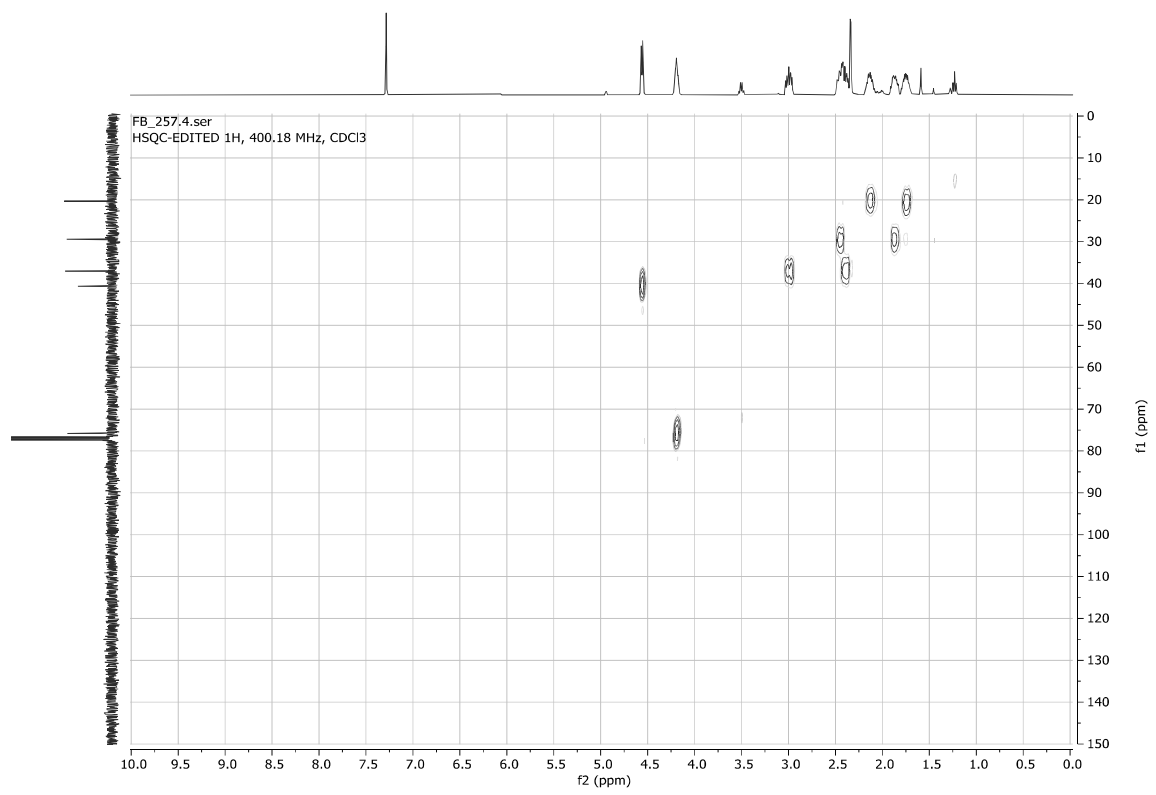


3-Hydroxy-2-iodocyclohexan-1-one **3v** (*Et₂O* peaks visible at 3.48 and 1.21 ppm)

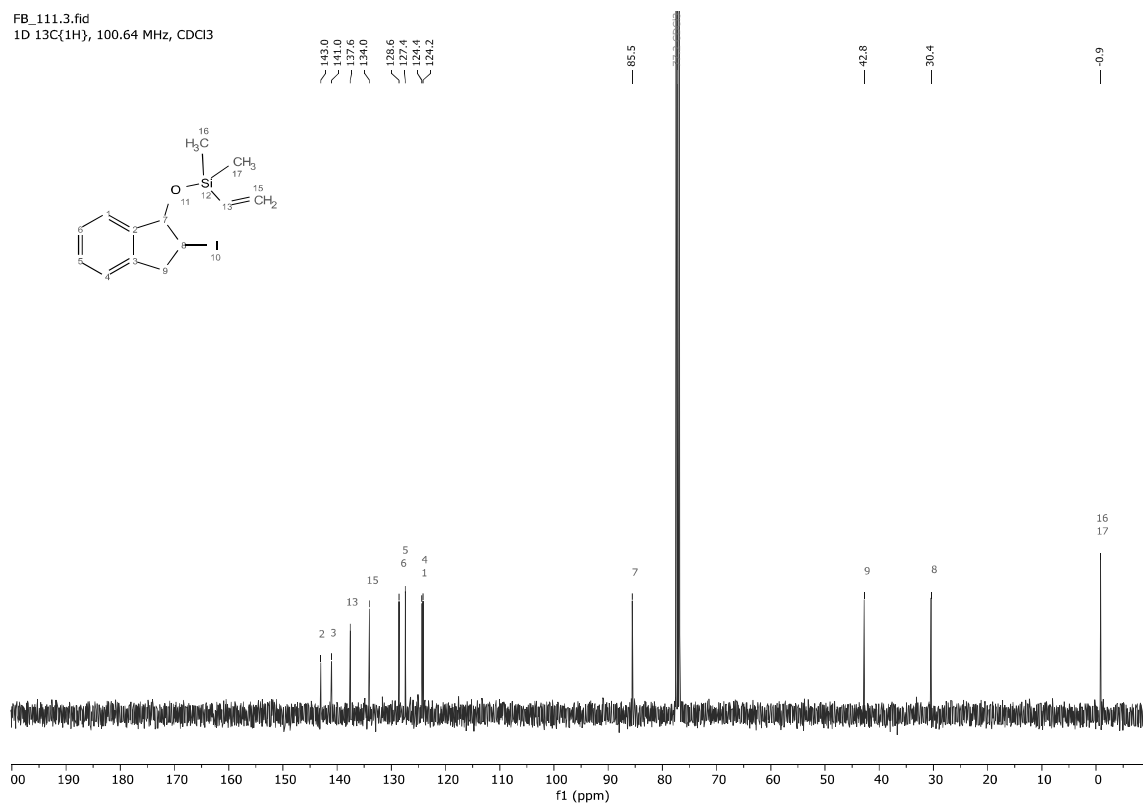
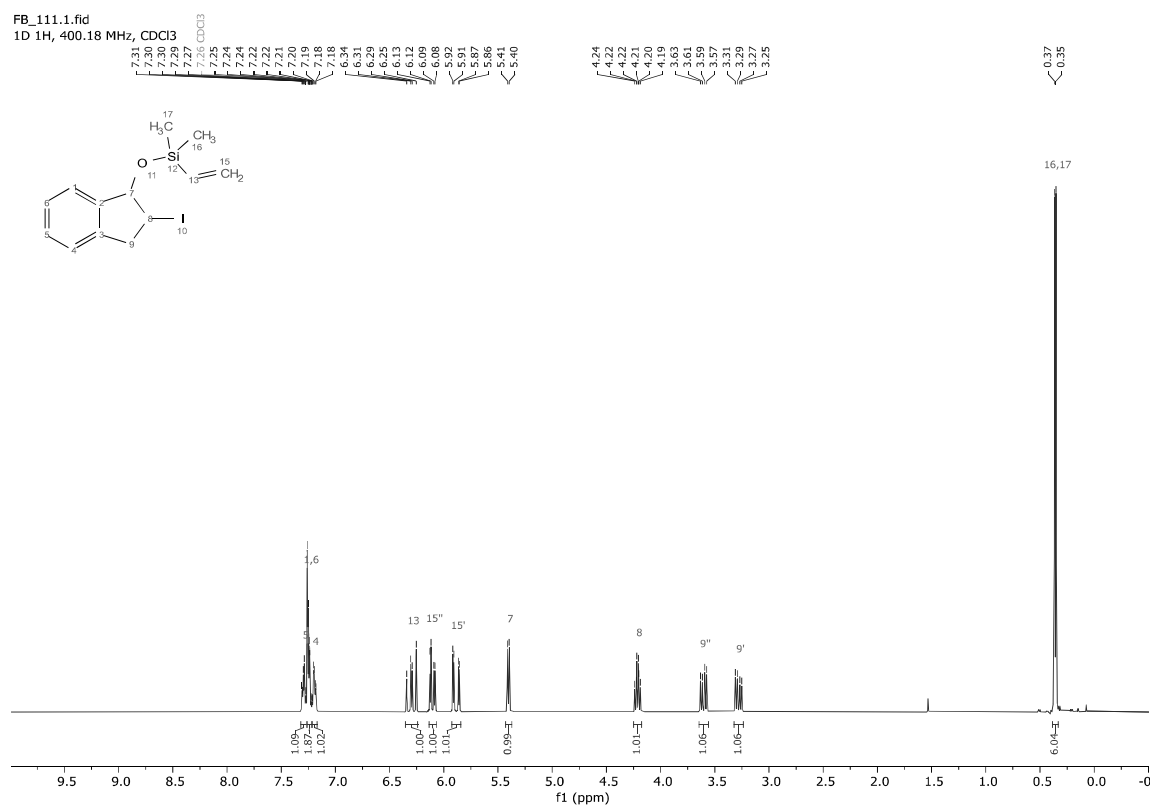


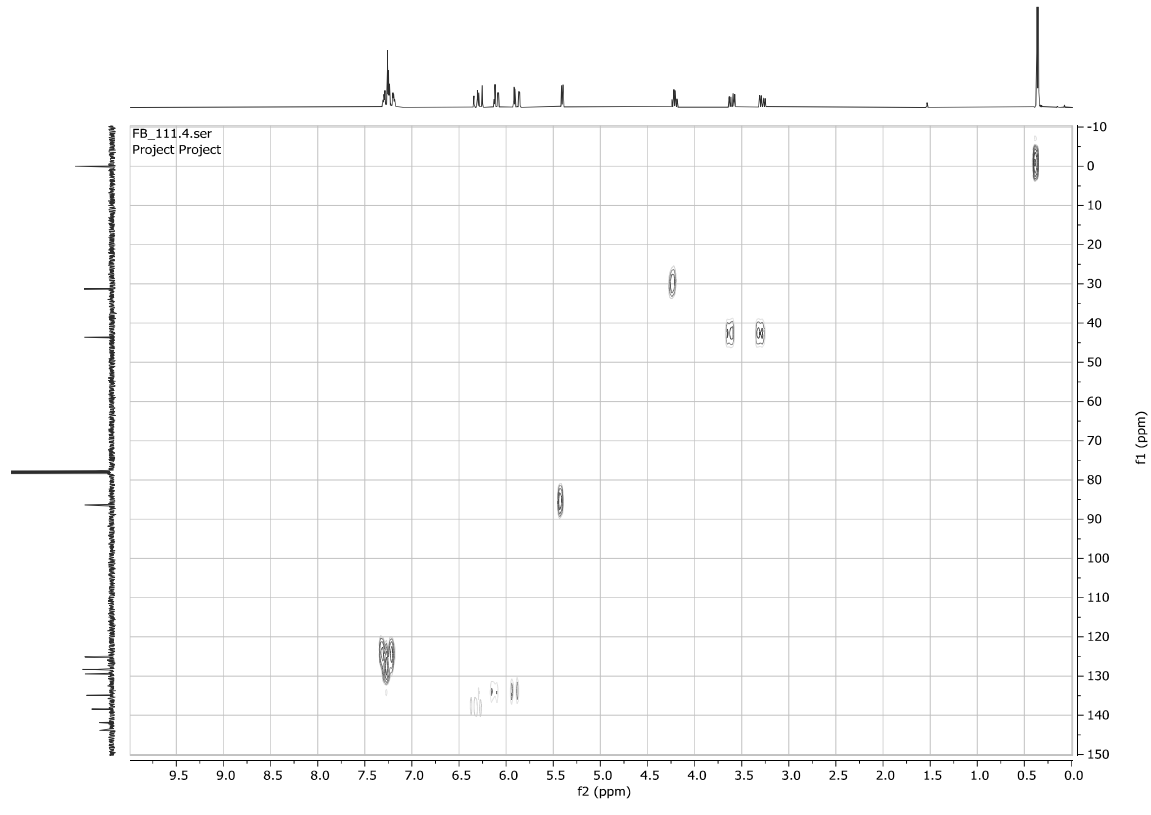
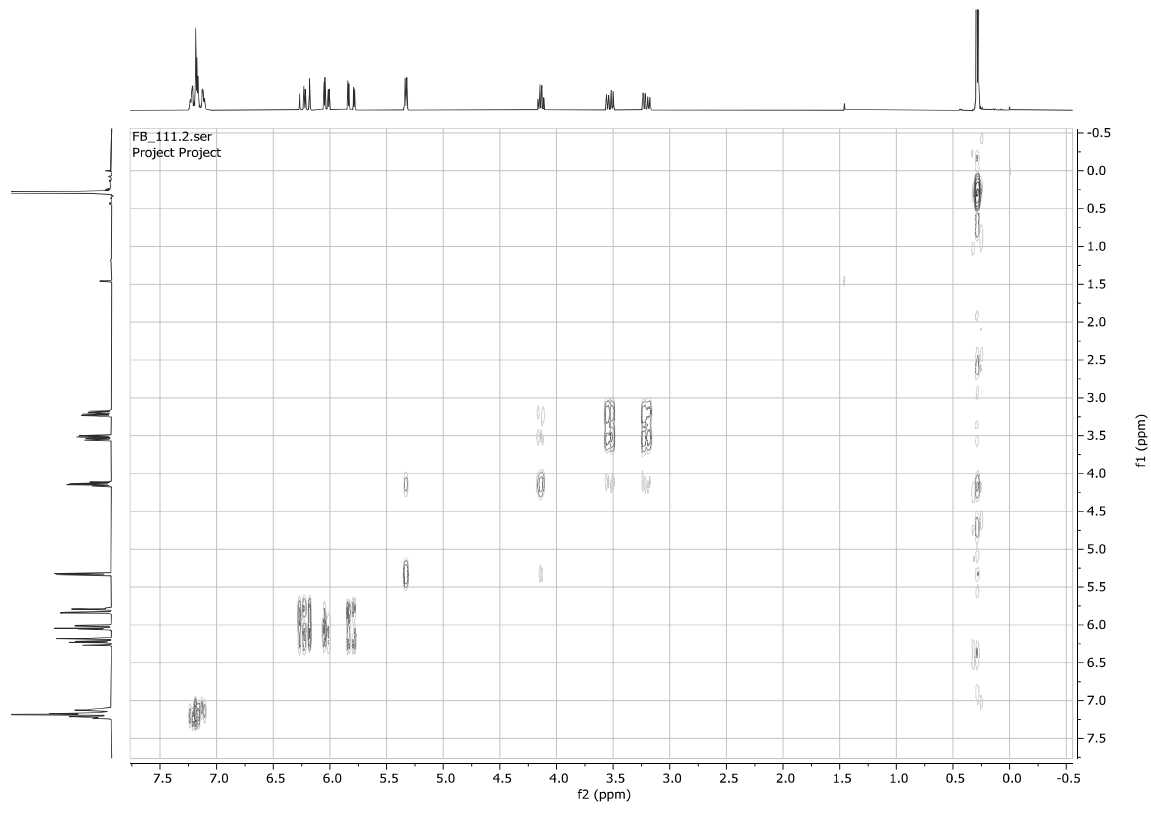
FB_257.3.fid
1D 13C(1H), 100.64 MHz, CDCl3

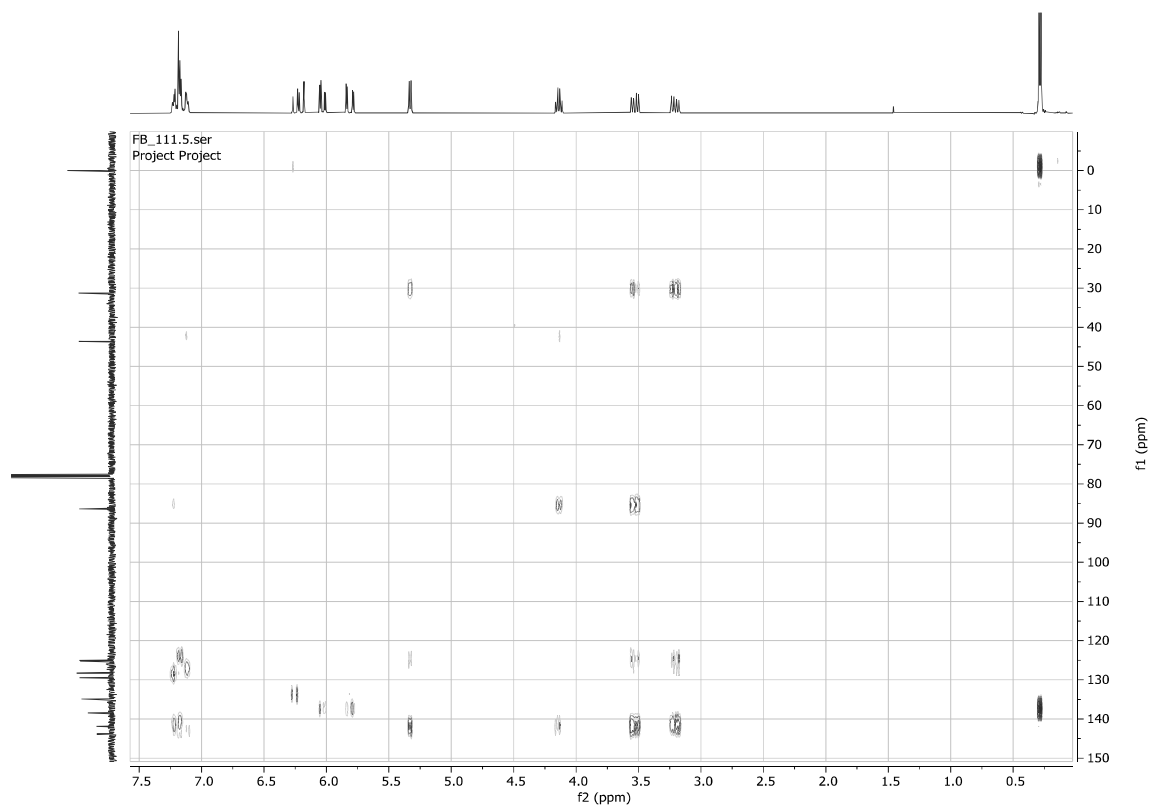




((2-Iodo-2,3-dihydro-1H-inden-1-yl)oxy)dimethylvinylsilane 4a

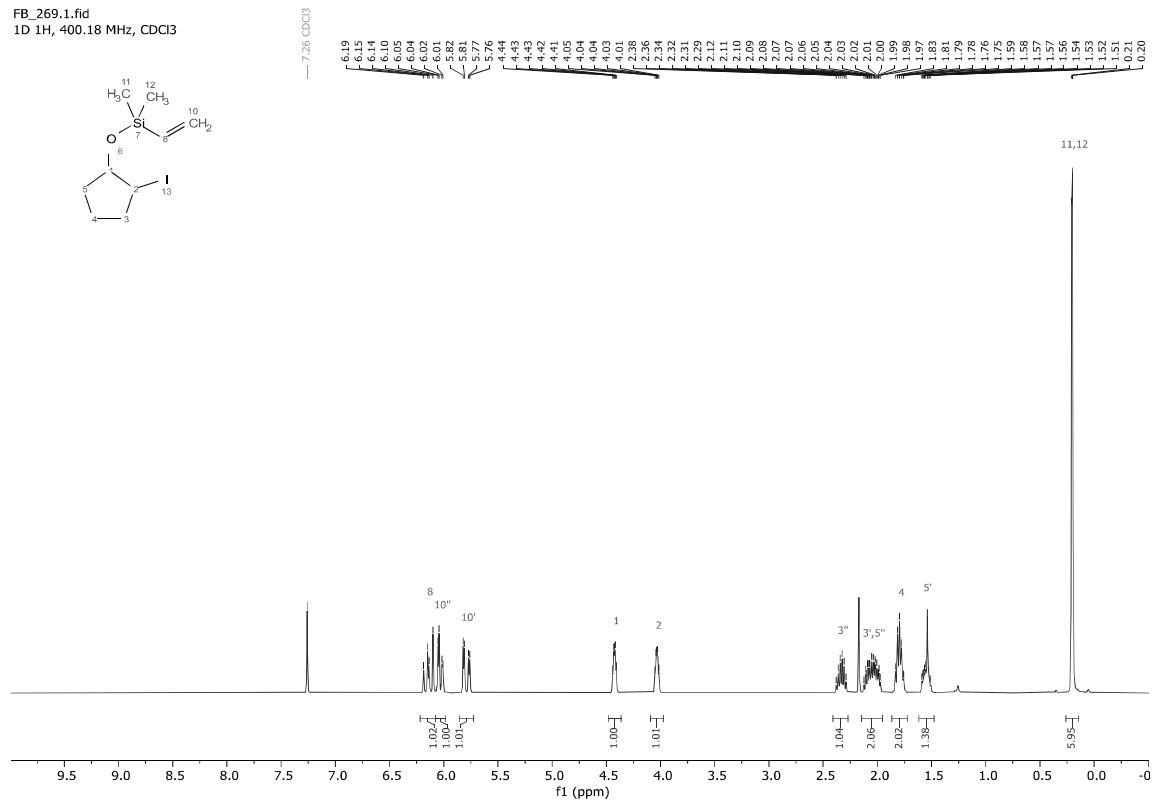




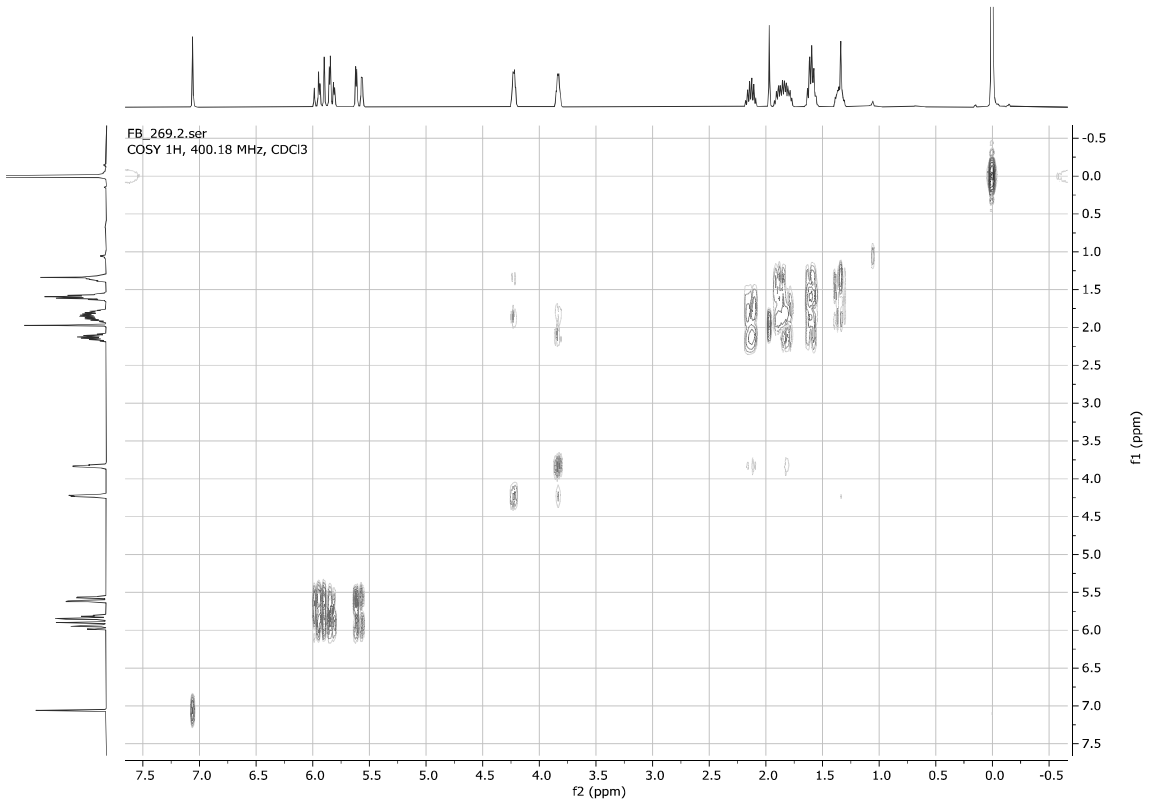
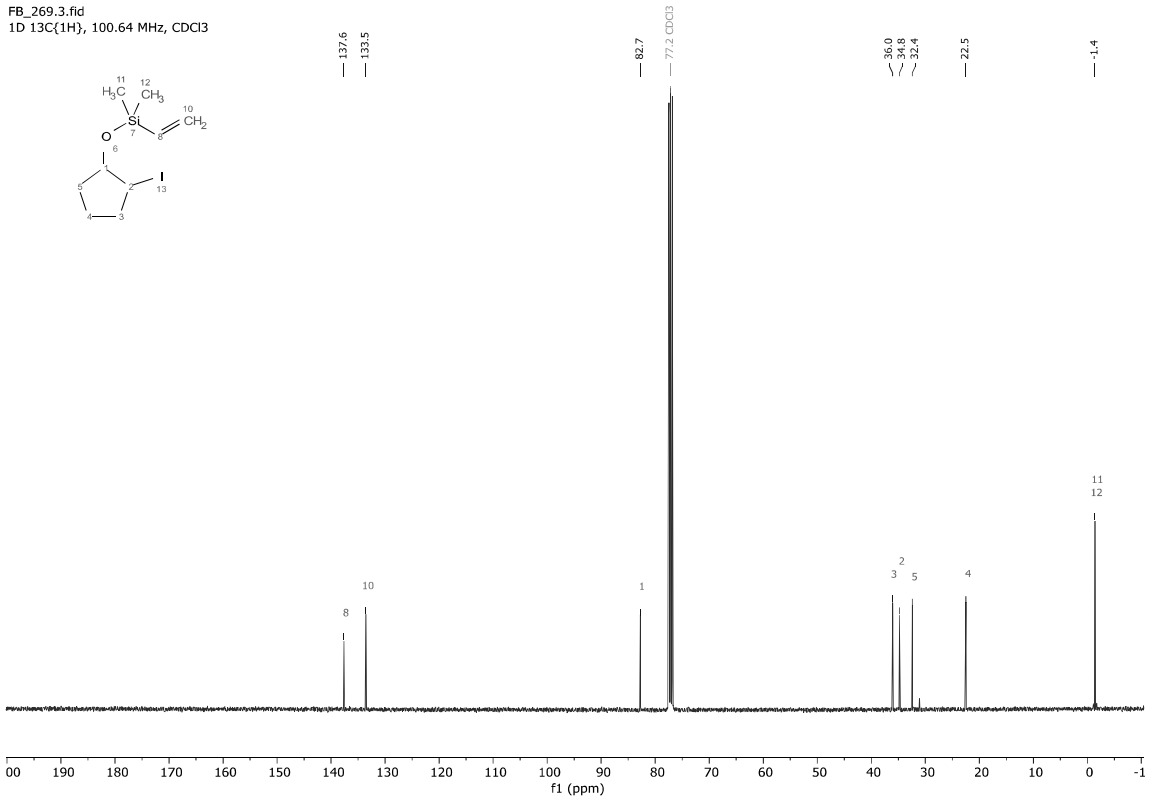


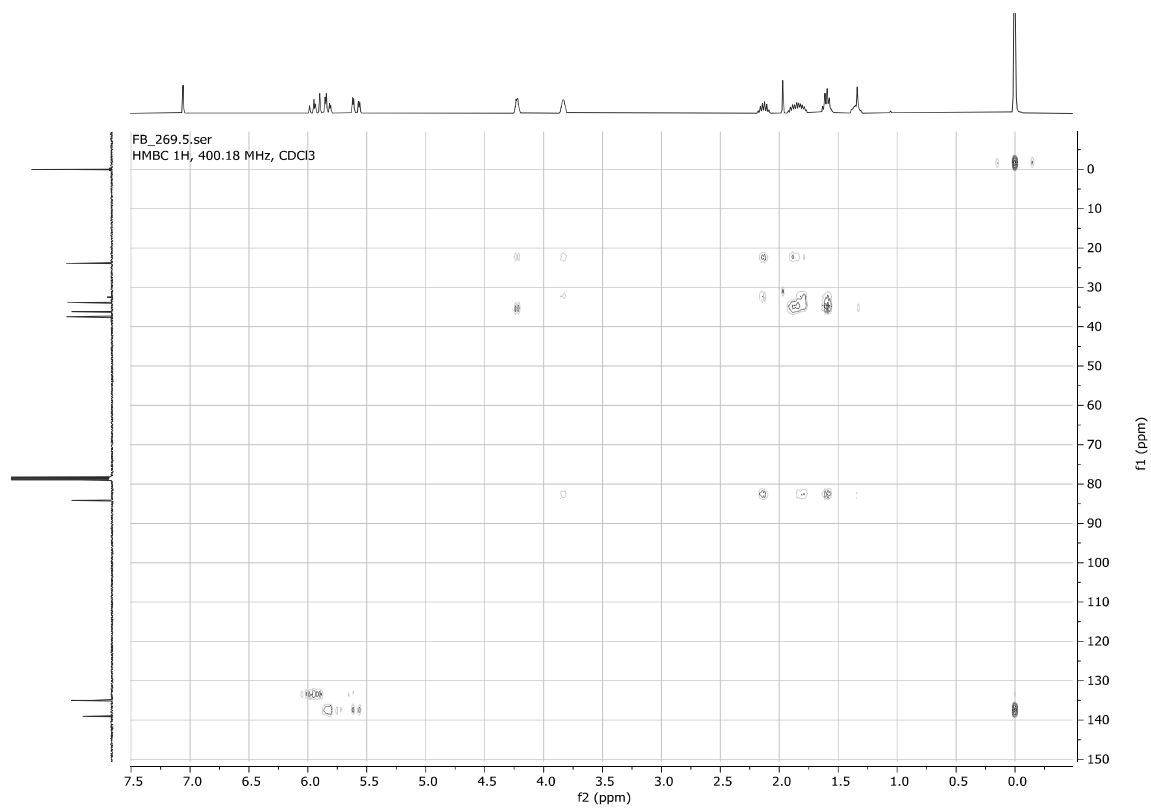
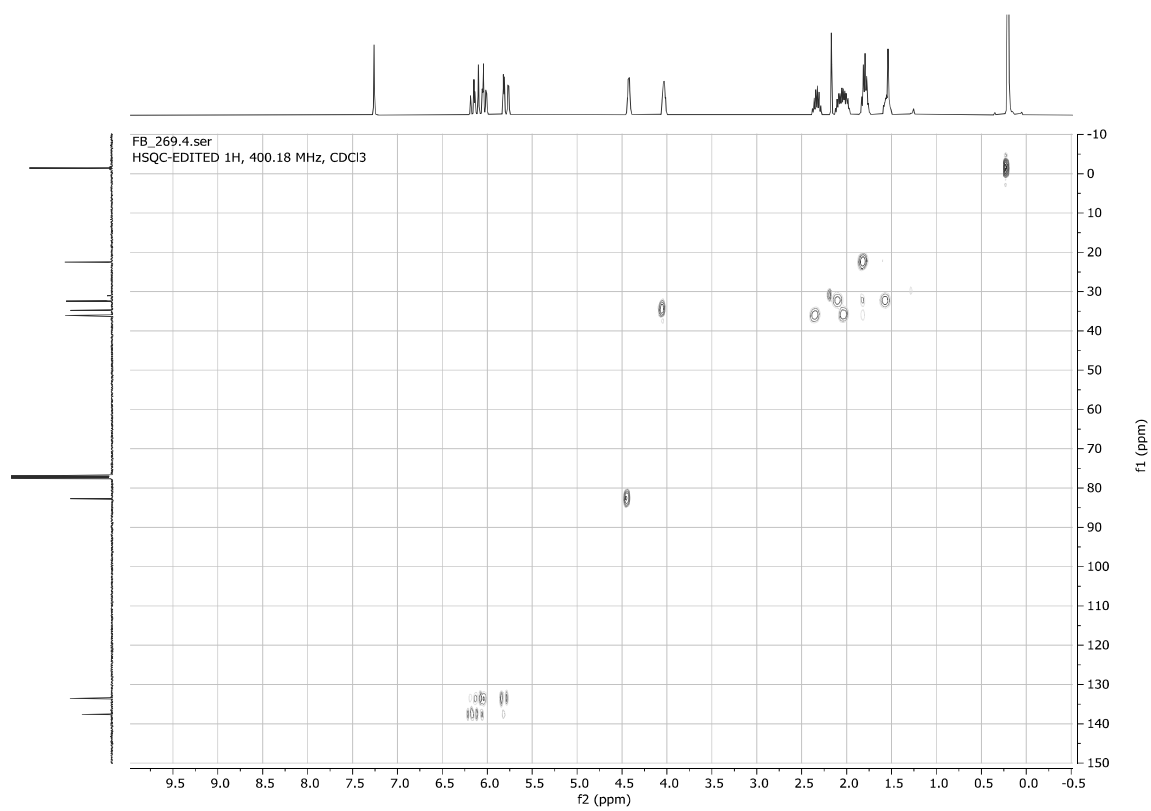
(2-Iodocyclopentyl)dimethylvinylsilane **4b**

FB_269.1.fid
1D 1H, 400.18 MHz, CDCl₃



FB_269.3.fid
1D 13C{1H}, 100.64 MHz, CDCl3

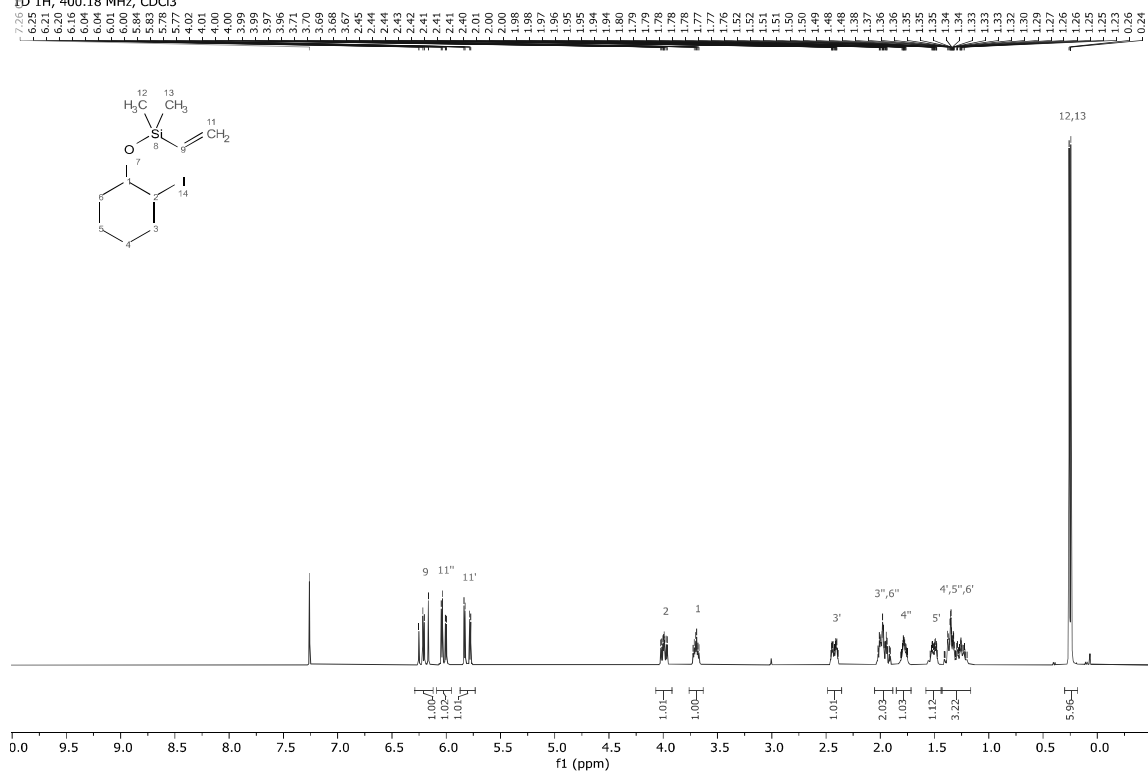




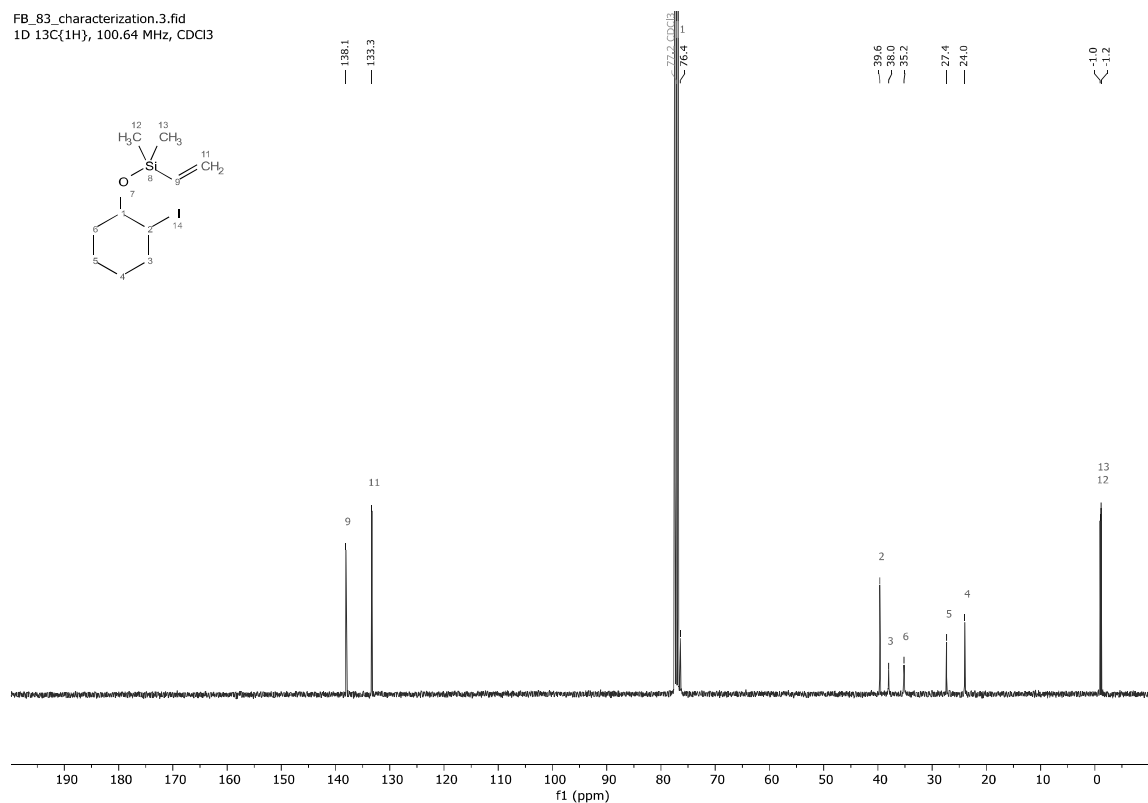
(2-Iodocyclohexyloxy)dimethylvinylsilane **4c**

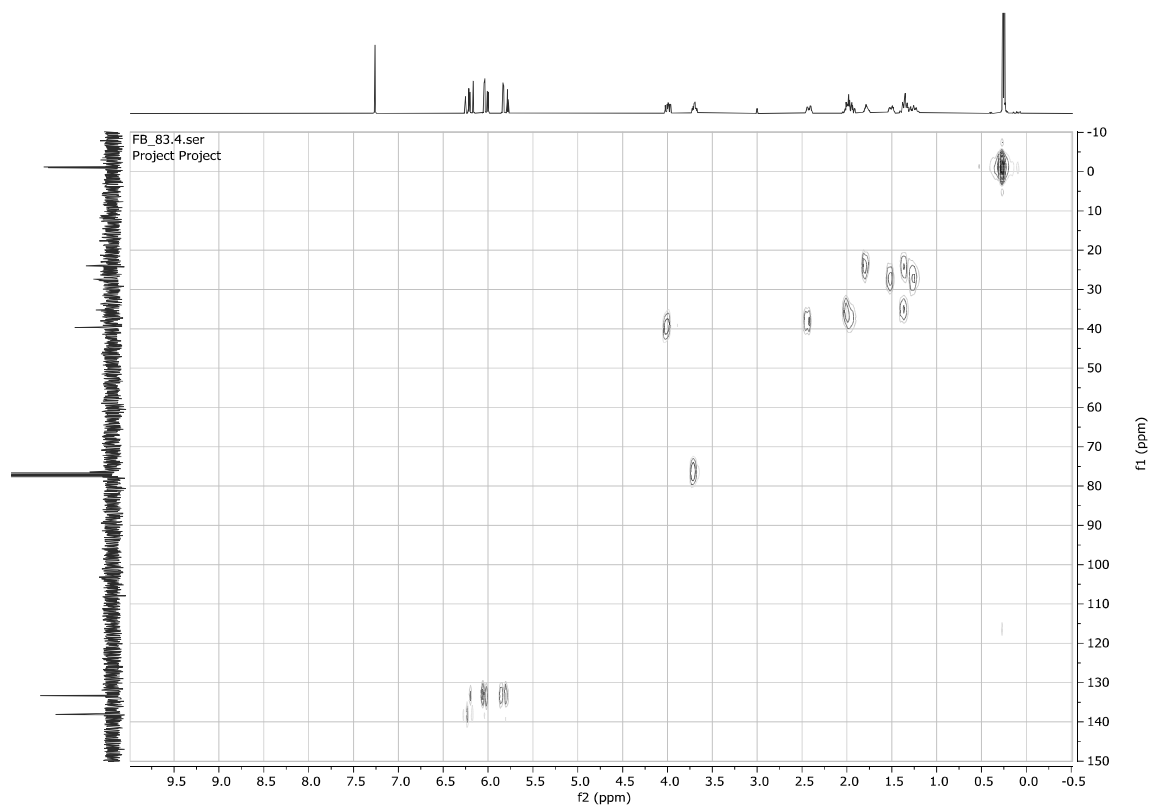
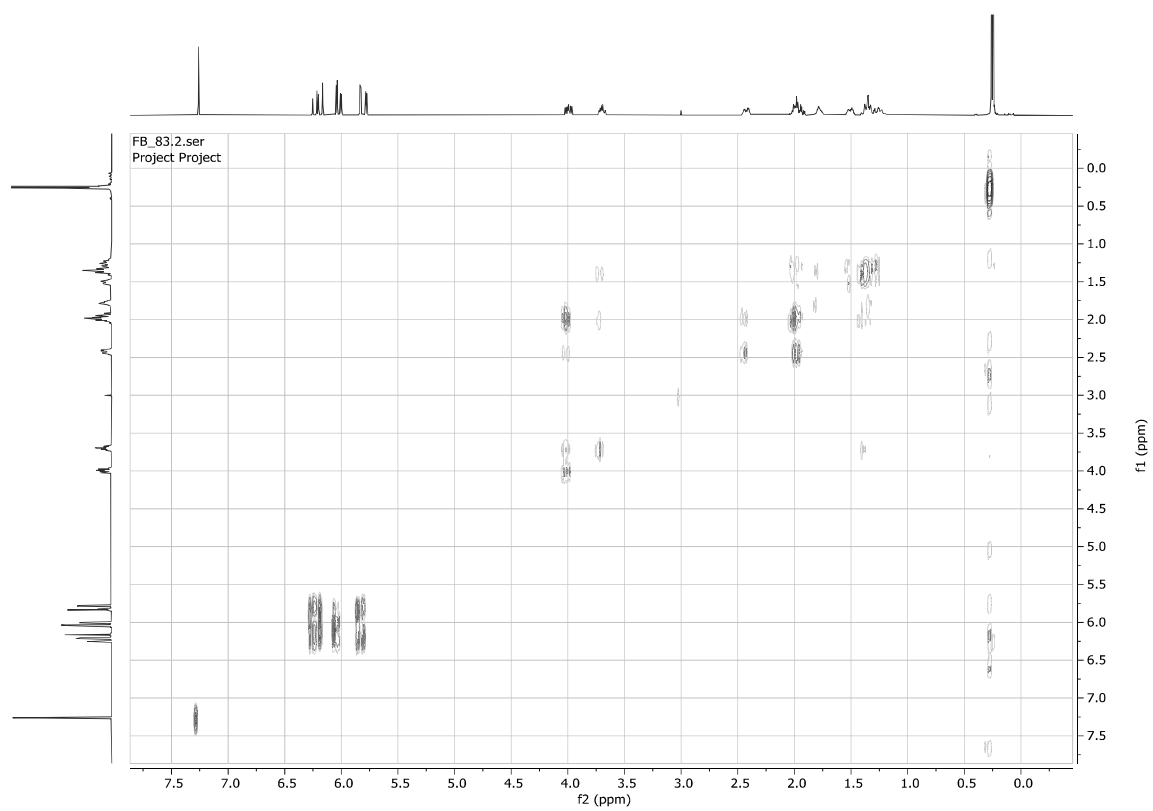
FB_83_characterization.1.fid

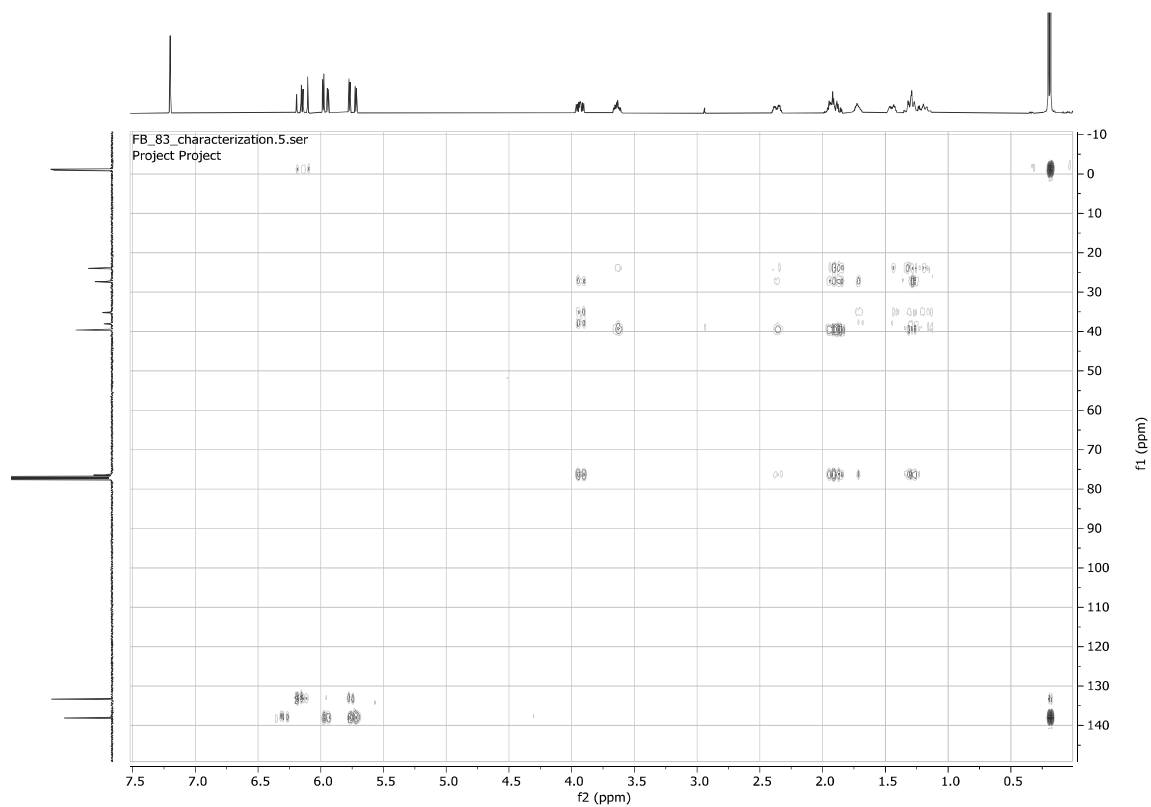
1D 1H, 400.18 MHz, CDCl₃



FB_83_characterization.3.fid
1D 13C(1H), 100.64 MHz, CDCl₃

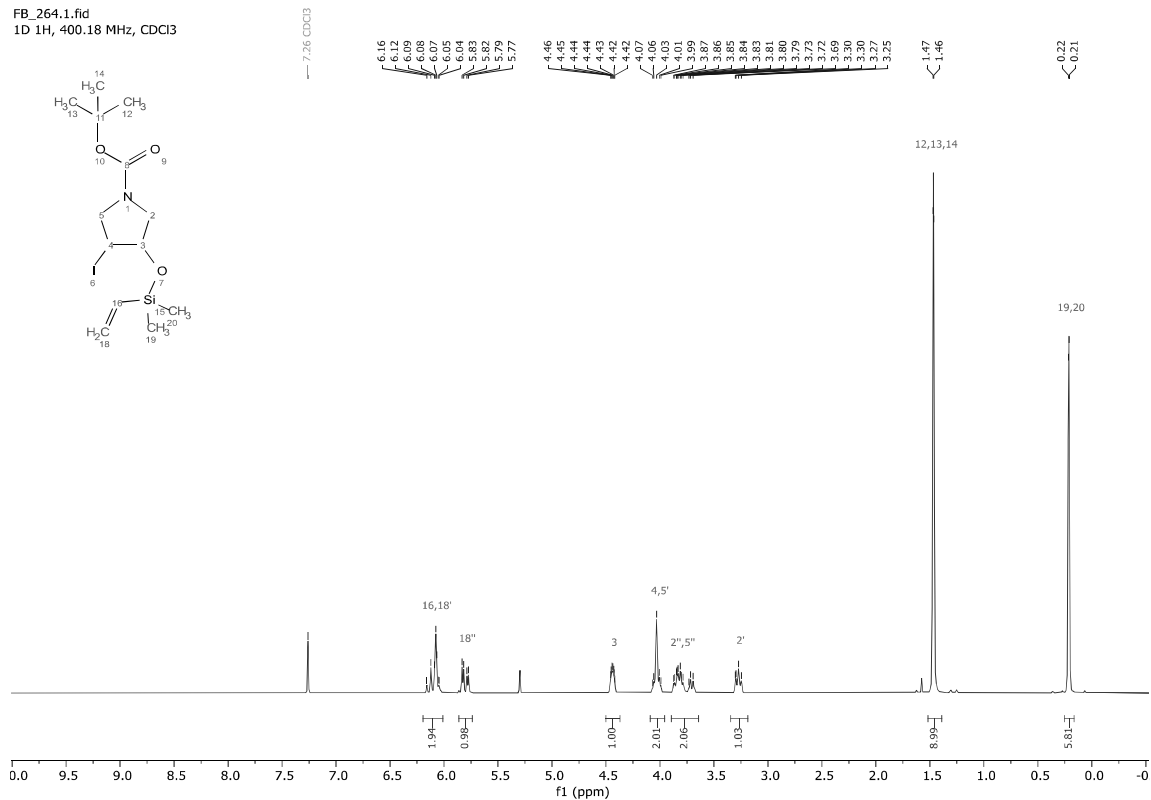




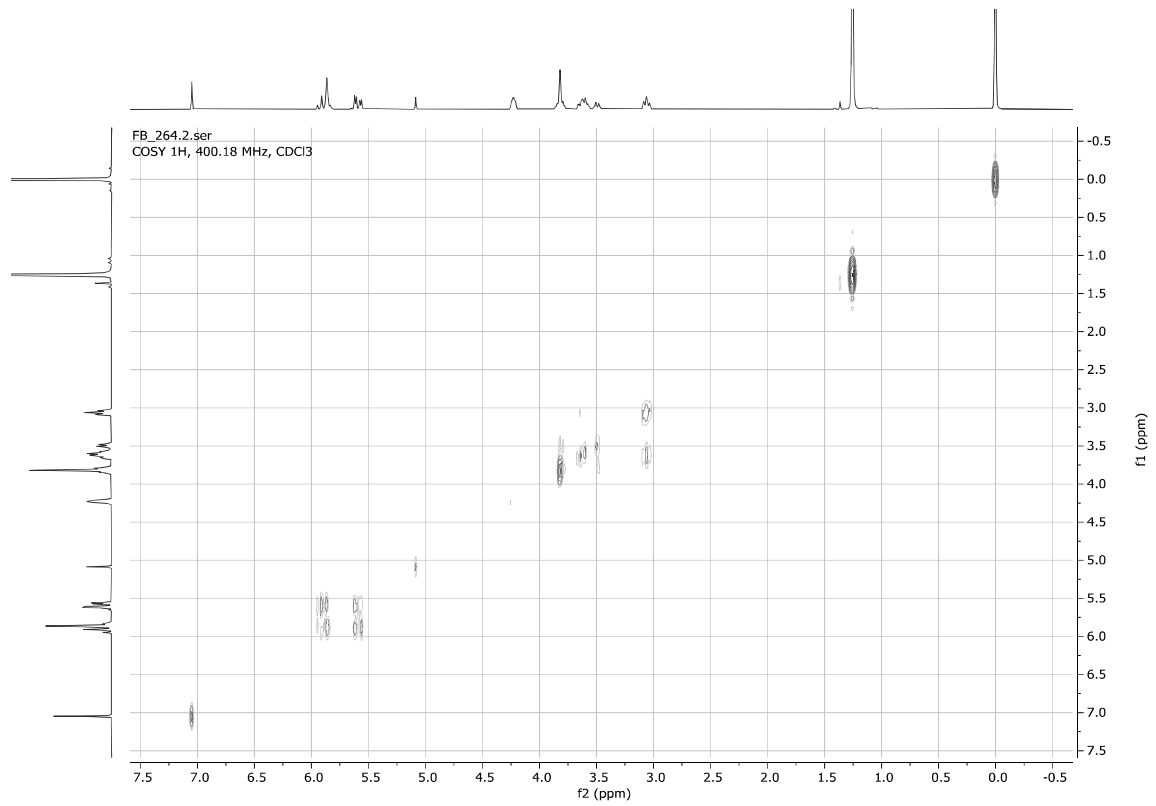
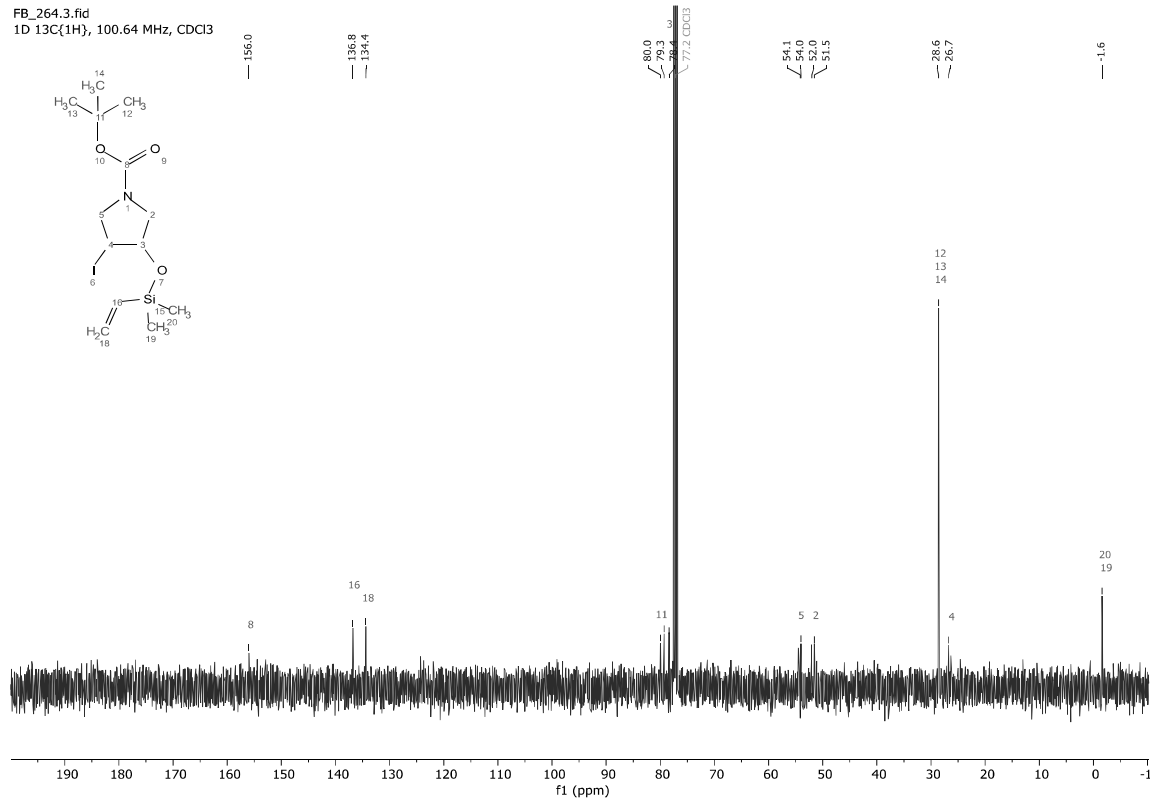


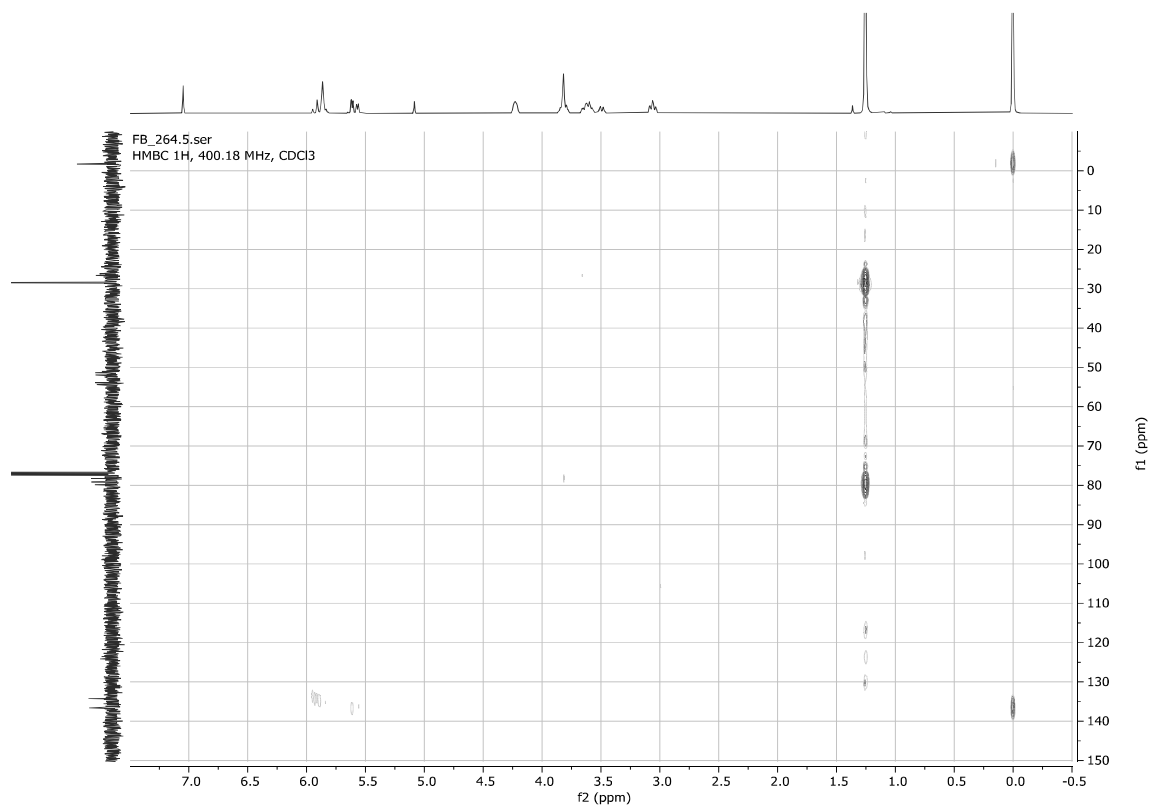
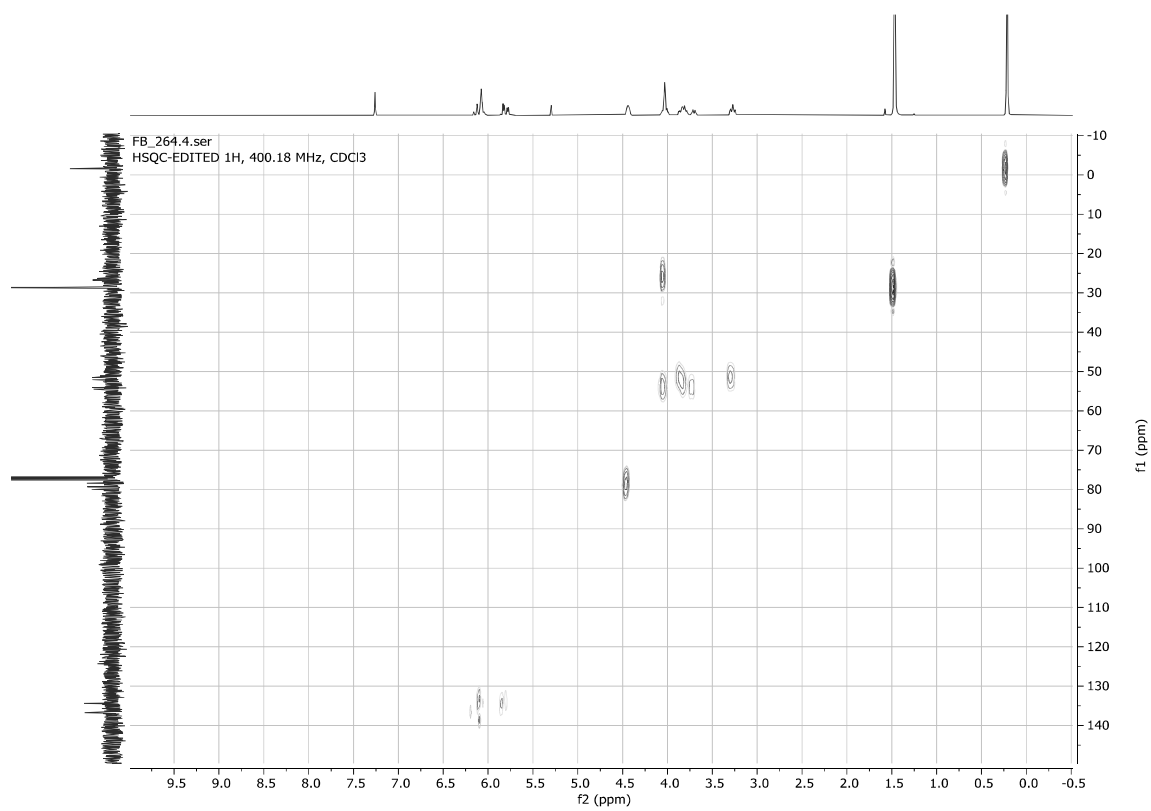
tert-Butyl 3-((dimethylvinylsilyl)oxy)-4-iodopyrrolidine-1-carboxylate **4d** (mixture of rotamers)

FB_264.1.fid
1D 1H, 400.18 MHz, CDCl₃

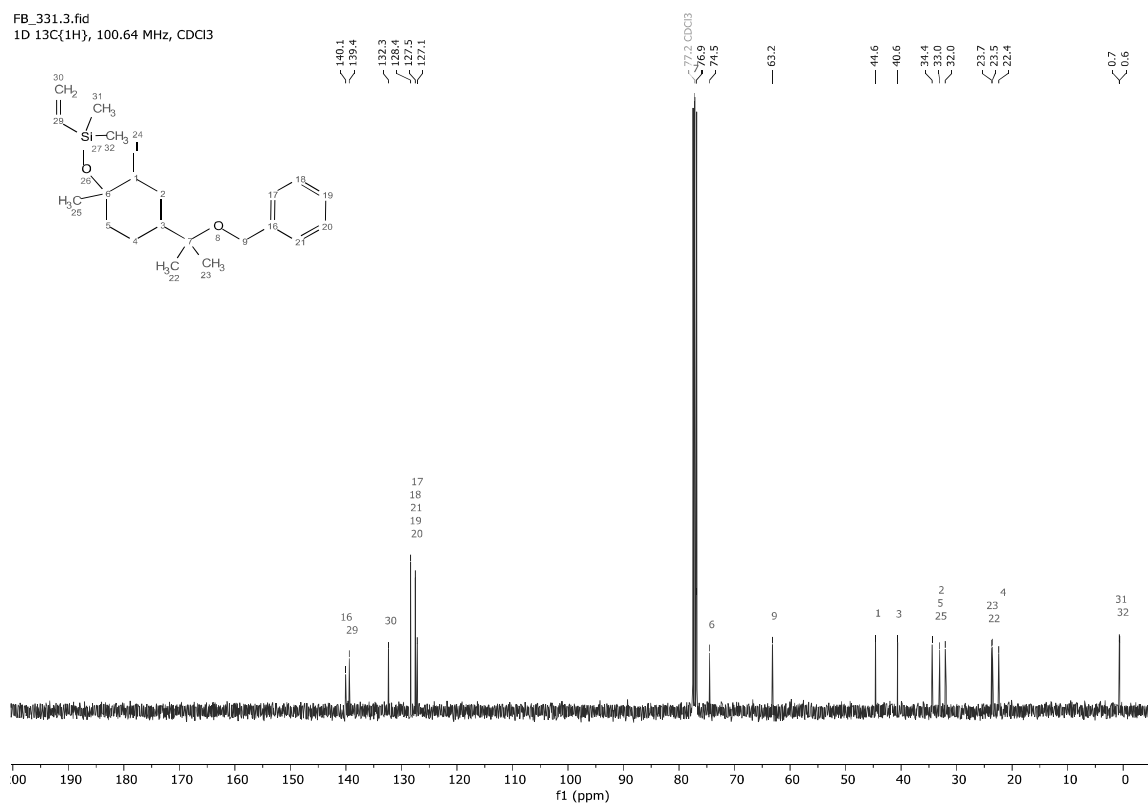
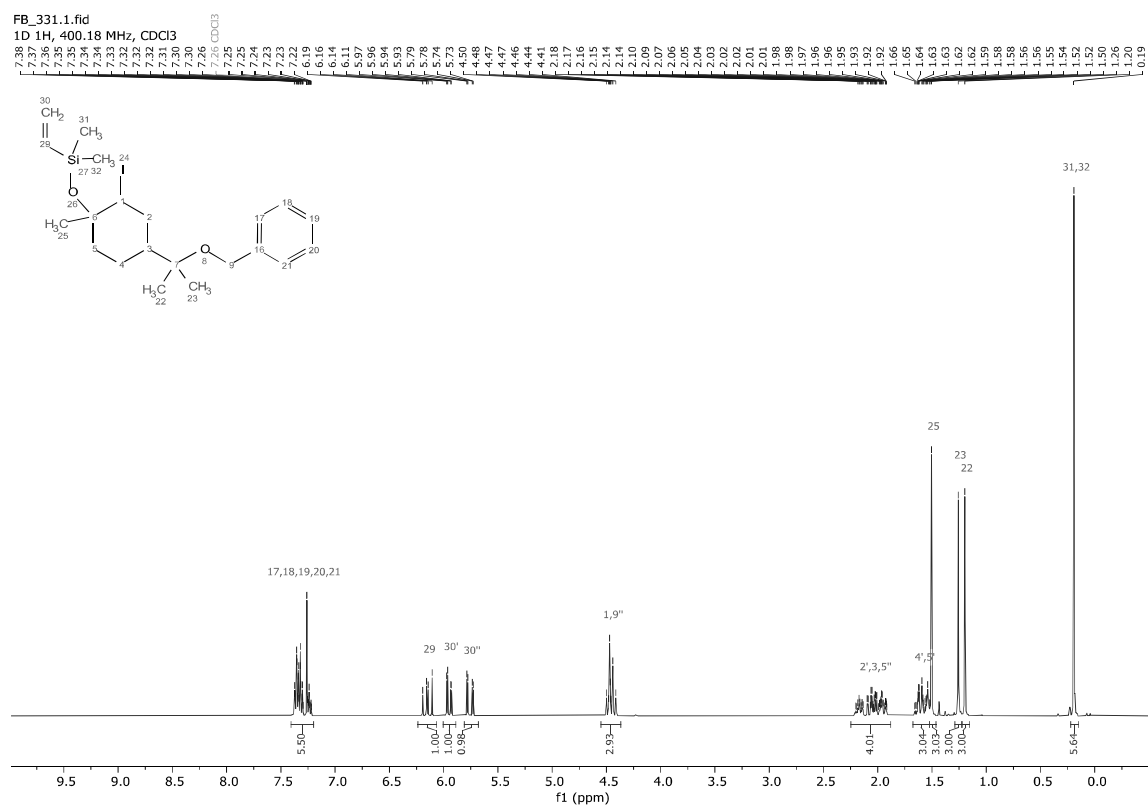


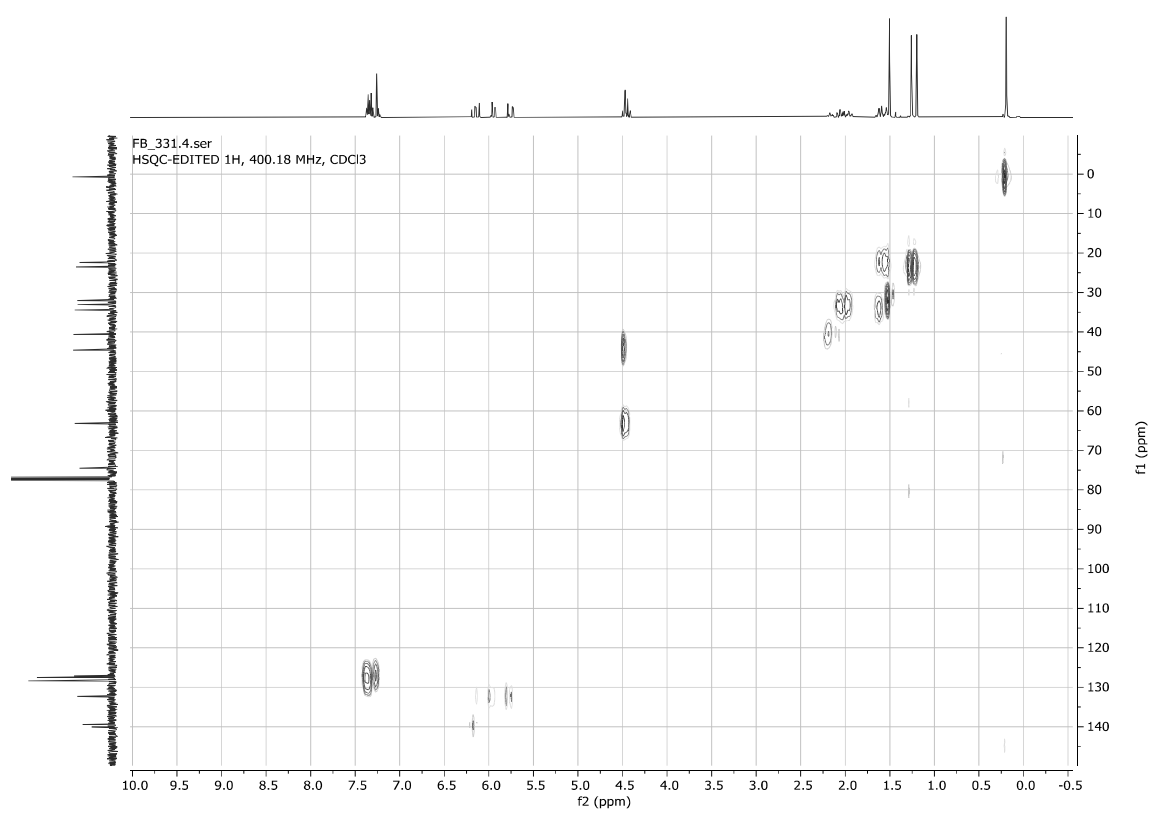
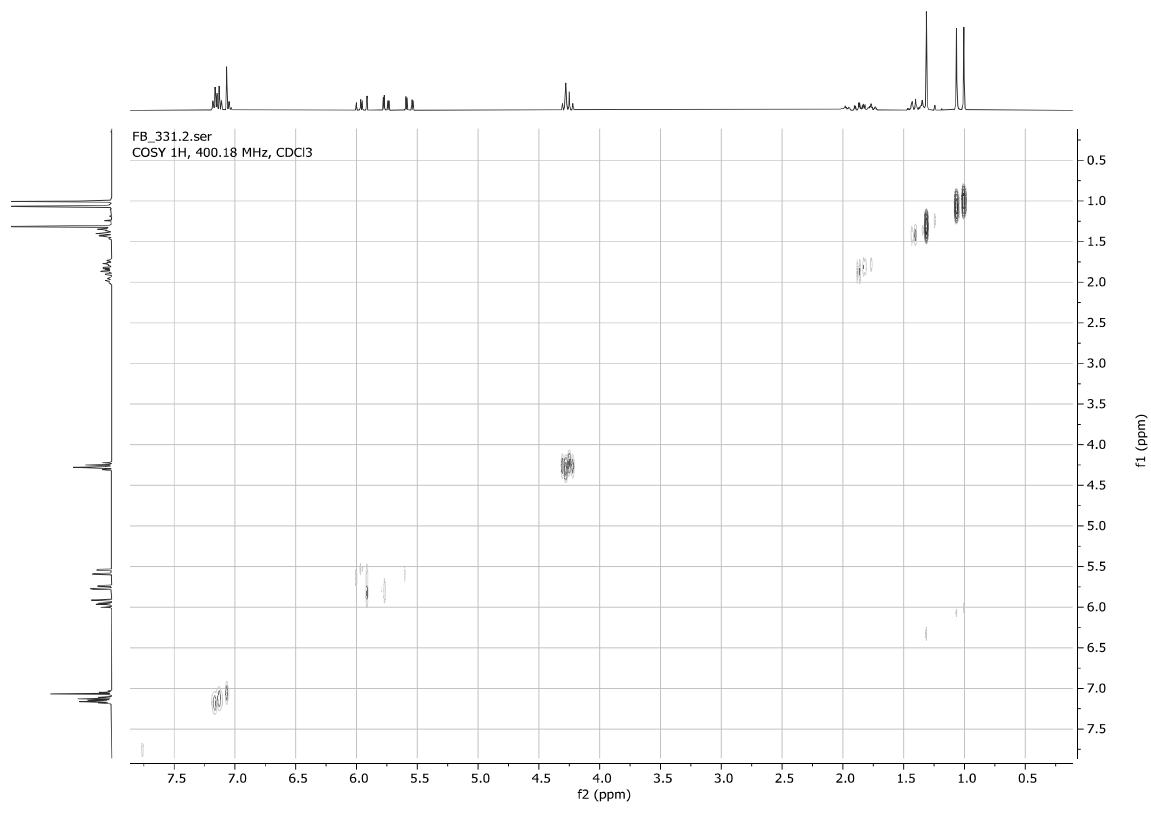
FB_264.3.fid
1D 13C{1H}, 100.64 MHz, CDCl3

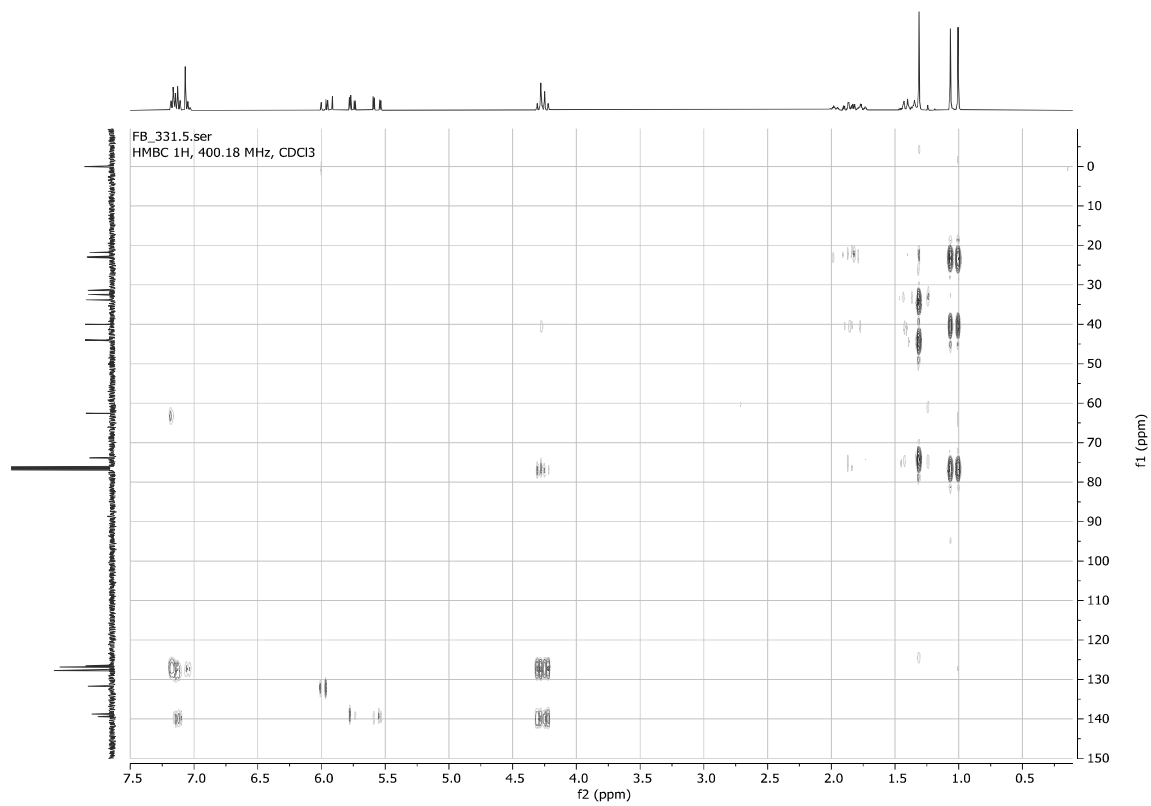




((4-(2-Benzyloxy)propan-2-yl)-2-iodo-1-methylcyclohexyl)oxydimethylvinylsilane **4e**

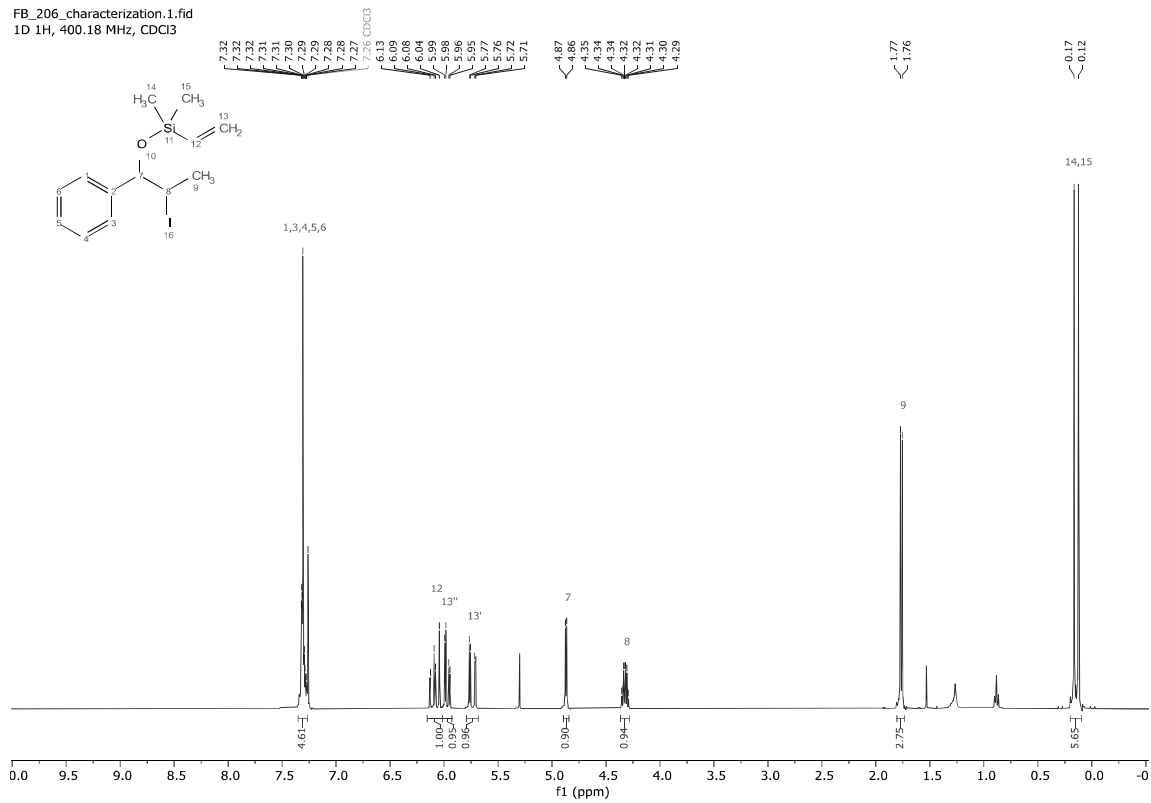




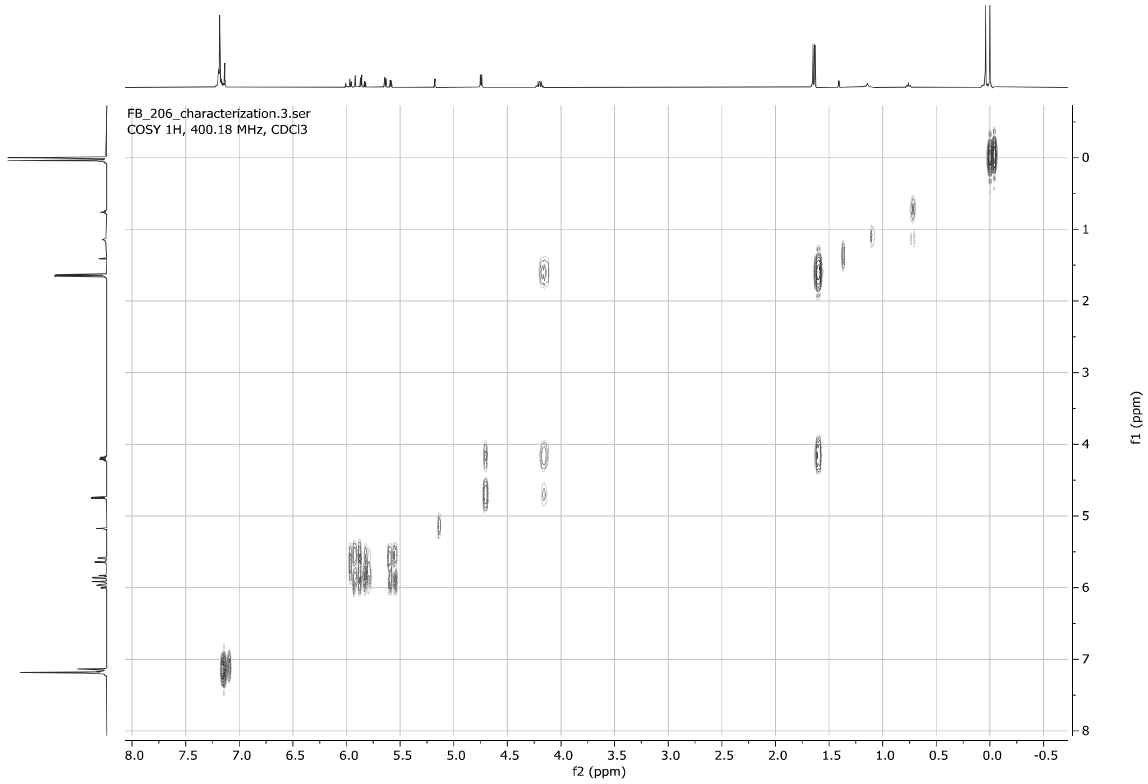
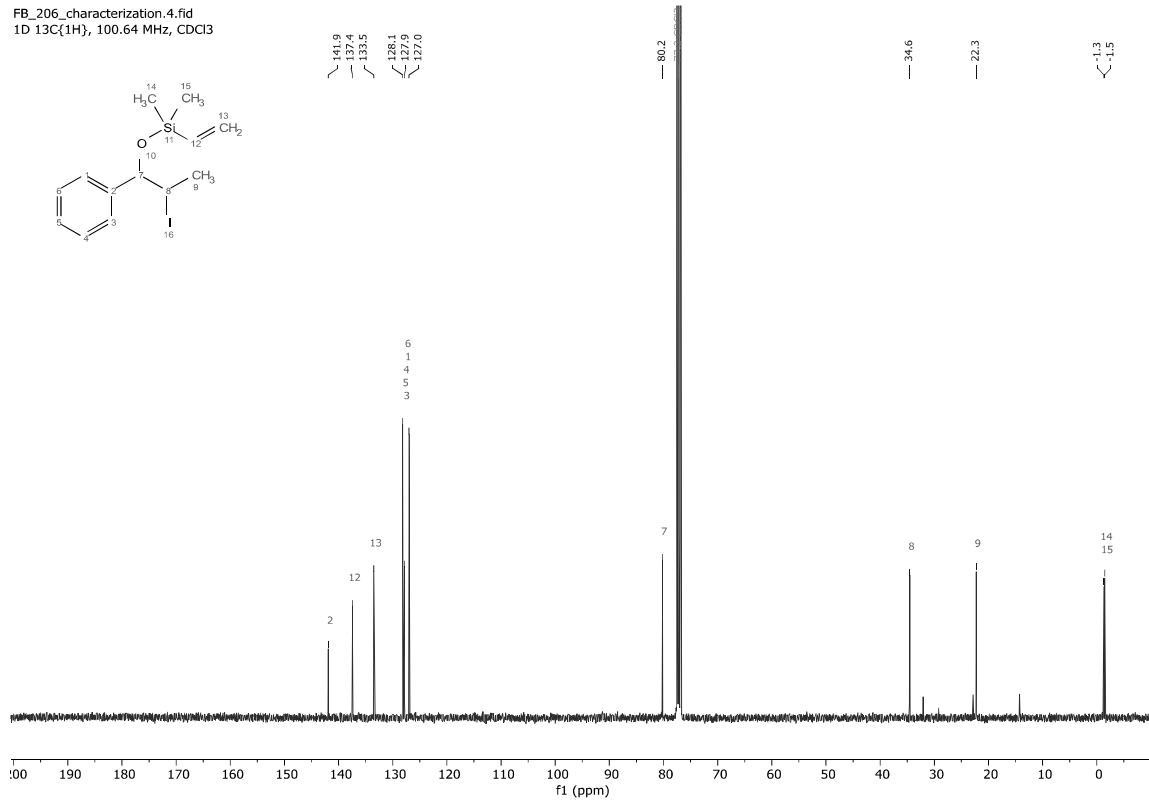


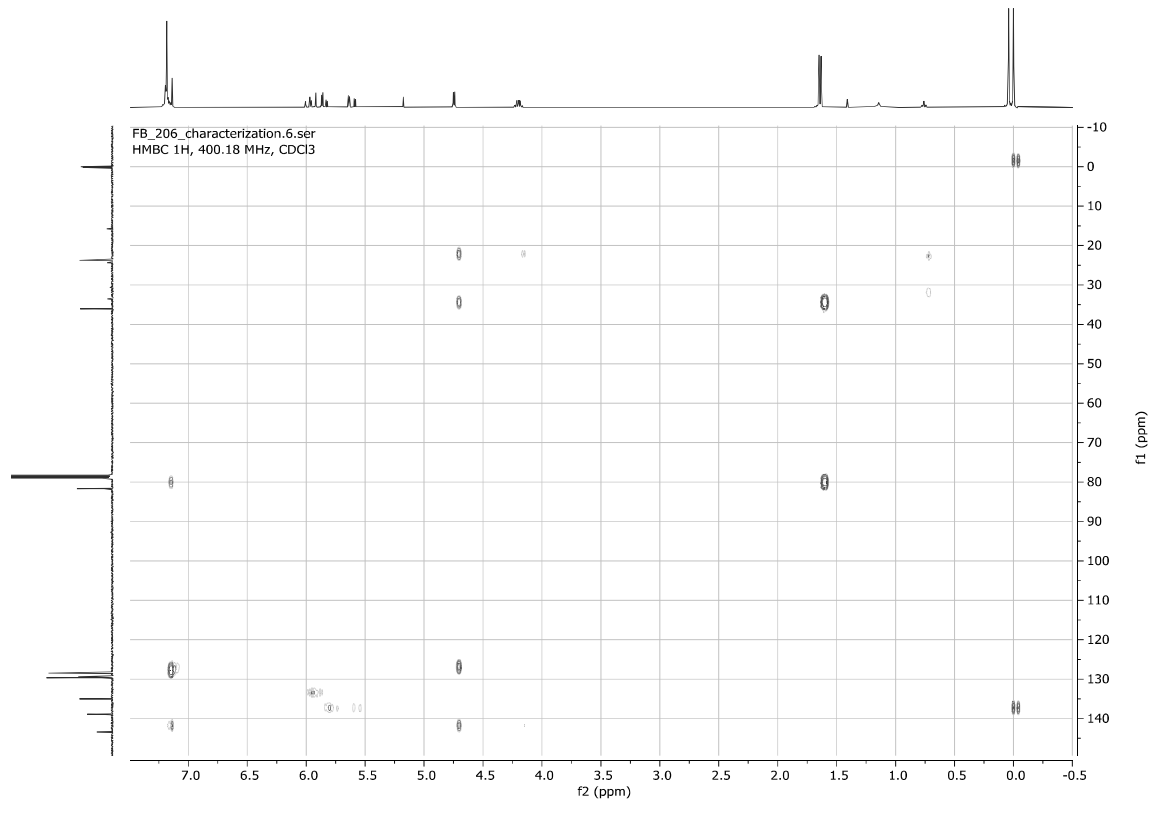
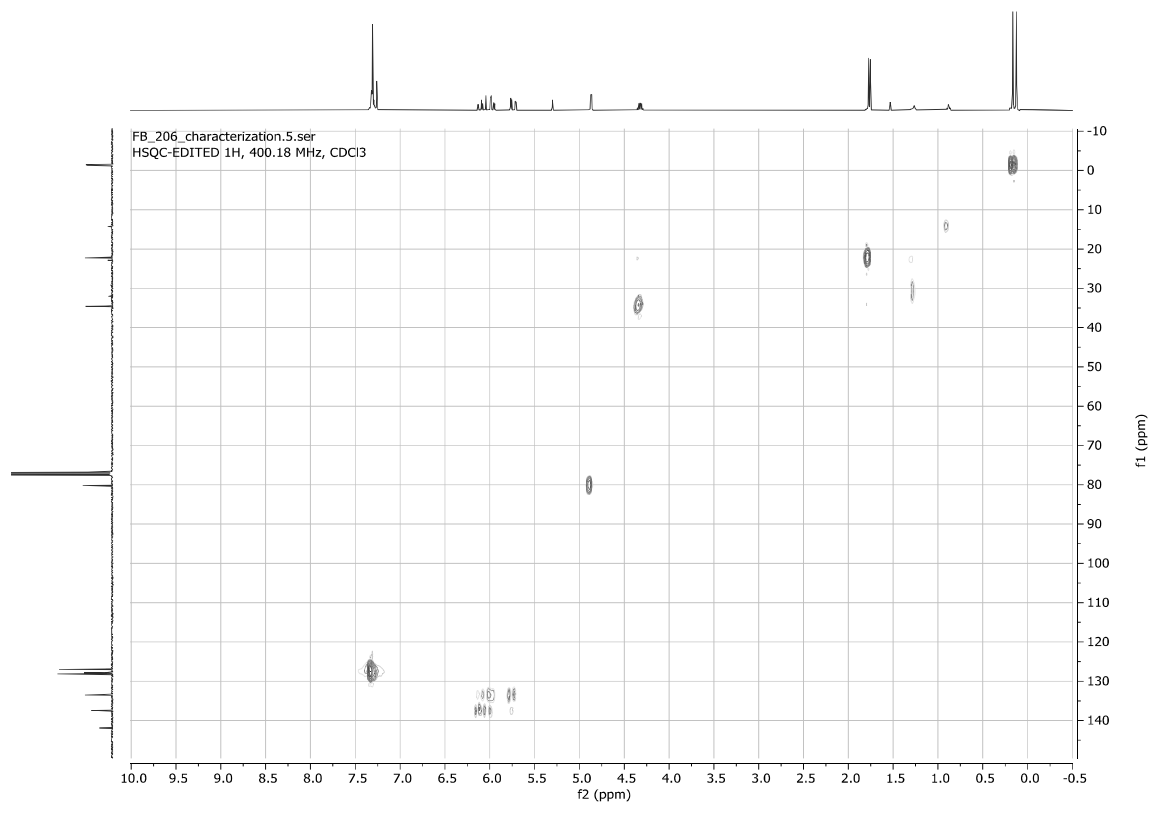
(2-Iodo-1-phenylpropoxy)dimethylvinylsilane **4f**

FB_206_characterization.1.fid
1D 1H, 400.18 MHz, CDCl3



FB_206_characterization.4.fid
1D ¹³C{¹H}, 100.64 MHz, CDCl₃

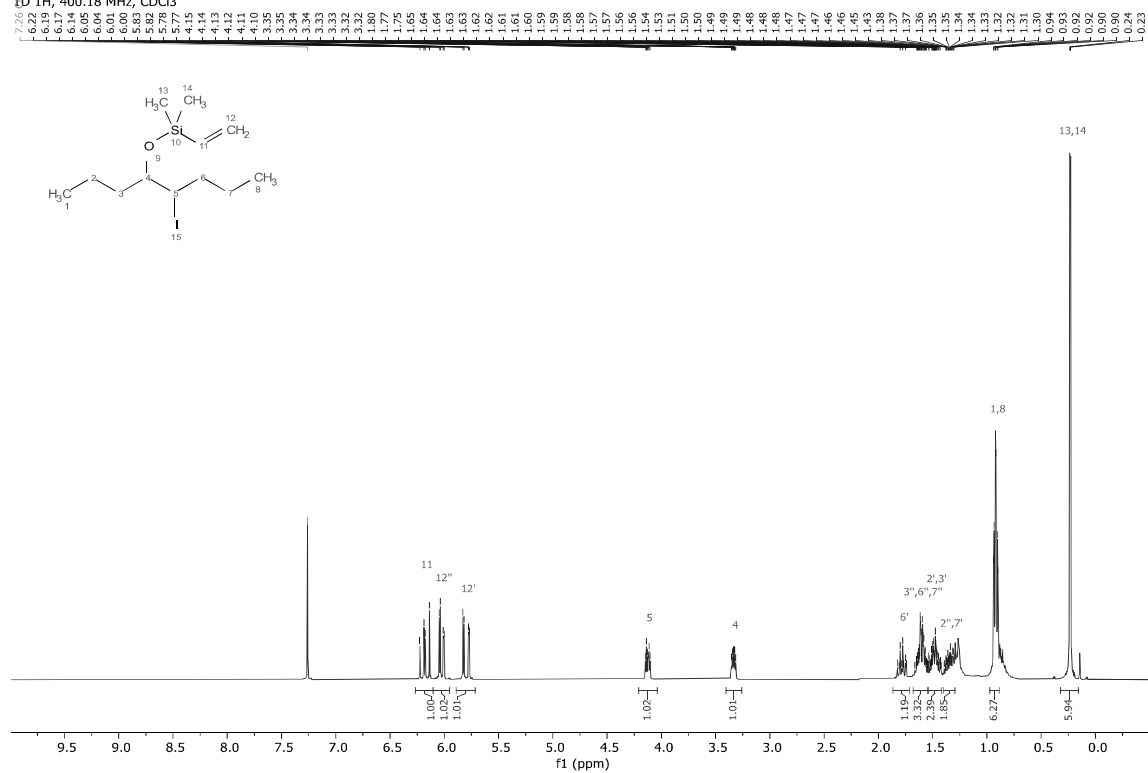




((5-Iodooctan-4-yl)oxy)dimethylvinylsilane **4g**

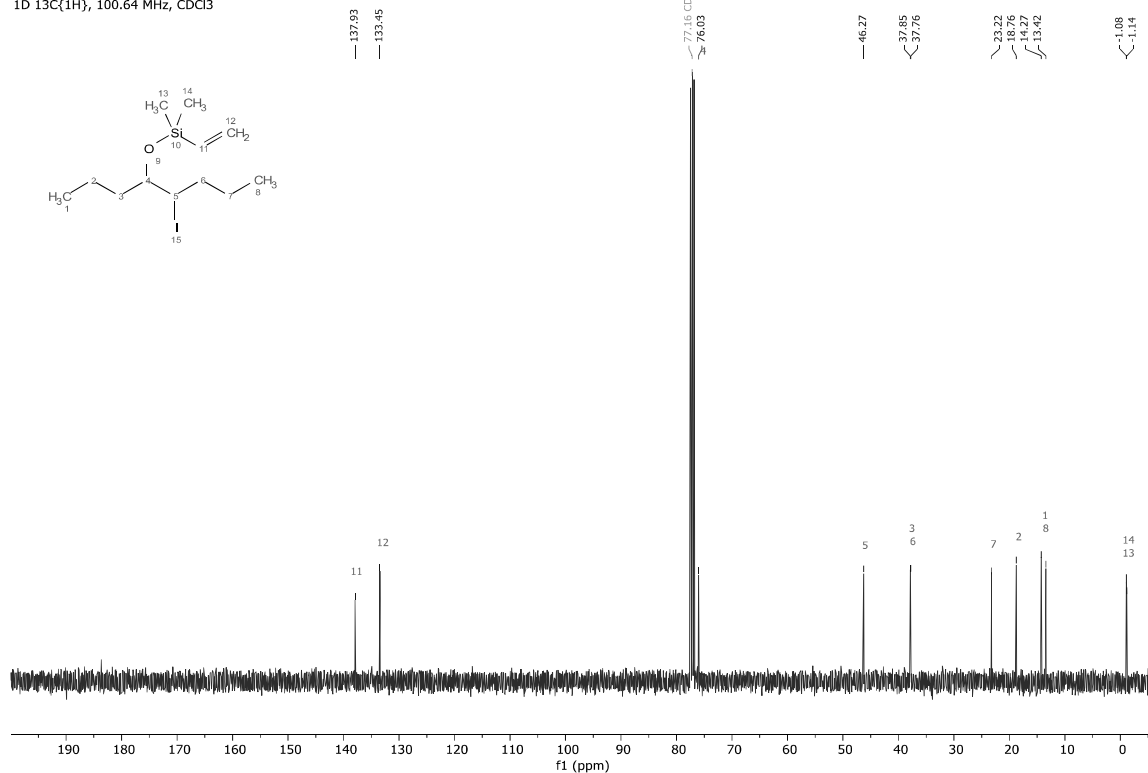
FB_152.1.fid

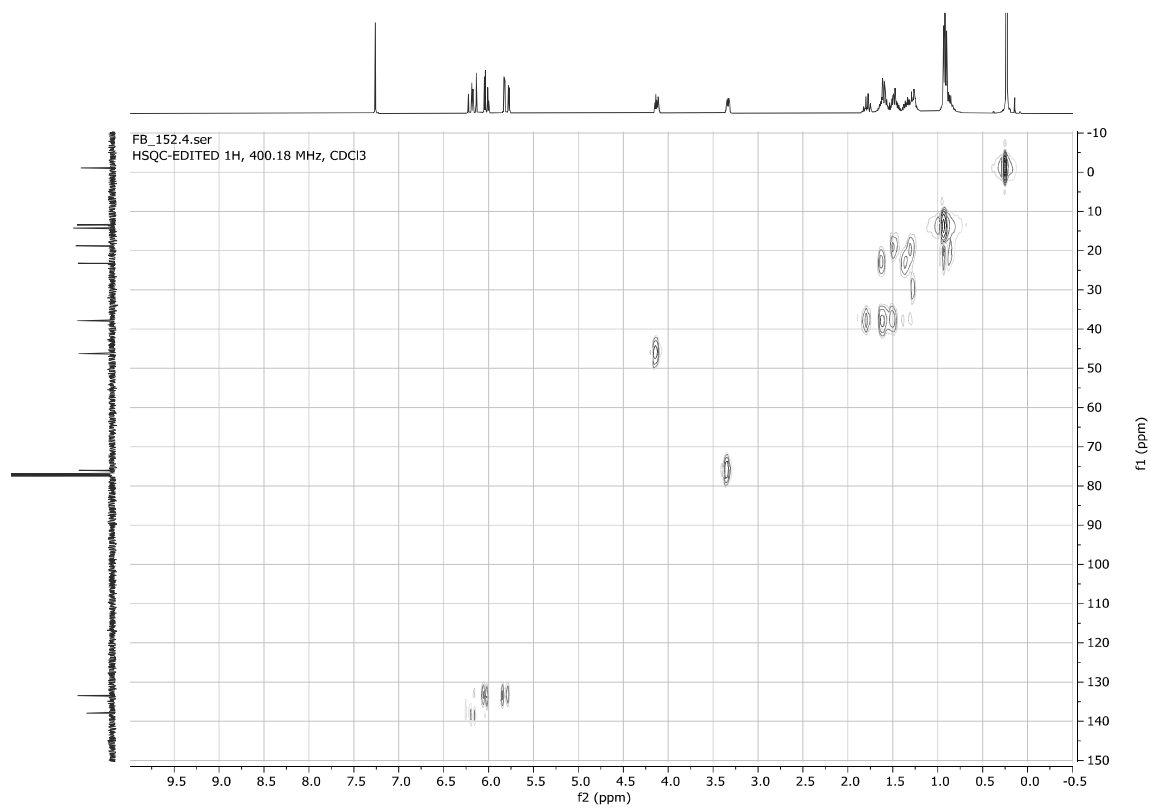
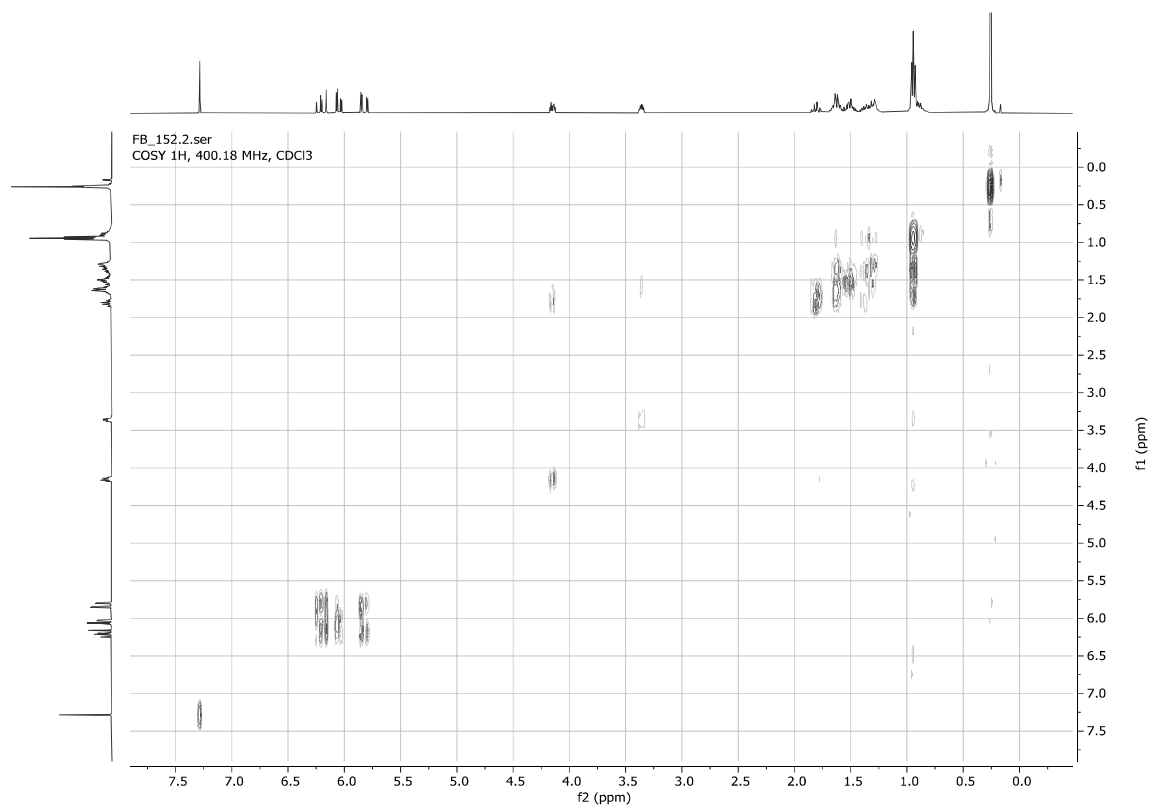
1D 1H, 400.18 MHz, CDCl₃

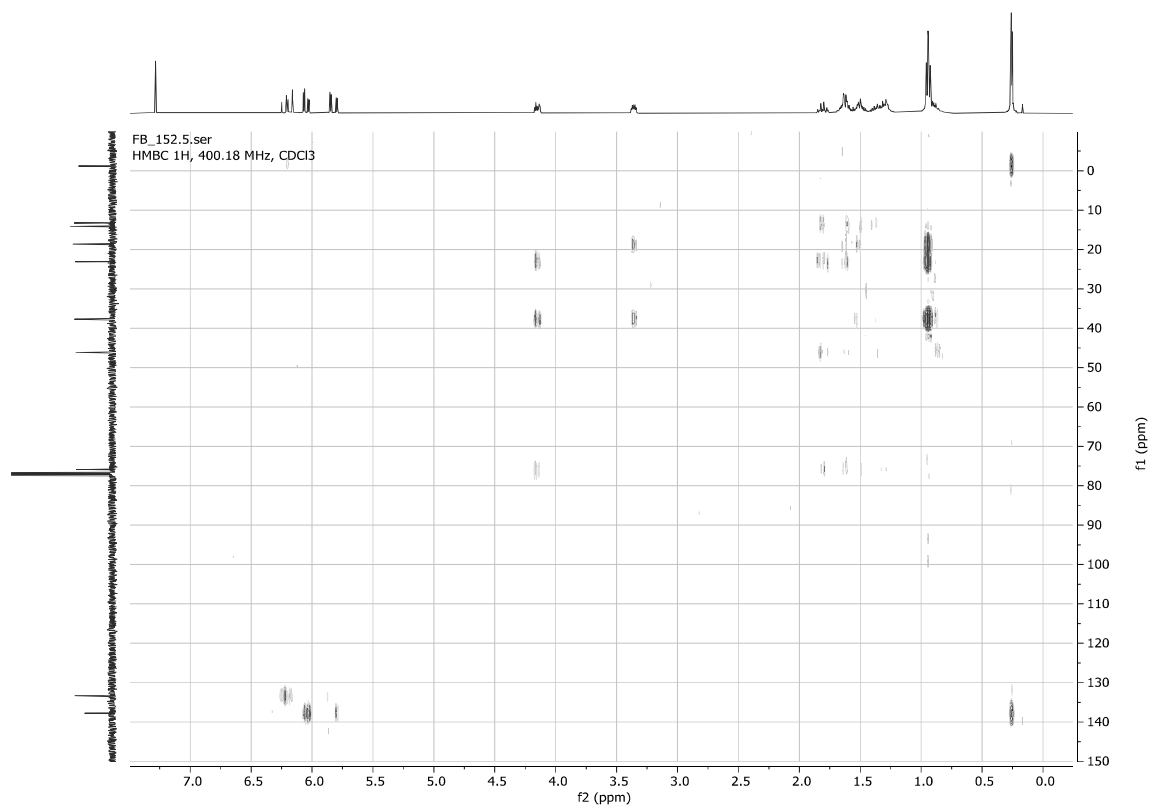


FB_152.3.fid

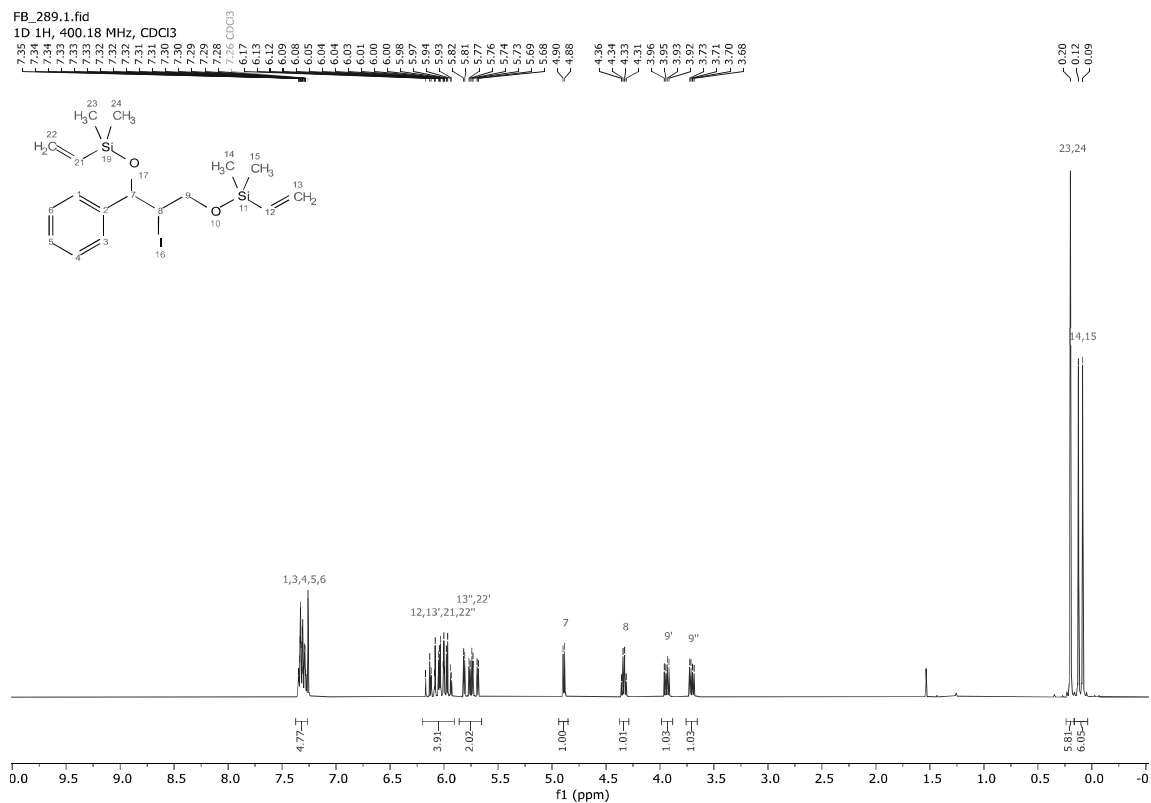
1D 13C(1H), 100.64 MHz, CDCl₃



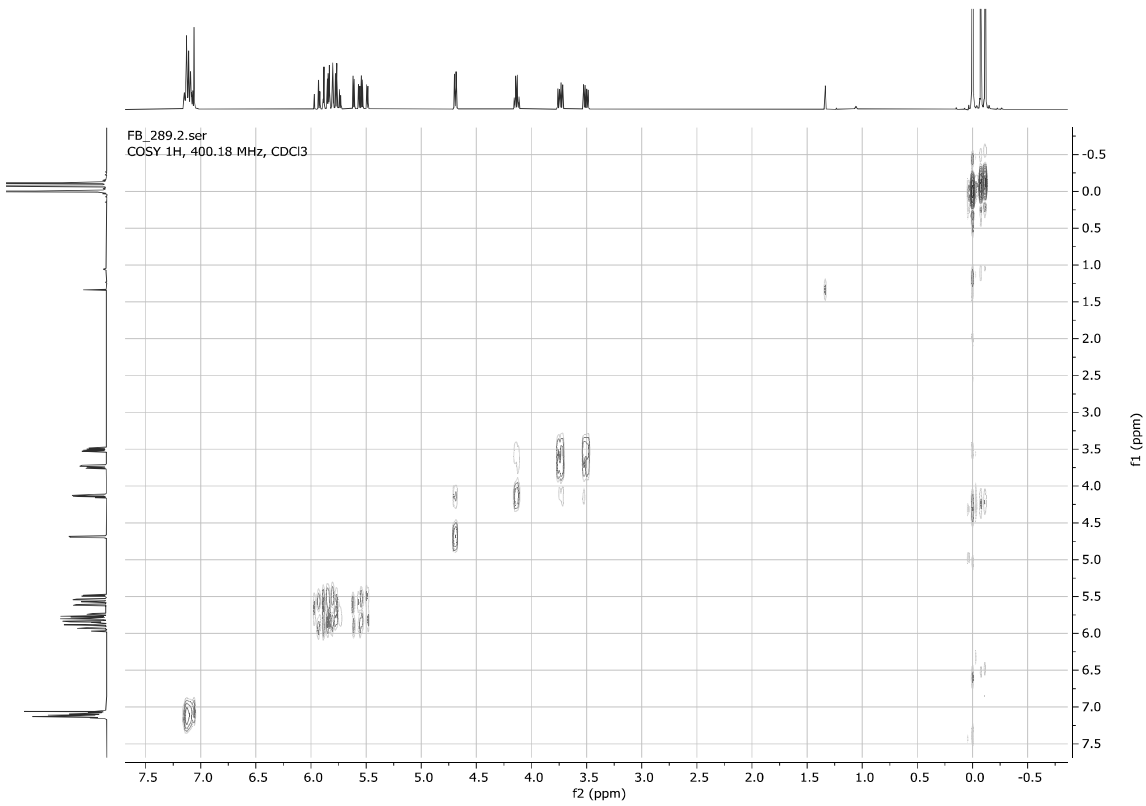
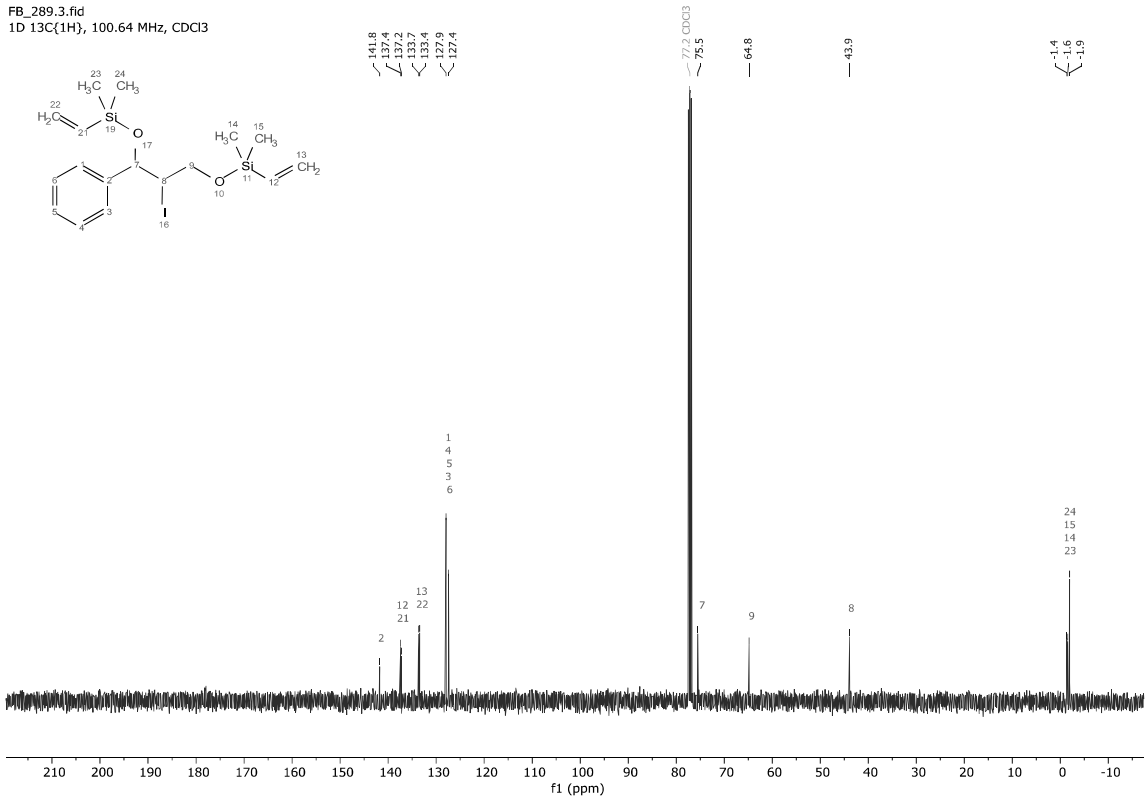


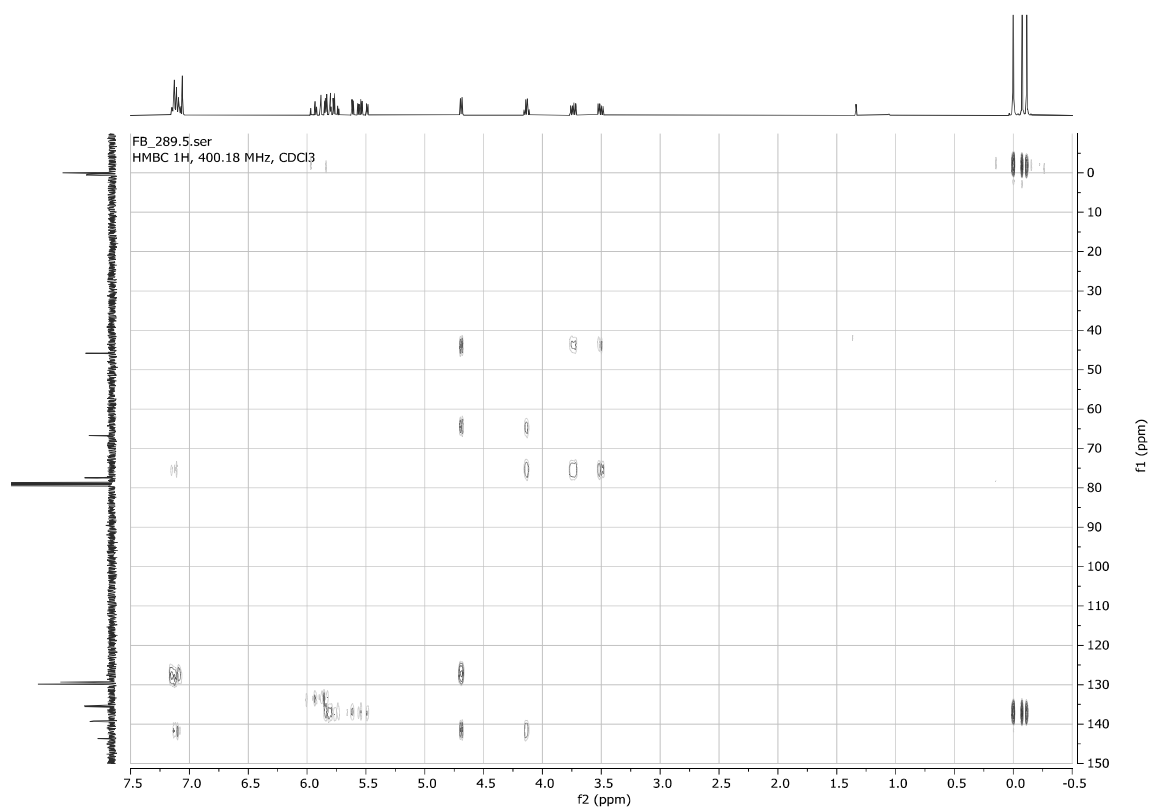
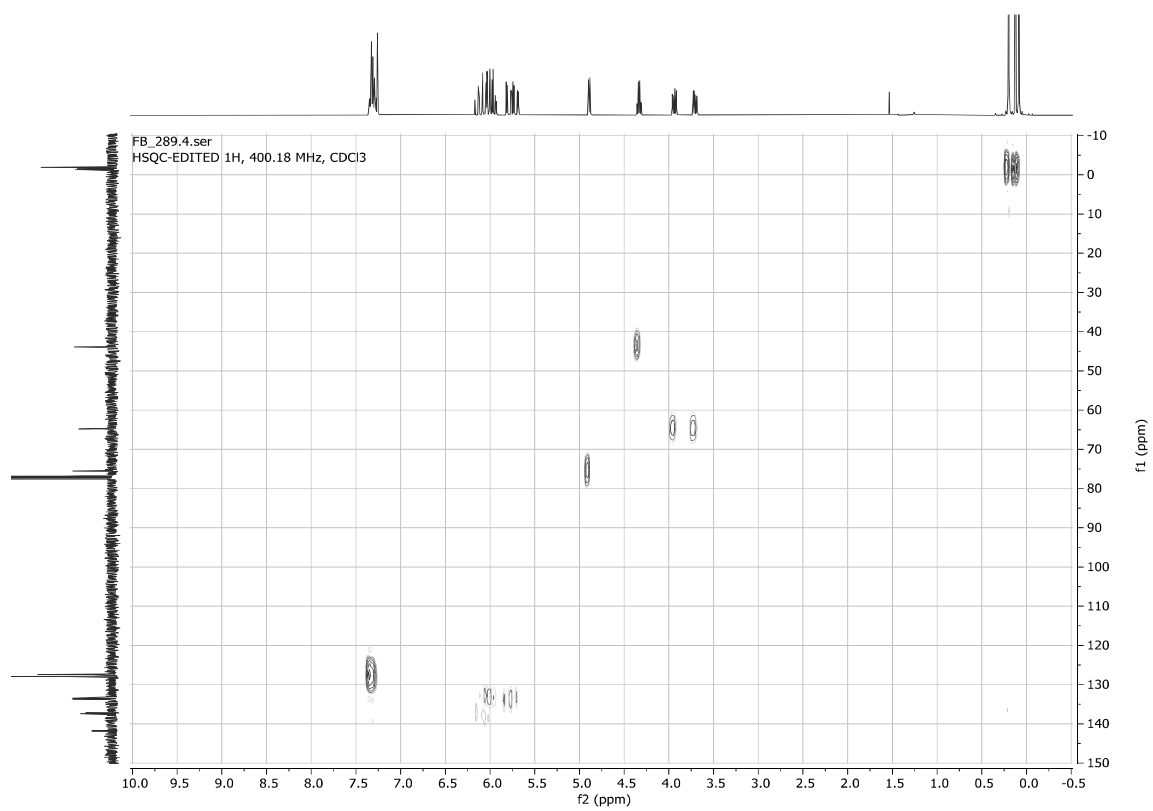


6-Iodo-3,3,9,9-tetramethyl-5-phenyl-4,8-dioxia-3,9-disilaundeca-1,10-diene **4h**



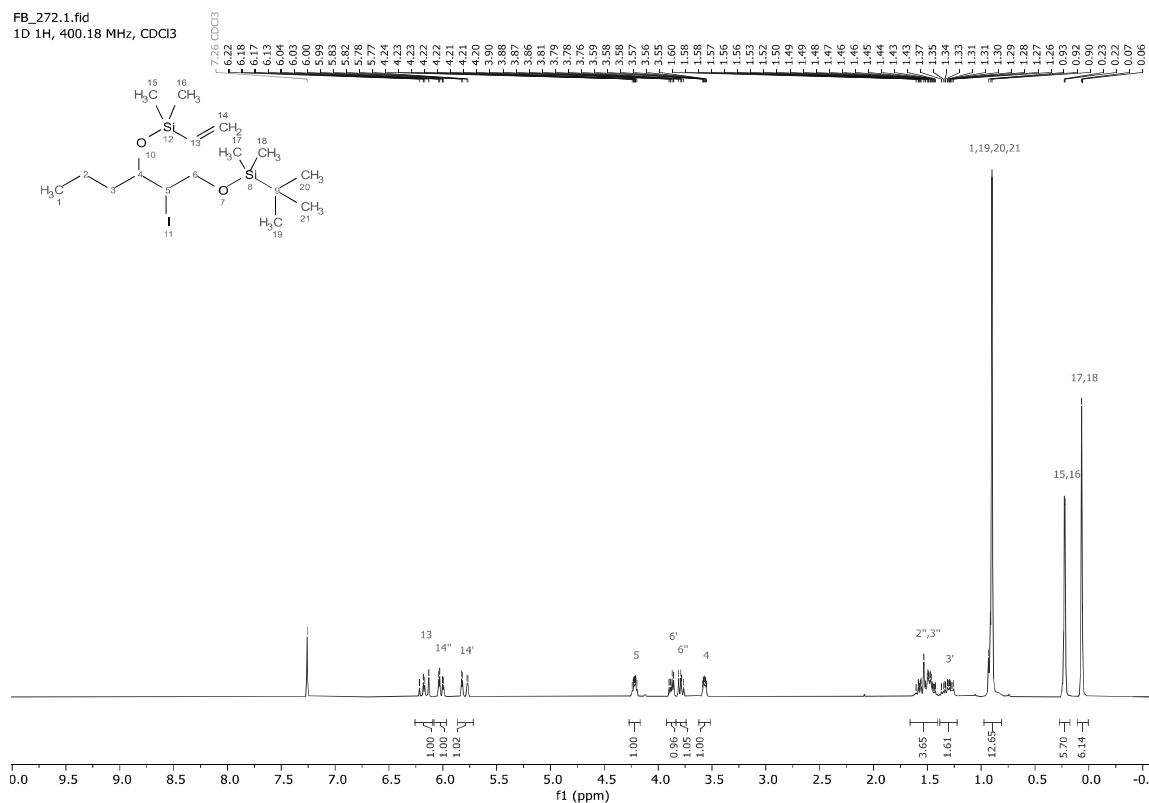
FB_289.3.fid
1D 13C{1H}, 100.64 MHz, CDCl3



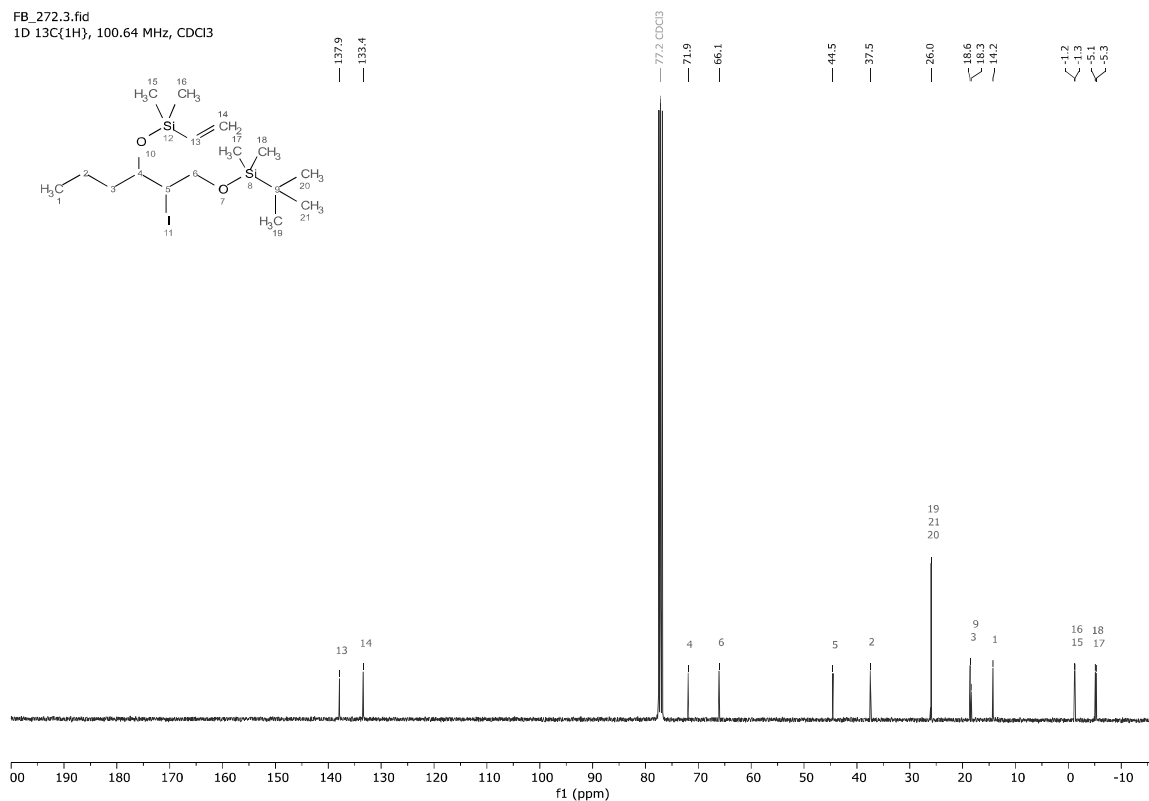


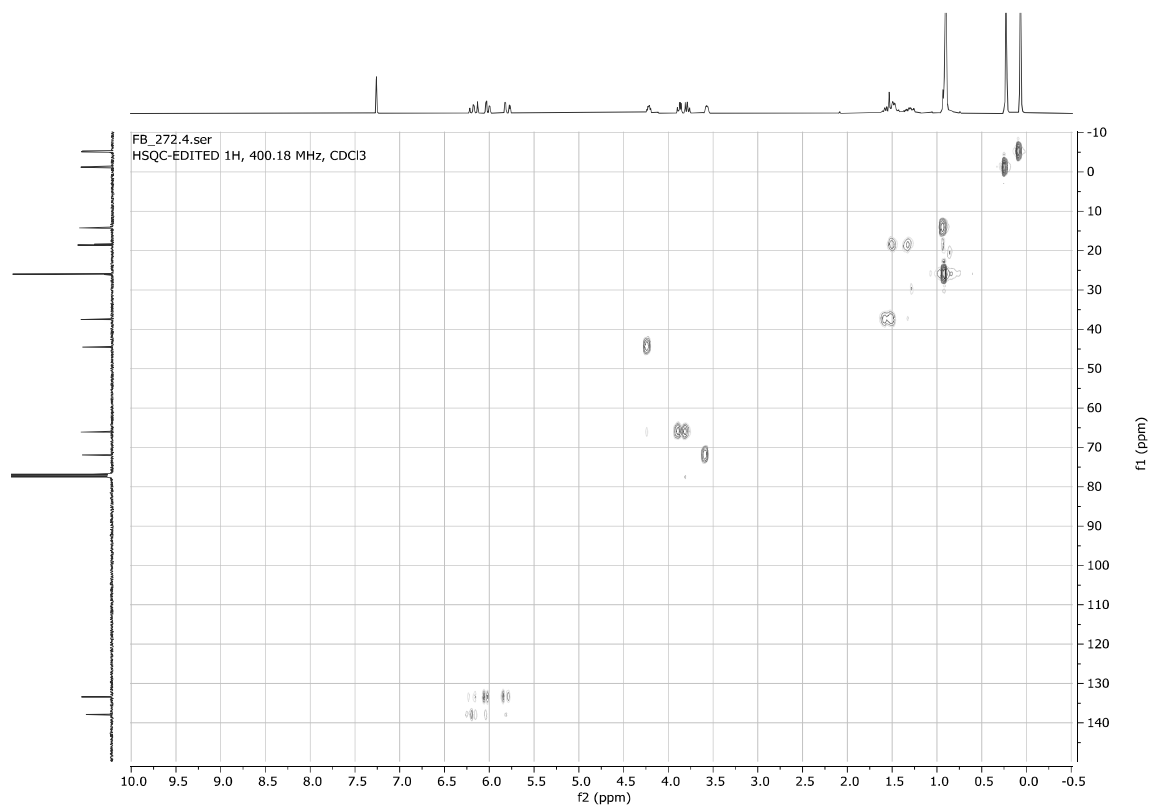
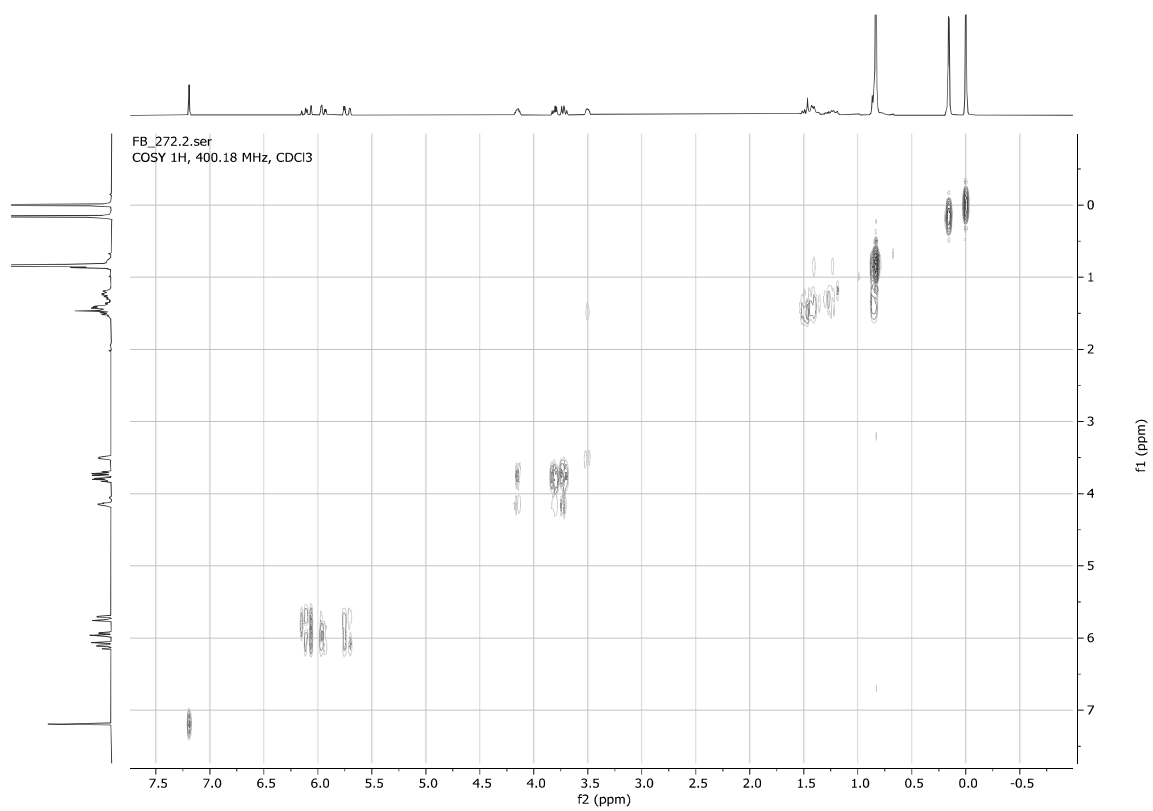
1-((*tert*-Butyldimethylsilyloxy)-2-iodohexan-3-oxy)dimethylvinylsilane **4i**

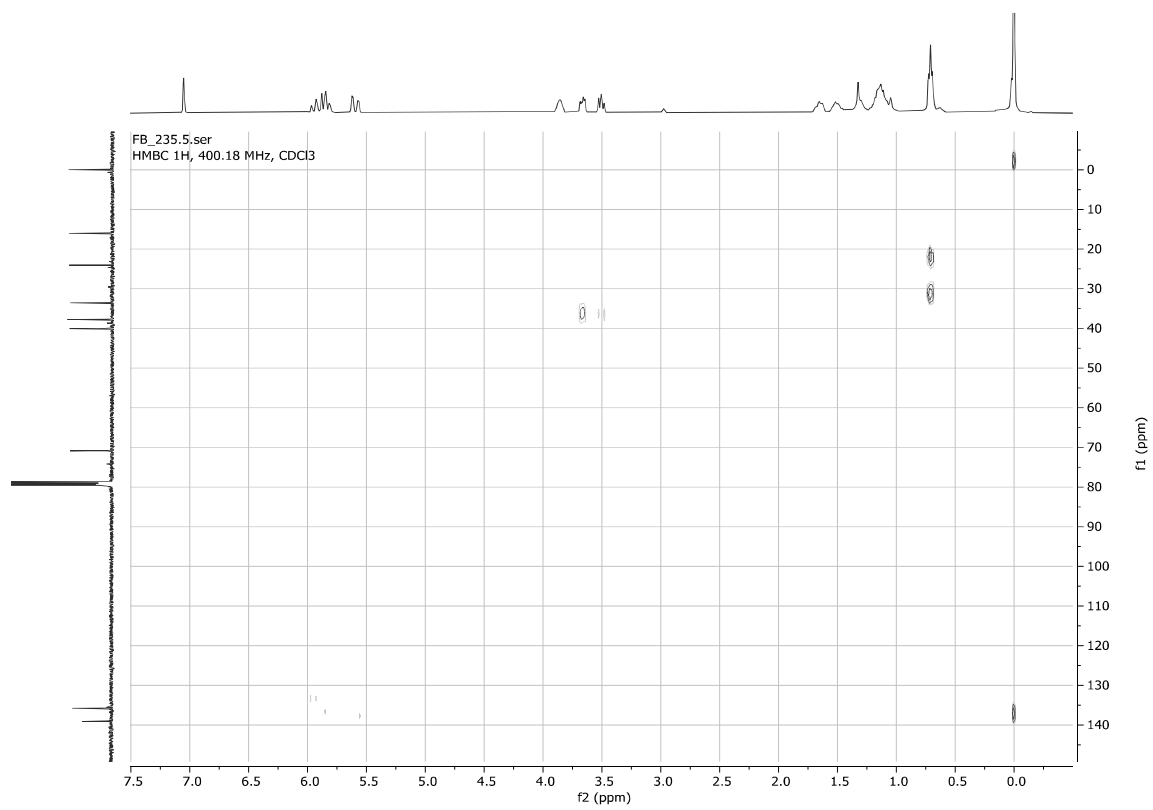
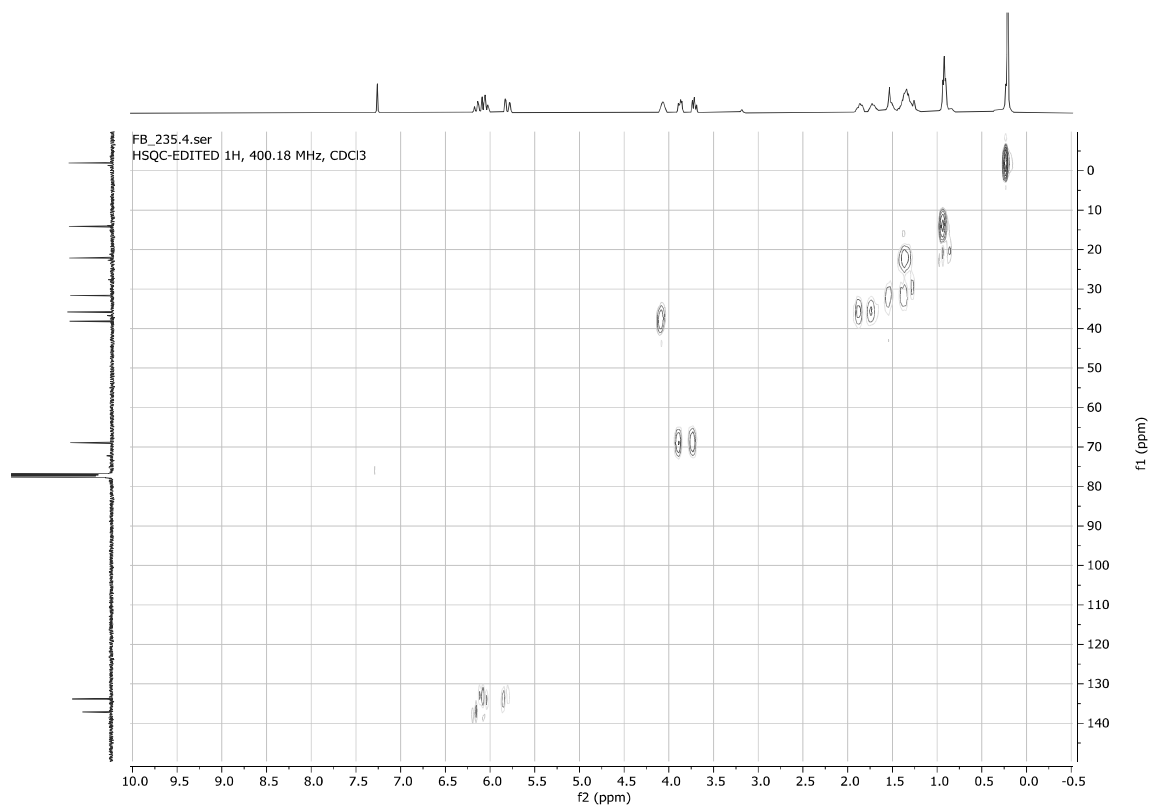
FB_272.1.fid
1D 1H, 400.18 MHz, CDCl₃



FB_272.3.fid
1D 13C{1H}, 100.64 MHz, CDCl₃

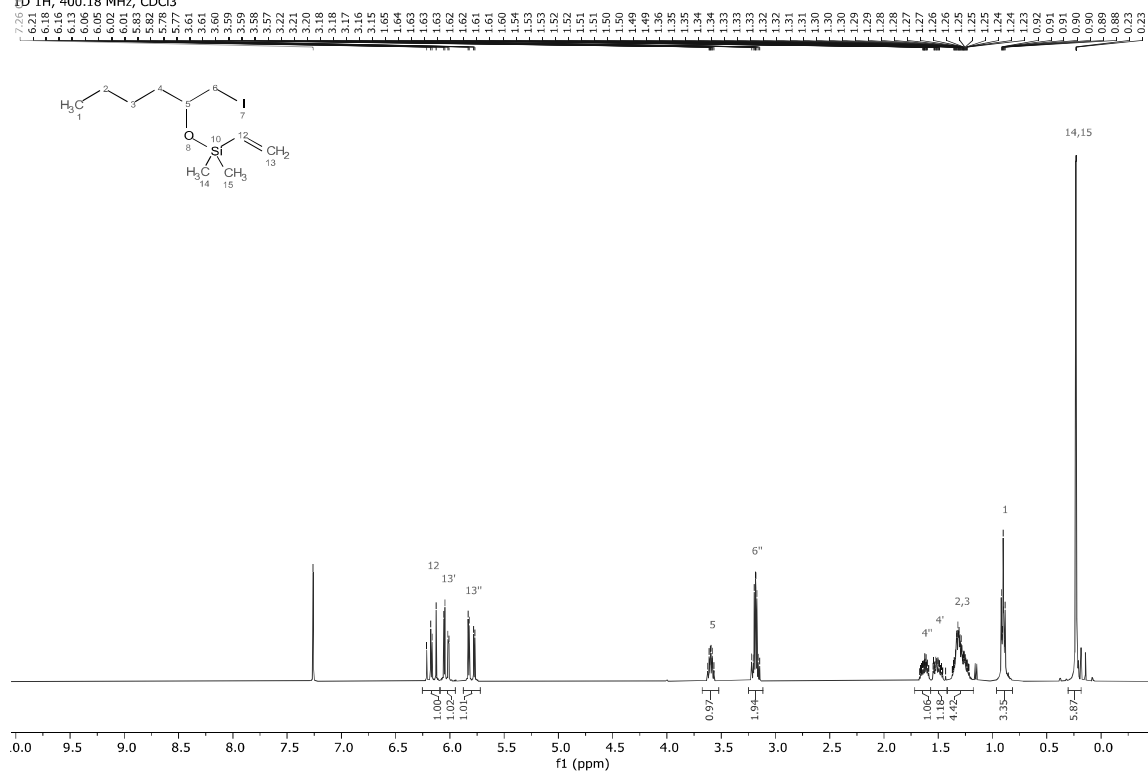




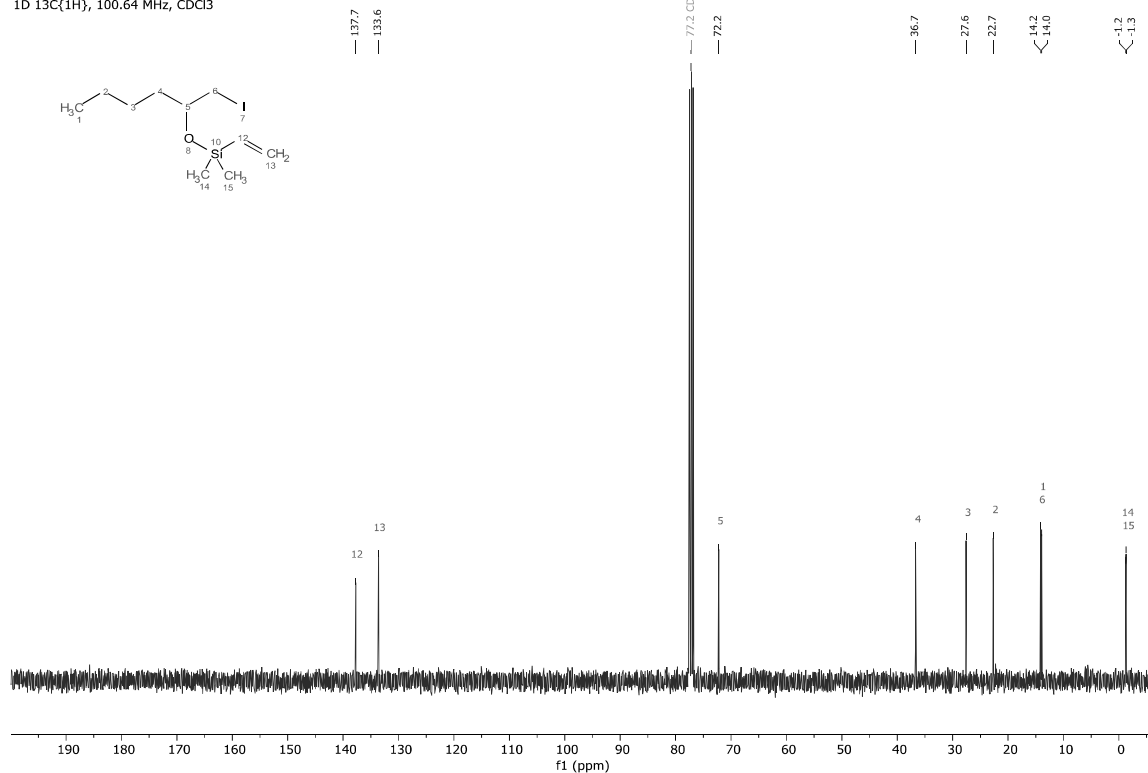


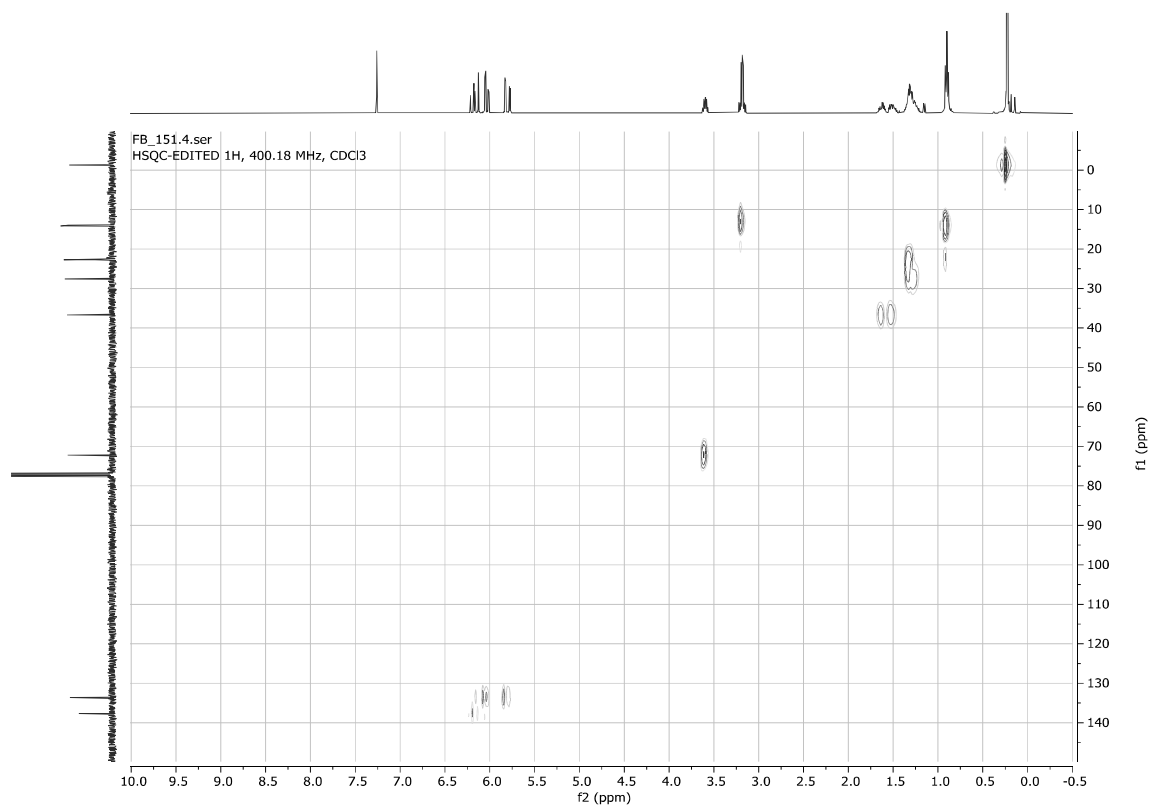
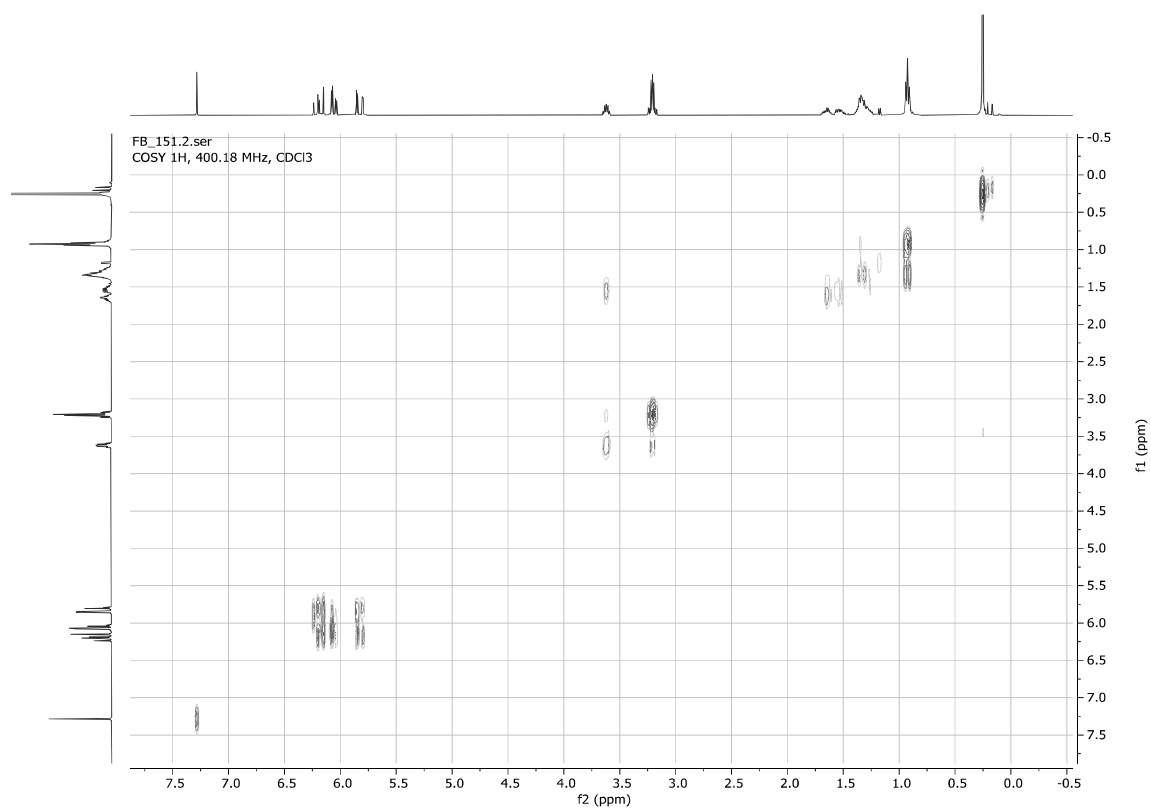
((1-Iodohexan-2-yl)oxy)dimethylvinylsilane **4k**

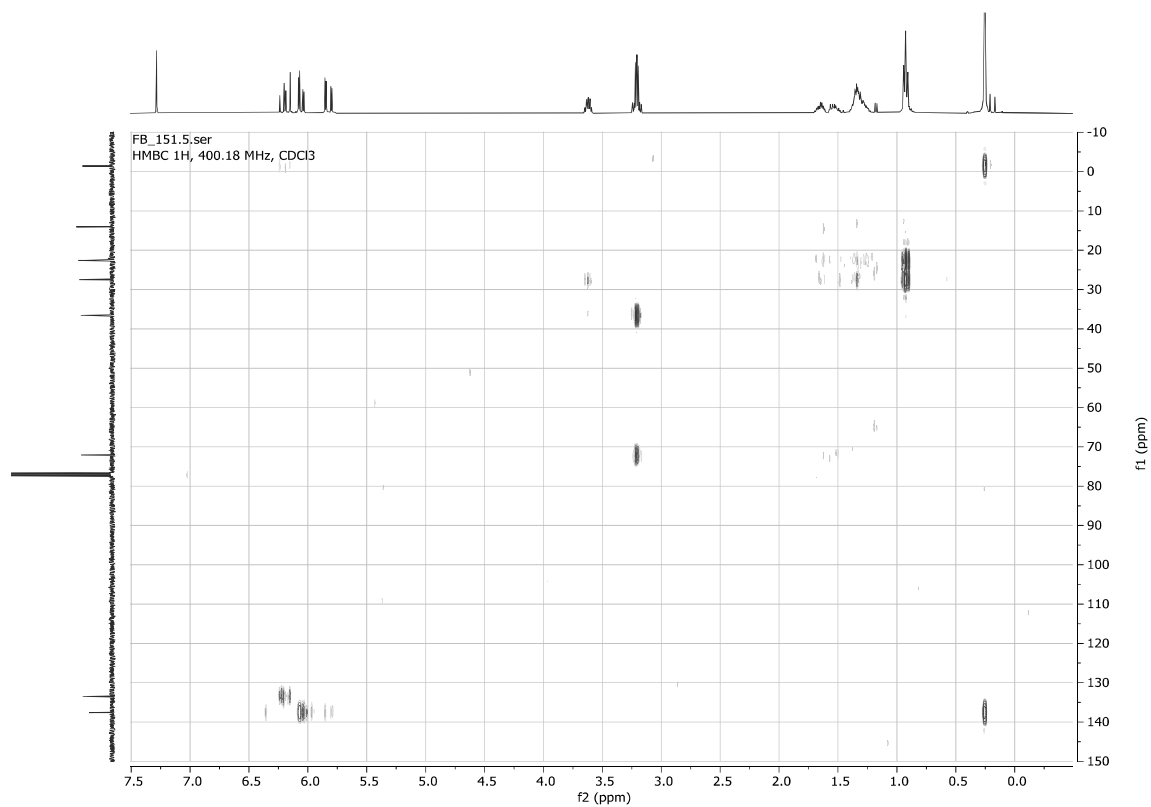
FB_151.1.fid
1D 1H, 400.18 MHz, CDCl3



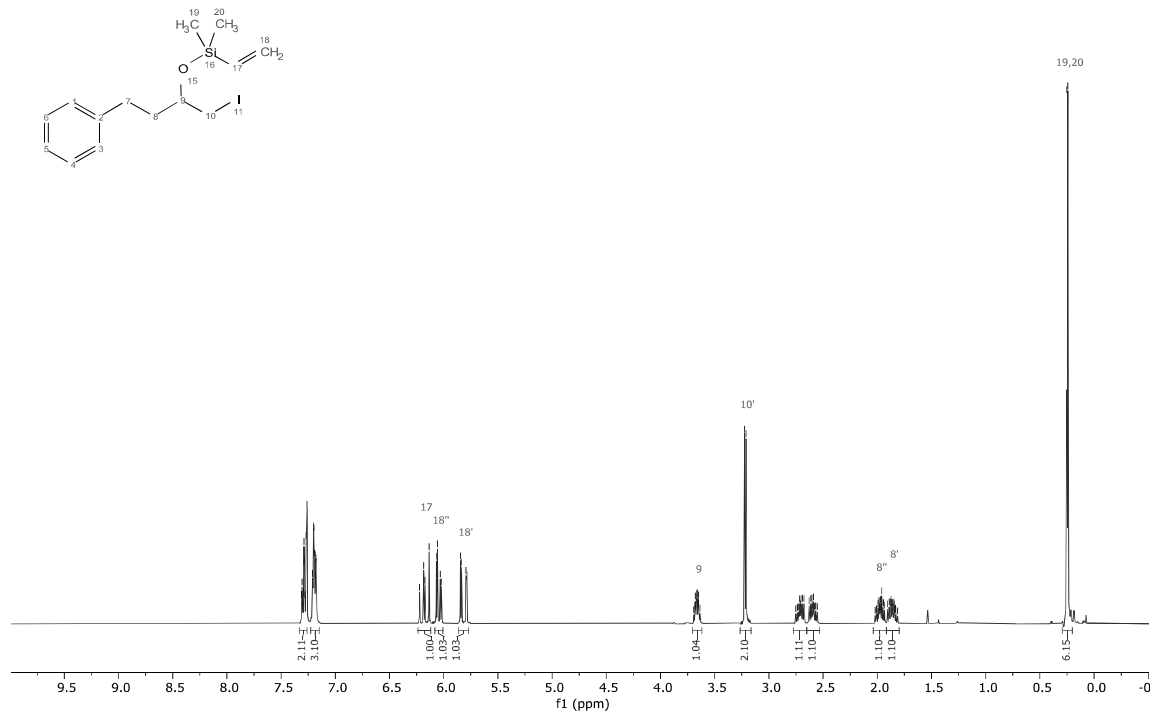
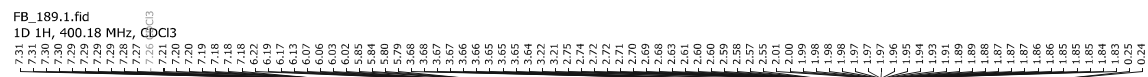
FB_151.3.fid
1D 13C(1H), 100.64 MHz, CDCl3



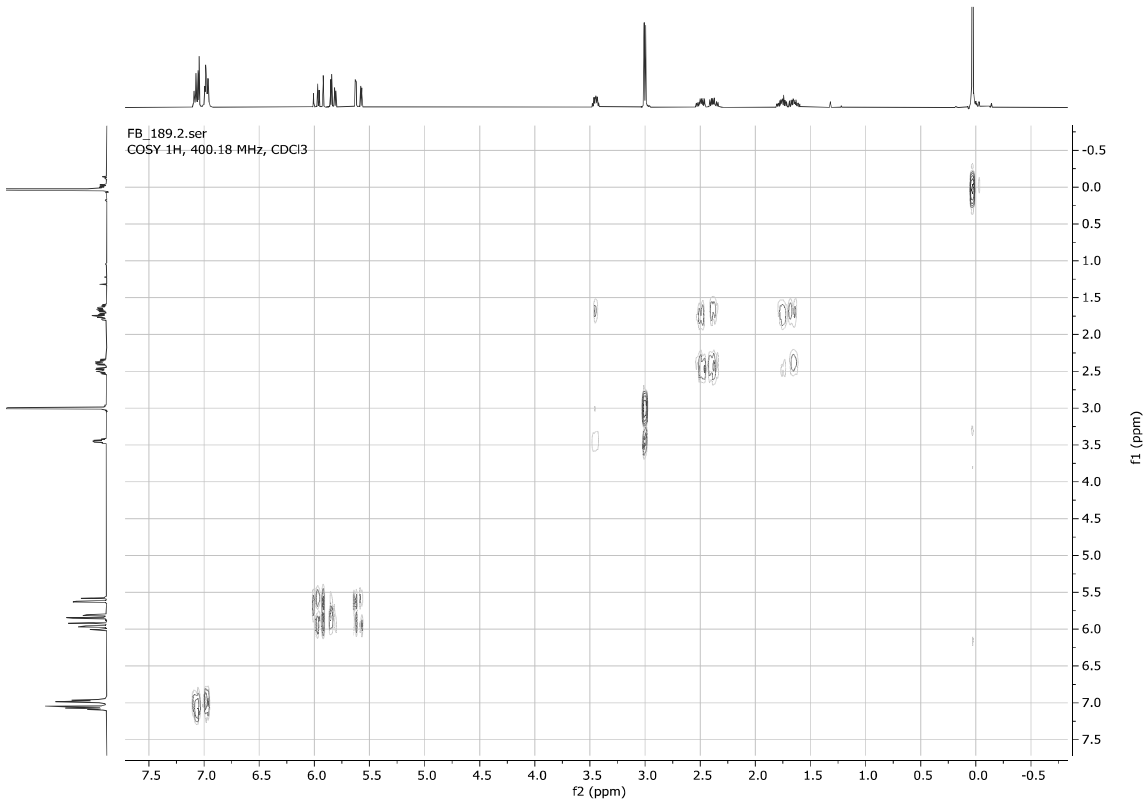
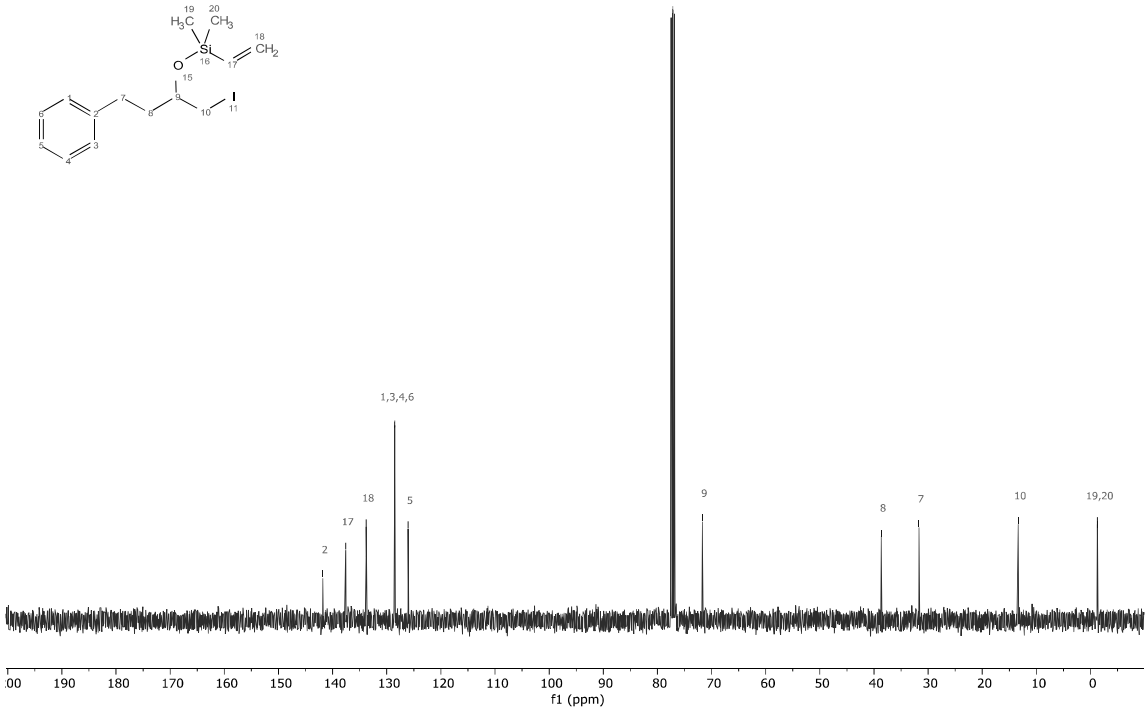


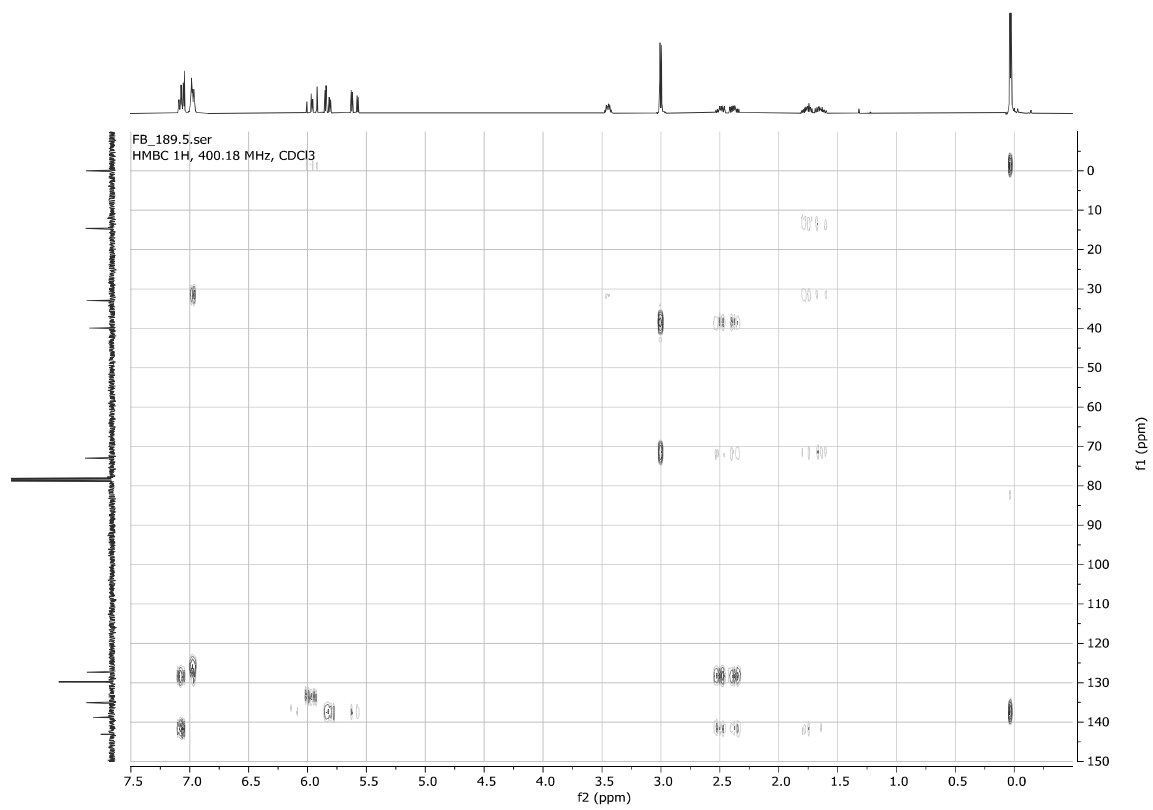
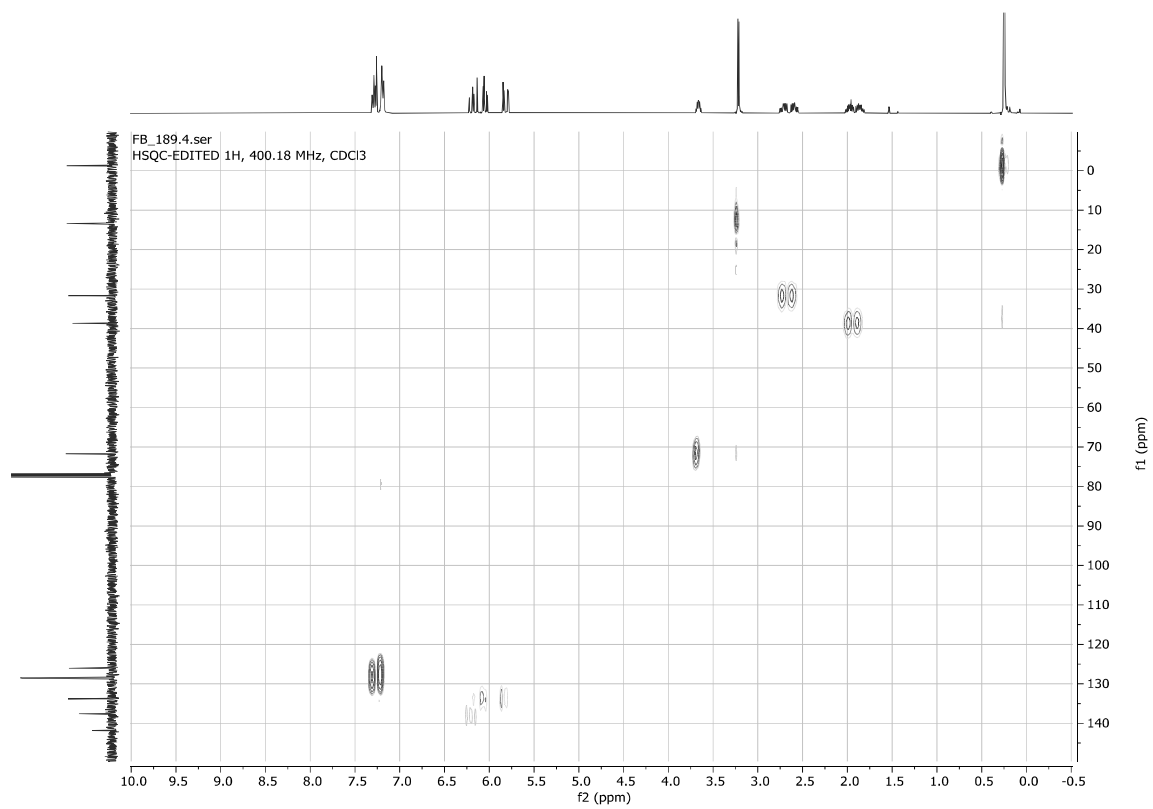


((1-Iodo-4-phenylbutan-2-yl)oxy)dimethylvinylsilane 4l



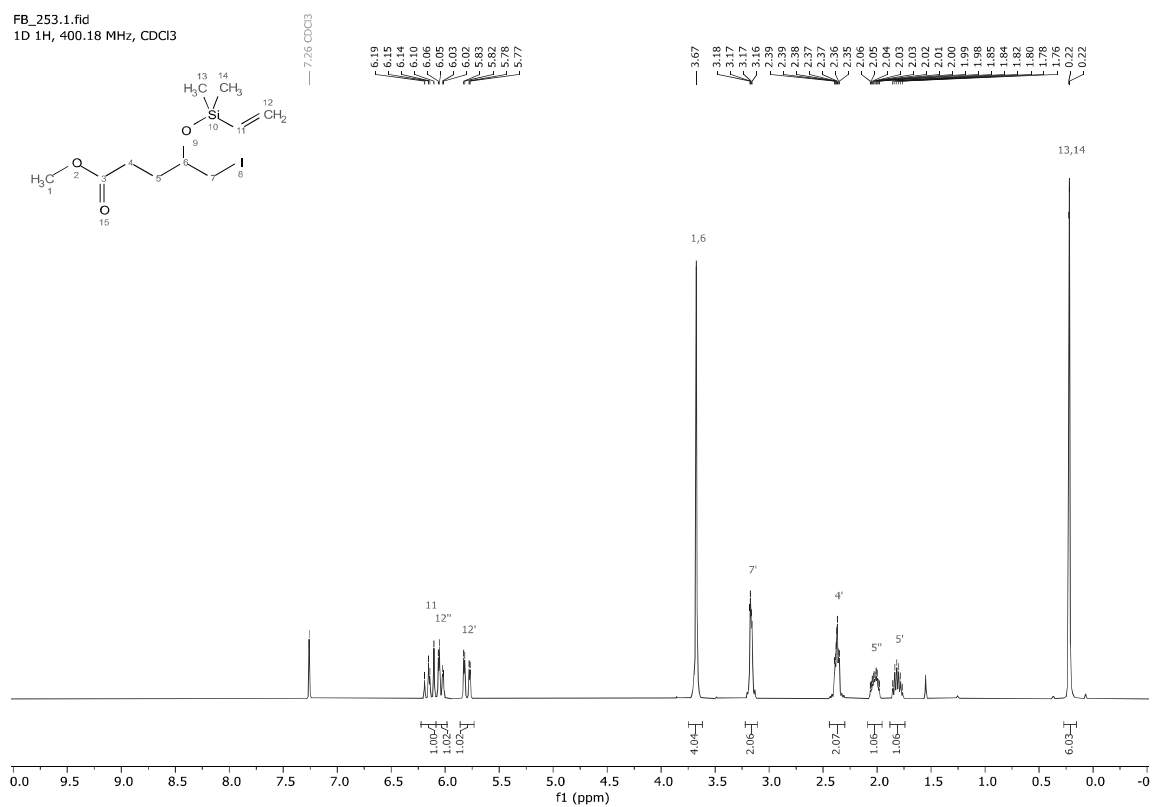
FB_189.3.fid
1D 13C{1H}, 100.64 MHz, CDCl3



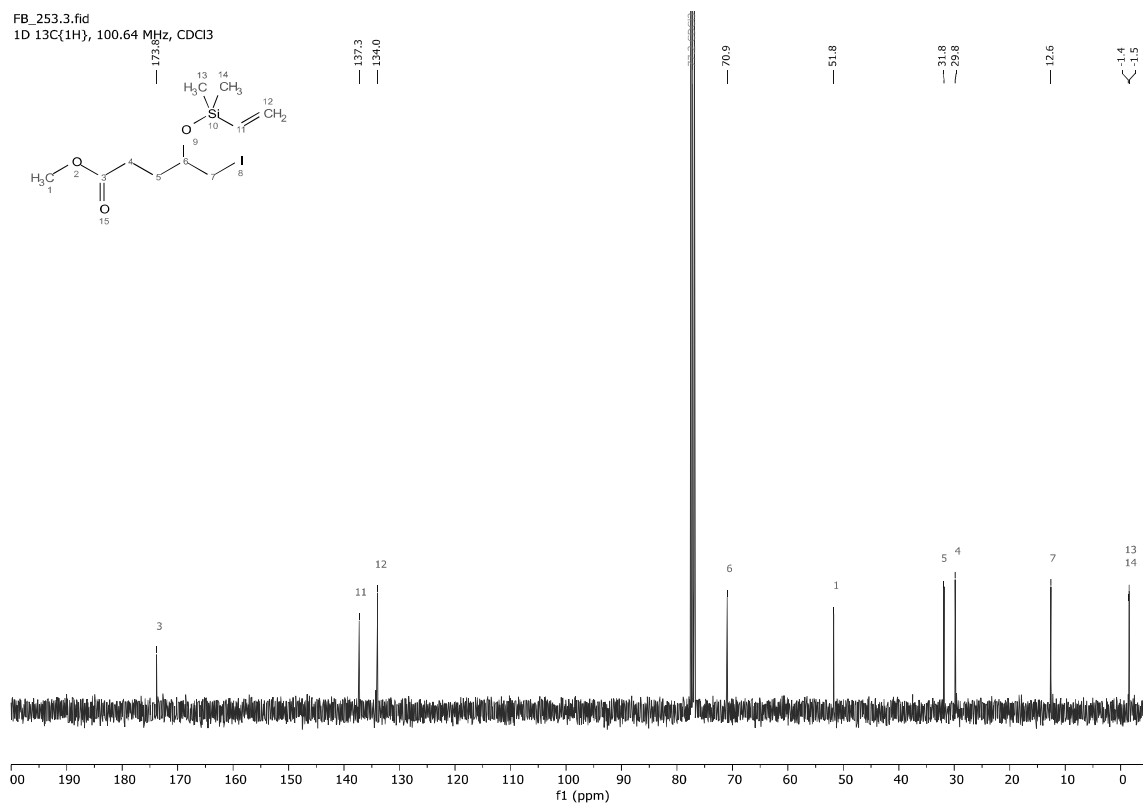


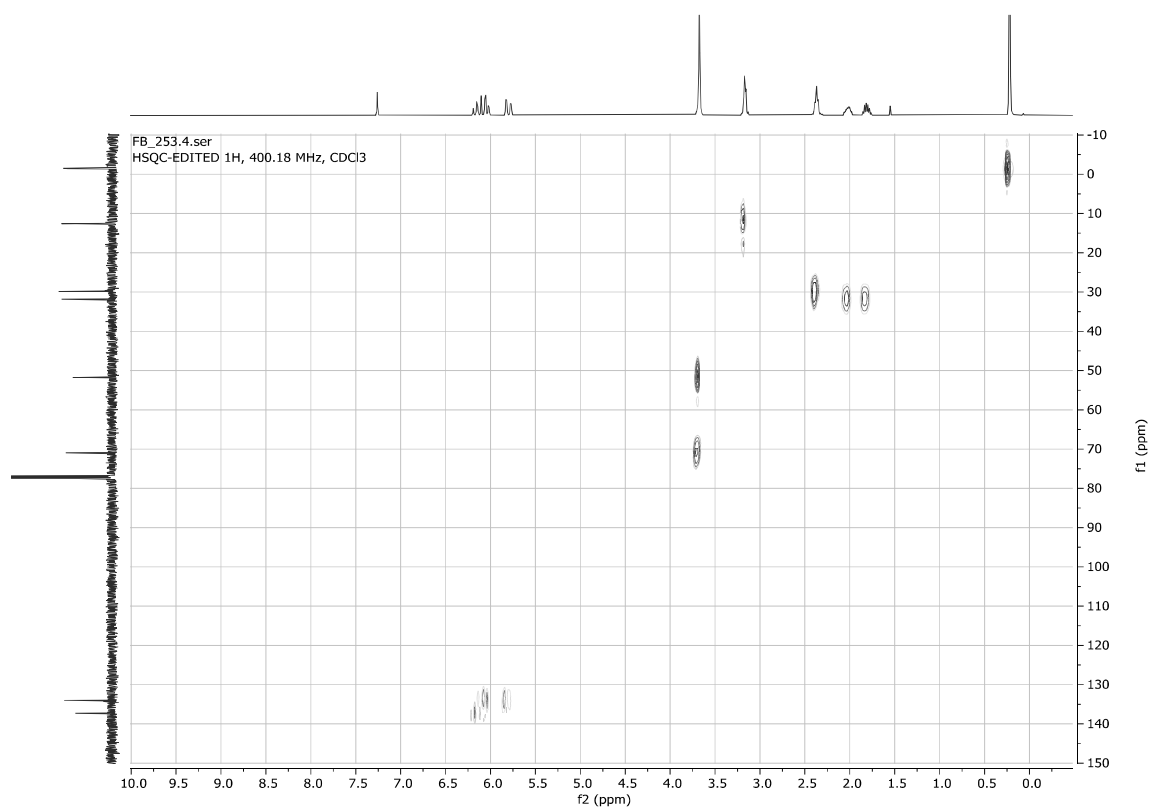
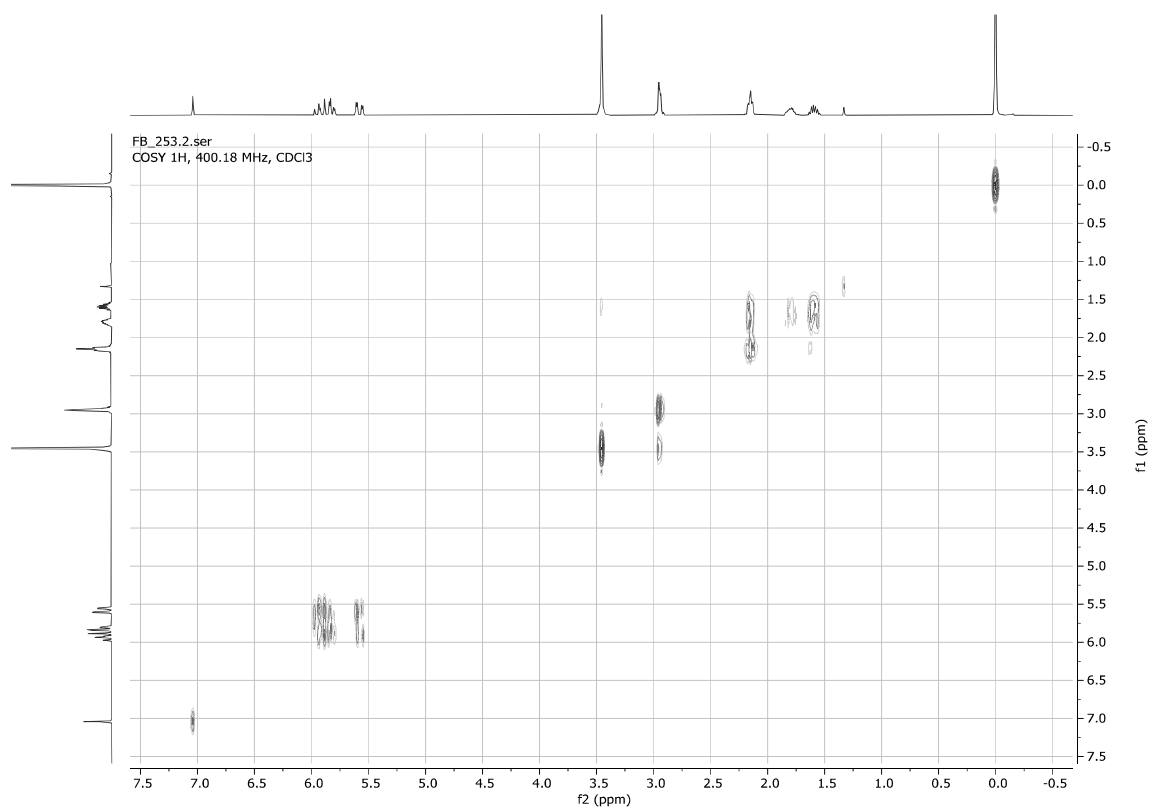
Methyl 4-((dimethylvinylsilyl)oxy)-5-iodopentanoate **4m**

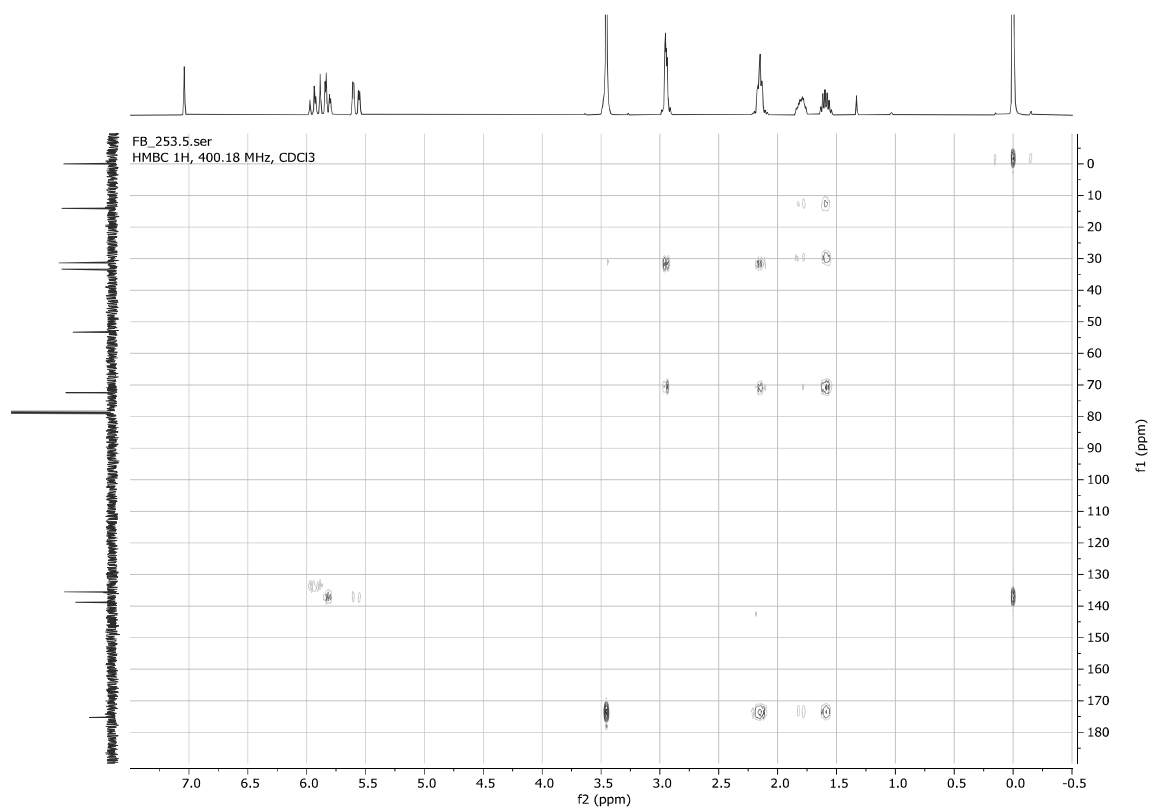
FB_253.1.fid
1D 1H, 400.18 MHz, CDCl₃



FB_253.3.fid
1D 13C(1H), 100.64 MHz, CDCl₃

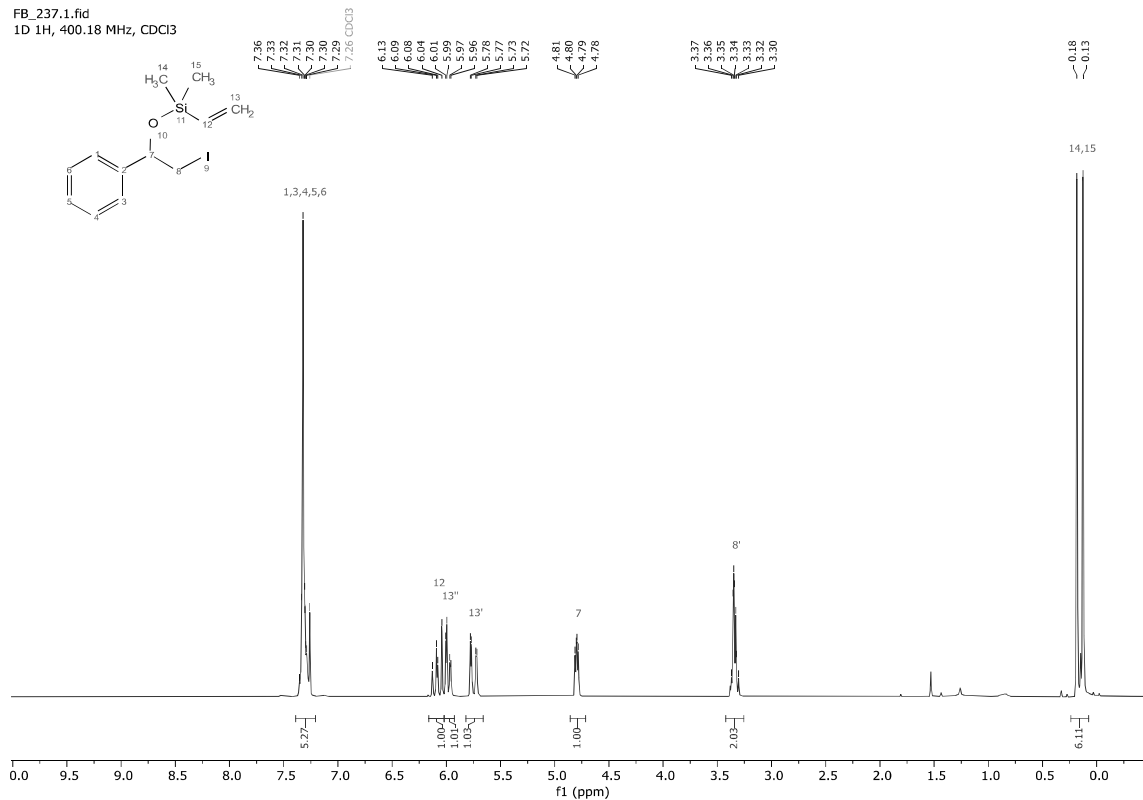




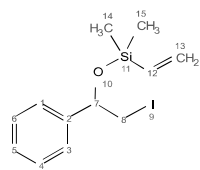


(2-Iodo-1-phenylethoxy)dimethylvinylsilane **4n**

FB_237.1.fid
1D 1H, 400.18 MHz, CDCl3



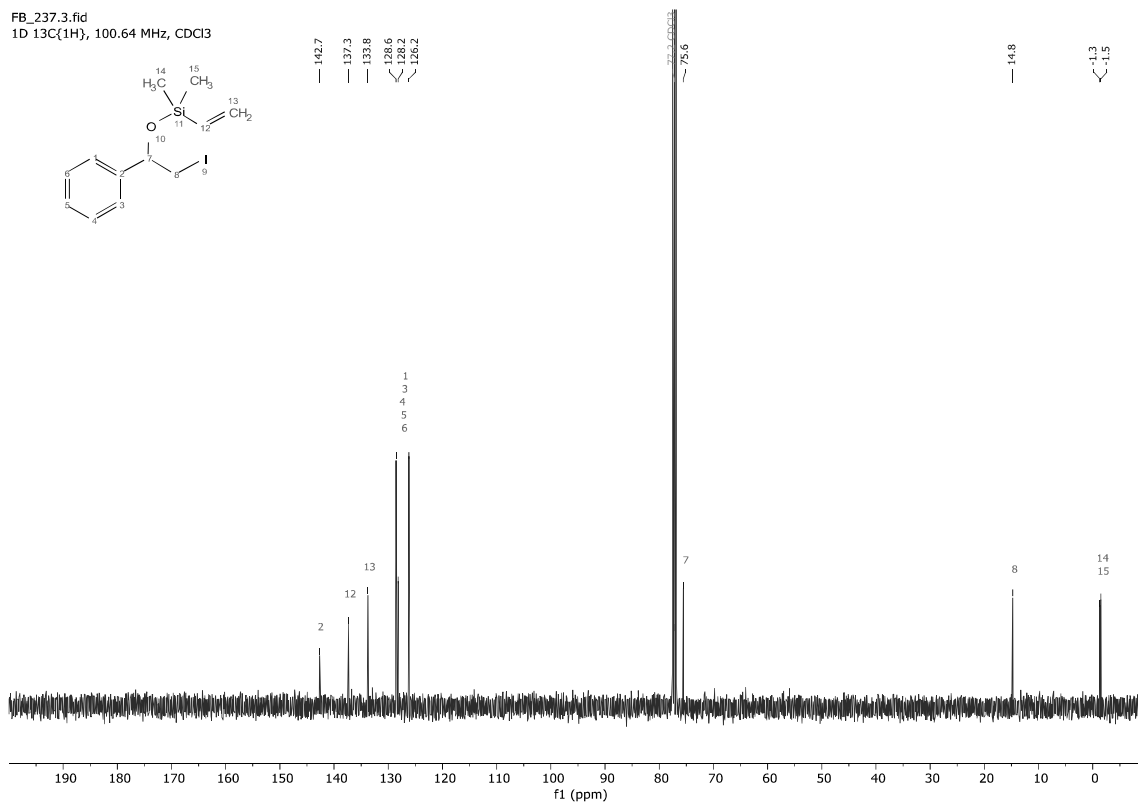
FB_237.3.fid
1D 13C{1H}, 100.64 MHz, CDCl3



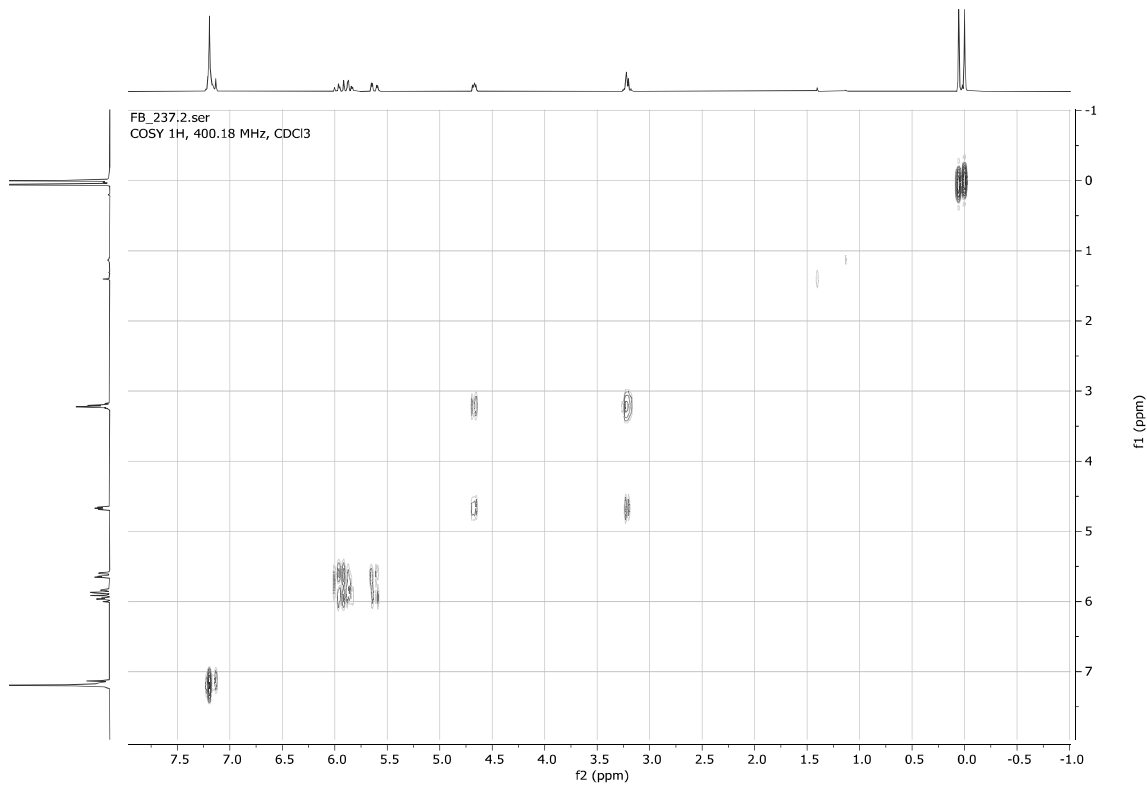
142.7
137.3
133.8
128.6
126.2

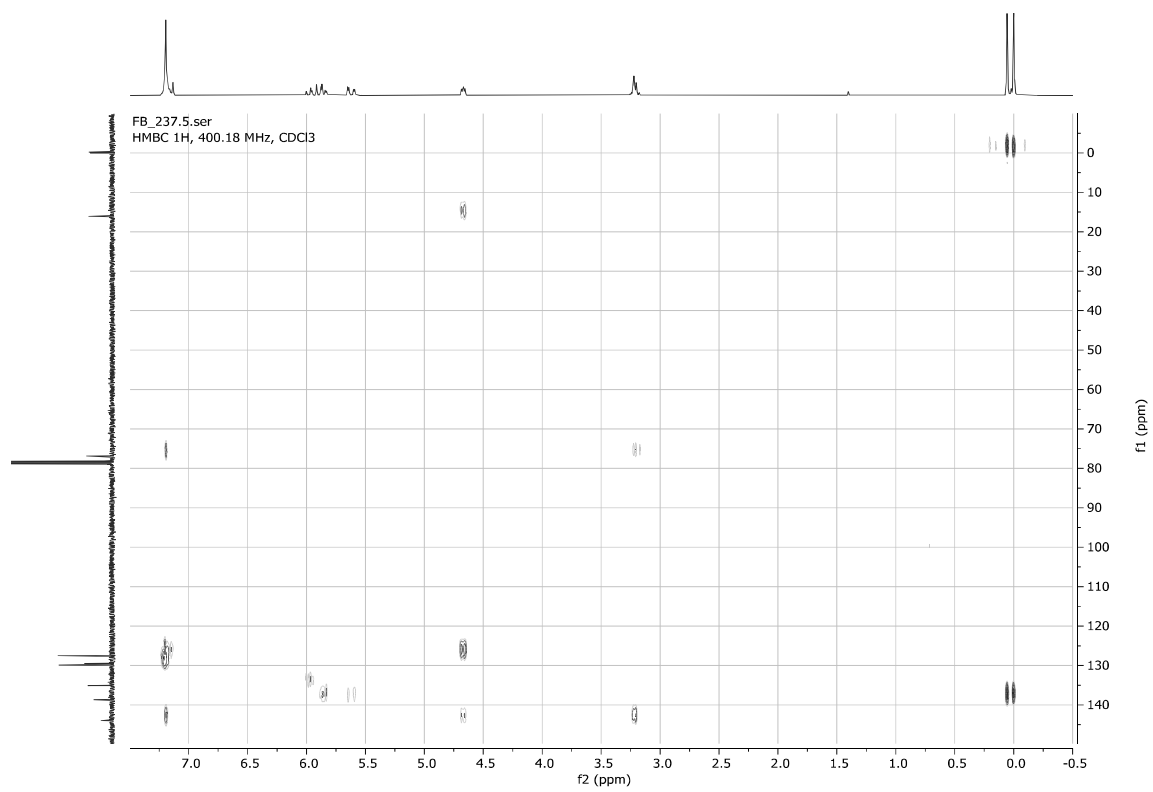
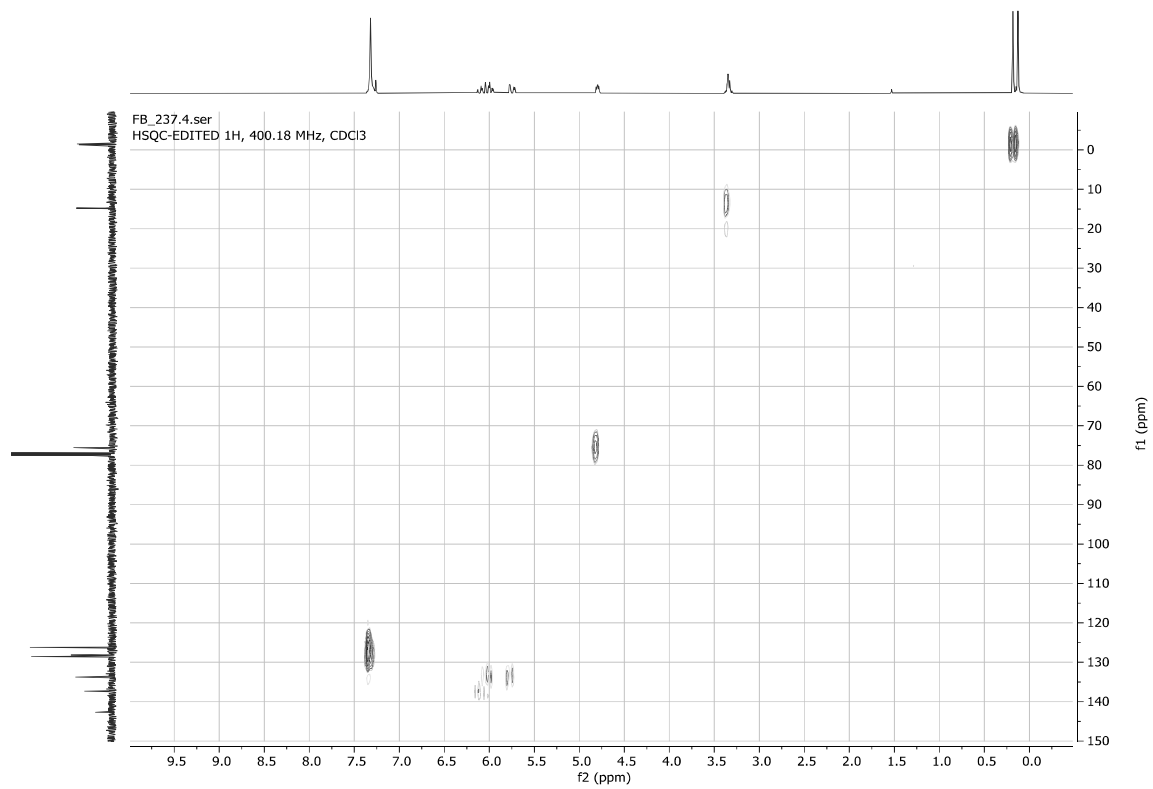
14.8

1.3
1.3



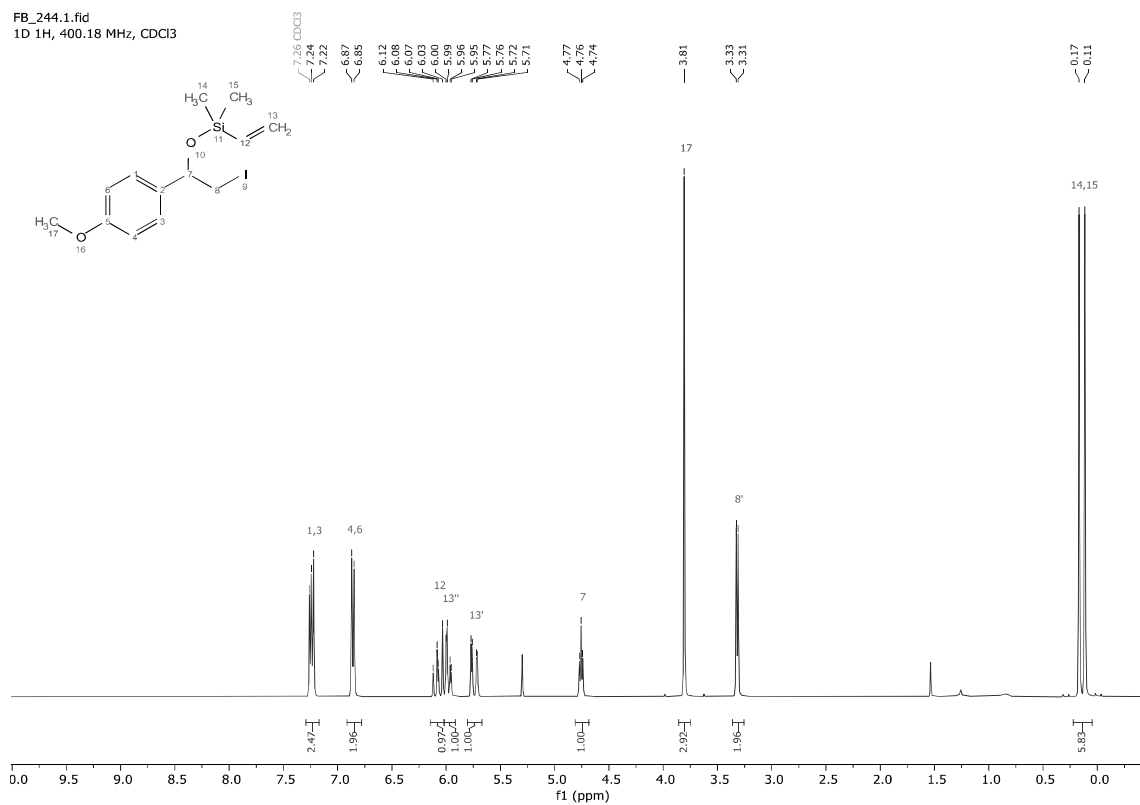
FB_237.2.ser
COSY 1H, 400.18 MHz, CDCl3



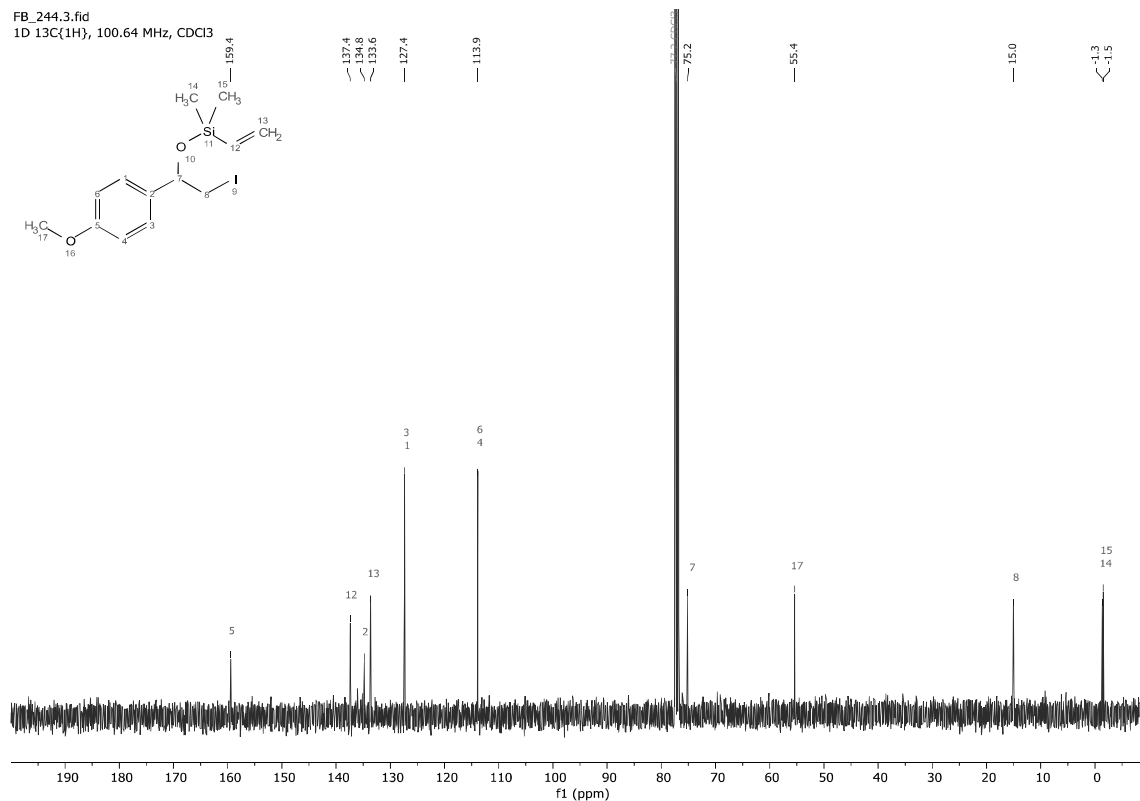


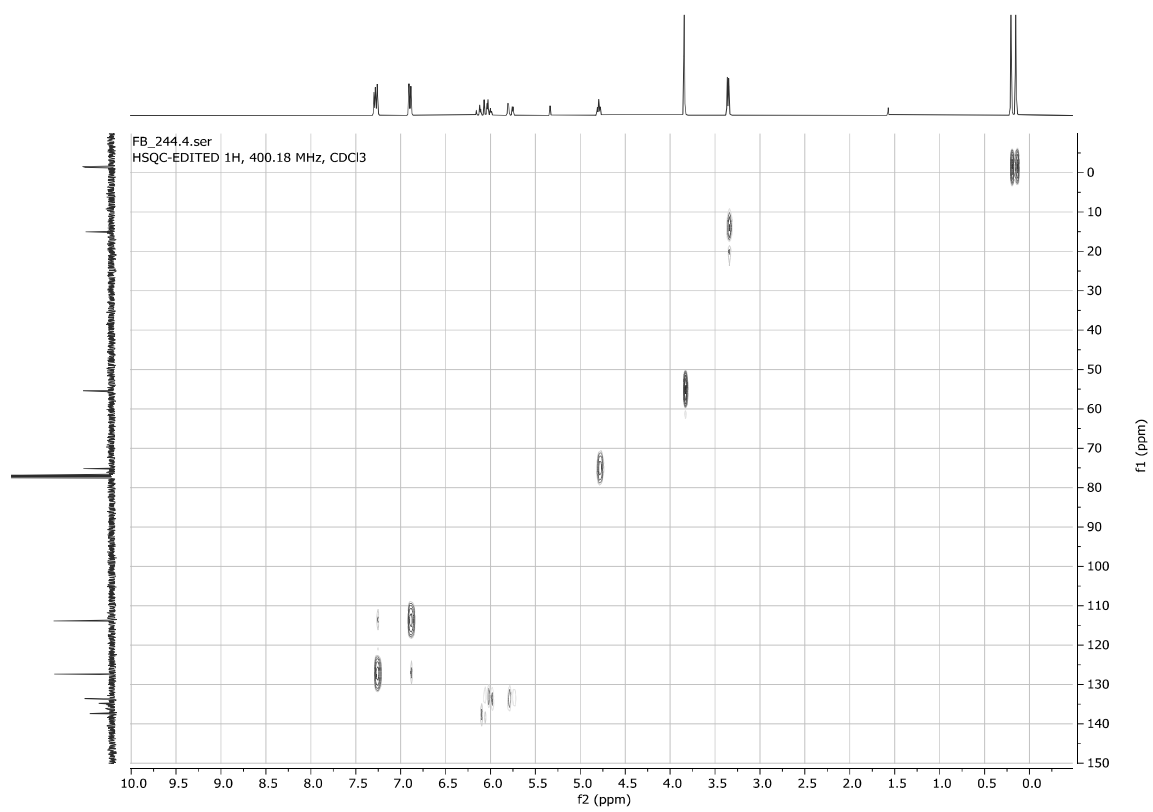
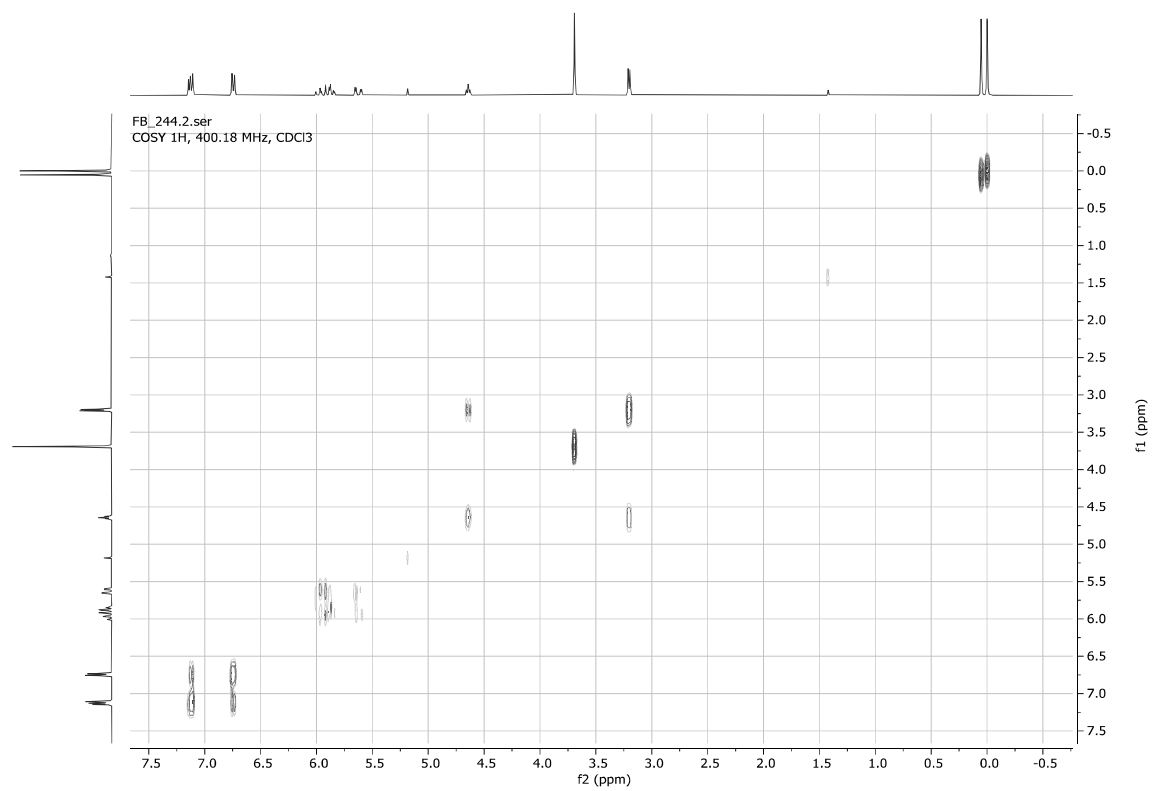
(2-Iodo-1-(4-methoxyphenyl)ethoxy)dimethylvinylsilane **4o**

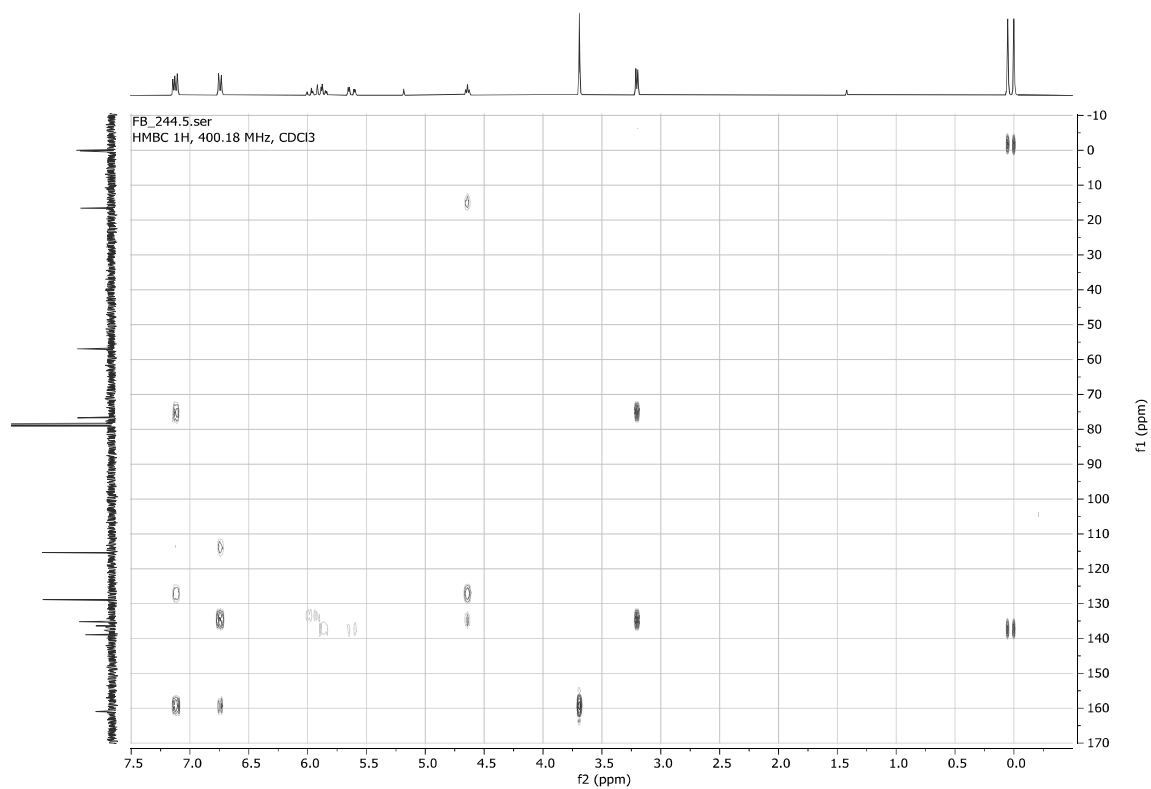
FB_244.1.fid
1D 1H, 400.18 MHz, CDCl3



FB_244.3.fid
1D 13C(1H), 100.64 MHz, CDCl3

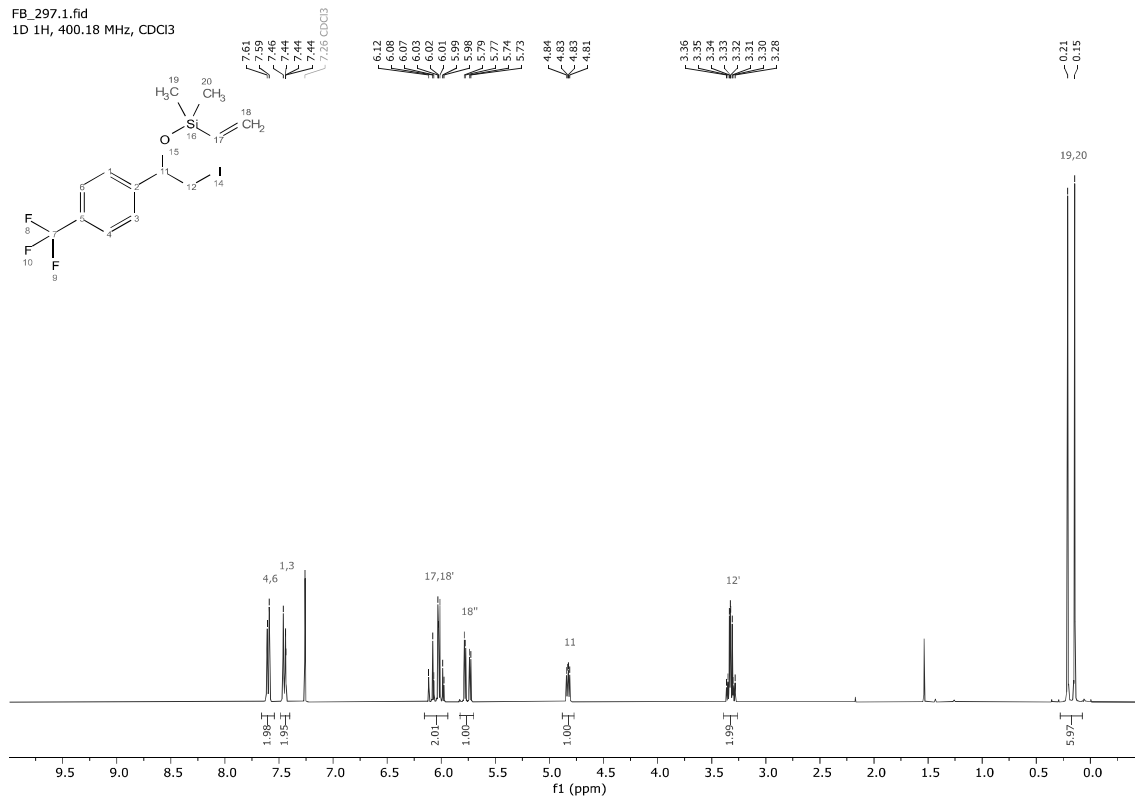




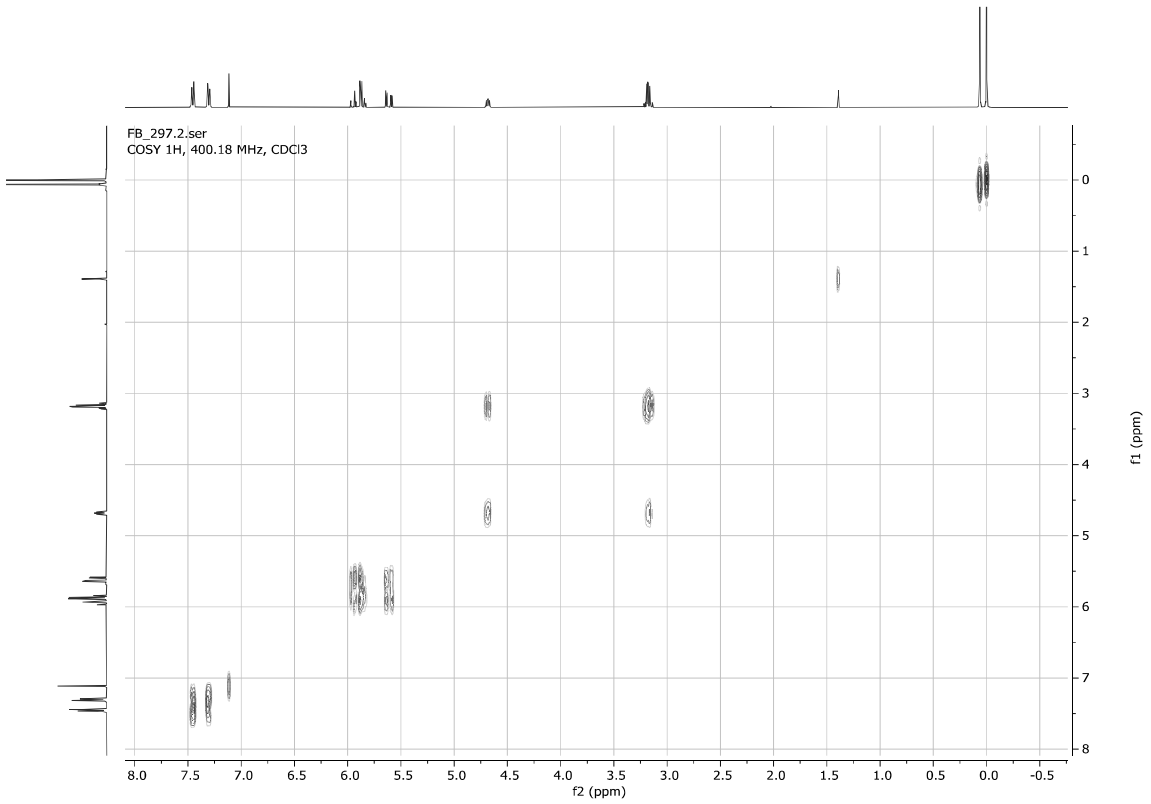
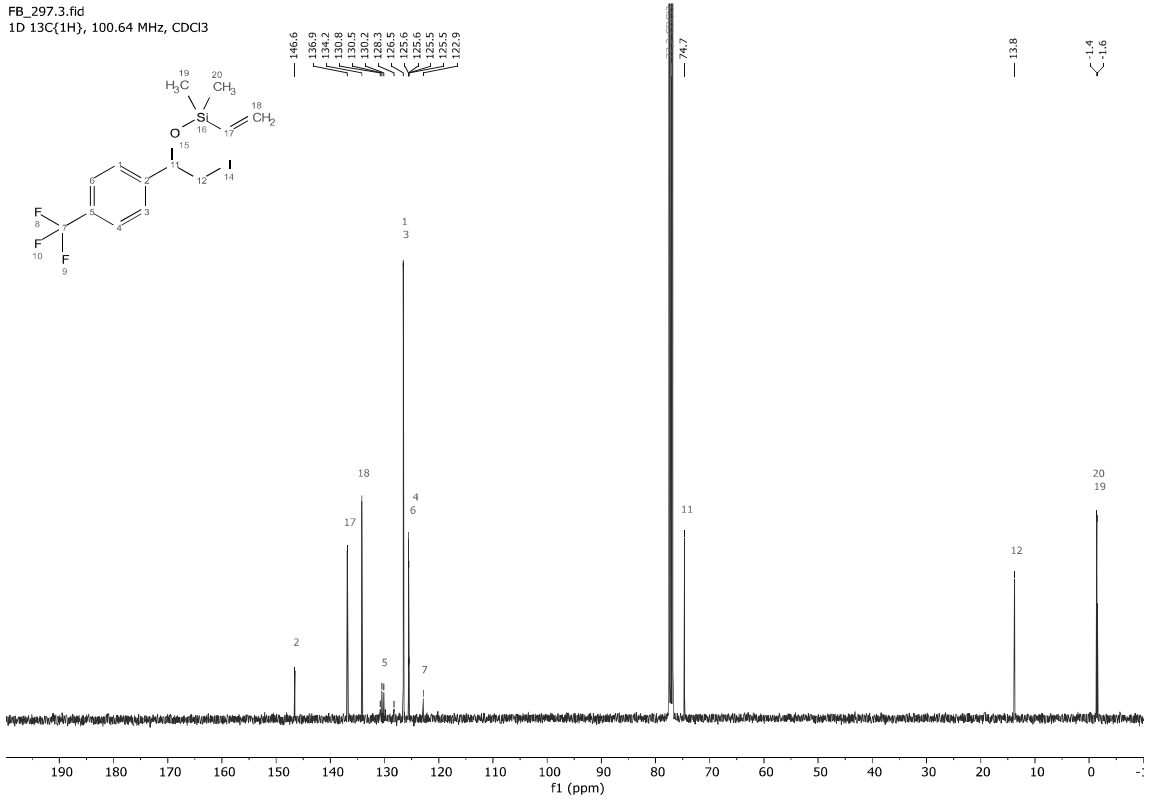


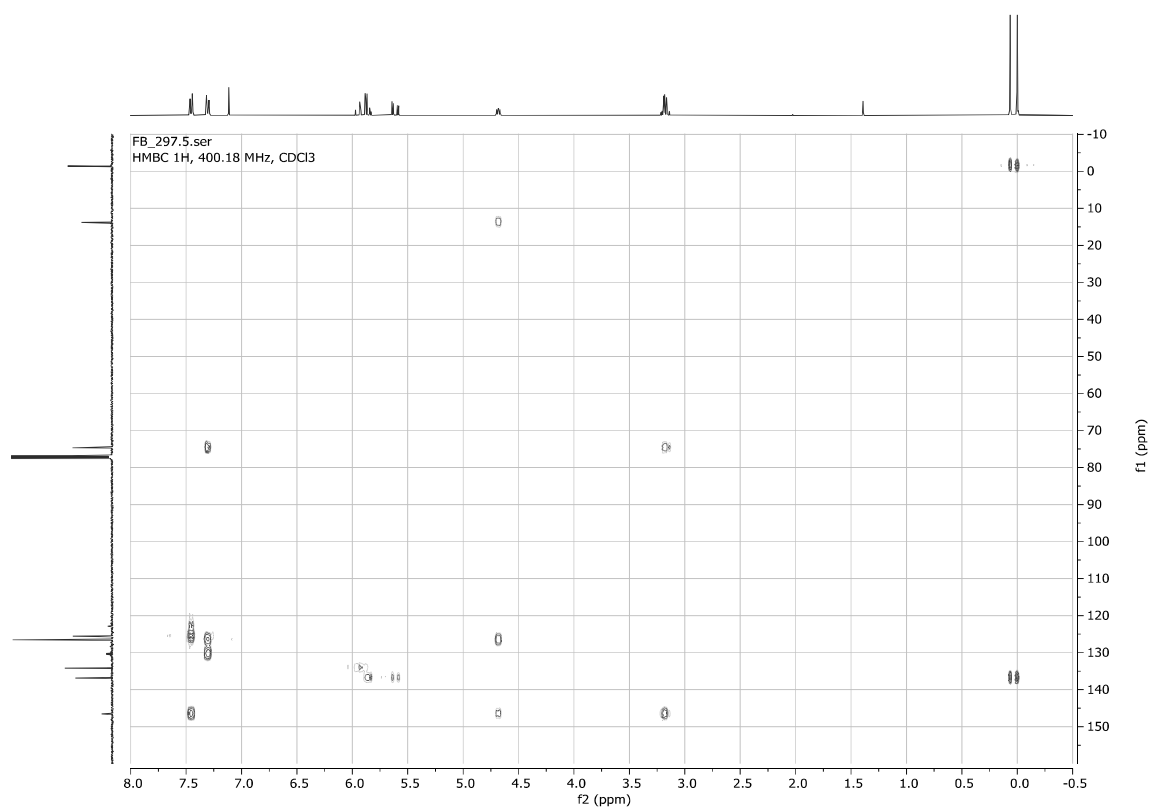
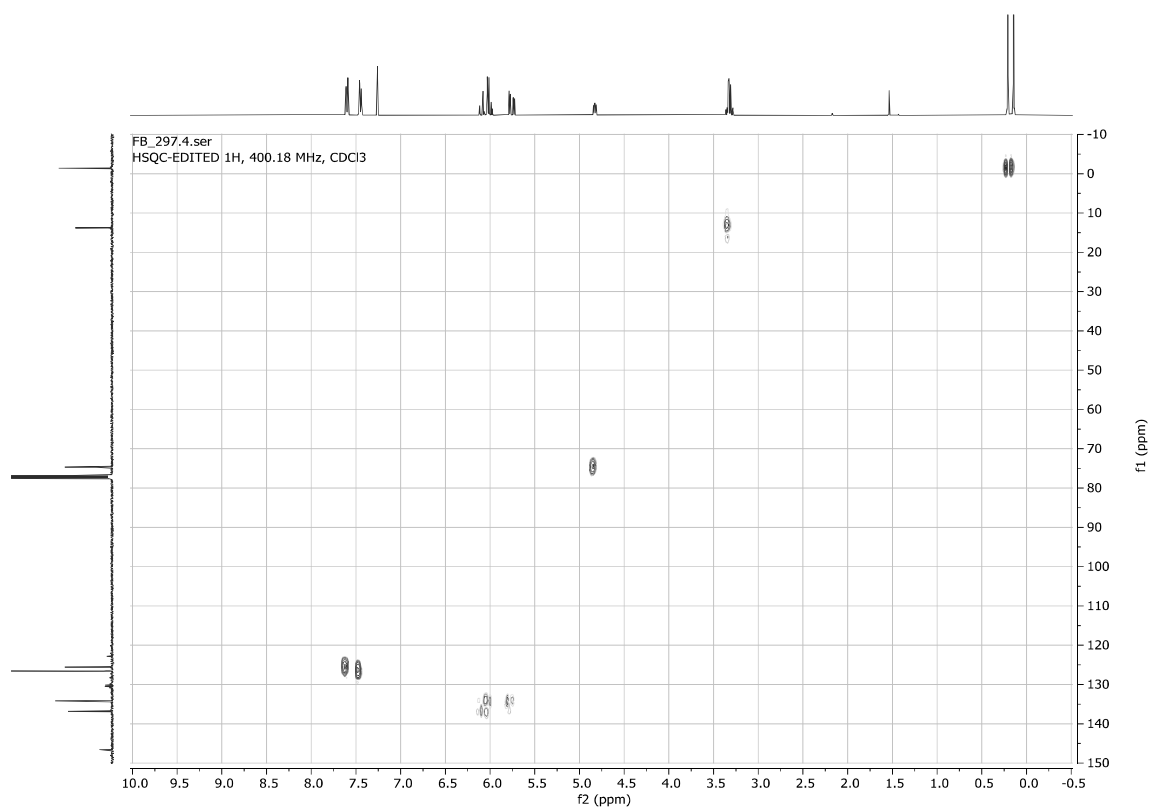
(2-Iodo-1-(4-(trifluoromethyl)phenyl)ethoxy)dimethylvinylsilane **4p**

FB_297.1.fid
1D 1H, 400.18 MHz, CDCl3



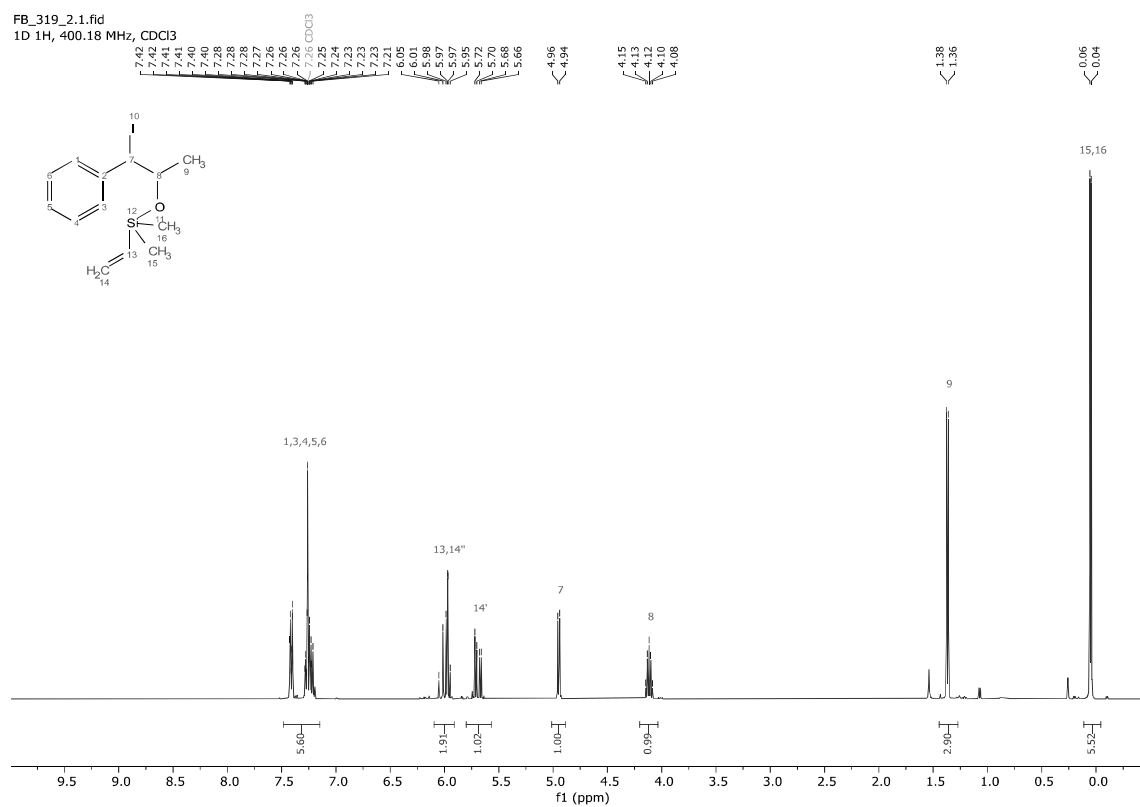
FB_297.3.fid
1D 13C{1H}, 100.64 MHz, CDCl3



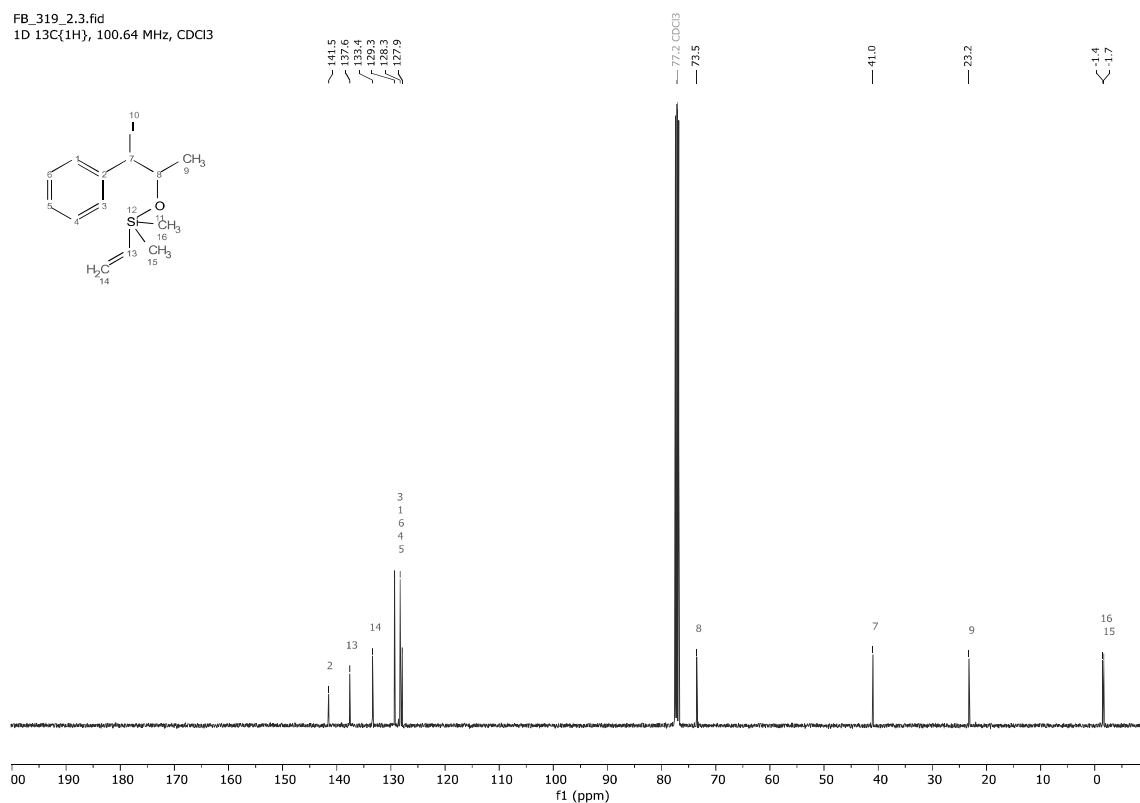


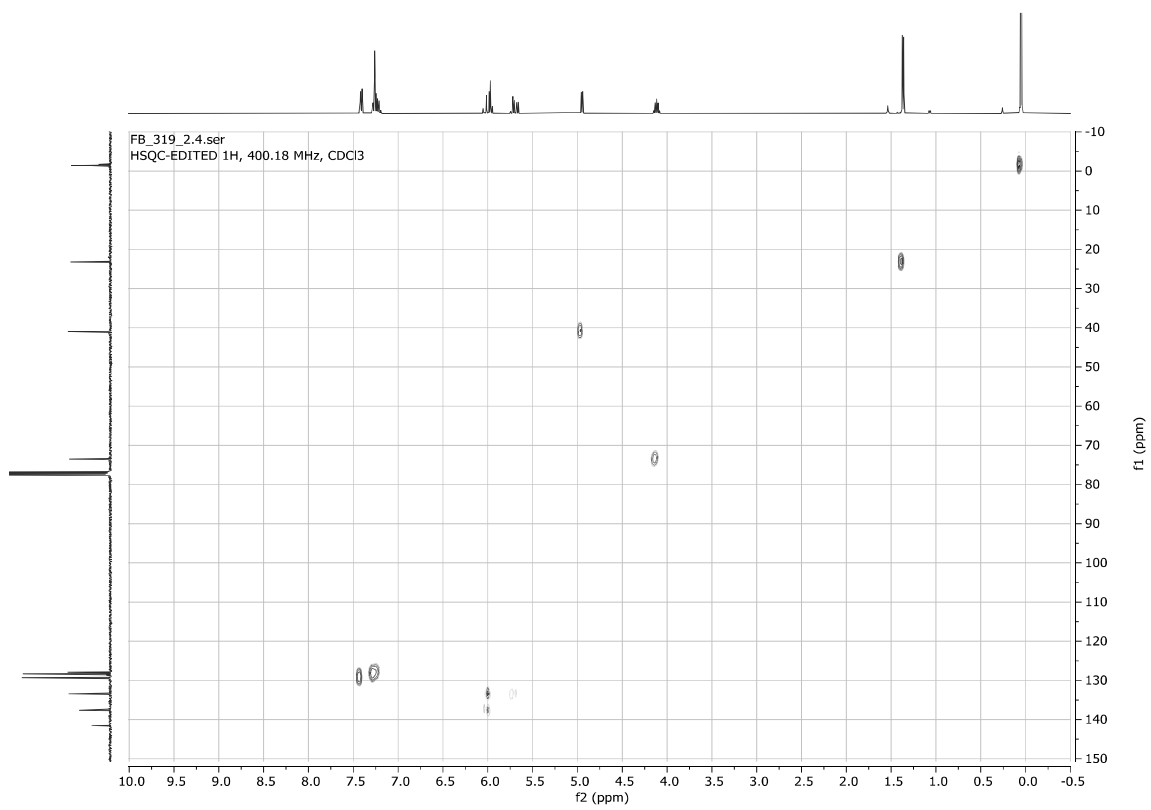
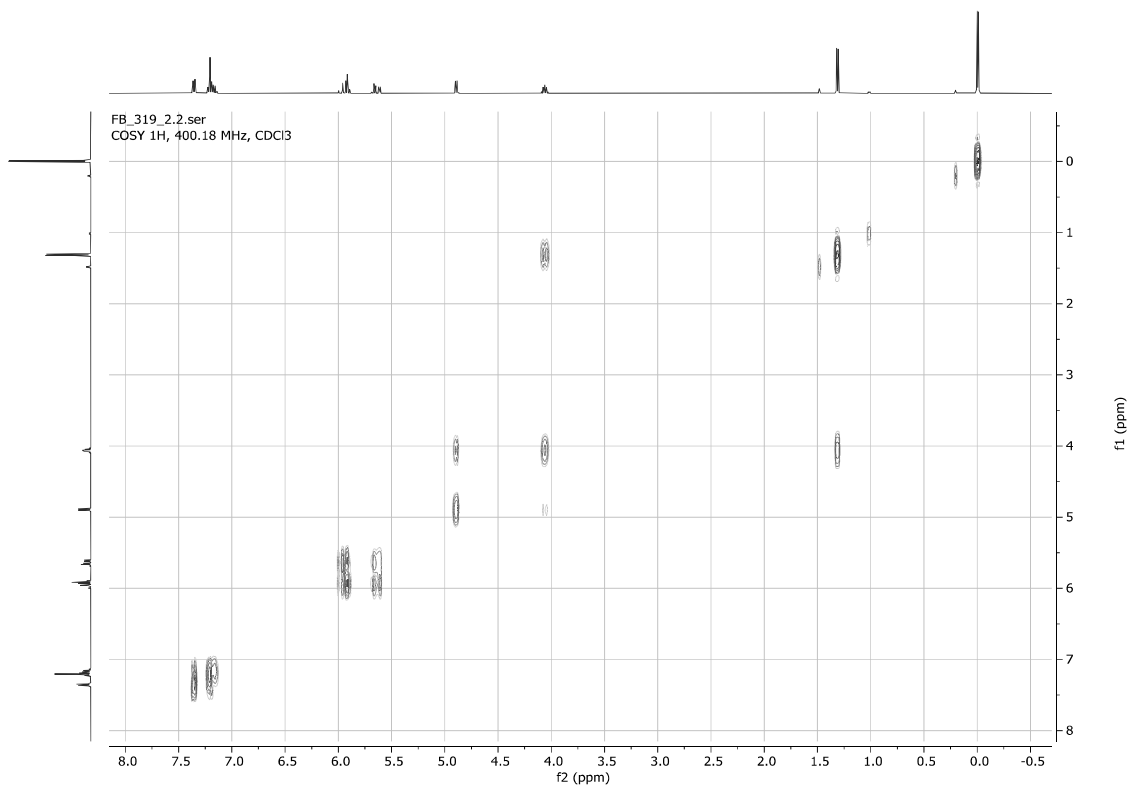
((1-Iodo-1-phenylpropan-2-yl)oxy)dimethylvinylsilane **4q**

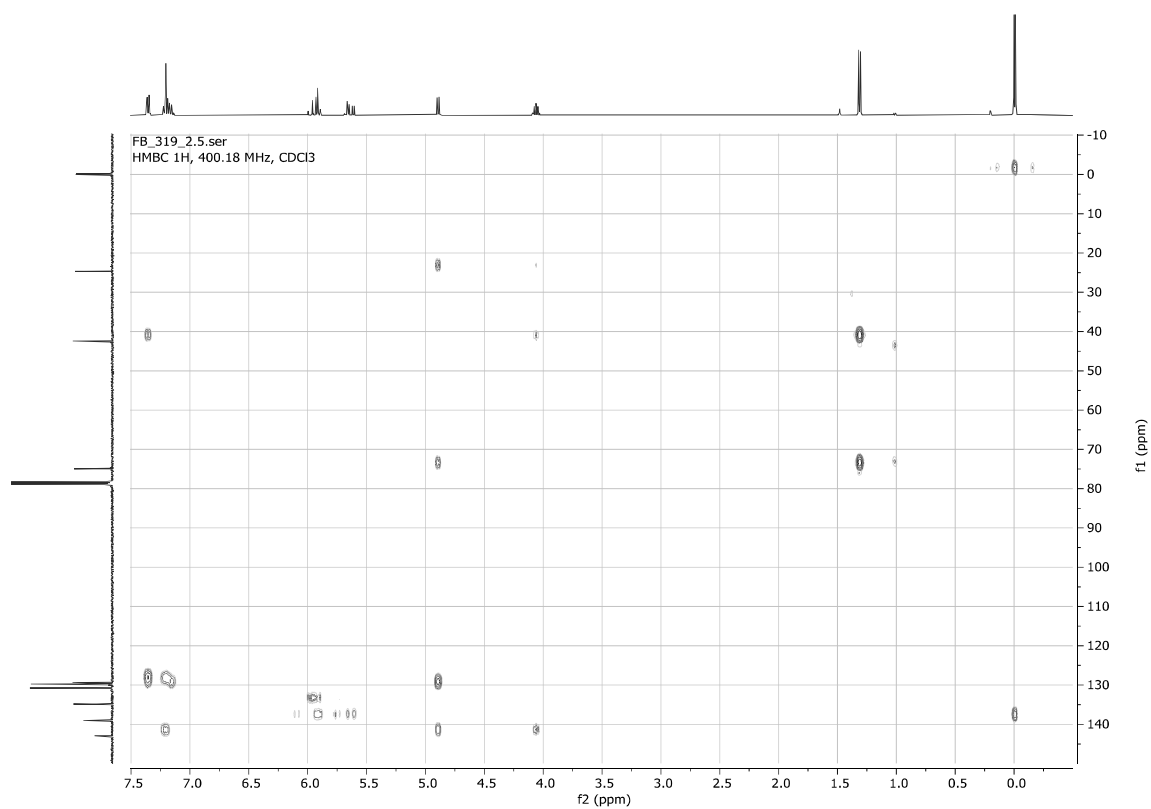
FB_319_2.1.fid
1D 1H, 400.18 MHz, CDCl₃



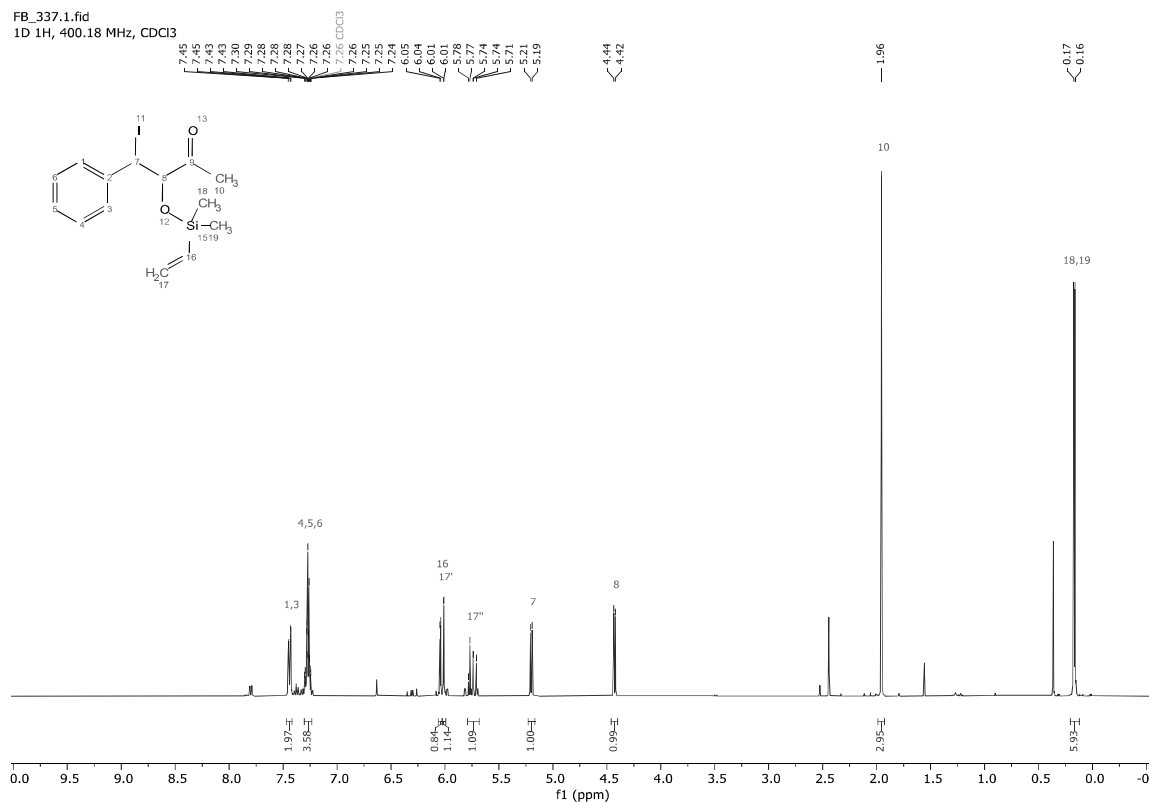
FB_319_2.3.fid
1D 13C(1H), 100.64 MHz, CDCl₃



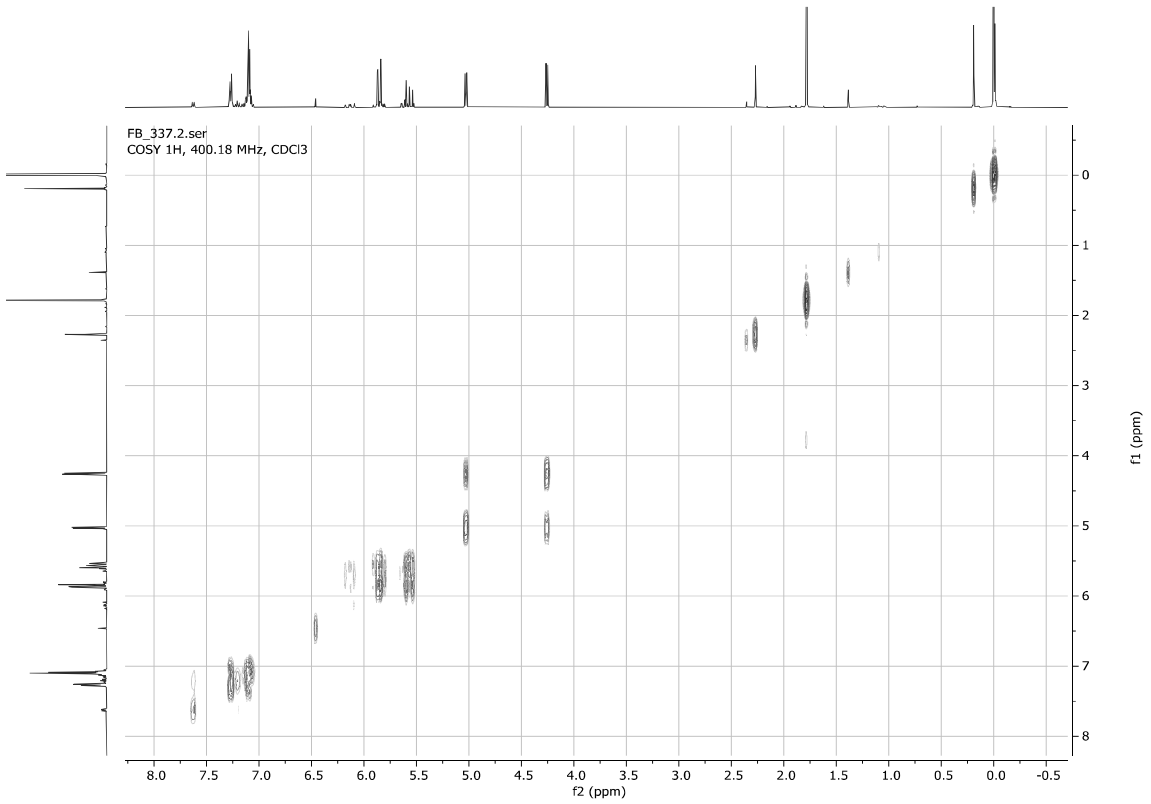
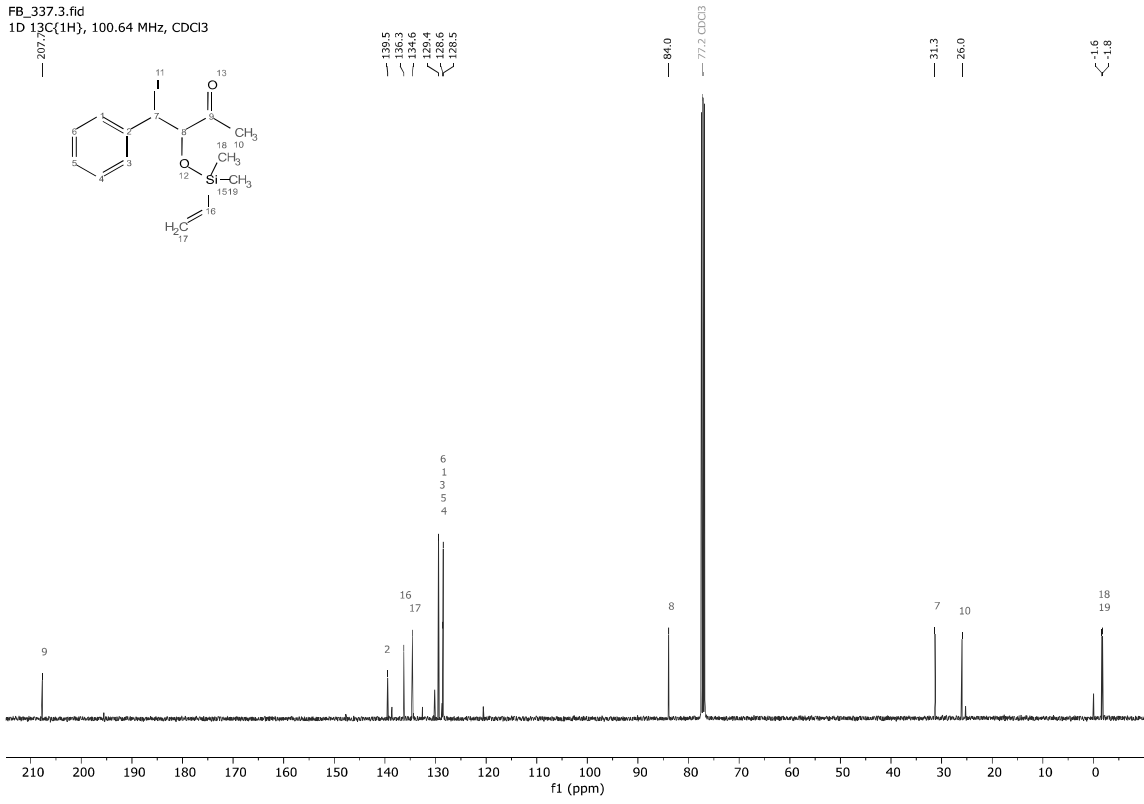


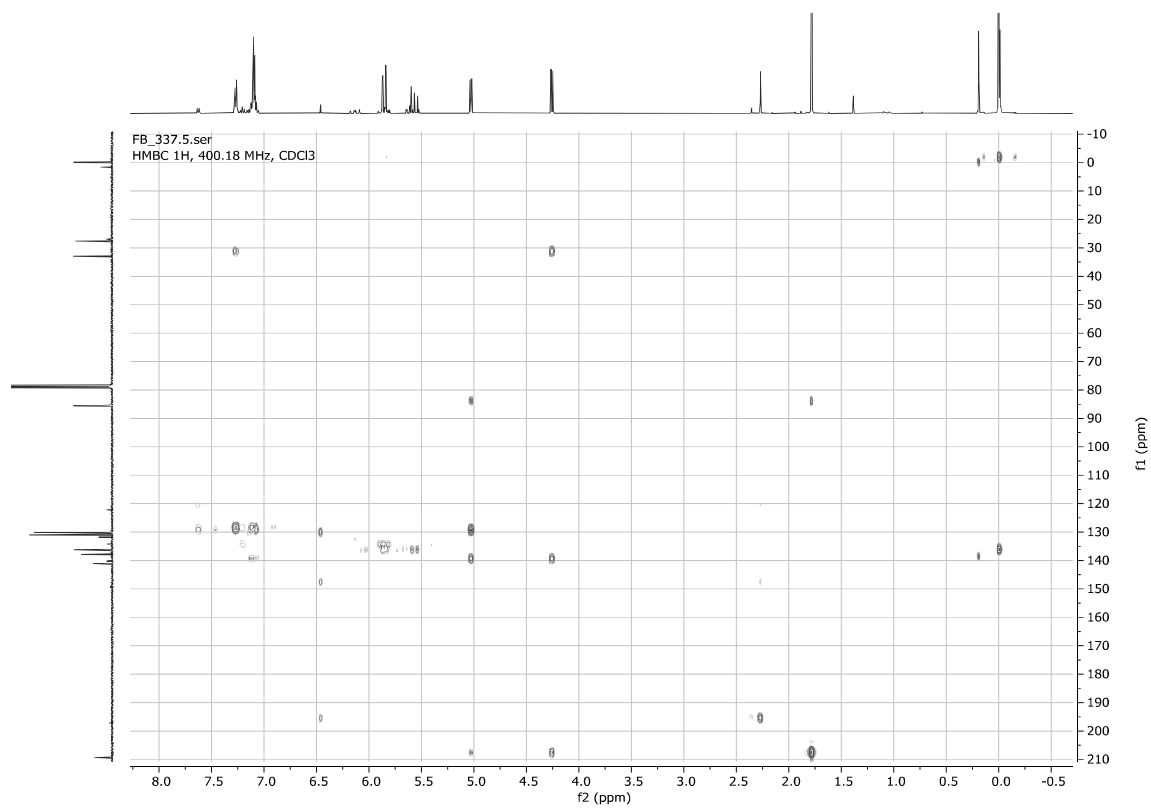
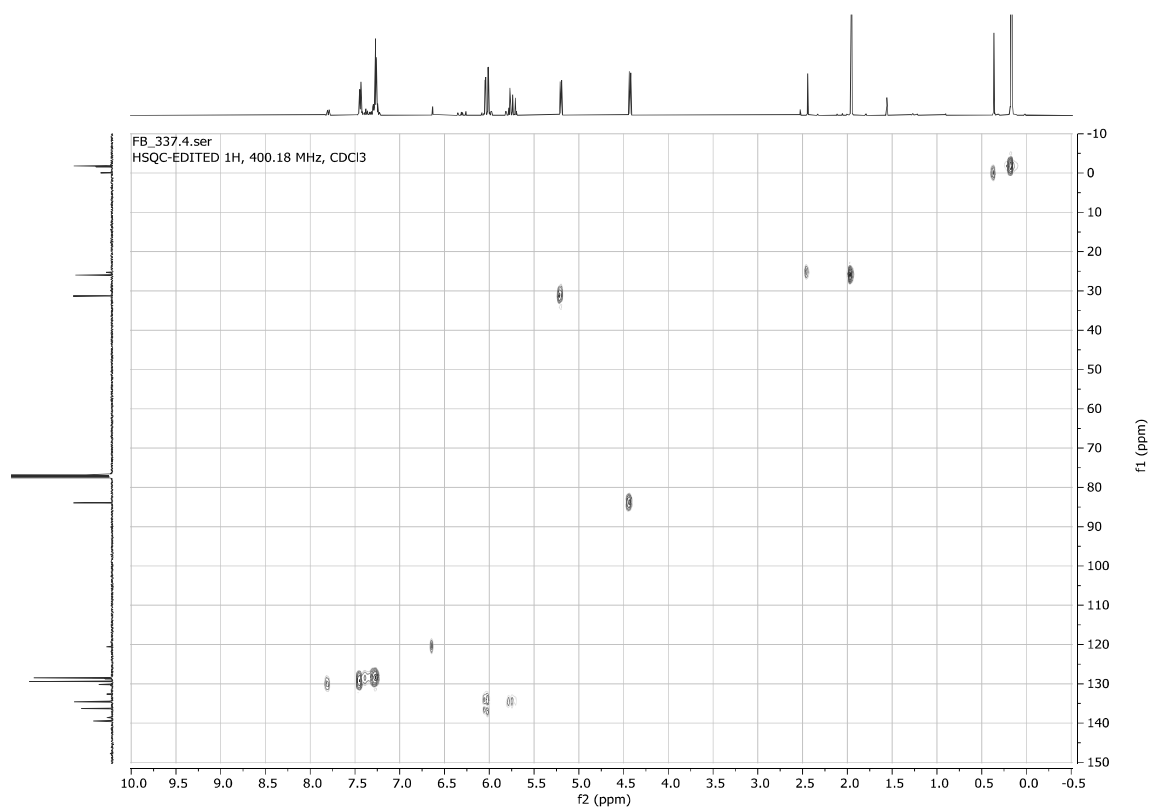


3-((Dimethylvinylsilyl)oxy)-4-iodo-4-phenylbutan-2-one **4r** (*inseparable 87:13 diastereomers mixture*)

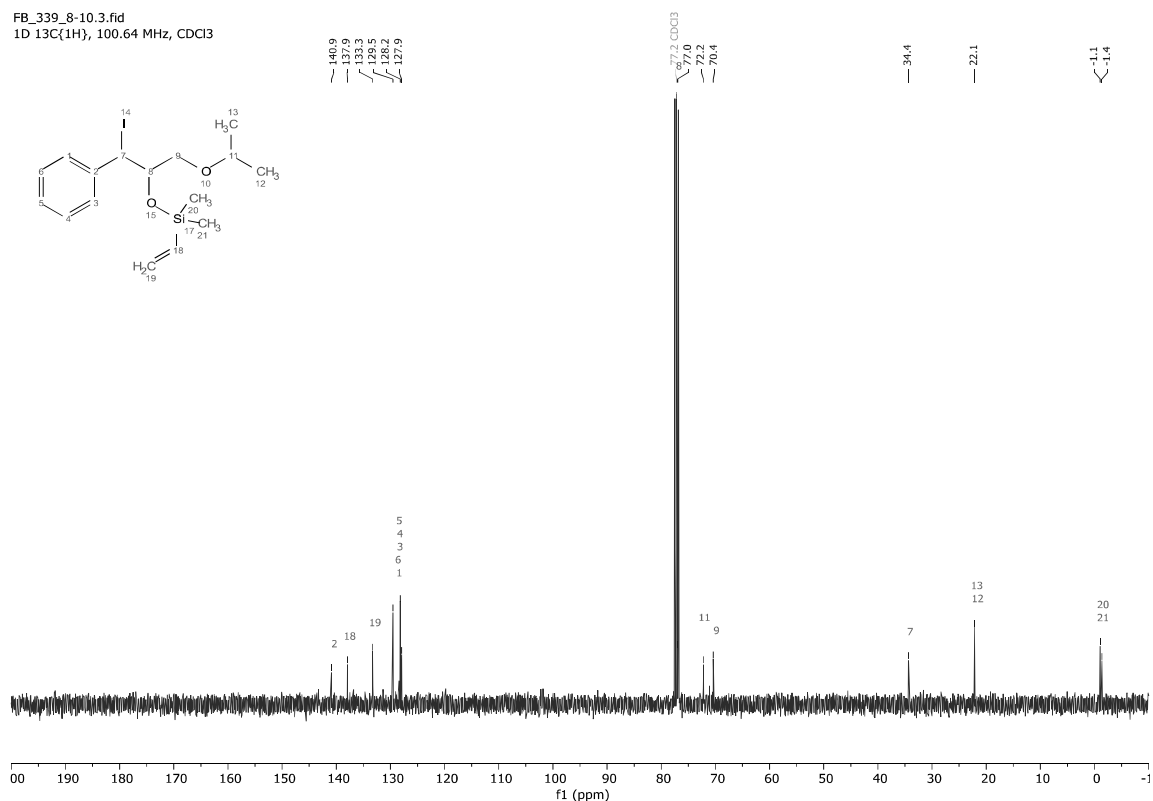
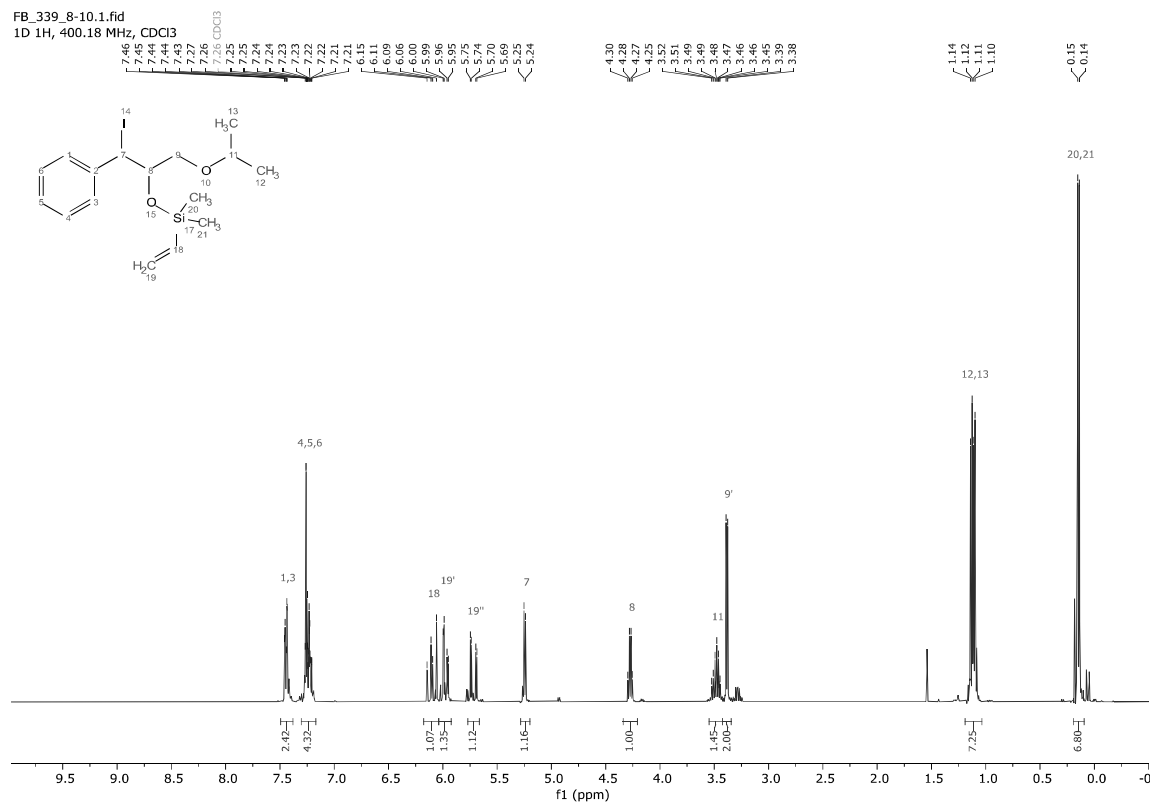


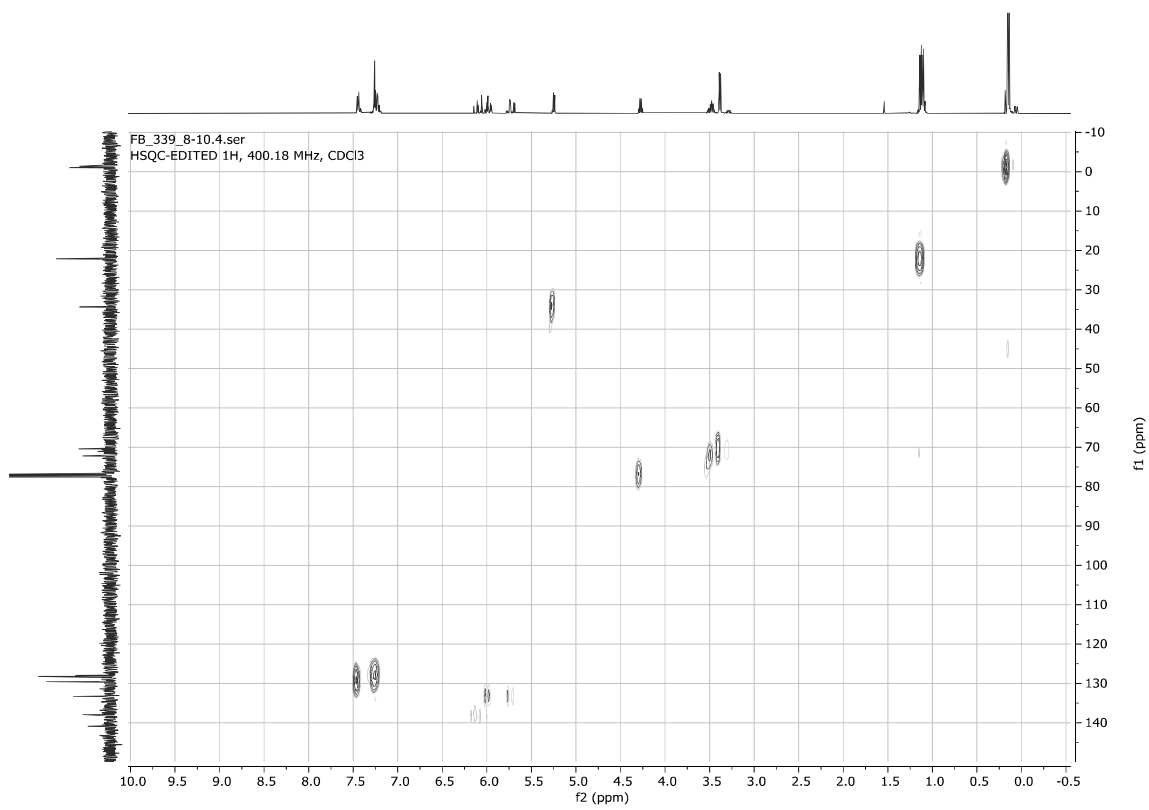
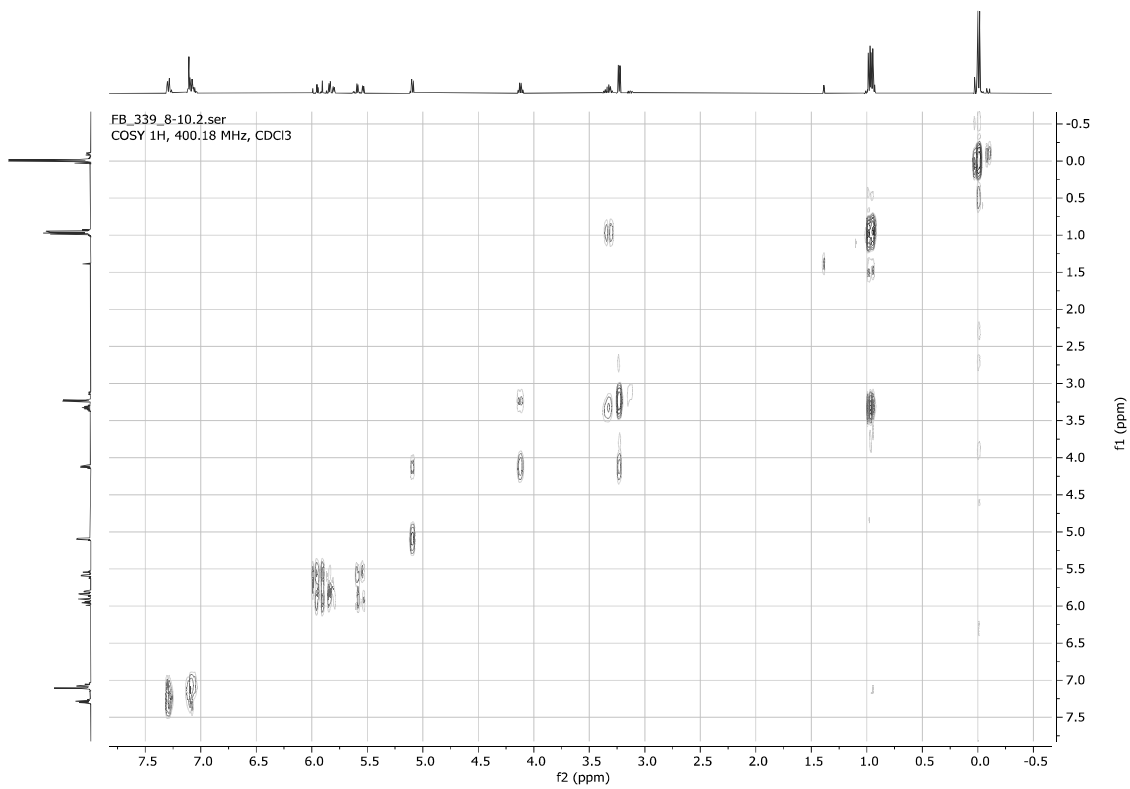
FB_337.3.fid
1D ¹³C{¹H}, 100.64 MHz, CDCl₃

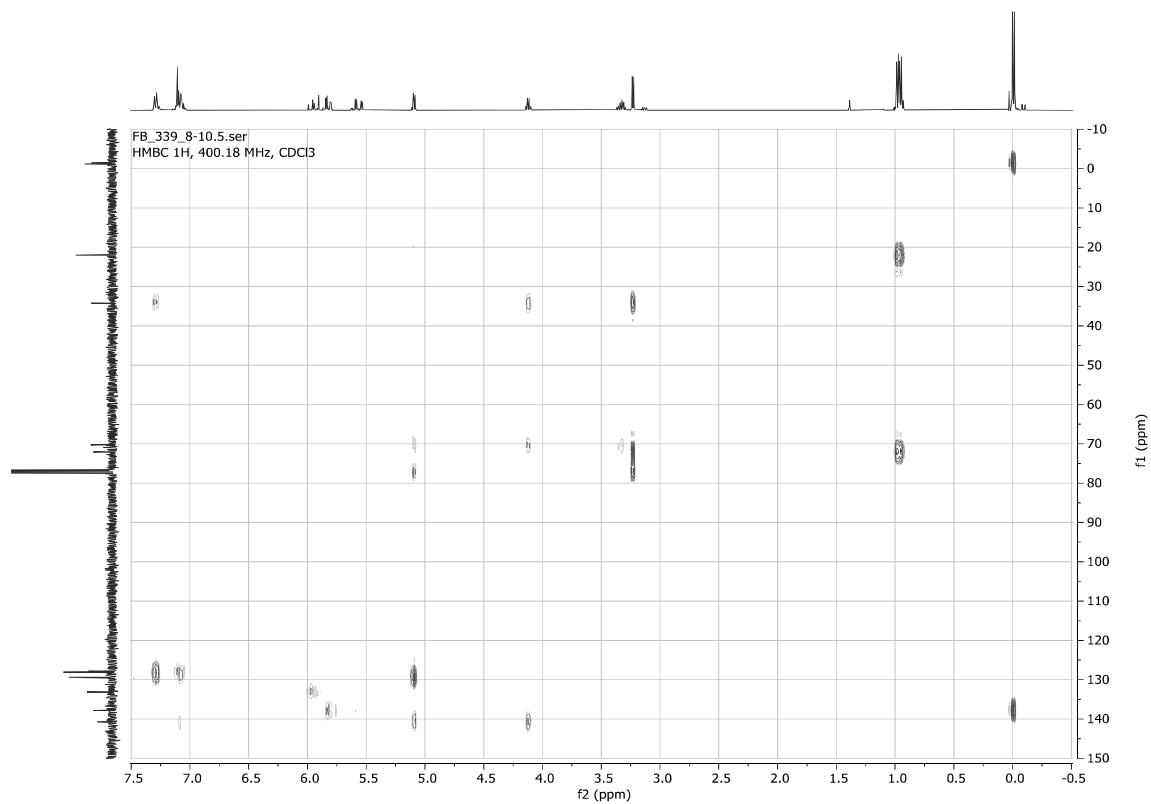




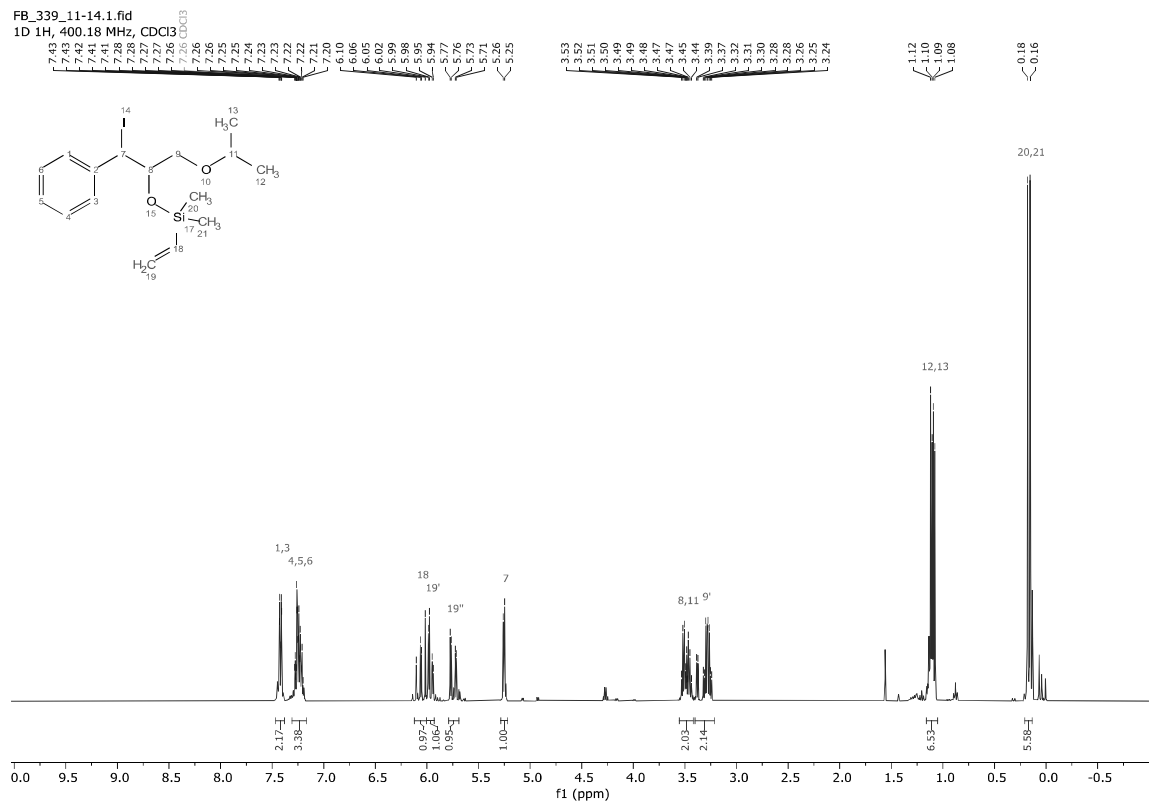
((1-Iodo-3-isopropoxy-1-phenylpropan-2-yl)oxy)dimethylvinylsilane **4s** (major of separable 80:20 diastereomers mixture)



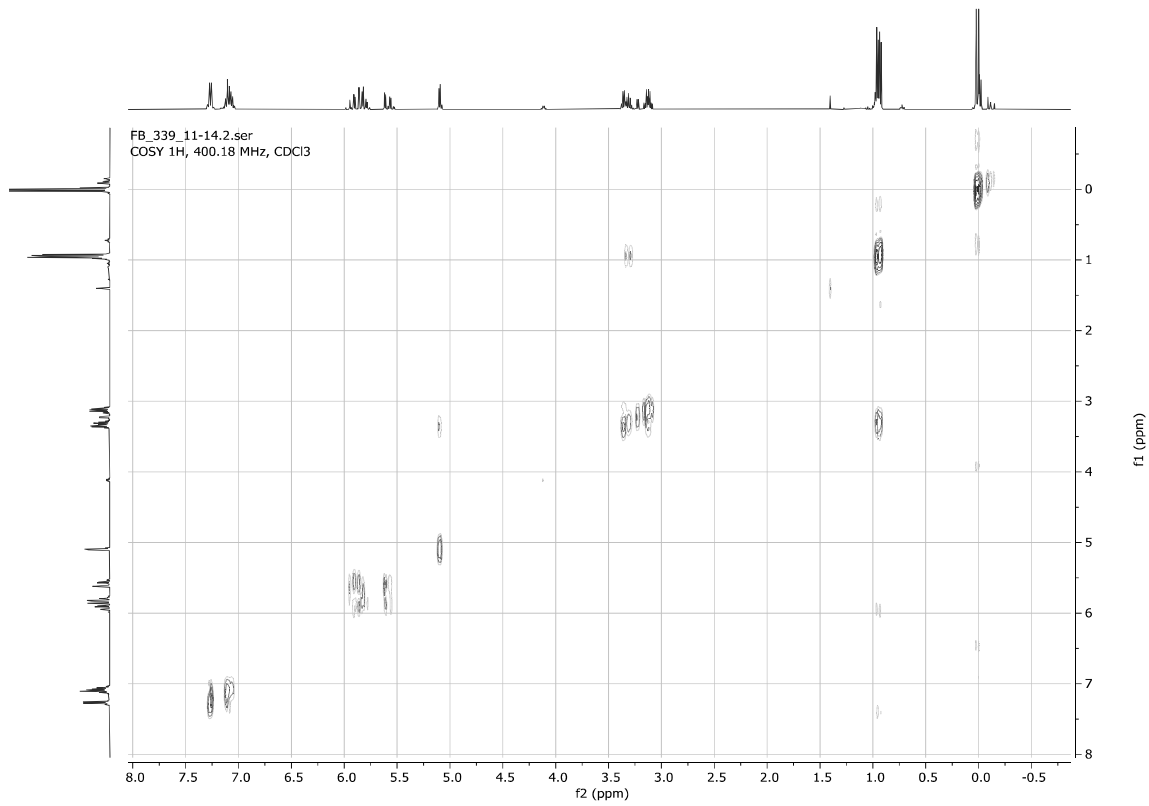
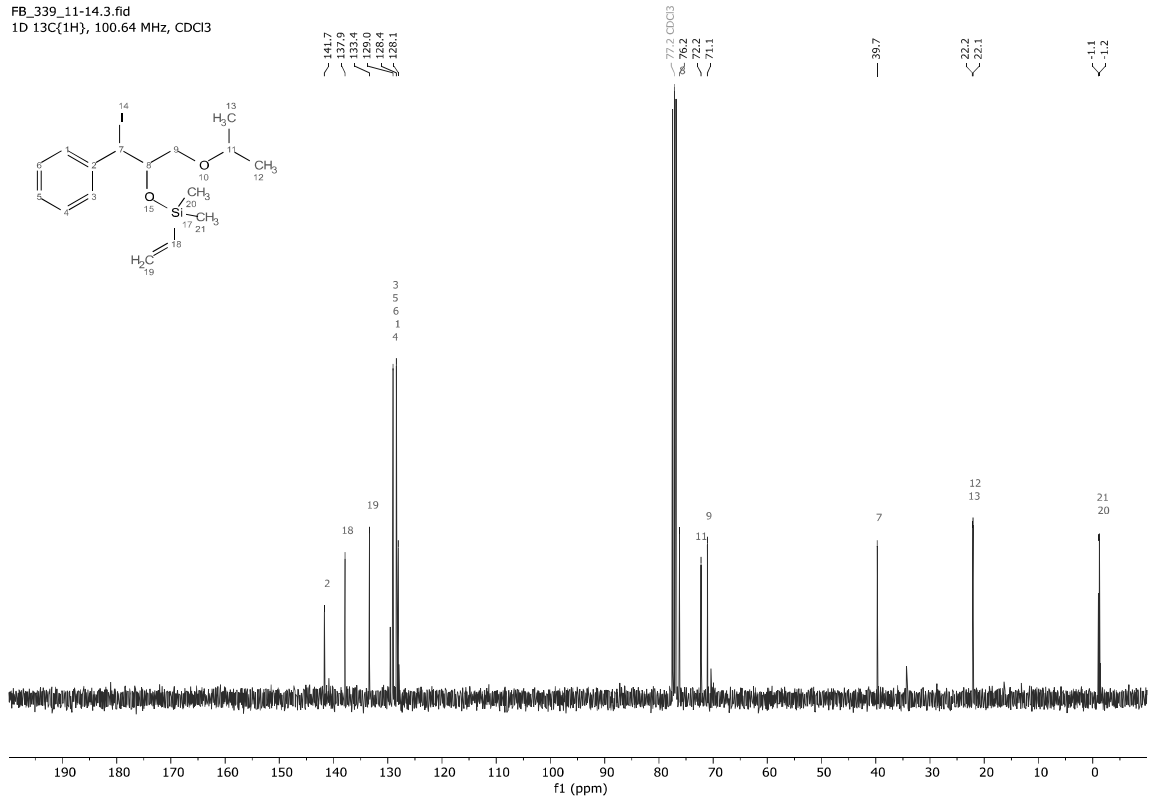


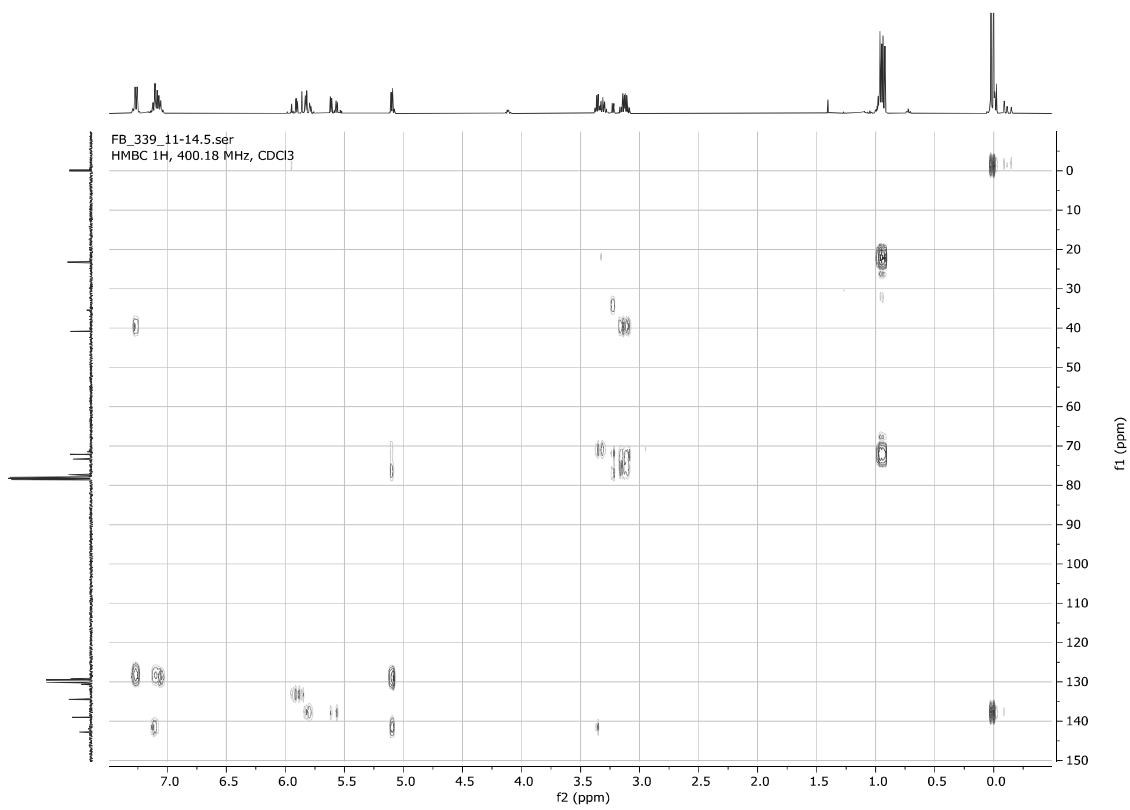
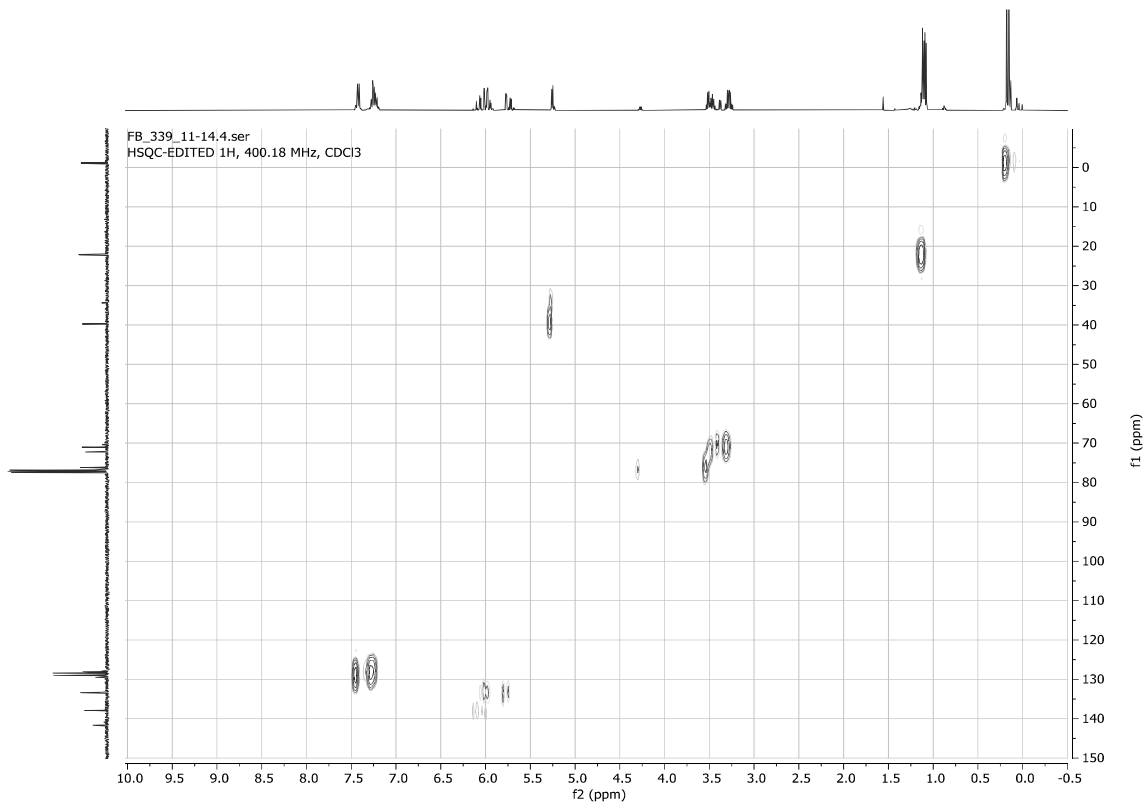


((1-Iodo-3-isopropoxy-1-phenylpropan-2-yl)oxy)dimethylvinylsilane **4s** (minor of separable 80:20 diastereomers mixture)



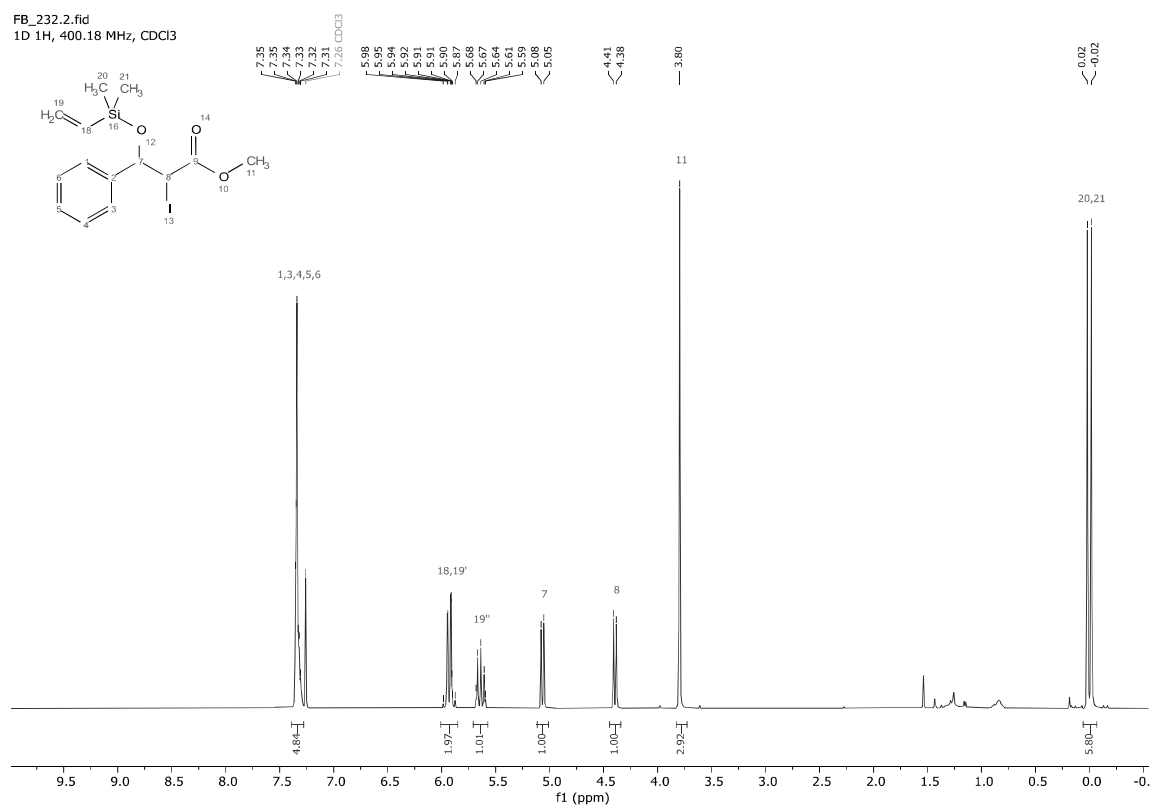
FB_339_11-14.3.fid
1D 13C{1H}, 100.64 MHz, CDCl3



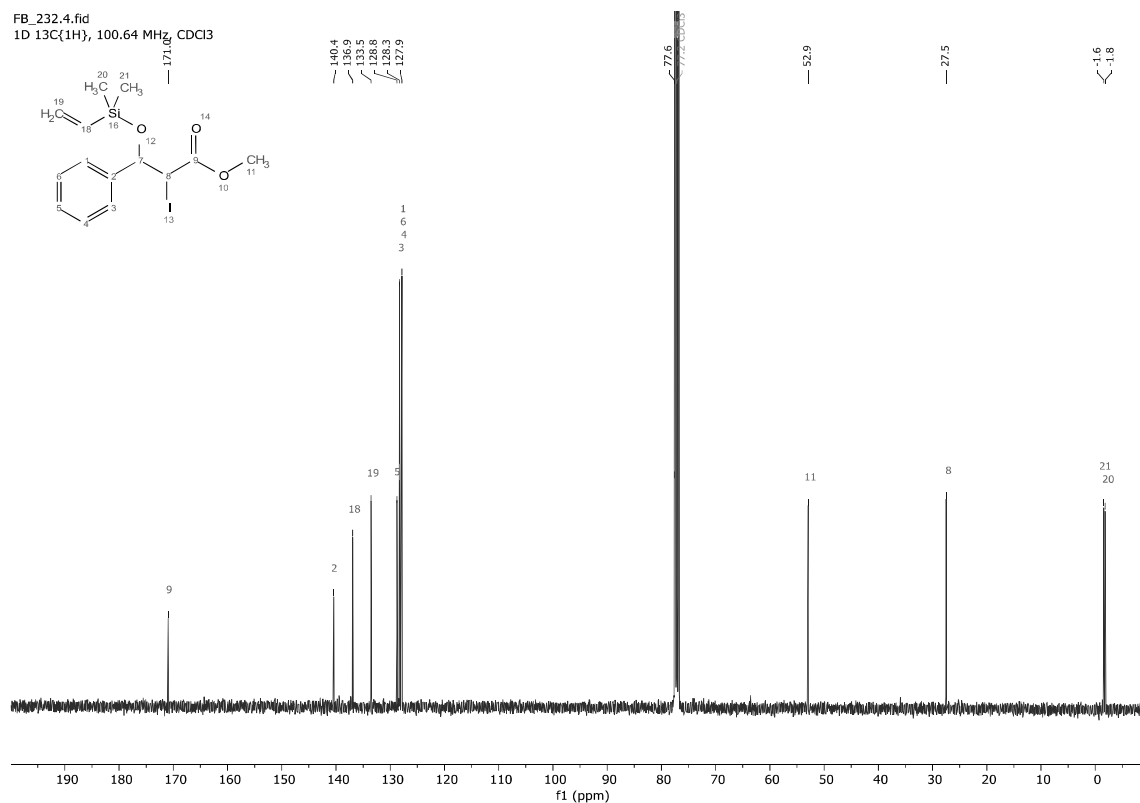


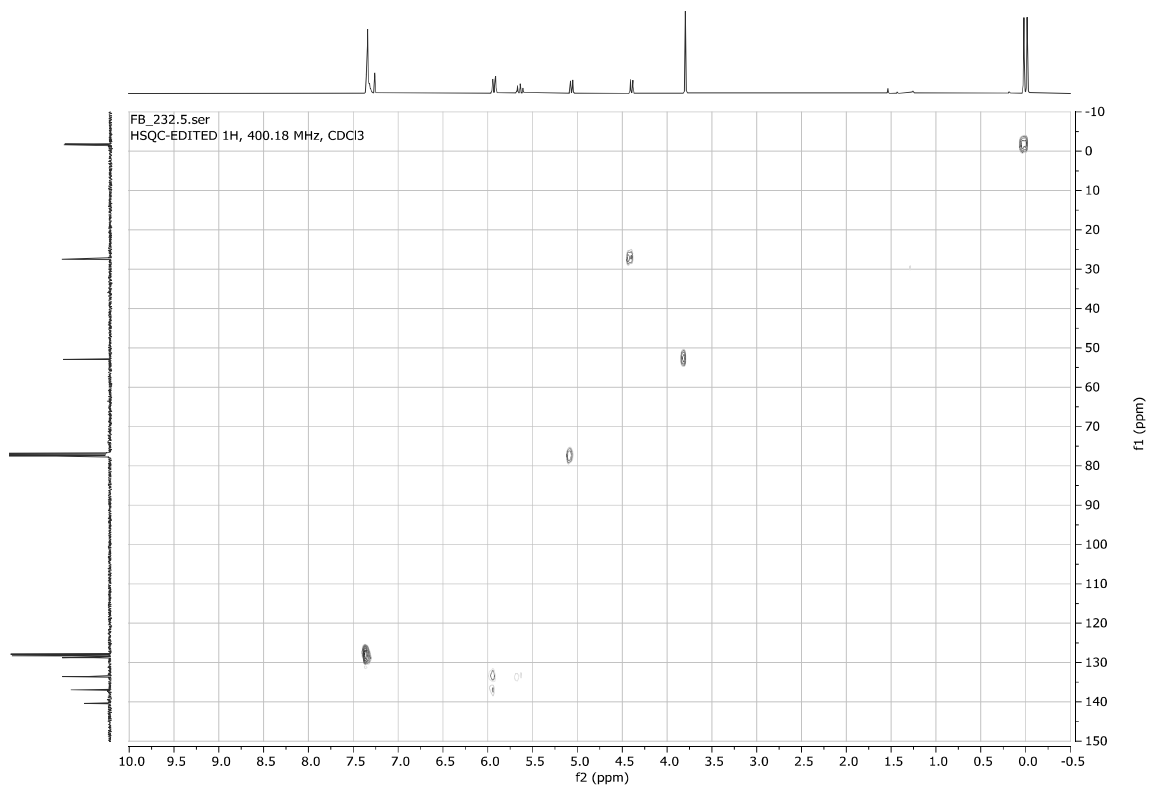
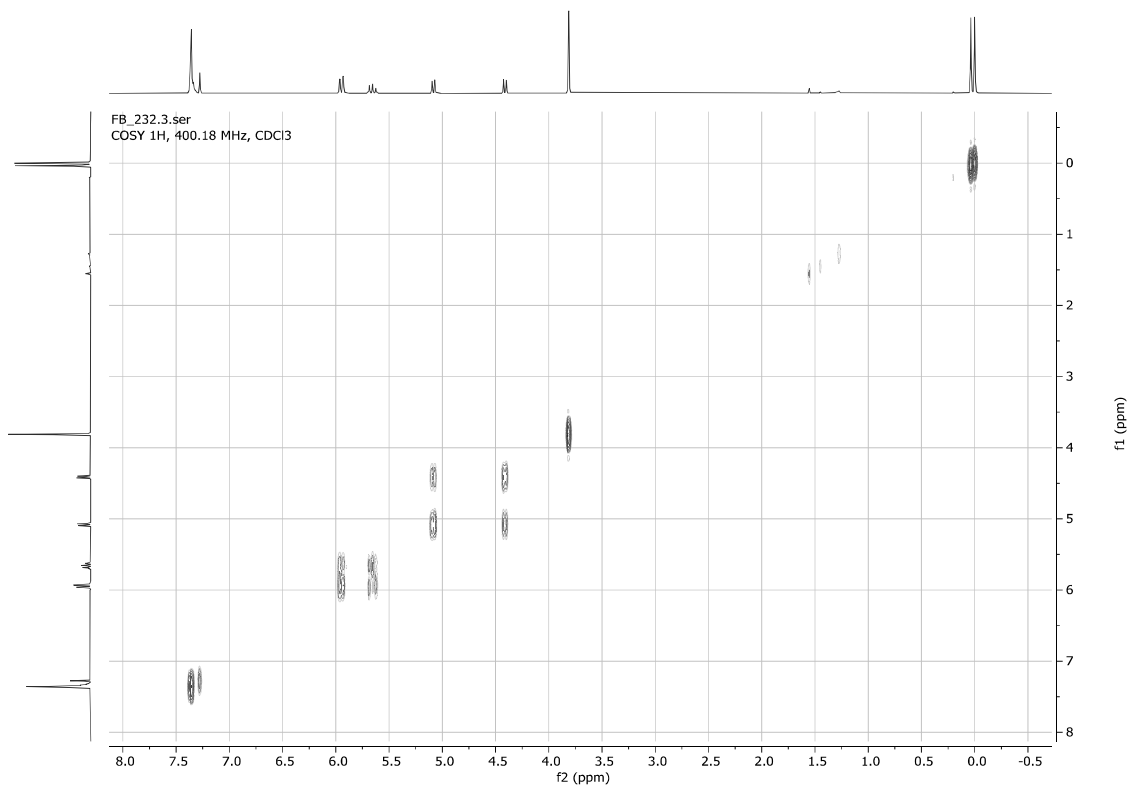
Methyl 3-((dimethylvinylsilyl)oxy)-2-iodo-3-phenylpropanoate **4t**

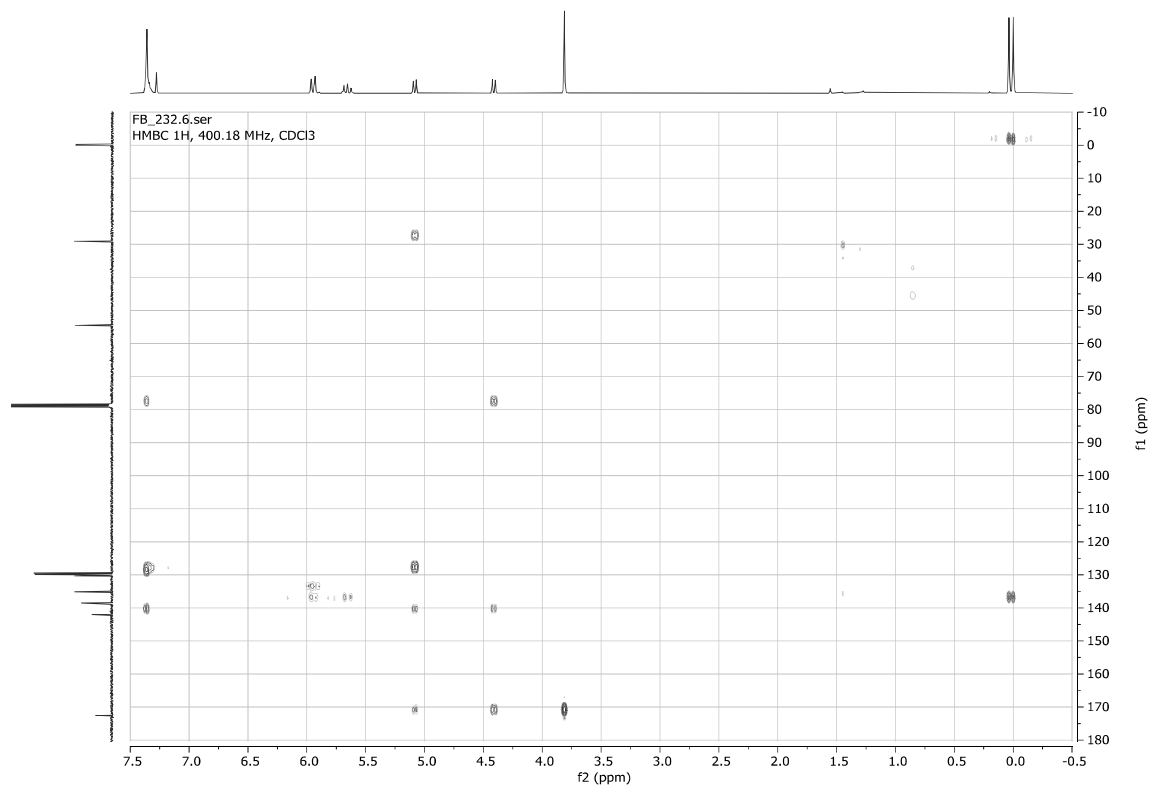
FB_232.2.fid
1D 1H, 400.18 MHz, CDCl3



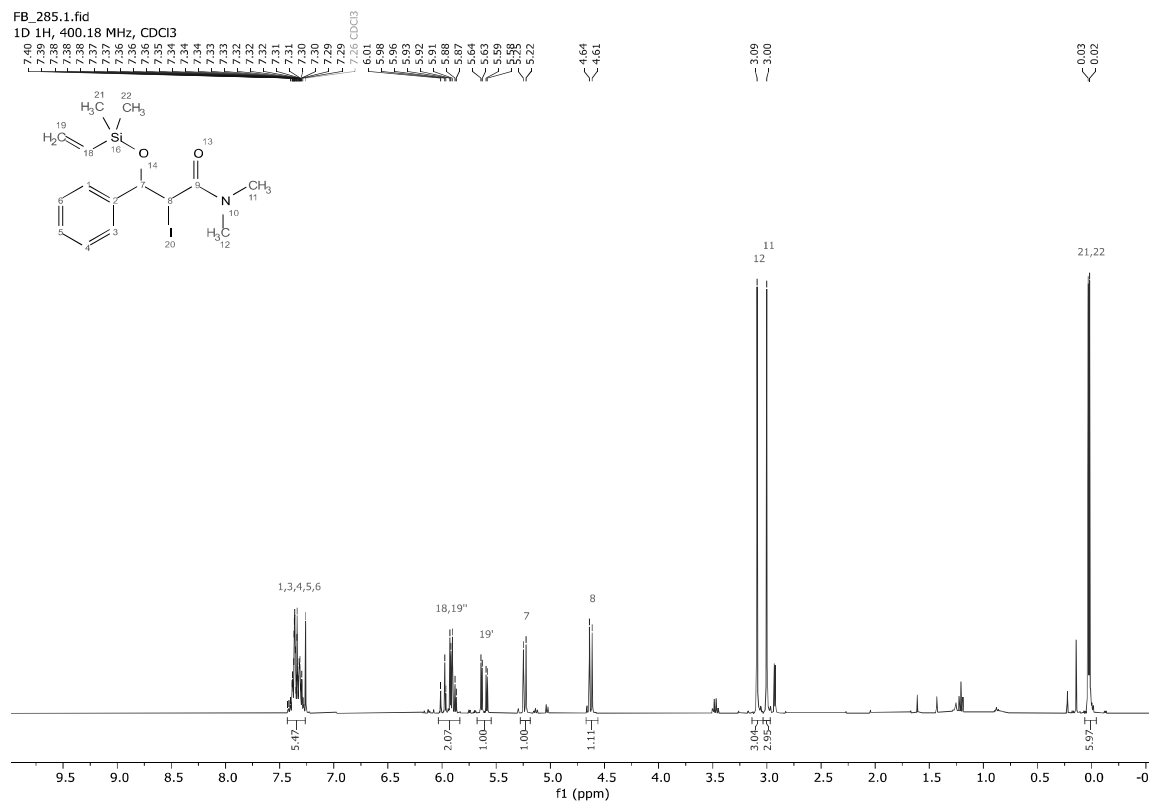
FB_232.4.fid
1D 13C{1H}, 100.64 MHz, CDCl3



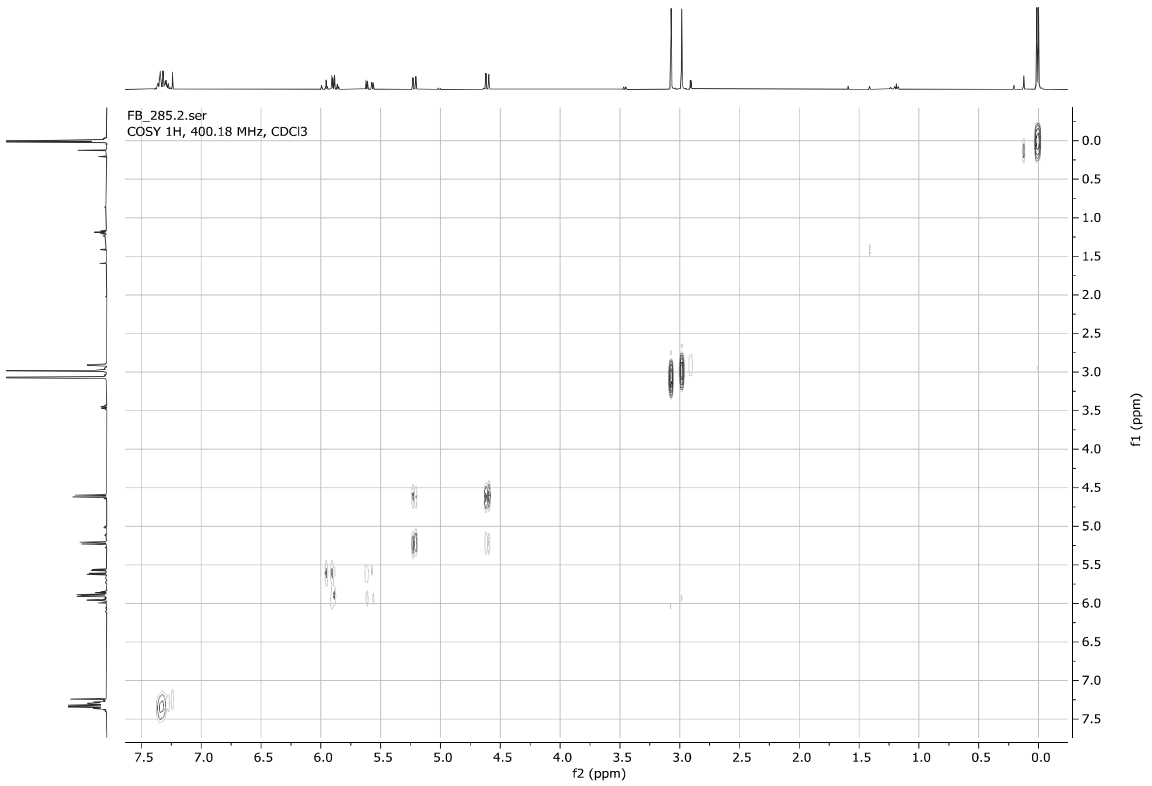
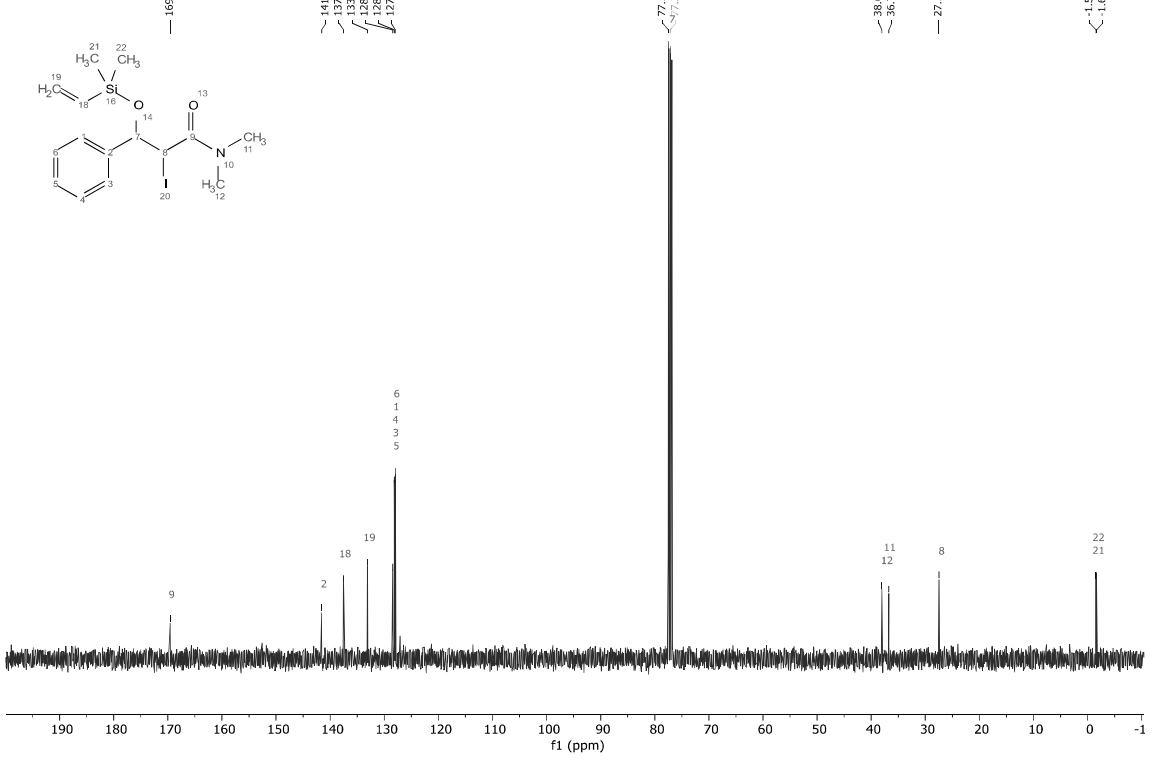


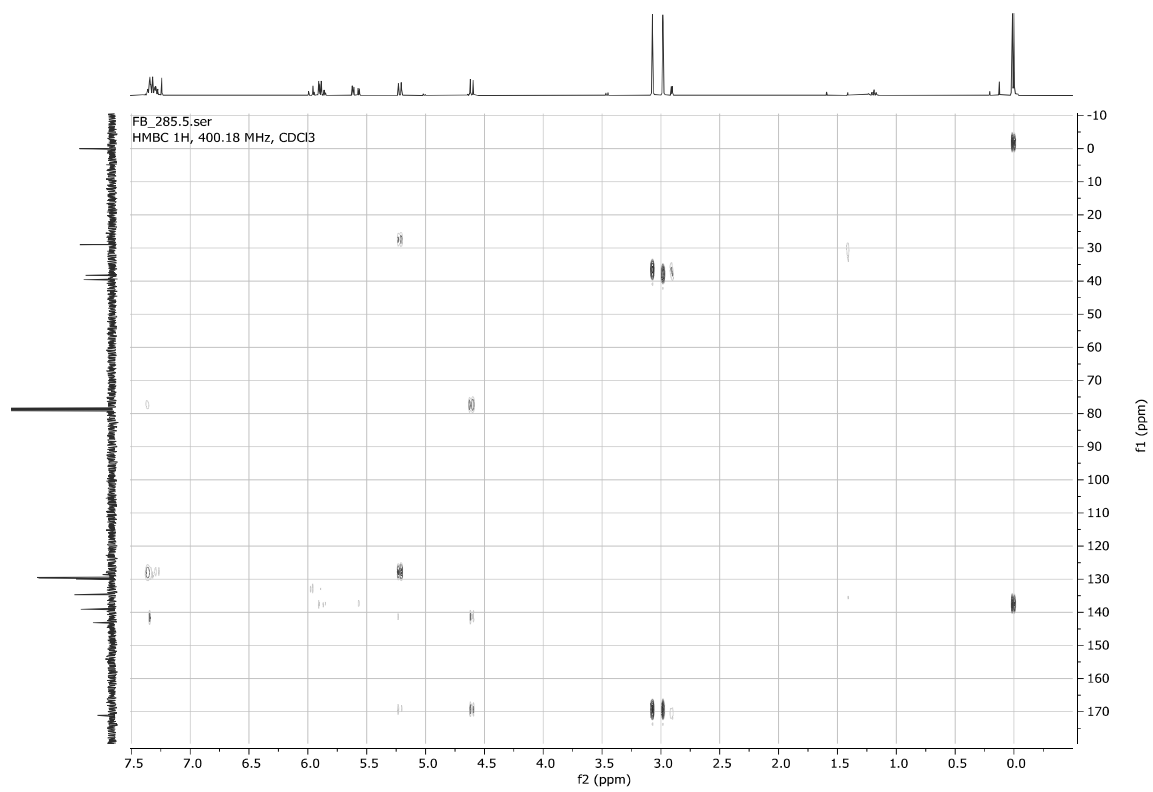
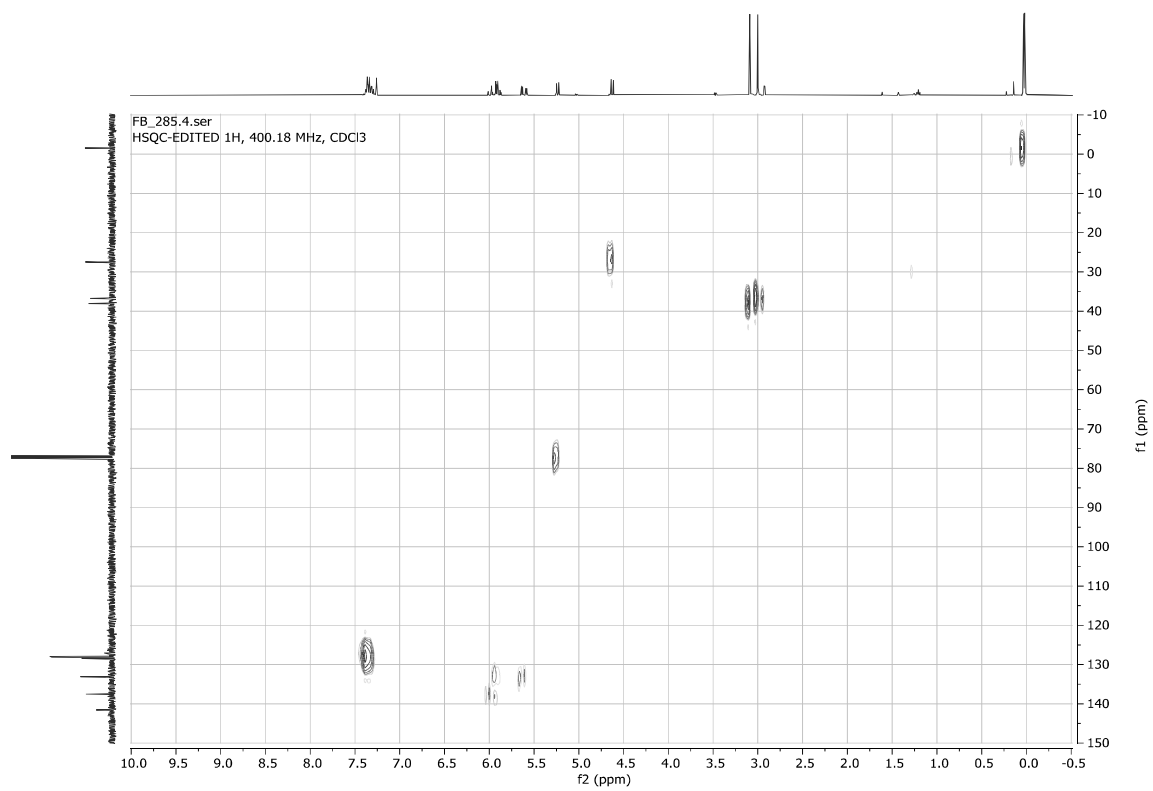


3-((Dimethylvinylsilyl)oxy)-2-iodo-*N,N*-dimethyl-3-phenylpropanamide **4u**



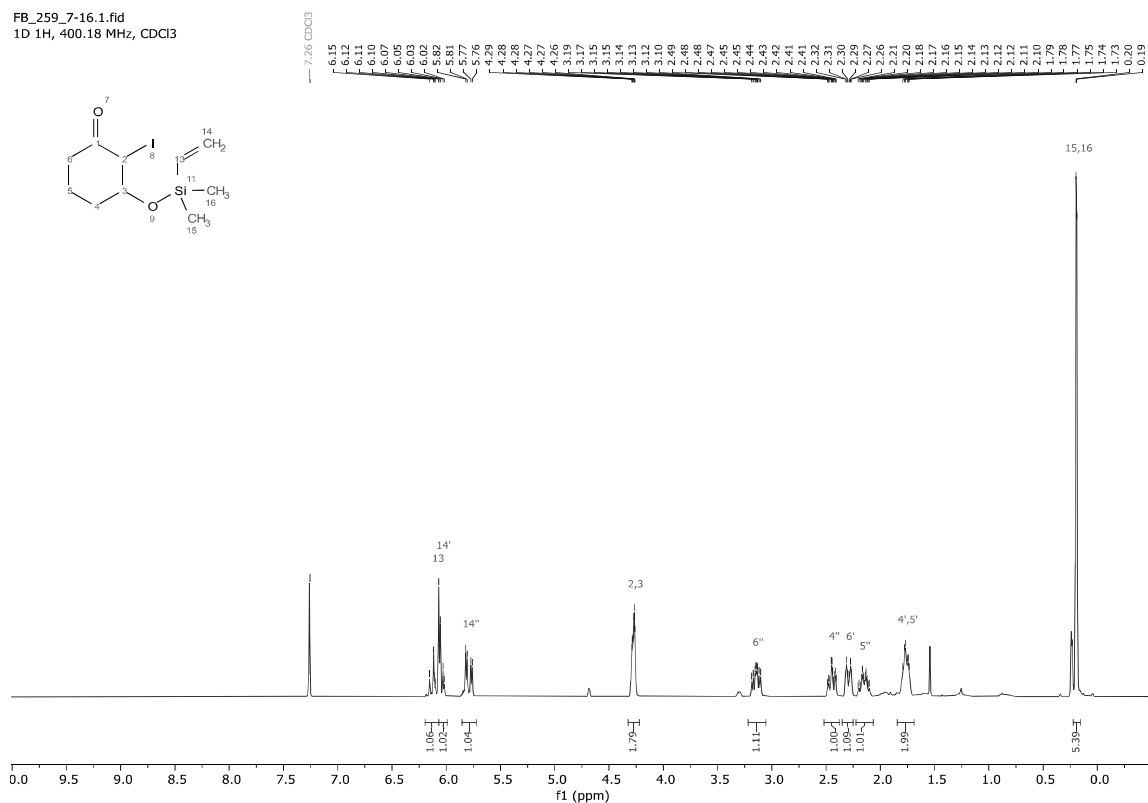
FB_285.3.fid
1D 13C{1H}, 100.64 MHz, CDCl3



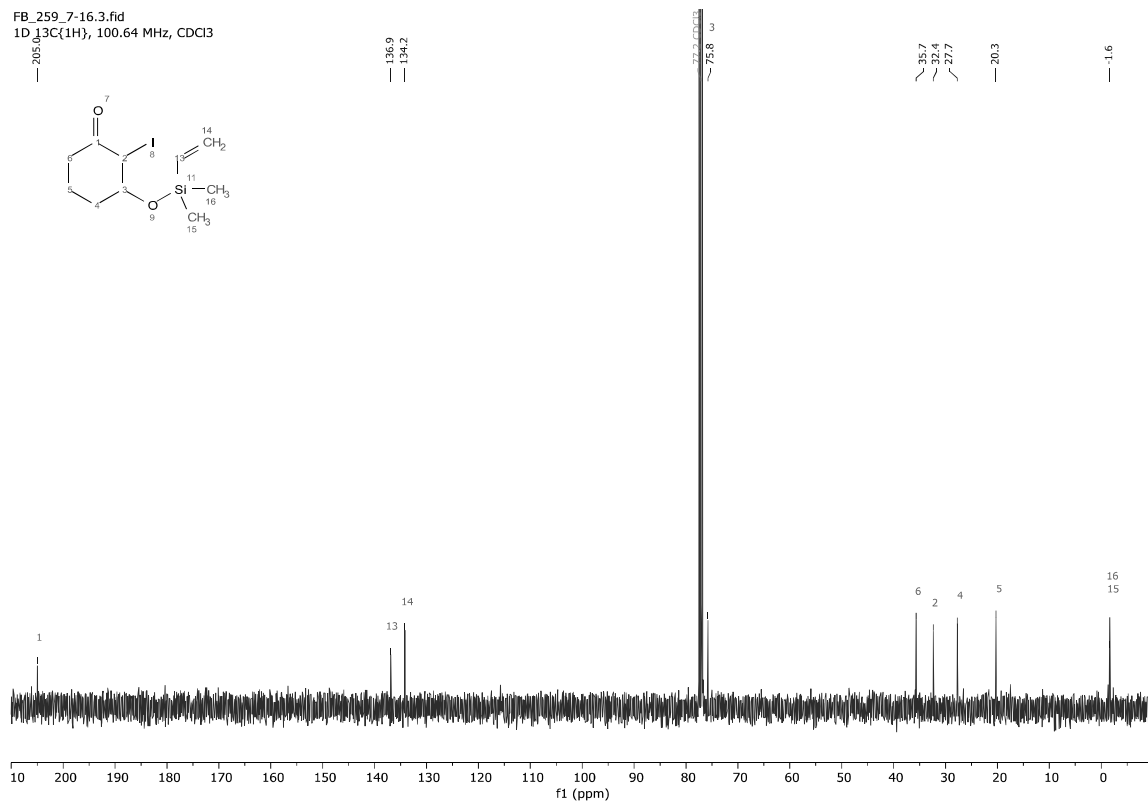


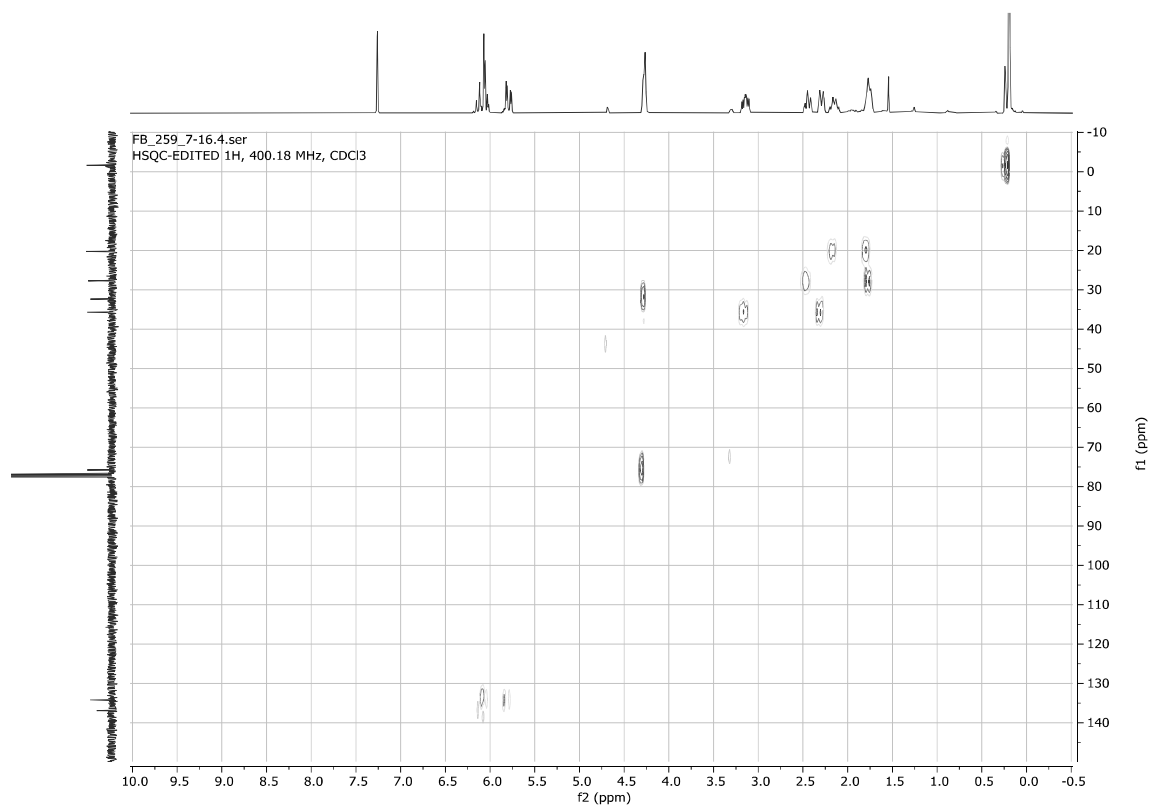
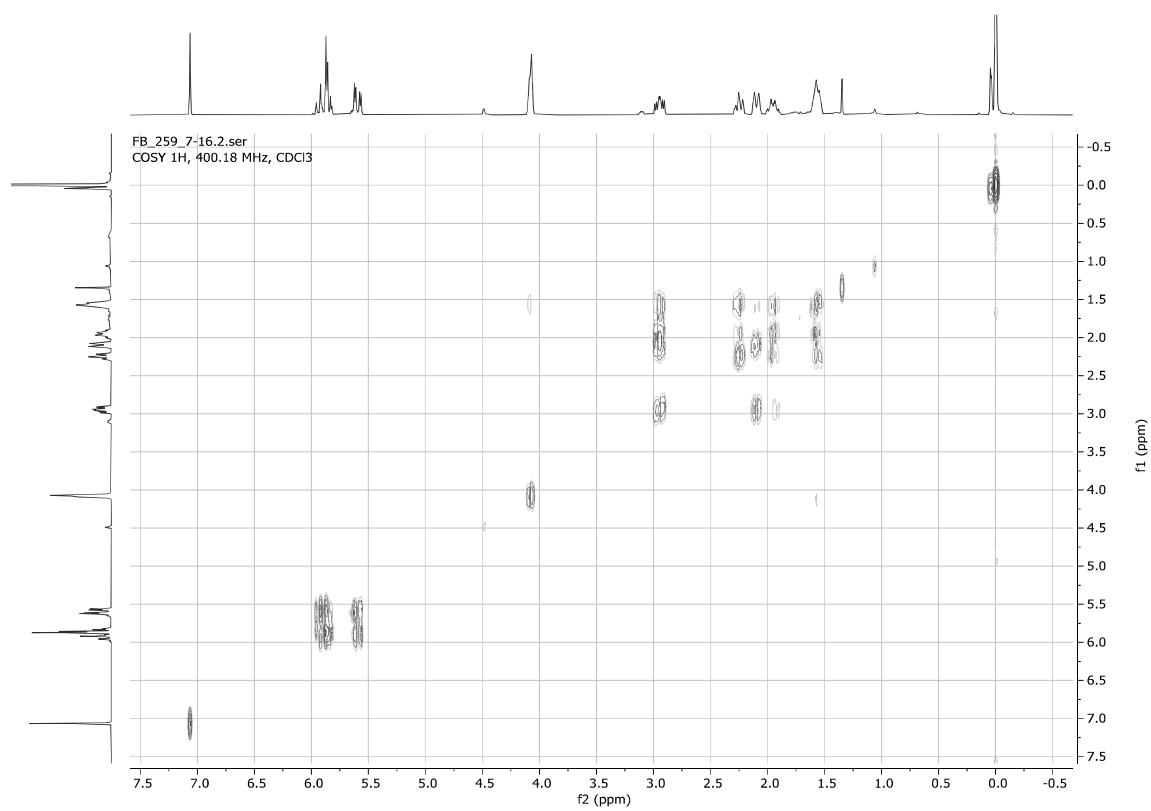
3-((Dimethylvinylsilyl)oxy)-2-iodocyclohexan-1-one **4v** (major of separable 71:29 diastereomers mixture)

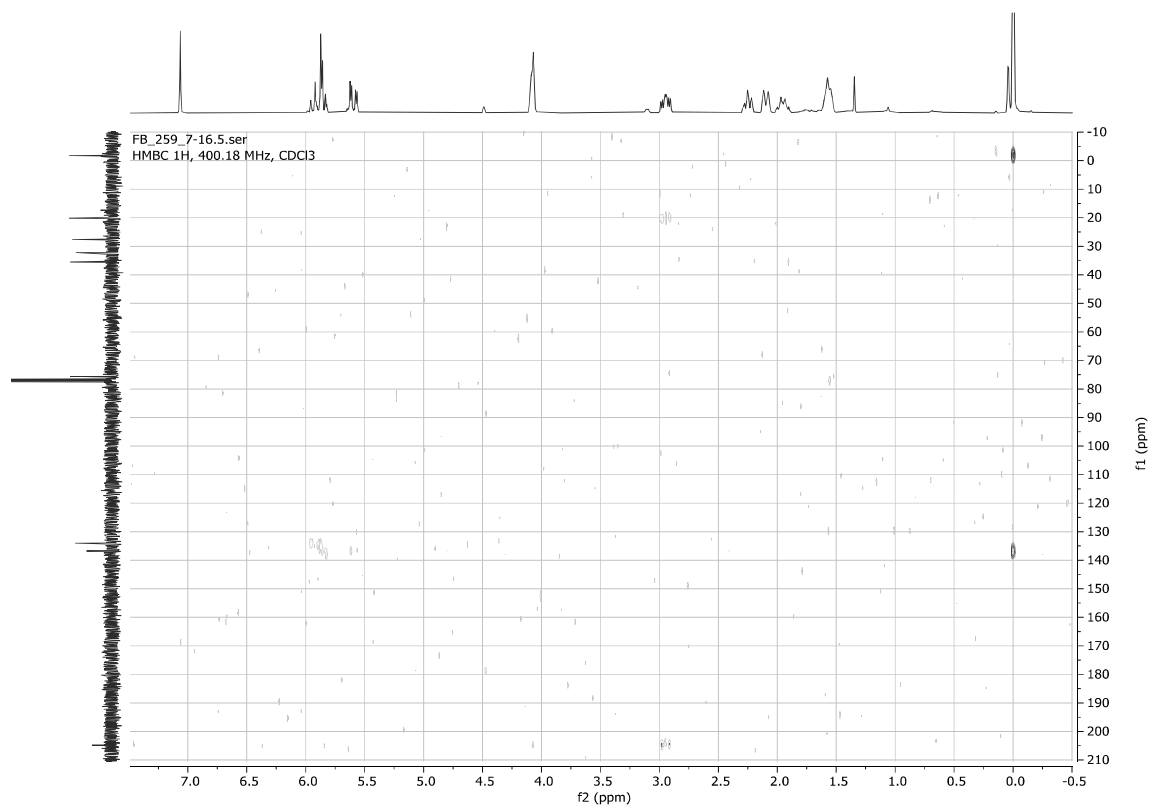
FB_259_7-16.1.fid
1D 1H, 400.18 MHz, CDCl3



FB_259_7-16.3.fid
1D 13C(1H), 100.64 MHz, CDCl3

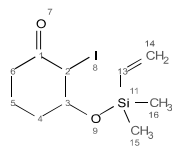
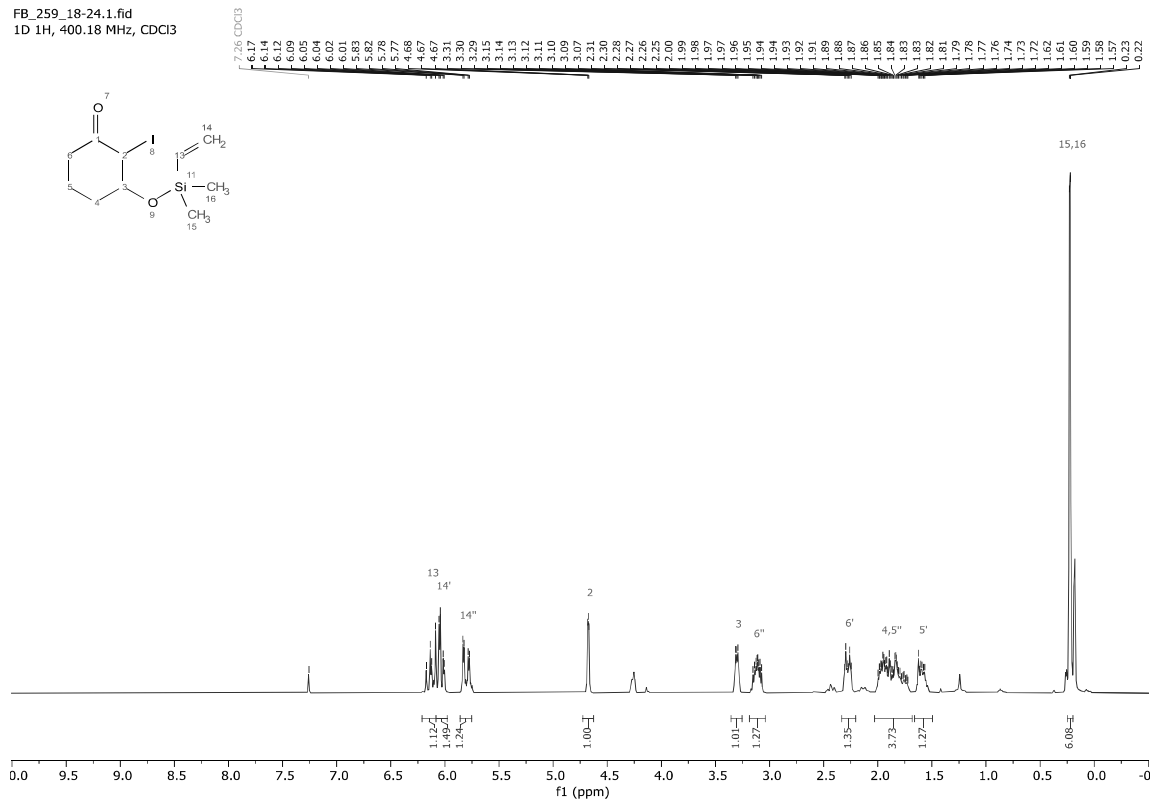




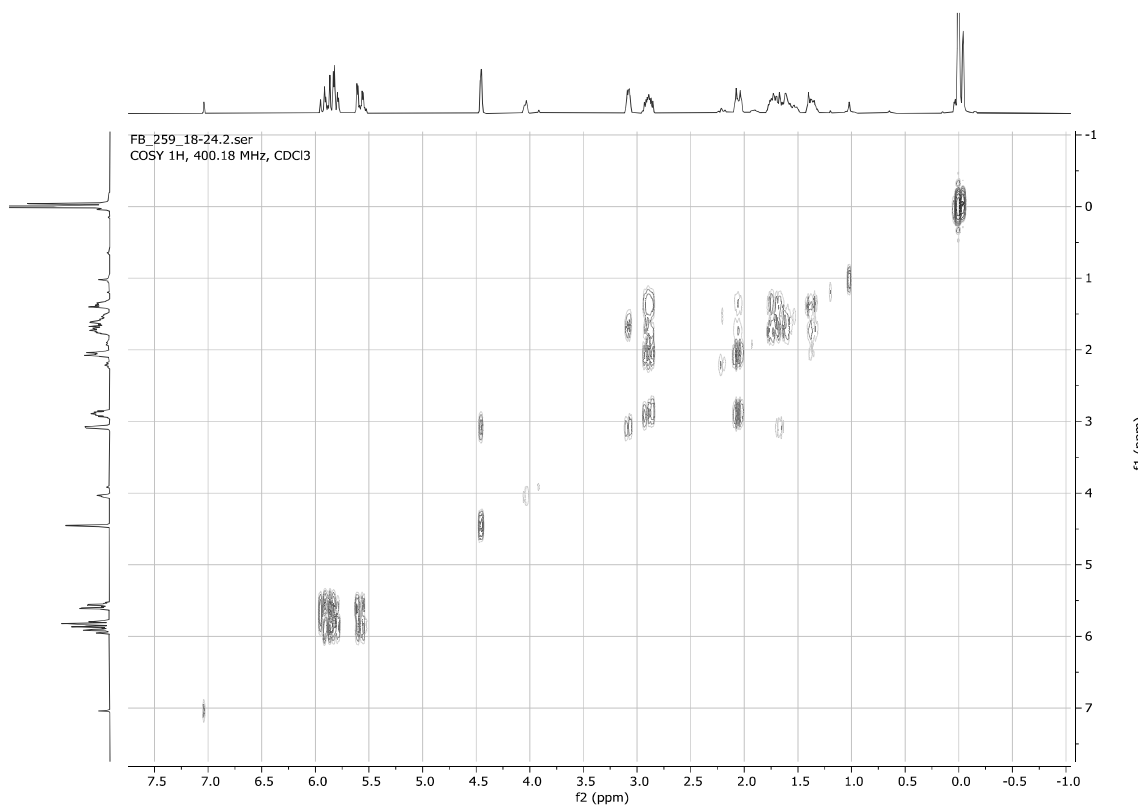
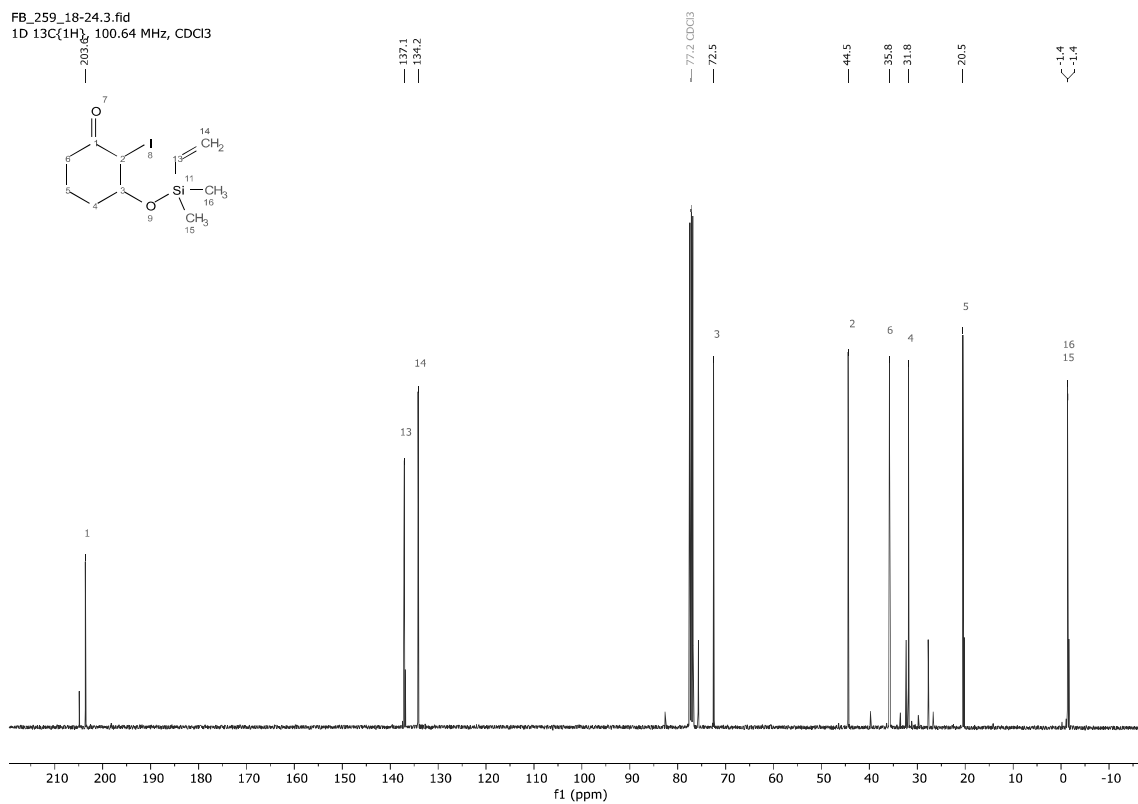


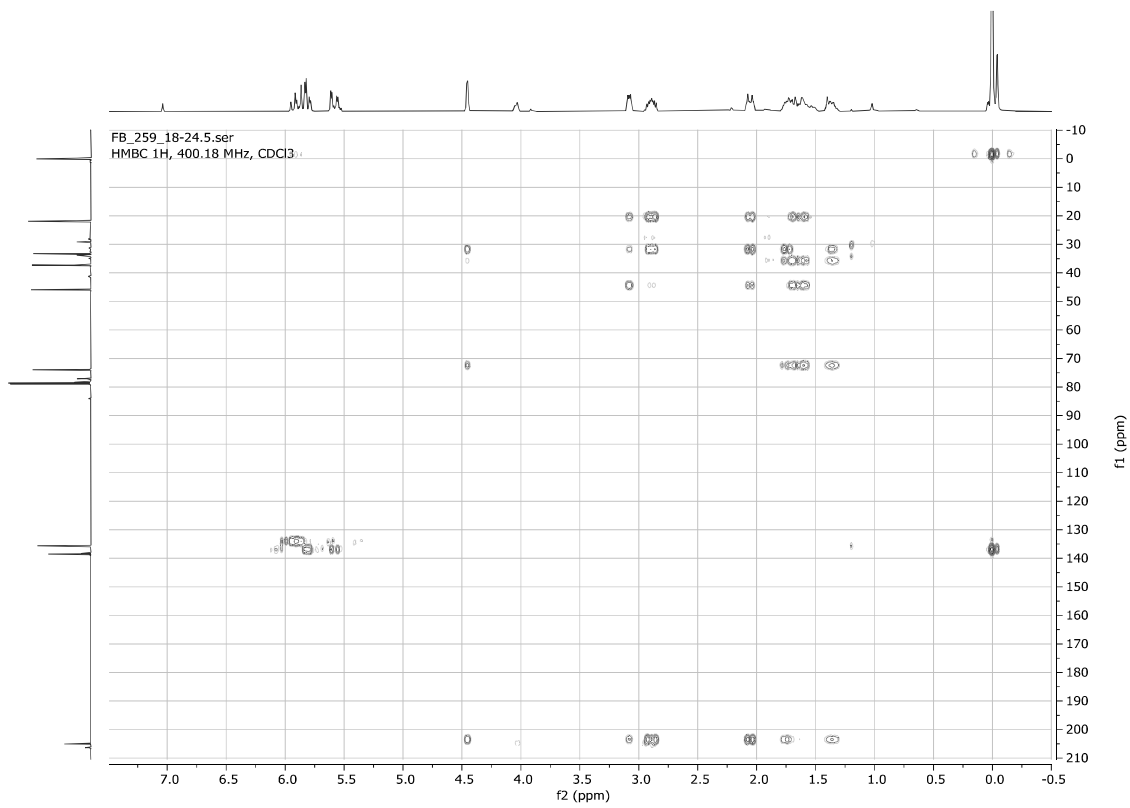
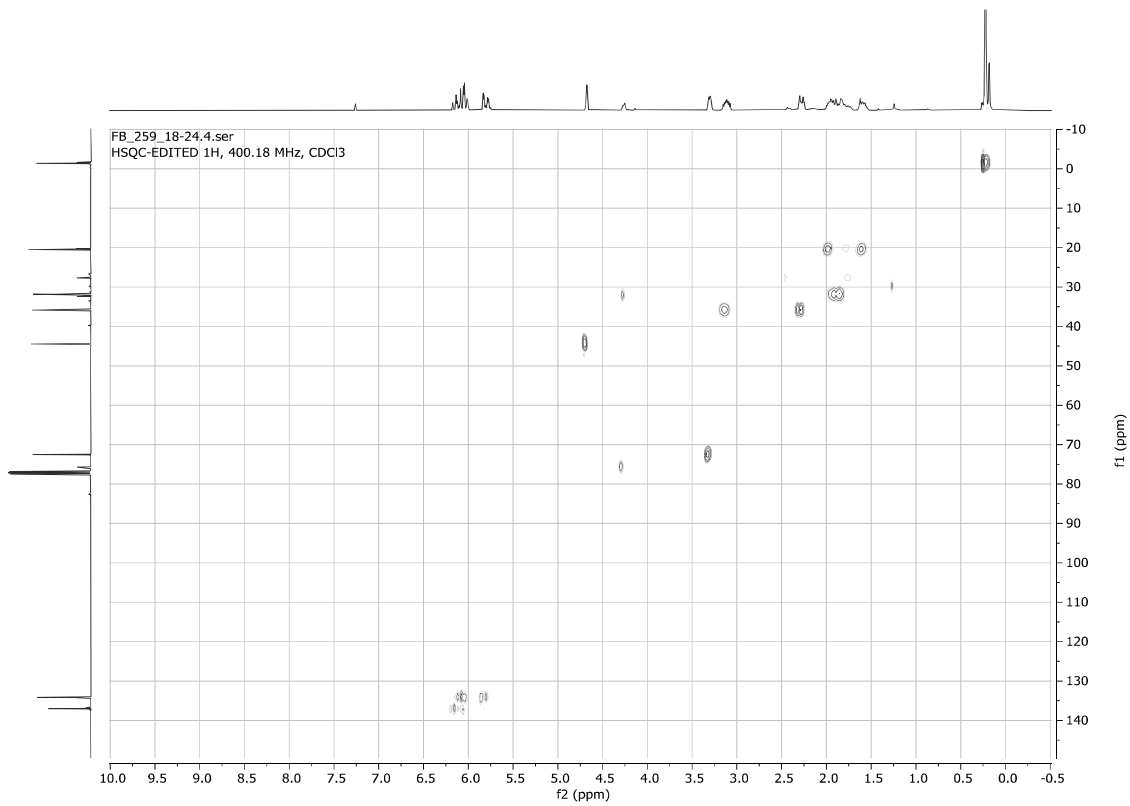
3-((Dimethylvinylsilyl)oxy)-2-iodocyclohexan-1-one **4v** (minor of separable 71:29 diastereomers mixture)

FB_259_18-24.1.fid
1D 1H, 400.18 MHz, CDCl3



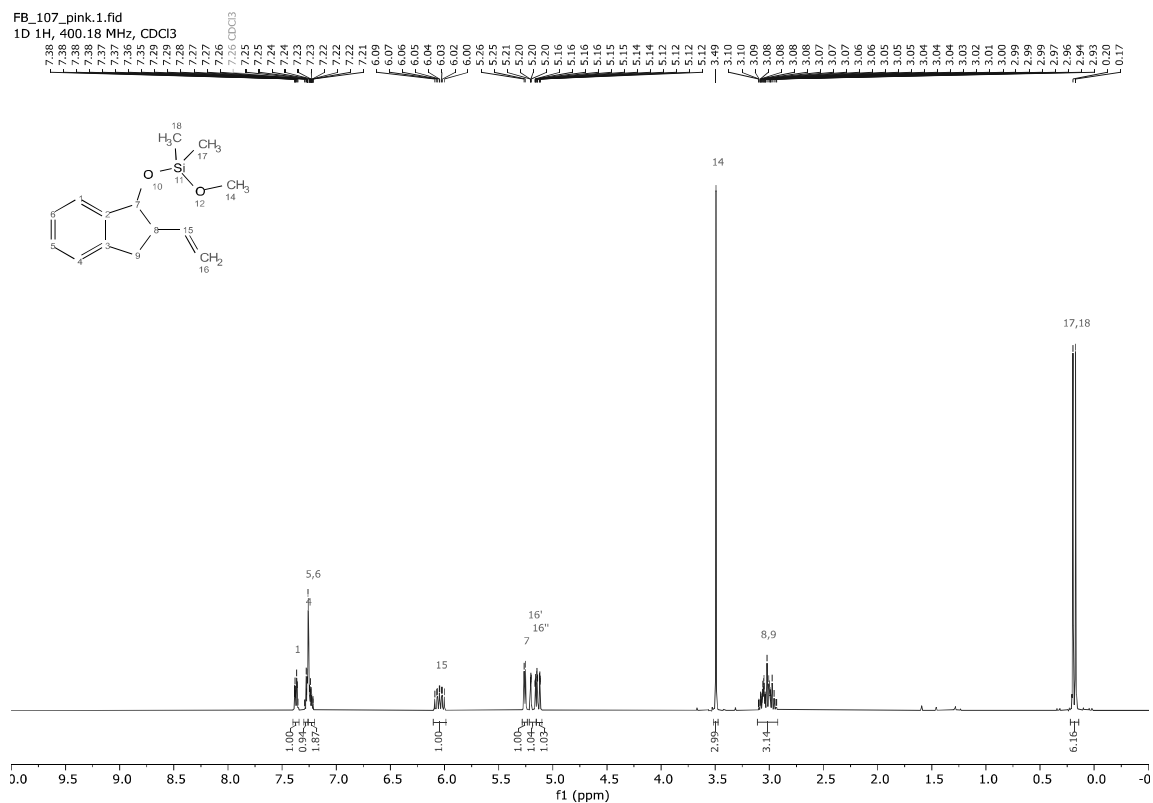
FB_259_18-24.3.fid
1D 13C{1H}, 100.64 MHz, CDCl3



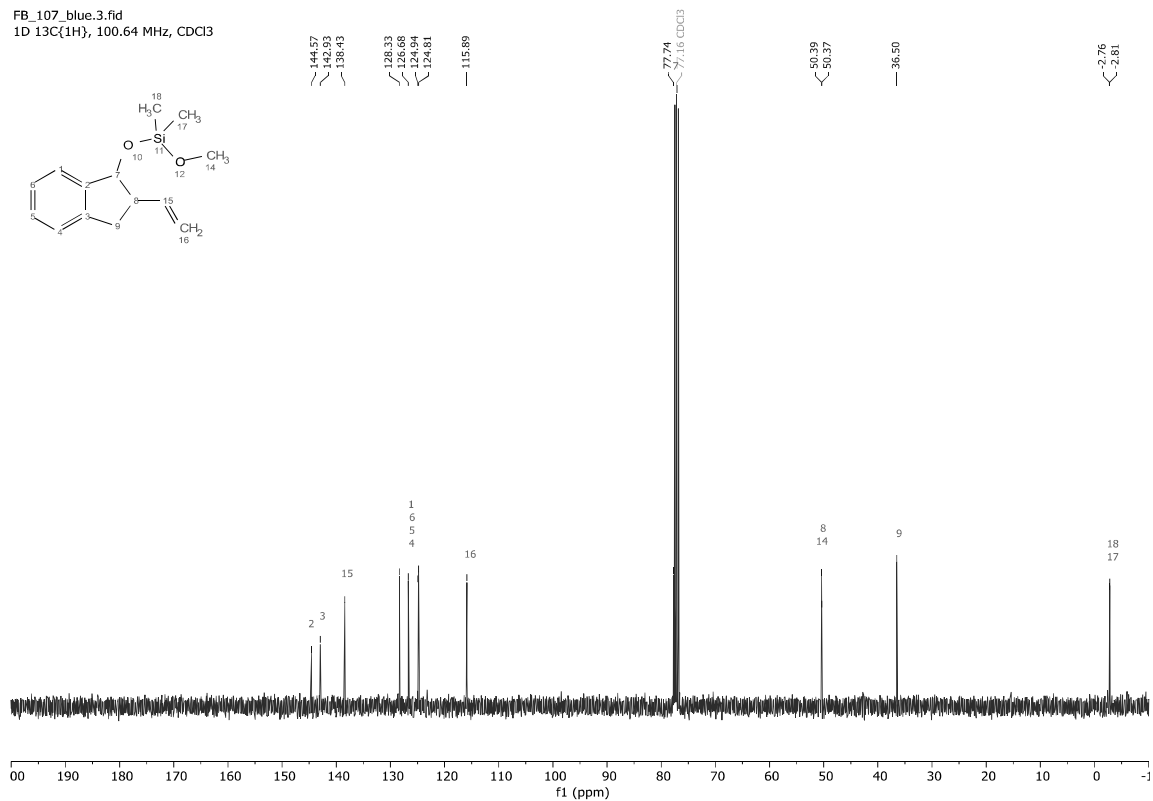


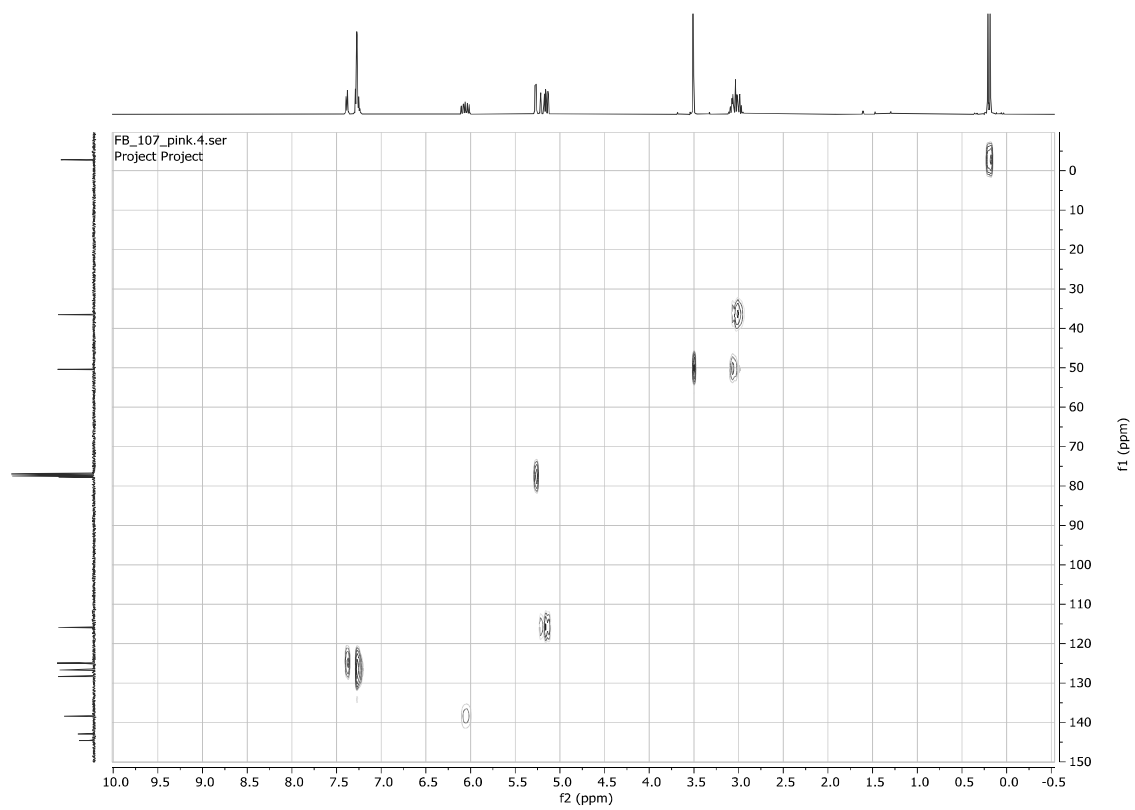
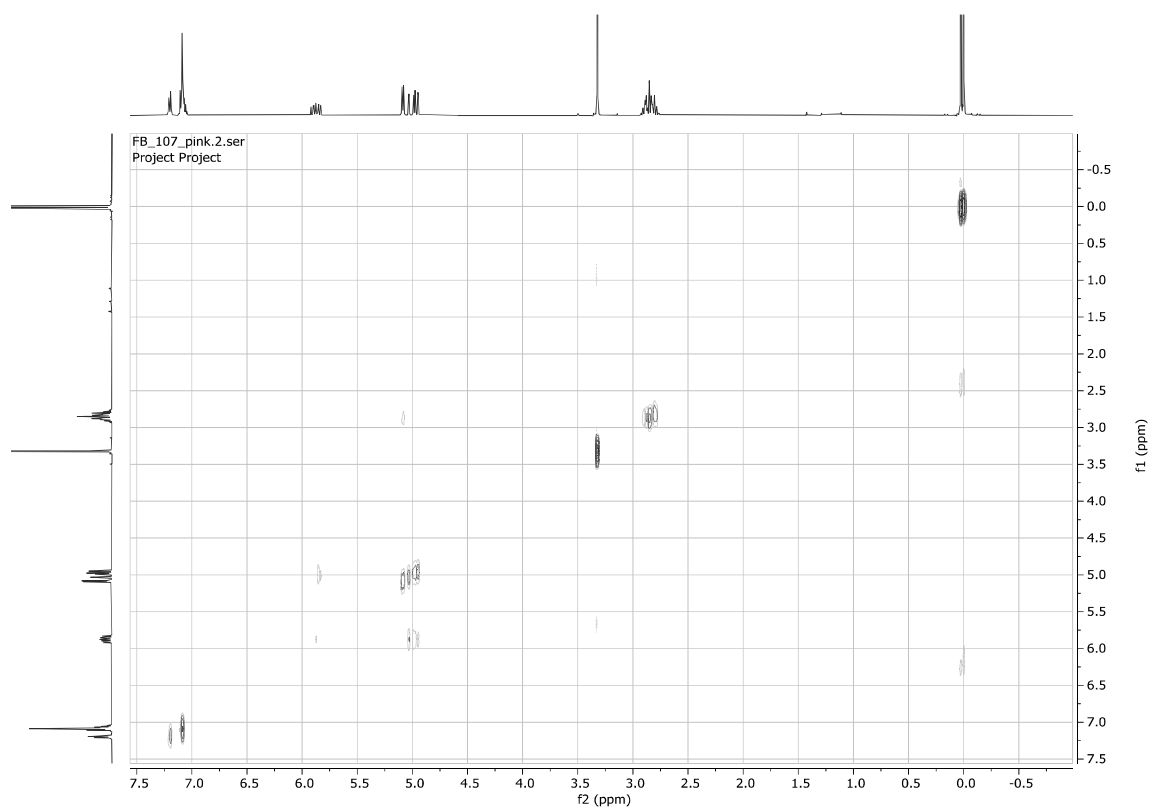
Metoxydimethyl((2-vinyl-2,3-dihydro-1H-inden-1-yl)oxy)silane 5a

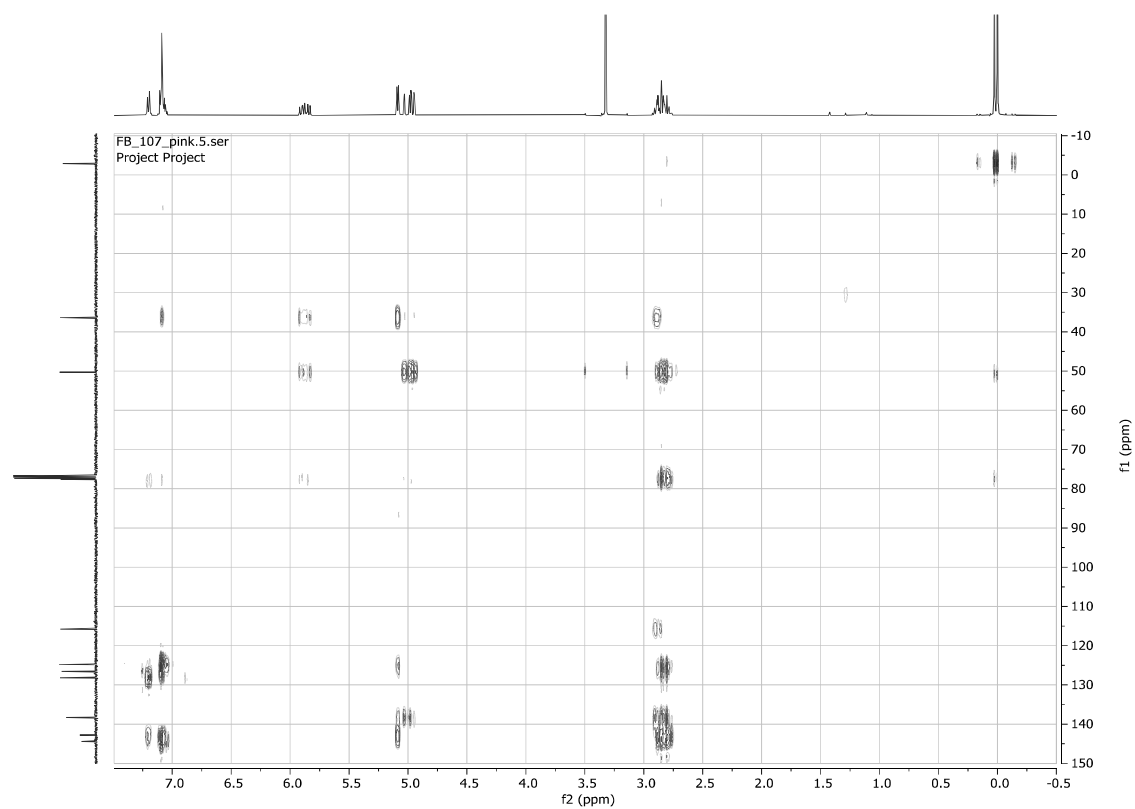
FB_107_pink.1.fid
1D 1H, 400.18 MHz, CDCl3



FB_107_blue.3.fid
1D 13C{1H}, 100.64 MHz, CDCl3

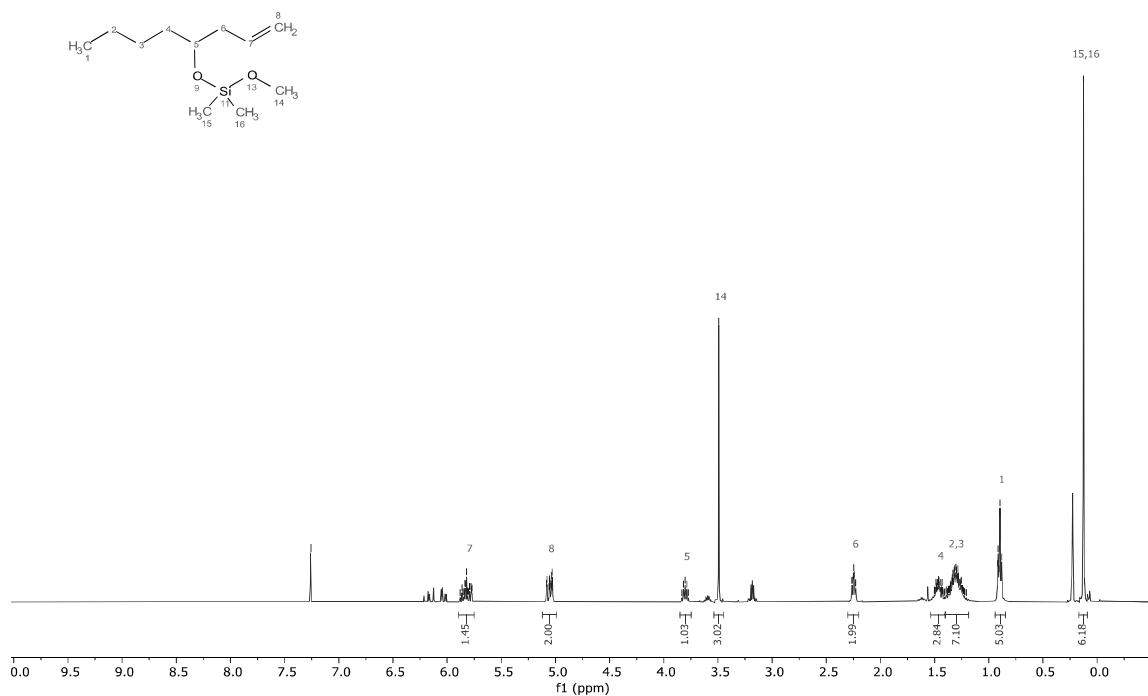




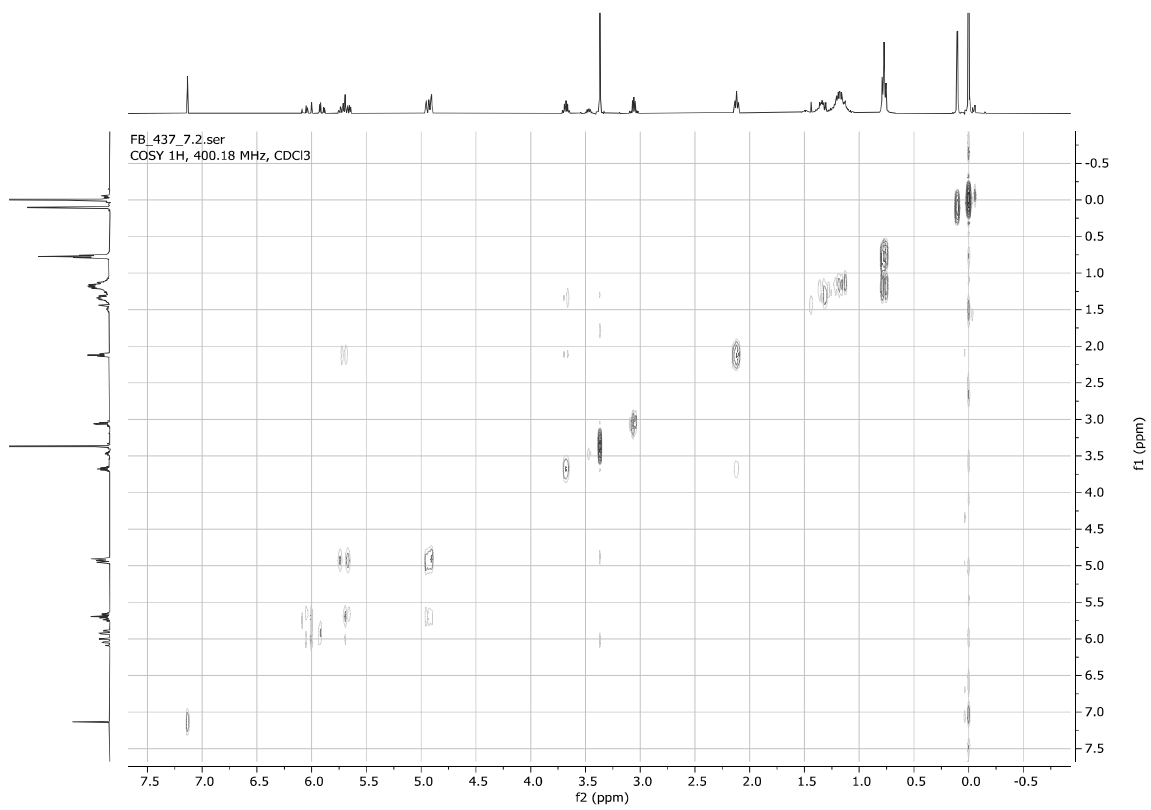
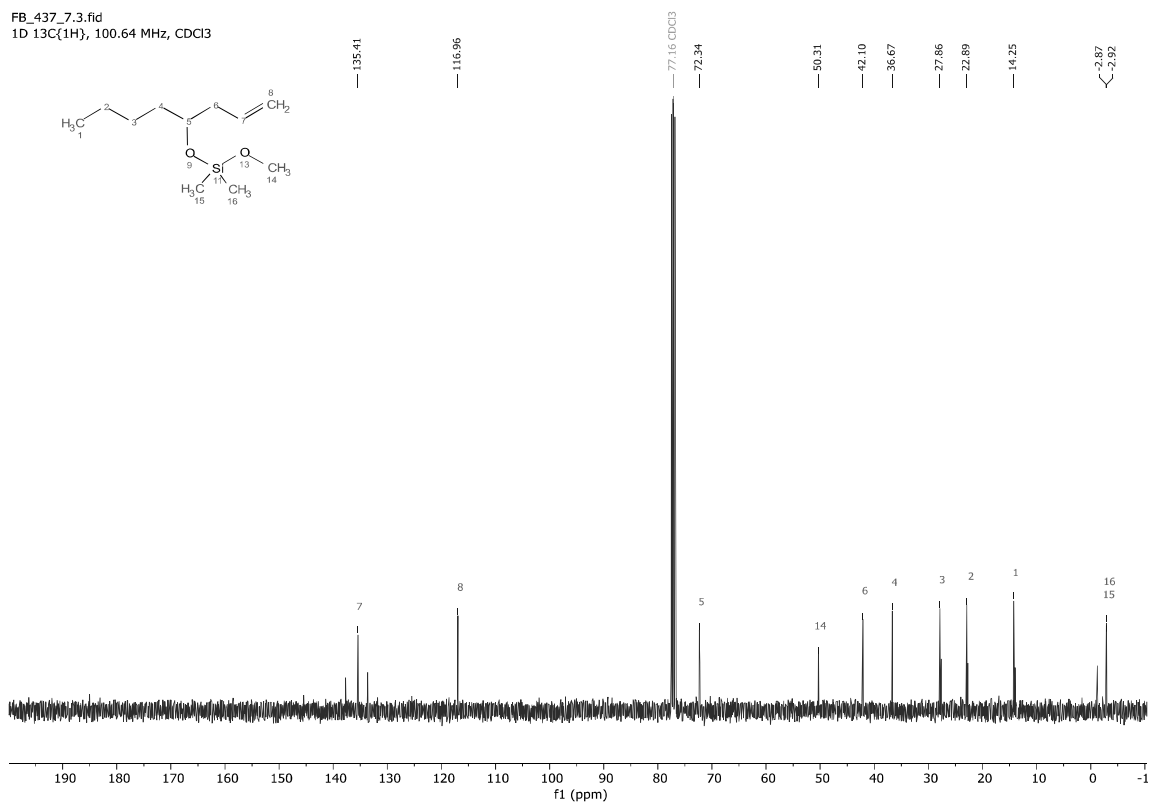


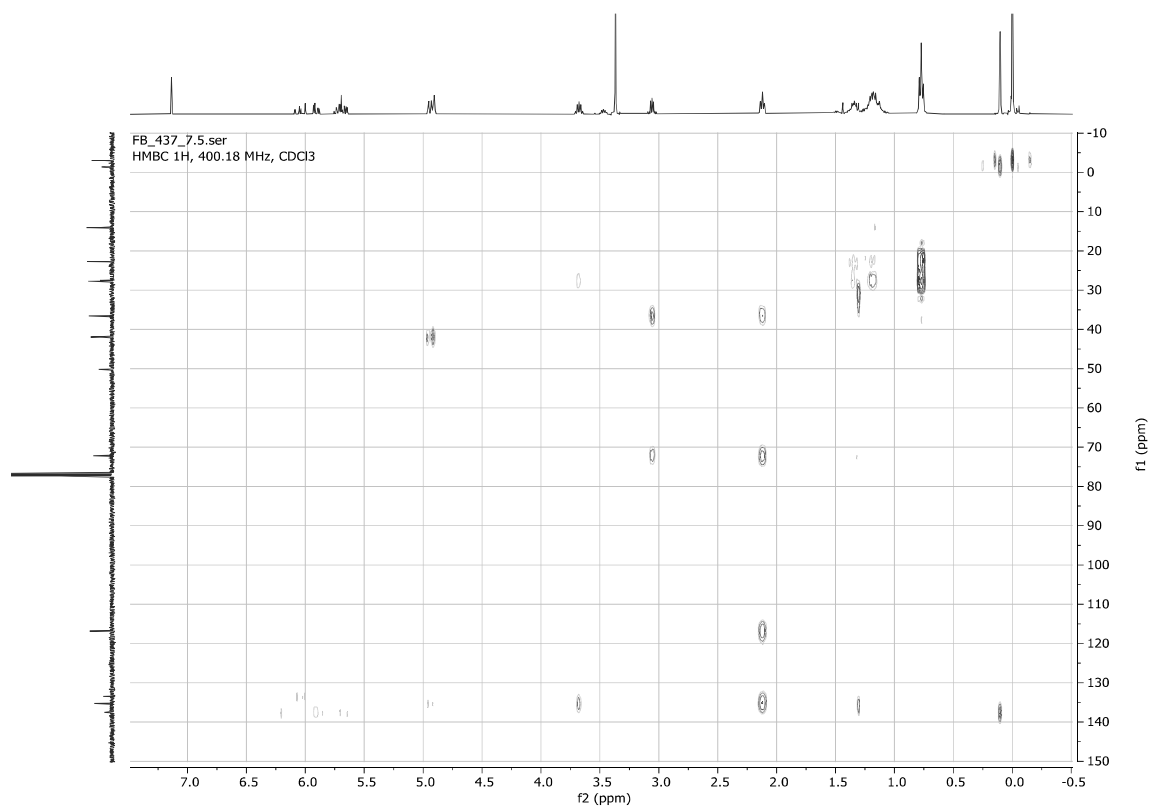
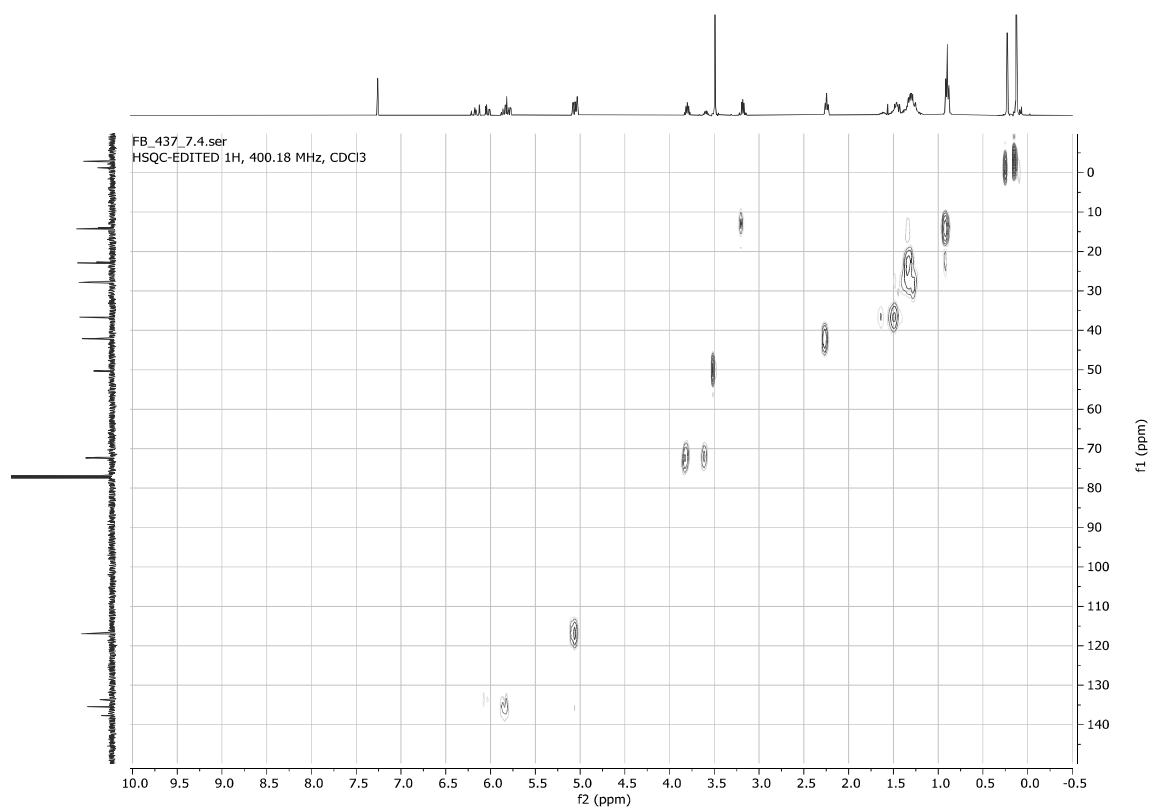
Inseparable 1:2 mixture of substrate **4k** and methoxydimethyl(oct-1-en-4-yloxy)silane **5k**

FB_437_7.1.fid
 1D 1H, 400.18 MHz, CDCl3

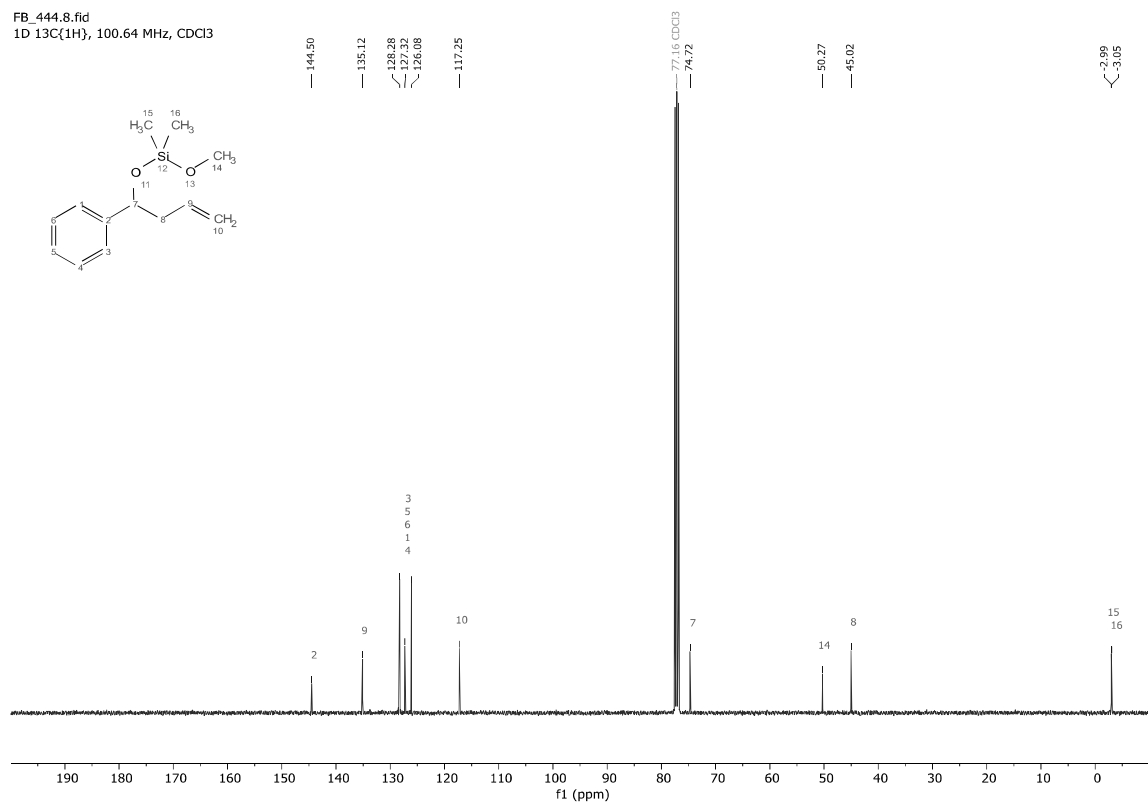
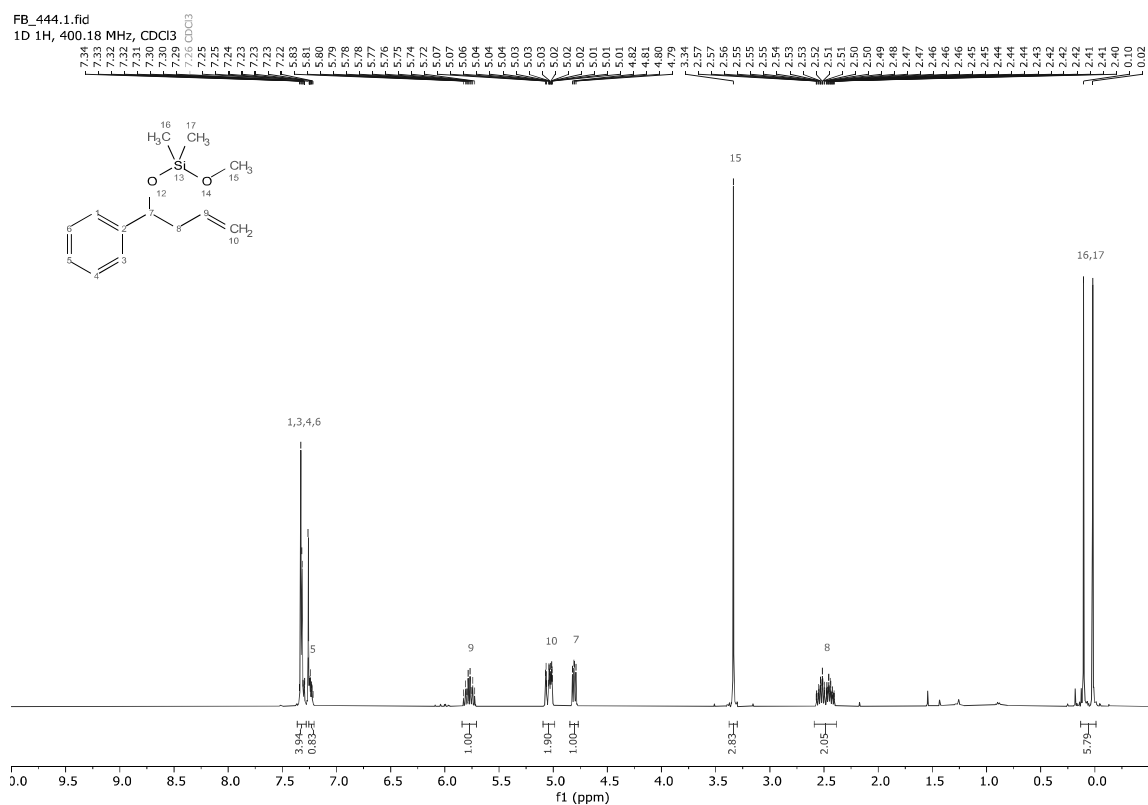


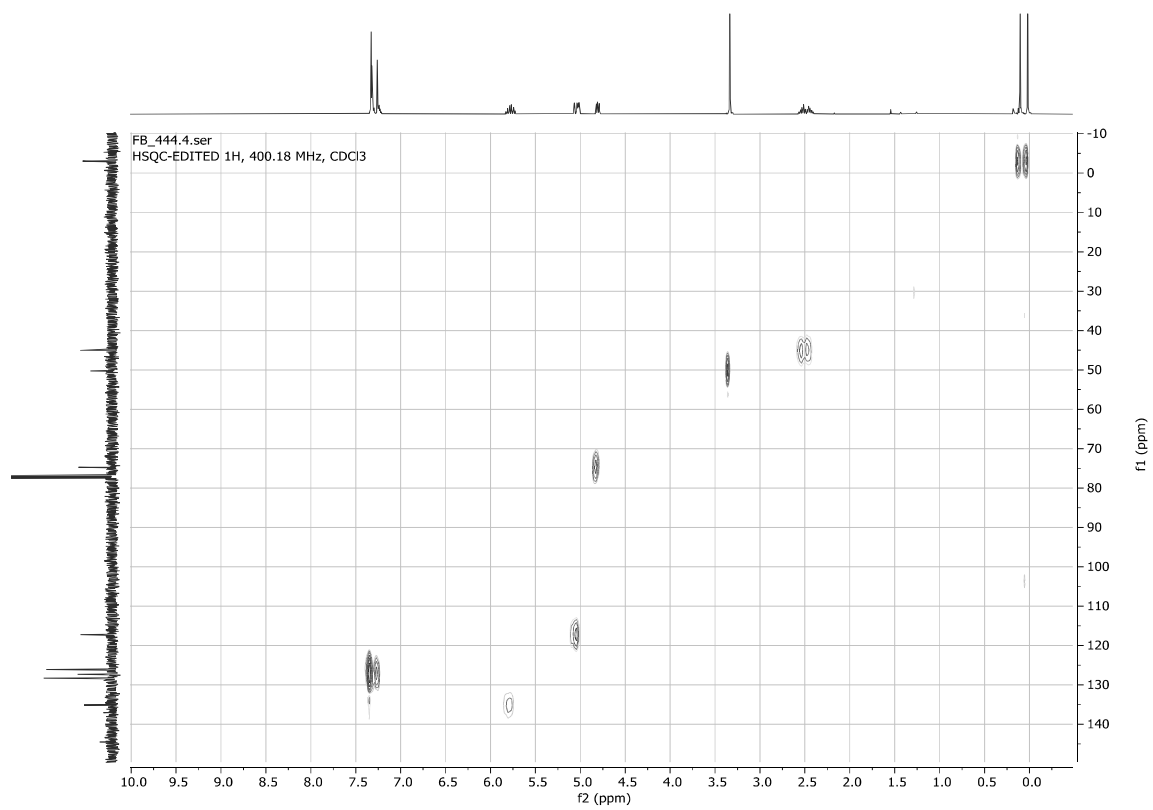
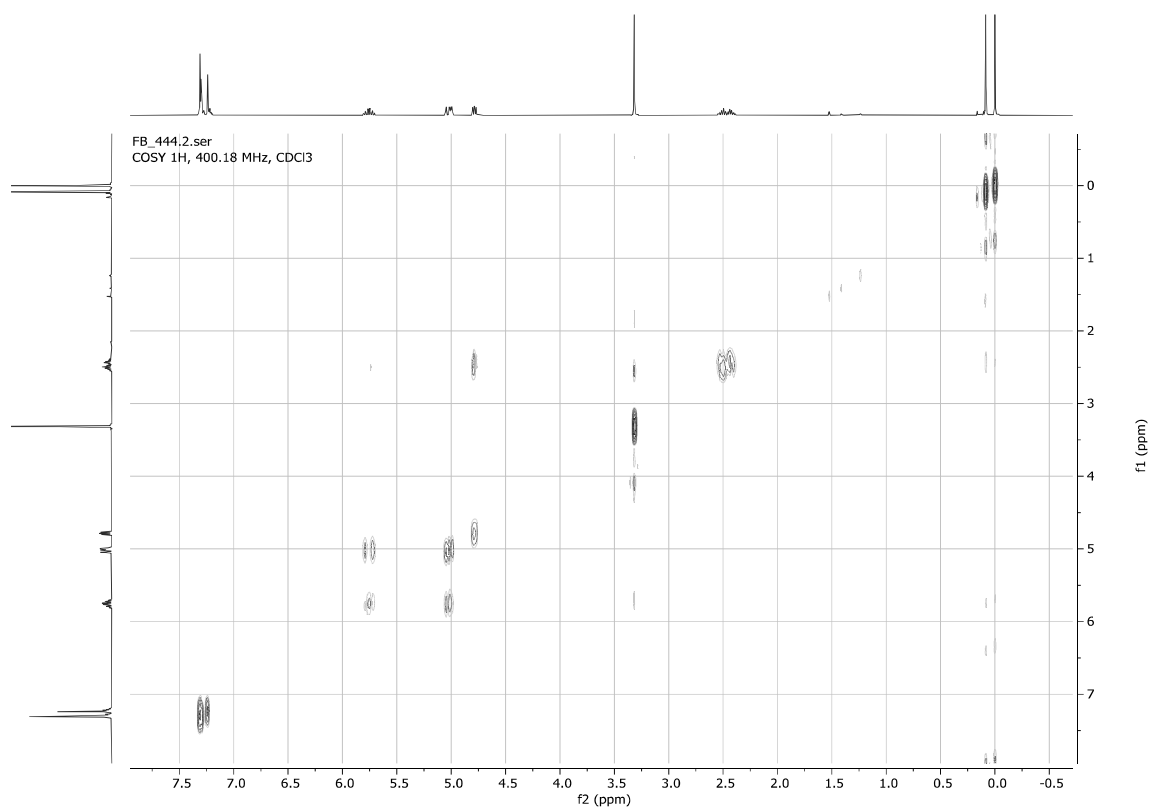
FB_437_7.3.fid
1D 13C{1H}, 100.64 MHz, CDCl3

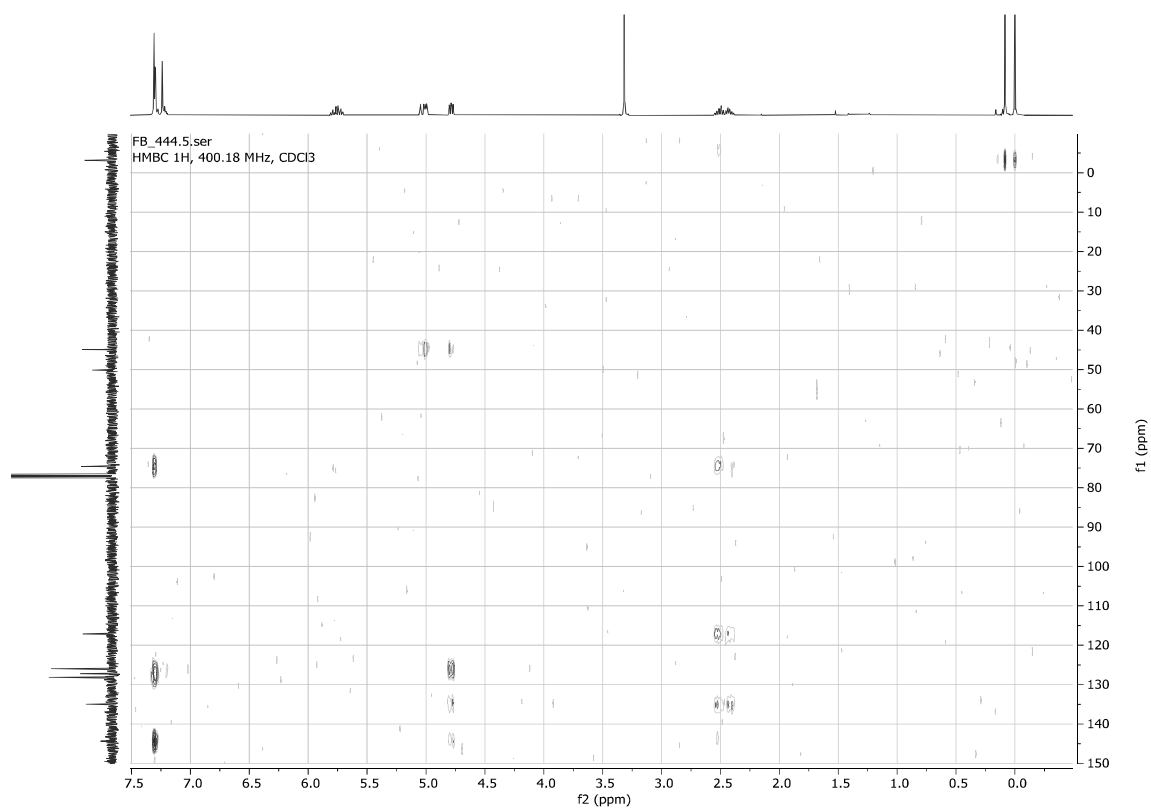




Methoxydimethyl((1-phenylbut-3-en-1-yl)oxy)silane **5n**

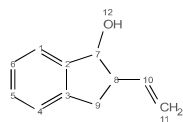






2-Vinyl-2,3-dihydro-1H-inden-1-ol **6a**

FB_225.1.fid
1D 1H, 400.18 MHz, CDCl3



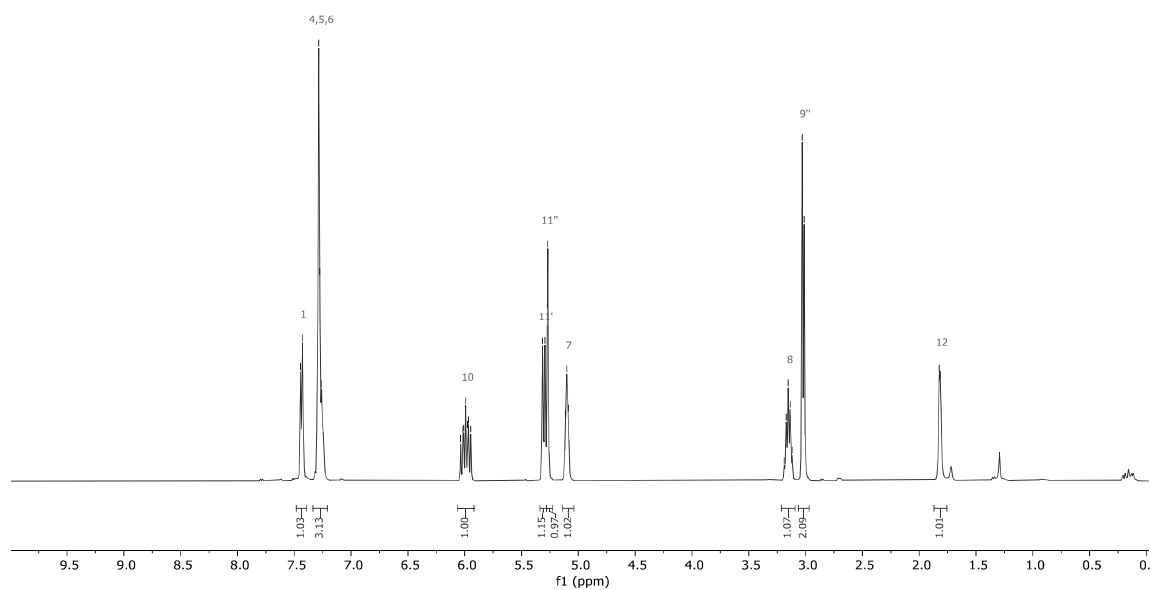
7.44
7.43
7.38
7.28
7.26 CDCl3

6.04
6.02
5.99
5.97
5.95

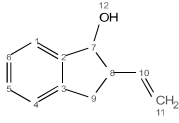
5.32
5.29
5.11
5.10
5.09

3.19
3.17
3.15
3.14
3.12
3.01

1.82
1.81



FB_225.3.fid
1D 13C{1H}, 100.64 MHz, CDCl3

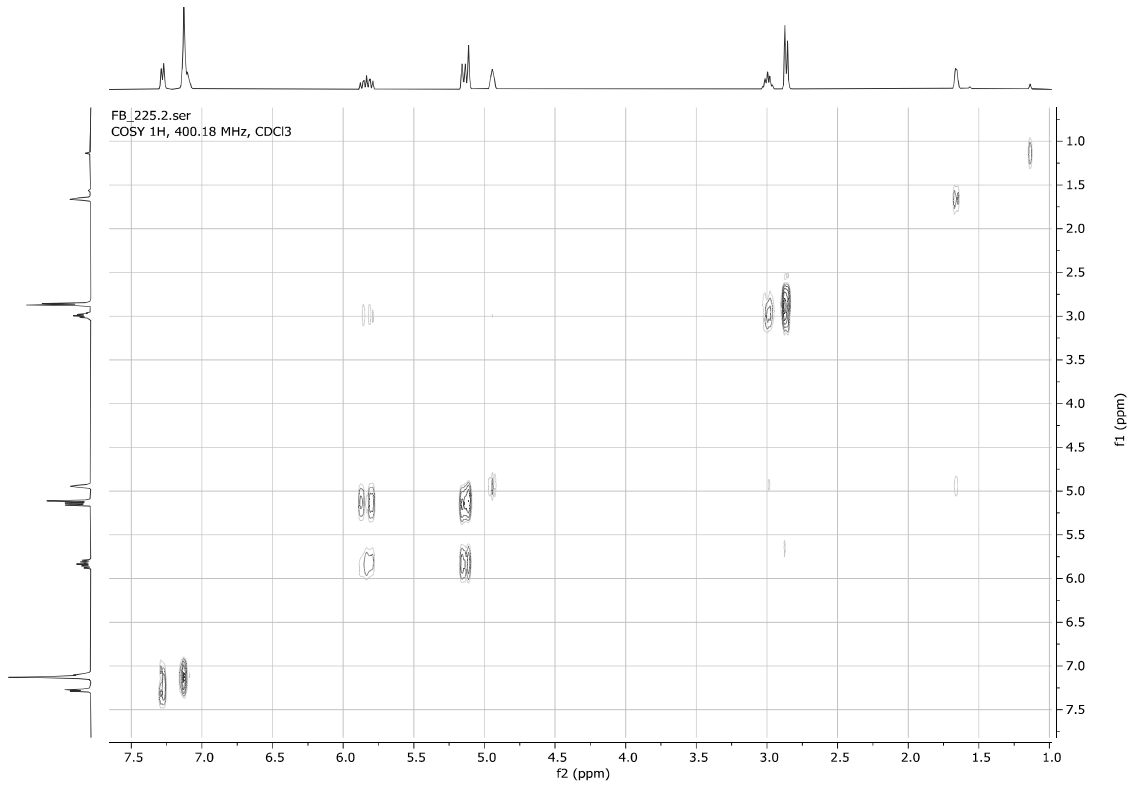
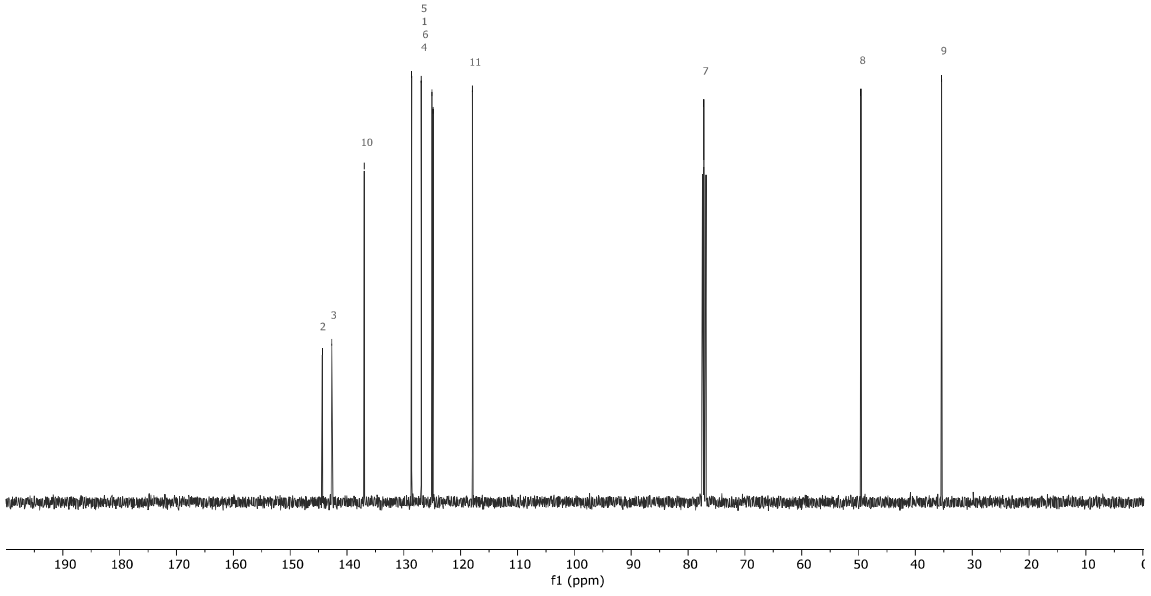


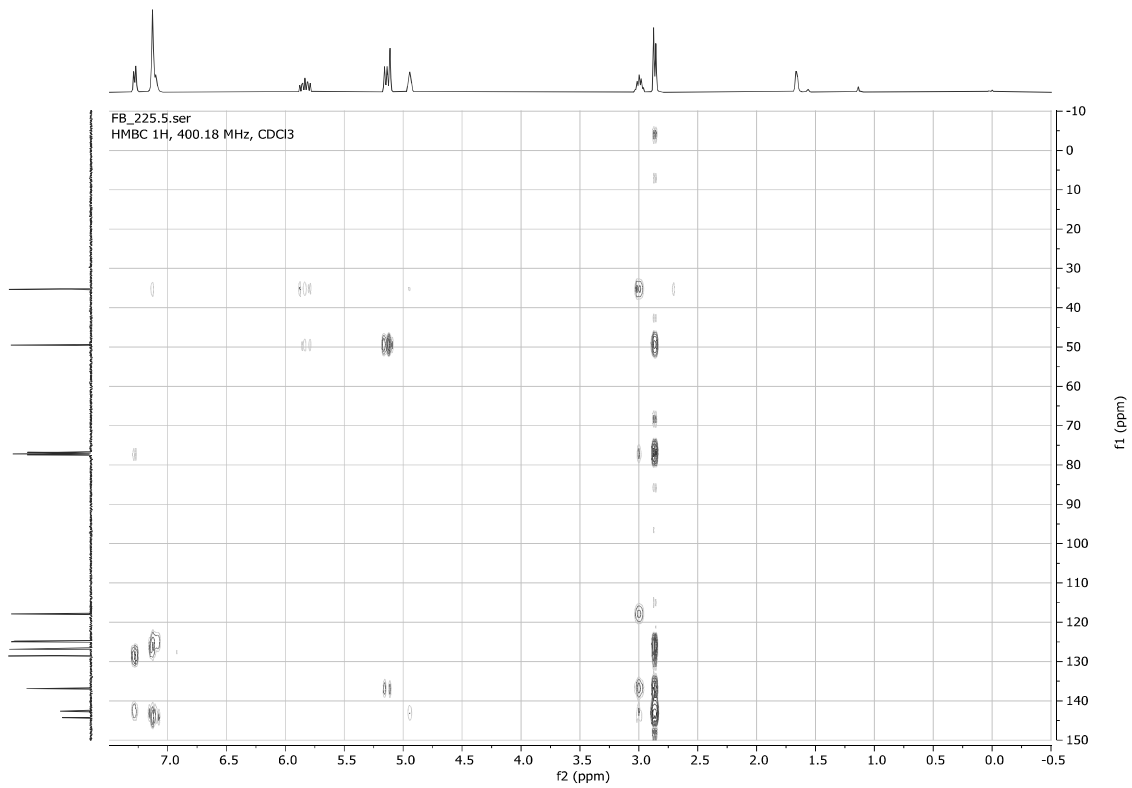
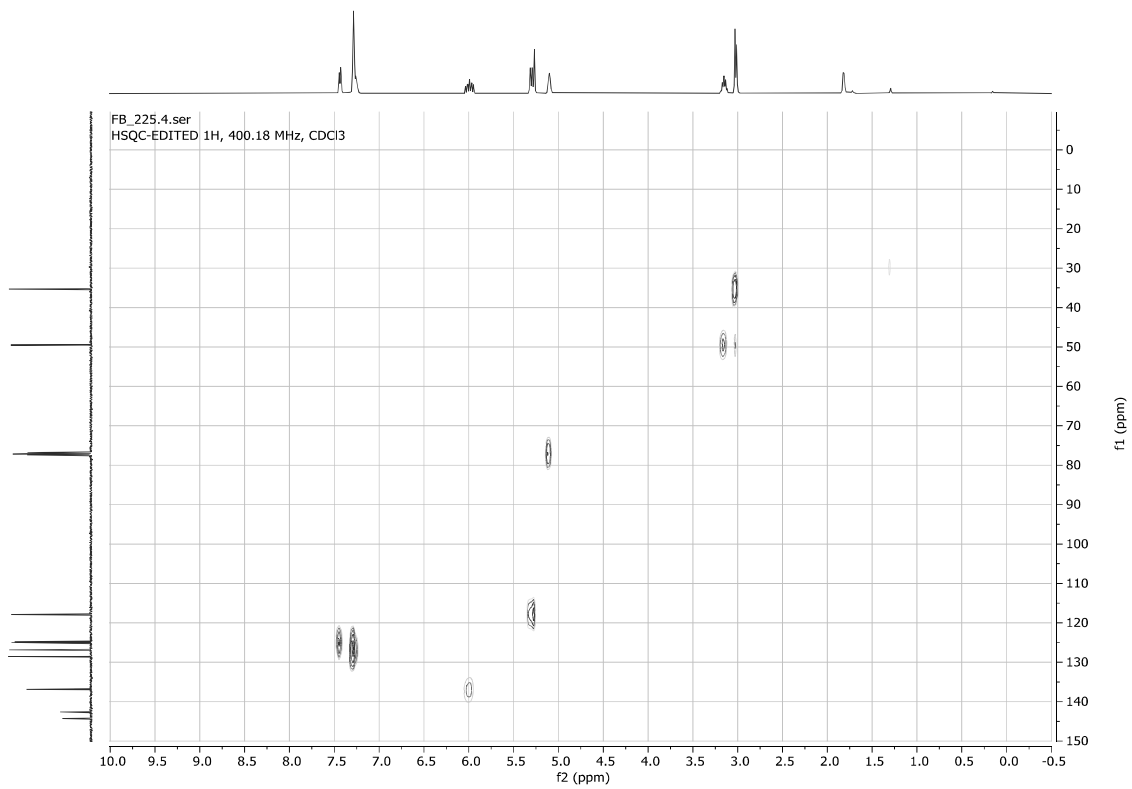
144.3
142.7
137.0
128.6
125.1
124.9
117.9

77.2
77.2 CDCl3

49.6

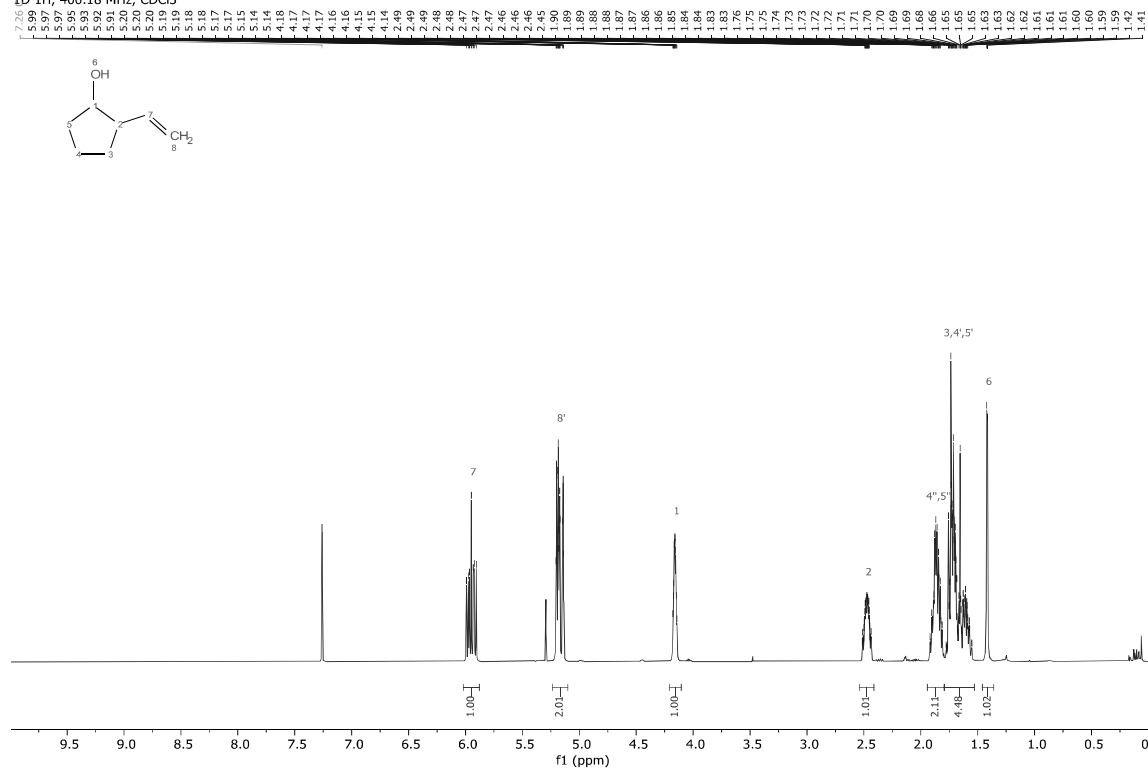
35.4



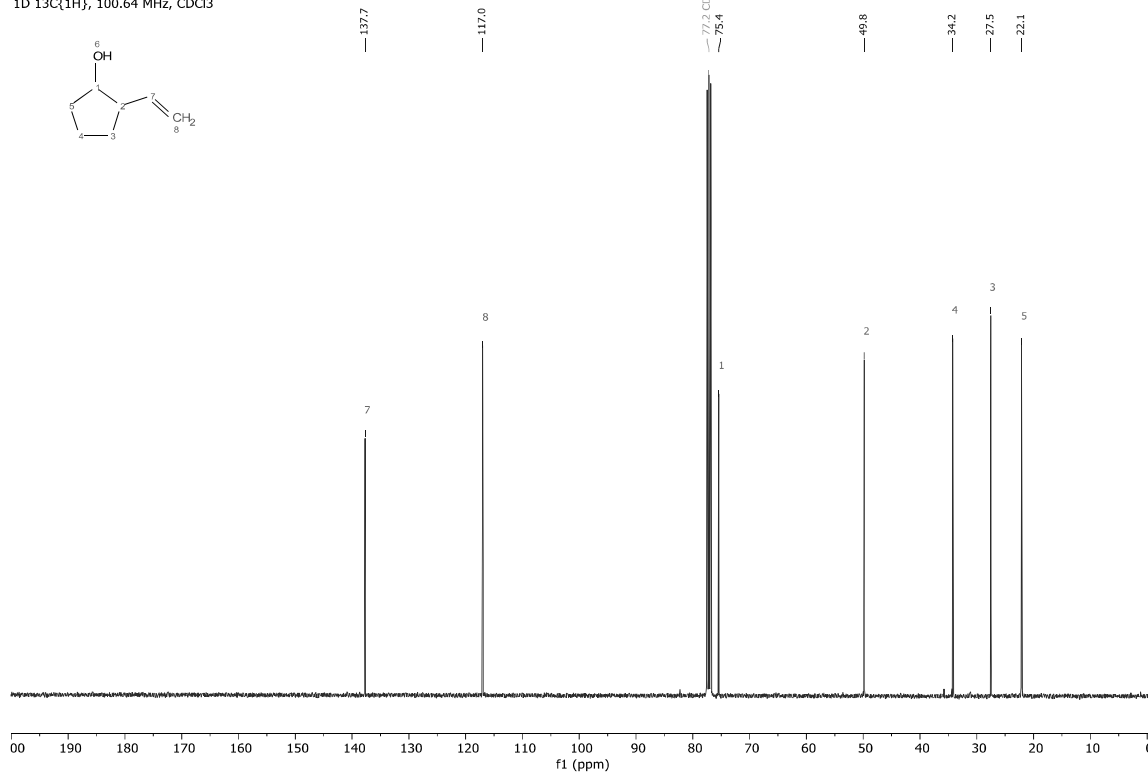


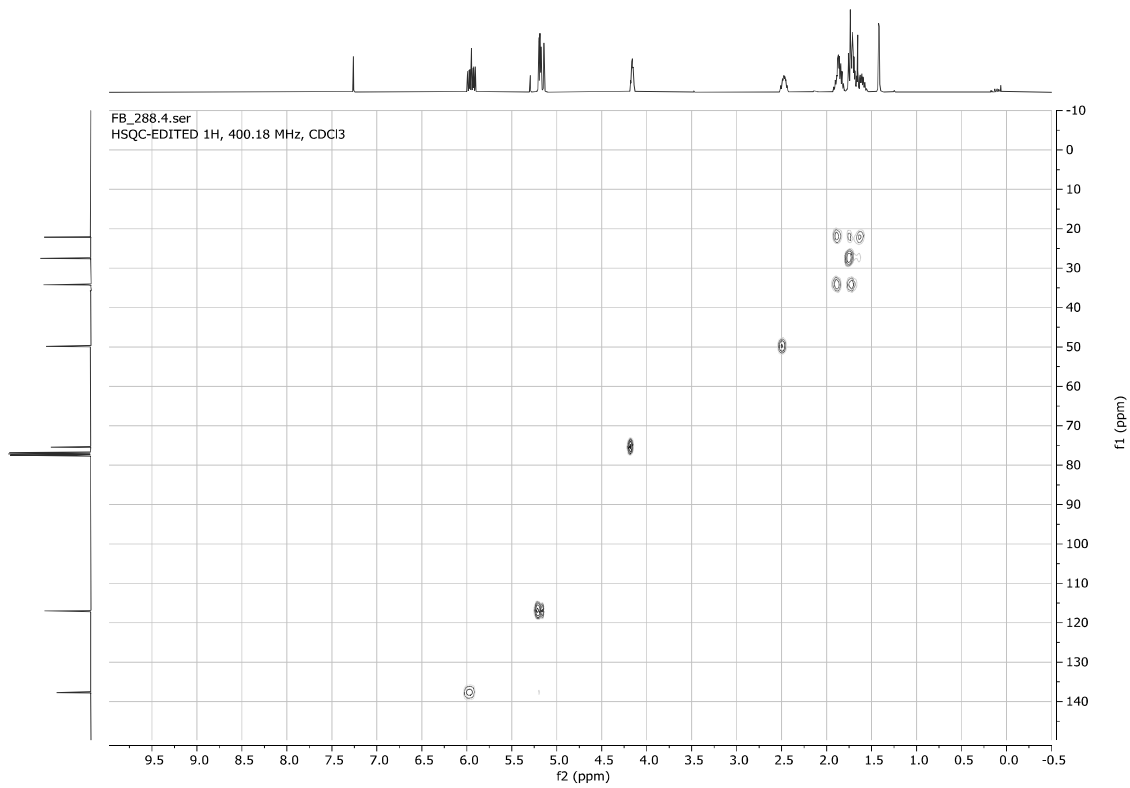
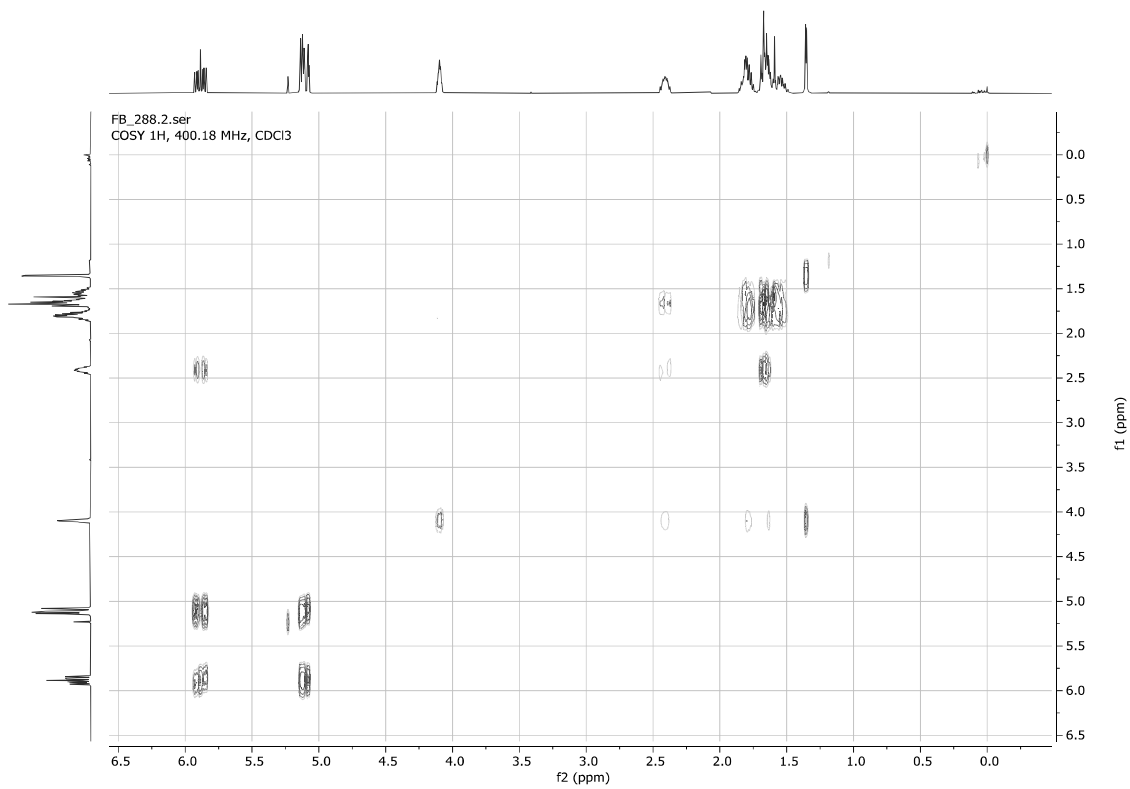
2-Ethynylcyclopentanol **6b**

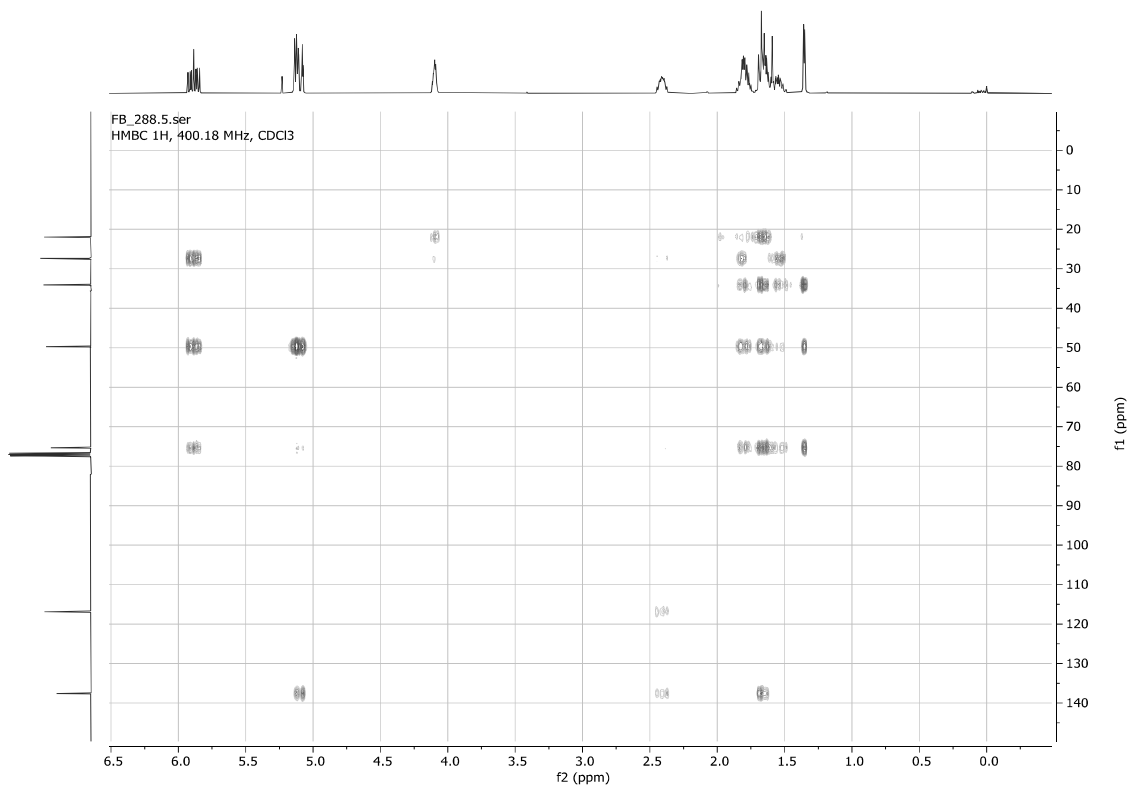
FB_288.1.fid
1D 1H, 400.18 MHz, CDCl3



FB_288.3.fid
1D 13C{1H}, 100.64 MHz, CDCl3

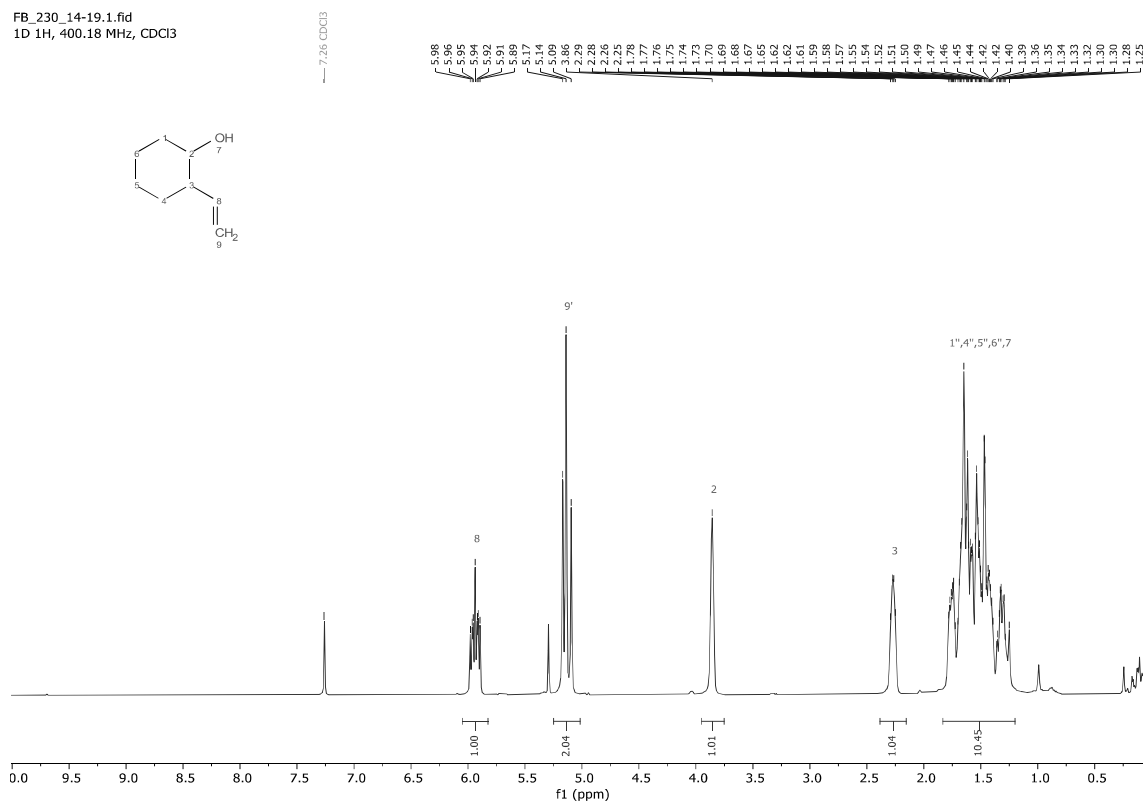
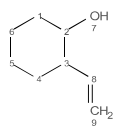




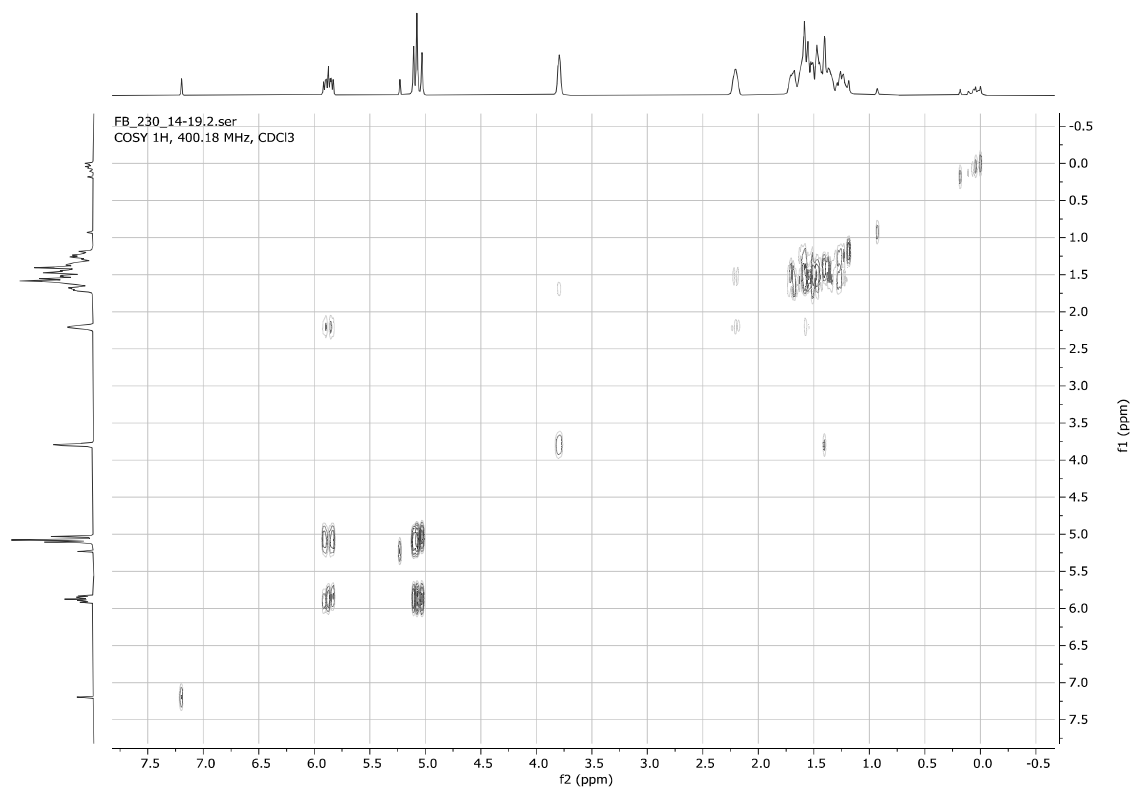
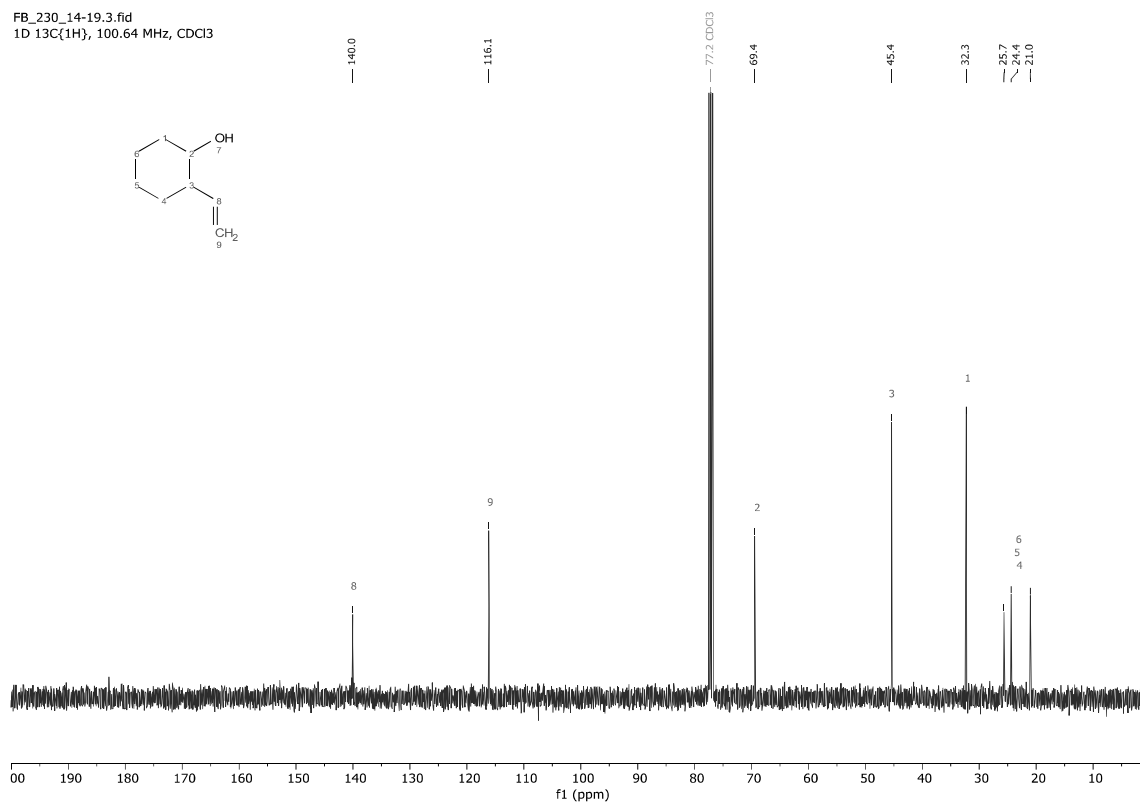


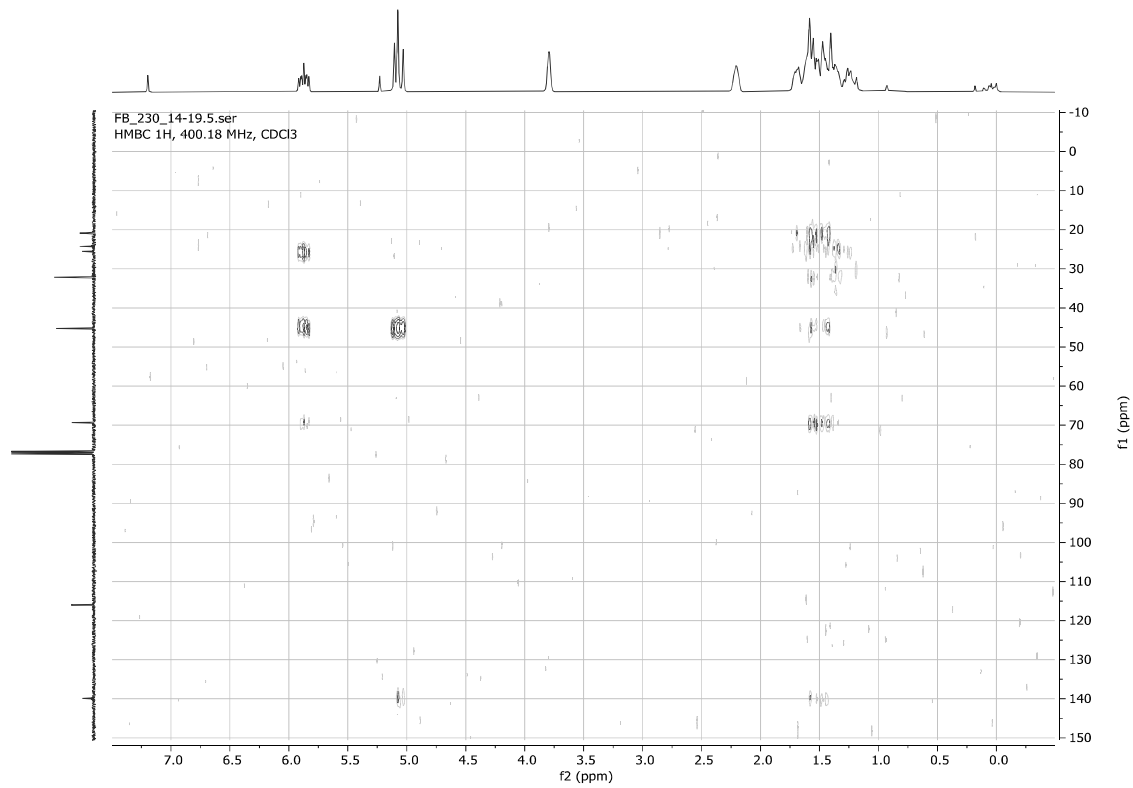
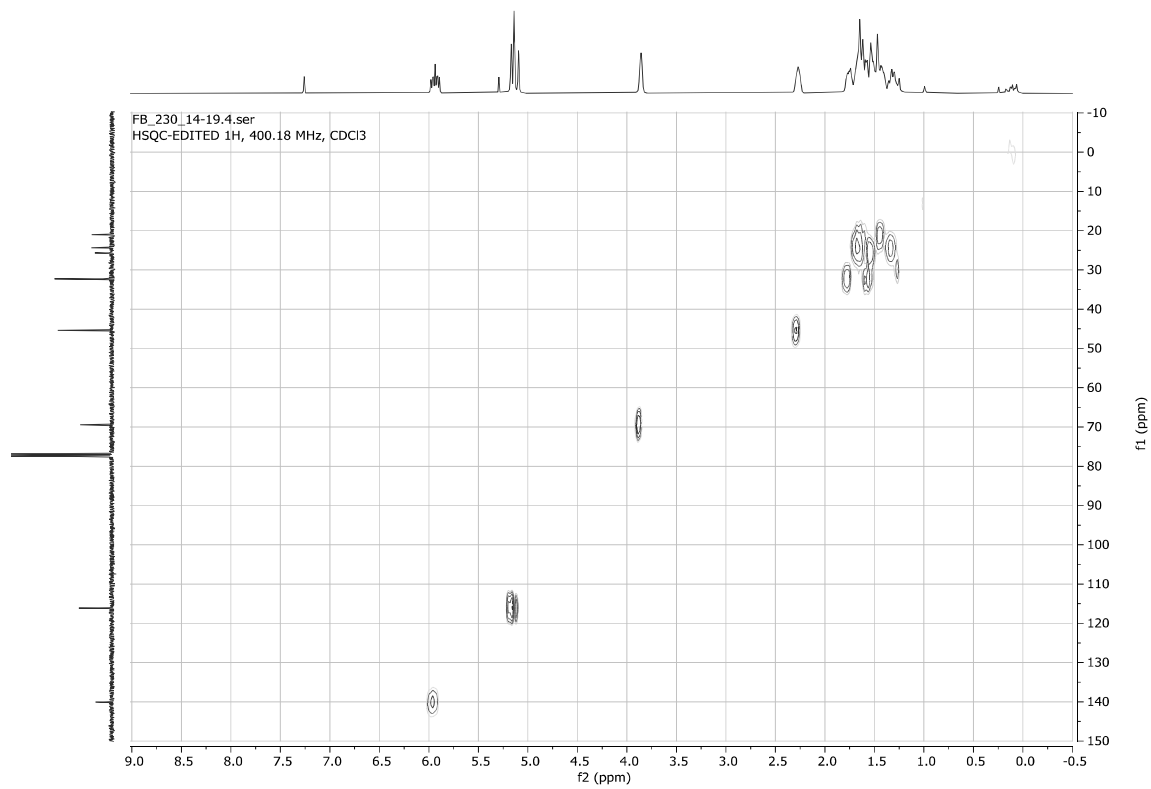
2-Vinylcyclohexan-1-ol **6c**

FB_230_14-19.1.fid
1D 1H, 400.18 MHz, CDCl3



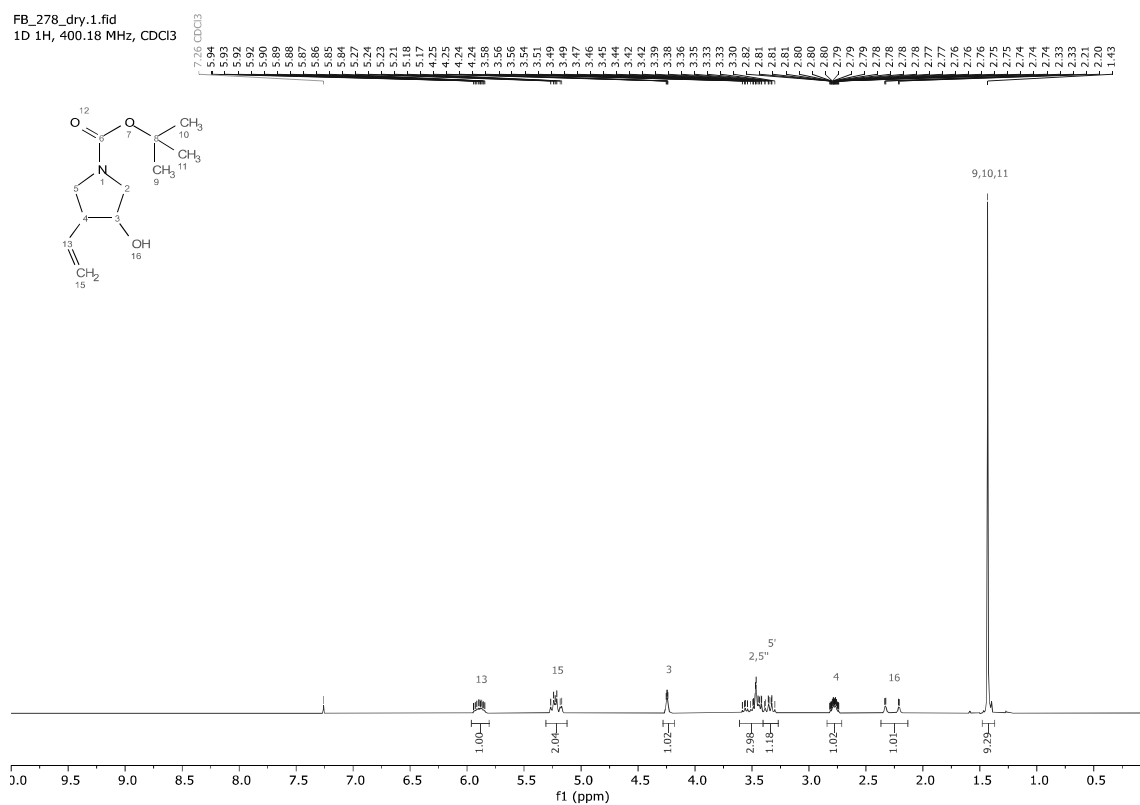
FB_230_14-19.3.fid
1D 13C{1H}, 100.64 MHz, CDCl3



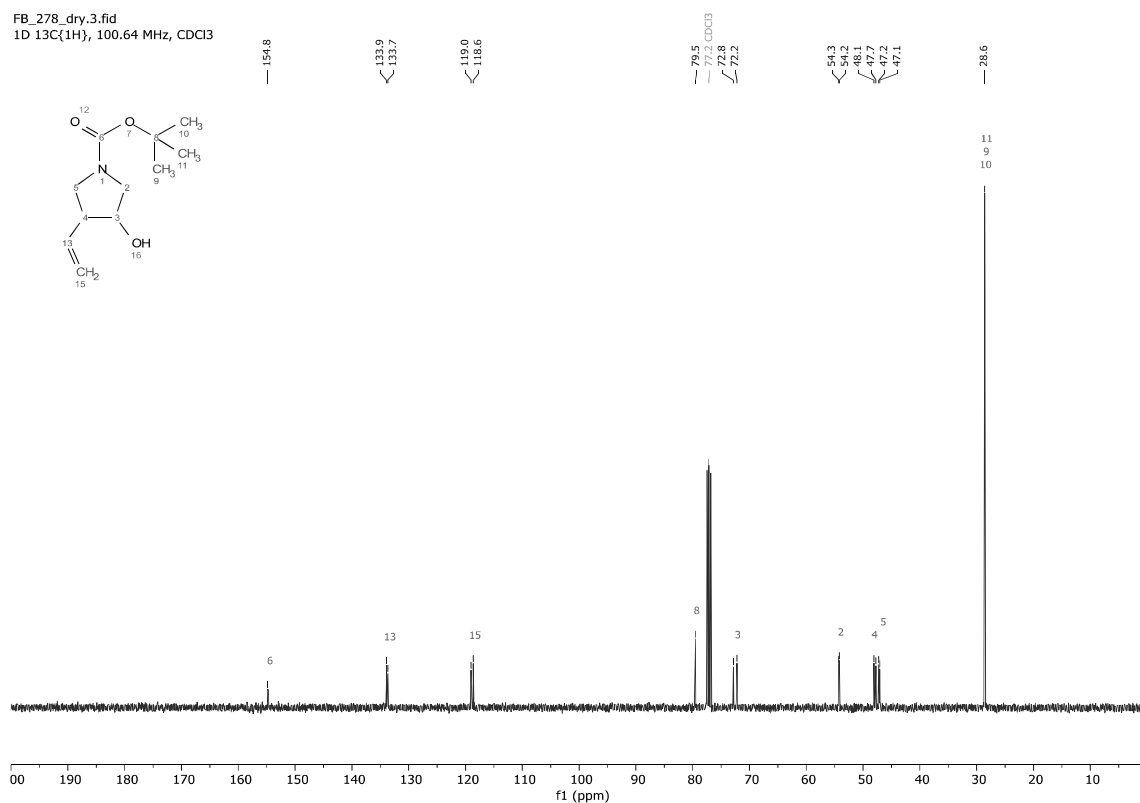


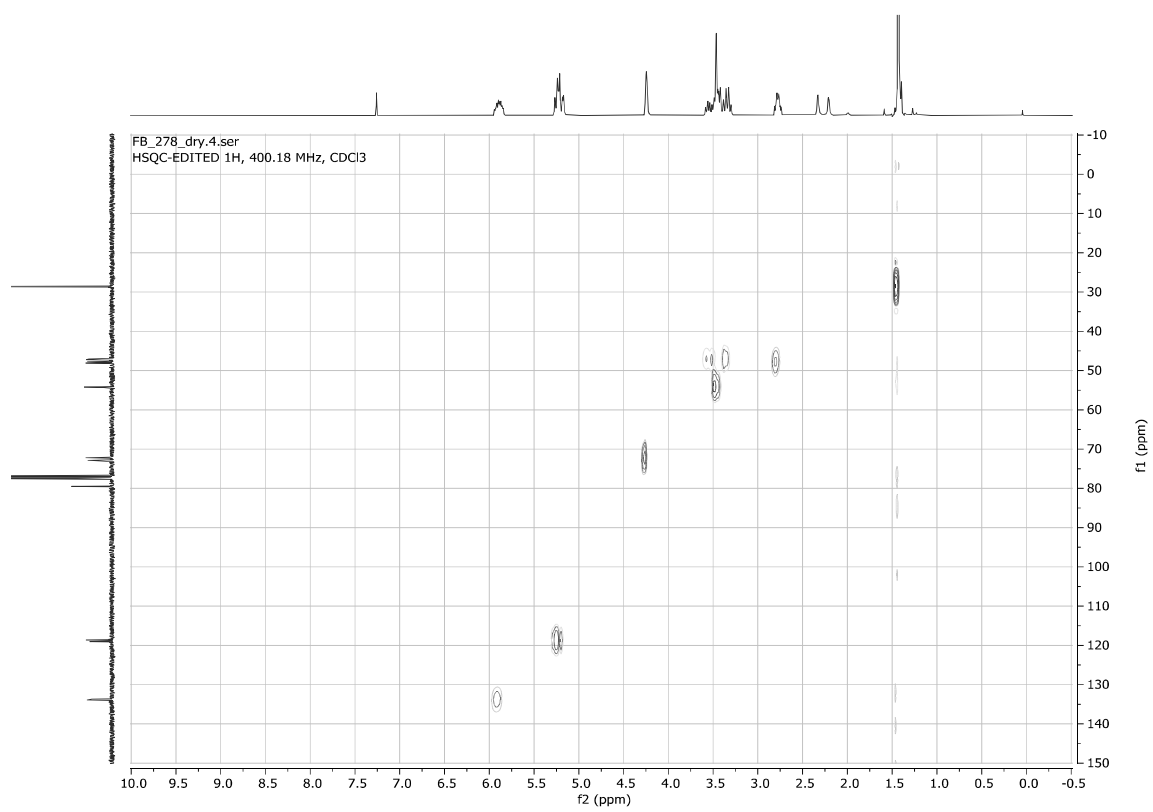
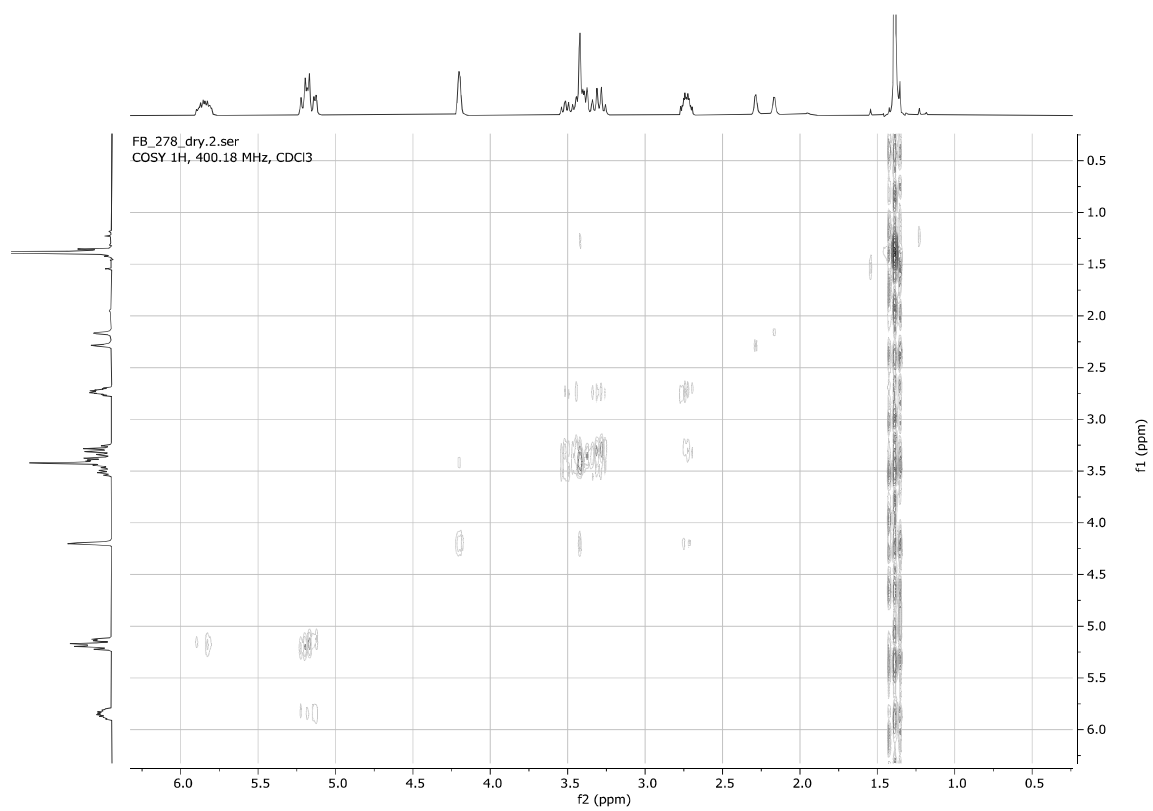
tert-Butyl 3-hydroxy-4-vinylpyrrolidine-1-carboxylate **6d** (mixture of rotamers)

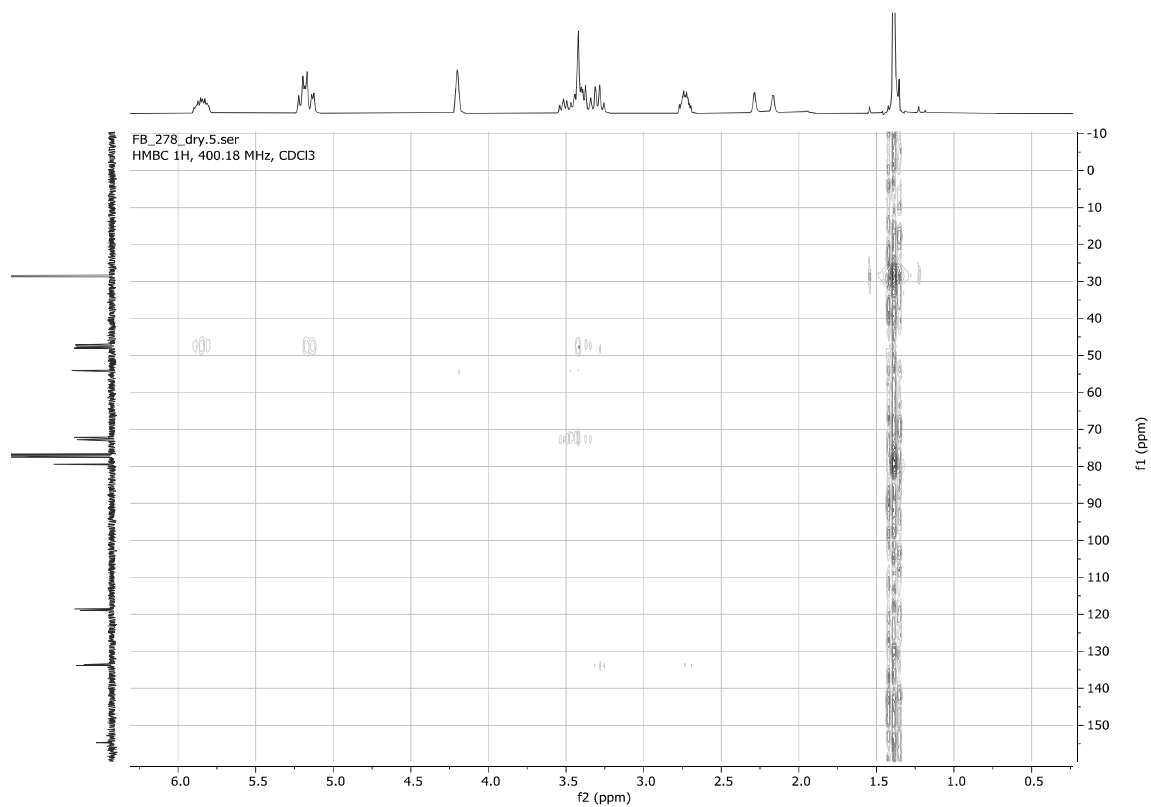
FB_278_dry.1.fid
1D 1H, 400.18 MHz, CDCl₃



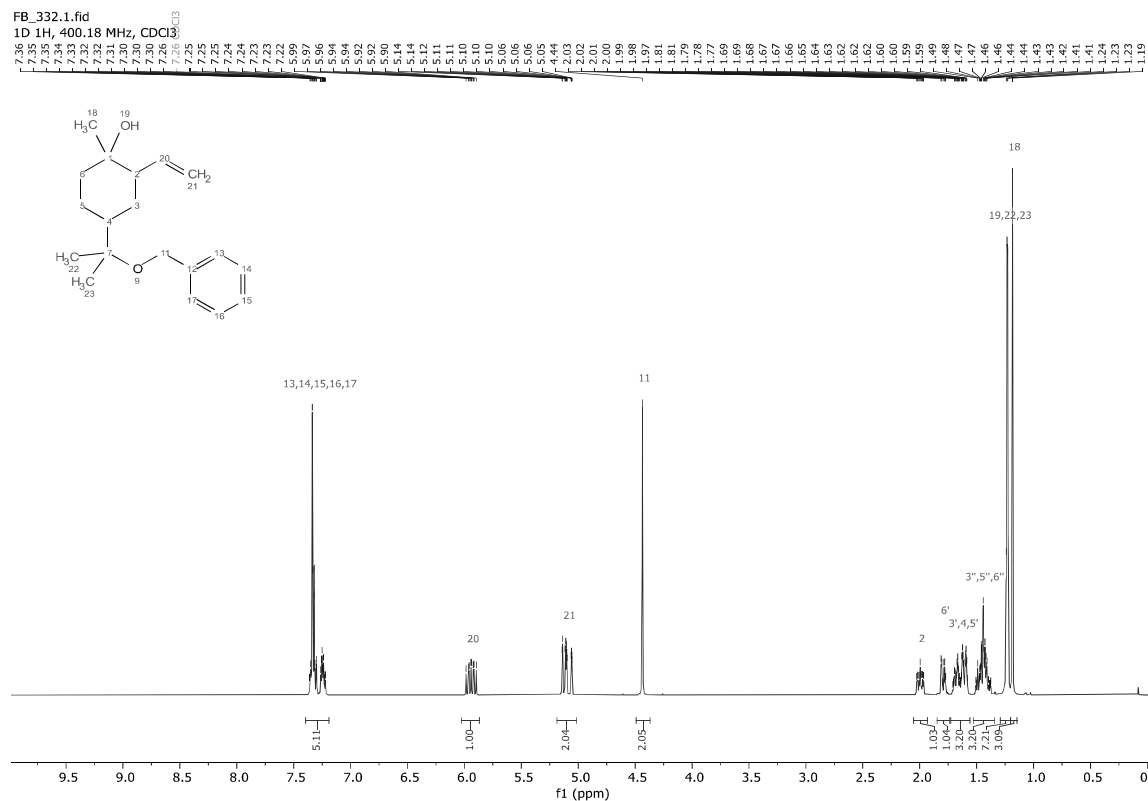
FB_278_dry.3.fid
1D 13C(1H), 100.64 MHz, CDCl₃



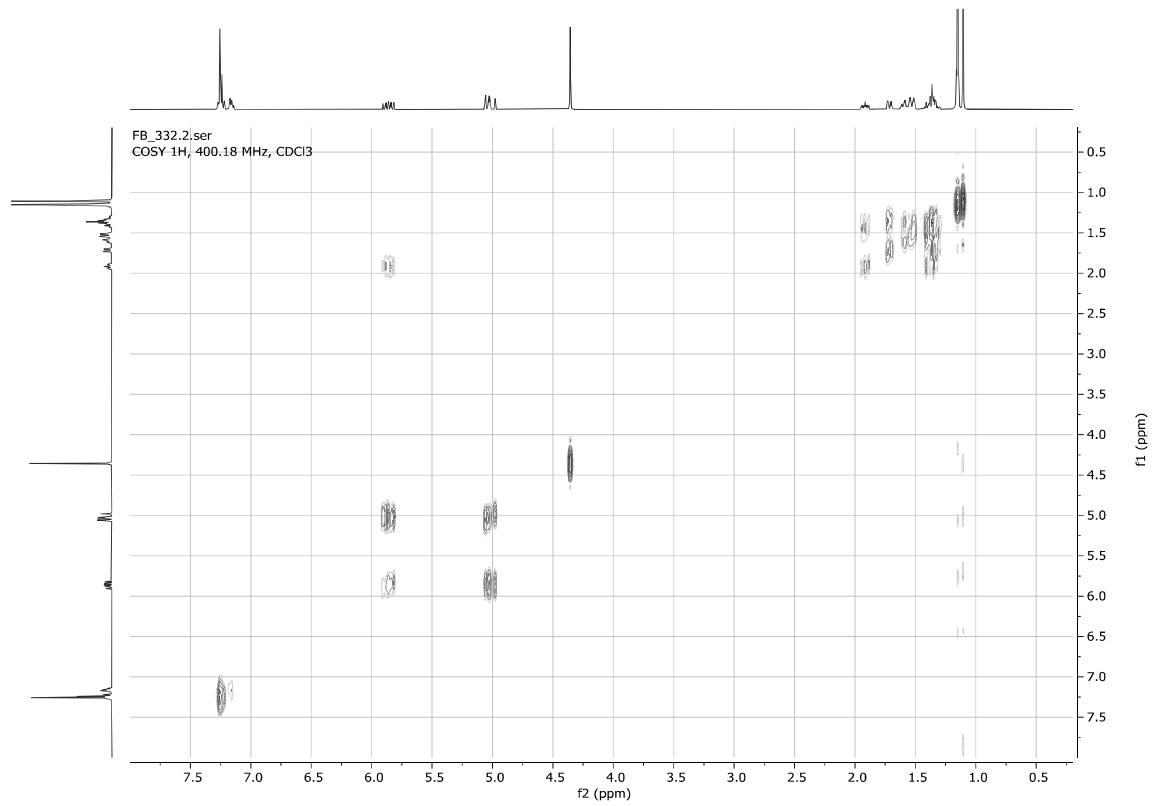
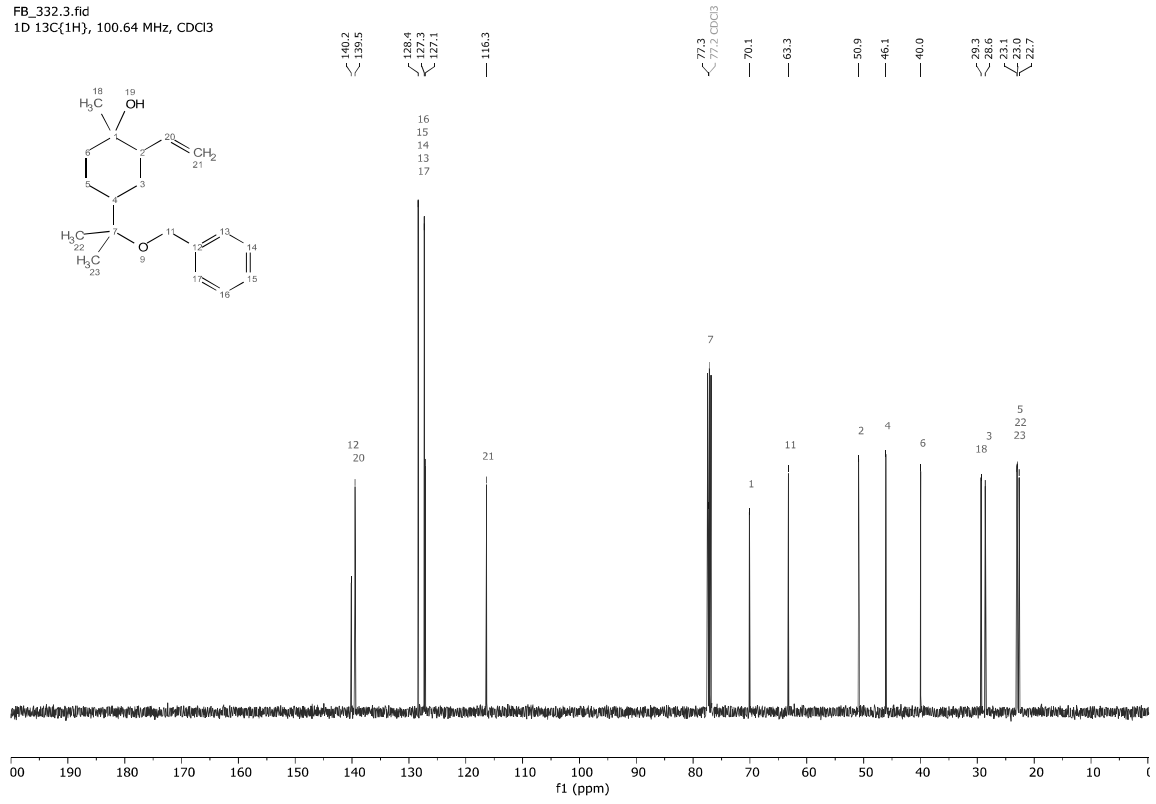


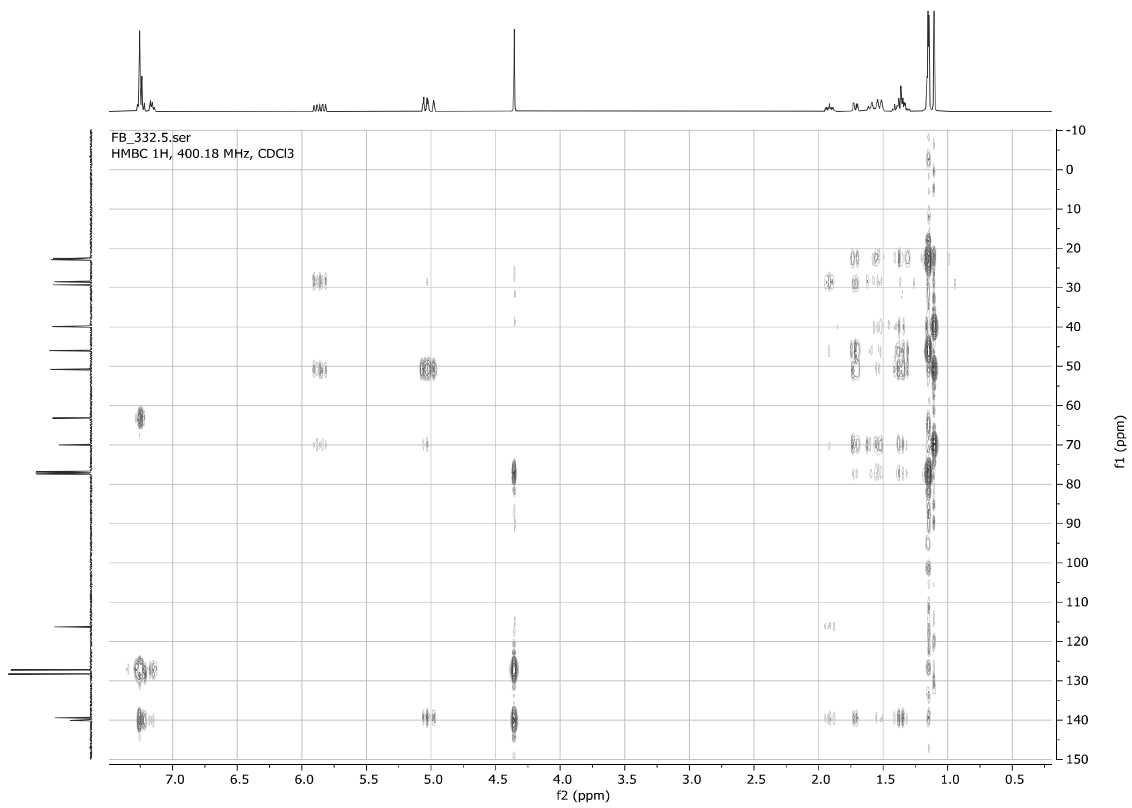
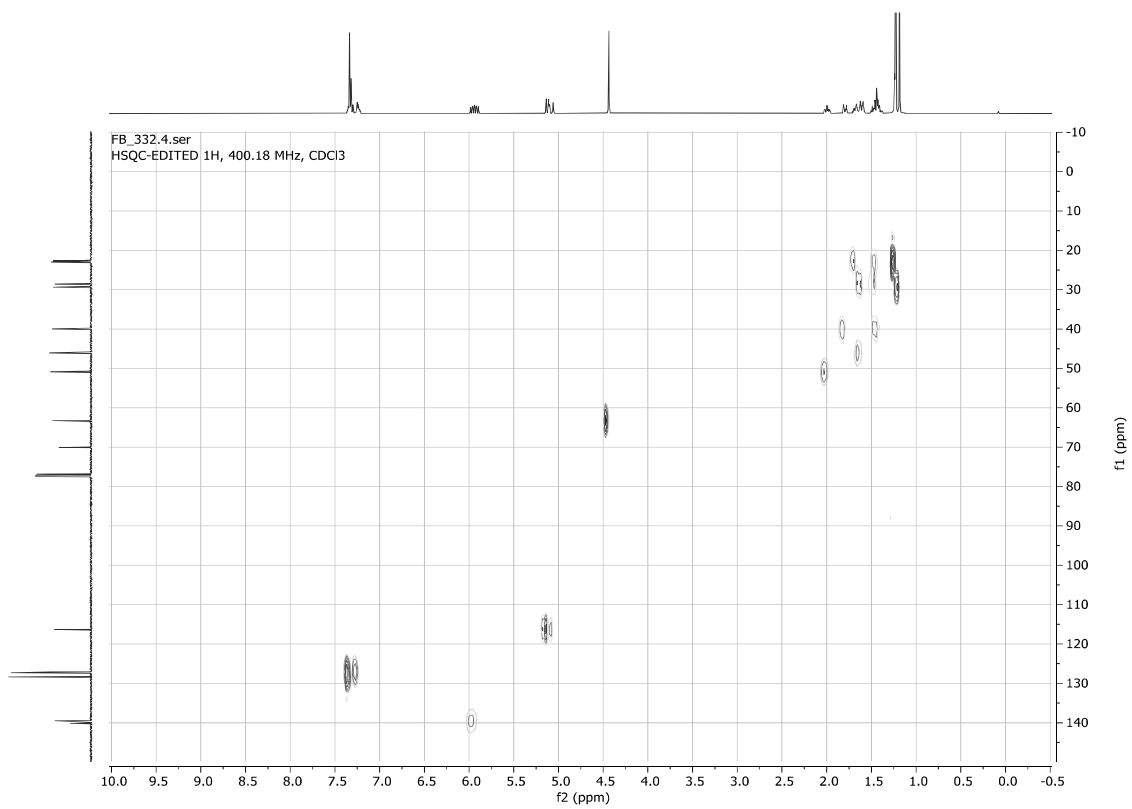


4-(2-Benzyloxy)propan-2-yl)-1-methyl-2-vinylcyclohexan-1-ol **6e**



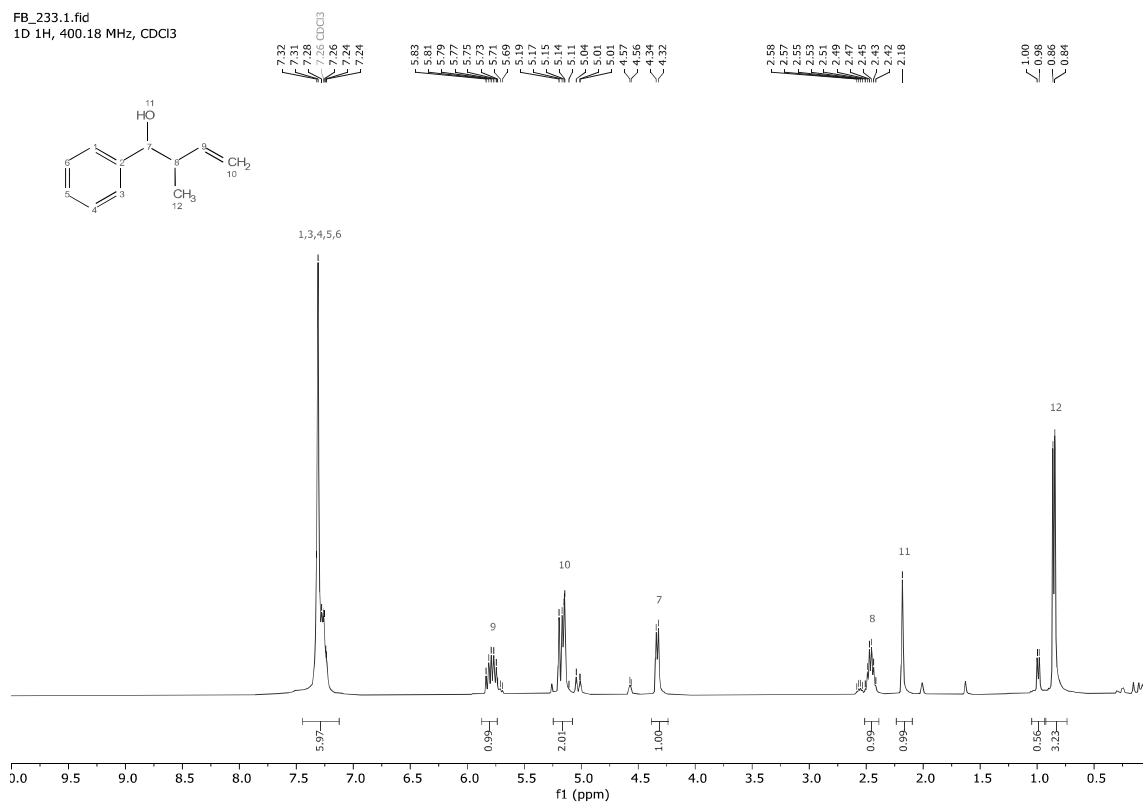
FB_332.3.fid
1D 13C{1H}, 100.64 MHz, CDCl3



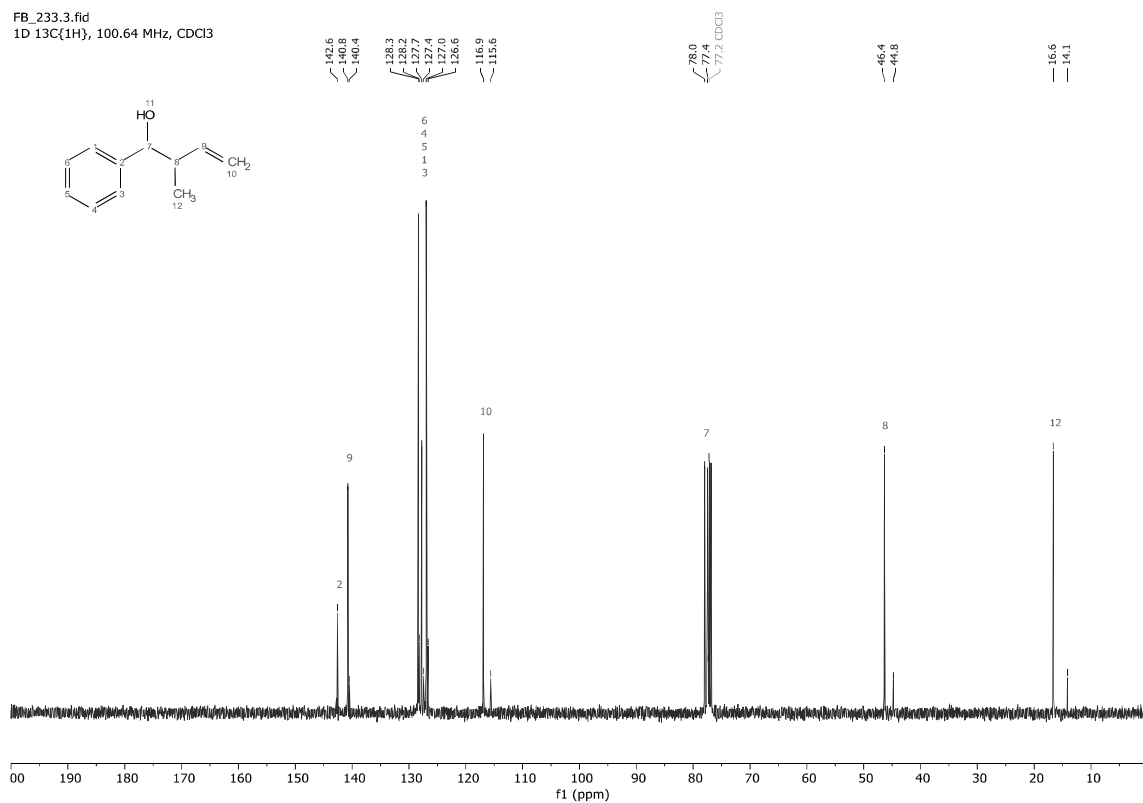


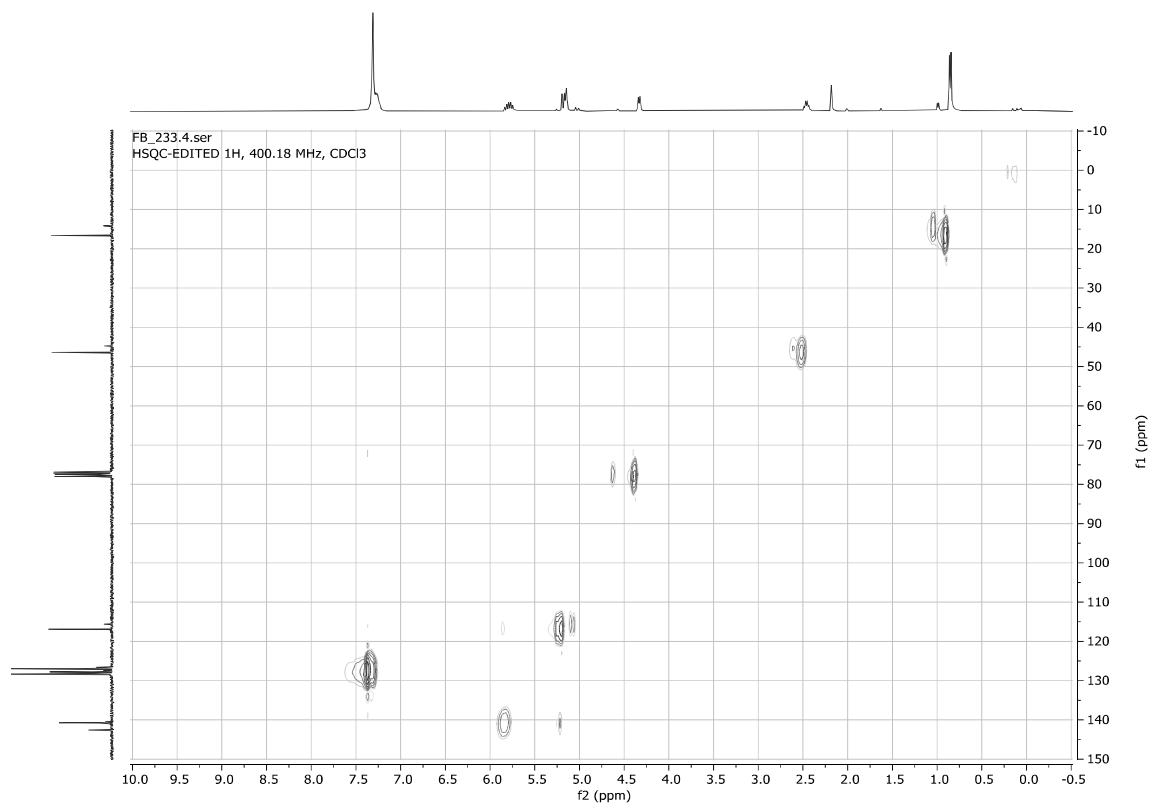
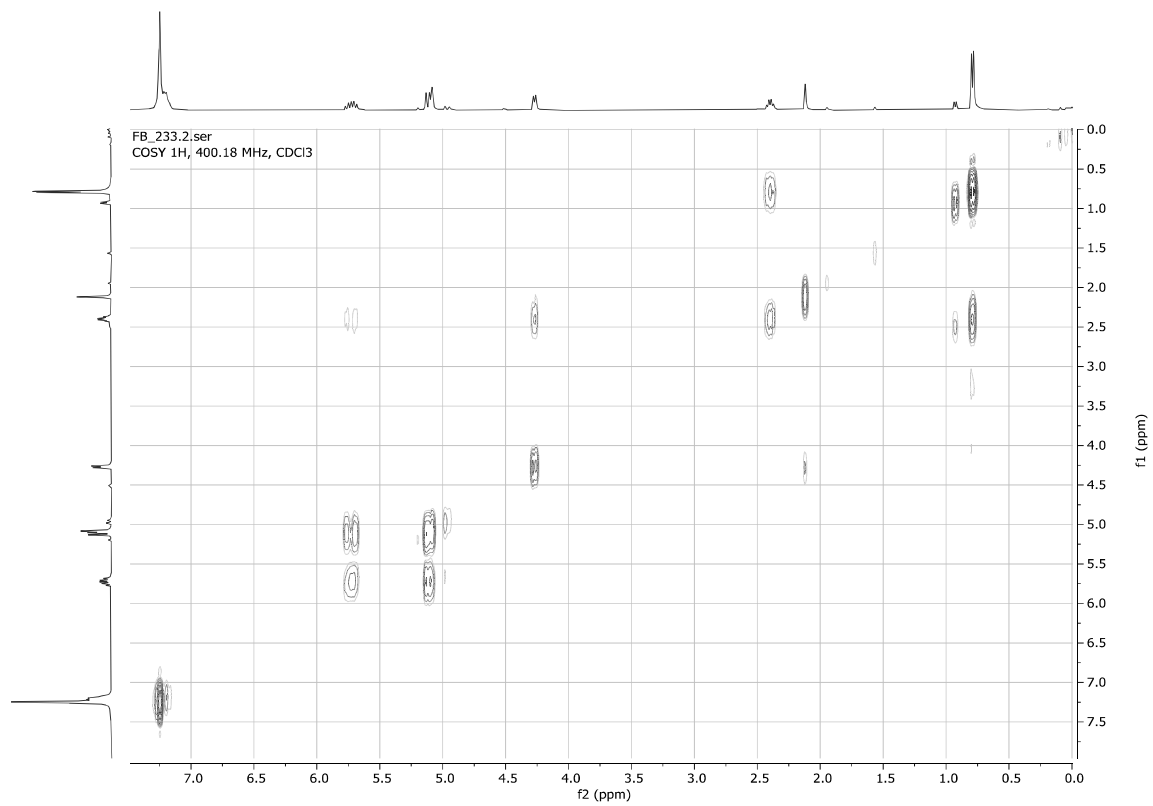
2-Methyl-1-phenylbut-3-en-1-ol **6f** (*inseparable 85:15 diastereomers mixture*)

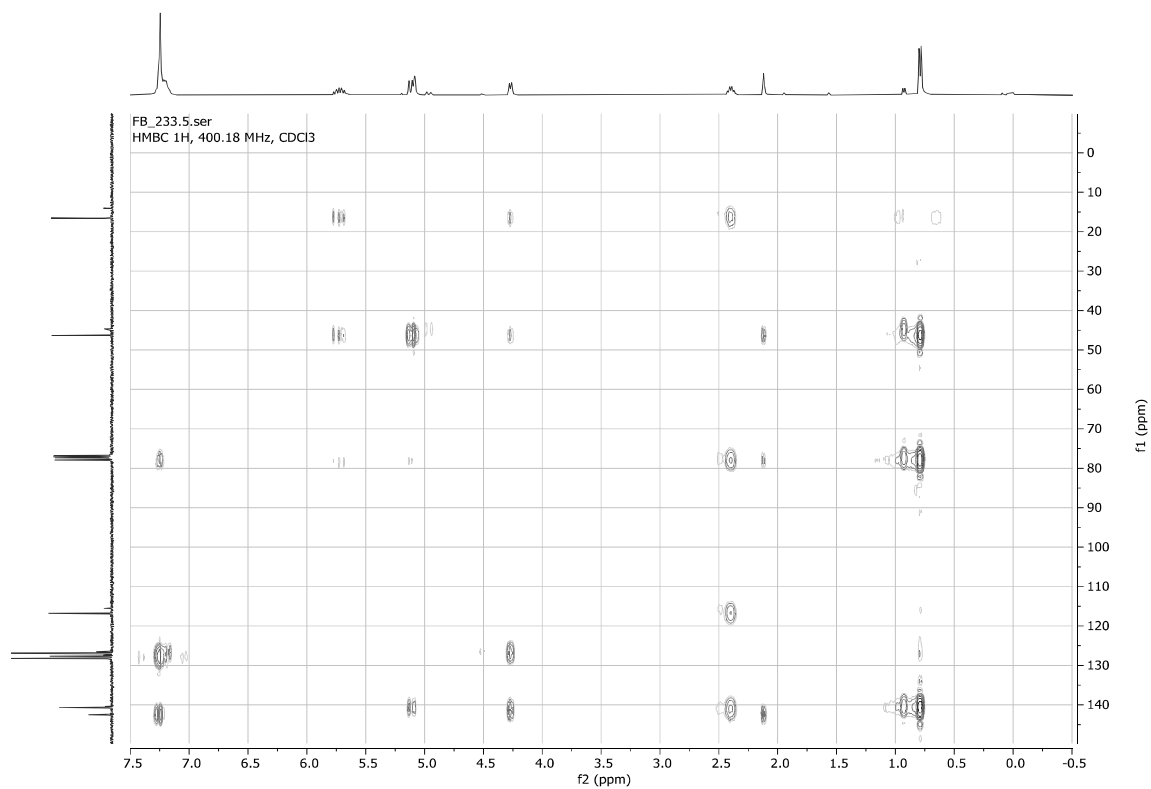
FB_233.1.fid
1D 1H, 400.18 MHz, CDCl3



FB_233.3.fid
1D 13C{1H}, 100.64 MHz, CDCl3

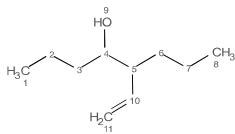
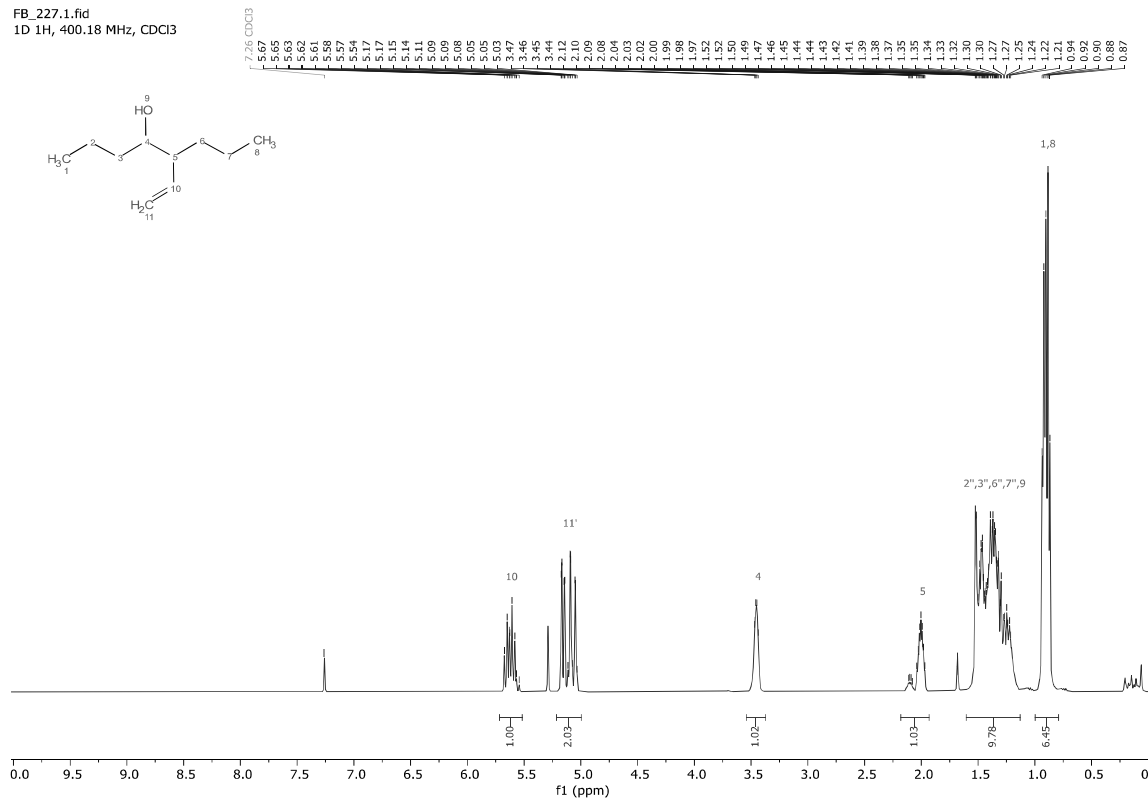




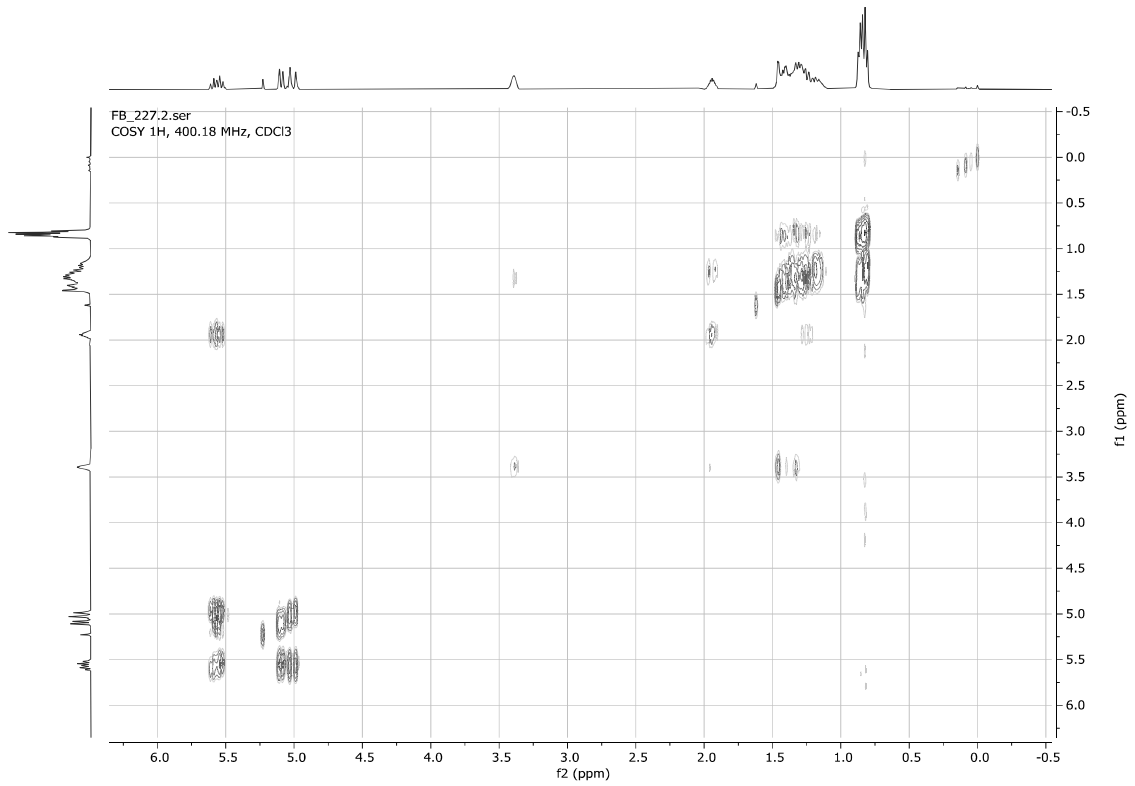
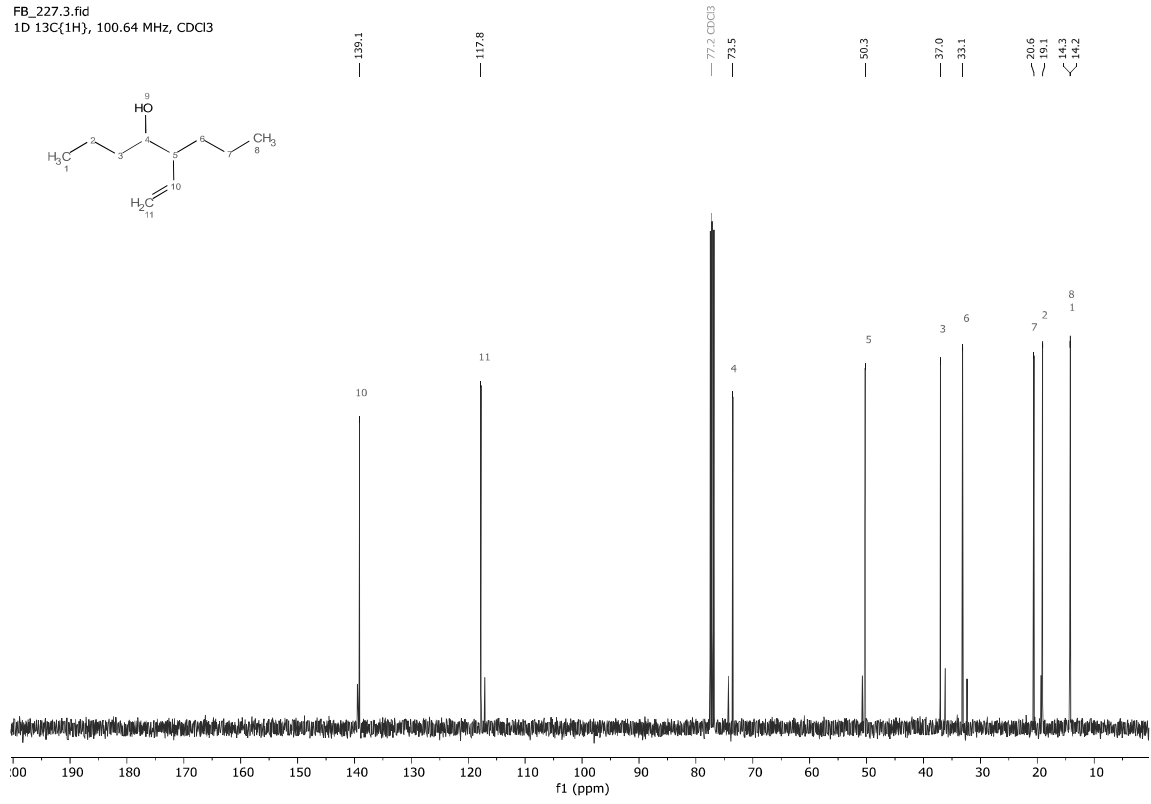


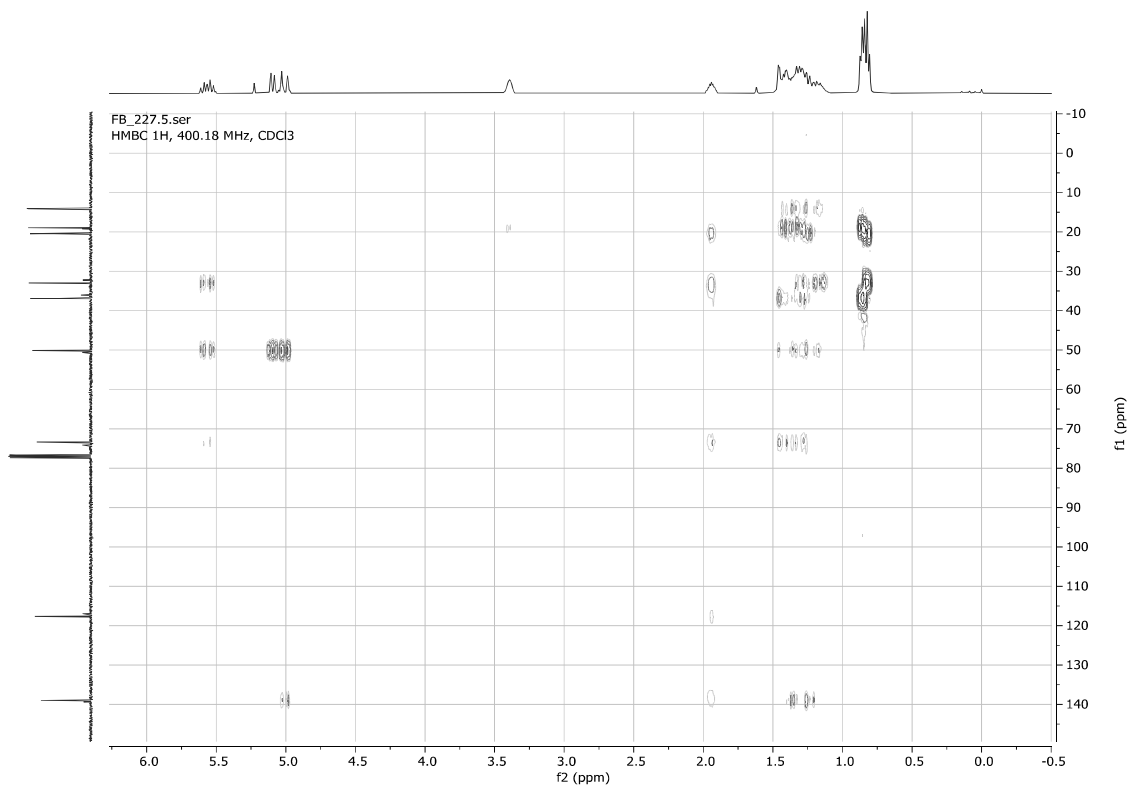
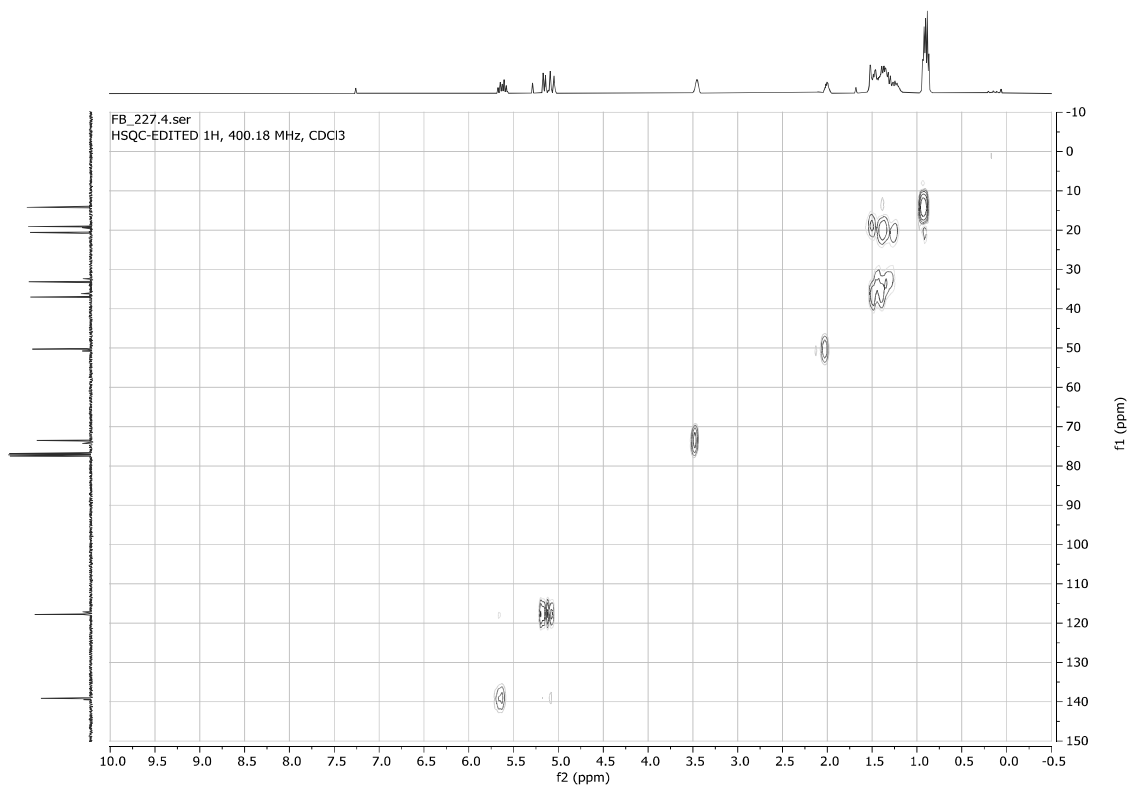
5-Vinyloctan-4-ol **6g** (*inseparable 86:14 diastereomers mixture*)

FB_227.1.fid
1D 1H, 400.18 MHz, CDCl3



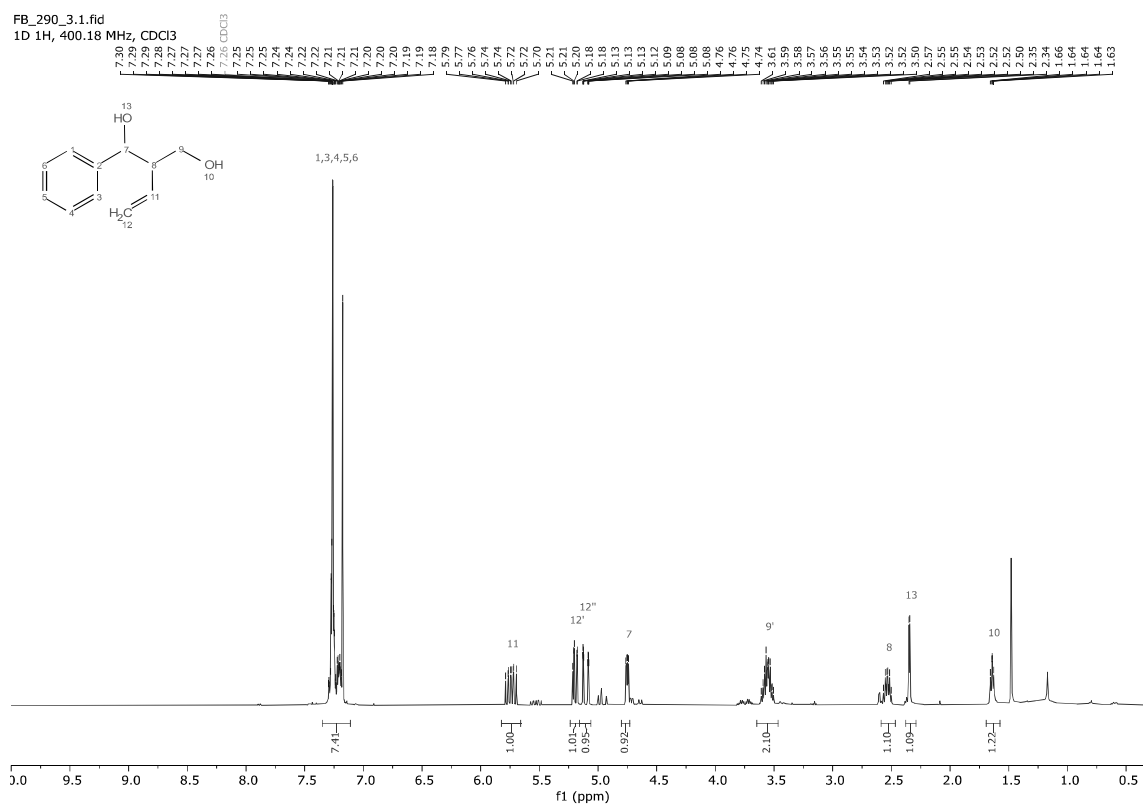
FB_227.3.fid
1D 13C{1H}, 100.64 MHz, CDCl3



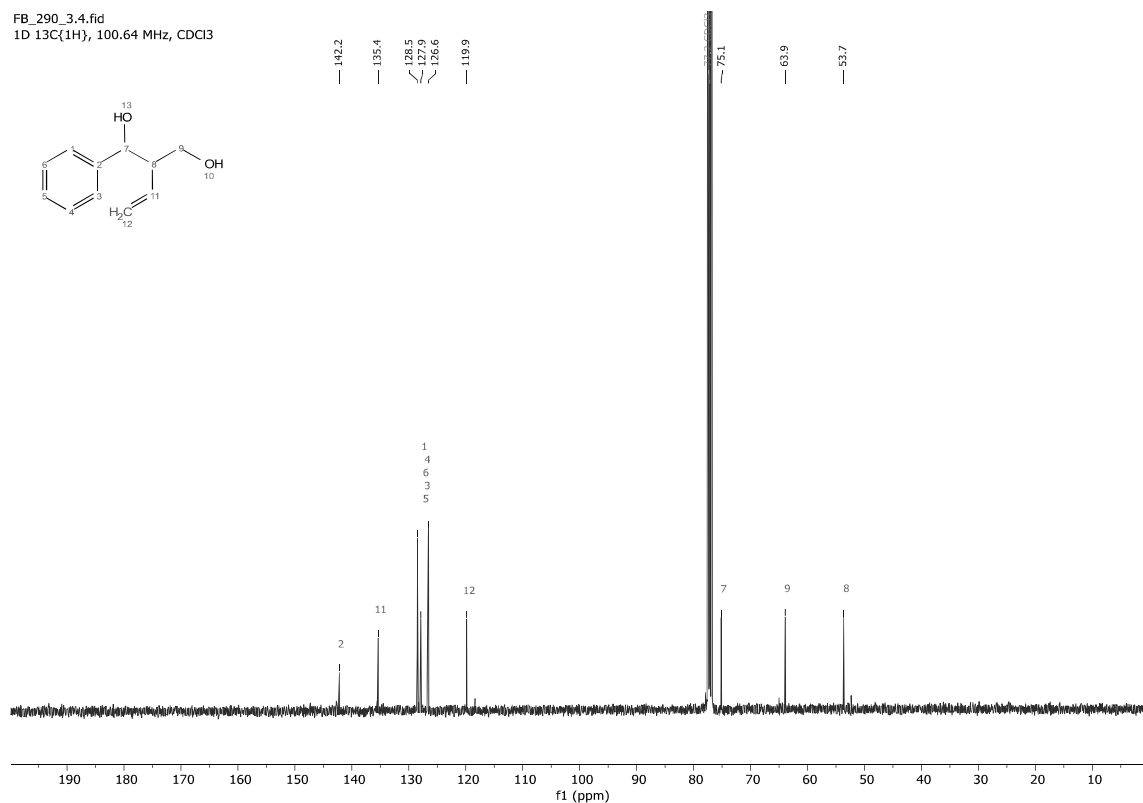


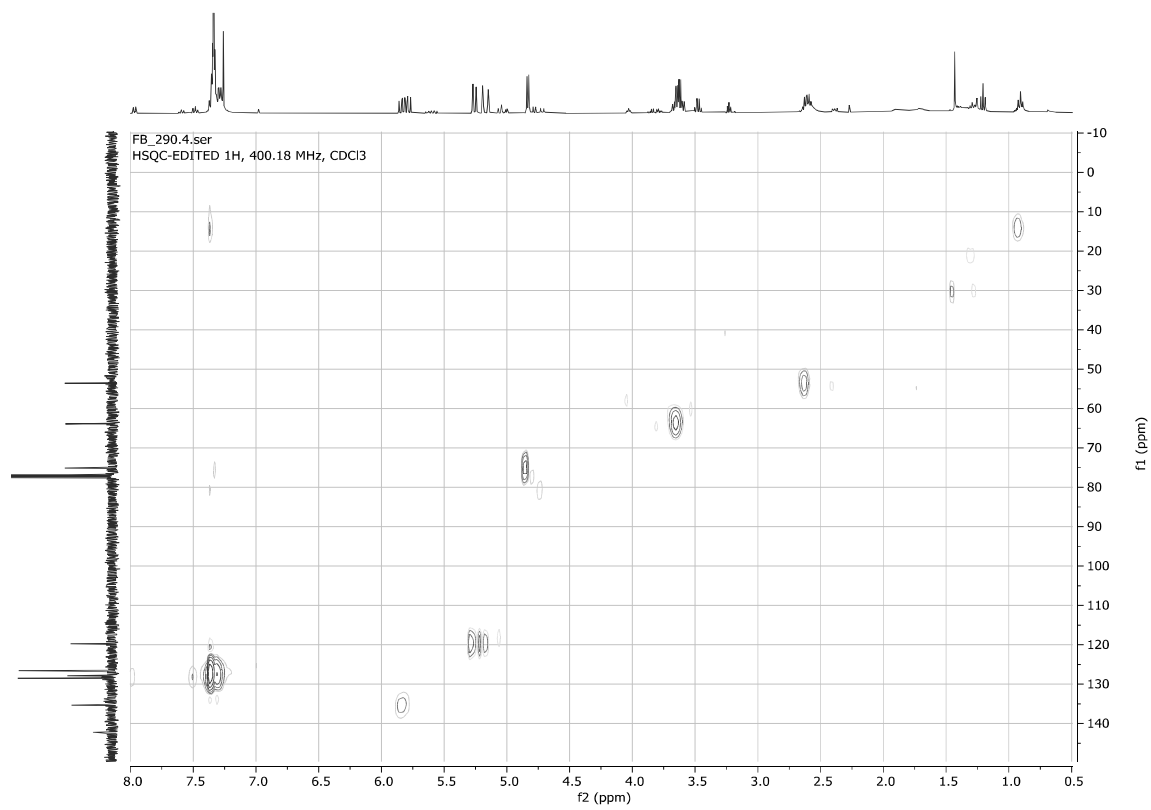
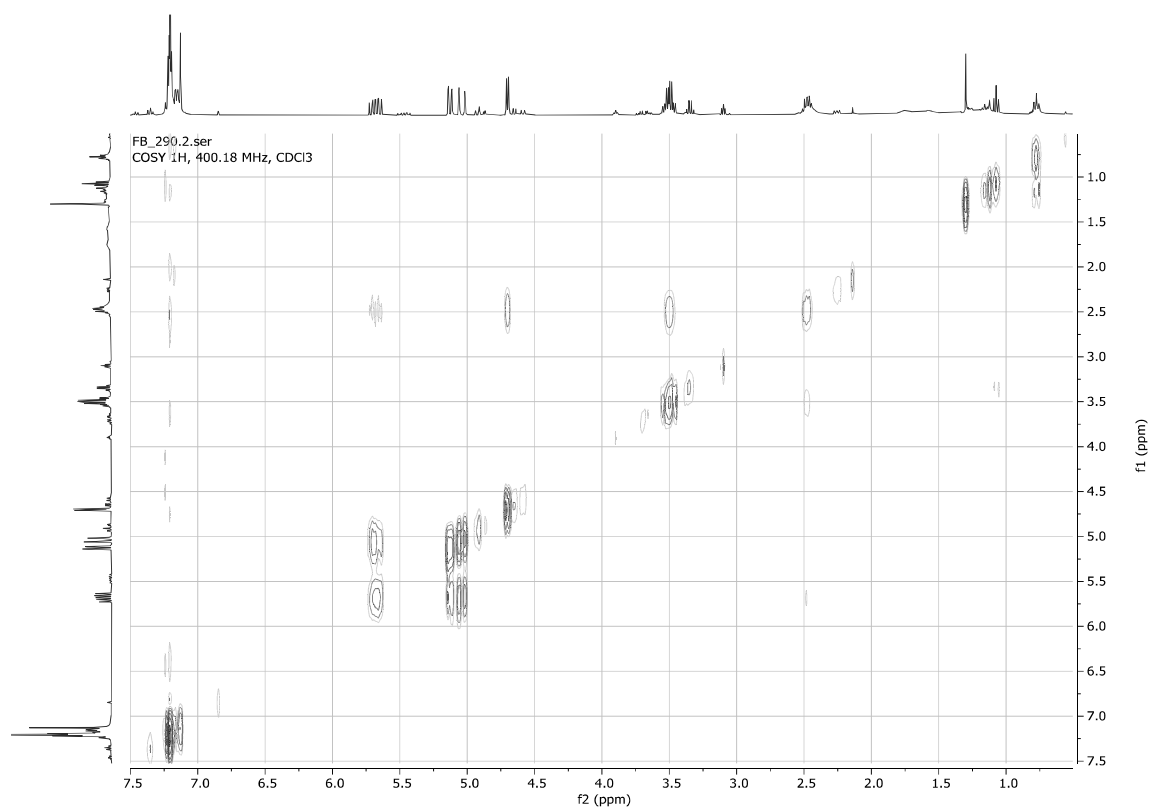
1-Phenyl-2-vinylpropane-1,3-diol **6h** (*inseparable 87:13 diastereomers mixture*)

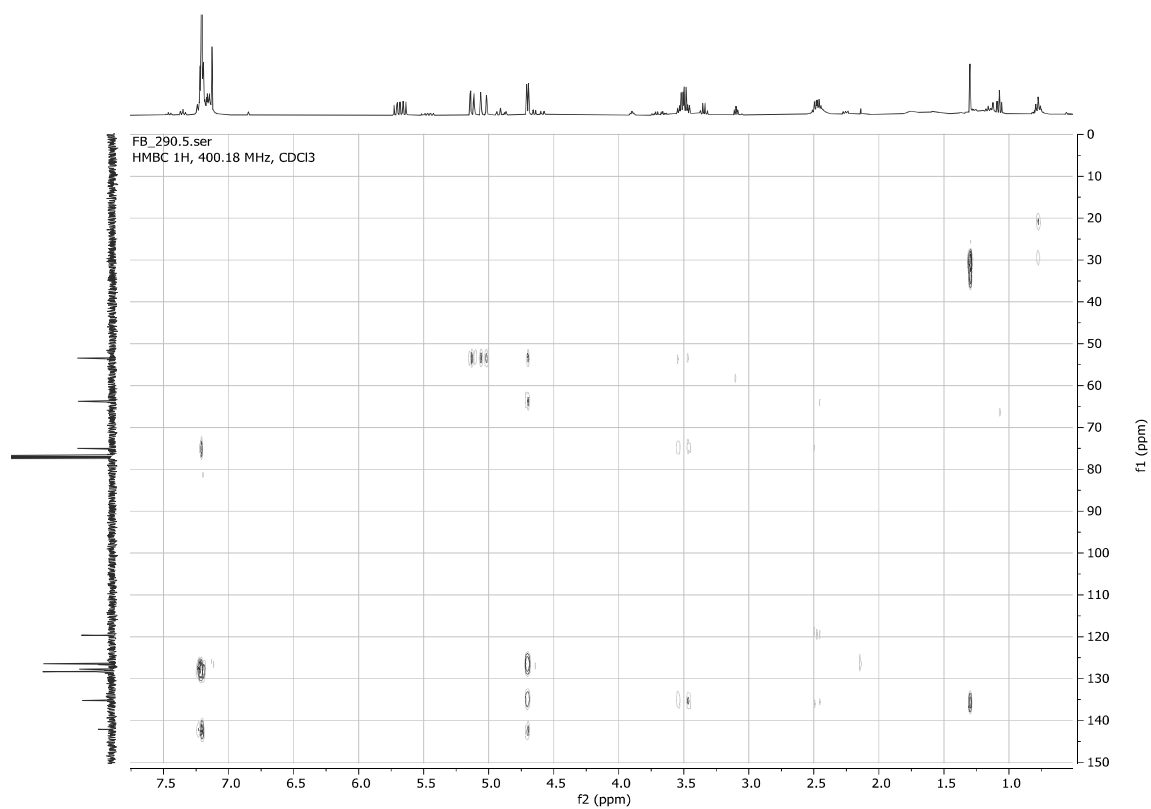
FB_290_3.1.fid
1D 1H, 400.18 MHz, CDCl3



FB_290_3.4.fid
1D 13C{1H}, 100.64 MHz, CDCl3



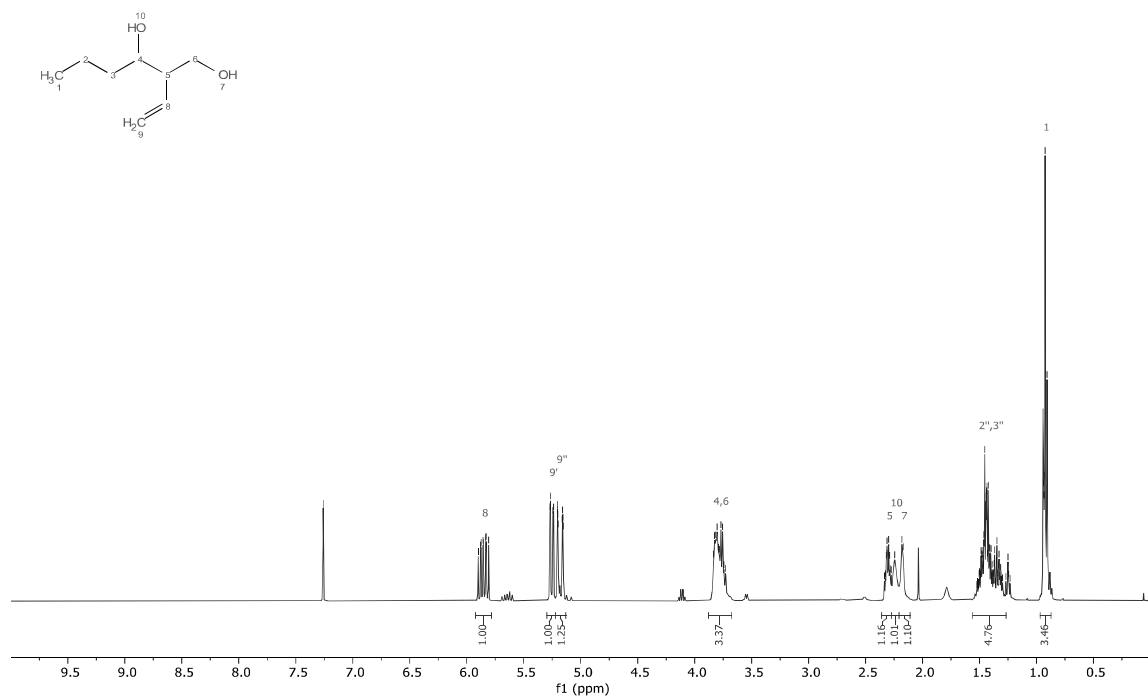




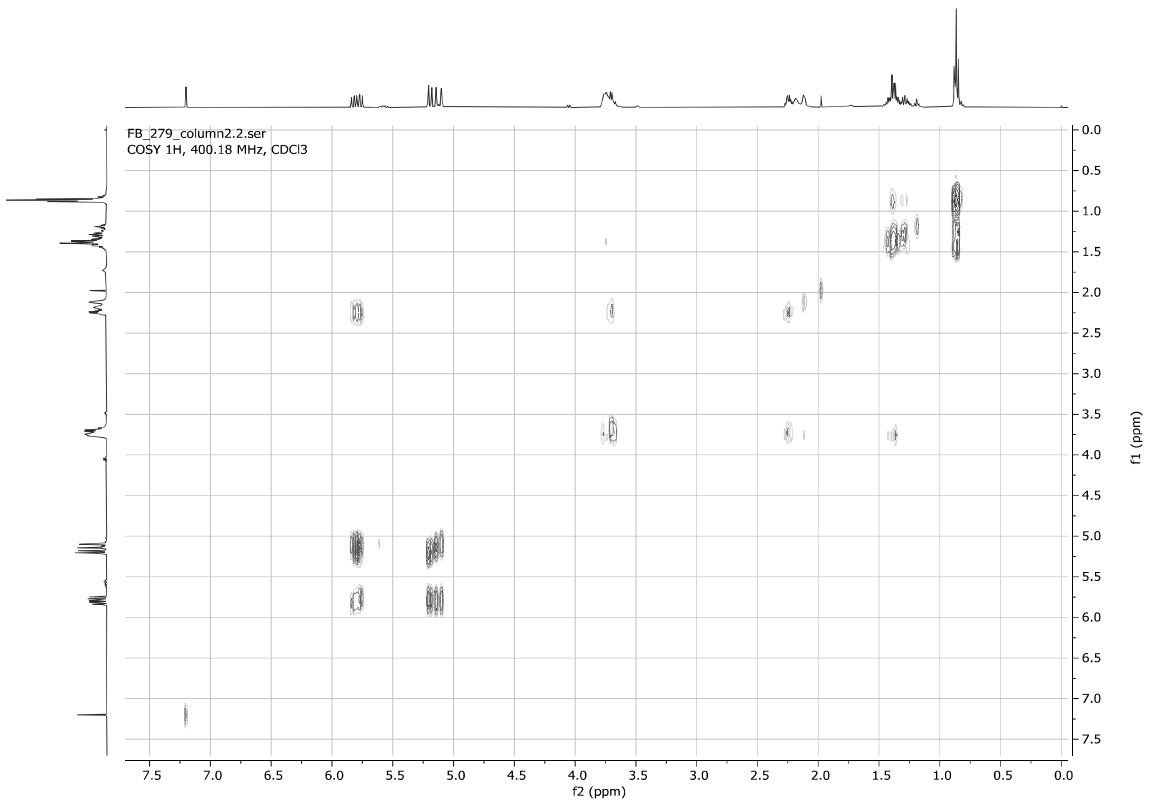
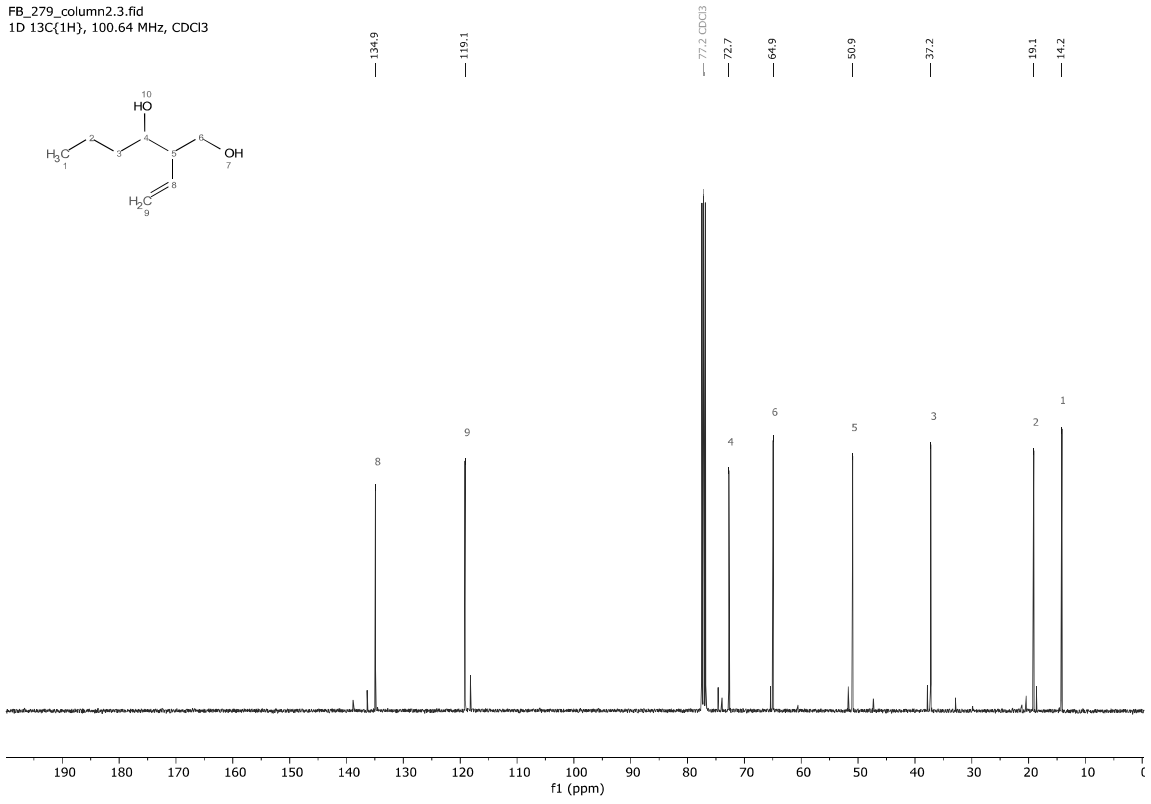
2-Vinylhexan-1,3-diol **6i** (inseparable 88:12 diastereomers mixture)

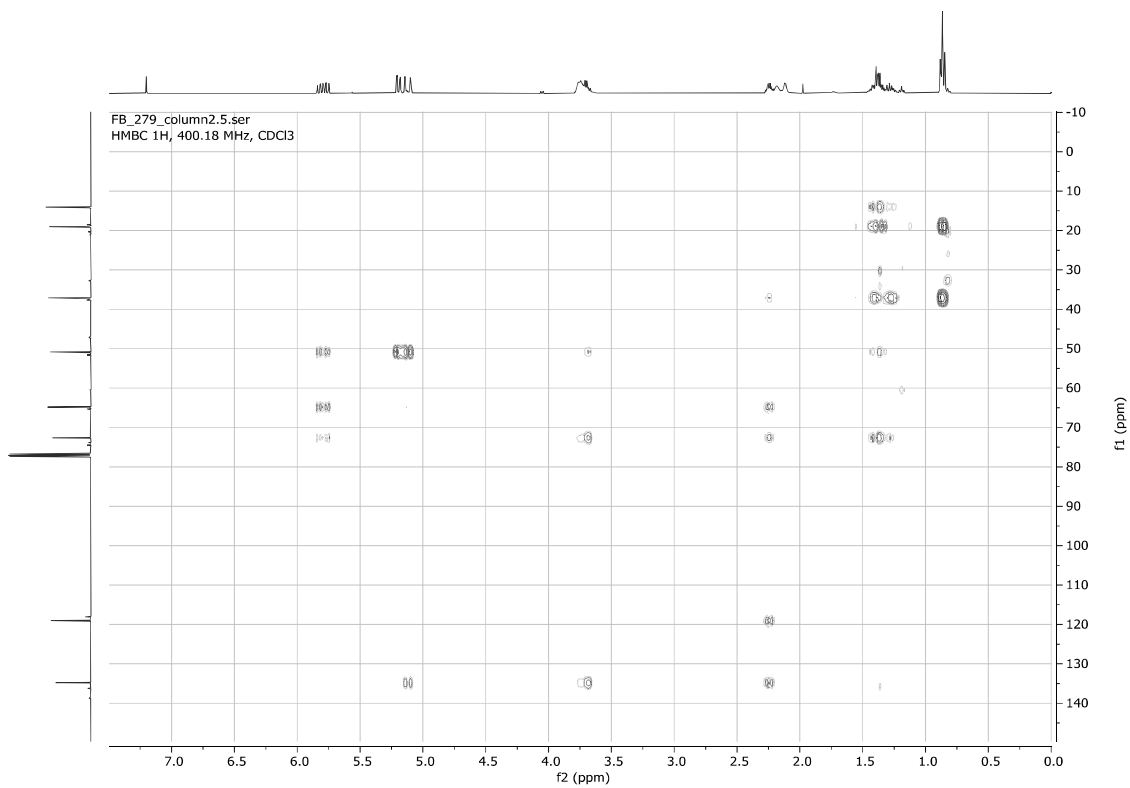
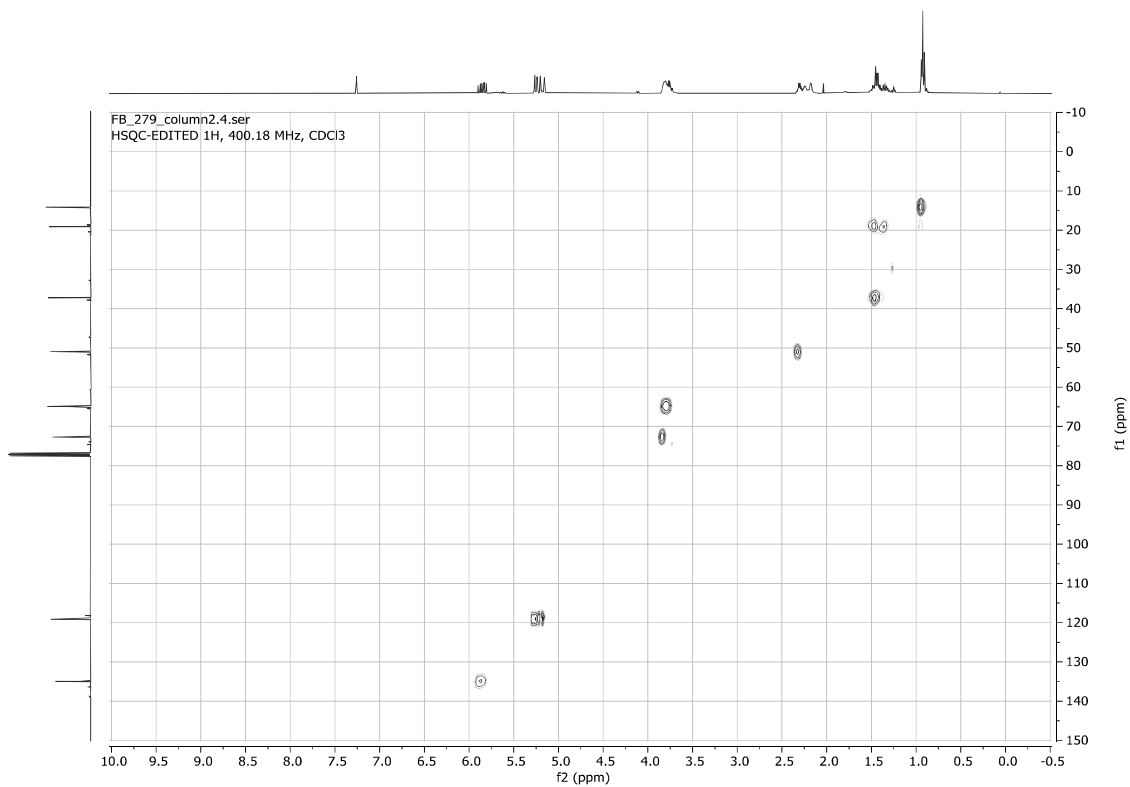
FB_279_column2.1.fid
1D 1H, 400.18 MHz, CDCl3

7.26	5.90	5.88	5.87	5.86	5.83	5.81	5.27	5.24	5.20	5.20	5.16	5.16	5.15	3.82	3.82	3.80	3.79	3.78	3.75	3.74	3.73	2.33	2.32	2.31	2.30	2.30	2.28	2.27	2.24	2.18	2.17	1.50	1.50	1.49	1.49	1.47	1.47	1.46	1.45	1.44	1.44	1.43	1.42	1.41	1.40	1.40	1.39	1.38	1.38	1.37	1.37	1.35	1.34	1.33	1.32	1.31	1.25	1.24	0.94	0.94	0.93	0.93	0.91
------	------	------	------	------	------	------	------	------	------	------	------	------	------	------	------	------	------	------	------	------	------	------	------	------	------	------	------	------	------	------	------	------	------	------	------	------	------	------	------	------	------	------	------	------	------	------	------	------	------	------	------	------	------	------	------	------	------	------	------	------	------	------	------



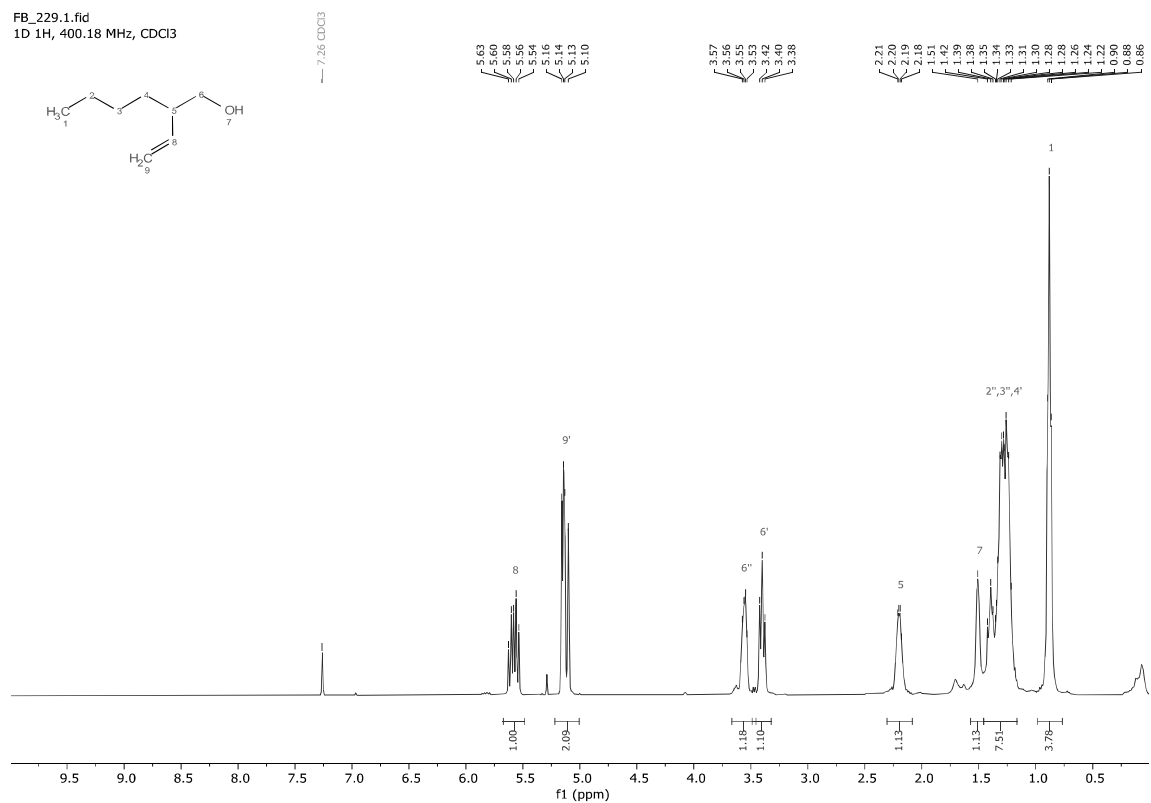
FB_279_column2.3.fid
1D 13C{1H}, 100.64 MHz, CDCl3



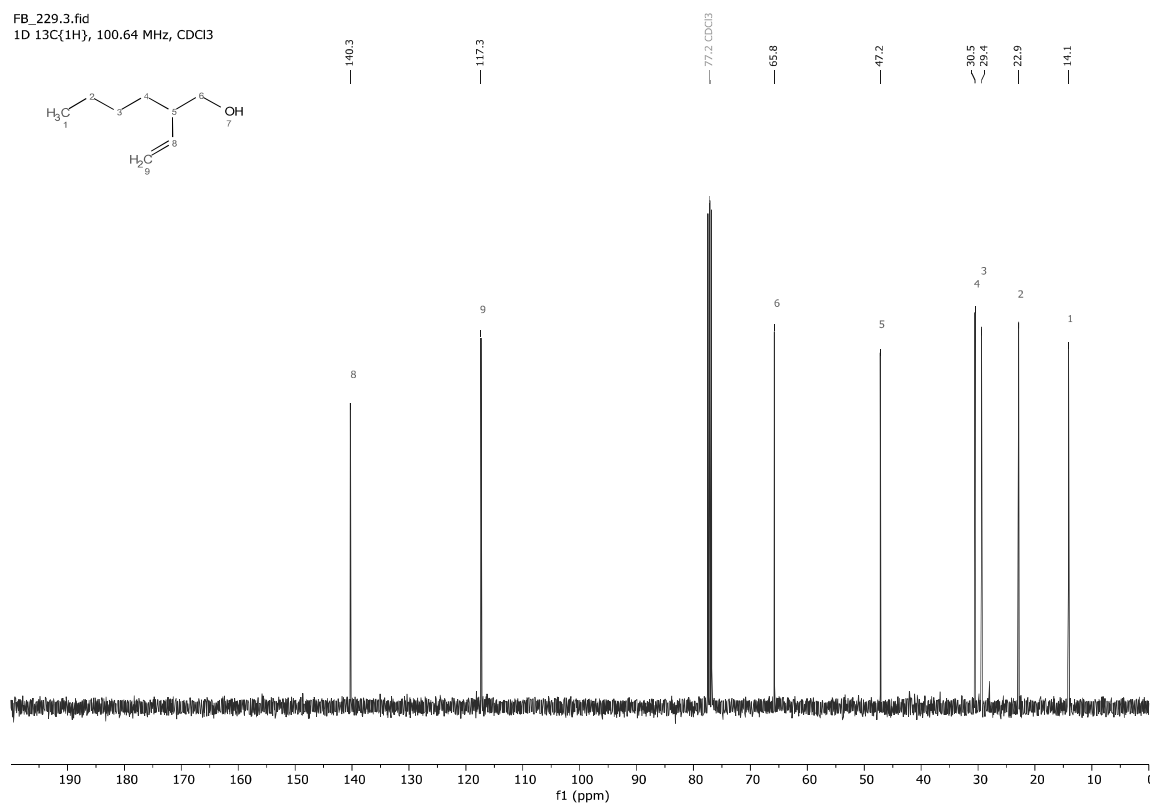


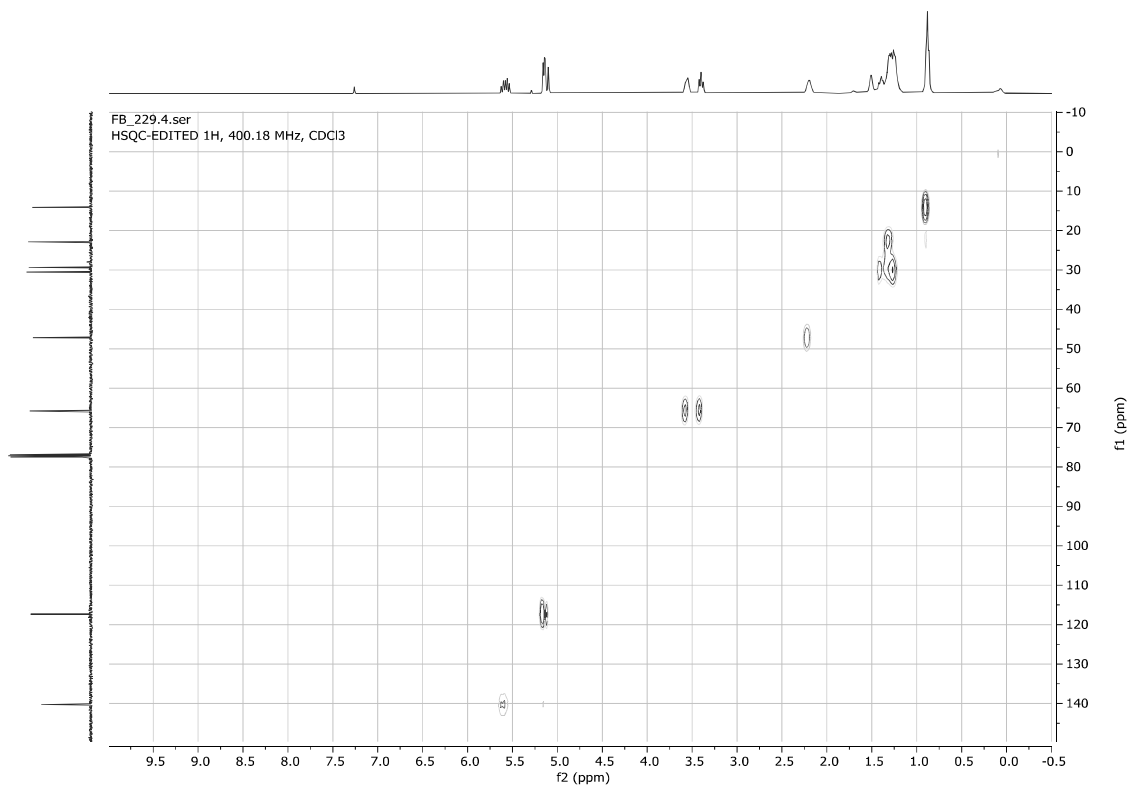
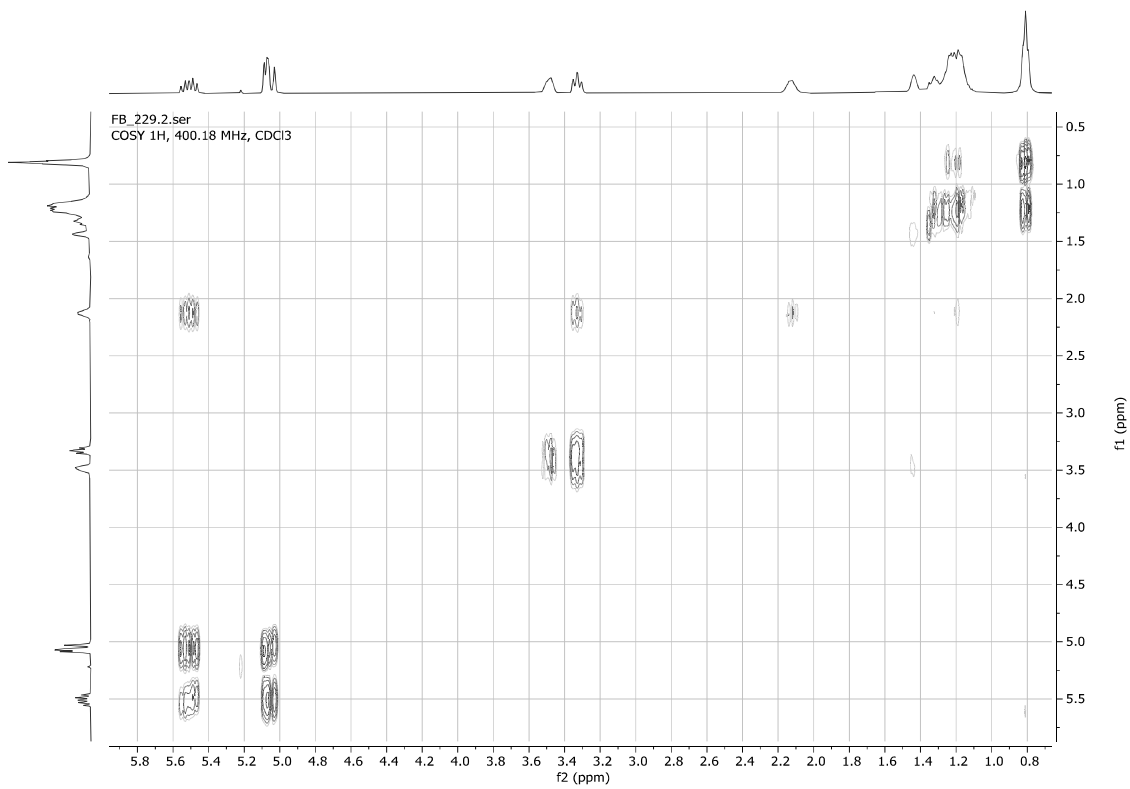
2-Vinylhexan-1-ol 6j

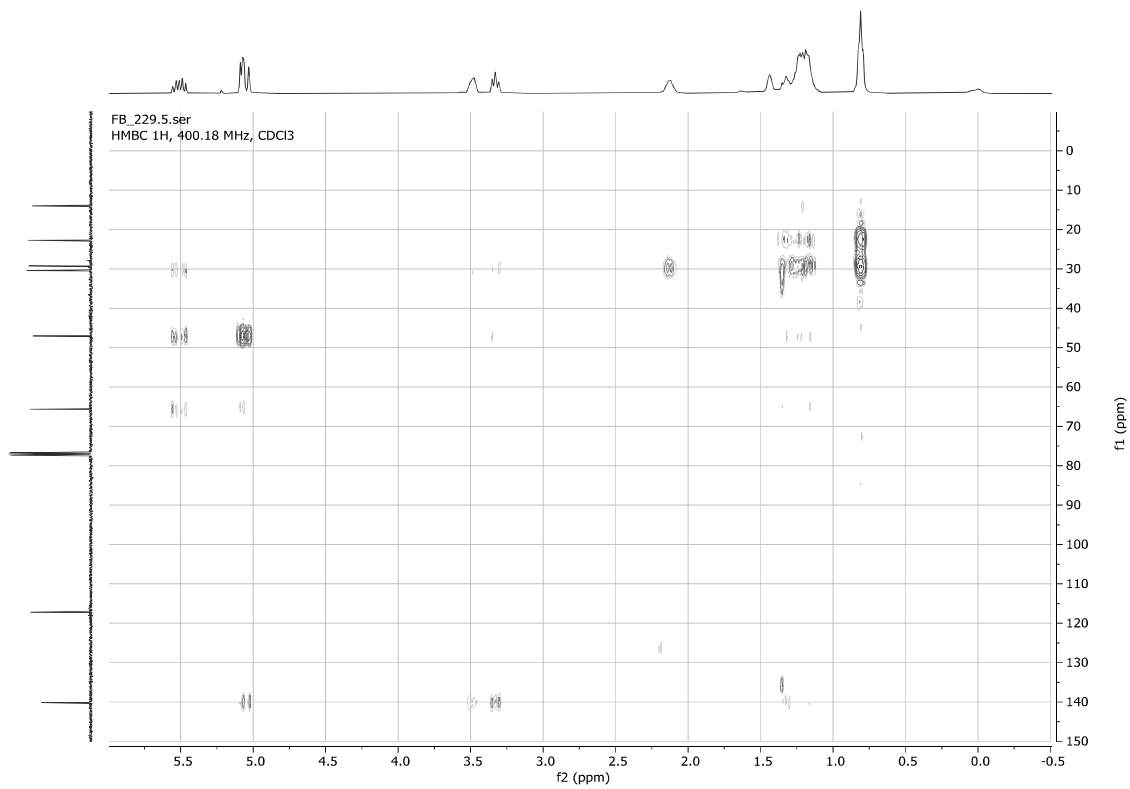
FB_229.1.fid
1D 1H, 400.18 MHz, CDCl3



FB_229.3.fid
1D 13C{1H}, 100.64 MHz, CDCl3

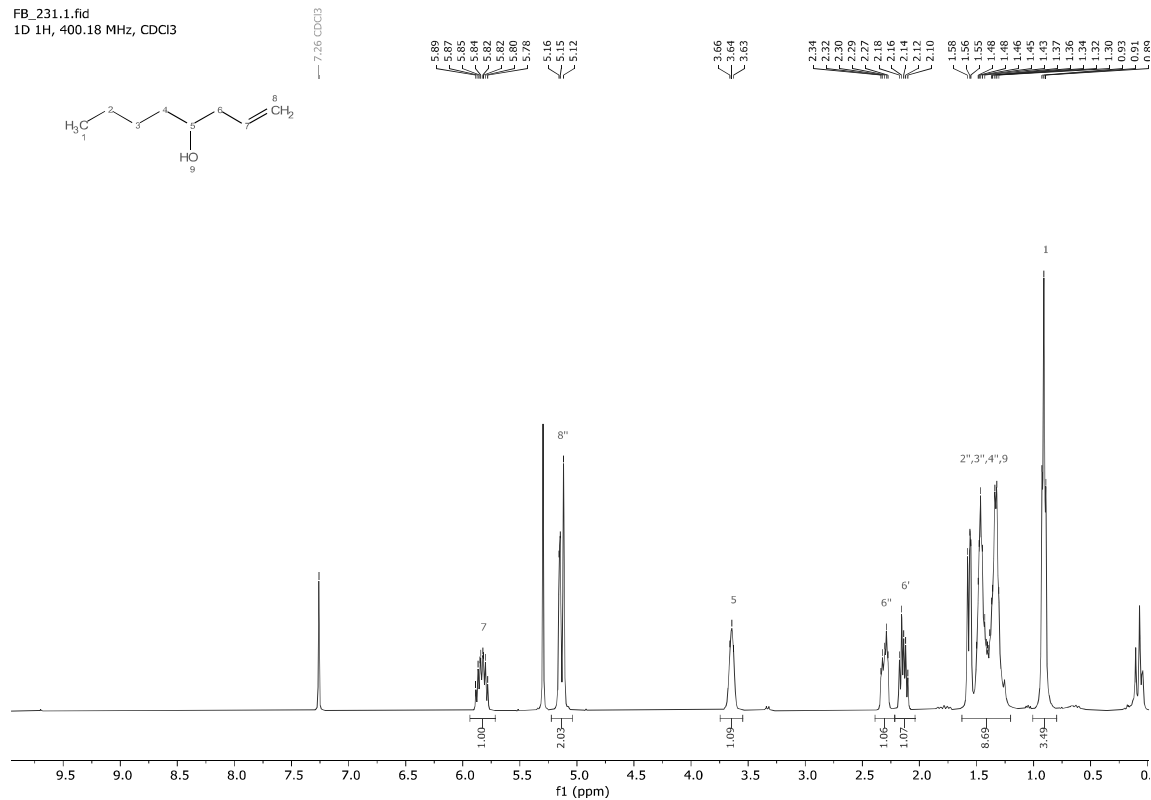




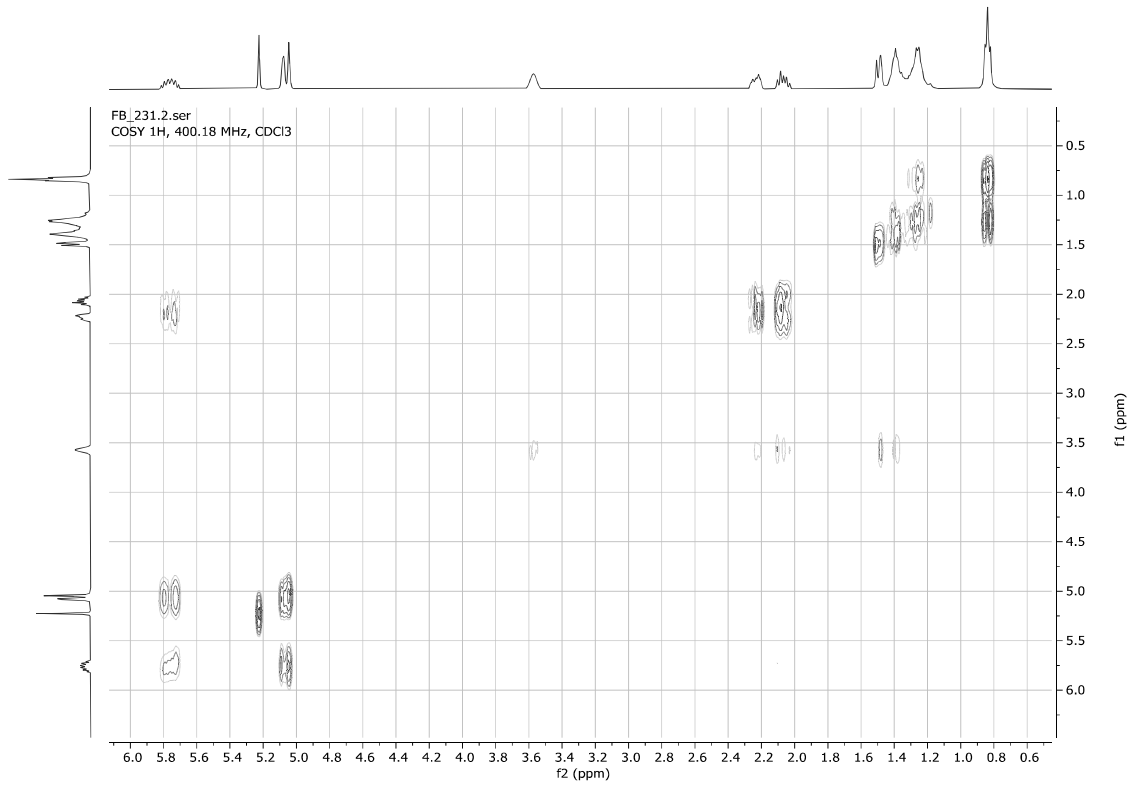
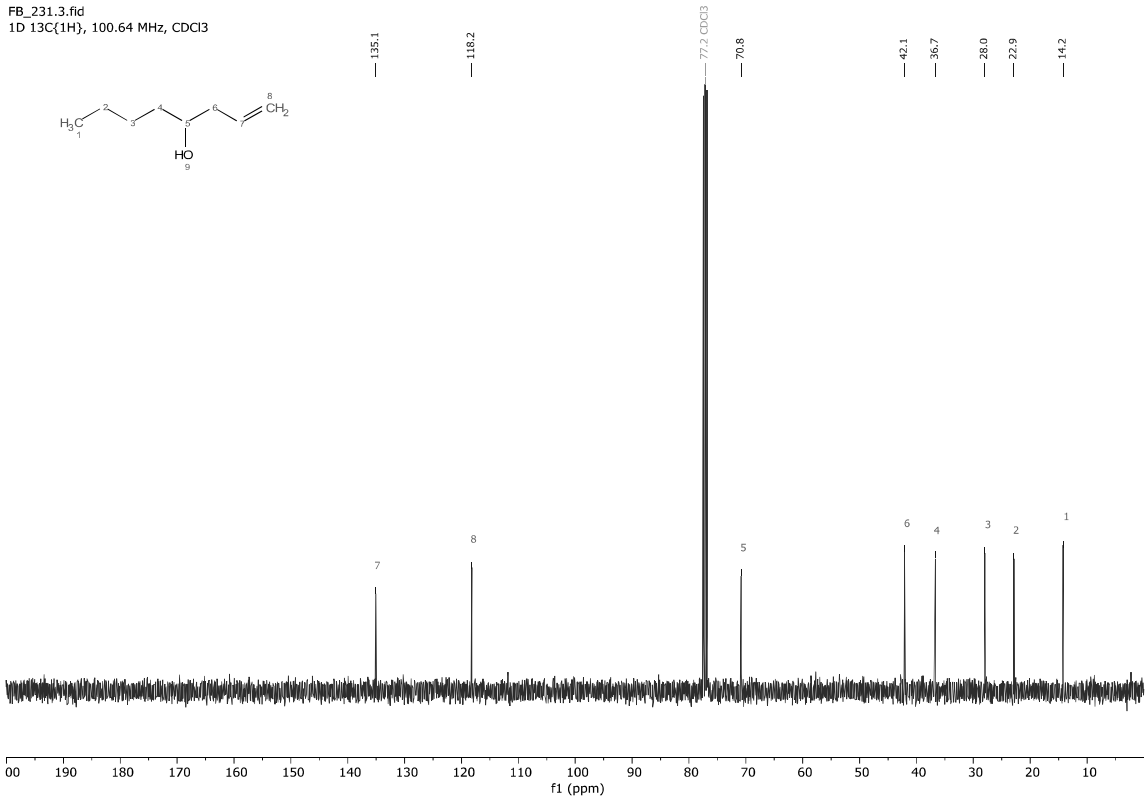


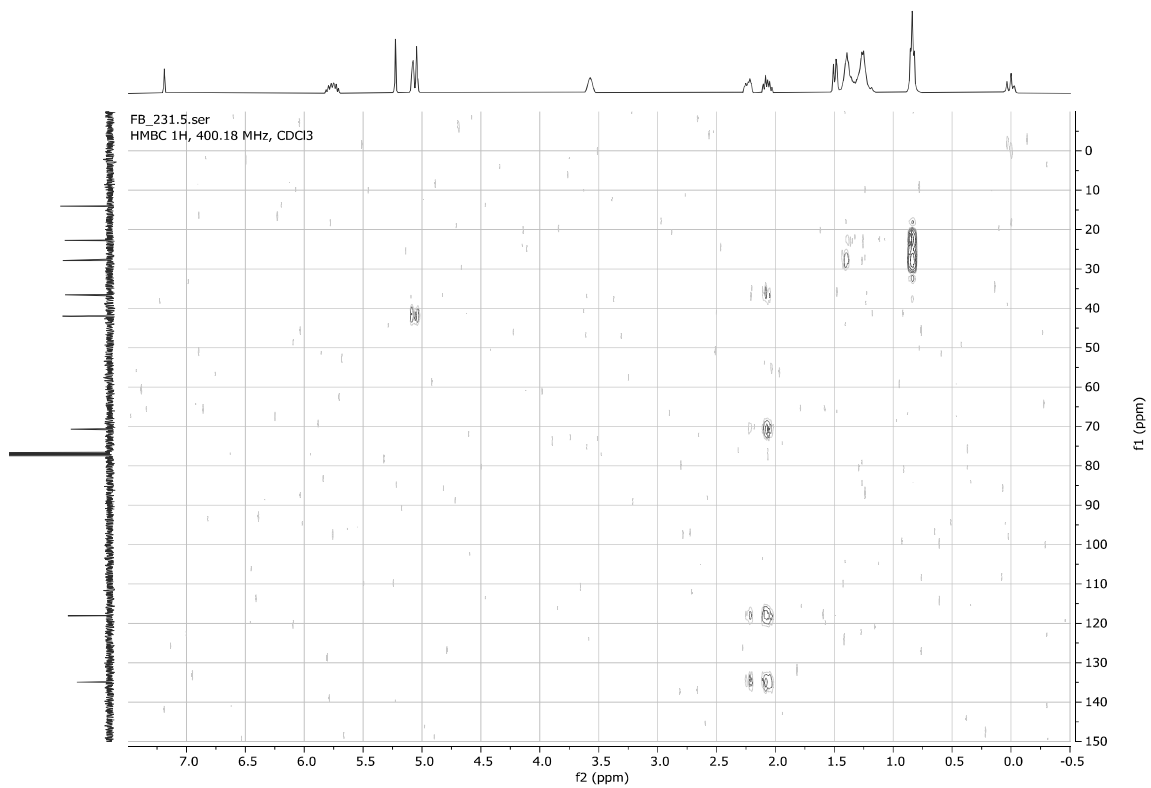
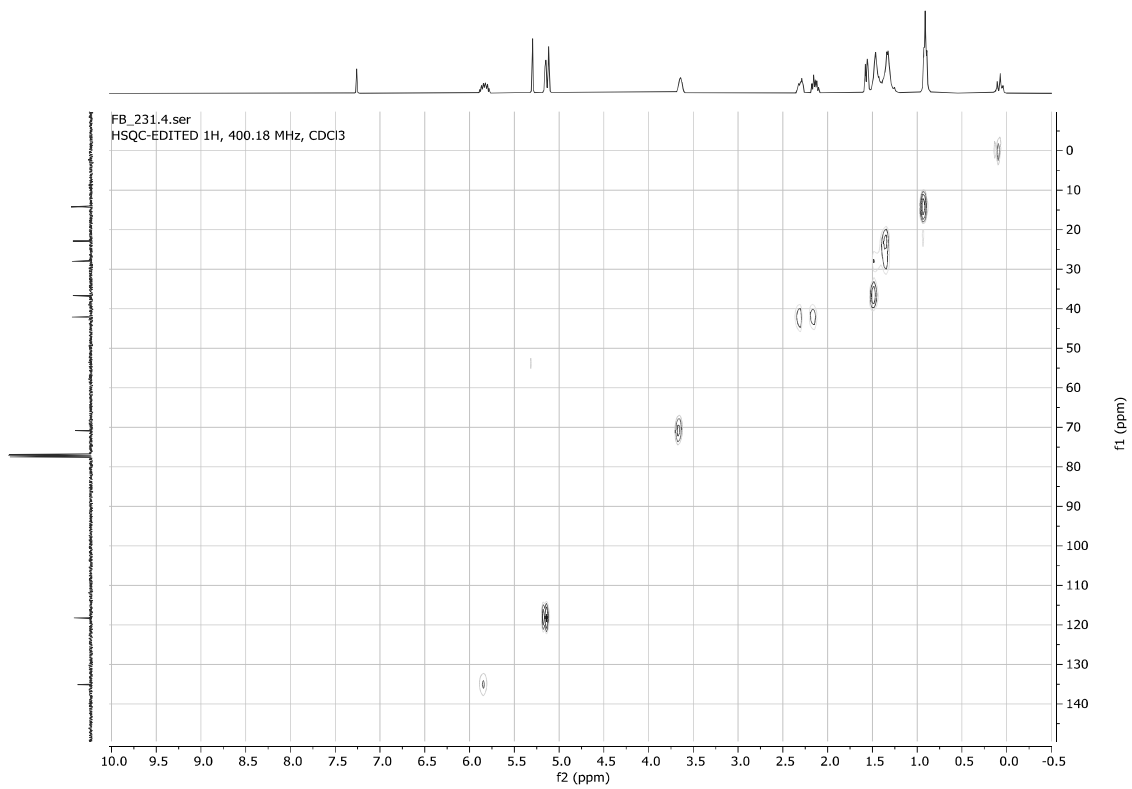
Oct-1-en-4-ol **6k**

FB_231.1.fid
1D 1H, 400.18 MHz, CDCl3



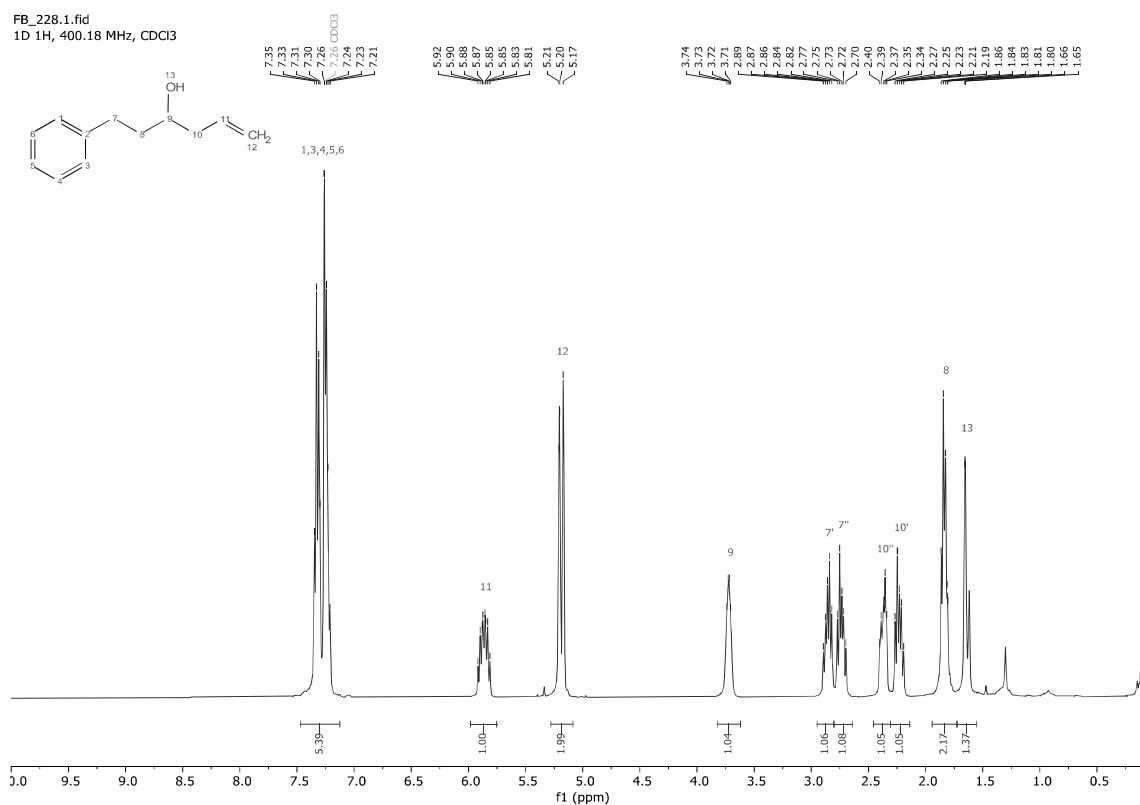
FB_231.3.fid
1D 13C{1H}, 100.64 MHz, CDCl3



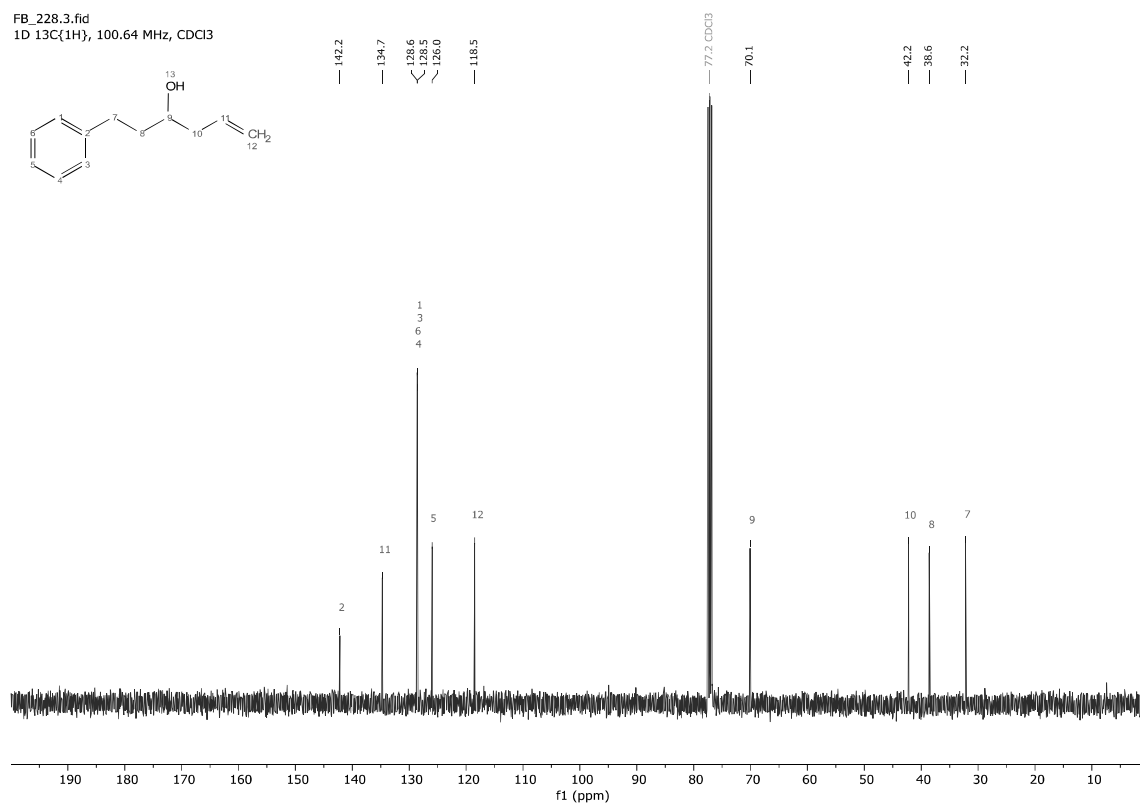


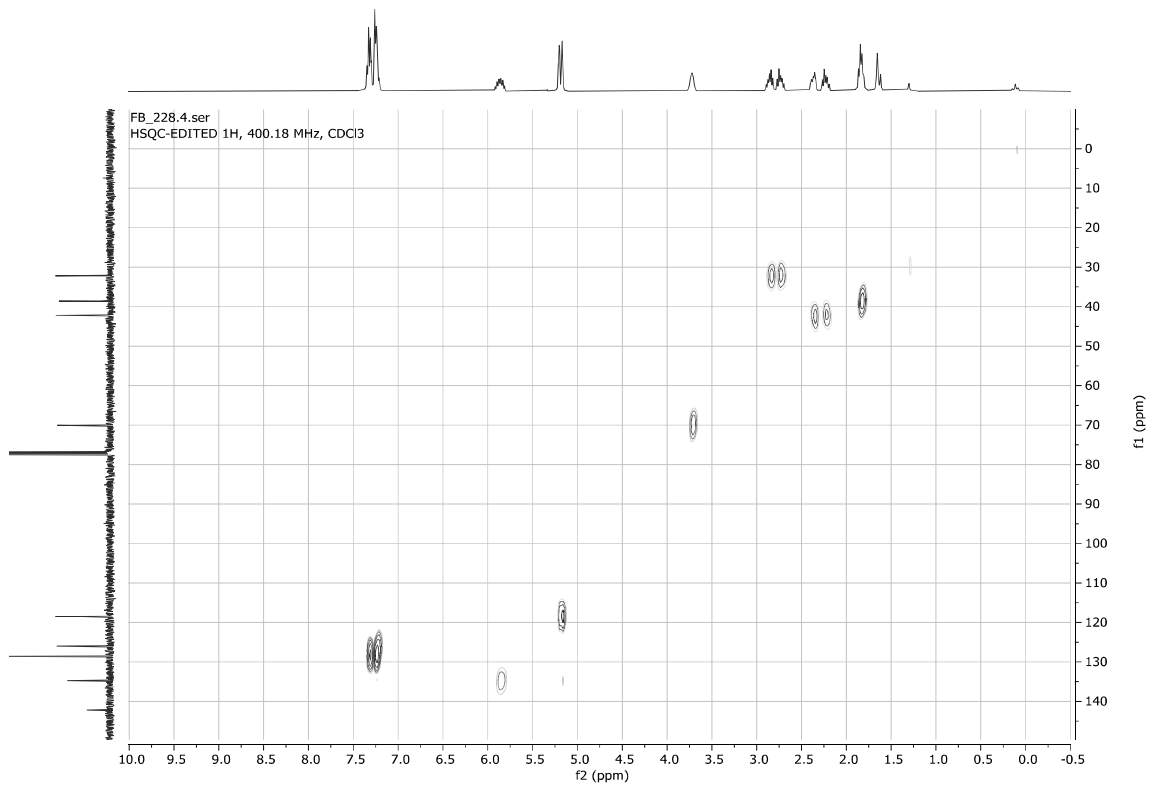
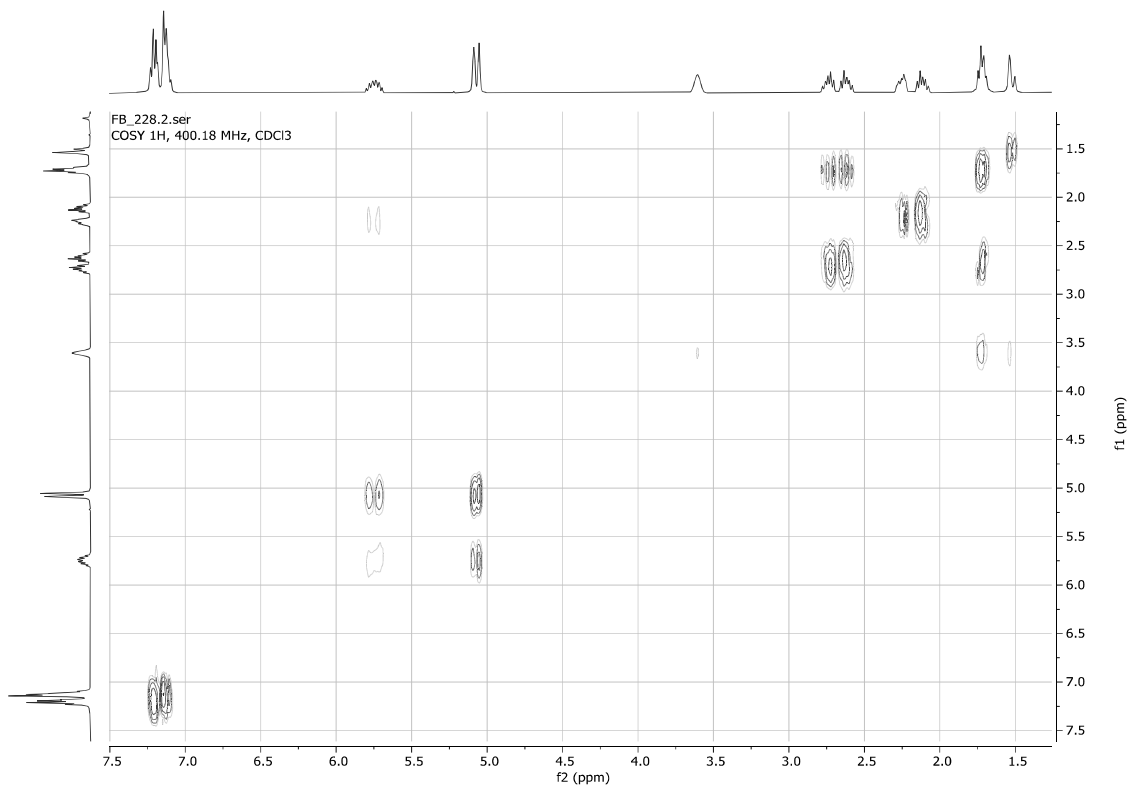
1-Phenylhex-5-en-3-ol **6l**

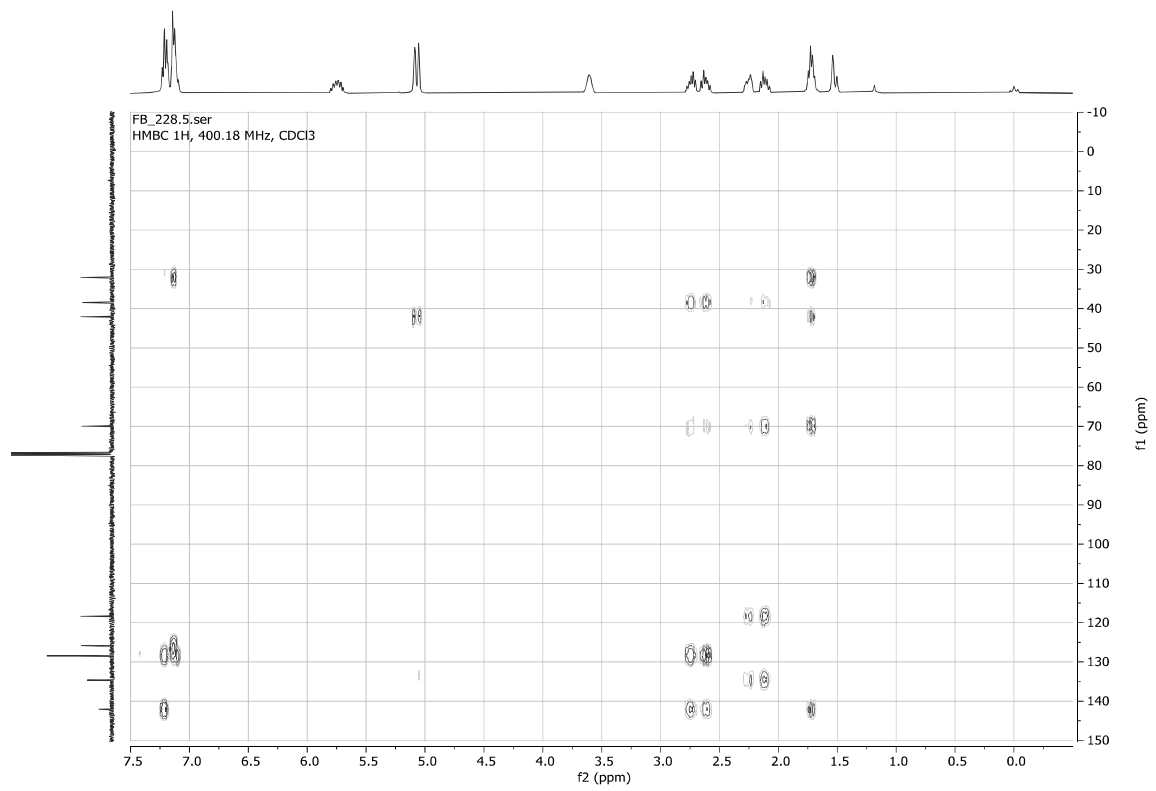
FB_228.1.fid
1D 1H, 400.18 MHz, CDCl₃



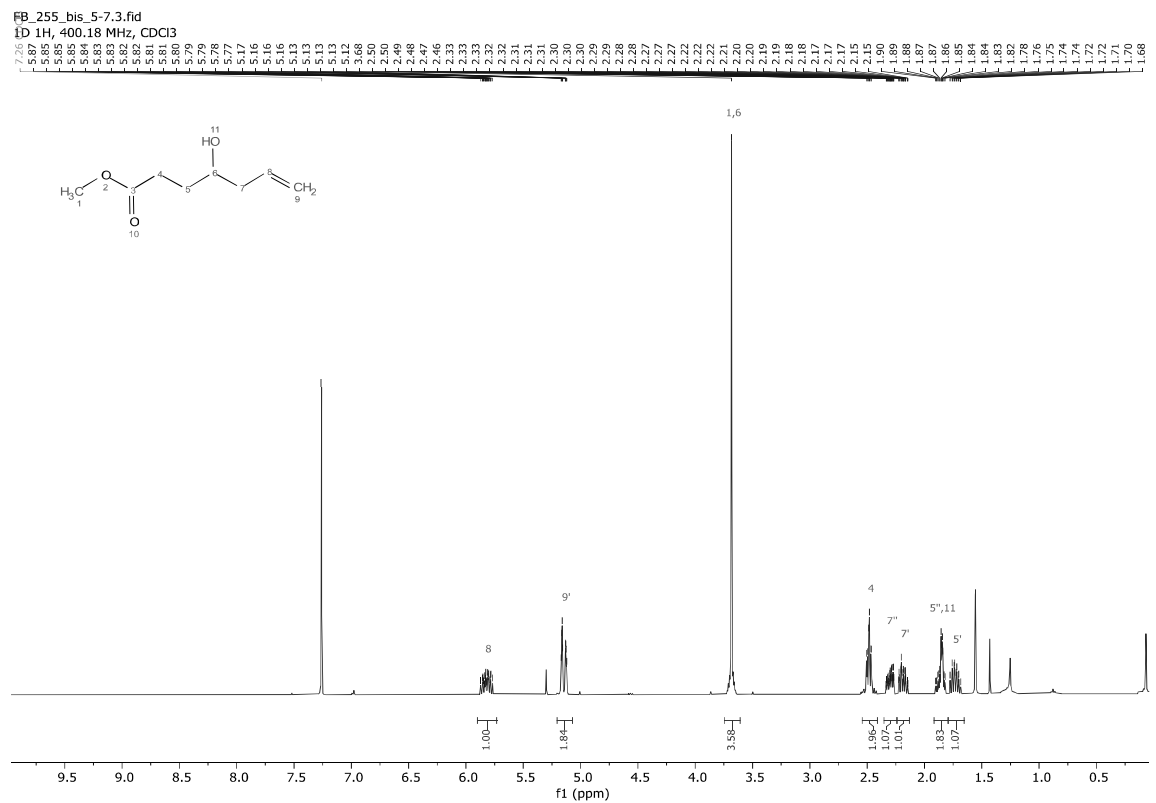
FB_228.3.fid
1D 13C(1H), 100.64 MHz, CDCl₃



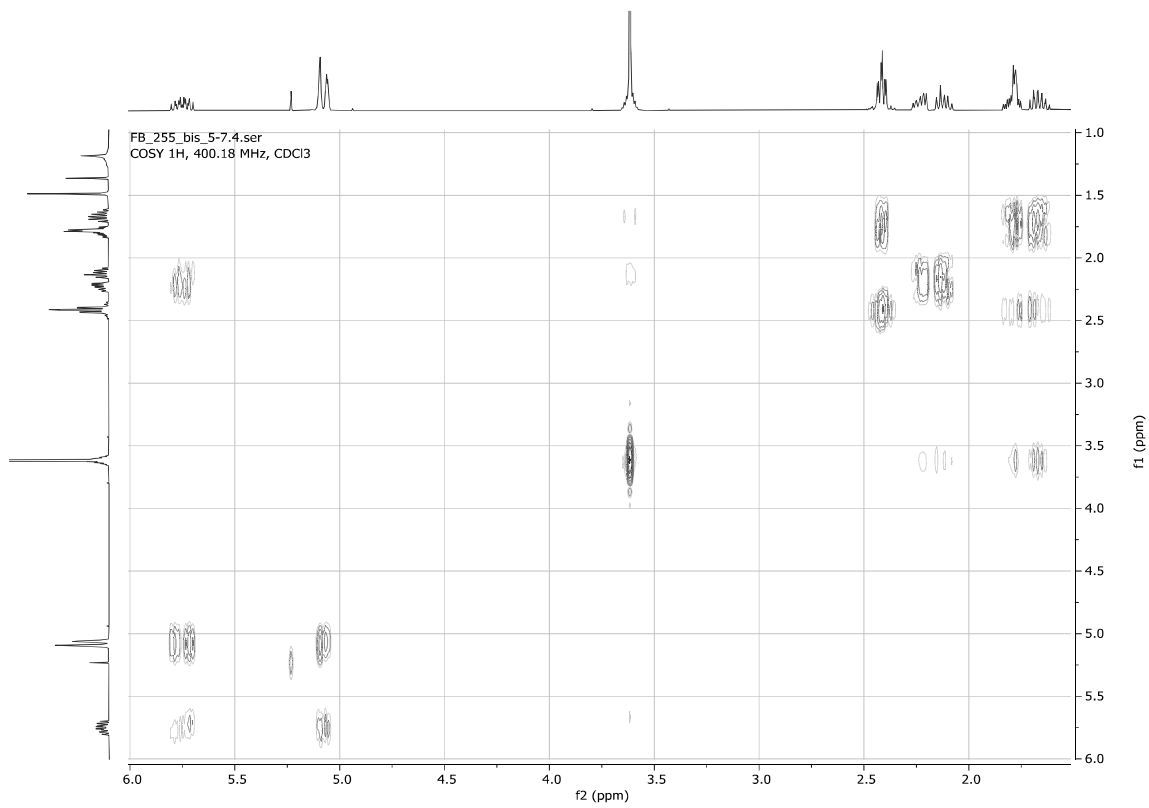
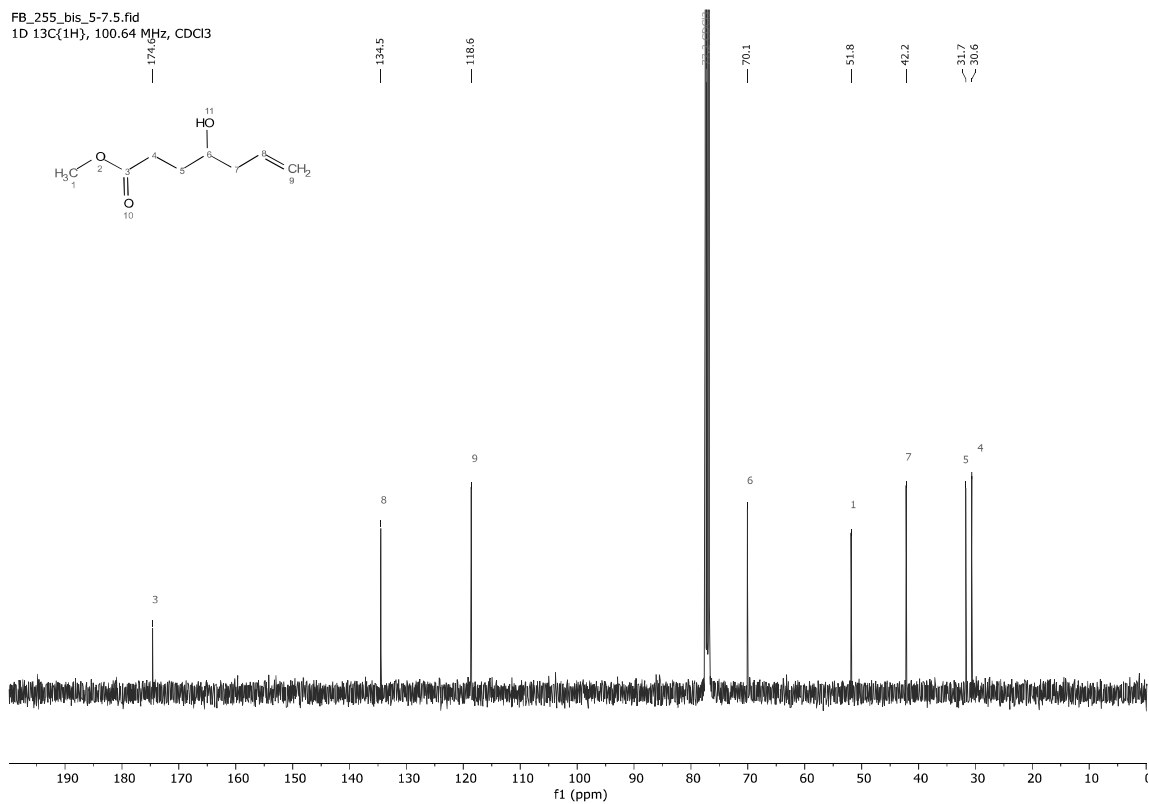


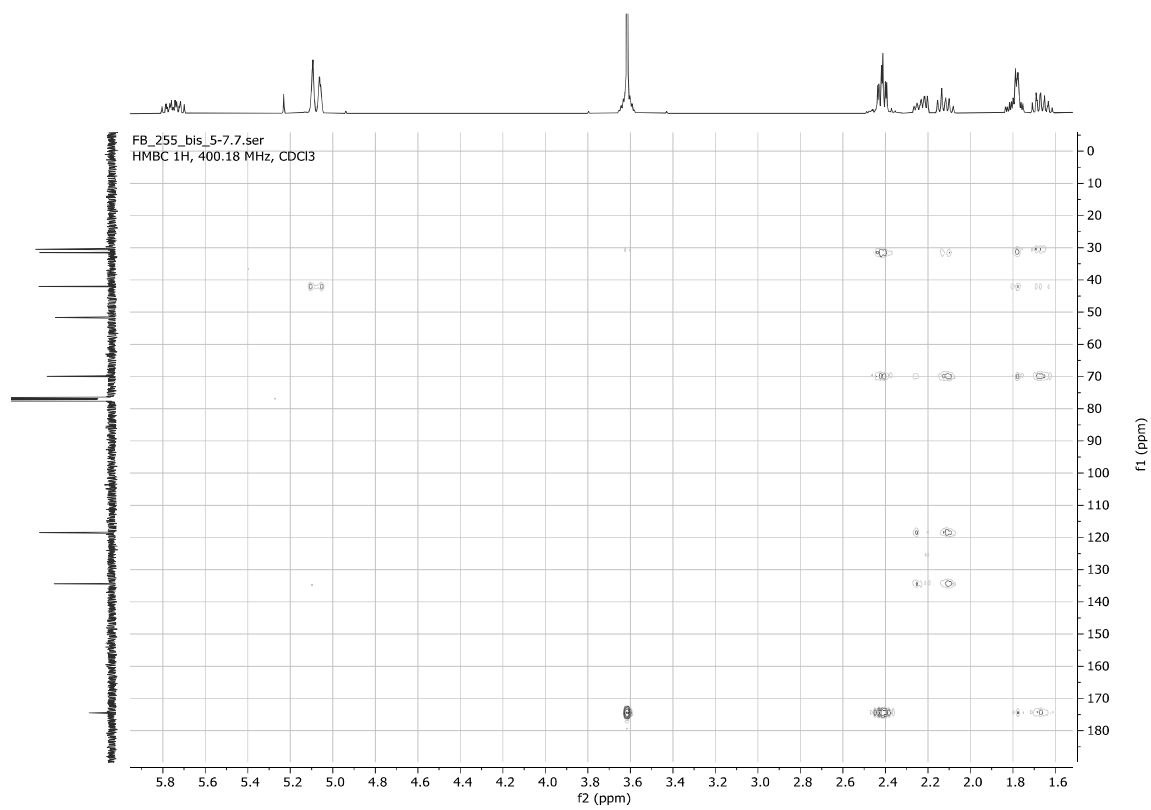
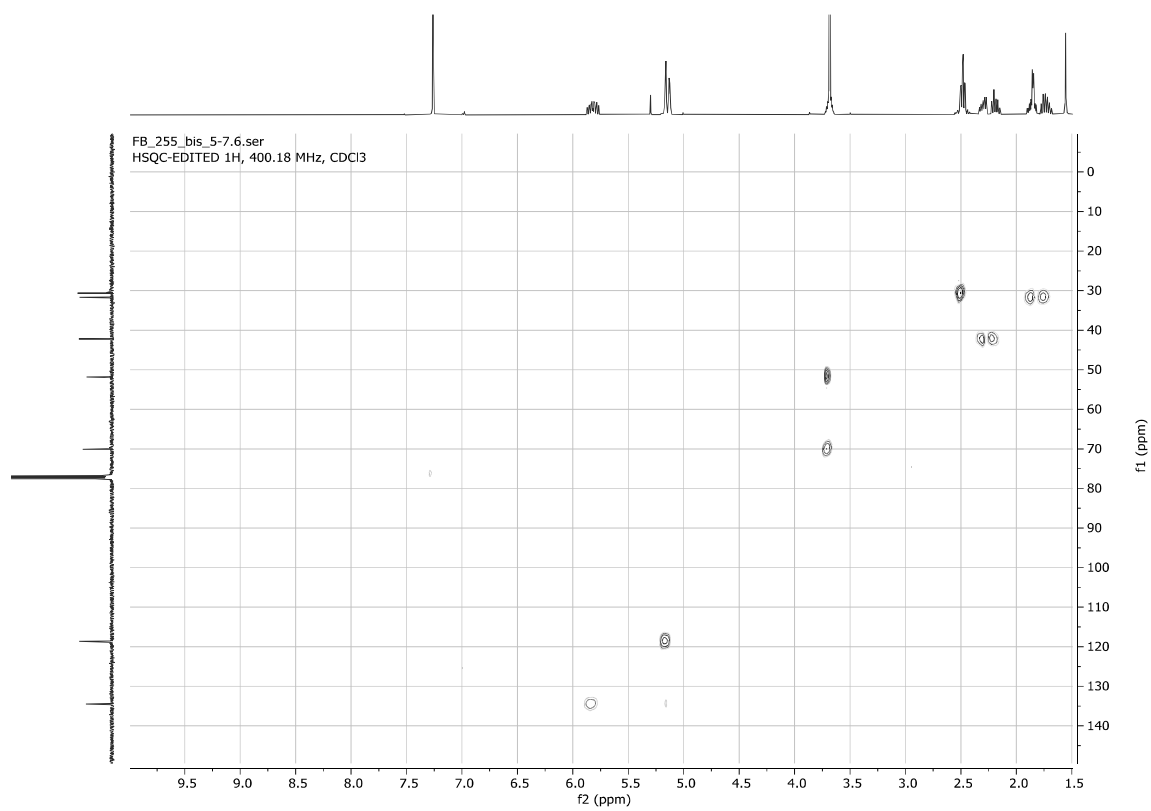


Methyl 4-hydroxyhept-6-enoate 6m



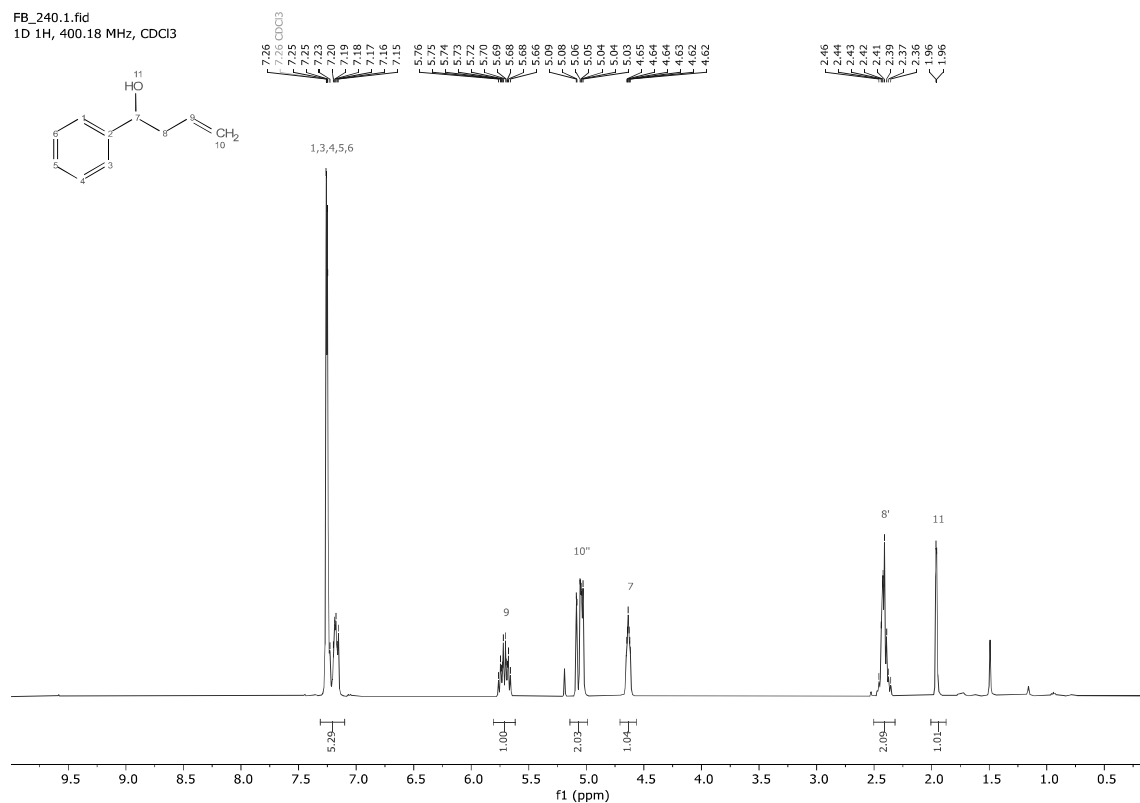
FB_255_bis_5-7.5.fid
1D 13C{1H}, 100.64 MHz, CDCl3



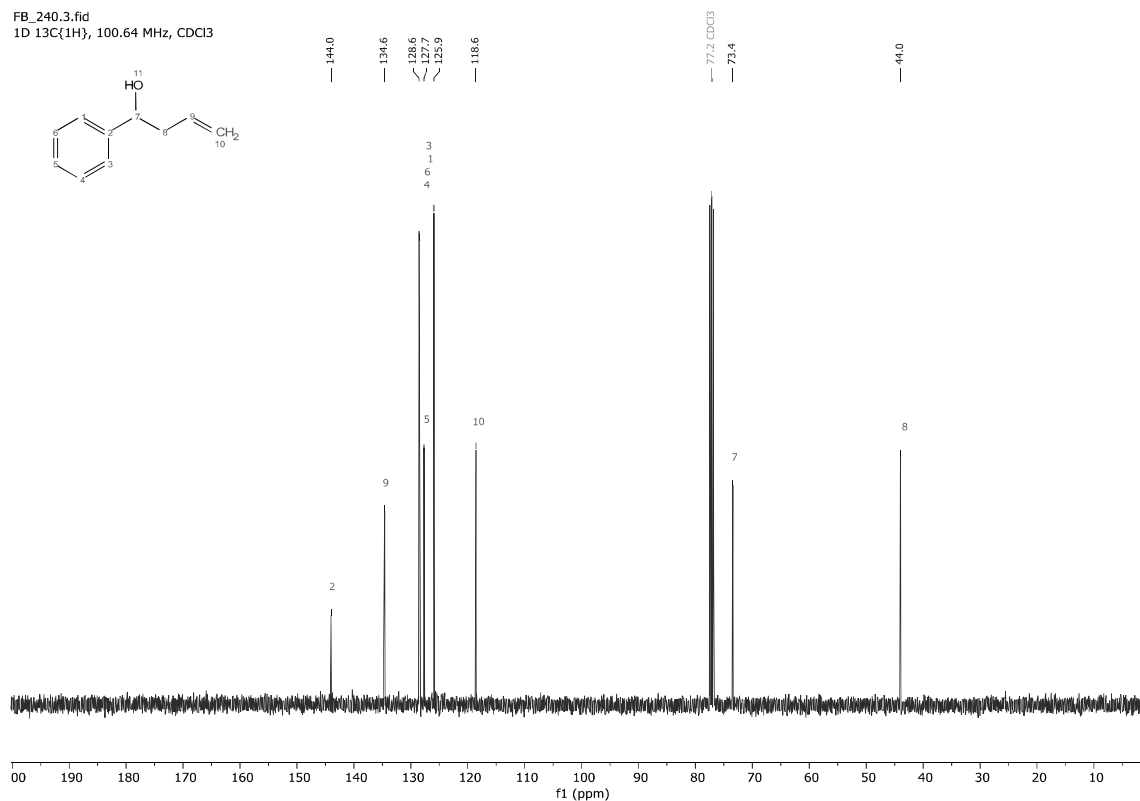


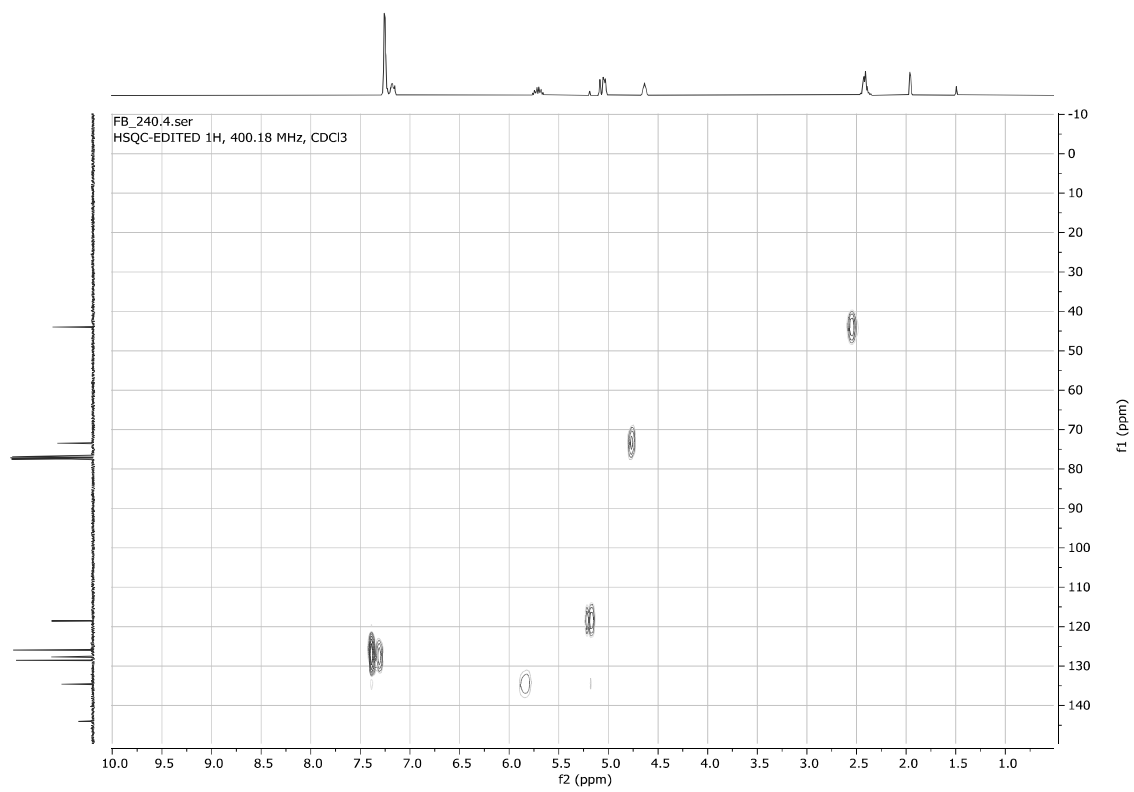
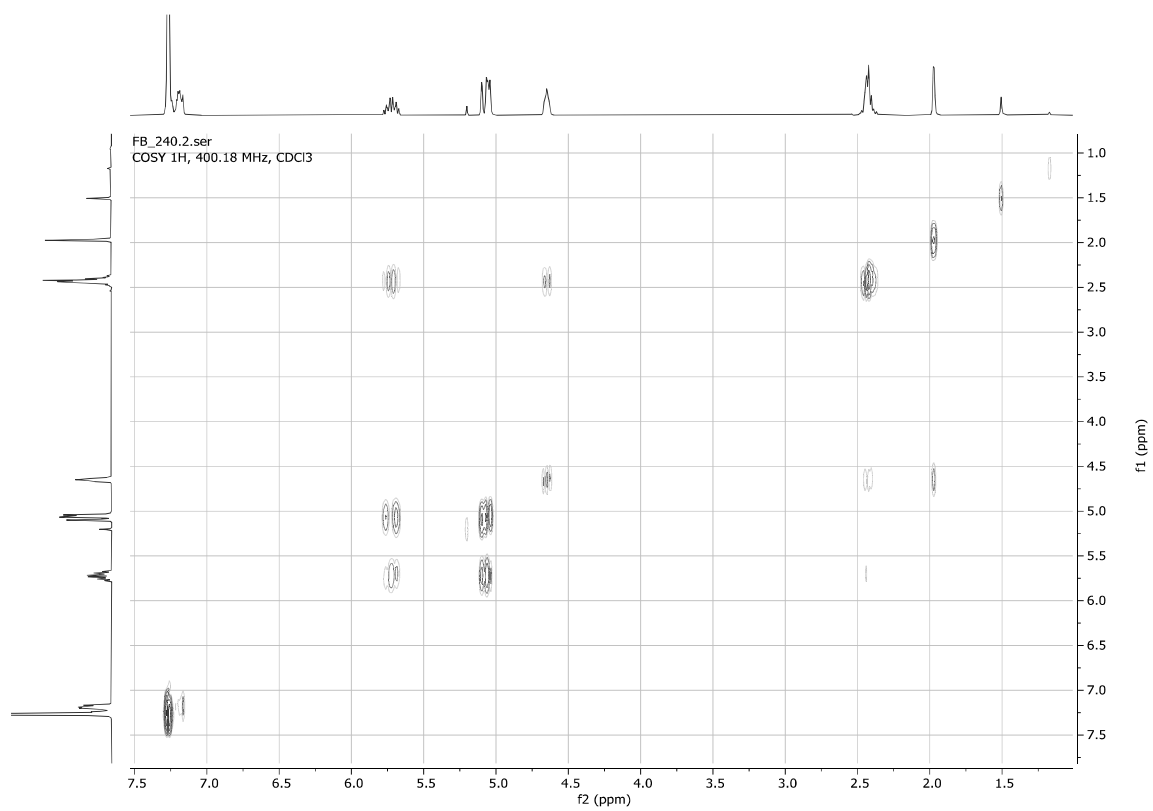
1-Phenylbut-3-en-1-ol **6n**

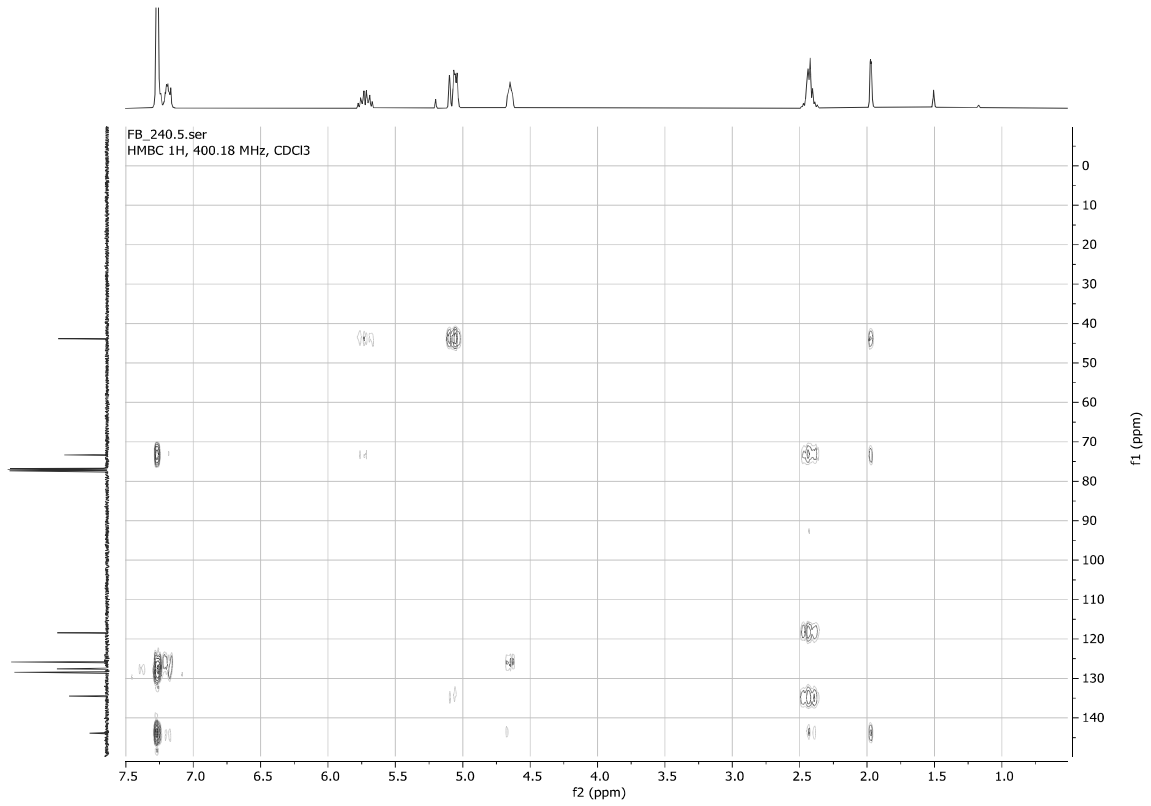
FB_240.1.fid
1D 1H, 400.18 MHz, CDCl₃



FB_240.3.fid
1D 13C{1H}, 100.64 MHz, CDCl₃

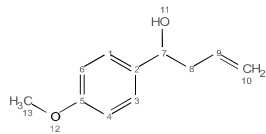
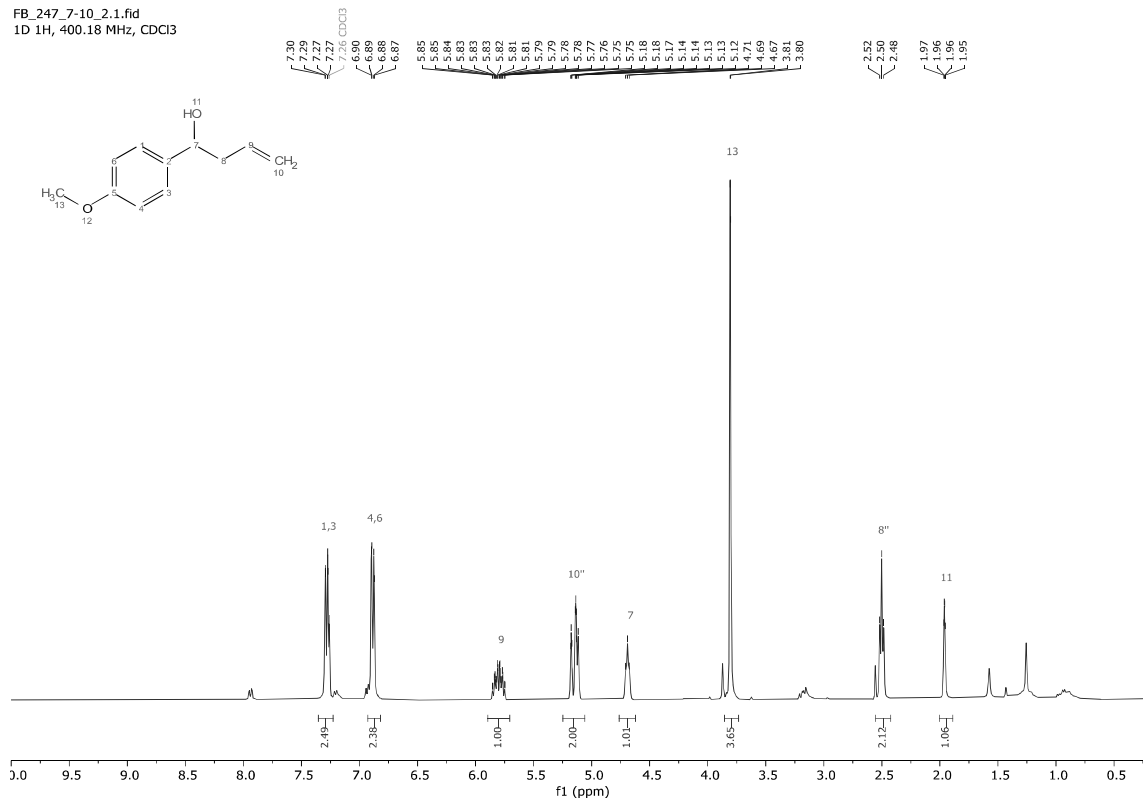




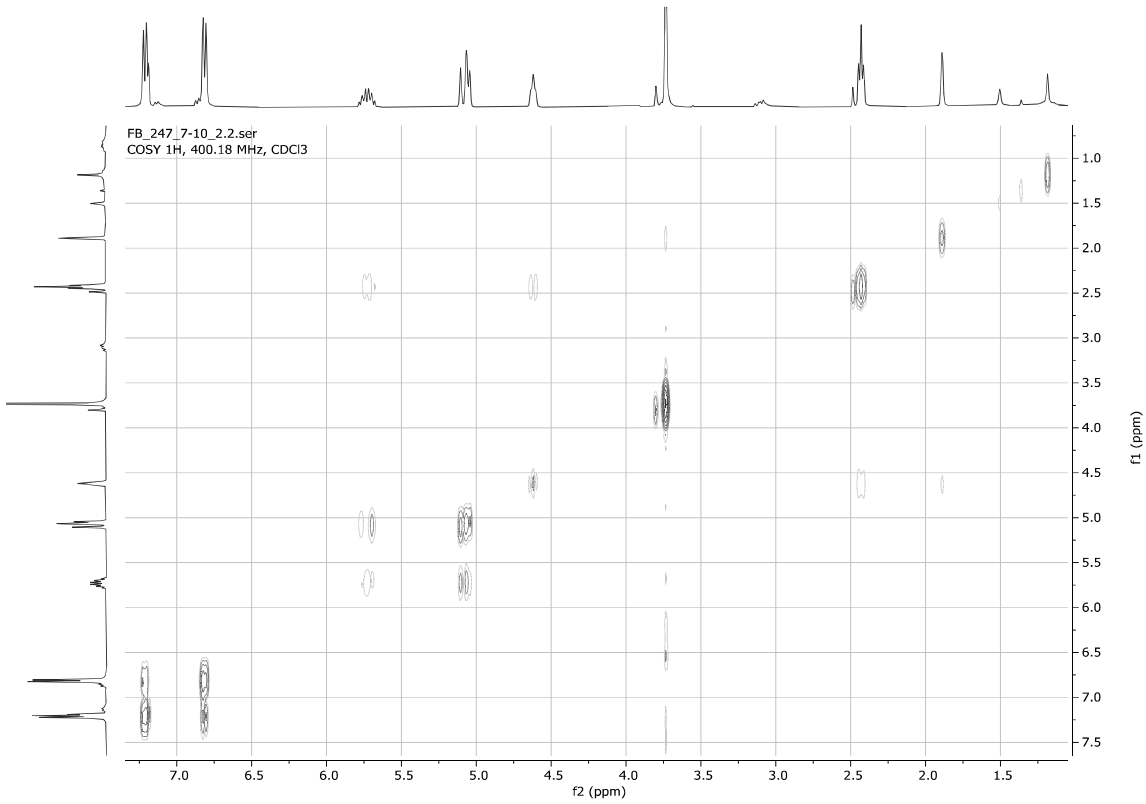
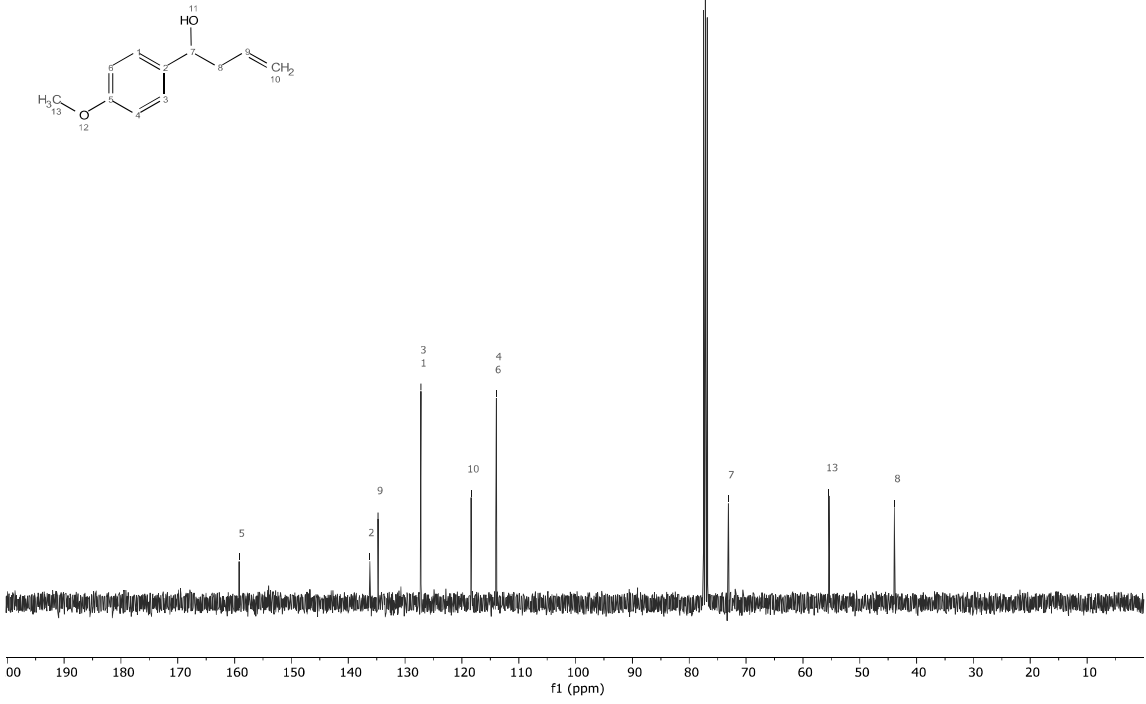


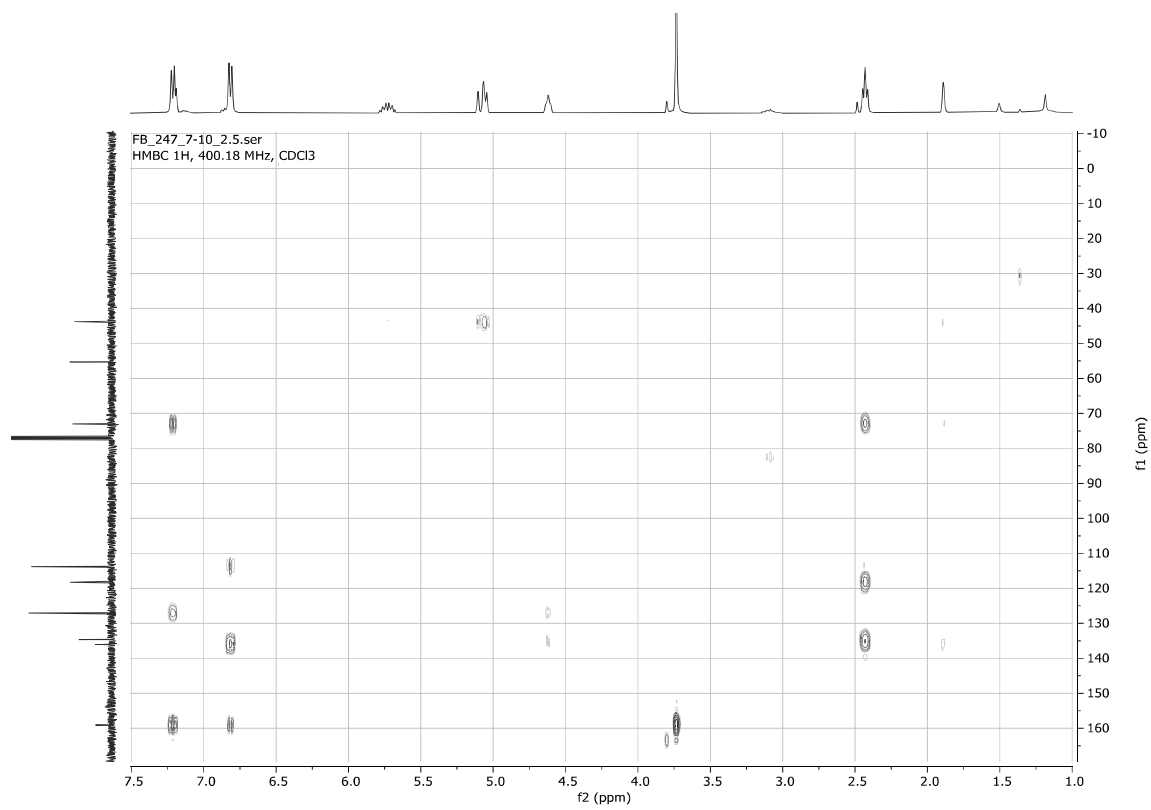
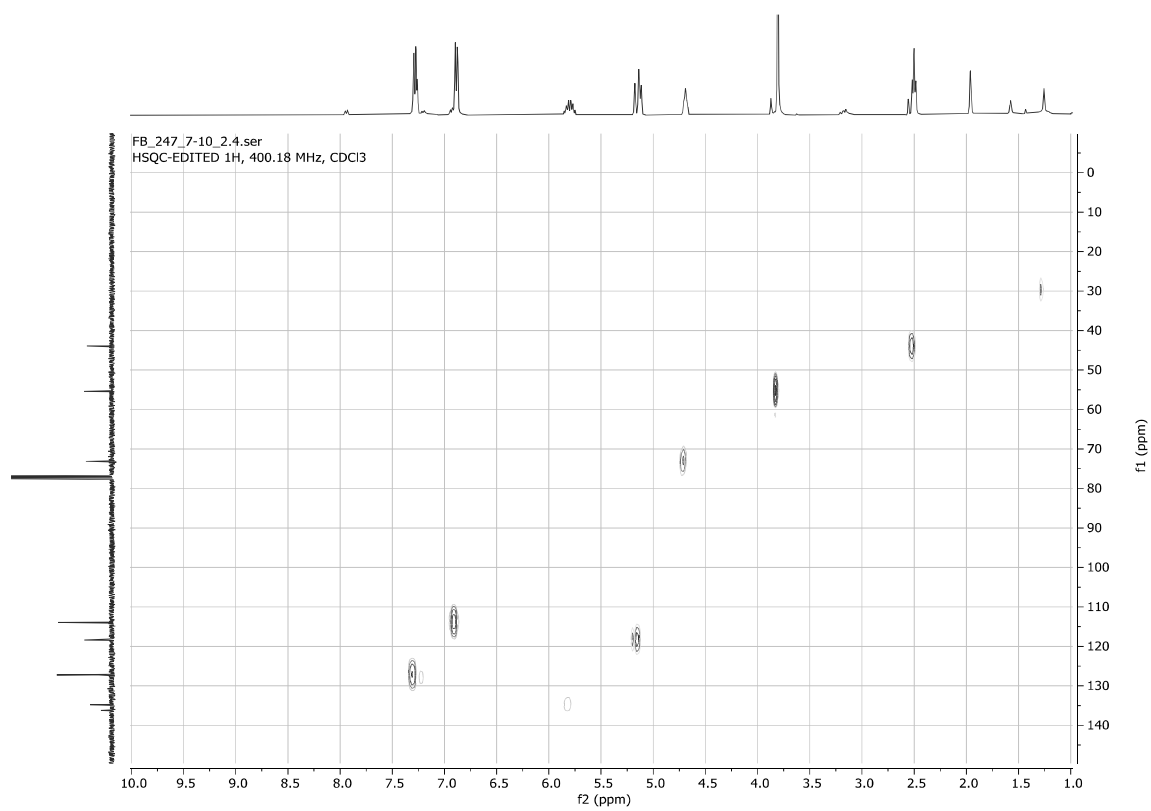
1-(4-Methoxyphenyl)but-3-en-1-ol **6o**

FB_247_7-10_2.1.fid
1D 1H, 400.18 MHz, CDCl3



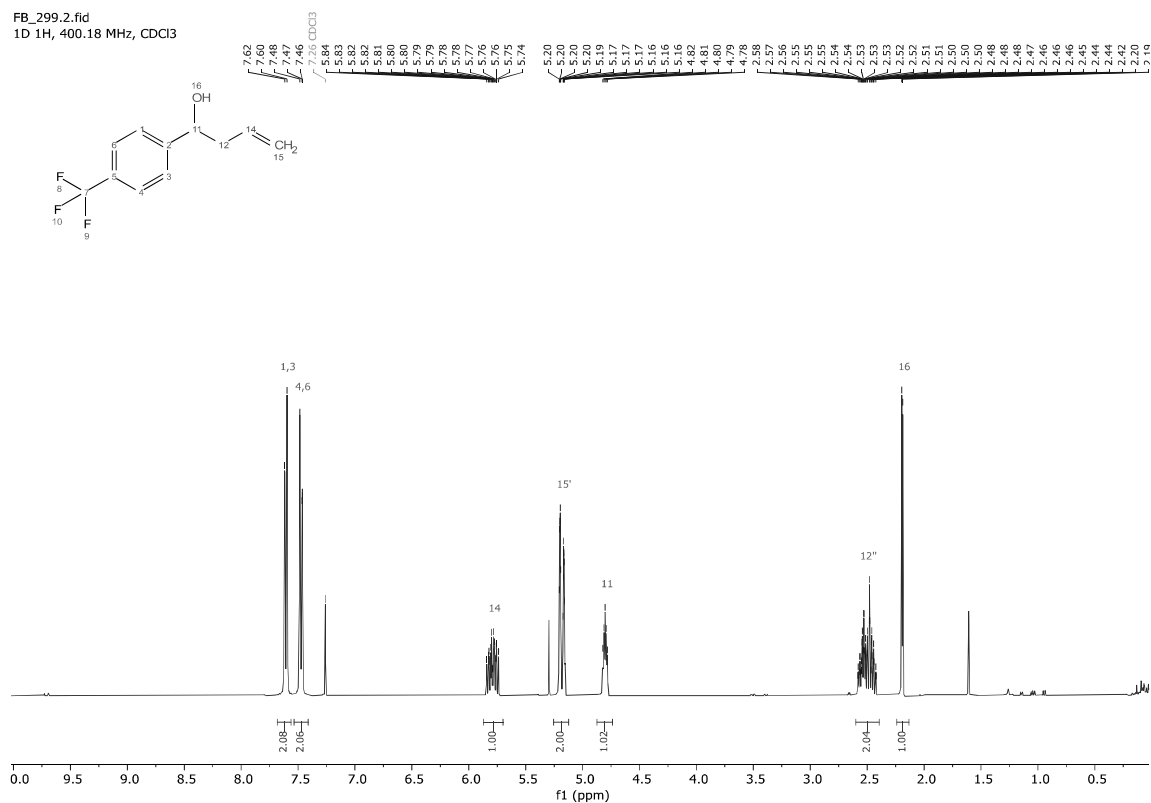
FB_247_7-10_2.3.fid
1D 13C{1H}, 100.64 MHz, CDCl3



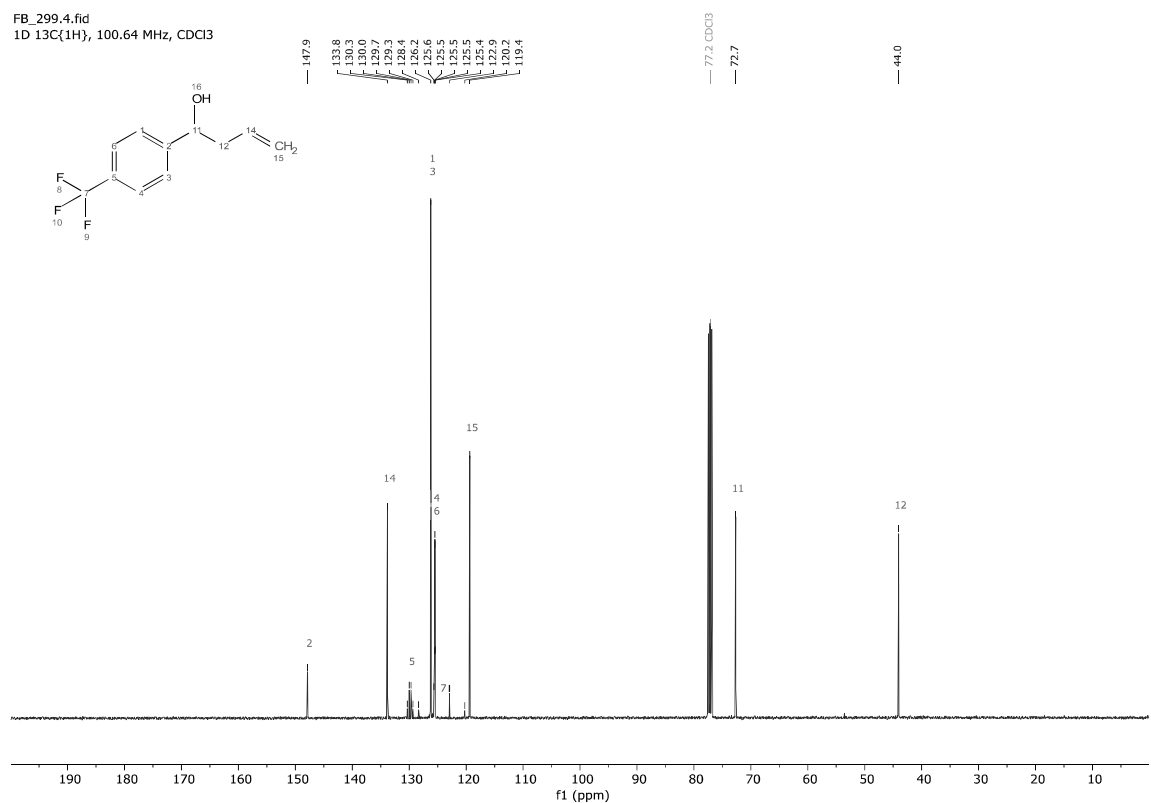


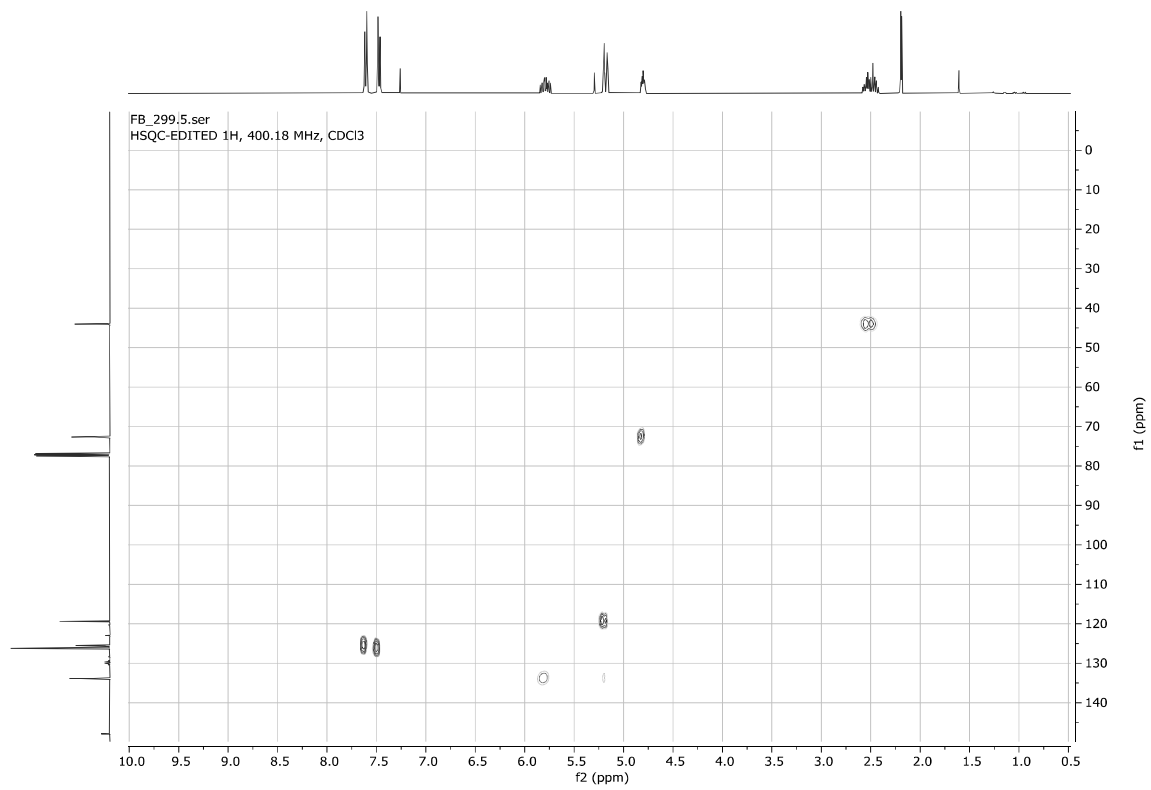
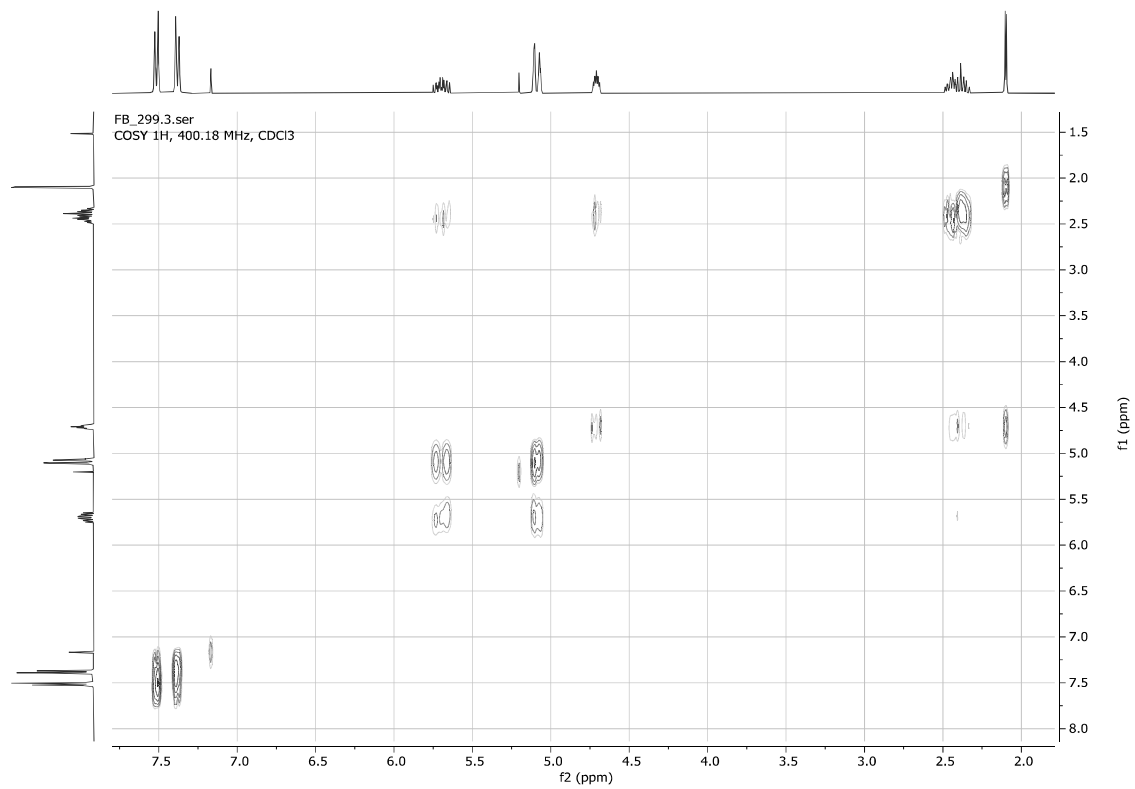
1-(4-(Trifluoromethyl)phenyl)but-3-en-1-ol **6p**

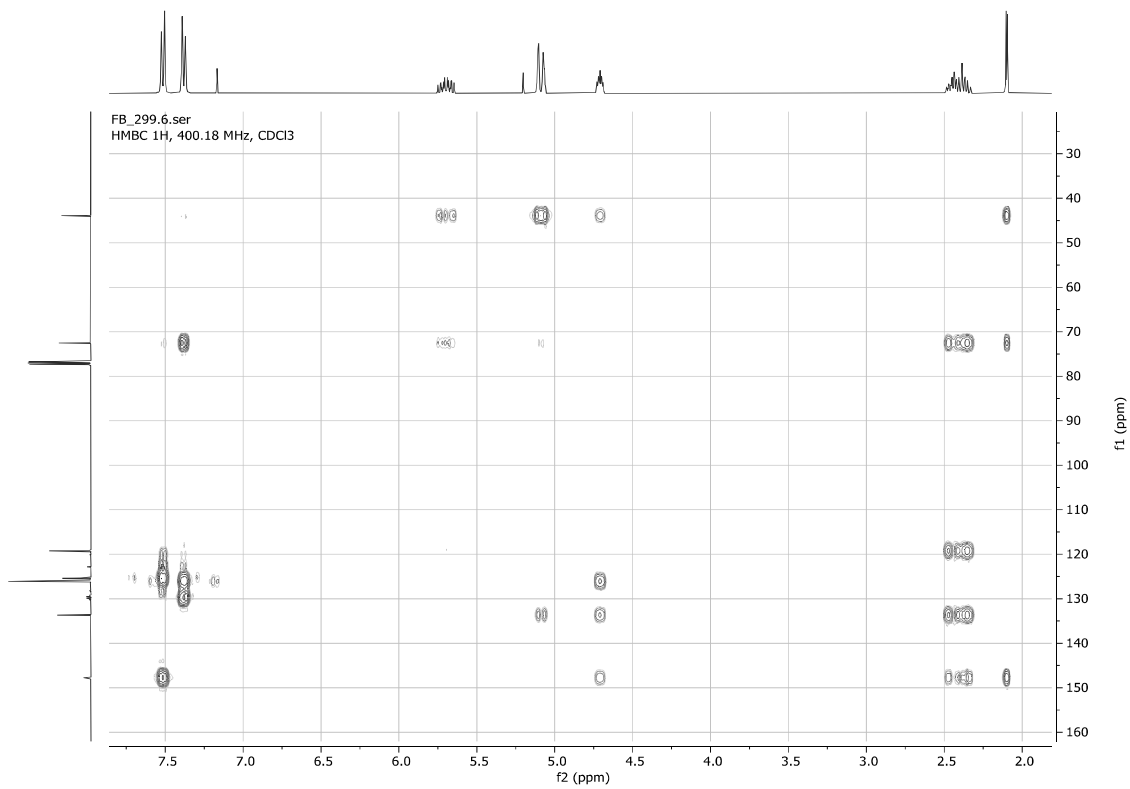
FB_299.2.fid
1D 1H, 400.18 MHz, CDCl3



FB_299.4.fid
1D 13C(1H), 100.64 MHz, CDCl3

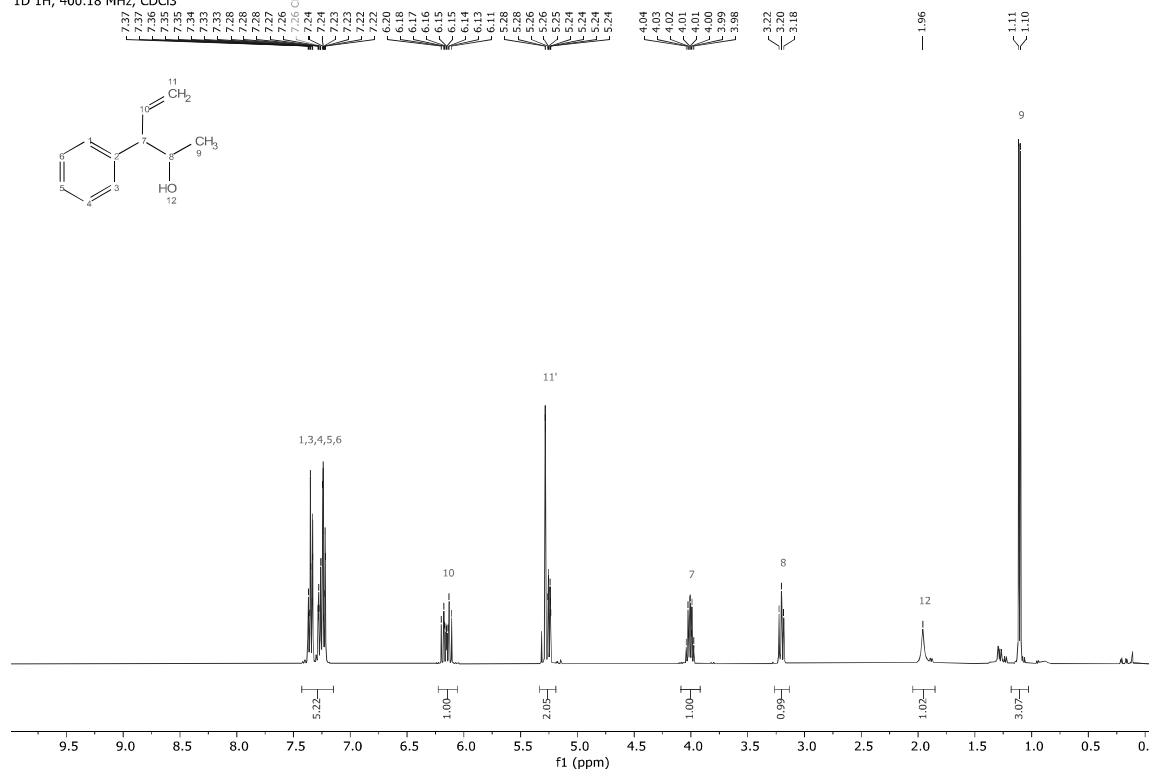
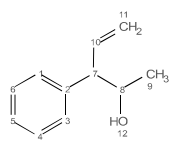




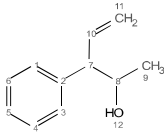


3-Phenylpent-4-en-2-ol **6q**

FB_324.1.fid
1D 1H, 400.18 MHz, CDCl3



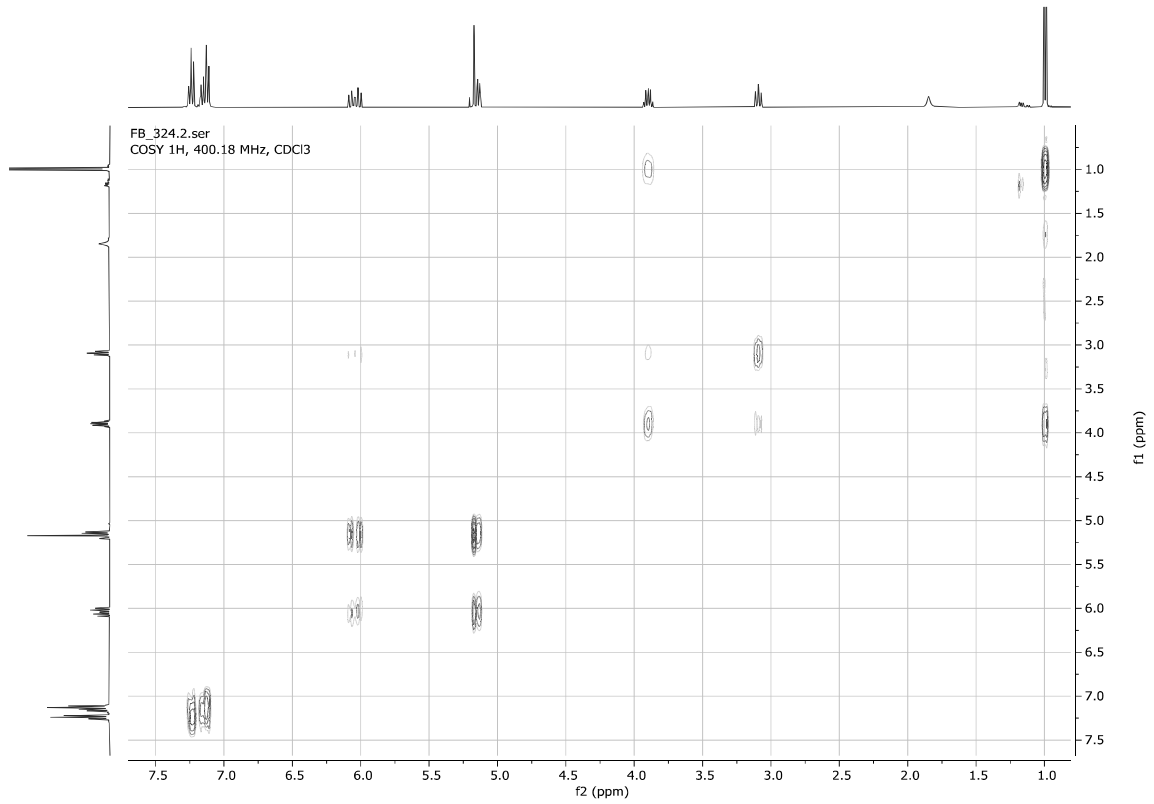
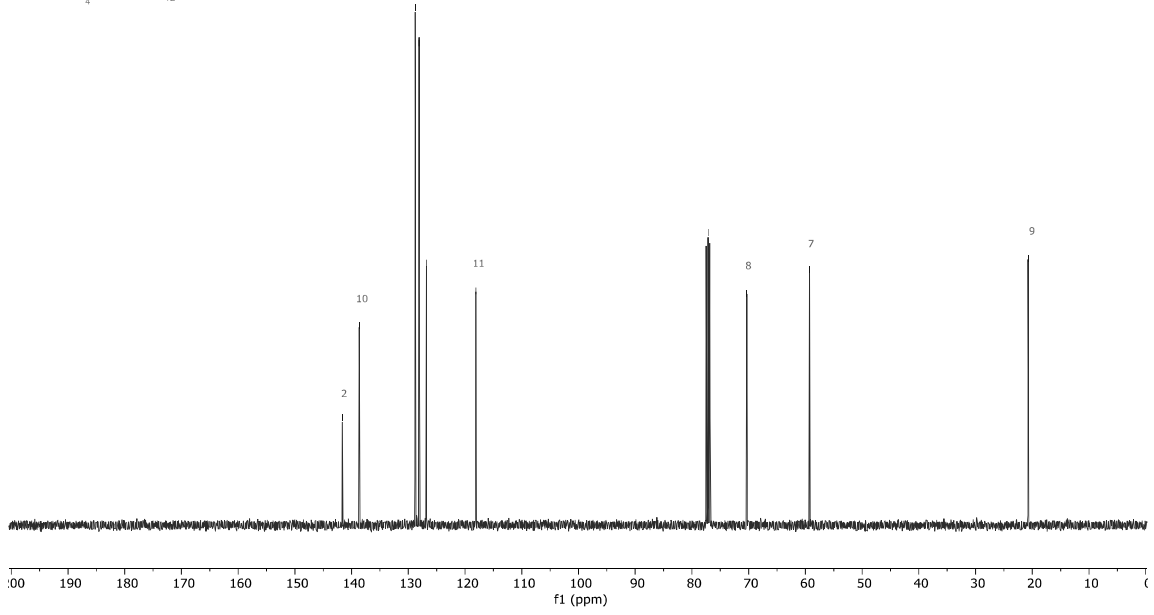
FB_324.3.fid
1D 13C{1H}, 100.64 MHz, CDCl3

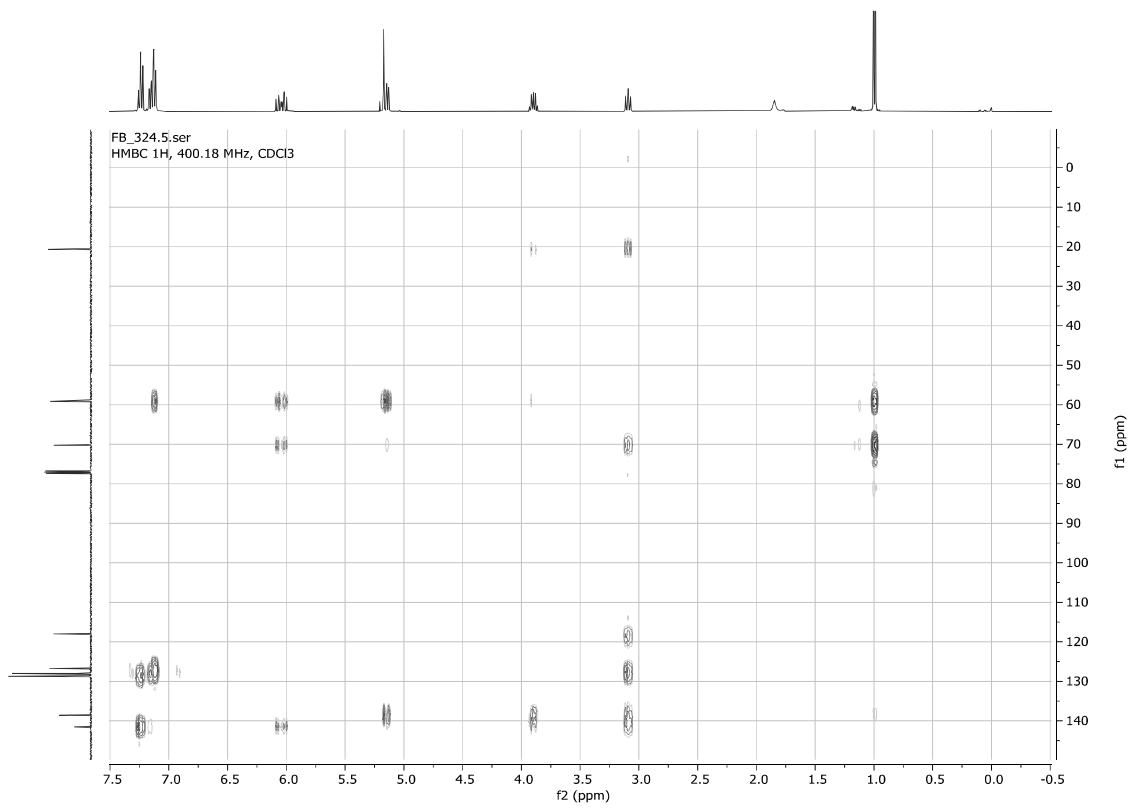
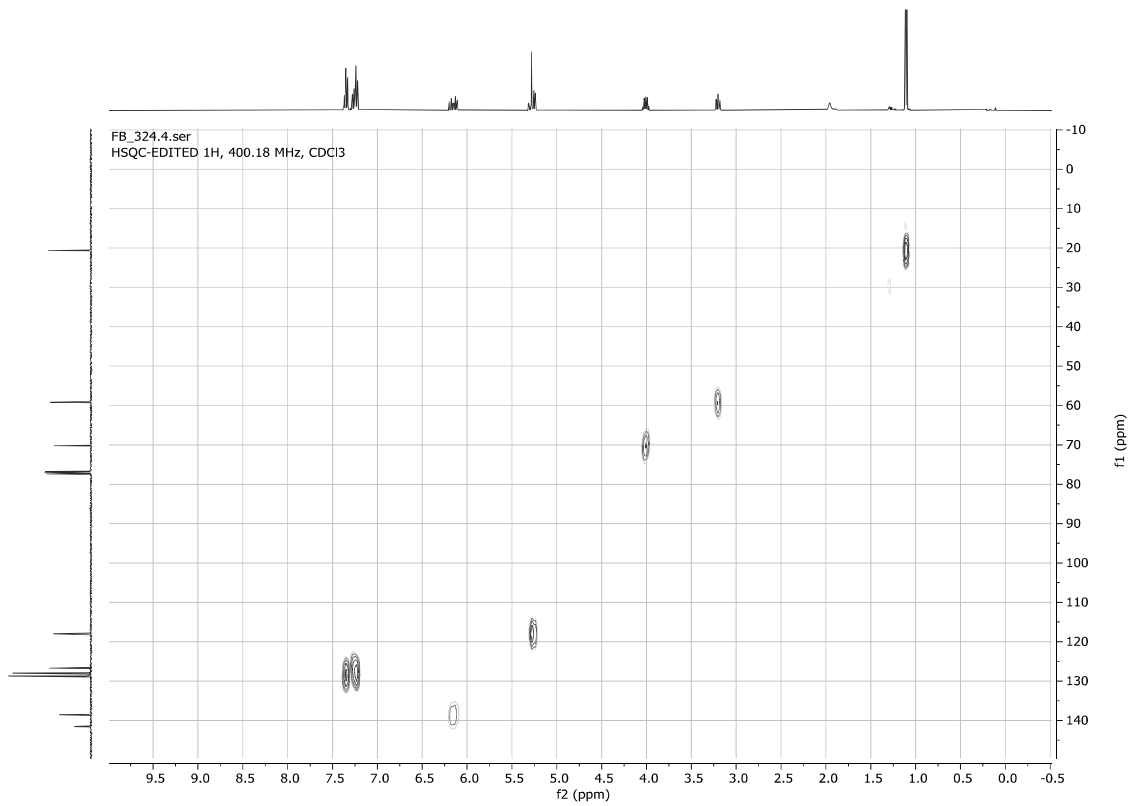


141.6
138.6
128.8
128.4
128.0
118.1

77.2 CDCl3
70.3
59.3

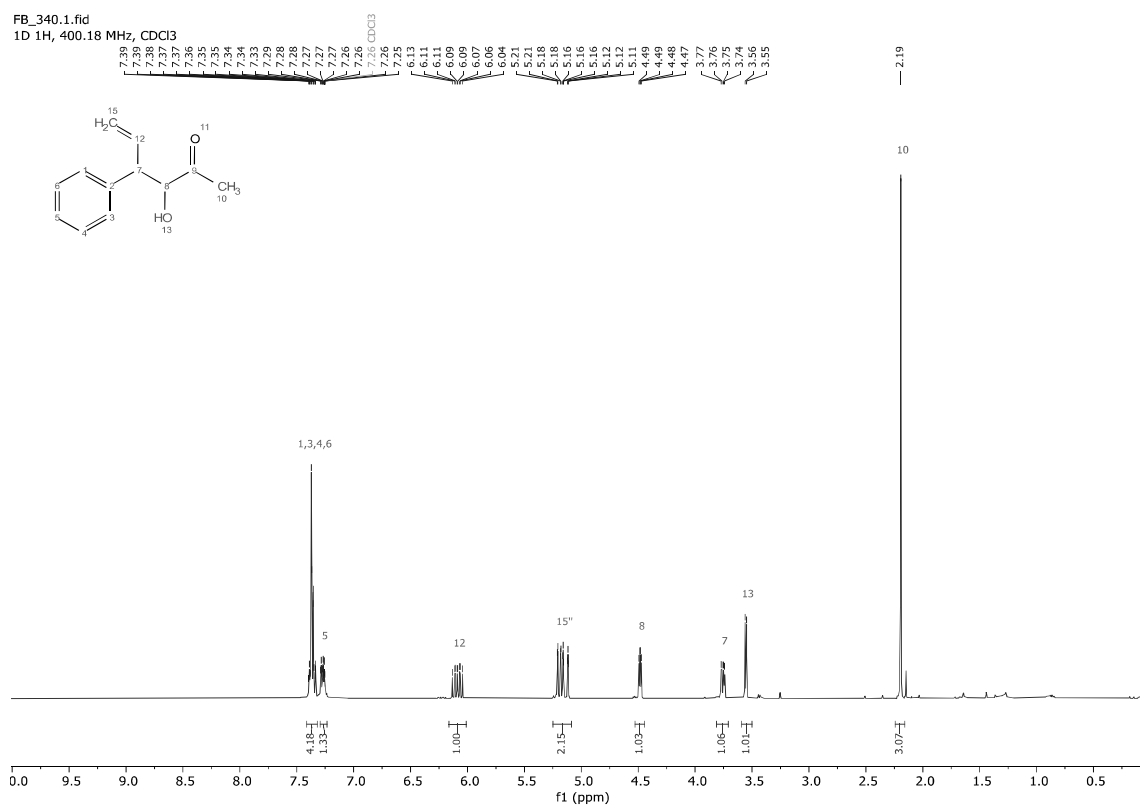
20.7



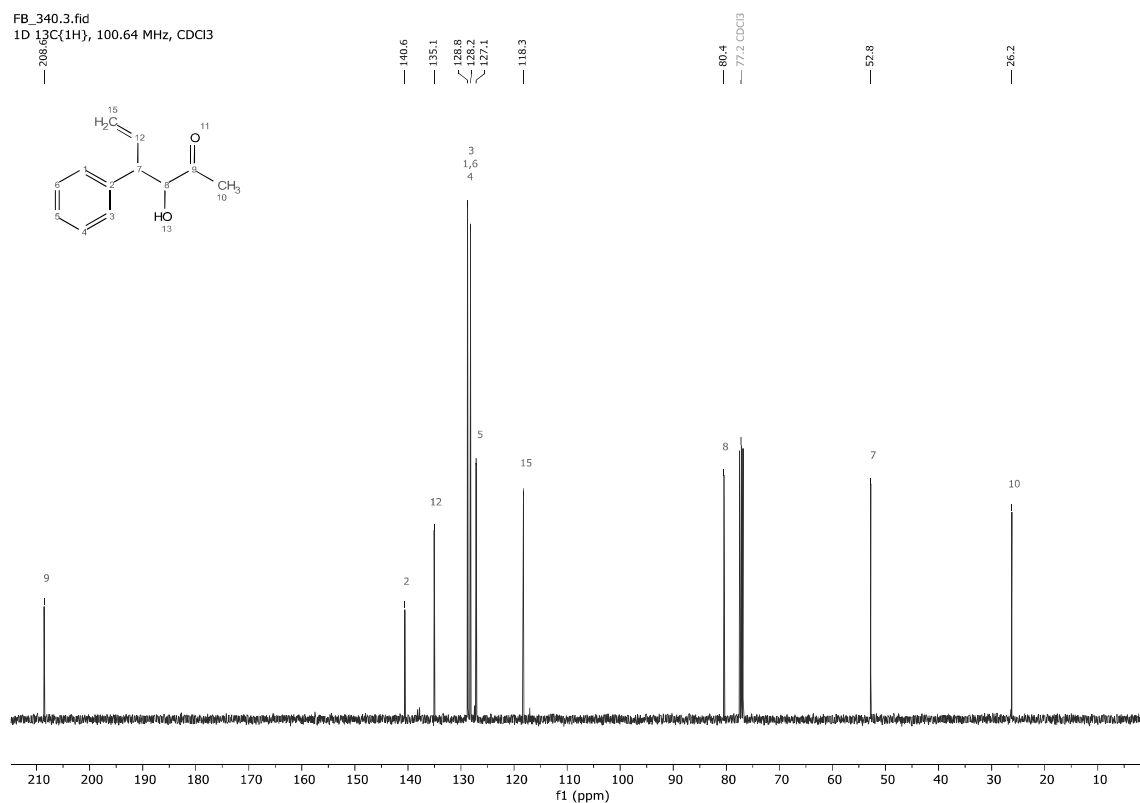


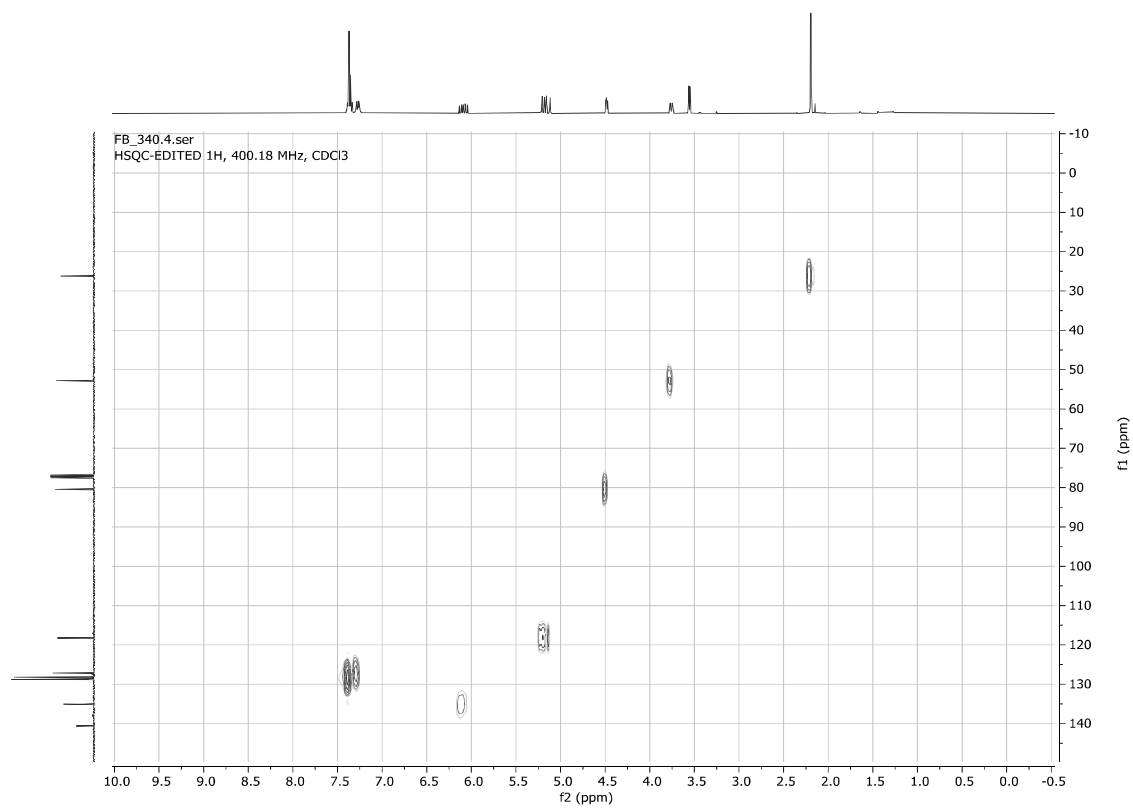
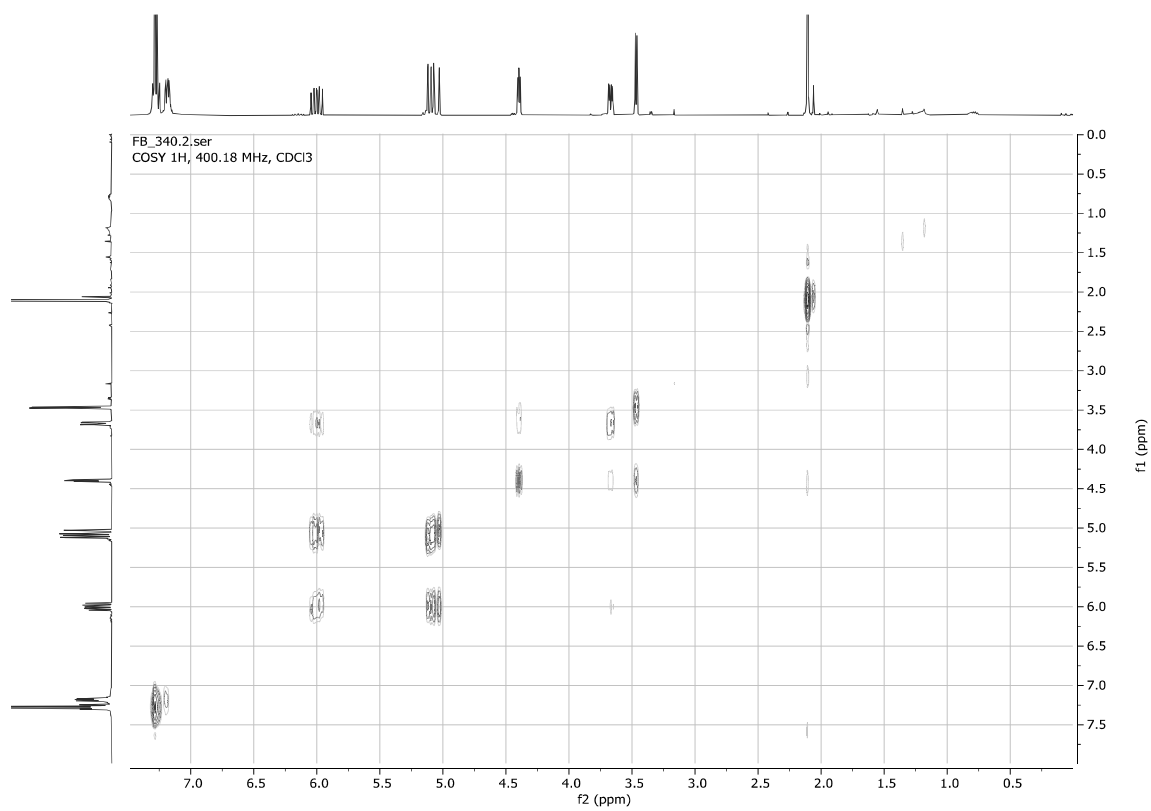
3-Hydroxy-4-phenylhex-5-en-2-one 6r

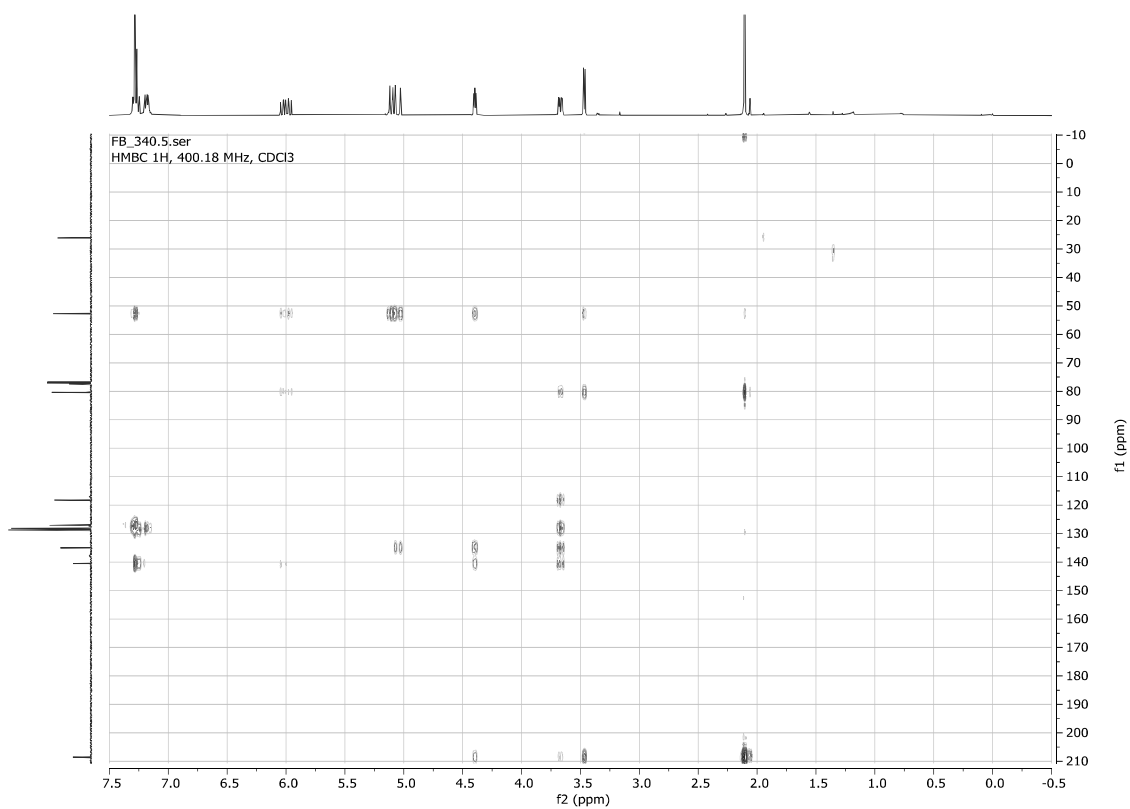
FB_340.1.fid
1D 1H, 400.18 MHz, CDCl3



FB_340.3.fid
1D 13C(1H), 100.64 MHz, CDCl3

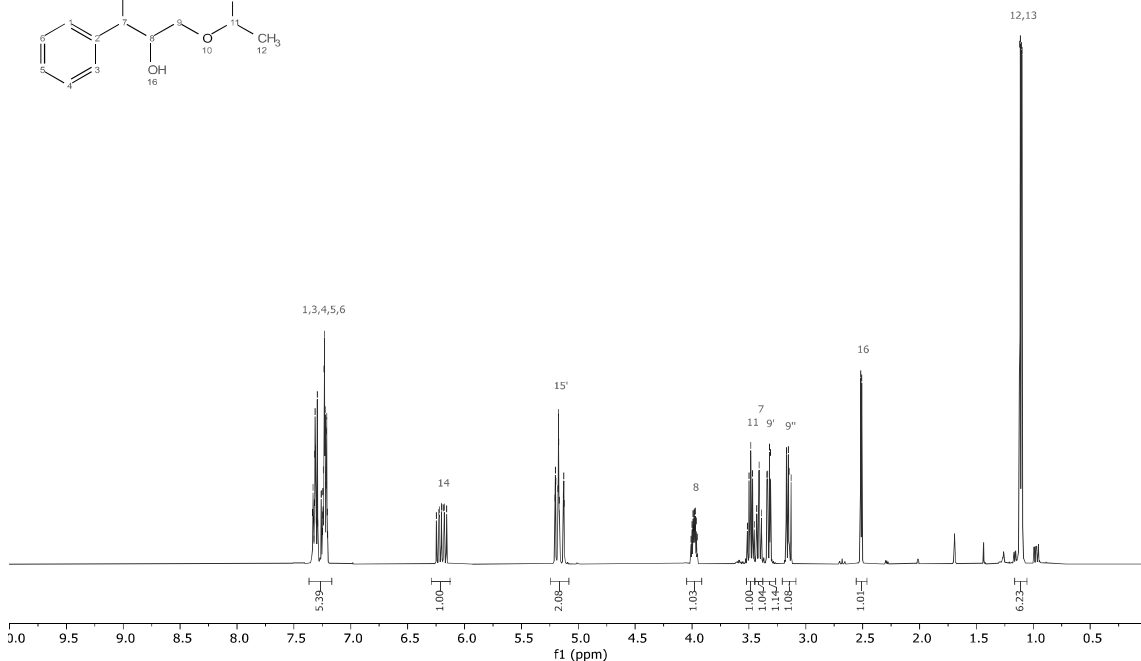
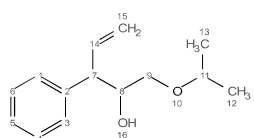




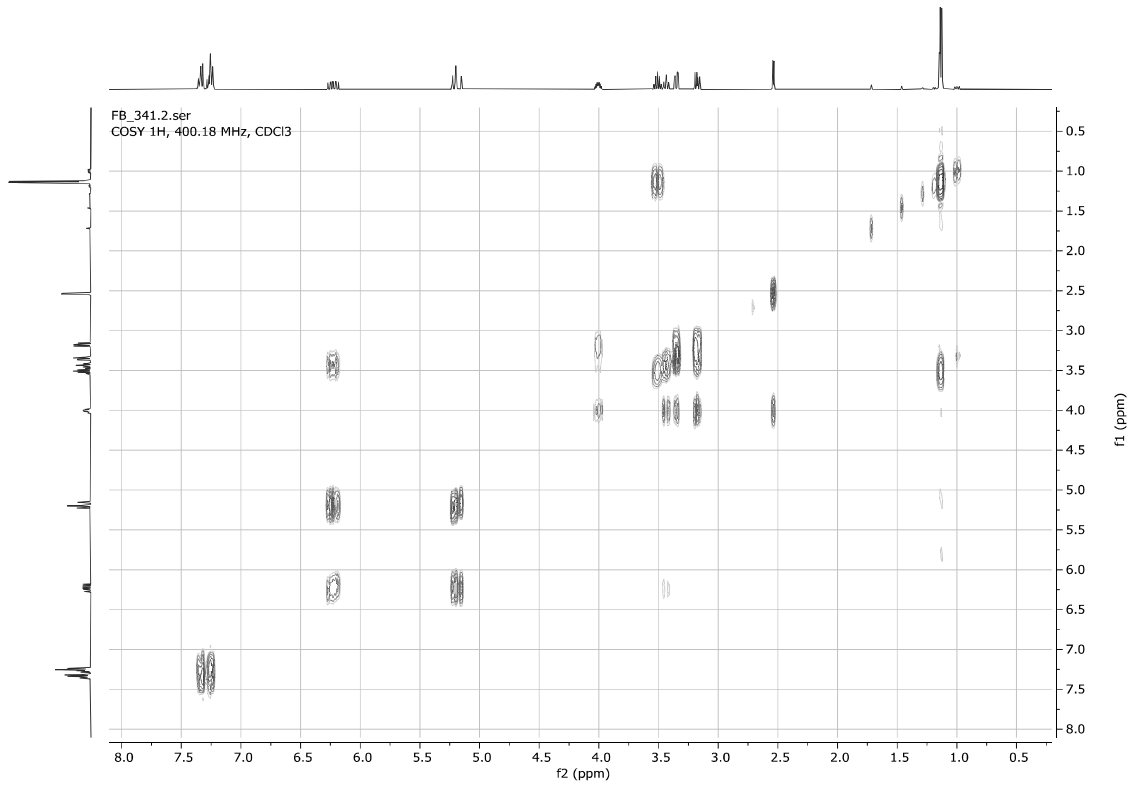
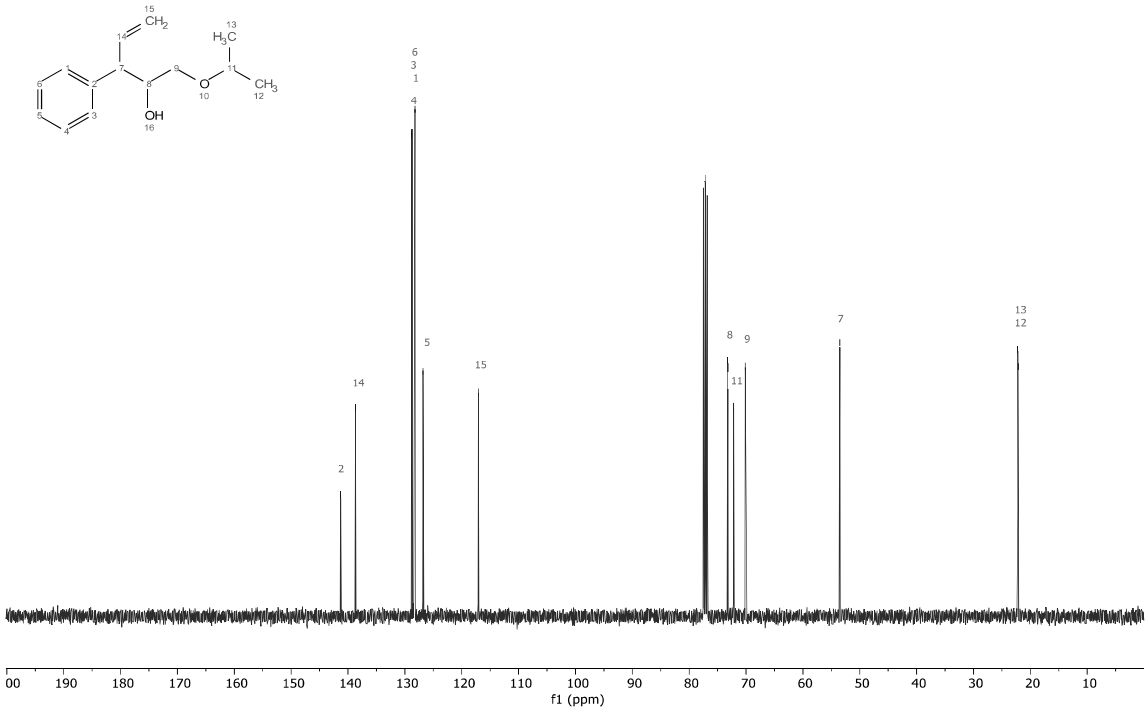


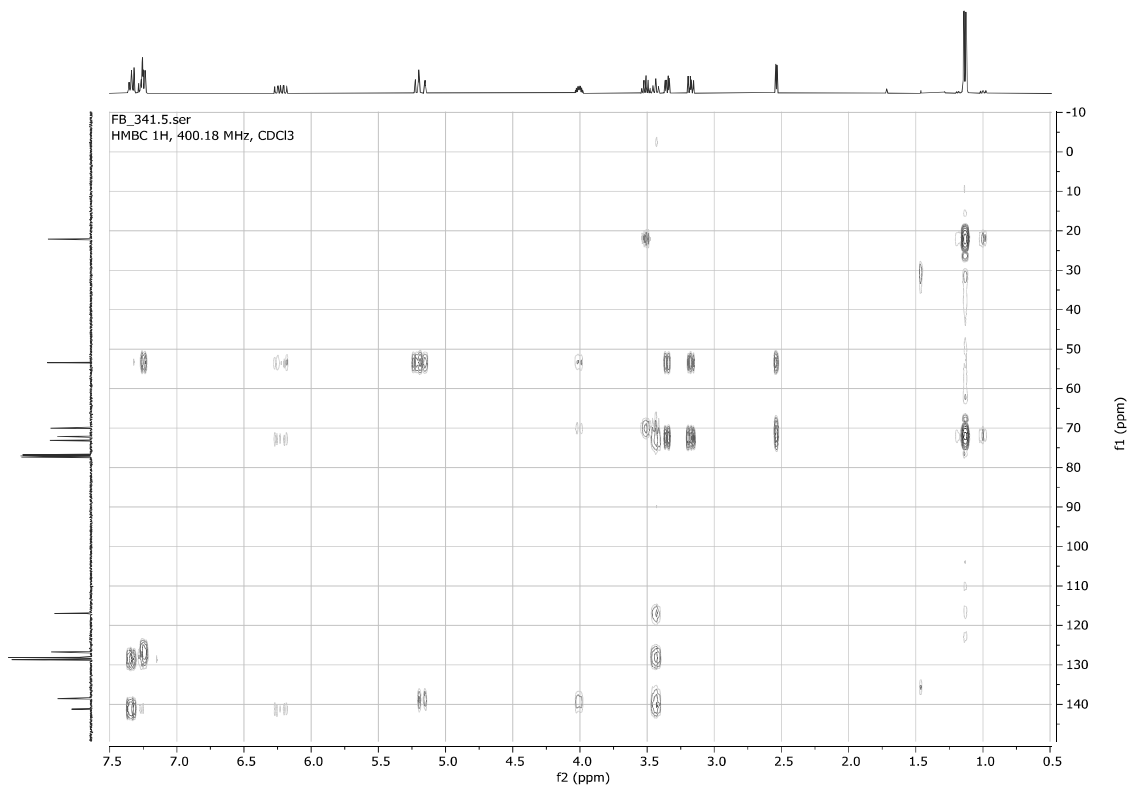
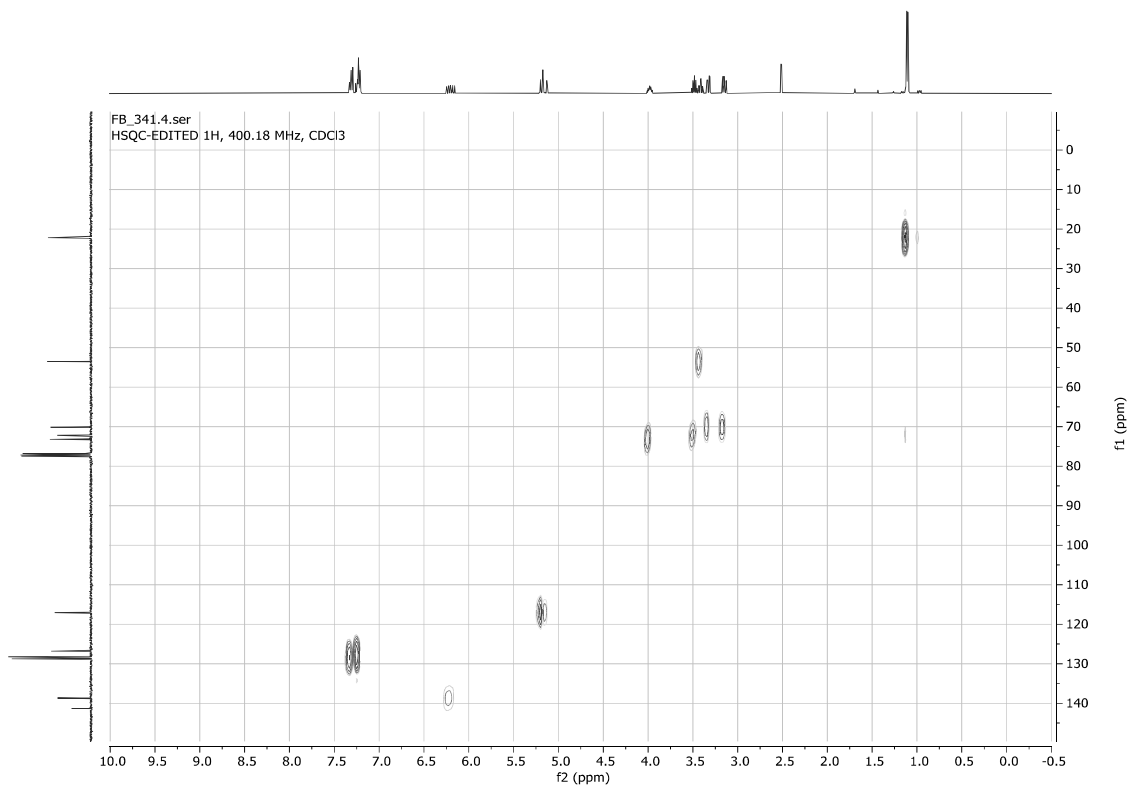
1-Isopropoxy-3-phenylpent-4-en-2-ol **6s**

FB_341.1.fid
 1D 1H, 400.18 MHz, CDCl3



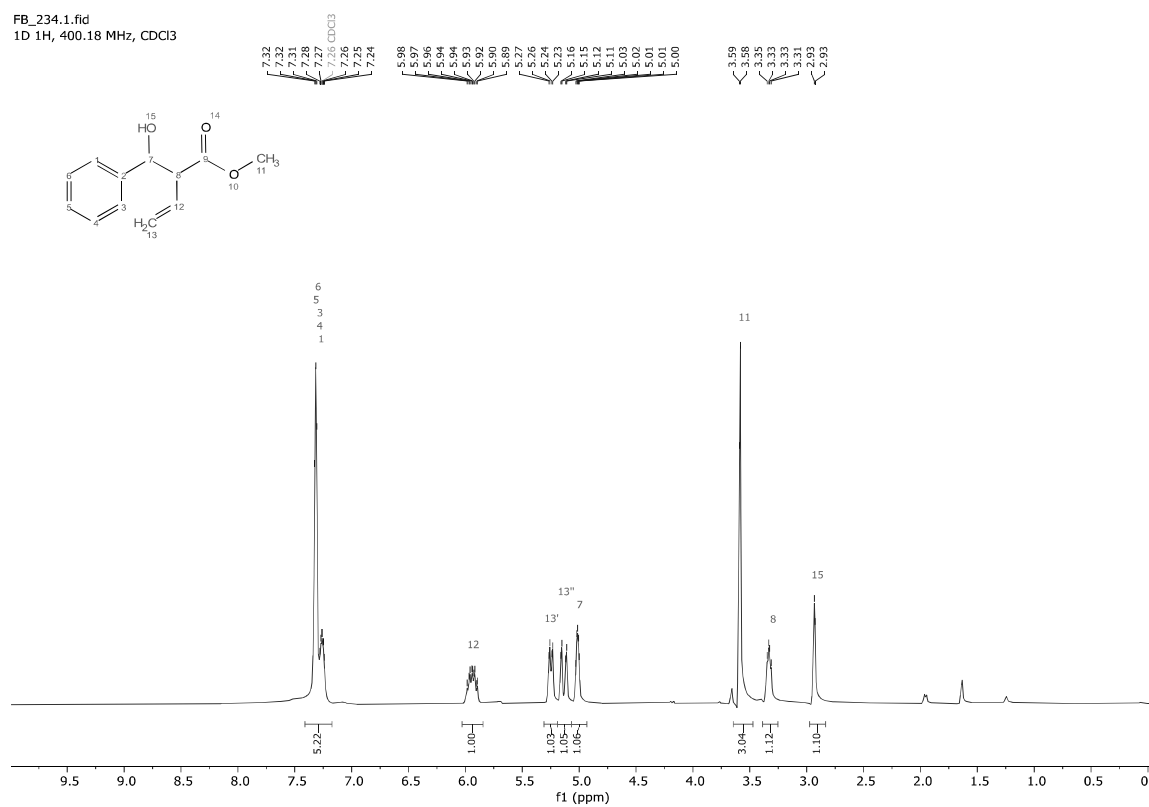
FB_341.3.fid
1D 13C{1H}, 100.64 MHz, CDCl3



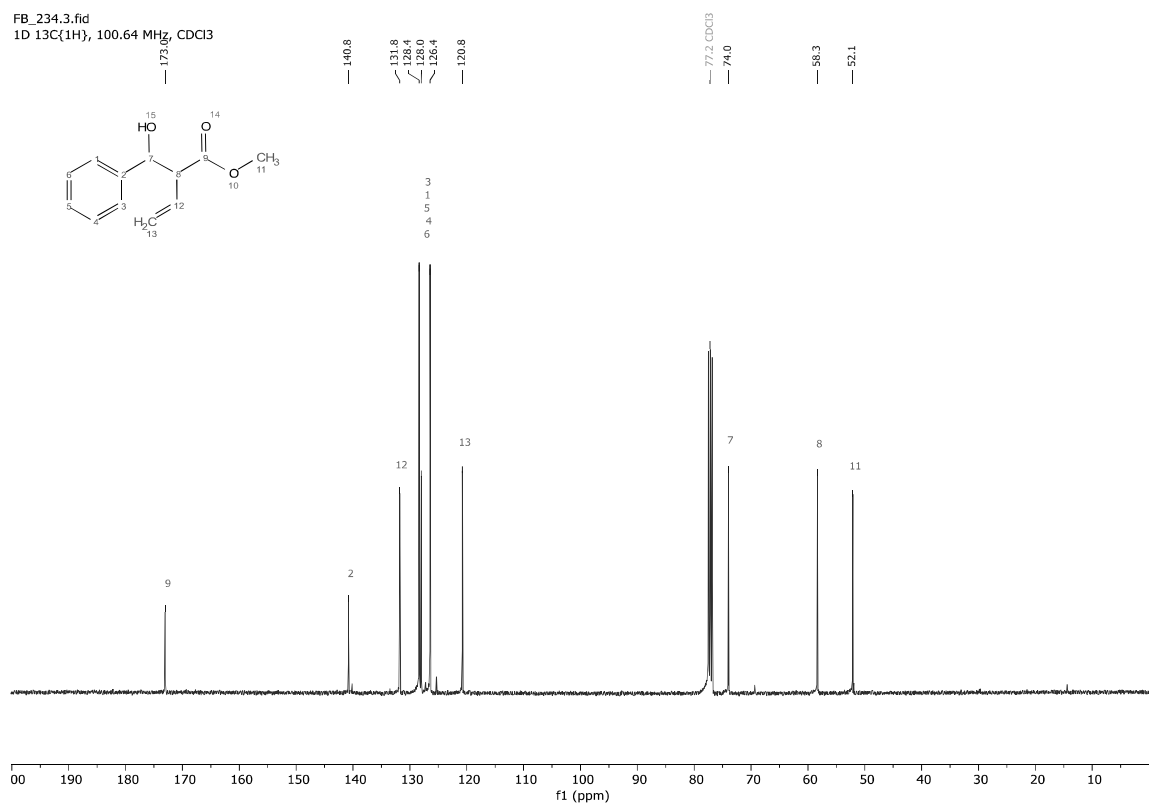


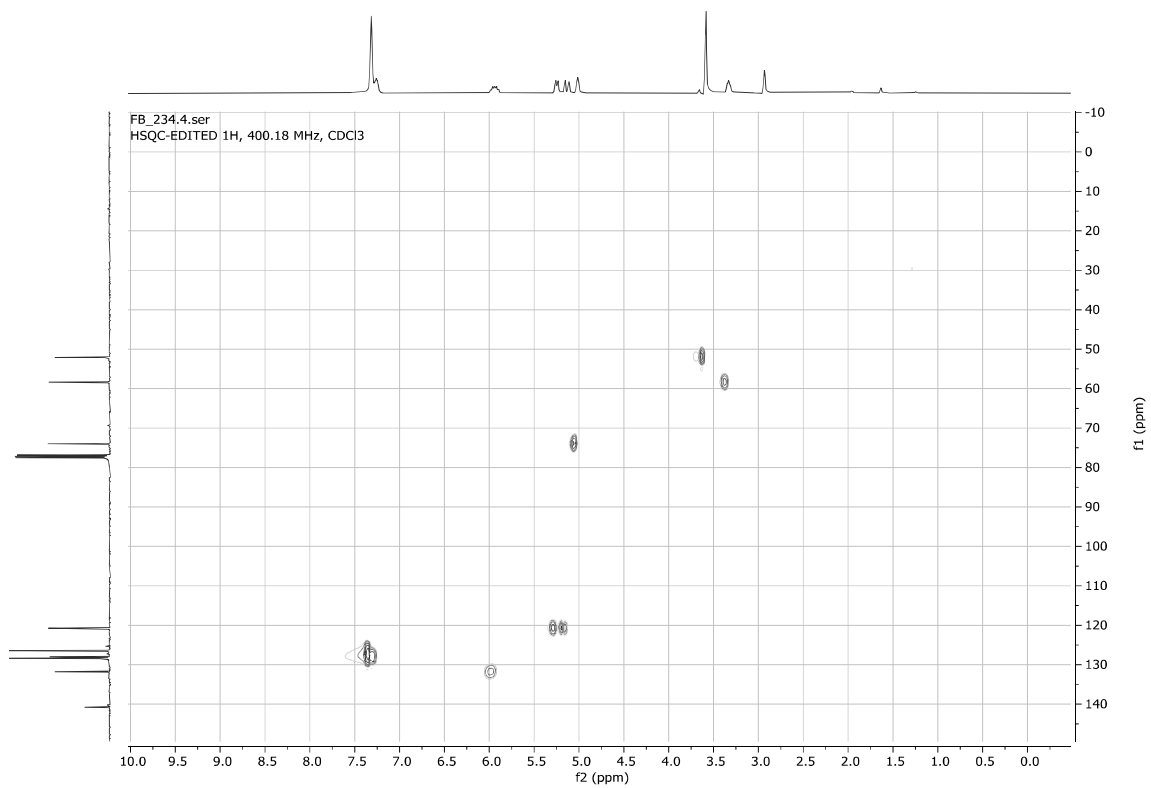
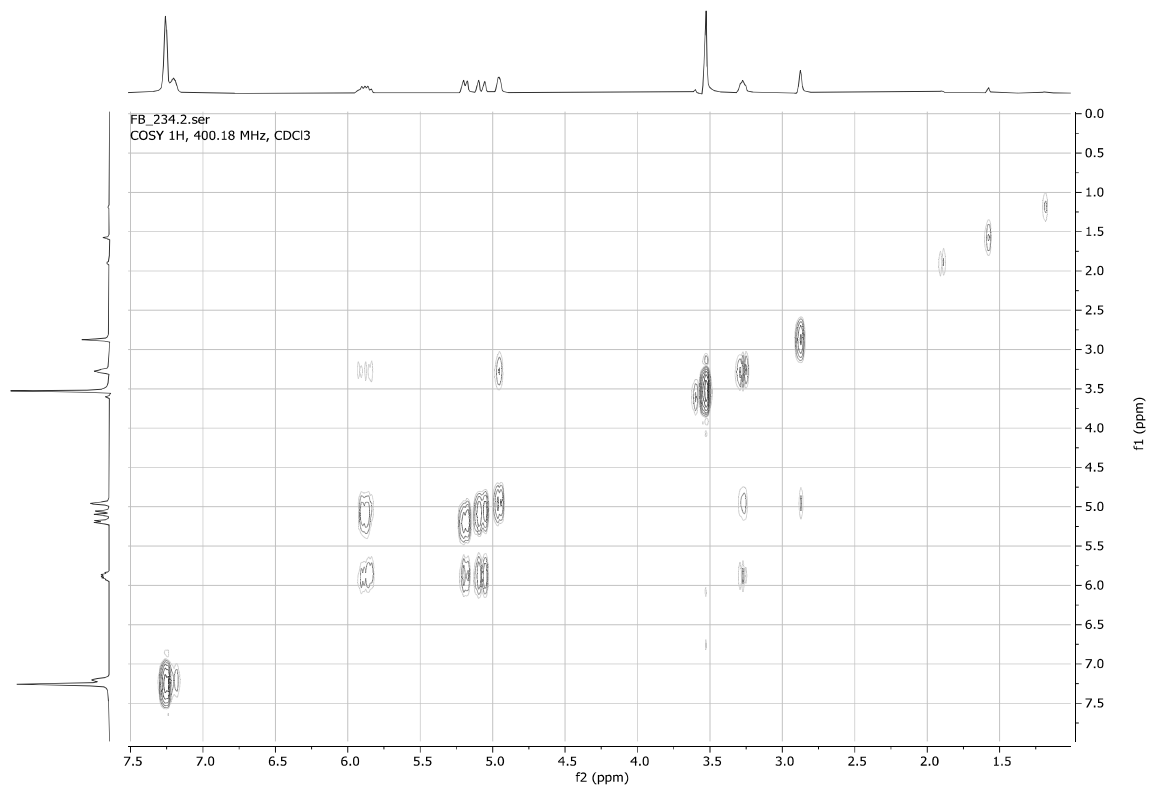
Methyl 2-(hydroxy(phenyl)methyl)but-3-enoate **6t**

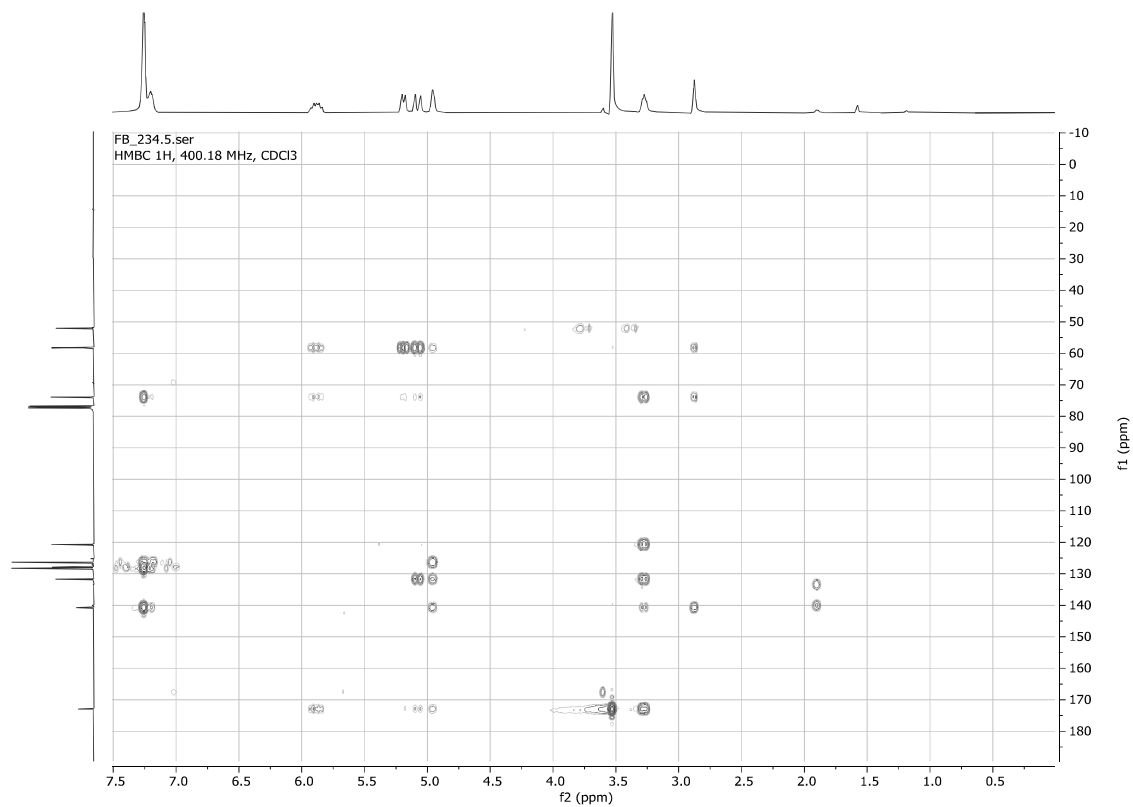
FB_234.1.fid
1D 1H, 400.18 MHz, CDCl₃



FB_234.3.fid
1D 13C(1H), 100.64 MHz, CDCl₃

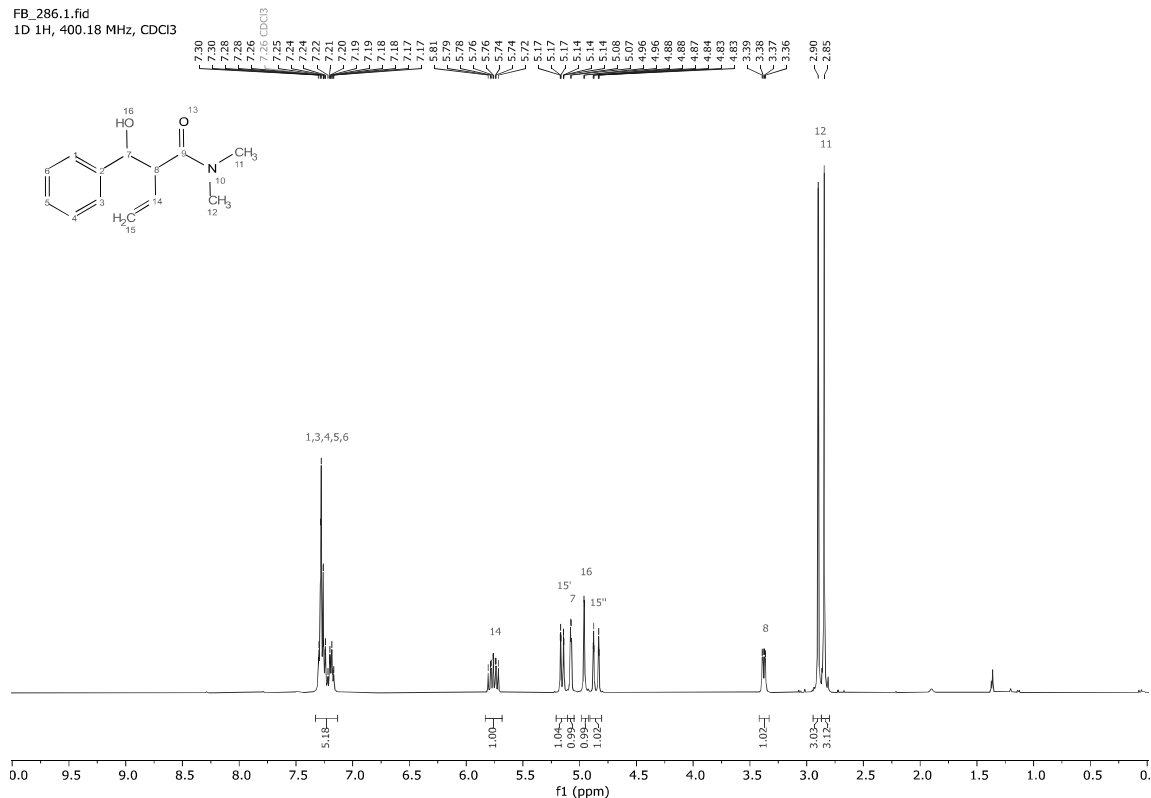




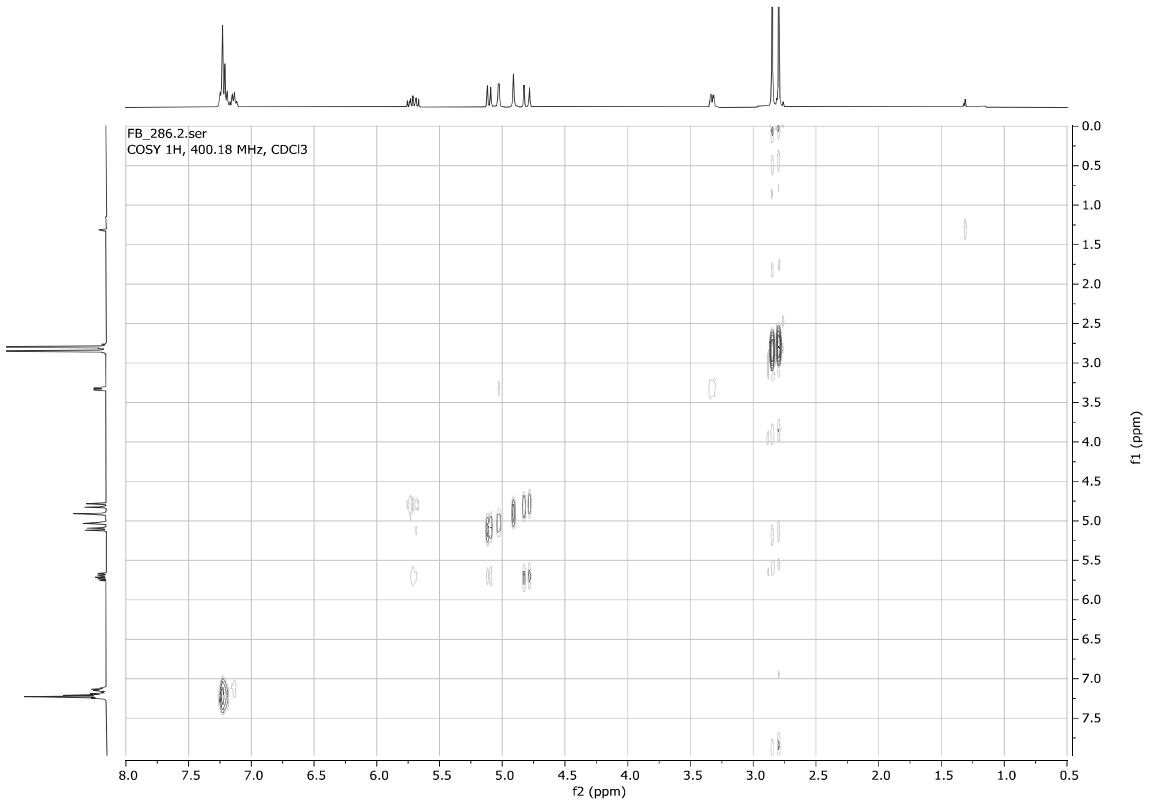
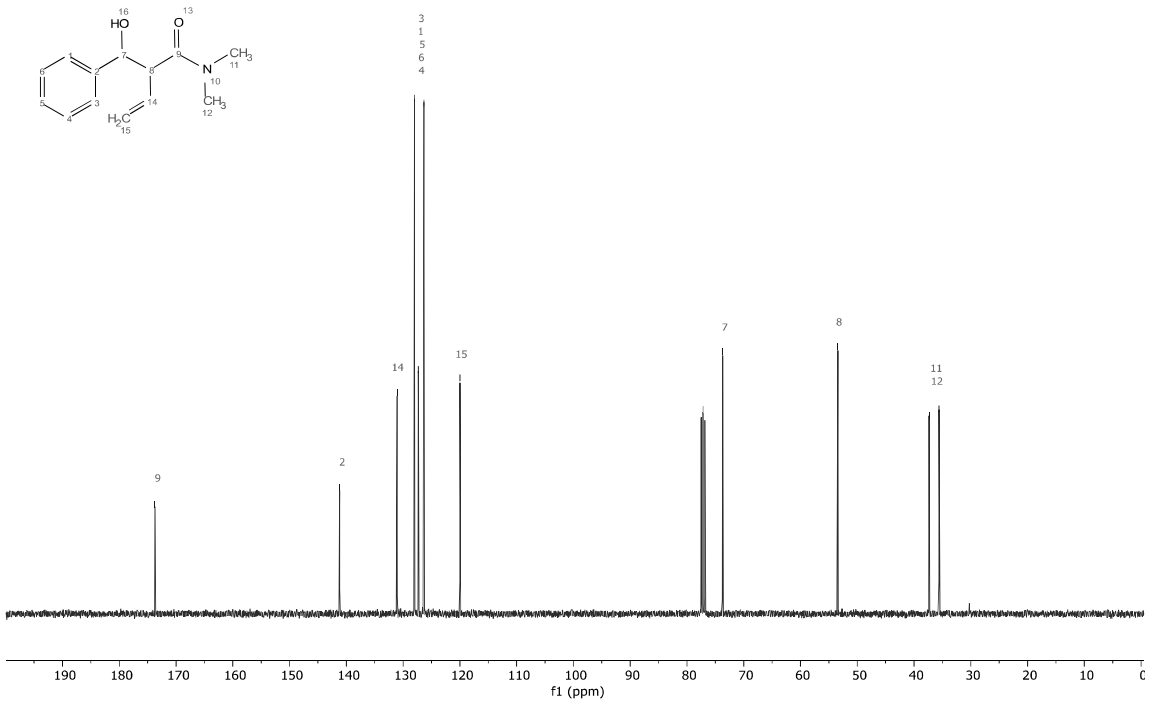


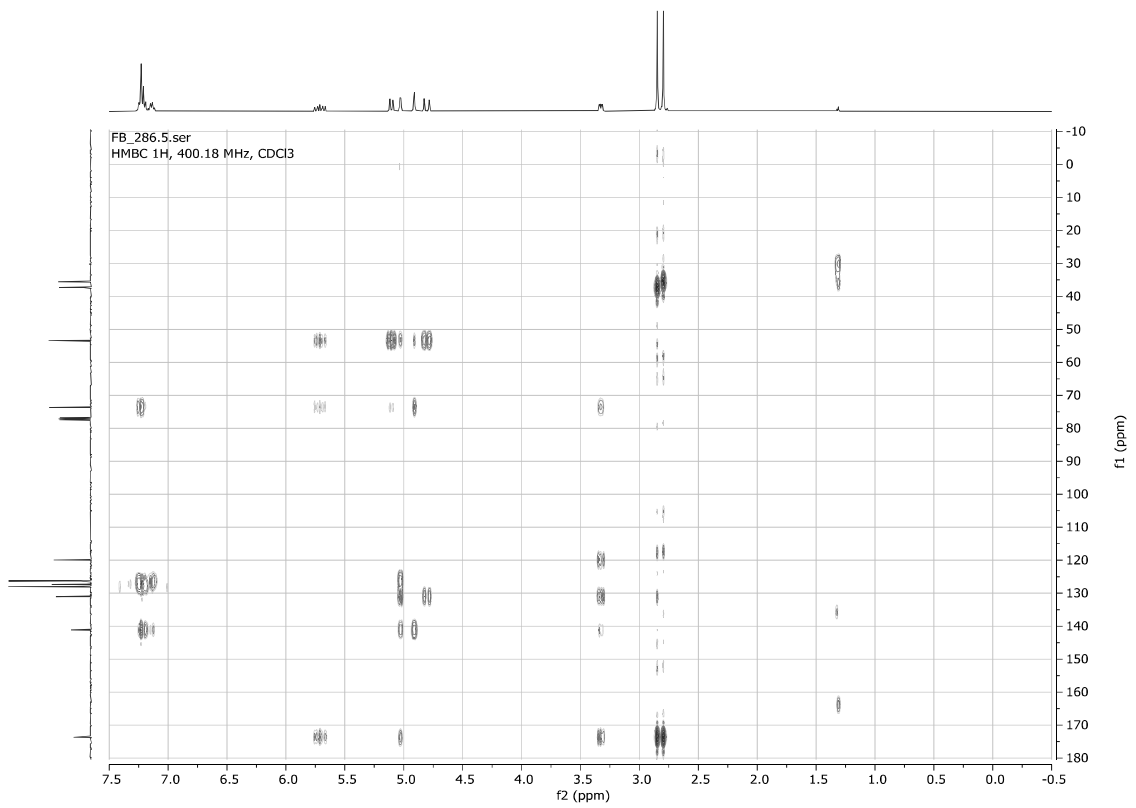
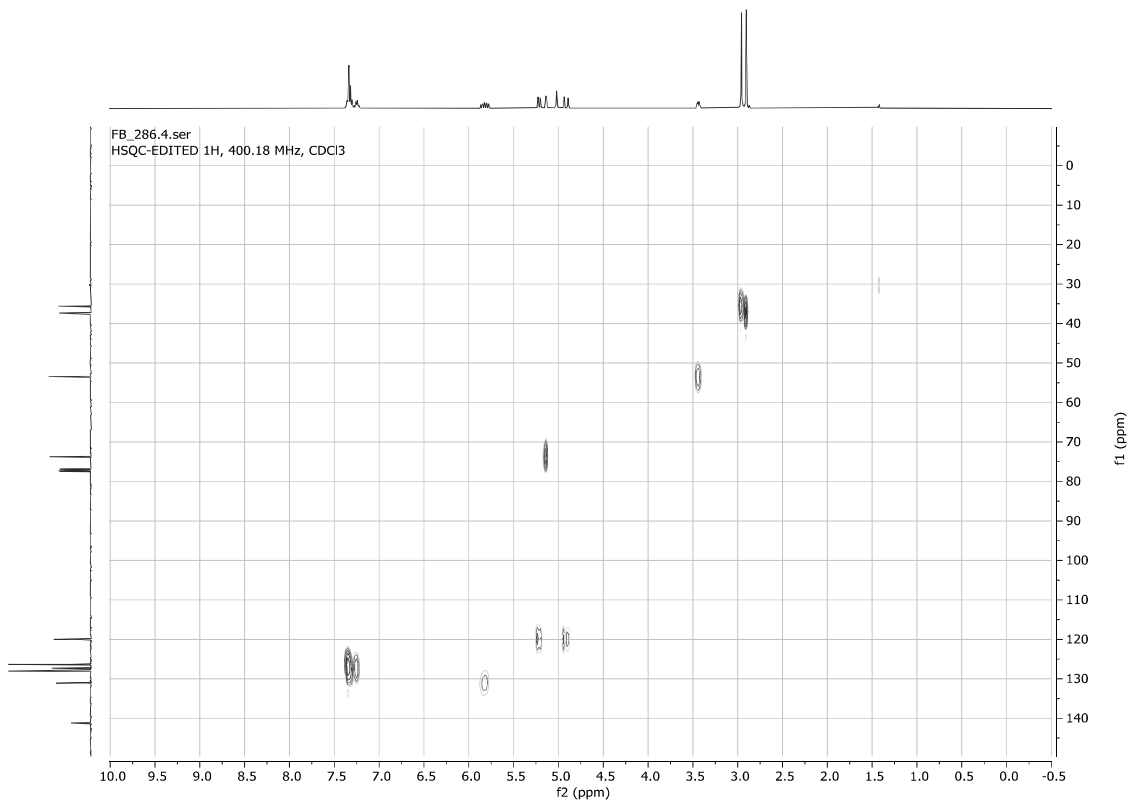
2-(Hydroxy(phenyl)methyl)-*N,N*-dimethylbut-3-enamide **6u**

FB_286.1.fid
1D 1H, 400.18 MHz, CDCl3



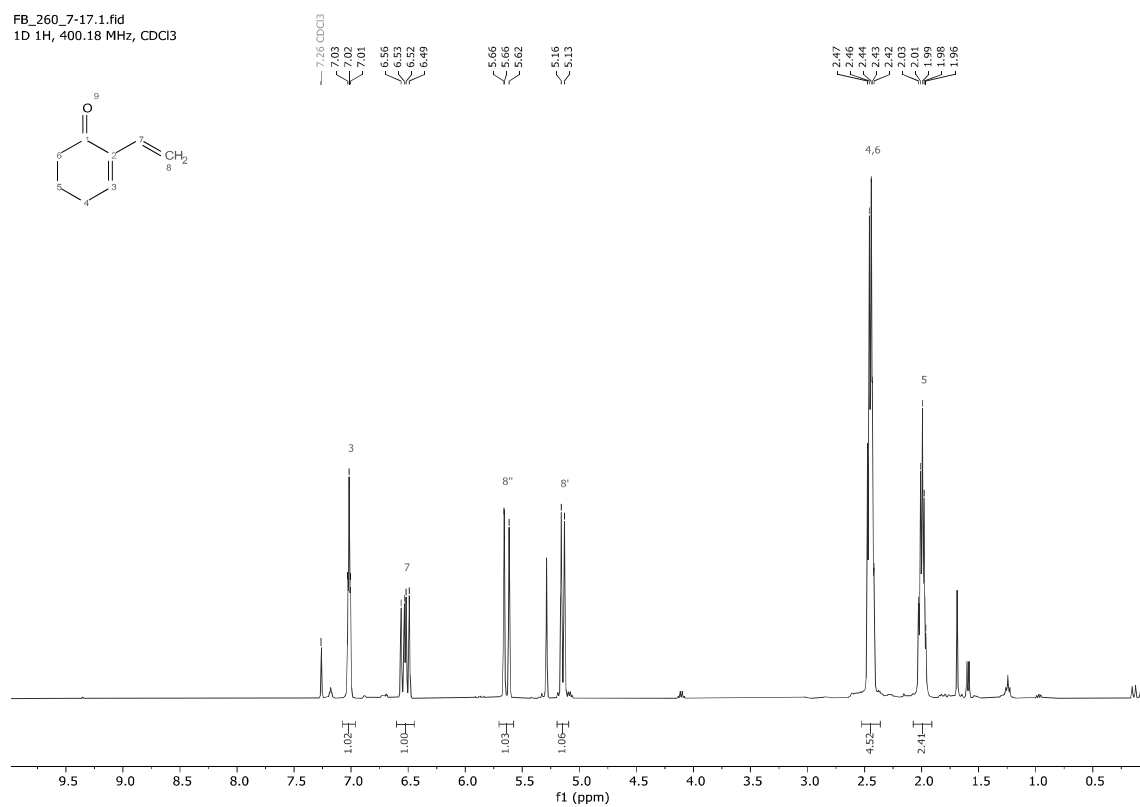
FB_286.3.fid
1D 13C{1H}, 100.64 MHz, CDCl3



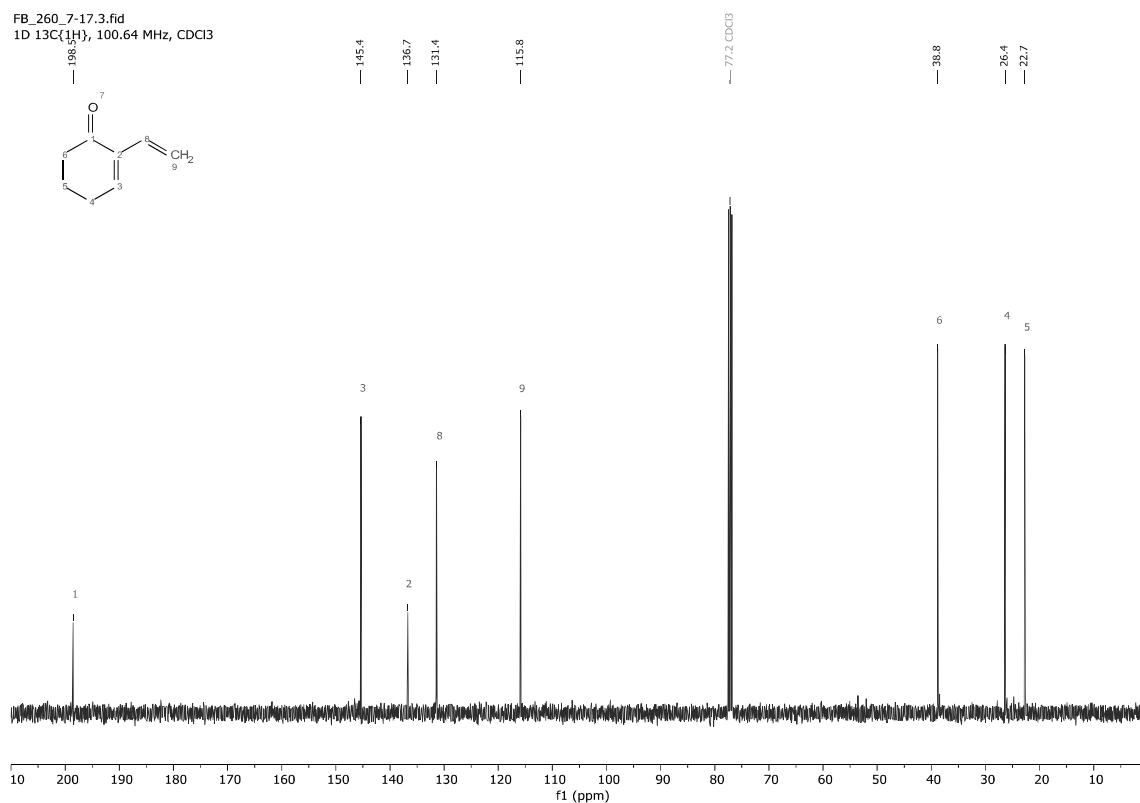


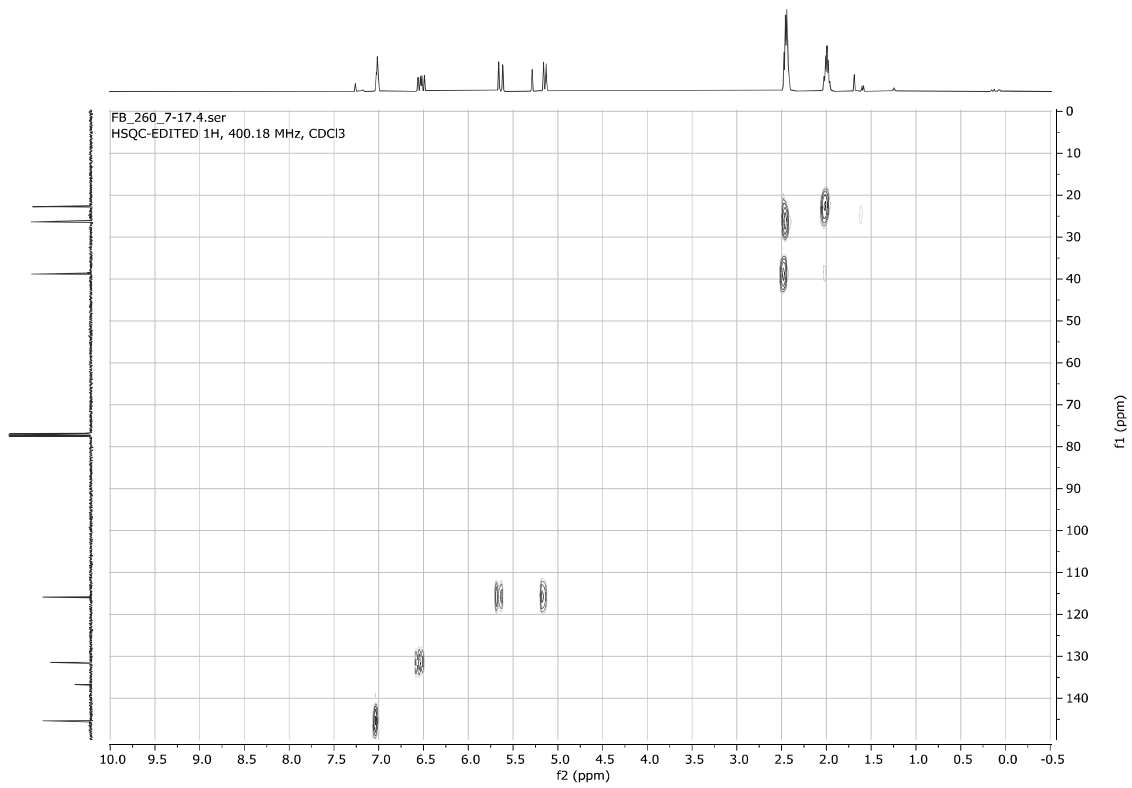
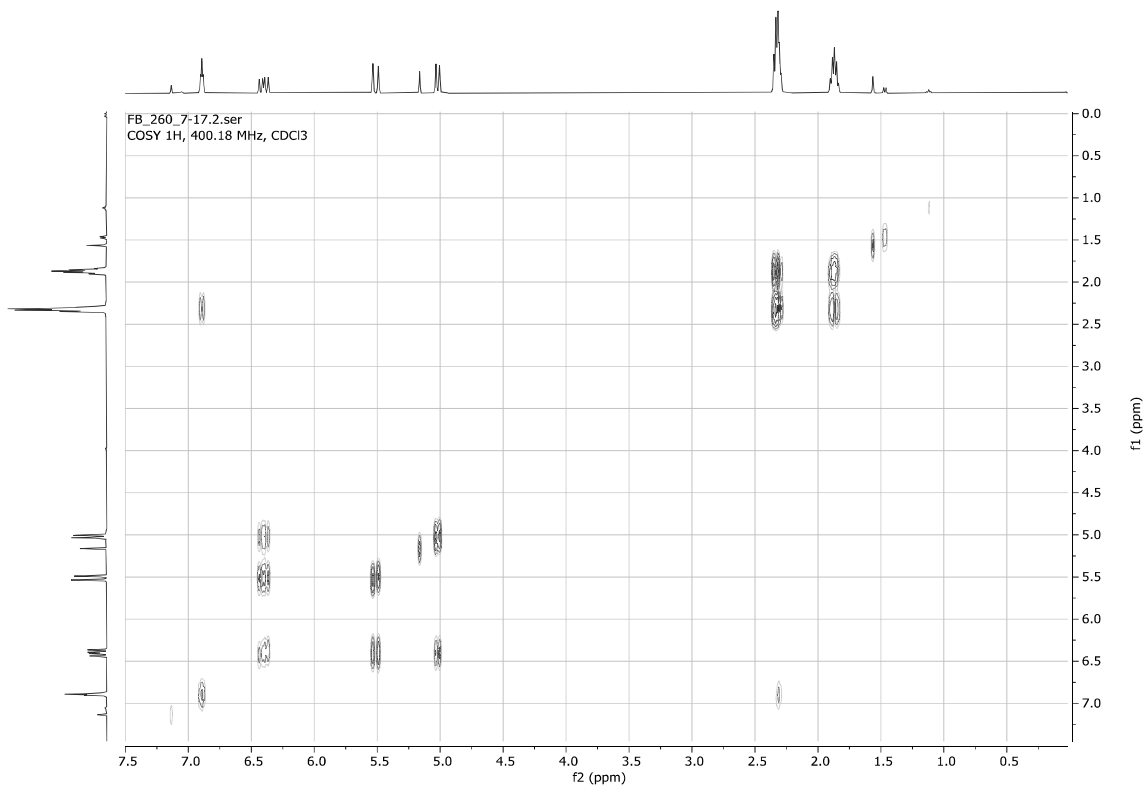
2-Vinyl-2-cyclohexenone **6v**

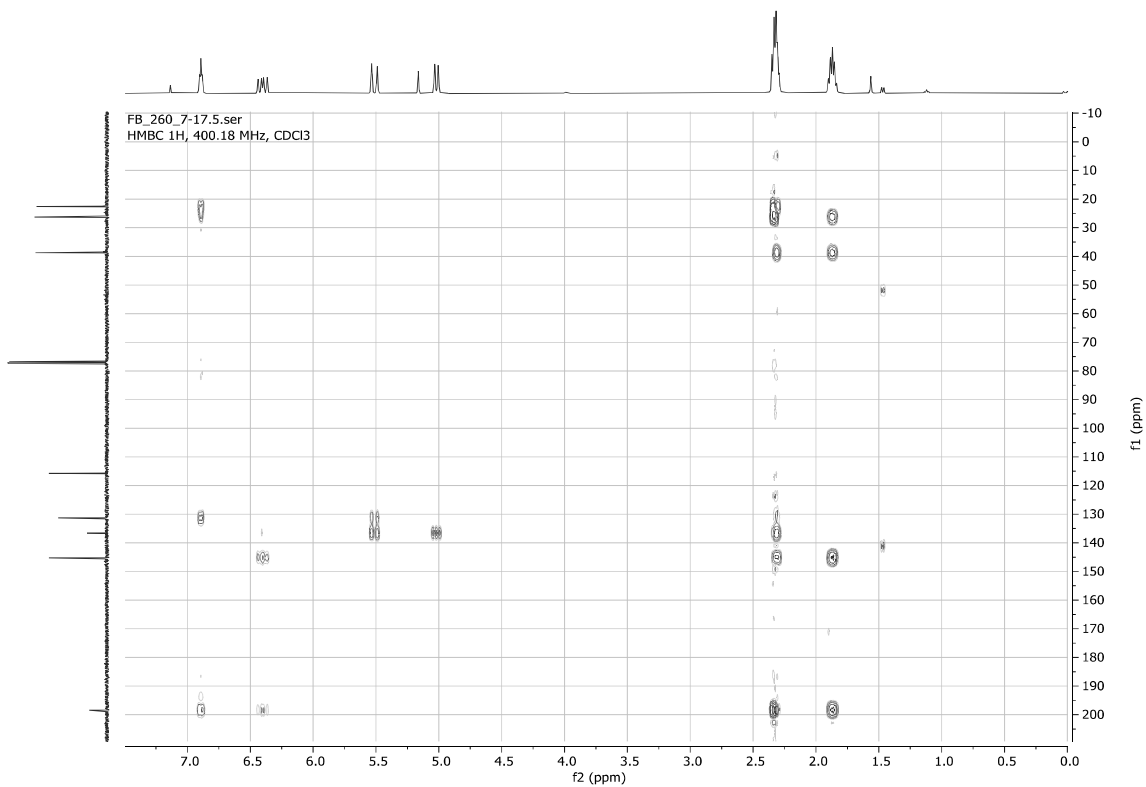
FB_260_7-17.1.fid
1D 1H, 400.18 MHz, CDCl₃



FB_260_7-17.3.fid
1D 13C(1H), 100.64 MHz, CDCl₃

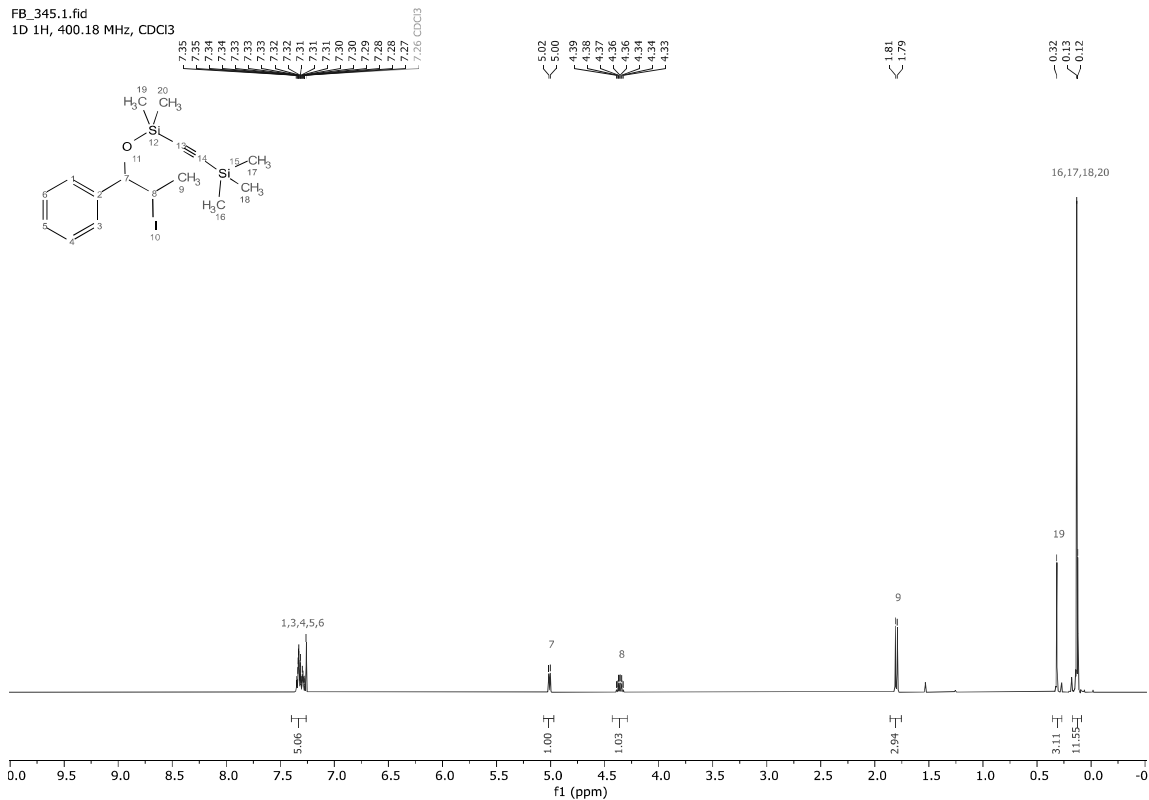




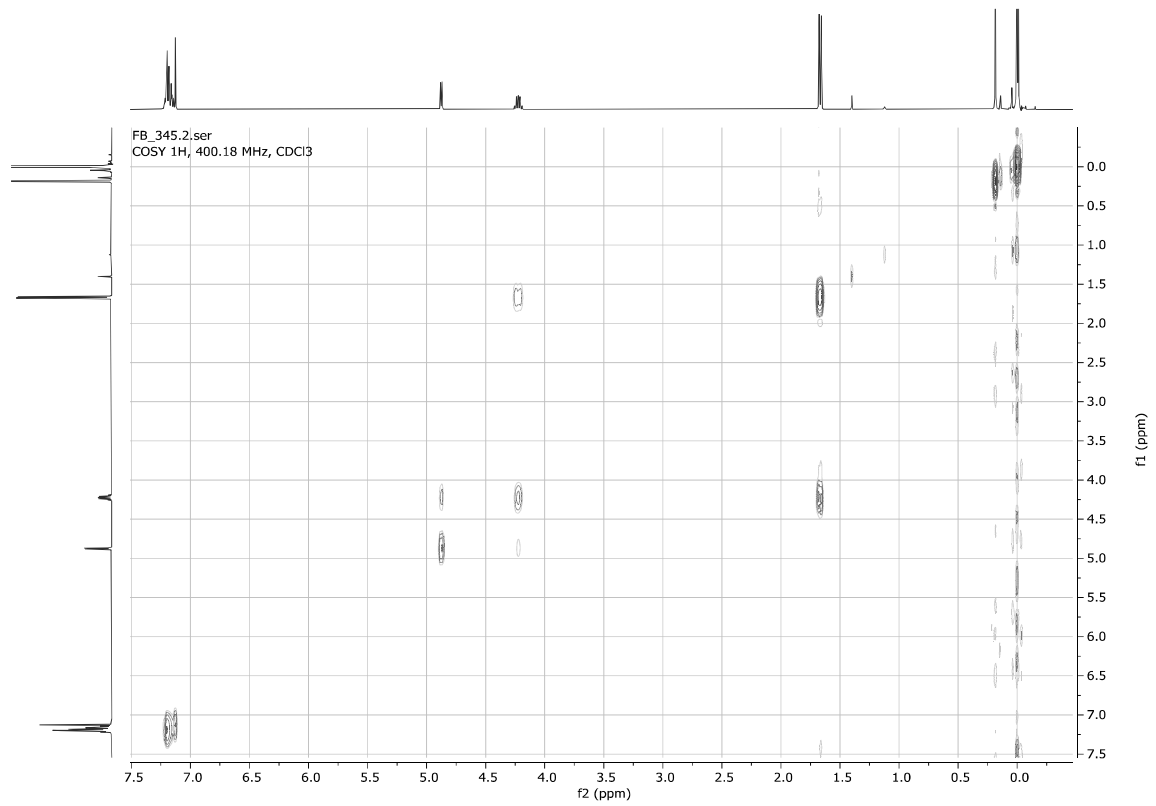
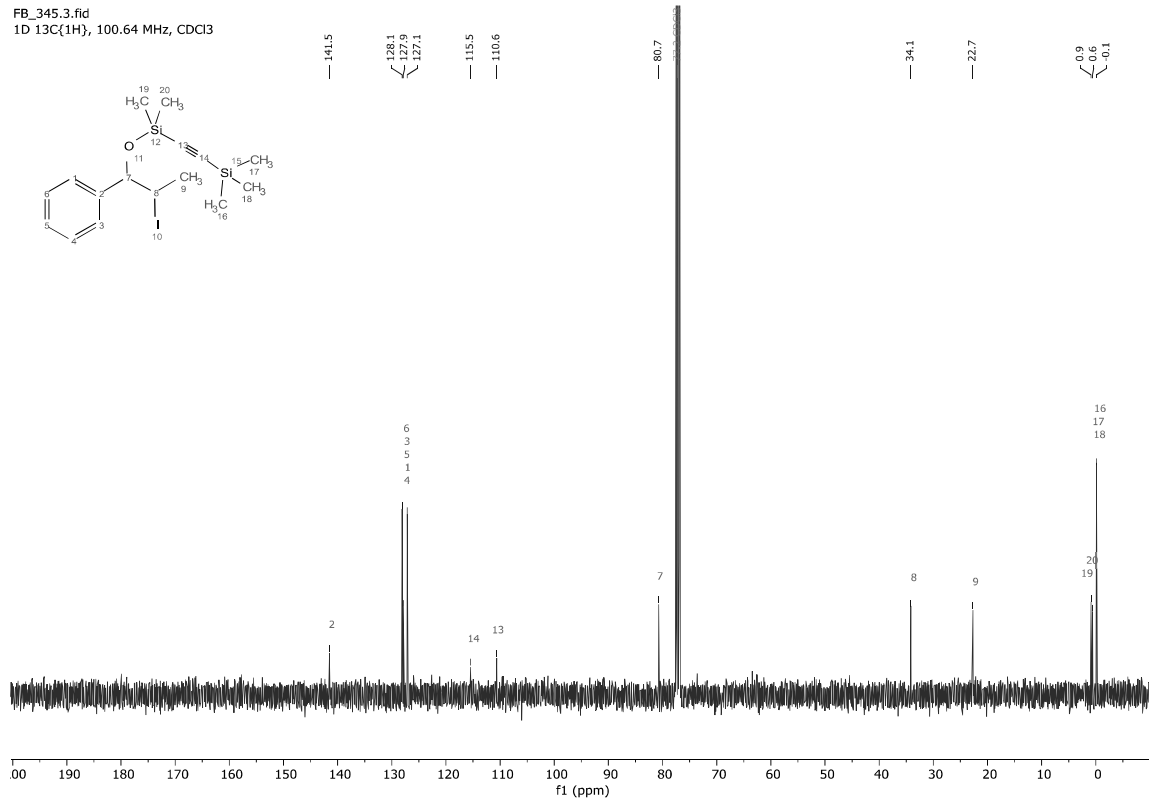


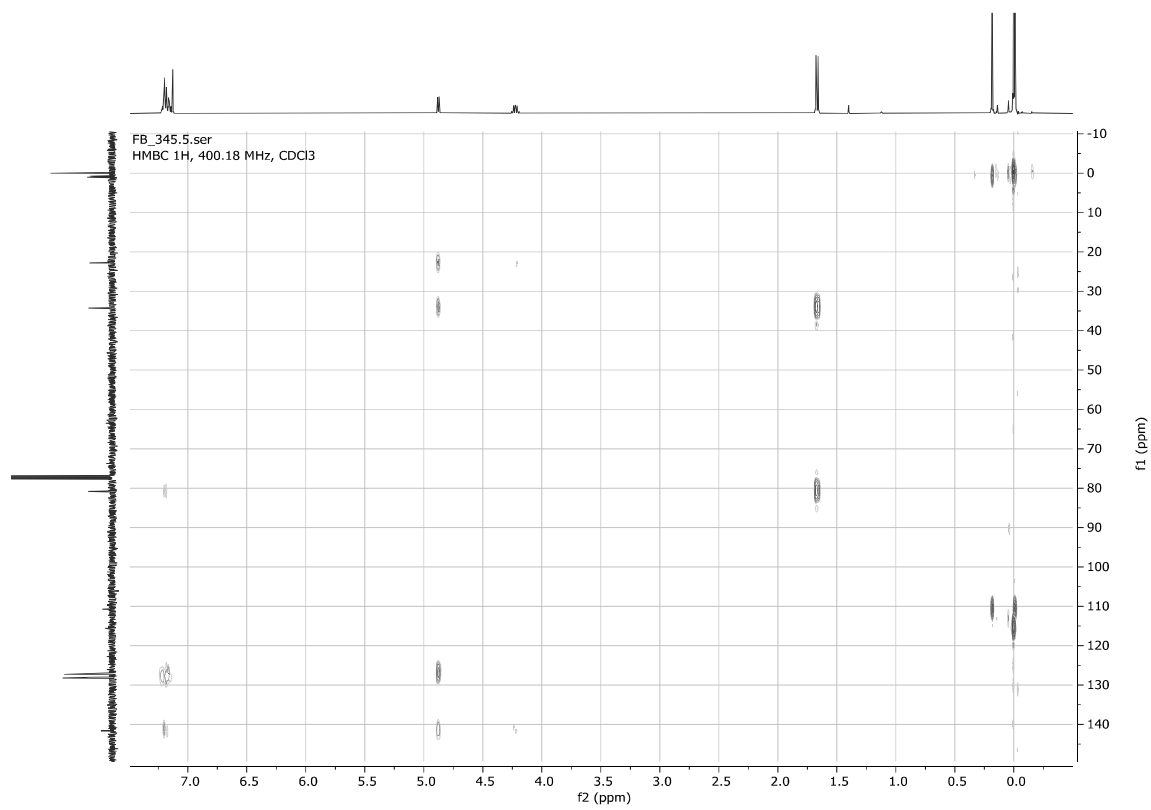
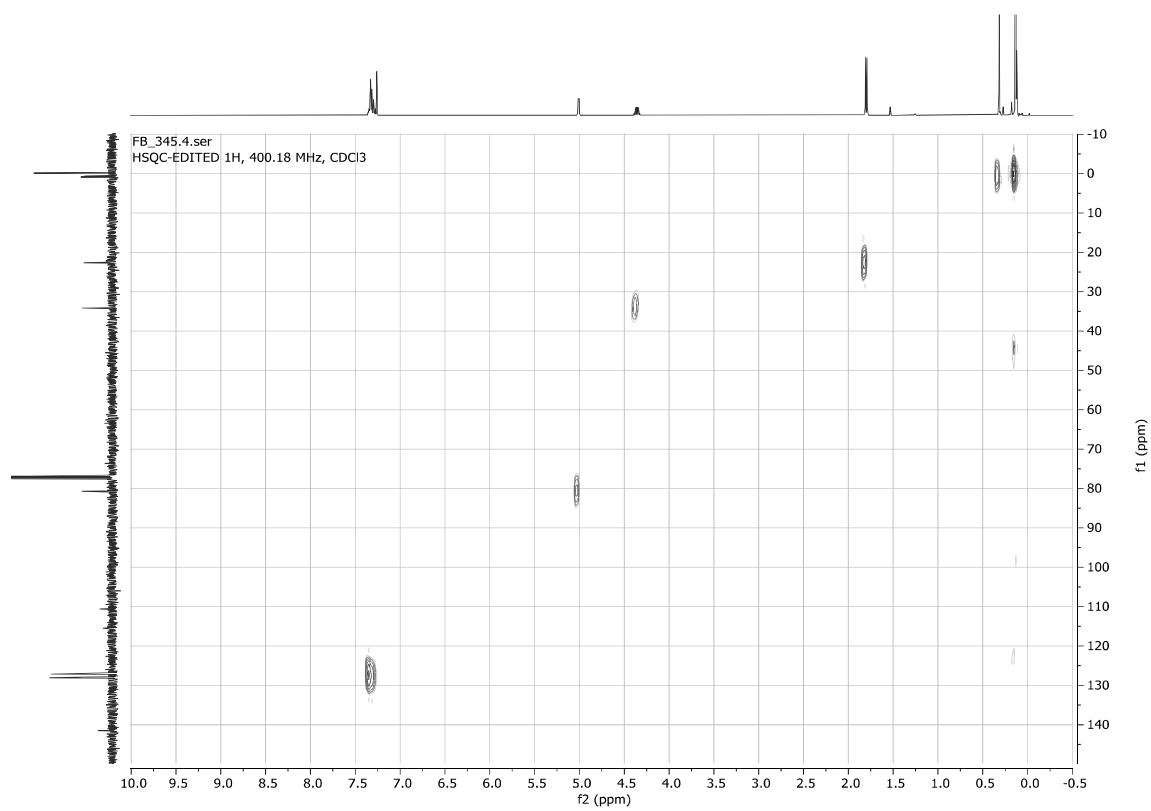
(2-Iodo-1-phenylpropoxy)dimethyl(trimethylsilyl)ethylsilane **7f**

FB_345.1.fid
1D 1H, 400.18 MHz, CDCl3



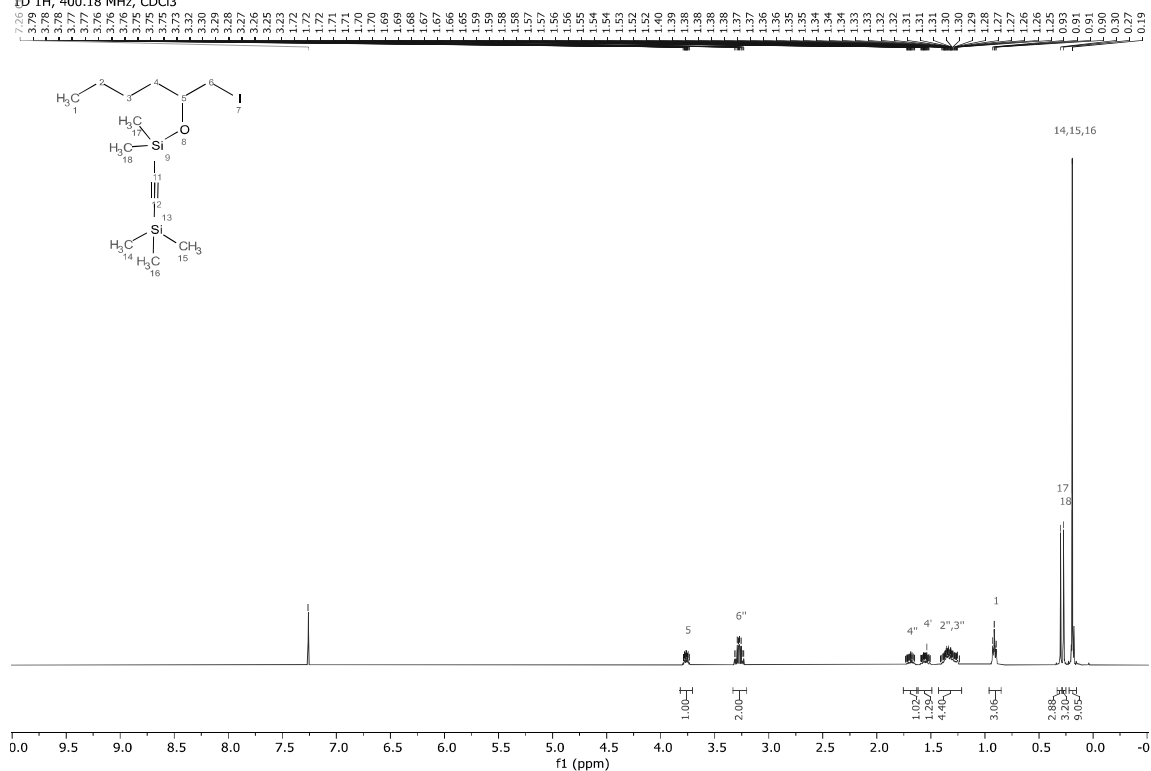
FB_345.3.fid
1D 13C{1H}, 100.64 MHz, CDCl3



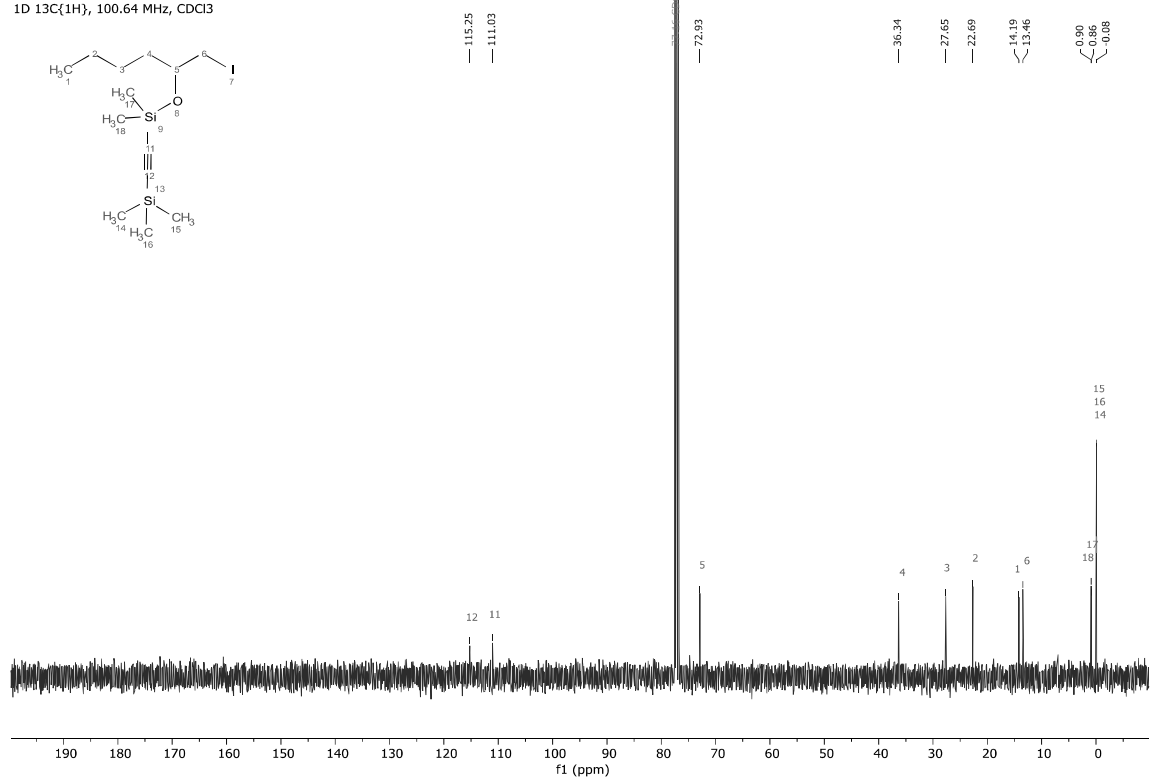


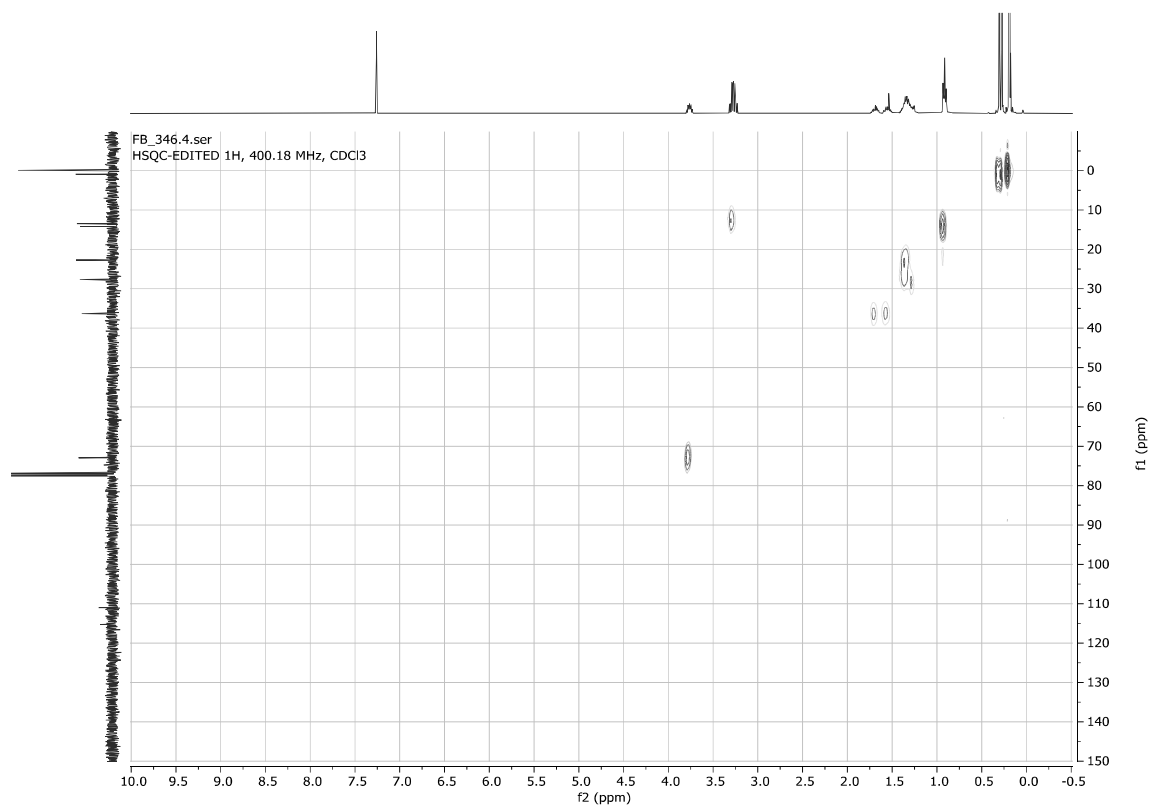
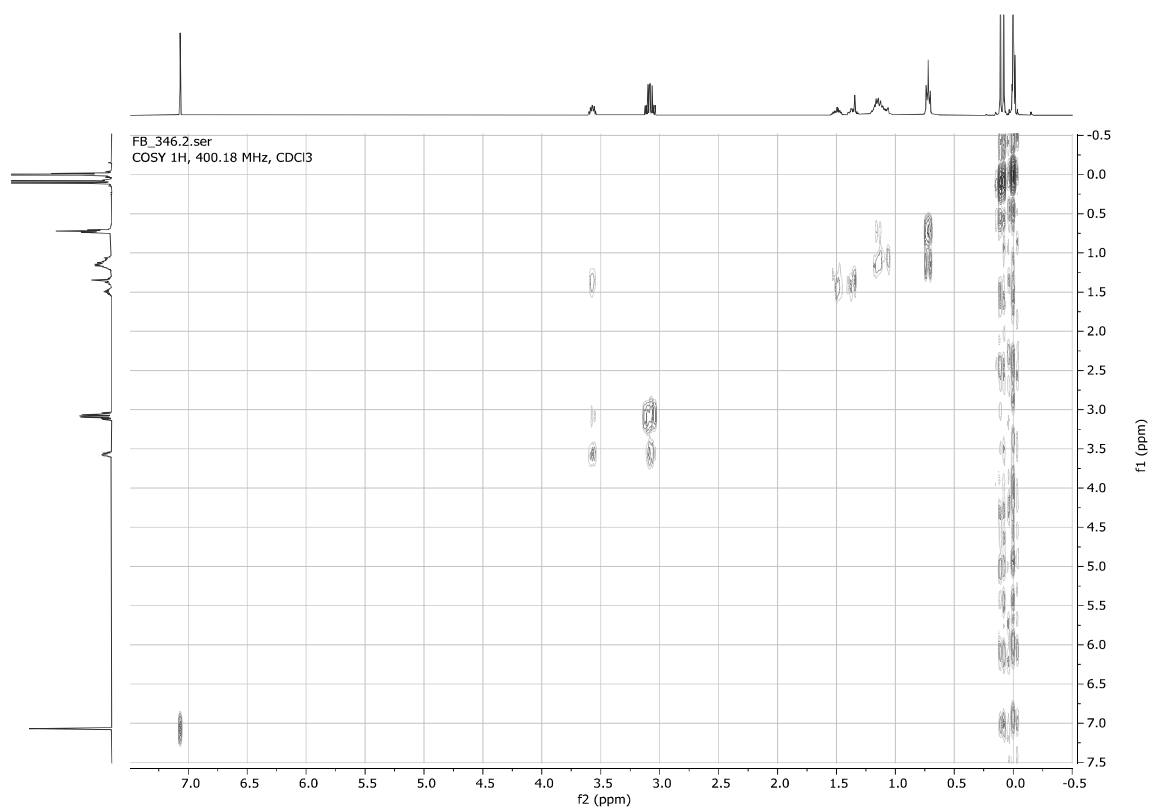
((1-Iodohexan-2-yl)oxy)dimethyl(trimethylsilyl)ethynylsilane 7k

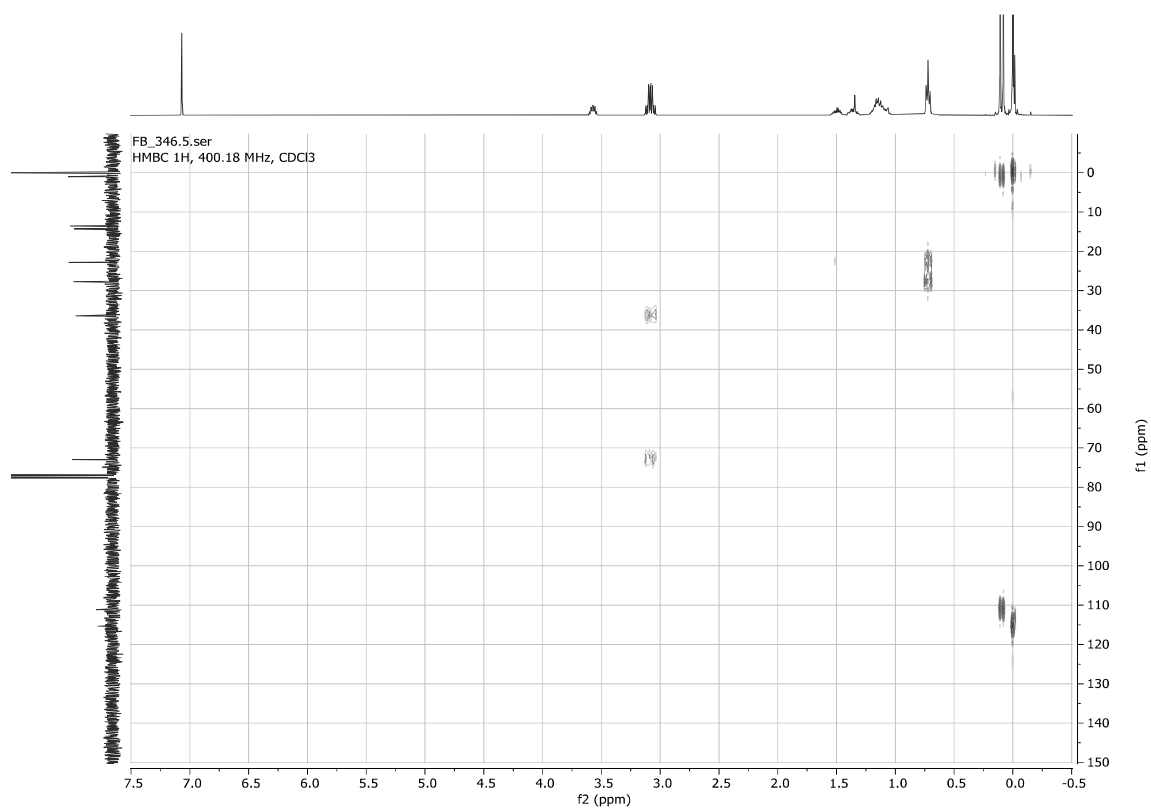
FB_346.1.fid
1D 1H, 400.18 MHz, CDCl3



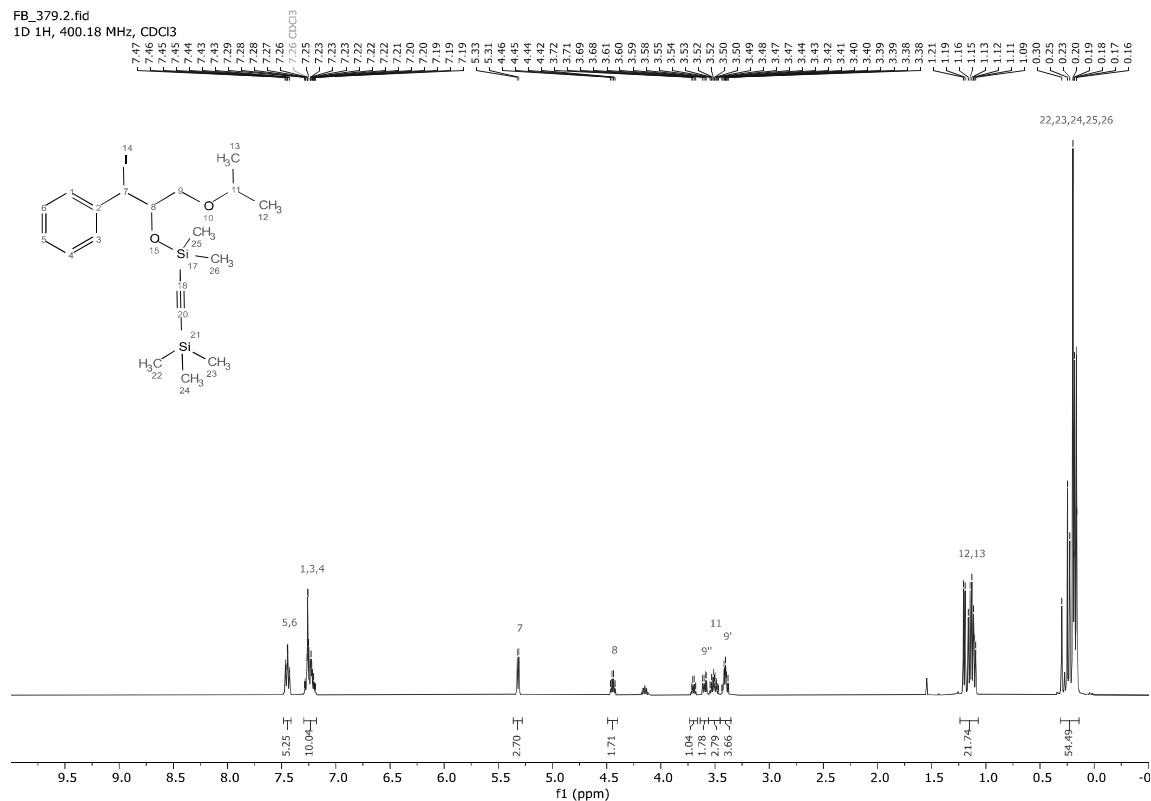
FB_346.3.fid
1D 13C(1H), 100.64 MHz, CDCl3



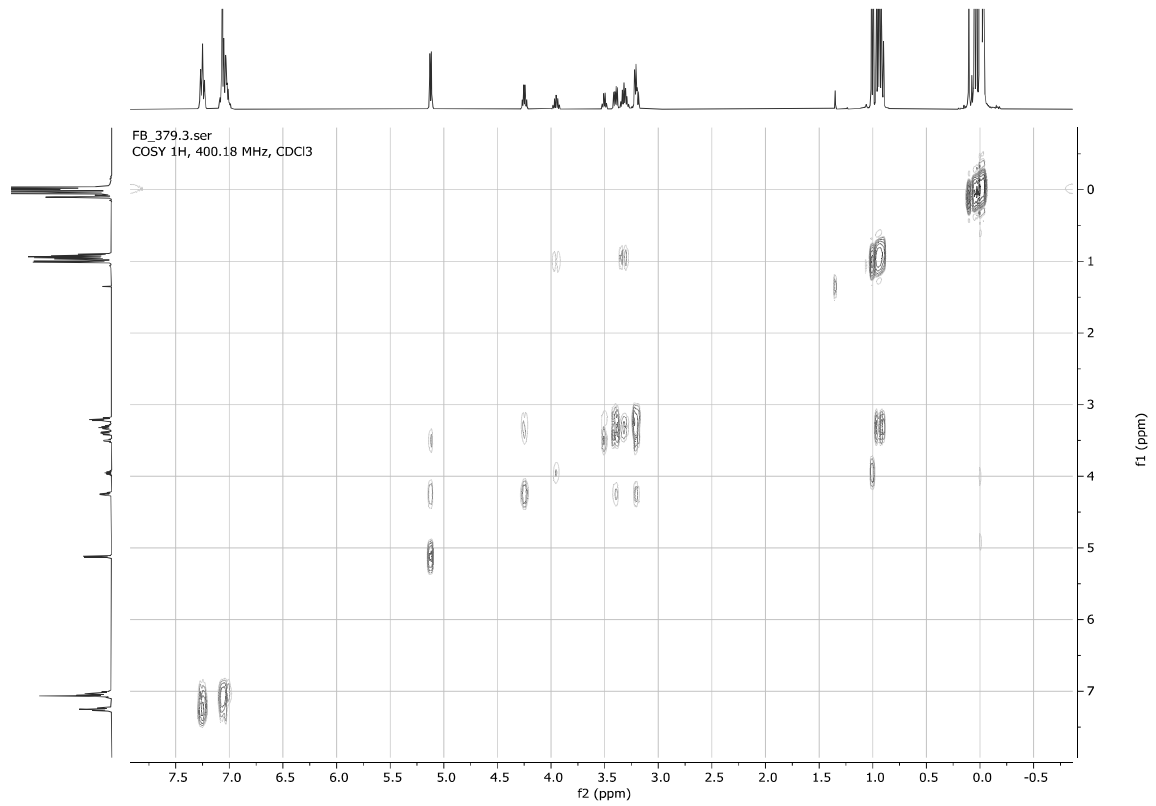
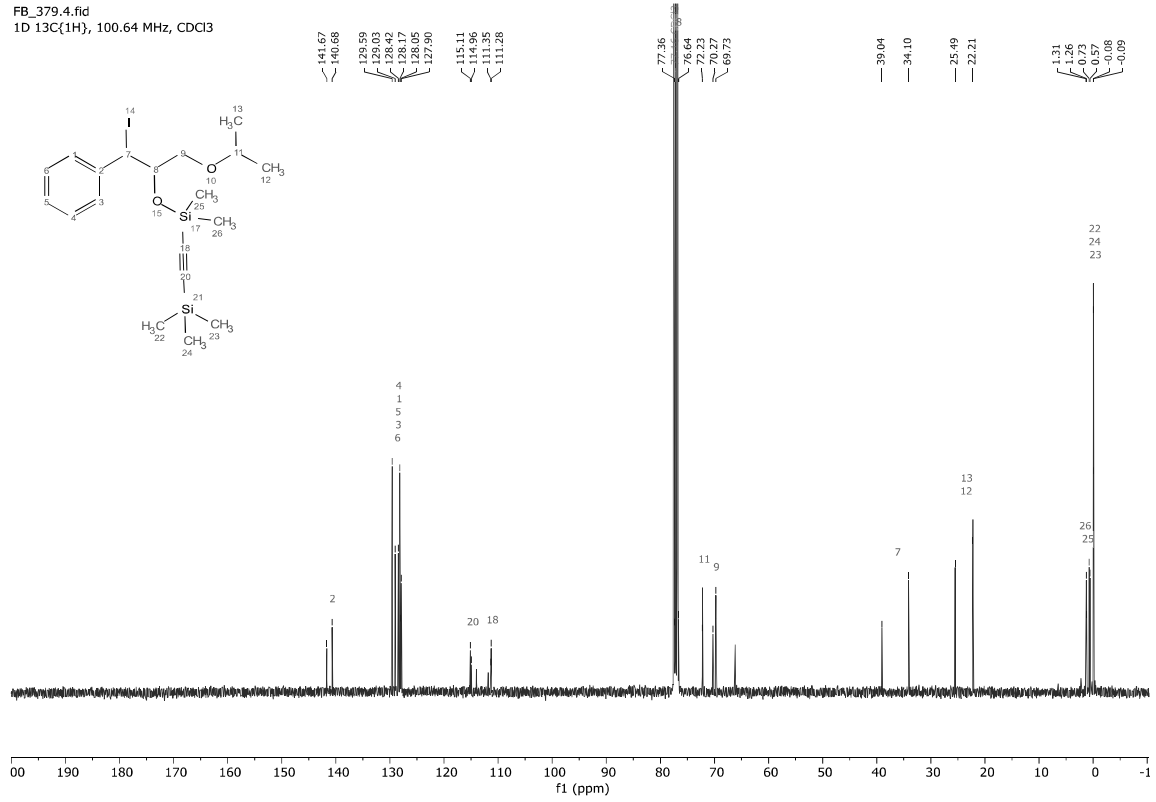


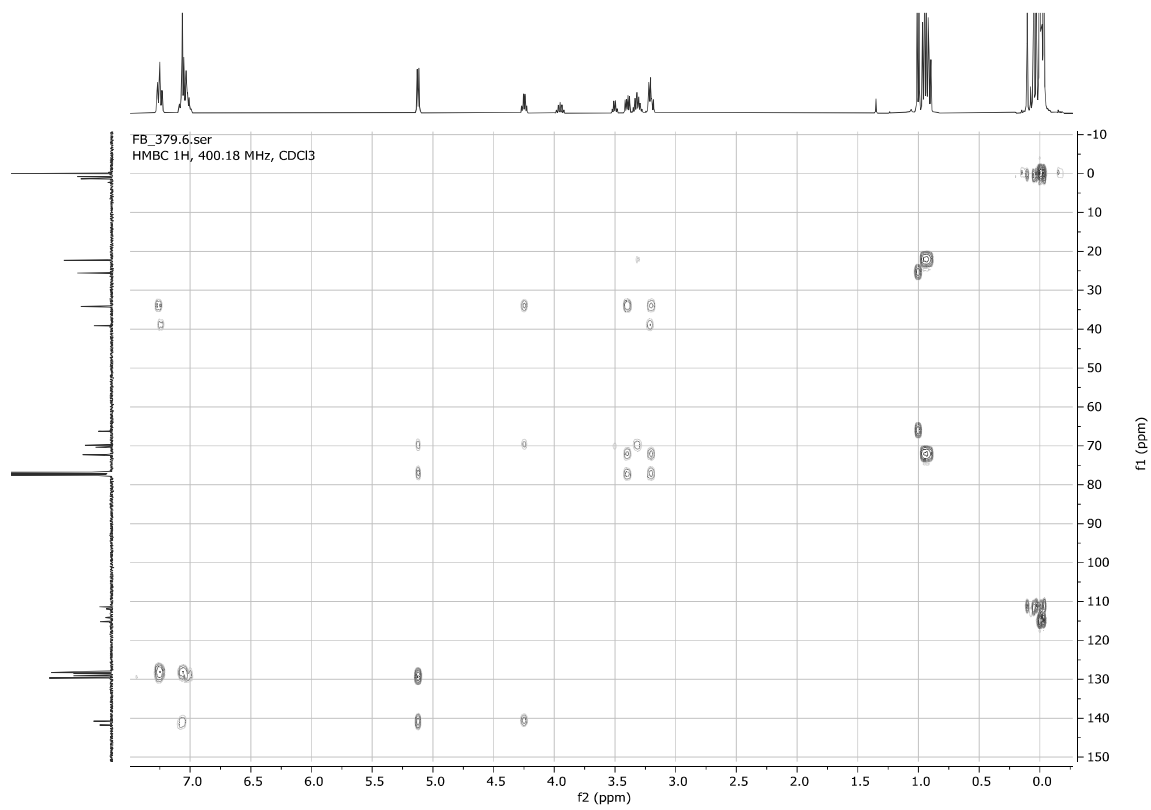
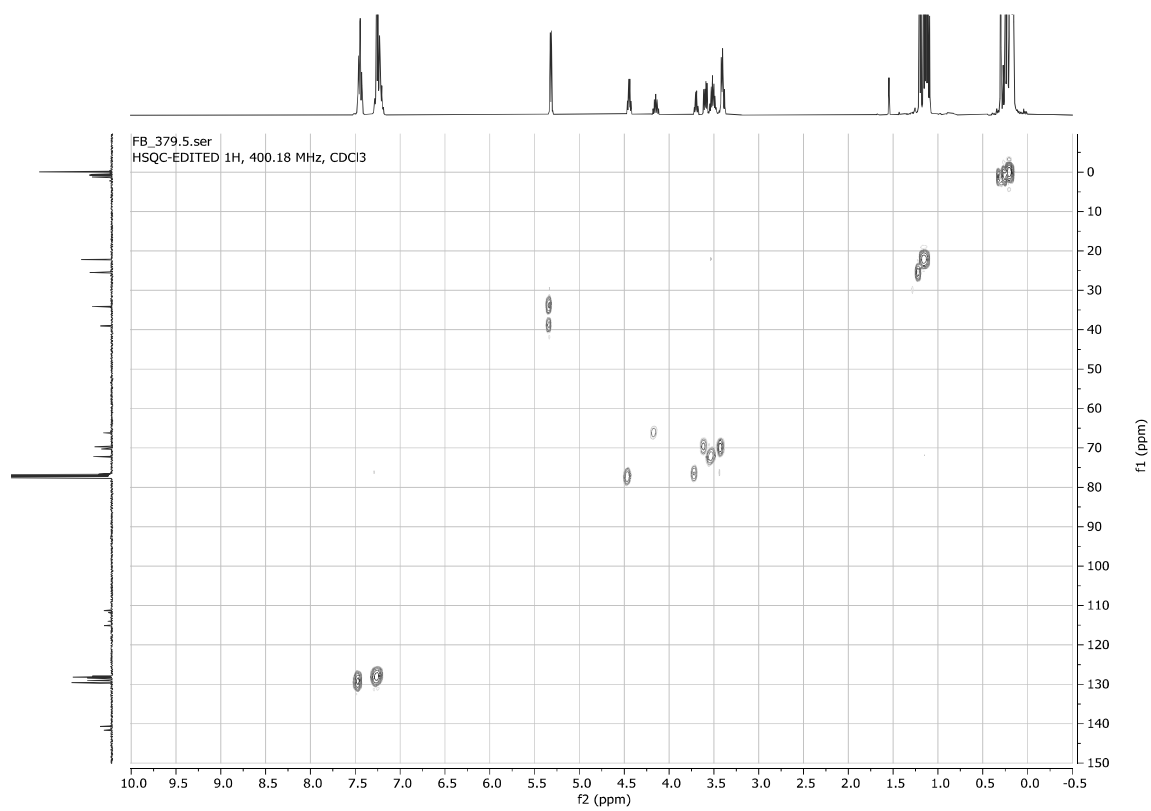


((1-Iodo-3-isopropoxy-1-phenylpropan-2-yl)oxy)dimethyl(trimethylsilyl)ethynylsilane **7s** (*inseparable 62:38 diastereomers mixture*)



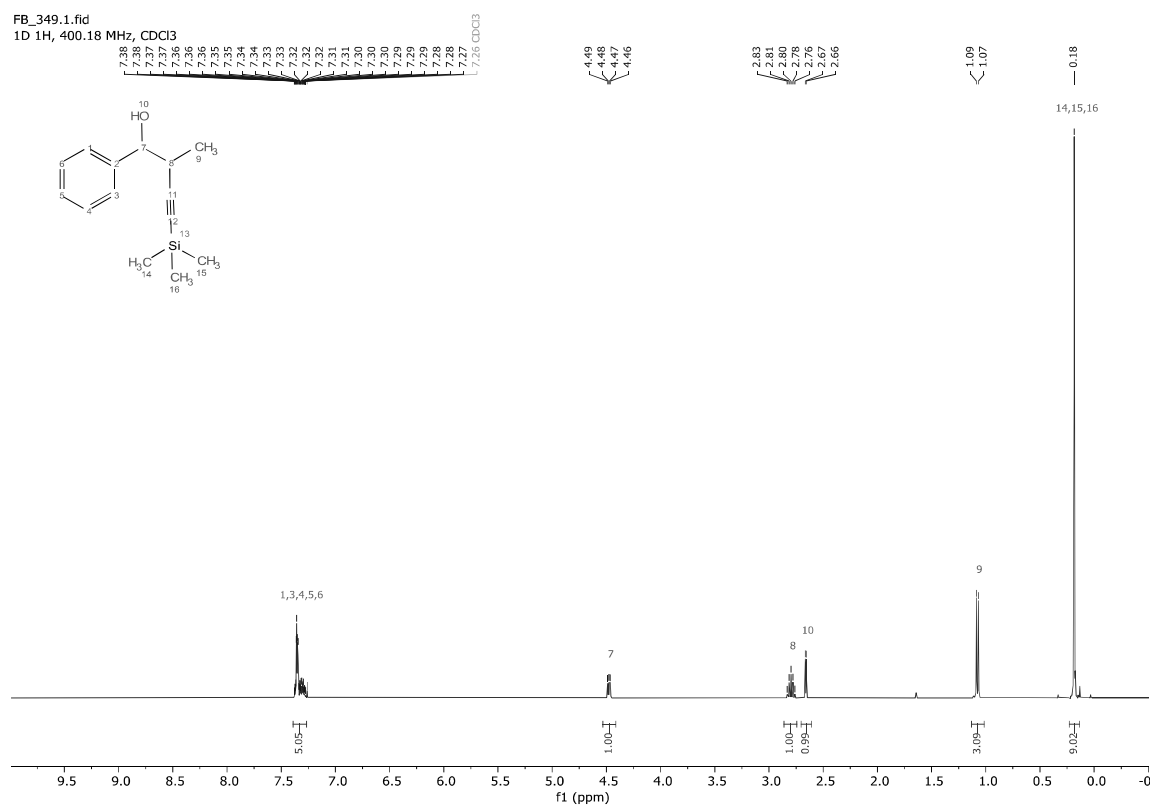
FB_379.4.fid
1D 13C{1H}, 100.64 MHz, CDCl3



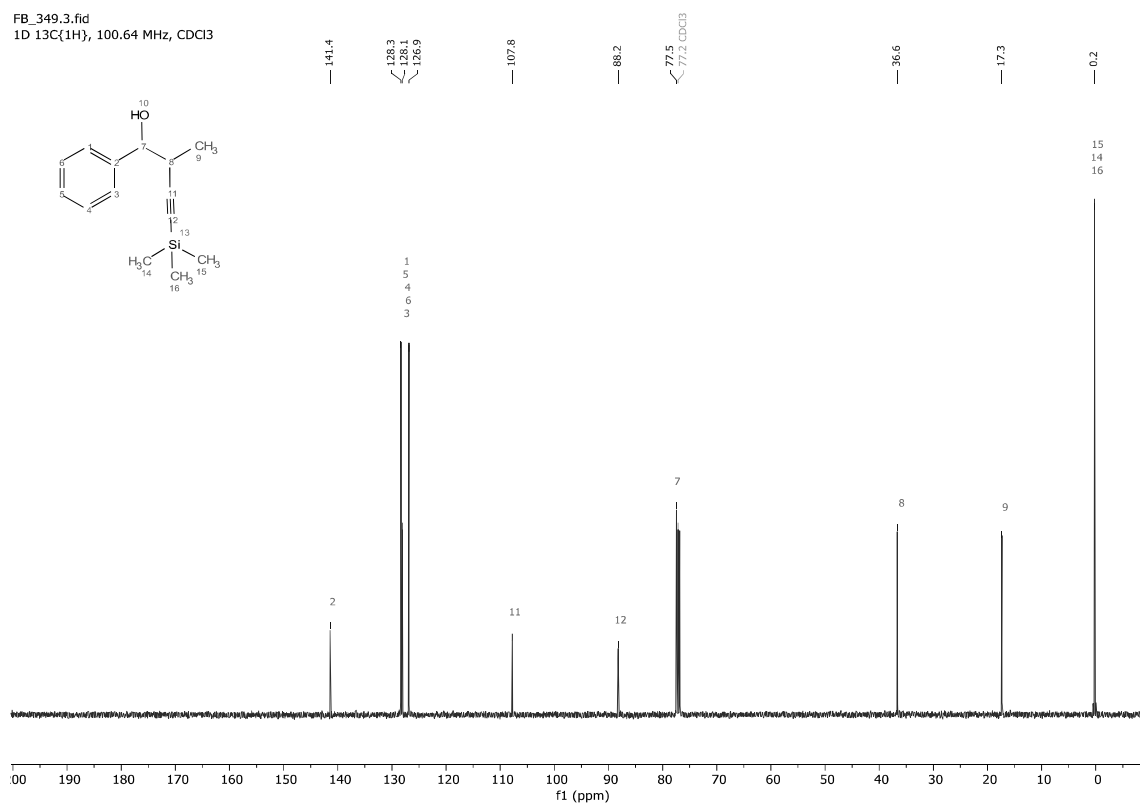


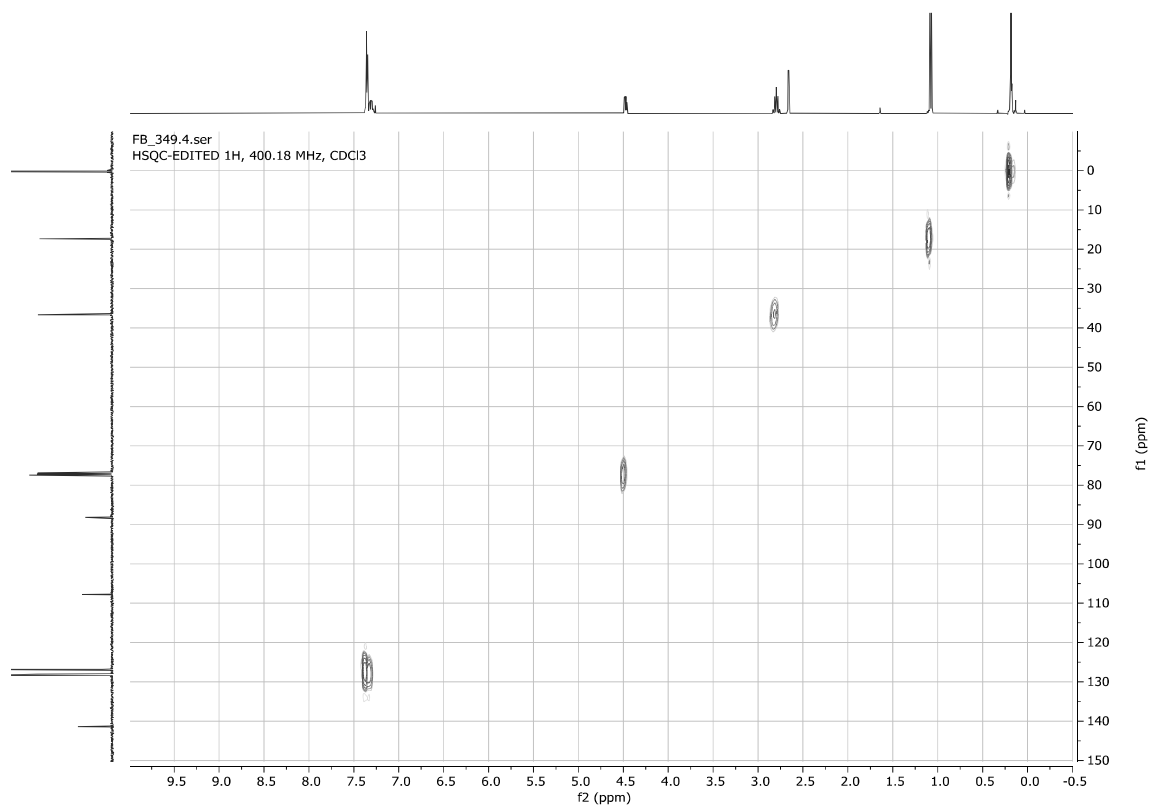
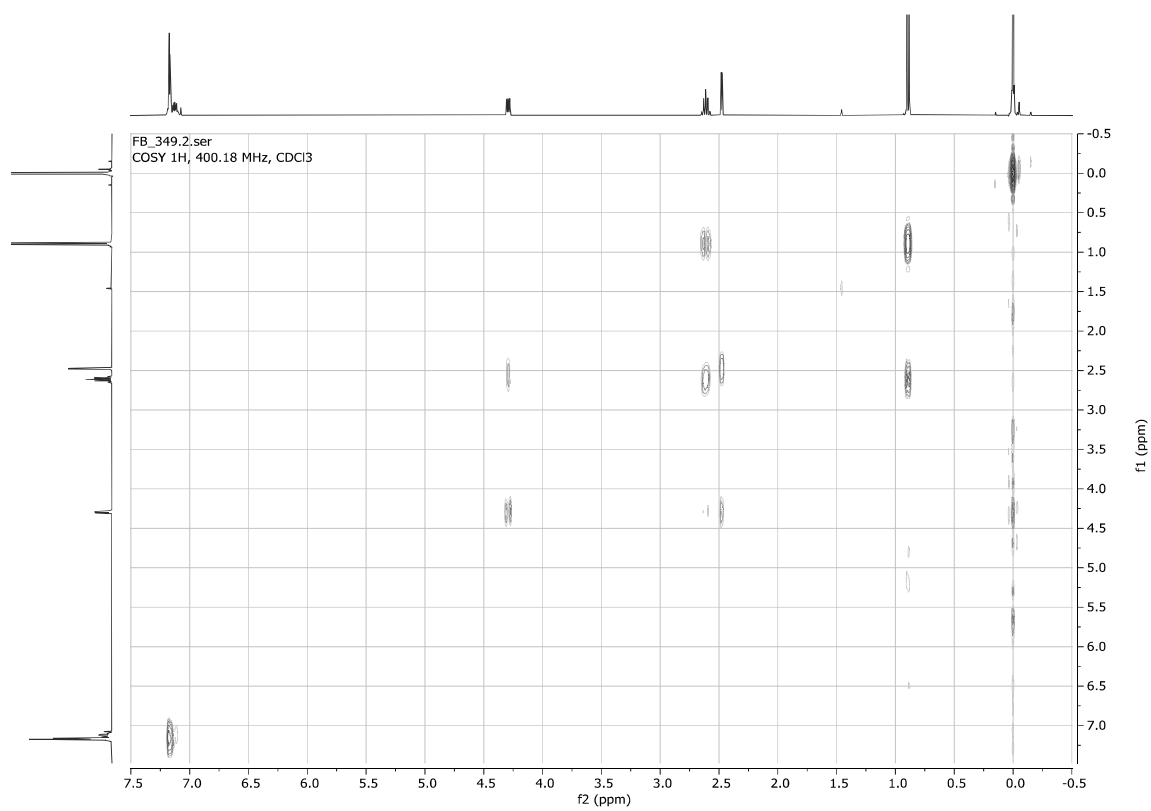
2-Methyl-1-phenyl-4-(trimethylsilyl)but-3-yn-1-ol **8f**

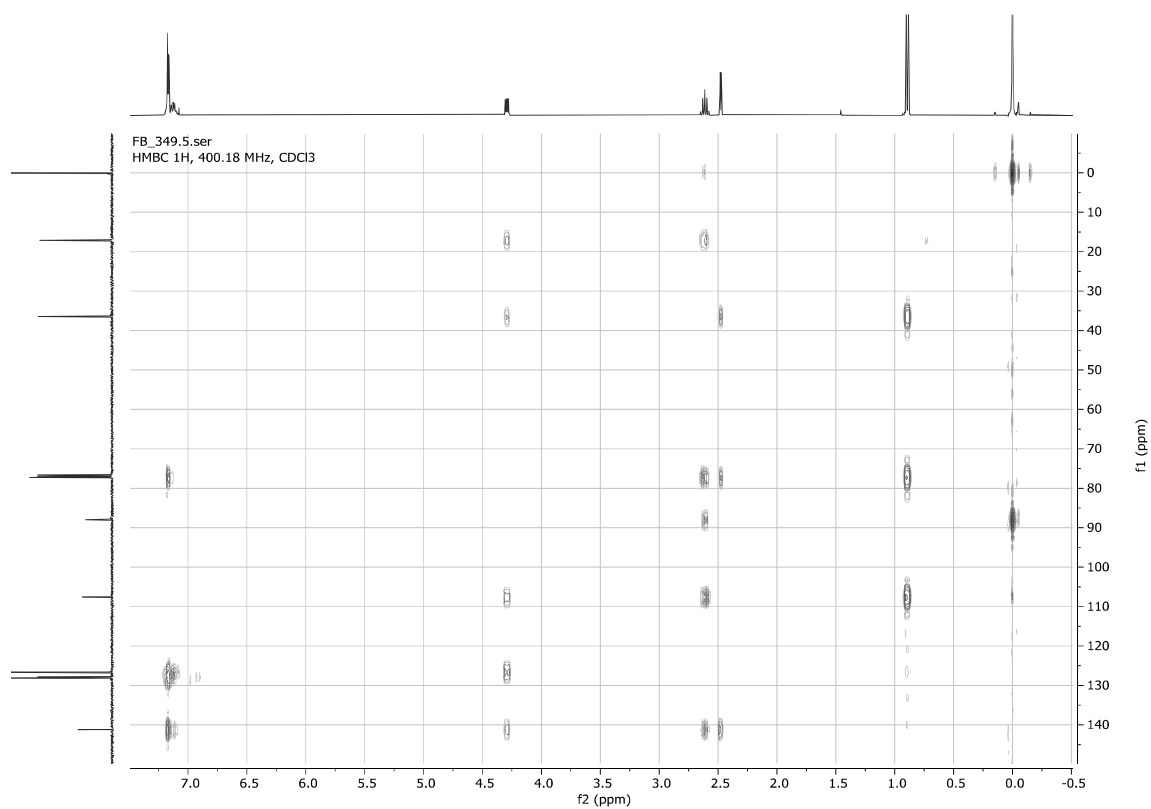
FB_349.1.fid
1D 1H, 400.18 MHz, CDCl3



FB_349.3.fid
1D 13C(1H), 100.64 MHz, CDCl3

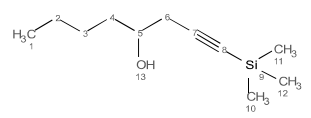
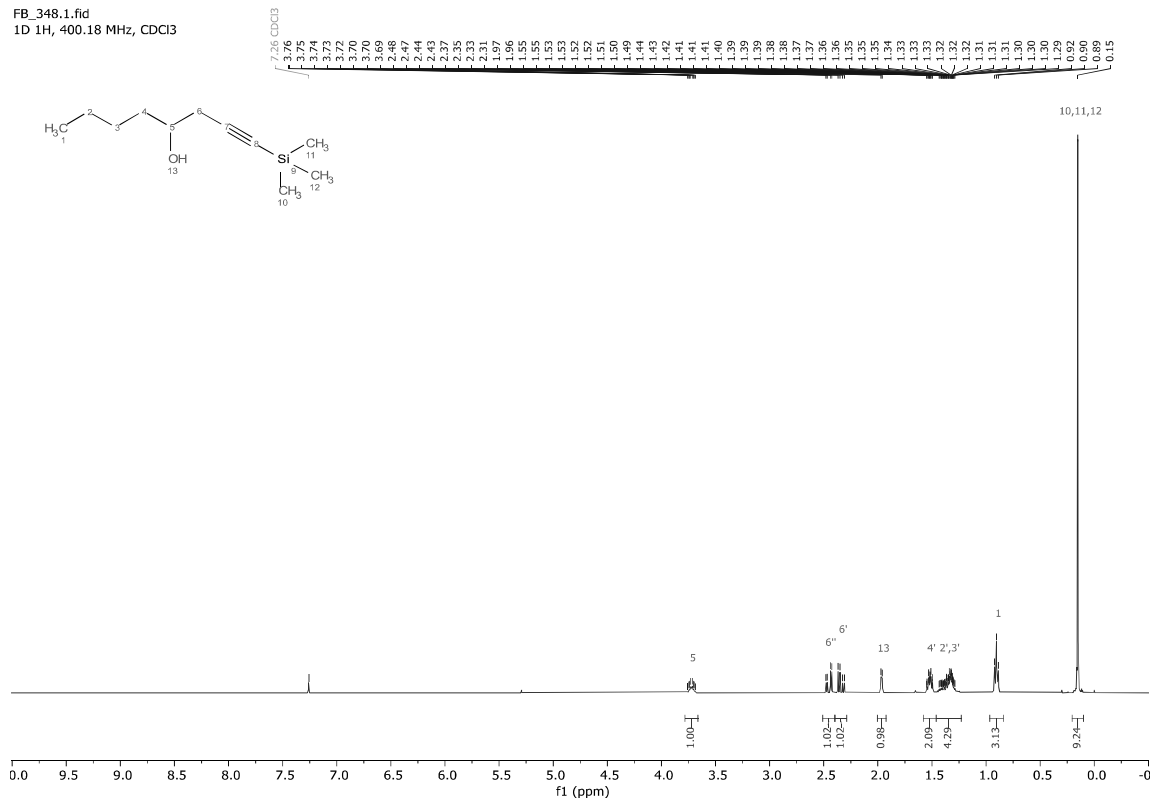




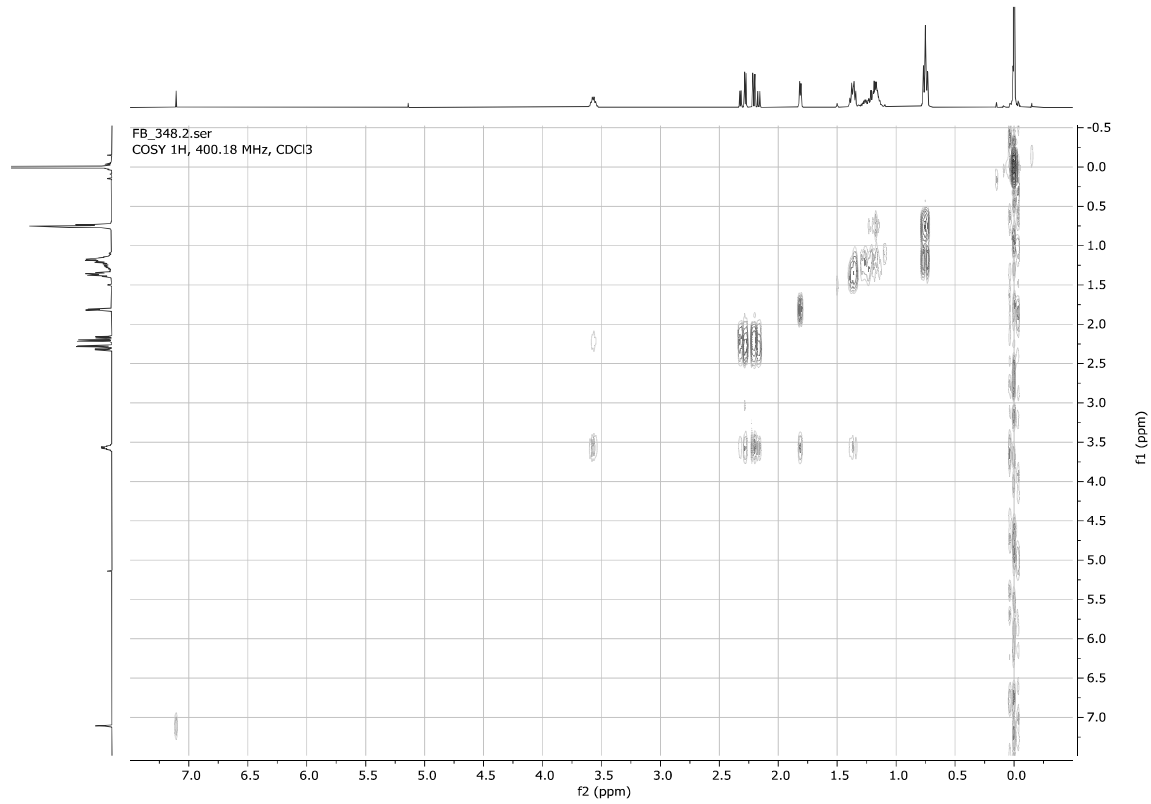
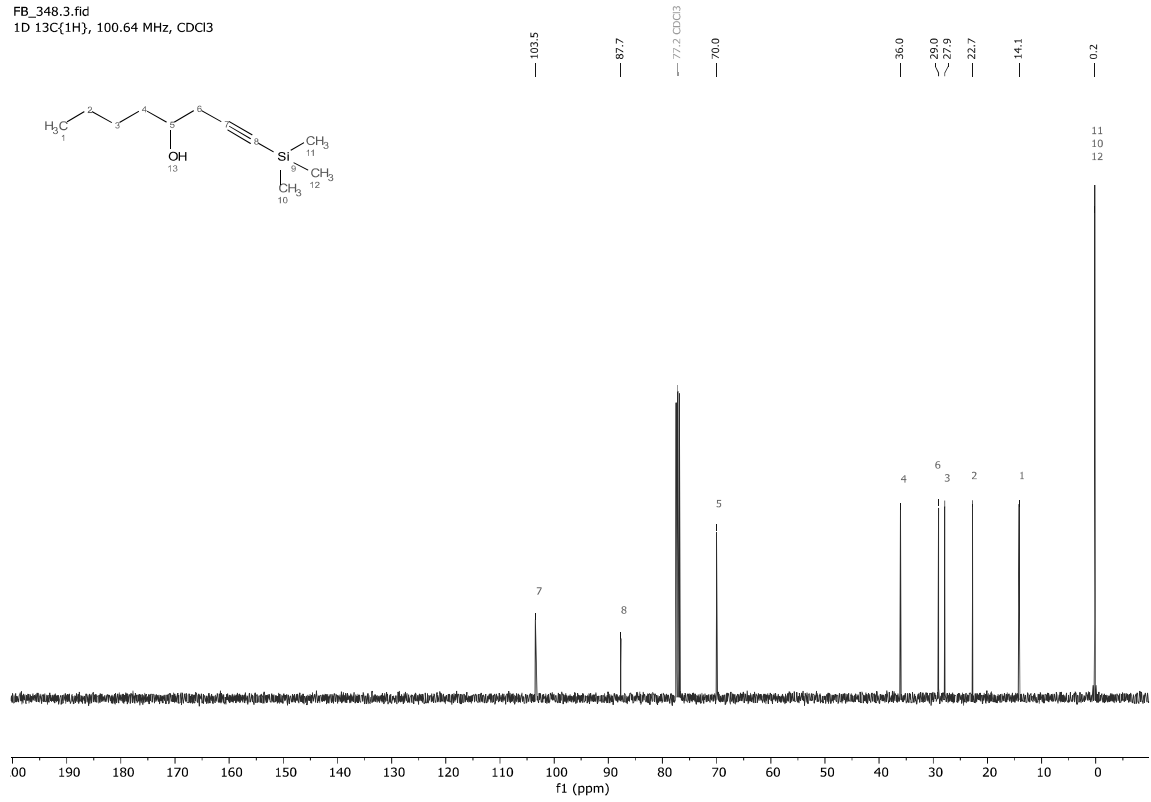


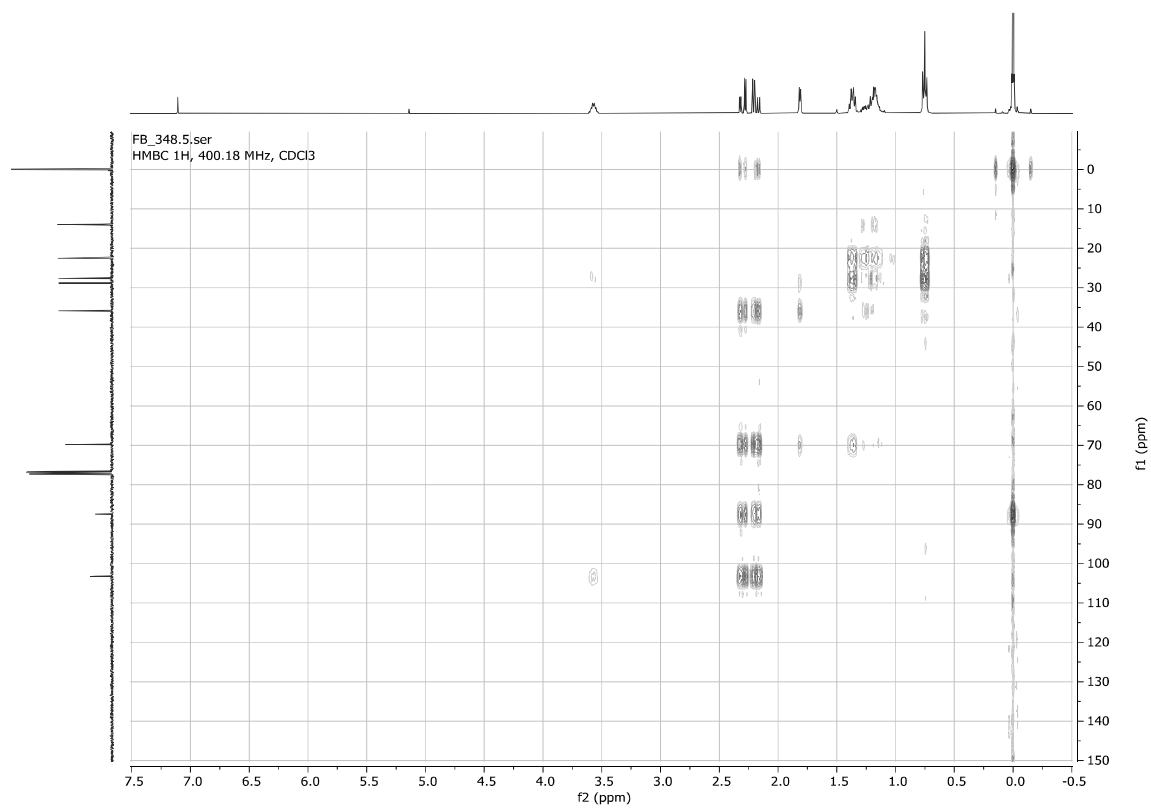
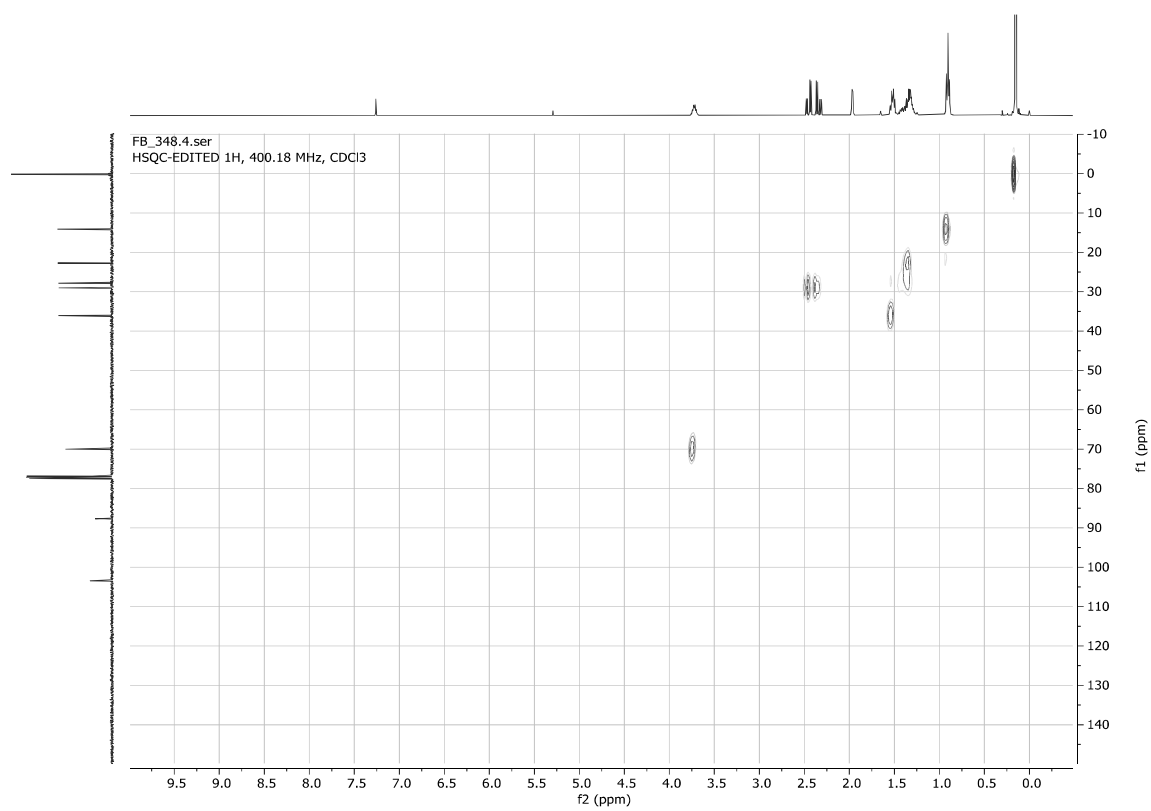
1-(Trimethylsilyl)oct-1-yn-4-ol **8k**

FB_348.1.fid
1D 1H, 400.18 MHz, CDCl3



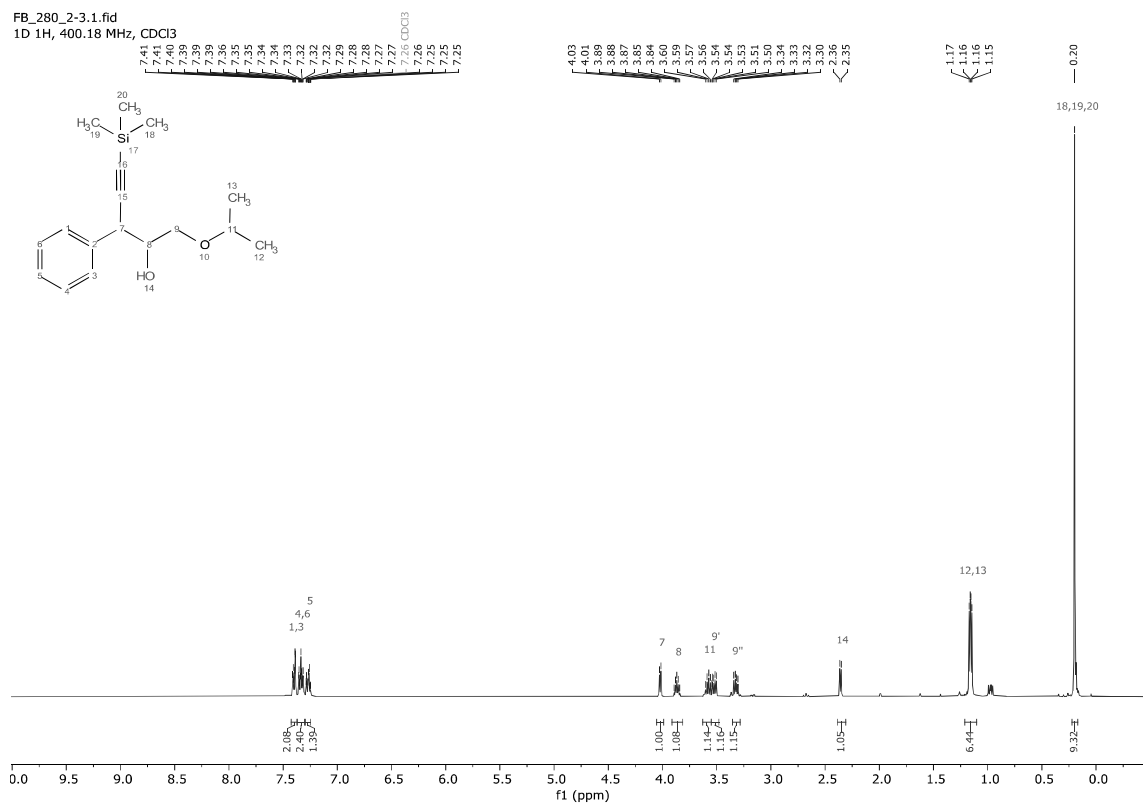
FB_348.3.fid
1D 13C{1H}, 100.64 MHz, CDCl3



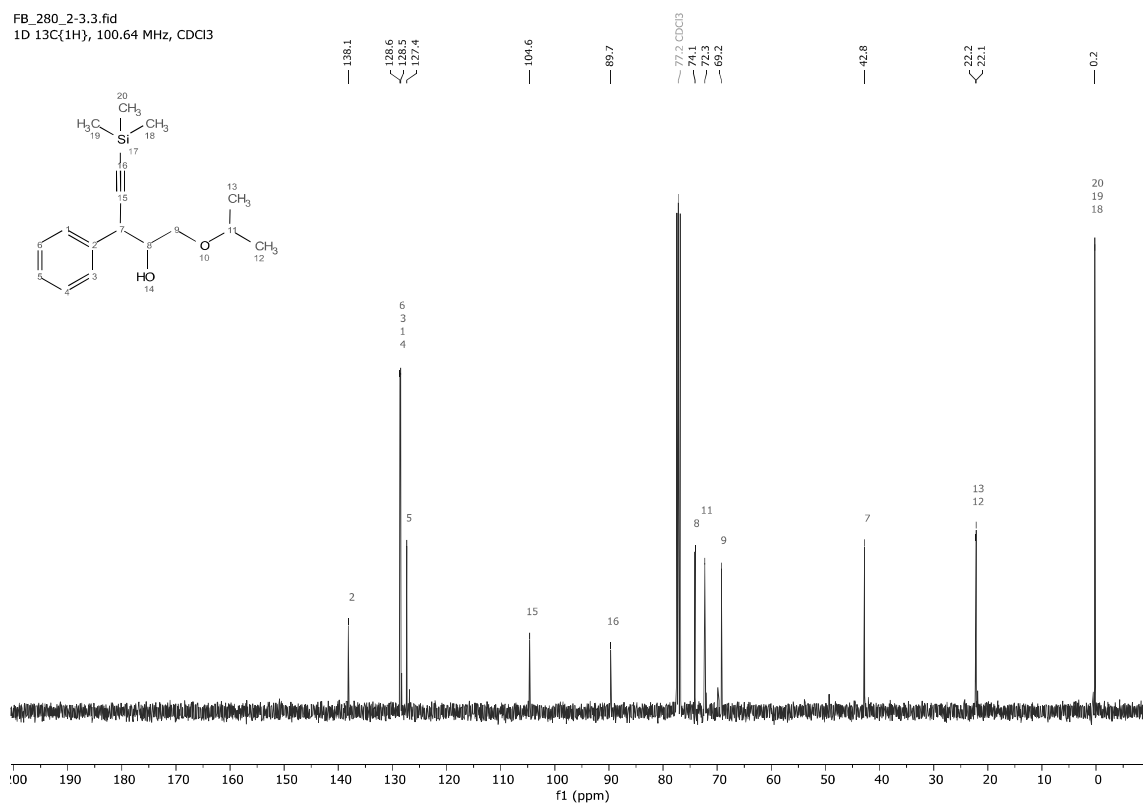


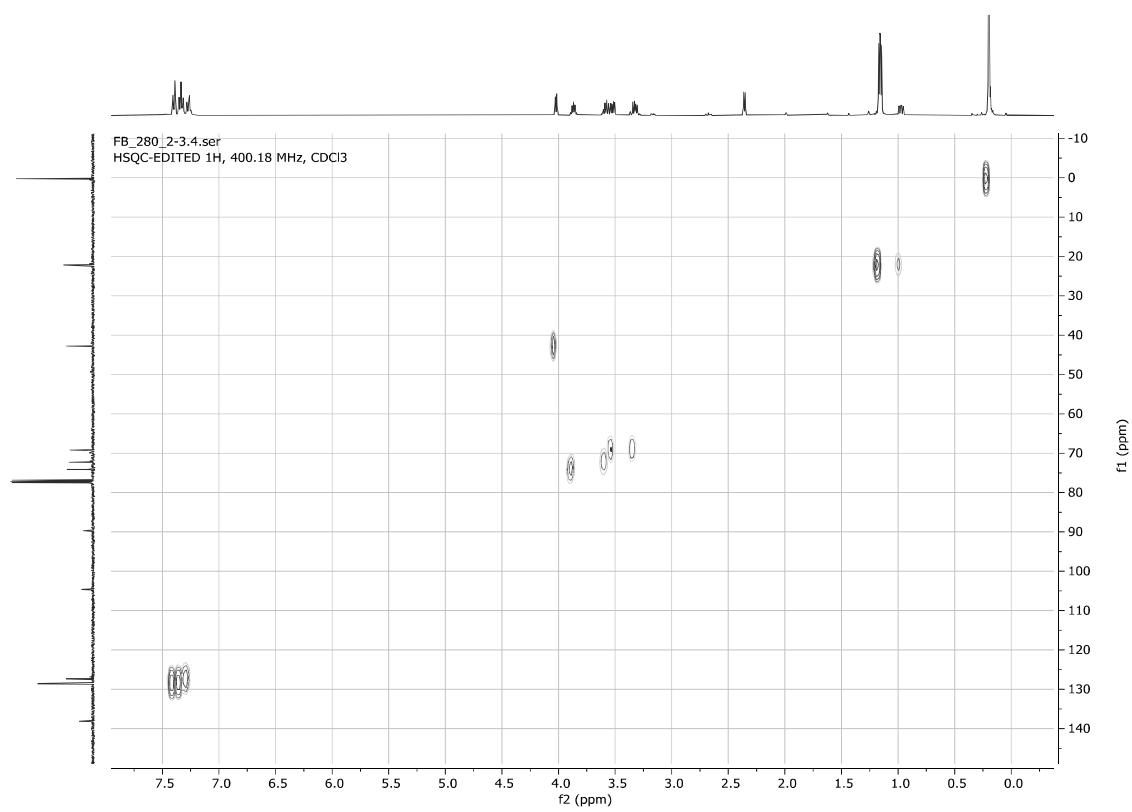
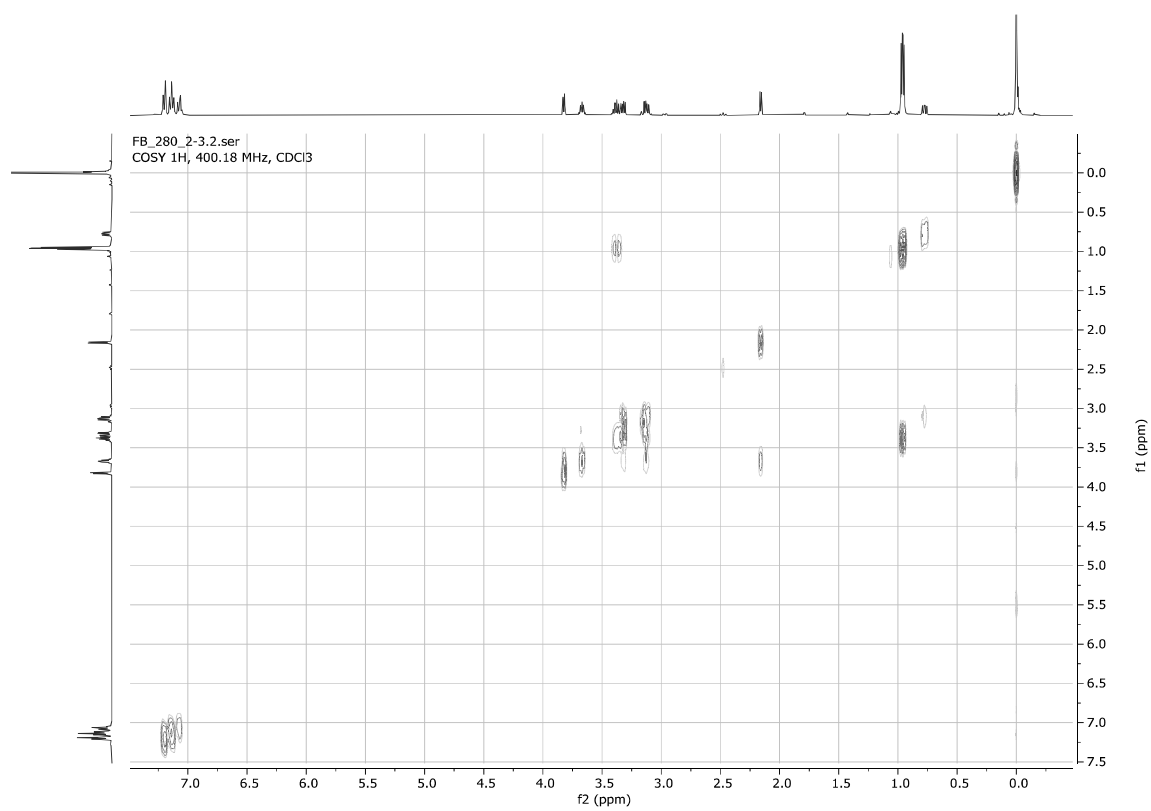
1-Isopropoxy-3-phenyl-5-(trimethylsilyl)pent-4-yn-2-ol **8s**

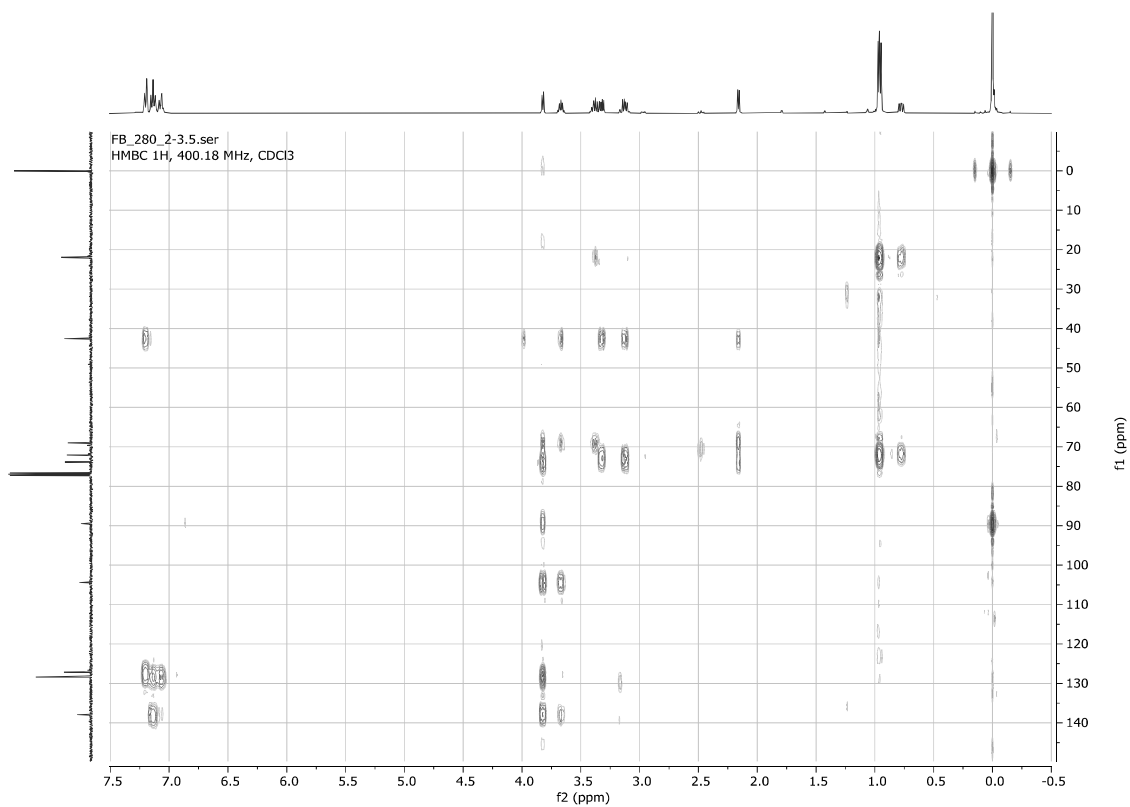
FB_280_2-3.1.fid
1D 1H, 400.18 MHz, CDCl3



FB_280_2-3.3.fid
1D 13C(1H), 100.64 MHz, CDCl3

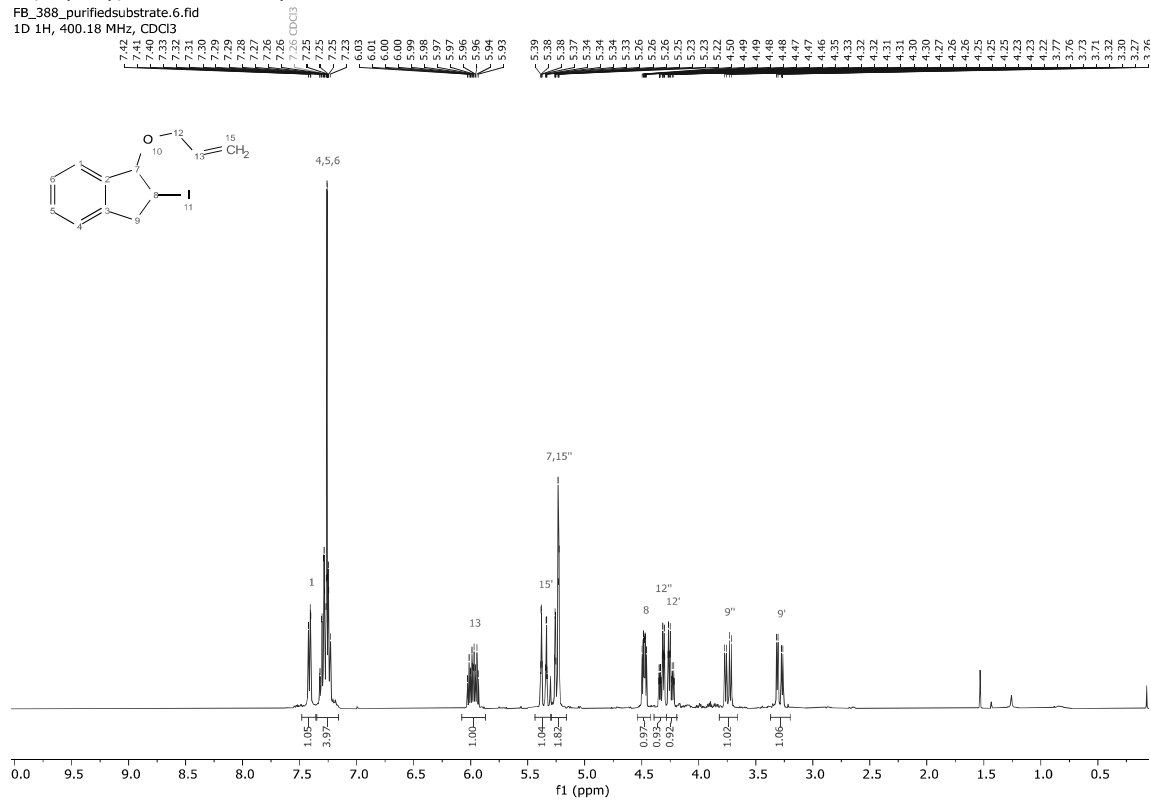




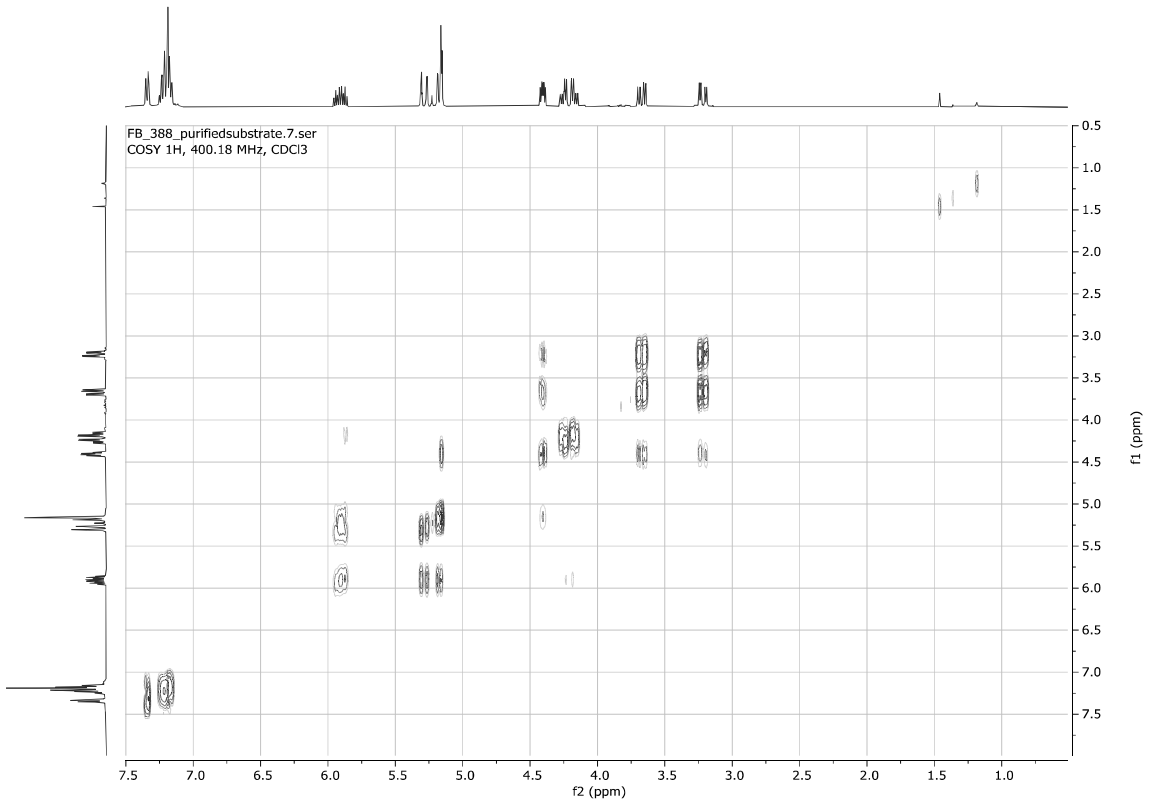
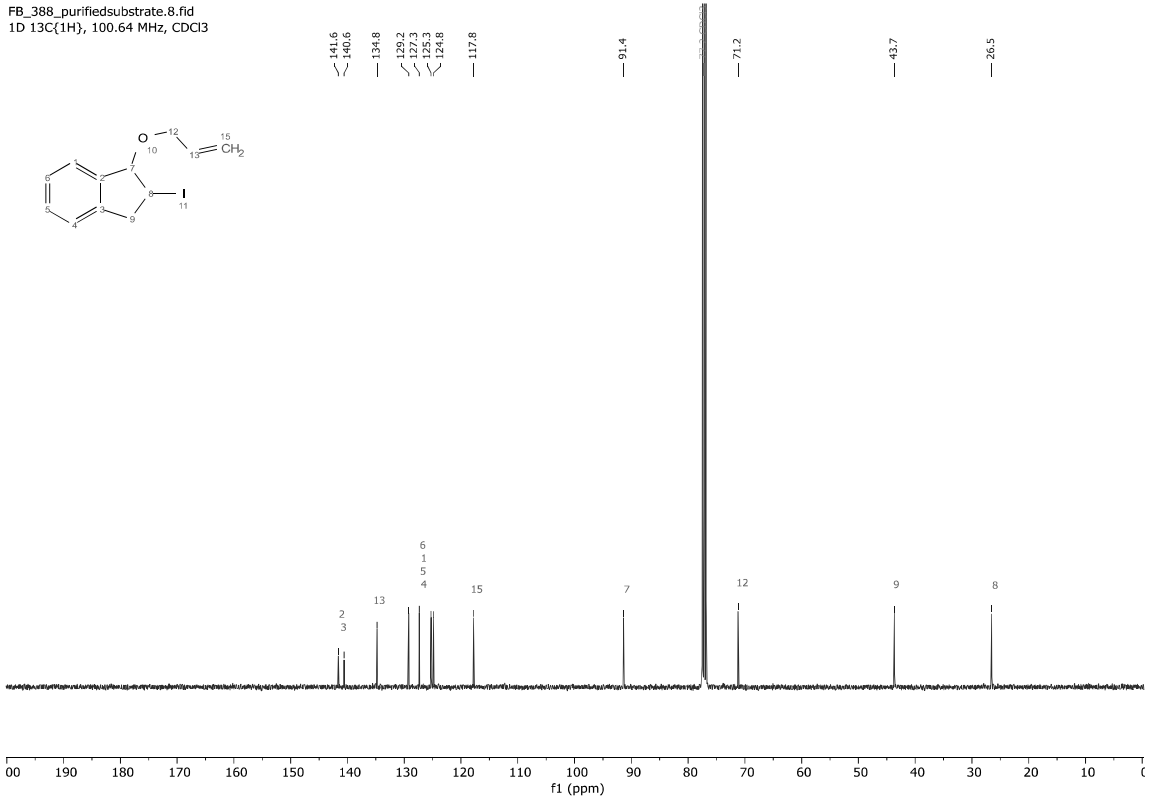


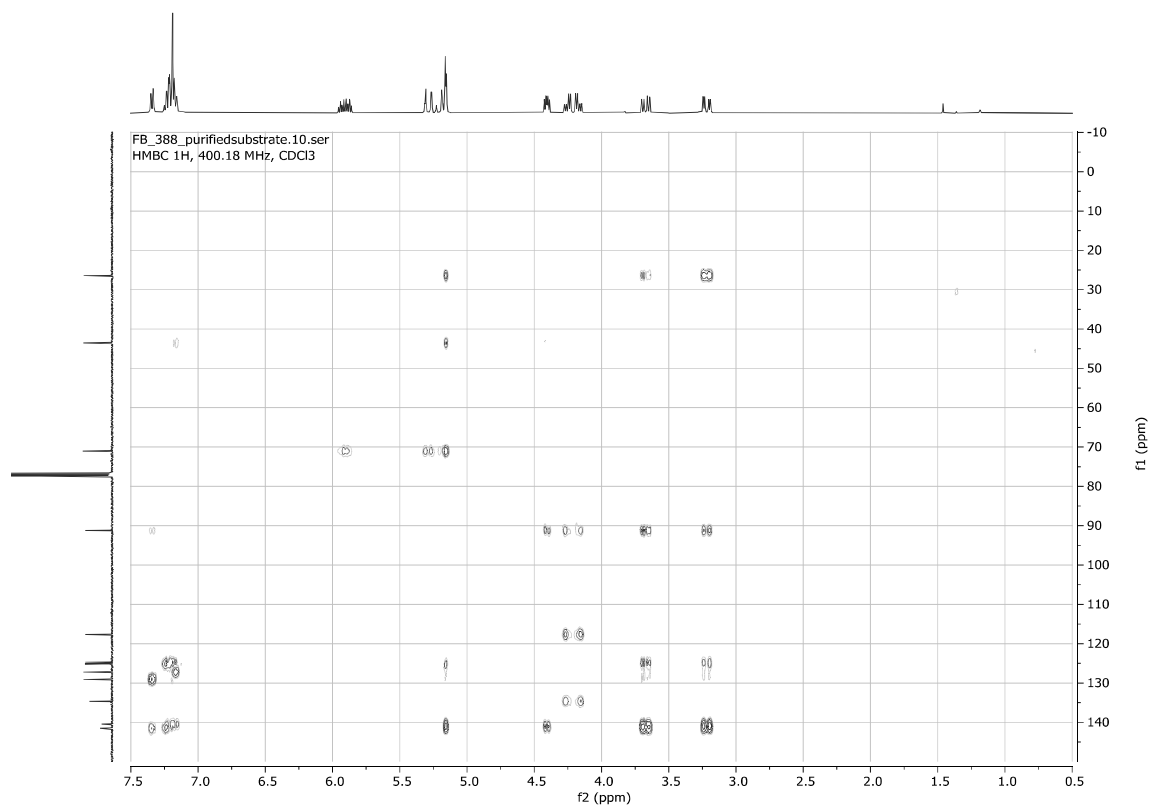
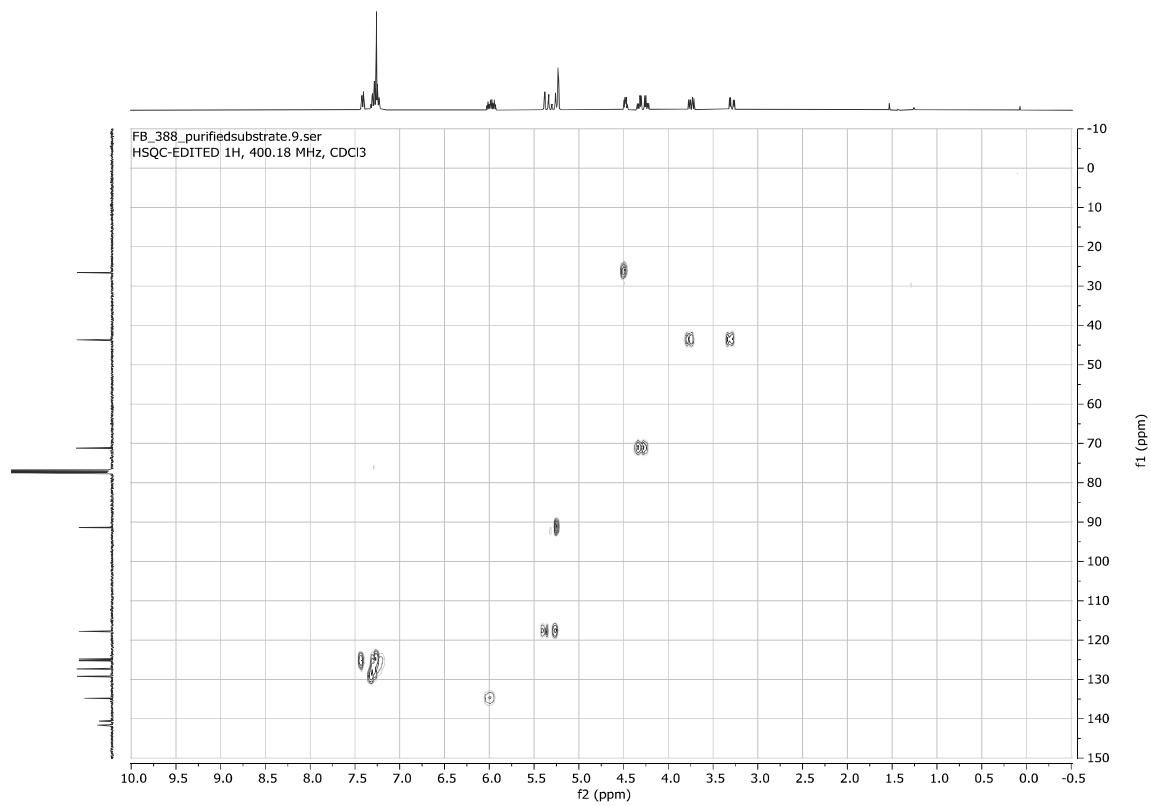
1-(Allyloxy)-2-iodo-2,3-dihydro-1H-indene 9

FB_388_purifiedsubstrate.6.fid
1D 1H, 400.18 MHz, CDCl3

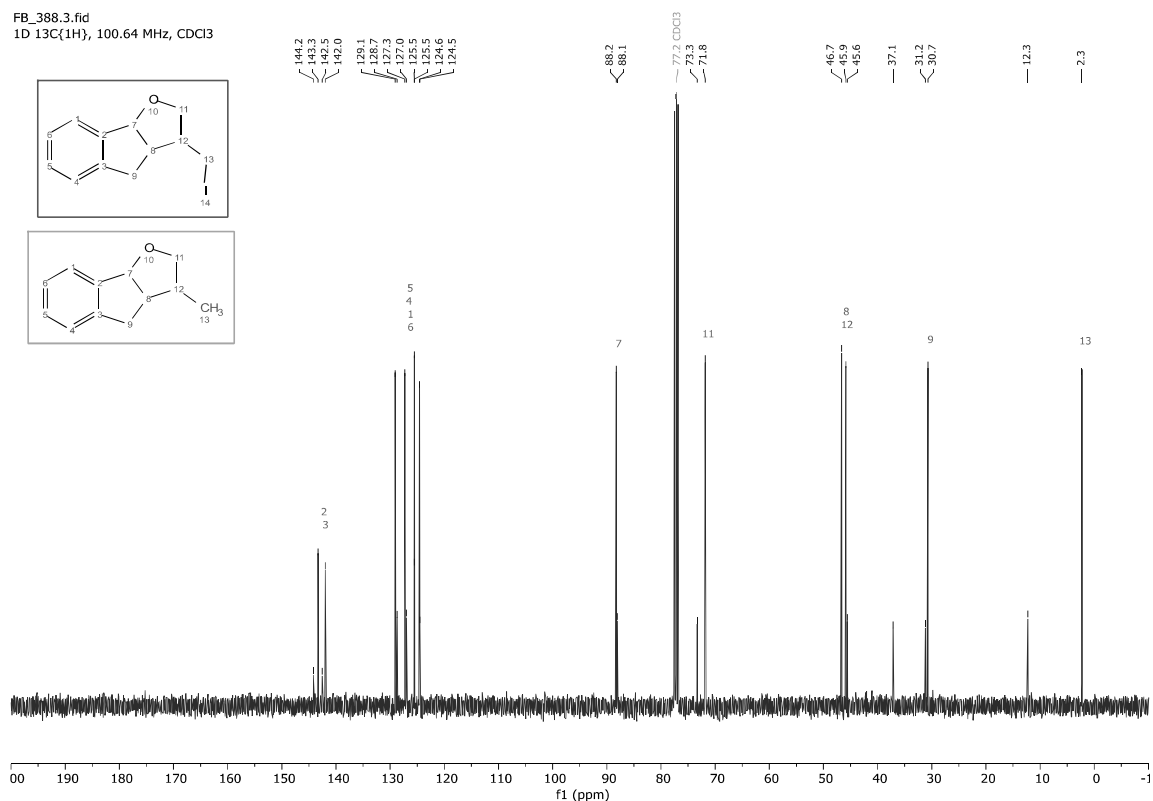
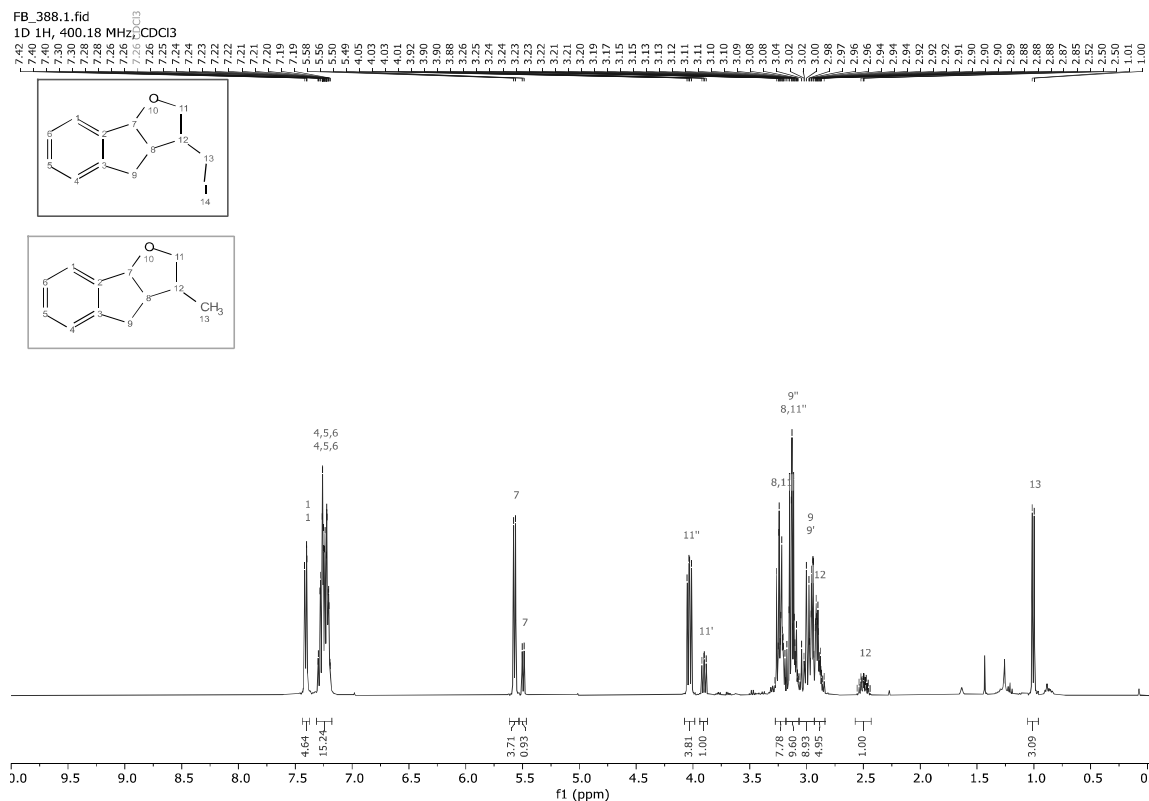


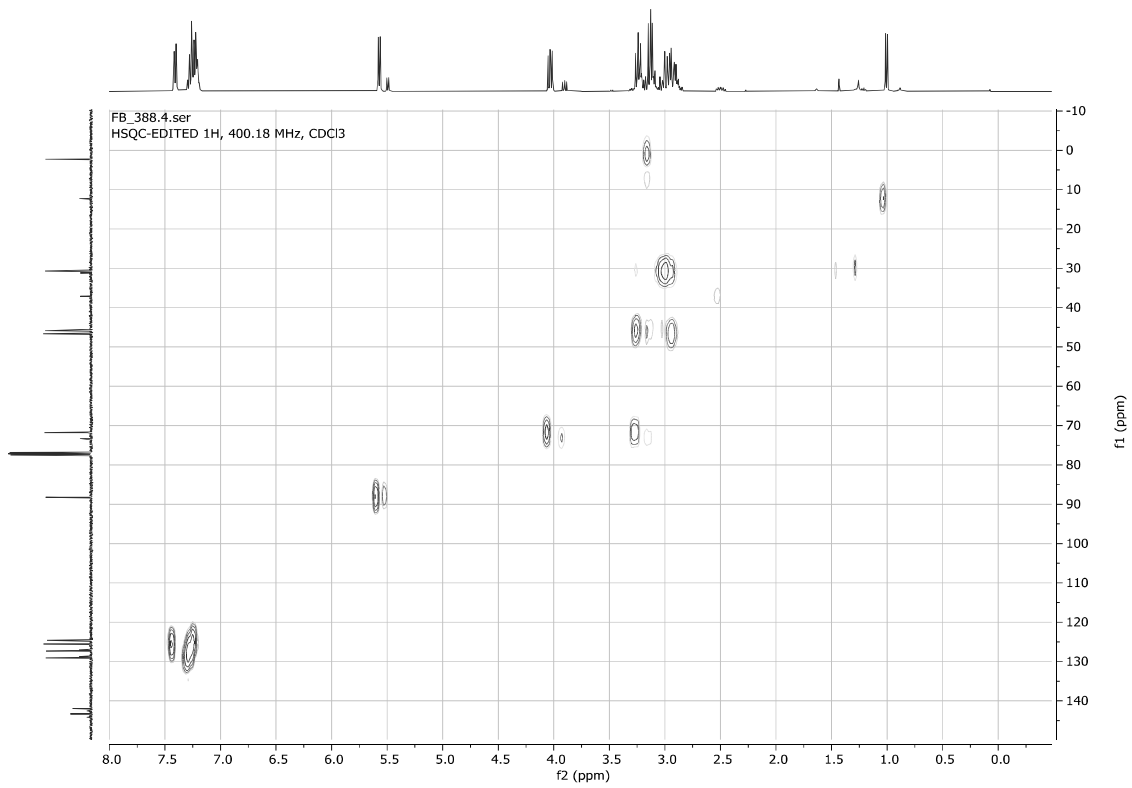
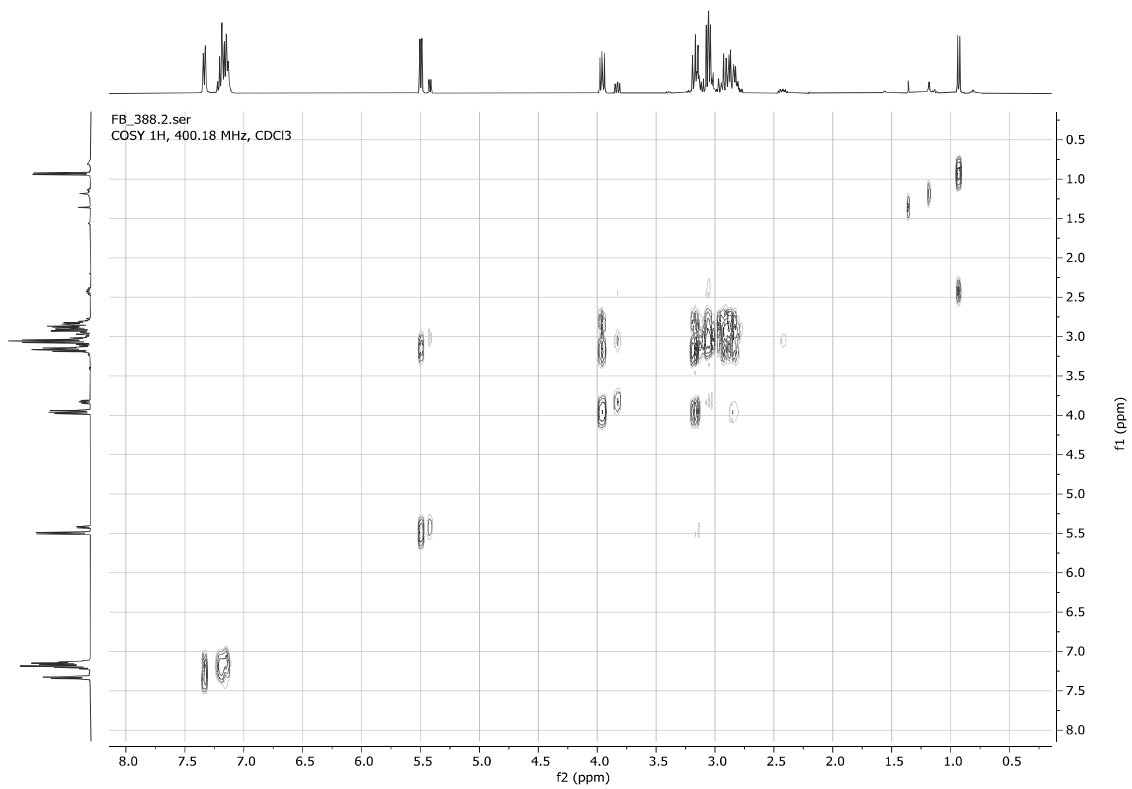
FB_388_purifiedsubstrate.8.fid
1D 13C{1H}, 100.64 MHz, CDCl3

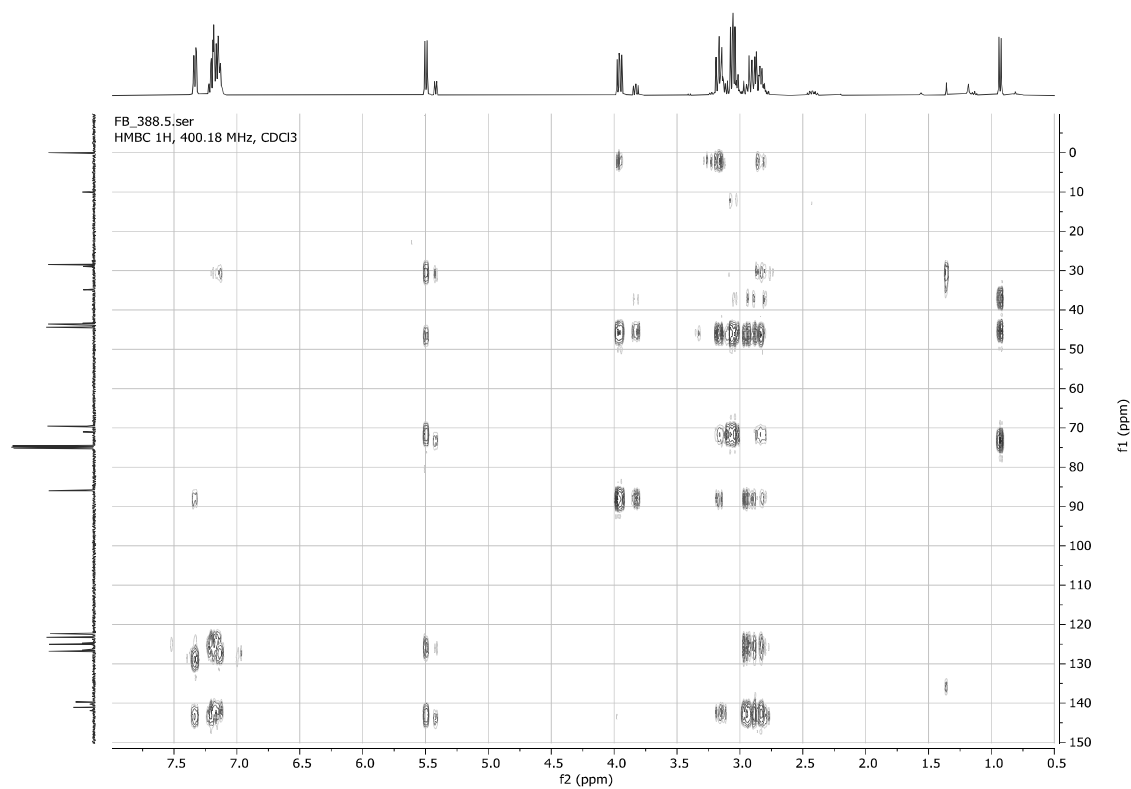




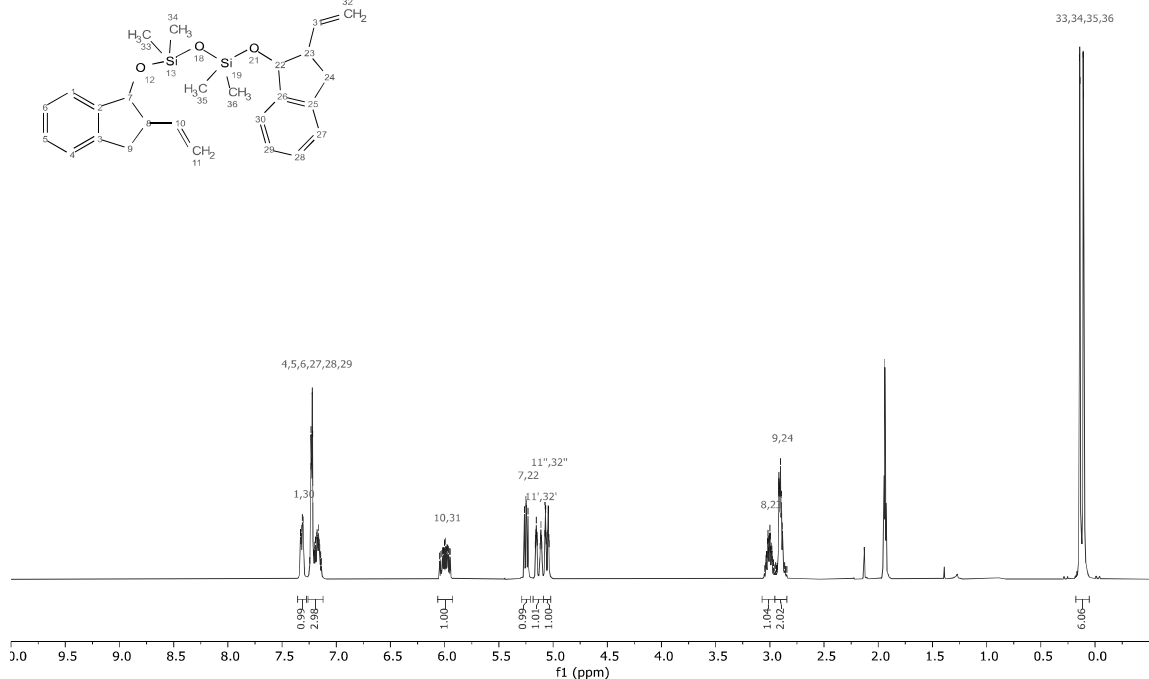
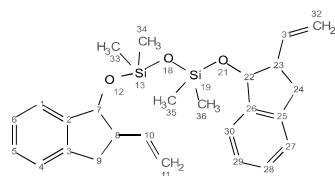
Inseparable 80:20 mixture of 3-(iodomethyl)-3,3a,4,8b-tetrahydro-2H-indeno[1,2-b]furan **10** and 3-methyl-3,3a,4,8b-tetrahydro-2H-indeno[1,2-b]furan **11**



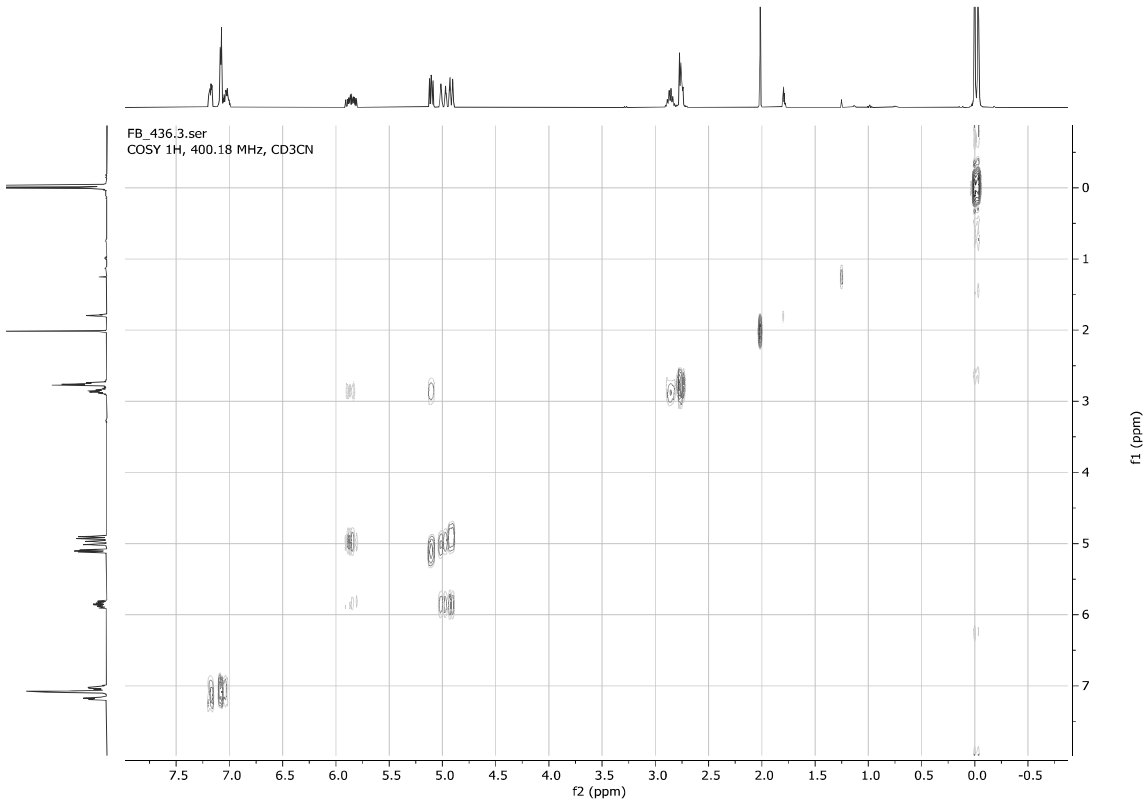
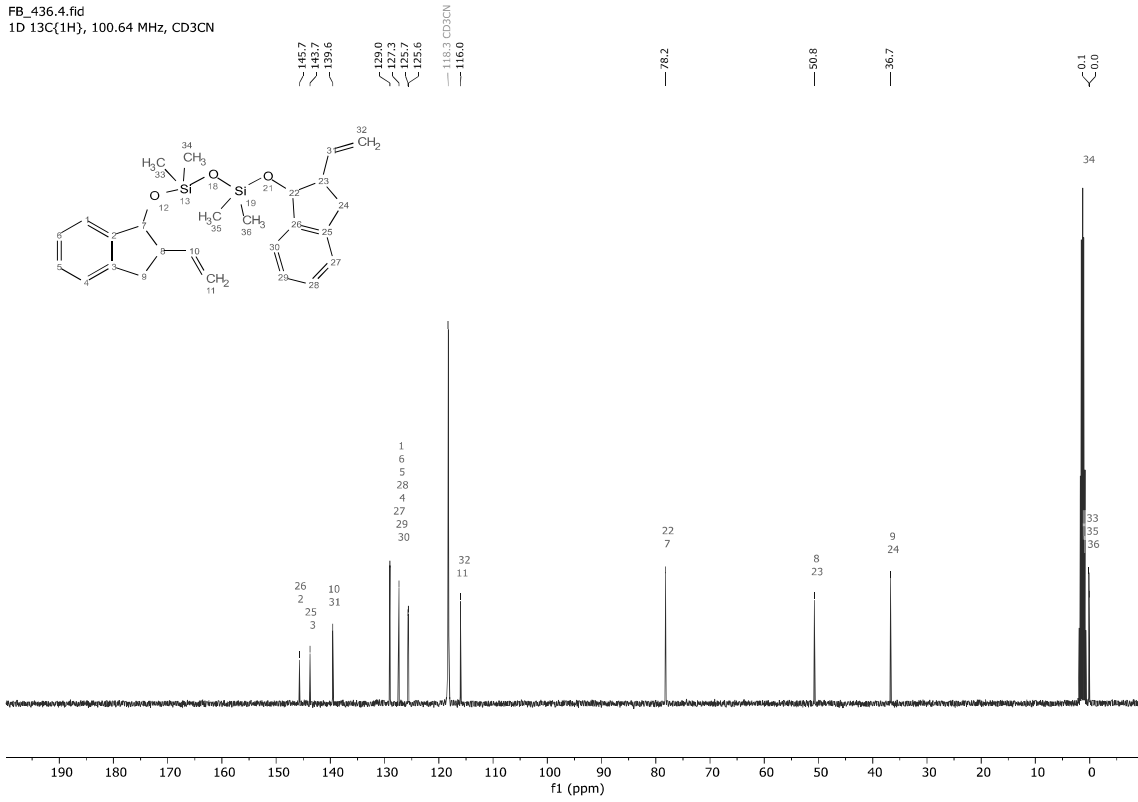


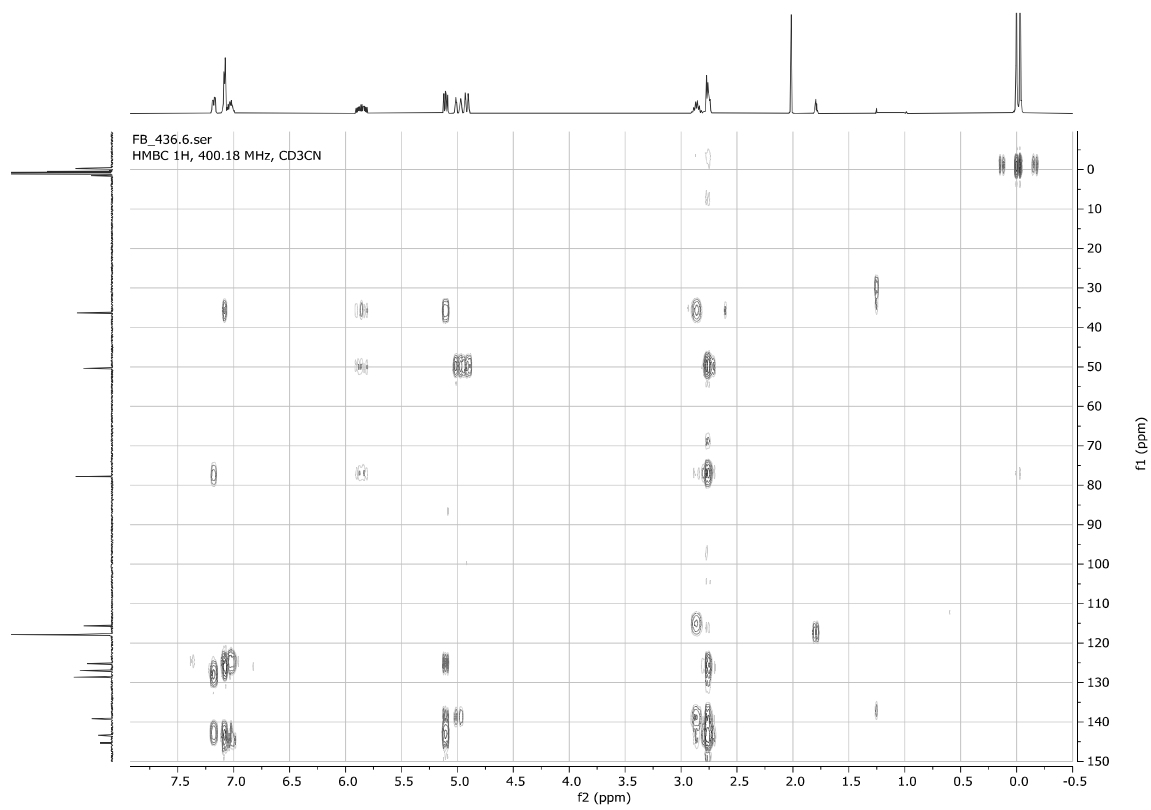
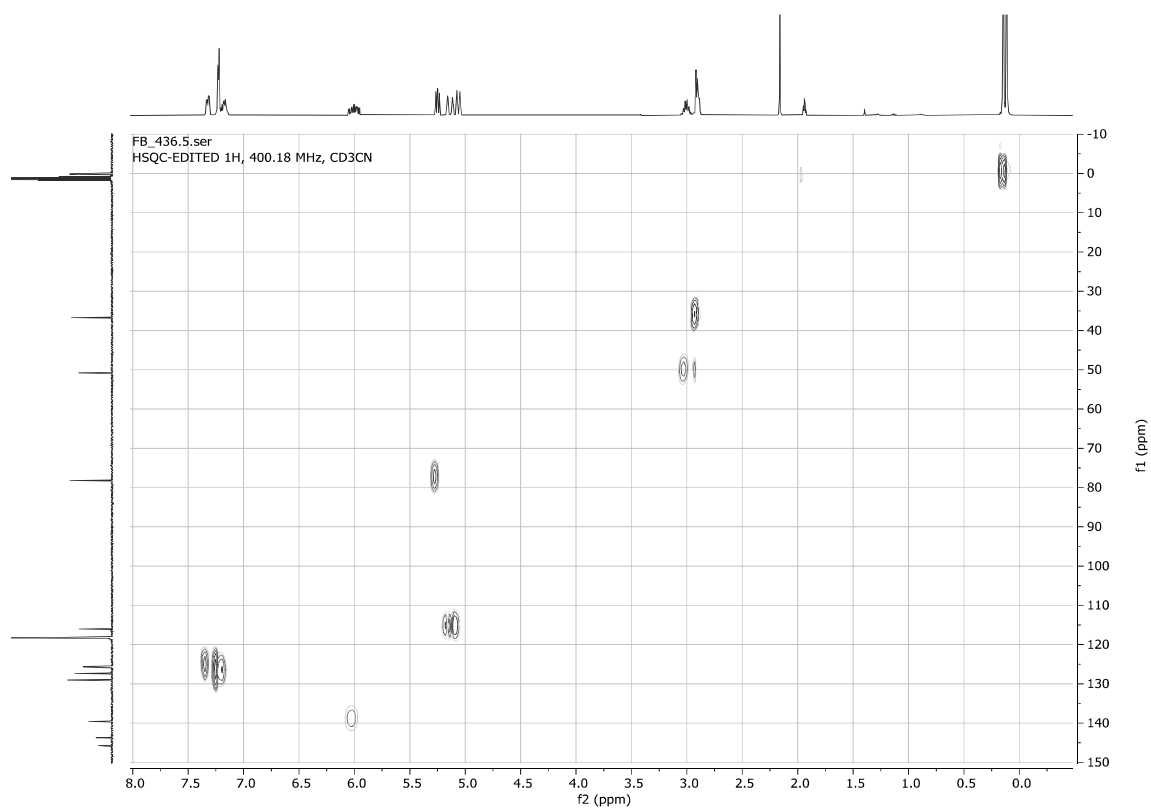


1,1,3,3-Tetramethyl-1,3-bis((2-vinyl-2,3-dihydro-1H-inden-1-yl)oxy)disiloxane **13a**



FB_436.4.fid
1D 13C{1H}, 100.64 MHz, CD3CN





Paper II

Light-promoted synthesis of complex α -iodoalkylsilanes

Floriane Baussière and Marius M. Haugland

Manuscript

Light-promoted synthesis of complex α -iodoalkylsilanes

Floriane Baussière^a and Marius M. Haugland^{a*}

^aDepartment of Chemistry, UiT The Arctic University of Norway, NO-9037 Tromsø, Norway

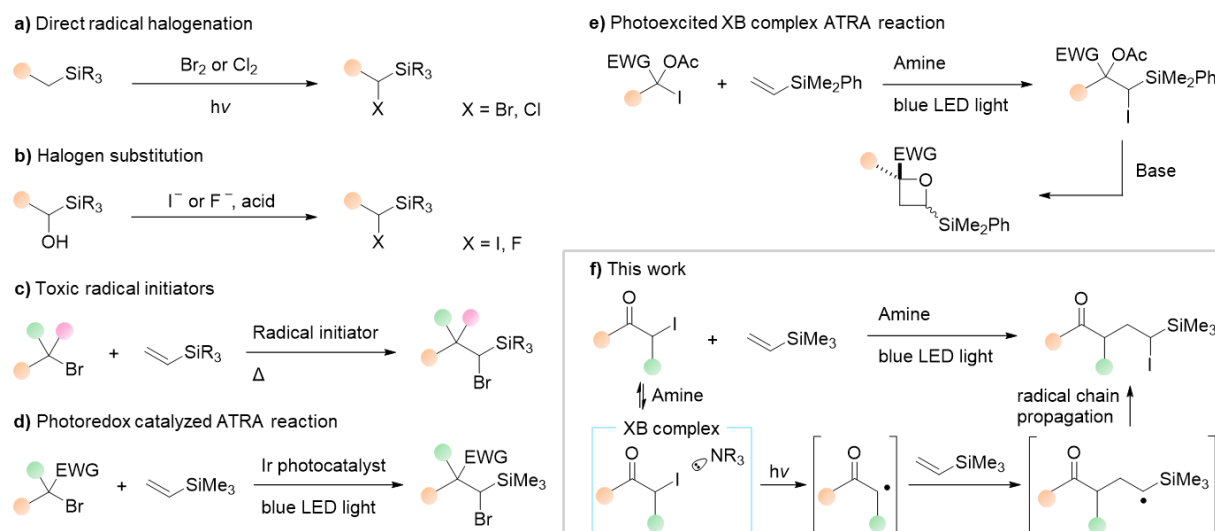
*Corresponding author

Abstract

The synthesis of α -iodoalkylsilanes is notoriously challenging. While atom transfer radical addition (ATRA) reactions between alkyl iodides and alkenyl silanes is an attractive synthetic strategy towards this category of compounds, only a few examples of such intermolecular radical reactions have been described. We report a protocol for the synthesis of α -iodoalkylsilanes under mild conditions through visible light-mediated and photocatalyst-free ATRA reaction between α -iodoketones and trimethylvinylsilane. The method was successfully applied to a selection of activated alkyl iodides and afforded the desired ATRA products in modest to excellent yields. We postulate that the radical reaction is initiated by photoexcitation of an iodide-amine XB complex and that the intermolecular ATRA reaction proceeds *via* radical chain propagation.

Introduction

α -Haloalkylsilanes are highly versatile intermediates that have found applications in a number of useful synthetic transformations.¹⁻⁸ Their use, however, is limited by the challenging synthesis of such compounds, which typically requires harsh conditions or highly reactive reagents.¹ α -Iodo- and α -fluoroalkylsilanes, in particular, are difficult to obtain as, unlike their bromide and chloride analogues, they cannot be prepared by direct radical halogenation of alkylsilanes (Scheme 1a).⁹⁻¹⁰ Indeed, the main synthetic strategy towards these compounds is halogen substitution of α -hydroxyalkylsilanes, which is limited by the access to such substrates (Scheme 1b).^{1,11}



Scheme 1. Typical synthetic strategies towards α -haloalkylsilanes by (a) radical halogenation, (b) halogen substitution, (c) traditional radical reactions and (d-e) recent visible light-mediated protocols. (f) This work.

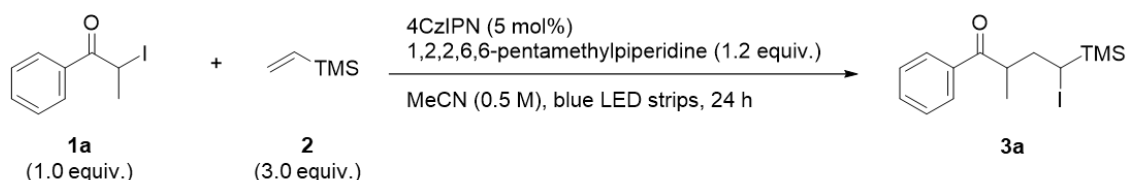
Atom transfer radical addition (ATRA) is a powerful synthetic strategy for the difunctionalization of alkenes.¹²⁻¹³ While a few examples of intermolecular ATRA reactions between alkyl halides and vinylsilanes have been reported, these protocols typically rely on the use of toxic radical initiators and heat to drive the radical reaction (Scheme 1c).¹⁴⁻¹⁷ In recent years, however, a photoredox catalyzed method has emerged for the ATRA reaction between activated alkyl bromides and trimethylvinylsilane under blue light irradiation (Scheme 1d).¹⁸ Very recently, the ATRA reaction between electron-deficient alkyl iodides and dimethylphenylvinylsilane mediated by visible light photoexcitation of halogen-bond (XB) complexes was reported as part of a study on the synthesis of oxetanes (Scheme 1e).¹⁹ While a limited selection of α -haloalkylsilanes was successfully synthesized using these light-mediated radical initiation protocols, the synthesis of α -haloalkylsilanes *via* ATRA reactions under mild conditions remains an attractive and largely underexplored strategy.

In this work, we present a visible light-mediated, photocatalyst-free method for the intermolecular ATRA reaction between α -iodoketones and trimethylvinylsilane (Scheme 1f).

Results and discussion

Radical nature of the reaction. To maximize the potential for the envisaged radical addition to the silane-substituted olefin, the electronically activated α -iodoketone **1** and trimethylvinylsilane **2** were chosen as reagents due to the polarity match between the electron deficient carbon-centered radical generated from **1** and the ambiphilic radical acceptor **2**.²⁰⁻²¹ Basing our initial conditions on typical reaction conditions for photoredox-catalyzed C-I σ bond cleavage,²² we began our investigation by testing whether the reaction was indeed a light initiated radical process (Table 1, entries 1-4). All reactions were performed in triplicates to ensure reliable results. While our initial conditions provided the desired ATRA product in reasonable 43-49% yields (entry 1), no conversion was observed when the reaction was performed in the dark (entry 2) or in the absence of amine (entry 3). Assuming that the reaction proceeded *via* an oxidative quenching cycle, which is reasonable given the relatively high reduction potential of 4CzIPN ($E_{1/2}$ (PC*/PC⁺) = -1.04 V vs SCE²³) and the use of activated alkyl iodides, this suggests that the radical addition intermediate (Scheme 1f) cannot turn over the catalytic cycle by being oxidized to a cation, as such a species would result in ATRA product **3a** after trapping by the halide anion. Moreover, it suggests that if the reaction is initiated by single electron reduction of the radical precursor **1a**, the reaction does not proceed *via* a radical chain mechanism, as this should lead to formation of **3a** in detectable quantities. Similar yields were obtained in the presence and absence of photocatalyst (entries 1 and 4), which suggests that formation of the C-centered radical from **1a** was not initiated by single electron transfer (SET) between the photocatalyst and the alkyl halide, nor by halogen-atom transfer (XAT) between a SET-generated α -aminoalkyl radical²⁴ and **1a**. Therefore, the photocatalyst was removed from the standard conditions as it was not believed to be involved in the mechanism of the reaction. Interestingly, reaction in the absence of both photocatalyst and amine resulted in 0-8% (NMR yield) of ATRA product **3a** (entry 5), which suggests that partial spontaneous C-I bond cleavage upon light irradiation can contribute to initiation. However, since the reaction operated in significantly higher yields in the presence of the amine, this spontaneous bond cleavage is not the main reaction pathway. Moreover, this result could be explained by contamination of the material with trace amounts of the amine, a hypothesis that cannot be excluded. The radical nature of the reaction was confirmed by the presence of adducts between 2,2,6,6-tetramethylpiperidine 1-oxyl (TEMPO) and radical intermediates when performing the reaction in the presence of TEMPO (see the Supporting Information).

Table 1. Study of the radical nature of the reaction^{a,b}



entry	deviation from standard conditions	yield (%)
1	none	43-49
2	no light	0
3	no amine	0
4	no photocatalyst	44-47
5 ^c	no amine, no photocatalyst	0-8

^aReaction scale: 0.30 mmol. ^bAll experiments were performed in duplicate. ^cYield determined by ¹H NMR with ethylene carbonate as internal standard.

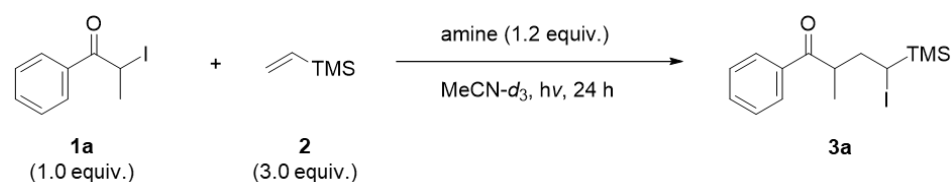
Influence of the amine. Next, we turned our attention to the nature of the amine. Based on our initial mechanistic discoveries (Table 1), we hypothesized that if the reaction did not proceed *via* SET or XAT, carbon-centered radicals were likely generated by fragmentation of excited-state XB complexes formed between **1a** and the amine.²⁵ While multiple nucleophilic partners have been reported to successfully form XB complexes with alkyl halides,²⁵ we focused on amines as potential halogen-bond acceptors due their established reactivity²⁶ and their wide commercial availability. Among the secondary and tertiary amines screened (Table 2, entries 1-9), 1,2,2,6,6-pentamethylpiperidine (PMP) provided the highest yield (entry 6).

Influence of the light source. A short irradiation source screening (Table 2, entries 6 and 10-12) confirmed the importance of blue light for the photoexcitation of the potential XB complex. Using a high intensity 456 nm lamp

(entry 11) provided slightly better yields than broad emission blue LED strips (entry 6). However, when repeated, reaction with the high intensity lamp only yielded 49% (entry 12). The similarity of yields achieved with these two sources of blue light suggests that either can be suitable for driving the desired ATRA reaction. However, based on literature precedence, we suspected that the optimal wavelength for XB complex excitation can be substrate dependent. Therefore, the broad emission light source was favored as the standard irradiation source.

Influence of the concentration. Further screening revealed that concentration was a crucial factor for the desired ATRA reaction (Table 2, entries 14-15). When the reaction mixture was concentrated from 0.5 M (entry 6) to 1 M (entry 14), a significant increase of yield was observed. Further increase of the concentration to 1.5 M (entry 15) showed no additional improvement in the yield, perhaps due to insufficient solubilization of the reagents. A final control experiment verified that high-intensity light irradiation at higher concentration also did not improve the yield (entry 16). We therefore set our standard concentration to 1 M to further evaluate the ATRA reaction.

Table 2. Optimization of the reaction conditions^a



entry	amine	irradiation source	concentration (M)	yield (%) ^b
1	DIPA	blue LED strips	0.5	46
2	2,2,6,6-tetramethylpiperidine	blue LED strips	0.5	13
3	Et ₃ N	blue LED strips	0.5	24
4	Bu ₃ N	blue LED strips	0.5	10
5 ^c	DIPEA	blue LED strips	0.5	8-32
6 ^c	PMP	blue LED strips	0.5	53-65
7	quinuclidine	blue LED strips	0.5	0
8	Bn ₃ N	blue LED strips	0.5	0
9	4-methoxytriphenylamine	blue LED strips	0.5	0
10 ^d	PMP	Kessil 370 nm	0.5	4
11 ^{d,e}	PMP	Kessil 456 nm	0.5	48-63
13	PMP	green LED strips	0.5	9
14^c	PMP	blue LED strips	1.0	72-83
15	PMP	blue LED strips	1.5	82
16 ^d	PMP	Kessil 456 nm	1.0	46

^aReaction scale: 0.30 mmol. ^bYield determined by ¹H NMR with ethylene carbonate as internal standard. ^cExperiment performed in triplicate. ^dReaction mixtures irradiated with Kessil lamps outside the photoreactor (see Fig. S2 in the Supporting Information). ^eExperiment performed in duplicate.

Influence of the substrate. Based on these results, we applied our optimized procedure to a selected range of secondary alkyl iodides **1a-e** (Table 3, entries 1-5). To our satisfaction, the protocol was successful for all substrates, albeit in low to moderate yields despite the generally high conversion of the substrates, which suggested degradation of the substrates or the products. Alternatively, we hypothesized that a side-reaction, such as polymerization, might operate. Further reaction optimization was therefore carried out to improve the general applicability of our synthesis method. Control experiments were performed for all substrates with and without PC, which confirmed that PC was not required for the desired ATRA reaction for all substrates (see the Supporting Information). A complementary screening of halogen-bond acceptors was performed with substrates **1b**, which confirmed PMP as the best reagent for our reaction (see the Supporting Information).

Influence of the temperature. Next, we hypothesized that varying the temperature might impact thermal side-reactions and therefore also yields. Substrates **1a-e** were subjected to our protocol at 0 °C (Table 3, entries 6-10), 20 °C (Table 3, entries 11-15) and 40 °C (Table 3, entries 16-20). To control the temperature, experiments were performed in a photoredox box connected to a circulation heater/chiller. Due to the nature of the setup, to maintain a broad emission light the irradiation source had to be switched from blue LED strips to high-intensity white light. Compared to the yields observed at 20 °C, reducing the temperature to 0 °C had a positive effect on the yield of **3e**, had little impact on **3c**, but was negative for **3a**, **3b** and **3d**. A slight drop of yield was observed for all substrates when the temperature was raised from 20 °C to 40 °C. Another aspect we investigated was side-

reactions by assessing the conversion of substrates **1a-e**. Unsurprisingly, higher temperatures resulted in higher consumption of the substrates. However, higher conversion did not correlate with higher yields. Overall, the best conversion-yield ratios were observed at 20 °C, which was therefore selected as the optimal reaction temperature.

Table 3. Study of the effect of temperature and light source on the synthesis of ATRA products 3a-e^a

$\text{1a-e (1.0 equiv.)} + \text{2 (3.0 equiv.)} \xrightarrow[\text{MeCN-d}_3, \text{ hv, 24 h}]{\text{PMP (1.2 equiv.)}} \text{3a-e}$

3a

3b

3c

3d

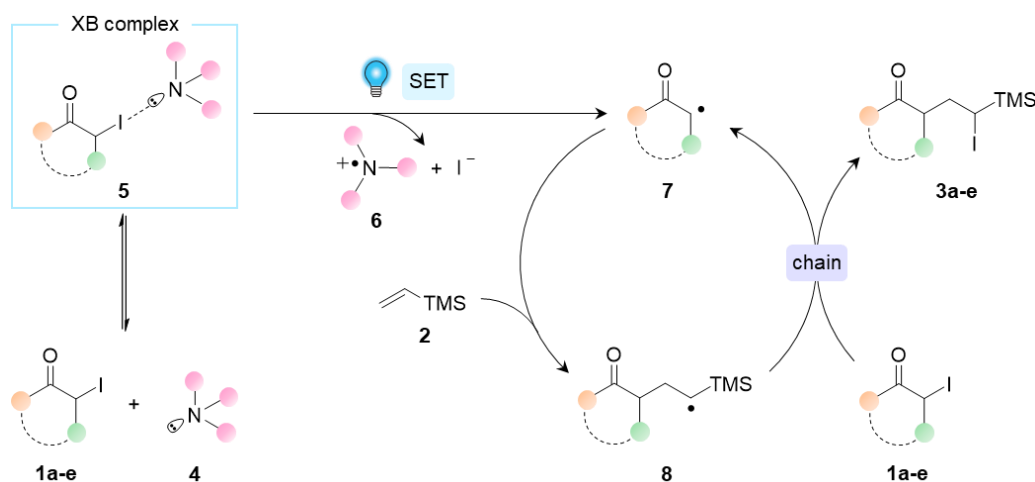
3e

entry	substrate	product	T (°C)	irradiation source	conversion (%) ^b	yield (%) ^b
1	1a	3a	34	blue LED strips	100	83
2	1b	3b	34	blue LED strips	84	10
3	1c	3c	34	blue LED strips	75	4
4	1d	3d	34	blue LED strips	67	26
5	1e	3e	34	blue LED strips	100	10
6	1a	3a	0	white light	100	11
7	1b	3b	0	white light	81	1
8	1c	3c	0	white light	90	21
9	1d	3d	0	white light	71	31
10	1e	3e	0	white light	100	69
11	1a	3a	20	white light	100	84
12	1b	3b	20	white light	86	7
13	1c	3c	20	white light	100	17
14	1d	3d	20	white light	72	52
15	1e	3e	20	white light	100	41
16	1a	3a	40	white light	100	78
17	1b	3b	40	white light	96	6
18	1c	3c	40	white light	100	7
19	1d	3d	40	white light	84	53
20	1e	3e	40	white light	100	37
21	1a	3a	20	390 nm	100	0
22	1b	3b	20	390 nm	100	4
23	1c	3c	20	390 nm	– ^c	– ^c
24	1d	3d	20	390 nm	100	31
25	1e	3e	20	390 nm	– ^c	– ^c
26	1a	3a	20	427 nm	100	25
27	1b	3b	20	427 nm	100	18
28	1c	3c	20	427 nm	100	8
29	1d	3d	20	427 nm	100	71
30	1e	3e	20	427 nm	100	62
31	1a	3a	20	456 nm	100	70
32	1b	3b	20	456 nm	100	18
33	1c	3c	20	456 nm	100	11
34	1d	3d	20	456 nm	100	66
35	1e	3e	20	456 nm	100	72

^aReaction scale: 0.30 mmol. ^bConversion/yield determined by ¹H NMR with ethylene carbonate as internal standard. ^cExperiment not performed.

Influence of the light source (2). Next, we investigated the impact of using narrow-spectrum high-intensity LED lamps as irradiation source (Table 3, entries 21-35). All high-intensity light sources provided full consumption of substrates **1a-e**. Lower yields were observed when the irradiation source was changed from white light to 390 nm LED light (Table 3, entries 21-25), mostly caused by side reactions and substrate decomposition leading to complex mixtures. The ATRA reaction was, however, a major productive pathway upon irradiation at 427 nm (Table 3, entries 26-30) and 456 nm (Table 3, entries 31-35), with 456 nm generating the overall best yields across the panel of substrates. While multiple light sources successfully initiated the desired ATRA reactions, the optimal wavelength seemed to be substrate dependent.

Mechanistic investigations. XB complexes can typically be identified by the presence of new bands in UV-vis spectra, as well as differences in chemical shifts in ^1H and ^{13}C NMR spectra.²⁵ In accordance with previous mechanistic studies involving the detection of XB complexes,²⁷⁻³⁰ we recorded the UV-vis spectra of solutions of **1a** alone as well as in combinations with the other reagents to mimic the reaction conditions (see the Supporting Information for all UV-vis spectra). To our surprise, no clear bathochromic shift was observable upon mixing **1a** and PMP, either in the presence or absence of **2**. In light of the importance of concentration for the ATRA reaction, we explain the absence of new absorption bands by a low equilibrium constant for the XB complex which results in complex formation below the limits of detection of the spectrometer. No XB complex was detected by NMR analysis either (see the Supporting Information for all NMR spectra), as no change was observed in the chemical shift of the α -proton of alkyl iodide **1a** by ^1H NMR in the presence and absence of PMP. Similarly, no change in the chemical shift of the α -carbon of **1a** could be detected by ^{13}C NMR upon addition of PMP. However, based on literature precedence and the fact that the desired ATRA reaction does not operate without irradiation with visible light or an amine being present (Table 1, entries 2 and 3), we postulate that the ATRA reaction proceeds *via* an XB radical chain mechanism (Scheme 2).²⁷⁻³⁰ XB complex **5** is formed by supramolecular σ -hole interaction between the iodide of the α -iodoketone radical precursor **1a-e** and the amine electron donor **4**. Upon visible light irradiation, SET takes place between the components of the photoexcited XB complex **5**, which fragments into aminium radical cation **6**, C-centered radical **7** and an iodine anion. Regioselective radical attack of **7** onto trimethylvinylsilane **2** results in α -silyl radical adduct **8**, which again affords the desired ATRA product **3a-e** *via* radical chain propagation.



Scheme 2. Postulated XB radical chain mechanism for ATRA reaction between α -iodoketones **1a-e** and trimethylvinylsilane **2**.

Conclusion

We have developed a mild, visible light-mediated, photocatalyst-free protocol for intermolecular ATRA reaction between α -iodoketones and trimethylvinylsilane. The method was successfully applied to a selection of activated alkyl iodides and afforded the desired α -iodoalkylsilane ATRA products in modest to excellent yields. The variability in isolated yields observed with different substrates, despite extensive screening of reaction conditions, suggests that the optimal conditions for this novel ATRA reaction are highly substrate specific. Although no direct evidence was found for an iodide-amine XB complex, we postulate that the desired ATRA reaction operates through an XB complex/radical chain propagation mechanism. We anticipate that this new protocol will enable access to a wider range of both simple and structurally complex α -iodoalkylsilanes, a group of highly useful intermediates in synthetic chemistry, under mild conditions from simple precursors.

Experimental section

For a detailed description of all chemical procedures, chemical analysis and supporting results, see the Supporting Information.

Author information

Corresponding author

Marius M. Haugland – Department of Chemistry, UiT The Arctic University of Norway, NO-9037 Tromsø, Norway; <https://orcid.org/0000-0001-7017-344X>
Email: marius.m.haugland@uit.no

Author

Floriane Baussière – Department of Chemistry, UiT The Arctic University of Norway, NO-9037 Tromsø, Norway

Author contributions

The manuscript was written through contributions from both authors. The experiments were performed by F. B.

Notes

The authors declare no competing financial interests.

Acknowledgements

The authors thank the Tromsø Research Foundation and UiT Centre for New Antibacterial Strategies (CANS) for a start-up grant (TFS project ID: 18_CANS).

References

1. Lawrence, N. J., *Science of Synthesis*. Thieme: 2002; Vol. 4.
2. van Delft, F. L.; de Kort, M.; van der Marel, G.; van Boom, J., Use of a Novel α -Hydroxyethylating Reagent in the Stereoselective Synthesis of Lincosamine. *J. Org. Chem.* **1996**, *61* (5), 1883-1885.
3. Hudrlik, P. F.; Agwaramgbo, E. L. O.; Hudrlik, A. M., Concerning the Mechanism of the Peterson Olefination Reaction. *J. Org. Chem.* **1989**, *54* (23), 5613-5618.
4. Cai, Y. Y.; Zhu, W. J.; Zhao, S. J.; Dong, C. J.; Xu, Z. C.; Zhao, Y. C., Difluorocarbene-Mediated Cascade Cyclization: The Multifunctional Role of Ruppert-Prakash Reagent. *Org. Lett.* **2021**, *23* (9), 3546-3551.
5. Schwarzwald, G. M.; Matier, C. D.; Fu, G. C., Enantioconvergent Cross-Couplings of Alkyl Electrophiles: The Catalytic Asymmetric Synthesis of Organosilanes. *Angew. Chem., Int. Ed. Engl.* **2019**, *58* (11), 3571-3574.
6. Stork, G.; Sofia, M. J., Stereospecific Reductive Methylation via a Radical Cyclization-Desilylation Process. *J Am Chem Soc* **1986**, *108* (21), 6826-6828.
7. Nishiyama, H.; Kitajima, T.; Matsumoto, M.; Itoh, K., Silylmethyl Radical Cyclization - New Stereoselective Method for 1,3-Diol Synthesis from Allylic Alcohols. *J. Org. Chem.* **1984**, *49* (12), 2298-2300.
8. Stork, G.; Mah, R., Introduction of angular methyl groups via radical cyclization. *Tetrahedron Lett.* **1989**, *30* (28), 3609-3612.
9. Hauser, C. R.; Hance, C. R., Preparation and Reactions of α -Halo Derivatives of Certain Tetra-substituted Hydrocarbon Silanes. Grignard Syntheses of Some Silyl Compounds. *J. Am. Chem. Soc.* **1952**, *74* (20), 5091-5096.
10. Tamao, K.; Kumada, M., Preparation of Certain Bromomethyl-Substituted and Iodomethyl-Substituted Disilanes. *J. Organomet. Chem.* **1971**, *30* (3), 329-337.

11. Barrett, A. G. M.; Flygare, J. A., Triply Convergent, Stereospecific Alkene Formation via Peterson Olefination. *J. Org. Chem.* **1991**, *56*, 638-642.
12. Muñoz-Molina, J. M.; Belderrain, T. R.; Pérez, P. J., Atom Transfer Radical Reactions as a Tool for Olefin Functionalization - On the Way to Practical Applications. *Eur. J. Inorg. Chem.* **2011**, (21), 3155-3164.
13. Prier, C. K.; Rankic, D. A.; MacMillan, D. W. C., Visible Light Photoredox Catalysis with Transition Metal Complexes: Applications in Organic Synthesis. *Chem. Rev.* **2013**, *113* (7), 5322-5363.
14. Vasil'eva, T. T.; Gapusenko, S. I.; Terent'ev, A. B.; Pinyaskin, V. V.; Strankevich, I. V.; Chistyakov, A. L.; Mysov, E. I., Radical-type addition of benzyl bromide to vinyl chloride: the kinetics and activation energy of the process. *Russ. Chem. Bull.* **1993**, *42*, 840-842.
15. Vasil'eva, T. T.; Gapusenko, S. I.; Vitt, S. V.; Terent'ev, A. B., Homolytic addition of benzyl bromide to unsaturated compounds in conditions of metal-complex initiation. *Bull. Russ. Acad. Sci.: Chem.* **1992**, *41*, 1841-1845.
16. Terent'ev, A. B.; Gapusenko, S. I.; Vasil'eva, T. T.; Vitt, S. V., Relative kinetics of the radical addition of benzyl bromide to unsaturated compounds. *Bull. Russ. Acad. Sci.: Chem.* **1992**, *41*, 1567-1571.
17. Sakurai, H.; Hosomi, A.; Kumada, M., Addition of trichloromethyl radicals to alkenylsilanes. *J. Org. Chem.* **1969**, *34* (6), 1764-1768.
18. Ehrnsberger, P. Photoredox-catalyzed ATRA reactions and related processes in a new light. University of Regensburg, 2021.
19. Gatazka, M. R.; Parikh, S. G.; Rykaczewski, K. A.; Schindler, C. S., Ketyl Radical Enabled Synthesis of Oxetanes. *Synthesis-Stuttgart* **2024**, *56* (16), 2513-2520.
20. Zard, S. Z., *Radical Reactions in Organic Synthesis*. Oxford University Press: 2003.
21. Fischer, H.; Radom, L., Factors Controlling the Addition of Carbon-Centered Radicals to Alkenes - An Experimental and Theoretical Perspective. *Angew. Chem., Int. Ed.* **2001**, *40* (8), 1340-1371.
22. Romero, N. A.; Nicewicz, D. A., Organic Photoredox Catalysis. *Chem. Rev.* **2016**, *116* (17), 10075-10166.
23. Motz, R. N.; Sun, A. C.; Lehnher, D.; Ruccolo, S., High-Throughput Determination of Stern-Volmer Quenching Constants for Common Photocatalysts and Quenchers. *ACS Org. Inorg. Au* **2023**, *3* (5), 266-273.
24. Julia, F.; Constantin, T.; Leonori, D., Applications of Halogen-Atom Transfer (XAT) for the Generation of Carbon Radicals in Synthetic Photochemistry and Photocatalysis. *Chem. Rev.* **2022**, *122* (2), 2292-2352.
25. Piedra, H. F.; Valdes, C.; Plaza, M., Shining light on halogen-bonding complexes: a catalyst-free activation mode of carbon-halogen bonds for the generation of carbon-centered radicals. *Chem. Sci.* **2023**, *14* (21), 5545-5568.
26. Matsuo, K.; Yoshitake, T.; Yamaguchi, E.; Itoh, A., Photoinduced Atom Transfer Radical Addition/Cyclization Reaction between Alkynes or Alkenes with Unsaturated α -Halogenated Carbonyls. *Molecules* **2021**, *26* (22).
27. Rrapi, M.; Batsika, C. S.; Nikitas, N. F.; Tappin, N. D. C.; Triandafillidi, I.; Renaud, P.; Kokotos, C. G., Photochemical Synthesis of Lactones, Cyclopropanes and ATRA Products: Revealing the Role of Sodium Ascorbate. *Chem. Eur. J.* **2024**.
28. Corti, V.; Dosso, J.; Prato, M.; Filippini, G., Photoinduced Cascade Reactions of 2-Allylphenol Derivatives toward the Production of 2,3-Dihydrobenzofurans. *J. Org. Chem.* **2023**, *88* (9), 6008-6016.
29. Marotta, A.; Fang, H.; Adams, C. E.; Marcus, K. S.; Daniliuc, C. G.; Molloy, J. J., Direct Light-Enabled Access to α -Boryl Radicals: Application in the Stereodivergent Synthesis of Allyl Boronic Esters. *Angew. Chem., Int. Ed. Engl.* **2023**, *62* (34), e202307540.

30. Mountanea, O. G.; Mantzourani, C.; Kokotou, M. G.; Kokotos, C. G.; Kokotos, G., Sunlight- or UVA-Light-Mediated Synthesis of Hydroxamic Acids from Carboxylic Acids. *Eur. J. Org. Chem.* **2023**, 26, e202300046.

Supporting Information for:

Light-promoted synthesis of complex α -iodoalkylsilanes

Floriane Baussière and Marius M. Haugland*

Department of Chemistry, UiT The Arctic University of Norway, 9037 Tromsø, Norway

*marius.m.haugland@uit.no

Contents

Experimental methods	2
Experimental setups	2
Synthesis of α -keto iodides (1a-e)	4
Procedure I	4
Procedure II	4
Characterization	4
Synthesis of ATRA products (3a-e)	5
Procedure 1. General procedure for synthesis of ATRA product 3a (Table 1 of the manuscript, isolated yields)	5
Procedure 2. General procedure for synthesis of ATRA products 3a-e (Table 3 of the manuscript, NMR yields)	5
Characterization	6
Additional reactions and results	8
Radical trapping with TEMPO	8
Synthesis of 3a-e in the presence of 4CzIPN	9
Halogen-bond acceptor screening for the synthesis of 3b	9
Mechanistic investigations	10
UV-vis analysis	10
NMR analysis	11
References	15
NMR spectra	16

Experimental methods

All reagents purchased from chemical suppliers were used as received. All air and/or water sensitive reactions were carried out under an atmosphere of argon in flame-dried glassware using standard Schlenk techniques. Anhydrous solvents were dried by pre-storing over activated 4 Å molecular sieves and purged by argon sparging. Light irradiation was performed with RGB LED strips (5.4 W) set to blue, EvoluChem™ LED 6200K white (18 W) and Kessil LED PR160L lamps. For experiments with blue LED strips, reaction flasks were placed 1 cm away from the light source (Figure S1). The intensity of all Kessil lamps was set to the maximum: 370 nm (max 43 W), 390 nm (max 52 W), 427 nm (max 45 W) and 456 nm (max 50 W). For experiments performed with Kessil lamps outside the photoreactor (main text, Table 2, entries 10, 11 and 15), reaction vials were placed 10 cm away from the light source (Figure S2) with an over-head fan to keep the temperature at 20 °C. All other experiments with EvoluChem™ LED 6200K white or Kessil LED PR160L lamps were performed in an EvoluChem PhotoRedOx Box TC™ (Figure S3) coupled with a Julabo 310F refrigerated bath equipped with a Julabo CORIO™ CD circulator. Reactions were monitored by thin-layer chromatography (TLC) on pre-coated aluminum-based plates (TLC Silica gel 60 F₂₅₄, Supelco). The plates were developed under UV irradiation (254 nm) or with vanillin or KMnO₄ staining and subsequent heating. Column chromatography was performed with silica gel (Silica gel 60, irregular 40–63 μm for flash chromatography, VWR Chemicals). ¹H NMR spectra were recorded at room temperature on a 400 MHz Bruker 9.4 Tesla Avance III HD system equipped with a SmartProbe (broad band). ¹³C NMR spectra (¹H decoupled) were recorded at room temperature on the same machine operating at 101 MHz. All chemical shifts (δ) are reported in parts per million (ppm) with internal reference to residual protons/carbons in CDCl₃ (δ 7.26/77.16) or MeCN-d₃ (δ 1.94/118.26). Coupling constants (*J*) are given in Hz with an accuracy of 0.1 Hz. Infrared (IR) spectra were recorded as thin films or liquids on an Agilent Technologies Cary 630 FTIR 318 spectrometer. Wavelength of maximum absorbance (*v*_{max}) are reported in wavenumbers (cm⁻¹). Only selected characteristic resonances are reported. High-resolution mass spectra (HRMS) were recorded on a Thermo Scientific Orbitrap Exploris 120 Mass spectrometer, using a dual electrospray ionization (ESI) probe. Pure compounds were directly injected as solutions in MeOH, while mixtures were first separated on a Thermo Scientific Vanquish UHPLC system equipped with a Accucore Vanquish C18+ 50x2.1 Particle size 1.5μ column coupled to the mass spectrometer. Melting points were recorded on a Stuart SMP50 Automatic Melting Point instrument.

Experimental setups

The different irradiation setups used in our investigation are represented in Figures S1-3.

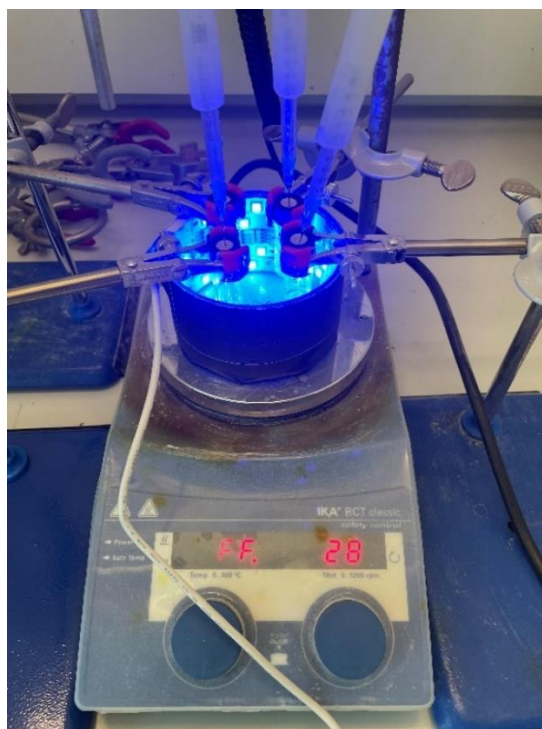


Figure S1. Blue LED strips setup. Reaction vials were placed 1 cm away from the side of a crystallization dish filled with RGB LED strips set to blue.

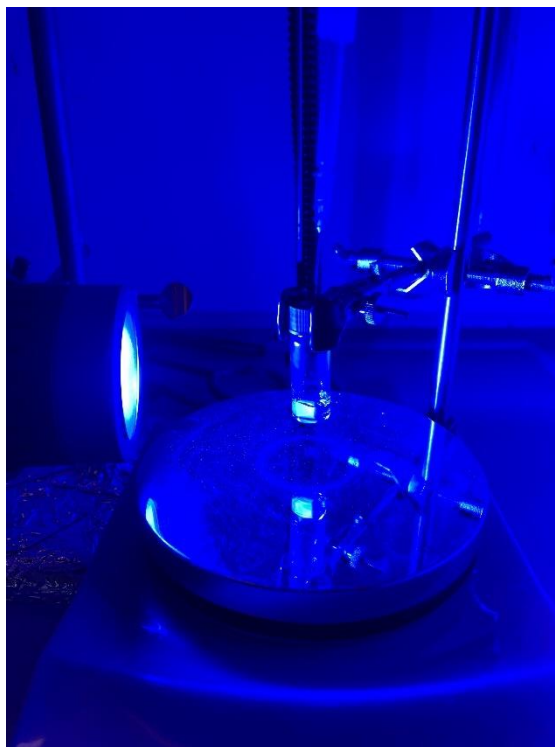


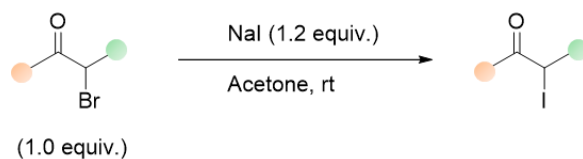
Figure S2. Kessil lamp outside photoreactor setup. Reaction vials were placed 10 cm away from the irradiation source of choice. A fan (not visible on figure) was placed above the setup to maintain room temperature.



Figure S3. Photoreactor setup. The photoreactor was placed onto a stirring plate, topped with the light source of choice, and filled with a thermostatic mixture (glycerol/H₂O 2:1) kept at set temperature by recirculating through the cooling/heating bath unit (not visible on figure). Reaction vials were immersed in the thermostatic fluid and held in place by the holder, which allowed an even light irradiation of all reaction mixtures.

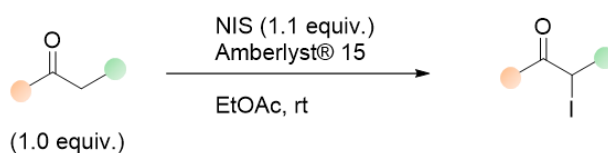
Synthesis of α -keto iodides (**1a-e**)

Procedure I



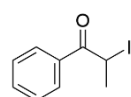
Based on a literature procedure,¹ a solution of sodium iodide (1.2 equiv.) in acetone (0.2 M with respect to the α -bromo ketone) was added to a solution of α -bromo ketone (1.0 equiv.) in acetone (0.2 M with respect to the α -bromo ketone), and the mixture was stirred in the dark at room temperature. Upon completion as indicated by TLC, the mixture was filtered through Celite[®]. The filtrate was reduced *in vacuo*, redissolved in CH_2Cl_2 and filtered once more. The filtrate was washed with an aqueous 10% $\text{Na}_2\text{S}_2\text{O}_3$ solution before being dried over anhydrous Na_2SO_4 and reduced *in vacuo*. The crude material was purified by column chromatography to afford the wanted α -keto iodide.

Procedure II

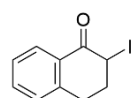


Based on a literature procedure,² *N*-iodosuccinimide (1.1 equiv.) was added to a mixture of ketone (1.0 equiv.) and Amberlyst[®] 15 hydrogen form (1.5 g) in EtOAc (0.1 M with respect to the ketone). The reaction mixture was stirred in the dark at room temperature. Upon completion as indicated by TLC, the mixture was filtered and concentrated *in vacuo*. The crude material was purified by column chromatography to afford the wanted α -keto iodide.

Characterization

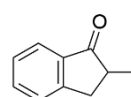


2-Iodo-1-phenyl-1-propanone 1a was synthesized from 2-bromopropiophenone (1.5 mL, 9.60 mmol, 1.0 equiv.), sodium iodide (1.72 g, 11.50 mmol, 1.2 equiv.) in acetone (96 mL) according to Procedure I. The crude material was purified by column chromatography (Et_2O /pentane 7%) to afford α -iodo ketone **1a** (2.29 g, 8.80 mmol, 92%) as a light-yellow solid. ¹H NMR (400 MHz, CDCl_3) δ 8.07–7.95 (2H, m, ArH), 7.62–7.53 (1H, m, ArH), 7.48 (2H, m, ArH), 5.50 (1H, q, $J = 6.7$ Hz, CHI), 2.08 (3H, d, $J = 6.7$ Hz, CH_3); ¹³C NMR (CDCl_3 , 101 MHz) δ 194.9, 133.8, 133.7, 128.9 (2C), 128.8 (2C), 22.2, 18.2. Data consistent with literature values.¹



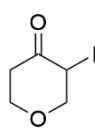
2-Iodo-3,4-dihydronaphthalen-1(2H)-one 1b was synthesized from α -tetralone (0.69 mL, 5.03 mmol, 1.0 equiv.), *N*-iodosuccinimide (1.18 g, 5.30 mmol, 1.1 equiv.), Amberlyst[®] 15 hydrogen form (1.5 g) in EtOAc (50 mL) according to Procedure II. The crude was purified by column chromatography (EtOAc/pentane 5%) to afford α -iodo ketone **1b** (0.96 g, 3.54 mmol, 70%) as an orange solid. ¹H NMR (400 MHz, CDCl_3) δ 8.10 (1H, dd, $J = 7.9, 1.4$ Hz, ArH), 7.51 (1H, td, $J = 7.5, 1.5$ Hz, ArH), 7.35 (1H,

t, $J = 7.6$ Hz, ArH), 7.29 (1H, d, $J = 7.7$ Hz, ArH), 5.02 (1H, t, $J = 3.8$ Hz, CHI), 3.15 (1H, ddd, $J = 16.3, 11.2, 4.5$ Hz, CH_2), 2.88 (1H, dt, $J = 17.2, 4.0$ Hz, CH_2), 2.29 (1H, dq, $J = 15.0, 3.9$ Hz, CHICH_2), 2.19–2.10 (1H, m, CHICH_2); ¹³C NMR (CDCl_3 , 101 MHz) δ 192.0, 142.9, 134.1, 129.5, 128.9, 128.9, 127.2, 32.8, 30.8, 28.0. Data consistent with literature values.³

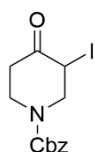


2-Iodo-1-indanone 1c was synthesized from 1-indanone (0.60 mL, 5.04 mmol, 1.0 equiv.), *N*-iodosuccinimide (1.18 g, 5.26 mmol, 1.1 equiv.), Amberlyst[®] 15 hydrogen form (1.5 g) in EtOAc (50 mL) according to Procedure II. The crude was purified by column chromatography (EtOAc/pentane 10%) to afford α -iodo ketone **1c** (1.10 g, 4.25 mmol, 84%) as a brown solid. ¹H NMR (400 MHz, CDCl_3) δ 7.86 (1H,

d, $J = 7.8$ Hz, ArH), 7.72–7.60 (1H, m, ArH), 7.45–7.41 (2H, m, ArH), 4.95 (1H, dd, $J = 7.4, 2.7$ Hz, CHI), 3.89 (1H, dd, $J = 18.4, 7.4$ Hz, CH₂), 3.48 (1H, dd, $J = 18.4, 2.6$ Hz, CH₂); ¹³C NMR (CDCl₃, 101 MHz) δ 201.6, 151.4, 135.8, 133.0, 128.3, 126.6, 125.2, 39.7, 19.4. Data consistent with literature values.⁴



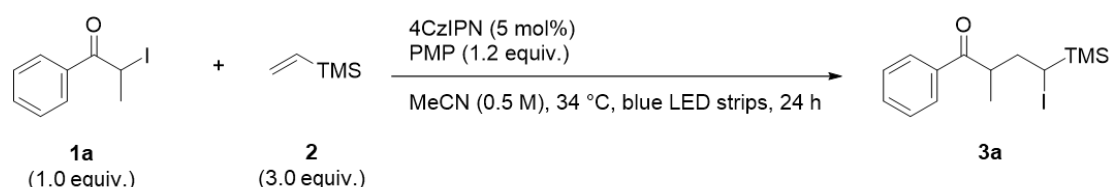
3-Iodotetrahydro-4H-pyran-4-one 1d was synthesized under inert atmosphere from tetrahydro-4H-pyran-4-one (0.46 mL, 5.00 mmol, 1.0 equiv.), *N*-iodosuccinimide (1.18 g, 5.26 mmol, 1.1 equiv.), Amberlyst® 15 hydrogen form (1.5 g) in dry EtOAc (50 mL) according to Procedure II. The crude was purified by column chromatography (EtOAc/pentane 25%) to afford α-iodo ketone **1d** (0.76 g, 3.36 mmol, 67%) as a yellow-brown solid. *R*_f 0.37 (EtOAc/pentane 25%); m.p. 32–34 °C; IR (liquid, $\nu_{\max}/\text{cm}^{-1}$) 2967, 2856, 1715, 1357, 1271, 1208, 1185, 1128, 1086, 1029, 964, 843, 689; ¹H NMR (400 MHz, CDCl₃) δ 4.67 (1H, ddd, $J = 6.4, 4.7, 1.5$ Hz, CHI), 4.14 (1H, dd, $J = 12.5, 4.7$ Hz, CHICH₂), 4.06–3.92 (3H, m, 2 x OCH₂, CHICH₂), 3.21 (1H, dt, $J = 14.9, 6.0$ Hz, COCH₂), 2.59 (1H, dtd, $J = 14.9, 6.0, 1.5$ Hz, COCH₂); ¹³C NMR (CDCl₃, 101 MHz) δ 199.4, 75.1, 68.4, 39.9, 30.8; HRMS (ESI) calc. for C₅H₇IO₂Na ([M+Na]⁺) 248.9383, found 248.9384.



Benzyl 3-iodo-4-oxo-1-piperidinecarboxylate 1e was synthesized from benzyl 4-oxo-1-piperidinecarboxylate (1.17 g, 5.00 mmol, 1.0 equiv.), *N*-iodosuccinimide (1.18 g, 5.26 mmol, 1.1 equiv.), Amberlyst® 15 hydrogen form (1.5 g) in EtOAc (50 mL) according to Procedure II. The crude was purified by column chromatography (EtOAc/pentane 35%) to afford α-iodo ketone **1e** (1.20 g, 3.33 mmol, 67%) as a thick yellow oil. *R*_f 0.30 (EtOAc/pentane 35%); IR (liquid, $\nu_{\max}/\text{cm}^{-1}$) 1692, 1427, 1221, 1140, 1094, 986, 735, 697; ¹H NMR (400 MHz, CDCl₃) δ 7.39–7.36 (5H, m, ArH), 5.24–5.17 (2H, m, COOCH₂), 4.60–4.54 (1H, m, CHI), 4.17–3.78 (3H, m, CH₂), 3.66–3.52 (1H, m, CH₂), 3.29–3.19 (1H, m, CH₂), 2.43 (1H, dt, $J = 15.3, 5.3$ Hz, CH₂); ¹³C NMR (CDCl₃, 101 MHz) δ 200.7, 155.0, 136.1, 128.7 (2C), 128.5 (2C), 128.3, 68.1, 51.6, 43.4, 37.1 (d, $J = 55.7$ Hz), 27.9; HRMS (ESI) calc. for C₁₃H₁₄INO₃Na ([M+Na]⁺) 381.9911, found 381.9911.

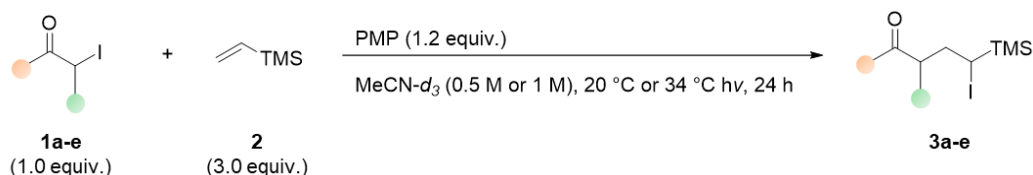
Synthesis of ATRA products (3a-e)

Procedure 1. General procedure for synthesis of ATRA product 3a (Table 1 of the manuscript, isolated yields)



Standard conditions: 1,2,2,6,6-Pentamethylpiperidine (PMP, 65 μL, 0.36 mmol, 1.2 equiv.) was added to a mixture of **1a** (78 mg, 0.30 mmol, 1.0 equiv.), **2** (0.13 mL, 0.90 mmol, 3.0 equiv.) and 4CzIPN (12 mg, 0.016 mmol, 5 mol%) in dry MeCN (0.6 mL) under Ar. The reaction mixture was irradiated with blue LED strips for 24 h (temperature inside the reaction vessel: 34 °C) before being reduced *in vacuo*. The crude was purified by column chromatography (Et₂O/pentane 4%) to afford ATRA product **3a** as a colorless oil.

Procedure 2. General procedure for synthesis of ATRA products 3a-e (Table 3 of the manuscript, NMR yields)



PMP (0.36 mmol, 1.2 equiv.) was added to a mixture of α-iodo substrate **1** (0.30 mmol, 1.0 equiv.), **2** (0.90 mmol, 3.0 equiv.) and ethylene carbonate (internal standard, 0.08 mmol, 0.25 equiv.) in dry MeCN-*d*₃ (0.3 mL or 0.6 mL) under Ar. The reaction mixture was stirred 1 min before transferring a few drops of it into an NMR tube containing CDCl₃ (0.5 mL). The NMR sample was analyzed by ¹H NMR to determine the exact initial substrate/internal

standard ratio of the reaction mixture. The reaction vial was irradiated with the appropriate light source at a set temperature. After 24 h, the light was switched off, and CDCl_3 (1 mL) was added to the reaction mixture to solubilize any potential precipitate. A few drops of the reaction mixture were transferred into an NMR tube containing CDCl_3 (0.5 mL) and the sample was analyzed by ^1H NMR. The NMR yield (Table S1) was calculated from the substrate/product integrals ratio when setting the internal standard's peak integral to 1.00 in spectra acquired both before and after reaction.

Table S1. Summary of the yields of the ATRA reactions with substrates **1a-e** under the conditions tested.^a

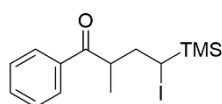
irradiation source	3a yield (%)	3b yield (%)	3c yield (%)	3d yield (%)	3e yield (%)
blue LED strip	83 ^b	10 ^b	4 ^b	26 ^b	10 ^b
white light	11 ^d ; 84 ^e ; 78 ^f	1 ^d ; 7 ^e ; 6 ^f	21 ^d ; 17 ^e ; 7 ^f	31 ^d ; 52 ^e ; 53 ^f	69 ^d ; 41 ^e ; 37 ^f
390 nm	0	4	— ^c	31	— ^c
427 nm	25	18	8	71	62
456 nm	70	18	11	66	72

^aYields determined by ^1H NMR with ethylene carbonate as internal standard. ^bReaction performed at 34 °C. ^cExperiment not performed.

^dReaction performed at 0 °C. ^eReaction performed at 20 °C. ^fReaction performed at 40 °C.

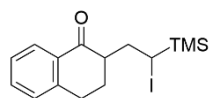
Characterization

For the purpose of characterization, ATRA products **3b-e** were isolated from reactions performed according to Procedure 2, which were part of the reaction conditions screening (Table S1). To this end, reaction mixtures of reactions that afforded the desired products in moderate to good amounts according to NMR yields were further concentrated *in vacuo*, and the crudes were purified by column chromatography to afford ATRA products **3b-e**.



4-Iodo-2-methyl-1-phenyl-4-(trimethylsilyl)butan-1-one 3a was synthesized according to Procedure 1 (standard conditions). The crude was purified by column chromatography (Et_2O /pentane 4%) to afford separable 11:9 diastereomers of ATRA product **3a** (*Diastereomer I*: 29 mg, 0.08 mmol, 27%; *Diastereomer 2*: 24 mg, 0.07 mmol, 22%; overall

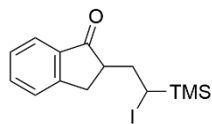
isolated yield: 49%) as colorless oils. *Diastereomer I*: R_f 0.36 (Et_2O /pentane 4%); **IR** (liquid, $\nu_{\text{max}}/\text{cm}^{-1}$) 2960, 1679, 1449, 1249, 1219, 968, 857, 836, 702, 687; **^1H NMR** (400 MHz, CDCl_3) δ 8.09–8.02 (2H, m, 2 x ArH), 7.62–7.54 (1H, m, ArH), 7.54–7.45 (2H, m, 2 x ArH), 4.03 (1H, dqd, $J = 10.0, 7.1, 2.7$ Hz, CHCH₃), 3.03 (1H, dd, $J = 13.1, 2.3$ Hz, CHI), 2.29 (1H, ddd, $J = 14.8, 10.3, 2.3$ Hz, CH₂), 1.70 (1H, ddd, $J = 14.8, 13.2, 2.7$ Hz, CH₂), 1.22 (3H, d, $J = 7.2$ Hz, CH₃), 0.18 (9H, s, 3 x Si(CH₃)); **^{13}C NMR** (CDCl_3 , 101 MHz) δ 204.0, 136.9, 133.3, 128.9 (2C), 128.6 (2C), 42.8, 37.2, 22.8, 19.4, -2.2 (3C); **HRMS** calc. for $\text{C}_{14}\text{H}_{21}\text{IOSiNa}$ ($[\text{M}+\text{Na}]^+$) 383.0299, found 383.0298. *Diastereomer II*: R_f 0.30 (Et_2O /pentane 4%); **IR** (liquid, $\nu_{\text{max}}/\text{cm}^{-1}$) 2961, 1681, 1598, 1449, 1363, 1249, 1179, 1079, 970, 855, 835, 700; **^1H NMR** (400 MHz, CDCl_3) δ 8.07–8.00 (2H, m, 2 x ArH), 7.61–7.54 (1H, m, ArH), 7.51–7.47 (2H, m, 2 x ArH), 3.83 (1H, dqd, $J = 9.7, 6.7, 2.8$ Hz, CHCH₃), 3.29 (1H, dd, $J = 13.5, 2.5$ Hz, CHI), 2.07 (1H, ddd, $J = 15.0, 13.5, 2.8$ Hz, CH₂), 1.56 (1H, ddd, $J = 15.0, 10.3, 2.5$ Hz, CH₂), 1.17 (3H, d, $J = 6.7$ Hz, CH₃), 0.16 (9H, s, 3 x Si(CH₃)); **^{13}C NMR** (CDCl_3 , 101 MHz) δ 203.9, 136.0, 133.2, 128.9 (2C), 128.6 (2C), 42.3, 36.8, 21.3, 14.8, -2.1 (3C); **HRMS** calc. for $\text{C}_{14}\text{H}_{21}\text{IOSiNa}$ ($[\text{M}+\text{Na}]^+$) 383.0299, found 383.0298.



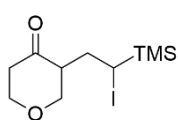
2-(2-Iodo-2-(trimethylsilyl)ethyl)-3,4-dihydronaphthalen-1(2H)-one 3b was synthesized according to Procedure 2 (456 nm, 20 °C). Upon NMR yield determination (18%), the reaction mixture was reduced *in vacuo*, and the crude was purified by column

chromatography (EtOAc /heptane 0-5%) to afford separable 13:12 diastereomers of ATRA product **3b** (*Diastereomer I*: 19 mg, 0.05 mmol, 8%; *Diastereomer II*: 19 mg, 0.05 mmol, 9%; overall isolated yield: 17%) as colorless oils. *Diastereomer I*: R_f 0.46 (EtOAc /heptane 10%); **IR** (thin film, $\nu_{\text{max}}/\text{cm}^{-1}$) 2951, 2928, 2861, 1682, 1602, 1456, 1361, 1249, 1224, 935, 910, 836, 733; **^1H NMR** (400 MHz, CDCl_3) δ 7.98 (1H, dd, $J = 7.9, 1.5$ Hz, ArH), 7.47 (1H, td, $J = 7.5, 1.5$ Hz, ArH), 7.30 (1H, t, $J = 7.6$ Hz, ArH), 7.24 (1H, d, $J = 7.8$ Hz, ArH), 3.72 (1H, dd, $J = 12.6, 2.4$ Hz, CHI), 3.18 (1H, ddd, $J = 16.7, 11.8, 4.8$ Hz, CCH₂), 3.06–2.84 (2H, m, COCH, CCH₂), 2.30 (1H, ddd, $J = 15.0, 9.1, 2.4$ Hz, CH₂CHI), 2.21–2.08 (1H, m, CH₂), 2.05–1.89 (1H, m, CH₂), 1.62 (1H, ddd, $J = 14.9, 12.6, 2.3$ Hz, CH₂CHI), 0.21 (9H, s, Si(CH₃)₃); **^{13}C NMR** (CDCl_3 , 101 MHz) δ 200.7, 144.0, 133.4, 132.9, 128.9, 127.3, 126.8, 49.1, 36.2, 30.9, 29.4, 24.8, -2.1 (3C); **HRMS** (ESI) calc. for $\text{C}_{15}\text{H}_{21}\text{IOSiNa}$ ($[\text{M}+\text{Na}]^+$) 395.0299, found 395.0299. *Diastereomer II*: R_f 0.44 (EtOAc /heptane 10%); **IR** (thin film, $\nu_{\text{max}}/\text{cm}^{-1}$) 2951, 2858, 1684, 1602, 1456, 1310, 1250, 1223, 861, 842, 742; **^1H NMR** (400 MHz, CDCl_3) δ 8.04 (1H, dd, $J = 7.8, 1.5$ Hz, ArH), 7.47 (1H, td, $J = 7.5, 1.5$ Hz, ArH), 7.31

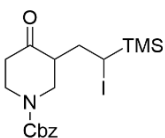
(1H, t, $J = 7.7$ Hz, ArH), 7.28–7.20 (1H, m, ArH), 3.17 (1H, dd, $J = 14.0, 2.6$ Hz, CHI), 3.12–2.93 (2H, m, CCH₂), 2.90–2.82 (1H, m, COCH), 2.59 (1H, ddd, $J = 15.4, 14.0, 3.4$ Hz, CH₂CHI), 2.39–2.23 (1H, m, CH₂), 1.73–1.56 (1H, m, CH₂), 1.45 (1H, ddd, $J = 15.4, 10.2, 2.7$ Hz, CH₂CHI), 0.20 (9H, s, Si(CH₃)₃); ¹³C NMR (CDCl₃, 101 MHz) δ 199.9, 144.0, 133.4, 132.7, 128.8, 127.5, 126.8, 49.0, 32.6, 28.8, 26.6, 20.3, -2.0 (3C); HRMS (ESI) calc. for C₁₅H₂₁IOSiNa ([M+Na]⁺) 395.0299, found 395.0299.



2-(2-Iodo-2-(trimethylsilyl)ethyl)-2,3-dihydro-1H-inden-1-one 3c was synthesized according to Procedure 2 (456 nm, 20 °C). Upon NMR yield determination (11%), the reaction mixture was reduced *in vacuo*, and the crude was purified by column chromatography (EtOAc/heptane 0-5%) to afford separable 9:11 diastereomers of ATRA product **3c** (*Diastereomer I*: 1 mg, 2.8 μ mol, 1%; *Diastereomer II*: 1 mg, 2.8 μ mol, 1%; overall isolated yield: 2%) as colorless and light-yellow oils, respectively. *Diastereomer I*: R_f 0.32 (EtOAc/heptane 5%); IR (thin film, $\nu_{\max}/\text{cm}^{-1}$) 2953, 2924, 2851, 1703, 1609, 1466, 1297, 1249, 1204, 1043, 837, 740, 719; ¹H NMR (400 MHz, CDCl₃) δ 7.74 (1H, d, $J = 7.7$ Hz, ArH), 7.59 (1H, td, $J = 7.4, 1.2$ Hz, ArH), 7.45 (1H, dt, $J = 7.6, 0.9$ Hz, ArH), 7.42–7.31 (1H, m, ArH), 3.89 (1H, dd, $J = 12.2, 3.0$ Hz, CHI), 3.52 (1H, dd, $J = 17.2, 8.0$ Hz, CCH₂), 3.00 (1H, tt, $J = 8.6, 4.6$ Hz, COCH), 2.80 (1H, dd, $J = 17.2, 4.3$ Hz, CCH₂), 2.12 (1H, ddd, $J = 15.1, 8.8, 3.0$ Hz, CH₂CHI), 1.96 (1H, ddd, $J = 15.2, 12.2, 5.0$ Hz, CH₂CHI), 0.17 (9H, s, Si(CH₃)₃); ¹³C NMR (CDCl₃, 101 MHz) δ 208.5, 153.5, 136.8, 134.9, 127.6, 126.6, 124.1, 48.2, 37.0, 34.3, 21.9, -2.0 (3C); HRMS (ESI) calc. for C₁₄H₁₉IOSiNa ([M+Na]⁺) 381.0142, found 381.0142. *Diastereomer II*: R_f 0.28 (EtOAc/heptane 5%); IR (thin film, $\nu_{\max}/\text{cm}^{-1}$) 2953, 2929, 1741, 1701, 1608, 1466, 1368, 1247, 1215, 1095, 1032, 869, 835, 749; ¹H NMR (400 MHz, CDCl₃) δ 7.77 (1H, d, $J = 7.7$ Hz), 7.60 (1H, td, $J = 7.4, 1.2$ Hz), 7.47 (1H, dt, $J = 7.7, 1.0$ Hz), 7.43–7.33 (1H, m), 3.41 (1H, dd, $J = 16.9, 7.9$ Hz, CCH₂), 3.27–3.10 (2H, m, COCH, CHI), 2.68 (1H, dd, $J = 17.0, 4.4$ Hz, CCH₂), 2.43 (1H, ddd, $J = 14.9, 13.7, 3.6$ Hz, CH₂CHI), 1.43 (1H, ddd, $J = 14.9, 11.2, 2.6$ Hz, CH₂CHI), 0.18 (9H, s, Si(CH₃)₃); ¹³C NMR (CDCl₃, 101 MHz) δ 208.3, 153.2, 137.2, 135.0, 127.7, 126.7, 124.1, 50.0, 34.9, 32.0, 21.5, -2.0 (3C); HRMS (ESI) calc. for C₁₄H₁₉IOSiNa ([M+Na]⁺) 381.0142, found 381.0143.



3-(2-Iodo-2-(trimethylsilyl)ethyl)tetrahydro-4H-pyran-4-one 3d was synthesized according to Procedure 2 (blue LED strip, 34 °C). Upon NMR yield determination (26%), the reaction mixture was reduced *in vacuo*, and the crude was purified by column chromatography (EtOAc/pentane 15%) to afford separable 13:12 diastereomers of ATRA product **3d** (*Diastereomer I*: 10 mg, 0.03 mmol, 10%; *Diastereomer II*: 10 mg, 0.03 mmol, 10%; overall isolated yield: 20%) as colorless oils. *Diastereomer I*: R_f 0.40 (EtOAc/pentane 15%); IR (thin film, $\nu_{\max}/\text{cm}^{-1}$) 2956, 2847, 1715, 1368, 1250, 1204, 1149, 1101, 1045, 861, 841; ¹H NMR (400 MHz, CDCl₃) δ 4.27–4.22 (1H, m, CH₂O), 4.16–4.11 (1H, m, CHCH₂O), 3.70 (1H, td, $J = 11.3, 3.1$ Hz, CH₂O), 3.43–3.25 (2H, m, CHCH₂O, CHI), 3.07–3.00 (1H, m, COCH), 2.73–2.65 (1H, m, COCH₂), 2.39–2.34 (1H, m, COCH₂), 2.13–2.06 (1H, m, CH₂CHI), 1.32–1.24 (1H, m, CH₂CHI), 0.17 (9H, s, Si(CH₃)₃); ¹³C NMR (CDCl₃, 101 MHz) δ 208.2, 73.1, 69.1, 53.3, 43.1, 30.3, 22.4, -2.2 (3C); HRMS (ESI) calc. for C₁₀H₁₉IO₂SiNa ([M+Na]⁺) 349.0091, found 349.0090. *Diastereomer II*: R_f 0.28 (EtOAc/pentane 15%); IR (thin film, $\nu_{\max}/\text{cm}^{-1}$) 2963, 2853, 2850, 1715, 1368, 1251, 1238, 1220, 1153, 1101, 869, 840; ¹H NMR (400 MHz, CDCl₃) δ 4.32–4.22 (2H, m, CH₂O, CHCH₂O), 3.71 (1H, td, $J = 11.4, 3.3$ Hz, CH₂O), 3.29 (1H, t, $J = 10.6$ Hz, CHCH₂O), 2.99–2.90 (2H, m, COCH, CHI), 2.71–2.65 (1H, m, COCH₂), 2.41 (1H, dt, $J = 14.3, 3.0$ Hz, COCH₂), 2.30–2.22 (1H, m, CH₂CHI), 1.50–1.43 (1H, m, CH₂CHI), 0.16 (9H, s, Si(CH₃)₃); ¹³C NMR (CDCl₃, 101 MHz) δ 208.0, 71.4, 68.7, 52.3, 42.7, 29.0, 18.5, -2.1 (3C); HRMS (ESI) calc. for C₁₀H₁₉IO₂SiNa ([M+Na]⁺) 349.0091, found 349.0090.

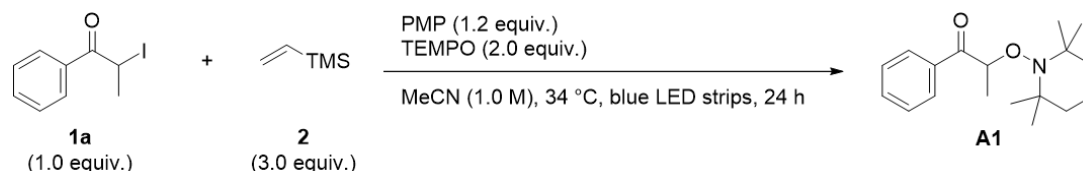


Benzyl 3-(2-iodo-2-(trimethylsilyl)ethyl)-4-oxopiperidine-1-carboxylate 3e was synthesized according to Procedure 2 (427 nm, 20 °C). Upon NMR yield determination (62%), the reaction mixture was reduced *in vacuo*, and the crude was purified by column chromatography (EtOAc/pentane 20%) to afford separable 23:27 diastereomers of ATRA product **3e** (*Diastereomer I*: 34 mg, 0.07 mmol, 25%; *Diastereomer II*: 40 mg, 0.09 mmol, 29%; overall isolated yield: 54%) as colorless oils. *Diastereomer I*: R_f 0.31 (EtOAc/pentane 20%); IR (thin film, $\nu_{\max}/\text{cm}^{-1}$) 2953, 2899, 1697, 1422, 1362, 1308, 1273, 1219, 1134, 1108, 1040, 979, 836, 732, 697; ¹H NMR (400 MHz, CDCl₃) δ 7.48–7.28 (5H, m, ArH), 5.20 (2H, s, OCH₂), 4.32 (2H, s, CH₂N, CHCH₂N), 3.33–3.24 (2H, m, CH₂N, CHI), 2.93 (2H, s, COCH, CHCH₂N), 2.59–2.52 (1H, m, COCH₂), 2.40–2.36 (1H, m, COCH₂), 2.07 (1H, s, CH₂CHI), 1.41 (1H, s, CH₂CHI), 0.17 (9H, s, Si(CH₃)₃); ¹³C NMR (CDCl₃, 101 MHz) δ 208.8, 155.2, 136.4, 128.7 (2C), 128.4, 128.2 (2C), 67.8, 51.7, 49.3, 44.3, 41.4, 31.7, 22.4, -2.0 (3C); HRMS (ESI) calc. for C₁₈H₂₆INO₃SiNa ([M+Na]⁺) 482.0619, found 482.0620. *Diastereomer II*: R_f 0.21

(EtOAc/pentane 20%); IR (thin film, $\nu_{\max}/\text{cm}^{-1}$) 2954, 2894, 1697, 1426, 1363, 1275, 1250, 1226, 1109, 993, 910, 836, 731, 697; $^1\text{H NMR}$ (400 MHz, CDCl_3) δ 7.43–7.33 (5H, m, ArH), 5.20 (2H, q, $J = 12.4$ Hz, OCH_2), 4.32–4.14 (2H, m, CH_2N , CHCH_2N), 3.46–3.24 (1H, m, CH_2N), 2.97–2.85 (3H, m, COCH , CHCH_2N , CHI), 2.56–2.54 (1H, m, COCH_2), 2.48–2.42 (1H, m, COCH_2), 2.26–2.18 (1H, m, CH_2CHI), 1.48–1.44 (1H, m, CH_2CHI), 0.15 (9H, s, $\text{Si}(\text{CH}_3)_3$); $^{13}\text{C NMR}$ (CDCl_3 , 101 MHz) δ 208.7, 155.2, 136.4, 128.7 (2C), 128.4, 128.2 (2C), 67.8, 51.2, 46.6, 43.8, 40.8, 31.7, 18.4, -2.4 (3C); HRMS (ESI) calc. for $\text{C}_{18}\text{H}_{26}\text{INO}_3\text{SiNa}$ ($[\text{M}+\text{Na}]^+$) 482.0619, found 482.0620.

Additional reactions and results

Radical trapping with TEMPO



PMP (65 μL , 0.36 mmol, 1.2 equiv.) was added to a solution of **1a** (78 mg, 0.30 mmol, 1.0 equiv.), **2** (0.13 mL, 0.90 mmol, 3.0 equiv.) and TEMPO (94 mg, 0.60 mmol, 2.0 equiv.) in dry MeCN (0.3 mL) under Ar. The reaction mixture was irradiated with blue LED strips for 24 h before being reduced *in vacuo*. The resulting crude was analyzed by LC/HRMS (solvent A: 100% H_2O + 0.1% TFA, solvent B: 90% MeCN + 10% H_2O + 0.1% TFA; 9 min method: 1 min 0% B, 6 min ramping to 90% B, 1 min hold 90% B, 1 min 0% B; column temperature: 45 $^\circ\text{C}$; detection by UV 220 nm and 254 nm), with the mass of the peak at 4.30 min corresponding to the **1a**-TEMPO adduct **A1** (Figure S4), thus confirming the radical nature of the reaction. HRMS (ESI) calc. for $\text{C}_{18}\text{H}_{28}\text{NO}_2$ ($[\text{M}+\text{H}]^+$) 290.2115, found 290.2115.

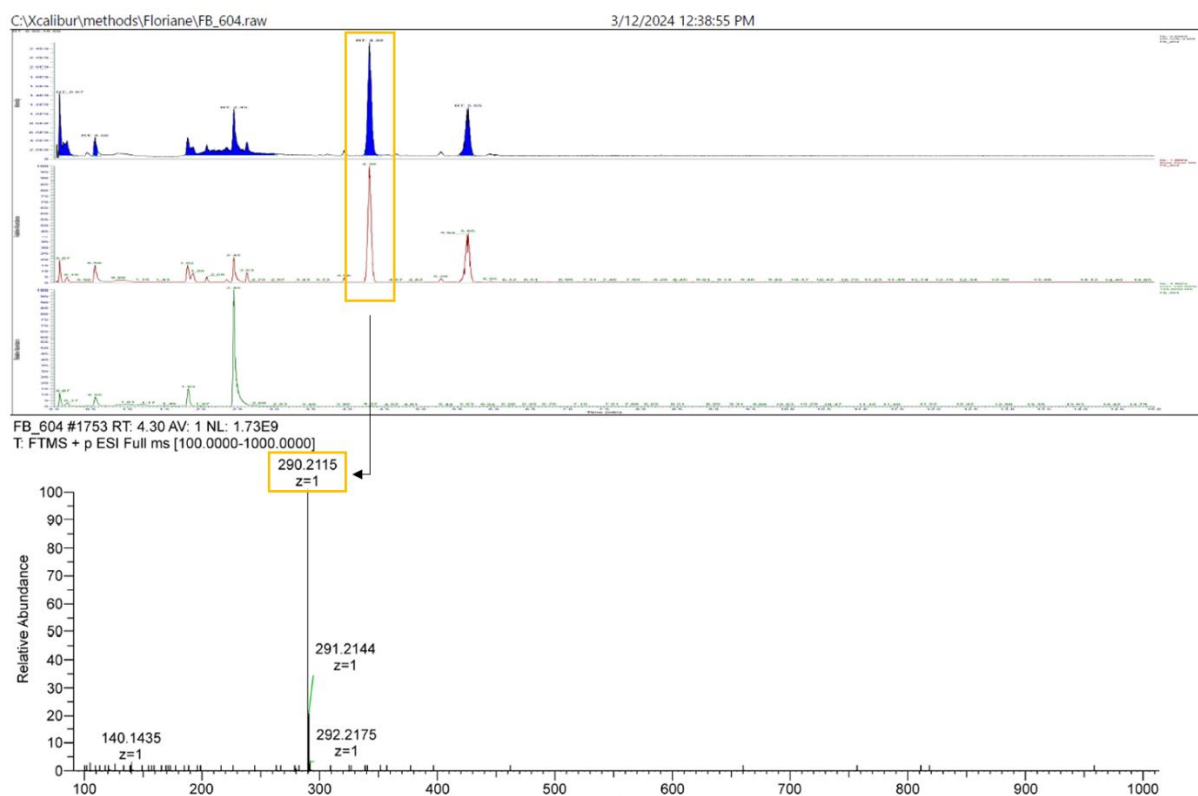
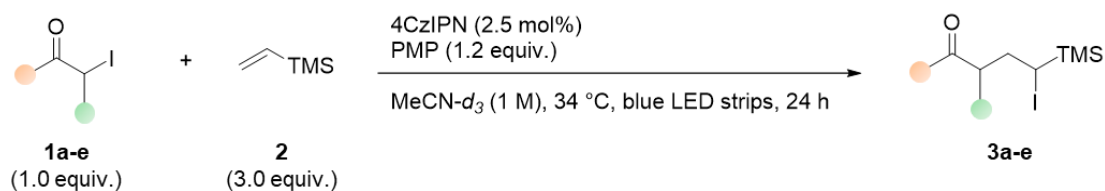


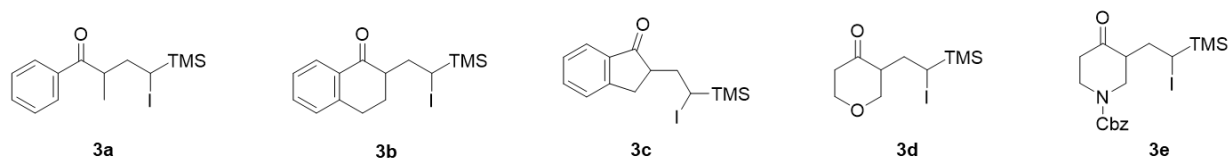
Figure S4. LC/HRMS analysis of the crude mixture after 24 h light irradiation in presence of TEMPO. The highlighted peak of the chromatogram corresponds to the highlighted mass, which matches the mass of **1a**-TEMPO adduct **A1**.

Synthesis of **3a-e** in the presence of 4CzIPN



PMP (0.36 mmol, 1.2 equiv.) was added to a mixture of α -iodo substrate **1** (0.30 mmol, 1.0 equiv.), **2** (0.90 mmol, 3.0 equiv.), 4CzIPN (2.5 mol%) and ethylene carbonate (internal standard, 0.08 mmol, 0.25 equiv.) in dry MeCN- d_3 (0.3 mL) under Ar. The reaction mixture was stirred 1 min before transferring a few drops of it into an NMR tube containing CDCl₃ (0.5 mL). The NMR sample was analyzed by ¹H NMR to determine the exact initial substrate/internal standard ratio of the reaction mixture. The reaction vial was irradiated with blue LED strips at 34 °C. After 24 h, the light was switched off, and CDCl₃ (1 mL) was added to the reaction mixture to solubilize any potential precipitate. A few drops of the reaction mixture were transferred into an NMR tube containing CDCl₃ (0.5 mL) and the sample was analyzed by ¹H NMR. The NMR yield was calculated from the substrate/product integrals ratio when setting the internal standard's peak integral to 1.00 in spectra acquired both before and after reaction. NMR yields of ATRA products **3a-e** are reported below (Table S2).

Table S2. Synthesis of ATRA products **3a-e** with photocatalyst 4CzIPN present in the reaction mixture^a

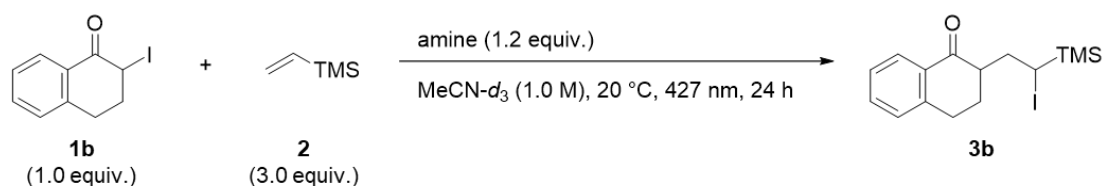


product	3a	3b	3c	3d	3e
yield (%) ^b	88	10	9	43	85

^aReaction scale: 0.30 mmol. ^bYield determined by ¹H NMR with ethylene carbonate as internal standard.

Halogen-bond acceptor screening for the synthesis of **3b**

A second amine screening was performed to investigate the interaction between the halogen-bond acceptor and low yielding substrate **1b**, and to test additional amines known to form XB complexes with alkyl halides⁵⁻⁸ that were not part of the initial screening.



The amine (0.36 mmol, 1.2 equiv.) was added to a mixture of **1b** (0.30 mmol, 1.0 equiv.), **2** (0.90 mmol, 3.0 equiv.) and ethylene carbonate (internal standard, 0.08 mmol, 0.25 equiv.) in dry MeCN- d_3 (0.3 mL) under Ar. The reaction mixture was stirred 1 min before transferring a few drops of it into an NMR tube containing CDCl₃ (0.5 mL). The NMR sample was analyzed by ¹H NMR to determine the exact initial substrate/internal standard ratio of the reaction mixture. The reaction vial was placed in the photoreactor, and the mixture was irradiated at 427 nm at 20 °C. After 24 h, the light was switched off, and CDCl₃ (1 mL) was added to the reaction mixture to solubilize any potential precipitate. A few drops of the reaction mixture were transferred into an NMR tube containing CDCl₃ (0.5 mL) and the sample was analyzed by ¹H NMR. The NMR yield was calculated from the substrate/product integrals ratio when setting the internal standard's peak integral to 1.00 in spectra acquired both before and after the reaction. The yields are reported below (Table S3).

Table S3. Amine screening in the synthesis of **3b**^a

amine	yield (%) ^b
PMP	18
4-phenylpyridine	0
2,6-lutidine	0
Et ₃ N	3
<i>N,N,N',N'</i> -tetraethylethylenediamine	5
quinuclidine	0
4-methoxytriphenylamine	0
triphenylamine	0
tribenzylamine	2

^aReaction scale: 0.30 mmol. ^bYield determined by ¹H NMR with ethylene carbonate as internal standard.

Mechanistic investigations

UV-vis analysis

The UV-vis spectra of a solution of **1a** in MeCN ($5 \cdot 10^{-5}$ M) was recorded, as well as the ones of 1.0:1.2 and 1.0:3.0:1.2 mixtures of **1a**/PMP and **1a**/**2**/PMP, respectively, in MeCN ($5 \cdot 10^{-5}$ M with respect to **1a**) (Figure S5). No evident bathochromic shift was visible upon mixing **1a** and PMP. Therefore, the same analysis was performed at higher concentration ($5 \cdot 10^{-3}$ M) to investigate whether an XB complex could be observed (Figure S6). However, no new absorption band due to halogen-bonding between **1a** and PMP was visible in the blue light range at this concentration either. These results suggested no XB complex between **1a** and PMP could be detected.

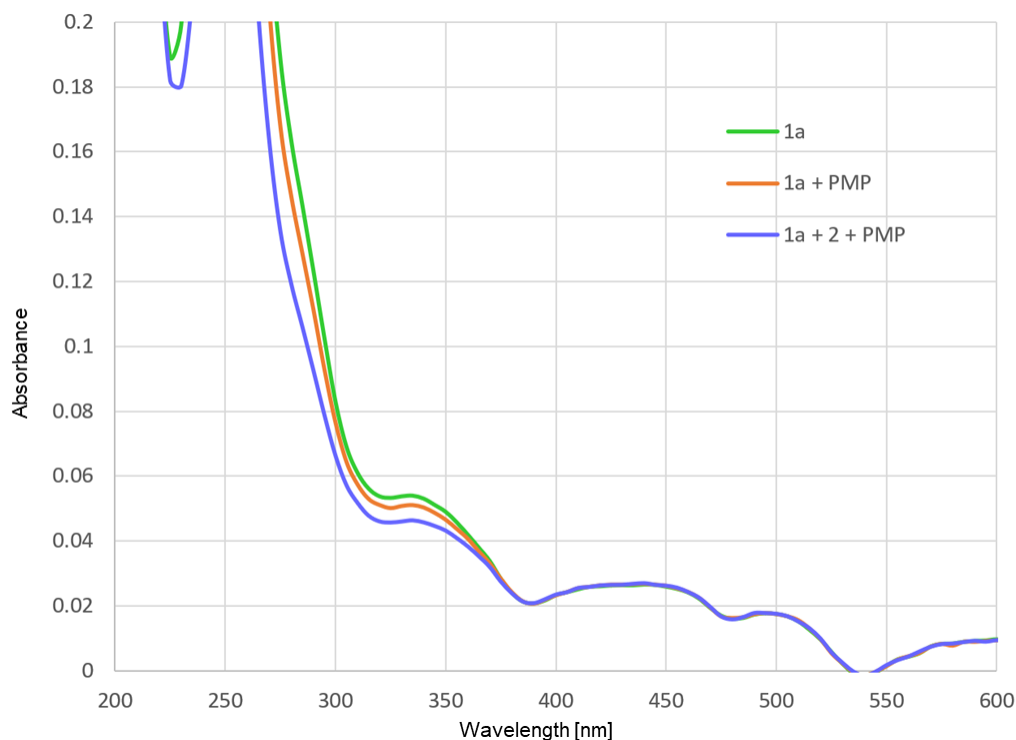


Figure S5. UV-vis analysis of a $5 \cdot 10^{-5}$ M solution of **1a** (green); a 1.0:1.2 mixture of $5 \cdot 10^{-5}$ M **1a** and PMP (orange); and a 1.0:3.0:1.2 mixture of $5 \cdot 10^{-5}$ M **1a**, **2** and PMP (blue). All mixtures were prepared in MeCN.

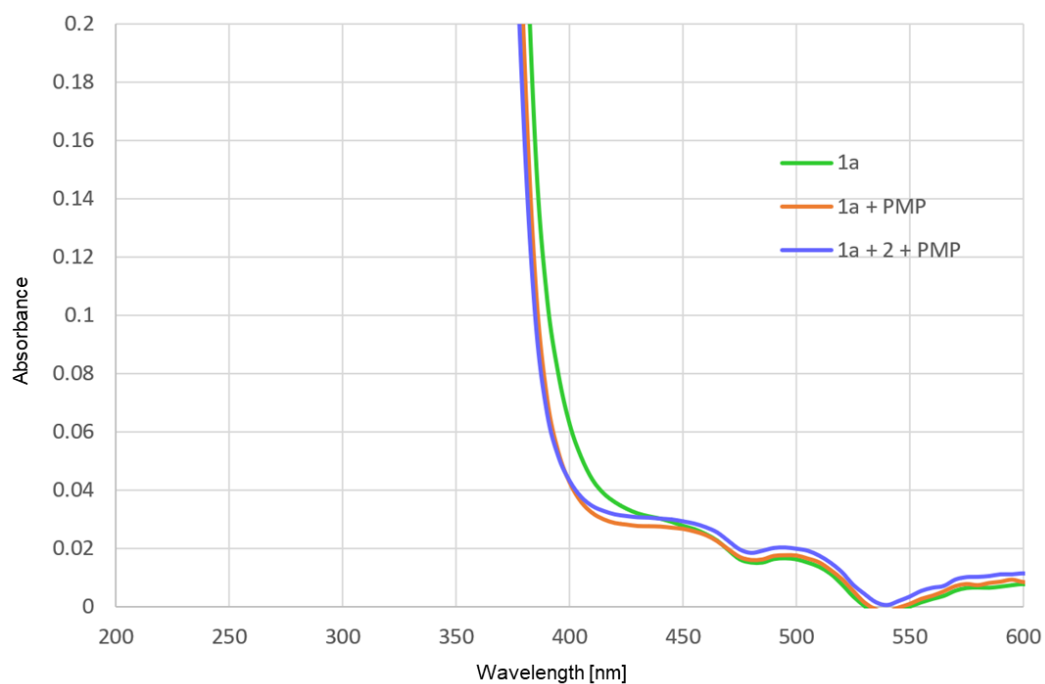


Figure S6. UV-vis analysis of a $5 \cdot 10^{-3}$ M solution of **1a** (green); a 1.0:1.2 mixture of $5 \cdot 10^{-3}$ M **1a** and PMP (orange); and a 1.0:3.0:1.2 mixture of $5 \cdot 10^{-3}$ M **1a**, **2** and PMP (blue). All mixtures were prepared in MeCN.

NMR analysis

NMR samples of the different reagents (**1a**, PMP and **2**) by themselves and as mixtures in ratios comparable to the ones in the reaction conditions were prepared in MeCN- d_3 and analyzed by ^1H NMR and ^{13}C NMR. The aim of these NMR analyses was to observe chemical shifts in the mixtures containing **1a** and PMP that would indicate the formation of a XB complex. On ^1H NMR, the chemical shift of the proton adjacent to the iodide (quadruplet at 5.71 ppm when analyzing pure **1a**, following the two main peaks of the signal on all spectra) was monitored. No significant difference of chemical shift was observed between **1a** on its own, in mixture with PMP (Figure S7), in mixture with **2** (Figure S8), and in mixture with both (Figure S9). Similarly, no significant difference of chemical shift of the carbon bearing the iodine of **1a** (20.3 ppm for **1a** on its own) was visible on ^{13}C NMR when comparing the spectra of pure **1a**, in mixture with PMP (Figure S10), in mixture with **2** (Figure S11), and in mixture with both (Figure S12). These results suggested no XB complex between **1a** and PMP could be detected.

^1H NMR analysis

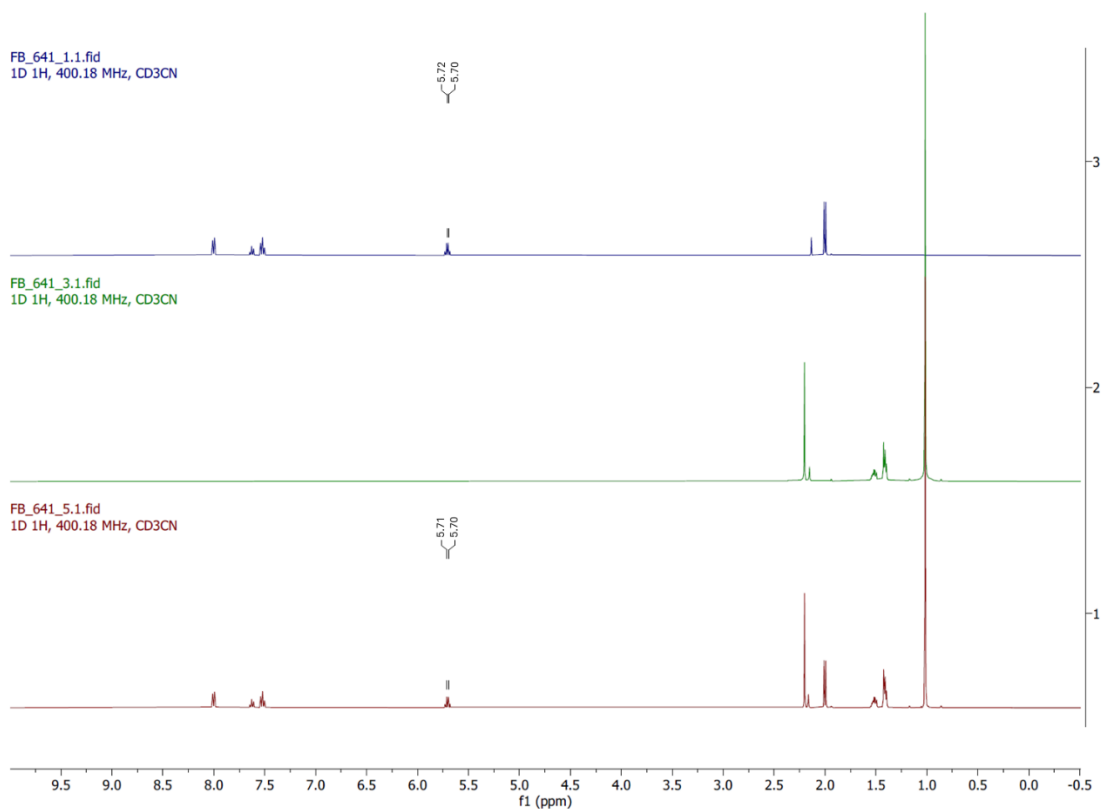


Figure S7. ^1H NMR analysis in $\text{MeCN-}d_3$: (3) **1a**, (2) PMP, (1) **1a**/PMP (1.0:1.2).

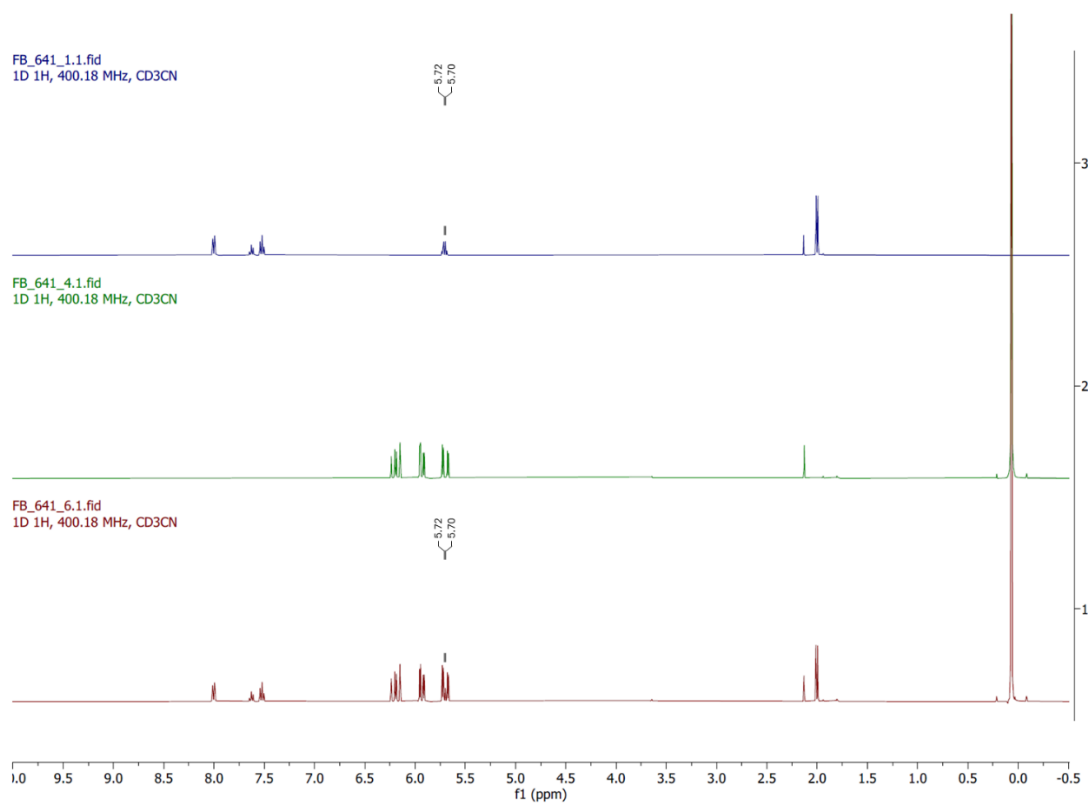


Figure S8. ^1H NMR analysis in $\text{MeCN-}d_3$: (3) **1a**, (2) **2**, (1) **1a**/**2** (1.0:3.0).

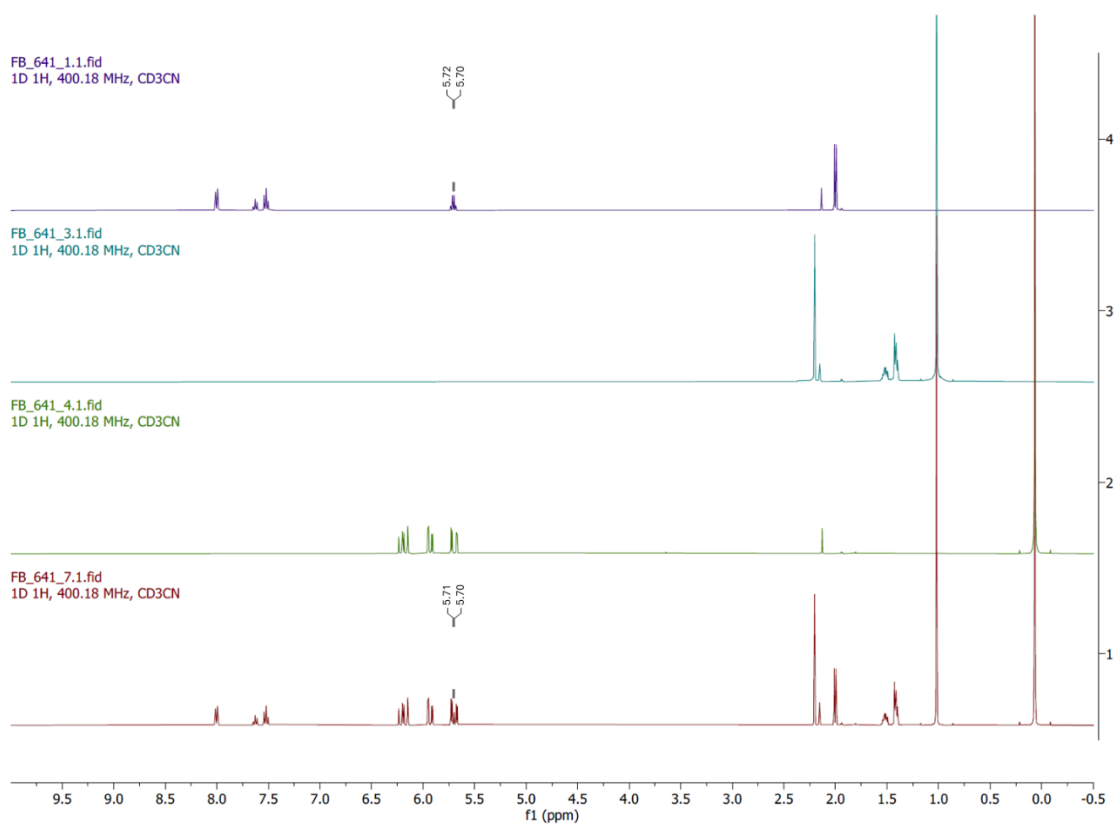


Figure S9. ^1H NMR analysis in $\text{MeCN-}d_3$: (4) **1a**, (3) PMP, (2) **2**, (1) **1a**/PMP/**2** (1.0:1.2:3.0).

^{12}C NMR analysis

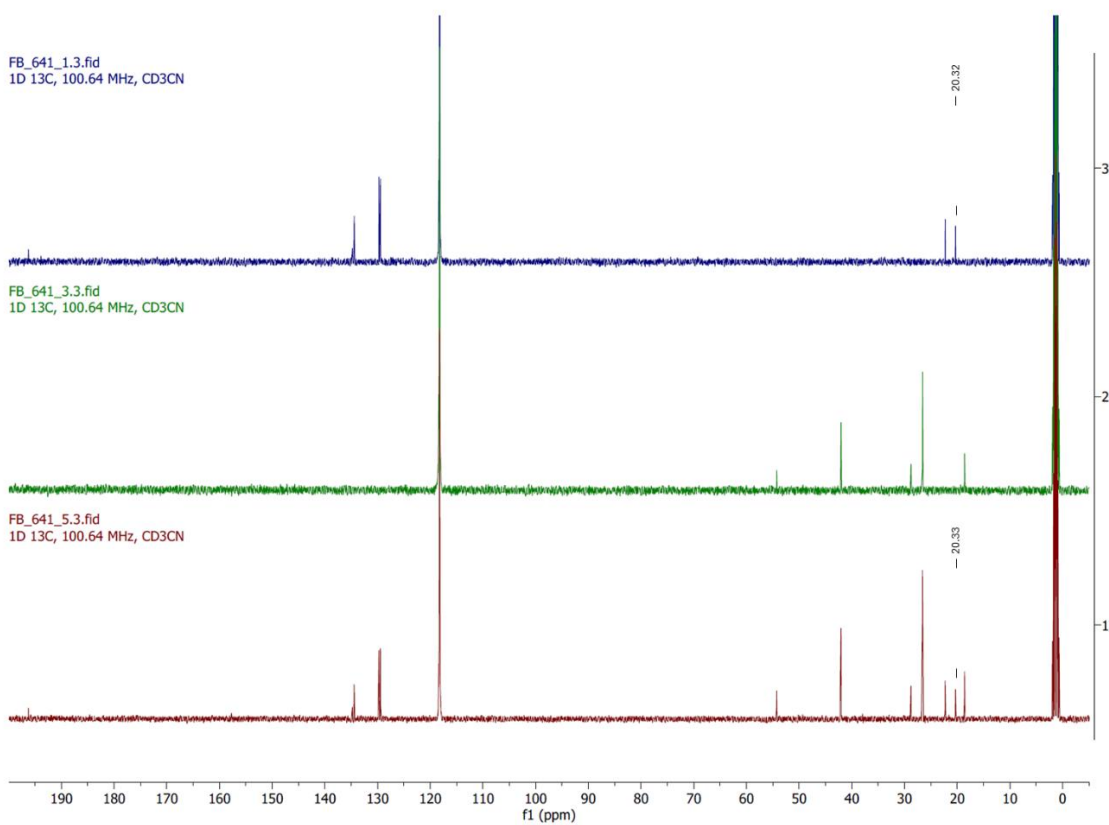


Figure S10. ^{13}C NMR analysis in $\text{MeCN-}d_3$: (3) **1a**, (2) PMP, (1) **1a**/PMP (1.0:1.2).

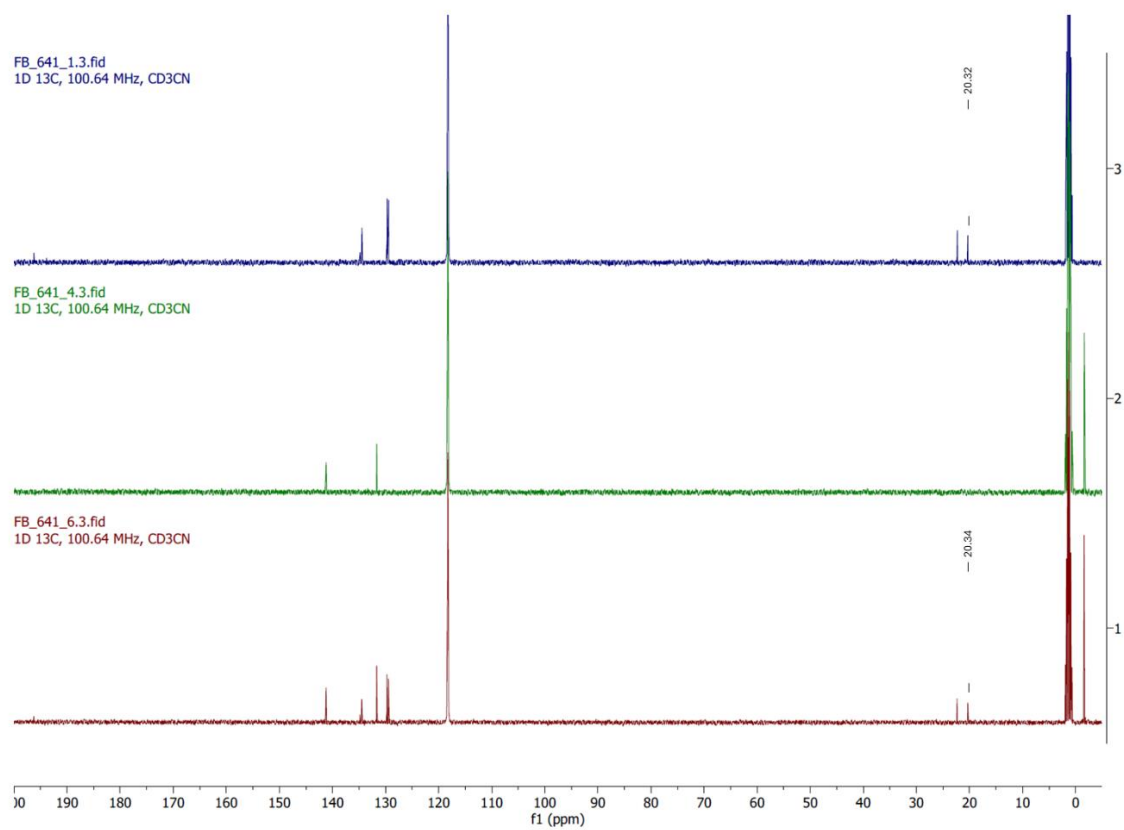


Figure S11. ^{13}C NMR analysis in $\text{MeCN-}d_3$: (3) **1a**, (2) **2**, (1) **1a**/**2** (1.0:3.0).

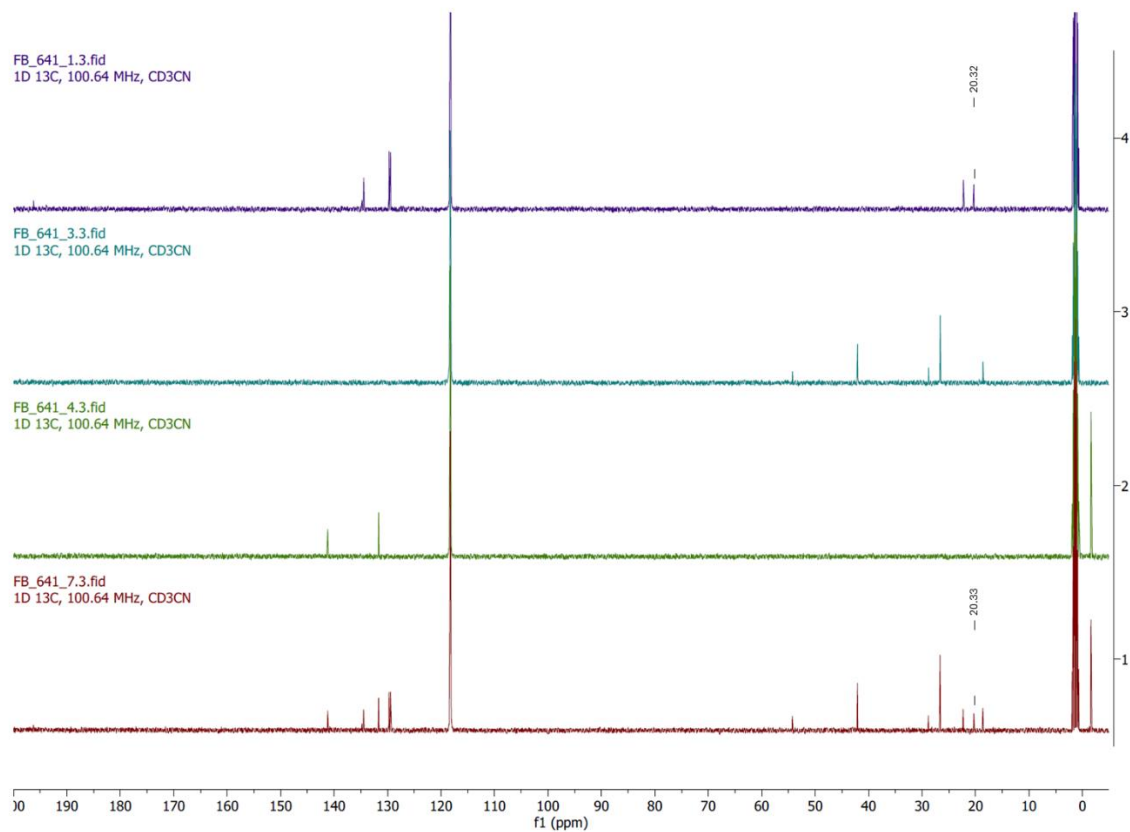


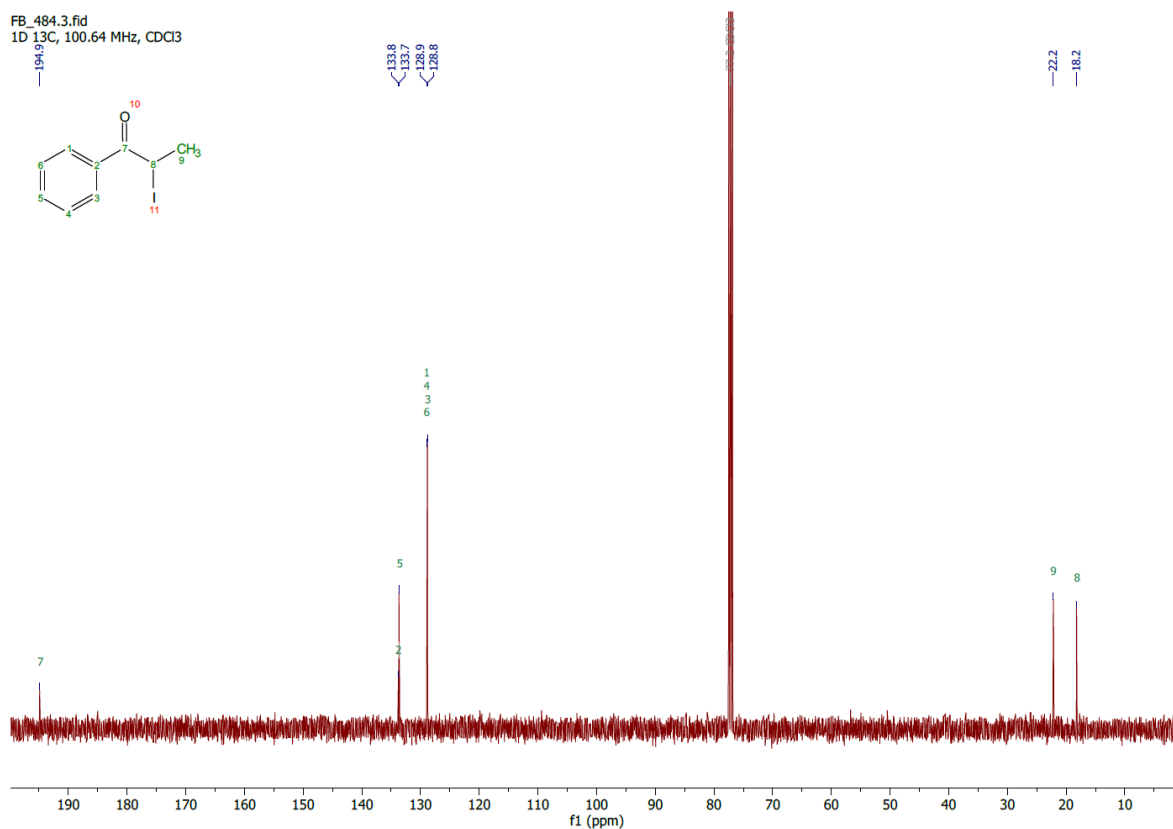
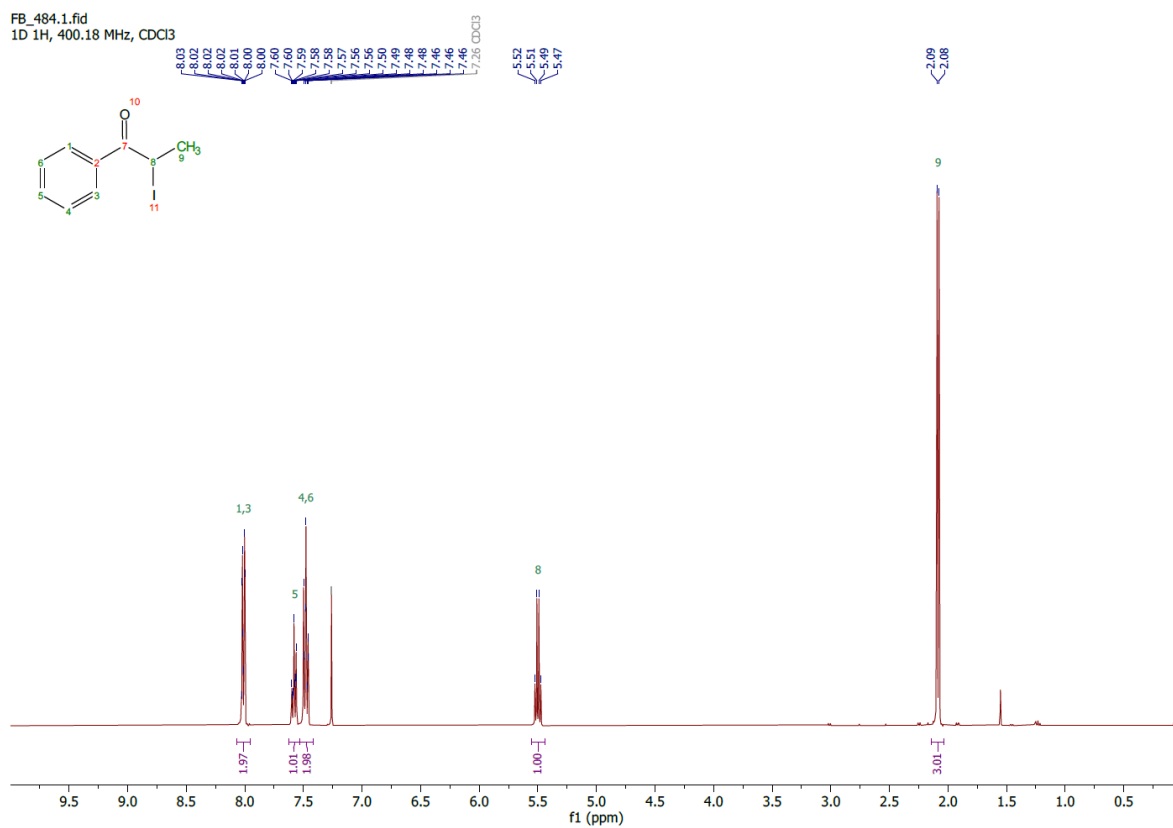
Figure S12. ^{13}C NMR analysis in $\text{MeCN-}d_3$: (4) **1a**, (3) PMP, (2) **2**, (1) **1a**/PMP/**2** (1.0:1.2:3.0).

References

1. Saiter, J.; Guérin, T.; Donnard, M.; Panossian, A.; Hanquet, G.; Leroux, F. R., Direct Trifluoromethoxylation without OCF-Carrier through In Situ Generation of Fluorophosgene. *Eur. J. Org. Chem.* **2021**, 2021 (22), 3139-3147.
2. Meshram, H. M.; Reddy, P. N.; Sadashiv, K.; Yadav, J. S., Amberlyst-15-promoted efficient 2-halogenation of 1,3-keto-esters and cyclic ketones using N-halosuccinimides. *Tetrahedron Lett.* **2005**, 46 (4), 623-626.
3. Fang, J. X.; Li, L. S.; Yang, C.; Chen, J. P.; Deng, G. J.; Gong, H., Tandem Oxidative Ring-Opening/Cyclization Reaction in Seconds in Open Atmosphere for the Synthesis of 1-Tetralones in Water-Acetonitrile. *Org. Lett.* **2018**, 20 (22), 7308-7311.
4. Yusubov, M. S.; Yusubova, R. Y.; Funk, T. V.; Chi, K. W.; Kirschning, A.; Zhdankin, V. V., m-Iodosylbenzoic Acid as a Convenient Recyclable Hypervalent Iodine Oxidant for the Synthesis of α -Iodo Ketones by Oxidative Iodination of Ketones. *Synthesis-Stuttgart* **2010**, (21), 3681-3685.
5. Matsuo, K.; Yamaguchi, E.; Itoh, A., In Situ-Generated Halogen-Bonding Complex Enables Atom Transfer Radical Addition (ATRA) Reactions of Olefins. *J. Org. Chem.* **2020**, 85 (16), 10574-10583.
6. Matsuo, K.; Kondo, T.; Yamaguchi, E.; Itoh, A., Photoinduced Atom Transfer Radical Addition Reaction of Olefins with α -Bromo Carbonyls. *Chem. Pharm. Bull.* **2021**, 69 (8), 796-801.
7. Marotta, A.; Fang, H.; Adams, C. E.; Marcus, K. S.; Daniliuc, C. G.; Molloy, J. J., Direct Light-Enabled Access to α -Boryl Radicals: Application in the Stereodivergent Synthesis of Allyl Boronic Esters. *Angew. Chem. Int. Edit.* **2023**, 62 (34), e20237540.
8. Wang, Y. X.; Wang, J. H.; Li, G. X.; He, G.; Chen, G., Halogen-Bond-Promoted Photoactivation of Perfluoroalkyl Iodides: A Photochemical Protocol for Perfluoroalkylation Reactions. *Org. Lett.* **2017**, 19 (6), 1442-1445.

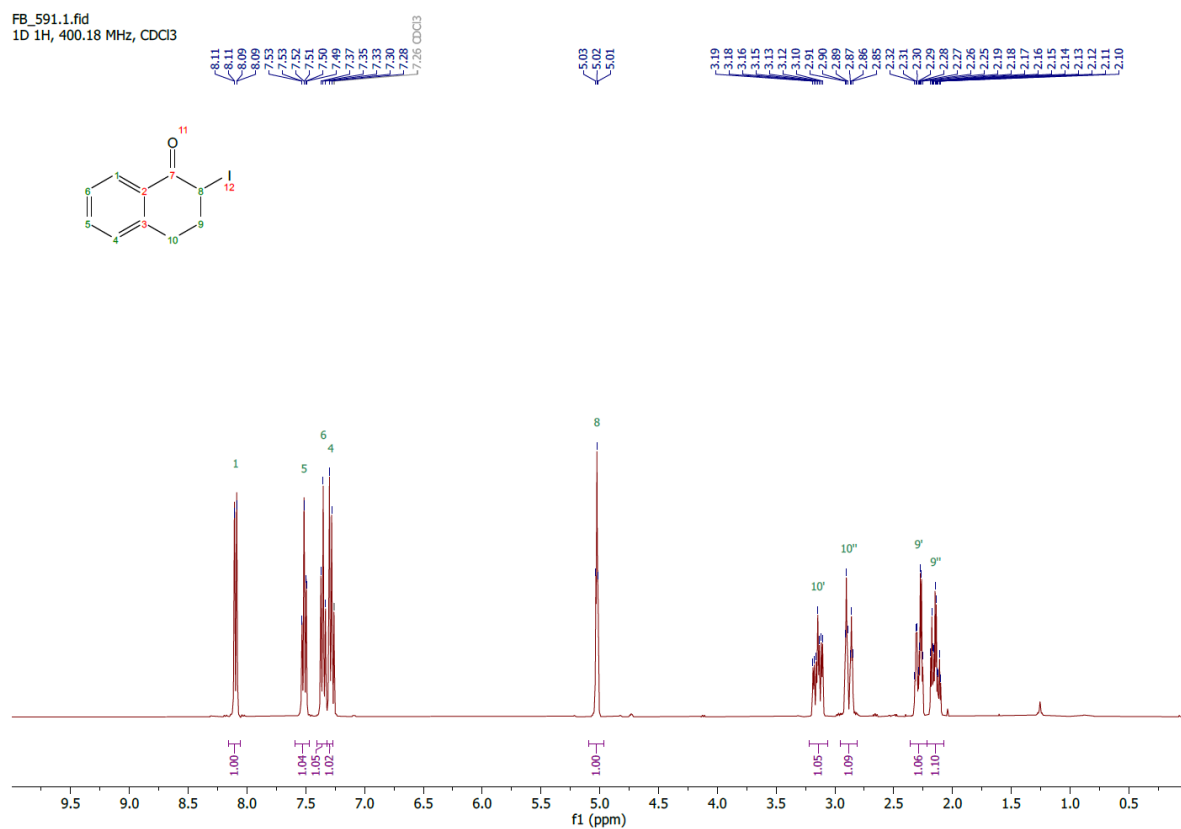
NMR spectra

2-Iodo-1-phenyl-1-propanone **1a**

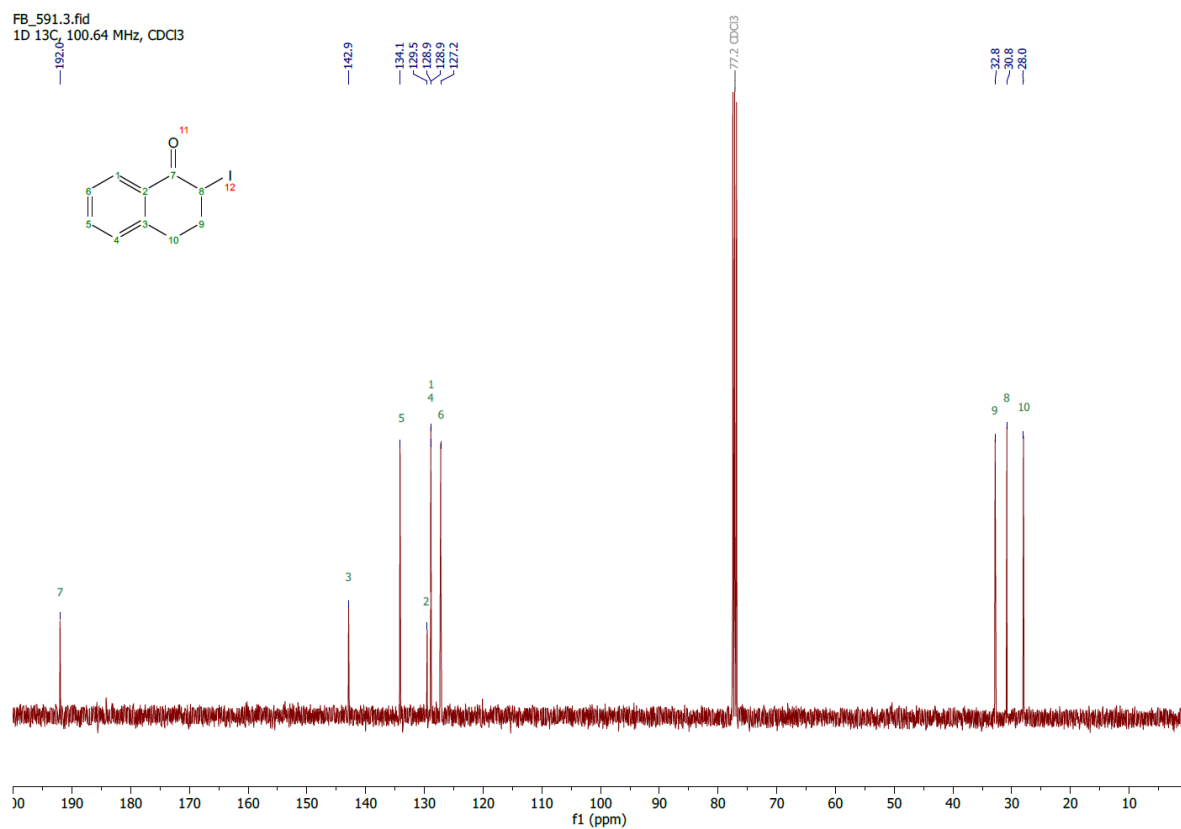


2-Iodo-3,4-dihydronaphthalen-1(2H)-one **1b**

FB_591.1.fid
1D 1H, 400.18 MHz, CDCl3

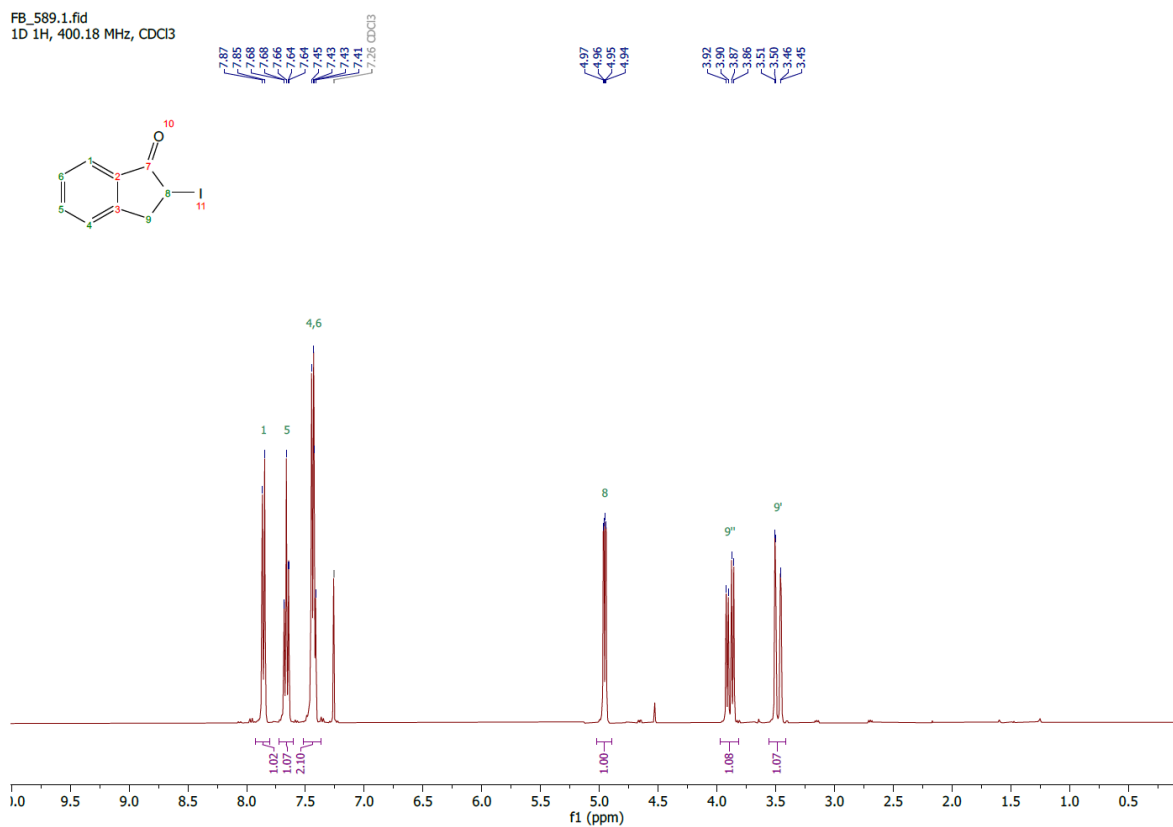


FB_591.3.fid
1D 13C, 100.64 MHz, CDCl3

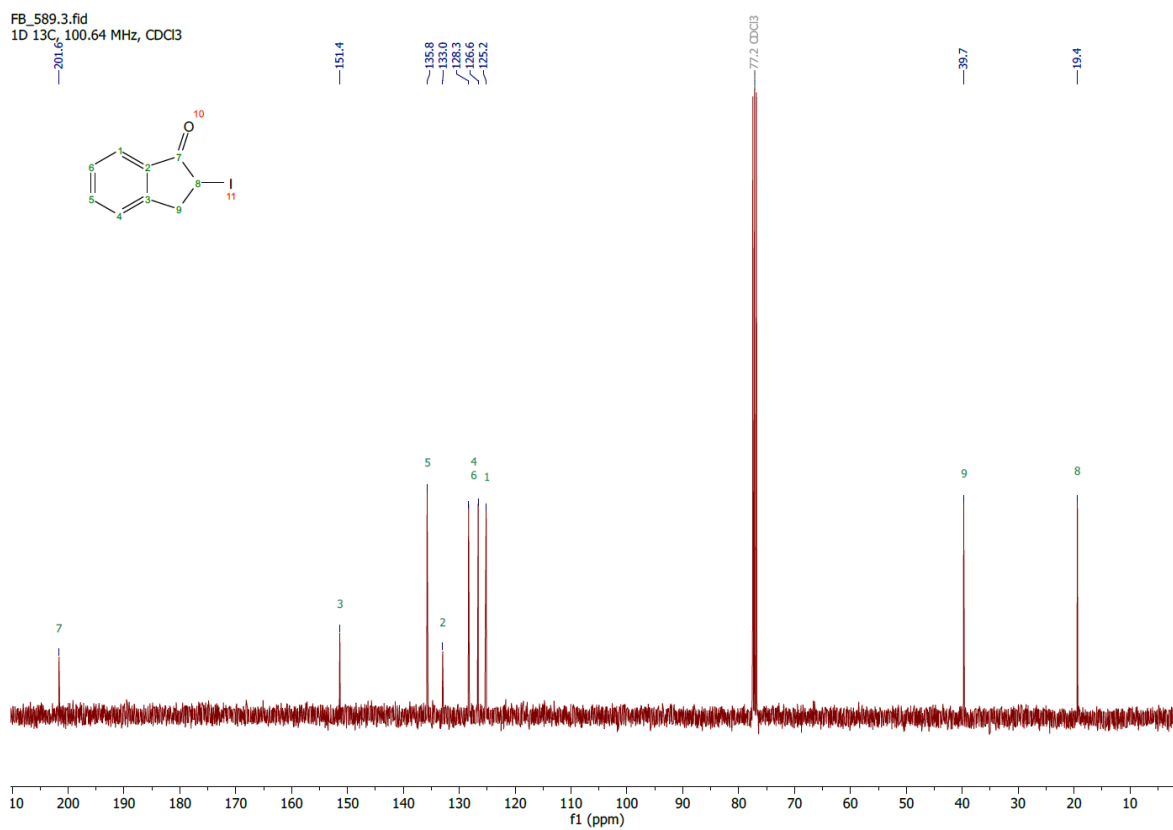


2-Iodo-1-indanone **1c**

FB_589.1.fid
1D 1H, 400.18 MHz, CDCl₃

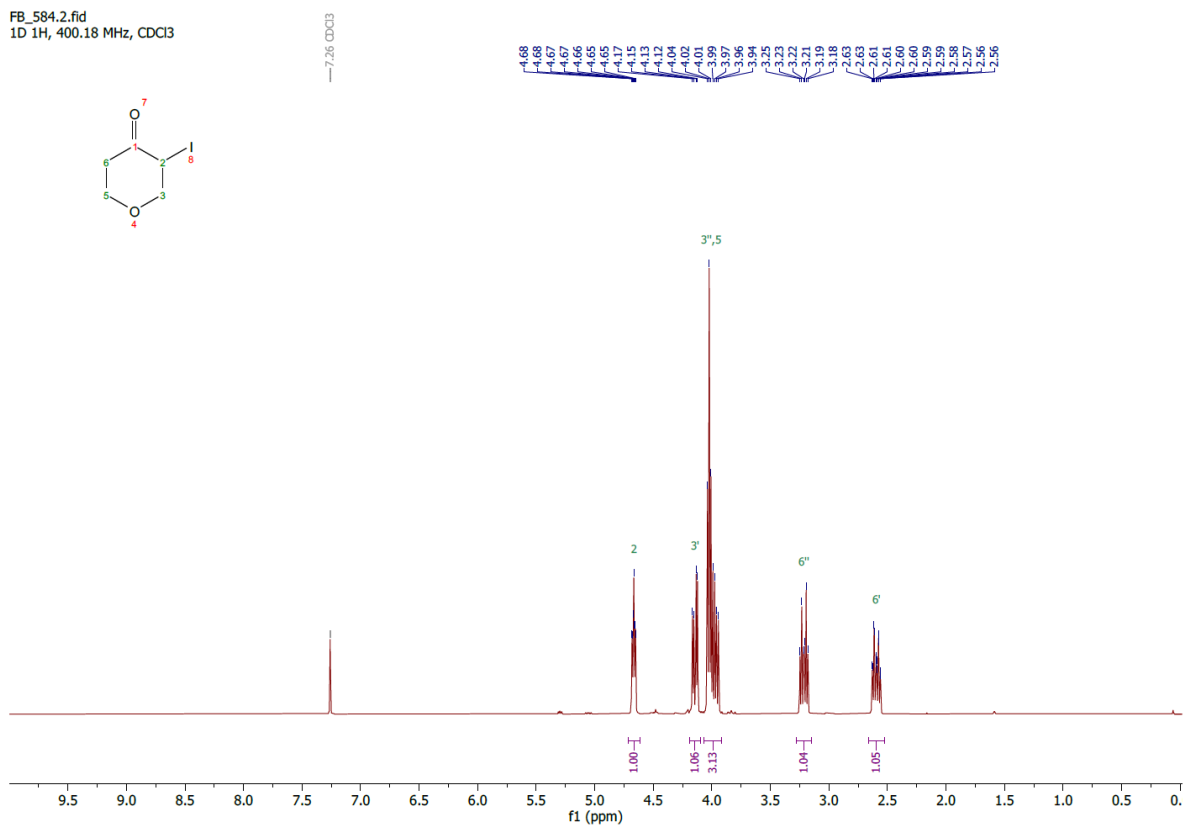


FB_589.3.fid
1D 13C, 100.64 MHz, CDCl₃

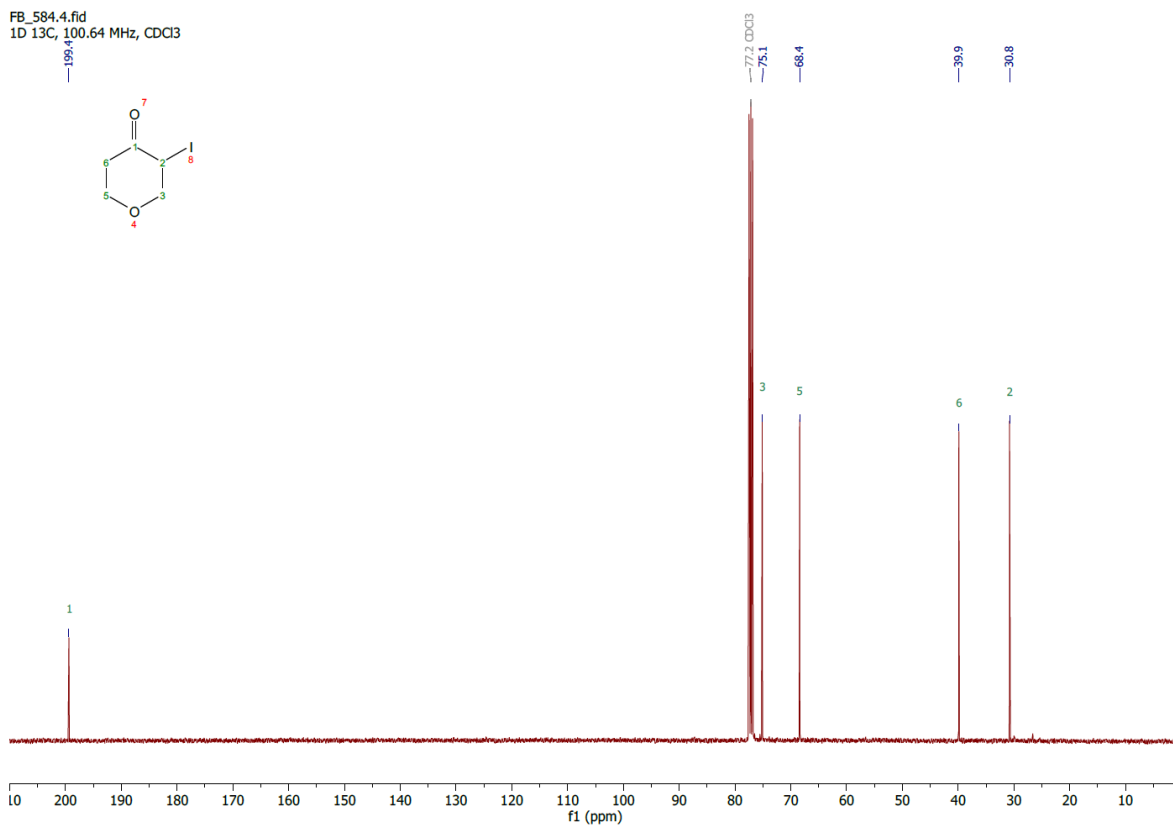


3-Iodotetrahydro-4H-pyran-4-one **1d**

FB_584.2.fid
1D 1H, 400.18 MHz, CDCl₃

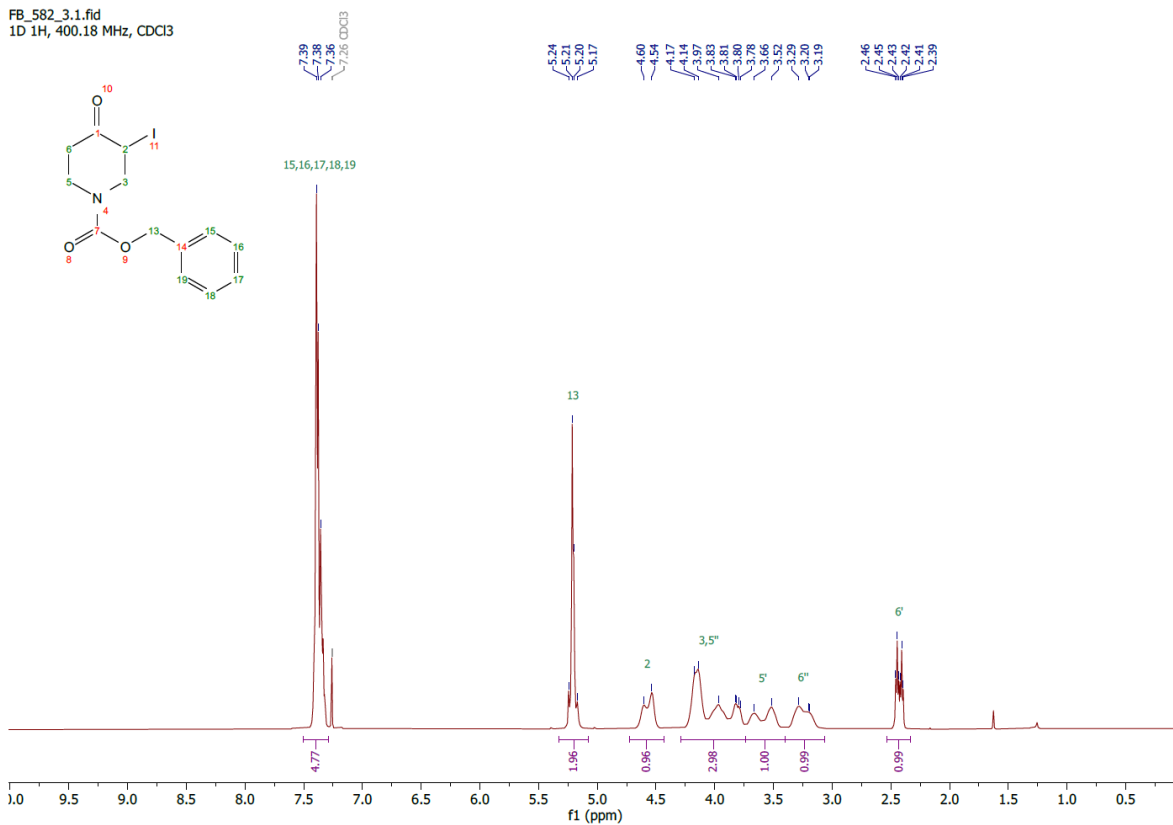


FB_584.4.fid
1D 13C, 100.64 MHz, CDCl₃

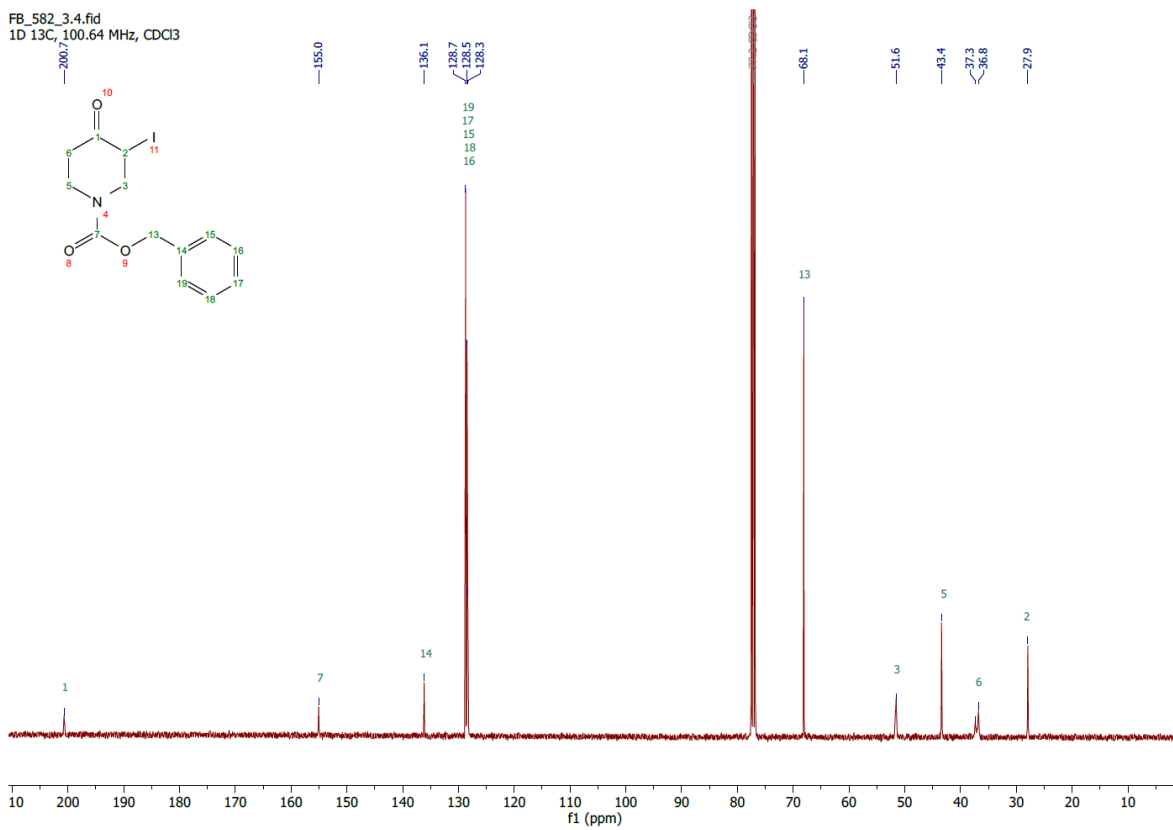


Benzyl 3-iodo-4-oxo-1-piperidinecarboxylate **1e**

FB_582_3.1.fid
1D 1H, 400.18 MHz, CDCl3

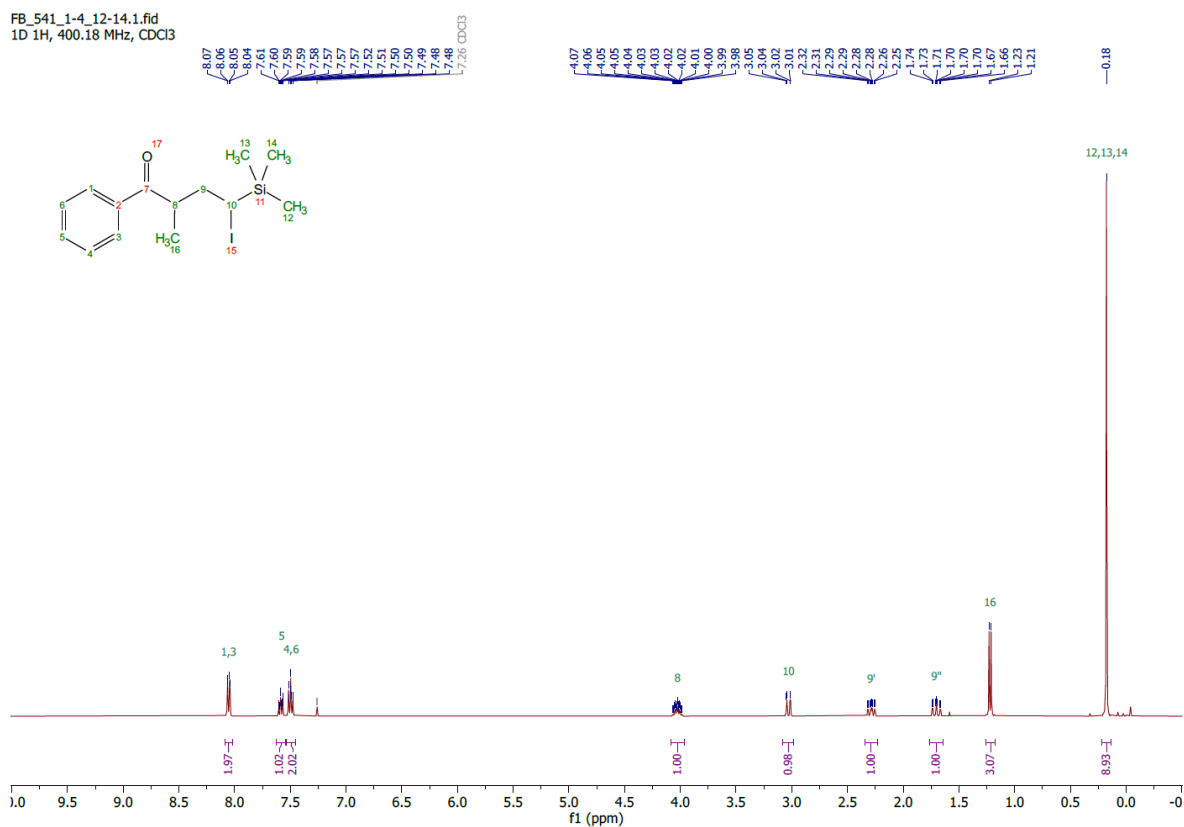


FB_582_3.4.fid
1D 13C, 100.64 MHz, CDCl3

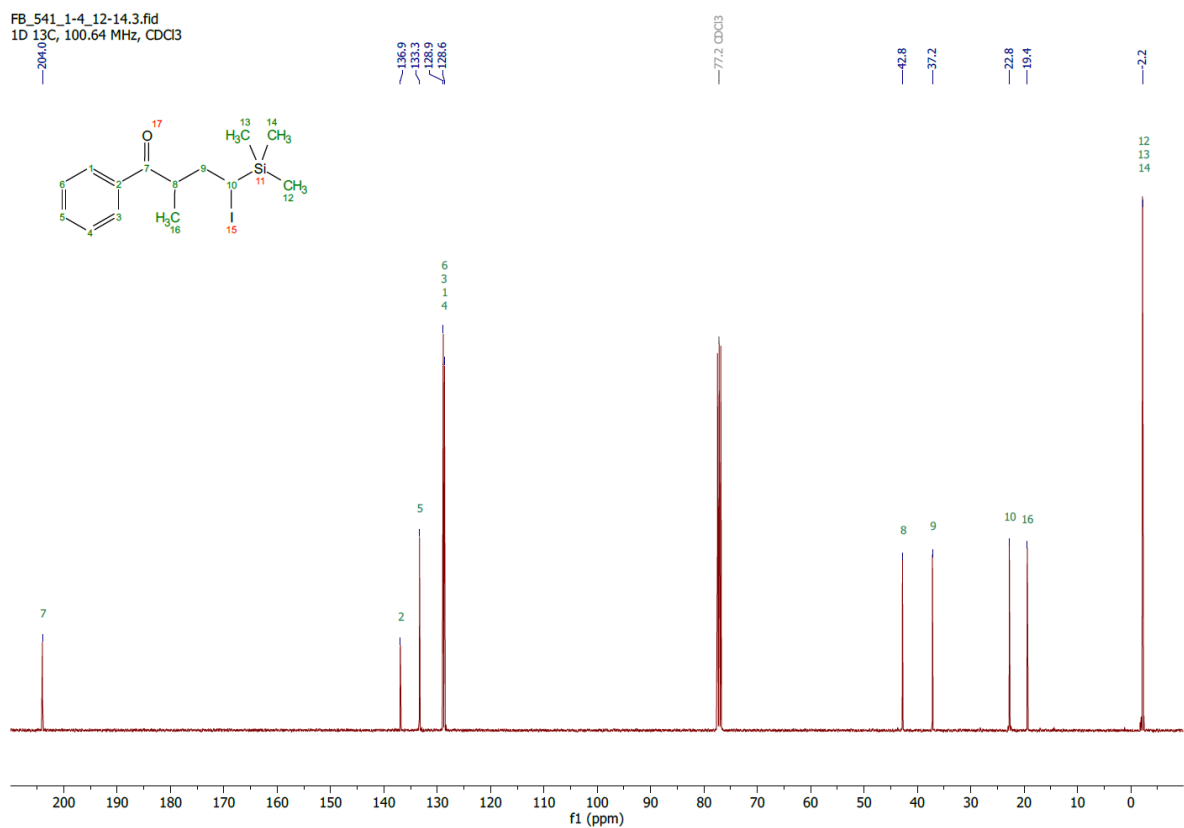


4-Iodo-2-methyl-1-phenyl-4-(trimethylsilyl)butan-1-one **3a** (diastereomer I)

FB_541_1-4_12-14.1.fid
1D 1H, 400.18 MHz, CDCl₃

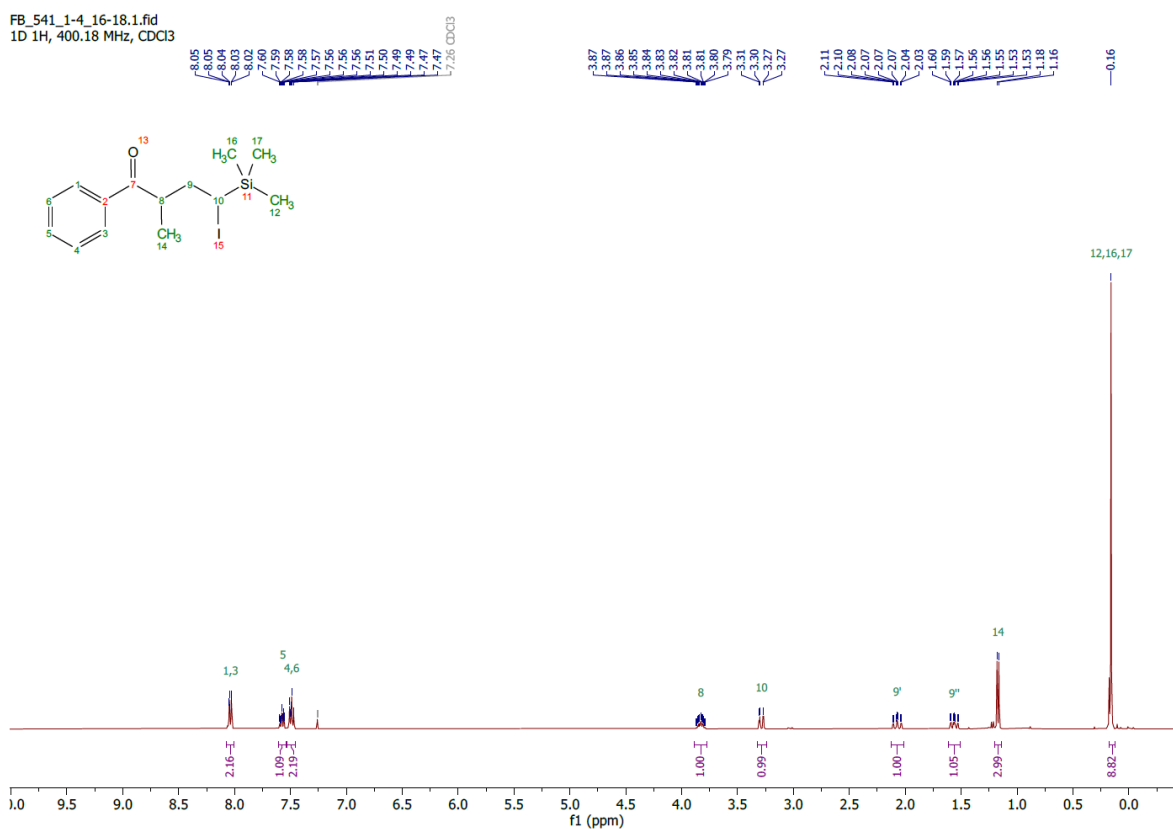


FB_541_1-4_12-14.3.fid
1D 13C, 100.64 MHz, CDCl₃

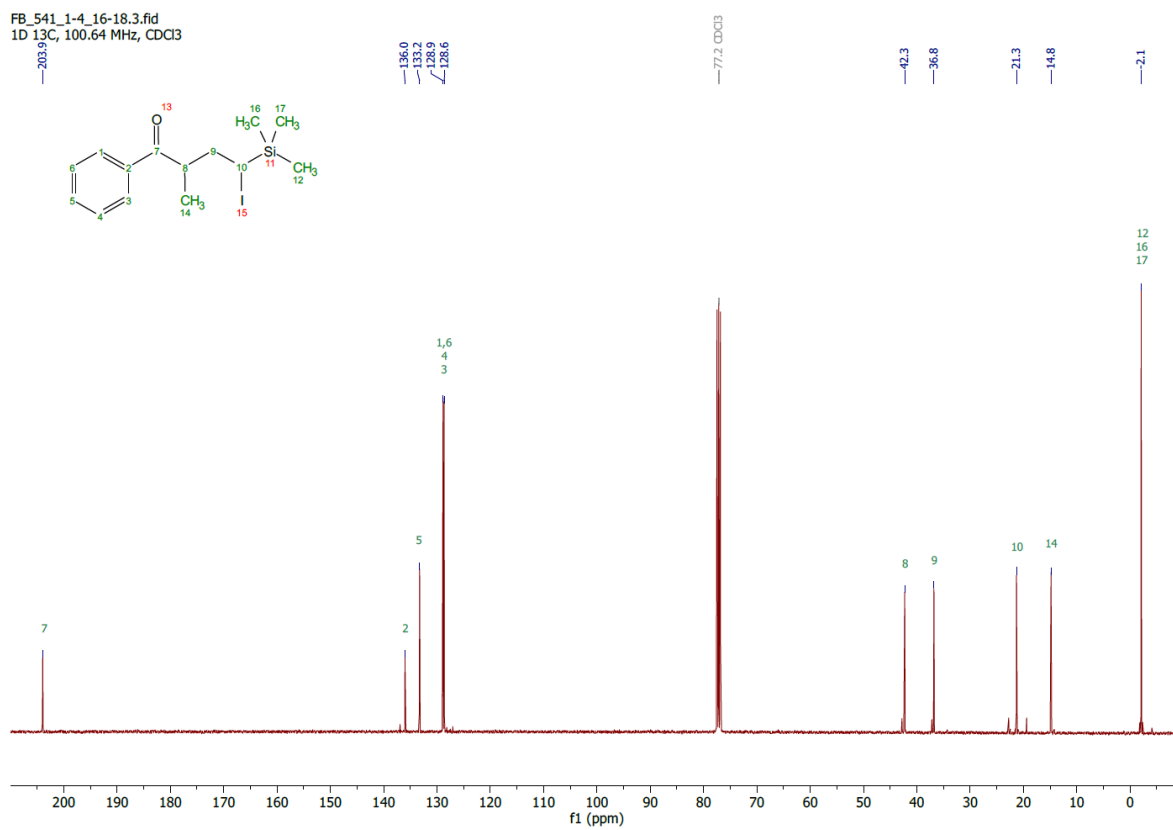


4-Iodo-2-methyl-1-phenyl-4-(trimethylsilyl)butan-1-one **3a** (*diastereomer II*)

FB_541_1-4_16-18.1.fid
1D 1H, 400.18 MHz, CDCl₃

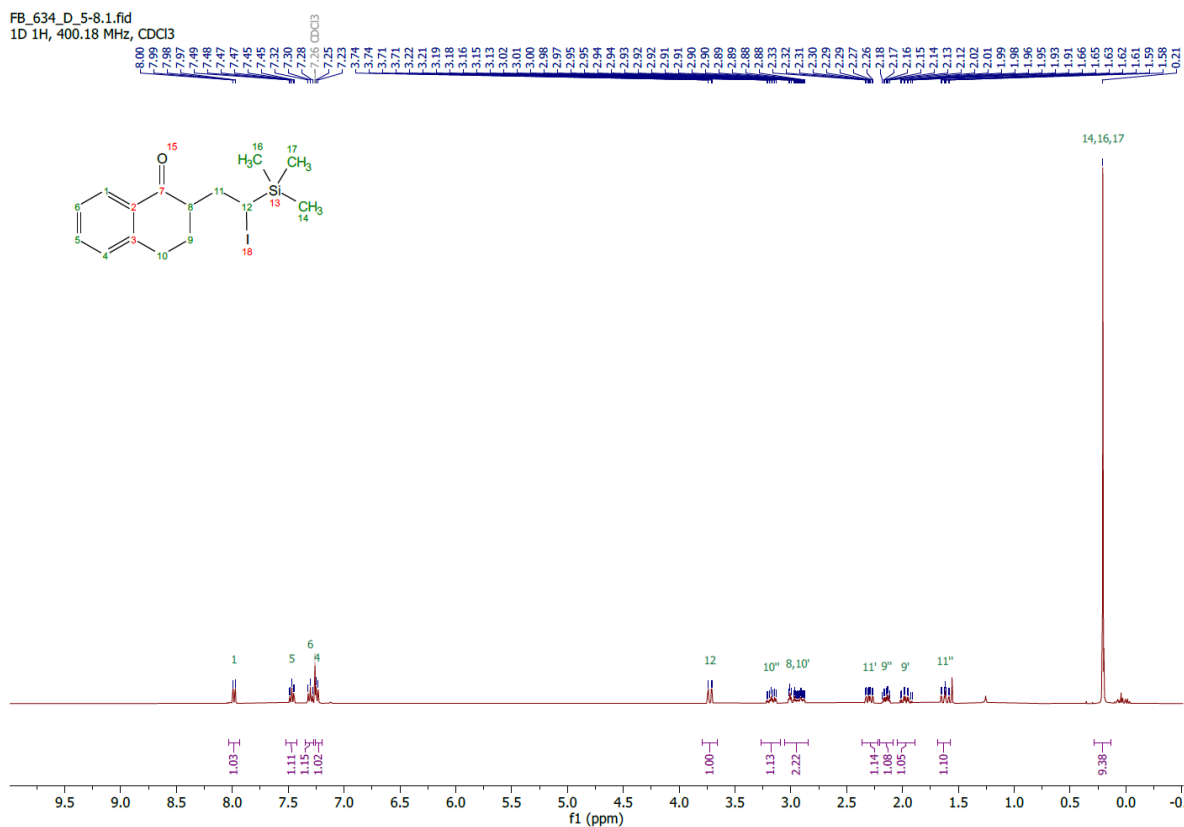


FB_541_1-4_16-18.3.fid
1D 13C, 100.64 MHz, CDCl₃

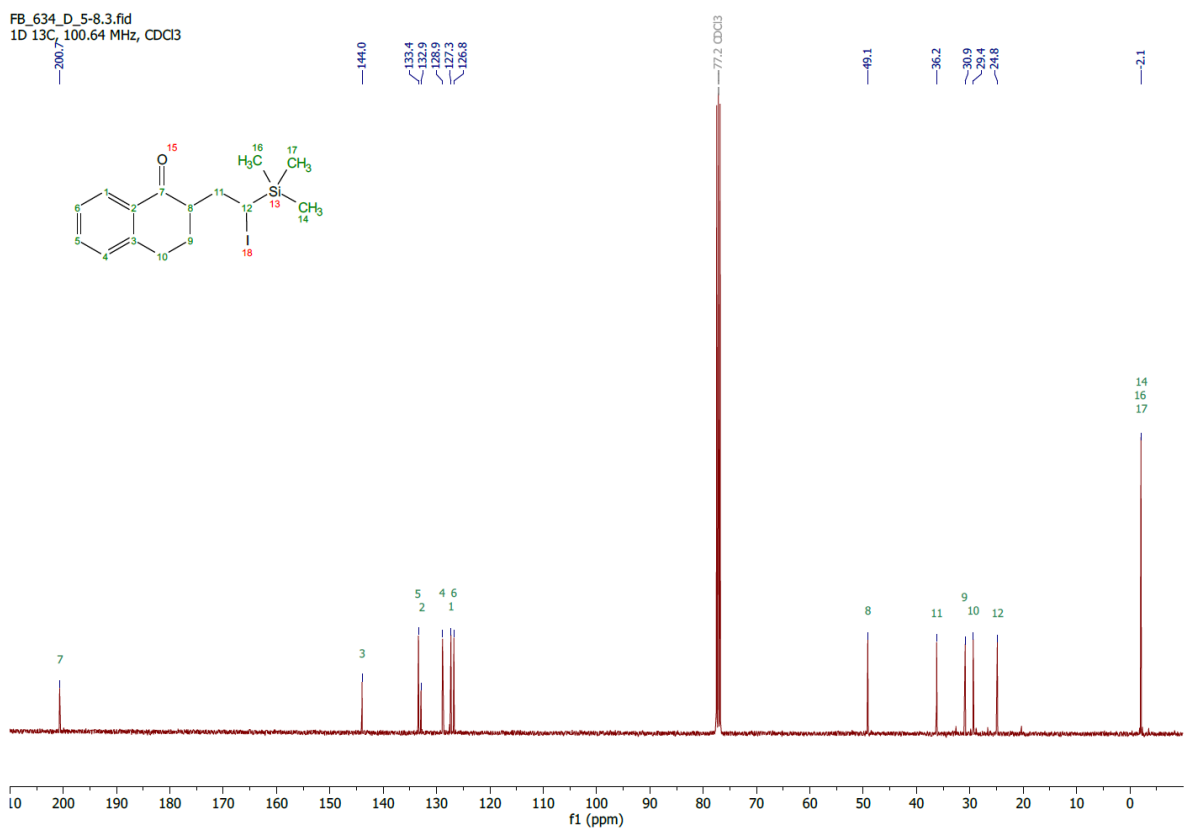


2-(2-Iodo-2-(trimethylsilyl)ethyl)-3,4-dihydronaphthalen-1(2H)-one **3b** (diastereomer I)

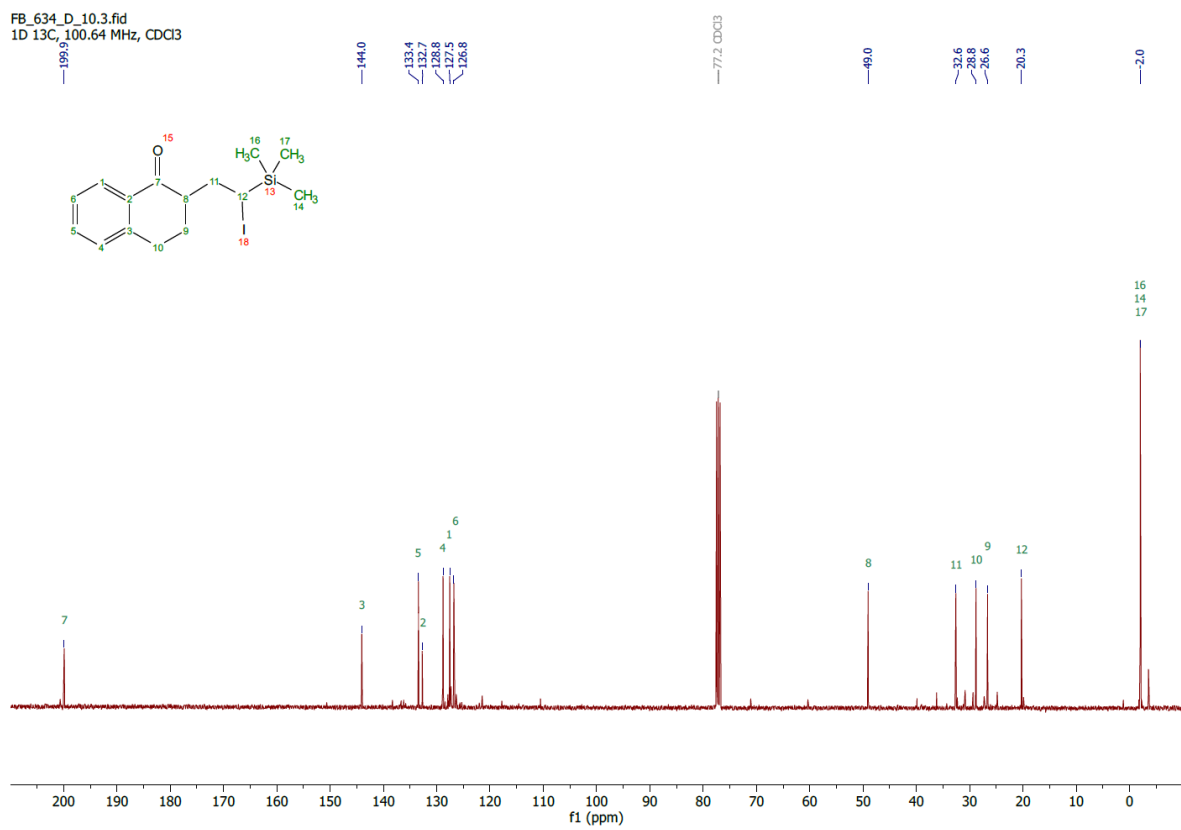
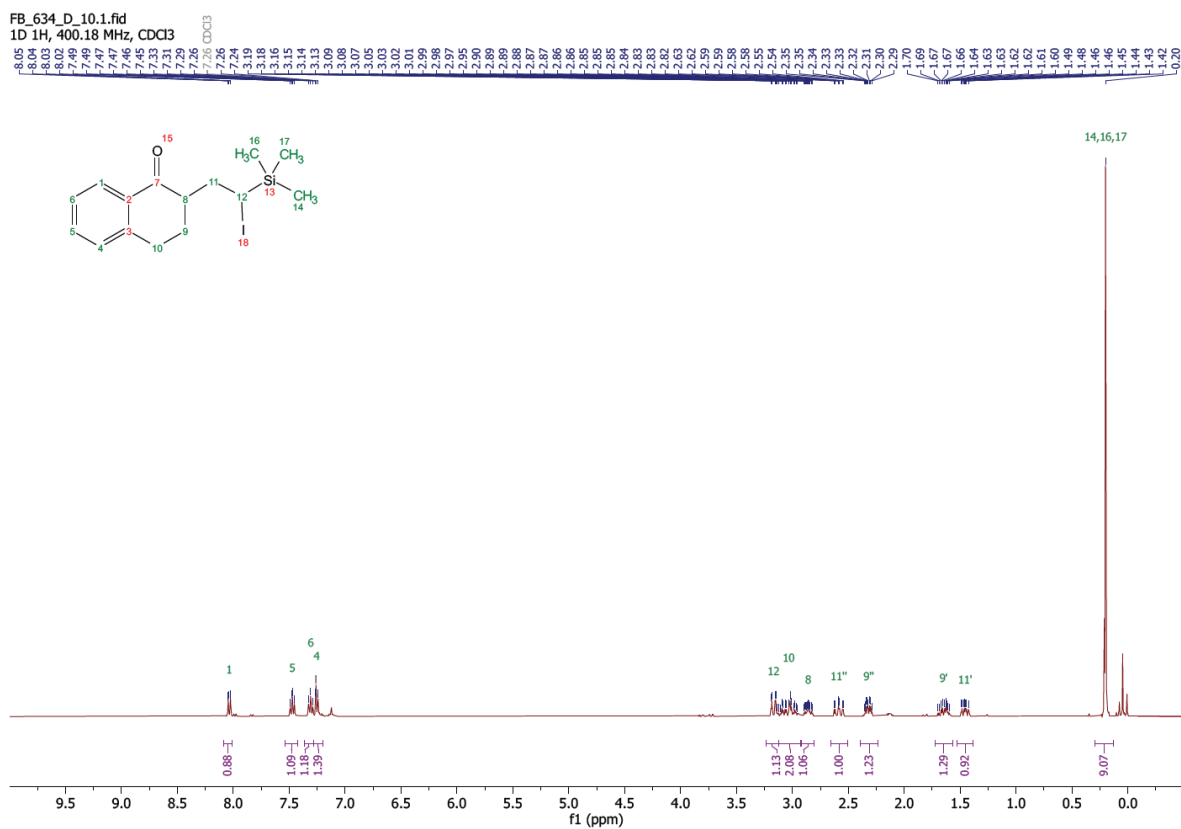
FB_634_D_5-8.1.fid
1D 1H, 400.18 MHz, CDCl3



FB_634_D_5-8.3.fid
1D 13C, 100.64 MHz, CDCl3

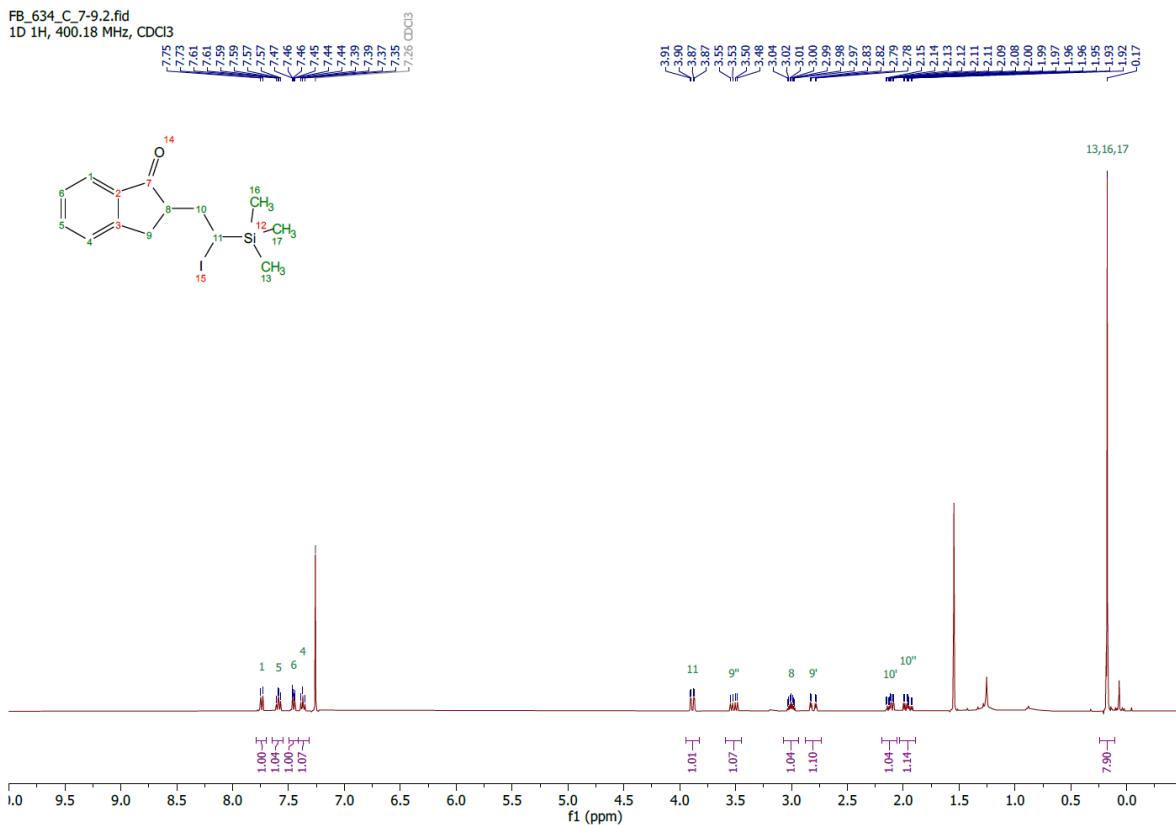


2-(2-Iodo-2-(trimethylsilyl)ethyl)-3,4-dihydronaphthalen-1(2H)-one **3b** (diastereomer II)

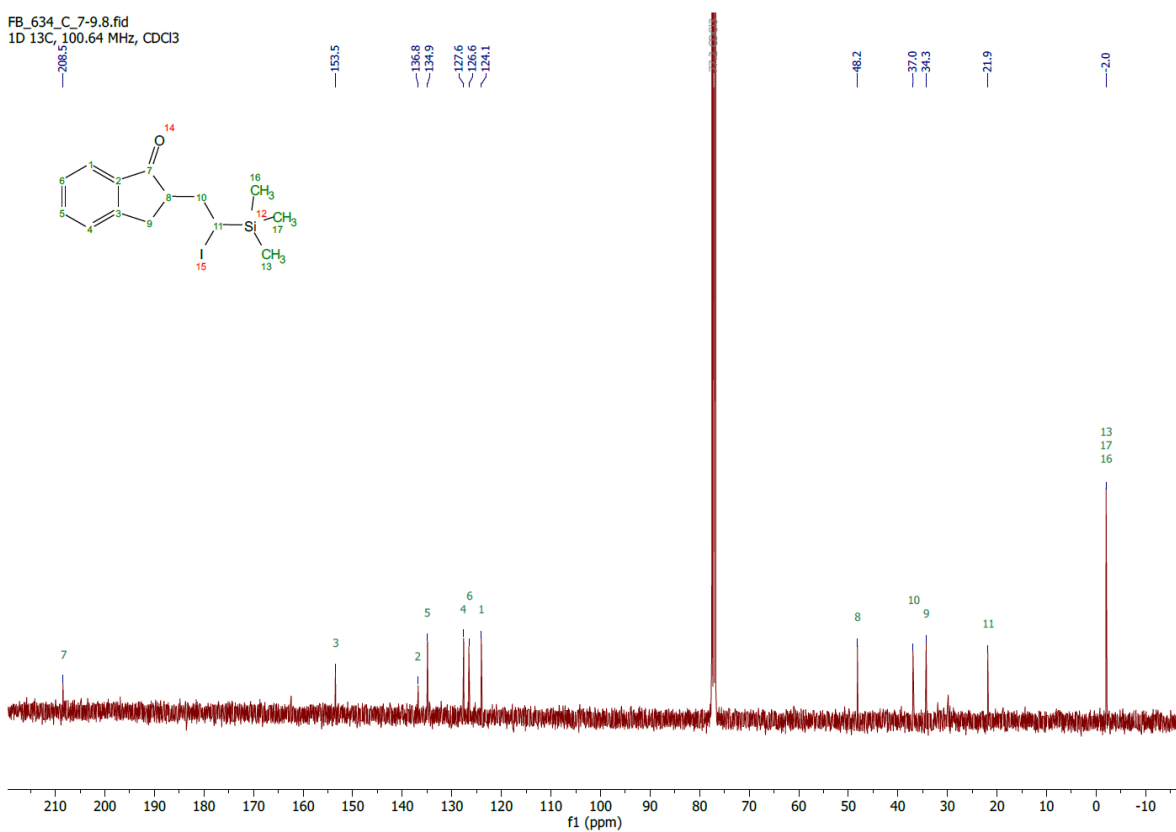


2-(2-Iodo-2-(trimethylsilyl)ethyl)-2,3-dihydro-1H-inden-1-one **3c** (*diastereomer I*)

FB_634_C_7-9.2.fid
1D 1H, 400.18 MHz, CDCl3

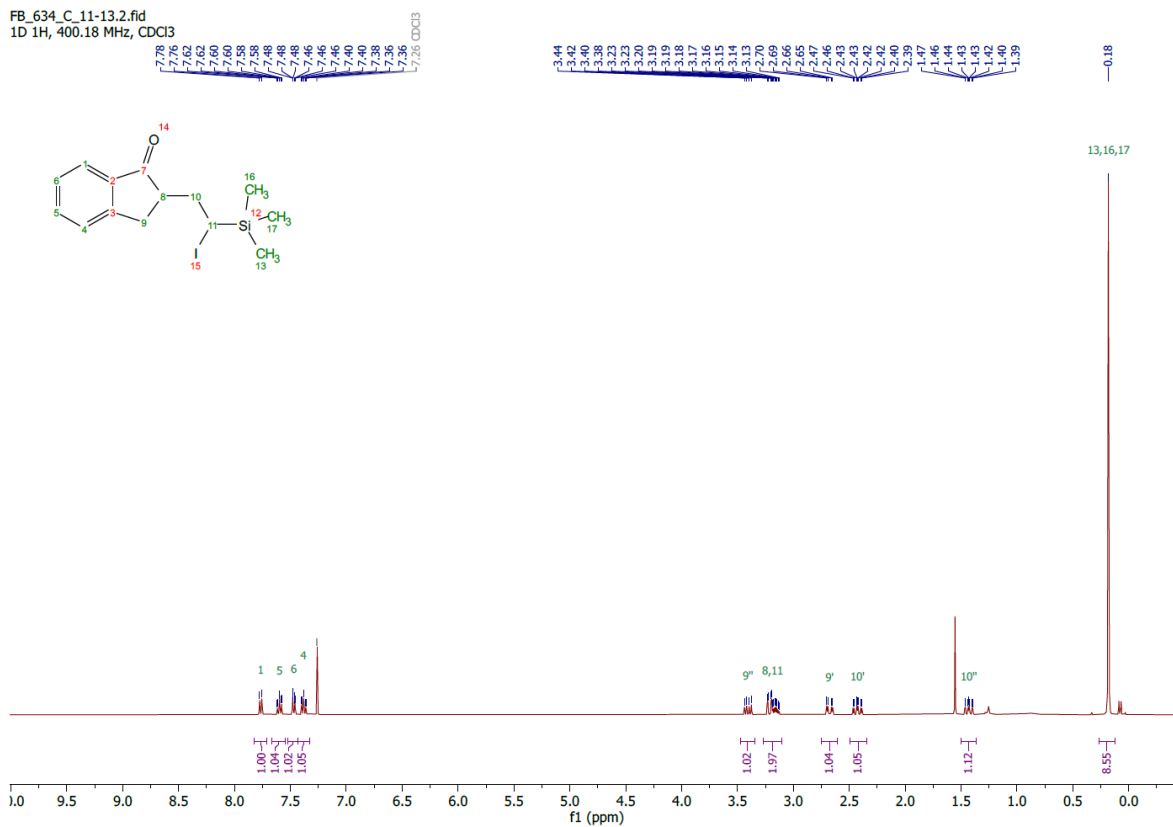


FB_634_C_7-9.8.fid
1D 13C, 100.64 MHz, CDCl3

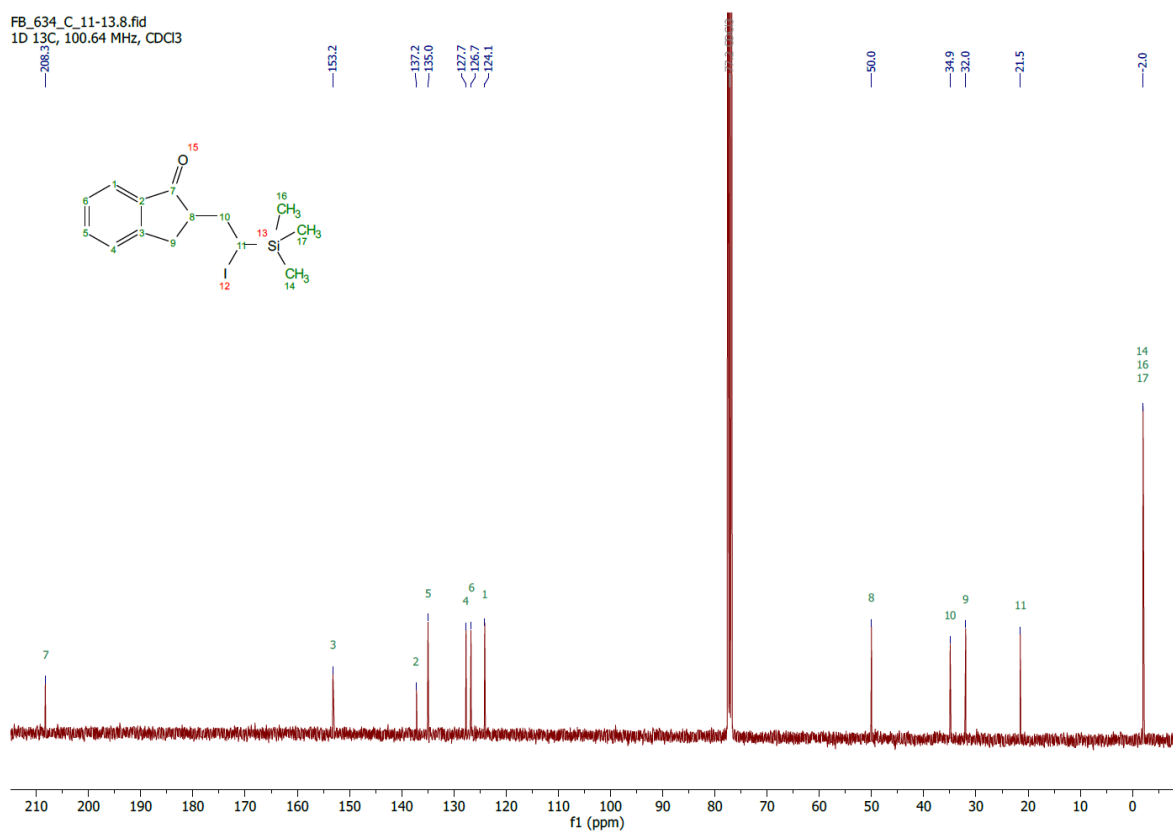


2-(2-Iodo-2-(trimethylsilyl)ethyl)-2,3-dihydro-1H-inden-1-one **3c** (*diastereomer II*)

FB_634_C_11-13.2.fid
1D 1H, 400.18 MHz, CDCl3

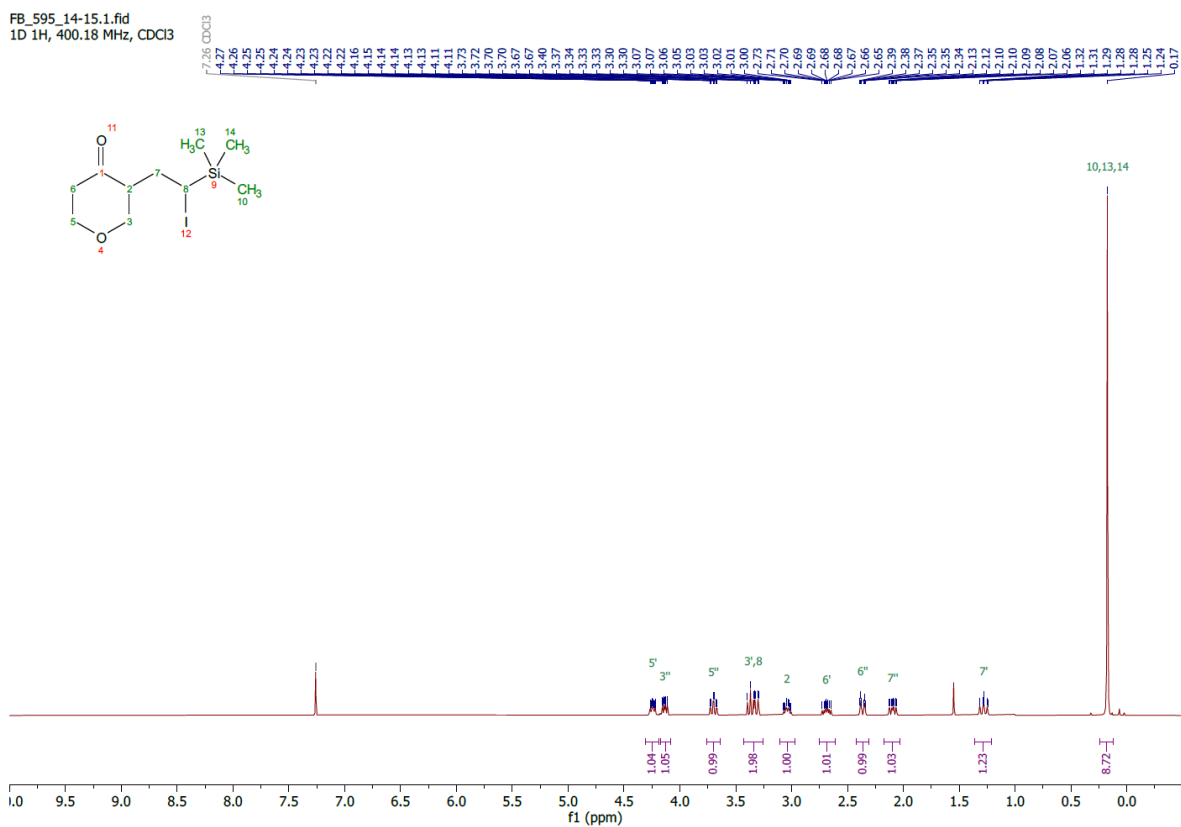


FB_634_C_11-13.8.fid
1D 13C, 100.64 MHz, CDCl3

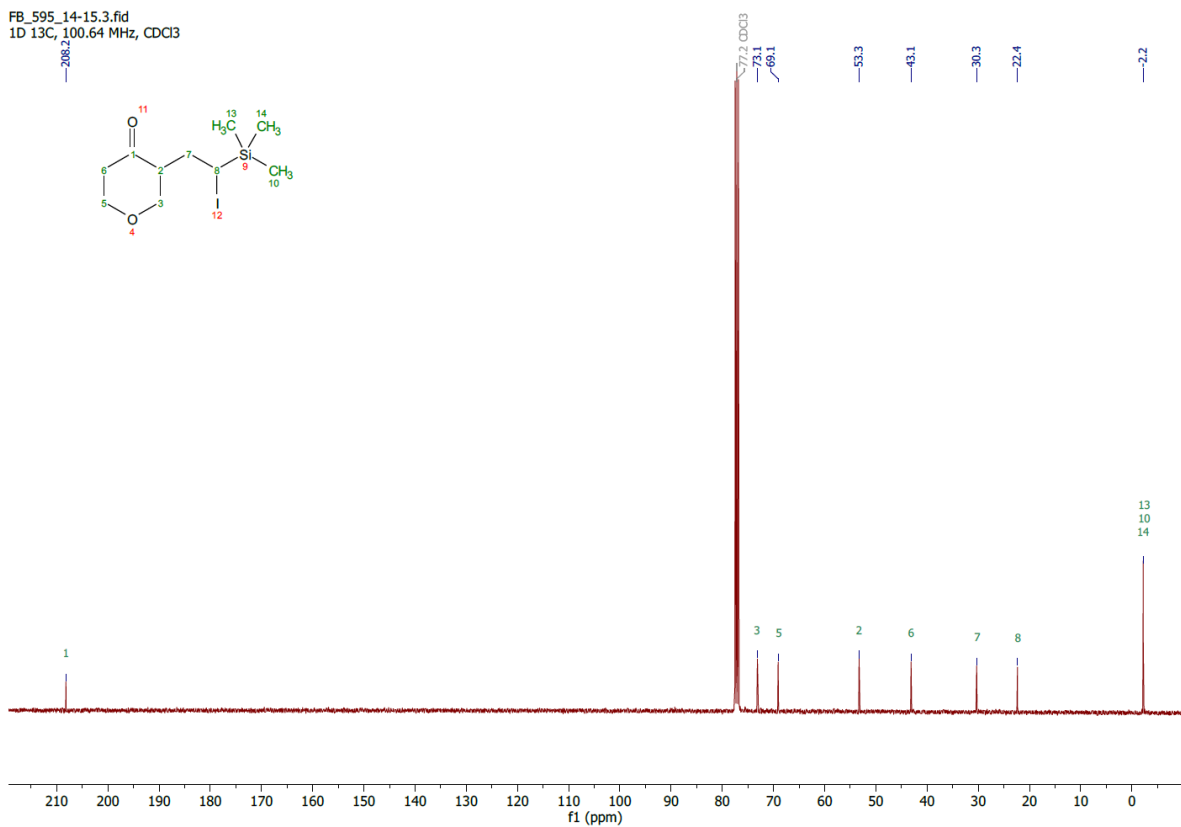


3-(2-Iodo-2-(trimethylsilyl)ethyl)tetrahydro-4H-pyran-4-one **3d** (diastereomer I)

FB_595_14-15.1.fid
1D 1H, 400.18 MHz, CDCl₃

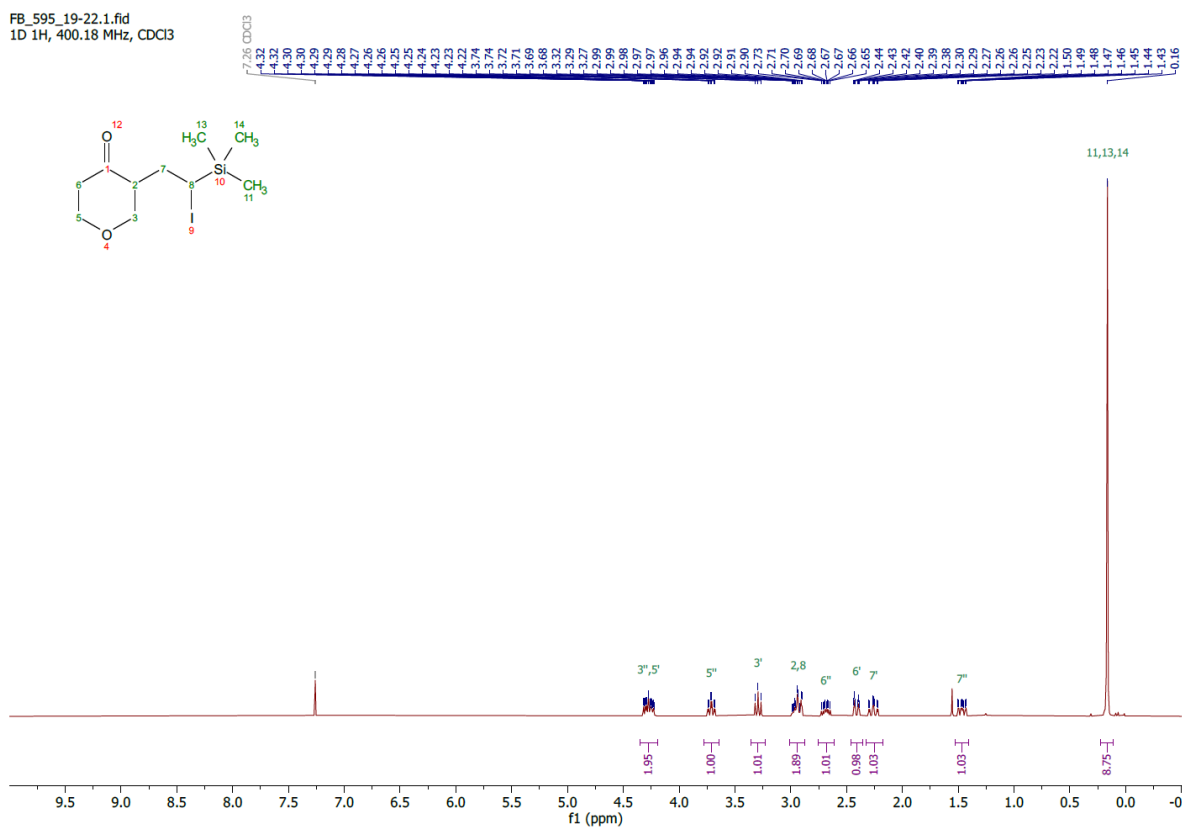


FB_595_14-15.3.fid
1D 13C, 100.64 MHz, CDCl₃

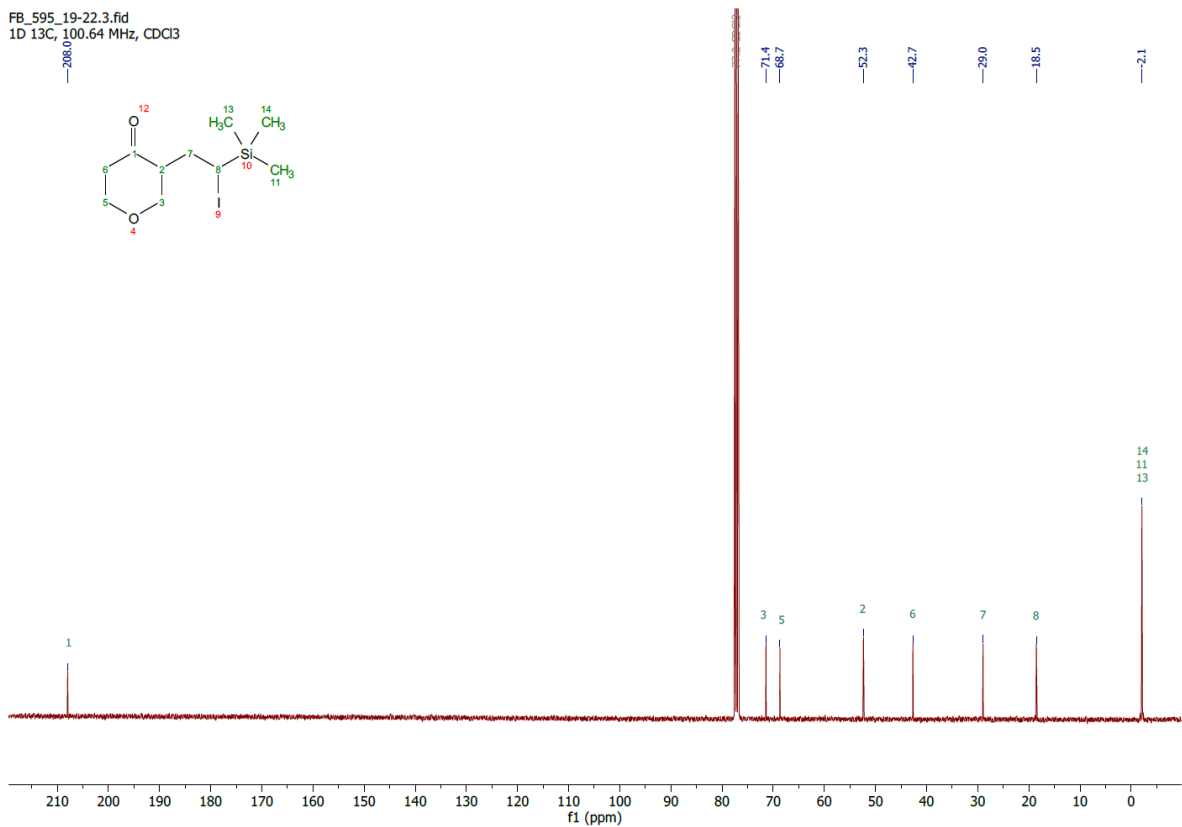


3-(2-Iodo-2-(trimethylsilyl)ethyl)tetrahydro-4H-pyran-4-one **3d** (diastereomer II)

FB_595_19-22.1.fid
1D 1H, 400.18 MHz, CDCl3

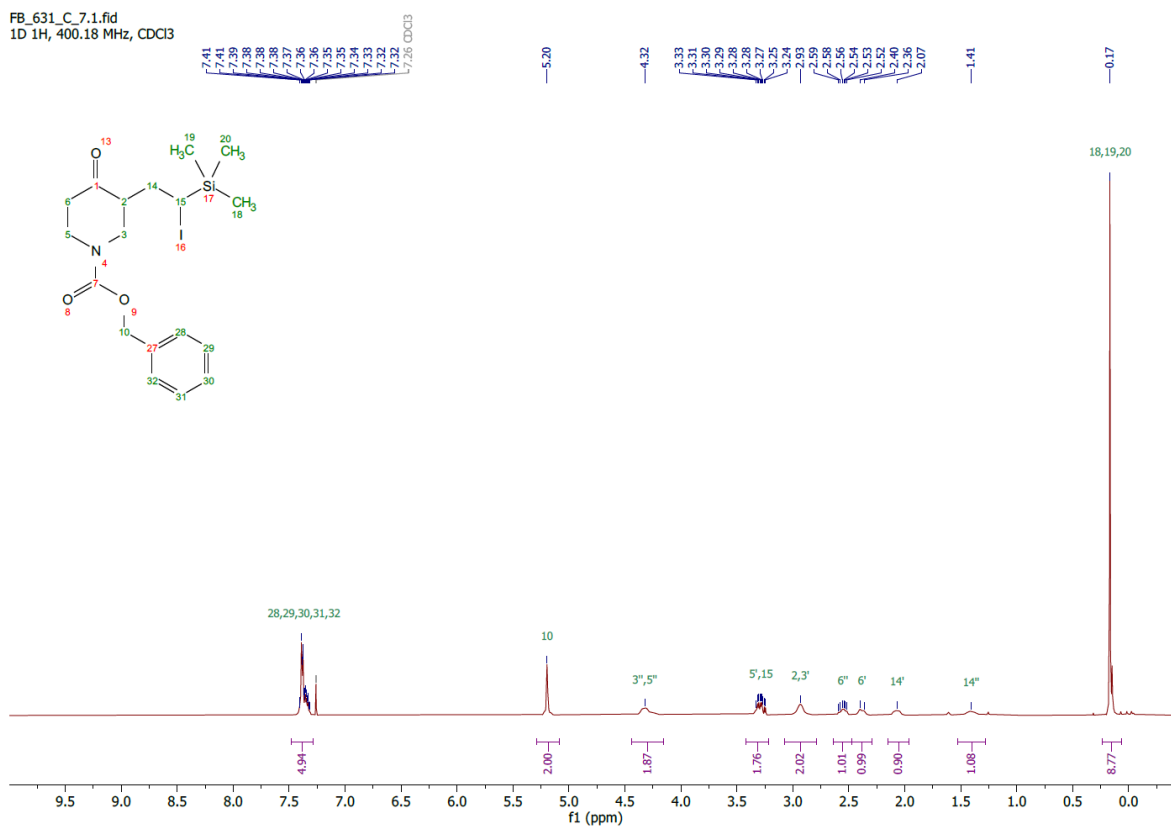


FB_595_19-22.3.fid
1D 13C, 100.64 MHz, CDCl3

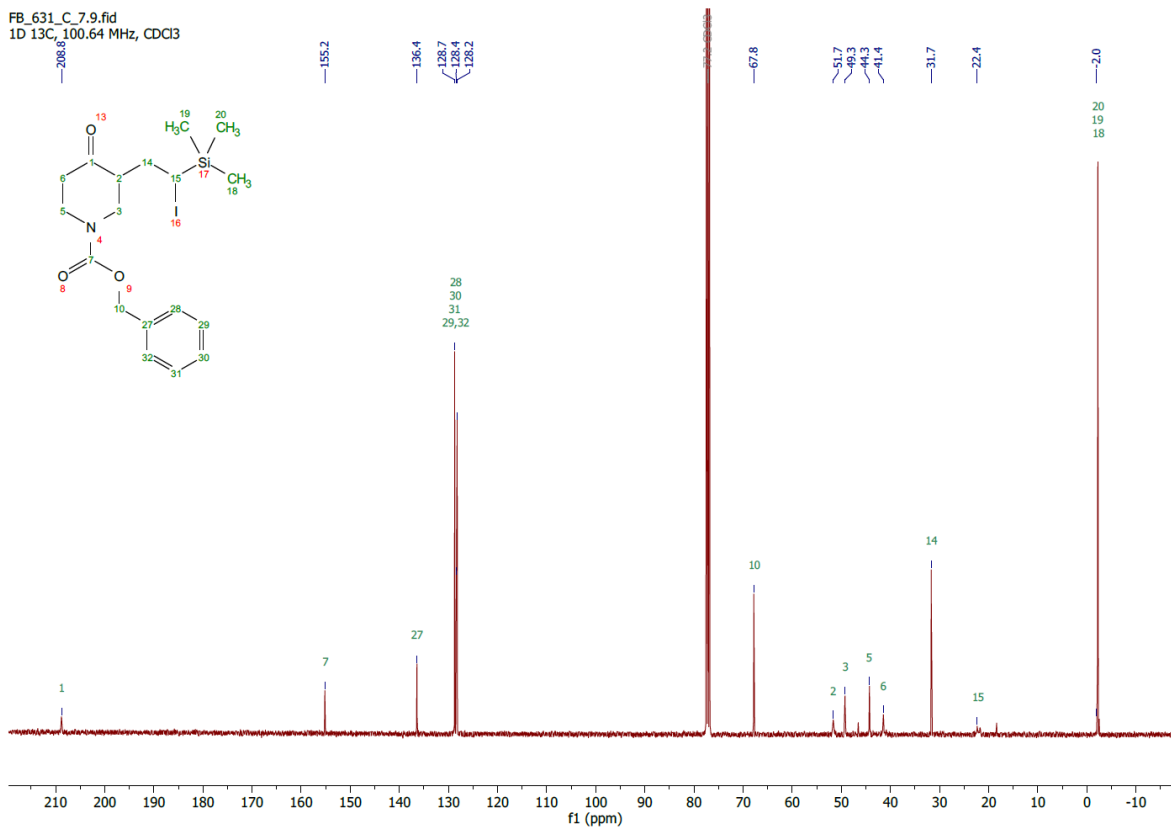


Benzyl 3-(2-iodo-2-(trimethylsilyl)ethyl)-4-oxopiperidine-1-carboxylate **3e** (*diastereomer I*)

FB_631_C_7.1.fid
1D 1H, 400.18 MHz, CDCl3

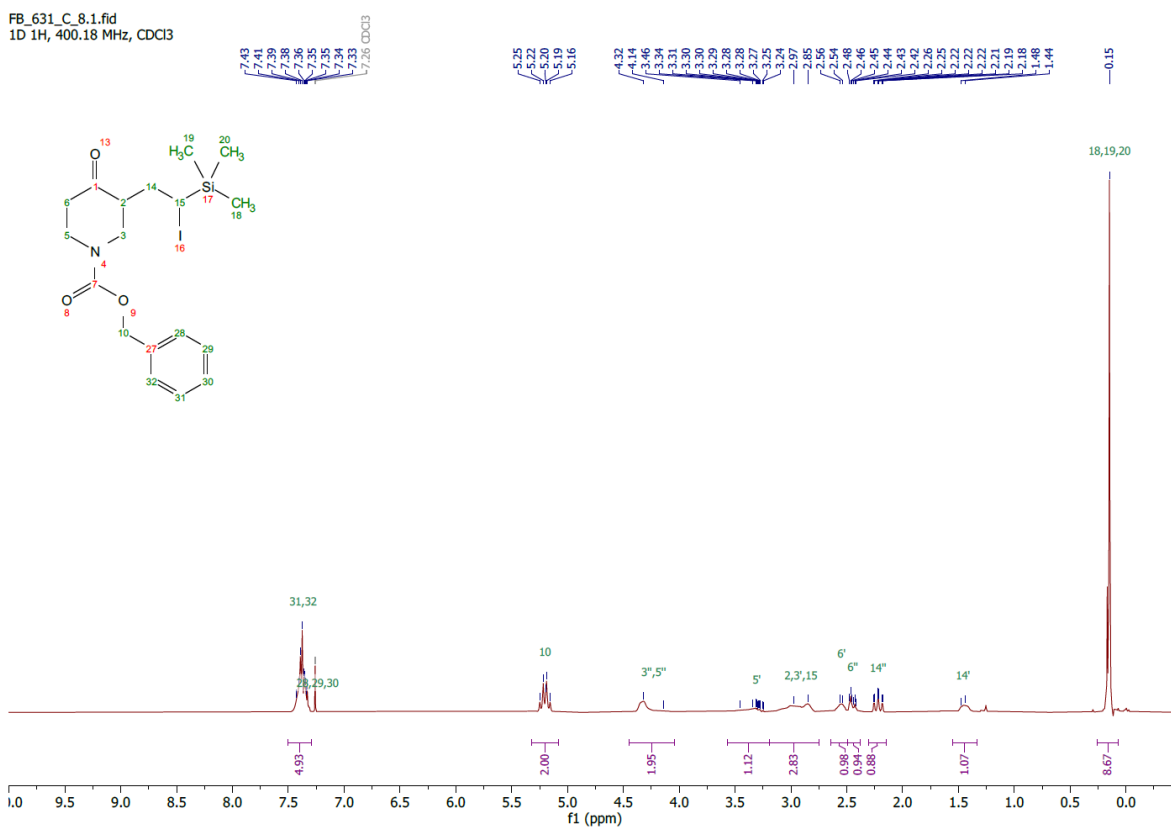


FB_631_C_7.9.fid
1D 13C, 100.64 MHz, CDCl3



Benzyl 3-(2-iodo-2-(trimethylsilyl)ethyl)-4-oxopiperidine-1-carboxylate **3e** (*diastereomer II*)

FB_631_C_8.1.fid
1D 1H, 400.18 MHz, CDCl3



FB_631_C_8.9.fid
1D 13C, 100.64 MHz, CDCl3

